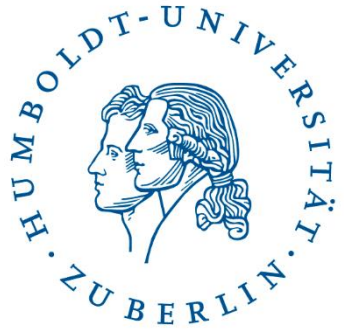

Chemoselective synthesis of functional drug conjugates

Dissertation zur Erlangung des akademischen Grades doctor rerum naturalium (Dr. rer. nat.)

im Fach: Chemie
Spezialisierung: Organische und Bioorganische Chemie

eingereicht an der
Mathematisch-Naturwissenschaftlichen Fakultät der Humboldt-Universität zu Berlin
von

M. Sc. Marc-André Kasper

Präsidentin der Humboldt-Universität zu Berlin
Prof. Dr.-Ing. Dr. Sabine Kunst

Dekan der Mathematisch-Naturwissenschaftlichen Fakultät
Prof. Dr. Elmar Kulke

Berlin, Juni 2019

Gutachter/innen:

1. Prof. Dr. Christian Hackenberger
2. Prof. Dr. Dorothea Fiedler
3. Prof. Dr. Jeffrey W. Bode

Tag der mündlichen Prüfung: 22.10.2019

I. Declaration

The present work has been accomplished in the time between the 1st of November 2014 until the 30th of June 2019 under the supervision of Prof. Dr. Christian P. R. Hackenberger at the Institut für Chemie of the Humboldt Universität zu Berlin and the Leibniz-Forschungsinstitut für molekulare Pharmakologie.

I hereby declare, that I have authored the present dissertation independently and only by means of the stated resources in accordance to § 7 paragraph 3 of the doctoral degree regulations of the faculty of mathematics and natural sciences, published in the official gazette of the Humboldt-Universität zu Berlin AMB No. 42/2018 from the 11th of July 2018. I have not applied for a doctor's degree elsewhere and do not hold a corresponding doctor's degree.

Berlin,

Marc-André Kasper

Die vorliegende Arbeit wurde in der Zeit vom 01.11.2014 bis zum 30.06.2019 unter der Leitung von Prof. Dr. Christian P. R. Hackenberger am Institut für Chemie der Humboldt Universität zu Berlin sowie am Leibniz-Forschungsinstitut für molekulare Pharmakologie angefertigt.

Hiermit erkläre ich, die vorliegende Dissertation selbstständig und nur unter Verwendung der angegebenen Hilfsmittel, gemäß § 7 Absatz 3 der Promotionsordnung der Mathematisch-Naturwissenschaftlichen Fakultät, veröffentlicht im Amtlichen Mitteilungsblatt Nr. 42/2018 vom 11. Juli 2018 angefertigt zu haben. Ich habe mich nicht anderweitig um einen Doktorgrad in dem Promotionsfach beworben und besitze keinen entsprechenden Doktorgrad.

Berlin,

Marc-André Kasper

II. Publications, patents, talks and posters

The work that has been performed during the doctoral studies of the author resulted so far in the following publications, patents, talks and posters:

A. Publications

1) Nicole Nischan, Marc-André Kasper, Thresen Mathew, Christian P.R. Hackenberger*
Org. Biomol. Chem. **2016**, 14, 7500-7508
Bis(arylmethyl)-substituted unsymmetrical phosphites for the synthesis of lipidated peptides via Staudinger-phosphite reactions

2) Henry D. Herce*, Dominik Schumacher*, Anselm F.L. Schneider, Anne K. Ludwig, Florian A. Mann, Marion Fillies, Marc-André Kasper, Stefan Reinke, Eberhard Krause, Heinrich Leonhardt, M. Cristina Cardoso*, Christian P.R. Hackenberger*
Nat. Chem. **2017**, 9, 762-771
Cell-permeable nanobodies for targeted immunolabelling and antigen manipulation in living cells.

3) Andreas Stengl, Marcus Gerlach, Marc-André Kasper, Christian P.R. Hackenberger, Heinrich Leonhardt, Dominik Schumacher*, Jonas Helma*
Org. Biomol. Chem. **2019**, 17, 4964-4969
TuPPL: Tub-tag mediated C-terminal protein–protein-ligation using complementary click-chemistry handles

4) Marc-André Kasper, Maria Glanz, Andreas Stengl, Martin Penkert, Simon Klenk, Tom Sauer, Dominik Schumacher, Jonas Helma, Eberhard Krause, M. Cristina Cardoso, Heinrich Leonhardt, Christian P. R. Hackenberger*
Angew. Chem. Int. Ed. **2019** DOI: 10.1002/anie.201814715
Cysteine-Selective Phosphonamidate Electrophiles for Modular Protein Bioconjugations

Also published as:
Angew. Chem. **2019** DOI: 10.1002/ange.201814715
Cysteinselektive phosphonamidatbasierte Elektrophile für modulare Biokonjugationen

5) Marc-André Kasper†, Maria Glanz†, Andreas Oder, Peter Schmieder, Jens P. von Kries, Christian P. R. Hackenberger*
Chem. Sci. **2019**, 10, 6322-6329
Vinylphosphonites for Staudinger-induced chemoselective peptide cyclization and functionalization
† authors contributed equally

6) Marc-André Kasper, Andreas Stengl, Philipp Ochtrop, Marcus Gerlach, Tina Stoschek, Dominik Schumacher, Jonas Helma, Martin Penkert, Eberhard Krause, Heinrich Leonhardt*, Christian P. R. Hackenberger*
Angew. Chem. Int. Ed. **2019** DOI: 10.1002/anie.201904193
Ethynylphosphonamidates for the rapid and cysteine selective generation of efficacious Antibody-Drug-Conjugates

B. Patents

1) Marc-André Kasper, Maria Glanz, Tom Sauer, Dominik Schumacher, Jonas Helma, Andreas Stengl, Heinrich Leonhardt, Christian P. R. Hackenberger
WO 2018041985 A1
Chemoselective thiol-conjugation with alkene or alkyne-phosphonamidates

2) Alice Baumann, Marc-André Kasper, Stephen Byrne, Jonas Helma, Heinrich Leonhardt, Tina Stoschek, Marcus Gerlach, Jonas Helma, Dominik Schumacher, Christian P. R. Hackenberger
PCT/EP2019/055509
Chemoselective Thiol-Conjugation with Alkene or Alkyne-Phosphonothiolates and -Phosphonates

C. Talks

1) Marc-André Kasper*, Maria Glanz, Andreas Stengl, Martin Penkert, Dominik Schumacher, Jonas Helma, Eberhard Krause, Heinrich Leonhardt, Christian P. R. Hackenberger
*Invited speaker: Bundesanstalt für Materialforschung und -prüfung (BAM), Berlin, Germany, 8th of May **2017**.
"P5-Labelling" for the construction of antibody-drug-conjugates

2) Marc-André Kasper, Maria Glanz, Andreas Stengl, Dominik Schumacher, Jonas Helma, Heinrich Leonhardt, Christian P. R. Hackenberger
12th Australian Peptide Conference, Noosa Heads, Australia, 16th of October **2017**
„P5-labelling" - Chemoselectively Induced Cysteine-Conjugation to Unsaturated Phosphonamidates

3) Marc-André Kasper*, Andreas Stengl, Dominik Schumacher, Jonas Helma, Heinrich Leonhardt, Christian P. R. Hackenberger
2nd Joint FMP/MDC Technology Transfer Workshop, Berlin, Germany, 09th of November **2017**
P5-labelling for next-generation Antibody-Drug-Conjugates
* Winner of the FMP Transfer Award and 2nd prize in the audience award

4) Marc-André Kasper*, Andreas Stengl, Philipp Ochtrop, Dominik Schumacher, Jonas Helma, Heinrich Leonhardt, Christian P. R. Hackenberger
*Invited Speaker: European Antibody Congress 2018, Basel, Switzerland, 30th of October **2018**
Chemoselectively induced bioconjugation for stable and homogeneous ADCs

D. Posters

1) Marc-André Kasper, Maria Glanz, Christian P. R. Hackenberger
EMBO Conference: Chemical Biology 2016, Heidelberg, Germany, 31st of August – 3rd of September **2016**
Exploiting the electrophilic and nucleophilic reactivity of phosphorus building blocks for the chemoselective modification of proteins

2) Dominik Schumacher, Marc-André Kasper, Henry D. Herce, Maria Glanz, Jonas Helma, M. Cristina Cardoso, Heinrich Leonhardt, Christian P. R. Hackenberger
Bürgenstock - Conference, Brunnen, Switzerland, 30th of April – 4th of May **2017**
New chemoselective reactions for the generation of cell-permeable protein and antibody-conjugates

3) Maria Glanz, Marc-André Kasper, Jordi Bertran-Vicente, Christian P. R. Hackenberger
7th Chemical Protein Synthesis Meeting, Haifa, Israel, 4th – 7th of September **2017**
Development of New Cysteine-Selective Bioconjugation Methods Based on Electrophilic Phosphorous(V) Compounds

4) Marcus Gerlach, Tina Stoschek, Hans Mescheder, Marc-André Kasper, Andreas Stengl, Christian P. R. Hackenberger, Heinrich Leonhardt, Dominik Schumacher, Jonas Helma
   7th Chemical Protein Synthesis Meeting, Haifa, Israel 4th – 7th of September **2017**
   Tub-Tag labelling: Chemoenzymatic protein functionalization by Tubulin Tyrosine Ligase enables next-generation Antibody-Drug-Conjugates

5) Marc-André Kasper, Sergej Schwagerus, Christian P. R. Hackenberger
   12th GDCh Scientific Forum Chemistry 2017 – Anniversary Congress "GDCh – 150 Years", Berlin, Germany, 10th – 14th of September **2017**
   Highly cysteine-selective protein modification with unsaturated phosphonamidates: Staudinger-induced conjugate addition

6) Marc-André Kasper*, Maria Glanz, Henry D. Herce, M. Cristina Cardoso, Christian P. R. Hackenberger
   6th Modern Solid Phase Peptide Synthesis and its Applications Symposium, Frazer Island, Australia, 12th – 14th of October **2017**
   Chemoselectively Induced Cysteine-Conjugation to Unsaturated Phosphonamidates for the Side-Selective Generation of Peptide-Protein Conjugates
   *Poster Prize Award

7) Marc-André Kasper*, Andreas Stengl, Jonas Helma, Dominik Schumacher, Heinrich Leonhardt, Christian P. R. Hackenberger
   12th Australian Peptide Conference, Noosa Heads, Australia, 15th – 19th of October **2017**
   „P5-labelling" - Chemoselectively Induced Cysteine-Conjugation to Unsaturated Phosphonamidates
   *Poster Prize Award

8) Andreas Stengl, Hans Mescheder, Marcus Gerlach, Tina Stoschek, Harald Polzer, Marc-André Kasper, Binje Vick, Heinrich Flaswinkel, Elisabeth Kremmer, Irmela Jeremias, Karsten Spiekermann, Christian P. R. Hackenberger, Heinrich Leonhardt, Jonas Helma, Dominik Schumacher
   SFB 1243 Cancer evolution symposium Munich, Germany, 1st-3rd of March **2018**
   Next-generation Antibody Drug Conjugates (ADCs) for targeted therapy of Acute Myeloid Leukemia (AML)

9) Andreas Stengl, Marcus Gerlach, Tina Stoschek, Hans Mescheder, Ricarda Trapp, Marc-André Kasper, Christian P. R. Hackenberger, Dominik Schumacher, Jonas Helma, Heinrich Leonhardt
PEGS 2018, Boston, Massachusetts, United States of America, 30th of April – 4th of May **2018**
The Tub-Tag®: A Tool for Site-Specific Protein Conjugation with Application in Antibody-Drug-Conjugates (ADC) Development

10) Marc-André Kasper, Philipp Ochtrop, Andreas Stengl, Jonas Helma-Smets, Dominik Schumacher, Heinrich Leonhardt, Christian P. R. Hackenberger
FMP/MDC PostDoc Day 2018, Berlin, Germany, 1st of June **2018**
„P5-labelling" - Chemoselectively Induced Cysteine-Conjugation to Unsaturated Phosphonamidates

11) Alice Baumann, Marc-André Kasper, Maria Glanz, Sergej Schwagerus, Andreas Stengl, Jonas Helma, Dominik Schumacher, Heinrich Leonhardt, Christian P. R. Hackenberger
ArmChemFront 2018 Frontiers in Chemistry, Yerevan, Armenia, 21th – 25th of October **2018**
A cysteine-selective bioconjugatio method based on electrophilic phosphorous(V) compounds

12) Marcus Gerlach†, Marc-André Kasper†, Tina Stoschek, Philipp Ochtrop, Andreas Stengl, Hans-Christian Mescheder, Stefanie Boldt, Heinrich Leonhardt, Jonas Helma, Christian Hackenberger, Dominik Schumacher
8th Chemical Protein Synthesis (CPS) Meeting, Berlin, Germany, 16th-19th of june **2019**
Novel enzymatic and chemical strategies for stable Antibody Drug Conjugates
† authors contributed equally

13) Alice Baumann†*, Maria Glanz†*, Marc-André Kasper†*, Sergej Schwagerus†*, Christian Hackenberger
8th Chemical Protein Synthesis (CPS) Meeting, Berlin, Germany, 16th-19th of june **2019**
Cysteine-selective bioconjugations based on electrophilic phosphorous(V) reagents
† authors contributed equally
*Poster Prize Award

III. Acknowledgements

First of all, I would like to thank Prof. Dr. Christian Hackenberger for supervising the work during my doctoral studies. I am truly thankful for always having an open door to discuss about research, for trusting my decisions, for giving me enough freedom to develop my own ideas, and most importantly for always being so supportive. I highly appreciate all the great chances to present our work outside and within the FMP.

I also would like to thank Prof. Dr. Dorothea Fiedler and Prof. Dr. Jeffrey Bode for taking their precious time to review this thesis.

I had the honor to collaborate with outstanding researchers from other institutes within the last years. The work for this thesis would not have been possible without the support and expertise from Dominik Schumacher and Jonas Helma, founders of the start-up project Tubulis-Technologies. Furthermore I thank Andreas Stengl, Prof. Dr. Heinrich Leonhardt, Prof. Dr. Karsten Spiekermann, Maike Roas, Marcus Gerlach and Tina Stoschek for the fruitful collaboration within the ADC projects.

I would also like to mention the inspiring working atmosphere and good collaborations within the FMP. I always enjoyed the open doors of all the other research groups when it came to starting a new project or using the great facilities. Thanks to Peter Schmieder, Brigitte Schlegel, Nils Trieloff and Monika Beerbaum for the support in interpreting NMR spectra, setting up experiments and maintaining the instruments. Another big thank you goes to the MS-facility, especially to Eberhard Krause, Martin Penkert, Michael Schümann, Heike Stephanowitz and Fan Liu for setting up the MS-experiments and all the help with data analysis. Furthermore I would like to acknowledge Martin Lehmann, Burkhard Wiesner and Jenny Eichhorst for performing cellular imaging experiments and very helpful discussions on cell biology.

Manny thanks go to the students I was allowed to supervise. Thank you, Arif Celik, Brian Rusi, Don Shenal Munasinghe, Jan Ole Kaufmann and Sebastian Trunschke for the great time, laboratory skills and delicious cakes and cookies. Lukas Lassak deserves a special notice for his relentless efforts in solving difficult column purification problems and for making our lab a healthier place to work in.

I was really blessed with great colleagues that were always helpful and supportive and made working much more fun. Very special thanks go to all current and former members of our group: Alec Michels, Alice Baumann, Anett Hauser, Anselm Schneider, Antoine Wallabregue, Beate Kindt, Bingjia Yan, Christian Stieger, Dagmar Krause, Debasish Bhowmick, Dominik Schumacher, Don Shenal Munasinghe, Florian Mann, Ines Kretzschmar, Jacob Gorenflos, Jennifer Trümpler, Jordi Bertran-Vicente, Katrin Wittig, Kristin Kemnitz-Hassanin, Kristina Siebertz, Lutz Adam, Maria Glanz, Marianne Dreißigacker,

Acknowledgements

Martin Penkert, Nicole Nischan, Olaia Nieto García, Oliver Reimann, Philipp Ochtrop, Reihaneh Safavi-Sohi, Sebastián Florez Rueda, Sergej Schwagerus, Simon Klenk, Simon Reiske, Tom Sauer, Wenyi Li. Thank you, Philipp and Dominik for proofreading this thesis and Philipp for the good company on trips to Basel and Munich. See you in the Jägerklause. Thank you Kristin for your patience with untidy PhD-students and for driving us home after Maibowle. Thanks to Maria, Simon, Lutz and Philipp: You managed to turn unpleasant office work into a lot of fun. Sorry Lutz for stealing all your pens. Special thanks to “the experts”: Flo, Jordi and Olli for never ending expertise, advice and long fun nights out. A big hug goes to Simon for being the best Lab and office mate you can think of. Thank you for scientific advice, a fun trip to Cologne and enjoying the best Scotch together.

I would also like to thank all my friends outside of work. Especially: Frederik Finnmann, Marvin George, Peter Carl, Philipp Ulita, Philipp Zimmermann, Sebastian Wahl, Simon Bürger, Timm Schwaar and Viktoria Steck. You all know why you are mentioned.

Finally I would like to thank my family. I am grateful to have such supportive parents who made my studies possible and always stand by my side with good advice and distraction from working life. I am truly grateful for my older sister Marie together with Olli, Larina and Lia. I always enjoy coming home to Wendeburg.

My last and foremost thank you goes to Sophie. Only your endless patients in listening to my stories and complains about work and the beautiful time we spend together outside of work always brought me and my motivation back on track.

„Die Kuben der großen Bahnachsen verhalten sich wie die Quadrate der Umlaufzeit“

3. Kepplersches Gesetz (Sinngemäß), Johannes Keppler, 17. Jahrhundert.

1. Table of contents

2. Abbreviations

ADC	antibody drug conjugate
ADCC	antibody-dependent cellular cytotoxicity
Ar	aryl
AML	acute myeloid leukemia
BOC	*tert*-butyloxycarbonyl
CDC	complement-dependent cytotoxicity
CDR	complementarity determining region
CPP	cell penetrating peptide
CoA	coenzyme A
CUAAC	copper-catalyzed azide alkyne cycloaddition
Cy5	cyanine5
DABCO	1,4-diazabicyclo[2.2.2]octane
DAR	drug to antibody ratio
DIPEA	*N*,*N*-diisopropylethylamine
DMF	dimethylformamide
DMSO	dimethylsulfoxide
DNA	deoxyribonucleic acid
DTT	dithiothreitol
E. coli	*Escherichia coli*
EDANS	5-((2-aminoethyl)amino)naphthalene-1-sulfonic acid
EDC	1-ethyl-3-(3-dimethylaminopropyl) carbodiimide
EDTA	ethylenediaminetetraacetic acid
eGFP	enhanced green fluorescent protein
EPL	expressed protein ligation
EPR	enhanced permeability and retention
Fab	fragment antigen binding antibody
Fc	fragment crystallizable region
FDA	food and drug administration
FMOC	fluorenylmethyloxycarbonyl
FRET	förster resonance energy transfer
GSH	glutathione
HPLC	high-performance liquid chromatography

IEDDA	inverse electron demand Diels–Alder reaction
IgG	immunoglobulin G
HOMO	highest occupied molecular orbital
LUMO	lowest unoccupied molecular orbital
MALDI	matrix-assisted laser desorption/ionization
MeCN	acetonitrile
MIP	molecularly imprinted polymers
MMAE	monomethylauristatin E
MMAF	monomethylauristatin F
MS	mass spectrometry
MWCO	molecular weight cut-off
NCL	native chemical ligation
NHS	*N*-hydroxysuccinimide
NMR	nuclear magnetic resonance
PBS	phosphate-buffered saline
PEG	poly ethylene glycol
PTM	post translational modification
scFv	single-chain variable fragment
SDS/PAGE	sodium dodecyl sulfate–polyacrylamide gel electrophoresis
SPAAC	strain-promoted azide alkyne cycloaddition
SPANC	strain-promoted azide nitrone cycloaddition
SPhR	Staudinger-phosphonite reaction
SPPS	solid-phase peptide synthesis
TCEP	tris(2-carboxyethyl)phosphine
TCO	*trans*-cyclooctene
TFA	trifluoroacidic acid
THF	tetrahydrofurane
THPTA	tris(benzyltriazolylmethyl)amine
TPPTS	triphenylphosphine trissulfonate
Tris	tris(hydroxymethyl)aminomethane
t-RNA	transfer ribonucleic acid
UPLC	ultra-performance liquid chromatography

3. Abstract

3.1. English

Chemoselective transformations constitute a particularly powerful class of chemical reactions, when applied to both: Classical organic synthesis as well as modern bioconjugation reactions. A chemoselective reaction allows on the one hand a facile transformation of functional organic compounds without the need of tedious protecting group manipulations and facilitates on the other hand the attachment of modifications to a distinct site of a biomolecule. While the former can significantly decrease the number of synthetic steps that are necessary to obtain a desired product, the latter is essential for a plethora of applications in the life sciences, in particular for the investigation of biological processes and the development of targeted therapeutics.

The present work introduces a novel modular reaction sequence of two chemoselective manipulations in a row. It is shown that vinyl- and ethynylphosphonamidates react selectively with cysteine residues on biomolecules such as proteins and antibodies. Most importantly, it is demonstrated that those electrophilic phosphonamidates can be incorporated into a given molecule in another preceding chemoselective Staudinger-phosphonite reaction (SPhR) from unsaturated phosphonites and azides. During this reaction, an electron-rich phosphonite is transformed into an electron-deficient phosphonamidate that is thereby activated for the subsequent thiol addition. The described technique thereby extends the existing repertoire of bioconjugations by introducing a new concept in protein synthesis: A chemoselective reaction that induces reactivity for a subsequent bioconjugation. The SPhR enables the synthesis of various functional electrophilic phosphonamidates, including biotin derivatives, fluorescent dyes, functional peptides and pharmaceutically active drugs. Together with the subsequent attachment to cysteine residues, the method facilitates the generation of highly functional protein and antibody conjugates in only two chemical steps. The thiol addition is reasonably fast with second order rate constants of up to 0.62 $M^{-1}s^{-1}$ and highly selective for the addition to cysteine over all other proteinogenic amino acids when ethynylphosphonamidates are used. Vinylphosphonamidates on the other hand are slower in the reaction with cysteine and less selective but can be tuned in cysteine reactivity by the attachment of electron withdrawing substituents to the phosphonamidate ester residue. Since retro-thiol addition is not observed, phosphonamidate-adducts hold an excellent conjugate stability in the presence of human serum, cell lysate and other thiols in excess.

Bioconjugations that are used to obtain therapeutic conjugates have to fulfil crucial criteria, including high selectivity for a given amino acid, clean reaction products and excellent stability of the protein

adducts in biological environments. Those properties drastically influence the performance and safety profile of a medication. Since phosphonamidate conjugations to cysteine hold all these features, it is described in the second part of the present work how ethynylphosphonamidates can be employed for the conjunction of tumor-sensing antibodies and cytotoxic drugs to generate Antibody-Drug-Conjugates (ADCs). A simple synthetic protocol starting from unengineered antibodies, using only a slight excess of the desired drug in a one-pot synthesis protocol is introduced. In a direct comparison to the maleimide containing FDA-approved Adcetris®, phosphonamidate linked ADCs show a superior behaviour in terms of linkage stability in serum, combined with an increased *in vivo* efficacy in a tumor xenograft mouse model. Taken together, the method described herein combines simple synthetic access with high selectivity, superior conjugate stability and the possibility to synthesize highly efficacious drug conjugates and is therefore likely to have a great contribution to the field of targeted therapeutics.

3.2. Deutsch

Chemoselektive Umwandlungen, angewendet auf klassische organische Synthese, wie auch auf moderne Biokonjugationsreaktionen stellen eine besonders leistungsstarke Klasse von chemischen Reaktionen dar. Eine chemoselektive Reaktion erlaubt einerseits eine mühelose Umwandlung von organischen Verbindungen ohne aufwändige Schutzgruppenmanipulationen und ermöglicht andererseits die Anbindung einer Modifikation an einer definierten Stelle eines Biomoleküls. Während Ersteres die Anzahl von synthetischen Schritten, die benötigt werden um ein gewünschtes Produkt zu synthetisieren drastisch reduzieren kann, ist letzteres unerlässlich für eine Vielzahl von Anwendungen im Bereich der Lebenswissenschaften, insbesondere bei der Untersuchung von biologischen Prozessen und der Entwicklung von zielgerichteten Therapien.

In der vorliegenden Arbeit wird eine neuartige Reaktionssequenz von zwei aufeinanderfolgenden chemoselektiven Umwandlungen vorgestellt: Es wird gezeigt, dass Vinyl- und Ethynylphosphonamidate chemoselektiv mit Cysteinen von Biomolekülen, wie Proteinen und Antikörpern reagieren. Im Besonderen wird weiterhin aufgezeigt, dass diese elektrophilen Phosphonamidate durch eine vorhergehende chemoselektive Staudinger-Phosphonit Reaktion zwischen Aziden und ungesättigten Phosphoniten in das gewünschte Molekül eingebaut werden können. Hierbei wird ein elektronenreiches Phosphonit in ein elektronenarmes Phosphonamidat umgewandelt, welches somit für die nachfolgende Thiol-Addition aktiviert wird. Die beschriebene Methode erweitert dadurch das bestehende Repertoire von Biokonjugationen durch die Einführung eines neuen Konzepts in der Proteinsynthese: Eine chemoleselektive Reaktion, die Reaktivität für eine nachfolgende Biokonjugation induziert. Die Staudinger-Phosphonit-Reaktion ermöglicht die

Herstellung von verschiedenen funktionalen elektrophilen Phosphonamidaten, wie zum Beispiel Biotinderivaten, fluoreszierenden Farbstoffen, funktionalen Peptiden und Wirkstoffmolekülen mit pharmakologischer Aktivität. Mit der nachfolgenden Addition an Cysteine können somit hoch-funktionale Konjugate von Proteinen und Antikörpern in nur zwei chemischen Schritten hergestellt werden. Die Thiol-Addition ist angemessen schnell mit einer Geschwindigkeitskonstante zweiter Ordnung von bis zu 0.62 $M^{-1}s^{-1}$ und hoch-selektiv für die Modifikation von Cystein in Gegenwart von allen anderen proteinogenen Aminosäuren, wenn Ethynylphosphonamidate verwendet werden. Obwohl Vinylphosphonamidate langsamer in der Reaktion und weniger selektiv für Cysteine sind, kann die Reaktivität hier durch die Anbindung von elektronenziehenden Substituenten an den Phosphonamidatester-Substituenten justiert werden. Da keine Rückreaktion der Thiol-Addition beobachtet wird, weisen Phosphonamidat-Addukte eine herausragende Stabilität in Gegenwart von humanem Serum, Zelllysat oder einem Überschuss von anderen Thiolen auf.

Werden Biokonjugationen verwendet um therapeutische Konjugate herzustellen, müssen entscheidende Kriterien erfüllt sein, wie zum Beispiel eine hohe Selektivität für eine bestimmte Aminosäure, saubere Reaktionsprodukte und eine hervorragende Stabilität der Protein-Addukte in biologischen Umgebungen. Diese Eigenschaften beeinflussen die Leistungsfähigkeit und die Sicherheit eines Medikaments maßgeblich. Da Phosphonamidat-Konjugationen an Cysteine all diese Eigenschaften mitbringen, wird im zweiten Teil dieser Arbeit beschrieben wie Ethynylphosphonamidate für die Anbindung von zytotoxischen Wirkstoffen an tumor-bindende Antikörper genutzt werden können um sogenannte Antikörper-Wirkstoff-Konjugate herzustellen. Ein einfaches Syntheseprotokoll für die Herstellung, ausgehend von einem nicht gentechnisch veränderten Antikörper mit nur geringen Überschüssen des gewünschten Wirkstoffs wird vorgestellt. Phosphonamidat-verbundene Antikörper-Wirkstoff-Konjugate zeigen im direkten Vergleichen zum zugelassenen, Maleimid-verbundenen Adcetris® überlegende Eigenschaften, wie eine erhöhte Stabilität in Serum, kombiniert mit einer erhöhten *in vivo* Wirksamkeit in einem Tumor Xenograft Mausmodel. Zusammenfassend verbindet die hier vorgestellte Methode einen einfachen synthetischen Zugang mit hoher Selektivität, überragender Konjugat-Stabilität und der Möglichkeit hochwirksame Wirkstoffkonjugate herzustellen und wird daher aller Voraussicht nach einen großen Beitrag zum Gebiet der zielgerichteten Therapie leisten.

4. Introduction

4.1. Motivation

Despite tremendous research efforts world-wide with breakthroughs in the development of new medications for the treatment of neoplastic diseases in the last decades, cancer is still one of the most life-threatening diseases with an estimated account for 9.6 million death globally in 2018 according to the world health organization.[1]

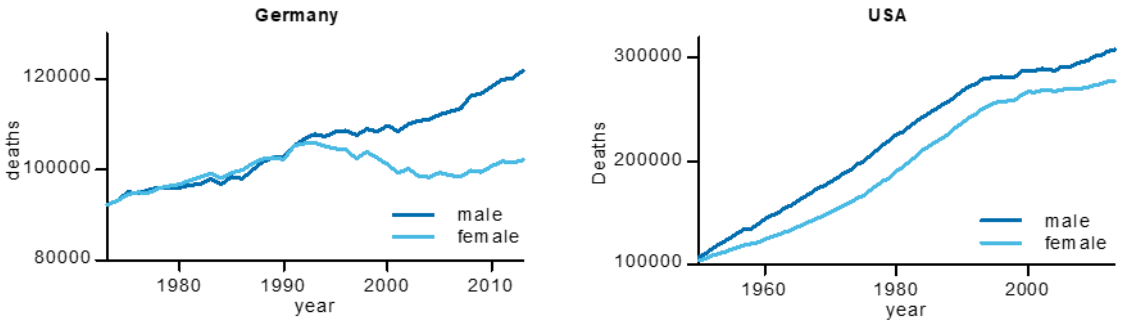

Figure 1: Mortality from all cancer types in Germany and the USA. Depicted are numbers of deaths for men (blue) and women (light blue) caused by malignant diseases per year. Data originates from the GLOBOCAN 2018 database, part of the international agency for research on cancer's (IARC's) global cancer observatory.

The development of novel treatment options for a lot of malignant diseases led to a 25-year decline in mortality rate for diagnosed cases.[2] However, due to a steady increase in diagnosed cases, cancer is the second leading cause of death and is estimated to surpass cardiovascular disease, expected to become the leading cause of death in industrial countries within the next ten years (Figure 1).[3] The increasing cancer burden is attributed to several factors such as population growth, ageing and changing prevalence of certain causes of cancer linked to social and economic development.[2]

4.2. Cancer treatment

The growing number of diagnosed neoplasms have spurred research-efforts to develop novel treatment options that prolong life expectancy of patients or even completely cure the disease. Even though cytotoxic agents (chemotherapeutics) still remain an important therapy option, recent break-through in understanding tumor biology have let to the development of more targeted approaches. Important novel therapy options include angiogenesis inhibitors, laser therapy, hyperthermia, photodynamic therapy, bone marrow and peripheral blood stem cell transplantations. Furthermore, biological therapies have been developed, including interferons, interleukins, monoclonal antibodies, vaccines and gene therapy.[4]

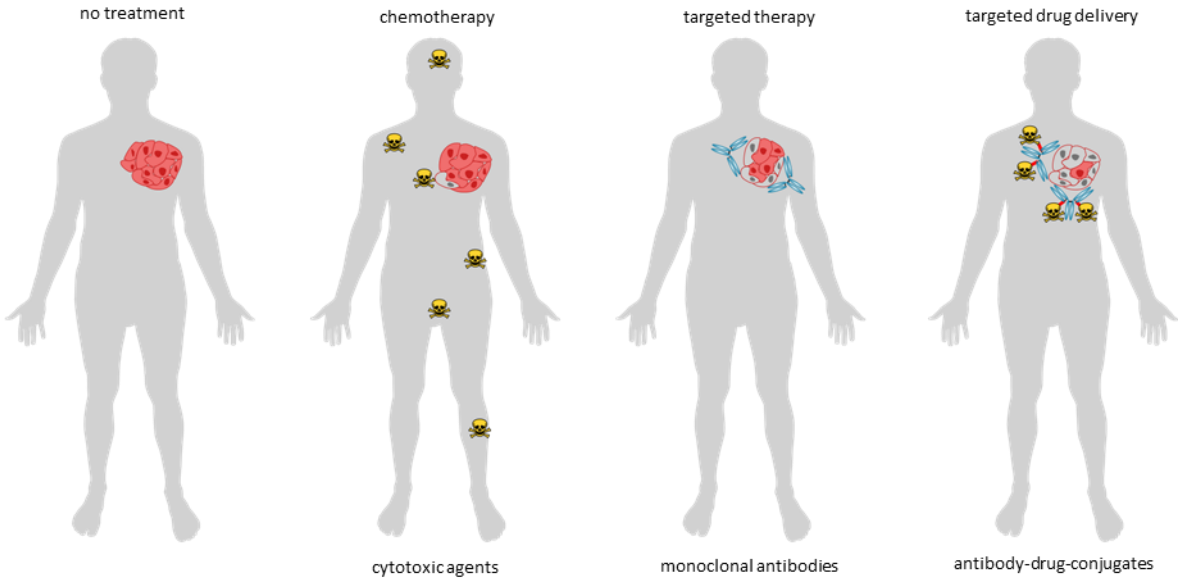

Figure 2: Examples for systemically applied drugs to treat cancer. Schematic representation (body: grey, tumor: red, antibody: blue, cytotoxic agent: yellow). Idealized scenario: Targeted drug delivery combines the effectiveness of chemotherapy with tumor specificity of targeted therapy.

This introduction will discuss oncological developments of systemically applied drugs starting from early unspecific chemotherapy, going on to more targeted approaches including modern immunotherapy, finally leading towards advanced drug delivery approaches. Here, focus will be set on directed delivery of highly effective toxins to the site of the tumor with the aid of antibody-drug-conjugates (ADCs) among others (Figure 2).

4.2.1. Chemotherapy

Until the first half of the 20th century surgery and radiotherapy were the only available options for the treatment of cancer. With medical oncology as a growing research area from the 1940s onwards, it became clear that a chemical treatment in addition to tumor removal is able to enhance the probability of patient survival also with advanced cancer types.[5] Chemotherapy was born with the initial experiments in treating non-Hodgkin's lymphoma with nitrogen mustards and the first cure of a solid tumor in humans employing the anti-folate drug methotrexate in 1958.[6] From then on, a broad range of structurally diverse chemical compound classes have been approved for the treatment of cancer. The most prominent classes include nucleobase and nucleoside analogues[7], inorganic platinum based compounds[8], various natural products[9] and different combinations of those.[6]

The majority of these classical cytotoxic chemotherapeutics preferentially damage proliferating cells.[10] Since malignant cells are usually rapidly dividing, these agents preferentially kill cancer cells while sparing healthy tissue.[11] However, higher levels of proliferation are also common in various normal cells such as those of the bone marrow and the gastrointestinal tract. As a consequence, chemotherapy has to be administered close to the maximum tolerated dose (MTD) to achieve a

significant therapeutic effect. Expanding the limited therapeutic window due to systemic toxicity remains the biggest challenge in treatment with cytotoxic substances.[12]

4.2.2. Targeted therapy

To overcome severe side effects of common unspecific chemotherapy, extensive efforts have been undertaken to find drugs with new mechanisms of action exploiting more cancer specific characteristics than only enhanced proliferation. Thus, due to deeper understandings of tumor signaling pathways, new targets on the surface of malignant cells were identified which are believed to play a critical role for cancer growth and survival.[13] Many of those targets represent receptor kinases that show characteristic mutations in certain cancer types when compared to healthy cells. Targeting those mutant kinases is most promising if tumor proliferation is directly dependent on kinase activity.[14] Here, great success has been achieved with the small molecule tyrosine kinase inhibitor imatinib (Gleevec®) in the treatment of chronic myeloid leukemia and gastrointestinal stromal tumors with extraordinary response rates in patients.[15] However, regularly acquired resistance to such specific modes of actions[16] and severe off-target toxicity due to insufficient selectivity for a specific kinase are well-known issues in the development of novel kinase inhibitors for targeted cancer therapeutics.[17]

As an alternative to such small molecule inhibitors, monoclonal antibodies (mAbs, Figure 3) have become more and more important in the field of specific cancer treatment. Highly specific monoclonal antibodies can be raised against certain molecular markers on the tumor surface that are important in tumor proliferation or progression.[18] In the best case, those markers, or tumor antigens, are overexpressed on the malignant cell and less abundant on healthy tissue. Typical antigens are cell-surface proteins, glycoproteins or carbohydrates.[12] After binding those tumor antigens, the killing of a malignant cell can result from different mechanisms of action, such as receptor blockage of growth factors, specific effects of an antibody on tumor vasculature and stroma or by immune mediated cell killing mechanisms, were the immune system of the patient is stimulated to attack the cancer cell such as complement-dependent cytotoxicity (CDC), (ADCC) and regulation of T cell function.[19] More recently, monoclonal antibodies were raised against immune checkpoints, regulators of the immune system that prevent t-cells from attacking the tumor. The field of immune checkpoint therapy was born and honored with the Nobel Prize in medicine for James P Allison and Tasuku Honjo in 2018.[20]

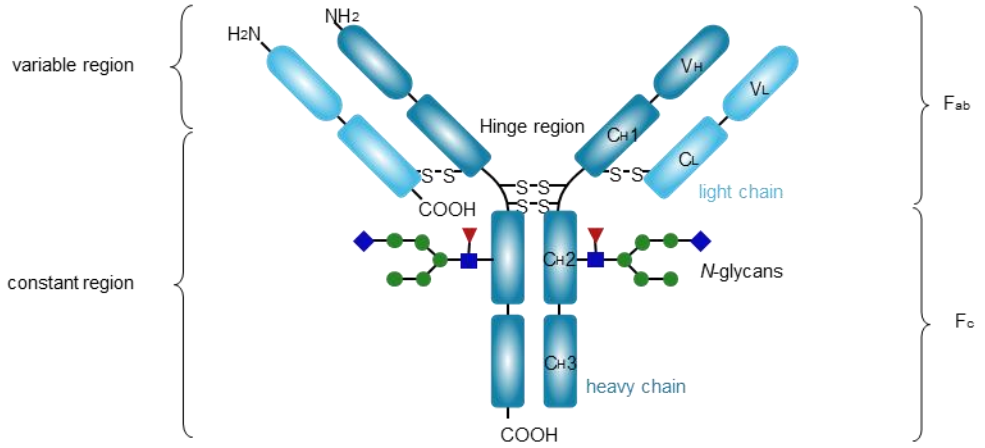

Figure 3: Structure of an immunoglobulin G1 (IgG1) antibody. Monoclonal antibodies consist of two heavy chains (dark blue) that are composed of the variable (V_H) and the constant (C_H1-3) region and two light chains (light blue) that are composed of the variable (V_L) and constant (C_L) region, connected via four disulfide bonds. *N*-glycosylation site is present at the conserved N297 residue of the Fc region. Two epitope binding sites are present in the variable regions. Figure adapted from Chudasama et al.[21]

Despite the recent success of therapeutical monoclonal antibodies, with increasing counts of FDA approvals every year[22], many antibodies still fall short of expectations, since they lack efficacy when applied as single agents. To overcome this inefficacy, especially in the treatment of solid tumors, many mAbs are only approved in combination with classical chemotherapy. The drawback of those combination therapies remains the toxicity of the unspecific chemotherapy which narrows the therapeutic window and leads to serious side effects in the patient.[12]

4.2.3. Targeted drug delivery

A concept that increases the efficacy of targeted therapy while retaining its high specificity is targeted drug delivery. Here, a highly potent cytotoxic molecule gets covalently attached to a targeting unit in order to improve selectivity and efficacy as well as avoiding biodistribution issues that are associated with chemotherapy and targeted therapy. In addition to side effect reduction, targeted therapy facilitates the usage of highly toxic warheads that are not tolerated in their unconjugated form and allow the administration of lower doses, since the drug can accumulate specifically in the targeted cell without unspecific damage of healthy tissue.[23] This concept of delivering toxic payloads to malignant cells using a targeting agent was first described in 1913 by Paul Ehrlich, who predicted a “haptophore” that can specifically deliver a “toxophore” selectively to a tumor site.[24]

A huge variety of different targeting ligands have been applied to specific drug delivery, ranging from small molecules of a few hundred Dalton (Da) to full length IgG antibodies with sizes of around 150 kDa. Small molecule targeting units that are applied to conjugates in recent clinical trials include carbohydrates such as β-D-glucose,[25] short peptides like NGR[26] and urea linked dimers of glutamate (DUPA).[23, 27] Probably the most prominent example for small molecule targeting is the vitamin folic acid that binds to the folate receptor with a very high affinity ($K_D \sim 10^{-10}$ M). The folate receptor alpha

is overexpressed in many human tumors, including cancers of the ovary, lung, kidney, endometrium, colon, and breast[28] and therefore an interesting target for drug delivery with several cytotoxic and diagnostic conjugates in recent clinical trials.[23]

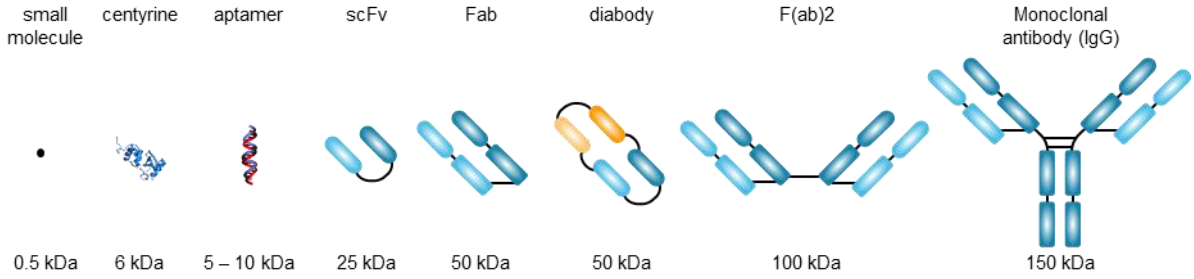

Figure 4: Selection of targeting ligands that have been applied to drug delivery in increasing order of size. Depicted are average molecular weights. Figure is adapted from Srinivasarao et al.[23]

However, besides plenty advantages of small-molecule targeting units in drug delivery such as the generation of highly defined products, ease of manufacturing and oral availability for some of the constructs, their biggest drawback remains their pharmacokinetics. Molecules with a molecular weight of far less than 40 kDa are readily released from circulation in the patient by renal filtration.[29] A strategy to improve the pharmacokinetics of small molecule targeting units is to increase their size by the attachment of a water-soluble polymer such as polyethylene glycol (PEG).[30] On the other hand, polymers itself can function as guiding ligands by selective target binding with molecularly imprinted polymers (MIPs)[31] or other mechanisms such as the enhanced permeability and retention (EPR) effect that describes the phenomenon that nanoparticles ranging from 10 to 100 nm can accumulate in solid tumors.[32] Other targeting ligands overcome the issue of rapid plasma clearance by relying on larger protein and oligonucleotide scaffolds including nucleic acids aptamers[33], full length IgG antibodies[21], antibody fragments such as Fab fragments[34], diabodies[35] or single-chain variable fragment (*scFv*)[36] and antibody mimetics such as affibodies[37] or centyrins[38] (Figure 4).

4.3. Antibody-Drug-Conjugates for cancer treatment

Among the aforementioned scaffolds, full length IgG-monoclonal antibodies bound to cytotoxic warheads have attracted the most attention in the field of targeted drug delivery in recent years.[39] These Antibody-Drug-Conjugates (ADCs) combine the antitumor potency of small-molecule drugs with the high selectivity, stability and prolonged circulation times of mAbs.[40] Recent success of those ADCs in clinical development include the approval of inotuzumab ozogamicin (Besponsa™)[41] and the re-approval of gemtuzumab ozogamicin (Mylotarg™).[42] Together with brentuximab vedotin (Adcetris®) and trastuzumab emtansine (Kadcyla®) (Figure 5), approved in 2010 and 2013, respectively there are four ADCs currently on the market and more than 80 candidates in recent clinical trials. [40] This clearly underlines the high potential of this compound class. [43]

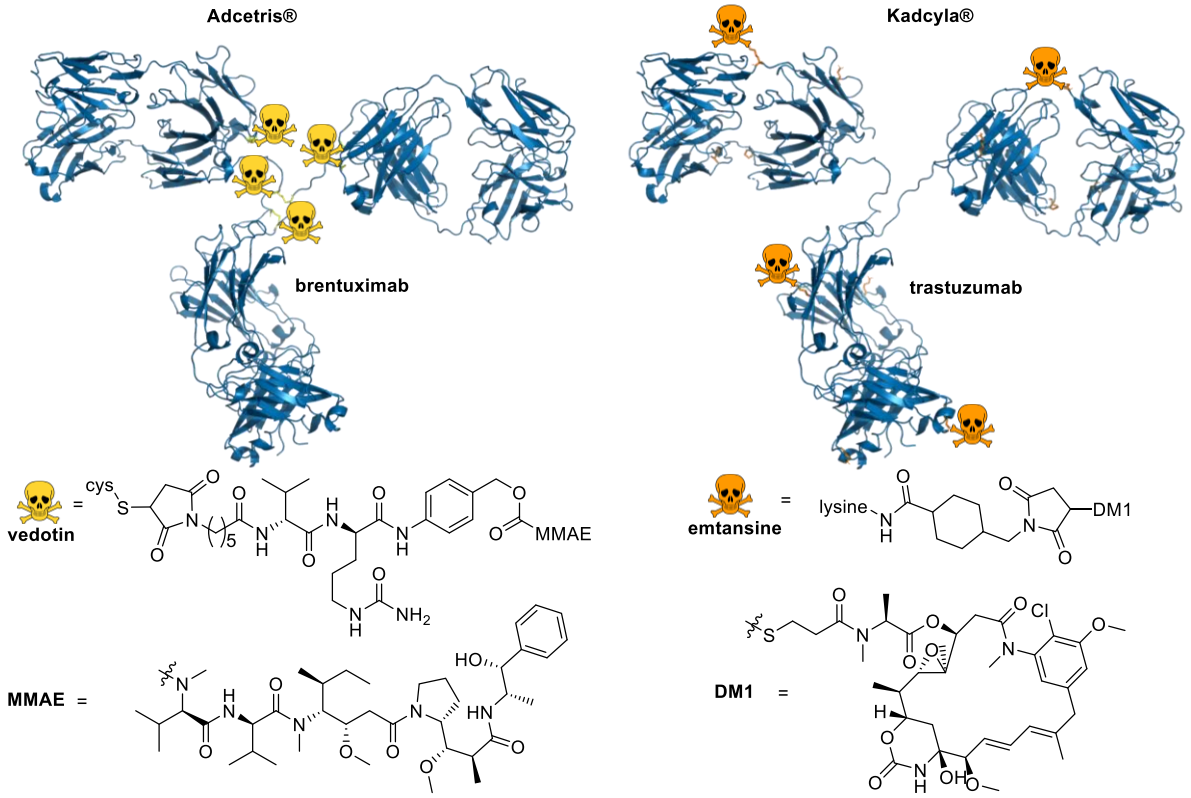

Figure 5: Comparison of two FDA-approved ADCs Adcetris® and Kadcyla®. Toxins are connected to cysteine residues (yellow) in the antibody's Hinge region for Adcetris® and to lysine residues (orange) all over the antibody structure for Kadcyla®. Antibody structure rendered using PyMol from structural data of Harris et al.[44]

Before first approvals were conceivable, a long list of failures had to be overcome in the development of ADCs for cancer treatment. First *in vitro* evaluated ADCs in the 1980s on antigen positive cell lines revealed only moderate activity and insufficient selectivity for the targeted cell line.[12] Nevertheless, researchers proceeded with first *in vivo* evaluations with human xenograft models in mice, showing a superior efficacy when compared to the unconjugated drug.[45] Encouraged by these results, two Phase I studies were initiated to evaluate a methotrexate-antibody conjugate in patients with non-small-cell lung cancer.[46] However, all first clinical trials with ADCs were discontinued due to a lack of efficacy and severe side effects such as strong immune responses against the murine antibodies that were used back then.[47] Afterwards, all parts of the ADC have been careful analyzed, which led to the identification of several factors that were improved, before Mylotarg™ was approved by the FDA as the first ADC for the treatment of Acute Myeloid Leukemia (AML) in 2000.

4.3.1. Technological requirements on ADCs

Learning from these early setbacks in ADC development, recent focus in the improvement of next-generation ADCs is put on all three parts: the antibody, the cytotoxic payload, and the linker that connects the two parts. Here, requirements for a safe and efficacious therapeutic are enormously

high.[48] Figure 6 summarizes the most important demands on all three parts of an ADC that will be discussed in detail in the following chapters.

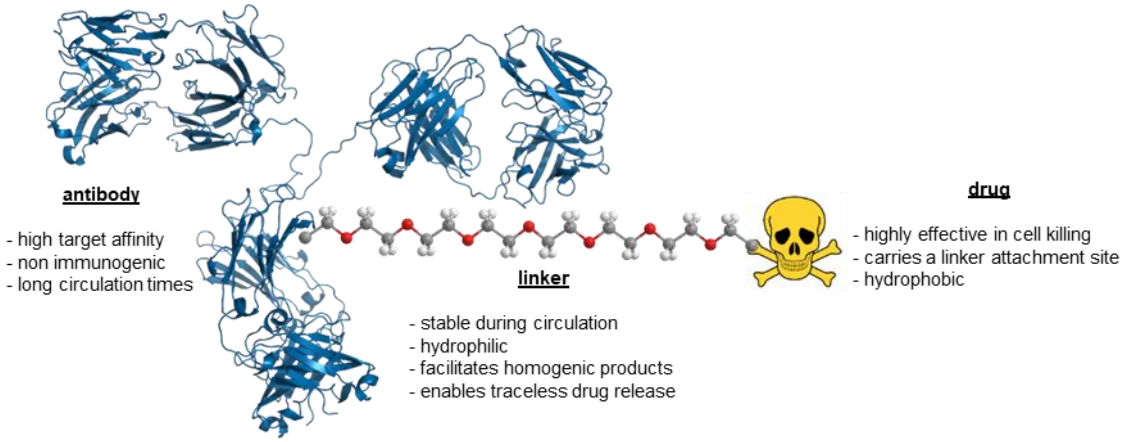

Figure 6: Demands on the three parts of an ADC: the antibody, the linker and the drug. Figure depicts are rough overview about what has been investigated. Not all requirements are compulsory to ensure a safe medication. Antibody structure rendered from structural data of Harris et al.[44]

4.3.1.1. Monoclonal antibodies

The selection of a suitable mAb is crucial for the generation of a safe ADC, since it has to ensure a good selectivity for tumor- over non-malignant cells. Therefore selection of a suitable antigen that is targeted by the mAb is very important. First of all, the targeted antigen should be homogenously expressed on the cell surface of all tumor cells in a high copy number of more than 10^5/cell with a significantly higher expression level compared to normal cells. In addition, receptor internalization upon binding is beneficial to ensure an intracellular delivery of the cytotoxic molecule to its side of action.[12] However, recent studies also include non-internalizing targets, which necessitates an extracellular release of the drug followed by diffusion in the cytosol.[49]

Furthermore, the mAb itself should bind the targeted receptor with a good affinity, typically in the range of 0.1-1.0 nM.[48] It has been shown that high affinities can hamper deep tumor penetration and therefore lower the efficacy in the treatment of solid tumors.[50] Finally, the antibody should be chimeric, humanized or most preferably even fully human to prevent an immune response in the patient[40] and prolong the circulation half-life in humans.[51] As indicated in Figure 7, in chimeric antibodies, the constant region of the originated species is replaced with the human form. In humanized antibodies typically everything is replaced, except for the complementarity determining regions (CDRs).

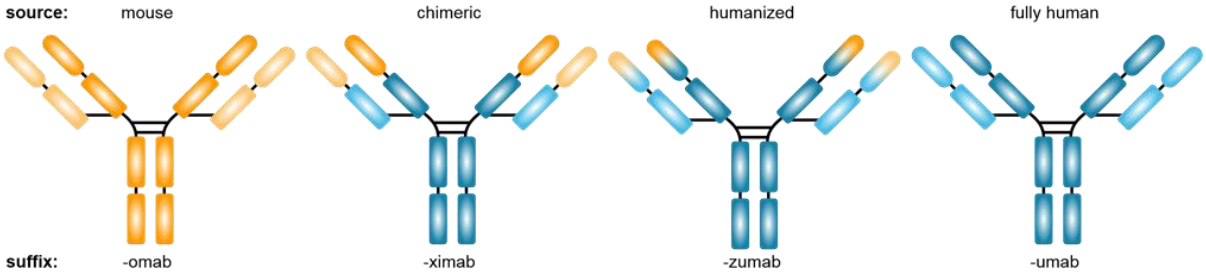

Figure 7: Monoclonal antibodies with increasing degree of humanization and the assigned suffixes that have been used until 2017.

The use of the suffixes depicted in Figure 7 have been discontinued for newly introduced monoclonal antibodies in 2017 because of increasing complexity in assigning the antibodies origin due to a lot of technological production advances.[52]

4.3.1.2. Cytotoxic payloads

Apart from choosing a suitable antibody, the choice of an appropriate cytotoxic payload defines the efficacy of the final ADC. Many clinical evaluations of ADCs with promising *in vitro* efficacy, employing drugs with a fifty percent growth inhibition concentration (IC_{50}) in the submicromolar range, such as doxorubicin[53] failed due to a lack of efficacy in the patient.[54] Further studies in cancer patients have revealed that tumor uptake of the ADC is below 0.01% of the injected dose per gram of tumor.[12] This data suggested that drugs, applied to ADCs must be highly efficient in cell killing at low intracellular concentrations with a low nanomolar to picomolar affinity for its target (IC_{50}).[48] Furthermore, commonly applied toxins are usually hydrophobic to enable unimpeded diffusion through cellular membranes ensuring endosomal escape and allowing toxin diffusion into neighboring cells, causing the so called bystander effect. Since solid tumors often express the target antigen in a heterogeneous manner, this bystander effect can enable cell killing also of antigen-negative cancer cells.[49] Finally, the chemical structure of the drug must allow the attachment of a linker that enables conjugation to the antibody while retaining its potency.[40] The cytotoxic compounds used in most of the marketed ADCs and in current clinical development (as of 2019) are either auristatins or maytansinoids, which are potent antimitotic microtubule-disrupting agents or derivatives of DNA damaging agents like calicheamicin, duocarmycin, indolinobenzodiazepine or pyrrolobenzodiazepine (PBD)-dimers (Figure 8).[48] Other, less commonly applied drugs used in ADCs include α-amanitin that kills cells by inhibiting RNA polymerase II[55] and analogues of the topoisomerase inhibitor camptothecin.[56]

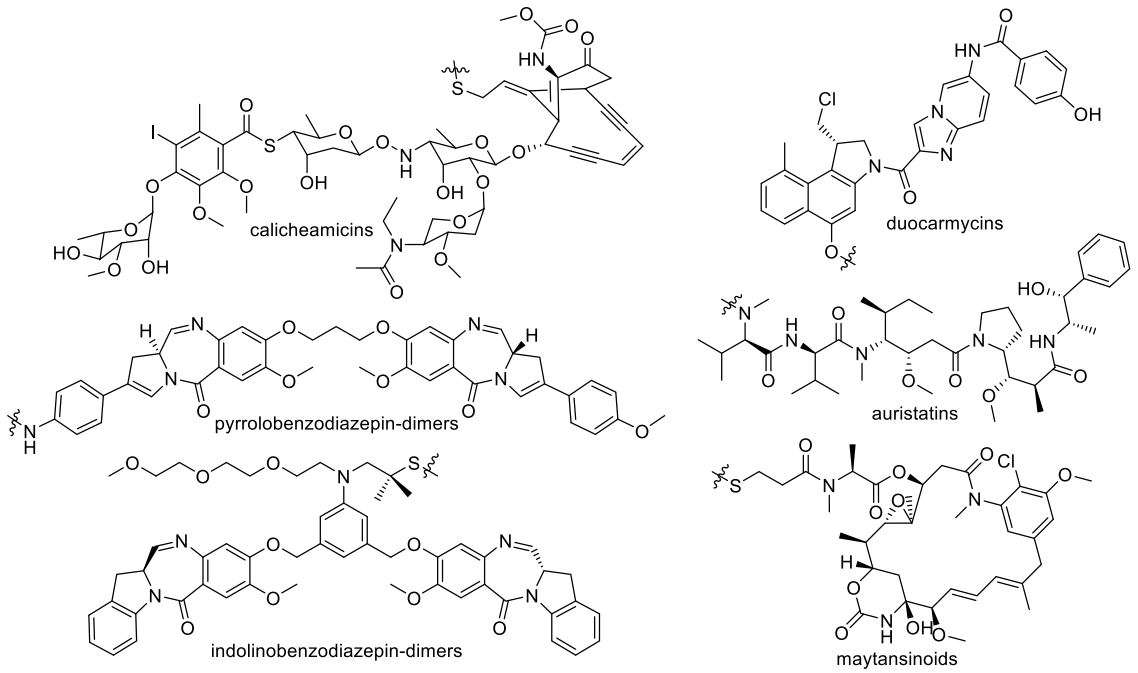

Figure 8: Examples for structures of cytotoxic payloads for ADCs in recent clinical trials. Depicted are derivatives of the most important toxin classes. Attachment site to the antibody is marked with a waved line.

Next to the nature of the drug itself, another important parameter for efficacy and stability of an ADC is the drug to antibody ratio (DAR). ADCs with a low drug load (i.e. low DAR) do not deliver enough cytotoxic payload into the targeted cell and are therefore ineffective. On the other hand it has been shown that a high loading of the antibody with hydrophobic drug molecules can increase unspecific uptake into non-targeted cells and therefore contribute to off-target toxicity and accelerated plasma clearance.[57] Furthermore, high DAR-species can be rapidly recognized by the immune system.[58] Hence, the DAR of the majority of ADCs in clinical development is often limited to a maximum of 4.[59]

4.3.1.3. Linker technology

The third part that allows improvement in ADC synthesis is the applied linker technology to connect the already discussed mAb and payload. Requirements on linkage technology are exceptionally high, since linkage stability drastically influences the safety profile of the final product. A premature release of the highly potent cytotoxin during circulation in the blood stream leads to severe off-target toxicity in the patient.[40] Therefore, the linker has to be tightly bound to the antibody as well as to the warhead. However, an inherent lability at the site of the warhead that allows a traceless release of the drug upon cellular uptake can also be desirable.

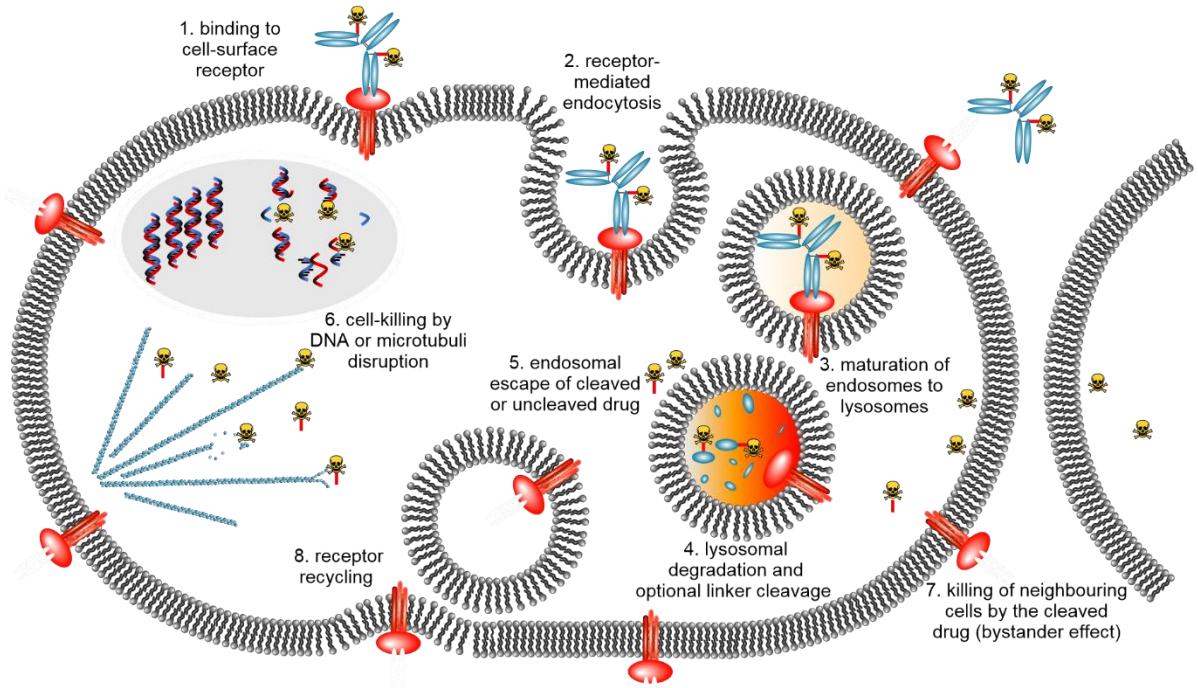

Figure 9: Mechanism of ADC mediated killing of target-receptor overexpressing cells. After binding to the targeted receptor (1), the ADC gets internalized into endosomes (2) that ripen to proteolytically active lysosomes (3). Antibody degradation and optional linker cleavage (4) facilitates drug release into the cytoplasm (5). Cleaved and uncleaved drug molecules act at the intracellular target (6). Cleaved drugs may freely diffuse into neighboring cells and enable the bystander effect (7). Receptor can be recycled to the cell-surface (8).

Usually, a linker is considered as cleavable if it facilitates a traceless release of the drug molecule after uptake into the targeted cell. Both, cleavable and non-cleavable linker, have been applied to approved ADCs and constructs in recent clinical trials.[12] In case of non-cleavable linker systems, the antibody is proteolytically degraded after receptor mediated uptake in the lysosomes to release the linker–drug moiety attached to one residual amino acid of the antibody (Figure 9).[60] Depending on the structure-activity relationship of the applied drug, a non-cleavable linker can be applied, if this cellular metabolite of the conjugated drug remains active in cell killing. In a recent study it has been shown that the auristatin MMAE, the toxin used in Adcetris®, remains active in its uncleaved form, while a cleavage is crucial in case of a PBD dimer that is attached via its DNA-binding imine.[61] Non-cleavable linker system also impair the aforementioned bystander effect (Figure 9), since the charge from the attached amino acid remaining after antibody lysis, reduces membrane permeability of the drug.[62] On the other hand, cleavable linkers are inherently labile and have to balance the need for good stability in circulation to ensure a safe ADC and efficient cleavage upon delivery into the target cell to preserve the payloads potency.[12] Apart from the mechanism of action triggering an intracellular cleavage, the drug's site of attachment is crucial to facilitate a traceless release. Self-immolative linker systems based on cyclization or 1,6-elimination mechanisms have been developed to combine various cleavage strategies with common functional groups such as primary, secondary and tertary amines, pyridines,[63] alcohols and thiols in drug molecules.[23]

One strategy to induce intracellular release is to use acid labile chemical moieties between drug and antibody. Hydrazones, for example, are stable to the neutral conditions during circulation (pH 7.4) but cleave in the acidic endosomal environment (~pH 5) after receptor mediated uptake.[64] Prominent examples using hydrazones include the approved ADCs Besponsa™ and Mylotarg™ (Scheme 1).[48] However, it has been shown in clinical trials that unspecific release during blood circulation is an issue for hydrazone linked ADCs.[65] In fact, Mylotarg's commonly triggered side effects have been attributed to the instability of its hydrazone linker that caused drug release during circulation.[66]

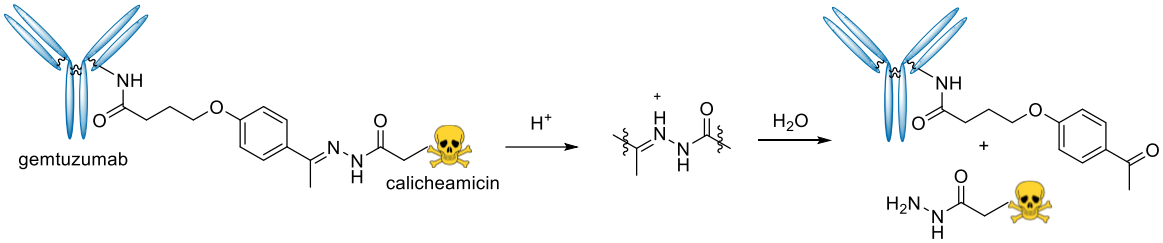

Scheme 1: Acidic release mechanism of the hydrazone linkage in Mylotarg™.

Other linker systems, applied to ADCs in recent clinical trials, incorporate disulfide bridges that can be selectively reduced in the presence of high intracellular concentrations (~2−10 mM) of glutathione.[23] For drugs that do not contain sulfhydryl groups, disulfides can be combined with self-immolative structures that release primary, secondary and more recently also tertiary amines after reduction (Scheme 2).[23, 63] A premature drug release of this systems, for example by disulfide reduction mediated by cysteine containing serum proteins in the bloodstream and interstitial fluids, can be prevented with short linker length to protect the disulfide with the protein structure of the antibody[67] or by the incorporation of sterically hindered disulfides.[23] In an anti-CD22 antibody based PBD-dimer delivery system, it has been shown that the stability of disulfide bridges can be optimized to limit premature cleavage by incorporation of various bulky groups such as methyl or cyclobutyl in α-position to the disulfide (Scheme 2).[68] However, very sterically hindered disulfides are also known to impair efficient intracellular reductive cleavage,[67] therefore careful optimization is required to find a structure that balances both needs.

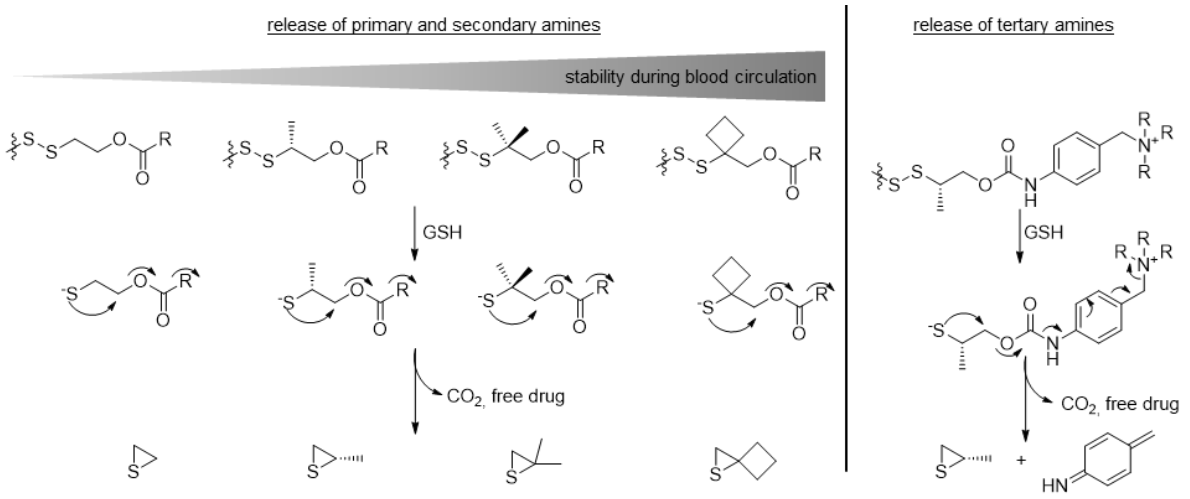

Scheme 2: Linker systems based on reductively cleavable disulfides for the traceless release of amino-modified drug molecules. Sterically hindered disulfides are less prone to be cleaved during blood circulation. Cyclization to form a thiirane and release of CO_2 can be exploited to facilitate a traceless release of primary- and secondary amines (left).[23] Additional 1,6-elimination linker enables release of tertary amines (right).[63] Attachment site to the antibody is marked with a waved line. R depicts the drug molecule.

Since the composition of hydrolytic enzymes in the blood stream widely varies from those that are intracellularly abundant, cleavable linkers can also be designed from structural motives that are selectively recognized and cleaved by intracellular enzymes. Moreover, many hydrolytic enzymes are upregulated in malignant cells, whose activities can be exploited to further increase selectivity by an increased drug release in the targeted cell.[69] Cleavage motives that are recognized by cathepsins, a protein family that is predominantly expressed in acidic lysosomes are often applied to ADCs. Adcetris® for example is equipped with a cathepsin B cleavable valine–citrulline linker, which is known to be more than 100 times more stable than other commonly used cleavable linkers during blood circulation.[70] Coupled to a 4-amino benzyl structure that facilitates a 1,6-elimination cascade, this linker enables the traceless release of MMAE after enzyme mediated cleavage (Scheme 3a).[70a] When the cleavage side is attached to quarternary ammonium salts via a 1,6-elimination linker, cathepsin B cleavage furthermore facilitates the release of drugs containing tertiary amines.[63] Apart from cathepsins, the glycosidase β-glucuronidase has also been utilized for the release of various toxins, including MMAE, MMAF and doxorubicin (Scheme 3b). As an example, the anti-CD30 antibody, equipped with a β-glucuronide linker to release a cytotoxic payload after deglycosylation and 1,6-elimination displayed pronounced antitumor activity in a subcutaneous lymphoma tumor model in mice.[71]

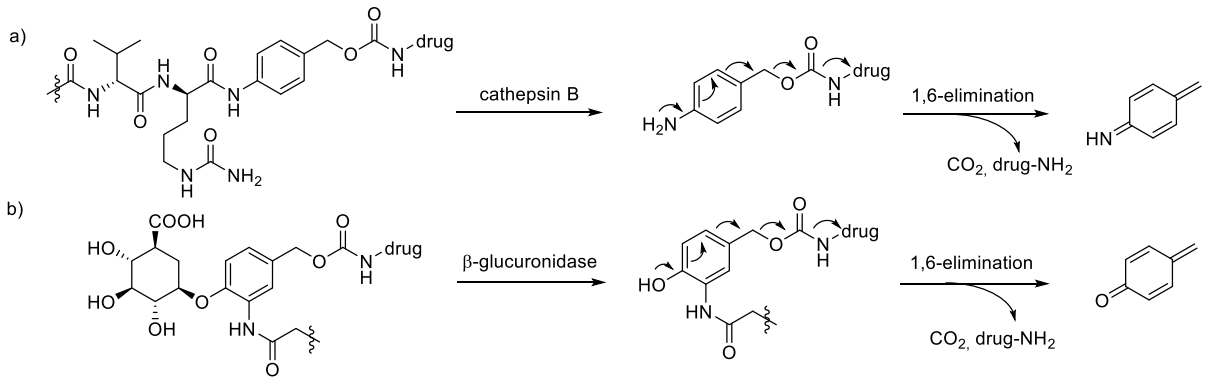

Scheme 3: Mechanism of enzyme mediated traceless drug release. a) Valine-citrulline cleavage side for cathepsin B cleavage. b) β-glucuronide self-immolative linker for glucuronidase cleavage. 1,6-elimination systems facilitate traceless release. Attachment site to the antibody is marked with a waved line.

In addition to the incorporation of cleavable systems, linker technology can also be optimized to increase the overall stability of ADCs. As mentioned in the previous chapter, severe issues can arise from the hydrophobic nature of drugs commonly applied to ADCs. In addition to unspecific uptake into non-targeted cells, the formation of High Molecular Weight Species (HMWS) or so called aggregates is a general issue in the field of antibody based therapeutics.[72] Aggregates impair the pharmacokinetic profile and efficacy[73] and can drastically increase the risk of immunogenicity in the patient[74]. To overcome problems that are usually associated with HMWS, hydrophilic linker systems, mostly based on PEGylation, have been developed that compensate for the hydrophobic nature of the drug.[57, 75] However, it has been recently demonstrated that long solubilizing PEG-chains negatively impair the pharmacokinetic profile of the final product if installed between the antibody and the drug molecule. Long polymeric PEG chains increase the solvent exposure of the drug, causing enhanced exposure to proteases and inadvertent hydrophobic interactions.[57, 75] In addition to PEG based systems, incorporation of quarternary ammonium salts or glucoronides into the linker has been also shown to be beneficial in terms of hydrophilicity.[63]

4.3.1.4. Antibody modification strategies for the construction of ADCs

Aside from linker polarity and the possibility of a traceless drug release, the mode of linker-drug attachment to the antibody fundamentally influences the stability and homogeneity of the ADC and therefore determines its therapeutic window and the pharmacokinetics.[21, 39] Since the antibody structure itself is proteogenic, a big variety of different chemoselective reactions being developed for protein modification, have also been applied to the construction of ADCs. First examples for the construction of ADC were based on conjugation to the native occurring lysine residues. However, as typical antibodies carry approximately 70 accessible lysine residues that all can be statistically modified, lysine conjugation yields in a broad mixture of different antibody species that vary in degree and site of modification.[76] Since such heterogeneity can drastically narrow the therapeutic window of

an ADC,[77] conjugation techniques allowing a better control of the conjugation side are desirable. To overcome this issue, targeting of less abundant amino acids such as methionine[78] and especially cysteine has become more and more important for the modification of antibodies.[79] Next to lysine, cysteine is one of the most commonly exploited amino acid for antibody conjugation. It has been shown that the four interchain disulfide bonds of an IgG antibody can be selectively reduced to yield eight free cysteine residues that can subsequently be modified with thiol selective conjugation techniques.[70a] It is thought that the antibody stability and structure is not impaired by these modifications, since antibody assembly is primarily dependent on non-covalent affinities of the antibody subunits to each other.[80] Other approaches for the modification of native antibodies not relying on the reactivity of certain amino acids, target the glycan structure at the conserved N297 residue of the Fc region. Here, modification can either be achieved by a selective transformation of the glycan structure into a chemical reporter, as for example an aldehyde that can be subsequently modified with hydrazides[81] or by an enzymatic removal of the glycans followed by modification of the unique asparagine residue with a transglutaminase.[82] Furthermore, the Z-domain that is derived from the immunoglobulin-binding domain of protein A has been used in proximity based labelling techniques to specifically modify amino acids in the Fc-part of the antibody.[83]

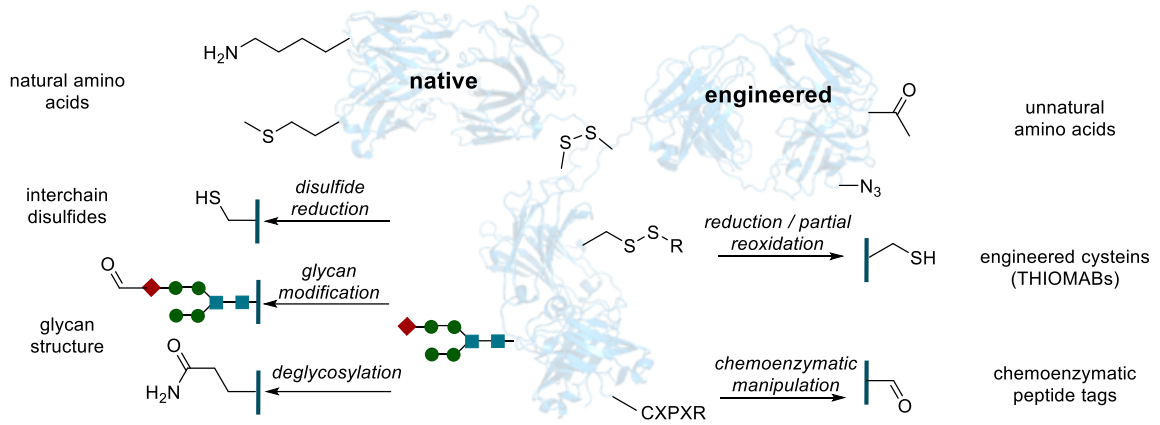

Figure 10: Typical residues that can be utilized for the modification of antibodies starting from either native (left) or biochemically engineered antibodies (right). Figure inspired by Chudasama et al.[21]

Another way to generate highly homogenous ADCs with defined DARs is to use genetic engineering. Amber suppression for instance can be employed to install unnatural amino acids into the primary structure of an expressed antibody, carrying bioorthogonal handles that enable site-specific payload attachment.[39] On the one hand, this approach is very versatile since it allows a simple prepositioning of the desired drug attachment site within the antibody structure. On the other hand amber suppression is associated with low expression yields.[84] Alternatively, additional cysteine residues can be engineered into the sequence to generate so called Thiomab™ antibodies, which can be selectively modified, since all the other cysteines of the antibody are trapped in disulfides.[77] Other strategies that

are not impairing the antibodies expression yields are dealing with the incorporation of certain peptide tags to the antibody that allow the incorporation of a chemical reporter by an enzyme-directed modification.[21] An overview of the most important antibody modification strategies can be found in Figure 10. The protein-modification strategies behind those methods are discussed in detail in the next chapters.

4.4. Chemoselective strategies for the modification of native proteins

The chemical attachment of synthetic molecules at distinct sites of a protein to add a functionality that is not defined by the genetic code, represents an essential process not only in the area of targeted drug delivery but also in fundamental research of basic biological processes.[85] In principle, protein modification can be achieved by two strategies: Incorporation of an unnatural chemoselective handle with the aid of unnatural amino acids or chemoenzymatic labelling techniques or by exploiting the specific reactivity of native proteinogenic amino acids.[86] Even though the former yields highly uniformly proteins, the incorporation of unnatural residues requires tedious biochemical manipulations like amber suppression techniques, selective pressure incorporation or site directed mutagenesis. Therefore protein modifications targeting natural occurring residues can be more straightforward for certain applications. One drawback of those approaches is that there are only residue specific, leading to heterogeneous mixtures of proteins with a different degree of modification including several regioisomers.[87] However, decent amounts of homogeneity can be achieved by targeting low abundant amino acids or the aid of affinity based protein modification techniques.[88]

4.4.1. Chemical modification of lysine residues and the N-terminus

The nucleophilicity of the primary amines of lysine and the N-termini of proteins has been exploited for a number of successful protein modification reactions. Due to its high natural abundance, targeting lysine residues is particularly attractive when selectivity for a distinct site of a protein is dispensable or when a high copy number of modifications per proteins is desired.[86a] In fact, three of the four FDA-approved ADCs are conjugated via lysine residues.[48]

Active esters of carboxylic acids have been applied in various examples to form amide bonds with primary amines irreversibly in slightly basic aqueous systems. The most prominent examples for such activated acids are *N*-hydroxysuccinimide esters (NHS). Several NHS derivatives of commonly used protein labels such as fluorescent dyes, biotin probes or crosslinking agents are commercially available. Selectivity for the N-terminus over the modification of lysine can be achieved with careful control of the pH,[89] or if the N-terminal amino acid is cysteine, by prior incubation with MESNA.[90] Furthermore, sulfonic acid modified NHS-derivatives have been applied for increased water solubility.[87b] NHS esters

have been applied for the modification of trastuzumab's lysine residues and subsequent attachment of DM1 to produce the FDA approved ADC Kadcyla®.[91] Selectivity for the amine group over the more nucleophilic sulfhydryl group of cysteine is attributed to NHS-ester being a harder electrophile and therefore preferably react with the harder amine of lysine.[86a] The same is true for isocyanates and isothiocyanantes that readily react with amines to form urea or thiourea, respectively,[92] even though more basic conditions are required when compared to NHS esters.[93] An alternative, well-established modification utilizes a reductive amination reaction. Here aldehydes react with primary amines of proteins to imines that can be subsequently reduced to secondary amines in the presence of a reduction agent that is stable under aqueous conditions such as sodium cyanoborohydride (Scheme 4).[94]

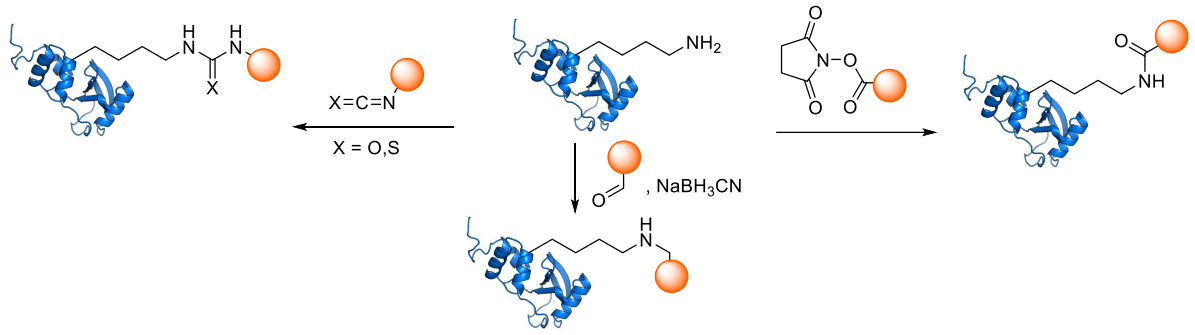

Scheme 4: Overview of different chemical protein modifications selective for amino residues. Iso-(thio)cyanates: left; NHS-esters right and reductive amination strategies: bottom.

Other reagents for the modification of amines that have been developed more recently are based on a 6π-aza-electrocyclization reaction and show selectivity of accessible lysine residues over the N-terminus. Here an unsaturated *E*-ester aldehyde reacts with primary amines to yield 1,2-dihydropyridines in an irreversible reaction.[95] In a very recent study, Bernardes and coworkers claim that a modification of a single lysine residue on native proteins can be achieved with sulfonyl acrylate reagents.[96] Another method that has been extensively used in the modification of the N-terminus is native chemical ligation (NCL).[97] In NCL, an N-terminal cysteine reacts with a thioester followed by an intramolecular *S*- to *N*-acyl shift to form a native peptide bond. NCL is one of the most important methods for the construction of synthetic proteins from either expressed N-terminal cysteine containing proteins or from expressed protein thioesters than termed expressed protein ligation (EPL).[98] In a similar manner, N-terminal serine or threonine residues can form native peptide bonds with C-terminal salicylaldehyde ester, which is known as the serine/threonine ligation.[99] Other strategies rely on the incorporation of an aldehyde or ketone to the N-terminus that can be selectively modified in a subsequent reaction step. This has been achieved by oxidation of N-terminal serine or threonine residues with sodium periodate[100] or by treatment of the native protein with pyridoxal-5-phosphate under slightly acidic conditions.[101]

4.4.2. Chemical modification of cysteine

In contrast to most of the other amino acids, cysteine is relatively low abundant with only 2.26% over all other amino acids in mammals.[102] Chemical protein modification via cysteine is therefore a promising strategy for a lot of biochemical applications, since it can allow functionalization of a distinct site of a protein (Figure 11). The unique nucleophilic properties of its sulfhydryl group has been utilized in the development of several cysteine selective modification techniques. Since the pKa of cysteine is ranging from 7.4 to 9.1 under physiological conditions,[103] depending on the protein conformation and its microenvironment, the highly reactive thiolate anion can be modified already under slightly basic conditions.[104]

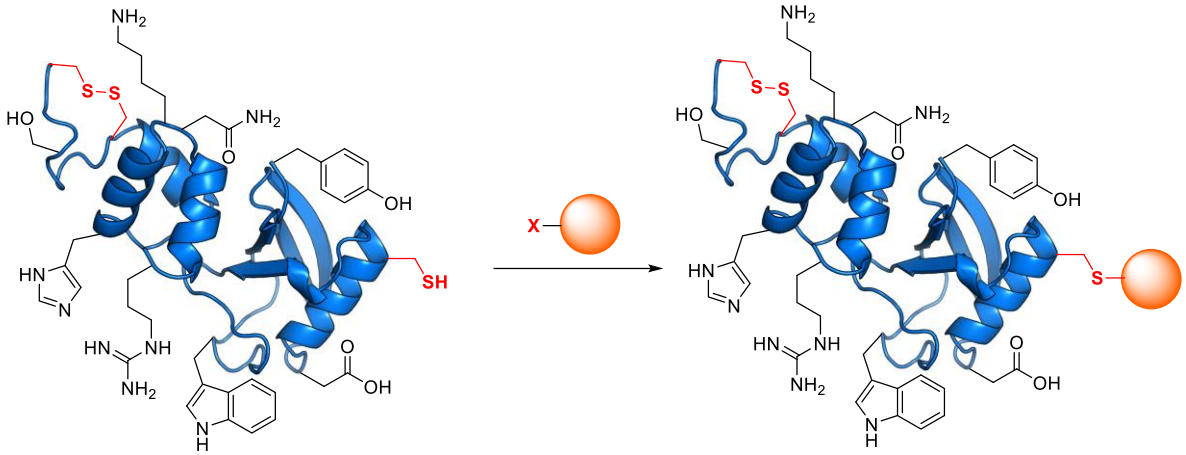

Figure 11: Selective chemical protein modification through cysteine next to all other naturally occurring nucleophilic functional groups and disulfides. X depicts the chemical warhead that facilitates the reaction. Figure adapted from Gunnoo et al.[104b]

Another unique characteristic of cysteines is that two cysteine residues within a protein structure can oxidize to either form an intramolecular disulfide bond or ensure a covalent intermolecular fusion of two protein fragments. This post-translational modification (PTM) occurs in the vast majority of proteins and plays key roles in protein folding and structural integrity since it stabilizes its tertiary and quarternary structure.[105] Furthermore, the ability to form disulfide bonds has been exploited in protein synthesis. On the one hand disulfides protect cysteine residues from reactions with electrophiles, thereby allowing the modification of a certain cysteine residue next to others that are trapped in disulfides.[106] On the other hand selective reduction of disulfides and subsequent modification with electrophiles can also be employed for conjugation. This concept has been applied for the construction of ADCs, with the FDA approved Adcetris® as its most prominent example.[70b] Here, a partial reduction strategy was applied that reduces only two of four native interchain disulfide bonds to generate four cysteine residues that can be subsequently modified with maleimides to synthesize an ADC with an average DAR of 4.[107]

4.4.2.1. Maleimides and related compounds

Within the variety of different compound classes that have been employed for the purpose of cysteine selective modification reactions, maleimides are by far the most used ones.[104b] The reaction with sulfhydryl groups proceeds via a conjugate addition of the thiolate anion to the double bond that is electrophillically activated by two neighboring carbonyls. Such conjugate additions of nucleophiles to activated olefins and alkynes has been first described by Michael in 1887 and ever since exploited in a plethora of different reactions in organic chemistry.[108] In maleimides, the release of ring-strain upon product formation provides an additional driving force towards product formation and makes the thiol-maleimide reaction one of the most efficient Michael-type additions,[109] with second order rate constants of more than 700 $M^{-1}s^{-1}$.[110] After the first reactions have been described in the 1950s[111], maleimides have become enormously popular in selective protein modification via cysteine. Maleimide-linkage has been employed for the synthesis of FDA approved therapeutics such as the two ADCs Kadcyla® and Adcetris®[40] and for the PEGylation of an anti-TNF construct for the treatment of Crohn's disease and arthritis.[112] Other than that, fluorescently labelled maleimides have been used for analytical purposes such as mapping of cysteine[113] and proteomic analyses with small reagents such as *N*-Ethyl maleimide.[114] Despite the huge success that is also reflected in the great variety of maleimide reagents that are commercially available, there are also drawbacks of this technology that have been described. One issue that is scarcely discussed in the literature constitutes side-reactions of maleimides with other nucleophilic amino acids than cysteine such as lysine and histidine.[115] In some applications this might be negligible, since the reaction of maleimide reagents with sulfhydryl groups is rapid and allows the addition of almost stoichiometric amounts of labelling reagent to the protein. However, it has been shown recently that the issue of unselective labelling can limit the applicability of maleimide labelling in certain applications. This was demonstrated by a loss of activity of the retro-aldolase RA-CM after maleimide labelling due to unspecific modification of a catalytically active lysine residue.[116] Another problem that is discussed more often in the context of maleimide labelling is the stability of the thio-succinimide bond that is formed upon thiol addition. It is known, that a retro-Michael reaction in solution can reform the unconjugated maleimide (Scheme 5).[117] Since the equilibrium of this reaction is far on the side of the Michael-adduct, this might be less problematic for most *in vitro* applications. However, it can be a drastic issue when the conjugate is exposed to other external thiols in solution that can reattach to the released maleimide. This thiol exchange reaction is particularly problematic in the context of targeted therapeutics, since the conjugates are exposed to cysteine containing proteins like albumin during circulation in the blood stream.[118] Here, a retro-Michael addition can lead to drugs conjugated to endogenous proteins as well as free drug molecules

and can therefore cause severe side effects and narrow the therapeutic window of the therapeutic conjugate.[119]

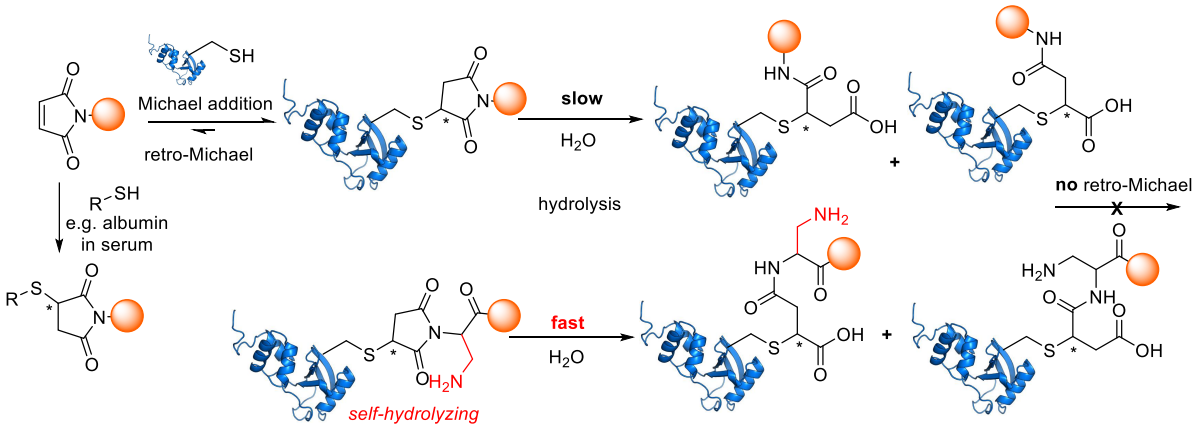

Scheme 5: Structures and chemistry of thiol-reactive maleimides. Reversible thiol-maleimide conjugation reaction (retro-Michael) can cause maleimide transfer to external thiols such as albumin's cysteine in serum. Retro-Michael can be avoided by succinimide hydrolysis. Self-hydrolyzing maleimides have an increased hydrolysis rate. Stars indicate stereo centers (usually racemic).

During optimization of the maleimide linkage, it has been shown that retro-Michael reaction does not occur in the hydrolyzed ring-opened form of the thio-succinimide adduct.[120] This phenomenon has been exploited in the construction of maleimide linked ADCs that are stable to thiol exchange, either by forcing the hydrolysis under slightly basic conditions at elevated temperature[121] or by the development of so called self-hydrolyzing maleimides. Here, a basic amino-group in close proximity to the thio-succinimide ring induces its hydrolysis after thiol-addition even at neutral pH and room temperature by intramolecular catalysis (Scheme 5).[122] It should be noted that several different regio- and stereoisomers are being formed after hydrolysis, which increases the heterogeneity of the final conjugates.[123] Other structurally refined Michael systems that were developed based on maleimide chemistry to form stable thiol adducts include exocyclic maleimides that are readily available by a solvent-free Wittig transformation (Scheme 6).[124]

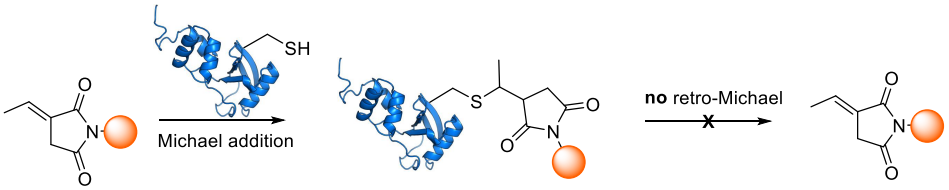

Scheme 6: Exocyclic maleimides form thiol adducts irreversibly.

Furthermore, maleimides that carry one or two additional leaving groups at the double-bond, so called next-generation maleimides (NGMs) have been designed within the last ten years. Here, cysteine modification occurs via an addition elimination mechanism forming a thio-maleimide bond. Mono-bromomaleimides for example have been shown to rapidly react selectively with cysteine residues.[125] Phenol substituted maleimides show a comparable reactivity with only slightly decreased kinetics.[126] The resulting thio-maleimide adducts are even more unstable than their saturated counterparts and

can be employed to either reform the unmodified cysteine by incubation with TCEP or treated with a base to form dehydroalanine.[125] The double bond of the thio-maleimide that is formed after the first addition can undergo a subsequent thiol addition, which makes these reagents suitable for disulfide rebridging. However it should be noted that the second addition is reversible and can eliminate one or the other thiol (Scheme 7).[126]

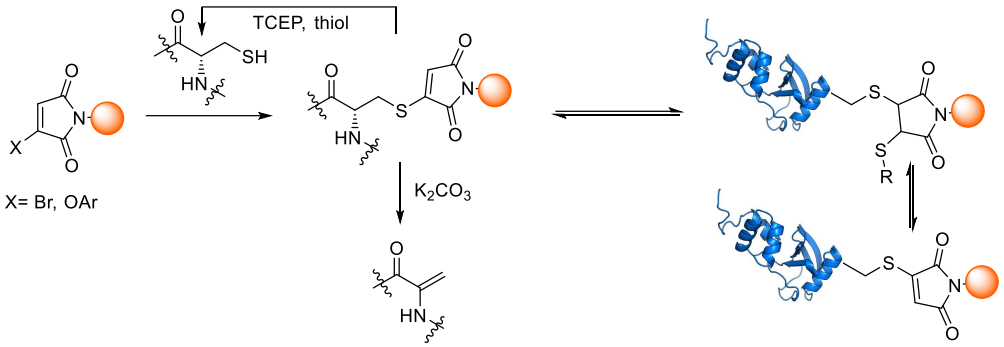

Scheme 7: Monosubstituted maleimides with leaving groups form thio-maleimide with cysteine residues. Reaction is reversible by the reaction with TCEP, Retro-addition is caused by addition of a second thiol. Thio-maleimide adducts that can be eliminated to form dehydroalanine under strongly basic conditions.

Another class of maleimides allowing disulfide rebridging are disubstituted maleimides. Disulfide rebridging involves the reduction of native occurring disulfide bonds in peptides and proteins followed by the attachment of a covalent junction to generate a structural mimic that is less prone to reduction and therefore increases protein stability. A functional rebridging agent additionally offers the possibility to add a modification to the stabilized disulfide such as a PEG- or a fluorescent tag.[104b] A broad variety of different leaving groups have been tested in the reaction of disubstituted maleimides with reduced disulfides. There, the leaving-group ability is determining the rate of the reaction with diodo- >dibromo- >dichloromaleimides. Dithiophenylmaleimides are advantageous since they tolerate the addition of TCEP to the reaction mixture, leading to a higher disulfide conversion due to prevention of reoxidation.[127] The addition of cysteine to disubstituted maleimides is generally reversible in the presence of external thiols allowing the intracellular release of a cargo that is connected via a disubstituted maleimide. This has been demonstrated with rhodamine–GFP conjugates by monitoring FRET intensities after cellular uptake.[128]

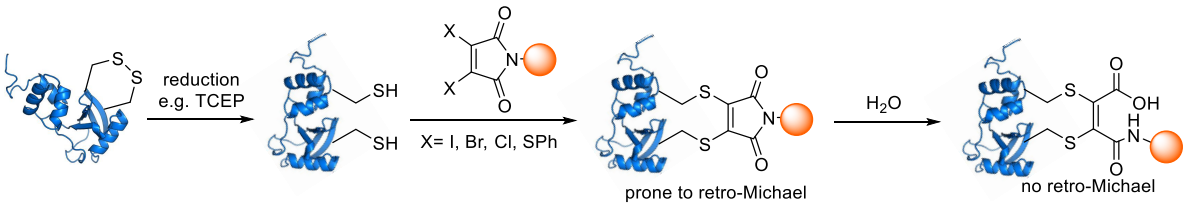

Scheme 8: Disulfide rebridging with disubstituted maleimides. Conjugates can be stabilized by ring hydrolysis.

The instability of NGMs due to retro-Michael reaction can be circumvented by hydrolysis of the maleimide to the open-ring form, analogously to simple maleimides (Scheme 8).[129] Even though two different regioisomers can be formed during hydrolysis, the generation of different diastereomers is not an issue in this case. NGMs have been applied to broad variety of applications,[104b] including rebridged ADCs from native trastuzumab and doxorubicin with control over the drug loading in a range between 0 and 4.[129a] Furthermore, near homogenous ADCs have been synthesized from an antibody containing an additional cysteine residue (THIOMAB™) in combination with NGMs.[130]

Another compound class inspired by dibromomaleimides are dibromopyridazinediones that are readily available by treating certain dibromomaleimides with hydrazine.[131] Dibromopyridazinediones react analogously to disubstituted maleimides with reduced disulfides (Scheme 9) and have been applied to the construction of various ADCs with DARs.[132] Since both nitrogen atoms of the pyridazinedione core have to be alkylated to be cysteine reactive, dibromopyridazinediones offer the possibility of the introduction of either one or two different modifications to a reduced disulfide on a protein or antibody.[132a] In accordance to dibromomaleimide adducts, dibromopyridazinediones conjugates are also prone to be cleaved in the presence of other thiols in solution. Inspired by the observation that both nitrogen atoms have to be alkylated to be reactive for cysteine, dibromopyridazinediones have been developed that allow a selective TCEP mediated cleavage of one of the substituents after the conjugation to the protein. The resulting *N*-monosubstituted dibromopyridazinediones proofed stable to thiol exchange.[133]

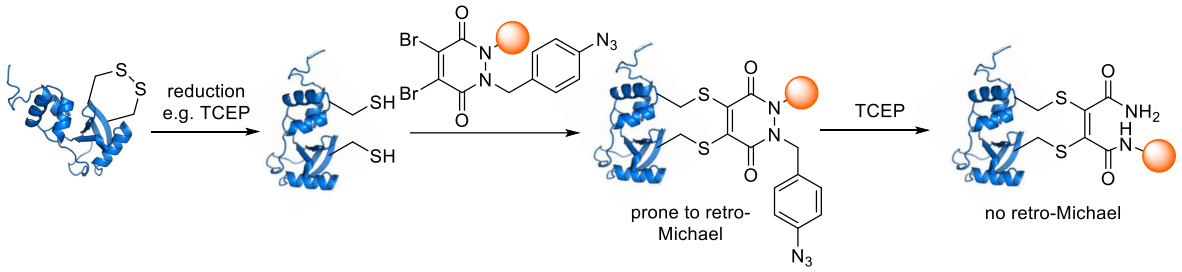

Scheme 9: Dibromopyridazinediones for disulfide rebridging. Conjugates can be stabilized by the selective removal of one *N*-substituent, as demonstrated for a 4-azido benzyl substituent that can be cleaved after cysteine rebridging by azide reduction and subsequent 1,6-elimination.

4.4.2.2. α,β-unsaturated carbonyl reagents

Due to the high reactivity of α,β-unsaturated carbonyl compounds towards thiols in a Michael addition reaction, a great variety of these compound classes have been employed for cysteine selective conjugation reactions on peptides and proteins. While derivatives of acrylic acid esters are more often applied in the field of polymer modification in material sciences,[134] early examples of protein modification include unsubstituted acrylamide that has been utilized to cap cysteine residues before protein sequencing in the Edman-degradation.[135] Structurally more refined α,β-unsaturated carbonyl

compounds have been developed by Bernardes and coworkers. To circumvent the reversibility of thiol additions to maleimides the group developed carbonylacrylic reagents that retain the high reactivity of maleimides while exhibiting a good stability when exposed to external thiols (Scheme 10). Both, carbonylacrylic -acids and -amides react rapidly with small molecule cysteine derivatives. The reaction is considered to be stoichiometric, since it proceeds with a high degree of cysteine labelling using equimolar amounts of reagent to protein. It has been successfully applied to the modification of a Thiomab™ variant of Trastuzumab that retained its function upon modification.[136] However, it should be mentioned that a stereocenter is formed upon conjugation which might impair the practicability for certain applications.

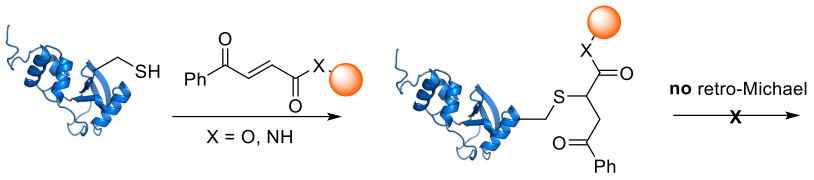

Scheme 10: Carbonylacrylic reagents form stable adducts with cysteine residues.

Other than that, α,β-unsaturated aryl ketones that carry an additional β-aryl sulfone have been used for disulfide rebridging reactions. Here, the conjugated double bond gets attacked by a cysteine residue, which initiates an elimination of sulfinic acid, reforming a conjugated double bond that can subsequently be attacked by a second cysteine (Scheme 11). This reaction can form a three-carbon bridge between the two sulfur atoms of a disulfide after reduction and has been applied successfully to PEGylation of therapeutically relevant proteins with retained activity.[137] Based on those findings, latent α,β-unsaturated bis-sulfone reagents have been developed, in which elimination of a first sulfinic acid occurs that generates the previously described unsaturated mono aryl sulfone reagent *in situ* (Scheme 11).[138]

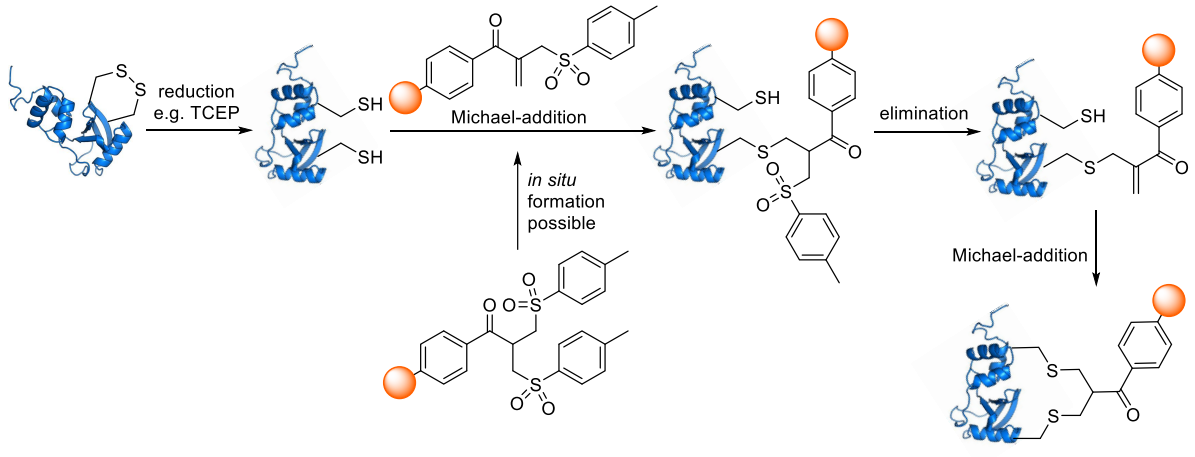

Scheme 11: Disulfide rebridging with α,β-unsaturated carbonyl reagents carrying an additional β-sulfonyl group that is susceptible to elimination. Reagents can also be generated *in situ* from bis-sulfones.

Next to alkenes, electron-deficient alkynes have also been introduced as reagents for chemoselective cysteine modification. Alkynoic amides, esters and alkynones have been shown to selectively modify cysteine residues in peptides under slightly basic aqueous conditions. A second thiol can be added to the generated vinyl sulfide linkage to give a dithioacetal, which is prone to eliminate one or the other thiol spontaneously (Scheme 12). Due to this, the addition is highly reversible in solution in the presence of other thiols. This has been exploited in the development of a biotinylated probe that allows for the enrichment of cysteine containing peptides from a peptide mixture followed by a mild thiol mediated elution with a high recovery.[139]

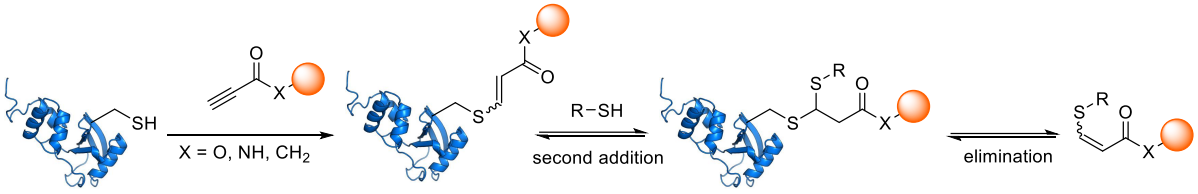

Scheme 12: Electron-deficient alkynes for reversible cysteine modifications.

Aside from classical carbonyl based Michael-acceptors, α,β-unsaturated sulfone reagents have been developed, were the carbonyl moiety is exchanged with an electron-withdrawing sulfone.[140] Vinylsulfone reagents have been shown to selectively modify cysteine residues in an almost quantitative manner and form a chemically stable thioether bond upon conjugation. Even though cross-reactivity with lysine and histidine was observed with these reagents under more basic conditions[140] they still comprise an interesting compound class, since no additional stereocenter is formed upon conjugation. This makes the technology attractive for certain applications such as ^{18}F-labelling.[141]

4.4.2.3. Unsaturated Phosphorus (V) reagents

Due to the electron withdrawing nature of phosphorus(V) substituents[142] it could be assumed that α,β-unsaturated compounds such as *P*-vinyl and *P*-ethynyl phosphorus(V) reagents can react with sulfhydryl groups in a conjugate addition reaction. However, despite from the work that is described in this thesis, there is only one literature example describing a conjugate thiol addition to α,β-unsaturated phosphorus(V) reagents. Gao et al. have synthesized *P*-vinylphosphonates and phosphonamidates from aminoglycosides and tested their reactivity towards an addition of sulfhydryl containing coenzyme A in order to design potent inhibitors for the enzyme aminoglycoside *N*-6'-acetyltransferase which is one of the key players in antibiotic resistance. However, it was reported that none of the tested conditions for the addition of CoA was successful in the addition to a vinylphosphonamidate. Switching to a vinylphosphonate for the conjugate addition was successful and provided the desired product in moderate yield (Scheme 13).[143]

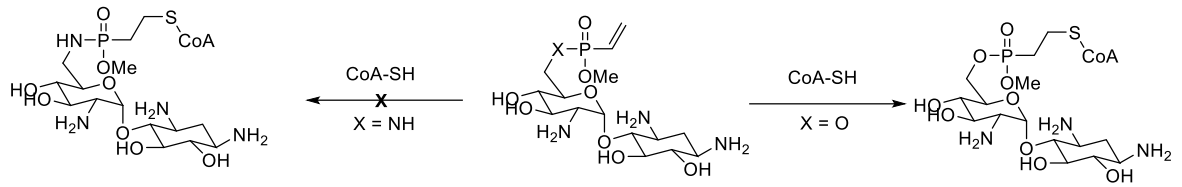

Scheme 13: Observations by Gao et al.: Vinylphosphonamidates are unreactive towards a conjugated thiol addition, whereas Vinylphosphonates do react. [143]

4.4.2.4. Alkylation with haloalkyl reagents

Alkylation with α-halo carbonyls with its most prominent example of iodoacetamides was first mentioned in 1935 and belongs to one of the earliest methods that have been developed for cysteine selective modifications.[144] Due to the ease of applicability conjugation of iodo-, bromo-, and chloroacetamides have been widely applied to cysteine modification (Scheme 14a). Iodoacetamide still is the reagent of choice to cap cysteine residues prior to proteomic analyses.[145] However, side-reactions with other nucleophilic side chains such as lysine and histidine have been reported and can lead to misinterpretation of MS-based proteomic analyses due to mass artifacts.[146] This issue can be solved by using less reactive chloroacetamide.[147] Due to the decreased electrophilicity of chloroacetamide, compared to their corresponding iodo counterparts, chloroacetamides have been used in proximity based protein labelling techniques.[148] The use of bromoacetamides for cysteine modification can constitute a compromise between sufficient reactivity and selectivity.

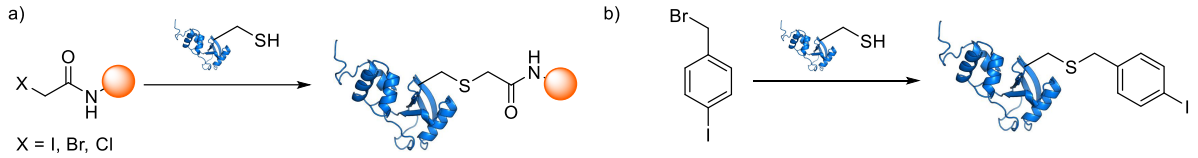

Scheme 14: Selective cysteine alkylation with haloalkyl compounds. a) Iodo- bromo- and chloroacetamides. b) 4-Iodobenzyl bromide.

Bromoacetamides have also been applied to therapeutic protein conjugates, for example to connect a folate moiety to a single cysteine-containing cytotoxic protein.[149] Due to the high stability of the thioether-bond, bromoacetamides have been also applied to the synthesis of ADCs with increased serum stability. Efficacy, potency and toxicity characteristics were however not distinguishable from maleimide linked ADC isotypes.[118] Other than acetamides, benzyl halides can also be applied for the modification of cysteine, as demonstrated by Chalker et al. (Scheme 14b).[150]

4.4.2.5. Metal catalyzed arylation

Most of the methods that are described above yield in alkylated or vinylated cysteine residues. In contrast to this, methods for arylation of sulfhydryl-groups in aqueous systems are relatively rare. Most prominently, Vinogradova et al. have described Pd(II)-complexes that allow a rapid selective arylation of cysteine residues in peptides and proteins (Scheme 15), tolerating a broad pH-range, with high

stability of the formed products towards acids, bases, oxidants and excess of external thiols. The reactivity, selectivity and stability of the palladium complex is determined by the carefully chosen RuPhos ligand that facilitates a specific electronic environment to prevent cross-reactivity with other nucleophilic residues like tyrosine for instance. The method has been successfully applied to peptide stapling and the synthesis of a linker-free ADC by direct attachment of an aromatic drug to trastuzumab's interchain forming cysteine residues.[151]

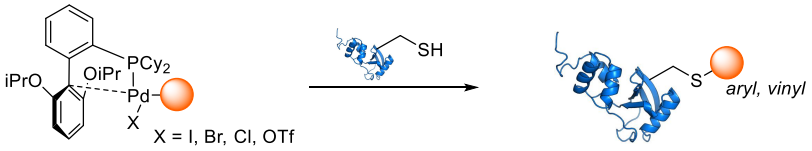

Scheme 15: Arylation of cysteine residues with Pd(II) reagents.

Other metal based reagents for cysteine modification include gold(III) complexes that yield arylated cysteine residues[152] and rhodium complexes that catalyze the alkylation of cysteine with diazo compounds.[153] Both methods yield in stable bonds and the applicability for protein modification has been demonstrated. Challenges however remain since selectivity is often an issue and purification of the final conjugates from remaining metal ions, which is crucial for therapeutic applications, can be tedious.[104b]

Very recently, conjugation to antibodies-cysteine residues based on Pt(II)-reagents has been introduced. Since it is well-known that chloro complexes of platinum (II) form stable complexes with thiols under physiological conditions, diamino-chloro platinum(II) complexes have been employed for the linkage of cytotoxic drugs to antibodies by disulfide rebridging (Scheme 16).[154]

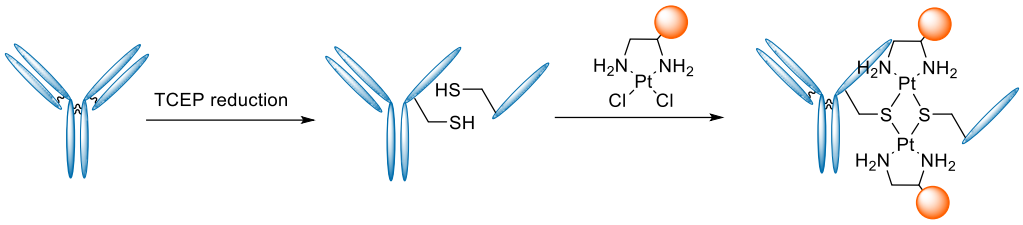

Scheme 16: Diamino-chloro platinum(II) complexes rebridging of antibody's interchain disulfides. For demonstrative reasons, modification of only one disulfide is depicted in the scheme; however, all four disulfides do react.

This linkage technology delivered efficacious ADCs that proofed to be efficient *in vivo* and less susceptible to thiol exchange than maleimide conjugation.

4.4.2.6. Perfluoroarylation

Based on the finding that sulfhydryl groups react with perfluoroaryl compounds in a nucleophilic aromatic substitution (S_NAr), Pentelute and coworkers developed a cysteine-selective modification reaction with hexafluorobenzene and decafluorobiphenyl. In their study they showed that the first

thiol-substitution to the aromatic systems favors a subsequent substitution in para position and therefore avoids mono-substitution of the perfluoroaromatic systems. Consequently, the method was applied to peptide cyclization of sequences containing two cysteine residues (Scheme 17).[155] Macrocyclication is a useful tool in peptide synthesis, since cyclized peptidic structures show enhanced biophysically properties, such as increased stability towards proteases[156] and restricted conformational flexibility.[157] Derda and coworkers refined the system of Pentelute by using decafluor-diphenylsulfone reagents, which are also capable of cyclizing peptides containing two cysteines (Scheme 17). These compounds modify cysteine residues with an unusual high reaction rate of up to 180 $M^{-1}s^{-1}$, making this reaction to one of the fastest cysteine modifications known in the literature to date.[158]

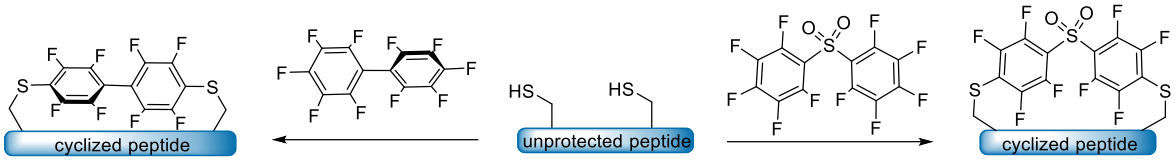

Scheme 17: Hexafluorobenzene (left) and decafluora-diphenylsulfon (right) for macrocyclization of peptides containing two cysteines.

Based on the findings that glutathione *S*-transferase catalyzes the reaction of the sulfhydryl-group of glutathione to various electrophiles, it was found out that this enzyme can be repurposed to transfer perfluoroaromatic structures to glutathione and also to glutathione-tagged polypeptides. Exploiting this concept, it has been shown that it is possible to modify the cysteine in the GSH-tag selectively next to other cysteine residues in the polypeptide that remained unmodified.[159] Even though site specific modification of cysteine residues is very desirable, this method is limited by the isopeptide bond of the GSH-tag, which hampers a general applicability to commonly expressed proteins. This issue has been solved by the development of a short genetically encodable peptide tag (Phe-Cys-Pro-Phe) which promotes the reaction with perfluoroaromatic probes in aqueous systems (Scheme 18). Zhang et al. demonstrated that this π-Clamp motif facilitates the modification of one cysteine site in proteins containing other endogenous cysteine residues.[160]

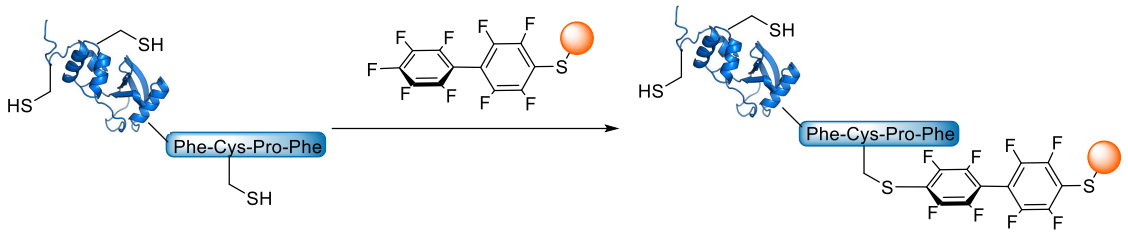

Scheme 18: π-Clamp-mediated site-selective cysteine conjugation to the Phe-Cys-Pro-Phe-motif.

4.4.2.7. Modification with hypervalent iodine species

Based on findings from Waser and coworkers that ethynyl benziodoxolone (EBX) hypervalent iodine reagents selectively alkynylate thiols in the presence of various functional groups,[161] those reagents have also been applied to selective cysteine alkynylation on proteins (Scheme 19).[162] In a proteome wide cysteine modification it could be shown that EBX reagents can incorporate an azide handle selectively on cysteine residues within living cells. A significantly higher cysteine selectivity has been described in a direct comparison experiment with iodoacetamides.

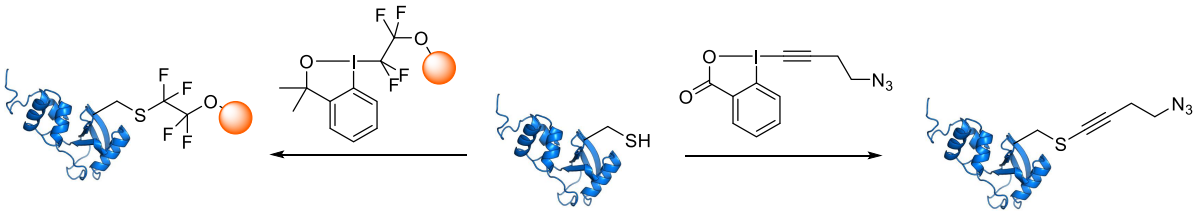

Scheme 19: Selective modification of cysteine with hypervalent iodine species. Tetrafluoroethyl-substituted hypervalent iodine (left) and ethynyl benziodoxolone (EBX) (right).

Fluoroalkyl derivatives of hypervalent iodine species are known to transfer the trifluoromethyl group and other fluoroalkyl-species to various nucleophiles including S-, P-, O-, N- and C-functionalities.[163] Inspired by this, Togni and coworkers developed tetrafluoroethylated hypervalent iodine reagents for selective cysteine modification (Scheme 19).[116] Superior selectivity was proven by labelling of a retro-aldolase that carries a hyper-reactive lysine residue in the active pocket. The enzyme activity remained intact upon cysteine labelling using fluoroalkylation reagents and dropped due to unspecific lysine modification with maleimide and iodoacetamide reagents.

4.4.2.8. Protein modification via disulfides

Since disulfides are readily cleaved in the reductive environment of the cytosol, attachment of functional moieties to proteins can be useful if an intracellular release of the cargo from the protein is desired.[164] To this end, several methods have been developed to selectively form a disulfide bond between a protein cysteine and a thiol containing modifier.

The simplest way to promote the formation of a disulfide bond between a cysteine residue and another sulfhydryl group is coincubation of the two thiols followed by oxidation. Even though this can be very convenient since air can serve as an oxidant and no additional reagents are required for the reaction, long reaction times and homodimer formation of either the protein or the modifier can be problematic.[104a] To circumvent undesired dimerization, specific disulfide formation can be achieved by directed disulfide exchange. Here, one reaction partner can be activated as an electrophilic disulfide preventing the formation of homodimers. After removal of the activation agent, the sulfhydryl group of the second reaction partner can attack the activated disulfide to form the desired disulfide bond

(Scheme 20). Electron-deficient aromatic disulfides, such as 5,5'-dithiobis(2-nitrobenzoic acid) known as Ellman's reagent,[165] that has been primary developed for quantification of free sulfhydryl groups or 2,2'-dithiobis(5-nitropyridine) (DTNP)[166] can serve as activation reagents.

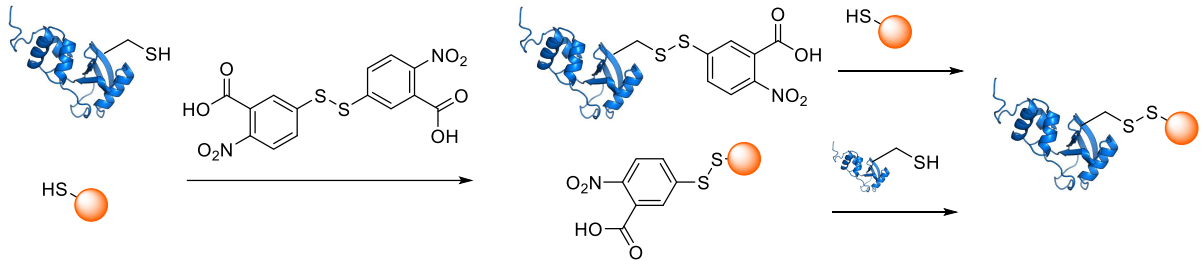

Scheme 20: Disulfide formation on proteins using Ellman's reagent. Either the protein or the modifier can be activated.

Exploiting this approach, several reductively cleavable protein constructs have been developed, including protein-protein[166] and protein-peptide conjugates[167] as well as several examples of ADCs.[168] Apart from forming disulfides with other cysteine residues, the activated electrophilic disulfide can also react with phosphites to install phosphocysteine residues site specifically.[169]

Due to possible intracellular release triggered by high amounts of glutathione in the cytoplasm (typically 1 to 11 mM), the application of disulfide linkages to drug delivery is of particular interest. However, even though the blood plasma is generally expected to be an environment in which disulfide exchange reactions are minimal, undesired cleavage during blood circulation can still occur due to reactive cysteine residues of blood proteins such as Cys34 of albumin.[164] To circumvent the problem of premature disulfide release during circulation, steric interference next to the disulfide bond in form of methyl groups for instance can be introduced.[23] In another example Pillow et al. have shown that a site-specific disulfide formation at certain sites of a Thiomab™ antibody can yield ADCs that are stable during blood circulation. In this case the protein structure in the surrounding of the conjugation site prevents premature disulfide reduction.[67]

4.4.2.9. Transformation of cysteine residues to dehydroalanine

The conversion of nucleophilic cysteine residues to electrophilic dehydroalanine that can be further derivatized by several modifiers, has been studied extensively by the Davis group.[104a] Next to methods that require organic solvents, elevated temperatures and/or strong basic conditions for the conversion and are therefore incompatible with many proteins, a bis-alkylation-elimination sequence turned out to be ideal for the generation of dehydroalanine residues in proteins.[170] 2,5-Dibromohexanediamide was identified as the most suitable reagent for the alkylation or dialkylation of cysteine residues followed by the elimination to dehydroanaline under slightly elevated temperatures (Scheme 21a). The generated Michael-system of dehydroanaline has been exploited extensively for the attachment of various functional moieties to different proteins. Several PTMs were incorporated for instance to

yield mimics of methylated and acylated lysine residues as well as phosphorylated and glycosylated serine mimics.[171] Brik and coworkers have applied the method to the synthesis of electrophilic diubiquitin activity probes for the characterization of several deubiquitinating enzymes.[172] More recently, dehydroanaline served also as a precursor for radical mediated modifications. Since this allows for the incorporation of C-C-bonds that depict native bonds in a great variety of natural occurring amino acid residues and PTM carrying amino acids, this method allows for the chemical transformation of dehydroalanine to other natural- and non-natural occurring amino acid residues (Scheme 21b).[173]

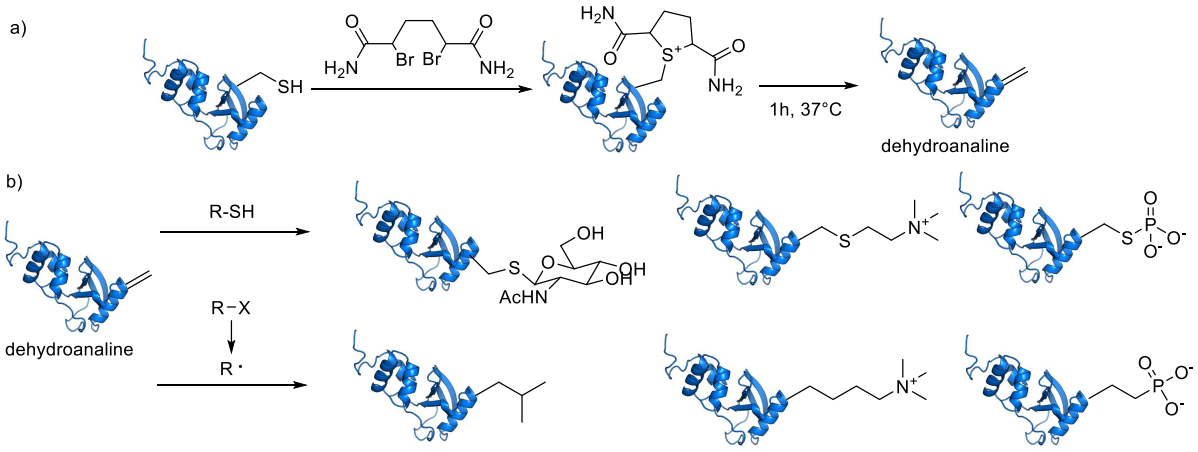

Scheme 21: Modification of cysteine residues via dehydroanaline formation. a) 2,5-Dibromohexanediamide for selective reaction of cysteine residues to yield dehydroanaline. b) Subsequent thiol addition or radical mediated *C-C*-bond formation.

One disadvantage of protein modification via dehydroanaline is the loss of cysteines chiral center after the formation of a sp^2-hybridized carbon. After subsequent modification of the double bond, the absolute configuration is depending on the tertiary structure of the protein and is therefore hard to predict.[174] It has been shown that the two diastereoisomers that arise after thiol addition to the dehydroanaline can be separated by HPLC.[175]

4.4.2.10. The thiol-ene reaction

The previous methods described above rely on the principle that an electrophilic reagent is attacked by the nucleophilic sulfhydryl group of cysteine to form a covalent bond. However, since sulfhydryl groups tend to generate thiyl radicals under photoirradiation conditions, selective conversion of cysteine residues can also be achieved by radical transformations.[176] In contrast to thiolates, thiyl radicals can also react with electron-rich alkenes and alkynes in a chain reaction. Propagation of these chain reactions proceeds via hydrogen abstraction by the carbon radical from another sulfhydryl group which leads to the formation of a new thiyl radical. The process is terminated by disulfide formation between two thiyl radicals (Scheme 22a).[177] Although requirements for protein modifications such as rapid kinetics, orthogonality to a lot of functional groups and reactivity in aqueous systems, are

fulfilled,[178] it has been mostly applied in the field of polymer chemistry. Described reactions on proteins mostly use alkene modified structures like homoallylglycine modified-[179] or farnesylated proteins.[180] However, several examples exploit the thiol-ene reaction also for the modification of protein cysteines with electron-rich alkenes. Strieter and coworkers successfully synthesized ubiquitin trimers from an ubiquitin mutant carrying two cysteine residues and allyl amide modified variants to yield unnatural isopeptide bonds that were recognized by deubiquitinating enzymes.[181] In another example radical addition of cysteine to *N*-vinylacetamide gave acetyl-thialysine which served as a mimic of acetyl-lysine (Scheme 22b).[182]

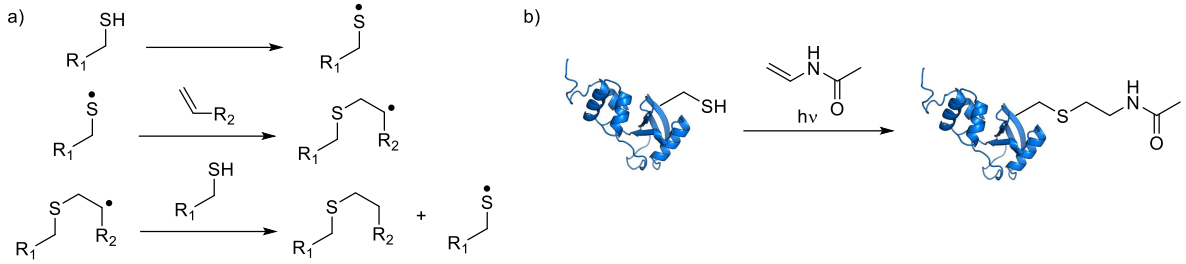

Scheme 22: Thiol-ene reaction for cysteine selective modifications. a) Mechanism of the thiol-ene reaction. b) Application to generate an acetyl-lysine mimic.

4.4.3. Selective modification of amino acids other than lysine and cysteine

In the previous chapters, the focus was set on protein modification reactions suitable for the selective targeting of the most commonly used amino acid residues lysine and cysteine. However, amino acid residues that are weakly nucleophilic under ambient conditions such as serine or threonine can also be selectively modified even though applied reaction conditions are often incompatible with the tertiary structure of most proteins.[123] Thus, the following chapter will focus on modification reactions that can be applied under conditions that are tolerated by most proteins.

Following cysteine, tryptophan is the second lowest abundant amino acid with only about 1% occurrence. However, about 90% of the endogenous proteins contain at least one tryptophan, making this residue very attractive for the development of a residue specific labelling.[123] Antos et al. developed a method for a selective tryptophan labelling with metallocarbenoids. They showed that metallocarbenoids, derived from stabilized vinyl diazo compounds, and a rhodium source selectively modify tryptophan residues on myoglobin without any cross-reactivity with other amino acid residues. In this reaction, two isomers, a 2-alkylated and a *N*-alkylated indole are formed upon conjugation (Scheme 23).[183] Rate acceleration was achieved by addition of hydroxylamine hydrochloride to the conjugation reaction, which is assumed to stabilize highly reactive metal intermediates.

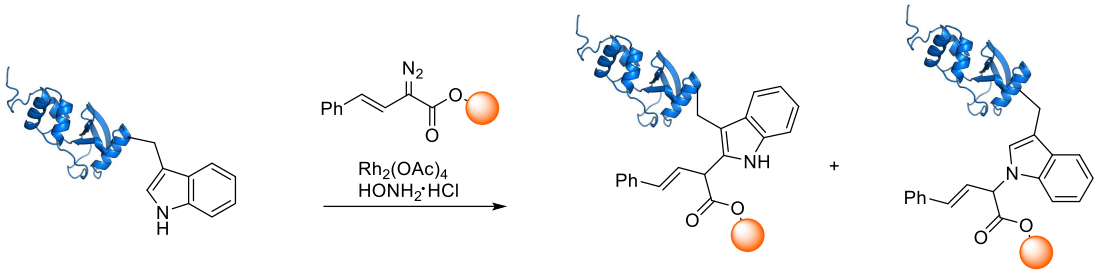

Scheme 23: Selective tryptophan labelling with rhodium metallocarbenoids.

Further additive screening led to the discovery of *N-tert*-butylhydroxylamine, which was able to promote the formation of rhodium carbenoids under mild aqueous conditions of pH 6.[184] A transition metal-free method for tryptophan-selective labelling based on organoradicals was developed by Kanai and coworkers. It was shown that the stable radical 9-azabicyclo[3.3.1]nonane-3-one-*N*-oxyl reacts selectively with tryptophan at ambient temperature and near neutral pH.[185]

Another residue that is particularly attractive for modification reactions is the tyrosine residue. The phenolic moiety of tyrosine constitutes a unique reactivity that is mostly orthogonal to that of cysteine, lysine and carboxylate-containing residues. Moreover, because of its amphiphilic nature, tyrosine residues are often less abundant on the protein surface and are therefore suitable for the attachment of only few modifications to a protein.[186] Francis and coworkers have developed a three-component Mannich-type reaction that uses *in situ* formed imines from formaldehyde and electron-rich anilines to modify tyrosine following an electrophilic aromatic substitution pathway. The reaction proceeds under mild pH and room-temperature at micromolar concentrations and represents one of the first carbon-carbon bond forming reactions on proteins.[186] The same group also developed a tyrosine *O*-allylation protocol based on π-allyl intermediates derived from allylic acetate and carbamate precursors.[187] Another method with increased kinetics relies on an oxidative coupling of dialkyl anilines mediated by cerium(IV) ammonium nitrate. However, it should be noted that tryptophan residues do also react.[188]

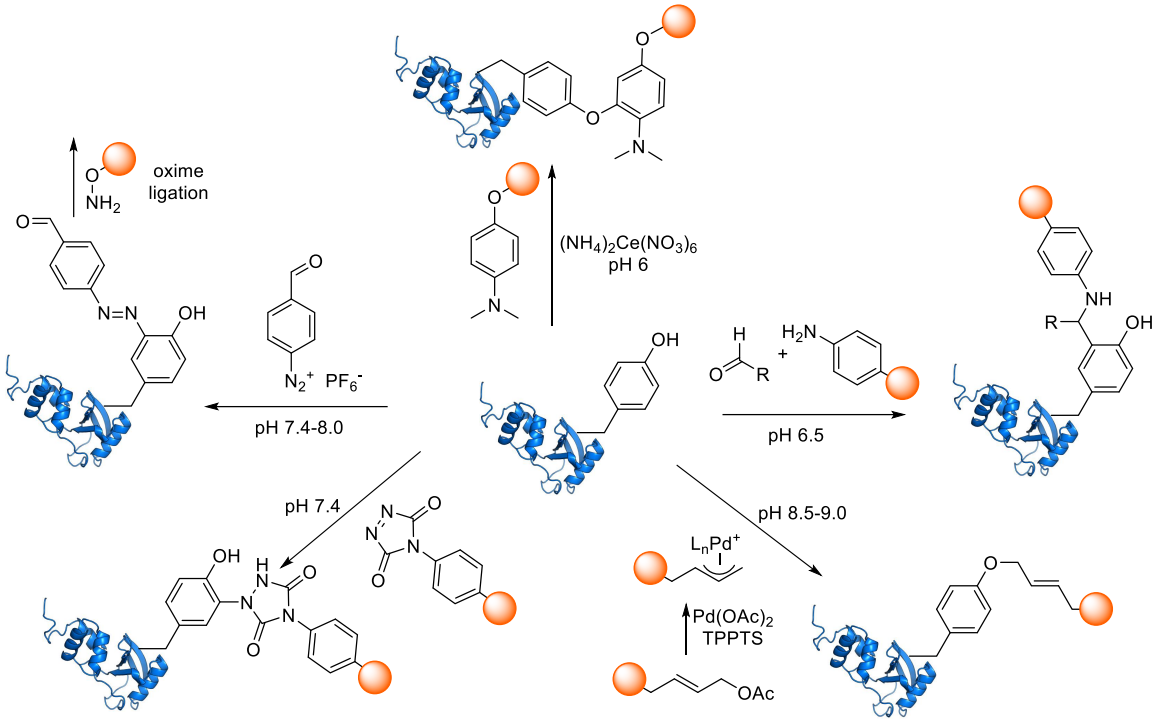

Scheme 24: Overview for different protein modification strategies through tyrosine.

Other strategies for tyrosine modification include diazodicarboxamide reagents that react with phenolic residues on proteins through an aqueous ene-type reaction in a broad pH range.[189] A bench stable diazonium hexafluorophosphate reagent has been employed to selectively attach an aldehyde to a proteins tyrosine residue which can be further modified with oxime ligation strategies.[190] An overview of the most important tyrosine modification strategies is depicted in Scheme 24. Furthermore, enzymatic oxidation of tyrosine residues to 1,2-quinones with the aid of mushroom tyrosinase has been applied for selective modification. Subsequent modification of the 1,2-quinone residue by strain-promoted quinone–alkyne cycloaddition has also been applied to the synthesis of ADCs.[191]

Histidine is the only amino acid with a pKa in the physiological range and is therefore often crucial for protein function, taking part in many mechanisms were abstraction or donation of a proton is necessary.[192] Therefore, one has to take into account that histidine modification might impair the protein function. Epoxides have been described to selectively react with the imidazole side chain of histidine, even though high pH and elevated temperature are necessary to achieve sufficient labelling.[193] Adusumalli et al. recently introduced a method using an epoxide attached to an aldehyde via linker of variable length that reacts intramolecularly with histidine in a proximity induced manner after being trapped by reversible intermolecular imine forming reaction with nearby lysine residues. The authors claim specific modification in dependence of the linker length on one particular protein histidine site.[194]

Since methionine is the second rarest amino acid in vertebrates, with a low level of surface exposure and a unique thioether functional group, selective modification of this residue offers a valuable strategy for selective protein modification of native proteins. However, only a limited set of selective modification strategies is available so far. Selective alkylation of methionine to sulfonium salts has only been achieved with highly electrophilic reagents at low pH, which limited the applicability as a general tool for protein modification.[195] Very recently, a redox-based modification strategy, named ReACT, developed by Lin et al. was introduced that allows a highly specific modification of methionine under neutral aqueous conditions. Here, an oxaziridine reagent reacts with the thioether bond of methionine to form a sulfimide (Scheme 25).[78]

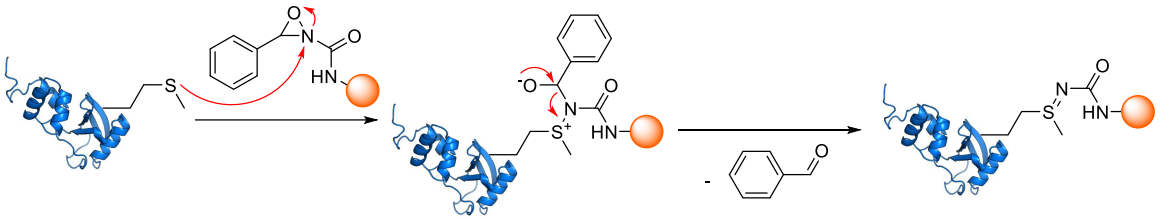

Scheme 25: The ReACT strategy for chemoselective methionine bioconjugation.

The method was successfully applied to the attachment of azide and alkyne handles to different proteins, including BSA, calmodulin as well as GFP- and HER2-binding Fab fragments with and without engineered methionine residues that were further derivatized via CuAAC. An ADC, consisting of an α-Her2 Fab linked to MMAE exhibited increased cytotoxicity to an Her2 expressing cell line.[78] In another very recent report, Taylor et al. introduced hypervalent iodonium salts that selectively alkylate the thioether of methionine to sulfonium salts. The reaction proceeds fast in water in micromolar concentrations and additionally enables the incorporation of a protein modifier, together with a diazo-group that can be subsequently modified. [196]

Addressing the carboxylic acid groups of glutamic and aspartic acids as well as the C-terminus has been rarely used for protein bioconjugations. Most probably due to the relatively high abundance and their low reactivity in aqueous systems. Carboxylic acid functions, activated with water-soluble diimides such as 1-ethyl-3-(3-dimethylaminopropyl) carbodiimide (EDC), can be reacted with amines to form stable amide bonds. To prevent protein cross-linking with lysine residues, it is important to use amines with a low pKa that follow modification pH 8.0.[197] More recently, Raines and coworkers introduced diazo reagents for a selective modification of carboxylic acid residues in proteins. Since this modification turns negatively charged carboxylic acids into uncharged ester residues, this concept is particularly interesting for the purpose of intracellular protein delivery. Inside the cell, the introduced esters can be selectively hydrolyzed by intracellular esterases, thus reforming the native protein.[198]

4.4.4. Affinity-based protein modifications

In addition to the principles, discussed in the last chapters that achieve selectivity for a certain amino acid residue by relying on different reactivities of functional groups, proteins can also be selectively modified in a specific spatial region with the aid of the proximity effect. Here, latent electrophiles are guided to the protein of interest by an affinity ligand where different nucleophilic amino acid side chains in the area of the ligand's binding side can react to form a covalent bond.[88]

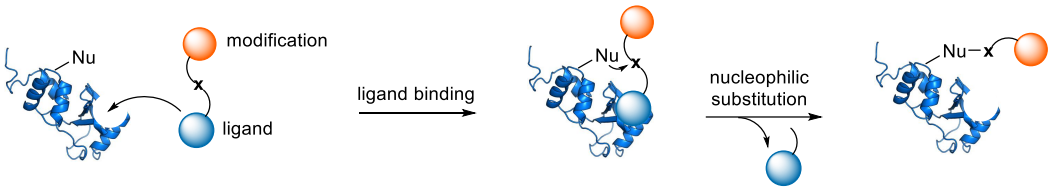

Scheme 26: Principle of the protein modification based on affinity probes. The ligand binds to the protein of interest to bring a reactive electrophile x in close proximity to the protein. Nucleophilic amino acids (Nu) react to form a covalent bond to attach the modification. Figure adapted from Sakamoto et al.[88]

Electrophilic warheads that have been employed for this strategy include tosyl groups,[199] acyl imidazoles[200] and phenyl esters.[201] In addition to those, several structurally refined electrophiles have been developed in the last decades that vary in reactivity and selectivity for the targeted nucleophilic amino acid.[88] The concept has been further expanded by Hamachi and coworkers that attached DMAP as a nucleophilic catalyst to the guiding ligand that promotes an acyl transfer from an electrophilic modifier to the protein. This circumvents the problem of intramolecular decomposition in cases where the ligand carries nucleophilic residues by itself.[202] Even though this concept enables a region specific modification of native proteins, it's limited to proteins with an identified ligand and the exact amino acid side that is modified is often hard to predict.

4.5. Modification of engineered proteins

Even though a lot of effort has been made to develop a plethora of useful methods that allows a specific modification of certain amino acid side chains, all these approaches are only residue specific and will always lead to multiple modification sides in proteins when more than one surface exposed targeted side chain is present. Truly site-specific modification is only possible by the incorporation of bioorthogonal functional groups or chemical reporters, carrying a unique reactivity over all other natural occurring functionalities (Scheme 27).[85b]

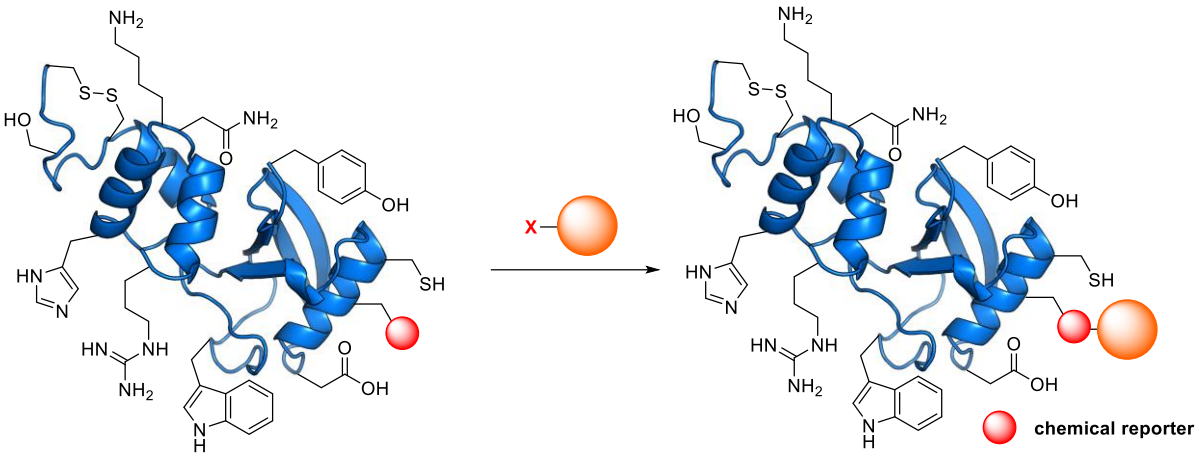

Scheme 27: Selective chemical protein modification of unnatural functionalities.

There are several biochemical methods available that allow the incorporation of very different non-natural functional groups into proteins and a multitude of chemoselective reactions have been developed in the last decades to specifically modify these residues.[92]

4.5.1. Incorporation of unnatural chemoselective handles into proteins

A very straightforward way to incorporate a non-canonical amino acid into a protein is to subject the expressing cells to media containing an unnatural amino acid with structural similarity to a canonical amino acid that tolerated by the translational machinery.[85b] The promiscuous activity of methionyl-tRNA synthetase has been widely exploited for the incorporation of a variety of methionine analogues. Protein expression yields are increased when the used *E. coli* strain is auxotrophic, meaning it is unable to synthesize methionine by itself.[203] At first demonstrated for selenomethionine, which can almost quantitatively replace methionine in protein synthesis,[204] the method has been exploited for the incorporation of a variety of bioorthogonal functional groups. Most prominent examples for methionine surrogates include homopropargylglycine, homoallylglycine[205] and azidohomoalanine.[206] Even though auxotrophic expression is generally associated with high protein expression yields, remaining drawbacks include amino acid scope and lack of site-specificity. Since all of the natural occurring methionine sites are exchanged by their non-canonical counterpart, the method is only residue specific.[85b]

More structural diversity of the unnatural amino acid and true site specificity can be achieved by genetic code expansion and reprogramming techniques that facilitate incorporation of unnatural amino acids into proteins beyond the canonical 20 amino acids. Genetic code expansion utilizes an aminoacyl–tRNA synthetase/tRNA pair that is orthogonal to natural occurring pairs. A promiscuous synthetase specifically transfers the non-canonical amino acids onto a tRNA that is complementary to a blank codon.[207] In case of the widely used amber suppression technique, the stop codon UAG gets

repurposed for the incorporation of the unnatural amino acid.[208] The method has been applied in bacteria and mammalian cells as well as *in vivo* in *Drosphila melanogaster*.[209] Several different amino acids, carrying various functionalities have been incorporated site-specifically into proteins by means of genetic code expansion.[210] Important examples that can be employed for subsequent protein modification include ketones, azides, terminal alkynes, strained alkynes, alkenes, strained alkenes and tetrazines.[87a] Aside from its excellent site-specificity, a major drawback of amber suppression is the competition with the termination of the protein, which is the natural function of the Stop codon. This leads to truncated proteins at the modification side and usually limits the number of incorporated unnatural amino acids to one per protein. [211]

To overcome the low expression yields in genetic code expansion approaches, site-specific modification can be also achieved with peptide tags consisting of canonical amino acids that are recognized by certain enzymes for a specific chemoenzymatic incorporation of the chemical reporter.[212] Here, the promiscuity of natural occurring enzymes that catalyze the covalent modification of proteins with small-molecule cofactors is exploited. Short peptide sequences, derived from the natural protein substrate are often sufficient for recognition by the enzyme and can be conveniently fused to the protein of interest. Small structural variations of the cofactors are often accepted by the enzyme and therefore allow incorporation of non-natural chemical reporters for subsequent labelling. Prominent examples include the formylglycine generating enzyme that transforms a cysteine residue in the CXPXR motive into an aldehyde,[213] Sortase A, recognizing the pentapeptide LPXTG to fuse an oligoglycine motive that can carry different modifications[214] or transglutaminases that are able to transfer a wide variety of unbranched primary amines to the carboxamide residue of glutamine to generate an isopeptide bond.[215] More recently, Schumacher et al. have introduced the Tub-Tag, a fourteen amino acid peptide sequence that gets recognized by the tubulin tyrosine ligase to transfer unnatural tyrosine substrates that can carry various chemical reporters such as azides or aldehydes.[216] These chemoenzymatic approaches are attractive due to high yielding protein expressions and often rapid labelling reactions, however applications are often limited since tags have to be fused to specific parts of the proteins such as either the C- or the N-terminus.[212]

4.5.2. Chemoselective reactions for site-specific protein modifications

The above mentioned techniques are often used to introduce unnatural functionalities into a given protein of interest that can subsequently be addressed wit chemoselective reagents. These chemoselective reagents have been incorporated in proteins have to fulfill several important criteria to ensure site specific labelling. First of all, they should not interfere with any other functional group

that is present in native proteins and yield in stable covalent linkages. Furthermore, to preserve the structural integrity of the modified protein, the reaction must proceed under physiological conditions such as ambient temperature, nearly neutral pH and aqueous conditions.[217] A chemoselective reaction is termed bioorthogonal if the reactants are non-toxic and do not interfere with any other *in-vivo* process.[218] Several reactions based on very different chemical principles that fulfill those criteria have been developed in the last decades. An overview of the most important bioorthogonal reactions is given in the next chapters.

4.5.2.1. Aldehyde and ketone condensations

One of the first chemical reporters that have been explored for site specific protein modification is the carbonyl functionality.[219] Aldehydes and ketones can be selectively reacted with nucleophiles that hold a strong α-effect such as alkoxyamines[220], hydrazines[221] or hydrazides[222] (Scheme 28). The reaction proceeds under slightly acidic conditions (usually pH 4-6) and is irreversible under physiological pH for most examples.[222] Rather slow reaction kinetics with second-order rate constants of 10^{-4} to 10^{-3} $M^{-1}s^{-1}$ require often high concentrations or huge excess of one or the other reaction partner to achieve sufficient labelling yields.[218] Rate enhancement for the reaction of hydroxylamines with aldehydes to form oximes can be achieved by the addition of aniline.[223] Reactions in a cellular context are often limited to the cell surface due to the necessity of acidic conditions and interference with intracellular aldehyde- and ketone- bearing metabolites.[224]

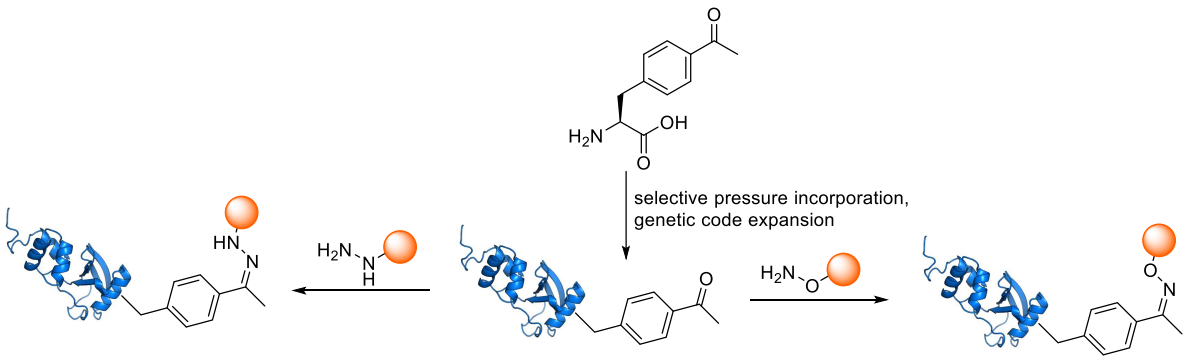

Scheme 28: Modification of carbonyl-modified proteins with hydrazines (left) and hydroxylamines (right). *p*-Acetylphenylanalin can be incorporated by selective pressure incorporation and genetic code expansion techniques.[87a]

4.5.2.2. Inverse-electron demand Diels-Alder reactions

One on of the biggest limitation of bioorthogonal reactions when performed in complex environments such as living animals is the reaction rate.[218] Since most of the known protein conjugation reactions follow second order kinetics, reactions with inherently slow reaction kinetics require high concentrations, that are not feasible to achieve sufficient labelling *in vivo*. The fastest bioorthogonal reaction known is based on the reaction between 1,2,4,5-tetrazines and strained alkenes and alkynes

that react in an inverse-electron demand Diels–Alder reaction (IEDDA) to yield dihydropyridazines and pyridazines. The release of gaseous nitrogen as the only byproduct, which is the driving force of the reaction and precludes reversibility.[225] Based on earlier observations of such reactions[226], the groups of Fox and Hilderbrand simultaneously reported on its applicability as a bioorthogonal reaction with unprecedented fast kinetics in 2008.[227] The rate constant of the IEDDA can be tuned by either increasing the electron density, introducing ring strain to the dienophile or by changing the electron deficiency of the tetrazine. Most of the reports from the last decade focus on manipulating the reaction rate by expanding the scope of dienophiles. Fox and coworkers at first reported *trans*-cyclooctene (TCO) (Scheme 29a) whereas Hilderbrand's concept focuses on norbornenes as dienophiles (Scheme 29b). Both of which exhibit second order rate constants in the range of 10^3 $M^{-1}s^{-1}$. The reaction proceeds through a Diels-Alder- followed by a retro-Diels-Alder pathway with the release of nitrogen as a driving force (Scheme 29c).[225] Other dienophiles that have been applied include simple terminal alkenes,[228] bicyclooctynes (BCN),[229] cyclopropenes[230] and vinylboronic acids[231], all exhibiting different reactivities towards tetrazines. The applicability of highly reactive dienophiles can be limited by decreased stability in the presence of thiols or simply prolonged storage, especially in aqueous buffers. Robillard et al. showed that TCO isomerizes in mouse serum to form the unreactive *cis*-isomer at 37°C with a half-life of 3.26 hours.[232]

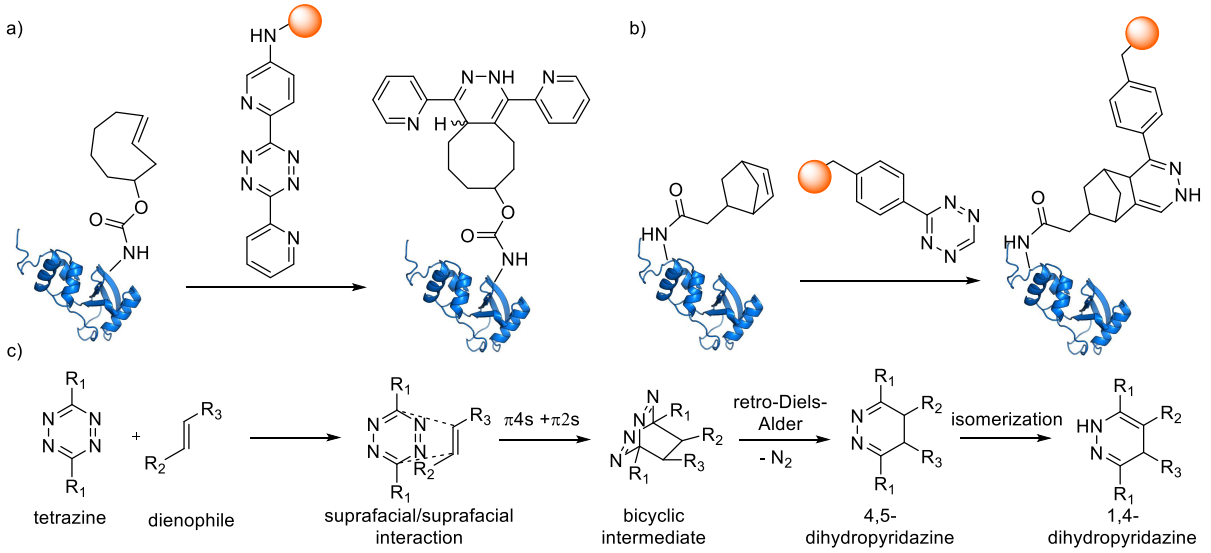

Scheme 29: Chemical protein modification with tetrazines. a) *trans*-Cyclooctene modified protein in the reaction with a dipyridyltetrtazine. b) Norbornene modified protein in the reaction with a phenyltetrazine. c) Mechanism of the IEDDA. Mechanism adapted from Oliveira et al.[225]

Similar to the developments that led to cyclooctynes with improved reactivity in SPAAC, further structural refinements of the TCO by introducing ring strain also yielded dienophiles that are even more rapid in IEDDA. Taylor et al. demonstrated that fusion of a *cis*- cyclopropane to the TCO increases the reaction rate with a tetrazine 20-fold.[233] Computational analysis led to the discovery of dioxolane-

fused d-TCO-derivatives that react with a second order rate constant of more than 300 000 $M^{-1}s^{-1}$ in pure water.[234] Stability studies revealed that d-TCOs display enhanced stability towards isomerization and are more easily prepared than other strained alkenes.

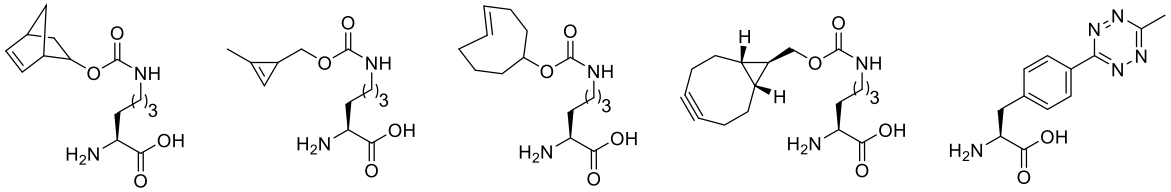

Figure 12: Selection of unnatural amino acids that can be genetically incorporated into proteins via genetic code expansion for IEDDA.

Most importantly, several unnatural amino acids allow for the incorporation of several dienophiles as well as tetrazines into proteins via genetic code expansion (Figure 12). Rapid reaction kinetics and high selectivity together with a feasible site-specific incorporation of one or the other reaction partner into proteins have turned IEDDA into the most promising method for protein modification in biological media with a myriad of applications.[225] Prominent examples include tracking and imaging of fast biological processes,[235] fluorescent tagging of low abundant proteins in living cells[236] and protein profiling *in vivo*. [237] Due to the absorption in the visible-light range, tetrazines also act as quenchers towards a series of fluorophores. A unique absorption change upon IEDDA reaction facilitates a turn-on in fluorescence of a conjugated dye upon conjugation with the biomolecule. This can results in a strong signal and minimizes background fluorescence.[238]

4.5.2.3. 1,3-dipolar cycloaddition reactions for site-specific protein modification

In contrast to carbonyl compounds, azides are nearly absent from biological systems and are therefore very attractive chemical reporters for the development of bioorthogonal reactions.[218] The first description of an azido modified compound tracks back to the middle of the 19th century when Griess was the first one to describe the synthesis of phenyl azide.[239] Since then, the unique reactivity of this functionality has been further explored and exploited in the development of several groundbreaking reactions in organic chemistry and chemical biology. Azides do not hydrolyze under ambient conditions, are resistant towards oxidation and only slightly prone to reduction in the presence of high intracellular thiol concentrations. In contrast to sodium azide that is a well-known cytotoxin, organic azide are usually considered as non-toxic.[240] Decomposition by light irradiation is only known for phenyl azides, which have been therefore employed as photo-crosslinking reagents.[241] The most important chemical property probably is the irreversible formation of gaseous dinitrogen upon chemical reaction, which acts as a powerful driving force. This unique feature enables the reaction with electrophiles, soft nucleophiles and radicals.[242]

In addition, azides are also 1,3-dipoles that can undergo [3+2] cycloaddition reactions with dipolarophiles such as alkynes.[224] This reaction is known since the late 19th century,[243] but was significantly refined by Huisgen more than five decades ago.[244] The reaction yields stable triazole adducts which are chemically stable towards oxidation, reduction as well as hydrolysis under acidic and basic conditions.[245] Thus triazoles are desirable linker systems for protein modifications. Even though thermodynamically favored, organic azides react with unactivated alkynes without the addition of a catalyst only under elevated temperature or high pressure. To overcome this issue, the groups of Sharpless and Meldal almost simultaneously reported that reaction rates can be significantly increased by copper(I)-catalysis.[246] The catalyzed reaction proceeds at room temperature without the need of oxygen exclusion when adding a source of Cu(I) or Cu(II) with a reduction agent such as sodium ascorbate. It should be noted that the 1,4-tetrazole regioisomer is almost exclusively formed under copper catalysis, whereas a 1:1 mixture of the two possible 1,4- and 1,5-regioisomers are produced in the thermal reaction (Scheme 30a). The reaction mechanism includes several different reactive copper complexes as intermediates. Recently, Jin et al. reported that dinuclear copper complexes are more pronounced during the reaction. However mononuclear complexes were also identified, suggesting that two different catalytic cycles are involved (Scheme 30b). A high functional group tolerance was already observed in the first reports of the copper catalyzed azide-alkyne cycloaddition (CuAAC). Together with high yields, broad scope, insensitivity towards oxygen and water as well as simple reaction workup, the CuAAC fulfills all requirements for a “Click”-reaction[247] and has therefore been successfully applied for the modification of azide and alkyne modified proteins for the first time by Wang et al.[248] Until today, CuAAC is one of the most important techniques for the chemoselective modification of macromolecules with applications in protein-,[249] nucleic acid-,[250] dendrimer-, and polymer synthesis.[251] Further improvements have been achieved by the development of new ligands that allow a reduced copper content in the ligation reaction.[252] Recently, a new tris(triazolylmethyl)amine ligand has been developed that even allows CuAAC modification within *E. Coli* and mammalian cells.[253]

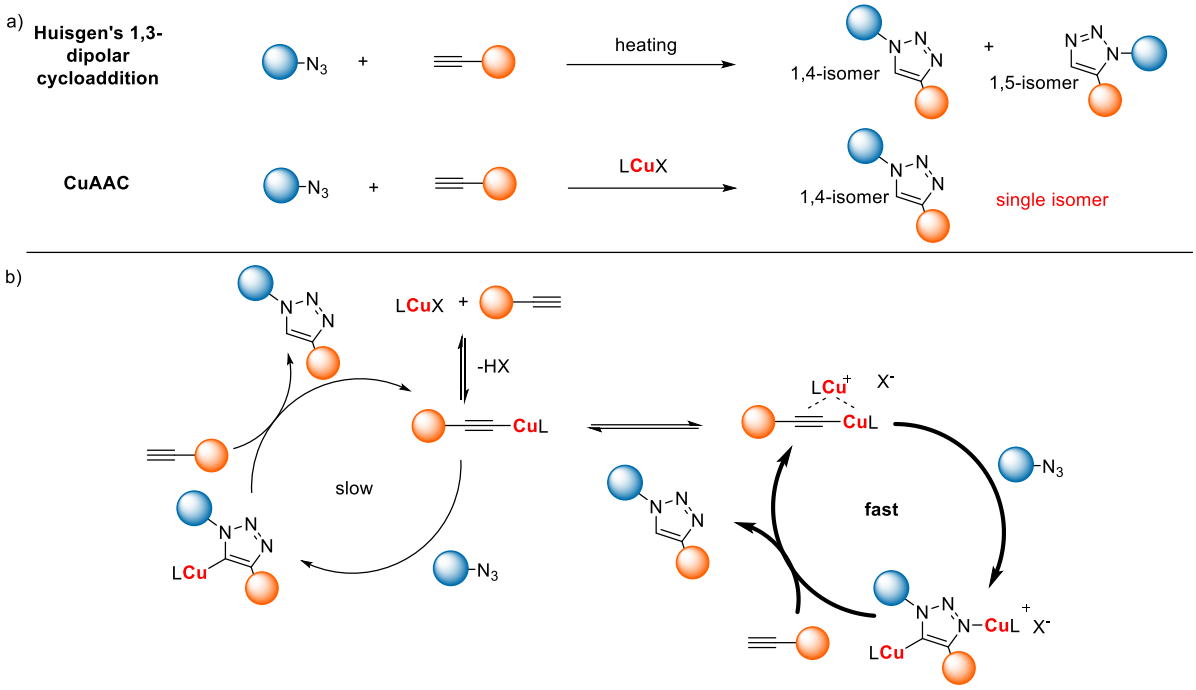

Scheme 30: Copper-mediated azide-alkyne cycloaddition (CuAAC). a) Regioisomer-differences between temperature-mediated Huisgen cycloaddition and CuAAC. b) Mechanism adapted from Jin et al.[254]

Even though novel ligands enable the use of significantly reduced amounts of copper in the ligation reactions, the primary disadvantage of the CuAAC remains coppers cytotoxicity[255], which limits the applicability to living cells and *in-vivo* ligations. A concept to improve the reaction kinetics in absence of a copper catalyst involves activation of the alkyne for the reaction. One possible modification of the alkyne is based on the attachment of electron-withdrawing groups such as esters.[256] However, the resulting α,β-unsaturated carbonyl compounds are also reactive towards thiols in a Michael-type addition and therefore limit the applicability in the presence of other thiols *in vivo*.[224] Based on early observations from Wittig and Krebs who described an explosive reaction between strained alkynes such as cyclooctyne with phenyl azide to form a triazole,[257] Agard et al. developed the Strain-promoted azide-alkyne cycloaddition (SPAAC) that proceeds under physiological conditions without the need of copper addition.[258] In the initial study, a biotinylated cyclooctyne (OCT) was synthesized and selective labelling of an *N*-azidoacetyl sialic acid containing glycoprotein was demonstrated in absence of copper. Driving force of the reaction is the release of ring strain that accounts for approximately 18 kcal/mol. In contrast to acyclic alkynes, substantial bond angle distortion destabilizes the ground state of cyclooctynes, which leads to a lower activation energy for the cycloaddition reaction.[259]

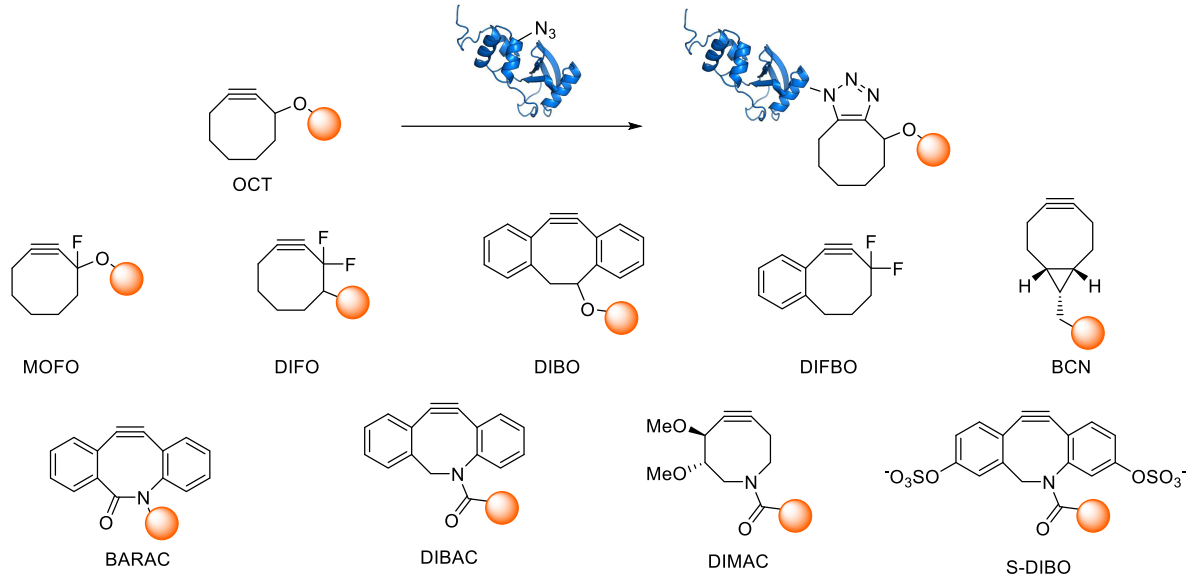

Scheme 31: SPAAC with cyclooctyne (OCT) and improved cyclooctyne derivatives with increased reactivity and water-solubility.

However, the rather slow kinetics in the reaction with azides, with a second-order rate constant in the range of 10^{-3} M^{-1} s^{-1} was still a drawback of the first cyclooctyne derivatives.[85b] To overcome this issue, electron-withdrawing substituents were attached to the strained alkyne to lower the LUMO and thereby increasing its interaction energy with the HOMO of the azide.[260] The attachment of fluorine atoms to generate mono- and difluorinated cyclooctynes, MOFOs[261] and DIFOs[262] increased the rate of the reaction by 4- and 60-fold, respectively. Further developments led to the discovery of benzo-substituted cyclooctynes such as dibenzo- (DIBOs)[263], difluorobenzo- (DIFBOs)[264], aza-dibenzo-cyclooctynes (DIBACs)[265], biarylazacyclooctynones (BARACs)[266] and Bicyclononynes (BCNs)[267] to increase the overall ring-strain (Scheme 31). Even though all of these reagents are superior in terms of reaction kinetics over unmodified cyclooctynes and have found applications in imaging azide-containing proteins in complex biological systems such as live cells[268] or *C. elegans*[269] efficient labelling failed to translate to more complex organisms. In mice for instance, it has been shown that DIFO derivatives bind to the highly abundant murine serum albumin (MSA) and therefore prevents selective target labelling.[270] This result already points to common problems that are associated with SPAAC, as for instance hydrophobicity of the cyclooctyne[271] and cross-reactivity with thiols of cysteines that are attacking the alkyne in a thiol-yne reaction.[272] To decrease hydrophobicity, Sletten et al. attached methoxy groups to the cyclooctyne producing DIMAC with increased water solubility but diminished reactivity in the cycloaddition.[273] Sulfation of DIBAC also yielded in S-DIBO cyclooctynes with increased water solubility and decreased cell-permeability, which can be advantageous in certain applications.[274]

Other than azides, also nitrones can react in a [3+2] cycloaddition reaction called SPANC (strain promoted alkyne- nitrone cycloaddition). Van Delft and coworkers developed a method that applies a

three-step one-pot protocol for the transformation of N-terminal serine residues into a nitrone that reacts subsequently with a cyclooctyne. Nitrones are up to 30 times faster than azides in the cycloaddition reaction.[275]

4.6. Chemoselective modifications based on Staudinger-type reactions

4.6.1. Staudinger reduction and related reactions

Reactions of organic azides with phosphines were first described 100 years ago by Staudinger, who observed a vigorous reaction between phenylazide and triphenylphosphine to form a iminophosphorane that could be hydrolyzed under acidic conditions to form an amine and phosphine oxide.[276] Since then, this reduction of an organic azide to an amine by phosphines is known as the Staudinger reaction. The reaction sequence is initiated by a nucleophilic attack of the phosphine to the terminal nitrogen atom of the azide to form a phosphazide. The release of gaseous nitrogen from the molecule to form the iminophosphorane proceeds via a cyclic four-membered transition state without any participation of radicals or nitrenes.[277] The iminophosphorane structure can be also described as an aza-ylide with a highly nucleophilic nitrogen that can undergo several transformations with electrophiles. Whereas it rapidly hydrolyzes in the presence of water to form the reduced amine, it can also be alkylated with alkyl halides to yield secondary amines after hydrolysis.[278] Furthermore, it is also known to react with aldehydes, amides and cyanates to form imines, amidines and carbodiimides in aza-Wittig-type reactions, respectively (Scheme 32).[279]

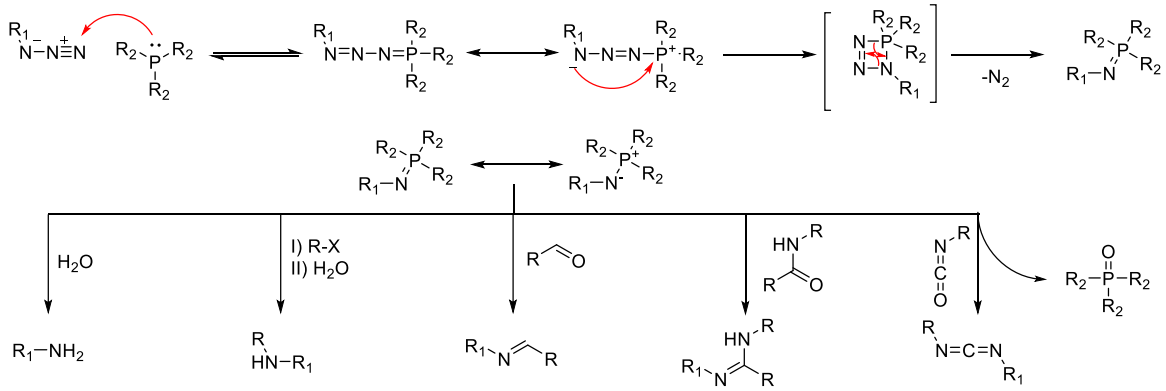

Scheme 32: Mechanism of the Staudinger reaction and subsequent reactivity with a plethora of nucleophiles.

4.6.2. Staudinger ligations

Due to the clean formation of an iminophosphorane that proceeds rapidly also in aqueous systems with high yields, Bertozzi and coworkers aimed at applying this reaction for a chemoselective ligation. To circumvent the amine formation by hydrolysis, an electrophilic trap in form of an ester can be installed onto the phosphine that facilitates an intramolecular reaction with the iminophosphorane to yield a stable amide bond (Scheme 33).[280] The bioorthogonality of this Staudinger ligation has been

demonstrated by selective cell-surface labelling of azido containing carbohydrates that have been incorporated by metabolic glyco-engineering. Other than this, an auxotrophically expressed azidohomoalanine containing protein has been selectively modified in cell lysate utilizing the Staudinger ligation.[281] More sophisticated phosphines, carrying an additional coumarin have also been synthesized by the Bertozzi group. Since those structures have been shown to become fluorescent when transformed from a phosphine to a phosphine oxide, they are utilized as specific fluorogenic labels of azido containing proteins.[282]

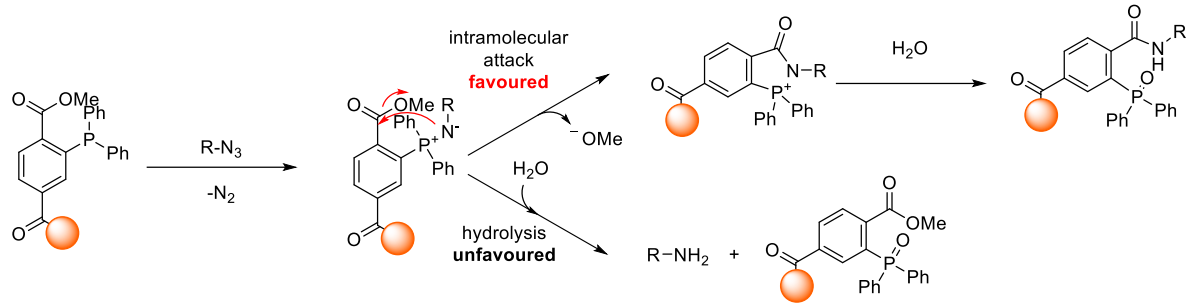

Scheme 33: Mechanism of the Staudinger ligation. An intramolecular reaction of the imminophosphorane via a five-membered transition state is favored over hydrolysis.

Despite from the high efficiency and selectivity of the Staudinger ligation in the reaction with azides to form the ligated product, there remains one drawback, which is the attached unnatural phosphine oxide residue. Since the formation of a native amide bond is beneficial in a peptide ligation, efforts have been made to develop a method were the phosphine oxide is released from the molecule during the reaction. This has been achieved almost simultaneously by the groups of Raines[283] and Bertozzi[284], who developed the traceless Staudinger ligation. In this reaction, the phosphine carries an acylated leaving group such as a phenol, a thiophenol, or an imidazole. After reaction with the azide and liberation of dinitrogen, an acyl transfer to the nucleophilic iminophosphorane takes place, followed by liberation of the phosphine oxide upon hydrolysis and generation of a native peptide bond (Scheme 34).[285]

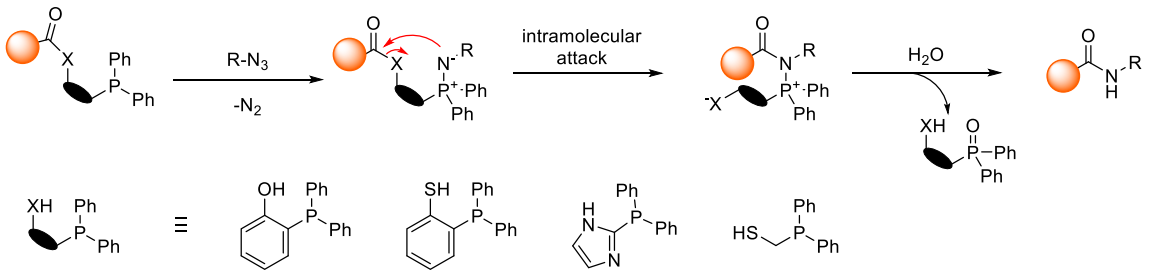

Scheme 34: Mechanism of the traceless Staudinger ligation with successfully applied phosphines.

A phenol group proved to be the most effective aromatic leaving group in the reaction,[284] whereas the aliphatic methylene bridged thiol has been shown to be even more efficient in forming the native peptide bond.[285] In cases were the azides originate from enantiomeric pure α-azido acids, the

stereochemistry is retained after traceless Staudinger ligation.[286] Due to its high efficiency paired with an excellent selectivity the traceless Staudinger ligation has found application in many different fields such as organic synthesis, peptide cyclization and protein synthesis. David et al. used the technique in an intramolecular cyclization reaction to generate medium-sized lactams,[287] whereas Hackenberger and coworkers expanded this idea and applied the concept to the synthesis of cyclic peptides.[288] Both studies report the utilization of diphenylphosphinomethanethiol which is a highly reactive linker for the ligation but also prone to oxidation under ambient conditions. Borane-phosphine Lewis acid-base pairs are known to prevent phosphine oxidation in the presence of air,[289] therefore borane adducts have been used in these studies to address this issue. Borane removal prior to Staudinger ligation can be achieved with bases such as DABCO or in the presence of strong acids such as TFA (Scheme 35).[290]

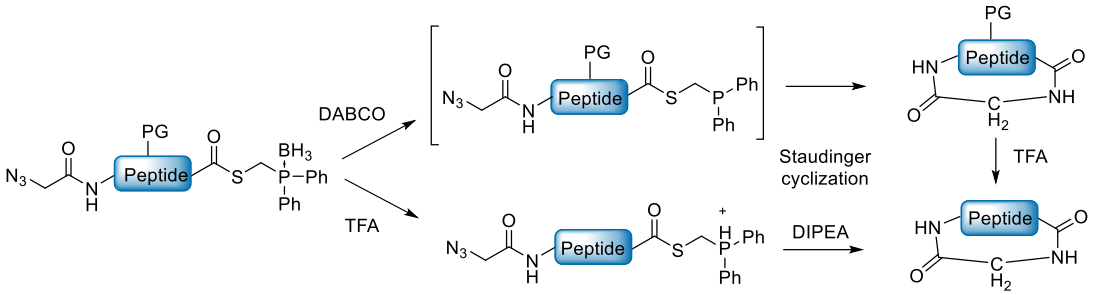

Scheme 35: Acid and base mediated Borane deprotection of phosphines followed by intramolecular Staudinger ligation on peptides.

Application of this approach to protein synthesis has been achieved by Nilsson et al. who ligated two protected synthetic peptide fragments on resin by traceless Staudinger ligation in high yields, followed by NCL of this peptide to a biosynthetically produced protein fragment of RNAse A. The resulting protein proved to be fully functional RNAse A.[291]

4.6.3. Staudinger phosphite and phosphonite reactions

Analogously to the reaction of phosphines and azides that form iminophosphoranes, other phosphorous(III) species such as phosphites, phosphonites or phosphinites can also react with azides to yield in products with *P-N* double bonds after release of dinitrogen (Scheme 36). The first description of an imidate formation from phosphites and phosphonites in the reaction with phenyl azide goes back to a report from 1956.[292] Afterwards several studies on phosphonimidate formation by Staudinger reactions can be found in the literature that describe the influence of the P-(III)-substituent on the rate of the Staudinger reaction[293] or employ imidates as amino protecting groups in organic syntheses for instance.[294]

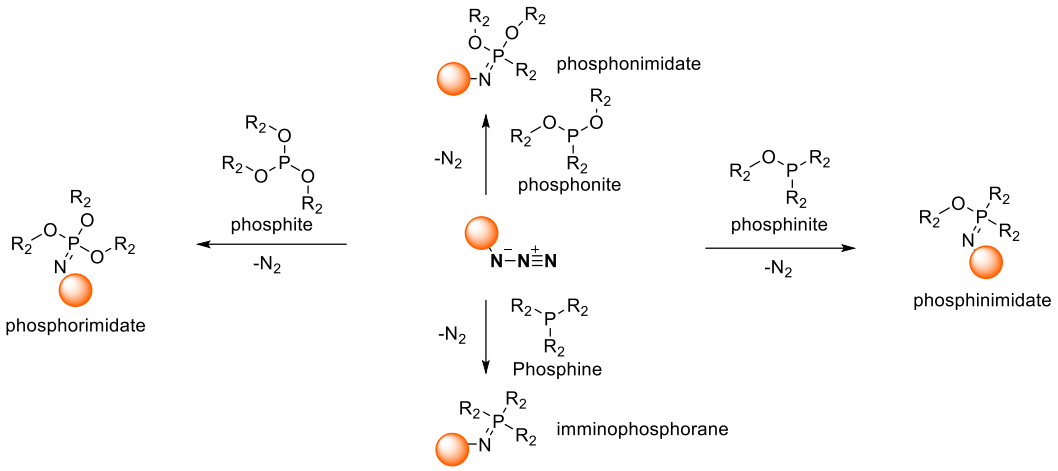

Scheme 36: Reaction of organic azides with differently substituted P(III)-reagents.

Even though cleavage of *P-C*-bonds has been described under harsh reaction conditions,[295] those bonds are generally considered as stable under ambient conditions. In contrast to this, *P-O*-bonds are generally considered as more labile.[296] Hence, phosphor- and phosphonimidates can undergo different rearrangement and hydrolysis pathways that are not possible with their iminophosphorane counterparts. Mapp and coworkers for example described a [3,3]-sigmatropic rearrangement of allylic phosphorimidates that were synthesized from azides and phosphites to generate *N-N*-disubstituted phosphoramidates. This strategy provides synthetic access to allylic amines from allylic alcohol- and azide precursors after hydrolysis (Scheme 37).[297] Based on findings from Iley and coworkers, who first described a possible rearrangement of phosphorimidates to *N-N*-disubstituted phosphoramidates that is not depending on allylic O-substituents,[298] Wilkening et al. found out that this reaction can be promoted by Lewis acid catalysis (Scheme 37). Here, a one-pot protocol was developed where the phosphorimidate is formed from azides and phosphites with a subsequent addition of boron trifluoride to generate the desired *N-N*-disubstituted phosphoramidates in high yields.[299] In another comprehensive synthetic study, this concept was also extended to phosphinimidates that yield *N-N*-disubstituted phosphinamidates after rearrangement.[300] Based on earlier observations,[298] it was shown that the reaction can also be catalyzed by alkyl halides instead of boron trifluoride.

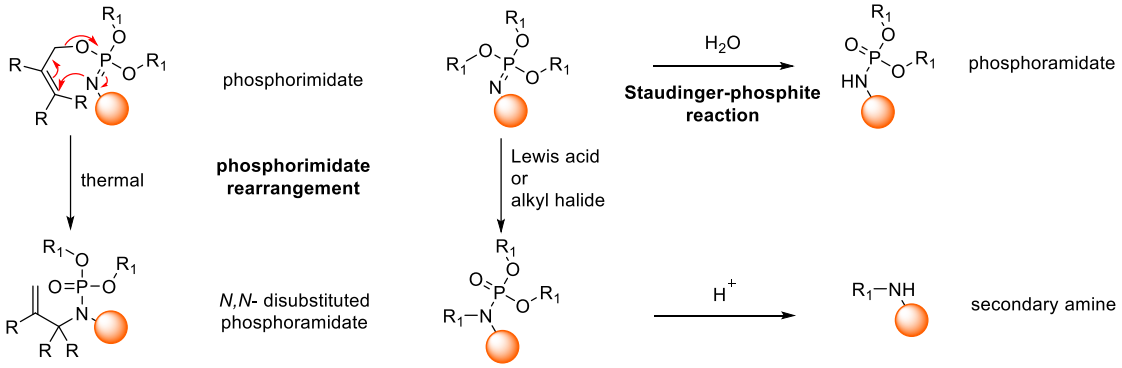

Scheme 37: Reactivity of phosphonimidates in rearrangement reactions and towards hydrolysis.

It has been observed that phosphorimidates hydrolyze under aqueous conditions to form phosphoramidates.[292, 301] In contrast to the classical Staudinger reaction with phosphines, here the *P*-*N*-bond stays intact and one alcohol substituent is liberated instead of the amine. Based on those observations, the Hackenberger group developed the Staudinger-phosphite reaction as a chemoselective labelling method for azide containing proteins. It has been shown that azido modified small molecules, peptides and proteins react with phosphites under aqueous conditions to form the desired phosphoramidates in high yields. The conjugated products proved stable over several days in solution at neutral pH.[302] Modification of peptides via Staudinger-phosphite reaction can be either performed on resin or in solution after cleavage of the peptide.[303]

The Staudinger-phosphite reaction has been extensively applied to protein and peptide synthesis for the introduction of very different functional moieties. For example, PEG-phosphites have been synthesized and site-specifically attached to azido-modified peptides and proteins.[304] The procedure allows efficient installation of PEG-phosphoramidates on proteins even in highly complex media such as cell lysate.

Since the cleavage of the phosphoramidate ester residue yields a phosphorylated amino group, the Staudinger-phosphonite reaction has also been employed for the site-specific incorporation of post-translational phosphorylations and their mimics (Scheme 38a). A phosphotyrosine analog was installed on a protein starting from a *p*-azido phenylalanine residue that has been reacted with a photocleavable PEG-phosphite, followed by phosphodiester cleavage, using light irradiation.[302] In another study, a similar approach was used to chemoselectively install phospholysine on peptides, leading to the development of a MS-based proteomic detection method for those rare post-translational modifications.[305] Furthermore, phosphoramidate-linked carbohydrates have been attached via the Staudinger-phosphonite reaction to access glycosylated peptides (Scheme 38b). In these studies, glycosylation has been achieved with phosphitylated peptides and azido modified sugars[306] or vice versa with carbohydrate modified phosphites and peptides bearing an azide handle.[307]

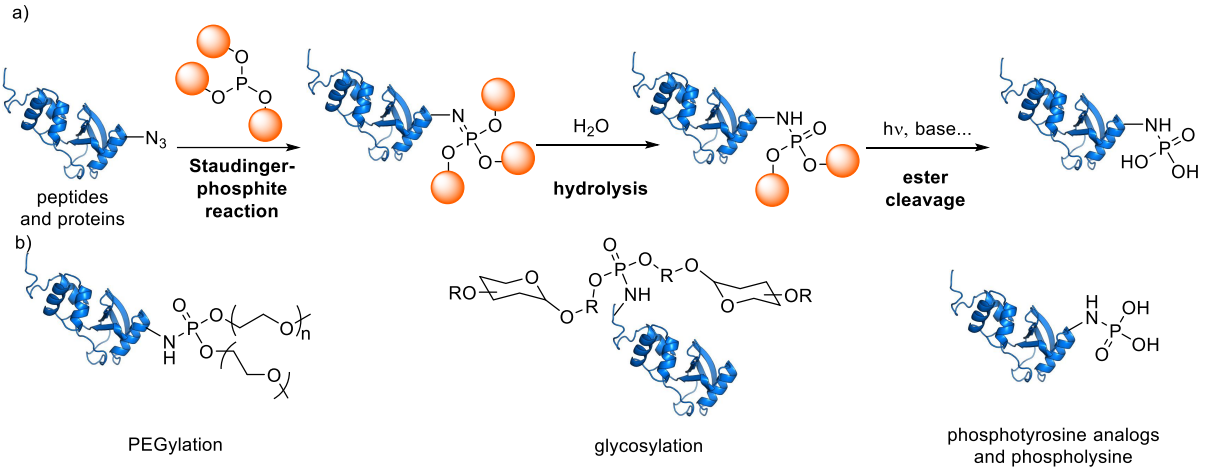

Scheme 38: Staudinger-phosphonite reaction on peptides and proteins. a) Reaction principle with subsequent phosphoramidate ester cleavage. b) Examples for site-specific incorporation of unnatural modifications and PTMs.

All the examples described so far utilize symmetrical phosphites for the reaction with the azide that carry three equal substituents. However, ligation products from those phosphites always yield doubly modified molecules, since only one substituent is released from the molecule upon hydrolysis. To overcome this issue, protocols based on unsymmetrical phosphites have been developed that facilitate the introduction of a single functionality (Scheme 39). In this case, two good leaving groups were attached to the phosphonite together with the desired modifier.[308]

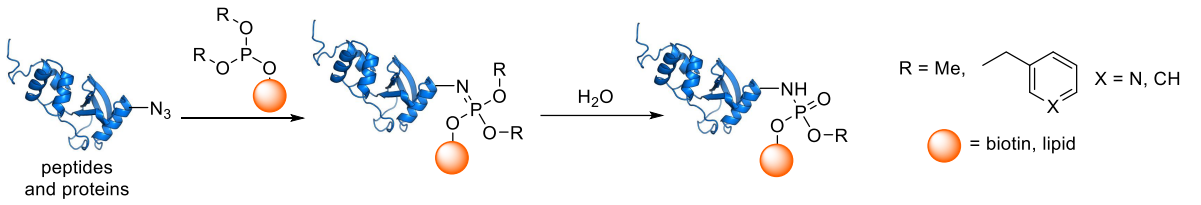

Scheme 39: Staudinger-phosphite reaction with unsymmetric phosphites.

Besides azides that have been extensively explored, other electrophiles are also known to yield phosphorus(V) species in the reaction with phosphorus(III) reagents. A famous example that has been at first described by Michaelis[309] in the late 19th century and further elaborated by Arbuzov, is the reaction of alkyl halides with phosphites to give phosphonates.[310] In a more recent example, Bertran-Vicente et al. have discovered electrophilic disulfides in the reaction with phosphites to yield phosphorothiolates. It could be shown that the reaction with unprotected, activated cysteine peptides is chemoselective and can introduce a native phosphocysteine residue after phosphodiester cleavage (Scheme 40).[169]

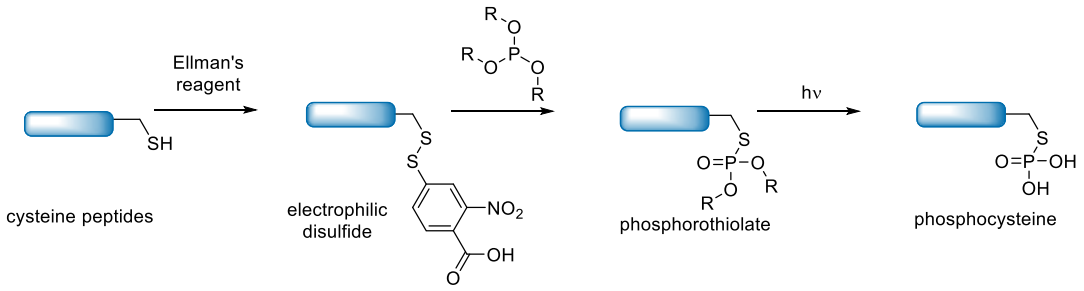

Scheme 40: Reaction of phosphites with electrophilic disulfides for the chemoselective installation of phosphocysteine.

Further developments in the area of chemoselective reactions based on phosphorus(III) reagents led to the discovery of the Staudinger-phosphonite reaction (SPhR) that yields phosphonamidates. Mono modification of an azide containing molecule is easily achieved when the desired modifier is installed on the phosphonite via a non-hydrolyzable *P-C*-bond. However, reactions with phosphonites in the presence of air can be more challenging since auto oxidation of phosphonites is known to be more rapid in comparison to other P(III)-species such as phosphites or phosphinites.[311] Because of this, first attempts were performed with monosilylated phosphonites since they can be readily synthesized from stable phosphinic acid ester precursors. Subsequent azide addition in a one pot procedure yields the desired phosphonamidate in very good yields.[299] Moreover, carbon substituents with sp^2-hybridization have been shown to increase phosphonites stability over alkyl substituted derivatives. Hence, C-phenyl substituted phosphonites have been used in the first example that was applied on proteins (Scheme 41).[312] Further increase of the stability in aqueous buffer was achieved by the introduction of small solubilizing ethylene glycol chains. It could be demonstrated that the reaction is chemoselective for azide residues and facilitates the modification of p-azidophenylalanine carrying proteins.

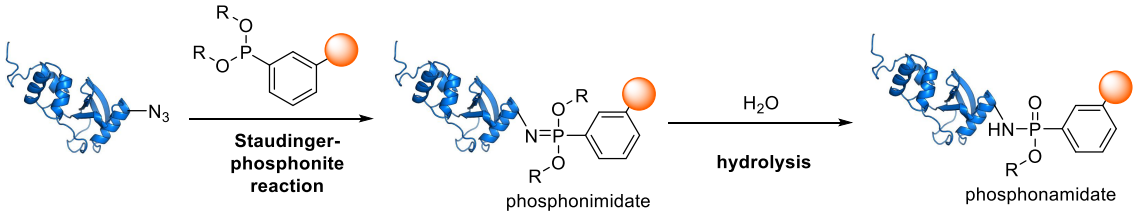

Scheme 41: Principle of the Staudinger-phosphonite reaction.

Encouraged by this first successful development of the Staudinger-phosphonite reaction as a chemoselective transformation, borane protected ethynylphosphonites have been synthesized that facilitate a modular stepwise conjugation of two different azide containing building blocks (Scheme 42). Here, copper-catalyzed azide-alkyne cycloaddition (CuAAC) was employed to form a triazole from the alkyne moiety in the first step. The borane-adduct ensured selectivity by preventing the phosphorus from reacting with the azide in the first place and likewise protected the P(III) from oxidation by air. Subsequent borane removal from the isolated triazole-phosphonites with DABCO and

Staudinger-phosphonite reaction with azides yielded triazole-phosphonamidates as the formal coupling product of two azides in high yields.[313]

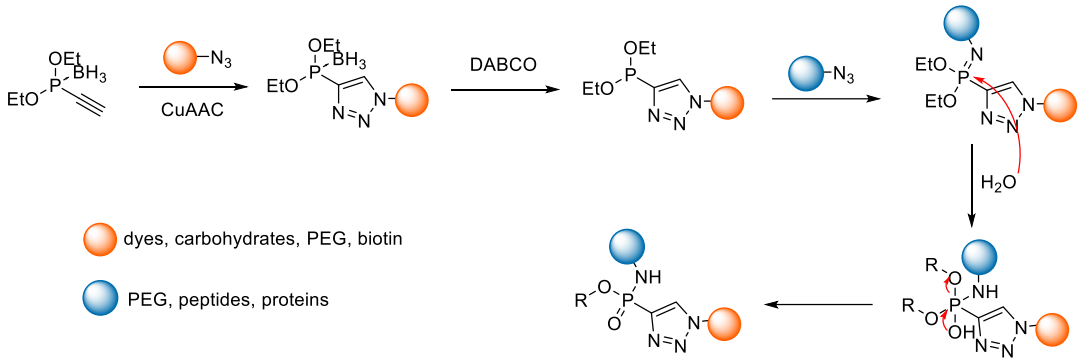

Scheme 42: Borane protected ethynylphosphonites for the sequential coupling of two azide containing building blocks.

Again, incorporation of ethylene glycol substituents to the ethynylphosphonites increased the stability in aqueous systems and therefore facilitated modification of azide containing proteins in the second Staudinger transformation.[314]

5. Objectives

The chemical modification of proteins with functional synthetic molecules constitutes an essential process in chemical biology and the life sciences in general. Traceable fluorescence-[315] tags or spin probes[315] have been attached to proteins to study their biological role applying methods like fluorescence microscopy or NMR. Furthermore, post translational modifications were installed to get a deeper insight into their function[316] and reactive crosslinkers and warheads were incorporated to synthesize activity based protein-probes that enable investigation of potential interaction partners[317]. Also drugs have been ligated to antigen binding proteins[23] and antibodies[48] to achieve a guided delivery to the side of action for a new generation of targeted therapeutics. All these applications require reliable protein bioconjugation techniques with different demands such as control over the attachment site, stability of the linkage, sufficient reaction kinetics, facile applicability in terms of reaction conditions and simple synthetic access.[85a, 86a, 318] Requirements on bioconjugation techniques for the synthesis of targeted therapeutics such as ADCs are exceptionally high, since the safety profile of the final medication is highly depending on the product's homogeneity as well as on the linkage stability between ligand and drug.[39] Despite many advances that have been achieved in recent decades there is still a great demand on adding methodologically novel chemical protein modification methods to the toolbox that enable a straightforward synthetic access combined with a high selectivity for the protein's modification site and linkage stability that is sufficient for targeted drug delivery applications. Consequently, two main goals were defined for this thesis:

1. Development of a modular cysteine-selective bioconjugation method based on electron-deficient phosphonamidates that can be chemoselectively incorporated via the Staudinger-phosphonite reaction.

2. Evaluation of this bioconjugation technique in the context of targeted drug delivery with a general focus on ADCs in terms of applicability, sufficient linkage stability and finally *in vitro* and *in vivo* efficacy.

Project 1: Chemoselective synthesis of phosphonamidate electrophiles for cysteine modification

Due to the relatively low natural abundance and the unique nucleophilic reactivity of its sulfhydryl group, protein conjugation via cysteine often constitutes a good compromise between highly site specific but cumbersome modification of unnatural residues and straightforward but rather unselective targeting of other proteinogenic amino acids. Despite recent developments of novel reagent classes for the selective modification of cysteine, remaining challenges include cross-reactivity

with other nucleophilic amino acids, integrity of the formed bond, especially in the presence of other thiol nucleophiles, and pretentious syntheses of the thiol reactive warhead (See chapter 4.4.2).

The aim of this research project was the development of a cysteine selective modification technique based on unsaturated vinyl- and ethynylphosphonamidate-electrophiles. Most importantly, it was envisioned that the Staudinger-phosphonite reaction can be employed to incorporate the desired phosphonamidates from vinyl- and ethynylphosphonites in a chemoselective manner into azide-containing molecules without elaborative protecting group manipulations. Since this process turns the electron-rich double or triple bond of the phosphonite into an electron-deficient unsaturated phosphonamidate, it was anticipated that the first Staudinger-phosphonite reaction induces reactivity for the subsequent thiol addition to cysteine. The overall goal was to evaluate the two synthetic steps in terms of feasibility, scope, functional group tolerance, modularity, reaction kinetics, selectivity, conjugate stability and finally applicability to protein modifications to establish a new, robust method for cysteine selective protein synthesis.

Project 2: Evaluation of phosphonamidates as part of linker systems for ADCs

Antibody-drug-conjugates combine the high efficiency of cytotoxic drugs with the tumor selectivity of monoclonal antibodies and represent therefore an emerging class of cancer therapeutics. In theory they are able to broaden the therapeutic window of commonly applied chemotherapy by specifically delivering toxins to the cancer site, while sparing healthy tissue. However, problems arise from unspecific uptake of the conjugates into healthy cells, pharmacokinetic issues caused by aggregation of the strongly hydrophobic drug molecules and insufficient linkage stability during blood circulation. The pharmacological consequences of the latter still needs to be investigated in detail, but a premature loss of drug from the antibody is assumed to diminish antitumor activity and cause severe side effects (see chapter 4.3).

Aim of this research project was the synthesis and pharmacological evaluation of phosphonamidate-linked ADCs, applying the methodology that has been developed in project 1 within this thesis. It was envisioned that native antibodies serve as a starting point to attach the cysteine reactive phosphonamidate drug molecules after reduction of the inter-chain disulfide bonds, as previously described for maleimide reagents, among others. After successful synthesis and characterization, it was aimed to evaluate the ADCs in terms of selective *in vitro* activity in cellular based assays, stability of the phosphonamidate linkage during blood circulation and finally *in vivo* antitumor efficacy in xenograft mouse models. The overall goal was to provide sufficient amounts of pharmacological data with direct comparisons to commonly applied linker technologies to overcome known limitations of current methods in ADC synthesis.

6. Results and Discussion

6.1. Chemoselectively installed ethynylphosphonamidates for modular, cysteine-selective modifications of proteins

Selective protein modification exploiting the exceptional nucleophilic properties of the sulfhydryl group of cysteine constitutes a highly attractive concept in protein synthesis. Requirements on new reagents that are developed for the purpose of cysteine modification are particularly high and include decent reactivity under aqueous conditions at close to neutral pH, fast reaction kinetics at ambient temperature and a good selectivity in the presence of all other proteinogenic amino acids. In addition to that, an excellent linkage stability and straightforward synthetic incorporation of the thiol reactive moiety into complex molecules is highly desirable. Even though a plethora of different cysteine modification techniques has been developed in recent years (chapter 4.4.2), there is no outstanding method that satisfies all criteria equally and surpasses all the others.

The good functional group tolerance of Staudinger-type transformations between P(III) reagents including phosphines, phosphites and phosphonites with azides already lead to the development of various chemoselective reactions (chapter 4.6). The aim of the work described in this chapter was to pursue with previous achievements on the SPhR and exploit this method for the chemoselective synthesis of phosphonamidate electrophiles for the modification of sulfhydryl groups. In particular, ethynylphosphonites were used for the synthesis of ethynylphosphonamidates and the potential of this compound-class to modify cysteine residues on proteins was evaluated with the following main goals:

a) Development of the SPhR with ethynylphosphonites and various azide-modified building blocks to synthesize ethynylphosphonamidates in the presence of different unprotected functional groups.
b) Evaluation of the potential of ethynylphosphonamidates to modify cysteine residues with a focus on selectivity, linkage stability, reaction kinetics and applicability to proteins in general and antibodies.
c) Exploration of the unique features of the phosphonamidate linker structure, which includes the incorporation of functional handles to the ethynylphosphonamidate ester residue and the potential to yield a single diastereoisomer after the conjugation to cysteine residues.

6.1.1. Chemoselective synthesis of *O*-ethyl-ethynylphosphonamidates and subsequent Cysteine-selective bioconjugation

This chapter was published in the following journal:

Marc-André Kasper, Maria Glanz, Andreas Stengl, Martin Penkert, Simon Klenk, Tom Sauer, Dominik Schumacher, Jonas Helma, Eberhard Krause, M. Cristina Cardoso, Heinrich Leonhardt and Christian P. R. Hackenberger*

"Cysteine-selective phosphonamidate electrophiles for modular protein bioconjugations"

Angew. Chem. Int. Ed. **2019**, *58* (34), 11625-11630.
Publication date (online): March 4th, 2019
The article is available online at:
https://onlinelibrary.wiley.com/doi/abs/10.1002/anie.201814715?af=R

*Corresponding author

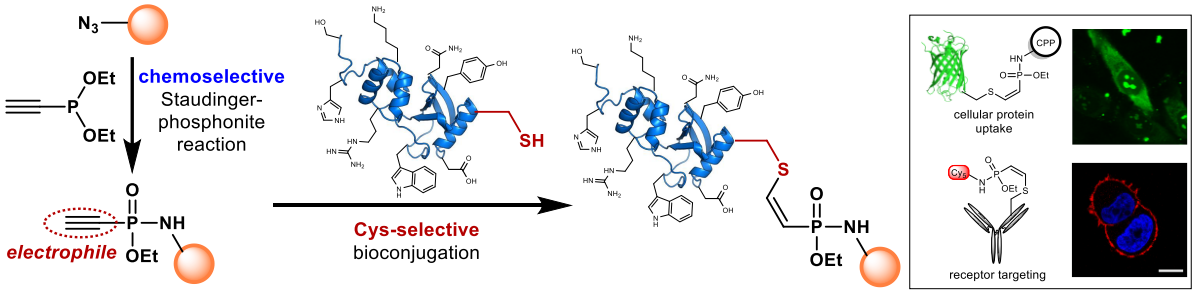

Figure 13: Principle of the SPhR with ethynylphosphonites to generate ethynylphosphonamidates and subsequent cysteine conjugation with proteins and its application to cellular protein uptake and receptor imaging.

Abstract

We describe a new technique in protein synthesis that extends the existing repertoire of methods for protein modification: A chemoselective reaction that induces reactivity for a subsequent bioconjugation. Hereby, an azide building block reacts first with an ethynylphosphonite via the Staudinger-phosphonite reaction (SPhR) to an ethynylphosphonamidate. The resulting electron-deficient triple bond subsequently undergoes a cysteine-selective reaction with proteins or antibodies. We demonstrate that ethynylphosphonamidates hold excellent cysteine-selective reactivity combined

with a superior stability of the thiol adducts. This turns our technique into a versatile and powerful tool for the facile construction of stable, functional protein conjugates.

Responsibility assignment

Christian P. R. Hackenberger designed and conceived the project. The author developed the SPhR with ethynylphosphonites and the subsequent cysteine modification, synthesized and characterized phosphonamidates and azide precursors, conceived and performed stability- and kinetic studies, developed the antibody modification with phosphonamidates and synthesized, purified and analyzed the antibody conjugates. Maria Glanz developed the SPhR with ethynylphosphonites on peptides, synthesized and characterized the cyclic peptides, performed stability studies, developed the phosphonamidate addition to proteins, expressed eGFP and performed the cellular imaging studies with eGFP. Andreas Stengl expressed and purified trastuzumab and performed cellular imaging with AFCs. Martin Penkert and Eberhard Krause conceived and performed two-dimensional MS experiments. Simon Klenk performed DFT calculations. Tom Sauer performed initial experiments on the SPhR and the subsequent thiol addition. Dominik Schumacher designed and cloned the eGFP mutant. Jonas Helma and Heinrich Leonhardt designed the cellular imaging experiments with AFCs. M. Cristina Cardoso contributed to the design of the cellular imaging studies with eGFP. The author wrote the manuscript and translated it into German supported by Christian P. R. Hackenberger.

Summary of content

A method for the chemoselective modification of cysteine residues in proteins and antibodies, making use of electrophilic ethynylphosphonamidates, is presented. Most importantly, the cysteine selective handle can be installed into azide-containing small molecule building blocks and unprotected peptides in a chemoselective manner with a high functional group tolerance, making use of the SPhR with electron-rich ethynylphosphonites. The electrophilic reactivity for cysteine is induced by this first step, forming the electron-deficient ethynylphosphonamidate. The investigations began with the development of a protocol to synthesize ethynylphosphonamidates from commercially available phosphorus precursors for the SPhR. A one-pot protocol, starting from diethyl chlorophosphite and ethynyl magnesiumchloride followed by azide addition and hydrolysis was developed that produces ethynylphosphonamidates in good isolated yields from 44% to 80% for phenyl azides. Functional groups such as carboxylic acids, amines and NHS esters were well tolerated and excellent isolated yields were reported for the reaction on unprotected peptides. Furthermore, it has been shown that amino- and NHS-containing ethynylphosphonamidates can be employed as modular building blocks to incorporate the thiol reactive moiety into other functional molecules such as fluorescent dyes in high yields avoiding the use of potentially unstable phosphorus (III) reagents that might be deterrent for

some laboratories. Next, cysteine addition studies to the ethynylphosphonamidates were performed with a glutathione model substrate, revealing decently fast reaction with a second order rate constant of 0.62 $M^{-1} \cdot s^{-1}$. An outstanding selectivity for the *Z*-addition product of more than 97% in aqueous solvent systems was supported by DFT calculations that unveiled a higher activation barrier for the *E*-product. To test the feasibility of cysteine modification on proteins, the interchain disulfide bonds of the monoclonal antibody trastuzumab were reduced, subsequently alkylated with a biotinyl ethynylphosphonamidate and successful conjugation was monitored by anti-biotin western blotting. Even though more equivalents had to be applied in comparison to other tested cysteine reactive reagents to achieve similar labelling degrees, a superior selectivity for cysteine over all other proteinogenic amino acids was solely observed for ethynylphosphonamidates. This was further confirmed by tandem-MS experiments after trypsin digestion of the antibodies. A good conjugate integrity under physiological conditions could be demonstrated in a FRET based stability study. The cysteine adducts proofed stable in PBS, human serum and freshly prepared cellular lysate over several days. Only very harsh conditions of pH 0 cleaved the *P*-*N*-bond over 24 hours. Since linkage-lability in the presence of external thiols is particularly problematic for pharmacological applications, stability studies in the presence of excess glutathione and serum proteins was tested and directly compared to state-of-the-art maleimide conjugation, revealing a superior integrity of the ethynylphosphonamidate-thiol adducts. Finally, the method was applied to the synthesis of a two functional conjugates, an antibody-fluorophore conjugate and a cyclic cell penetrating peptide eGFP conjugate. Both syntheses proceeded smoothly to yield the desired protein conjugates in two straightforward chemical steps and the conjugates proofed functional on a cellular level, exemplified by fluorescence microscopy.

Manuscript and supporting information

The manuscript and Supporting Information are printed from: Marc-André Kasper, Maria Glanz, Andreas Stengl, Martin Penkert, Simon Klenk, Tom Sauer, Dominik Schumacher, Jonas Helma, Eberhard Krause, M. Cristina Cardoso, Heinrich Leonhardt and Christian P. R. Hackenberger: Cysteine-selective phosphonamidate electrophiles for modular protein bioconjugations. Angewandte Chemie International Edition. 2019.

Protein Modification

International Edition: DOI: 10.1002/anie.201814715
German Edition: DOI: 10.1002/ange.201814715

Cysteine-Selective Phosphonamidate Electrophiles for Modular Protein Bioconjugations

*Marc-André Kasper, Maria Glanz, Andreas Stengl, Martin Penkert, Simon Klenk, Tom Sauer, Dominik Schumacher, Jonas Helma, Eberhard Krause, M. Cristina Cardoso, Heinrich Leonhardt, and Christian P. R. Hackenberger**

Dedicated to Professor Hans-Ulrich Reißig on the occasion of his 70th birthday

Abstract: *We describe a new technique in protein synthesis that extends the existing repertoire of methods for protein modification: A chemoselective reaction that induces reactivity for a subsequent bioconjugation. An azide-modified building block reacts first with an ethynylphosphonite through a Staudinger-phosphonite reaction (SPhR) to give an ethynylphosphonamidate. The resulting electron-deficient triple bond subsequently undergoes a cysteine-selective reaction with proteins or antibodies. We demonstrate that ethynylphosphonamidates display excellent cysteine-selective reactivity combined with superior stability of the thiol adducts, when compared to classical maleimide linkages. This turns our technique into a versatile and powerful tool for the facile construction of stable functional protein conjugates.*

Chemical attachment of synthetic molecules to a distinct site of a protein is essential for a plethora of applications in the life sciences, in particular for the investigation of biological processes and the development of targeted therapeutics.[1] Protein modification can in principle be achieved by one of two strategies: incorporation of unnatural amino acids or peptide sequences, which possess distinct reactivities to chemical or enzymatic reactions, or reactions that rely on specific chemical properties of the side chains of proteinogenic amino acids.[2] The former requires sometimes tedious biochemical manipulations such as amber suppression or additional enzymatic transformations, while the latter is only residue-specific and can produce protein mixtures with a different degree of modification and several regioisomers being formed.[3] Despite recent advancements in the engineering of new residue-specific reactions, including the modification of tyrosine,[4] tryptophan,[5] and methionine,[6] the targeting of cysteine (Cys) residues for chemical protein modification still offers many advantages. Cys residues have a low natural abundance in a reduced form on accessible protein surfaces and can be readily incorporated into a given protein or antibody through facile mutagenesis.[7] Moreover, the unique nucleophilic properties of its sulfhydryl group have been exploited in the development of several Cys-selective modification techniques,[7,8] including metal-catalyzed reactions[9] and radical transformations.[10] Several compound classes have been employed, including the prominent electrophilic maleimides[11] and α-halo acetamides,[8] as well as a recent report on perfluorophenyl reagents.[12]

Among other techniques, maleimides remain the most widely used method for chemical modification on Cys residues,[7] mostly due to their rapid kinetics in reactions with sulfhydryl groups.[13] However, one of the biggest drawbacks of maleimide conjugates is their instability caused by a retro-Michael addition in the presence of external thiols.[14] Recently developed alternatives include self-hydrolyzing maleimides,[15] structurally refined Michael-type acceptors such as carbonyl acrylic derivatives,[16] or exocyclic maleimides.[17] These Michael-type acceptors yield stable sulfhydryl adducts; however, challenges remain, since stereo- or regioisomers are formed[18] and their incorporation into functional molecules usually requires protecting-group manipulations.

Previous work from our laboratory has shown that phosphonamidates can be chemoselectively installed into a given azide-containing protein with high functional-group tolerance through a Staudinger-phosphonite reaction (SPhR).[19] By taking advantage of this, we have used borane-protected ethynylphosphonites for the sequential coupling of two azide-containing molecules, including probes, polymers, or proteins.[20] Based on these findings, we now report a method that enables the chemoselective installation of a highly Cys-selective handle into a given azide-containing molecule through SPhR with unprotected ethynylphosphonites. Most importantly, the chemoselective

[*] M.-A. Kasper, M. Glanz, M. Penkert, S. Klenk, T. Sauer, Dr. D. Schumacher, Dr. E. Krause, Prof. Dr. C. P. R. Hackenberger
Chemical Biology Department
Leibniz-Forschungsinstitut für Molekulare Pharmakologie (FMP)
Robert-Rössle-Strasse 10, 13125 Berlin (Germany)
E-mail: hackenbe@fmp-berlin.de

M.-A. Kasper, M. Glanz, M. Penkert, S. Klenk, Dr. D. Schumacher, Prof. Dr. C. P. R. Hackenberger
Department of Chemistry, Humboldt Universität zu Berlin
Brook-Taylor-Str. 2, 12489 Berlin (Germany)

A. Stengl, Dr. D. Schumacher, Dr. J. Helma, Prof. Dr. H. Leonhardt
Department of Biology II, and Center for Integrated Protein Science Munich, Ludwig-Maximilians-Universität München
Großhadenerstr. 2, 82152 Martinsried (Germany)

Prof. Dr. M. C. Cardoso
Department of Biology, Technische Universität Darmstadt
Schnittspahnstrasse 10, 64287 Darmstadt (Germany)

Supporting information and the ORCID identification number(s) for the author(s) of this article can be found under: https://doi.org/10.1002/anie.201814715.

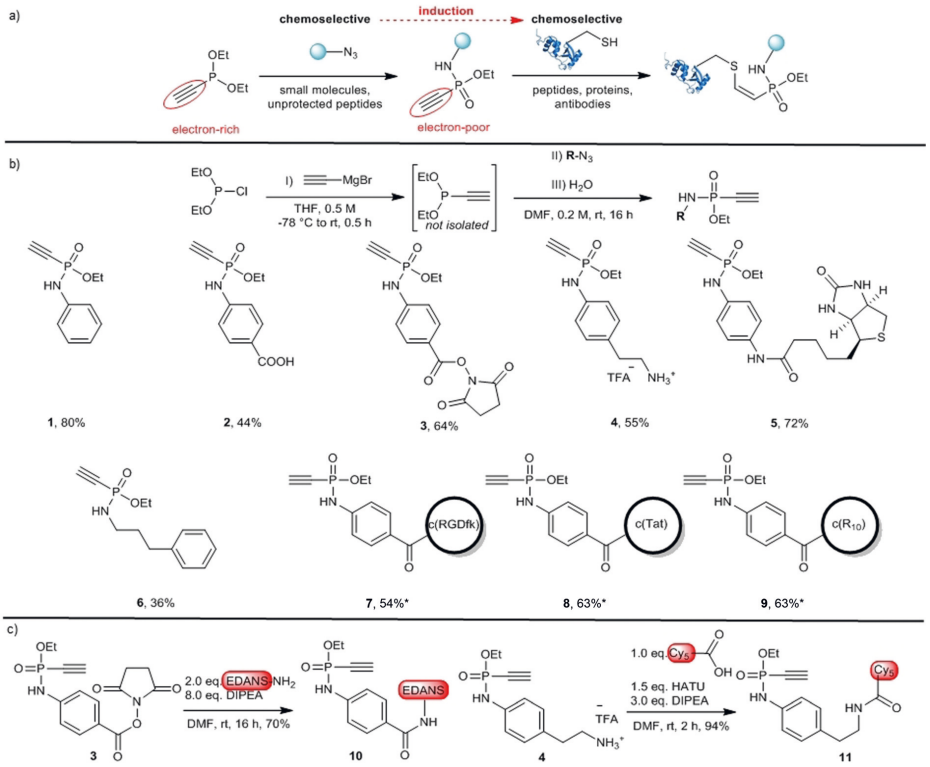

Figure 1. a) Principle of chemoselective reactivity induction for Cys. b) Yields of isolated product from one-pot SPhR with different unprotected azides. Unless stated otherwise 1.2 equiv of phosphonite were used with respect to the azide; reactions were carried out in THF at room temperature overnight. * 4 equiv phosphonite were used, reactions were carried out in DMSO. c) Modular building blocks (**3**, **4**) to attach ethynylphosphonamidates to other functional modules via amide bonds.

SPhR turns the electron-rich triple bond of an ethynylphosphonite into an electron-poor ethynylphosphonamidate and thereby induces reactivity for subsequent thiol addition (Figure 1 a). With this unique reaction sequence of two subsequent chemoselective transformations, we developed a modular method that simplifies the attachment of functional molecules to proteins and antibodies with superior stability.

At the outset of our studies, we validated our proposed concept by reacting readily available diethyl ethynylphosphonite with different azides containing various functional groups. In comparison to other P^{III} species such as phosphites, auto-oxidation of phosphonites is more rapid.[21] This issue was previously addressed by isolating air-stable borane protected phosphonites that had to be deprotected with strong bases prior SPhR.[19,20] Now, we developed a one-pot synthesis starting from commercially available diethyl chlorophosphite and ethynylmagnesium bromide followed by azide addition and hydrolysis without isolation of the phosphonite intermediate (Figure 1 b. We observed that polar aprotic solvents generally worked best for the SPhR as they gave the best yields and ensured solubility of all tested azides. The desired ethynylphosphonamidates **1**–**6** were isolated in good overall yields, with a better performance in the formation of N-phenylphosphonamidates compared to the alkyl derivative **6**. Nucleophilic functional groups such as amines, alcohols, carboxylic acids, and electrophilic NHS esters were well tolerated. Even unprotected azide-containing peptides, including cyclic RGD and cyclic cell-penetrating peptides (cCPPs) could be converted into the desired ethynylphosphonamidates **7**–**9** in very good yields of isolated product, with HPLC analysis verifying the formation of a single reaction product.

The purified ethynylphosphonamidates showed excellent stability in solution at neutral pH over several days (Figure S1 in the Supporting Information) and could be stored at 4 °C for several months without any observable decomposition. Furthermore, we were able to demonstrate that compounds **3** and **4** can be further used as modular building blocks to attach ethynylphosphonamidates to other functional modules in high yields, as exemplified by the synthesis of phosphonami-

date derivatives of the fluorescent dyes EDANS (**10**) and Cy5 (**11**) in 70% and 94% yield of isolated product, respectively (Figure 1c).

Previously, Gao et al. observed that vinylphosphonamidates do not undergo thiol addition under their tested conditions.[22] Since we envisioned ethynylphosphonamidates to be more reactive, we carried out model reactions with the *N*-phenyl derivative **1** and glutathione under varying pH conditions and monitored the progress by UPLC-UV. It was observed that the conversion rate increases from pH 7.4 to 9.0 with only a slight increase from pH 8.5 to 9.0 (Figure S2 in the Supporting Information). Considering decreased protein stability at higher pH, we decided to continue our studies at pH 8.5. Full conversion to the desired thiol adduct was observed at pH 8.5 after 30 minutes at a concentration of 10 mM *N*-phenyl derivative **1** (Figure 2a and Figure S2 in the Supporting Information). The second-order rate constant for the thiol addition reaction was determined by fluorescence HPLC with the *N*-phenyl-EDANS-phosphonamidate derivative **10** at a concentration of 0.1 mM to $0.62 \pm 0.01\,M^{-1}s^{-1}$ (Figure S3 in the Supporting Information). It should be noted that the thiol adduct is formed with a high *Z* selectivity (>97%) in aqueous systems, as studied for the addition of ethanethiol to **1** (Figure S4 in the Supporting Information). Similar observations for the formation of the *Z* isomer have been made for other electron-deficient alkynes earlier.[23] DFT calculations revealed a higher activation barrier for the *E* product and can therefore explain the high *Z* selectivity (Figure S5 in the Supporting Information).

To test the applicability of our reaction to the construction of protein conjugates, we proceeded in a proof-of-principle study with the Her2-addressing IgG monoclonal antibody trastuzumab. For antibody modification, we applied a previously described protocol, which reduces and alkylates interchain disulfide bonds of IgG antibodies.[24] In our studies, we probed the modification of trastuzumab with different electrophilic biotin derivatives, including a maleimide, an iodoacetamide, and the ethynylphopshonamidate **5**. All antibody modifications were carried out at concentrations between 3 and 6 μM. Anti-biotin western-blot analysis revealed labeling of the light and heavy chains with DTT-reduced trastuzumab for all of the tested biotin derivatives when using the reported conditions of 1.1 equiv. of labeling reagent per free Cys.[24] Probably due to slower reaction kinetics ($0.62\,M^{-1}s^{-1}$ for phosphonamidates vs. $734\,M^{-1}s^{-1}$ for maleimides),[25] decreased labelling efficiency was observed for **5** compared to the maleimide derivative (Figure S6 in the Supporting Information). Therefore, we screened various phosphonamidate equivalents and monitored the degree of modification by intact protein MS. Optimal conditions for the phosphonamidate labelling were identified with 10 equiv of phosphonamidate per free Cys, which corresponds to 80 equiv with respect to the antibody (Figure S7 in the Supporting Information). Side reactions of other nucleophilic amino acid residues with common Cys-labeling techniques have been reported earlier[26] and have been shown to be very problematic in certain applications.[27,26b] To confirm the chemoselectivity of the phosphonamidate labeling technique, reactions were carried out without prior reduction of the antibody disulfide bonds. Compared to other Cys-conjugation techniques at neutral pH, outstanding selectivity for Cys residues was observed for the labeling reaction with 1.1 equiv ethynylphosphonamidate per free cysteine residue at pH 8.5 when carried out without prior reduction of the antibody disulfide bonds (Figure S6 in the Supporting Information). In contrast to a maleimide reagent, even a larger excess of 10 equiv ethynylphosphonamidate per free cysteine did not lead to any unspecific labeling (Figure 2b). The selectivity was further confirmed by mass spectrometry (LC-MS/MS) after trypsin digestion of the modified antibody. Only interchain-disulfide-forming cysteines were modified after reduction and alkylation with an excess of **1**, and no modification on any amino acid was found without prior reduction (Figure S8 in the Supporting Information). Taken together, the intrinsic Cys selectivity of this reaction allows ethynylphosphonamidates to be employed in bioconjugation reactions even in larger

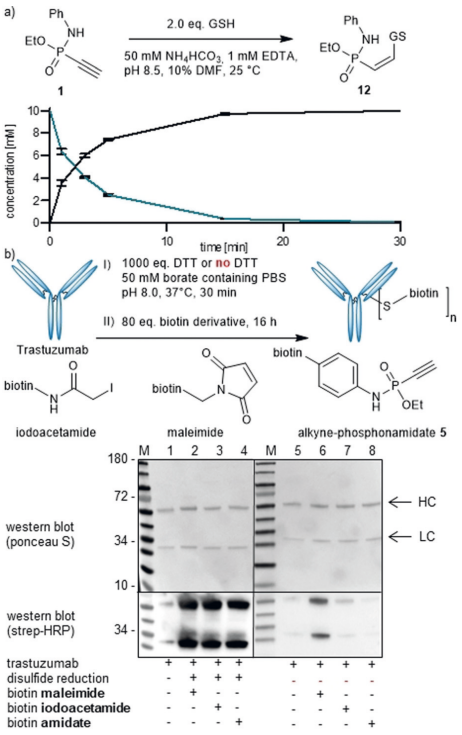

Figure 2. a) Reaction of glutathione (GSH) with phosphonamidate **1**. 10 mM phosphonamidate were reacted with 20 mM GSH at pH 8.5 (NH_4HCO_3-buffer). Concentrations of the starting material **1** (cyan) and product **12** (black) over time are sown as a mean and error from three independent measurements, as monitored by UPLC-UV. b) Trastuzumab modification with three different Cys-reactive biotin derivatives. Reactions were carried out with 80 equiv biotin derivative. Western-blot analysis: Lanes 1 and 5: untreated antibody. Lanes 2–4: prior DTT treatment. Lanes 6–8: Control reactions without prior DTT treatment. HC = Antibody heavy chain, LC = light chain.

excess without running into the risk of unselective labeling, which is advantageous when the exact concentration of the protein or antibody probe is difficult to determine.

The linkage stability of the Cys conjugates is crucial for many applications and in particular for drug delivery applications to prevent hazardous off-target effects, especially during circulation in the blood stream.[7] To test the stability of our phosphonamidate–thiol adducts a fluorescence-quenching assay was carried out in which a fluorescent signal was generated upon cleavage of the conjugates (Figure 3a). Quenched probes were synthesized through the addition of a DABCYL-modified peptide to the fluorescent phosphonamidate **10**. The phosphonamidate adducts show a high stability in PBS buffer, HEK cell lysate, and human serum over several days. Since P–N bonds are generally susceptible to hydrolysis under acidic conditions,[28] very harsh conditions of pH 0 were applied, which led to to cleave the phosphonamidate adduct within 24 h (Figure 3b). Previously, thiol adducts of electron-deficient alkynes such as propynamides were described as susceptible to exchange with other thiols.[23] However, with the ethynylphosphonamidates, high stability upon exposure to excess thiols was observed, with a superior performance in a direct comparison to a maleimide conjugate (Figure S9 in the Supporting Information). Next, we probed the stability of phosphonamidite- versus maleimide-labelled antibodies under physiologically relevant concentrations of serum proteins. This is of particular importance, since the transfer of maleimide-modified drugs to serum albumin has been described before and poses a serious risk for off-target toxicity when applied to drug delivery.[14,29] Biotin-modified antibodies were exposed to bovine serum albumin (BSA) at 37 °C under physiological conditions and the potential transfer to BSA was monitored by western blotting (Figure 3c and Figure S10 in the Supporting Information). After several days of incubation, a significant transfer of the biotin to BSA was observed for the maleimide linkage whereas the phosphonamidate linkage was stable under the tested conditions. Taken together with the previously described stability experiments with quenched fluorescent probes, these results clearly point to excellent stability of the phosphonamidate conjugates, especially when compared to conventional maleimide-linked conjugates.

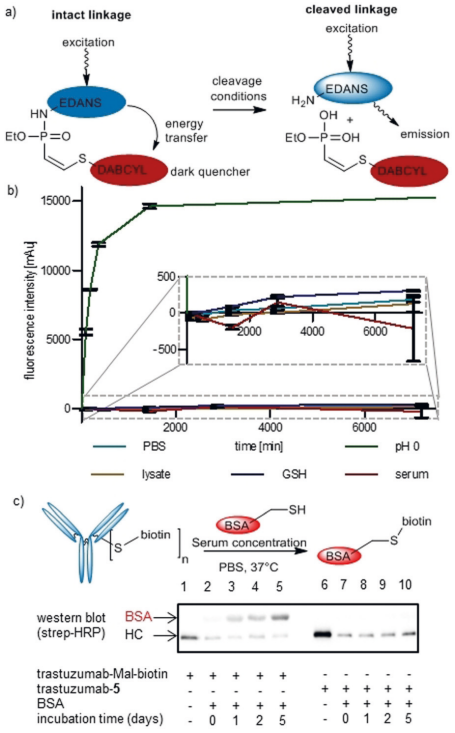

Figure 3. a) Set-up of the fluorescence-quenching assay for stability measurements of the thiol adducts. b) Fluorescence increase was monitored over time. Measurements were performed at least in triplicate. Cyan: PBS, green: pH 0 (1 N HCl), brown: cell-lysate, blue: GSH (1000 equiv of glutathione in PBS), red: human serum. c) Transfer of the antibody modification to serum proteins. Trastuzumab–biotin conjugates were incubated at a concentration of 3 μM with 500 μM BSA in PBS at 37 °C. Lane 1: Untreated maleimide conjugate. Lanes 2–5: BSA-exposed maleimide adduct after 0, 1, 2 and 5 days. Lane 6: Untreated phosphonamidate conjugate. Lanes 7–10: BSA-exposed phosphonamidate adduct after 0, 1, 2 and 5 days.

Encouraged by the outstanding thiol selectivity and the high stability of the Cys–phosphonamidate adducts, we proceeded with the functional evaluation of phosphonamidite-based antibody conjugates. We modified trastuzumab, an anti-Her2 antibody, with the fluorescent Cy5 phosphonamidate **11** to generate an antibody–fluorophore conjugate (AFC). Trastuzumab modification was carried out by using the above-mentioned reduction and alkylation of the interchain disulfide bonds (Figure 4a). Successful modification was confirmed by in-gel fluorescence measurements of the antibody heavy and light chains (Figure S11 in the Supporting Information). Immunostaining experiments with the AFC constructs show excellent target selectivity for the Her2-receptor on the outer cell membrane (Figure 4b). This experiment clearly shows that our modification strategy does not affect the antibody's performance and provides a simple conjugation approach for diagnostic reagents.

Finally, we applied our strategy to the attachment of cCPPs to eGFP for functional protein delivery into living cells, in a manner similar to that previously described.[30] An eGFP mutant with a single addressable cysteine was obtained by consecutive point mutation of Cys 70 to Met and Ser 147 to Cys, and the mutant protein was almost quantitatively modified with 20 equiv of the phosphonamidate cTAT or cR_{10} peptides **8** and **9** after reaction for three hours at 37 °C in PBS at a protein concentration of 100 μM (Figure 4c,d). With the eGFP–cCPP conjugates in hand, we performed cellular uptake studies monitored by live-cell microscopy in HeLa cells. Unconjugated eGFP was not taken up, whereas a green fluorescence signal was detected in the cytosol and the nucleoli for both eGFP–cCPP conjugates following incubation with 50 μM of the constructs, which is in accordance with previous observations using CuAAC conjugation for the

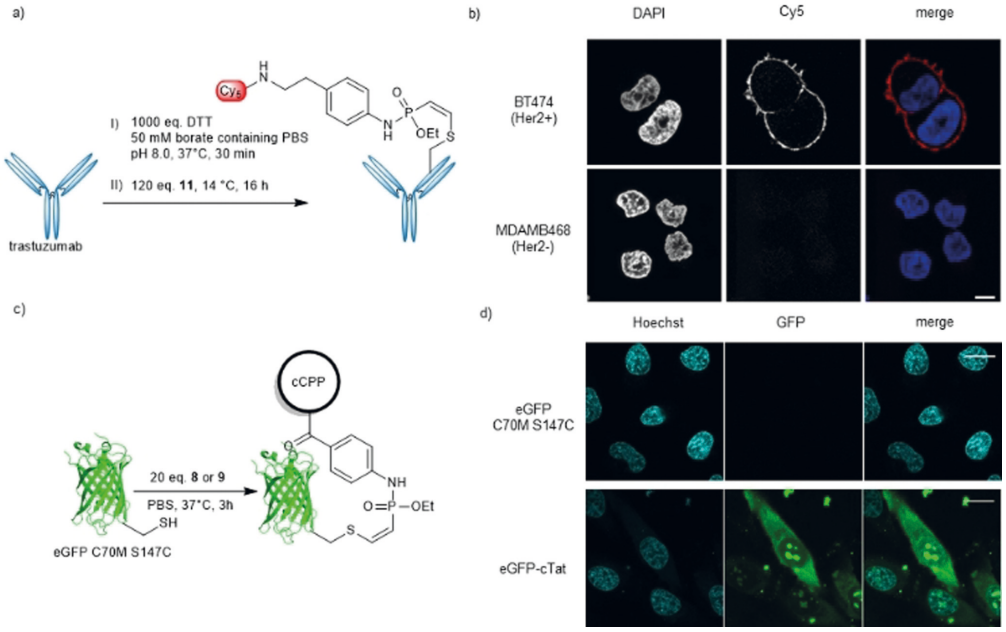

Figure 4. a) Synthetic scheme for phosphonamidate attachment of the Cy5 fluorophore to trastuzumab (anti-Her2 antibody) to generate an AFC. b) Immunostaining of fixed cells either over-expressing the cell-surface receptor Her2 (BT474) or exhibiting low Her2 expression levels (MDAMB468). The merged images show the signal from the DNA stain DAPI in blue and the Cy5 signal in red. Scale bar: 10 μm. c) Synthetic scheme for the attachment of phosphonamidite-modified cCPPs **8** and **9** to a eGFP mutant with a single addressable cysteine. d) Fluorescence imaging of HeLa cells after incubation with eGFP alone and eGFP–cTat at 50 μM. Images show the GFP channel in green and the Hoechst 33342 nuclear stain in blue. Scale bar: 20 μm. For further information see the Supporting Information.

attachment of cTAT (Figure 4e).[30a] With these results, we demonstrated that our method enables the straightforward synthesis of functional protein–cCPP conjugates for intracellular protein delivery.

In summary, we present a unique reaction sequence that first incorporates a thiol-reactive ethynylphosphonamidate into a given molecule through an initial chemoselective SPhR and subsequently modifies Cys residues smoothly in aqueous systems with outstanding selectivity towards sulfhydryl groups. This approach enables the facile conjugation of complex molecules to proteins, as exemplified by the conjugation of biotin, fluorophores, and peptides to antibodies and proteins. In contrast to the widespread maleimide labeling, our thiol adducts showed excellent stability to thiol exchange with GSH and albumin in the presence of human serum and cell lysate. The applicability of our method was demonstrated by the synthesis of a functional AFC for selective staining of antigen-presenting cells and eGFP–CPP conjugates for efficient protein delivery into cells. This method combines facile synthetic access with high flexibility, chemoselectivity, and superior linkage stability and is therefore a powerful and versatile tool for selective protein conjugation.

Acknowledgements

We thank K. K. Hassanin for excellent technical assistance, B. Keller for discussion on the computational modelling and P. Schmieder for helpful discussions on NMR-spectra. This work was supported by grants from the Deutsche Forschungsgemeinschaft (SPP1623) to C.P.R.H. (HA 4468/9-1) and H.L. (LE 721/13-2), (RTG1721) to H.L., the Einstein Foundation Berlin (Leibniz-Humboldt Professorship), the Boehringer-Ingelheim Foundation (Plus 3 award) and the Fonds der Chemischen Industrie to C.P.R.H. A.S. was trained and supported by the graduate school GRK1721 of the Deutsche Forschungsgemeinschaft (DFG).

Conflict of interest

The technology described in the manuscript is part of a pending patent application by M.-A.K., M.G., T.S., D.S., J.H., A.S, H.L and C.P.R.H.

Keywords: bioconjugation · bioorganic chemistry · bioorthogonal chemistry · cysteine-selective modification · protein modification

How to cite: *Angew. Chem. Int. Ed.* **2019**, *58*, 11625 – 11630
Angew. Chem. **2019**, *131*, 11751 – 11756

[1] a) R. D. Row, J. A. Prescher, *Acc. Chem. Res.* **2018**, *51*, 1073 – 1081; b) N. Krall, F. P. da Cruz, O. Boutureira, G. J. L. Bernardes, *Nat. Chem.* **2016**, *8*, 103; c) E. M. Sletten, C. R. Bertozzi, *Angew. Chem. Int. Ed.* **2009**, *48*, 6974 – 6998; *Angew. Chem.* **2009**, *121*, 7108 – 7133.
[2] C. D. Spicer, B. G. Davis, *Nat. Commun.* **2014**, *5*, 4740.
[3] a) K. Lang, J. W. Chin, *Chem. Rev.* **2014**, *114*, 4764 – 4806; b) E. Baslé, N. Joubert, M. Pucheault, *Chem. Biol.* **2010**, *17*, 213 – 227.
[4] H. Ban, J. Gavrilyuk, C. F. Barbas, *J. Am. Chem. Soc.* **2010**, *132*, 1523 – 1525.
[5] J. M. Antos, M. B. Francis, *J. Am. Chem. Soc.* **2004**, *126*, 10256 – 10257.
[6] S. Lin, X. Yang, S. Jia, A. M. Weeks, M. Hornsby, P. S. Lee, R. V. Nichiporuk, A. T. Iavarone, J. A. Wells, F. D. Toste, C. J. Chang, *Science* **2017**, *355*, 597 – 602.
[7] S. B. Gunnoo, A. Madder, *ChemBioChem* **2016**, *17*, 529 – 553.
[8] J. M. Chalker, G. J. L. Bernardes, Y. A. Lin, B. G. Davis, *Chem. Asian J.* **2009**, *4*, 630 – 640.
[9] E. V. Vinogradova, C. Zhang, A. M. Spokoyny, B. L. Pentelute, S. L. Buchwald, *Nature* **2015**, *526*, 687.
[10] C. E. Hoyle, C. N. Bowman, *Angew. Chem. Int. Ed.* **2010**, *49*, 1540 – 1573; *Angew. Chem.* **2010**, *122*, 1584 – 1617.
[11] J. E. Moore, W. H. Ward, *J. Am. Chem. Soc.* **1956**, *78*, 2414 – 2418.
[12] C. Zhang, M. Welborn, T. Zhu, N. J. Yang, M. S. Santos, T. Van Voorhis, B. L. Pentelute, *Nat. Chem.* **2016**, *8*, 120.
[13] L.-T. T. Nguyen, M. T. Gokmen, F. E. Du Prez, *Polym. Chem.* **2013**, *4*, 5527 – 5536.
[14] B.-Q. Shen, K. Xu, L. Liu, H. Raab, S. Bhakta, M. Kenrick, K. L. Parsons-Reponte, J. Tien, S.-F. Yu, E. Mai, D. Li, J. Tibbitts, J. Baudys, O. M. Saad, S. J. Scales, P. J. McDonald, P. E. Hass, C. Eigenbrot, T. Nguyen, W. A. Solis, R. N. Fuji, K. M. Flagella, D. Patel, S. D. Spencer, L. A. Khawli, A. Ebens, W. L. Wong, R. Vandlen, S. Kaur, M. X. Sliwkowski, R. H. Scheller, P. Polakis, J. R. Junutula, *Nat. Biotechnol.* **2012**, *30*, 184 – 189.
[15] P. A. Szijj, C. Bahou, V. Chudasama, *Drug Discovery Today* **2018**, *30*, 27 – 34.
[16] B. Bernardim, P. M. S. D. Cal, M. J. Matos, B. L. Oliveira, N. Martínez-Sáez, I. S. Albuquerque, E. Perkins, F. Corzana, A. C. B. Burtoloso, G. Jiménez-Osés, G. J. L. Bernardes, *Nat. Commun.* **2016**, *7*, 13128.
[17] D. Kalia, P. V. Malekar, M. Parthasarathy, *Angew. Chem. Int. Ed.* **2016**, *55*, 1432 – 1435; *Angew. Chem.* **2016**, *128*, 1454 – 1457.
[18] O. Koniev, A. Wagner, *Chem. Soc. Rev.* **2015**, *44*, 5495 – 5551.
[19] M. R. J. Vallée, P. Majkut, I. Wilkening, C. Weise, G. Müller, C. P. R. Hackenberger, *Org. Lett.* **2011**, *13*, 5440 – 5443.
[20] a) M. R. J. Vallée, L. M. Artner, J. Dernedde, C. P. R. Hackenberger, *Angew. Chem. Int. Ed.* **2013**, *52*, 9504 – 9508; *Angew. Chem.* **2013**, *125*, 9682 – 9686; b) M. R. J. Vallée, P. Majkut, D. Krause, M. Gerrits, C. P. R. Hackenberger, *Chem. Eur. J.* **2015**, *21*, 970 – 974.
[21] W.-S. Hwang, J. T. Yoke, *J. Org. Chem.* **1980**, *45*, 2088 – 2091.
[22] F. Gao, X. Yan, K. Auclair, *Chem. Eur. J.* **2009**, *15*, 2064 – 2070.
[23] H.-Y. Shiu, T.-C. Chan, C.-M. Ho, Y. Liu, M.-K. Wong, C.-M. Che, *Chem. Eur. J.* **2009**, *15*, 3839 – 3850.
[24] S. O. Doronina, B. E. Toki, M. Y. Torgov, B. A. Mendelsohn, C. G. Cerveny, D. F. Chace, R. L. DeBlanc, R. P. Gearing, T. D. Bovee, C. B. Siegall, J. A. Francisco, A. F. Wahl, D. L. Meyer, P. D. Senter, *Nat. Biotechnol.* **2003**, *21*, 778 – 784.
[25] F. Saito, H. Noda, J. W. Bode, *ACS Chem. Biol.* **2015**, *10*, 1026 – 1033.
[26] a) C. F. Brewer, J. P. Riehm, *Anal. Biochem.* **1967**, *18*, 248 – 255; b) M. L. Nielsen, M. Vermeulen, T. Bonaldi, J. Cox, L. Moroder, M. Mann, *Nat. Methods* **2008**, *5*, 459 – 460.
[27] J. Václavík, R. Zschoche, I. Klimánková, V. Matoušek, P. Beier, D. Hilvert, A. Togni, *Chem. Eur. J.* **2017**, *23*, 6490 – 6494.
[28] J. Bertran-Vicente, R. A. Serwa, M. Schümann, P. Schmieder, E. Krause, C. P. R. Hackenberger, *J. Am. Chem. Soc.* **2014**, *136*, 13622 – 13628.
[29] J. F. Ponte, X. Sun, N. C. Yoder, N. Fishkin, R. Laleau, J. Coccia, L. Lanieri, M. Bogalhas, L. Wang, S. Wilhelm, W. Widdison, J. Pinkas, T. A. Keating, R. Chari, H. K. Erickson, J. M. Lambert, *Bioconjugate Chem.* **2016**, *27*, 1588 – 1598.
[30] a) N. Nischan, H. D. Herce, F. Natale, N. Bohlke, N. Budisa, M. C. Cardoso, C. P. R. Hackenberger, *Angew. Chem. Int. Ed.* **2015**, *54*, 1950 – 1953; *Angew. Chem.* **2015**, *127*, 1972 – 1976; b) H. D. Herce, D. Schumacher, A. F. L. Schneider, A. K. Ludwig, F. A. Mann, M. Fillies, M.-A. Kasper, S. Reinke, E. Krause, H. Leonhardt, M. C. Cardoso, C. P. R. Hackenberger, *Nat. Chem.* **2017**, *9*, 762 – 771.

Manuscript received: December 29, 2018
Accepted manuscript online: March 4, 2019
Version of record online: April 29, 2019

Angewandte Chemie
Eine Zeitschrift der Gesellschaft Deutscher Chemiker

Supporting Information

Cysteine-Selective Phosphonamidate Electrophiles for Modular Protein Bioconjugations

*Marc-André Kasper, Maria Glanz, Andreas Stengl, Martin Penkert, Simon Klenk, Tom Sauer, Dominik Schumacher, Jonas Helma, Eberhard Krause, M. Cristina Cardoso, Heinrich Leonhardt, and Christian P. R. Hackenberger**

anie_201814715_sm_miscellaneous_information.pdf

Table of contents

1. Supplementary Figures

1.1. Figure S1

pH-dependent stability of ethynylphosphonamidate **8** (0.3 mM). Stability was monitored by UPLC-UV by integration of the UV peaks in relation to an internal standard (tryptophan, 0.15 mM) over several days. Shown are mean and error of three independent measurements (n=3). Conditions: pH 1.0: 0.1 M HCl; pH 2.0: TFA in H_2O; pH 7.4: PBS; pH 9.0: 100 mM NH_4HCO_3, pH 12: 0.01 M NaOH.

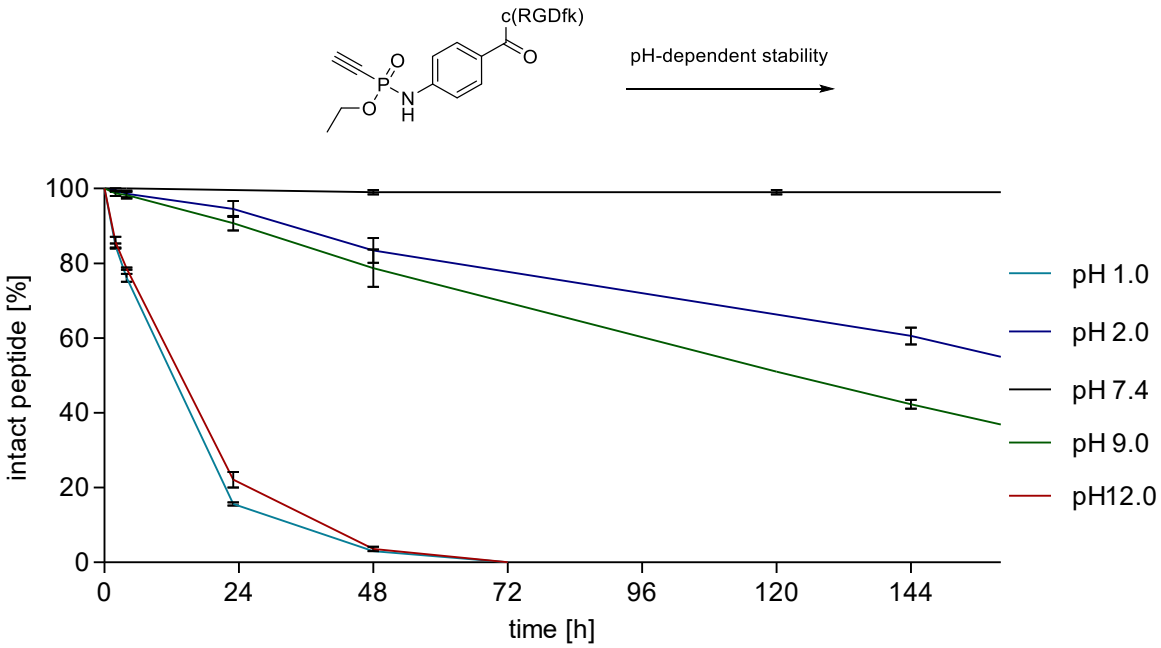

1.2. Figure S2

Glutathione addition to phosphonamidates. A) Concentration of starting material Ethyl-*N*-phenyl-*P*-ethynylphosphonamidate (**1**) under varying pH conditions over time monitored by UPLC/MS (pH 8.0, 8.5 and 9.0: 50mM NH_4HCO_3, 1mM EDTA; pH 7.4: Dulbecco's PBS, 1mM EDTA). Values were calculated by integration of the peaks in relation to an internal standard (inosin). Sample were drawn from the reaction mixture and immediately diluted into 50 mM NaOAc buffer at pH 3.5 to stop the reaction and subjected to UPLC analysis. Peaks were assigned by MS. Shown are mean and error of three independent measurements (n=3). B) Exemplaric UPLC/UV trace (254 nm) of the addition reaction at pH 8.5 after 0, 1, 5 and 30 min. Extinction of the starting material is lower than extinction of the glutathione adduct at 254 nm. C) Concentration of starting material **1** (black) and glutathione adduct (red) over time. Reaction performed at pH 8.5. Shown are mean and error of three independent measurements (n=3).

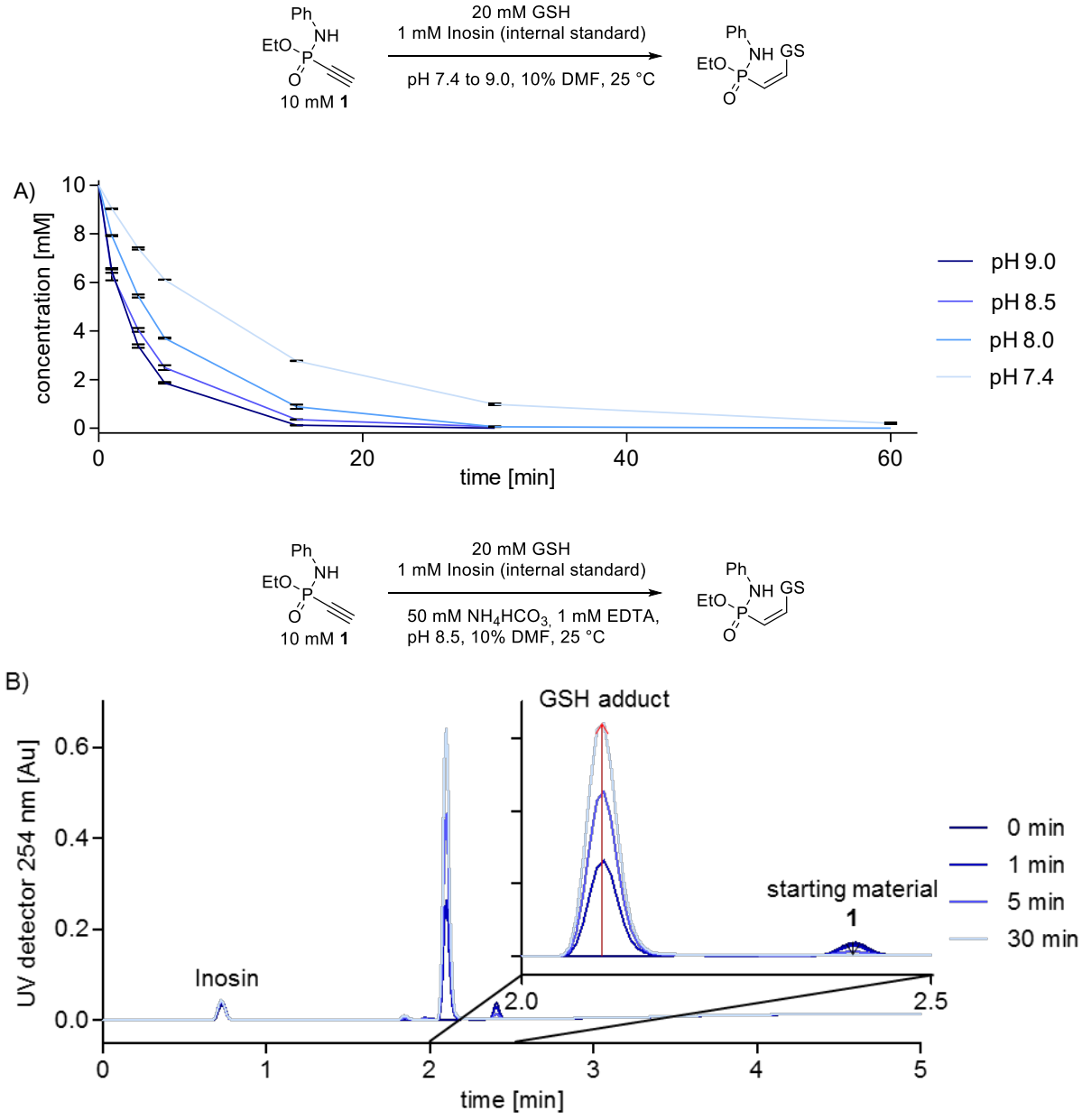

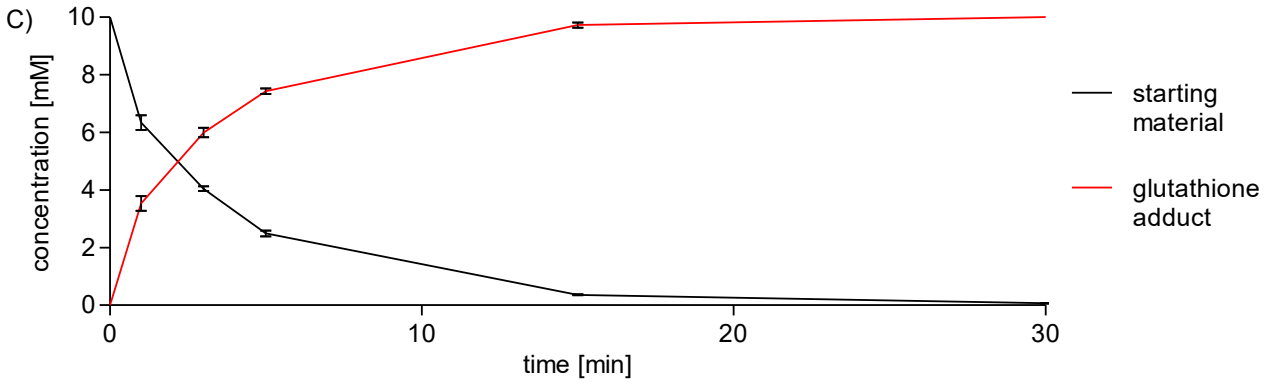

1.3. Figure S3

Determination of the second-order rate constant of the reaction between glutathione and EDANS phosphonamidate **11**. A) Reaction conditions. Reactions were performed in a volume of 0.5 ml. The first sample (t=0) was drawn before the addition of glutathione. Samples were taken after 15, 30, 60, 120, 240 and 480 min. Samples were drawn in a volume of 20 µl and immediately diluted into 80 µl of 50 mM NaOAc buffer at pH 3.5 to stop the reaction. Those samples were subjected to fluorescent HPLC analyses, injecting 20 µl each. B) Mathematic consideration for the determination of a second order rate constant with equal concentrations of the two reactants. C) Concentration of starting material over time. Calculated by integration of the peaks in relation to the internal standard (EDANS). Shown are mean and error of three independent measurements. (n=3) D) Graph: 1/c over time and

linear plot. Slope is the second order rate constant. Shown are mean and error of three independent measurements.

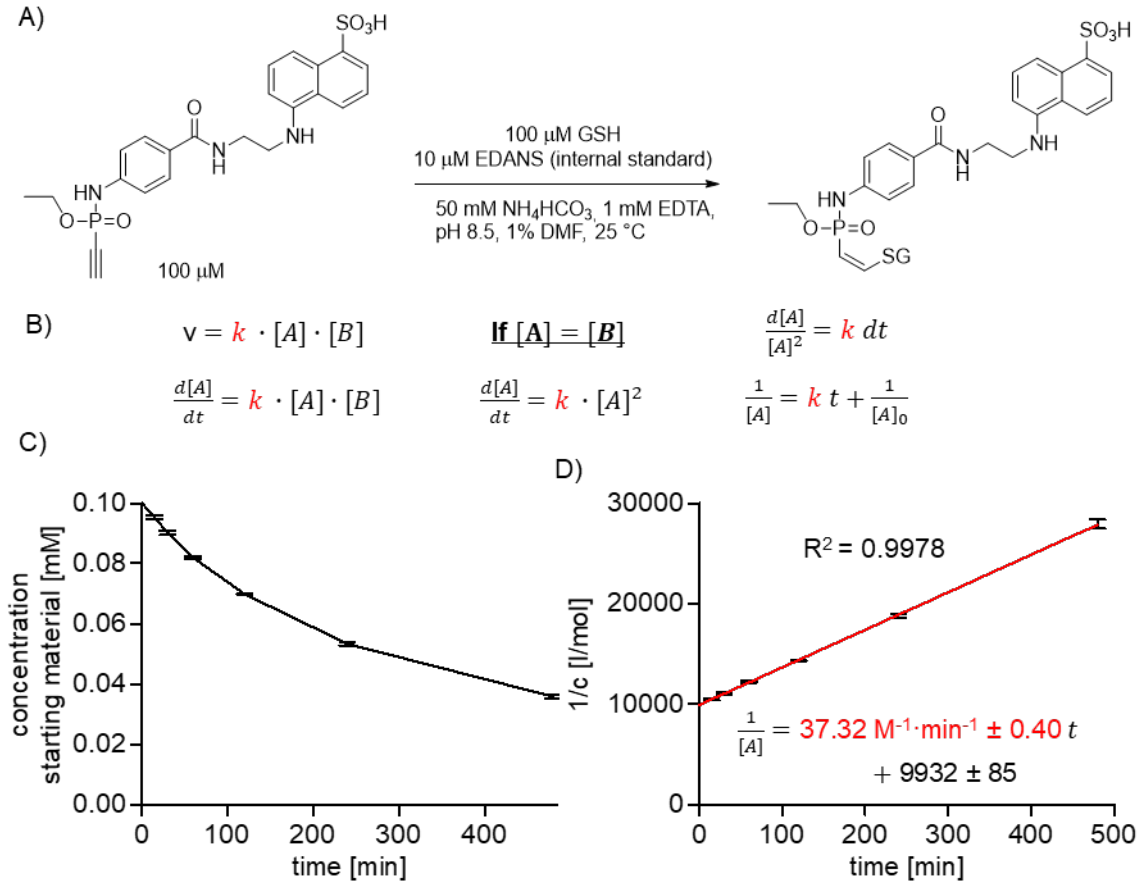

1.4. Figure S4

E/*Z*-selectivity of the thiol addition in dependence of the solvent system and different bases. a) Values measured by ^{31}P-NMR-signal integration of the crude reaction mixtures. b) ^{31}P peaks were assigned by comparison to spectra of isolated *E*- and *Z*-products (See chapter 4.18, 4.19 and 5 for synthesis details and NMR-spectra). The *E*-Product was synthesized via radical mediated thiol addition. Here, we measured almost identical *H-H* and *H-P*-coupling constants in comparison to a previously described *E*-thiol adduct of a phosphonate.[1] For the *Z*-product that was synthesized via base mediated thiol addition on the other hand, a lower $^{3}J_{HH}$ and a much higher $^{3}J_{PH}$ coupling constant was measured.

a)

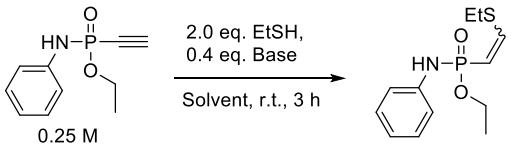

Entry	Base	DMSO E/Z	DMF/H_2O (1:1) E/Z
1	$MeNH_2$	5:95	3:97
2	Li_2CO_3	3:97	2:98
3	Na_2CO_3	6:94	1:99
4	K_2CO_3	12:88	2:98
5	Cs_2CO_3	17:83	2:98

b)

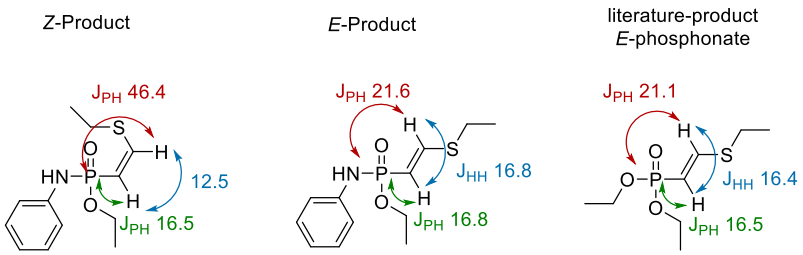

1.5. Figure S5

Computed *E* (red) and *Z* (blue) reaction paths for the addition of sodium methylthiolate to methylphosphonamidate. Calculations were performed with *O*-methyl substituted phosphonamidates and methyl thiol to simplify the calculations. The *E* addition pathway exhibits a 6.9 kcal/mol higher activation barrier than the *Z* pathway. (See chapter 6 for details)

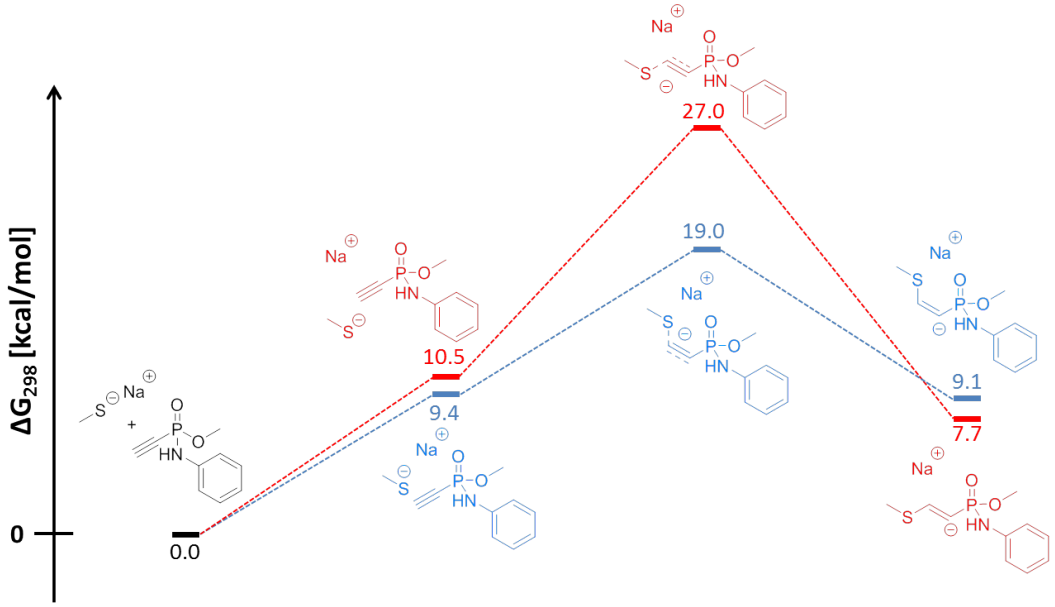

1.6. Figure S6

Trastuzumab modification with three different Cys-reactive biotin derivatives, applying the general procedure described in 3.2. Disulfide reduction was carried out with 1000 eq. DTT in 50 mM borate containing PBS for 30 min at 37°C. Excess DTT was removed with Zeba™ Spin Desalting Columns. Labelling was conducted with 8.8 eq. biotin derivative with a final DMSO content of 1% in a Buffer containing 50 mM NH_4HCO_3 and 1mM EDTA, pH 8.5 at 14°C for the phosphonamidate and PBS containing 1mM EDTA, pH 7.4 at 4°C for the maleimide and iodoacetamide labelling. Western blot analysis: Lane 1: untreated antibody. Lane 2-4: prior DTT treatment. Lane 5-7: Control reactions without prior DTT treatment. See chapter 3.1 for trastuzumab expression details)

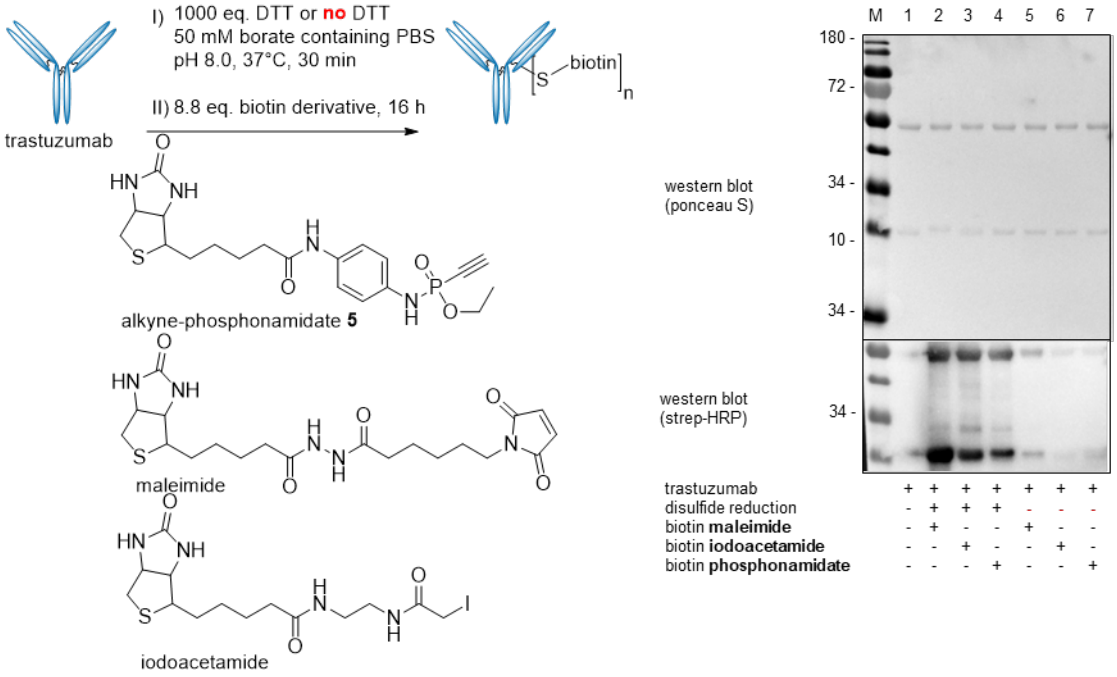

1.7. Figure S7

Influence of the phosphonamidate equivalents on the degree of antibody modification. Reactions were carried out, applying the general procedure described in 3.2 with varying equivalents of **5**. The degree of modification was calculated with the MS intensities with intact protein MS (See chapter 2.11) after deglycosylation and reduction (See chapter 3.3). An exemplary spectrum of the reaction with 80 eq. **5** is shown below (left: raw spectrum, right: deconvoluted). It should be noted that the degree of modification does not exceed 1 for the LC and 3 for the HC, clearly underlining the selectivity for inter-chain forming Cys-residues LC: Light Chain; HC: Heavy Chain, mod: modification with **5** (See chapter 3.1 for trastuzumab expression details).

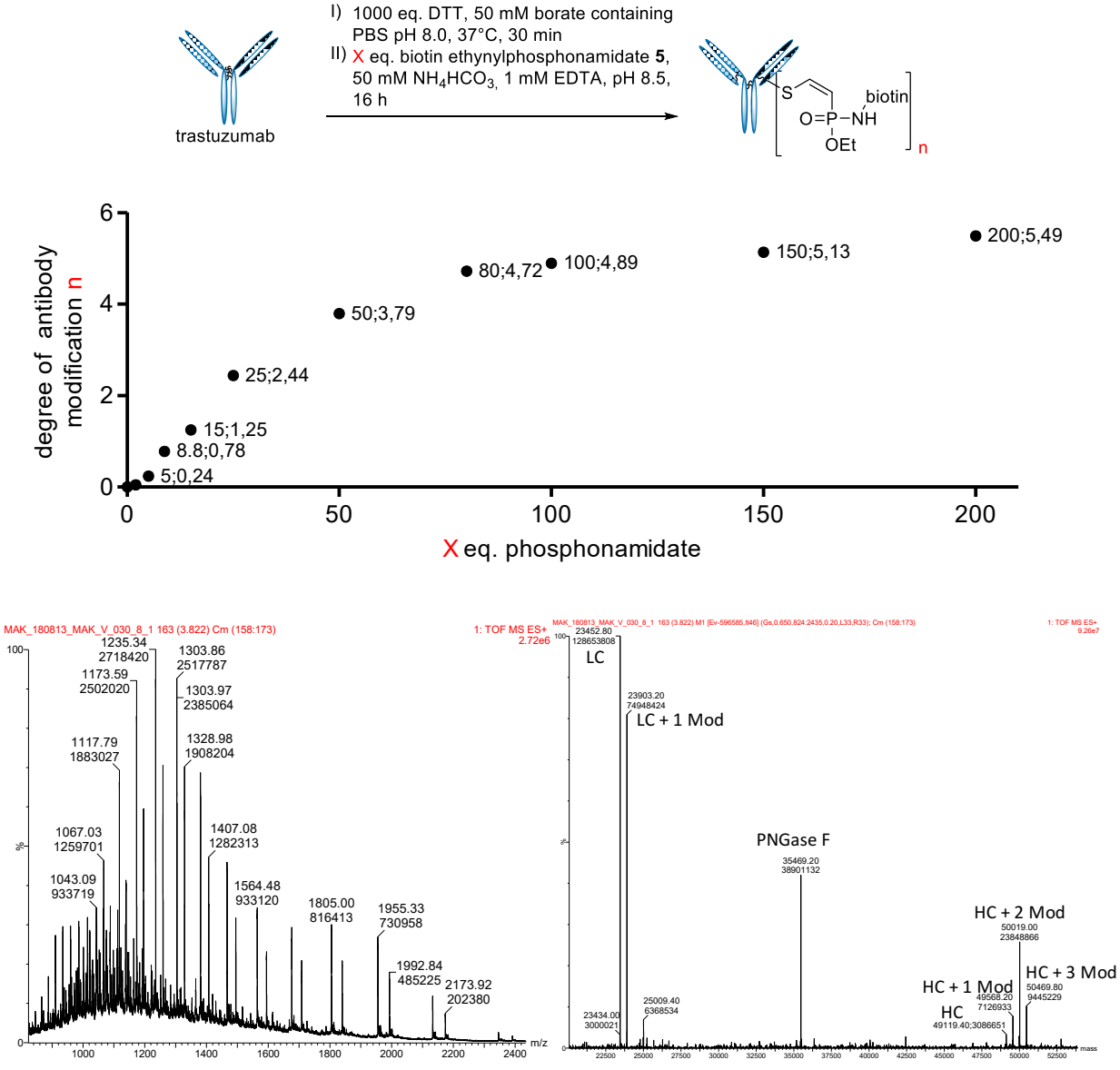

1.8. Figure S8

MS/MS experiments of trastuzumab, modified with Ethyl-*N*-phenyl-*P*-ethynylphosphonamidate (**1**), with and without prior reduction of the antibody as described in general procedure 2. In-gel digest of heavy and light chain separately after reducing SDS/Page as described earlier.[2] Oxidation of methionine, alkylation of cysteine via iodoacetamide and the phosphonamidate on Y, S, T, C, K, H & R were searched as variable modifications. (See chapter 2.9. for MS/MS details).

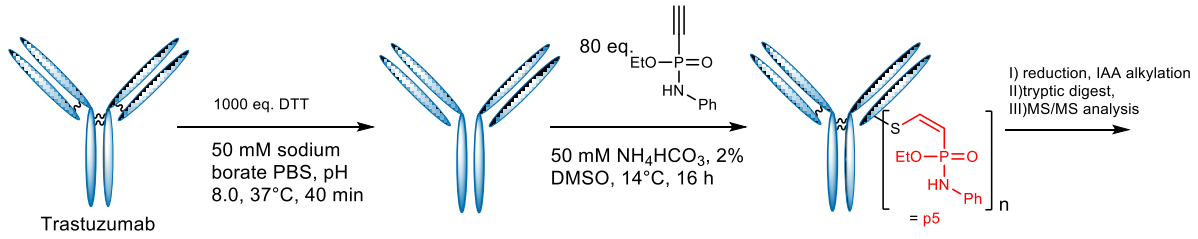

Light Chain: Sequence coverage: 94.39%; MS/MS recorded
Modifications: O: Methionine oxidation; C: Carbamidomethyl; p5: *N*-phenyl-phosphonamidate

```
  O                   C
DIQMTQSPSSLSASVGDRVTITCRASQDVNTAVAWYQQKPGKAPKLLIYSASFLYSGVPSRFSGSR
                    C
SGTDFTLTISSLQPEDFATYYCQQHYTTPPTFGQGTKVEIKRTVAAPSVFIFPPSDEQLKSGTASV
 C                                                              C
VCLLNNFYPREAKVQWKVDNALQSGNSQESVTEQDSKDSTYSLSSTLTLSKADYEKHKVYACEVTH
             p5
QGLSSPVTKSFNRGEC
```

Peptide spectrum match of the modified peptide SFNRGEp5C (HCD MS/MS spectrum):

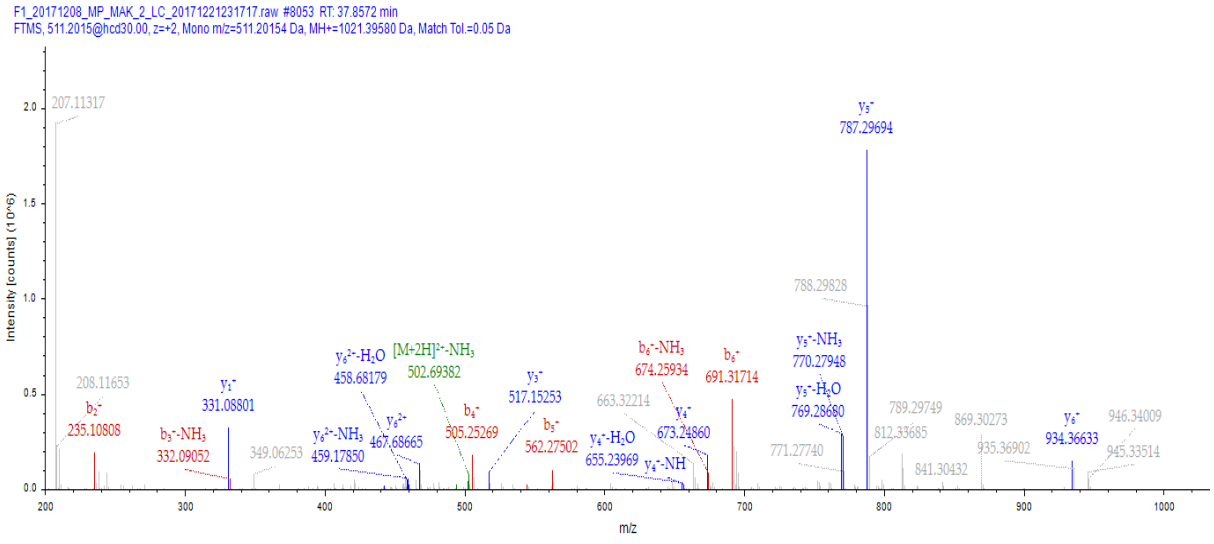

Peptide spectrum match of the modified peptide SFNRGEp5C (EthcD MS/MS spectrum):

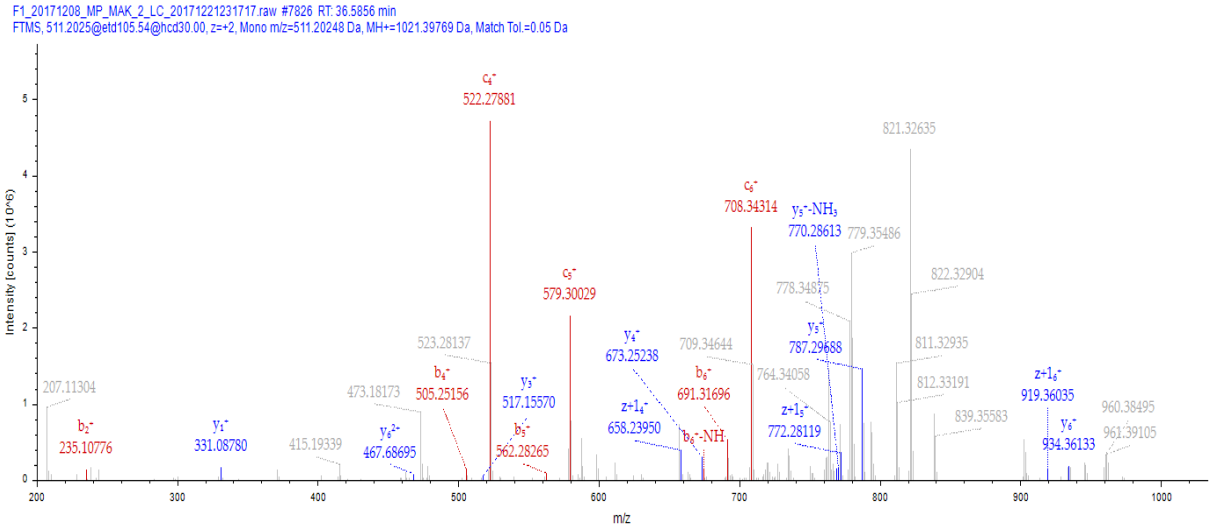

Heavy chain: Sequence coverage: 64.52%; MS/MS recorded

Modifications: O: Methionine oxidation; C: Carbamidomethyl; p5: *N*-phenyl-phosphonamidate

```
                              C
EVQLVESGGGLVQPGGSLRLSCAASGFNIKDTYIHWVRQAPGKGLEWVARIYPTNGYTRYADSVKGRFTISA
             O                C
DTSKNTAYLQMNSLRAEDTAVYYCSRWGGDGFYAMDYWGQGTLVTVSSASTKGPSVFPLAPSSKSTSGGTAA
  C
LGCLVKDYFPEPVTVSWNSGALTSGVHTFPAVLQSSGLYSLSSVVTVPSSSLGTQTYICNVNHKPSNTKVDK
               C  C
        C      p5 p5                          O          C
KVEPPKSCDKTHTCPPCPAPELLGGPSVFLFPPKPKDTLMISRTPEVTCVVVDVSHEDPEVKFNWYVDGVEV

HNAKTKPREEQYNSTYRVVSVLTVLHQDWLNGKEYKCKVSNKALPAPIEKTISKAKGQPREPQVYTLPPSRE
            C
LTKNQVSLTCLVKGFYPSDIAVEWESNGQPENNYKTTPPVLDSDGSFFLYSKLTVDKSRWQQGNVFSCSVMH

EALHNHYTQKSLSLSPGK
```

Peptide spectrum match of the modified peptide THTp5CPPcamCPAPELLGGPSVFLFPPKPK (EThcD MS/MS spectrum)

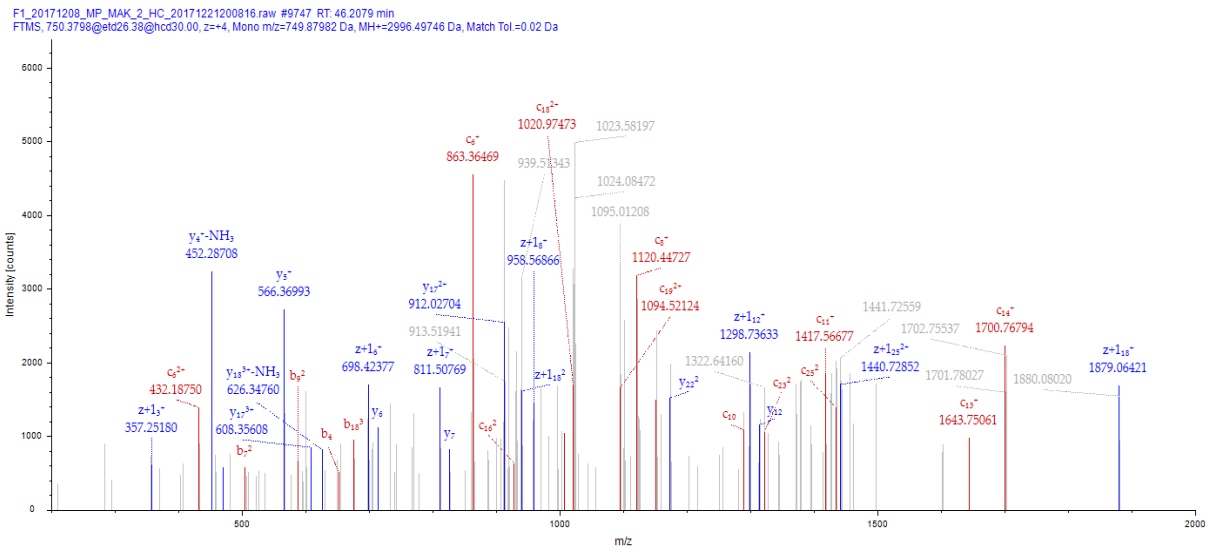

Peptide spectrum match of the modified peptide THTcamCPPp5CPAPELLGGPSVFLFPPKPK (EThcD MS/MS spectrum)

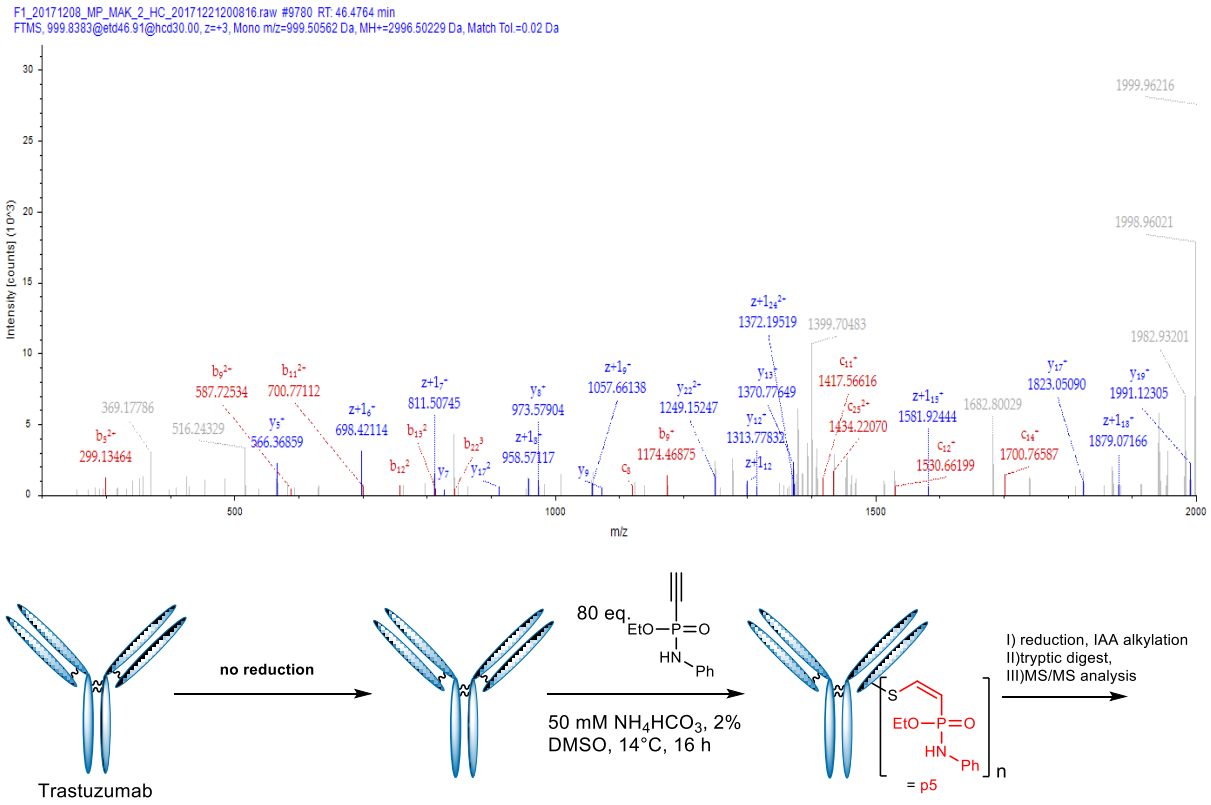

Light Chain: Sequence coverage: 92.06%

Modifications: O: Methionine oxidation; C: Carbamidomethyl; p5: *N*-phenyl-phosphonamidate

```
   O                    C
DIQMTQSPSSLSASVGDRVTITCRASQDVNTAVAWYQQKPGKAPKLLIYSASFLYSGVPSRFSGSR
                     C
SGTDFTLTISSLQPEDFATYYCQQHYTTPPTFGQGTKVEIKRTVAAPSVFIFPPSDEQLKSGTASV
 C                                                              C
VCLLNNFYPREAKVQWKVDNALQSGNSQESVTEQDSKDSTYSLSSTLTLSKADYEKHKVYACEVTH
                C
QGLSSPVTKSFNRGEC
```

Heavy Chain: Sequence coverage: 64.52%

Modifications: O: Methionine oxidation; C: Carbamidomethyl; p5: *N*-phenyl-phosphonamidate

```
                      C
EVQLVESGGGLVQPGGSLRLSCAASGFNIKDTYIHWVRQAPGKGLEWVARIYPTNGYTRYADSVKGRFTISA
          O           C          O
DTSKNTAYLQMNSLRAEDTAVYYCSRWGGDGFYAMDYWGQGTLVTVSSASTKGPSVFPLAPSSKSTSGGTAA
  C
LGCLVKDYFPEPVTVSWNSGALTSGVHTFPAVLQSSGLYSLSSVVTVPSSSLGTQTYICNVNHKPSNTKVDK
       C     C  C                      O         C
KVEPPKSCDKTHTCPPCPAPELLGGPSVFLFPPKPKDTLMISRTPEVTCVVVDVSHEDPEVKFNWYVDGVEV

HNAKTKPREEQYNSTYRVVSVLTVLHQDWLNGKEYKCKVSNKALPAPIEKTISKAKGQPREPQVYTLPPSRE
          C                                                        C  O
LTKNQVSLTCLVKGFYPSDIAVEWESNGQPENNYKTTPPVLDSDGSFFLYSKLTVDKSRWQQGNVFSCSVMH

EALHNHYTQKSLSLSPGK
```

1.9. Figure S9

Fluorophore-quencher based assay to investigate the stability of phosphonamidate-thiol adducts. A: Structure of the phosphonamidate linked dye-quencher conjugate. B: Structure of the maleimide linked dye-quencher conjugate C: Principle of the fluorescence-quencher based readout. Conjugates were incubated at room temperature at a concentration of 10 µM. Measurements were performed at least in triplicates in a 96-well plate (n≥3). Normalization of the graphs by subtraction of the intensity at t=0min for each value. D: Fluorescence measurements for the phosphonamidate linkage (blue) and the maleimide linkage (orange) lysate was freshly prepared from HEK-cells, lysed in PBS. Serum originated from human blood. Glutathione was dissolved in 10 mM in PBS and pH was adjusted to 7.4. (See chapter 3.4 for details)

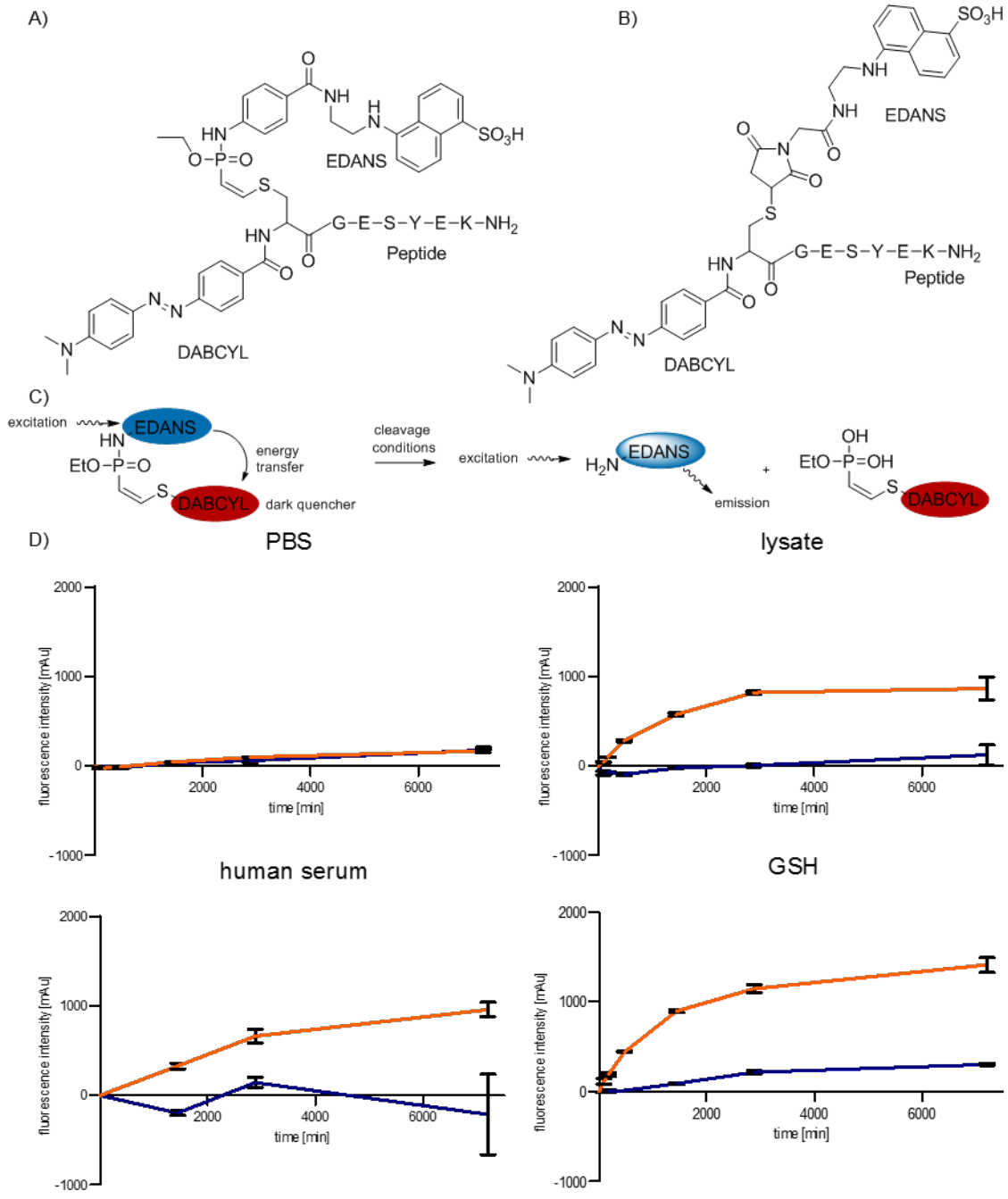

1.10. Figure S10

Stability of trastuzumab-biotin-conjugates towards modification transfer to serum proteins. Conjugates were incubated at a concentration of 3 µM in PBS with a final concentration of 3 µM and 0.5 mM BSA at 37 °C. Samples were drawn after 0, 1, 2 and 5 days, deep frozen in liquid N_2 and finally subjected to SDS/Page and western blot analysis. (See Chapter 3.5 for details)

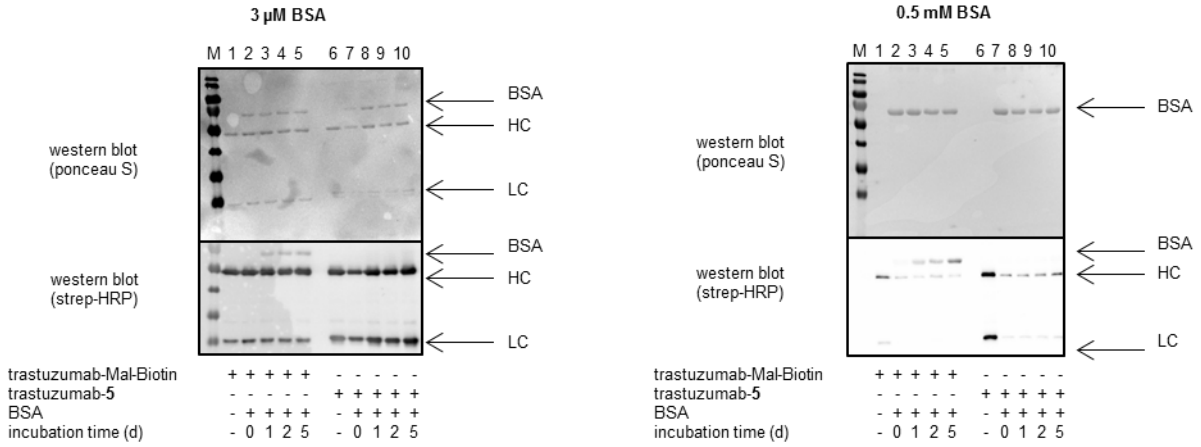

1.11. Figure S11

SDS-Page analysis and fluorescence microscopy of trastuzumab-phosphonamidate-Cy5 conjugates. Depicted are immunostainings of fixed cells over expressing the cell surface receptor Her2 (SKBR3). The antibody-flurophore-conjugate (AFC) Tras-P5-Cy5 shows clear localization to the plasma membrane for Her2+ cell lines. The merged images show the DAPI signal in blue and the Tras-phosphonamidate-Cy5 signal in red. Scale bar represents 10 µM. (See Chapter 3.6 for conjugation and microscopy details)

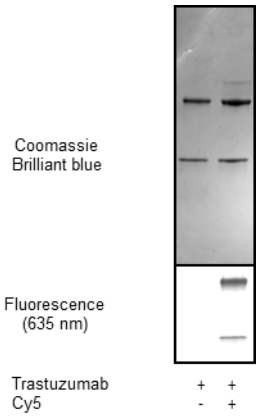

1.12. Figure S12

Fluoresence imaging of HeLa-cells after incubation with eGFP alone and eGFP-cR_{10} at 50 µM. Images show GFP channel in green and Hoechst 33342 in blue. Scale bar represents 20 µm.

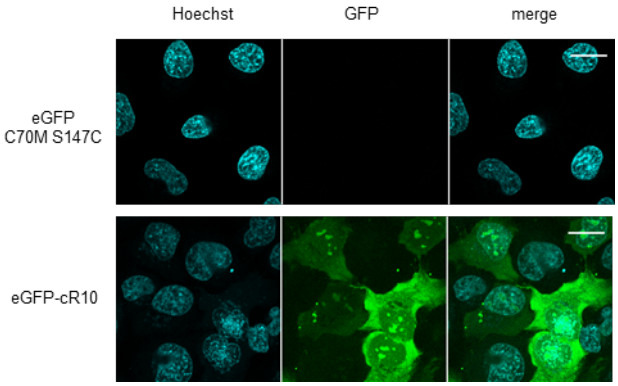

2. General Information

2.1. Chemicals and solvents

Chemicals and solvents were purchased from Merck (Merck group, Germany), TCI (Tokyo chemical industry CO., LTD., Japan) and Acros Organics (Thermo Fisher scientific, USA) and used without further purification. Dry solvents were purchased from Acros Organics (Thermo Fisher scientific, USA).

2.2. Flash- and thin layer chromatography

Flash column chromatography was performed, using NORMASIL 60® silica gel 40-63 µm (VWR international, USA). Glass TLC plates, silica gel 60 W coated with fluorescent indicator F254s were purchased from Merck (Merck Group, Germany). Spots were visualized by fluorescence depletion with a 254 nm lamp or manganese staining (10 g K_2CO_3, 1.5 g $KMnO_4$, 0.1 g NaOH in 200 ml H_2O), followed by heating.

2.3. Preparative HPLC

Preparative HPLC was performed on a Gilson PLC 2020 system (Gilson Inc, WI, Middleton, USA) using a VP 250/32 Macherey-Nagel Nucleodur C18 HTec Spum column (Macherey-Nagel GmbH & Co. Kg, Germany). The following gradients were used: Method C: (A = H_2O + 0.1% TFA (trifluoroacetic acid), B = MeCN (acetonitrile) + 0.1% TFA, flow rate 30 ml/min, 5% B 0-5 min, 5-90% B 5-60 min, 90% B 60-65 min. Method D: 0.1% TFA, flow rate 18 ml/min, 5% B 0-5 min, 5-90% B 5-60 min, 90% B 60-65 min, using a VP 250/21 Macherey-Nagel Nucleodur C18 HTec Spum column (Macherey-Nagel GmbH & Co. Kg, Germany)

2.4. Semi-preparative HPLC

Semi-preparative HPLC was performed on a Shimadzu prominence HPLC system (Shimadzu Corp., Japan) with a CBM20A communication bus module, a FRC-10A fraction collector, 2 pumps LC-20AP, and a SPD-20A UV/VIS detector, using a VP250/21 Macherey-Nagel Nucleodur C18 HTec Spum column (Macherey-Nagel GmbH & Co. Kg, Germany). The following gradients were used: Method E: (A = H2O + 0.1% TFA, B = MeCN + +0.1% TFA), flow rate 10 ml/min, 5% B 0-5 min, 5-99% B 5-65 min, 99% B 65-75 min.

2.5. NMR

NMR spectra were recorded with a Bruker Ultrashield 300 MHz spectrometer and a Bruker Avance III 600 MHz spectrometer (Bruker Corp., USA) at ambient temperature. Chemical shifts δ are reported in ppm relative to residual solvent peak ($CDCl_3$: 7.26 [ppm]; DMSO-d6: 2.50 [ppm]; acetone-d6: 2.05 [ppm]; CD_3CN 1.94 [ppm]; 4.79 D_2O [ppm] for ^{1}H-spectra and $CDCl_3$: 77.16 [ppm]; DMSO-d6: 39.52 [ppm]; acetone-d6: 29.84 [ppm]; CD3CN 1.32 [ppm]; for ^{13}C-spectra . Coupling constants *J* are stated in Hz. Signal multiplicities are abbreviated as follows: s: singlet; d: doublet; t: triplet; q: quartet; m: multiplet.

2.6. UPLC-UV/MS

UPLC-UV/MS traces were recorded on a Waters H-class instrument equipped with a quaternary solvent manager, a Waters autosampler, a Waters TUV detector and a Waters Acquity QDa detector with an Acquity UPLC BEH C18 1.7 µm, 2.1 x 50 mm RP column with a flow rate of 0.6 mL/min (Waters Corp., USA). The following gradient was used: A: 0.1% TFA in H_2O; B: 0.1% TFA in MeCN. 5% B 0 - 0.5 min, 5-95% B 0.5-3 min, 95% B 3-3.9 min, 5% B 3.9-5 min.

2.7. Analytical HPLC

Analytical fluorescence HPLC was conducted on a Shimadzu prominence HPLC system (Shimadzu Corp., Japan) with a CBM-20A communication bus module, a SIL-20A auto sampler, 2 pumps LC-20AT, and a SPD-M20A UV/VIS detector, a CTO-20A column oven and a RF-10AXL fluorescence detector, using an Agilent Eclipse C18 5 µm, 250 x 4.6 mm RR-HPLC column (Agilent Technologies, USA) with a flow rate of 1.0 ml/min. The following gradients were used: (A = H2O + 0.1% TFA, B = MeCN + +0.1% TFA), flow rate 1.0 ml/min, 2% B 0-5 min, 2-45% B 5-35 min, 45-95% B 35-36 min, 95% B 36-40 min, 95 to 2% B 40-41 min, 2% B 41-45 min. Fluorescence spectra with Ex/Em 336/490 were recorded.

2.8. HR-MS

High resolution ESI-MS spectra were recorded on an Agilent 6220 TOF Accurate Mass coupled to an Agilent 1200 LC (Agilent Technologies, USA) and were measured at 35°C between 100- 2000 m/z. The used column was an Accucore RP-MS (30 x 2,1 mm; 2.6 µm particle size) eluted with a flow of 0.8 mL/min and the following gradient (A = water, B = acetonitrile): 95%A + 5%B for 0.2 min, then 95% A + 5% B to 1% A + 99% B until 1.1 min, then 1% A + 99% B until 2.5 min.

2.9. Analytical HPLC-MS/MS

After in-gel digestion peptides were dissolved in water and analyzed by a reversed-phase capillary liquid chromatography system (Dionex Ultimate 3000 NCS-3500RS Nano, Thermo Scientific) connected to an Orbitrap Fusion mass spectrometer (Thermo Fisher Scientific, Germany). LC separations were performed with an in-house packed C18 column for reversed phase separation (column material: Poroshell 120 EC-C18, 2.7 µm (Agilent Technologies, USA) at an eluent flow rate of 300 µL/min using a gradient of 2-40% B in 38 min. Mobile phase A contained 0.1% formic acid in water, and mobile phase B 0.1% formic acid in acetonitrile. FT survey scans were acquired in a range of 350 to 1500 m/z with a resolution of 60000 (FMHM) and an AGC target value of 4e5. Precursor ions with charge states 2-4 were isolated with a mass selecting quadrupole (isolation window m/z 1.6). Precursor ions were fragmented in alternating mode using EThcD and HCD. HCD MS/MS spectra were acquired with 30% NCE. EThcD fragmentation was performed using charge dependent ETD parameters and the supplemental activation (sa) was set to 30%. For both fragmentation types the maximum injection time was set to 500 ms to collect 5e4 precursor ions. Fragment ion spectra were acquired with a resolution of 15000 (FWHM).

MS raw data were processed with Proteome Discoverer 2.2 software (Thermo Fisher Scientific, Germany). The non-fragment filter was applied with following parameters: Precursor ions and charged reduced precursors were removed within a 1 Da window and neutral losses within a 0.5 Da window. MS/MS spectra were search against a database containing trastuzumab heavy and light chain and some common contaminants using Sequest. Precursor mass tolerance and fragment mass tolerance were set to 6 ppm and 0.02 Da, respectively. Oxidation of methionine, alkylation of cysteine via iodoacetamide and the phosphonamidate (Y, S, T, C, K, H & R) were searched as variable modifications. Target Decoy PSM Validator was used to filter peptide spectrum matches (PSMs) with a false-discovery rate (FDR) of 0.05. Peptide spectrum matches displaying modification sites were manually verified.

2.10. Size-exclusion chromatography

Protein purification by size-exclusion chromatography was conducted with an ÄKTA FPLC system (GE Healthcare, United States) equipped with a P-920 pump system, a UPC-900 detector, a FRAC-950 fraction collector and a 5 ml HiTrap® desalting column, with a flow of 1.5 ml/min.

2.11. Intact protein MS

Intact proteins were analyzed using a Waters H-class instrument equipped with a quaternary solvent manager, a Waters sample manager-FTN, a Waters PDA detector and a Waters column manager with an Acquity UPLC protein BEH C4 column (300 Å, 1.7 µm, 2.1 mm x 50 mm). Proteins were eluted at a clomun temperature of 80°C with a flow rate of 0.3 mL/min. The following gradient was used: A: 0.01% FA in H_2O; B: 0.01% FA in MeCN. 5-95% B 0-6 min. Mass analysis was conducted with a Waters XEVO G2-XS QTof analyzer. Proteins were ionized in positive ion mode applying a cone voltage of 40 kV. Raw data was analyzed with MaxEnt 1.

2.12. MALDI-TOF MS

MALDI-TOF MS of intact protein samples was conducted with a Bruker Microflex™ LT benchtop system (Bruker, United States). Using a matrix of saturated DHAP (2',6'-Dihydroxyacetophenone) in acetonitrile.

2.13. Solid-Phase-Peptide Synthesis (SPPS)

SPPS was carried out manually or on a Tribute-UV peptide synthesizer (Protein technologies, USA) via standard Fmoc-based protocols.

3. Experimental procedures

3.1. Trastuzumab production

Trastuzumab expression and purification was executed as previously published with an additional final purification by gel filtration on a Superdex 200 Increase 10/300 from GE (GE life sciences, USA) with PBS and flow rate of 0.75 ml/min.[3]

3.2. General procedure for antibody modification with phosphonamidates via reduction and alkylation of inter-chain disulfides

Trastuzumab modification was carried out by incubating freshly expressed antibody (typical concentration c = 0.5 to 1.0 mg/ml) with 1000 eq. of DTT in a buffer containing 50 mM sodium borate in PBS (pH 8.0) with a total volume of 80 µl at 37 °C for 40 min. Excess DTT removal and buffer exchange to a solution containing 50 mM NH_4HCO_3 and 1mM EDTA (pH 8.5) was conducted afterwards using 0.5 mL Zeba™ Spin Desalting Columns with 7K MWCO (Thermo Fisher Scientific, USA). The desired

phosphonamidate, dissolved in DMSO was added quickly to reach a final DMSO content of no more than 5%. The mixture was shaken at 850 rpm and 14 °C for 16 hours. Excess reagent was again removed by buffer exchange to sterile PBS using 0.5 mL Zeba™ Spin Desalting Columns with 7K MWCO or size exclusion chromatography.

3.3. Deglycosylation, reduction and MS-analysis of trastuzumab conjugates

40 µl of the crude antibody modification mixture were purified by size-exclusion chromatography, eluting with 100 mM $NaHCO_3$ and 500 mM NaCl. The antibody containing fractions were pooled and concentrated by spin-filtration to 40 µl (MCWO: 10 kDa, 0.5 ml, Sartorius, Germany). 2 µl RapiGest™ solution (1% in H_2O) (Waters Corp., USA) were added and the solution was heated to 60 °C for 30 min. The solution was allowed to cool to room temperature, 1 µl PNGase-F solution (Pomega, Germany, Recombinant, cloned from Elizabethkingia miricola 10 u/µl) was added and the solution was incubated at 37 °C over night. Disulfide bridges were reduced by addition of 2 µl DTT solution (70 mM in H_2O) and incubation at 37°C for 30 min. Samples were diluted with 120 µl 1% HCl and subjected to intact protein MS.

3.4. Stability studies of the Dabcyl-EDANS adducts

Stability studies were conducted in 96-well plate (Corning 3615, black with clear, flat bottom) at least in triplicates. 5 µl of a 200 µM Stock solution of the Dabcyl-EDANS adducts and 95 µl of the respective test solutions were added to each well.

HEK cell lysate was generated from approximately $3,9*10^7$ cells, lysed in 2 mL PBS by sonification (final protein concentration: 1.7 mg/ml). Cells were grown on three 75 cm^2 cell culture plates, washed twice with PBS and harvested with a cell scraper. Human serum was purchased from Sigma Aldrich. Glutathione was dissolved at a concentration of 10 mM in PBS and the pH was adjusted to 7.4. 1N HCl studies were conducted at 200 µM, neutralized to pH 7 and diluted to 10 µM before fluorescence measurements.

Fluorescence was measured on a Tecan Safire plate reader. Excitation: 360 nm, emission: 508 nm, bandwidth: 5nm at 20 °C.

3.5. Incubation of trastuzumab-biotin conjugates with BSA

Trastuzumab-biotin conjugates were incubated at a concentration of 3 µM in PBS with a final concentration of 0.5 mM BSA at 37 °C. Samples were drawn after 0, 1, 2 and 5 days, deep frozen in liquid nitrogen and finally subjected to SDS-Page and western blot analysis.

3.6. Synthesis of trastuzumab-Cy5 conjugates and fluorescence microscopy

Trastuzumab-Cy5 conjugates were synthesized according to the general procedure 1 with the following slight modifications: the phosphonamidate equivalents (Cy5-*O*-ethyl-*P*-alkynyl-phosphonamidate) were raised to 130, and the DMSO content was raised to 5% to solubilize the Cy5. Samples were subjected to SDS-Page analysis and fluorescence microscopy.

BT474, SKBR3 and MDAMB468 were seeded on sterile cover slips and incubated ON at 37 °C, 5 % CO2 for cell attachment. Cells were washed three times with 1x PBS prior to fixation for 10 min in 1x PBS/4% PFA (formaldehyde). Fixation was stopped by the addition of an equal volume 1 x PBST (PBS + 0.05 % Tween20) followed by two more washes with PBST. AFCs were added to a final concentration of 5 µg/mL and incubated for 1 h at rt. Unbound AFC was removed by three washes with PBS. Images were acquired on a Leica SP5 confocal microscopy system equipped with a 63x1.40 oil immersion objective.

Laserlines 405 nm and 594 nm were used in combination with standard DAPI and Cy5 filter settings. Image processing was carried out with ImageJ 1.5.1h software extended by the Fiji processing package.

3.7. eGFP C70M S147C production

The eGFP mutant C70MS147C was generated allowing for single cysteine conjugation experiments. Even though this mutant obtains two cysteines (C48 and C147), the cysteine at position 48 was shown to be not addressable for different conjugation methods (data not shown).
For construction of the bacterial expression constructs coding for His-tagged eGFPC70MS147C, eGFP was cloned from pGEXeGFP (provided by Roland Kühne, FMP Berlin) into pET28a using XhoI and NdeI restriction endonuclease sites. The mutations were introduced with classical PCR by the use of complementary primer pairs (GTACAACTACAACTGCCACAACGTC and GACGTTGTGGCAGTTGT AGTTGTAC).
The protein was expressed in E. coli BL21(DE3) using LB medium containing 100 µg/mL ampicillin (LBAMP). Cells were grown at 37 °C, 180 rpm until OD_{600} reached approx. 0.8, induced with 0.3 mM IPTG and incubated at 18 °C for 19 h. Lysis was performed in Dulbecco's PBS (137 mM NaCl, 2.7 mM KCl, 10 mM Na2HPO4 and 1.8 mM KH2PO4) using a high-pressure homogenizer (Microfluidics LM10 Microfluidizer) and debris centrifuged at 20.000 g for 30 min. The protein was purified with a BioRad NGC system (BioRad, USA) using a 5 mL HisTrap FF (GE Healthcare, USA) column, peak fractions were collected and desalted to Dulbecco's PBS using a HiPrep 26/10 Desalting column (GE Healthcare, USA). Thrombin (1 µL/mL; Thrombin restriction grade, Merck Millipore, Germany) was added to the protein fractions and incubated for 16 h at 16 °C. The protein was concentrated to 1 mL using Vivaspin 20 (cut-off 19 kDa; Merck Millipore, Germany) and subjected to a final size exclusion chromatography using a Superdex 75 10/300 GL column (GE Healthcare, USA). The protein concentration was determined by NanoDrop® at 280 nm (ε = 21890 M-1 cm-1). The expressed protein was isolated in 15-20 mg yield for 1 L expression. Peak fractions were pooled, 0.1 mM PMSF added and aliquots were shock-frozen and stored at -80 °C until further use.

Deconvoluted HRMS: 27765 Da (calcd. MW: 27766 Da)

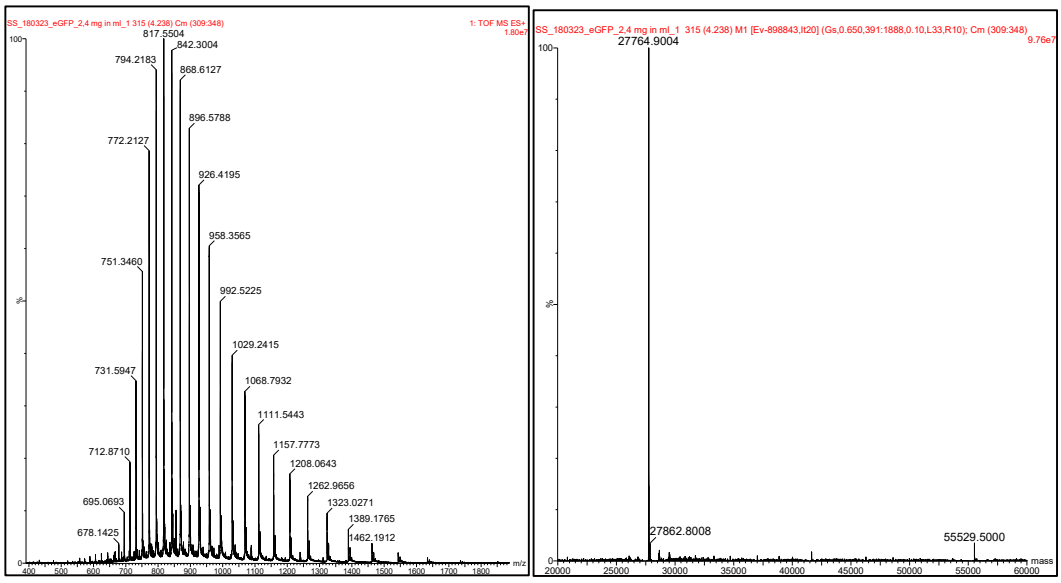

Protein sequence: His-tag highlighted in green; protease cleavage site highlighted in blue; eGFP highlighted in grey; C70M and S147C highlighted in red.

MGSSHHHHHHSSGLVPRGSHMGSIQMVSKGEELFTGVVPILVELDGDVNGHKFSVSGEGEGDATYGKLTLKFICTT
GKLPVPWPTLVTTLTYGVQMFSRYPDHMKQHDFFKSAMPEGYVQERTIFFKDDGNYKTRAEVKFEGDTLVNRIEL
KGIDFKEDGNILGHKLEYNYNCHNVYIMADKQKNGIKVNFKIRHNIEDGSVQLADHYQQNTPIGDGPVLLPDNHYL
STQSALSKDPNEKRDHMVLLEFVTAAGITLGMDELYK

3.8. Addition of the CPP-phosphonamidate peptides 8 and 9 to eGFP

To eGFP C70M S147C buffered in PBS, ethynylphosphonamidate-peptides (20 eq.) were added to give the final protein concentration of 100 µM protein and 2 mM peptide. The reaction mixture was shaken at 37°C and 800 rpm for 3 h. The excess peptide was removed by spinfiltration using Amicon Spin filters with a 10 kDa MWCO (Sartorius, Germany). The sample was filtered five times with PBS at 14000 rpm for 5 min to remove excess Peptide.

Cyclic-(Tat)-eGFP

Peptide **8** (3.06 mg as TFA-salt, 1.13 µmol, 20 eq.) was reacted with eGFP C70M S147C (56.3 nmol) according to the above stated procedure. After removal of excess peptide by spin filtration the sample was analyzed by MALDI-TOF after acetone precipitation and re-solvation in 10 mM ammonium bicarbonate buffer. Quantitative conversion to the product was observed.

MALDI TOF: expected (in Da): 29795.2 (M+H+); found (in Da): 29851.4 (M+H+)

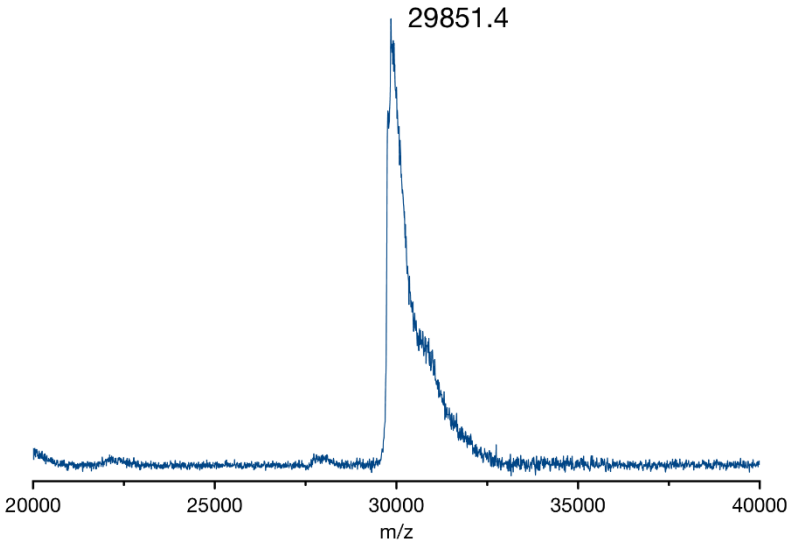

Cyclic-(R_{10})-eGFP

Peptide **9** (3.94 mg as TFA-salt, 1.13 µmol, 20 eq.) was reacted with eGFP C70M S147C (56.3 nmol) according to the above stated procedure. After removal of excess peptide by spin filtration the sample was analyzed by MALDI-TOF after acetone precipitation and re-solvation in 10 mM ammonium bicarbonate buffer. Quantitative conversion to the product was observed.

MALDI TOF: expected (in Da): 30106.4 ($M+H^+$); found (in Da): 30128.0 ($M+Na^+$).

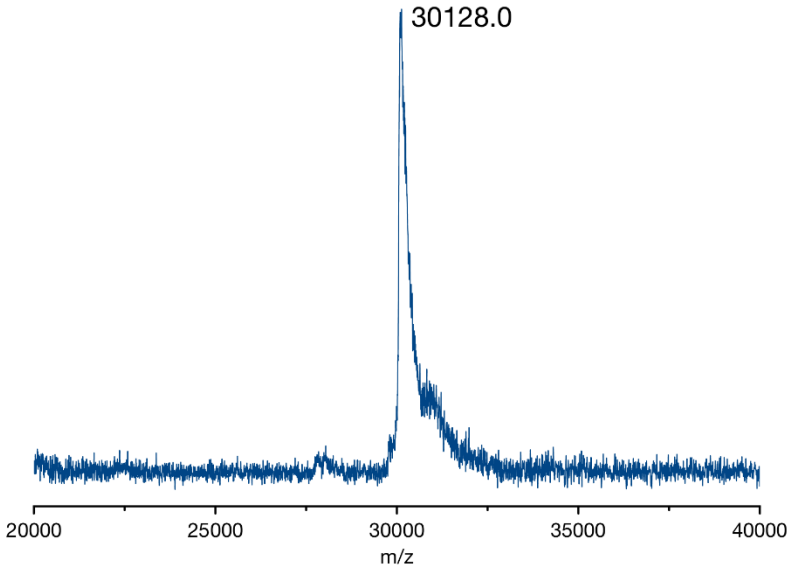

3.9. Cellular uptake experiments

All cellular uptake experiments were carried out with HeLa (ATCC CCL-2) cells cultured in Dulbecco's MEM medium supplemented with 10% FBS and 1% Penicillin Streptomycin. 70 000 cells were seeded in an uncoated glass bottom 8-well µ-slide (Ibidi) 24 hours prior to treatment. The cellular uptake was carried out by gently washing cells three times with HEPES buffer pH 7.5 (5 mM HEPES, 140 mM NaCl, 2.5 mM KCl, 5 mM glycine). The peptide-protein conjugate buffered in the same HEPES buffer was added to the cells in 200 µl at 50 µM and incubated for at 37°C in a 5% CO_2 atmosphere. After one hour cells were gently washed with 25 mM HEPES in Dulbecco's MEM supplemented with 10% FKS and cells were rested for 30 minutes at 37°C. The cell nucleus was stained with Hoechst 33342 and cells imaged with a Zeiss 710 confocal microscope.

4. Organic Synthesis

4.1. General procedure 1 for the synthesis of *O*-ethyl-ethynylphosphonamidates

A 25-ml Schlenk flask was charged with 173 µl diethyl chlorophosphite (1.20 mmol, 1.2 eq.) under an argon atmosphere, cooled to –78 °C and 2.00 ml ethynylmagnesium bromide solution (0.5 M in THF, 1.00 mmol, 1.0 eq.) was added drop wise. The solution was allowed to warm to room temperature and 1.00 mmol of azide (1.0 eq.) dissolved in 3.0 ml of THF or DMF was added and stirred over night at room temperature. 5 ml of water were added and stirred for another 2 h. The reaction mixture was extracted with EtOAc, the combined organic fractions dried ($MgSO_4$) and solvents were removed under reduced pressure. The crude product was purified by flash column chromatography on silica gel or preparative reversed phase HPLC.

4.2. Ethyl-*N*-phenyl-*P*-ethynylphosphonamidate (1)

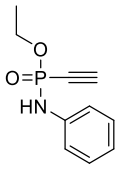

The compound was synthesized according to the general procedure 1 from 1.45 ml diethyl chlorophosphite (10.07 mmol) and 1.00 g phenyl azide (8.39 mmol). The crude phosphonamidate was purified by flash column chromatography on silicagel (50% *n*-hexan in EtOAc) and obtained as a yellowish solid. (1.4 g, 6.74 mmol, 80.3%)

^{1}H NMR (600 MHz, Chloroform-*d*) δ = 7.33 – 7.25 (m, 2H), 7.20 (d, *J*=7.6, 1H), 7.16 – 7.10 (m, 2H), 7.05 – 6.94 (m, 1H), 4.35 – 4.10 (m, 2H), 2.91 (d, *J*=12.9, 1H), 1.39 (t, *J*=7.1, 3H). ^{13}C NMR (151 MHz, Chloroform-*d*) δ = 139.18, 129.28, 122.23, 118.16 (d, *J*=7.6), 87.77 (d, *J*=48.8), 76.39 (d, *J*=272.9), 62.13 (d, *J*=5.1), 16.17 (d, *J*=7.4). ^{31}P NMR (243 MHz, Chloroform-*d*) δ = -8.75. HR-MS for $C_{10}H_{13}NO_2P^+$ $[M+H]^+$ calcd.: 210.0678, found 210.0680.

4.3. Ethyl-*N*-(4-carboxy-phenyl)-*P*-ethynylphosphonamidate (2)

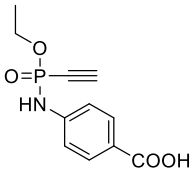

The compound was synthesized according to the general procedure 1 from 1.06 ml diethyl chlorophosphite (7.36 mmol) and 1.00 g 4-azidobenzoic acid (6.13 mmol). The crude phosphonamidate was purified by flash column chromatography on silicagel (5 to 20% MeOH in EtOAc) and obtained as a white solid. (0.68 g, 2.67 mmol, 43.5%)

^{1}H NMR (300 MHz, Acetone-d_6) δ 8.11 – 8.00 (m, 1H), 7.97 (d, *J* = 8.6 Hz, 2H), 7.30 (d, *J* = 8.6 Hz, 2H), 4.32 – 4.11 (m, 2H), 3.87 (d, *J* = 12.9 Hz, 1H), 1.36 (t, *J* = 7.1 Hz, 3H).^{13}C NMR (75 MHz, Acetone-d_6) δ = 167.65, 145.51 (d, *J*=1.5), 131.93, 124.63, 118.04 (d, *J*=7.8), 90.15 (d, *J*=47.6), 77.28 (d, *J*=267.2), 62.98 (d, *J*=5.1), 16.38 (d, *J*=7.1).^{31}P NMR (122 MHz, Acetone-d_6) δ -11.05. HR-MS for $C_{11}H_{13}NO_4P^+$ $[M+H]^+$ calcd.: 254.0577, found 254.0586.

4.4. Ethyl-*N*-(4-(2,5-dioxo-1-pyrrolidinyl)oxy-carbonyl-phenyl)-*P*-ethynylphosphonamidate (3)

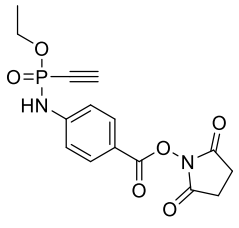

The compound was synthesized according to the general procedure 1 from 173 µl diethyl chlorophosphite (1.20 mmol) and 260 mg 4-azidobenzoic-acid-*N*-hydroxysuccinimide ester 1.00 mmol). The crude phosphonamidate was purified by flash column chromatography on silicagel (100% EtOAc) and obtained as a yellowish solid. (225 mg, 0.64 mmol, 64.3%)

^{1}H NMR (300 MHz, Chloroform-*d*) δ = 8.05 (d, *J*=8.6, 2H), 7.37 (d, *J*=7.4, 1H), 7.16 (d, *J*=8.6, 2H), 4.38 – 4.13 (m, 2H), 2.96 (d, *J*=13.2, 1H), 2.90 (s, 4H), 1.40 (t, *J*=7.1, 3H).^{13}C NMR (75 MHz, Chloroform-*d*) δ = 169.59, 161.51, 145.64, 132.55, 118.38, 117.59 (d, *J*=8.0), 88.69 (d, *J*=50.2), 62.93 (d, *J*=5.2), 25.82, 16.24 (d, *J*=7.3).^{31}P NMR (122 MHz, Chloroform-*d*) δ = -10.65. HR-MS for $C_{15}H_{16}N_2O_6P^+$ $[M+H]^+$ calcd.: 351.0740, found 351.0749.

Synthetic route to 2-(4-Azidophenyl)-ethylamine hydrochloride

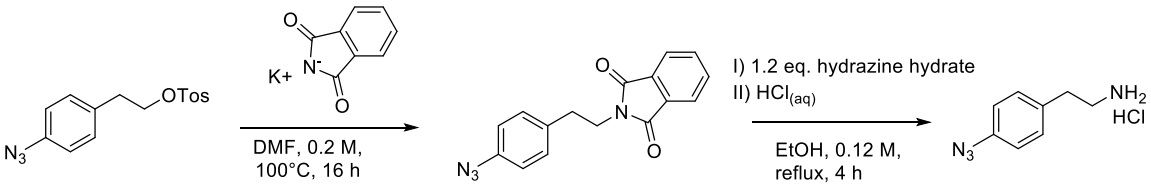

4.5. 2-(4-Azidophenyl)-ethyl phtalimide

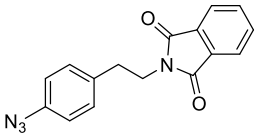

A 50-ml round-bottom flask was charged with 4.11 g of 2-(4-Azidophenyl)-ethyl-4-toluenesulfonate (12.95 mmol, 1.00 eq.), together with 3.60 g potassium phtalimide (19.42 mmol, 1.50 eq.) and dissolved in 60 ml DMF. The brown solution was stirred over night at 100 °C. All volatiles were removed under reduced pressure, 50 ml of water were added extracted three times with EtOAc, the combined organic fractions were washed two times with water, the organic layer was dried ($MgSO_4$) and all volatiles were removed under reduced pressure. The product was used in the next step without further purification. Pure product was obtained by flash column chromatography on silicagel (10% to 20% EtOAc in *n*-hexan) as a yellow solid (1.75 g, 5.99 mmol, 46.2%). ^{1}H NMR (600 MHz, Chloroform-*d*) δ = 7.85 (dd, *J*=5.4, 3.1, 2H), 7.73 (dd, *J*=5.4, 3.1, 2H), 7.25 (d, *J*=8.4, 2H), 6.96 (d, *J*=8.4, 2H), 3.93 (dd, *J*=8.3, 6.8, 2H), 3.00 (dd, *J*=8.3, 6.8, 2H). ^{13}C NMR (151 MHz, $CDCl_3$) δ = 168.12, 138.43, 134.76, 133.96, 132.00, 130.22, 123.26, 119.17, 39.14, 33.92.

4.6. 2-(4-Azidophenyl)-ethylamine hydrochloride

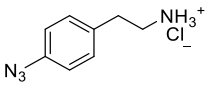

A 100-ml round-bottom flask was charged with 722 mg of 2-(4-Azidophenyl)-ethyl phtalimide (2.47 mmol, 1.00 eq.), 144 µl hydrazine hydrate (2.96 mmol, 1.20 eq.), dissolved in 20 ml of dry ethanol under argon atmosphere and the solution was refluxed for 4 h. Most of the solvent was removed under reduced pressure, 50 ml water was added and the suspension was basified with 1N NaOH. It was extracted three times with EtOAc, the combined organic fractions were washed two times with water, the organic layer was dried ($MgSO_4$) and all volatiles were removed under reduced pressure. Pure product was obtained by flash column chromatography on silicagel (10% MeOH in CH_2Cl_2 + 0.5% *N,N*-ethyldimethylamine) and lyohilisation from 1N HCl as yellowish solid (224 mg, 1.14 mmol, 46.2% over two steps). ^{1}H NMR (600 MHz, Deuterium Oxide) δ = 7.29 (d, *J*=7.6, 2H), 7.05 (d, *J*=7.6, 2H), 3.22 (t, *J*=7.2, 2H), 2.94 (t, *J*=7.2, 2H). ^{13}C NMR (151 MHz, D_2O) δ = 138.81, 133.24, 130.32, 119.40, 40.51, 32.13. NMR data was in accordance with literature values.[4]

4.7. Ethyl-*N*-(4-(2-aminoethyl)phenyl)-*P*-ethynylphosphonamidate TFA salt (4)

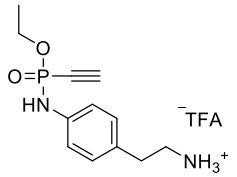

The compound was synthesized according to the general procedure 1 from 181 µl diethyl chlorophosphite (1.25 mmol) and 322 mg 2-(4-azidophenyl)ethyl amine hydrochloride (1.05 mmol). The crude phosphonamidate was purified by preparative RP-HPLC (Method C) and obtained as brown oil. (88 mg, 0.24 mmol, 22.9%)

^{1}H NMR (300 MHz, Acetonitrile-d_3) δ = 7.58 (s, 3H), 7.20 – 7.01 (m, 4H), 6.96 (d, *J*=8.5, 1H), 4.26 – 4.05 (m, 2H), 3.42 (d, *J*=12.8, 1H), 3.08 (d, *J*=7.8, 2H), 2.88 (dd, *J*=9.0, 6.4, 2H), 1.31 (t, *J*=7.1, 3H). ^{13}C NMR (75 MHz, Acetonitrile-d_3) δ = 161.38 (q, *J*=34.7), 139.20 (d, *J*=1.3), 131.75, 130.66, 119.63 (d, *J*=7.3), 90.09 (d, *J*=47.2), 77.02 (d, *J*=265.0), 63.54 (d, *J*=5.3), 41.92, 33.19, 16.41 (d, *J*=7.3). ^{31}P NMR (122 MHz, Acetonitrile-d_3) δ = -9.71. HR-MS for $C_{12}H_{18}N_2O_2P^+$ $[M+H]^+$ calcd.: 253.1100, found 253.1095.

4.8. *N*-(4-azidophenyl) biotinamide

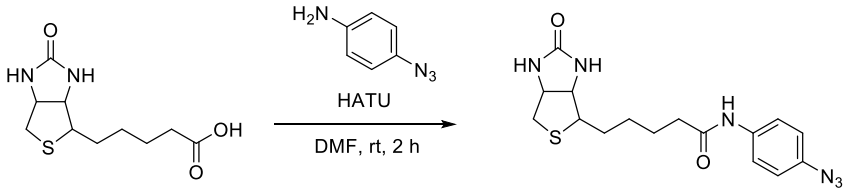

A 50-ml round-bottom flask was charged with 642 mg of D-biotin (2.63 mmol, 1.50 eq.) and 1.00 g of HATU (2.63 mmol, 1.50 eq.) under argon, dissolved in 5 ml of dry DMF and cooled to 0°C. 920 µl DIPEA (5.25 mmol, 3.0 eq.) were added and stirred for several min. A solution of 235 mg 4-azido aniline (1.75 mmol, 1.00 eq.) in 4 ml of dry DMF was added, the yellow solution was allowed to warm to room temperature and stirred for additional 2 h. The solvents were removed under reduced pressure and the crude product was purified by flash column chromatography on silicagel (5 to 12% MeOH in CH_2Cl_2). The product was obtained as white powder. (617 mg, 1,72 mmol, 98%)

^{1}H NMR (600 MHz, DMSO-d_6) δ = 9.96 (s, 1H), 7.64 (d, *J*=8.9, 2H), 7.07 (d, *J*=8.9, 2H), 6.44 (s, 1H), 6.37 (s, 1H), 4.42 – 4.28 (m, 1H), 4.21 – 4.08 (m, 1H), 3.21 – 3.07 (m, 1H), 2.84 (dd, *J*=12.4, 5.1, 1H), 2.60 (d, *J*=12.4, 1H), 2.31 (td, *J*=7.4, 1.8, 2H), 1.70 – 1.57 (m, 3H), 1.55 – 1.47 (m, 1H), 1.44 – 1.32 (m, 2H). ^{13}C NMR (151 MHz, DMSO) δ = 171.60, 163.20, 137.09, 134.00, 121.00, 119.83, 61.53, 59.69, 55.85, 40.31, 36.64, 28.70, 28.56, 25.55. HR-MS for C16H21N$_6$O2S$^+$ $[M+H]^+$ calcd.: 361.1441, found 361.1447.

4.9. Ethyl-*N*-(4-biotinamido-phenyl)-*P*-ethynylphosphonamidate (5)

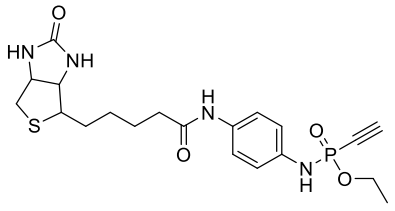

The compound was synthesized according to the general procedure 1 from 239 µl diethyl chlorophosphite (1.66 mmol) and 150 mg *N*-(4-azidophenyl) biotinamide (0.416 mmol). The crude phosphonamidate was purified by flash column chromatography on silicagel (12% MeOH in CH_2Cl_2) and obtained as white solid. (134 mg, 0.30 mmol, 71.5 %).

^{1}H NMR (600 MHz, DMSO-d_6) δ = 9.74 (s, 1H), 8.27 (d, *J*=8.6, 1H), 7.45 (d, *J*=8.6, 2H), 7.00 (d, *J*=8.6, 2H), 6.45 (bs, 2H), 4.39 – 4.30 (m, 2H), 4.19 – 4.01 (m, 3H), 3.17 – 3.10 (m, 1H), 2.84 (dd, *J*=12.4, 5.1, 1H), 2.60 (d, *J*=12.4, 1H), 2.28 (t, *J*=7.1, 2H), 1.73 – 1.55 (m, 3H), 1.55 – 1.46 (m, 1H), 1.44 – 1.32 (m, 2H), 1.29 (t, *J*=7.0, 3H). ^{13}C NMR (151 MHz, DMSO-d_6) δ = 171.21, 163.25, 135.56, 134.03, 120.64, 118.72 (d, *J*=7.4), 91.15 (d, *J*=44.8), 77.76 (d, *J*=257.8), 61.92 (d, *J*=3.6), 61.56, 59.72, 55.86, 40.31, 36.56, 28.71, 28.55, 25.65, 16.43 (d, *J*=6.8). ^{31}P NMR (243 MHz, DMSO) δ = -9.37. HR-MS for $C_{20}H_{28}N_4O_4PS^+$ $[M+H]^+$ calcd.: 451.1563, found 451.1565.

4.10. Ethyl-*N*-(3-phenyl-propyl)-*P*-ethynylphosphonamidate (6)

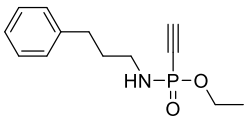

The compound was synthesized according to the general procedure 1 from 346 µl diethyl chlorophosphite (2.40 mmol) and 322 mg 3-phenyl-propyl azide (2.00 mmol). The crude phosphonamidate was purified by flash column chromatography on silicagel (50% *n*-hexan in EtOAc) and obtained as colourless oil. (180 mg, 0.72 mmol, 35.8%)

^{1}H NMR (300 MHz, Chloroform-*d*) δ = 7.33 – 7.25 (m, 2H), 7.24 – 7.16 (m, 3H), 4.20 – 4.05 (m, 2H), 3.31 (dd, *J*=11.8, 5.9, 1H), 3.07 – 2.93 (m, 2H), 2.88 (d, *J*=12.2, 1H), 2.68 (dd, *J*=8.7, 6.8, 2H), 1.88 (p, *J*=7.2, 2H), 1.35 (t, *J*=7.1, 3H). ^{13}C NMR (75 MHz, Chloroform-*d*) δ = 141.30, 128.33, 128.30, 125.87, 86.96 (d, *J*=45.5), 76.90 (d, *J*=257.0), 61.57 (d, *J*=5.1), 40.29, 32.84 (d, *J*=6.4), 32.78, 16.08 (d, *J*=7.3). ^{31}P NMR (122 MHz, Chloroform-*d*) δ = -2.23. HR-MS for $C_{13}H_{19}NO_2P^+$ $[M+H]^+$ calcd.: 252.1148, found 252.1154.

4.11. c(RGDfK)-azide

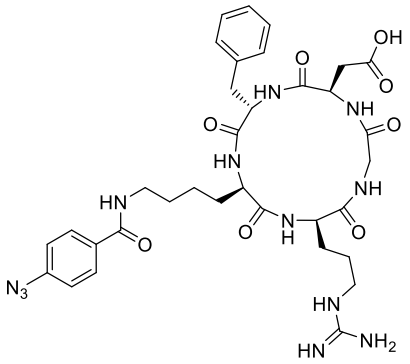

The cyclic RGDfK-azido peptide was synthesized manually on a NovaSynTGT alcohol resin with a loading of 0.26 mmol/g. First the resin was activated by stirring 480.7 mg resin in 2.5 ml toluene and 480 µl acetylchloride at 60°C for 3 h. Double coupling of Fmoc-Asp(OAll)-OH (123.56 mg, 0.3125 mmol, 2.5 eq) was performed in CH_2Cl_2 using DIPEA (212.6 µl, 1.25 mmol, 10 eq.) as activating base each for 1 h. Further amino acid couplings were performed by mixing amino acid (0.25 mmol, 2 eq.), HATU (0.25 mmol, 2 eq.) and DIPEA (0.5 mmol, 4 eq.) in DMF and coupling once for 30 min and once for one hour. Fmoc deprotection was accomplished with 20 % piperidine in DMF. After the final amino acid coupling the alloc deprotection was achieved by treating the resin with $Pd(P(Ph_3)_4)$ (433 mg, 0.375 mmol, 3 eq.) in chloroform/acetic acid/NMM (37:2:1;v:v:v) for 2 h in an argon atmosphere, followed by Fmoc deprotection and cyclisation with HATU (0.25 mmol, 2 eq.) and DIPEA (0.5 mmol, 4 eq.) in DMF for 16 h. To be able to install the aromatic azide on the lysine residue Fmoc-Lys(dde)-OH was used in the solid phase synthesis and was orthogonally deprotected on resin using 2% hydrazine in DMF three times for 3 min, followed by coupling of 4–azidobenzoic acid (81.65 mg, 0.5 mmol, 4 eq.) with HATU (190mg, 0.5 mmol, 4eq.) and DIPEA (1 mmol, 8 eq.) in DMF for 2 h. Cleavage from the resin was performed using

TFA/ CH_2Cl_2 (75:25;v:v) for 2.5 h. Precipitation was carried out in cold and dry ether. The crude was purified by preparative HPLC (Method C). LR-MS for $C_{34}H_{45}N_{12}O_3^+$ $[M+H]^+$ calcd.: 749.35, found 749.67.

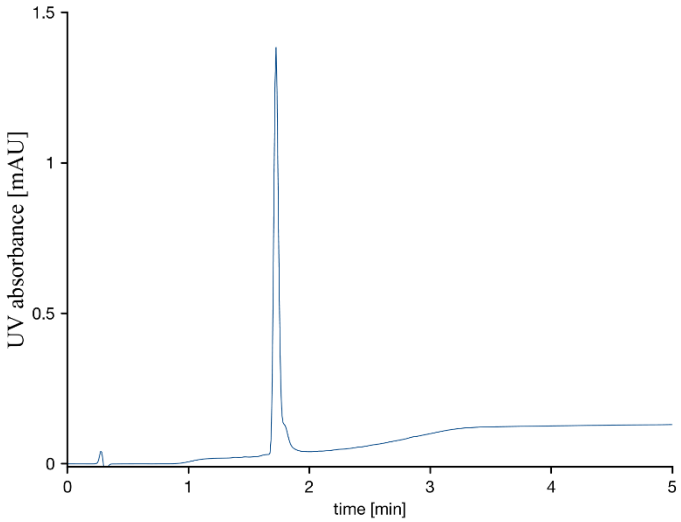

4.12. General procedure 2 for the synthesis of *O*-ethyl-alkynyl phosphonamidates from diethyl chlorophosphite with peptides

A 25-ml Schlenk flask was charged with 144 µl diethyl chlorophosphite (1.00 mmol, 5.0 eq.) under an argon atmosphere, cooled to –78 °C and 2.00 ml ethynylmagnesium bromide solution (0.5 M in THF, 1.00 mmol, 5.0 eq.) was added drop wise. The yellowish solution was allowed to warm to room temperature and 0.20 mmol of peptidic azide (1.0 eq.) dissolved in 5.0 ml of DMF or DMSO was added and stirred over night at room temperature. 5 ml of water were added and stirred for another 2 h. Solvents were removed under reduced pressure. The crude product was purified by preparative reversed phase HPLC.

4.13. Synthesis of c(RGDfK)-ethynylphosphonamidate 7

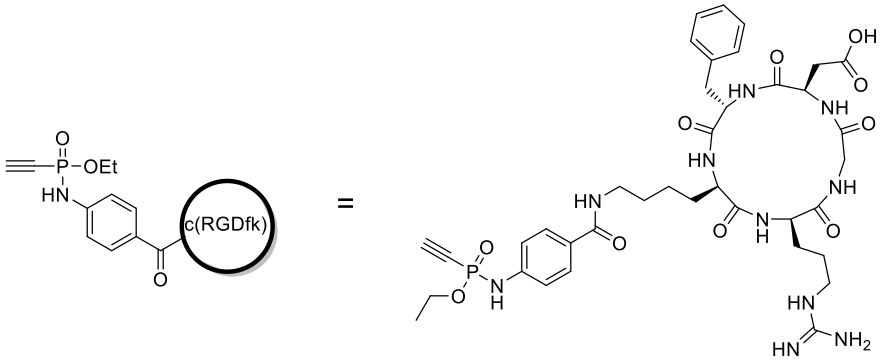

The compound was synthesized according to the general procedure 2 from 8.95 µl diethyl chlorophosphite (0.036 mmol, 4.0 eq.), 72 µl ethynylmagnesium bromide solution (0.5 M in THF, 0.036 mmol, 4.0 eq.) and 6.9 mg c(RGDfK)-azide (9.14 µmol, 1 eq.) . The crude phosphonamidate was purified by preparative HPLC (Method D) and obtained as a white solid after lyophilisation. (4.1 mg, 4.89 µmol, 53.5 % yield). HR-MS for $C_{38}H_{45}N_{10}O_{10}P^+$ $[M+H]^+$ calcd.: 839.3606, found 839.3636.

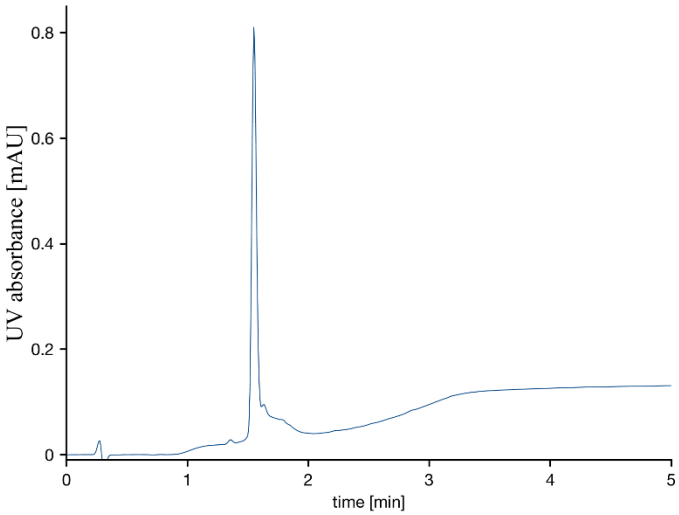

4.14. c-(Tat)-azide

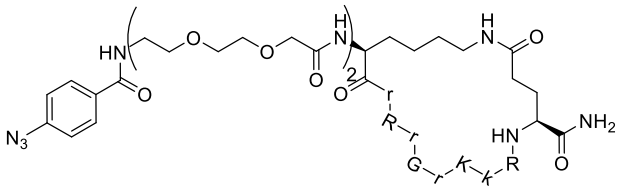

The cyclic-(Tat)-azido peptide was synthesized in a 0.1 mmol scale on a Rink amide resin with a loading of 0.78 mmol/g. The synthesis was carried out on a PTI synthesizer with single couplings of each amino acid (10 eq. amino acid for 40 min) in DMF. After the final PEG building block coupling the peptide, still Fmoc protected, was treated with Pd(PPh3)4 (24 mg, 20 µmol, 20 mol%) and phenylsilane (308 µl, 2.5 mmol, 2.5 eq.) in 4 ml dry CH_2Cl_2 for 1 h in order to cleave the alloc and allyl protecting groups in one step. After confirmation of full deprotection by test cleavage, cyclization with 2 eq. HATU 4 eq. DIPEA was carried for 4 h in DMF. The peptide was then Fmoc-deprotected using 20% piperidine in DMF and the 4-azidobenzoic acid (81.6 mg, 0.5 mmol, 5 eq.) was coupled to the *N*-terminus with HATU (190.1 mg, 0.5 mmol, 5 eq.) and DIPEA (170 µl, 1.0 mmol, 10 eq.) for 1 h. Finally the peptide was cleaved from the resin by treatment with 4 ml of a TFA:TIS:H2O (95:2.5:2.5) mixture for 3 h and precipitated in cold diethylether. The crude peptide was purified by preparative HPLC (Method D). The product was gained as white powder (30.0 mg as TFA-salt, 11.4 µmol, 11.4% yield) MS: m/z: 648.49 $[M+3H]^{3+}$ (calcd. m/z: 648.0569).

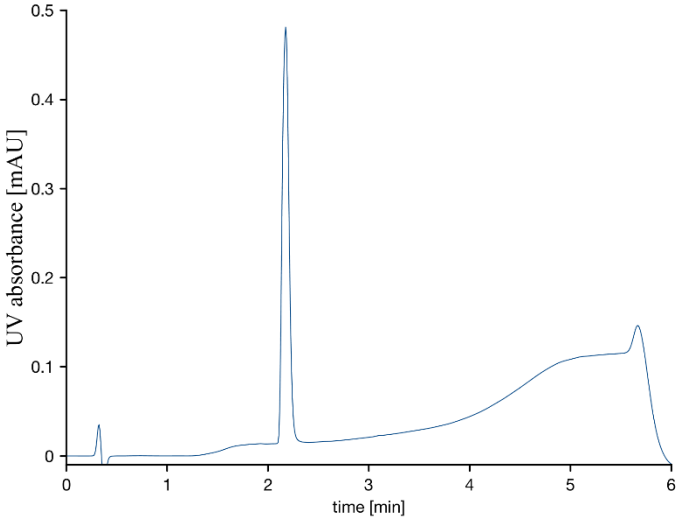

4.15. c-(Tat)-ethynylphosphonamidate 8

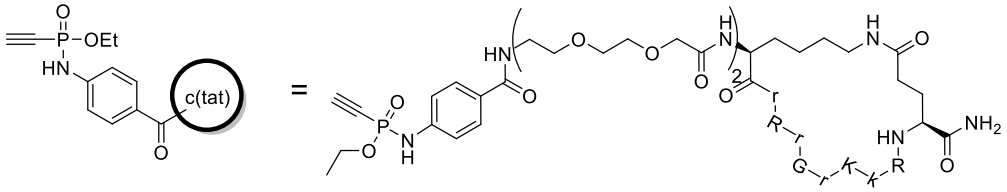

The compound was synthesized according to the general procedure 2 from 8.95 µl diethyl chlorophosphite (0.030 mmol, 4.0 eq.), 72 µl ethynylmagnesium bromide solution (0.5 M in THF, 0.030 mmol, 4.0 eq.) and 20 mg c(Tat)-azide (7.6 µmol, 1 eq.). The product was gained after semi-preparative HPLC (Method D) as white powder (13 mg, 4.8 µmol, 62.9% yield). HRMS: m/z: 678.0569 $[M+3H]^{3+}$ (calcd. m/z: 678.0610).

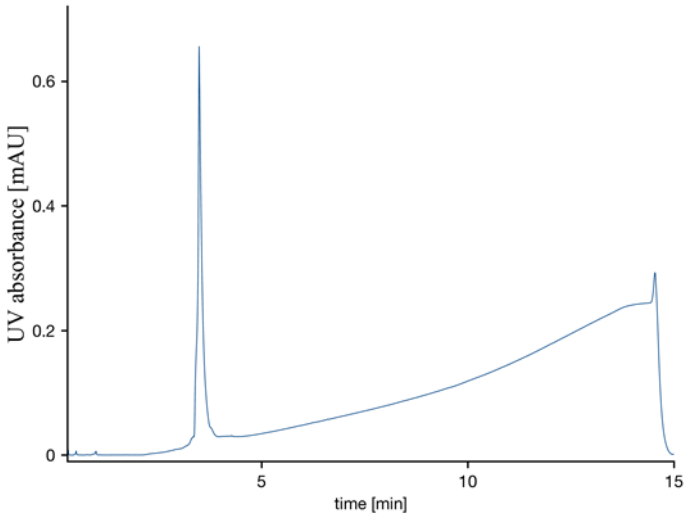

4.16. c(R_{10})-azide

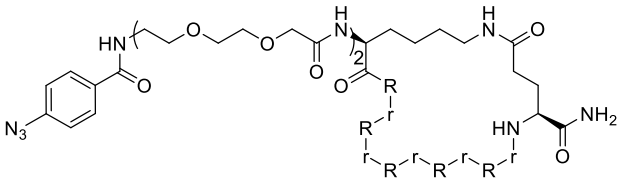

The cyclic-(R10)-azido peptide was synthesized in a 0.1 mmol scale on a Rink amide resin with a loading of 0.78mmol/g. The synthesis was carried out on a PTI synthesizer with double couplings of each amino acid (5 eq. amino acid for 40 min) in DMF. After the final PEG building block coupling the peptide, still Fmoc protected, was treated with Pd(PPh3)4 (24 mg, 20 µmol, 20 mol%) and phenylsilane (308 µl, 2.5 mmol, 2.5 eq.) in 4 ml dry CH_2Cl_2 for 1 h in order to cleave the alloc and allyl protecting groups in one step. After confirmation of full deprotection by test cleavage, cyclization with 2 eq. HATU 4 eq. DIPEA was carried out overnight in DMF. The peptide was then Fmoc-deprotected using 20% Piperidine in DMF and the 4-azidobenzoic acid (81.6 mg, 0.5 mmol, 5 eq.) was coupled to the *N*-terminus with HATU (190.1 mg, 0.5 mmol, 5 eq.) and DIPEA (170 µl, 1.0 mmol, 10 eq.) for 1 h. Finally the peptide was cleaved from the resin by treatment with 4 ml of a TFA:TIS:H2O (95:2.5:2.5) mixture for 3 h and precipitated in cold diethylether. The crude peptide was purified by preparative HPLC (Method D) and gained as white powder (62 mg as TFA-salt, 18.3 µmol 18.3% yield). MS: m/z: 752.35 $[M+3H]^{3+}$ (calcd. m/z: 751.7879)

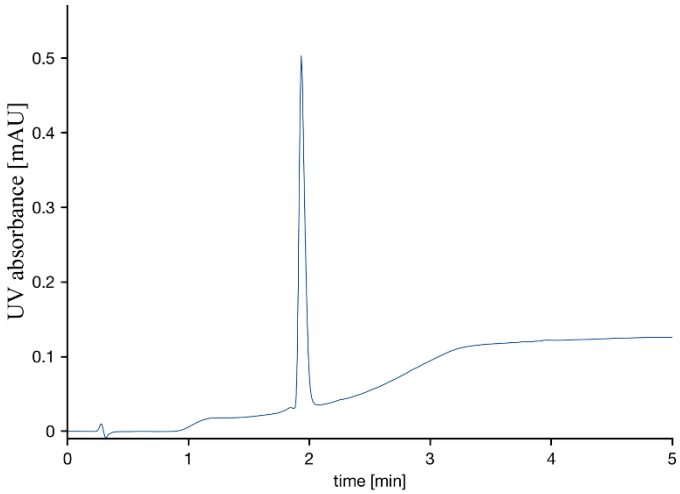

4.17. c-(R10)-ethynylphosphonamidate 9

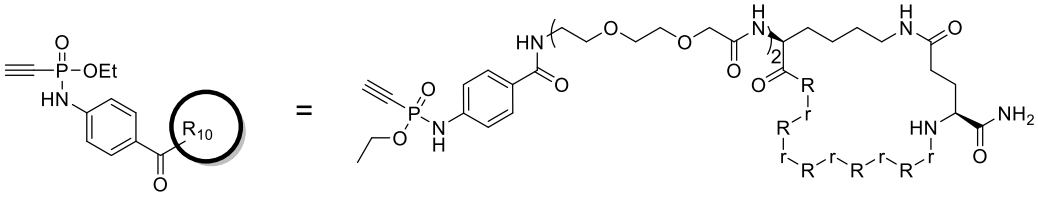

The compound was synthesized according to the general procedure 2 from 8.95 µl diethyl chlorophosphite (0.041 mmol, 4.0 eq.), 72 µl ethynylmagnesium bromide solution (0.5 M in THF, 0.041 mmol, 4.0 eq.) and 35 mg c(R10)-azide (7.6 µmol, 1 eq.). The product was gained after semi-preparative HPLC (Method D) as white powder (13 mg, 4.79 µmol, 62.9% yield). HRMS: m/z: 781.7965 $[M+3H]^{3+}$ (calcd. m/z: 781.7920).

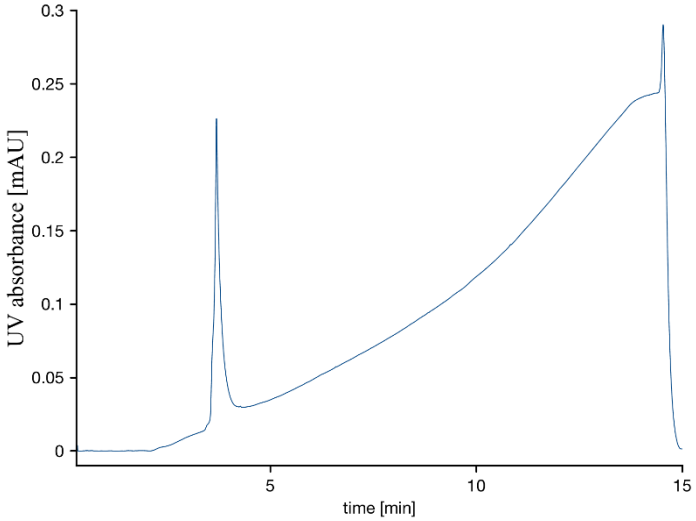

4.18. 5-((2-(*O*-Ethyl-*P*-ethynyl-phosphonamidato-*N*-benzoyl)ethyl)amino)naphthalene-1-sulfonic acid (10)

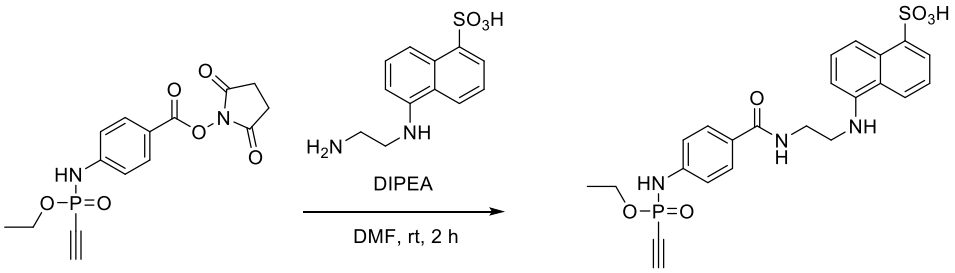

The reaction was carried out in DMF. 265 µl of a 100 mM solution of Ethyl-*N*-(4-(2,5-dioxo-1-pyrrolidinyl)oxy-carbonyl-phenyl)-*P*-ethynylphosphonamidate (0.0265 mmol, 1.00 eq.) and 1.06 ml of a 50 mM solution of 5-((2-Aminoethyl)aminonaphthalene-1-sulfonate (EDANS) (0.0530 mmol, 2.00 eq.) together with 795 µl DMF was premixed and 530 µl of a solution of 200 mM DIPEA (0.1060 mmol, 4.00 eq.) was added. The mixture was shaken for 2 h at room-temperature, all volatiles were removed under reduced pressure, the crude mixture was purified by semi-preparative HPLC using method D and the desired compound obtained as a white solid after lyophilisation. (9.30 mg, 0.0186 mmol, 70.0%)

^{1}H NMR (600 MHz, DMSO-d_6) δ = 8.78 (d, *J*=8.5, 1H), 8.57 (t, *J*=5.7, 1H), 8.36 (d, *J*=8.6, 1H), 8.11 (d, *J*=8.4, 1H), 7.99 (d, *J*=7.0, 1H), 7.80 (d, *J*=8.7, 2H), 7.43 (dd, *J*=8.5, 7.1, 1H), 7.38 (t, *J*=8.1, 1H), 7.14 (d, *J*=8.7, 2H), 6.92 (d, *J*=7.5, 1H), 4.43 (d, *J*=12.7, 1H), 4.21 – 4.05 (m, 2H), 3.62 (q, *J*=6.3, 2H), 3.46 (t, *J*=6.6, 2H), 1.31 (t, *J*=7.0, 3H). ^{13}C NMR (151 MHz, DMSO-d_6) δ = 167.03, 144.64, 143.48, 141.01, 130.59, 128.98, 127.65, 126.47, 125.13, 124.62, 123.86, 123.13, 119.62, 117.34 (d, *J*=7.8), 107.91, 91.69 (d, *J*=45.5), 77.26 (d, *J*=260.8), 62.31 (d, *J*=5.0), 45.51, 38.15, 16.42 (d, *J*=6.9). ^{31}P NMR (243 MHz, DMSO) δ = -10.35. HR-MS for $C_{23}H_{25}N_3O_6PS^+$ $[M+H]^+$ calcd.: 502.1196, found 502.1195.

4.19. Cy5-*O*-ethyl-*P*-alkynyl-phosphonamidate 11

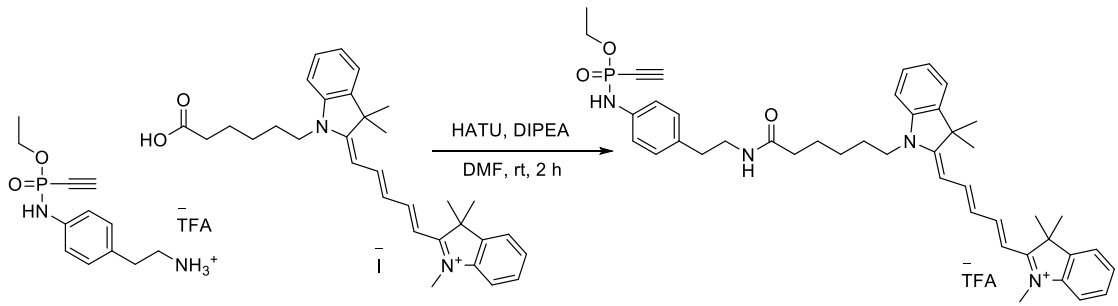

The Cy5-COOH was synthesized according to a procedure, previously published by our lab.[5] A 5-ml-round bottom flask was charged with 33.2 mg Cy5-COOH (0.0628 mmol, 1.00 eq.), 35.8 mg HATU (0.0942 mmol, 1.5 eq.) and 200 µl DMF. The deep blue solution was cooled to 0 °C and 32 µl DIPEA (0.1884 mmol, 3.0 eq.) were added. After 5 min a solution of 23 mg Ethyl-*N*-(4-(2-aminoethyl)phenyl)-*P*-ethynylphosphonamidate TFA salt (0.0628 mmol, 1.00 eq.) in 300 µl DMF were added drop-wise. The solution was allowed to warm to room-temperature and stirred for 2 h. All volatiles were removed under reduced pressure and the crude product was purified by flash column chromatography on silicagel (0% to 5% MeOH in CH_2Cl_2) and obtained as blue solid. (45 mg, 0.0590 mmol, 93.9 %).

^{1}H NMR (600 MHz, Chloroform-*d*) δ = 7.88 (td, *J*=13.0, 4.9, 2H), 7.43 – 7.33 (m, 4H), 7.23 (t, *J*=7.4, 2H), 7.15 – 7.07 (m, 4H), 7.01 (d, *J*=8.4, 2H), 6.72 (t, *J*=12.5, 1H), 6.46 (bs, 1H), 6.18 (dd, *J*=13.6, 8.5, 2H), 6.11 (q, *J*=7.6, 1H), 4.27 – 4.09 (m, 2H), 3.98 (t, *J*=7.6, 2H), 3.56 (s, 3H), 3.43 (q, *J*=6.9, 2H), 2.97 (d, *J*=12.8, 1H), 2.75 (t, *J*=7.5, 2H), 2.25 (t, *J*=7.3, 2H), 1.81 (p, *J*=8.0, 2H), 1.73 – 1.67 (m, 2H), 1.70 (s, 6H),

1.69 (s, 6H), 1.55 – 1.42 (m, 2H), 1.35 (t, *J*=7.1, 3H). ^{13}C NMR (151 MHz, CDCl3) δ = 173.64, 173.19, 173.11, 153.34, 152.99, 142.72, 141.90, 141.17, 140.89, 136.88, 133.32, 129.69, 128.78, 128.66, 126.32, 126.22, 125.34, 125.15, 122.21, 122.13, 118.60, 118.53, 110.83, 110.36, 103.77, 103.64, 88.54, 88.23, 75.27, 62.46, 49.40, 49.17, 44.22, 41.03, 35.94, 34.78, 27.96, 27.90, 27.84, 27.09, 26.32, 25.24, 16.17, 16.11, 16.04. ^{31}P NMR (243 MHz, CDCl3) δ = -9.08. HR-MS for $C_{44}H_{54}N_4O_3P^+$ $[M]^+$ calcd.: 717.3928, found 717.3895.

4.20. Ethyl-*N*-phenyl-*P*-(*Z*-ethylthioethenyl) phosphonamidate

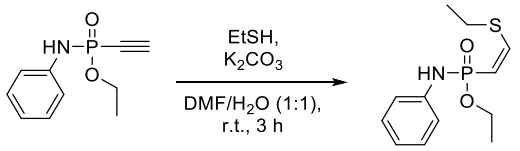

A 5-ml round bottom flask was charged with 50 mg Ethyl-*N*-phenyl-*P*-ethynylphosphonamidate (0.239 mmol, 1.0 eq.), 13.2 mg potassium carbonate (0.096 mmol, 0.4 eq.), 0.5 ml DMF and 0.5 ml water. 26.5 µl ethane thiol (0.359 mmol, 1.5 eq.) were added through a microliter syringe and the solution was stirred for 3 h at room temperature. All volatiles were removed under reduced pressure and the crude product was purified by flash column chromatography on silicagel (70% EtOAc in *n*-hexan to 100% EtOAc) and obtained as a yellowish solid. (56.0 mg, 0.206 mmol, 86.3%)

^{1}H NMR (600 MHz, Chloroform-*d*) δ 7.22 (t, *J* = 7.9 Hz, 2H), 7.12 (dd, *J* = 46.4, 12.5 Hz, 1H), 7.05 – 6.99 (m, 2H), 6.92 (t, *J* = 7.4 Hz, 1H), 6.65 (d, *J* = 6.1 Hz, 1H), 5.77 (dd, *J* = 16.5, 12.5 Hz, 1H), 4.40 – 3.97 (m, 2H), 2.73 (q, *J* = 7.4 Hz, 2H), 1.35 (t, *J* = 7.1 Hz, 3H), 1.26 (t, *J* = 7.4 Hz, 3H). ^{13}C NMR (75 MHz, Chloroform-d) δ 149.92, 140.44 (d, J = 1.0 Hz), 129.07, 121.03, 117.39, 117.30, 113.32, 110.94, 60.25 (d, J = 6.0 Hz), 29.42, 16.30 (d, J = 7.0 Hz), 15.40. ^{31}P NMR (122 MHz, CDCl3) δ 14.73. HR-MS for $C_{12}H_{19}NO_2PS^+$ $[M+H]^+$ calcd.: 272.0869, found 272.0856.

4.21. Ethyl-*N*-phenyl-*P*-(*E*-ethylthioethenyl) phosphonamidate

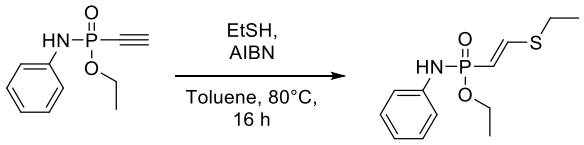

A 5-ml round bottom flask was charged with 40 mg Ethyl-*N*-phenyl-*P*-ethynylphosphonamidate (0.191 mmol, 1.0 eq.), 12.6 mg azobisisobutyronitrile (0.076 mmol, 0.4 eq.), 16.5 µl ethane thiol (0.229 mmol, 1.2 eq.) and 0.8 ml toluene. The brownish solution was heated to 80 °C over night. The reaction mixture was purified by flash column chromatography on silicagel (70% EtOAc in *n*-hexan to 100% EtOAc) and obtained as a yellowish solid. (22.0 mg, 0.081 mmol, 42.1%)

^{1}H NMR (300 MHz, Chloroform-*d*) δ 7.44 (dd, *J* = 21.6, 16.8 Hz, 1H), 7.28 – 7.20 (m, 2H), 7.03 – 6.90 (m, 3H), 6.33 (d, *J* = 6.0 Hz, 1H), 5.74 (t, *J* = 16.8 Hz, 1H), 4.40 – 3.85 (m, 2H), 2.75 (q, *J* = 7.4 Hz, 2H), 1.34 (t, *J* = 7.0 Hz, 3H), 1.28 (t, *J* = 7.4 Hz, 3H). ^{13}C NMR (75 MHz, Chloroform-*d*) δ 148.42 (d, *J* = 9.1 Hz), 140.34, 129.34, 121.23, 117.25, 117.16, 111.53, 109.13, 60.55 (d, *J* = 6.0 Hz), 25.76, 16.27 (d, *J* = 7.1 Hz), 13.64. ^{31}P NMR (122 MHz, $CDCl_3$) δ 15.42. HR-MS for $C_{12}H_{19}NO_2PS^+$ $[M+H]^+$ calcd.: 272.0869, found 272.0856.

4.22. DABCYl-Cys peptide

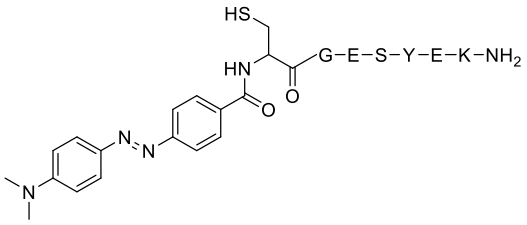

DABCYl-Cys peptide was synthesized by standard Fmoc-based chemistry in a linear synthesis by manual coupling. 0.1 mmol of Rink amide resin (subst: 0.4 mmol/g) was added to a reaction vessel and synthesis was performed with five-fold amino acid excess. Fmoc de-blocking was achieved by resin treatment with 20% piperidine in DMF twice for 5 min. Coupling was achieved by addition of HOBt/HBTU/DIPEA (5 eq./5 eq./10 eq) in DMF for 45 min. After the final Cys coupling, 5 eq. of the DABCYL acid was coupled with 5 eq. HATU and 10 eq. DIPEA in DMF for 45 min. The peptide was cleaved of the resin by addition of TFA/DTT/TIS (95/2.5/2.5, *w*,*w*,*w*) within 3 h. Subsequently, the peptide was precipitated by the addition of ice-cold diethyl ether. The precipitate was collected by centrifugation, dried and purified by preparative HPLC (method C). The peptide was obtained as a red solid in a yield of 35.8% (38.2 mg, 35.8 µmol). ESI-MS for $C_{48}H_{66}N_{12}O14S^{+}$ $[M+2H]^{+}$ calcd.: 533.23, found 533.34.

4.23. DABCYl-Cys peptide phosphonamidate EDANS adduct

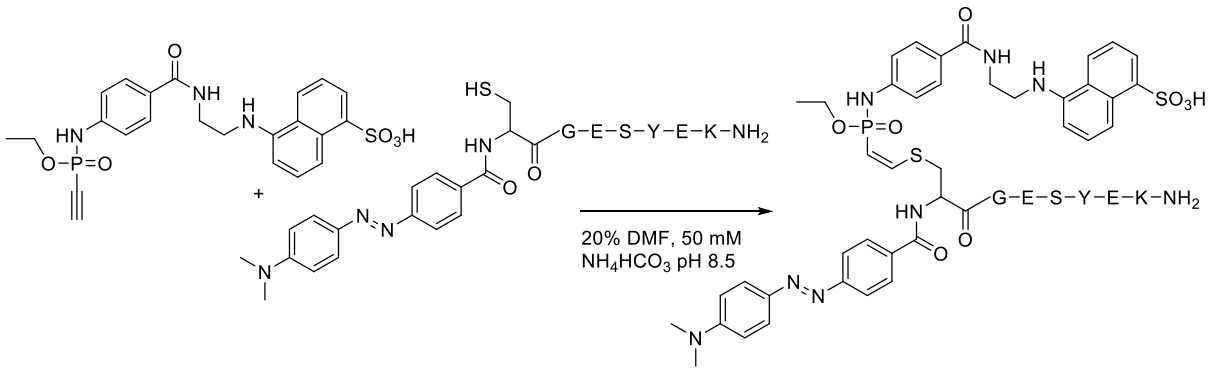

A 1.5-ml Eppendorf tube was charged with 263 µl of a solution of DABCYL-Cys peptide (20 mM) in 50 mM NH_4HCO_3 at a pH of 8.5. 158 µl 50 mM NH_4HCO_3 at a pH of 8.5 and 105 µl of a solution of EDANS phosphonamidate (100 mM) in DMF was added to give a final concentration of 20 mM peptide and 10 mM phosphonamidate in 20% DMF/Buffer. The tube was shaken at 800 rpm at room temperature for 3 h. All volatiles were removed under reduced pressure and the crude product purified by semi-preparative HPLC (method E). The peptide was obtained as a red solid. HR-MS for $C_{71}H_{90}N_{15}O_{20}PS_2^{2+}$ $[M+2H]^{2+}$ calcd.:783.7827, found 783.7804.

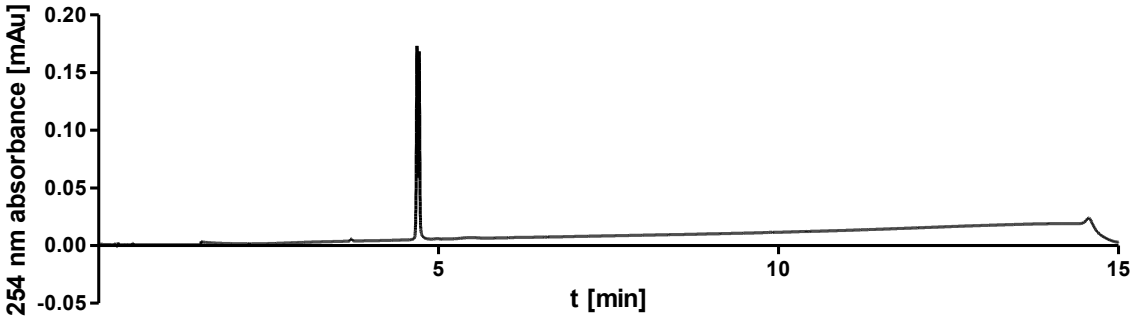

4.24. DABCYl-Cys peptid maleimide EDANS adduct

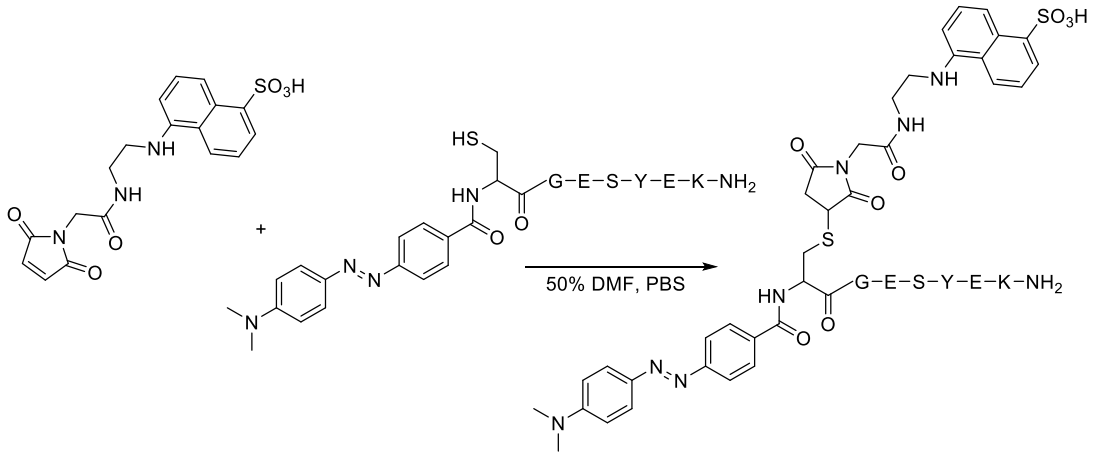

A 1.5-ml Eppendorf tube was charged with 188 µl of a solution of DABCYl-Cys peptide (20 mM) in PBS. 188 µl of a solution of EDANS maleimide (40 mM) in DMF was added to give a final concentration of 10 mM peptide and 20 mM maleimide in 50% DMF/buffer. The tube was shaken at 800 rpm at room temperature for 3 h. All volatiles were removed under reduced pressure and the crude product purified by semi-preparative HPLC (method E). The peptide was obtained as a red solid. HR-MS for $C_{66}H_{83}N_{15}O_{20}S_2^{2+}$ $[M+2H]^{2+}$ calcd. 734.7685, found. 734.7698.

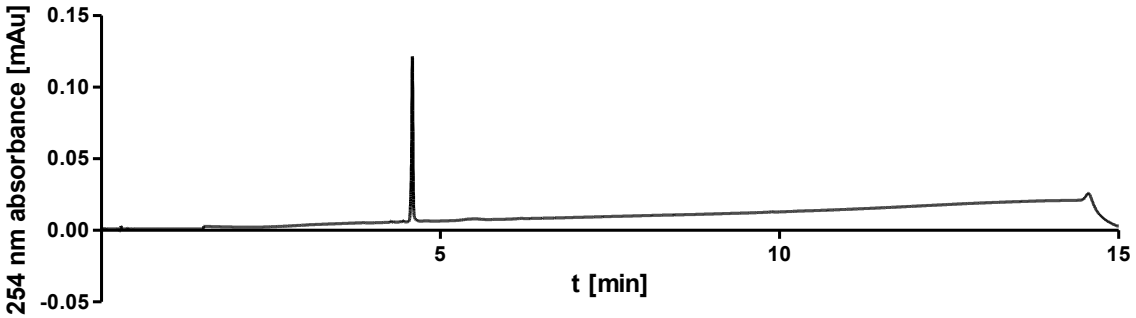

5. NMR spectra

Diethyl ethynylphosphonite (crude reaction mixture)

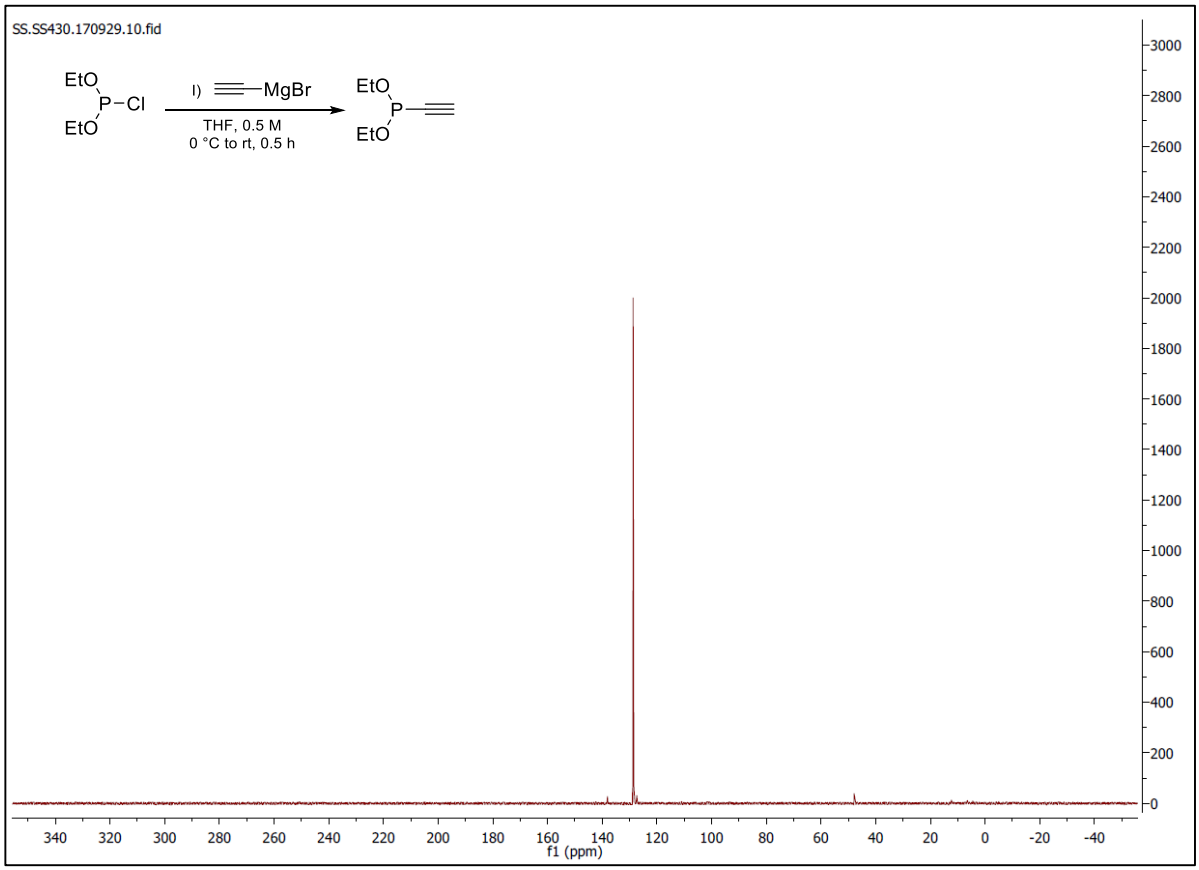

Ethyl-*N*-phenyl-*P*-ethynylphosphonamidate (**1**)

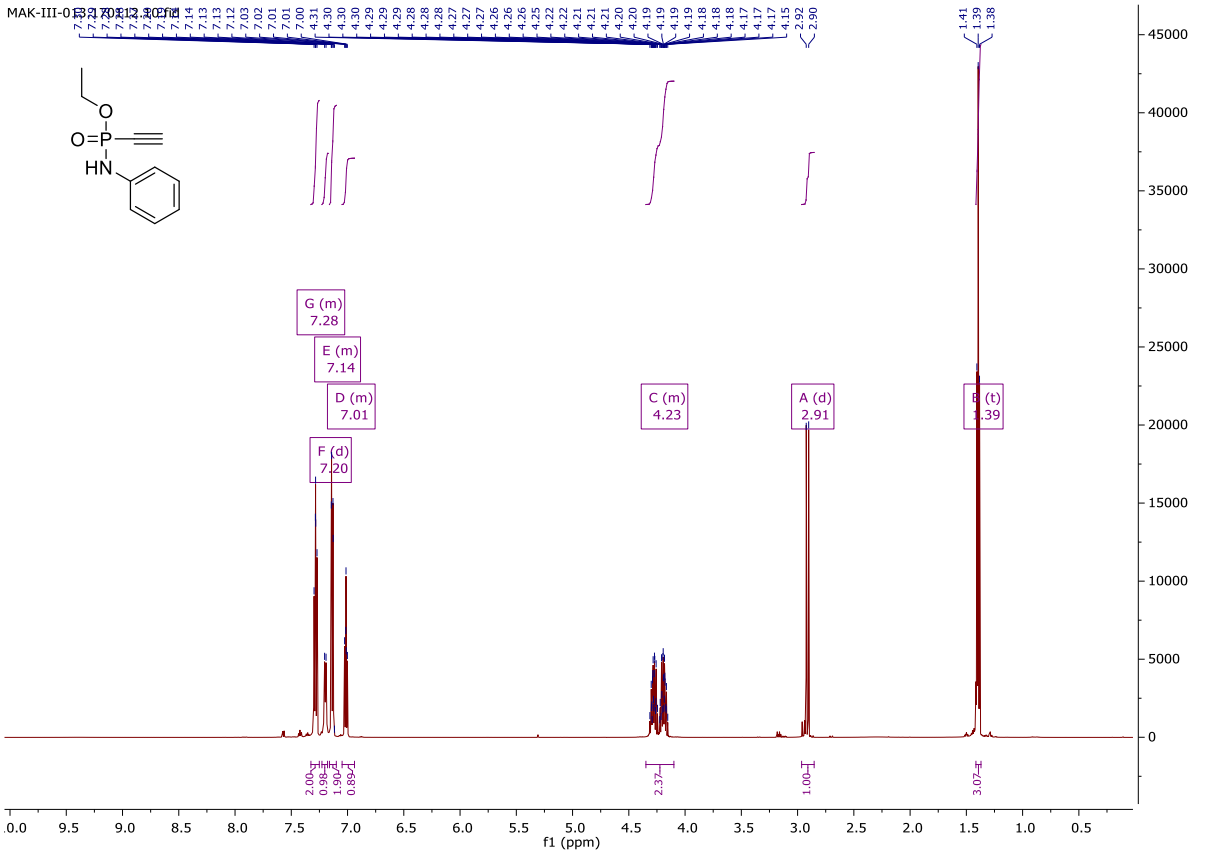

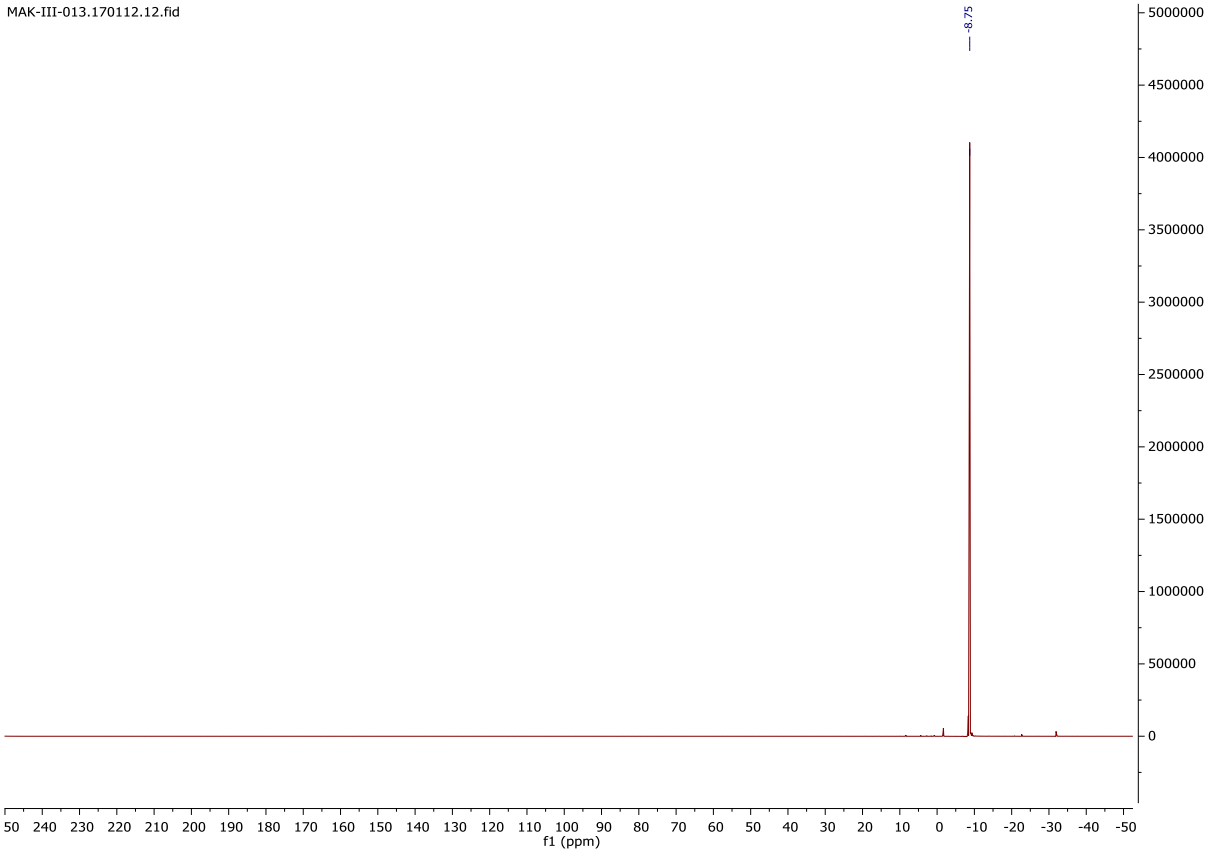

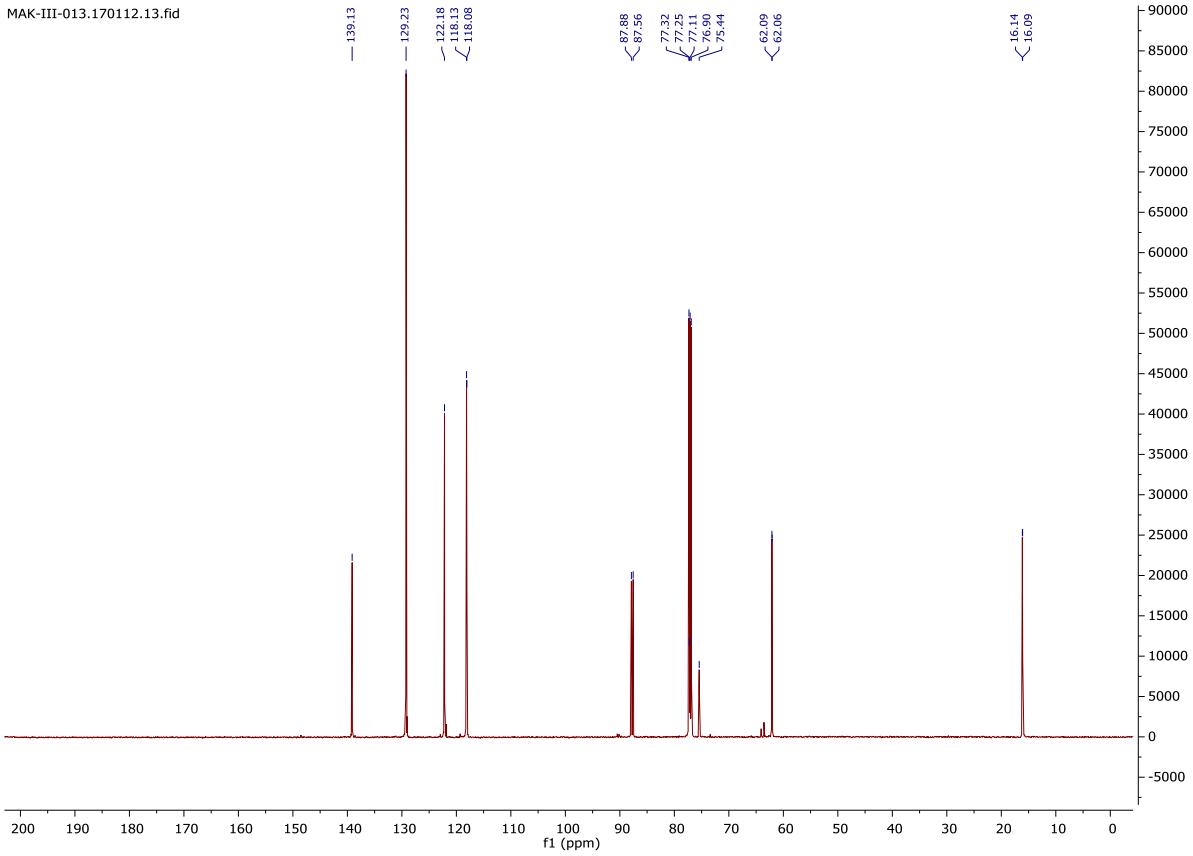

Ethyl-*N*-(4-carboxy-phenyl)-*P*-ethynylphosphonamidate (**2**)

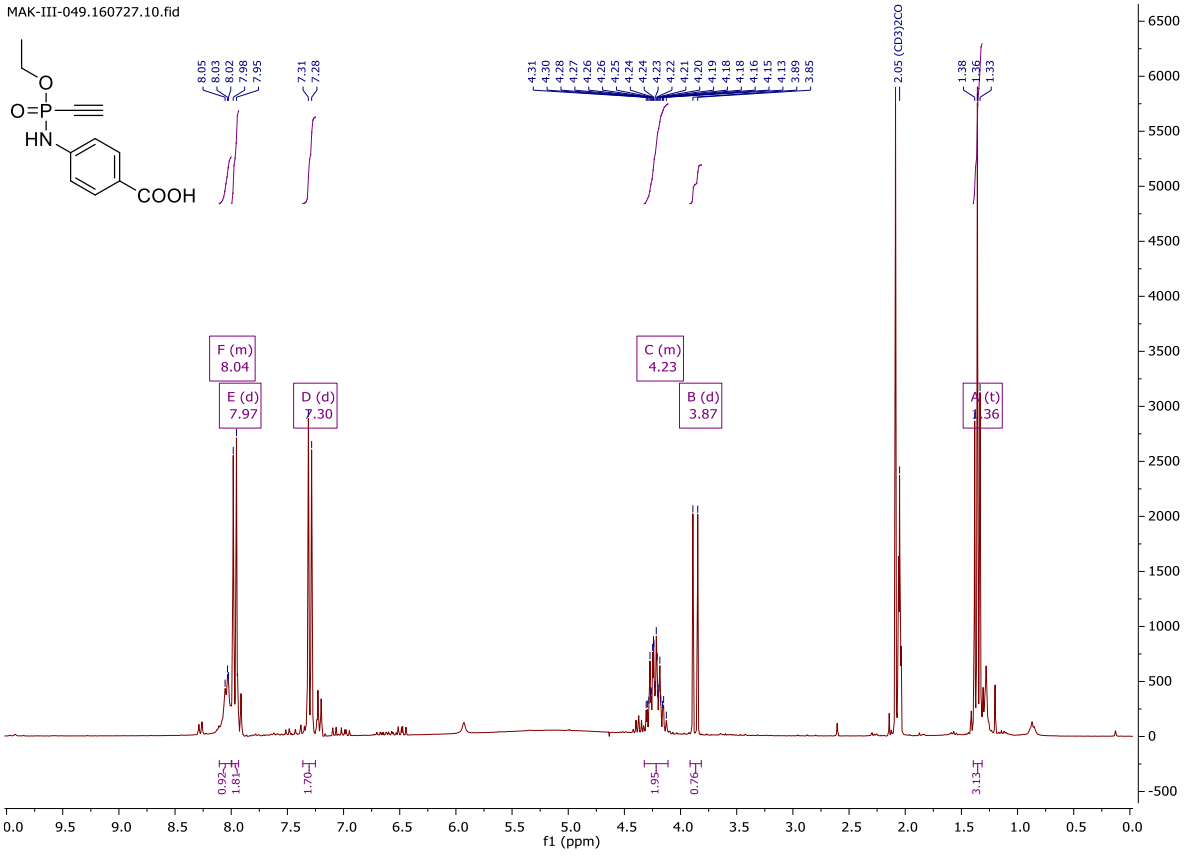

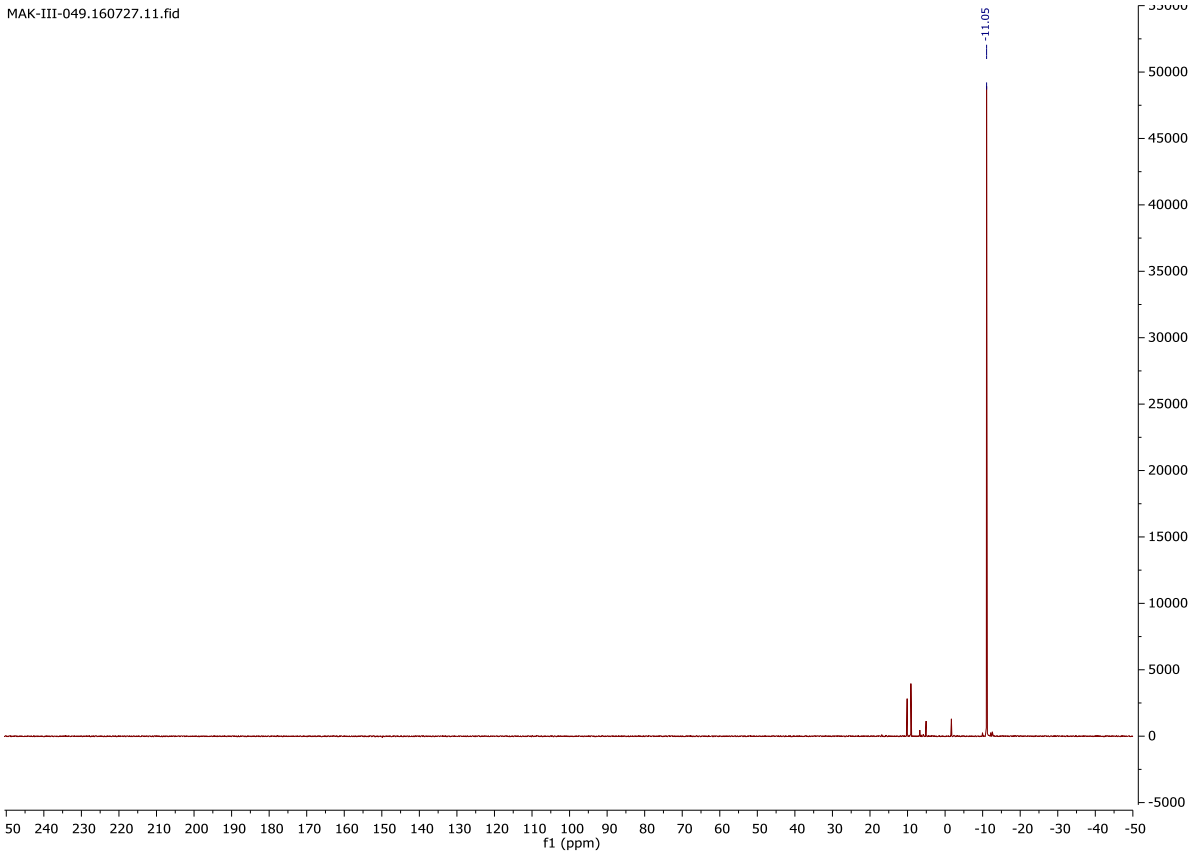
MAK-III-049.160727.11.fid
-11.05
f1 (ppm)

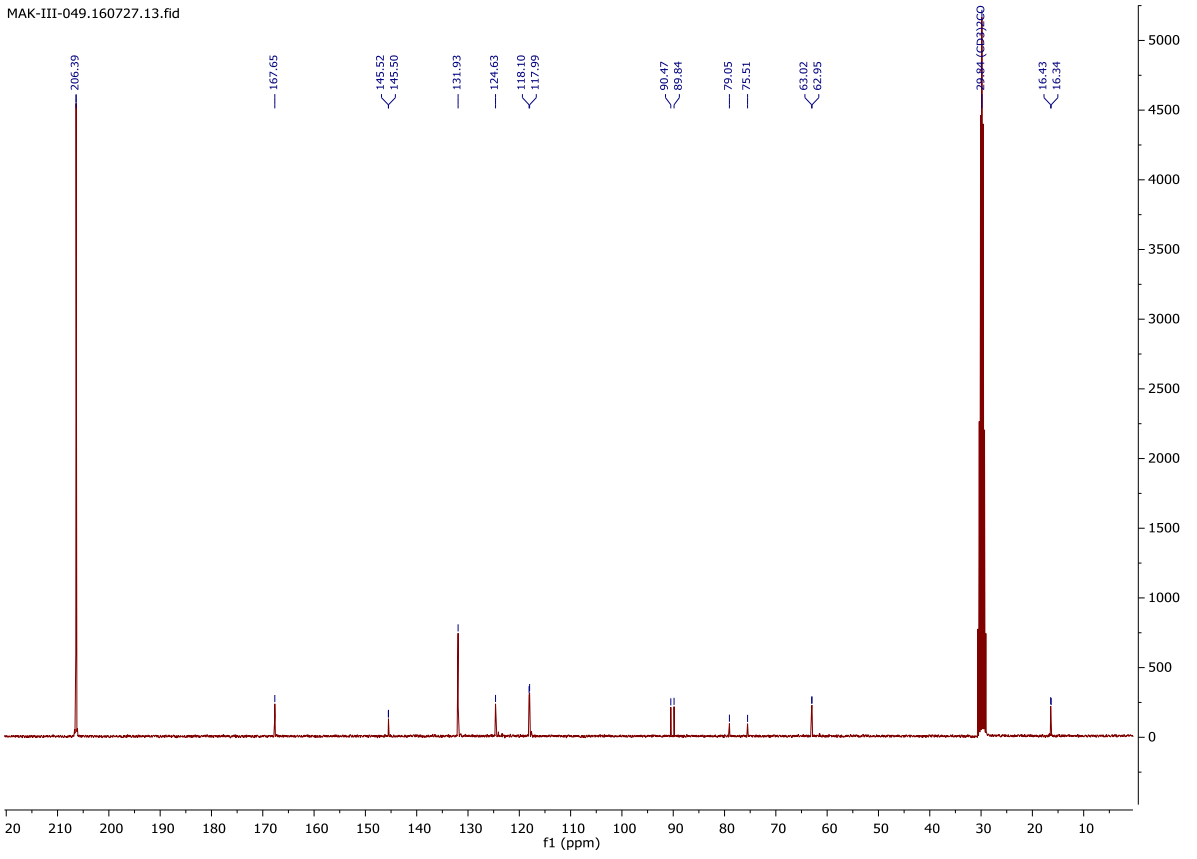
MAK-III-049.160727.13.fid
206.39
167.65
145.52
145.50
131.93
124.63
118.10
117.99
90.47
89.84
79.05
75.51
63.02
62.95
16.43
16.34
f1 (ppm)

Ethyl-*N*-(4-(2,5-dioxo-1-pyrrolidinyl)oxy-carbonyl-phenyl)-*P*-ethynylphosphonamidate (**3**)

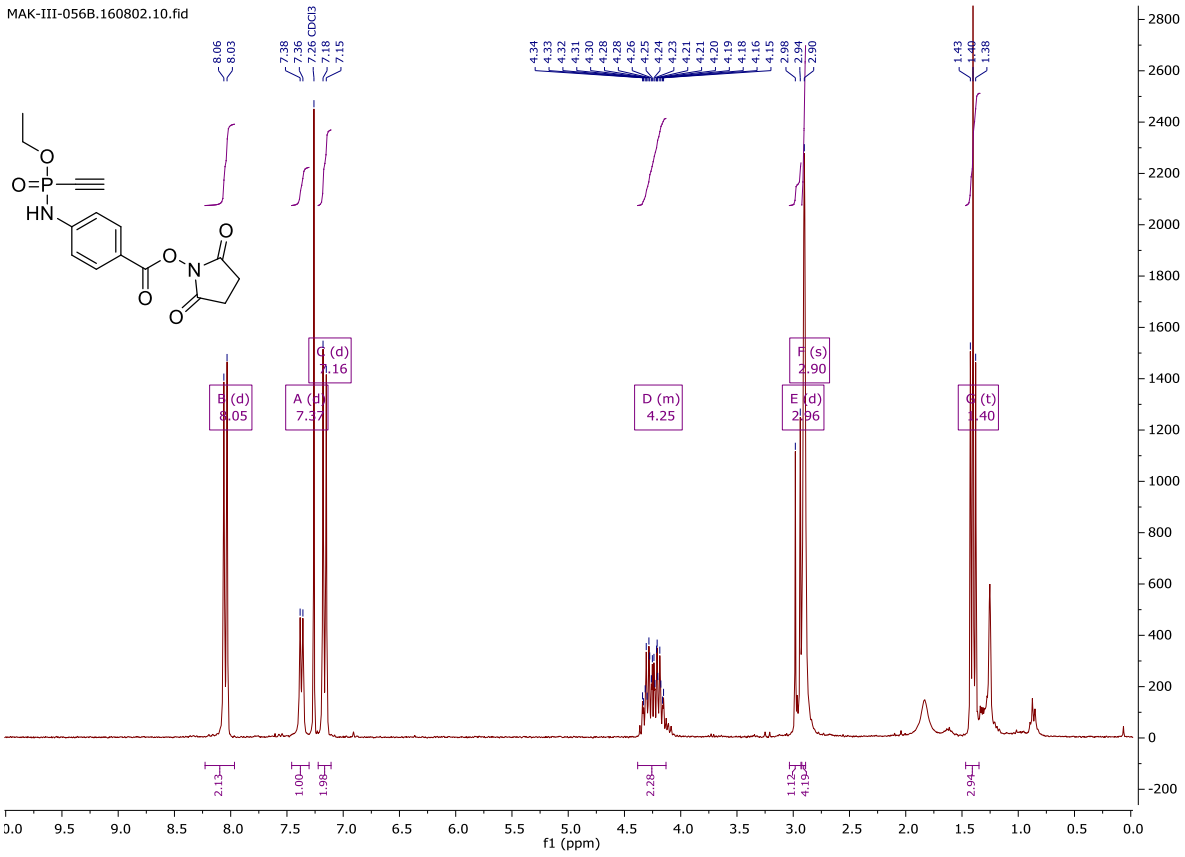

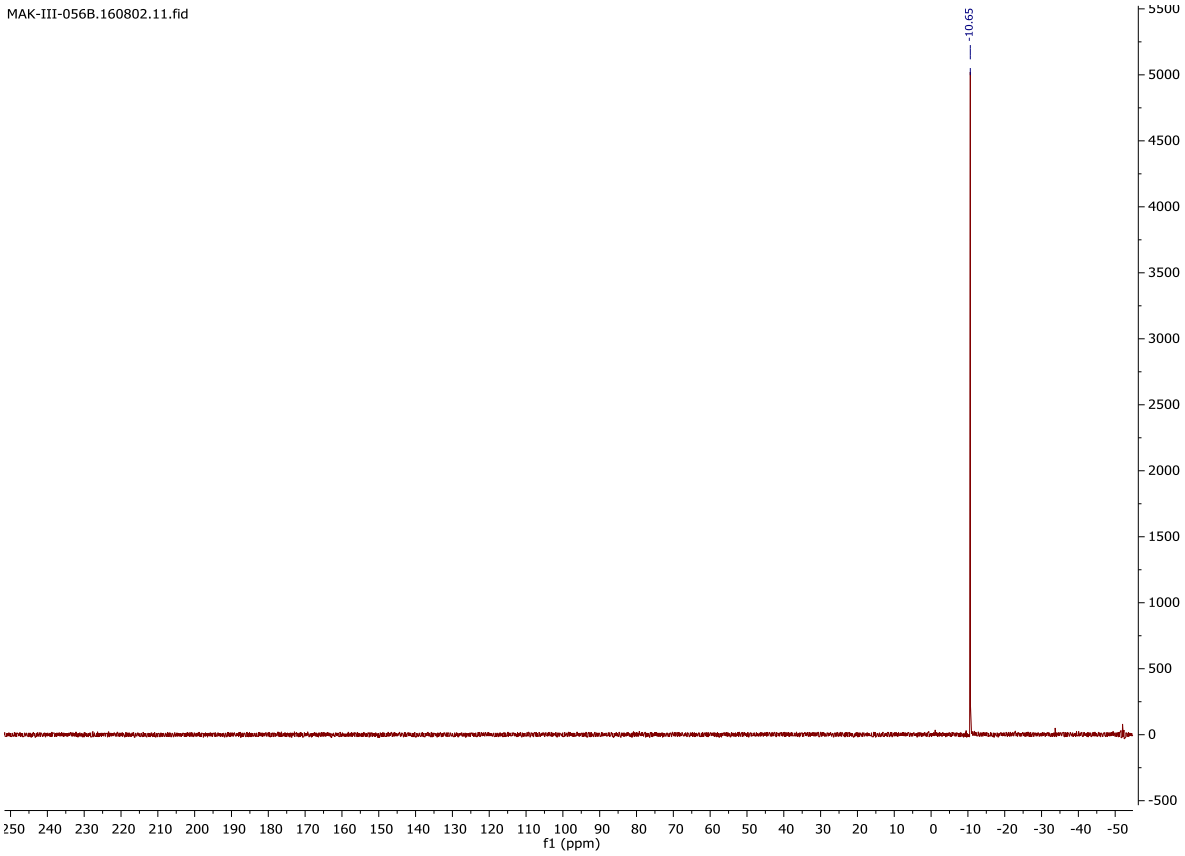

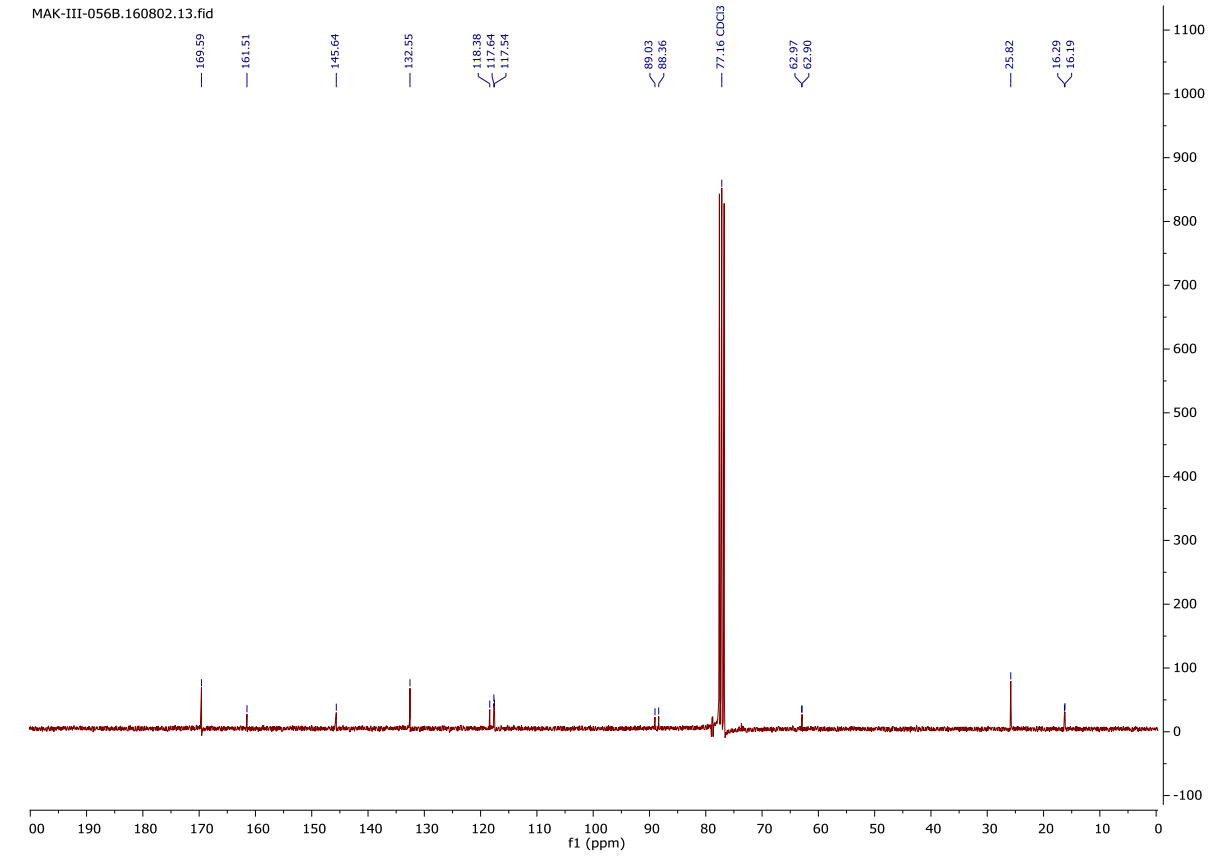

2-(4-Azidophenyl)-ethyl phtalimide

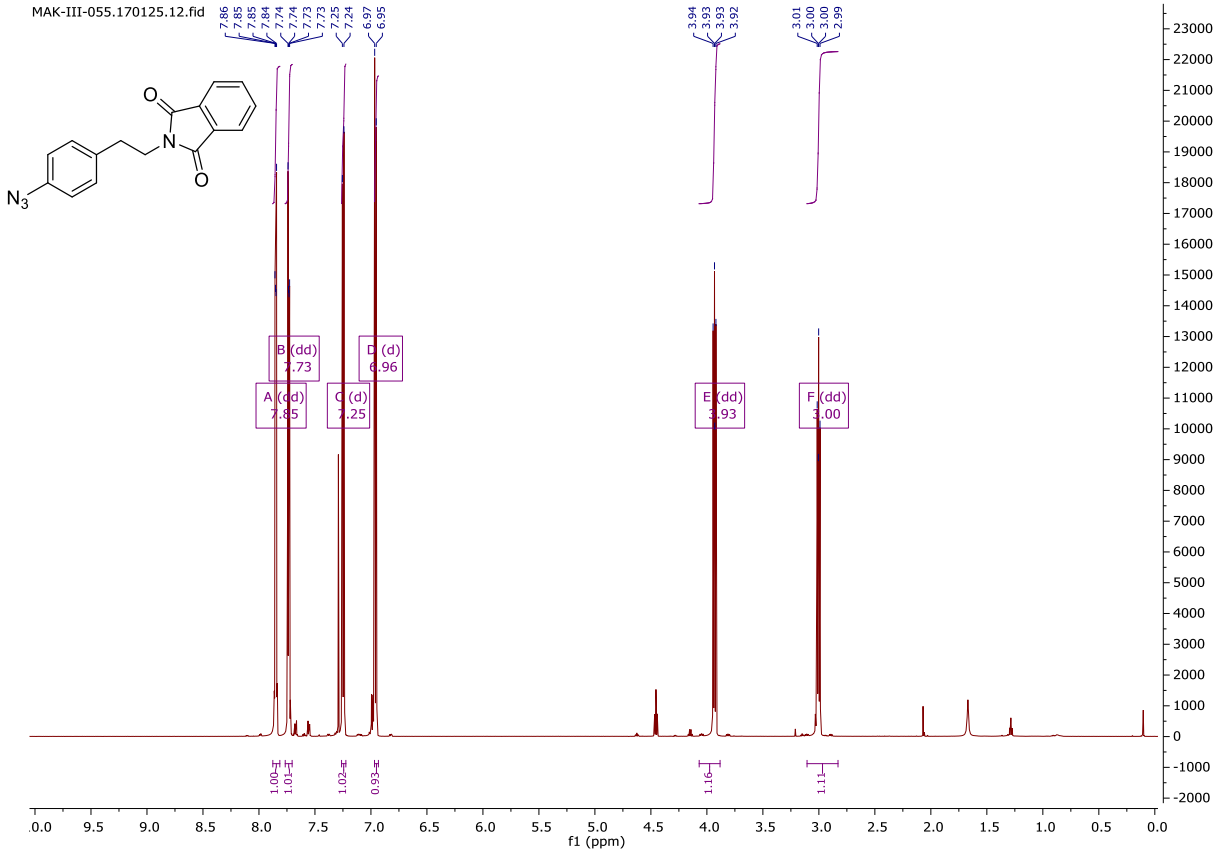

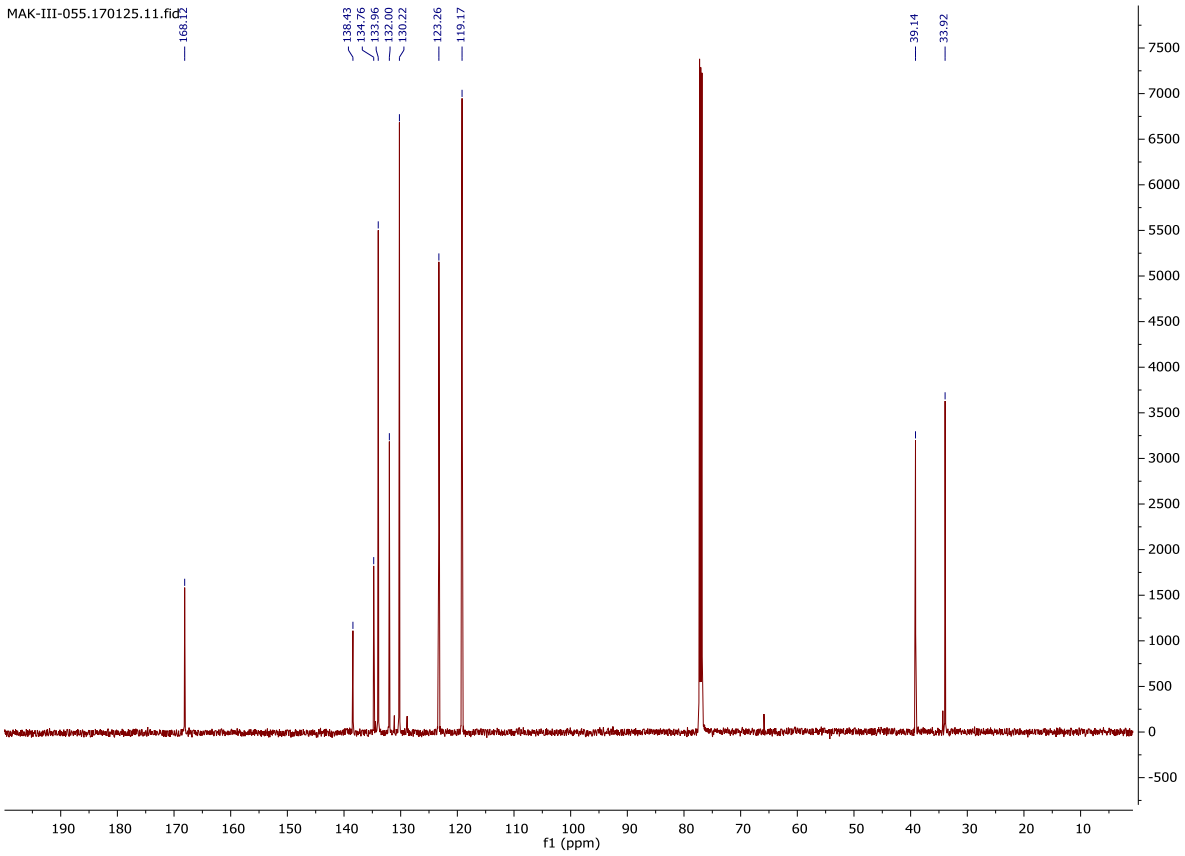

Ethyl-*N*-(4-(2-aminoethyl)phenyl)-*P*-ethynylphosphonamidate TFA salt (**4**)

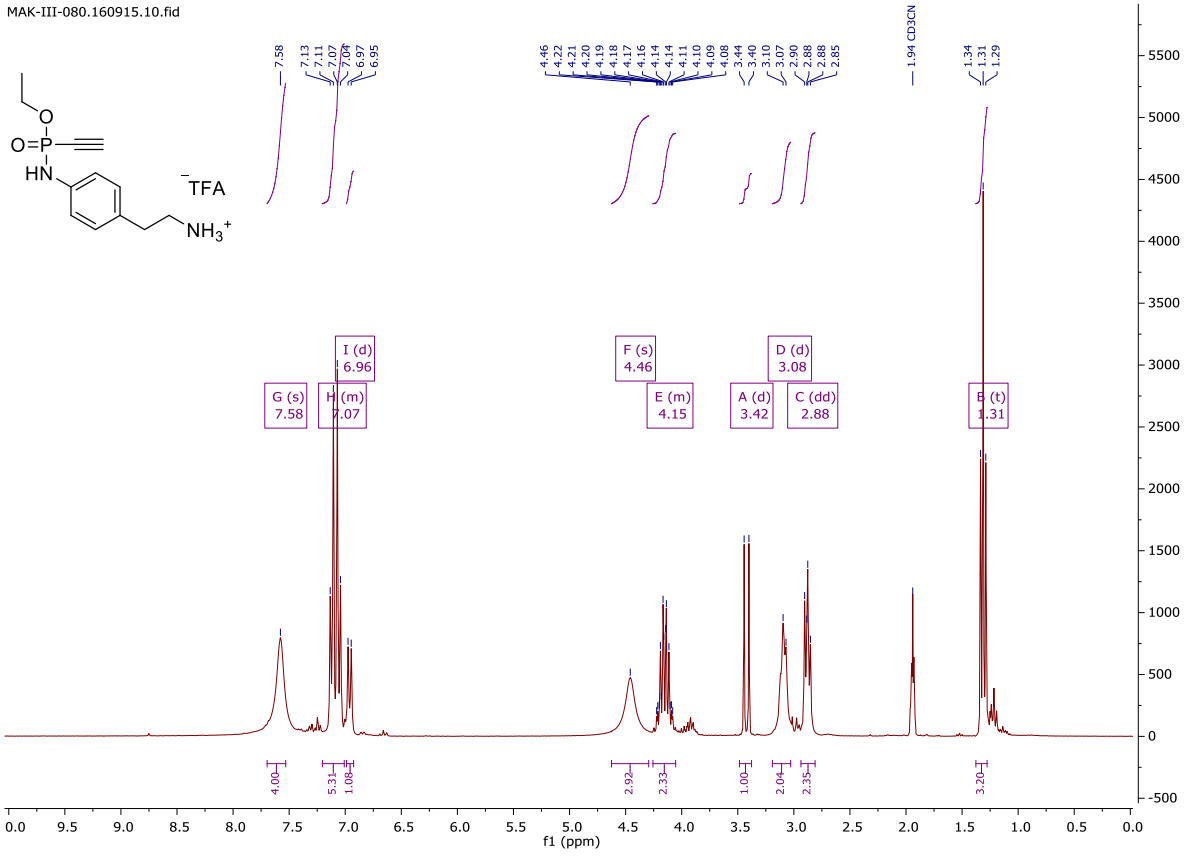

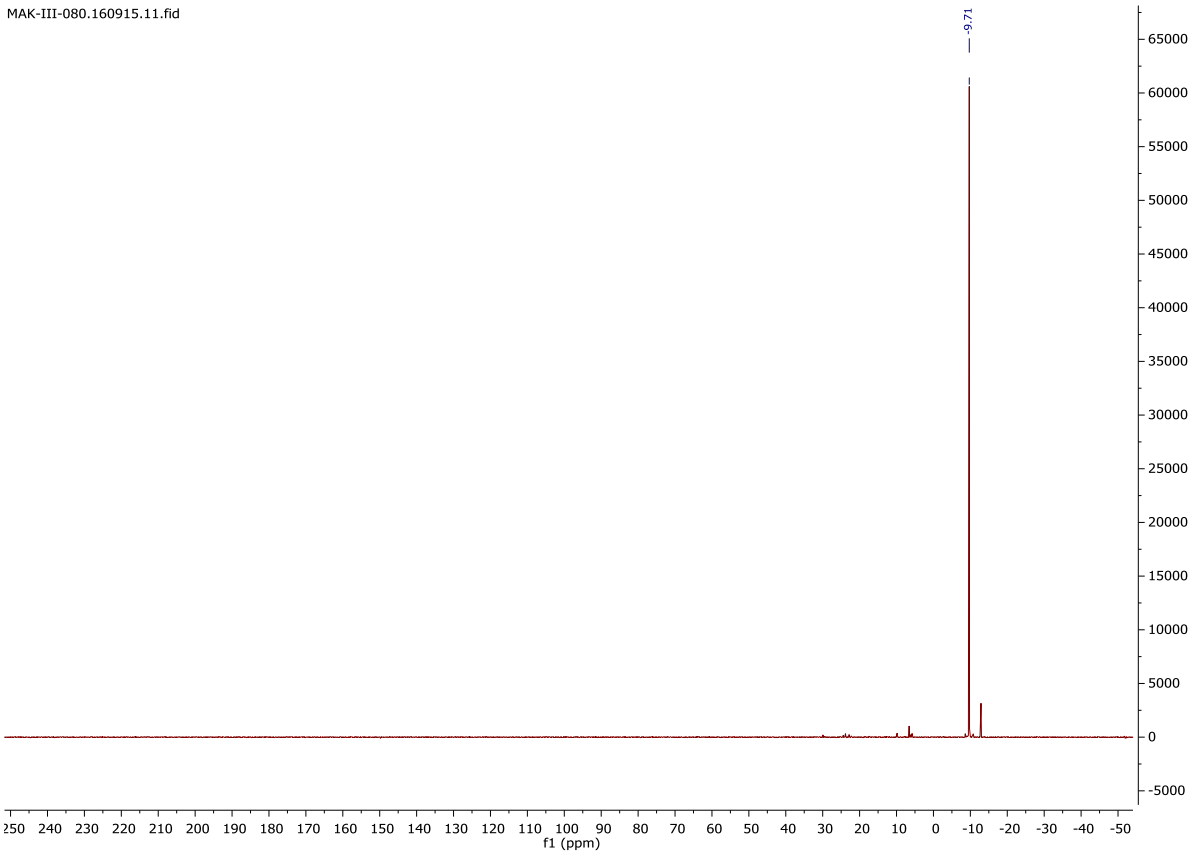
MAK-III-080.160915.11.fid
-9.71
f1 (ppm)

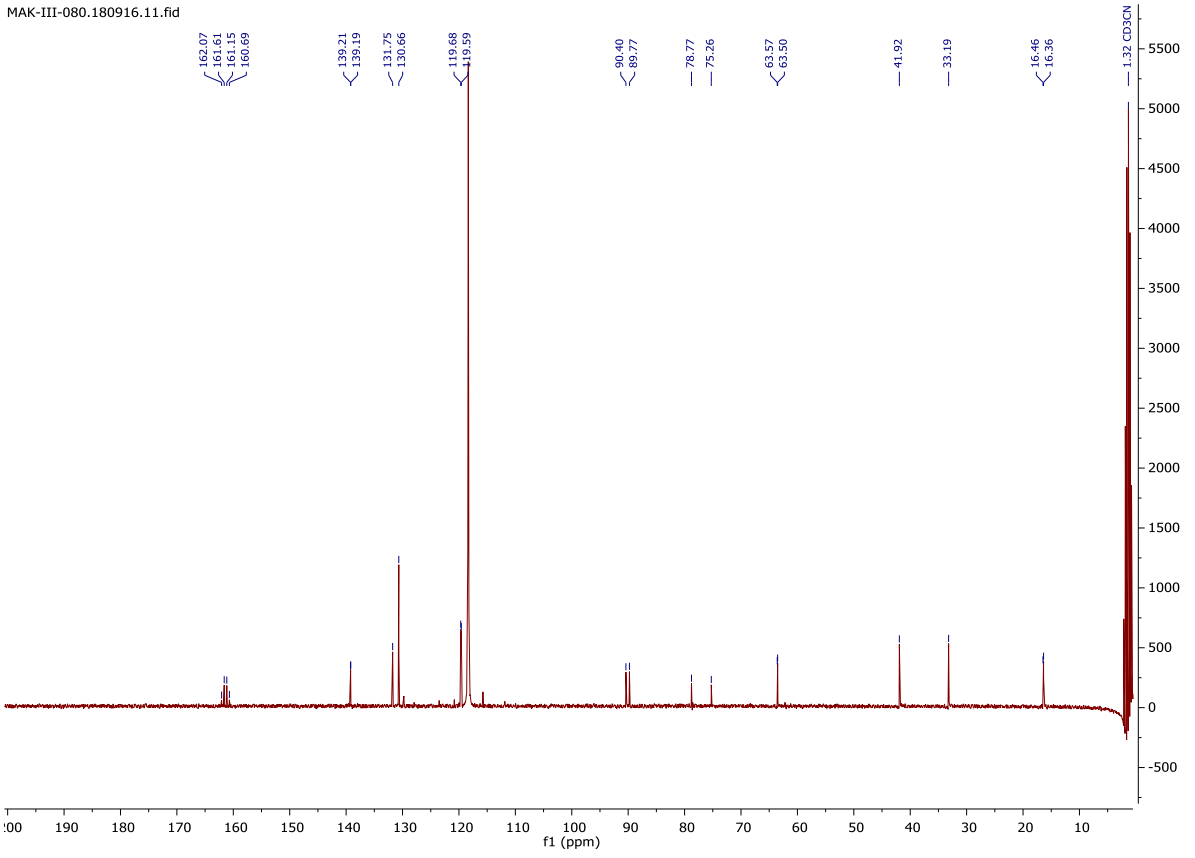
MAK-III-080.180916.11.fid
162.07
161.61
161.15
160.69
139.21
139.19
131.75
130.66
119.68
119.59
90.40
89.77
78.77
75.26
63.57
63.50
41.92
33.19
16.46
16.36
1.32 CD3CN
f1 (ppm)

N-(4-azidophenyl) biotinamide

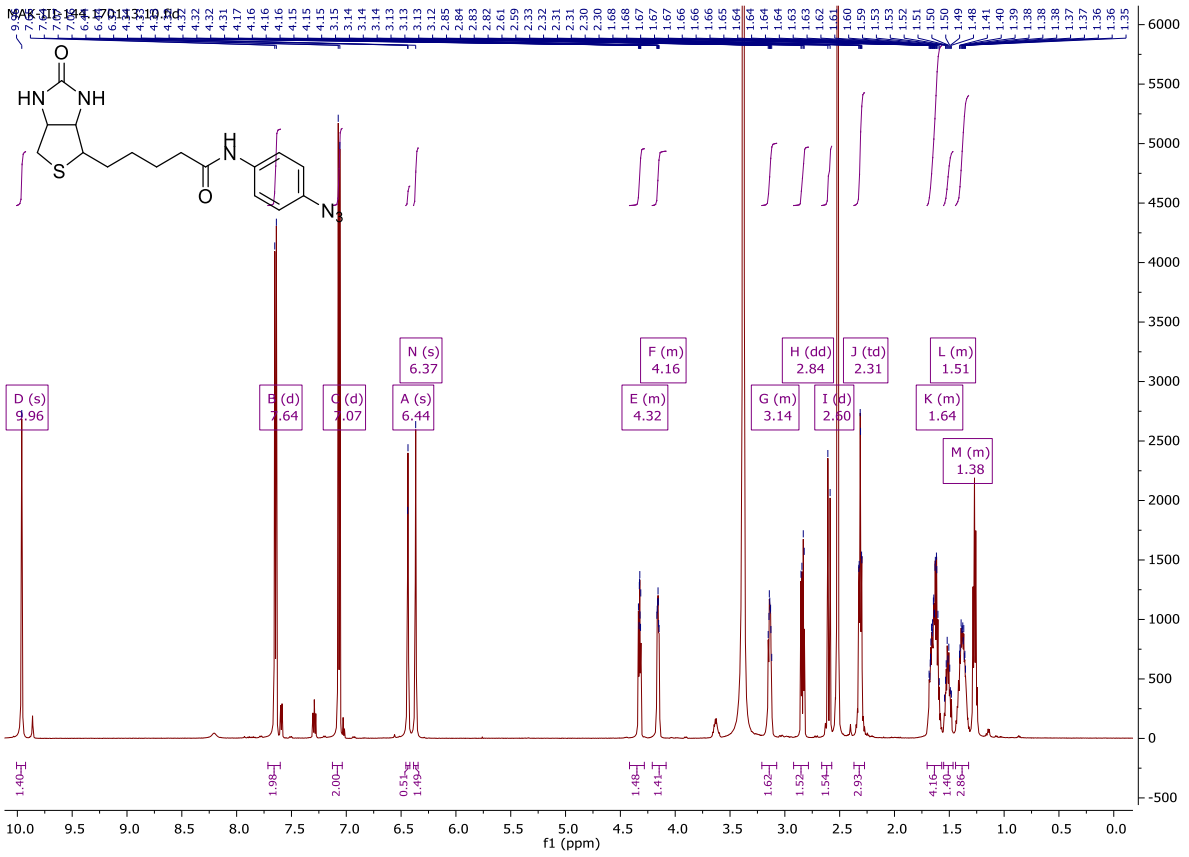

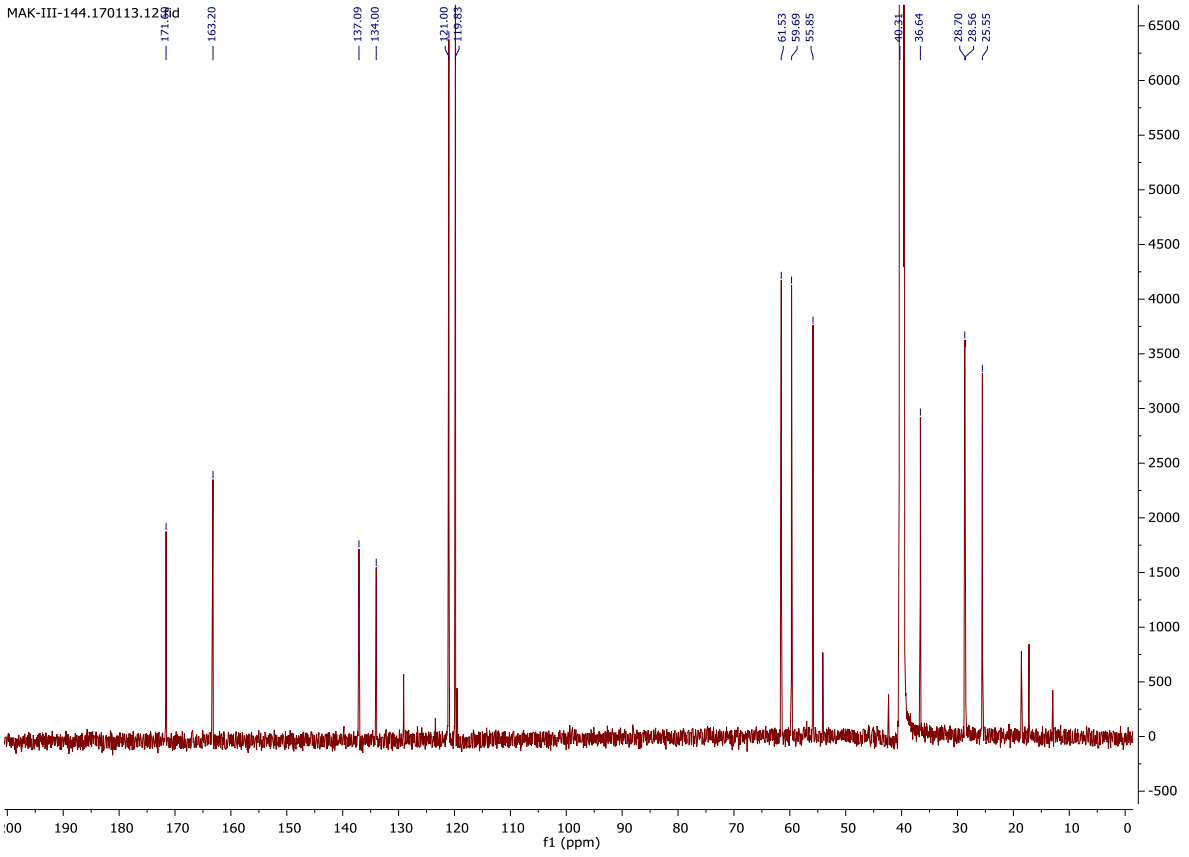

Ethyl-*N*-(4-biotinamido-phenyl)-*P*-ethynylphosphonamidate (**5**)

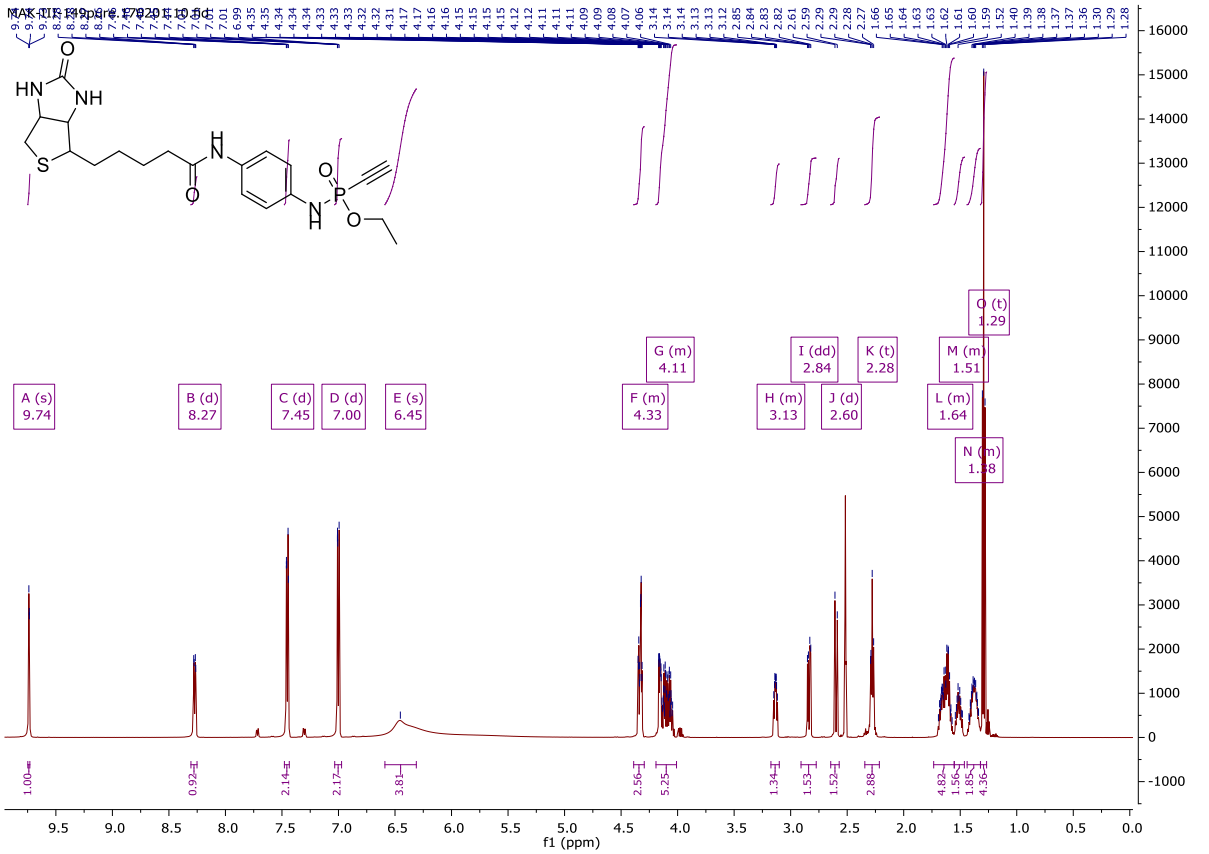

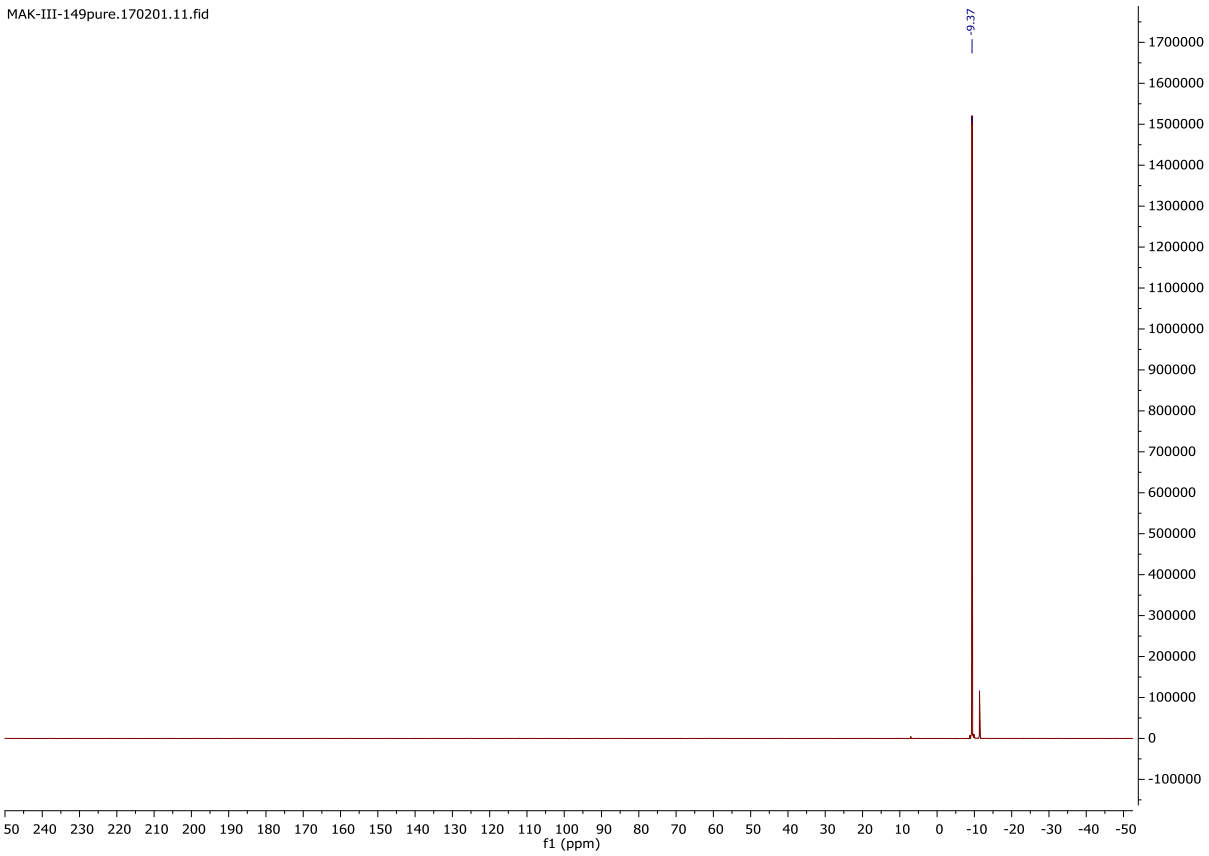

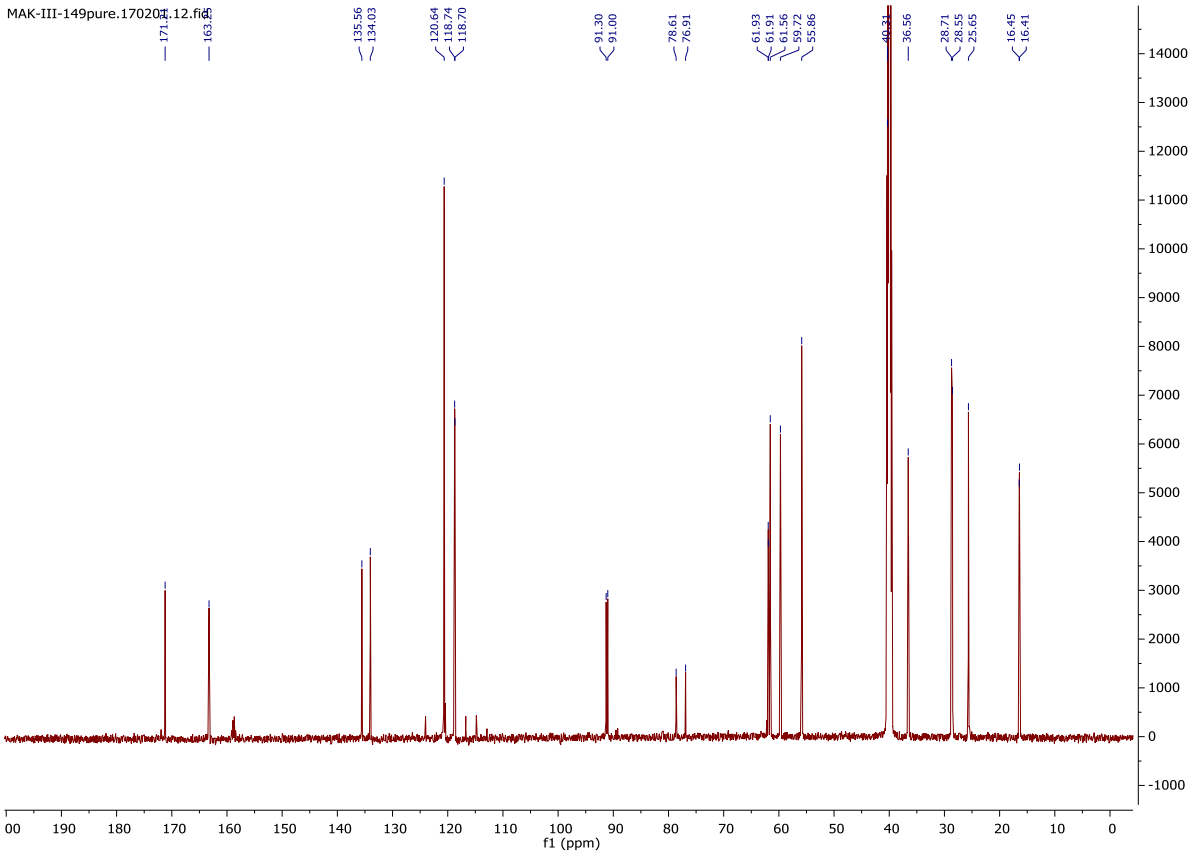

Ethyl-*N*-(3-phenyl-propyl)-*P*-ethynylphosphonamidate (**6**)

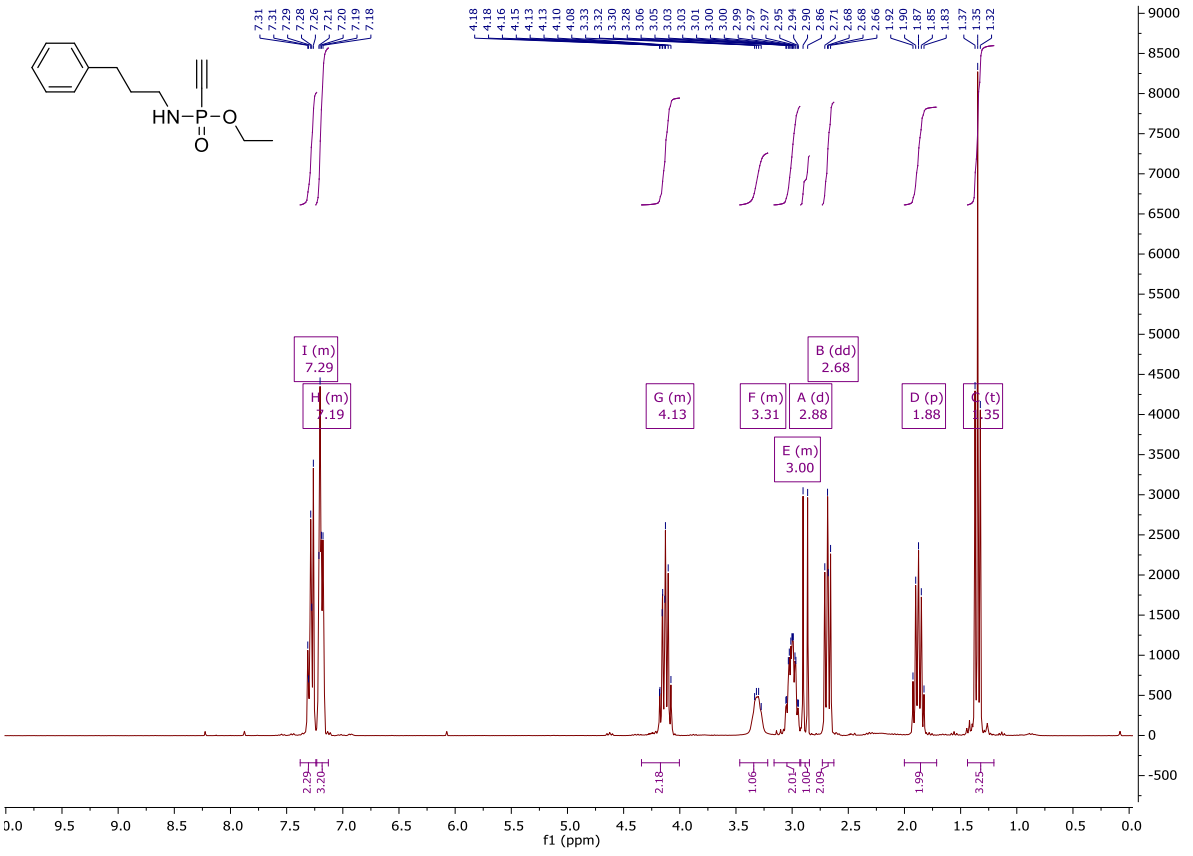

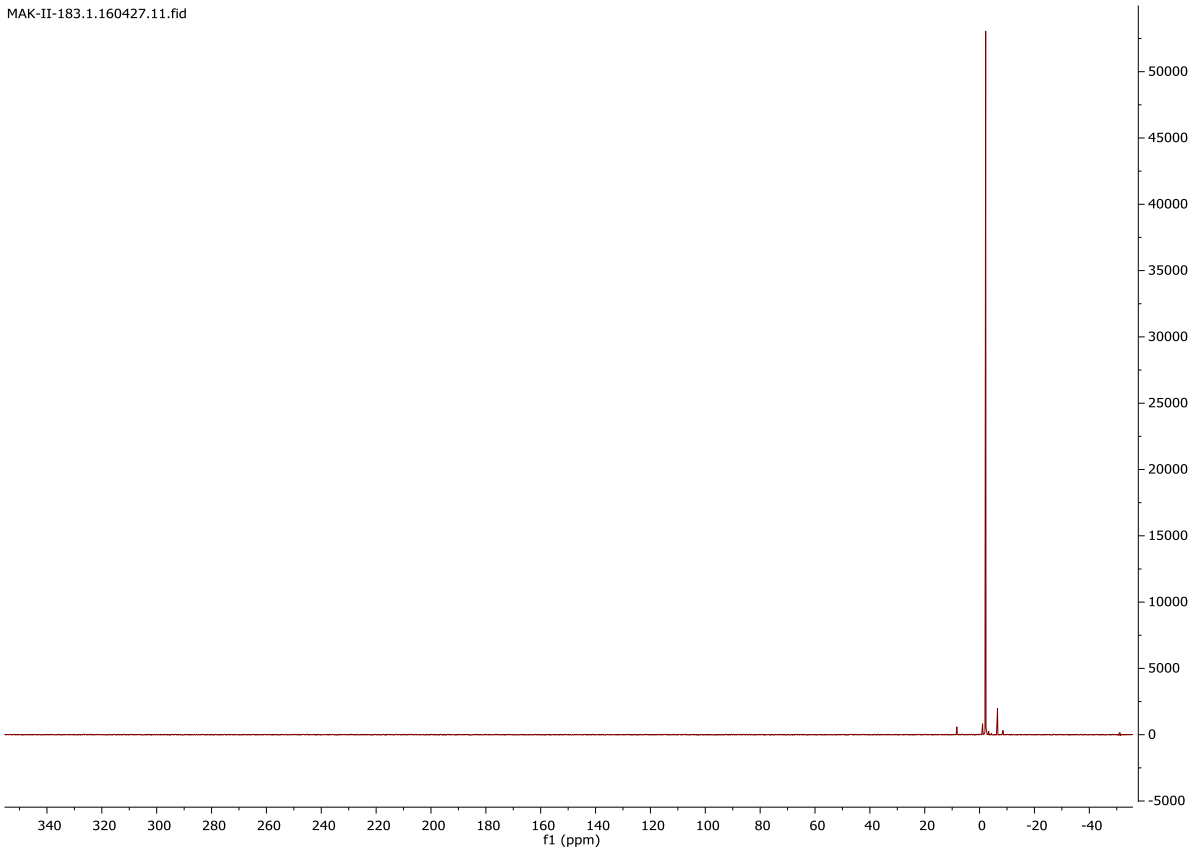
MAK-II-183.1.160427.11.fid
50000
45000
40000
35000
30000
25000
20000
15000
10000
5000
0
-5000
340 320 300 280 260 240 220 200 180 160 140 120 100 80 60 40 20 0 -20 -40
f1 (ppm)

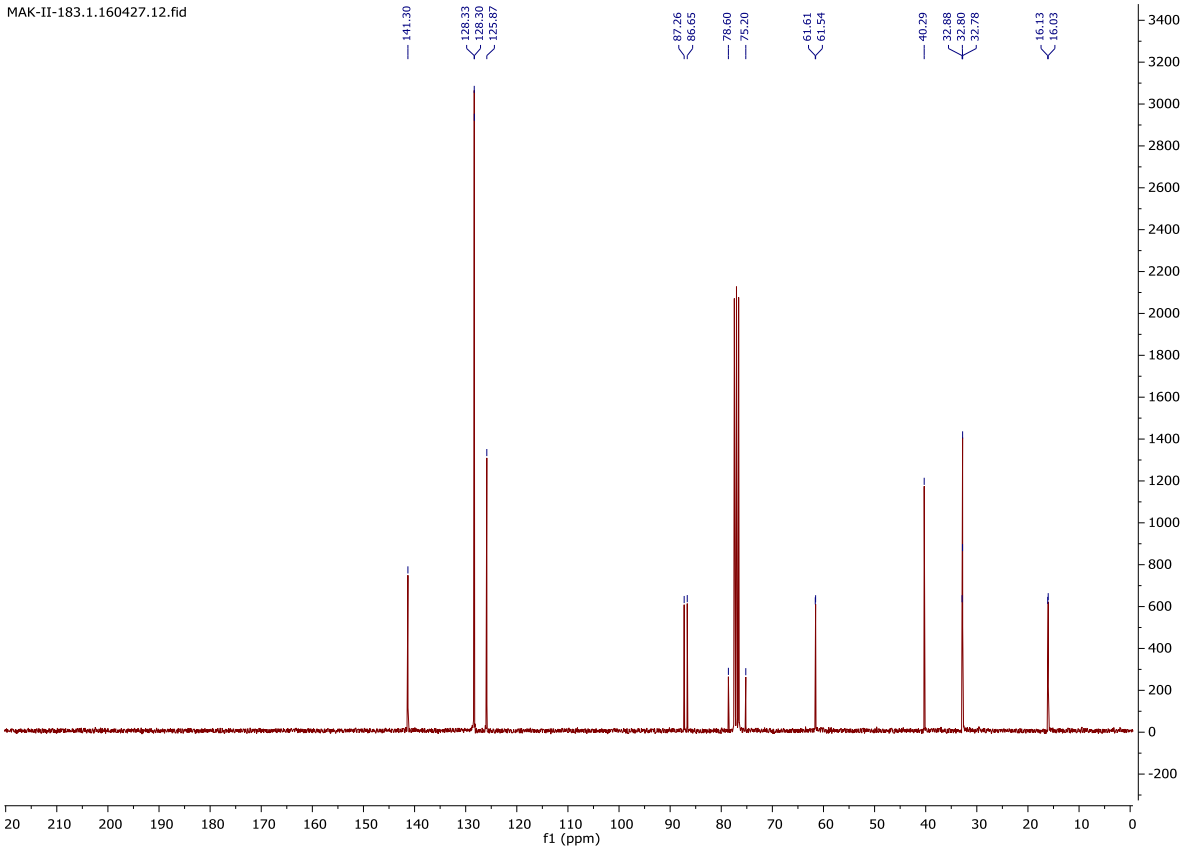
MAK-II-183.1.160427.12.fid
141.30
128.33
128.30
125.87
87.26
86.65
78.60
75.20
61.61
61.54
40.29
32.88
32.80
32.78
16.13
16.03
3400
3200
3000
2800
2600
2400
2200
2000
1800
1600
1400
1200
1000
800
600
400
200
0
-200
20 210 200 190 180 170 160 150 140 130 120 110 100 90 80 70 60 50 40 30 20 10 0
f1 (ppm)

5-((2-(*O*-Ethyl-*P*-ethynyl-phosphonamidato-*N*-benzoyl)ethyl)amino)naphthalene-1-sulfonic acid (**10**)

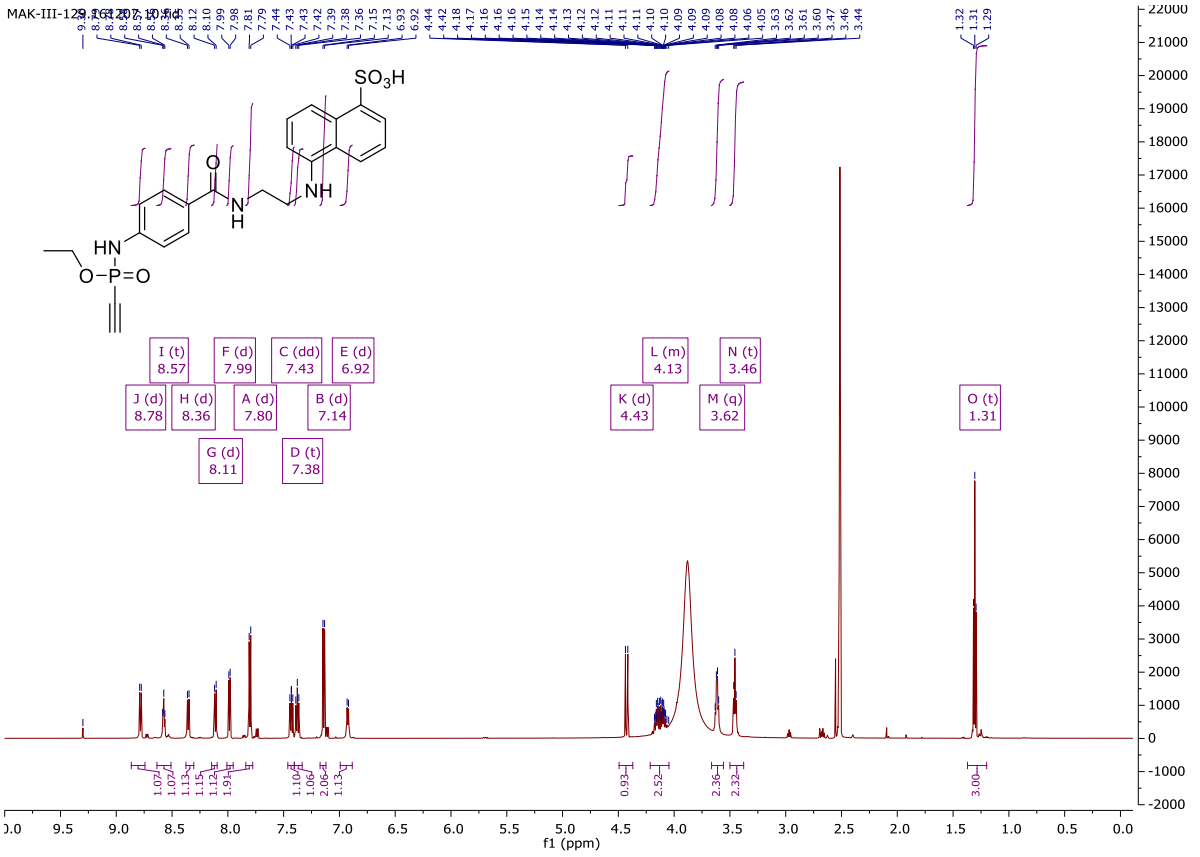

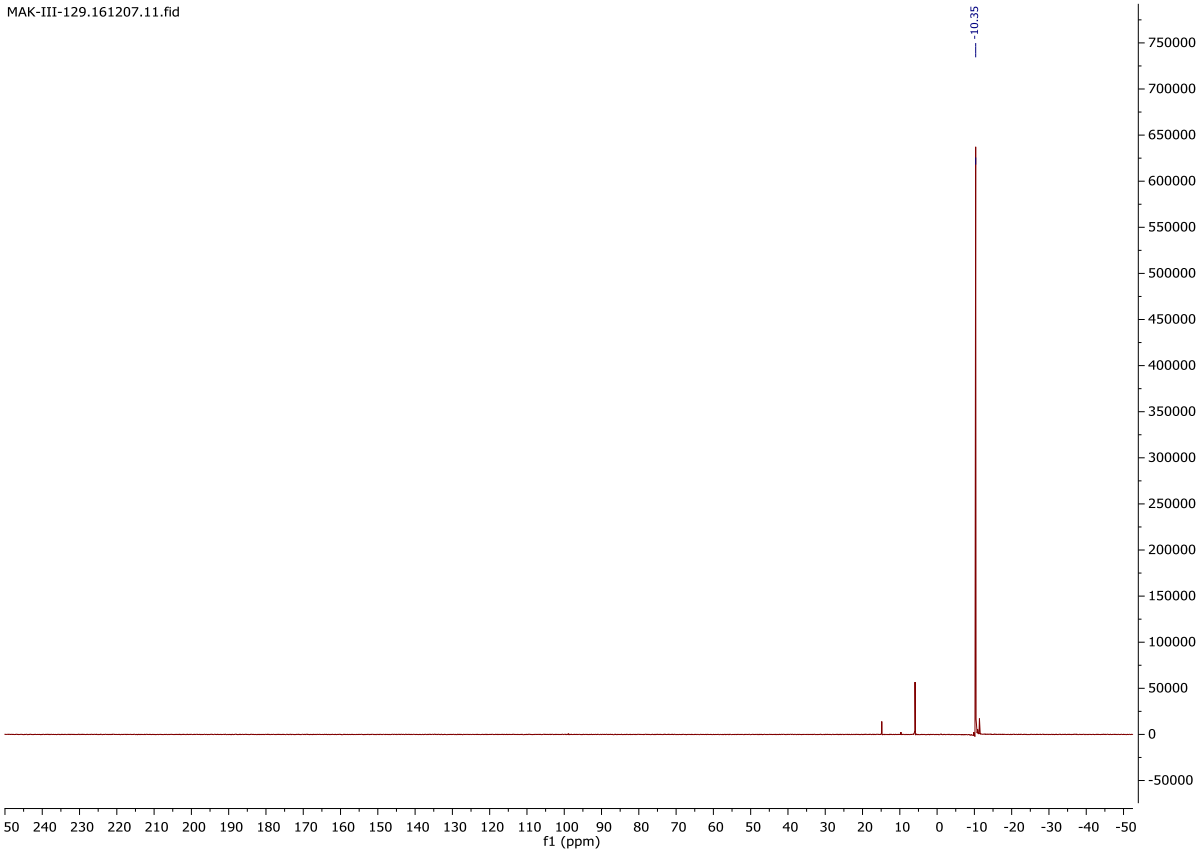

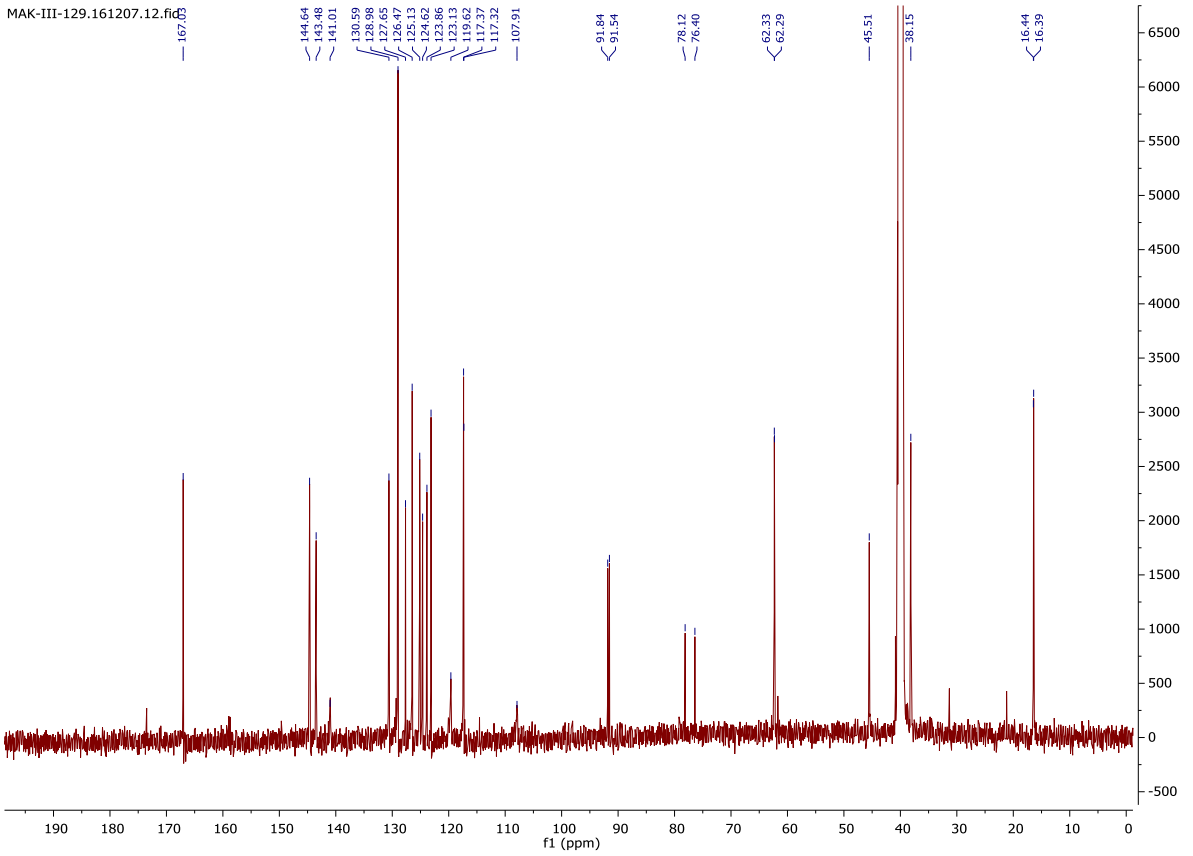

Cy5-*O*-ethyl-*P*-alkynyl-phosphonamidate (**11**)

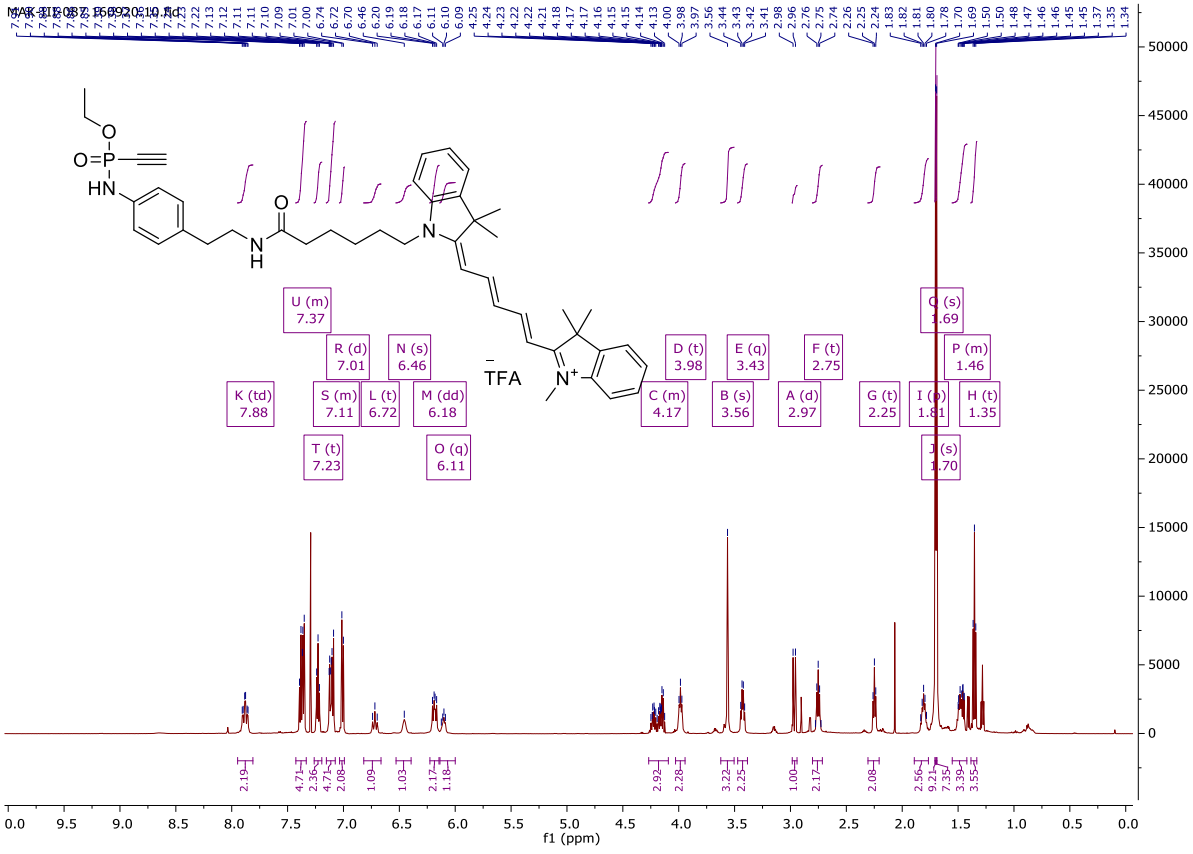

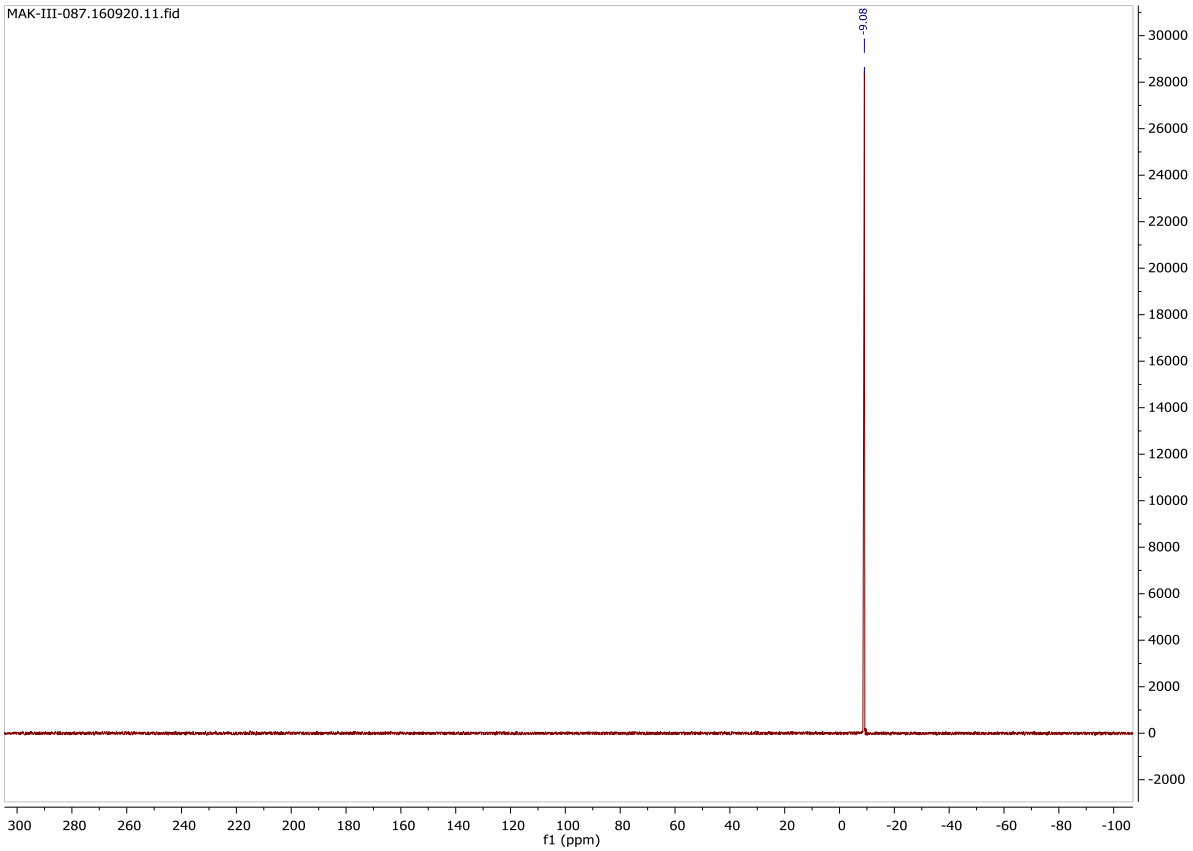
MAK-III-087.160920.11.fid
-9.08
f1 (ppm)

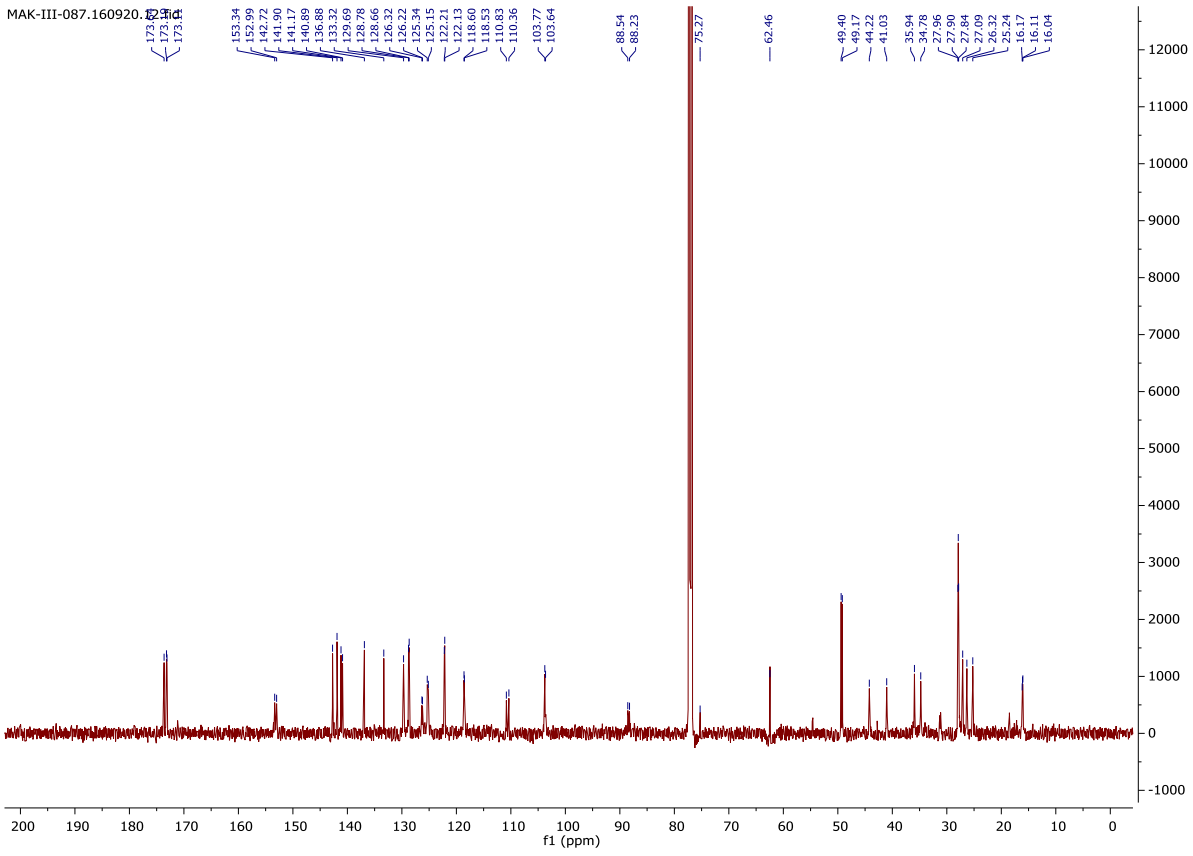
MAK-III-087.160920.12.fid
173.42
173.31
173.14
153.34
152.99
142.72
141.90
141.17
140.89
136.88
133.32
129.69
128.78
128.66
126.32
126.22
125.34
125.15
122.21
122.13
118.60
118.53
110.83
110.36
103.77
103.64
88.54
88.23
75.27
62.46
49.40
49.17
44.22
41.03
35.94
34.78
27.96
27.90
27.84
27.09
26.32
25.24
16.17
16.11
16.04
f1 (ppm)

Ethyl-*N*-phenyl-*P*-(*Z*-ethylthioethenyl) phosphonamidate

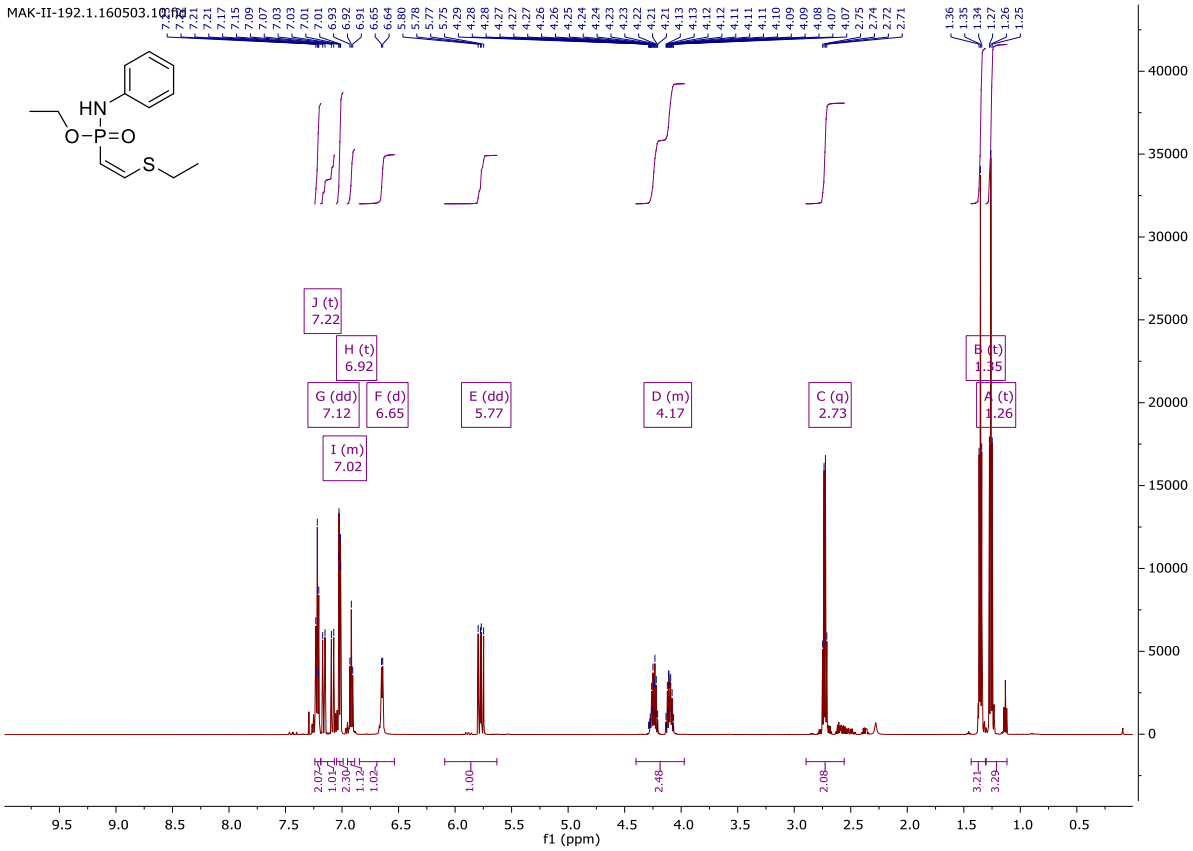

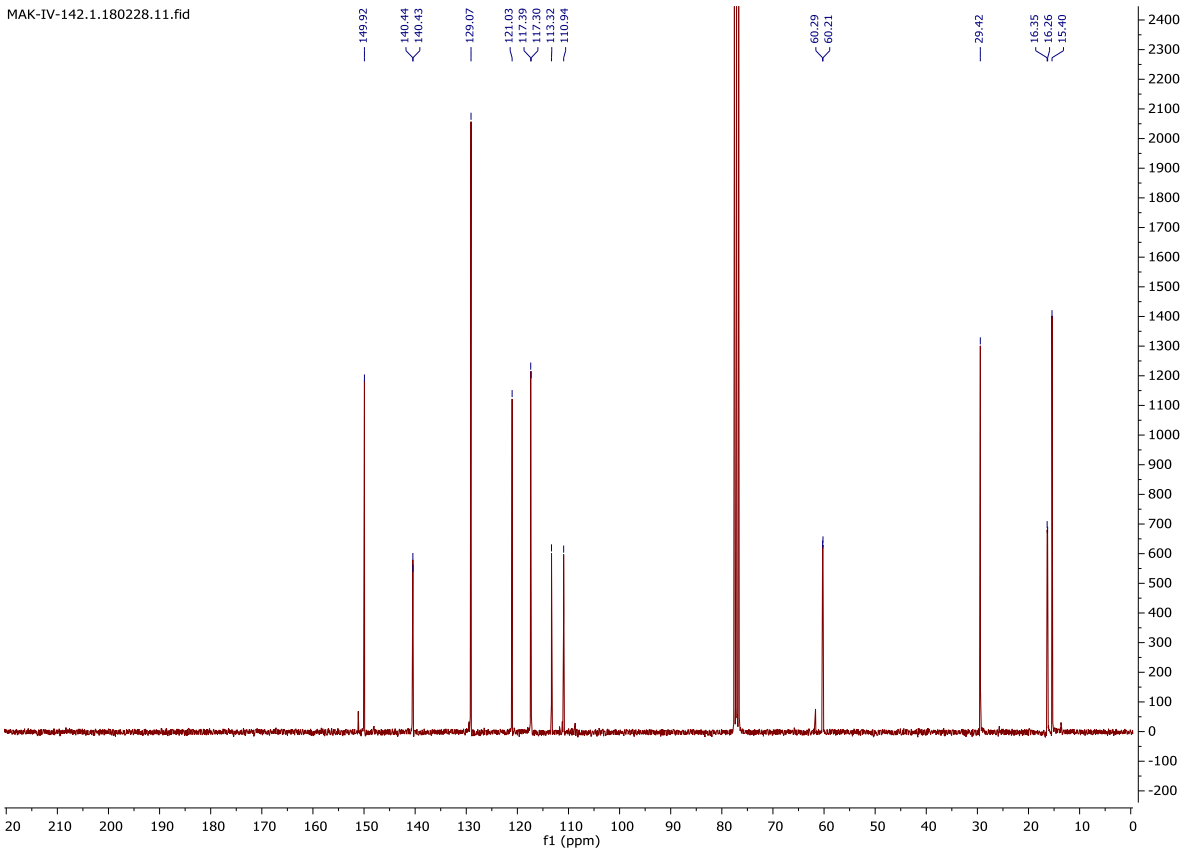

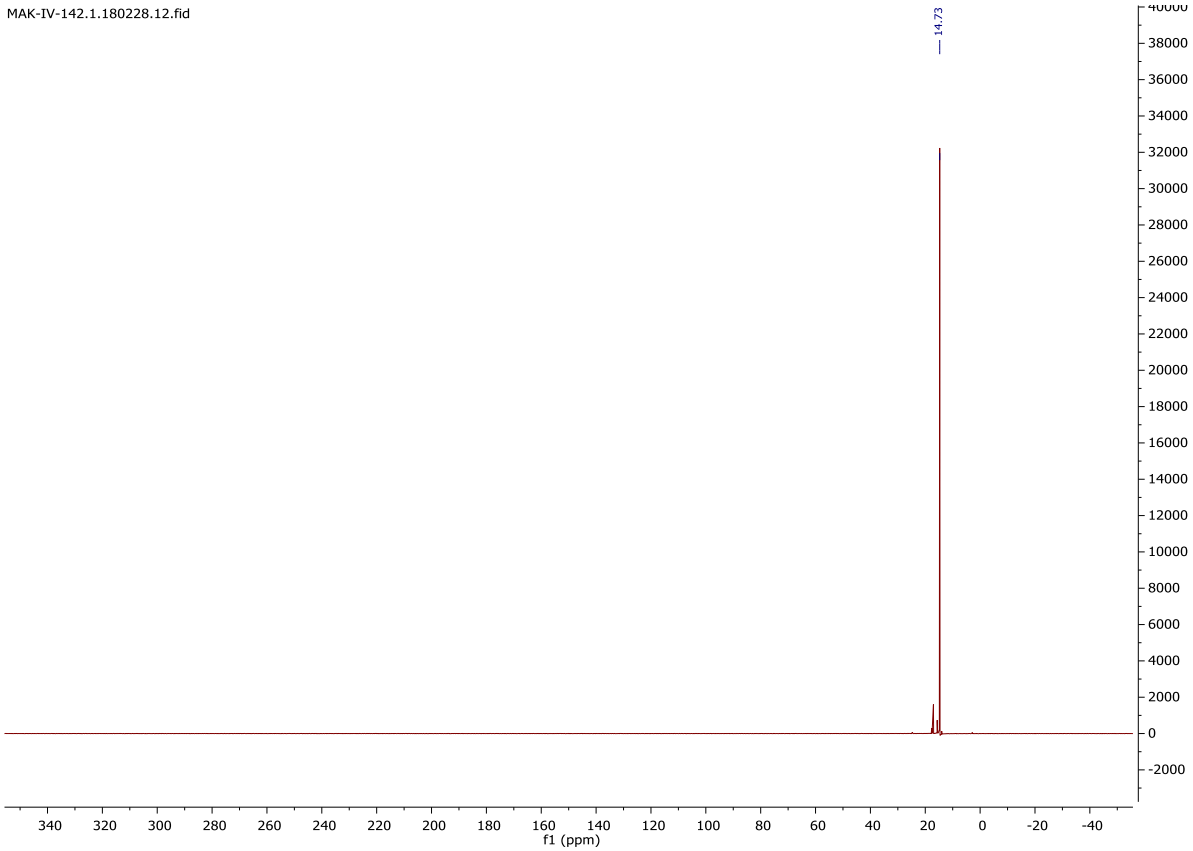

Ethyl-*N*-phenyl-*P*-(*E*-ethylthioethenyl) phosphonamidate

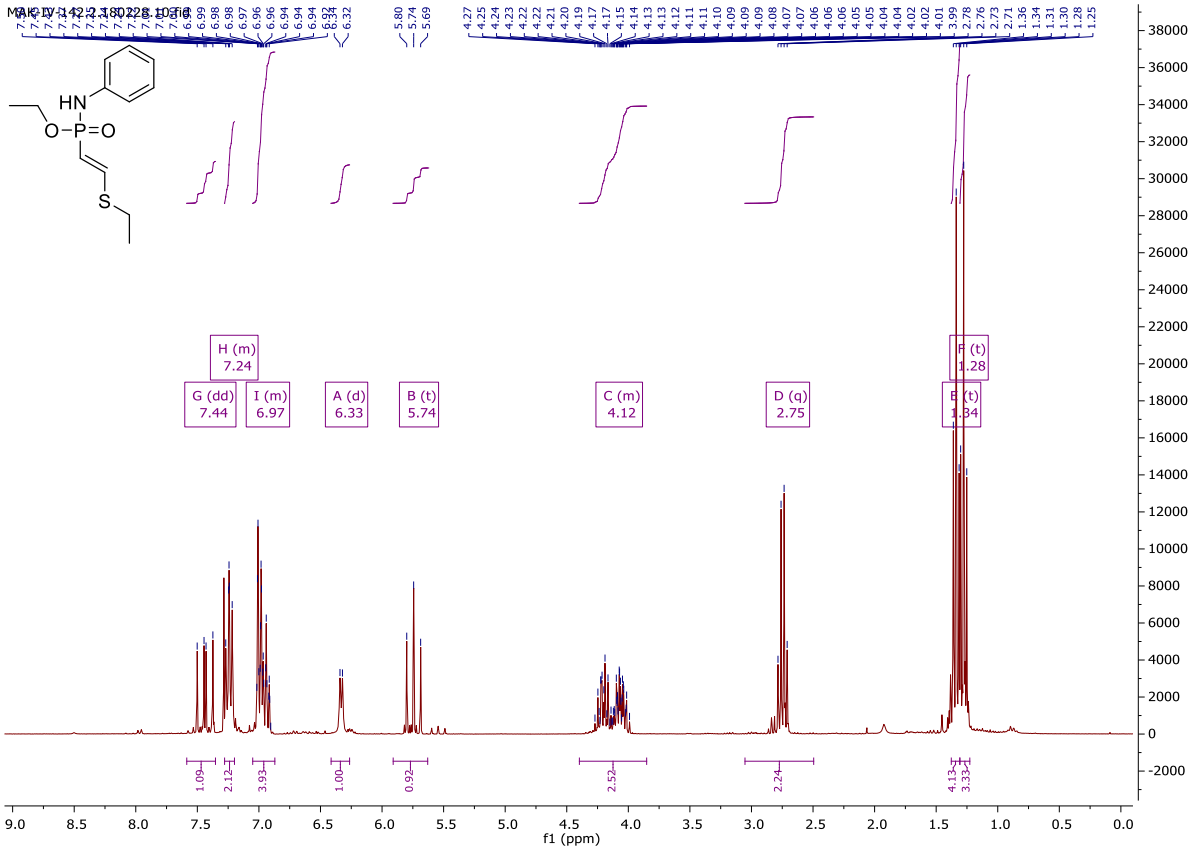

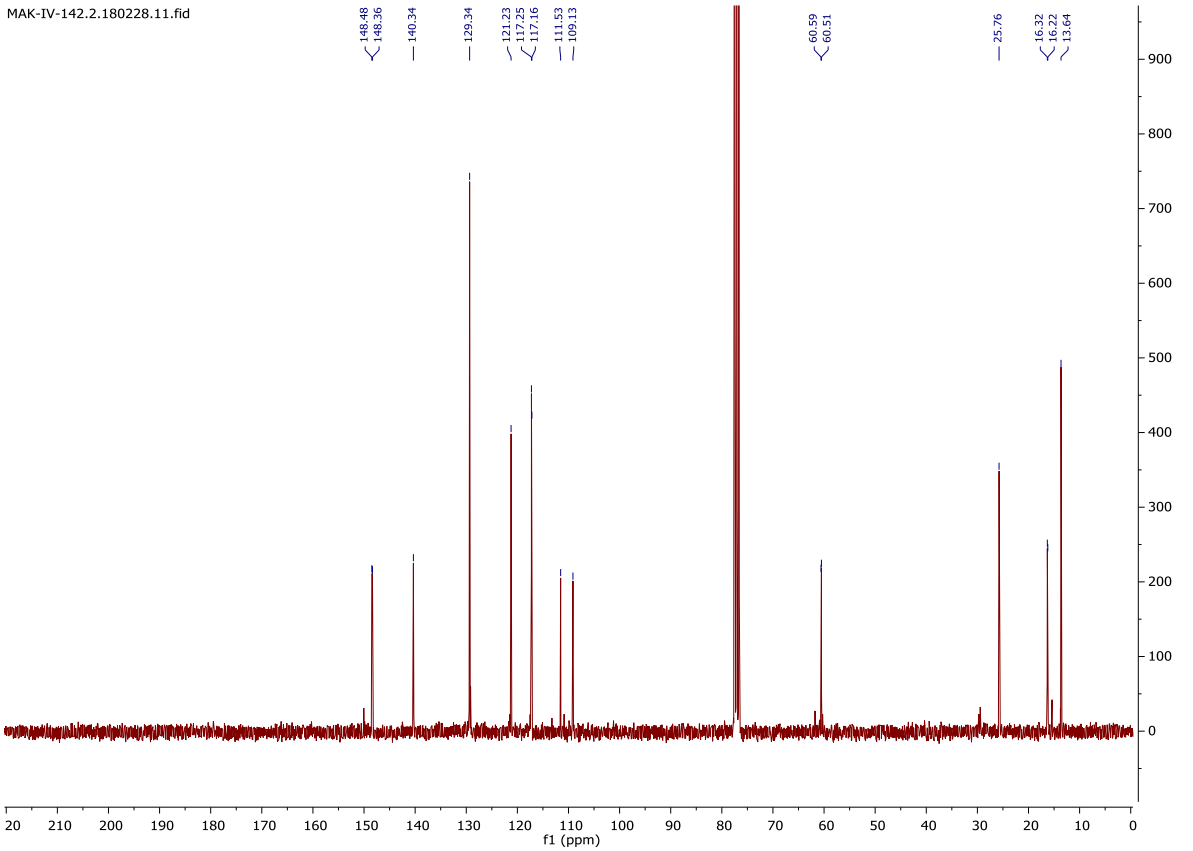
MAK-IV-142.2.180228.11.fid
148.48
148.36
140.34
129.34
121.23
117.25
117.16
111.53
109.13
60.59
60.51
25.76
16.32
16.22
13.64
f1 (ppm)

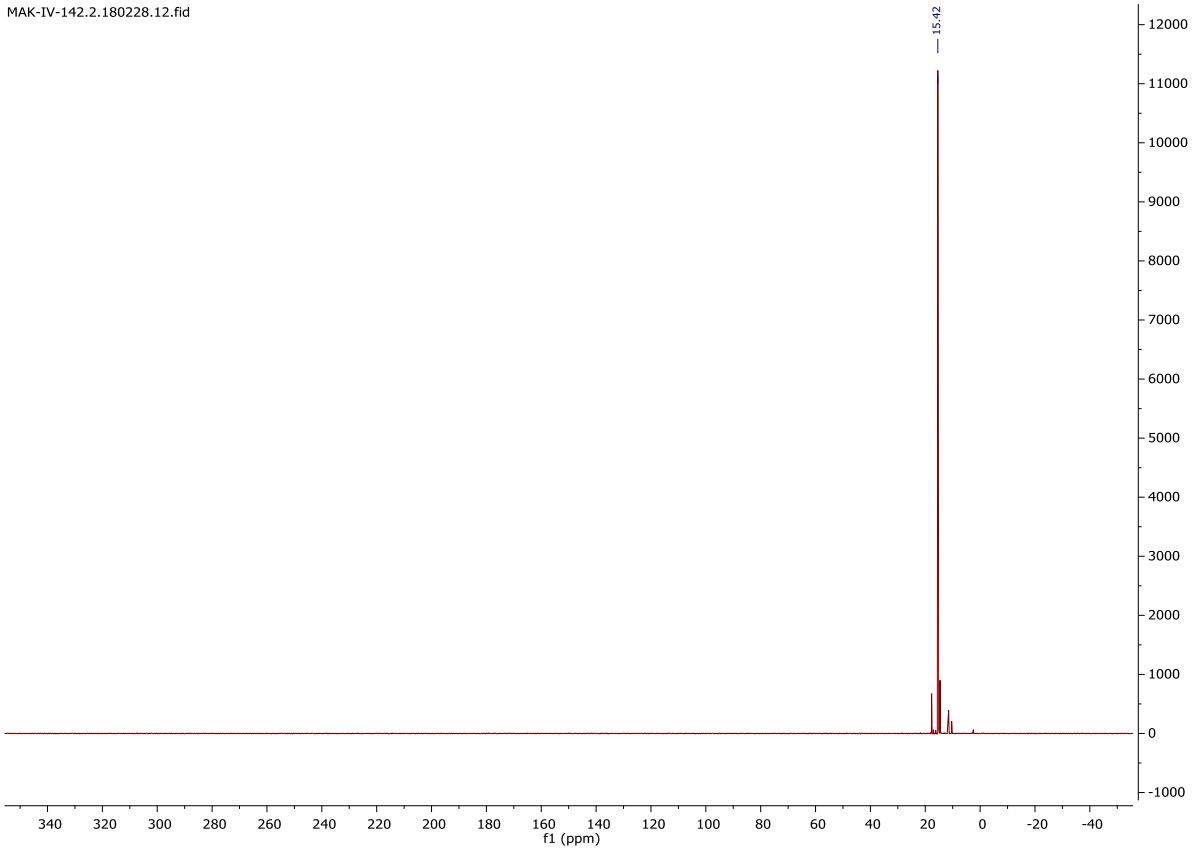
MAK-IV-142.2.180228.12.fid
15.42
f1 (ppm)

6. Computational Details

All DFT calculations were carried out with the *ORCA* program package (Version 3.0.3).[6] The *M06* functional[7] as well as the polarized and minimally augmented *ma-def2-TZVPP*[8] basis set was chosen for geometry optimizations and frequency calculations. This functional performed very well in a comparative study of different functionals for modelling Michael-type additions of thiols to olefins.[9] Minima and transition states were confirmed by frequency calculations, giving no or one imaginary frequency for minima or transition states, respectively. Connectivity of minima and transition states were verified by IRC calculations.

Free enthalpies *G* at 298 K and 1 atm were obtained as follows:

$$G_{298} = H - T \cdot S \quad (1)$$

$$G_{298} = [U + k_B \cdot T] - T \cdot S \quad (2)$$

$$G_{298} = [(E(\text{el}) + E(\text{ZPE}) + E(\text{therm.})) + k_B \cdot T] - T \cdot S \quad (3)$$

with $k_B \cdot T$ = 0.00094421 Eh = 0.59 kcal/mol. Electronic energies *E*(el) were obtained from single-point calculations using the *M06* functional, the *ma-def2-QZVPP* basis set and the COSMO(water) solvent model. Zero point energy *E*(ZPE) and thermal *E*(therm.) corrections to *E*(el) as well as entropy contributions *T·S* were taken from the performed frequency calculations.

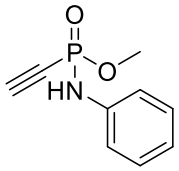

E(el)	-895.458852624575 Eh
E(ZPE)	0.17525247 Eh
E(therm.)	0.01160533 Eh
T·S	0.05031000 Eh

Cartesian Coordinates

P	-0.59808667893139	-0.79193299214631	-1.06157798293773
O	-0.84191595202287	0.20450774235482	-2.09483537170814
N	0.96965046103202	-1.19665078849081	-0.73992993344396
C	1.99671875829470	-0.31544052832699	-0.37033877145969
H	1.14036383293728	-2.17313573738952	-0.55927517552338
C	1.89123801209630	1.05546376836423	-0.58359136071128
C	3.14889631025628	-0.82858616203342	0.21610731821571
C	2.92669060040681	1.88986229494945	-0.20212312754092
C	4.18015324474254	0.01547912488830	0.58365963473391
C	4.07510913902655	1.38144998402923	0.38100548454480
H	3.23330177068336	-1.89685038938847	0.38329533780969
H	1.01060893451755	1.46055785984276	-1.06628035885925
H	2.83278599539945	2.95489222405636	-0.37390872197060
H	5.07181513090782	-0.40034204259692	1.03595841074113

H	4.88134685920472	2.04221125327538	0.67109348259601
O	-1.15697000366242	-2.25036866555863	-1.30763992232812
C	-2.51475846045912	-2.39856369228203	-1.70357045233556
H	-2.65961815297741	-3.44474888140695	-1.95998675137036
H	-2.73201335378030	-1.77390355104223	-2.57057450876158
C	-1.31886812180330	-0.30262653032260	0.46907926519826
C	-1.79617744806682	0.05443290614241	1.51156949293613
H	-2.21899399028480	0.37459086644969	2.43436972006966
H	-3.18410688751695	-2.13096806336774	-0.88296570789472

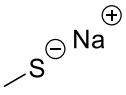

E(el)	-600.465161259222 Eh
E(ZPE)	0.03757793 Eh
E(therm.)	0.00502206 Eh
T·S	0.03488390 Eh

Cartesian Coordinates

H	1.014080	-6.973725	-1.066760
C	0.011793	-6.782643	-1.450494
S	-0.119700	-5.011348	-1.874077
H	-0.137387	-7.422987	-2.320414
Na	-2.417433	-4.527406	-2.723502
H	-0.699582	-7.073231	-0.676803

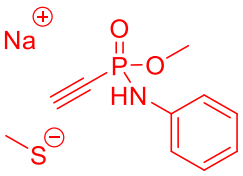

E(el)	-1495.926988297768 Eh
E(ZPE)	0.21416977 Eh
E(therm.)	0.01870608 Eh
T·S	0.06791930 Eh

Cartesian Coordinates

P	-0.15990138938735	-0.42890133226999	1.68066421387234
O	1.28905431940470	-0.55998260868668	1.44642303776843
N	-0.74787526262474	1.10218910608974	1.50582083119721
C	-0.52822641827539	1.78503626389223	0.27743199719787
H	-1.66132340572990	1.24877770195440	1.91111596027621

C	0.76633721846293	2.10196909523885	-0.11765538579724
C	-1.60038884359792	2.12557736147711	-0.53543827557891
C	0.97826992231358	2.74033788382037	-1.32837944090304
C	-1.38004766219673	2.78496999331815	-1.73198549524531
C	-0.09099391207539	3.08638351329645	-2.13706654720796
H	-2.60646344300938	1.85678843069678	-0.23397889204412
H	1.59224452939677	1.86231059178470	0.53967127485290
H	1.98857018908750	2.98144316166376	-1.63438353947903
H	-2.22100737873071	3.04213351296220	-2.36284710454076
H	0.08048729214691	3.58216808562844	-3.08332310574765
O	-0.67085571220736	-0.77331734645779	3.12410918190957
C	-0.36692682120073	-2.05110826576515	3.67686392339406
H	-0.80006172961555	-2.07716500499186	4.67267189974559
H	0.71272288944299	-2.18856873486798	3.74272427469574
C	-0.98868493807023	-1.45840366849309	0.54569293109351
H	-0.80346894473742	-2.84645787195382	3.06917486956848
C	-1.26145146444185	-2.03482879195294	-0.48034991707923
S	0.73169552106387	-1.89499206904874	-3.01729149891012
H	-1.45066474890741	-2.53967157647509	-1.40552983404055
C	-0.09891401953583	-0.31412096883020	-3.40818125130681
H	0.61109376202893	0.42462717350397	-3.78525876785612
H	-0.60339473757962	0.12309476988667	-2.53957185208112
H	-0.85154840840719	-0.47223873416687	-4.18221098601402
Na	1.72387359698248	-1.18076967125357	-0.73155250173993

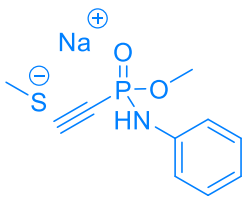

E(el)	-1495.928557055642 Eh
E(ZPE)	0.21391460 Eh
E(therm.)	0.01829736 Eh
T·S	0.06755280 Eh

Cartesian Coordinates

P	-0.36037976685003	0.13355232188078	0.61123685218097
O	1.10235359348308	0.02642981787580	0.46057187745980
N	-0.95877437078580	1.65959785670547	0.72183742296938

C	-0.75197407908927	2.72718413905645	-0.16305004559664
H	-1.60585506357871	1.82193129669133	1.47650460215438
C	0.01723713541010	2.58824521126833	-1.31288993602354
C	-1.33864275829865	3.95638608830814	0.11797571991568
C	0.18949356256277	3.66711486370590	-2.16182508042082
C	-1.15807743273044	5.02739170971521	-0.73649982473076
C	-0.39322013811892	4.89105122844698	-1.88308685914572
H	-1.93739974278876	4.06991078580137	1.01482005029815
H	0.48952203104070	1.64213148843627	-1.54383059140264
H	0.78957899076340	3.54381275378197	-3.05463164392604
H	-1.62027743256610	5.97774827229369	-0.50139049320000
H	-0.25302745117682	5.72980968695513	-2.55187755734917
O	-0.98351571778120	-0.46914587529734	1.91801829236482
C	-0.73167681332266	-1.84193492925137	2.25322153955814
H	-1.42667223794100	-2.10057363121747	3.04678733806946
H	0.29239616168492	-1.95143670560393	2.61028408911116
C	-1.10456297074447	-0.72790637966886	-0.70807884820319
C	-1.44888768891447	-1.53401809800798	-1.53234833648837
H	-0.88265875618574	-2.50016357178798	1.39253193013356
H	0.54192328428941	-6.36834119671117	-0.87890319109539
C	1.28667788503706	-5.57597213453699	-0.95686385438022
S	0.46916664296550	-3.95465138018539	-0.78960212308365
H	2.02881433482387	-5.73691151477983	-0.17444196993379
Na	1.91503910679568	-1.83187459415343	-0.55107612222325
H	1.77994767978370	-5.67348824456517	-1.92436664841333
H	-1.73817798776714	-2.25598926515594	-2.26140658859900

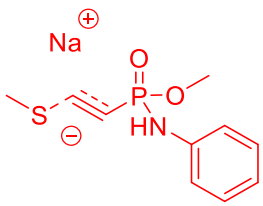

E(el)	-1495.903404154544 Eh
E(ZPE)	0.21390115 Eh
E(therm.)	0.01678484 Eh
T·S	0.06301100 Eh

Cartesian Coordinates

P	0.00432476169549	0.07439378080378	0.03483007911912

O	1.48979535952874	0.11784780285387	0.05205064051289
N	-0.67939745823217	1.60611201619863	0.04828214663593
C	-0.60945443107929	2.38124384695229	-1.12325255303219
H	-1.58117886616957	1.63058322624726	0.50200213429641
C	0.61360622824937	2.59007445787278	-1.75713533565964
C	-1.76173141661530	2.92304785645567	-1.68206632484857
C	0.66683917801570	3.29477411233949	-2.94627840900653
C	-1.69540030100169	3.64486249115244	-2.86070121379741
C	-0.48416662485819	3.82339269203808	-3.50826265088159
H	-2.71687440673611	2.76079990236050	-1.19505440196975
H	1.51362190011937	2.20057594014165	-1.29809859626996
H	1.62286197828597	3.44212827435099	-3.43379068812924
H	-2.60262773972388	4.05759098770230	-3.28387002267648
H	-0.43645805864117	4.37478281746018	-4.43807287728148
O	-0.67986115113054	-0.48578617052310	1.34579071774600
C	-0.36821074667098	-1.79693562996775	1.78523738148224
H	-0.89967750996454	-1.95741435947259	2.72024013978589
H	0.70462159416630	-1.90018077055168	1.95876675060872
C	-0.46684704394486	-0.83690250386103	-1.32368975748261
H	-0.69335476386363	-2.53821695305871	1.05206019661377
C	-0.65045308587053	-0.77389615595494	-2.55662789634114
S	0.57484080092058	-2.15153498080379	-3.99758282840588
H	-1.12272463635685	-0.26894759844267	-3.38904406858779
C	0.39887429035098	-1.08246105636445	-5.44454504796888
H	1.36623393151158	-0.82762080576871	-5.87393774378108
H	-0.09934965201922	-0.14697401098467	-5.16093725008649
H	-0.20435215622752	-1.57063932689784	-6.20876000056083
Na	2.01296002626197	-1.07716988227795	-1.87014252003342

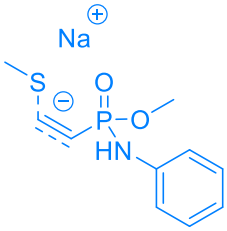

E(el)	-1495.916470890467 Eh
E(ZPE)	0.21408209 Eh
E(therm.)	0.01678282 Eh
T·S	0.06297910 Eh

Cartesian Coordinates

P	0.08297664804403	0.01268079694422	0.22619410842859
O	1.56057219538901	-0.00338119524710	0.37643233521234
N	-0.56131069757442	1.53901847869489	0.16657459276146
C	-0.38205278561491	2.44900896831032	-0.87821970791492
H	-1.37807676278223	1.68115426670683	0.73861484454082
C	0.71168435902738	2.36424981461287	-1.73521917347702
C	-1.31212103575827	3.46635483447016	-1.07089924698579
C	0.85279059993369	3.26938892224779	-2.77142945366212
C	-1.15503187877306	4.37246352691388	-2.10239923438397
C	-0.07514511209937	4.27801349231498	-2.96516596984354
H	-2.16699069977524	3.53872335758424	-0.40766352238659
H	1.45990779365444	1.59917728214409	-1.57382389319361
H	1.70668486306791	3.18578123447073	-3.43245835172661
H	-1.88993671422970	5.15625113648516	-2.23692905018631
H	0.04255052797643	4.98346325688275	-3.77697343661031
O	-0.72996702979485	-0.50343803831498	1.48141929991982
C	-0.54961782805538	-1.85137983206765	1.90346833831624
H	-1.22791876008619	-2.01703308233649	2.73643218877581
H	0.47688815158217	-2.01316906107841	2.23895533356830
C	-0.38491055143777	-0.92171674722083	-1.13745404367154
C	-0.27345422903572	-2.01721683261896	-1.71147087021387
H	-0.77961069471334	-2.54897751532011	1.09459529782401
H	0.50510643116304	-5.79725391568251	-2.20873160404509
C	0.98085515385962	-4.83442500913788	-2.38898907820844
S	1.02831584219300	-3.87211507839207	-0.85882302422860
H	1.97508043723897	-5.00945647481630	-2.79676115252502
Na	2.51917646309879	-1.66806334169796	-0.73028272176178
H	0.39157338639573	-4.30801916887146	-3.14974246849609
H	-0.53108807289377	-2.63278407598016	-2.55630033582618

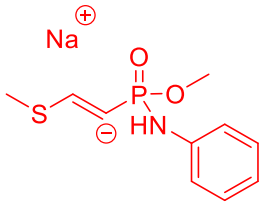

E(el)	-1495.936211350094 Eh
E(ZPE)	0.21581204 Eh
E(therm.)	0.01667476 Eh
T·S	0.06278790 Eh

Cartesian Coordinates

P	0.13190445789879	-0.39544362431027	1.57341806811963
O	1.36785884049088	0.09034133108148	2.26095635068092
N	-0.93135278554734	0.85227434258795	1.17561996490530
C	-0.67872828045422	1.78788077381042	0.17275917567321
H	-1.90385327488597	0.63980157528976	1.33386716151470
C	0.61049718258318	2.26786757669032	-0.05456872676165
C	-1.71749117563628	2.25139721012141	-0.63265842295178
C	0.84888729023589	3.15950796470553	-1.08437854437916
C	-1.46995653888793	3.15342698095931	-1.65055748902673
C	-0.18318994680054	3.60755675202598	-1.89288833332116
H	-2.72318705316351	1.88094155926185	-0.46441044945607
H	1.41374943050895	1.94175802639791	0.59440802495773
H	1.85817552566784	3.51671560494053	-1.25063517369336
H	-2.29146864117551	3.49570346169783	-2.26777009581932
H	0.01109557855656	4.30571687865122	-2.69635952136178
O	-0.86003157005055	-1.14793682555242	2.58076094913618
C	-0.36587481618504	-2.25707682981987	3.30054725818283
H	-1.14901518529915	-2.58235391798314	3.98252489117598
H	0.51628084442688	-1.97937510569729	3.88426003682387
C	0.59077743055756	-1.43843113282618	0.26996702126070
H	-0.11224971395133	-3.08044158849582	2.62773652612117
C	-0.03227714421668	-1.28865458763087	-0.89600355826189
S	0.39512405652662	-2.19890790235265	-2.34438024281346
H	-0.86276963520567	-0.60054862296691	-1.09834472771805
C	-0.55261708171232	-1.29416626908217	-3.58643971354119
H	-0.33667484130893	-1.74869211596690	-4.55119913393233
H	-0.25492070220577	-0.24628406750522	-3.61212847846134
H	-1.62227381905404	-1.36888855869870	-3.39438648209920

Na	2.80115156828766	-1.22266888933307	1.12326366504626

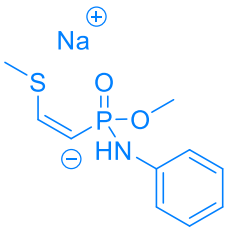

E(el)	-1495.931615683340 Eh
E(ZPE)	0.21522419 Eh
E(therm.)	0.01776208 Eh
T·S	0.06575200 Eh

Cartesian Coordinates

P	-0.18746350698823	-0.31429005717662	-0.55022791305267
O	1.23368130751095	-0.39773105025972	-1.02326320659152
N	-0.98909665388179	1.04344395489395	-1.08088584831332
C	-0.74115610021521	2.38451397898745	-0.80933236204473
H	-1.82740640102437	0.82595786330311	-1.59449350373988
C	0.44200790749066	2.81211498752494	-0.20929217096651
C	-1.69760166578076	3.33640027058733	-1.15854109816395
C	0.64031730345613	4.15600967308731	0.05133453584731
C	-1.48335078238488	4.67738586797046	-0.90431787582489
C	-0.31530095258042	5.09910366240952	-0.29017961091239
H	-2.61823022948042	3.01131792433970	-1.63059286051503
H	1.21054583782706	2.09090878508211	0.03869324231180
H	1.56276585713255	4.47042569490638	0.52450609010491
H	-2.24125186109238	5.39851926183271	-1.18499978047360
H	-0.15073786737756	6.14863916487608	-0.08416827162059
O	-0.22742307789983	-0.07019933209949	1.03166202204200
C	0.79761671524305	-0.55597249009913	1.87173218857205
H	0.54507038199053	-0.26186258882679	2.88892687412815
H	1.76277605441774	-0.12374126356874	1.59906964868359
C	-1.18034267585157	-1.59125524227056	-1.12832951288644
C	-1.12267508952716	-2.89001583208522	-0.95573478213874
H	0.87247015431527	-1.64704554211805	1.83057439639872
H	-1.33721520688497	-5.80489322230161	-0.01107463455198
C	-0.32398567144947	-5.54438060852389	-0.31159147736897
S	0.04483694350864	-3.83415699792097	0.14745026856292
H	0.37674632226972	-6.18749519182302	0.21668753872025

Na	1.37186982811735	-2.39354045190515	-1.88053935040992
H	-0.21142761901564	-5.70278395256589	-1.38368274787106
H	-1.76227925184500	-3.62812726625621	-1.44908979792551

7. References

[1] M. Mikolajczyk, B. Costisella, S. Grzejszczak, *Tetrahedron* **1983**, *39*, 1189-1193.

[2] A. Shevchenko, H. Tomas, J. Havli, J. V. Olsen, M. Mann, *Nat. Protoc.* **2007**, *1*, 2856.

[3] A. Stengl, D. Hörl, H. Leonhardt, J. Helma, *SLAS Discov.* **2017**, *22*, 309-315.

[4] A. J. Pérez, F. Wesche, H. Adihou, H. B. Bode, *Chem. Eur. J.* **2016**, *22*, 639-645.

[5] H. D. Herce, D. Schumacher, A. F. L. Schneider, A. K. Ludwig, F. A. Mann, M. Fillies, M.-A. Kasper, S. Reinke, E. Krause, H. Leonhardt, M. C. Cardoso, C. P. R. Hackenberger, *Nat. Chem.* **2017**.

[6] F. Neese, *Wiley Interdiscip. Rev.-Comput. Mol. Sci.* **2012**, *2*, 73-78.

[7] Y. Zhao, D. G. Truhlar, *Theor. Chem. Acc.* **2008**, *120*, 215-241.

[8] aF. Weigend, R. Ahlrichs, *Phys. Chem. Chem. Phys.* **2005**, *7*, 3297-3305; bJ. Zheng, X. Xu, D. G. Truhlar, *Theor. Chem. Acc.* **2011**, *128*, 295-305.

[9] J. M. Smith, Y. Jami Alahmadi, C. N. Rowley, *J. Chem. Theory Comput.* **2013**, *9*, 4860-4865.

6.1.2. Variation of the ethynylphosphonamidate ester residue for further functionalizations

All the work described in the previous chapter has been performed with *O*-ethyl substituted ethynylphosphonites and -phosphonamidates. One unique advantage of phosphonamidate based conjugations over other cysteine conjugation techniques is the possibility of a facile incorporation of a third functional *O*-substituent to the phosphonamidate core structure in a few chemical steps (Scheme 43).

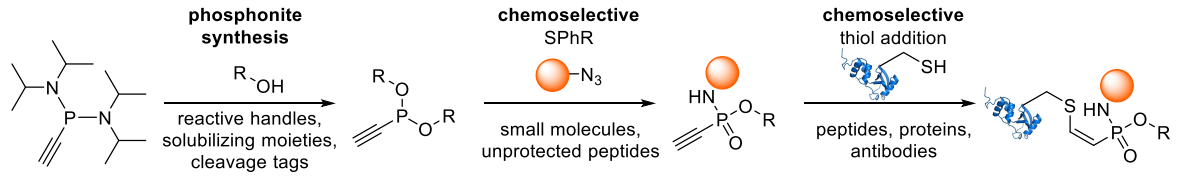

Scheme 43: Principle of the chemoselective SPhR with differently substituted ethynylphosphonites to convert azide building blocks into thiol reactive ethynylphosphonamidates with expanded functionality.

The development of linker systems which can be selectively cleaved by an external stimulus that is not affecting the integrity of an attached biomolecule constitutes an important tool in chemical biology.[319] Such controlled release systems can for example facilitate purification or enrichment of biomolecules by catch and release strategies[320] or enable a controlled release of drugs from the targeting protein after cellular uptake in drug delivery applications.[23] Due to the lability of *P-N*-bonds towards acidic conditions, phosphoramidates have been used before to release primary and secondary amines. Careful optimization of the phosphoramidate substituents, for example by the attachement of carboxylic acids or pyridinium substituents to the phosphoramidate core, can be used to tune the lability towards acidic hydrolysis.[321] Based on this observation with phosphoramidates, Siebertz et al. could show that cleavage of phosphonamidate ester residues to form phosphonamidic acids also induces lability of the *P-N*-bond. Therefore, a free amine can be released after a cleavage of the *O*-substituent of the phosphonamidate under slightly acidic conditions.[322] In the current chapter, this principle was translated to ethynylphosphonamidates to enable a cysteine selective protein modification technique that facilitates the release of the attached modification from the protein after an external stimulus such as light, reducing agents or even enzymes. For this, the attachment of various cleavable residues to the *O*-substituent of ethynylphosphonamidates was planned as depicted in Scheme 44.

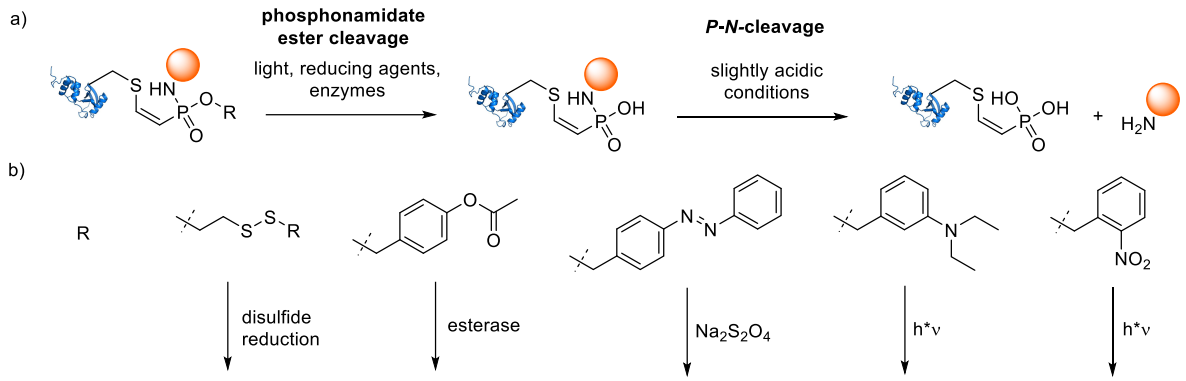

Scheme 44: Phosphonamidate ester for an induced cleavage of the *P-N*-bond. a) Cleavage of the phosphonamidate ester facilitates an amine release from the phosphonamidate under slightly acidic conditions. b) Various ester residues that can be cleaved under the influence of different stimuli.

In addition to cleavable residues, also other functional substituents were attached to ethynylphosphonamidates to expand their functionality. Polar oligo ethylene glycol units to increase aqueous solubility or alkynes as chemoselective handles for further chemoselective modifications via CuAAC were incorporated.

Goal of the following research project was the variation of the *O*-substituent of ethynylphosphonamidates via the synthetic route that is depicted in Scheme 43. Since this residue is preserved during SPhR with azides, we started our investigations by synthesizing different substituted ethynylphosphonites with various handles. Afterwards their reactivity with azides in the SPhR was tested. And the phosphonamidates were than probed for subsequent thiol addition and functionality of the handles in different model experiments.

6.1.2.1. Synthesis of *O*-substituted ethynylphosphonites

Synthesis of phosphonites is in principle possible via two different routes (Scheme 45). One possibility is alkylation of a disubstituted chlorophosphite with an organometallic reagent.[313-314] Disubstituted chlorophosphites are usually synthesized by substitution of phosphorus trichloride (**1**) with two equivalents of the desired alcohol in the presence of an amine base. However, mono- and triple substituted byproducts are usually formed.[322] Since separation of the desired product from these byproducts is often a heavy task, an alternative previously established route has been employed herein that starts with alkylation of bis(diisopropylamino)-chlorophosphine (**2**) to generate the phosphonamidite **3** followed by 1*H*-tetrazole mediated substitution of the diisopropylamino groups with the alcohol of choice.[312, 322]

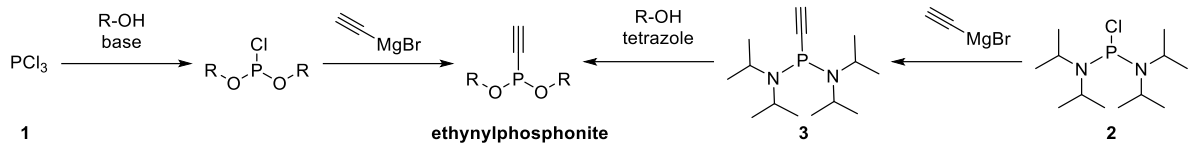

Scheme 45: Two different synthetic routes for the synthesis of ethynylphosphonites starting from phosphorus trichloride (left) or bis(diisopropylamino)-chlorophosphine (right).

A big issue in the synthesis of P(III) compounds is product isolation, which often fails due to rapid oxidation in the presence of air and hydrolysis of the *O*-substituents in the presence of water.[323] This can be in particular problematic for phosphonites, since their auto-oxidation is even more rapid in comparison to other P(III)-species such as phosphites or phosphinites.[311] The problem was addressed in chapter 6.1.1 by performing the subsequent SPhR in a one-pot reaction without isolation of the phosphonite intermediate. An alternative strategy includes the isolation of air-stable borane adducts of the P(III)-species, followed by borane deprotection with strong bases directly before SPhR, which has been applied earlier.[312-313] Here, it was found out that ethynylphosphonites with electron-donating substituents are stable enough to be isolated by column chromatography and stored at - 20 °C for several weeks, making any borane-adduct formation unnecessary. This proceeding worked for most of the phosphonites that did not carry electron-withdrawing substituents except from diethyl ethynylphosphonite that has been used for the SPhR in chapter 6.1.1. Several attempts to isolate this compound without borane attachment failed due to decomposition of the desired product.

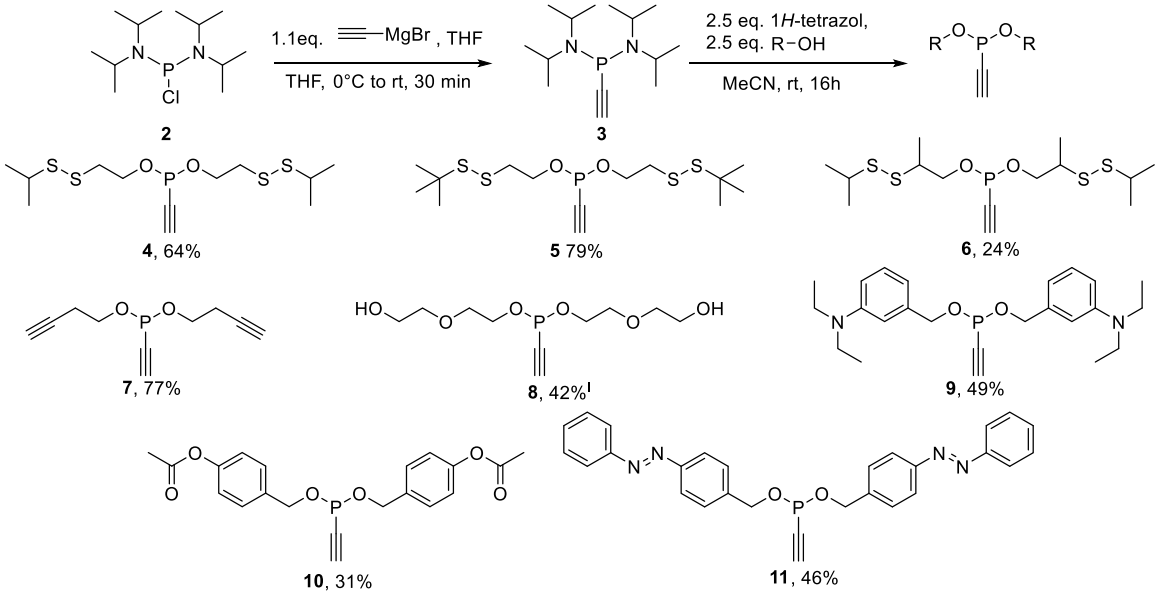

Scheme 46: Synthesis of differently substituted ethynylphosphonites from bis(diisopropylamino)chlorophosphine. Stated are isolated yields.* I) 10 equivalents of the alcohol were used.

* Compound **9** was synthesized and characterized by Brian Rusi as part of an internship in the Hackenberger laboratory under the supervision of the author

For the synthesis of the phosphonites that are depicted in Scheme 46, **2** was alkylated with ethynylmagnesium bromide, directly followed by addition of the alcohol and tetrazole without isolation of the phosphonamidite intermediate **3**. The desired phosphonites were isolated in excellent to moderate yields. It should be noted, that mass analysis of phosphonites failed for all of the tested compounds, possibly due to decomposition under ESI-conditions. It's remarkable that the disulfides in compound **4**-**6** were tolerated during synthesis and isolation without decomposition of the phosphonite product. This is surprising, since it is well known that P(III) compounds are able to react with disulfide bonds in a reducing manner.[324] Additionally, it was even possible to synthesize the highly hydrophilic phosphonite **8** with an unprotected alcohol being present, using an excess of the diol to avoid multimer formation or polymerization. An aryl ester- and a diazo functionality were also well tolerated in the reaction and yielded the desired phosphonites **10** and **11**.

In contrast to these findings, all attempts to isolate unprotected ethynylphosphonites with electron-withdrawing substituents failed due to rapid decomposition in the presence of air. To overcome this issue, all of the ethynylphosphonites unstable to air were isolated as borane adducts to stabilize the P(III)-species.[289, 312]

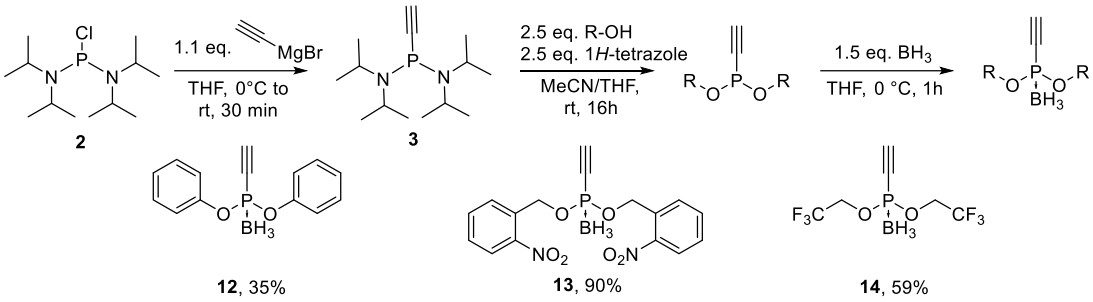

Scheme 47: One-Pot-Procedure for the synthesis of borane protected ethynylphosphonites from bis(diisopropylamino)chlorophosphine. Stated are isolated yields.*

A one pot procedure has been applied, were the borane was directly added to the reaction mixture of the phosphonite synthesis (See Scheme 47). After this, phosphonite borane adducts **12**-**14** were stable enough to be isolated by column chromatography in excellent yields to moderate yields.

6.1.2.2. Staudinger phosphonite reaction with ethynylphosphonites carrying various *O*-substituents

In the next step, differently substituted unprotected ethynylphosphonites were reacted in a SPhR with an azide to generate ethynylphosphonamidates with various *O*-Substituents. Following the observations from chapter 6.1.1 that the NHS-ester building block **15** holds a good reactivity in the

* Compounds **13** and **14** were synthesized and characterized by Arif Celik as part of his bachelor thesis in the Hackenberger laboratory under the supervision of the author

SPhR, **15** was chosen for the test reactions with different ethynylphosphonites. NHS-modified phosphonamidates isolated from this reaction have the additional advantage of a facile subsequent modification with functional amines as demonstrated with 5-((2-aminoethyl)amino)naphthalene-1-sulfonic acid (EDANS, **16**), a fluorescent dye carrying a primary amine.

SPhR with differently substituted phosphonites was carried out with one equivalent of azide **15** in DMF overnight without any further additive. The good stability of the electron-rich phosphonites towards air made an inert atmosphere for the reaction unnecessary. The desired phosphonamidates could be isolated for all of the tested substituents in good to moderate yields (Table 1). To probe the reactivity of the NHS-modified phosphonamidates towards amines, the building blocks **16**-**22** were reacted with EDANS in the presence of DIPEA in DMF. Fluorescently modified phosphonamidates **23**-**29** could be isolated from all of the tested NHS building blocks in good yields by preparative HPLC.

Table 1: SPhR of different ethynylphosphonites with azide **15** and subsequent amide bond modification with EDANS. Stated are isolated yields of the NHS- and the EDANS phosphonamidates.

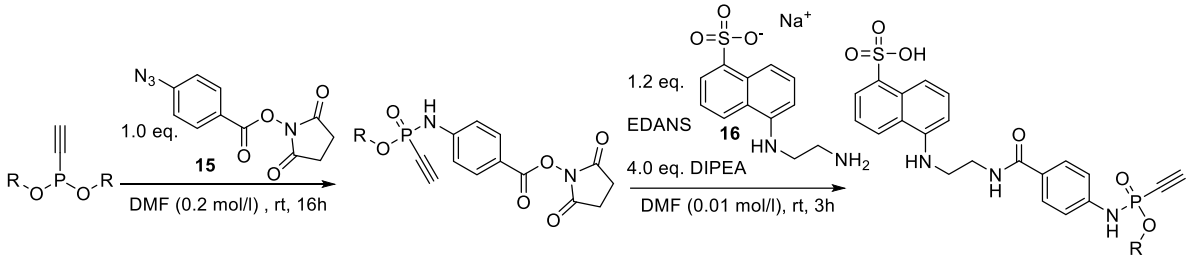

entry	R	phosphonite	NHS ester phosphonamidate	yield	EDANS phosphonamidate	yield
1	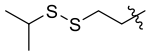	**4**	**16**	43%	**23**	67%
2	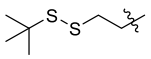	**5**	**17**	47%	**24**	62%
3	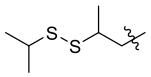	**6**	**18**	43%	**25**	40%
4	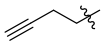	**7**	**19**	77%	**26**	74%
5	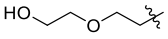	**8**	**20**	31%	**27**	56%
6	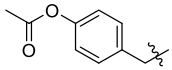	**10**	**21**	29%	**28**	30%
7	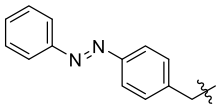	**11**	**22**	76%	**29**	51%

The phosphonites that were isolated as borane adducts had to be deprotected prior to SPhR in order to restore reactivity towards azides. Borane removal is usually carried out with strong bases such as DABCO.[312-313] A one-pot protocol has been developed that circumvents the isolation of unstable, unprotected ethynylphosphonites by a direct addition of the azide to the deprotection mixture in a one-pot manner, as also previously reported.[313]

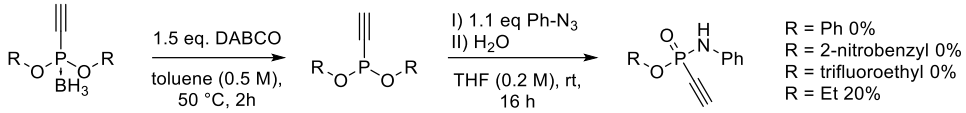

Scheme 48: Reaction of different phosphonites with electron withdrawing substituents after borane deprotection with phenyl azide. Stated are isolated yields.

Since the SPhR with ethynylphosphonites with electron withdrawing substituents proved to be difficult from the beginning, reactions were carried out with structurally simple phenyl azide and analyzed by ^{31}P-NMR and MS. However, no evidence for the formation of the desired phosphonamidate was found for the tested electron poor phosphonamidates, even though complete conversion of the phosphonites was observed in the NMR.* In contrast to this, the desired product could be isolated with diethyl ethynylphosphonite in 20% yield, demonstrating the general applicability of the protocol (Scheme 48). The synthesis of the diethyl ethynylphosphonite borane adduct has been described earlier.[325]

These results were surprising since electron-deficient 2-nitrobenzyl phosphonites, substituted with a triazole at the *C*-substituent instead of an alkyne have been employed in the SPhR earlier.[322] Therefore, further analyses of the formed side products from the reaction between diphenyl ethynylphosphonite (**12**) and phenyl azide were performed. It was found out that the phenol adduct **31** of the desired ethynylphosphonamidate **30** is the main reaction product, which could be isolated in 24% yield. This undesired reaction product probably originates from the addition of the liberated phenol during SPhR to the electron-deficient triple bond of the phosphonamidate (Scheme 49). It should be noted, that **31** was unreactive to thiols, as even an excess of glutathione added under basic conditions did not show any conversion.

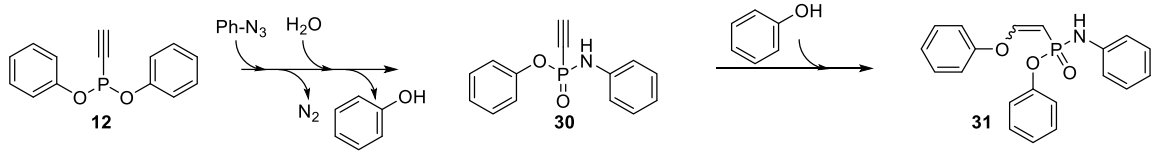

Scheme 49: Reaction between phenylazide and diphenyl ethynylphosphonite (**12**). Liberated phenol attacks the triple bond of the desired product **30** to form the phenyl enol ether **31**.

The undesired reattack of the liberated phenol might be explained by the high electrophilic character of the phosphonamidate **30**. Electron withdrawing substituents further increase the electrophilicity of ethynylphosphonamidates whereby reactivity for nucleophiles, other than cysteine increases. This leads to problems in the synthesis, as demonstrated with this example and could also promote undesired effects on the selectivity of the subsequent cysteine addition with proteins.

* Investigations of the SPhR with phosphonites **13** and **14** were performed by Arif Celik as part of his bachelor thesis in the Hackenberger laboratory under the supervision of Marc-André Kasper.

Since electron withdrawing substituents diminish the stability of ethynylphosphonites, lead to synthetic problems in the SPhR and most probably cause undesired side reactions with amino acid residues other than cysteine, electron withdrawing substituents were excluded in further reactions of azides with ethynylphosphonamidates.

6.1.2.3. Functional evaluation of cleavable phosphonamidate ester residues

After successful incorporation of different cleavable substituents to the ethynylphosphonamidate residue as described in the previous chapter, the functionality to release a phosphonamidic acid and subsequently a primary amine after cleavage of the *P*-*N*-bond was monitored in a HPLC and a FRET-based assay. Substituents were chosen that can be cleaved by different external stimuli. An overview of the different substituents with proposed cleavage mechanisms is depicted in Scheme 50.

It is known that 2-thiolethyl residues that are attached to good leaving groups such as carbamates cyclize spontaneously to release carbamic acids (see chapter 4.3.1.3). From this finding, it was anticipated that disulfide modified phosphonamidates such as **23**-**25** can release a phosphonamidic acid after disulfide reduction followed by thiirane formation (Scheme 50a). Disulfide modified phosphonamidate ester residues could thereof facilitate an intracellular release of an amine due to increased intracellular glutathione concentrations. This is in particular interesting for the traceless release of amino modified drugs in drug delivery applications, where the phosphonamidate moiety functions as cysteine selective linker and traceless release unit in one. Extracellular stability of those linker systems is crucial for drug delivery applications. Since the stability of disulfides is dependent on the sterically hindrance (see chapter 4.3.1.3, Scheme 2), disulfides with different methyl substitution patterns have been synthesized for this study.

The conversion of carboxylic acids into esters of pharmacologically active drugs to mask their hydrophilicity is a common approach in the development of prodrugs.[326] Lipophilic esters are able to pass cellular membranes, where they get hydrolyzed by intracellular esterases to release the active drug molecule. Based on this strategy it was envisioned that the benzoyl ester in **28** facilitates an intracellular release of a phosphonamidic acid after ester cleavage and 1,6,-elimination as depicted in Scheme 50b in a similar manner than previously described for other enzymatic cleavable linker systems that have been applied to drug delivery (see chapter 4.3.1.3).

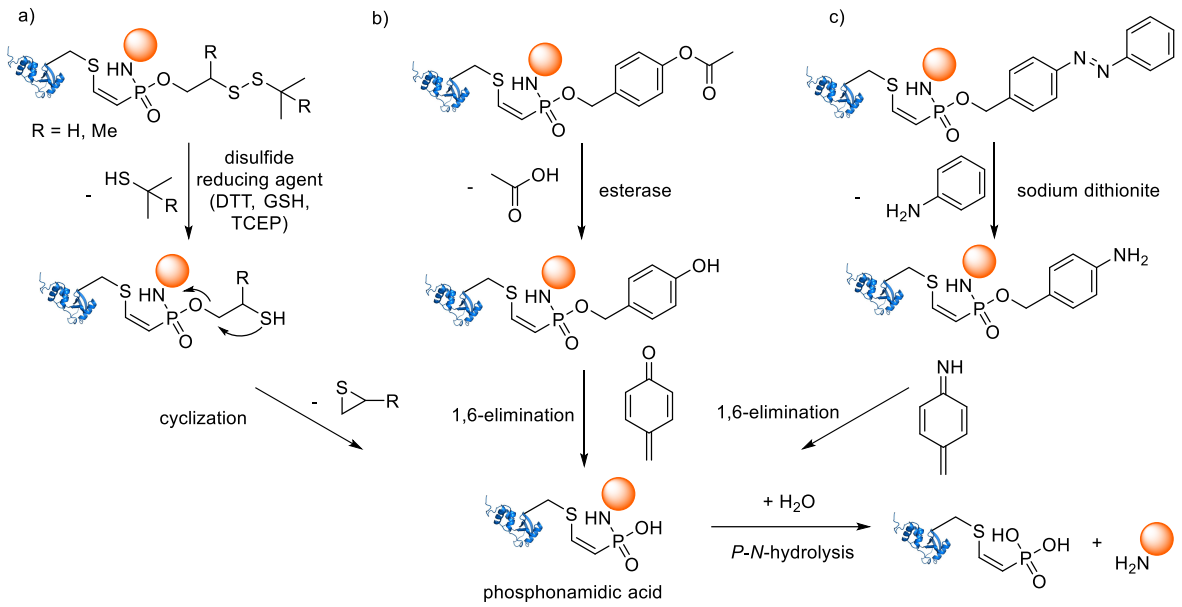

Scheme 50: Principles of the cleavage of different phosphonamidate ester substituents to release phosphonamidic acid which is prone to hydrolytic release of a primary amine from the *P-N*-bond.[322] a) Reductively cleavable substituent. b) Esterase-cleavable substituent. c) Dithionite-cleavable substituent.

Cleavable diazobenzene-based linker systems are commonly used as dithionite-cleavable affinity tags for enrichment strategies in chemical proteomics.[327] Building up on this, the diazo linkage in compound **29** was envisioned to release the desired phosphonamidic acid after selective reduction with dithionite, followed by 1,6-elimination (Scheme 50c). This could facilitate the development of novel phosphonamidate based selectively cleavable affinity tags for proteomic *in vitro* analyses.

To investigate the proposed release principles, a cysteine modified DABCYL-peptide was first added to the phosphonamidates **23**-**25** and **28** to synthesize water soluble EDANS-DABCYL-FRET pairs **32**-**35** that generate a fluorescent signal upon cleavage of the phosphonamidate linkage, as previously described in chapter 6.1.1 (Scheme 51). A non-cleavable ethyl-substituted derivative **36** was synthesized for control reactions from the EDANS-phosphonamidate, as described in chapter 6.1.1.

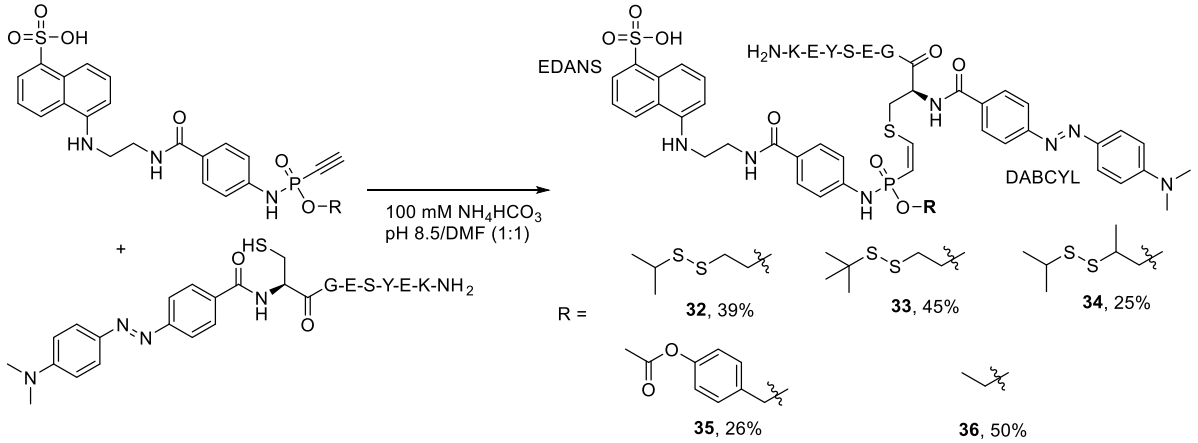

Scheme 51: Synthesis of phosphonamidate linked EDANS-DABCYL-FRET-Pairs with different cleavable **32**-**35** and one non cleavable phosphonamidate ester residue **36**. Peptide sequence is depicted in the amino acid one letter code. Stated are isolated yields after preparative HPLC.

In a first proof-of-principle study, peptides **32**-**34** were incubated with 10 equivalents of TCEP in PBS (Figure 14a). After incubation for one hour at 37 °C, the samples were analyzed by UPLC/MS and compared to control reactions were the constructs were exposed only to PBS for the same amount of time and at the same temperature. It could be observed that all of the disulfide-cleavable constructs **32**-**34** were fully consumed when exposed to 10 equivalents of TCEP and two new reaction products could be detected. No conversion of the starting material was observed in the control reactions without TCEP addition. In addition to that, no reaction at all was observed for the non-cleavable ethyl-substituted compound **36** (Figure 14b-e). The two peaks that arise for all of the samples under reductive conditions in the same ratio were identified by MS as the phosphonamidic acid **37** and the *P*-*N*-cleavage product, the phosphonic acid **38**. Firstly, these results confirm that 2-disulfido ethyl substituted phosphonamidates efficiently form the phosphonamidic acid upon disulfide reduction. The formation is selective for reducing conditions and does not occur for stably linked *O*-ethyl-phosphonamidate adducts. However the acidic UPLC conditions containing 0.1% TFA might promote the hydrolysis of the *P*-*N*-hydrolysis after the phosphonamidate ester cleavage. It is therefore difficult to assess, if the *P*-*N*-bond is cleaved during UPLC analysis or before during the reaction. It was previously demonstrated for other phosphonamidic acids that harsh acidic conditions need to be applied to cleave the *P*-*N*-bond.[322]

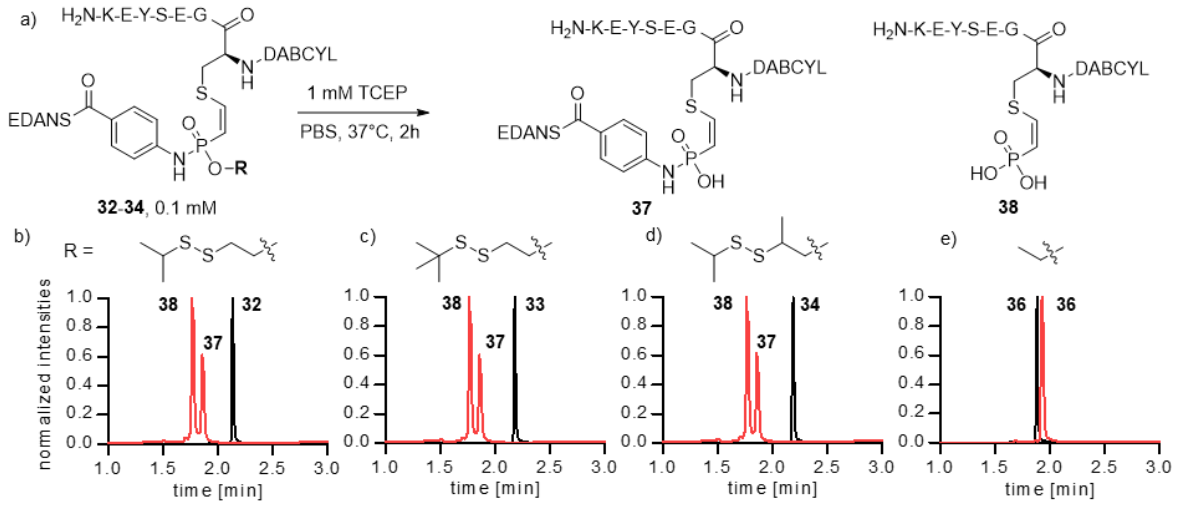

Figure 14: Exposure of the constructs **22**-**34** and **36** to 10 eq. of TCEP in PBS at 37 °C and analysis via UPLC/MS. Shown is the reaction-scheme with potential products **37** and **38** (a) and the normalized chromatograms of the reaction mixtures after incubation with TCEP in PBS (red) or in PBS only (black) for construct **32** (b), **33** (c), **34** (d) and **36** (e). Peaks were identified by MS. Traces in e correspond to the same compound, even though slightly shifted.

In a very similar experiment, peptide **35** was exposed to HeLa-cell-lysate and the reaction was monitored accordingly (Figure 15a). Here, cleavage occurred in the same way to form peptides **37** and **38** in similar ratios selectively for the ester-substituent over the ethyl substituted compound **36** and only in the presence of lysate (Figure 15b-c). Even though, this experiment also does not answer the

question of *P-N*-bond cleavage efficiency, it still suggests that the ester substituent of **35** can be cleaved intracellularly, while it is stable under PBS conditions.

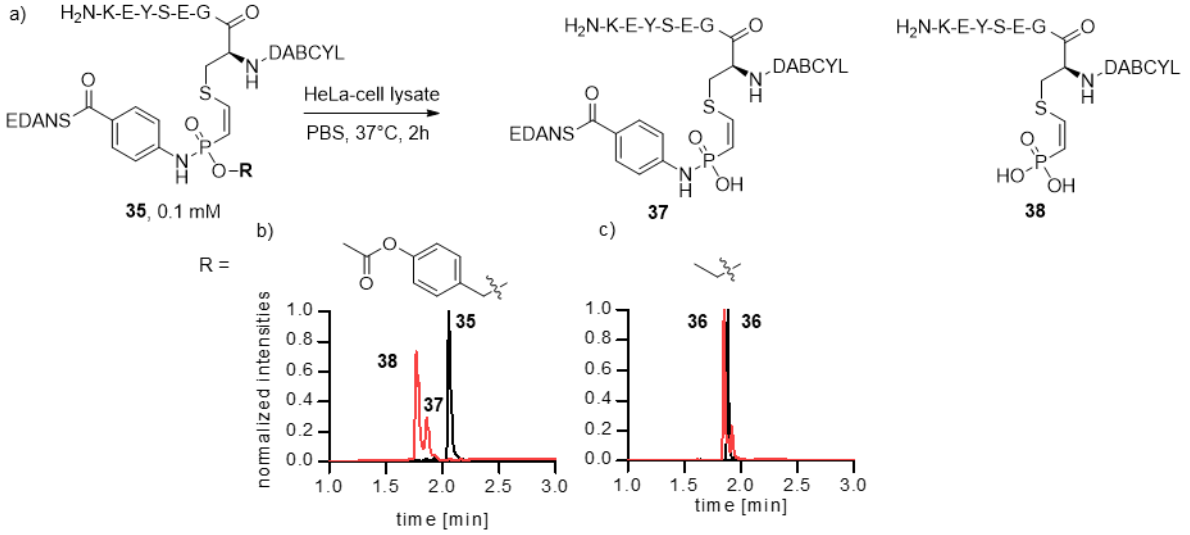

Figure 15: Exposure of the constructs **35** and **36** to freshly prepared HeLa-cell lysate in PBS at 37 °C and analysis via UPLC/MS. Shown is the reaction-scheme with potential products **37** and **38** (a) and the normalized chromatograms of the reaction mixtures after incubation with cell lysate (red) or in PBS only (black) for construct **35** (b) and **36** (c). Peaks were identified by MS. Traces in b correspond to the same compound, even though slightly shifted.

To exclude any bias of the acidic HPLC on the *P-N*-bond stability during the analysis, fluorescence measurements with the fluorescence-quencher-pairs **32** and **36** were carried out under neutral conditions. Here, the probe is still quenched after cleavage of the phosphonamidate ester substituent and a fluorescent signal is generated only after subsequent *P-N*-bond cleavage (Figure 16a). In a first experiment, the reductively cleavable probe **32** and the non-cleavable, ethyl substituted compound **36** were incubated with 10 eq. of TCEP in PBS at pH 7.4 and the fluorescence was monitored over time (Figure 16b). Even though, the previous HPLC based assay demonstrated that these conditions successfully cleave the disulfide containing phosphonamidate ester from **32** to liberate the phosphonamidic acid **37**, no increase in fluorescence was observed in a direct comparison to the non-cleavable variant **36** even after 24 hours (Figure 16c). In a second experiment, the pH was lowered after 4 hours of incubation with TCEP to 5.5. This time, compound **32** showed a steady increase in fluorescence, while the non-cleavable control did not increase over time, which suggests that the phosphonamidic acid is more prone towards acidic hydrolysis than the phosphonamidate ester (Figure 16d). Taken together, the fluorescence measurements underline that TCEP incubation of **32** delivers the phosphonamidic acid **37**. However, cleavage of the *P-N*-bond necessitates acidic conditions as previously reported.[322]

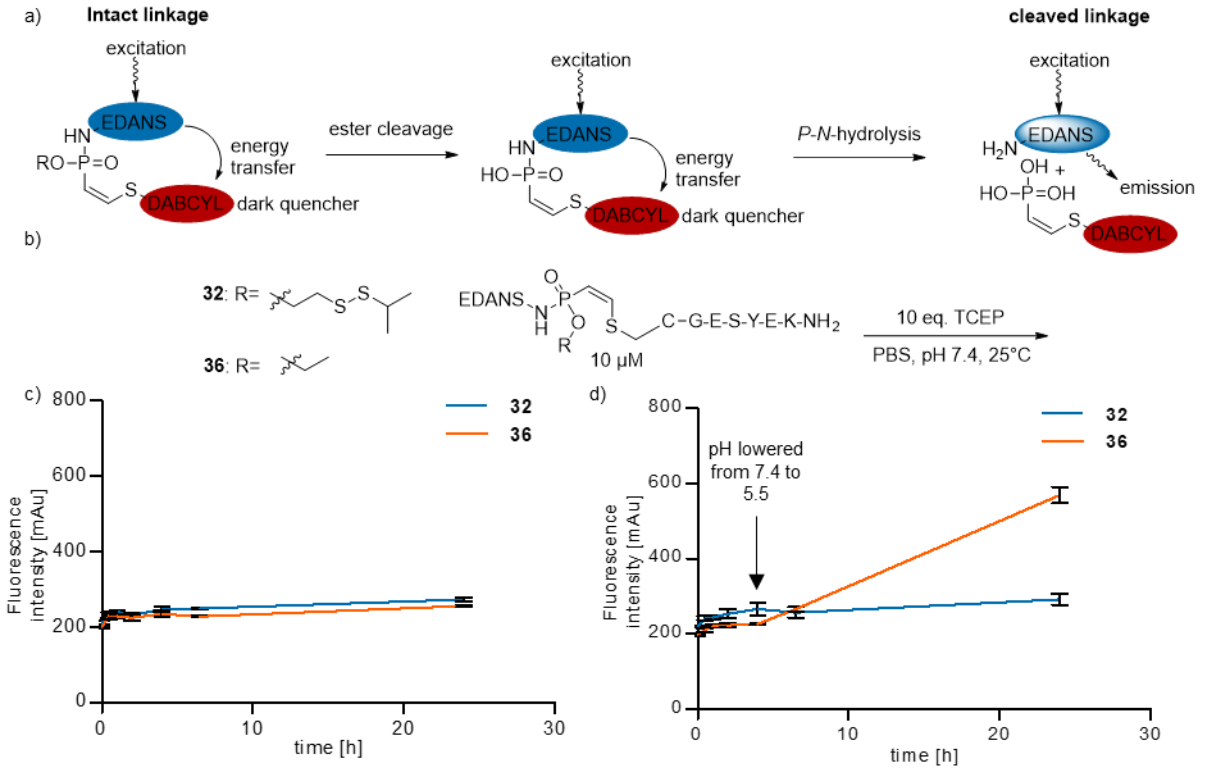

Figure 16: Stability measurements of the thiol adducts **32** and **36** after TCEP incubation. a) Set-up of the fluorescence-quenching assay. A fluorescent signal is only generated upon *P-N*-Bond cleavage. b) **32** and **36** were incubated at a concentration of 10 µM with 100 µM TCEP. c) EDANS-fluorescence intensity over time at pH 7.4. **32** (blue) and **36** (orange). d) EDANS-fluorescence intensity over time at pH 7.4, lowered to pH 5.5 after 4h **32** (blue) and **36** (orange). Excitation: 360 nm, emission: 508 nm, bandwidth: 5nm at 20 °C.

To sum up, it was demonstrated in this chapter that different phosphonamidate substituents can be cleaved by disulfide reduction (**32**-**34**) or by intracellular esterases (**35**) to release phosphonamidic acids under conditions were the control *O*-ethyl phosphonamidate **36** is stable. The *P-N*-bond of the phosphonamidic acid **37** is more prone towards acidic hydrolysis than the phosphonamidate ester in compound **32** to **36**. Future investigations should include studies that identify the exact pH window under which the *P-N*-cleavage occurs to be able to apply the strategy to intracellular drug release as described in chapter 4.3.1.3. Successful cleavage at pH 5.5, as depicted in Figure 16d, already suggest the applicability to an intracellular release in endosomes, where the pH can drop to 4.5–5.5 in late endosomes and lysosomes.[328]

6.1.2.4. Ethynylphosphonamidates for triple conjugations

To further expand the functional possibilities of the phosphonamidate ester residue, the building block **19** was evaluated for the ability to connect three functional moieties in an orthogonal fashion, as depicted in Figure 17a. The phosphonamidate ester residue carries in this case a stably linked terminal alkyne that enables a site selective attachment of a third functionality via CuAAC (See chapter 4.5.2.3) after cysteine labelling of a protein. In a proof of principle study, the NHS-ester of **19** was first reacted with the cyclic cell penetrating peptide (cCPP) cR_{10} **39** that carries an unmodified N-terminus (Figure

17b).* The R_{10} peptide is, like other arginine-rich peptides, able to enhance the transduction of functional proteins into living cells when covalently attached to the protein cargo.[167, 329] The aforementioned eGFP C70M S147C with a single addressable cysteine residue† was subsequently labelled with the phosphonamidate modified peptide **40** and successful conjugation confirmed by ESI-MS and the observation of an indicative mass-shift in the SDS-PAGE (Figure 17d-e).

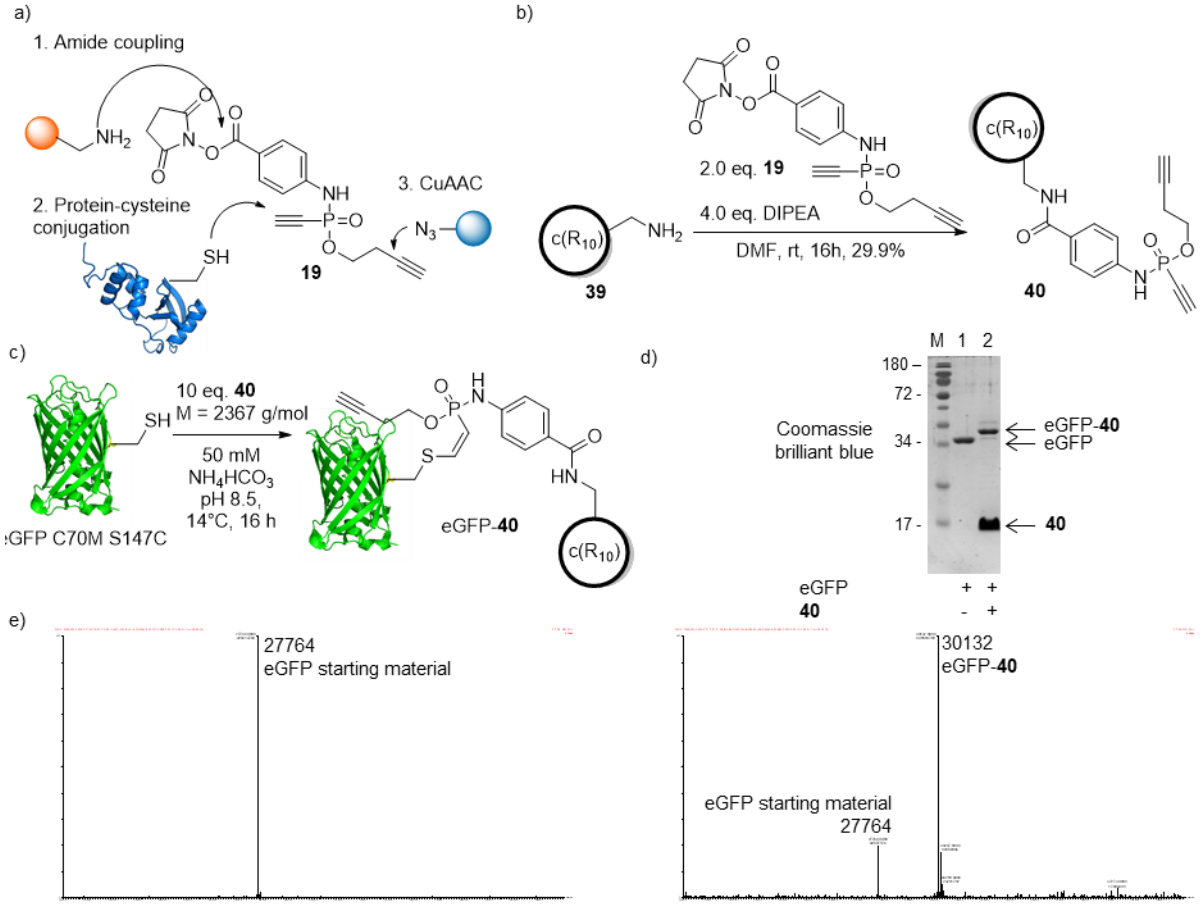

Figure 17: Compound **40** can be utilized as a functional building block to conjugate three different functionalities in an orthogonal manner. a) Principle of the triple conjugation. b) Functionalization of an amine containing cR_{10} **39** with **19**. Stated is the isolated yield after preparative HPLC. c) Conjugation of the modified peptide **40** to eGFP C70M S147C. d) Successful conjugation was monitored by an indicative SDS-PAGE gel shift. line 1: eGFP starting material. line 2: Reaction mixture after overnight incubation. e) Intact-protein MS analysis before (left) and after the reaction (right). A mass shift of 2367 Da is indicative for the desired thiol-addition product.

After successful conjugation of the cysteine eGFP to the peptide **40**, the accessibility of the terminal alkyne at the phosphonamidate ester residue was evaluated. For this, an azide containing Cy5 was attached, using a standard copper catalyzed cycloaddition protocol.

Azides are usually attached to the dye core via long alkyl chains[330] that add a lot of additional hydrophobicity to the molecule, diminish thereby water solubility and hamper protein conjugations

* cR10 was synthesized and purified by Ines Kretzschmar by standard SPPS

† eGFP C70M S147C was designed and cloned by Dr. Dominik Schumacher as part of his PhD thesis. Expression was performed by Kristin Kemnitz-Hassanin.

under aqueous conditions. The azide-modified Cy5 **45** with a short ethylene linker, used in this work has not been described so far. The synthetic route for **45** that has been applied is depicted in Scheme 52.*

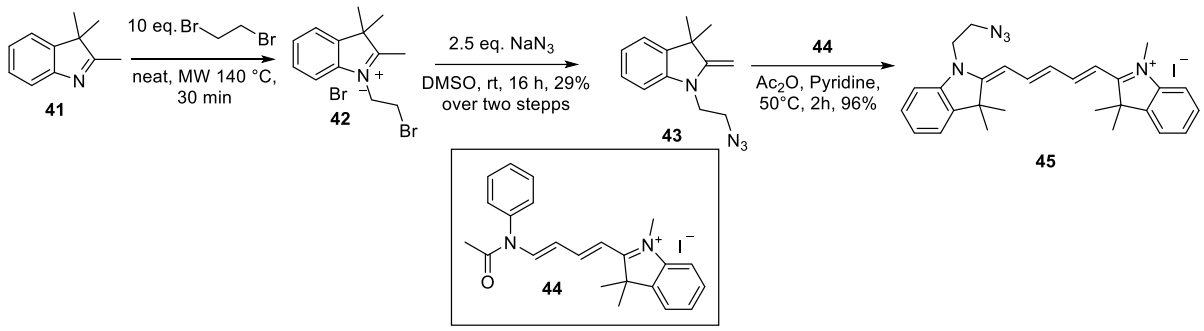

Scheme 52: Synthesis of Cy5-N_3 **45**. The Cy5 precursor **44** was synthesized according to a previously published procedure.[331]

The Cy5 dye core was synthesized based on a previously described procedure[331] from the intermediate **44** and the azido modified indoline **43** in very high yields. The synthesis of **43** was conducted from the commercial available trimethyl indol **41** by alkylation with dibromoethane followed by a nucleophilic substitution of the bromide with sodium azide in DMSO.

Copper-catalyzed cycloaddition of **45** to the modified eGFP proceeded smoothly to give the desired product in good conversion. Successful conjugation was proven by in-gel fluorescence after excitation of the Cy5 at 635 nm. In addition, intact protein ESI-MS revealed good labelling yields (Figure 18).

* Structure and synthesis of Cy5 azide is inspired by a Cy3 synthesis route, developed by Dr. Felix Hövelmann as part of his PhD thesis.

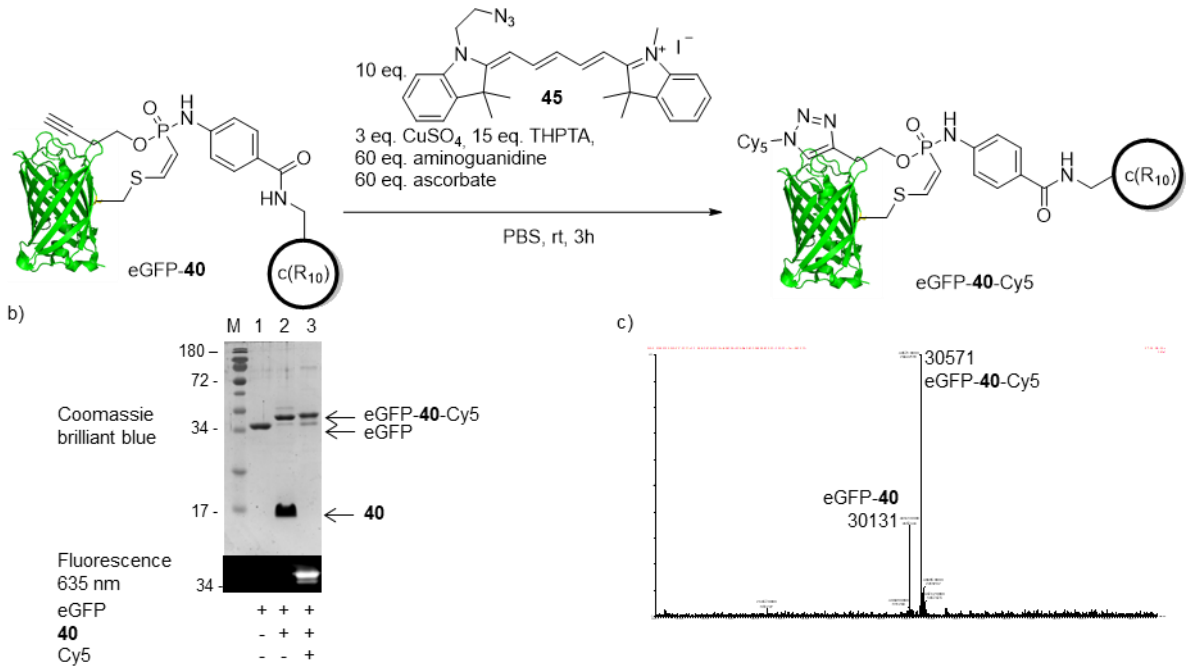

Figure 18: CuAAC of Cy5-N_3 **45** to eGFP, modified with **40**. a) Synthetic scheme. b) Successful conjugation was monitored by in-gel fluorescence measurements of an SDS-PAGE gel at 635 nm. line 1: eGFP starting material. line 2: Reaction mixture of the addition of **40** to eGFP. line 3: Reaction mixture of the CuAAC, depicted in a. c) Intact-protein MS analysis after CuAAC. A mass shift of 438 Da is indicative for the desired triazole product.

To sum up, it has been demonstrated that the installation of a terminal alkyne to the Phosphonamidate ester residue facilitates an additional side-specific attachment via CuAAC after the cysteine conjugation of the ethynylphosphonamidate. The functional building block **19** enables a triple conjugation of an amine, a protein thiol and an azide in a modular subsequent conjugation strategy. In the particular case, a cCPP, a Protein and a fluorescent dye were assembled, facilitating the observation of cellular uptake by fluorescence microscopy also of non-fluorescent proteins. Next Steps include the functional evaluation of the eGFP-**40**-Cy5 construct in terms of cell penetration and application of the concept to other non-fluorescent proteins.

6.1.3. Enantiomerically pure ethynylphosphonamidates

One unique feature of the thiol addition to ethynylphosphonamidates is the high *Z*-selectivity of the reaction in aqueous systems, as described in chapter 6.1.1. Due to this, enantiomerically pure ethynylphosphonamidates give rise to highly homogenous protein conjugates via cysteine, yielding a single diastereoisomer. This is impossible with other cysteine selective labelling reagents such as maleimides, since a stereocenter is formed upon thiol addition to the maleimide (Scheme 53).

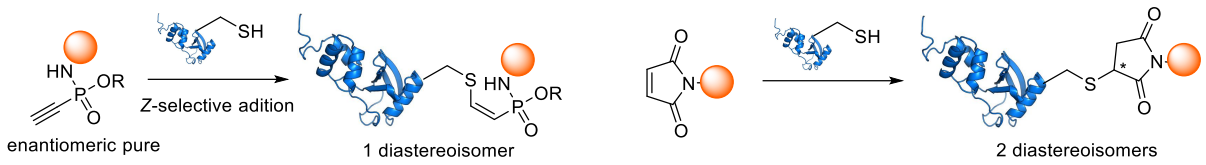

Scheme 53: enantiomeric pure ethynylphosphonamidates yield a single diastereoisomer after cysteine modification. Maleimides react with cysteine to form two diastereoisomers.

Here, it was tested if the two phosphonamidate enantiomers that originate from the SPhR can be separated by chiral HPLC. Baseline separation of the two enantiomers of compound **46** was possible after optimization of the HPLC conditions and it was observed that a one to one mixture is produced from the SPhR, as expected (Figure 19a). With semi-preparative chiral HPLC it was possible to isolate the two enantiomers from each other, as demonstrated by analytical chiral HPLC of the two isolated fractions (Figure 19b).*

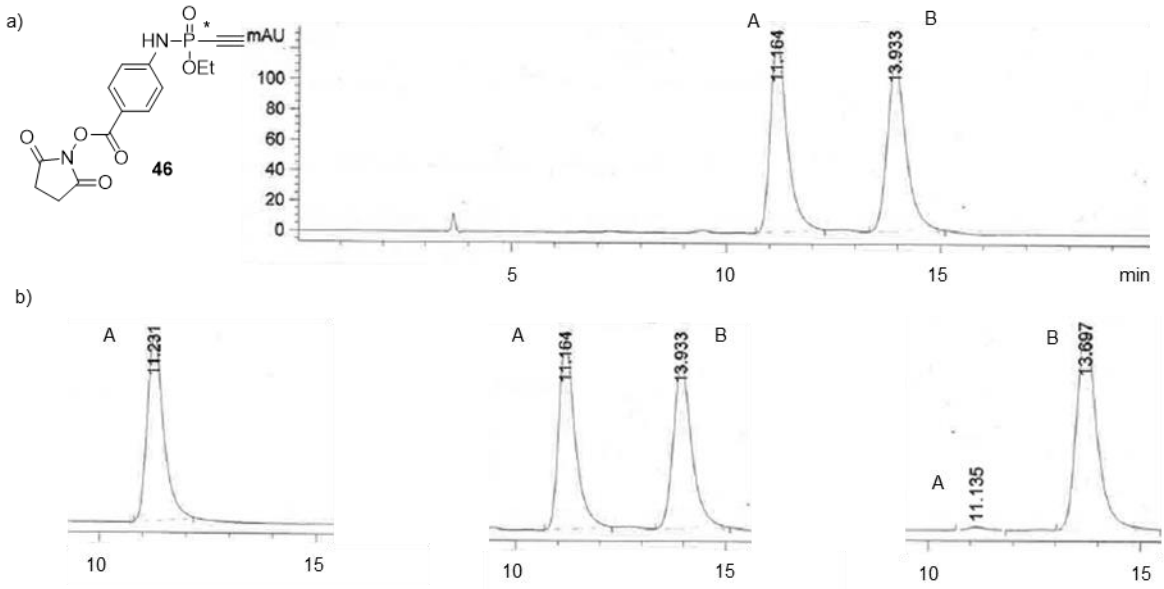

Figure 19: Phosphonamidate enantiomers can be separated by chiral HPLC. a) Chromatogram of the enantiomeric mixture of **46**, synthesized via standard conditions for the SPhR, as described in chapter 6.1.1. b) Zoom into the analytical chromatograms of enantiomer A (left) enantiomeric mixture (middle) and enantiomer B (right). Enantiomers were isolated by semi-preparative chiral HPLC.

With the enantiomerically pure building blocks of compound **46**, it is now in principle possible to attach a functionality to a protein's cysteine residue, yielding a single diastereoisomer.

* Semi-preparative and analytical chiral HPLC was performed by Christiane Groneberg in the laboratory of Mathias Christmann

6.2. Electrophilic vinylphosphonamidates with tunable reactivity for cysteine-selective modifications of proteins

As described in the previous chapter, ethynylphosphonamidates function as cysteine-selective electrophiles that can be chemoselectively incorporated starting from ethynylphosphonites by the SPhR. In the current chapter, vinylphosphonites are described for the transformation of azides into electron-deficient vinylphosphonamidates that subsequently modify cysteine residues in peptides and proteins. In contrast to ethynylphosphonamidates, which haven't been described before, some few literature examples that describe the compound class of vinylphosphonamidates can be found. Vinylphosphonamidates have been evaluated as monomers for polymerization[332], potential inhibitors for a hepatitis C virus polymerase[333], antimicrobials[334] and synthetic precursors[335]. Gao et al. were the only ones who reported vinylphosphonamidates as potential thiol acceptors for Coenzyme A. However, thiol adducts formation was not observed under their tested conditions (see chapter 0).[143] All previous synthetic attempts that have been described so far were based on nucleophilic substitution of vinylphosphonochloridate precursors with amines under basic conditions, whereas a method based on the SPhR has not been described so far. The aim of the work described in this chapter was the evaluation of vinylphosphonites as substrates for the SPhR with azide building blocks to synthesize vinylphosphonamidates for subsequent thiol addition to modify cysteine residues on biomolecules with the following main goals:

a) Development of the SPhR with differently substituted vinylphosphonites and various azide-modified building blocks to synthesize vinylphosphonamidates
b) Evaluation of the reactivity of vinylphosphonamidates for cysteine residues in dependence of the electronic nature of the phosphonamidate ester residue to identify suitable derivatives for the modification of proteins and antibodies.
c) Exploration of the unique features of the phosphonamidate linker structure, which includes the incorporation of functional handles to the vinylphosphonamidate ester residue

6.2.1. SPhR with vinylphosphonites to generate vinylphosphonamidates for cysteine modifications and chemoselective peptide cyclizations

This chapter was published in the following journal:

Marc-André Kasper†, Maria Glanz†, Andreas Oder, Peter Schmieder, Jens P. von Kries and Christian P. R. Hackenberger*

"Vinylphosphonites for Staudinger-induced chemoselective peptide cyclization and functionalization"

Chem. Sci. **2019**, 10, 6322-6329
Publication date (online):
The article is available online at: May 16th, 2019
https://pubs.rsc.org/en/content/articlelanding/2019/sc/c9sc01345h#!divAbstract

† These authors contributed equally
*Corresponding author

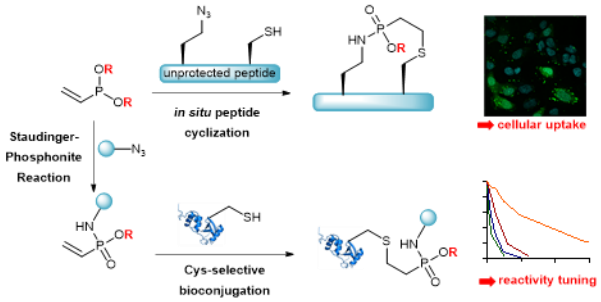

Figure 20: Vinylphosphonites enable the incorporation of vinylphosphonamidates via SPhR that subsequently modify cysteine residues on proteins and facilitate a chemoselective peptide cyclization. Altering the phosphonamidate's *O*-substituents allows for tuning the reactivity for sulfhydryl groups or promotes an increase in cellular uptake of stapled peptides.

Abstract:

In this paper, we introduce vinylphosphonites for chemoselective Staudinger-phosphonite reactions (SPhR) with azides to form vinylphosphonamidates for the subsequent modification of cysteine residues in peptides and proteins. An electron-rich alkene is turned into an electron-deficient vinylphosphonamidate, thereby inducing electrophilic reactivity for a following thiol addition. We show that by varying the phosphonamidate ester substituent we can fine-tune the reactivity of the thiol addition and even control the functional properties of the final conjugate. Furthermore, we

observed a drastic increase in thiol addition efficiency when the SPhR is carried out in the presence of the thiol substrate in a one-pot reaction. Hence, we utilize vinylphosphonites for the chemoselective intramolecular cyclization of peptides carrying an azide-containing amino acid and a cysteine in high yields. Our concept was demonstrated for the stapling of a cell-permeable peptidic inhibitor for protein–protein–interaction (PPI) between BCL9 and beta-catenin, which is known to create a transcription factor complex acting in embryonic development and cancer origin, and for macrocyclizing cell-penetrating peptides (CPPs) to enhance the cellular uptake of proteins.

Responsibility assignment:

Christian P. R. Hackenberger designed and conceived the project. The author developed the SPhR and the subsequent cysteine modification, synthesized and characterized all isolated phosphonites, the non-peptidic phosphonamidates and the azide precursors, conceived and performed stability studies and all kinetic studies, developed the antibody modification protocol with vinylphosphonamidates and synthesized, purified and analyzed the antibody conjugates. Maria Glanz developed the intramolecular peptide cyclization, synthesized and characterized all peptides, performed stability studies, expressed all proteins, synthesized the eGFP conjugates and performed all cellular imaging studies. Andreas Oder performed the HTRF assay. Peter Schmieder conceived and performed two-dimensional NMR experiments and analyzed the spectra. Jens P. von Kries designed and conceived the HTRF assay-experiments. The author wrote the manuscript supported by Maria Glanz and Christian P. R. Hackenberger.

Summary of content:

A method for the chemoselective transformation of azides with vinylphosphonites to synthesize electrophilic vinylphosphonamidates that are reactive for cysteine residues is presented. The SPhR turns an electron-rich phosphonite into an electron-deficient phosphonamidate and thereby induces reactivity for subsequent thiol addition. The method facilitates either a two-step approach where the cysteine-reactive vinylphosphonamidates is incorporated in the first step followed by protein modification or a one-step chemoselective intramolecular cyclization of peptides carrying an azide-containing amino acid and a cysteine. Described is the synthesis of various vinylphosphonites, carrying different *O*-substituents and subsequent SPhR with an aromatic and an aliphatic model azide. Vinylphosphonites were stabilized for isolation by borane adduct formation. Subsequent borane removal and SPhR with the azides was carried out applying a one-pot protocol. Different electrophilic vinylphosphonamidates with various *O*-substituents could be isolated applying this protocol and the reactivity with glutathione as a model cysteine substrate was tested afterwards. It could be

demonstrated that vinylphosphonamidates react significantly slower with sulfhydryl groups when compared to their ethynyl counterparts, but the reactivity can be increased by the attachment of electron withdrawing substituents at the phosphonamidate ester residue. The fastest vinylphosphonamidate tested in this study carried an *O*-trifluoroethyl- and a *N*-phenyl substituent and modified glutathione with a second-order rate constant of 0.021 $M^{-1}s^{-1}$. It could be shown that the phosphonamidate with this substitution pattern is able to modify cysteine residues on proteins, as demonstrated by alkylation of the interchain disulfide bonds of the therapeutically relevant antibody cetuximab. A good cysteine selectivity, using only slight reagent excess could be observed, whereas only small degrees of unselective lysine-labelling was observed with high excess of more than 100 equivalents with respect to the antibody. Furthermore, an intramolecular version of the chemically induced thiol addition for a chemoselective cyclization of peptides, carrying an azidohomoalanine and a cysteine residue, is presented. It is shown that the reactivity for the thiol addition is increased when the SPhR is carried out in the presence of a thiol. Vinylphosphonites facilitate thereby a high yielding chemoselective cyclization of azide functionalized cysteine peptides. The method was applied to the synthesis of a stapled peptide that is known to disrupt the protein-protein interaction between BCL-9 and β-Catenin. The helicity of the peptide is increased by the cyclization from 20% to 50%, as investigated by CD-spectroscopy and a homogeneous assay with time resolved fluorescence (HTRF) revealed that the PPI can be disrupted with concentrations in the submicromolar range. Exchanging the phosphonamidate's *O*-substituent from ethyl to a more lipophilic benzyl residue furthermore enhances the potential of the cyclized peptides to penetrate into cells. In addition to that, the technology was used to cyclize a cell-penetrating CR_{10} peptide, which was afterwards conjugated to eGFP. R_{10} that was cyclized with a vinylphosphonite sufficiently enhanced the uptake of eGFP into HeLa cells in a similar manner than the previously described lactam cyclized CR_{10}.

Manuscript and supporting information

Chemical Science

EDGE ARTICLE

View Article Online
View Journal | View Issue

Cite this: *Chem. Sci.*, 2019, **10**, 6322

All publication charges for this article have been paid for by the Royal Society of Chemistry

Received 19th March 2019
Accepted 10th May 2019

DOI: 10.1039/c9sc01345h

rsc.li/chemical-science

Vinylphosphonites for Staudinger-induced chemoselective peptide cyclization and functionalization†‡

Marc-André Kasper,§[ab] Maria Glanz,§[ab] Andreas Oder,[a] Peter Schmieder,[a] Jens P. von Kries[a] and Christian P. R. Hackenberger *[ab]

In this paper, we introduce vinylphosphonites for chemoselective Staudinger-phosphonite reactions (SPhR) with azides to form vinylphosphonamidates for the subsequent modification of cysteine residues in peptides and proteins. An electron-rich alkene is turned into an electron-deficient vinylphosphonamidate, thereby inducing electrophilic reactivity for a following thiol addition. We show that by varying the phosphonamidate ester substituent we can fine-tune the reactivity of the thiol addition and even control the functional properties of the final conjugate. Furthermore, we observed a drastic increase in thiol addition efficiency when the SPhR is carried out in the presence of a thiol substrate in a one-pot reaction. Hence, we utilize vinylphosphonites for the chemoselective intramolecular cyclization of peptides carrying an azide-containing amino acid and a cysteine in high yields. Our concept was demonstrated for the stapling of a cell-permeable peptidic inhibitor for protein–protein interaction (PPI) between BCL9 and beta-catenin, which is known to create a transcription factor complex playing a role in embryonic development and cancer origin, and for macrocyclization of cell-penetrating peptides (CPPs) to enhance the cellular uptake of proteins.

Introduction

Selective chemical modification of the sulfhydryl group of cysteine is an important tool in the life sciences.[1,2] Cysteine-selective reactions have been employed to covalently modify proteins in a residue specific manner for various applications including drug delivery,[3] incorporation of post-translational modifications[4] and activity based protein profiling.[5]

A plethora of different techniques have been developed in the past few decades that allow for selective modification of cysteine residues on peptides and proteins based on various reaction mechanisms. Michael additions to α,β-unsaturated carbonyl compounds in maleimides,[6] sulfone reagents[7] and recently developed carbonylacrylic reagents[8] are the most prominent examples. Other methods rely on SN_2-reactions of haloalkyl bonds such as iodoacetamides,[9] on alkynylation[10] and fluoroalkylation[11] with hypervalent iodine reagents, on nucleophilic aromatic substitution of perfluoroaromatic compounds[12] or on Pd-mediated cross-coupling.[13] The level of reactivity for cysteine in these methods is predetermined by the chemical nature of the reactive group itself. Alteration of this reactivity is often difficult and requires tedious chemical manipulations. However, certain applications such as activity based protein profiling[14] or covalent enzyme inhibition[15] often rely on reduced reactivity that allows for modification of the active site cysteine while sparing all other free nucleophiles in the proteome. Such decreased reactivity has for instance been achieved by substituting the highly reactive iodide in α-haloacetamides with a less reactive chloride.[16] Therefore, a cysteine selective modification method that utilizes easily tunable electrophilic warheads would be highly attractive for addressing challenges in peptide and protein chemistry.

Aside from protein modification, cysteine selective reactions have also been applied to peptide synthesis. One or two covalent linkages between cysteine residues in peptides enable the construction of macro or bicyclized peptides with enhanced biophysical and pharmacological properties.[17] Upon macrocyclization, peptidic structures can become more stable against proteases,[18] they can be locked in their structural conformation by covalently linking side chains and therefore restricting their conformational flexibility[19,20] or increasing their function by rigid constraint as shown for various cyclic bioactive[21] or cell penetrating peptides (cCPPs).[22] The groups of Pentelute and Derda introduced perfluoroaromatic linkages

[a]*Leibniz-Forschungsinstitut für Molekulare Pharmakologie (FMP), Chemical Biology Department, Robert-Rössle-Strasse 10, 13125 Berlin, Germany. E-mail: hackenbe@fmp-berlin.de*

[b]*Humboldt Universität zu Berlin, Department of Chemistry, Brook-Taylor-Str. 2, 12489 Berlin, Germany*

† This work is dedicated to Prof. Ron Raines on the occasion of his 60th birthday.

‡ Electronic supplementary information (ESI) available. See DOI: 10.1039/c9sc01345h

§ These authors contributed equally.

for the cyclization of peptides containing two cysteines.[23,24] Tricyclic peptides have also been synthesized by alkylation with tris-(bromomethyl)benzene[25] and very recently by the incorporation of two chemical bridges with a set of various dibromoalkyl reagents.[26] Such chemoselective modification strategies are advantageous over common cyclization techniques[27] such as lactamization,[28] since they can be applied after cleavage from the resin and preclude therefore tedious orthogonal protecting group strategies during SPPS. In addition, even cysteine containing proteins can be cyclized by applying chemoselective techniques, as recently demonstrated with the aid of a trimeric chloroacetamide.[29]

Based on the Staudinger-phosphonite reaction (SPhR), developed in our laboratory,[30] we recently introduced ethynylphosphonamidates as cysteine-selective electrophiles that can be chemoselectively incorporated starting from ethynylphosphonites.[31] In the current paper, we report vinylphosphonites as a new compound class for the transformation of azides into electron deficient alkenes that selectively modify cysteine residues in peptides and proteins. We observed that the SPhR with vinylphosphonites facilitates straightforward access to vinylphosphonamidates carrying different *O*-substituents. We discovered that the rate of the subsequent thiol addition can be drastically influenced by the electronic properties of these phosphonamidate ester substituents. In addition, we engineered an intramolecular variant of the chemically induced thiol addition for a chemoselective cyclization of peptides. We were able to demonstrate that azido modified cysteine peptides can be cyclized upon SPhR with vinylphosphonites in high yields (Scheme 1). In contrast to other chemoselective peptide cyclizations, which have been mainly used for head-to-tail cyclizations, including traceless Staudinger ligation,[32] α-ketoacid–hydroxylamine amide-ligation[33] or serine ligation,[34] the method presented herein can be straightforwardly applied to side-chain ring closure.

Results and discussion

Previously, Gao *et al.* have observed that methyl-substituted vinylphosphonamidates are unreactive in base mediated thiol additions,[35] probably due to decreased electrophilicity, compared to their ethynyl substituted counterparts.[31] We anticipated that the electrophilic reactivity of the double bond towards thiol-addition can be increased by attaching different electron-withdrawing substituents to the phosphonamidate ester moiety. Since this residue is preserved during SPhR with azides, we started our investigations by synthesizing different substituted vinylphosphonites. Here, we followed previously published procedures starting from either phosphorus trichloride (route I) or bis(diisopropylamino)-chlorophosphine (route II).[36] Several attempts to isolate unprotected vinylphosphonites failed due to product decomposition, hence we decided to isolate the phosphonites in their borane-protected form and use them directly as starting materials for the subsequent SPhR. Vinylphosphonite borane adducts proved to be stable during column chromatography and we were able to obtain four vinylphosphonites with ethyl, **1a**, phenyl, **1b** and electron withdrawing 2-nitrobenzyl, **1c**, and trifluoroethyl, **1d**, substituents (Fig. 1a).

With vinylphosphonites **1a–d** in hand, we continued our studies to perform the SPhR with two different model azides **2** and **3** to synthesize both *N*-phenyl **4a–d** and *N*-alkyl substituted vinylphosphonamidates **5a–d**. Here, we applied previously published procedures, either diethyl chlorophosphite alkylation with vinylmagnesium bromide[31] (route III) or borane deprotection with DABCO in toluene[37] (route IV), directly followed by azide addition and hydrolysis without isolation of the phosphonite intermediate. The SPhR was always carried out in dry solvents to prevent hydrolysis of the phosphonites. All of the tested phosphonites reacted smoothly under the tested conditions and the desired vinylphosphonamidates could be isolated by column chromatography. Electron withdrawing substituents were well tolerated in the reaction with the aryl azide **2** and with the alkyl azide **3** (Fig. 1b).

Next, we probed the reactivity of the synthesized vinylphosphonamidates towards thiol addition in aqueous solution under slightly basic conditions as previously performed for ethynylphosphonamidates[31] (Fig. 2a). For this, a time course for the addition of glutathione (GSH) to vinylphosphonamidates **4a–d** and **5a–d** in ammonium bicarbonate buffer was recorded.

Under the tested conditions (10 mM phosphonamidate and two equivalents of GSH) the *N*-phenyl vinylphosphonamidate **4a** showed a good conversion of 80% to the desired thiol adduct after 24 h. In contrast to **4a**, the comparable *N*-alkyl derivative **5a** was only converted 20% under the same conditions (Fig. 2b), which is in accordance with the observations of Gao *et al.* on the unreactivity of *N*-alkyl-*O*-methyl-vinylphosphonamidate towards thiols; however, the previously mentioned dealkylation of the phosphonamidate ester was not observed under conditions applied here. Since we assumed that such slow kinetics would limit the applicability to protein modification, for example by undesired disulfide formation of the peptide or protein substrate, we also tested compounds with electron-

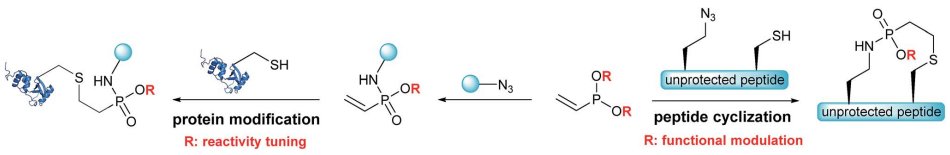

Scheme 1 Vinylphosphonites for intramolecular peptide cyclization and cysteine selective protein modification.

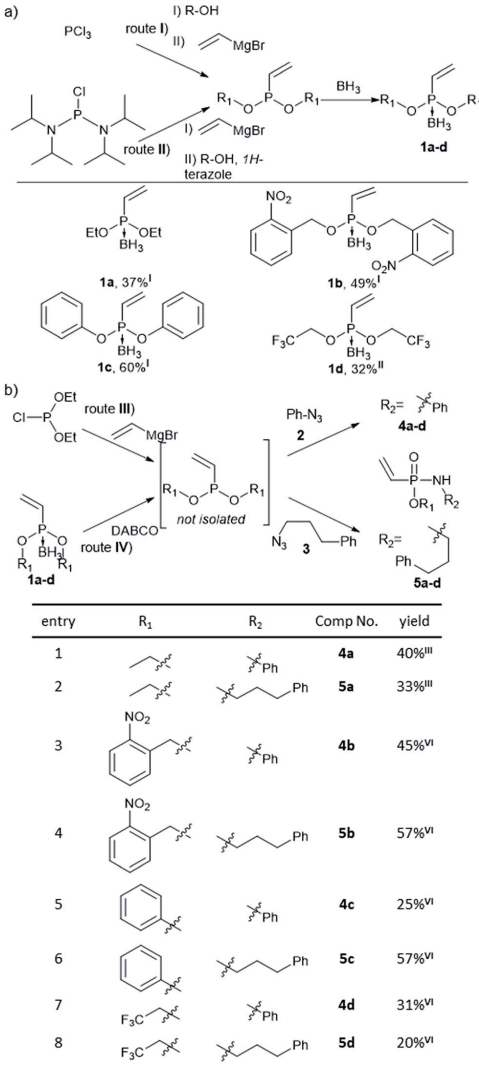

entry	R_1	R_2	Comp No.	yield
1		Ph	**4a**	40%III
2		Ph	**5a**	33%III
3	NO_2	Ph	**4b**	45%VI
4	NO_2	Ph	**5b**	57%VI
5		Ph	**4c**	25%VI
6		Ph	**5c**	57%VI
7	F_3C	Ph	**4d**	31%VI
8	F_3C	Ph	**5d**	20%VI

Fig. 1 (a) Synthesis of substituted vinylphosphonites from phosphorus trichloride (route I) or bis(diisopropylamino)chlorophosphine (route II). Stated are isolated yields. (b) One-pot SPhR with vinylphosphonites and azides. Synthesis from borane protected vinylphosphonites (route III) or diethyl chlorophosphite (route IV). Stated are isolated yields.

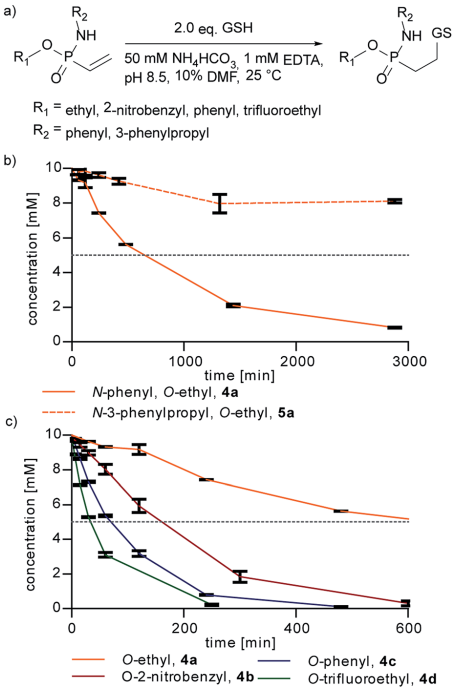

Fig. 2 (a) Reaction of glutathione (GSH) with differently substituted vinylphosphonamidates. 10 mM vinylphosphonamidates were reacted with 20 mM GSH at pH 8.5 (NH_4HCO_3 buffer). Concentration of the starting materials over time, mean and error from three independent measurements, monitored by UPLC-UV. (b) *N*-Phenyl *vs.* *N*-alkyl comparison. (c) Comparison of different *O*-substituents. Dotted line depicts 50% conversion.

deficient phosphonamidate ester substituents in the addition of glutathione. A conversion of 50% is reached after two and a half hours for 2-nitrobenzyl compound **4b** and after only 30 minutes for trifluoroethyl substituted **4d**. The *O*-phenyl compound **4c** shows an accelerating effect over alkoxy-substituents as well, reaching 50% conversion in only one hour (Fig. 2c). These results clearly show that the reactivity of vinylphosphonamidates can be tuned by varying the phosphonamidate ester residue. The corresponding *N*-alkyl substituted compounds **5a–d** also undergo rate enhancement with more electron withdrawing *O*-substituents, with a slower reaction compared to the *N*-phenyl substituted compounds **4a–d** in general (ESI Fig. S1‡). Notably, the glutathione adduct was the only detectable product by UPLC/MS and no other side product was observed for any of the tested phosphonamidates (ESI Fig. S2‡). The identity of the thiol-glutathione adducts of **4a** (ESI Fig. S3‡) and **4d** was confirmed by NMR characterization after isolation by preparative HPLC in 60% and 89% yield, respectively.

Further kinetic investigations of the thiol addition to **4d**, being the fastest compound tested in this study (ESI Fig. S1‡), revealed a second-order rate constant of 0.021 M^{-1} s^{-1} (ESI Fig. S4‡). Even though this is considerably slower than that of maleimides (734 M^{-1} s^{-1}),[38] ethynylphosphonamidates (0.62 M^{-1} s^{-1})[31] and recently introduced dinitroimidazoles,[39] the rate is still higher or in the range of other protein modification

reactions such as oxime, Staudinger or Pictet–Spengler ligations.[38] Next to reaction rates, an important aspect for many applications of cysteine selective protein modification reagents is susceptibility of the conjugate towards thiol exchange.[1] Maleimides are in particular known to undergo retro Michael addition, followed by transfer of the modification to other cysteine containing molecules in solution.[40] To prove the stability of the vinylphosphonamidate adducts in the presence of other thiols, we incubated the glutathione adducts of **4a** and **4d** with an excess of 100 equivalents of 2-mercaptoethanesulfonate. Even after one week of incubation, no thiol exchange could be observed for both of the constructs by UPLC/MS (ESI Fig. S5‡).

Next, we wanted to probe the reactivity of electron-poor vinylphosphonamidates towards cysteine modification on antibodies. For this, we synthesized a fluorescent EDANS-modified vinylphosphonamidate **6**, analogously to compound **4d**, with the *N*-phenyl-*O*-trifluoroethyl substitution pattern that has been identified to be superior in thiol addition kinetics. Based on a previously established protocol[31] we reduced the four interchain disulfide bonds of cetuximab to generate 8 free cysteine residues and probed the reactivity towards **6** (Fig. 3a). Successful labelling after reduction and incubation with 20 equivalents of reagent per antibody was confirmed by in-gel fluorescence (Fig. 3b). Intact protein MS revealed a decent degree of modification of 3.8 fluorophore molecules per antibody (ESI Fig. S6‡). To probe the cysteine selectivity, a control experiment without prior antibody reduction was performed and no modification could be detected after incubation with 20 equivalents of **6** by in-gel fluorescence and MS. Only upon exposure of the unreduced antibody to high reagent excesses of more than 50 equivalents per antibody, low degrees of modification were observed (Fig. 3b). The observation of unspecific labelling at higher reagent concentrations was further investigated by mass spectrometry (LC-MS/MS) after trypsin digestion of the reduced antibody modified with 100 eq. of **4d** (ESI Fig. S7‡). In addition to the inter-chain disulfide forming cysteines, a few lysine residues were also found to be modified. This cross-reactivity with lysine is also known for other cysteine labelling reagents such as iodoacetamides[41] and maleimides.[42] The findings are nevertheless contrary to our previously reported ethynylphosphonamidate reagents that exhibit excellent cysteine selectivity even with large reagent excesses.[31] To further broaden the scope of our method, we also synthesized a biotin-modified 2-nitrobenzyl-phosphonamidate with a structure that has the same substitution pattern as compound **4b**. Successful antibody labelling was confirmed by anti-biotin Western blot analysis. Analogously to the trifluoroethyl compound, only prolonged reaction times lead to minor labelling degrees without prior reduction of the antibody disulfide bonds (ESI Fig. S8‡). Taken together, we were able to show that vinylphosphonamidates can lead to efficient and selective modification of cysteine residues on proteins using only slight reagent excesses.

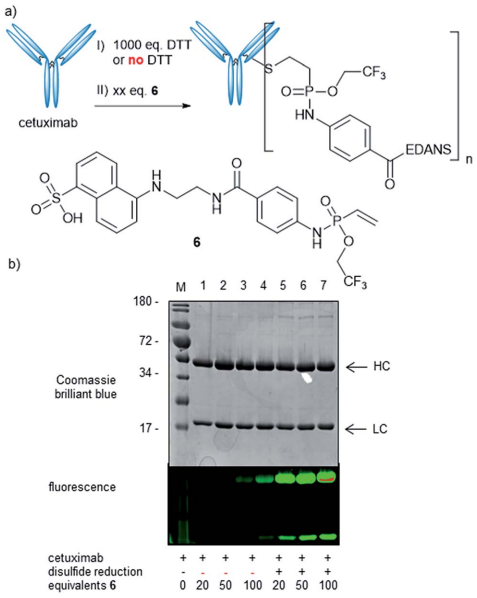

Fig. 3 Cetuximab modification with **6**. (a) Reduction and alkylation principles and structure of **6**. (b) Gel analysis: reactions were carried out with varying equivalents of **6**: Lane 1: untreated antibody. Lane 2–4: control reactions without prior DTT treatment. Lane 5–7: prior DTT treatment. HC: antibodies' heavy chain, LC: light chain.

We further anticipated that the SPhR with subsequent thiol addition could also be applied in an intramolecular reaction. Therefore we synthesized an azidohomoalanine- and cysteine-containing peptide, aiming to initiate a covalent cyclization. As the first proof of principle study, we chose to macrocyclize the BCL9 derived peptide **8a**, which has been reported to act as a potent PPI-inhibitor when stapled by ring closing metathesis (RCM).[43] We decided to replace the two olefinic amino acids in the *i*,*i*+4 position with azidohomoalanine and cysteine in order to keep the linker length (10 atoms) similar to that of the literature-known peptide **7** (Scheme 2). In our initial experiments we aimed to keep a double bond in the linker structure for more rigidity and hence used an ethyl-substituted ethynylphosphonite in the reaction with peptide **8a** in dry DMSO based on our previously published conditions.[31] However, we found that in order to promote the initial SPhR with the alkylazide of azidohomoalanine the reaction temperature had to be raised to 50 °C, upon which the macrocyclized product formed only in low amounts. A major side product observed by UPLC-UV/MS was a peptide with an additional 28 Da, which we attribute to the alkylation of the nitrogen of the phosphonamidate. Similar *N*-alkylated phosphoramidates were reported previously by us after the rearrangement of phosphorimidates under elevated temperatures.[44] We hypothesized that raising the reactivity of the phosphonite by using a more nucleophilic vinyl- as opposed to the ethynyl-phosphonite in the SPhR enables the use of lower reaction temperature and would thereby prevent the rearrangement to the alkylated byproduct. Therefore purified

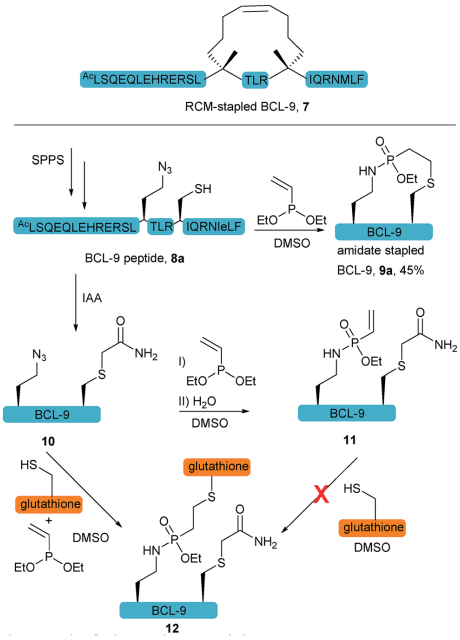

Scheme 2 Principle of the intramolecular peptide cyclization of an azido containing cysteine-BCL-9 derived peptide. Investigations with a capped cysteine peptide (**9**) revealed an accelerated thiol addition when SPhR is performed in the presence of thiols. SPhR on peptides is always carried out with the crude diethyl phosphonite, synthesized from diethyl chlorophosphite (route III).

peptide **8a** was reacted with crude diethyl vinylphosphonite (route III) after SPPS in an over-night reaction in DMSO. To our delight, we isolated the desired cyclized peptide **9a** after preparative HPLC as the main product in a very good yield of 45%. This result is particularly remarkable in light of the slow intermolecular thiol addition to *O*-ethyl-*N*-alkyl-vinylphosphonamidates such as **5a** as shown before (Fig. 2b). UPLC/MS showed a clean conversion towards the desired product without significant amounts of the side product (ESI Fig. S9‡).

To gain more insight into the *in situ* intramolecular cyclization, we capped the cysteine of peptide **8a** with iodoacetamide to form peptide **10**. This peptide was reacted with glutathione under two different reaction conditions (Scheme 2). First, glutathione was added in a one-pot reaction with peptide **10** (1.65 mM) and 5 eq. diethyl vinylphosphonite. Here, the thiol addition product **12** could be observed by LC-MS as the major product (ESI Fig. S10‡). In the second experiment, we reacted peptide **10** with 5 eq. vinyl phosphonite to form the phosphonamidate **11** after hydrolysis, as observed by LC-MS. After lyophilization peptide **11** was incubated with 1 eq. glutathione (1.65 mM) in DMSO for 24 hours. Under these conditions, no product formation could be observed by MS analysis (ESI Fig. S10‡). This experiment again points towards the decreased reactivity of ethyl-substituted vinylphosphonamidates in intermolecular reactions with thiol substrates (see Fig. 2a and ref. 35), and furthermore implies that the *in situ* process benefits from the reaction of thiols with a more reactive SPhR intermediate.

With the phosphonamidate-cyclized BCL9 peptide **9a** in hand we set out to investigate its stability and helicity. At first, **9a** was incubated at different pH values over several days and the stability monitored by UPLC. Under acidic conditions below pH 2 the P–N-bond gets cleaved within 24 hours, which is in accordance with our previous observations.[31] At neutral and basic pH, the phosphonamidate moiety proved to be stable over several days without any observable decomposition (Fig. 4a and b). Next, we evaluated the peptides' helical propensities by CD spectroscopy and could show a drastic increase in helicity upon cyclization from 20% to around 50% (Fig. 4d). To verify the ability to disrupt the PPI between purified BCL9 and β-catenin we used a homogeneous assay with time resolved fluorescence (HTRF), in which both interacting proteins were recognized by distinct antibodies *via* orthogonal tags and conjugated fluorophores suitable for energy transfer.[45] Disturbance of the protein–protein interaction causes a decreased FRET signal (ESI Fig. S11‡). Using this assay, we could show that the phosphonamidate cyclized peptides can disrupt the PPI at concentrations in the nM range (Fig. 4e). The IC_{50} values are almost identical to those reported for the RCM stapled BCL9 peptide.[43] Furthermore, we observed that the stereochemistry at cysteine seems to have an influence on the disruption behavior, with a superior inhibition constant observed for the D-enantiomer **9b** compared to that of the L-enantiomer **9a**.

Since peptide stapling is known to improve cellular uptake through endocytic vesicle trafficking[46] and the BCL-9 and β-catenin interaction takes place intracellularly in the cytoplasm and the nucleus,[45] we also tested the peptides' ability to penetrate cells. By treating HeLa cells with 10 μM mixture of 10% fluorescein labelled and 90% non-labelled peptides for three hours, we observed that peptide **9b** shows almost no uptake, whereas the RCM stapled peptide **7** is taken up readily. We attributed this to a recent observation from the Futaki lab, in which they show the importance of net hydrophobicity for the cellular uptake of stapled peptides.[47] In order to increase the hydrophobicity of our linkage, we synthesized peptide **13** with a more lipophilic *O*-benzyl-substituent at the phosphonamidate. For this, the SPhR of the azido peptide **8b** with a benzyl phosphonite was carried out at slightly elevated temperatures to ensure high conversions. The peptide was only synthesized in the D-cysteine variant due to the aforementioned improved disruption behavior towards the BCL-9 and β-catenin interaction. Isolated **13** showed comparable helicity to the ethyl substituted **9b** (Fig. 4d) and the benzyl-substituent did not hamper the peptides' ability to disrupt the PPI (Fig. 4e). In addition, we observed increased cellular uptake of benzyl substituted **13**, compared to **9b**, which nicely

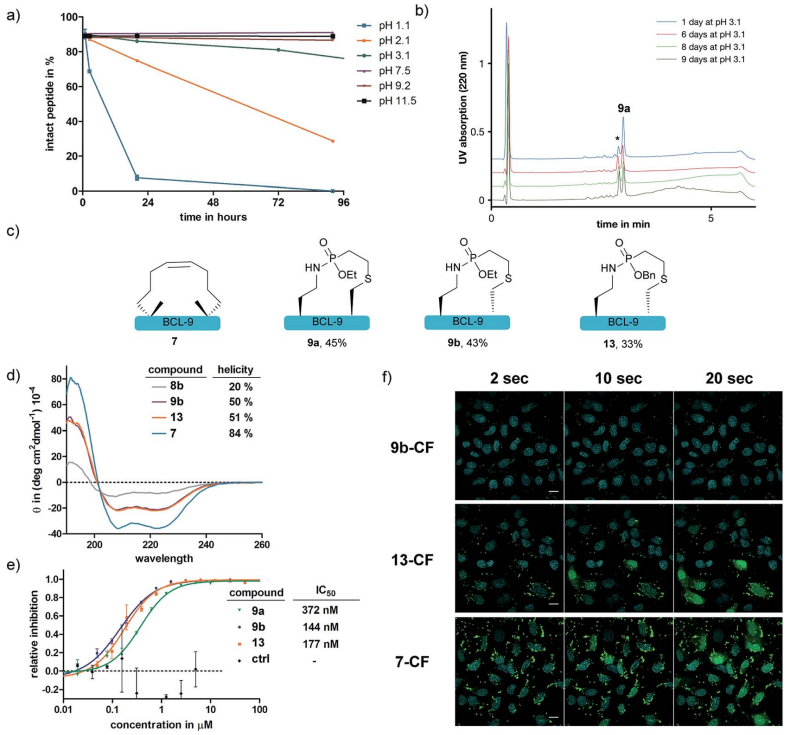

Fig. 4 (a) Stability of **9a** at different pH values. Shown are mean and error from three independent measurements, monitored by UPLC-UV. (b) UPLC-UV spectra of **9a** upon incubation at pH 3.1 over several days. *P–N-bond cleavage is the only degradation product observed. (c) Structures of differently cyclized BCL-9 peptides. Stated are isolated yields from the cyclization reaction. (d) CD-measurement of peptides. (e) HTRF assay shows disruption of PPI by peptidic inhibitors. (f) Cellular uptake studies of 10 μM mixture of 10% carboxy-fluorescein (CF)-labelled and 90% non-labelled peptides in HeLa cells. Confocal images with scale bar = 20 μm. Depicted is the overlay of fluorescein-fluorescence and Hoechst nucleus stain at different time points of laser (405/488 nm) irradiation.

illustrates the modularity of our method that allows a facile exchange of the *O*-substituent of phosphonamidates to modulate the functional properties of the peptide ligation products.

In addition to the side-chain-stapled peptides, we further expanded our novel cyclization method to a more general macrocyclization technique for enhancing the cellular uptake properties of protein conjugates. Therefore, we aimed for the cyclization of an R_{10} peptide, which is, like other arginine-rich peptides, able to enhance the transduction of functional proteins into living cells when covalently attached to the protein cargo.[48] We and others observed that the cellular transduction behavior is significantly improved for the cyclic version of cR_{10} when compared to its linear counterpart.[22,49,50] As an alternative to the previously applied cyclized R_{10}-CPP **14**, we synthesized peptide **15** containing a cysteine and an azidohomoalanine residue to replace the former lactam bridge after our novel cyclization technique. The linear unprotected peptide was reacted with the crude diethylvinylphosphonite (route III) in dry DMSO overnight to yield 48% of the *in situ* macrocyclized peptide **16** after purification. For conjugation of **16** to a protein cargo, the *N*-terminus of the peptide was capped with an ethynylphosphonamidate-NHS building block **17** [31] to yield **18** (Fig. 5a) for Cys-selective labeling reactions. Conjugation to eGFP that carries a single addressable cysteine proceeded quantitatively according to MALDI-TOF-MS (Fig. 5b). Cellular uptake of the protein was demonstrated by confocal fluorescence imaging after incubation of HeLa-cells with 30 μM conjugate for one hour at 37 °C in HEPES buffer and was compared to that of the standard lactam cyclized cR_{10}-eGFP conjugate. Cytosolic and nucleolar GFP fluorescence was observed and both protein–peptide-conjugates showed the same amount of transduced cells, indicating the feasibility of using our novel cyclization method as a macrocyclization technique (Fig. 5c).

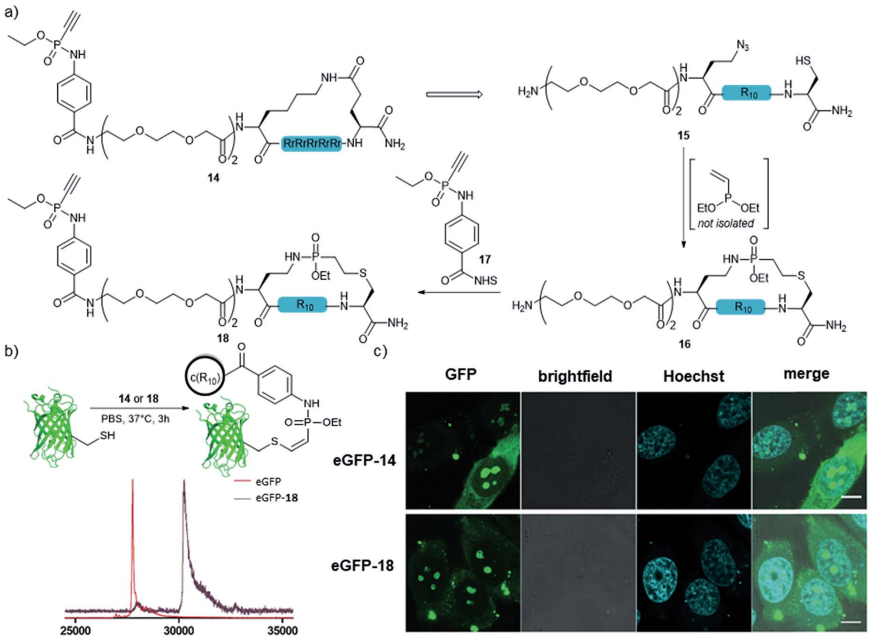

Fig. 5 (a) Principle of the Staudinger induced peptide cyclization with R_{10} and subsequent attachment of a thiol reactive handle. (b) Conjugation of cR_{10} to eGFP C70M S147C. Shown are MALDI-TOF-MS spectra before and after the reaction with 23. (c) Cellular uptake studies of 30 μM eGFP-**14** and eGFP-**18** in HeLa cells. Confocal images with scale bar = 10 μm.

Conclusions

In summary, we introduce the SPhR with vinylphosphonites as a versatile tool for the chemoselective cyclization of peptides. Furthermore, we demonstrate that variation of the phosphonite's *O*-substituent enables fine-tuning of the electrophilicity for intermolecular protein and antibody labeling. Additionally, this variation facilitates the incorporation of functional handles that can modulate the properties of the reaction product as demonstrated for the increased cellular uptake of phosphonamidate-cyclized BCL9 peptides. Finally, the high yielding peptide cyclization technique not only allows facile stapling of peptides but furthermore also facilitates a general macrocyclization strategy as shown for cCPPs. We believe that this tool will enable researchers to develop both novel cysteine reactive probes for applications where a narrow reactivity window is crucial and cyclic peptides with enhanced pharmacological properties that can be manipulated by phosphonamidate ester variation.

Conflicts of interest

The authors declare competing financial interests. The technology described in the manuscript is part of a pending patent application by M.-A. K., M. G. and C. P. R. H.

Acknowledgements

We thank H. Stephanowitz and Dr Fan Liu for performing tandem MS experiments, K. K. Hassanin for excellent technical assistance and Dr K. Licha for the provision of Cetuximab. This work was supported by grants from the Deutsche Forschungsgemeinschaft (SPP1623) to C. P. R. H. (HA 4468/9-1), the Einstein Foundation Berlin (Leibniz-Humboldt Professorship), the Boehringer-Ingelheim Foundation (Plus 3 award), the Leibniz Association with the Leibniz competition to C. P. R. H. and the Fonds der Chemischen Industrie to C. P. R. H.

Notes and references

1 S. B. Gunnoo and A. Madder, *ChemBioChem*, 2016, **17**, 529–553.
2 J. M. Chalker, G. J. L. Bernardes, Y. A. Lin and B. G. Davis, *Chem.–Asian J.*, 2009, **4**, 630–640.
3 S. O. Doronina, B. E. Toki, M. Y. Torgov, B. A. Mendelsohn, C. G. Cerveny, D. F. Chace, R. L. DeBlanc, R. P. Gearing, T. D. Bovee, C. B. Siegall, J. A. Francisco, A. F. Wahl, D. L. Meyer and P. D. Senter, *Nat. Biotechnol.*, 2003, **21**, 778–784.
4 J. Bertran-Vicente, M. Penkert, O. Nieto-Garcia, J.-M. Jeckelmann, P. Schmieder, E. Krause and C. P. R. Hackenberger, *Nat. Commun.*, 2016, **7**, 12703.

5 B. F. Cravatt, A. T. Wright and J. W. Kozarich, *Annu. Rev. Biochem.*, 2008, **77**, 383–414.
6 J. E. Moore and W. H. Ward, *J. Am. Chem. Soc.*, 1956, **78**, 2414–2418.
7 S. Brocchini, S. Balan, A. Godwin, J.-W. Choi, M. Zloh and S. Shaunak, *Nat. Protoc.*, 2006, **1**, 2241–2252.
8 B. Bernardim, P. M. S. D. Cal, M. J. Matos, B. L. Oliveira, N. Martínez-Sáez, I. S. Albuquerque, E. Perkins, F. Corzana, A. C. B. Burtoloso, G. Jiménez-Osés and G. J. L. Bernardes, *Nat. Commun.*, 2016, **7**, 13128.
9 D. R. Goddard and L. Michaelis, *J. Biol. Chem.*, 1935, **112**, 361–371.
10 D. Abegg, R. Frei, L. Cerato, D. Prasad Hari, C. Wang, J. Waser and A. Adibekian, *Angew. Chem.*, 2015, **127**, 11002–11007.
11 J. Václavík, R. Zschoche, I. Klimánková, V. Matoušek, P. Beier, D. Hilvert and A. Togni, *Chem.–Eur. J.*, 2017, **23**, 6490–6494.
12 C. Zhang, M. Welborn, T. Zhu, N. J. Yang, M. S. Santos, T. Van Voorhis and B. L. Pentelute, *Nat. Chem.*, 2015, **8**, 120.
13 E. V. Vinogradova, C. Zhang, A. M. Spokoyny, B. L. Pentelute and S. L. Buchwald, *Nature*, 2015, **526**, 687.
14 M. J. Niphakis and B. F. Cravatt, *Annu. Rev. Biochem.*, 2014, **83**, 341–377.
15 R. Lonsdale and R. A. Ward, *Chem. Soc. Rev.*, 2018, **47**, 3816–3830.
16 K. T. Barglow and B. F. Cravatt, *Chem. Biol.*, 2004, **11**, 1523–1531.
17 M. E. Otero-Ramirez, T. Passioura and H. Suga, *Biomedicines*, 2018, **6**, 116.
18 A. Celine and S. Claudio, *Curr. Med. Chem.*, 2002, **9**, 963–978.
19 L. D. Walensky, A. L. Kung, I. Escher, T. J. Malia, S. Barbuto, R. D. Wright, G. Wagner, G. L. Verdine and S. J. Korsmeyer, *Science*, 2004, **305**, 1466–1470.
20 L. D. Walensky and G. H. Bird, *J. Med. Chem.*, 2014, **57**, 6275–6288.
21 L. J. Walport, R. Obexer and H. Suga, *Curr. Opin. Biotechnol.*, 2017, **48**, 242–250.
22 G. Lättig-Tünnemann, M. Prinz, D. Hoffmann, J. Behlke, C. Palm-Apergi, I. Morano, H. D. Herce and M. C. Cardoso, *Nat. Commun.*, 2011, **2**, 453.
23 S. Kalhor-Monfared, M. R. Jafari, J. T. Patterson, P. I. Kitov, J. J. Dwyer, J. M. Nuss and R. Derda, *Chem. Sci.*, 2016, **7**, 3785–3790.
24 A. M. Spokoyny, Y. Zou, J. J. Ling, H. Yu, Y.-S. Lin and B. L. Pentelute, *J. Am. Chem. Soc.*, 2013, **135**, 5946–5949.
25 C. Heinis, T. Rutherford, S. Freund and G. Winter, *Nat. Chem. Biol.*, 2009, **5**, 502.
26 S. S. Kale, C. Villequey, X.-D. Kong, A. Zorzi, K. Deyle and C. Heinis, *Nat. Chem.*, 2018, **10**, 715–723.
27 N. A. Afagh and A. K. Yudin, *Angew. Chem., Int. Ed.*, 2010, **49**, 262–310.
28 L. Peng and P. R. Peter, *Curr. Top. Med. Chem.*, 2002, **2**, 325–341.
29 M. Pelay-Gimeno, T. Bange, S. Hennig and T. N. Grossmann, *Angew. Chem., Int. Ed.*, 2018, **57**, 11164–11170.
30 M. R. J. Vallée, P. Majkut, I. Wilkening, C. Weise, G. Müller and C. P. R. Hackenberger, *Org. Lett.*, 2011, **13**, 5440–5443.
31 M.-A. Kasper, M. Glanz, A. Stengl, M. Penkert, S. Klenk, T. Sauer, D. Schumacher, J. Helma, E. Krause, M. C. Cardoso, H. Leonhardt and C. Hackenberger, *Angew. Chem., Int. Ed.*, DOI: 10.1002/anie.201814715.
32 R. Kleineweischede and C. P. R. Hackenberger, *Angew. Chem., Int. Ed.*, 2008, **47**, 5984–5988.
33 T. Fukuzumi, L. Ju and J. W. Bode, *Org. Biomol. Chem.*, 2012, **10**, 5837–5844.
34 H. Y. Lam, Y. Zhang, H. Liu, J. Xu, C. T. T. Wong, C. Xu and X. Li, *J. Am. Chem. Soc.*, 2013, **135**, 6272–6279.
35 F. Gao, X. Yan and K. Auclair, *Chem.–Eur. J.*, 2009, **15**, 2064–2070.
36 K. D. Siebertz and C. P. R. Hackenberger, *Chem. Commun.*, 2018, **54**, 763–766.
37 M. R. J. Vallée, L. M. Artner, J. Dernedde and C. P. R. Hackenberger, *Angew. Chem., Int. Ed.*, 2013, **52**, 9504–9508.
38 F. Saito, H. Noda and J. W. Bode, *ACS Chem. Biol.*, 2015, **10**, 1026–1033.
39 Q. Luo, Y. Tao, W. Sheng, J. Lu and H. Wang, *Nat. Commun.*, 2019, **10**, 142.
40 J. F. Ponte, X. Sun, N. C. Yoder, N. Fishkin, R. Laleau, J. Coccia, L. Lanieri, M. Bogalhas, L. Wang, S. Wilhelm, W. Widdison, J. Pinkas, T. A. Keating, R. Chari, H. K. Erickson and J. M. Lambert, *Bioconjugate Chem.*, 2016, **27**, 1588–1598.
41 M. L. Nielsen, M. Vermeulen, T. Bonaldi, J. Cox, L. Moroder and M. Mann, *Nat. Methods*, 2008, **5**, 459–460.
42 C. F. Brewer and J. P. Riehm, *Anal. Biochem.*, 1967, **18**, 248–255.
43 K. Takada, D. Zhu, G. H. Bird, K. Sukhdeo, J.-J. Zhao, M. Mani, M. Lemieux, D. E. Carrasco, J. Ryan, D. Horst, M. Fulciniti, N. C. Munshi, W. Xu, A. L. Kung, R. A. Shivdasani, L. D. Walensky and D. R. Carrasco, *Sci. Transl. Med.*, 2012, **4**, 148ra117.
44 I. Wilkening, G. del Signore and C. P. R. Hackenberger, *Chem. Commun.*, 2008, 2932–2934.
45 A. Klaus and W. Birchmeier, *Nat. Rev. Cancer*, 2008, **8**, 387.
46 G. L. Verdine and G. J. Hilinski, in *Methods Enzymol*, ed. K. D. Wittrup and G. L. Verdine, Academic Press, 2012, vol. 503, pp. 3–33.
47 K. Sakagami, T. Masuda, K. Kawano and S. Futaki, *Mol. Pharm.*, 2018, **15**, 1332–1340.
48 N. Nischan, H. D. Herce, F. Natale, N. Bohlke, N. Budisa, M. C. Cardoso and C. P. R. Hackenberger, *Angew. Chem., Int. Ed.*, 2015, **54**, 1950–1953.
49 H. D. Herce, D. Schumacher, A. F. L. Schneider, A. K. Ludwig, F. A. Mann, M. Fillies, M.-A. Kasper, S. Reinke, E. Krause, H. Leonhardt, M. C. Cardoso and C. P. R. Hackenberger, *Nat. Chem.*, 2017, **9**, 762–771.
50 A. F. L. Schneider, A. L. D. Wallabregue, L. Franz and C. P. R. Hackenberger, *Bioconjugate Chem.*, 2019, **30**, 400–404.

Electronic Supplementary Material (ESI) for Chemical Science.

Vinylphosphonites for Staudinger-induced chemoselective peptide cyclization and functionalization

Marc-André Kasper[1,2†], Maria Glanz[1,2†], Andreas Oder[1], Peter Schmieder[1], Jens P. von Kries[1] and Christian P. R. Hackenberger[1,2,*]

[1]Leibniz-Forschungsinstitut für Molekulare Pharmakologie (FMP), Chemical Biology Department, Robert-Rössle-Strasse 10, 13125 Berlin (Germany)

[2]Humboldt Universität zu Berlin, Department of Chemistry, Brook-Taylor-Str. 2, 12489 Berlin (Germany)

*e-mail: hackenbe@fmp-berlin.de

† authors contributed equally

Supporting Information

1. Supplementary Figures

1.1. Figure S1

Glutathione addition to vinylphosphonamidates. (see chapter 3.1 for details) a) Concentration of starting materials **4b**, **4d**, **5b** and **5d** over time monitored by UPLC/MS (pH 8.5, 50 mM NH_4HCO_3, 1 mM EDTA). Values were calculated by integration of the peaks in relation to an internal standard (inosin). Sample were drawn from the reaction mixture and immediately diluted into 50 mM NaOAc buffer at pH 3.5 to stop the reaction and subjected to UPLC analysis. Peaks were assigned by MS. Shown are mean and error of three independent measurements (n=3). Solid line: *N*-phenyl substituents, dotted line: *N*-alkyl-substituents. b) Overview for all vinylphosphonamidates tested in this study in GSH addition under the same conditions. Stated is the time until 50% conversion is reached.

a)

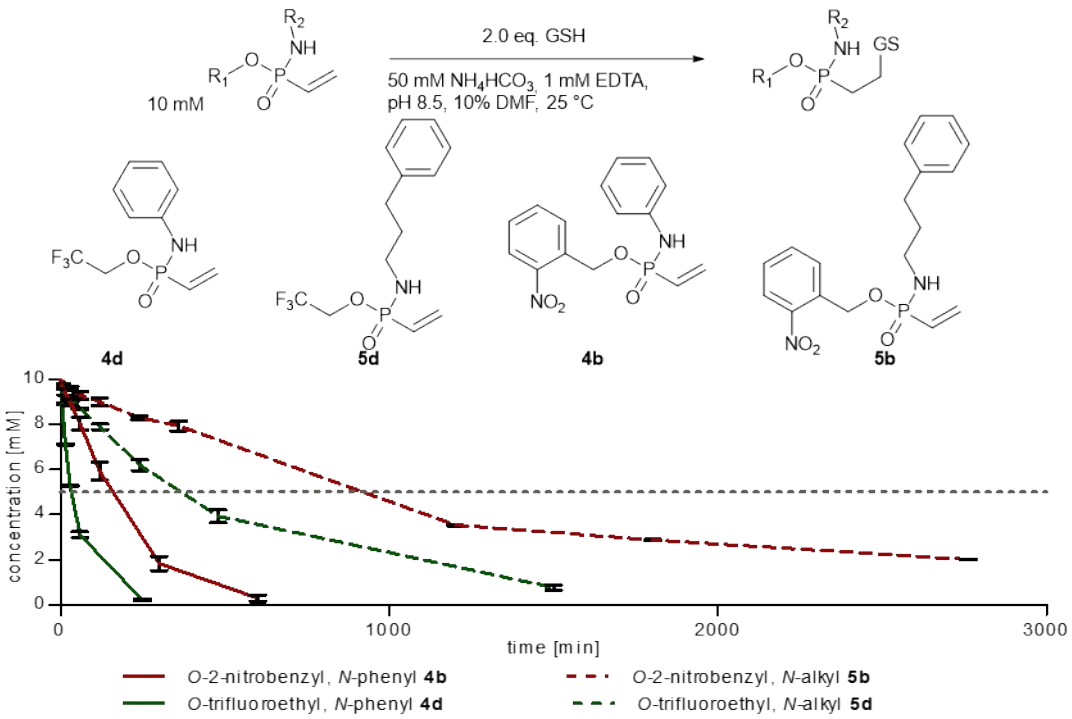

b)

entry	R_1	R_2	Comp No.	time until 50% conversion [min]
1			**4a**	650
2		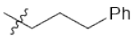	**5a**	n.d.
3	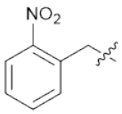		**4b**	160
4	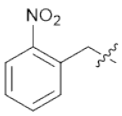	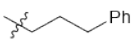	**5b**	900
5			**4c**	70
6			**4d**	30
7		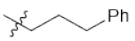	**5d**	360

1.2. Figure S2

UPLC traces of the reaction of compounds **4a**, **4b**, **4c**, **4d**, **5a**, **5b** and **5d** before (red) and after the reaction (black) with two equivalents of glutathione, as stated in chapter 3.1. Shown are the traces of t=0 and the last time point of the measurements that have been performed for the time-course curves in Fig. 2 and S1. The appearance of a single product-peak for each of the compounds suggests a clean conversion to the desired cysteine adduct without side reactions. Peaks were assigned by MS.

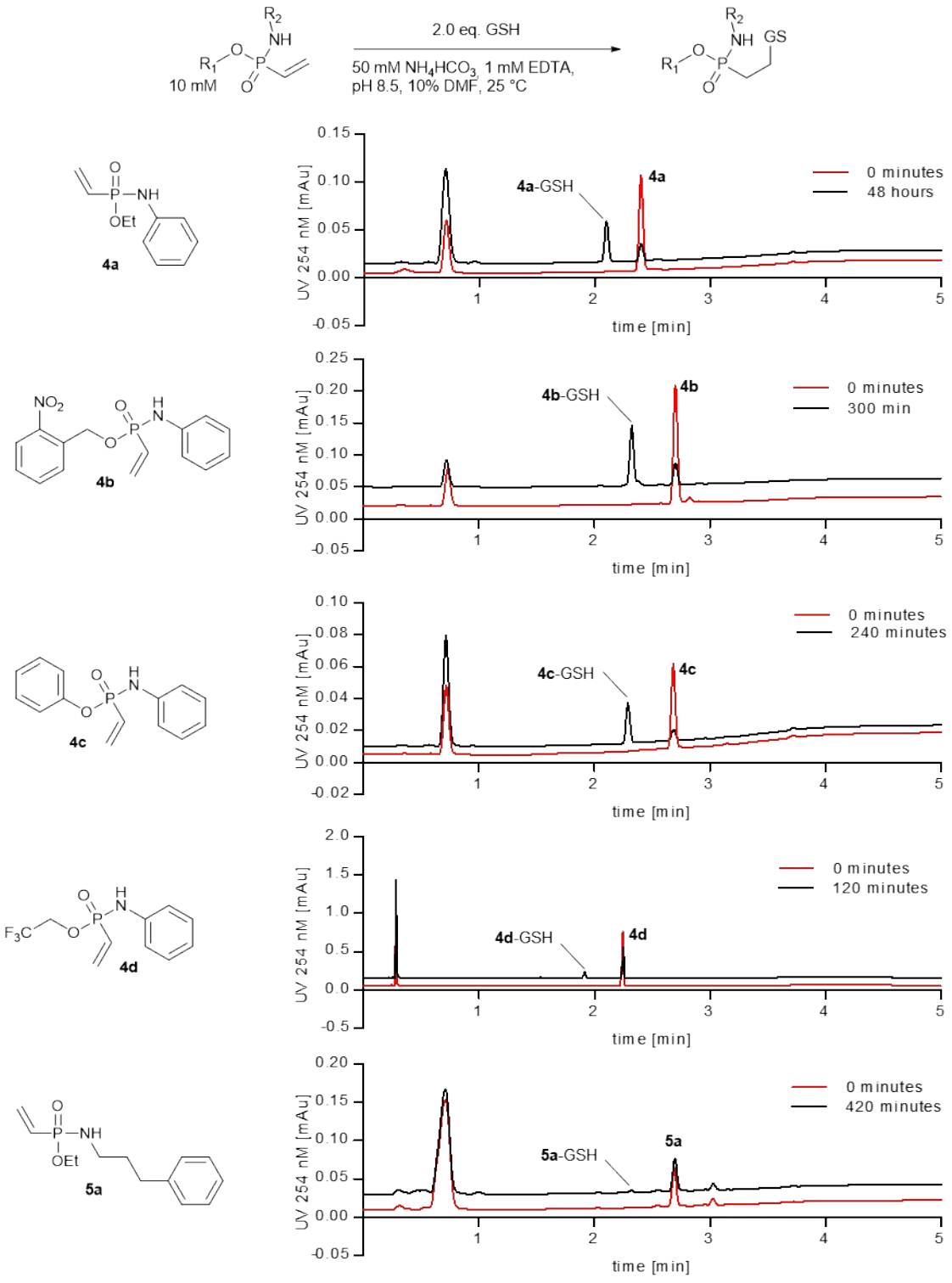

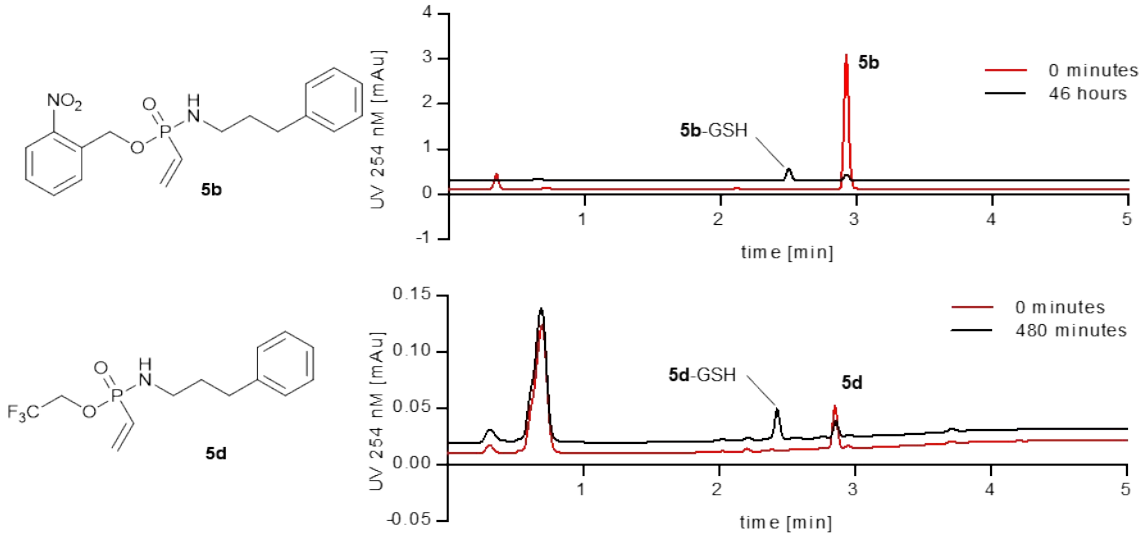
NO2
O
P
H
N
O
5b
UV 254 nM [mAu]
4
3
2
1
0
-1
5b
5b-GSH
0 minutes
46 hours
1
2
3
4
5
time [min]
F3C
O
P
O
H
N
5d
UV 254 nM [mAu]
0.15
0.10
0.05
0.00
-0.05
5d-GSH
5d
0 minutes
480 minutes
1
2
3
4
5
time [min]

1.3. Figure S3

Full assignment of the NMR-shifts of the gluthatione adduct to **4a** by two dimensional experiments. a) ^{1}H-^{1}H-COSY-spectrum with important highlighted correlations that underline the assignments of the ^{1}H-NMR-shifts. b) ^{1}H-^{13}C-HSQC-spectrum and assignment of the measured ^{13}C-NMR-shifts. c) ^{1}H-^{13}C-HMBC-spectrum. Three highlighted correlations demonstrate successful conjugation to the cysteine's sulfhydryl-group. d) ^{1}H-^{31}P-HMBC-spectrum. Four highlighted correlations underline that all three phosphorus substituents (EtO-, RCH_2- and PhNH-) are attached to the phosphorus core structure.

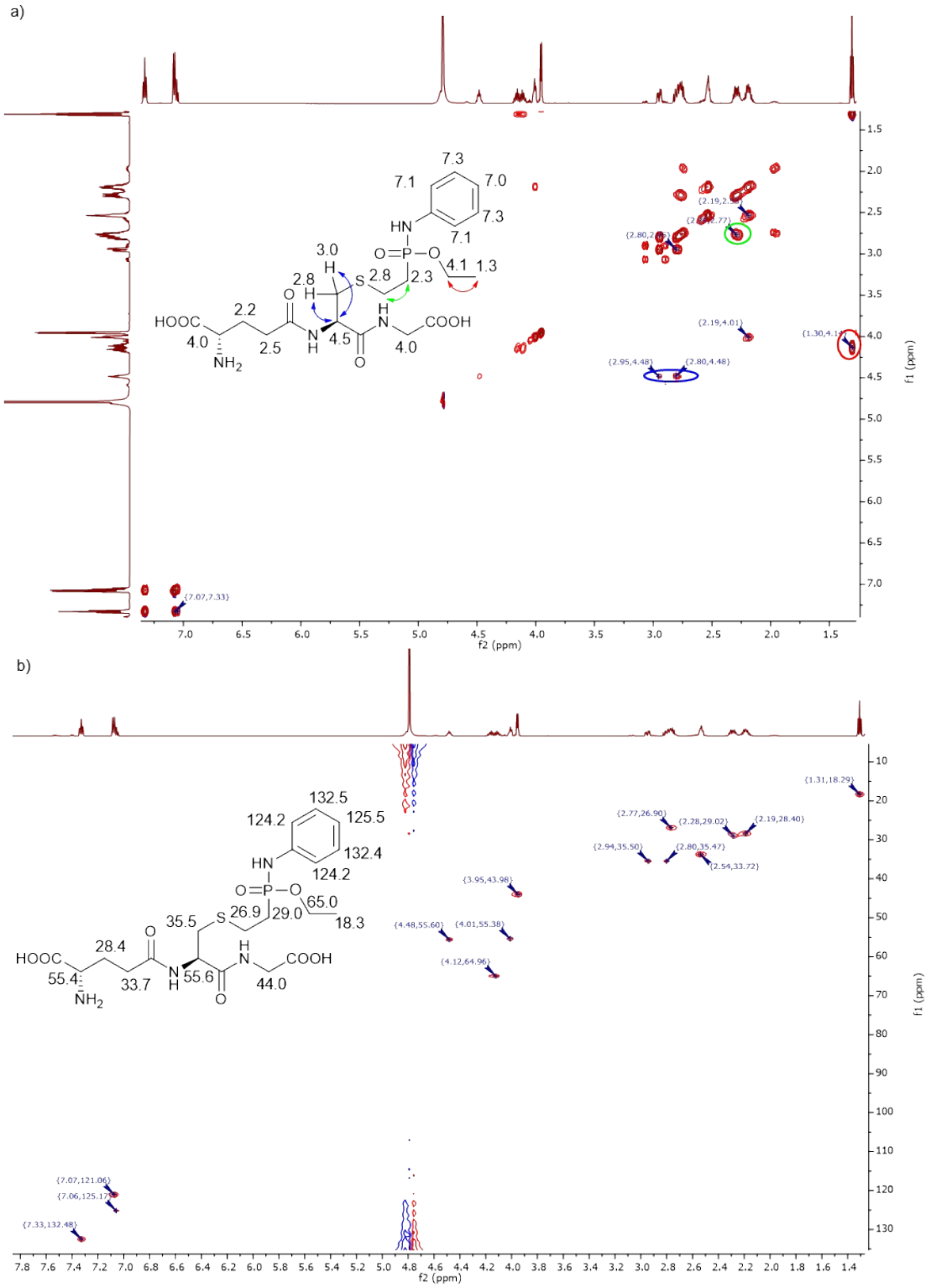

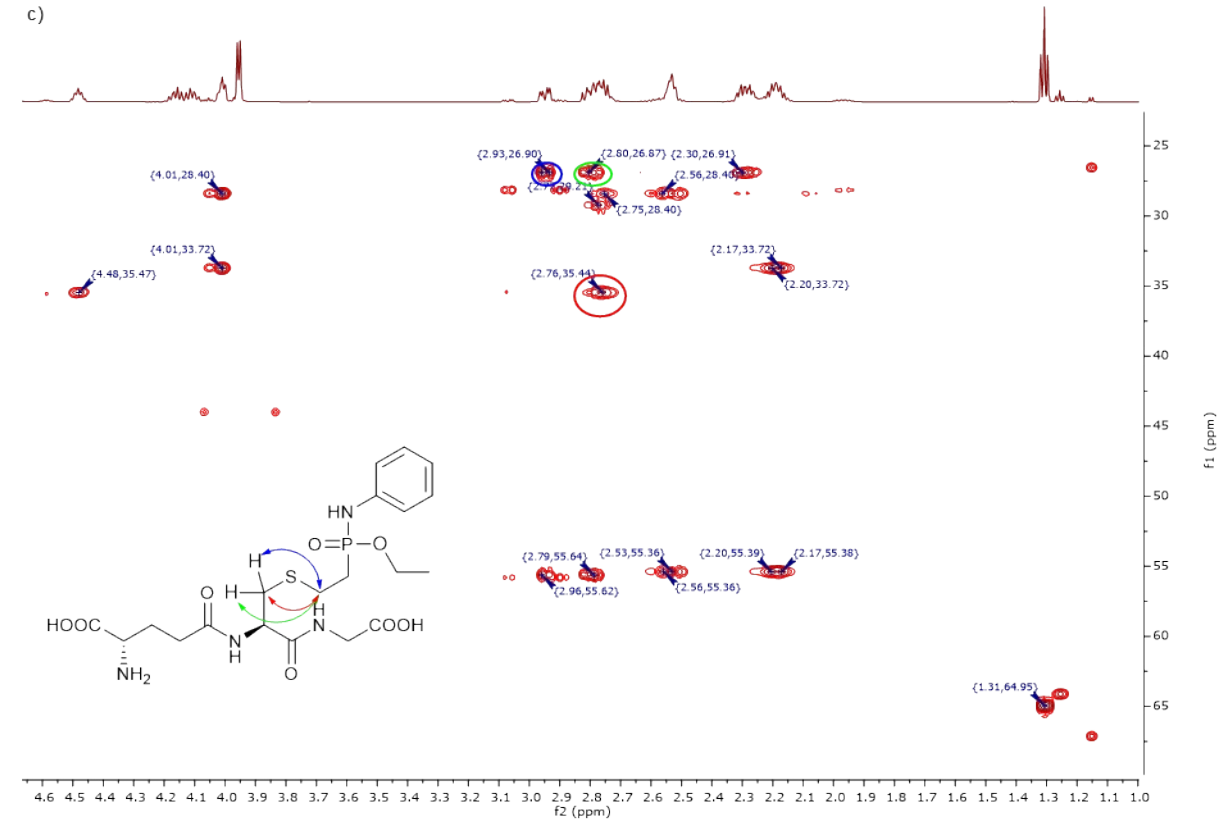
c)
{4.01,28.40}
{2.93,26.90}
{2.60,26.87}
{2.30,26.91}
{2.56,28.40}
{2.75,28.40}
{4.01,33.72}
{4.48,35.47}
{2.76,35.44}
{2.17,33.72}
{2.20,33.72}
{2.79,55.64}
{2.96,55.62}
{2.53,55.36}
{2.56,55.36}
{2.20,55.39}
{2.17,55.38}
{1.31,64.95}
HN
O=P–O
H
S
O
H
HOOC
N
H
NH2
H
N
COOH
O
f2 (ppm)
f1 (ppm)

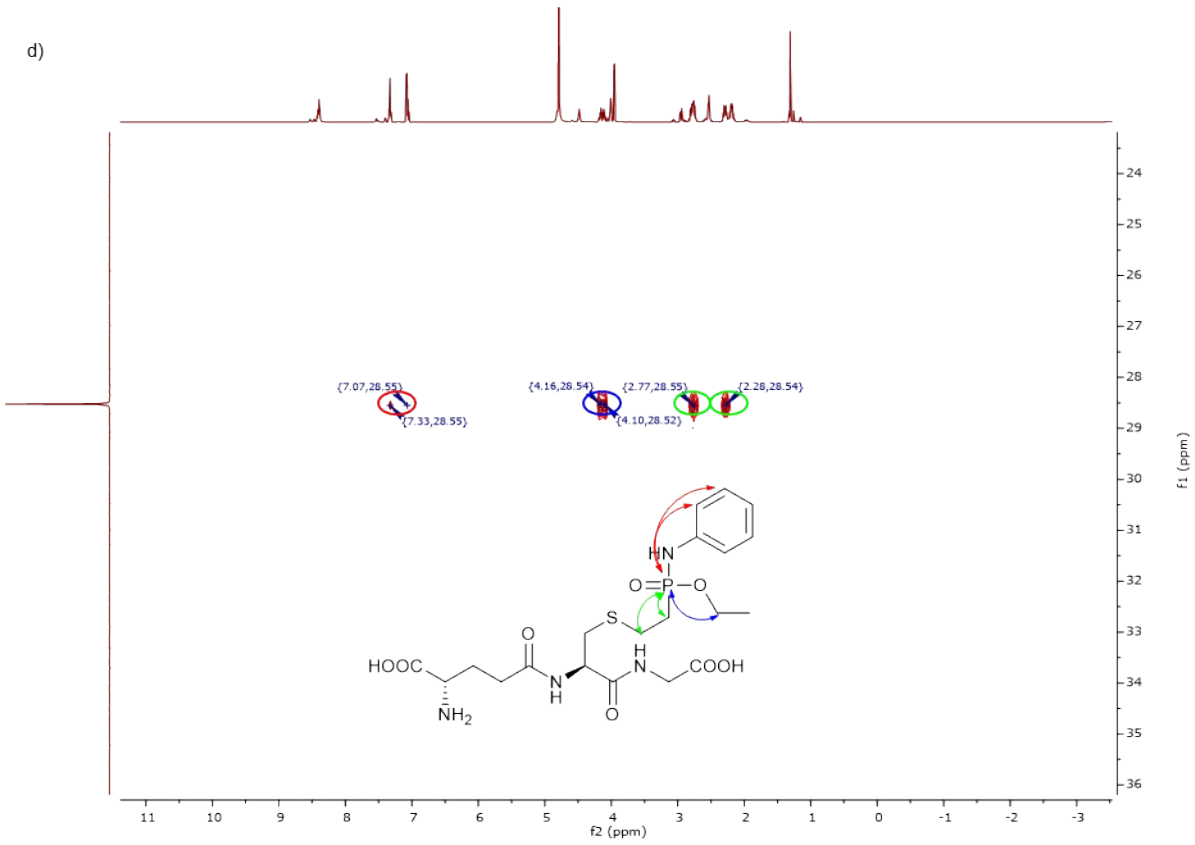
d)
{7.07,28.55}
{7.33,28.55}
{4.16,28.54}
{2.77,28.55}
{2.28,28.54}
{4.10,28.52}
HN
O=P–O
S
O
H
HOOC
N
H
NH2
N
COOH
O
f2 (ppm)
f1 (ppm)

1.4. Figure S4

Determination of the second-order rate constant of the reaction between glutathione and **4d**. a) Reaction conditions. Reactions were performed as described in chapter 3.1 in a volume of 0.2 ml, as stated in chapter 3.1. The first sample (t=0) was drawn before the addition of glutathione. Samples were taken after 5, 15, 30, 60, and 120 min. Samples were drawn in a volume of 20 µl and immediately diluted into 80 µl of 50 mM NaOAc buffer at pH 3.6 to stop the reaction. b) Mathematic consideration for the determination of a second order rate constant with equal concentrations of the two reactants. c) Concentration of starting material over time. Calculated by integration of the peaks in relation to the internal standard (inosine). Shown are mean and error of three independent measurements. (n=3) d) Graph: 1/c over time and linear plot. Slope is the second order rate constant. Shown are mean and error of three independent measurements.

a)

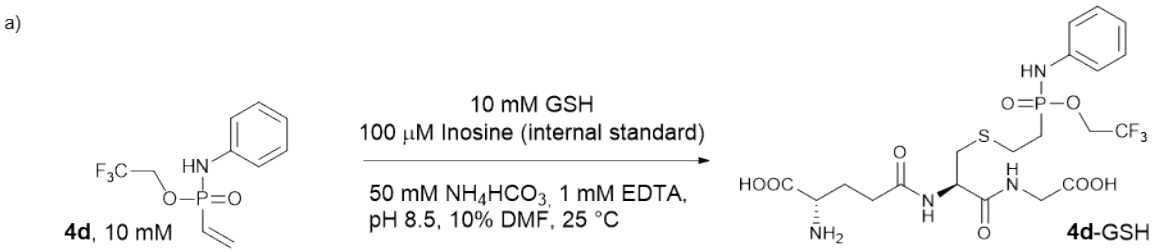

b)

$$v = k \cdot [A] \cdot [B] \qquad \textbf{If } [\mathbf{A}] = [\boldsymbol{B}] \qquad \frac{d[A]}{[A]^2} = k\,dt$$

$$\frac{d[A]}{dt} = k \cdot [A] \cdot [B] \qquad \frac{d[A]}{dt} = k \cdot [A]^2 \qquad \frac{1}{[A]} = k\,t + \frac{1}{[A]_0}$$

c)

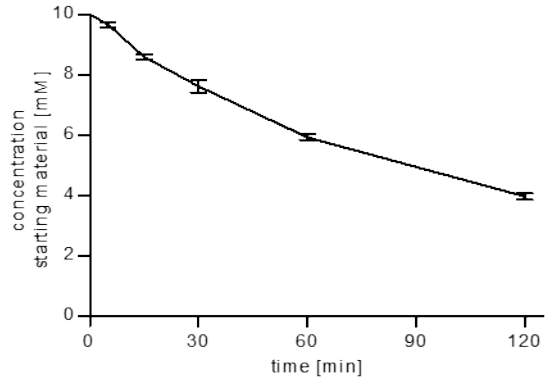

d)

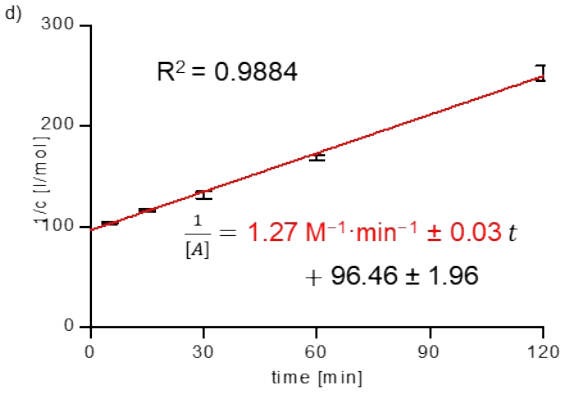

1.5. Figure S5

Incubation of the glutathione adducts of **4a** and **4d** with an excess of mesna to demonstrate stability towards thiol exchange. a) Conjugates were incubated at a concentration of 50 µM for 7 days at room temperature with 5 mM of mesna in PBS (100 eq.) and analyzed by UPLC/MS. Samples of 10 µl were analyzed after day 0, 2 and 7. No Signal was detected by MS over the whole chromatogramm for the **4a** and **4d**- Mesna adduct even after 7 days of incubation. b) Overlay of an isolated Mesna adduct to **4d** (black) and **4d**-GSH incubated with Mesna for 7 days. The difference in retention time underlines that the Mesna adduct is not formed by thiol exchange of **4d**-GSH.

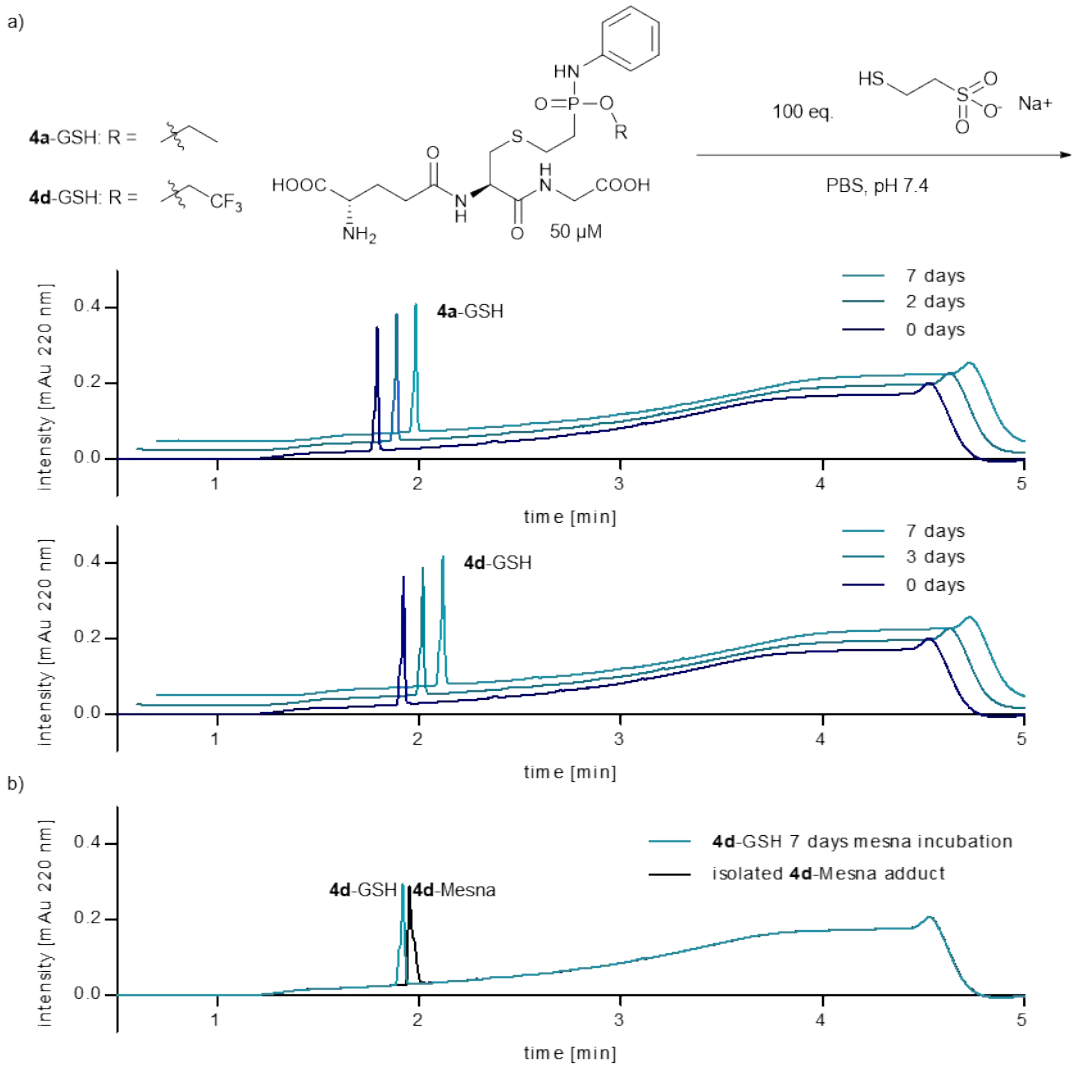

1.6. Figure S6

Modification of cetuximab with **6** and analysis with intact protein MS (See chapter 3.2 for synthesis details). Interchain reduction generates one free cysteine on the light chain and three on the heavy chain. MS-spectrum of cetuximab's heavy and light chain after deglycosylation with PNGase F and reduction with DTT as described in chapter 3.3. Shown are crude spectra before the deconvolution and Deconvoluted between 20000 and 60000 Da. Calculated delta mass for **6**: 557 Da. a) Unmodified cetuximab. b) cetuximab, incubated with 20 eq. **6** without prior reduction. No modification detected for heavy and light chain. c) cetuximab, incubated with 20 eq. **6** with prior reduction. Modification ratio calculated to 3.8 from the MS intensities as stated in chapter 3.3. HC: heavy chain, LC: light chain.

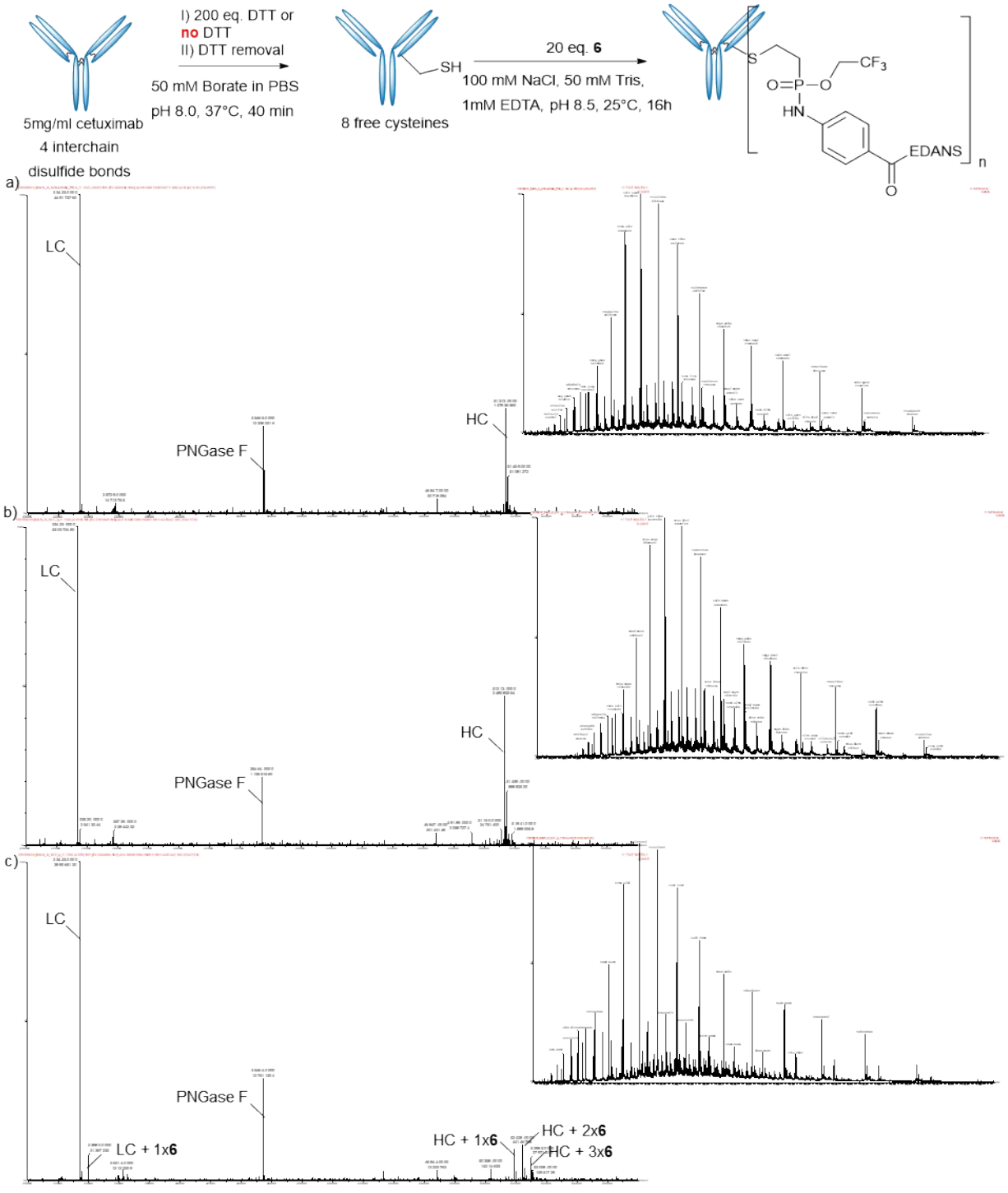

1.7. Figure S7

MS/MS experiments of cetuximab, modified with 100 eq. **4d** with prior reduction of the antibody as described in chapter 3.2. a) MS-spectrum of cetuximab's heavy and light chain after deglycosylation with PNGase F and reduction with DTT as described in chapter 3.3 to proof successful antibody modification. b) SDS Page analysis of the modified antibody. In-gel digestion for tandem-MS has been executed as described earlier.[1] Bands for HC and LC were excised and digested together. c) MS/MS results. Sequence coverage was determined using MASCOT. The phosphonamidate (delta-mass of **4d**) was searched on Y, S, T, C, K, H & R as variable modifications using maxquant. Aminoacids with a Probability of more than 0.7 are highlighted with a red M. (See chapter 2.9 for MS/MS details).

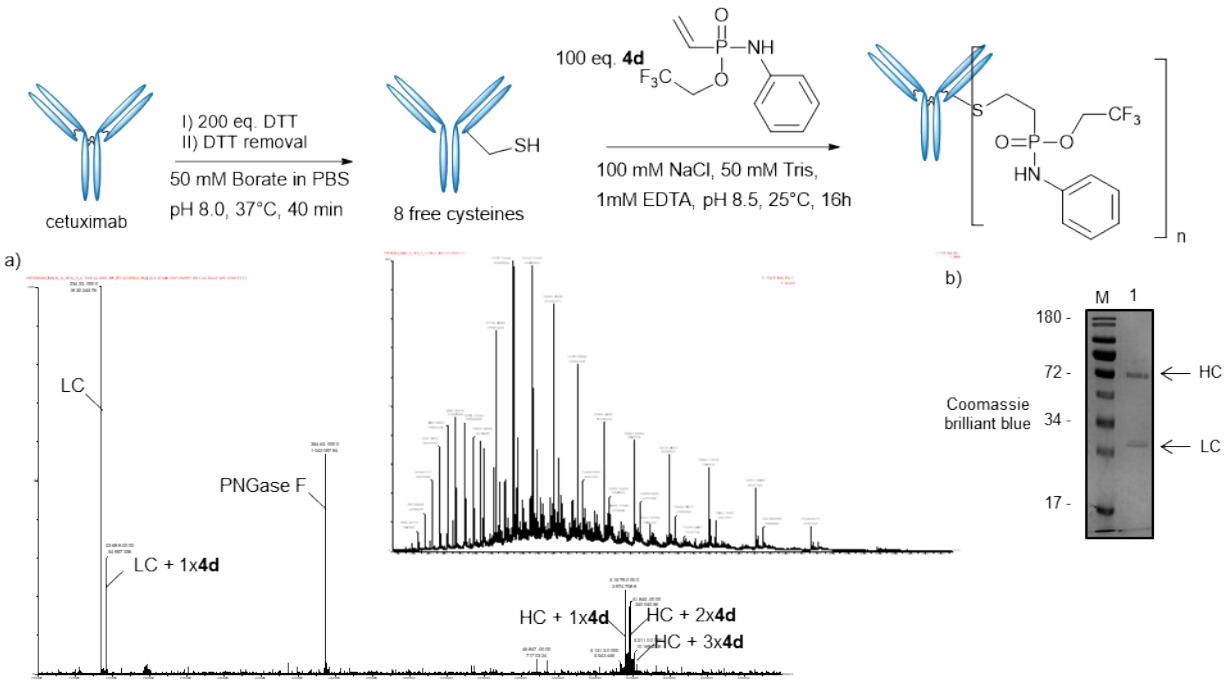

c)

Heavy Chain: Sequence coverage: 75%

1 QVQLKQSGPGLVQPSQSLSITCTVSGFSLTNYGVHWVRQSPGKGLEWLGVIWSGGNTDYNTPFTSRLSINKDNSKSQVFFKMNSLQSNDTAIYYCARALT

101 YYDYEFAYWGQGTLVTVSAASTKGPSVFPLAPSSKSTSGGTAALGCLVKDYFPEPVTVSWNSGALTSGVHTFPAVLQSSGLYSLSSVVTVPSSSLGTQTY

201 ICNVNHKPSNTKVDKRVEPKSCDKTHTCPPCPAPELLGGPSVFLFPPKPKDTLMISRTPEVTCVVVDVSHEDPEVKFNWYVDGVEVHNAKTKPREEQYNS

301 TYRVVSVLTVLHQDWLNGKEYKCKVSNKALPAPIEKTISKAKGQPREPQVYTLPPSREEMTKNQVSLTCLVKGFYPSDIAVEWESNGQPENNYKTTPPVL

401 DSDGSFFLYSKLTVDKSRWQQGNVFSCSVMHEALHNHYTQKSLSLSPGK

Light chain: Sequence coverage: 89%

1 DILLTQSPVILSVSPGERVSFSCRASQSIGTNIHWYQQRTNGSPRLLIKYASESISGIPSRFSGSGSGTDFTLSINSVESEDIADYYCQQNNNWPTTFGA

101 GTKLELKRTVAAPSVFIFPPSDEQLKSGTASVVCLLNNFYPREAKVQWKVDNALQSGNSQESVTEQDSKDSTYSLSSTLTLSKADYEKHKVYACEVTHQG

201 LSSPVTKSFNRGEC

1.8. Figure S8

Antibody modifications with vinylphosphonamidates by reduction and alkylation of interchain disulfide bonds as described in chapter 3.4. a) Synthesis of a biotin modified O-2-nitrobenzyl vinylphophonamidate that can be detected by western blotting. b) Principle of the antibody modification procedure. Reaction was carried out either with or without prior disulfide reduction as previously described.[2] c) Western blot analysis: Lane 1 and 6: untreated antibody. Lane 2-5: prior DTT treatment. Lane 7-10: Control reactions without prior DTT treatment.

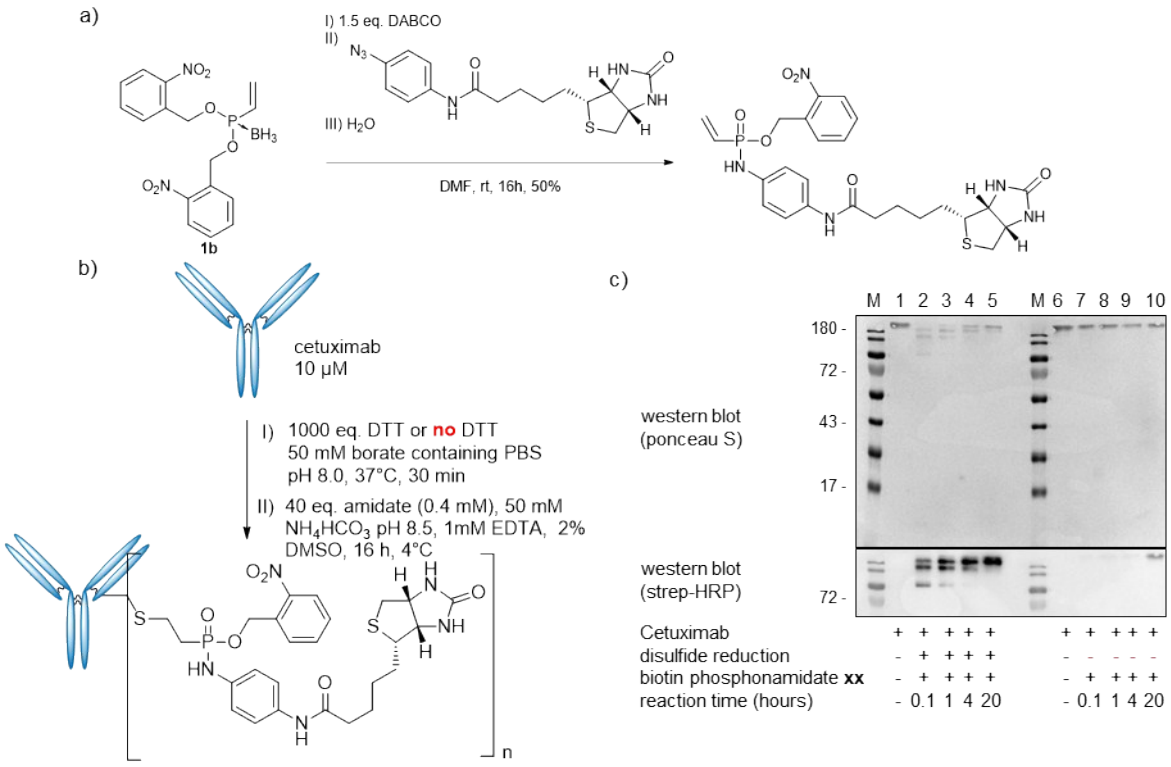

1.9. Figure S9

Reaction of azide and cysteine containing BCL-9 with a vinylphosphonite yields the cyclized product **9a**. a) Reaction scheme. b) UPLC-chromatogramm of the crude reaction mixture shows a clean conversion to two diastereoisomers (*racemic stereocenter at phosphorus). The mass fits the desired product. C) HMBC correlating ^{31}P-NMR and ^{1}H-NMR for the isolated product of the reaction. ^{31}P-shift matches the thiol addition product. In addition, ^{31}P-Correlations were assigned to the adjacent O-CH_2 and two CH_2 groups, which can only be present after thiol addition to the double bond of the vinylphosphonamidate. The correlation pattern matches the fully characterized and assigned NMR-Spectra of the GSH-thiol adduct to **4a** (See Figure S1).

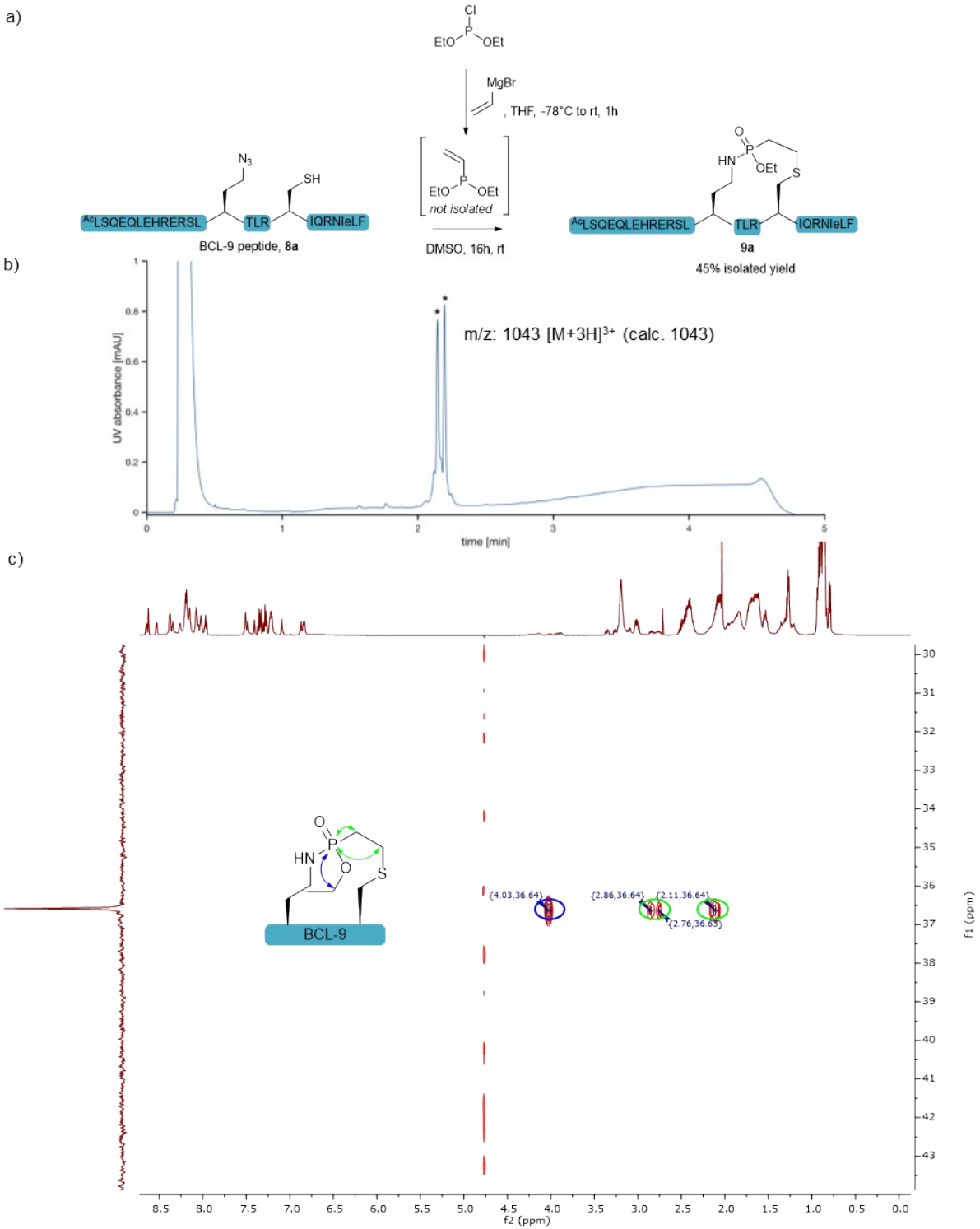

1.10. Figure S10

Thiol addition of unactivated vinylphosphonamidates proceeds with an intermediate of the SPhR. Depicted are mass-spectra after the respective reaction sequences. a) *In situ* addition of glutathione to the SPhR. b) Incubation of isolated phosphonamidate **11** with glutathione. c) Mechanistic assumption: Accelerated thiol addition to an intermediated of the SPhR such as the phosphonimidate. Mechanism adapted from Vallee et al.[3]

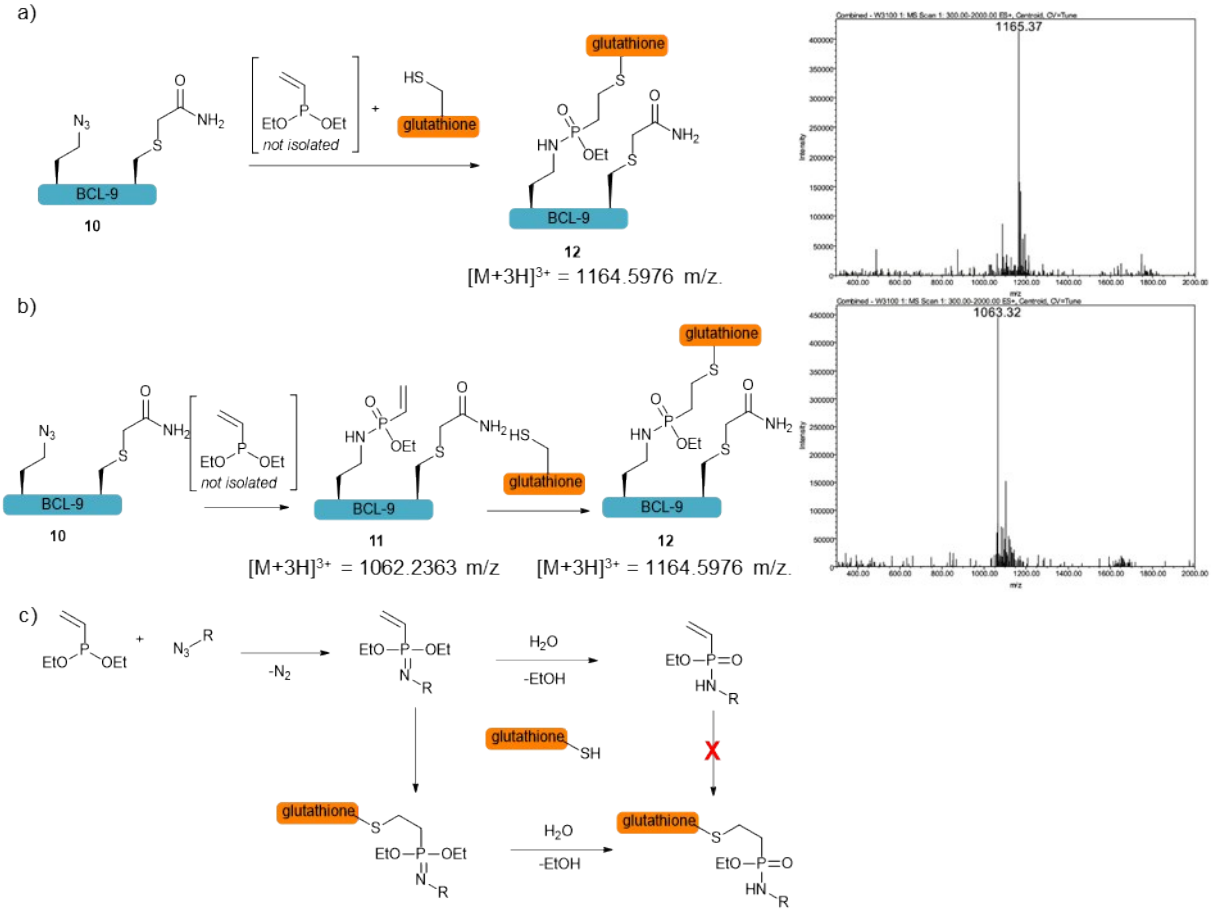

1.11. Figure S11

Principle of the HTRF assay. A FRET system is created between two fluorescently labeled antibodies recognizing a GST-tag on the β-Catenin and a His-tag on the BCL9 protein. If the proteins interact a FRET signal is generated upon antibody incubation that vanishes in case of disturbed interaction by a BCL-9 stapled peptide for instance. Protein expression and purification was performed as described in chapter 3.2 and 3.3. HTRF assay was performed as described in chapter 3.4.

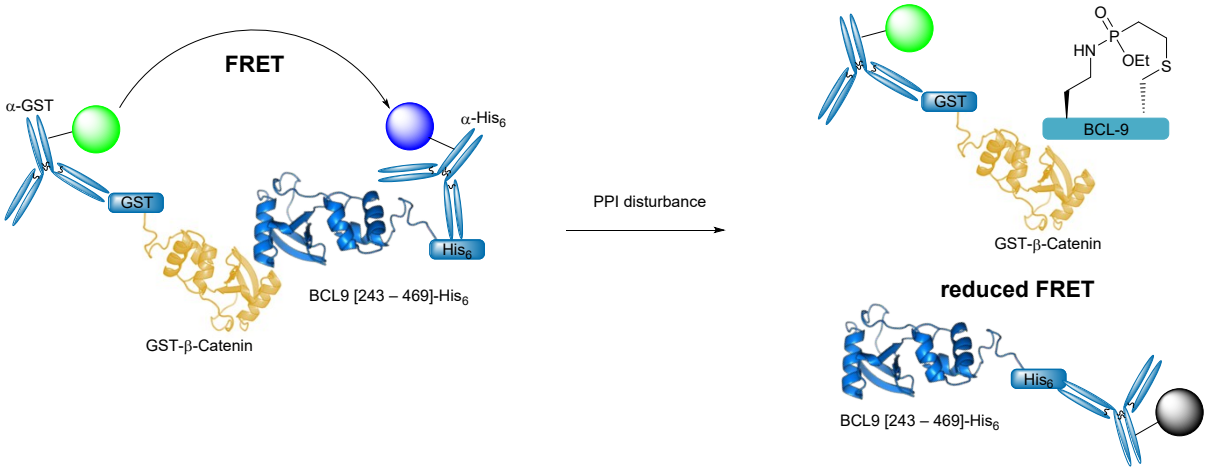

2. General Information

2.1. Chemicals and solvents

Chemicals and solvents were purchased from Merck (Merck group, Germany), TCI (Tokyo chemical industry CO., LTD., Japan) and Acros Organics (Thermo Fisher scientific, USA) and used without further purification. Dry solvents were purchased from Acros Organics (Thermo Fisher scientific, USA). Amino acids and resins for SPPS were purchased from Novabiochem (Merck, USA) or Iris Biotech GmbH (Germany).

2.2. Flash- and thin layer chromatography

Flash column chromatography was performed, using NORMASIL 60® silica gel 40-63 µm (VWR international, USA). Glass TLC plates, silica gel 60 W coated with fluorescent indicator F254s were purchased from Merck (Merck Group, Germany). Spots were visualized by fluorescence depletion with a 254 nm lamp or manganese staining (10 g K_2CO_3, 1.5 g $KMnO_4$, 0.1 g NaOH in 200 ml H_2O), followed by heating.

2.3. Preparative HPLC

Preparative HPLC was performed on a Gilson PLC 2020 system (Gilson Inc, WI, Middleton, USA) using a VP 250/32 Macherey-Nagel Nucleodur C18 HTec Spum column (Macherey-Nagel GmbH & Co. Kg, Germany). The following gradient was used: A = H_2O + 0.1% TFA (trifluoroacetic acid), B = MeCN (acetonitrile) + 0.1% TFA, flow rate 30 ml/min, 5% B 0-5 min, 5-90% B 5-60 min, 90% B 60-65 min

2.4. NMR

NMR spectra were recorded with a Bruker Ultrashield 300 MHz spectrometer and a Bruker Avance III 600 MHz spectrometer (Bruker Corp., USA) at ambient temperature. Chemical shifts δ are reported in ppm relative to residual solvent peak ($CDCl_3$: 7.26 [ppm]; DMSO-d6: 2.50 [ppm]; acetone-d6: 2.05 [ppm]; CD_3CN 1.94 [ppm]; 4.79 D_2O [ppm] for ^{1}H-spectra and $CDCl_3$: 77.16 [ppm]; DMSO-d6: 39.52

[ppm]; acetone-d6: 29.84 [ppm]; CD3CN 1.32 [ppm]; for ^{13}C-spectra . Coupling constants *J* are stated in Hz. Signal multiplicities are abbreviated as follows: s: singlet; d: doublet; t: triplet; q: quartet; m: multiplet.

2.5. UPLC-UV/MS

UPLC-UV/MS traces were recorded on a Waters H-class instrument equipped with a quaternary solvent manager, a Waters autosampler, a Waters TUV detector and a Waters Acquity QDa detector with an Acquity UPLC BEH C18 1.7 µm, 2.1 x 50 mm RP column with a flow rate of 0.6 mL/min (Waters Corp., USA). The following gradient was used: A: 0.1% TFA in H_2O; B: 0.1% TFA in MeCN. 5% B 0 - 0.5 min, 5-95% B 0.5-3 min, 95% B 3-3.9 min, 5% B 3.9-5 min.

2.6. SPPS

SPPS was carried out manually or on a Tribute-UV peptide synthesizer (Protein technologies, USA) via standard Fmoc-based protocols.

2.7. HR-MS

High resolution ESI-MS spectra were recorded on a Waters H-class instrument equipped with a quaternary solvent manager, a Waters sample manager-FTN, a Waters PDA detector and a Waters column manager with an Acquity UPLC protein BEH C18 column (1.7 µm, 2.1 mm x 50 mm). Samples were eluted with a flow rate of 0.3 mL/min. The following gradient was used: A: 0.01% FA in H_2O; B: 0.01% FA in MeCN. 5% B: 0-1 min; 5 to 95% B: 1-7min; 95% B: 7 to 8.5 min. Mass analysis was conducted with a Waters XEVO G2-XS QTof analyzer.

2.8. Intact protein MS

Intact proteins were analyzed using a Waters H-class instrument equipped with a quaternary solvent manager, a Waters sample manager-FTN, a Waters PDA detector and a Waters column manager with an Acquity UPLC protein BEH C4 column (300 Å, 1.7 µm, 2.1 mm x 50 mm). Proteins were eluted with a flow rate of 0.3 mL/min. The following gradient was used: A: 0.01% FA in H_2O; B: 0.01% FA in MeCN. 5-95% B 0-6 min. Mass analysis was conducted with a Waters XEVO G2-XS QTof analyzer. Proteins were ionized in positive ion mode applying a cone voltage of 40 kV. Raw data was analyzed with MaxEnt 1.

2.9. Analytical HPLC-MS/MS

After in-gel digestion peptides were dissolved in water and analyzed by a reversed-phase capillary liquid chromatography system (Dionex Ultimate 3000 NCS-3500RS Nano, Thermo Scientific) connected to an Orbitrap Fusion mass spectrometer (Thermo Fisher Scientific, Germany). LC separations were performed with an in-house packed C18 column for reversed phase separation (column material: Poroshell 120 EC-C18, 2.7 µm (Agilent Technologies, USA) at an eluent flow rate of 300 µL/min using a gradient of 2-40% B in 38 min. Mobile phase A contained 0.1% formic acid in water, and mobile phase B 0.1% formic acid in acetonitrile. FT survey scans were acquired in a range of 350 to 1500 m/z with a resolution of 60000 (FMHM) and an AGC target value of 4e5. Precursor ions with charge states 2-4 were isolated with a mass selecting quadrupole (isolation window m/z 1.6). Precursor ions were fragmented in alternating mode using EThcD and HCD. HCD MS/MS spectra were acquired with 30% NCE. EThcD fragmentation was performed using charge dependent ETD parameters and the supplemental activation (sa) was set to 30%. For both fragmentation types the maximum injection time was set to 500 ms to collect 5e4 precursor ions. Fragment ion spectra were acquired with a resolution of 15000 (FWHM).

2.10. MALDI-TOF-MS

Spectra were measured on a Bruker LT microflex using a 2,5-DHAP matrix. Proteins were precipitated in cold acetone and resolved in 10 mM Ammoniumbicarbonate buffer at pH 7.4. Protein sample (0.8 µl) was mixed with 2% TFA in water (0.8 µl) and matrix (0.8 µl). After addition of matrix the solution was transferred a MSP 96 target (polished steel BC).

2.11. Protein concentration determination

Protein concentrations were determined by absorption spectroscopy measurements at 280 nm using the extinction coefficient and molecular weight of the protein on a NanoDrop ND-1000. In addition or as alternative concentrations were determined by BCA assay (Thermo Fisher Scientific, USA) according to the manufacturers protocol.

2.12. Protein purification

Protein purification was accomplished either with an ÄKTA FPLC or a BioRad NGC system as stated below.

2.13. CD-spectroscopy

CD-spectroscopy was measured on a Jasco J-720 spectropolarimeter at 20°C and parameters set to: measured wavelength range 190 – 260 nm; data pitch of 0.1 nm; continuous scanning mode; 100 nm/min scanning speed; 1sec. response; 1.0 nm band width; 0.1 cm cell length; 5 accumulations.

3. Experimental procedures

3.1. Glutathione addition to differently substituted vinylphosphonamidates and analysis by UPLC/MS

Reaction buffer: 50 mM NH_4HCO_3, 1 mM EDTA pH 8.5. In an Eppendorf tube, 11 µl of a 200 mM phosphonamidate solution in DMF was mixed with 143 µl reaction buffer and 22 µl of a 10 mM solution of Inosin in a mixture of DMF and reaction buffer (1:1). A 16 µl sample was drawn for t=0. 40 µl of a solution containing 100 mM glutathione in reaction buffer (50 mM for rate constant determination), adjusted to pH 8.5 was added to the mixture to start the reaction. Sample were drawn from the reaction mixture after distinct time points and immediately diluted into 180 µl of a 50 mM NaOAc buffer at pH 3.5 to stop the reaction and subjected to UPLC analysis (10 µl per injection). Conversions were calculated by integration of the Peaks in relation to an internal standard (inosin). Peaks were assigned by MS. Exemplaric chromatograms of the reaction of glutathione with *O*-Phenyl-*N*-phenyl-*P*-vinyl-phosphonamidate (**4c**) after 0, 15, 30, 60, 120, 240 and 480 minutes are shown below.

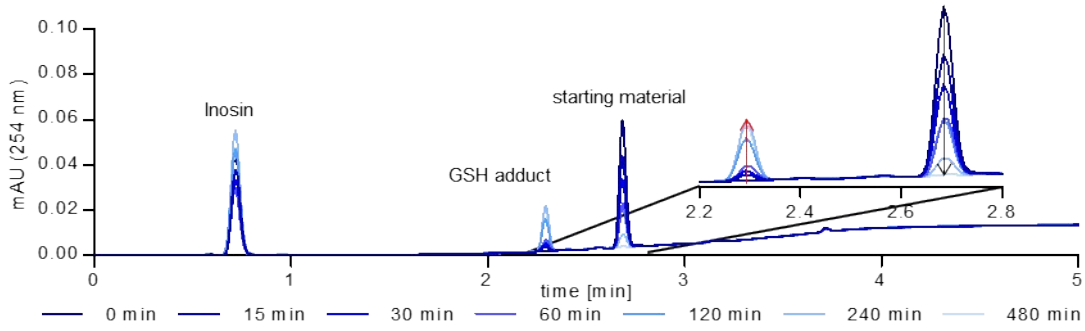

3.2. Cetuximab modification with 4d or 6

5 µl of a 70 mM solution of DTT in 50 mM sodium borate in PBS (pH 8.0) was added to 50 µl of a cetuximan solution of 5.0 mg/ml in 50 mM sodium borate in PBS (pH 8.0) and the mixture was incubated at 37 °C for 40 min. Excess DTT removal and exchange to the conjugation buffer (50 mM Tris, 1 mM EDTA, 100 mM NaCl, pH 8.5 at 14°C) was conducted afterwards using 0.5 mL Zeba™ Spin Desalting Columns with 7K MWCO (Thermo Fisher Scientific, USA). 50 µl of the reduced antibody solution (4.55 mg/ml, 30.30 µM antibody) were mixed quickly afterwards with desired amount of **4d** or **6** dissolved in DMSO to give a final amount of 5% DMSO. The mixture was shaken at 850 rpm and 25 °C for 16 hours.
The crude antibody modification mixtures were purified by size-exclusion chromatography with a 5 ml HiTrap® desalting column and a flow of 1.5 ml/min eluting with PBS over four column volumes. The antibody containing fractions were pooled and concentrated to 50 µl by spin-filtration to 40 µl (MWCO: 10 kDa, 0.5 ml, Sartorius, Germany).

3.3. Antibody analyses

2 µl of the samples, that were prepared as described in 3.2 were subjected to SDS-PAGE analysis.

For MS analysis, 5 µl of the samples were diluted with 15 µl PBS and 1 µl PNGase-F solution (Pomega, Germany, Recombinant, cloned from Elizabethkingia miricola 10 u/µl) was added and the solution was incubated at 37 °C for at least 2 hours. Disulfide bridges were reduced by addition of 2 µl DTT solution (70 mM in H_2O) and incubation at 37°C for 30 min. 10 µl of the samples were diluted with 190 µl of pure water and subjected to intact protein MS (see chapter 2.8), injecting 3 µl for each sample.

3.4. Cetuximab modification with biotin

Cetuximab modification was carried out by incubating the antibody (typical concentration c = 1.5 mg/ml, 10 µM) in a buffer containing 50 mM sodium borate and 10 mM DTT in PBS (pH 8.0) with a total volume of 80 µl at 37 °C for 30 min. Control reactions were carried out without DTT. Excess DTT removal and buffer exchange to a solution containing 50 mM NH_4HCO_3 and 1mM EDTA (pH 8.5) was conducted afterwards using 0.5 mL Zeba™ Spin Desalting Columns with 7K MWCO (Thermo Fisher Scientific, USA). 1.0 µl of a solution containing 20 mM vinyl phosphonamidate (40eq.) in DMSO was added quickly to 50 µl of the reduced antibody solution. 10 µl samples were drawn and deep frozen in liquid nitrogen to stop the reaction after 10 minutes, 1, 4 and 20 hours. 1.0 µl of the samples were subjected to SDS/PAGE and subsequent western-blot analysis.

3.5. Protein expression β-Catenin-GST

β-Catenin-GST (pGEX-Bcatfl was a gift from David Rimm (Addgene plasmid #24193)) was expressed in *E.coli* BL21 (DE3) with LB medium including 100 µg/ml Ampillicin. Cells were grown at 37°C at 180 rpm until OD_{600} reached 0.73 followed by induction with 0.2 mM IPTG and expression at 18°C at 180 rpm for 16 hours.

The cells were harvested by centrifugation at 4000 g for 15 minutes at 4°C. Cell lysis was carried out in Dulbecco's PBS with a sonicator at 30% for six minutes. Finally debris was centrifugation at 27000 g for 20 minutes. β-Catenin-GST was purified with a Bioscale™ Mini Profinity™ GST cartridge (5 ml) on a BioRad NGC system (Binding/Wash buffer: 50 mM Tris HCl pH 8.0/ 150 mM NaCl/ 0.1 mM EDTA; elution buffer: 50 mM Tris HCl pH 8.0/ 150 mM NaCl/ 0.1 mM EDTA/ 10 mM reduced glutathione). After elution the peak fractions were combined and dialyzed to Dulbecco's PBS. The protein was aliquoted at a concentration of 0.87 mg/ml, shock frozen and stored at -80°C. a) Purification of GST- β-Catenin. b) Pooled elution fractions rebuffered to PBS.

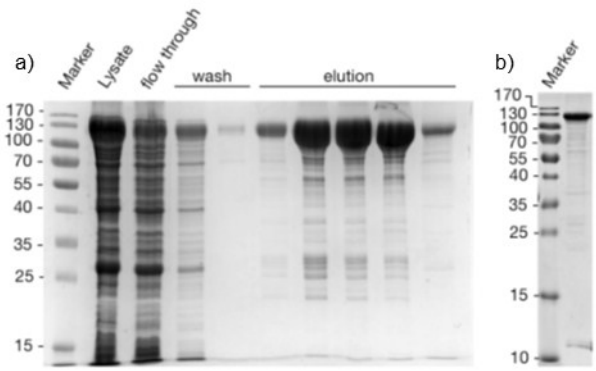

3.6. His_6-BCL9 (243 – 469) production

The cDNA for BCL9 was purchased from biocat (Gene ID 607) in a pCR-BluntII-TOPO vector.

PCR:

The Gene region of interest was amplified with BamHI and HindII restriction sites by PCR using complementary primer pairs (for conditions see table 8.4 and 8.5) (GTAGTGGATCCAACCAGGACCAGAATTCTTC and ATACGAAGCTTTTAC TGCTCGGGAGTCATATGGT) for cloning into the pET28a vector. Two PCRs were done in parallel.

Reaction mix of PCR:

ddH_2O	13.6 µl
Phu HF buffer (5x) (Thermo scientific, USA)	4 µl
template DNA (1 ng/µl)	1 µl
fwd primer mix (10 µM)	0.4 µl
rev primer mix (10 µM)	0.4 µl
dNTP mix (10 mM each) (Thermo scientific, USA)	0.4 µl
Phusion polymerase (Thermo scientific, USA)	0.2 µl

Cycle steps in mutagenesis PCR:

step	cycles	temp.[°C]	time
initial denaturation	1	98	30''
denaturation		98	10''
annealing	30	58	30''
extension		72	3'
final extension	1	72	10'
hold		4	∞

Digestion with restriction endonucleases

The PCR product as well as the target vector pET28a was digested with the restriction endonucleases BamHI and HindII for 70 minutes at 37°C. To the vector digestion, 1 µL of FastAP Themosensitive Alkaline Phosphatase (1 U/µl) was added and again incubated at 37°C for 15 minutes.

Reaction mix of restriction digestion:

	PCR product	vector
DNA	2 x 20 µl	16 µl (1 µg)
FastDigest™ buffer (10x)	5 µl	2
BamHI enzyme (10 U/µl)	1 µl	1
HindII enzyme (10U/µl)	1 µl	1
ddH_2O	3 µl	-

DNA purification

DNA fragments were purified by agarose gel electrophoresis (1% agarose in TAE buffer) at 120 V in 1x TAE buffer for 20 minutes. The samples were mixed with MidoriGreen Direct before loading, for visualization purposes. GeneRuler 1kb Plus DNA Ladder was used as size marker. The target DNA bands were excised from the agarose gel with a clean scalpel and purified with a GeneJET™ Gel Extraction Kit according to the manufacturer's protocol, but was eluted with 20µl ddH_2O contrary to the included elution buffer.

DNA ligation

The Ligation between vector and PCR product was done with T4 DNA ligase (Thermo Scientific USA) and the T4 Buffer (Thermo Scientific USA). The vector to insert ration was either 1:5 or 1:10 and was calculated according to length of both DNA parts and their respective concentration. The reation mixture was incubated at 16 °C for 16 hours and directly transformed into competent DH5α cells.

Reaction mix of Ligation:

vector DNA	50 – 100 ng
insert DNA	variable
T4 buffer (10x) (Thermo scientific, USA)	2 µl
T4 DNA ligase (Thermo scientific USA)	1 µl
ddH_2O	adjust to 20 µl

Clones were picked and cultured over night in LB_{Kana} at 37°C; 180 rpm and DNA was isolated with a GeneJET Plasmid Miniprep Kit (Thermo Scientific, USA) according to manufacturer's protocol, but again elution was done in 30 µl ddH_2O. DNA concentration was determined by Nanodrop and send to sequencing. DNA was stored at -20°C.

Protein expression and purification

Finally His-BCL9 (243 – 469) was expressed in *E.coli* BL21 (DE3) with LB medium including 100 µg/ml kanamycin. Cells were grown at 37°C at 180 rpm until OD_{600} reached 0.7 followed by induction with 0.5 mM IPTG and expression at 18°C at 180 rpm for 16 hours.

The cells were harvested by centrifugation at 4000 g for 15 minutes at 4°C. Cell lysis was carried out in Dulbecco's PBS with a sonicator at 30% for six minutes. Finally debris was centrifugation at 27000 g for 20 minutes. His-BCL9 (243 – 469) purified *via* 5 ml HisTrap™ FF column on a BioRad NGC system. Elution was performed in PBS with 500 mM Imidazole. Elution fractions containing the wanted protein were combined and further purified by size exclusion chromatography using a Superdex 75 10/300 GL column on a ÄKTA FPLC system. The product fractions were combined and concentrated with a Vivaspin 20 filter unit (MWCO 10 kDa) then shock frozen and stored at -80°C. a) Purification of BCL9-His6 *via* Ni-NTA beads. b) Further purification *via* SEC. D) MALDI-TOF spectra of pooled fractions.

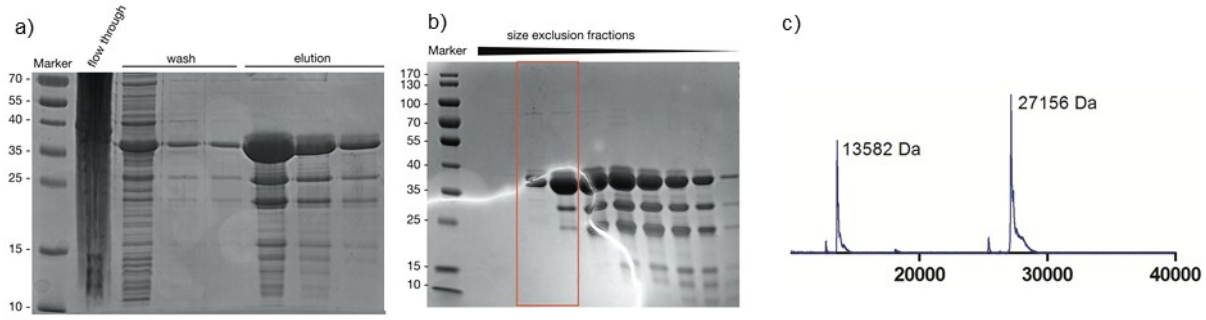

3.7. Homogeneous Time Resolved Fluorescence (HTRF) energy transfer assay

Beta-catenin-GST (7,5 nM) was first mixed with peptides at different peptide concentrations in PBS with 0.05% Tween 20, in reaction volumes of 5 µl in 384-well microtiter plates (ProxyPlate, PerkinElmer), followed by addition of BCL9-His (125nM), Anti-GST-Terbium (CisBio; 1:100) and Anti-His-XL665 (CisBio; 1:100) in PBS with 0.05% Tween 20 at final reaction volumes of 10 µl. Final assay concentrations were 3,75 nM for beta-catenin, 62,5 nM for BCL-9 and contained 1:200 dilutions for each antibody in PBS with 0,05% Tween-20. After mixing on a plate shaker for 15 seconds at 1500 rpm the plate was incubated for one hour at room temperature. The plate was read in an Envision plate reader using excitation at 320 nm and emission reading at 620/665 nm wavelengths using the prism software for data plotting. Positive control wells represent a mixture of both proteins and both antibodies. Negative control wells did not contain beta-catenin.

3.8. Cellular uptake experiments

All cell uptake experiments were carried out with HeLa (ATCC CCL-2) cells cultured in Dulbecco's MEM medium supplemented with 10% FBS and 1% Penicillin Streptomycin. 70 000 cells were seeded in an uncoated glass bottom 8-well µ-slide (Ibidi) 24 hours prior to treatment.
The cellular uptake with **FAM labeled peptides** was carried out by gently washing cells three times with DMEM without FBS. The FAM labeled peptides which were solved in DMSO (1 mM stock solution), were added to the medium after the final wash. The cells were incubated for at 37°C in a 5% CO_2 atmosphere for two hours. Then the cells were gently washed with 25 mM HEPES in Dulbecco's MEM supplemented with 10% FKS and cells were rested for 30 minutes at 37°C. The cell nucleus was stained with Hoechst 33342 and cells imaged with a Zeiss 710 confocal microscope.
The cellular uptake of **cR10-eGFP** was carried out by gently washing cells three times with HEPES buffer pH 7.5 (5 mM HEPES, 140 mM NaCl, 2.5 mM KCl, 5 mM glycine). The peptide-protein conjugate buffered in the same HEPES buffer was added to the cells in 200 µl at respective concentration and incubated for at 37°C in a 5% CO_2 atmosphere. After one hour cells were gently washed with 25 mM

HEPES in Dulbecco's MEM supplemented with 10% FKS and cells were rested for 30 minutes at 37°C. The cell nucleus was stained with Hoechst 33342 and cells imaged with a Zeiss 710 confocal microscope.
The percentage of cells that took up the GFP conjugate was determined by counting all cells showing nucleolar GFP relative to the total number of cells (all Hoechst stained nuclei). Each uptake experiment was repeated at least three times.

4. Organic and peptide synthesis

4.1. Diethyl vinylphosphonite borane (1a)

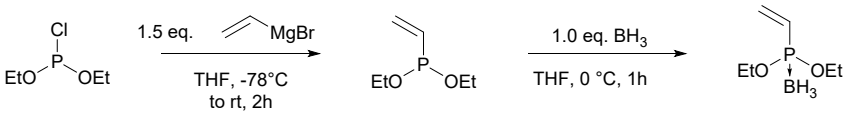

A 25-ml Schlenk flask was charged with 2.14 ml vinylmagnesium bromide (0.7 M in THF, 1.50 mmol, 1.5 eq.) under an argon atmosphere, cooled to -78 °C and 140 µl diethyl chlorophosphite (1.00 mmol, 1.0 eq.) were added drop wise. The yellowish solution was allowed to warm to 0 °C, stirred for another two hours and 1.00 ml of Borane (1.0 M in THF, 1.00 mmol, 1.0 eq.) were added and stirred for one more hour at 0°C. The organic solvents were removed under reduced pressure and the crude product was purified by flash column chromatography on silica gel (Hexane/EtOAc, 9:1) to yield the desired compound as colourless oil. (60 mg, 0.37 mmol, 37.0%)

^{1}H NMR (300 MHz, Chloroform-*d*) δ = 6.36 – 6.03 (m, 3H), 4.19 – 3.96 (m, 4H), 1.33 (t, *J*=7.1, 6H), 0.55 (ddd, *J*=190.3, 94.1, 16.6, 3H). ^{13}C NMR (75 MHz, Chloroform-*d*) δ = 134.62 (d, *J*=8.7), 130.12 (d, *J*=75.0), 63.16 (d, *J*=4.8), 16.59 (d, *J*=5.6). ^{31}P NMR (122 MHz, Chloroform-*d*) δ = 129.58 (dd, *J*=167.1, 82.6).

NMR data is in accordance with those reported in the literature.[4]

4.2. General procedure 1 for the synthesis of borane protected vinylphosphonites from phosphorous trichloride (route I)

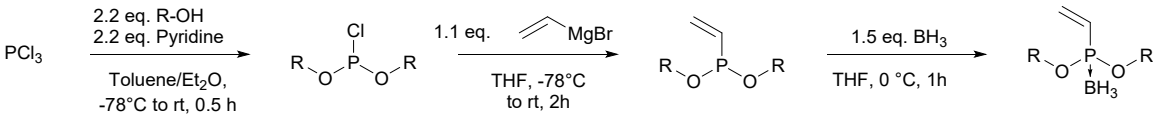

A flame-dried Schlenkflask was charged with 1.00 mmol (1.0 eq.) of phosphorous trichloride in 15 ml of dry toluene and cooled to -78 °C. 2.2 mmol of pyridine (2.2 eq.) and a solution of 2.2 mmol of the alcohol (2.2 eq.) in 3 ml Et2O were added drop wise. The resulting suspension was allowed to warm to room temperature, stirred for another 30 min and cooled again to -78 °C. 1.10 mmol (1.1eq.) of vinyl magnesiumbromide (1.0 M in THF) was added and the reaction was stirred at room temperature for two hours. Finally, 1.50 mmol (1.5 eq.) of borane (1.0 M in THF) were added at 0 °C and the suspension was stirred for another hour. The crude product was dry packed on a silica column for purification.

It should be noted, that mass analysis of borane protected phosphonites failed for all of the tested compounds, possibly due to decomposition under ESI-conditions.

4.3. Di(2-nitrobenzyl) vinylphosphonite borane (1b)

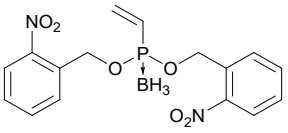

The compound was synthesized according to the general procedure 1 from 260 µl PCl_3 (3.00 mmol). The crude borane protected phosphonite was purified by flash column chromatography (Hexane/EtOAc, 4:1) and obtained as a yellowish solid. (555 mg, 1.48 mmol, 49.2%)

^{1}H NMR (300 MHz, Chloroform-d) δ = 8.10 (d, J=8.2, 2H), 7.77 – 7.63 (m, 4H), 7.57 – 7.44 (m, 2H), 6.51 – 6.18 (m, 3H), 5.45 (qd, J=14.8, 7.5, 4H), 1.42 – -0.02 (m, 3H). ^{13}C NMR (75 MHz, Chloroform-d) δ = 146.80, 136.84 (d, J=10.2), 132.52 (d, J=6.8), 129.10, 129.05, 128.67, 128.61 (d, J=74.3), 125.09, 65.56 (d, J=3.6). ^{31}P NMR (122 MHz, Chloroform-d) δ = 136.23 (dd, J=151.3, 56.0).

4.4. Diphenyl vinylphosphonite borane (1c)

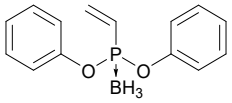

The compound was synthesized according to the general procedure 1 from 393 µl PCl_3 (4.50 mmol). The crude borane protected phosphonite was purified by flash column chromatography (Hexane/EtOAc, 4:1) and obtained as a colourless oil. (700 mg, 2.71 mmol, 60.3%)

^{1}H NMR (300 MHz, Chloroform-d) δ = 7.39 (td, J=7.7, 5.5, 4H), 7.30 – 7.17 (m, 6H), 6.67 – 6.18 (m, 3H), 1.48 – 0.01 (m, 3H). 13C NMR (75 MHz, Chloroform-d) δ = 151.27 (d, J=8.7), 137.01 (d, J=12.5), 129.70 (d, J=1.0), 129.05 (d, J=71.1), 125.35 (d, J=1.3), 120.90 (d, J=4.2). ^{31}P NMR (122 MHz, Chloroform-d) δ = 134.08 – 130.87 (m).

4.5. Bis(2,2,2-trifluoroethyl) vinylphosphonite borane (1d) (route II)

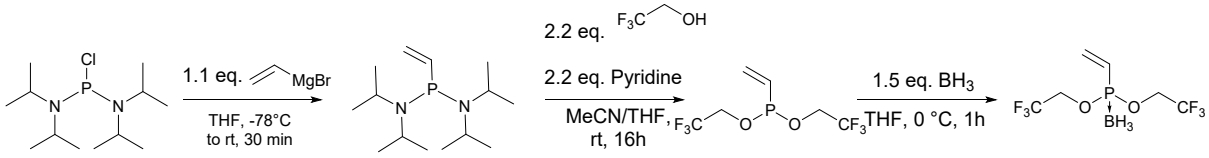

A flame-dried Schlenkflask was charged with 266 mg Bis(diisopropylamino)-chlorophosphine (1.0 mmol, 1.0 eq.), dissolved in 200 µl of dry THF and cooled to -78 °C. 1.1 ml of vinyl magnesiumbromide (1.0 M in THF, 1.10 mmol, 1.1eq.) were added and the reaction was stirred at room temperature for 30 minutes. A solution of 160 µl 2,2,2-Trifluoroethanol (2.20 mmol, 2.2 eq.) in 1 ml of MeCN and 4.9 ml tetrazole (0.45 M in MeCN, 2.20 mmol, 2.2 eq.) were added subsequently. The resulting suspension was stirred at room temperature overnight. Finally, 1.50 ml of borane (1.0 M in THF, 1.50 mmol, 1.5 eq.) were added at 0 °C and stirred for another hour. The crude product was dry packed on a silica column for purification (Hexane/CH2Cl2, 9:1 to 4:1) and obtained as a colourless liquid. (87 mg, 0.32 mmol, 32.2%)

^{1}H NMR (300 MHz, Chloroform-d) δ = 6.52 – 6.11 (m, 3H), 4.36 (p, J=8.1, 4H), 0.62 (ddd, J=203.0, 103.5, 15.0, 3H).^{13}C NMR (75 MHz, Chloroform-d) δ = 137.57, 127.48 (d, J=79.1), 122.37 (qd, J=276.0, 7.5), 63.60 (qd, J=37.7, 2.5). ^{19}F NMR (282 MHz, Chloroform-d) δ = 2.13. ^{31}P NMR (122 MHz, Chloroform-d) δ = 145.49 (dd, J=135.6, 65.1).

4.6. General procedure 2 for the synthesis of vinylphosphonamidates from diethyl chlorophosphite (route III)

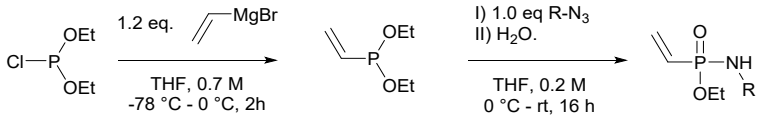

A 25-ml Schlenk flask was charged with 1.71 ml vinylmagnesium bromide (0.7 M in THF, 1.20 mmol, 1.2 eq.) under an argon atmosphere, cooled to -78 °C and 140 µl diethyl chlorophosphite (1.00 mmol, 1.0 eq.) were added drop wise. The yellowish solution was allowed to warm to 0 °C, stirred for another two hours and 1.00 mmol of azide (1.0 eq.) dissolved in 3.2 ml of THF was added and stirred over night at room temperature. 5 ml of water were added and stirred for another 24 h. The solvents were removed under reduced pressure and the crude product was purified by flash column chromatography on silica gel.

4.7. Ethyl-*N*-phenyl-*P*-vinylphosphonamidate (4a)

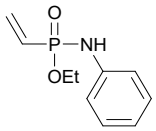

The compound was synthesized according to the general procedure 2 from 1.15 ml diethyl chlorophosphite (8 mmol). The crude phosphonamidate was purified by flash column chromatography (EtOAc) and obtained as a white solid. (675 mg, 3.20 mmol, 40.0%)

^{1}H NMR (600 MHz, Chloroform-d) δ = 7.24 (dd, J=8.5, 7.3, 2H), 7.05 – 7.01 (m, 2H), 6.99 (d, J=5.8, 1H), 6.94 (tt, J=7.3, 1.1, 1H), 6.33 – 6.23 (m, 2H), 6.10 (ddd, J=50.3, 9.6, 5.1, 1H), 4.29 – 4.04 (m, 2H), 1.35 (t, J=7.1, 3H). ^{13}C NMR (151 MHz, Chloroform-d) δ = 140.43, 134.44, 129.28, 127.51 (d, J=172.7), 121.26, 117.31 (d, J=6.6), 60.44 (d, J=6.2), 16.22 (d, J=7.0). ^{31}P NMR (122 MHz, Chloroform-d) δ = 15.68. HRMS for $C_{10}H_{15}NO_2P^+$ $[M+H]^+$ calcd.: 212.0835, found: 212.0839.

4.8. Ethyl-*N*-(3-phenyl-propyl)-*P*-vinyl-phosphonamidate (5a)

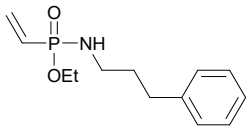

The compound was synthesized according to the general the general procedure 2 from 290 µl diethyl chlorophosphite (2 mmol). The crude phosphonamidate was purified by flash column chromatography (EtOAc) and obtained as a colourless oil. (165 mg, 0.65 mmol, 32.5%)

^{1}H NMR (300 MHz, Chloroform-d) δ = 7.28 (dd, J=8.1, 6.2, 2H), 7.23 – 7.11 (m, 3H), 6.28 – 5.89 (m, 3H), 4.04 (qt, J=10.2, 7.2, 2H), 2.92 (dq, J=9.1, 7.0, 2H), 2.84 – 2.70 (m, 1H), 2.70 – 2.60 (m, 2H), 1.82 (p, J=7.3, 2H), 1.31 (t, J=7.1, 3H). ^{13}C NMR (75 MHz, Chloroform-d) δ = 141.28, 132.98 (d, J=1.5), 128.42 (d, J=169.0), 128.34, 128.24, 125.88, 59.95 (d, J=5.7), 40.23, 33.53 (d, J=5.6), 32.86, 16.32 (d, J=6.7). ^{31}P NMR (122 MHz, Chloroform-d) δ = 20.82. HRMS for $C_{13}H_{21}NO_2P^+$ calcd.: 254.1304, found: 254.1312.

4.9. General procedure 3 for the synthesis of vinylphosphonamidates from borane protected vinylphosphonites (route IV)

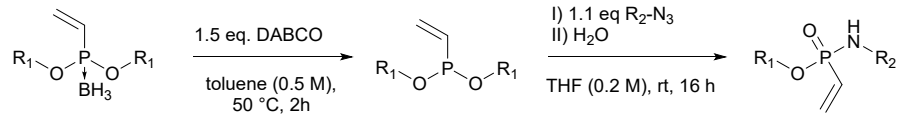

A flame-dried Schlenkflask was charged with 1.0 mmol (1.0 eq.) of the borane protected phosphonite under an argon atmosphere and dissolved in 2 ml of dry toluene. In an argon stream, DABCO (1.50 mmol, 1.5 eq.) was added and the solution was heated to 50 °C for 2 hours. The mixture was allowed to cool to room temperature and a solution of 1.1 mmol of the azide (1.1 eq.) in 3 ml dry THF or dry DMF was added. The resulting solution was stirred at room temperature overnight. Finally 1 ml of water was added and stirred for another two hours. The crude product was purified by column chromatographie.

4.10. 2-Nitrobenzyl-*N*-phenyl-*P*-vinyl-phosphonamidate (4b)

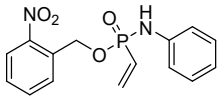

The compound was synthesized according to the general procedure 3 from 100 mg Di(2-nitrobenzyl) vinylphosphonite borane (**1b**) (0.266 mmol). The crude phosphonamidate was purified by flash column chromatography (30% hexane in EtOAc) and obtained as a colourless solid. (38 mg, 0.119 mmol, 44.7%)

^{1}H NMR (300 MHz, Chloroform-*d*) δ 8.12 (dd, *J* = 8.2, 1.3 Hz, 1H), 7.83 (dd, *J* = 7.9, 1.3 Hz, 1H), 7.68 (td, *J* = 7.6, 1.3 Hz, 1H), 7.50 (ddd, *J* = 8.1, 7.4, 1.5 Hz, 1H), 7.21 (dd, *J* = 8.5, 7.2 Hz, 2H), 7.09 – 6.82 (m, 3H), 6.61 – 6.00 (m, 4H), 5.57 (ddd, *J* = 67.1, 14.9, 7.6 Hz, 2H). ^{13}C NMR (75 MHz, Chloroform-*d*) δ 146.89, 139.47, 135.77, 135.75, 134.02, 132.72 (d, *J* = 7.6 Hz), 129.44, 128.80 (d, *J* = 3.3 Hz), 126.71 (d, *J* = 172.1 Hz), 125.01, 121.96, 117.63 (d, *J* = 6.5 Hz), 62.75 (d, *J* = 4.8 Hz). ^{31}P NMR (122 MHz, $CDCl_3$) δ 16.83. HRMS for $C_{15}H_{16}N_2O_4P^+$ $[M+H]^+$ calcd.: 319.0842, found: 319.0825.

4.11. 2-Nitrobenzyl-*N*-(3-phenyl-propyl)-*P*-vinyl-phosphonamidate (5b)

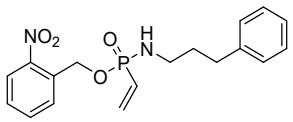

The compound was synthesized according to the general procedure 3 from 100 mg Di(2-nitrobenzyl) vinylphosphonite borane (**1b**) (0.266 mmol). The crude phosphonamidate was purified by flash column chromatography (20% hexane in EtOAc) and obtained as a yellowish solid. (55 mg, 0.153 mmol, 57.5%)

^{1}H NMR (300 MHz, Chloroform-*d*) δ 8.12 (d, *J* = 8.2 Hz, 1H), 7.77 (d, *J* = 7.8 Hz, 1H), 7.73 – 7.60 (m, 1H), 7.56 – 7.43 (m, 1H), 7.27 (t, *J* = 7.2 Hz, 2H), 7.23 – 7.10 (m, 3H), 6.55 – 5.88 (m, 3H), 5.43 (h, *J* = 7.4 Hz, 2H), 2.98 (dd, *J* = 9.4, 5.1 Hz, 3H), 2.65 (t, *J* = 7.7 Hz, 2H), 1.84 (p, *J* = 7.1 Hz, 2H). ^{13}C NMR (75 MHz, Chloroform-*d*) δ 141.14, 133.98 (d, *J* = 1.5 Hz), 133.88, 133.21 (d, *J* = 7.7 Hz), 128.75, 128.60, 128.53, 128.36, 128.24, 126.50, 125.91, 124.84, 62.30 (d, *J* = 4.4 Hz), 40.27, 33.45 (d, *J* = 5.5 Hz), 32.83. ^{31}P NMR (122 MHz, $CDCl_3$) δ 21.87. HRMS for $C_{18}H_{22}N_2O_4P^+$ $[M+H]^+$ calcd.: 361.1312, found: 361.1304.

4.12. Phenyl-*N*-phenyl-*P*-vinyl-phosphonamidate (4c)

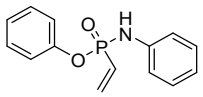

The compound was synthesized according to the general procedure 3 from 134 mg Diphenyl vinylphosphonite borane (**1c**) (0.519 mmol). The crude phosphonamidate was purified by flash column chromatography (50% hexane in EtOAc) and obtained as a yellowish oil. (34 mg, 0.131 mmol, 25.3%)

^{1}H NMR (600 MHz, Chloroform-*d*) δ 7.32 – 7.25 (m, 5H), 7.24 – 7.20 (m, 2H), 7.16 (t, *J* = 7.3 Hz, 1H), 7.10 – 6.96 (m, 3H), 6.56 – 6.12 (m, 3H), 5.64 (d, *J* = 5.7 Hz, 1H). ^{13}C NMR (151 MHz, Chloroform-*d*) δ 149.87 (d, *J* = 8.1 Hz), 139.26, 135.98, 129.71, 129.41, 126.99 (d, *J* = 173.3 Hz), 125.08, 122.19, 120.72 (d, *J* = 4.6 Hz), 118.06 (d, *J* = 6.5 Hz). ^{31}P NMR (243 MHz, $CDCl_3$) δ 12.74. HRMS for $C_{14}H_{15}NO_2P^+$ $[M+H]^+$ calcd.: 260.0835, found: 260.0836.

4.13. Phenyl-*N*-(3-phenyl-propyl)-*P*-vinyl-phosphonamidate (5c)

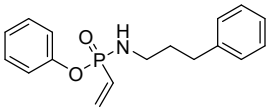

The compound was synthesized according to the general procedure 3 from 150 mg Diphenyl vinylphosphonite borane (**1c**) (0.581 mmol). The crude phosphonamidate was purified by flash column chromatography (30% EtOAc in hexane) and obtained as a white solid. (100 mg, 0.332 mmol, 57.1%)

^{1}H NMR (600 MHz, Chloroform-*d*) δ 7.35 – 7.28 (m, 4H), 7.26 – 7.19 (m, 3H), 7.19 – 7.13 (m, 3H), 6.41 – 6.01 (m, 3H), 3.20 – 2.92 (m, 3H), 2.63 (t, *J* = 7.7 Hz, 2H), 1.80 (pd, *J* = 7.1, 1.6 Hz, 2H). ^{13}C NMR (151 MHz, Chloroform-*d*) δ 150.63 (d, *J* = 7.9 Hz), 141.30, 134.03, 129.64, 128.43, 128.35, 127.98 (d, *J* = 172.0 Hz), 125.99, 124.55, 120.58 (d, *J* = 4.9 Hz), 40.48, 33.38 (d, *J* = 5.6 Hz), 32.87. ^{31}P NMR (243 MHz, $CDCl_3$) δ 18.79. HRMS for $C_{17}H_{21}NO_2P^+$ $[M+H]^+$ calcd.: 302.1304, found: 302.1315.

4.14. 2,2,2-trifluoroethyl-*N*-phenyl-*P*-vinyl-phosphonamidate (4d)

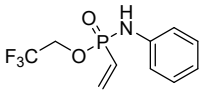

The compound was synthesized according to the general procedure 3 from 90 mg Bis(2,2,2-trifluoroethyl) vinylphosphonite borane (**1d**) (0.333 mmol). The crude phosphonamidate was purified by flash column chromatography (60 to 70% EtOAc in hexane) and obtained as a white solid. (27 mg, 0.102 mmol, 30.6%)

^{1}H NMR (300 MHz, Chloroform-*d*) δ 7.27 (dd, *J* = 9.3, 6.3 Hz, 2H), 7.13 – 6.86 (m, 3H), 6.65 (d, *J* = 6.2 Hz, 1H), 6.53 – 6.01 (m, 3H), 4.70 – 4.06 (m, 2H). ^{13}C NMR (75 MHz, Chloroform-*d*) δ 138.93, 136.50 (d, *J* = 1.7 Hz), 129.43, 125.70 (d, *J* = 172.5 Hz), 122.23, 117.68 (d, *J* = 6.7 Hz), 60.42 (qd, *J* = 37.7, 5.1 Hz), 51.28. ^{31}P NMR (122 MHz, $CDCl_3$) δ 17.93. ^{19}F NMR (282 MHz, $CDCl_3$) δ 2.69. HRMS for $C_{10}H_{12}F_3NO_2P^+$ $[M+H]^+$ calcd.: 266.0552, found: 266.0552.

4.15. 2,2,2-trifluoroethyl-*N*-(3-phenyl-propyl)-phenyl-*P*-vinyl-phosphonamidate (5d)

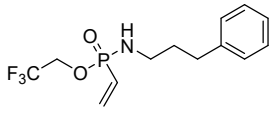

The compound was synthesized according to the general procedure 3 from 80 mg Bis(2,2,2-trifluoroethyl) vinylphosphonite borane (**1d**) (0.296 mmol). The crude phosphonamidate was purified by flash column chromatography (70 to 80% EtOAc in hexane) and obtained as a colourless oil. (18 mg, 0.059 mmol, 19.8%)

^{1}H NMR (300 MHz, Chloroform-*d*) δ 7.36 – 7.12 (m, 6H), 6.54 – 5.94 (m, 3H), 4.29 (dqt, *J* = 12.2, 8.4, 4.1 Hz, 2H), 2.96 (dt, *J* = 9.6, 7.1 Hz, 2H), 2.82 (d, *J* = 8.4 Hz, 1H), 2.66 (t, *J* = 7.7 Hz, 2H), 1.85 (p, *J* = 7.3 Hz, 2H). ^{13}C NMR (75 MHz, Chloroform-*d*) δ 141.00, 135.06 (d, *J* = 1.5 Hz), 128.41, 128.22, 126.69 (d, *J* = 170.2 Hz), 126.00, 60.48 (qd, *J* = 37.2, 4.6 Hz), 40.08, 33.40, 33.32, 32.79. ^{31}P NMR (122 MHz, $CDCl_3$) δ 22.94. ^{19}F NMR (282 MHz, $CDCl_3$) δ 2.40. HRMS for $C_{13}H_{18}F_3NO_2P^+$ $[M+H]^+$ calcd.: 308.1022, found: 308.1017.

4.16. Ethyl-*N*-phenyl-*P*-(2-(glutathionyl-thio)ethyl)-phosphonamidate

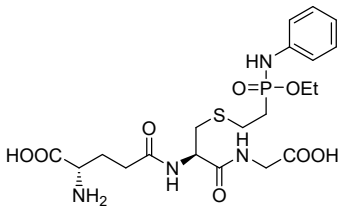

A 5-ml round-bottom-flask was charged with 12.2 mg Ethyl-*N*-phenyl-*P*-vinyl-phosphonamidate (**4a**) (0.058 mmol, 1.00 eq.) and 150 µl DMF. A solution containing 21.4 mg glutathione (0.070 mmol, 1.20 eq.) in 150 µl H_2O was adjusted to with potassium carbonate to pH 9.0 and added to the reaction mixture, which was stirred for 24h at room temperature. All volatiles were removed under reduced pressure and the crude product was purified by preparative HPLC and obtained as a colourless solid after lyophilization as a mixture of diastereoisomers (18 mg, 0.035 mmol, 60.3%).

^{1}H NMR (600 MHz, Deuterium Oxide) δ 7.53 – 7.22 (m, 2H), 7.15 – 6.89 (m, 3H), 4.44 (tt, J = 9.1, 4.5 Hz, 1H), 4.26 – 3.96 (m, 2H), 3.89 – 3.51 (m, 3H), 3.04 – 2.90 (m, 1H), 2.86 – 2.63 (m, 3H), 2.54 – 2.39 (m, 2H), 2.37 – 2.19 (m, 2H), 2.19 – 2.03 (m, 2H), 1.37 – 1.23 (m, 3H). ^{13}C NMR (151 MHz, Deuterium Oxide) δ 176.03, 174.84, 173.90, 171.74 (d, *J* = 3.7 Hz), 139.43, 129.79, 122.48, 118.34 (d, *J* = 6.1 Hz), 62.27 (d, *J* = 6.9 Hz), 54.15, 52.80 (d, *J* = 14.3 Hz), 43.33, 32.82 (d, *J* = 12.9 Hz), 31.45, 26.22, 26.08 (d, *J* = 124.0 Hz), 24.10 (d, *J* = 10.6 Hz), 15.54 (d, *J* = 6.4 Hz). ^{31}P NMR (243 MHz, D_2O) δ 31.68. HRMS for $C_{20}H_{32}N_4O_8PS^+$ $[M+H]^+$ calcd.: 519.1673, found: 519.1675.

4.17. 2,2,2-trifluoroethyl-*N*-phenyl-*P*-(2-(glutathionyl-thio)ethyl)-phosphonamidate

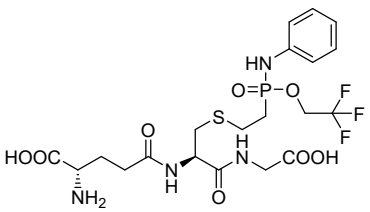

A 5-ml round-bottom-flask was charged with 17.2 mg 2,2,2-trifluoroethyl-*N*-phenyl-*P*-vinyl-phosphonamidate (**4d**) (0.065 mmol, 1.00 eq.) and 150 µl DMF. A solution containing 21.85 mg glutathione (0.072 mmol, 1.10 eq.) in 150 µl H_2O was adjusted to with potassium carbonate to pH 9.0

and added to the reaction mixture, which was stirred for 24h at room temperature. All volatiles were removed under reduced pressure and the crude product was purified by preparative HPLC and obtained as a colourless solid after lyophilization as a mixture of diastereoisomers (33 mg, 0.058 mmol, 89.0%).

^{1}H NMR (600 MHz, Deuterium Oxide) δ 7.27 (dd, *J* = 8.5, 7.3 Hz, 2H), 7.05 – 7.00 (m, 3H), 4.54 – 4.36 (m, 3H), 4.00 (td, *J* = 6.6, 3.4 Hz, 1H), 2.89 (dd, *J* = 14.1, 5.4 Hz, 1H), 2.80 – 2.66 (m, 3H), 2.49 (ddt, *J* = 9.7, 7.4, 3.1 Hz, 2H), 2.40 – 2.25 (m, 2H), 2.22 – 2.06 (m, 2H). ^{13}C NMR (151 MHz, Deuterium Oxide) δ 174.15, 172.76, 172.51 – 172.47 (m), 171.42, 138.58, 129.78, 123.02, 118.82 (d, *J* = 5.1 Hz), 60.93 (qd, *J* = 37.6, 5.1 Hz), 52.76 (d, *J* = 9.6 Hz), 52.17, 41.04, 32.70 (d, *J* = 6.8 Hz), 30.87, 26.41, 25.59, 25.41, 23.94. ^{31}P NMR (243 MHz, D_2O) δ 33.70. ^{19}F NMR (282 MHz, D_2O) δ 2.60, 1.91. HRMS for $C_{20}H_{29}F_3N_4O_8PS^+$ $[M+H]^+$ calcd.: 573.1390, found: 573.1391.

4.18. Trifluorethyl-*N*-(4-(2,5-dioxo-1-pyrrolidinyl)oxy-carbonyl-phenyl)-*P*-vinylphosphonamidate

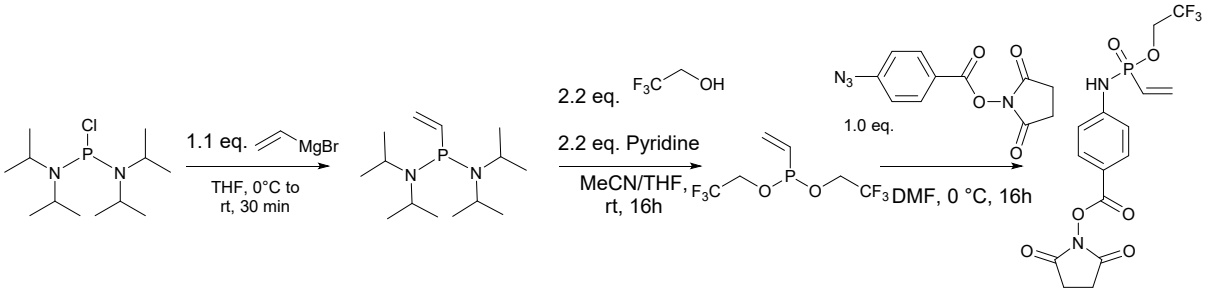

A flame-dried Schlenkflask was charged with 266 mg Bis(diisopropylamino)-chlorophosphine (1.0 mmol, 1.0 eq.), dissolved in 200 µl of dry THF and cooled to 0 °C. 1.1 ml of vinyl magnesiumbromide (1.0 M in THF, 1.10 mmol, 1.1eq.) were added and the reaction was stirred at room temperature for 30 minutes. A solution of 160 µl 2,2,2-Trifluoroethanol (2.20 mmol, 2.2 eq.) in 1 ml of MeCN and 4.9 ml tetrazole (0.45 M in MeCN, 2.20 mmol, 2.2 eq.) were added subsequently. The resulting suspension was stirred at room temperature overnight. Afterwards, 260 mg 4-azidobenzoic-acid-*N*-hydroxysuccinimide ester (1.0 mmol, 1.0 eq.), dissolved in 1 ml of dry DMF was added and the suspension was stirred overnight. All volatiles were removed under reduced pressure and the crude product was purified by silica column (EtOAc/n-hexane, 4:1) and obtained as a colourless solid. (223 mg, 0.55 mmol, 55.0%)

^{1}H NMR (300 MHz, Chloroform-*d*) δ 7.93 (d, *J* = 8.8 Hz, 3H), 7.06 (d, *J* = 8.8 Hz, 2H), 6.54 – 5.96 (m, 3H), 4.58 – 4.15 (m, 2H), 2.84 (s, 4H). ^{13}C NMR (75 MHz, Chloroform-*d*) δ 169.79, 161.35, 146.14, 137.44, 132.37, 126.35, 124.07, 117.83, 117.24 (d, *J* = 7.1 Hz), 60.76 (qd, *J* = 37.8, 5.1 Hz), 25.63. ^{31}P NMR (122 MHz, $CDCl_3$) δ 17.53. ^{19}F NMR (282 MHz, $CDCl_3$) δ 2.88. HRMS for $C_{15}H_{15}F_3N_2O_6P^+$ $[M+H]^+$ calcd.: 407.0614, found: 407.0614.

4.19. 5-((2-(*O*-trifluorethyl-*P*-vinyll-phosphonamidato-*N*-benzoyl)ethyl)amino)naphthalene-1-sulfonic acid (6)

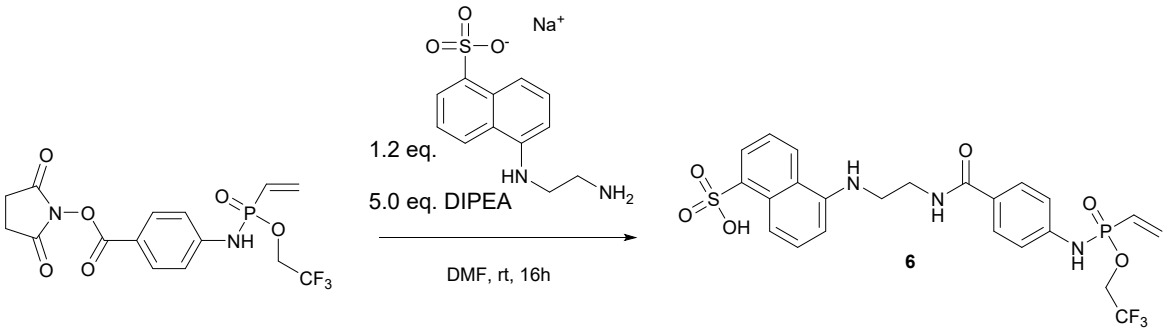

A 10-ml round-bottom-flask was charged with 50 mg Trifluorethyl-N-(4-(2,5-dioxo-1-pyrrolidinyl)oxy-carbonyl-phenyl)-P-vinylphosphonamidate (0.123 mmol, 1.0 eq.), 43 mg EDANS sodium salt (0.147 mmol, 1.2 eq.) and 1.2 ml DMF. 107 µl DIPEA (0.615 mmol, 5.0 eq.) were added and the solution was stirred overnight. The crude product was purified by preparative HPLC and obtained as a colourless solid after lyophilization (60.360,3 mg, 0.108 mmol, 88.0%). HRMS for $C_{23}H_{24}F_3N_3O_6P^+$ $[M+H]^+$ calcd.: 558.1070, found: 558.1071.

^{1}H NMR (600 MHz, DMSO-d_6) δ 8.55 (t, *J* = 8.7 Hz, 2H), 8.41 (s, 1H), 8.11 (d, *J* = 8.5 Hz, 1H), 8.00 (d, *J* = 7.1 Hz, 1H), 7.78 (d, *J* = 8.4 Hz, 2H), 7.42 (dt, *J* = 29.4, 7.9 Hz, 2H), 7.13 (d, *J* = 8.4 Hz, 2H), 6.99 (s, 1H), 6.44 – 6.16 (m, 3H), 4.76 – 4.46 (m, 2H), 3.61 (q, *J* = 6.3 Hz, 2H), 3.47 (t, *J* = 6.3 Hz, 2H). ^{13}C NMR (151 MHz, DMSO-d_6) δ 166.99, 153.70, 144.71, 144.02, 136.66, 130.59, 128.98, 128.24, 127.34, 127.15, 126.39, 125.19, 124.88, 124.78, 124.07 (d, *J* = 6.3 Hz), 123.10, 117.39, 117.34, 61.90 – 59.65 (m), 45.88, 38.01. ^{31}P NMR (243 MHz, DMSO) δ 17.26. ^{19}F NMR (282 MHz, DMSO) δ 4.13.

4.20. 2-Nitrobenzyl-*N*-(4-biotinamido-phenyl)-*P*-vinyl phosphonamidate

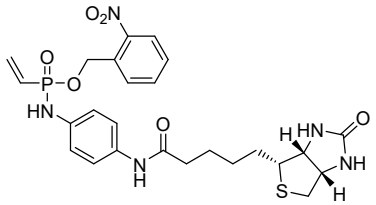

N-(4-azidophenyl) biotinamide was synthesized as previously described.[2] The above stated compound was synthesized according to the general procedure 3 from 302 mg Di(2-nitrobenzyl) vinylphosphonite borane (**1b**) (0.803 mmol, 1.50 eq.) in DMF. The crude phosphonamidate was purified by flash column chromatography (12-15% MeOH in CH_2Cl_2) and obtained as yellowish solid. (150 mg, 0.268 mmol, 50.1%)

^{1}H NMR (300 MHz, DMSO-d6) δ 9.76 (s, 1H), 8.13 (d, J = 8.1 Hz, 1H), 8.02 (d, J = 8.4 Hz, 1H), 7.85 – 7.73 (m, 2H), 7.69 – 7.54 (m, 1H), 7.40 (d, J = 8.8 Hz, 2H), 6.97 (d, J = 8.8 Hz, 2H), 6.61 – 5.99 (m, 5H), 5.37 (qd, J = 14.8, 7.4 Hz, 2H), 4.30 (dd, J = 7.8, 4.9 Hz, 1H), 4.22 – 4.00 (m, 1H), 3.15 – 3.01 (m, 1H), 2.82 (dd, J = 12.4, 5.1 Hz, 1H), 2.58 (d, J = 12.4 Hz, 1H), 2.25 (t, J = 7.3 Hz, 2H), 1.75 – 1.26 (m, 6H). ^{13}C NMR (75 MHz, DMSO-d_6) δ 171.02, 163.10, 147.09, 136.39, 135.17, 134.63, 133.42, 133.00 (d, *J* = 7.7 Hz), 129.84, 129.44, 128.97, 125.18, 120.54, 118.24 (d, *J* = 6.6 Hz), 62.45 (d, *J* = 4.1 Hz), 61.41, 59.56, 55.78, 48.97, 45.79, 36.44, 28.54 (d, *J* = 12.6 Hz), 25.56. ^{31}P NMR (122 MHz, DMSO) δ 16.30. HRMS for $C_{25}H_{31}N_5O_6PS^+$ $[M+H]^+$ calcd.: 560.1727, found: 560.1725.

4.21. Synthesis of RCM-BCL9-Nle peptide 7

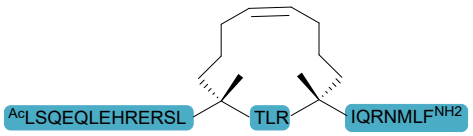

The RCM-BCL9 peptide was synthesized in a 0.05 mmol scale on a Rink Amide Resin with a loading of 0.78 mmol/g. Until the first olefinic amino acid the synthesis was carried out on a PTI synthesizer with single couplings (5 eq. amino acid for 40 minutes). Olefinic amino acids (2 eq.) were coupled manually with HATU (2eq.) and DIPEA (4 eq.) for two hours and full conversion was checked by trial cleavage. The three amino acids in between the olefinic ones were coupled manually (5 eg. for 40 minutes) all amino acids following the olefinic ones were coupled in double coupling steps with five equivalents for 40 minutes. After the second olefinic amino acids the synthesis was resumed by automated SPPS on the PTI synthesizer. The *N*-terminus was acetylated by treatment with a lutidine:acetic anhydride:DMF (5:6:89;v:v:v) for 10 minutes. To generate the hydrocarbon staple the resin was incubated with a 10 mM solution of bis(tricyclohexylphosphine)-benzylidene ruthenium (IV) (1st generation Grubb's catalyst) in 1,2-dichloroethane for one hour twice.

The final cleavage from resin was achieved by incubation with a mixture of TFA:TIS:H_2O (95:2.5:2.5;v:v:v) for two hours followed by precipitation in cold diethylether. The crude peptide was purified by preparative reverse phase C18 HPLC and the product was gained as white powder (14 mg, 3.9 µmol, 7.8% yield).

HRMS: m/z: 1019.5471 $[M+3H]^{3+}$ (calc. 1019.5881 m/z).

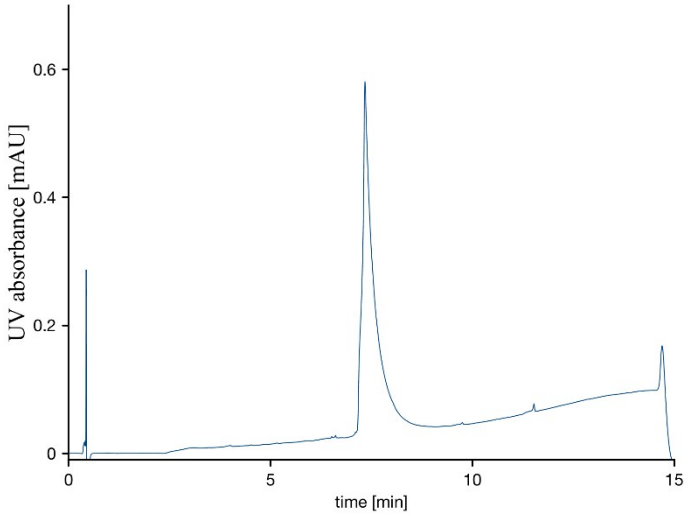

4.22. Synthesis of FAM RCM-BCL9-Nle peptide 7-CF

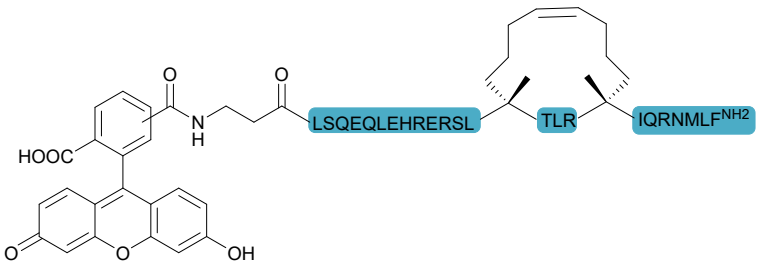

The FAM-RCM-BCL9 peptide was synthesized in a 0.05 mmol scale on a Rink Amide Resin with a loading of 0.78 mmol/g. Until the first olefinic amino acid the synthesis was carried out on a PTI synthesizer

with single couplings (5 eq. amino acid for 40 minutes). Olefinic amino acids (2 eq.) were coupled manually with HATU (2eq.) and DIPEA (4 eq.) for two hours and full conversion was checked by trial cleavage. The three amino acids in between the olefinic ones were coupled manually (5 eg. for 40 minutes) all amino acids following the olefinic ones were coupled in double coupling steps with five equivalents for 40 minutes. After the second olefinic amino acids the synthesis was resumed by automated SPPS on the PTI synthesizer and Fmoc-β-Ala was coupled *N*-terminally. To generate the hydrocarbon staple the resin was incubated with a 10 mM solution of bis(tricyclohexylphosphine)-benzylidene ruthenium (IV) (1st generation Grubb's catalyst) in 1,2-dichloroethane for one hour twice. Finally the peptide was fluorescein labeled by coupling 5-(6)-carboxyfluorescein succinimidyl ester (2 eq.) with DIPEA (3 eq.) as activating base for two hours.

The final cleavage from resin was achieved by incubation with a mixture of TFA:TIS:H_2O (95:2.5:2.5;v:v:v) for two hours followed by precipitation in cold diethylether. The crude peptide was purified by preparative reverse phase C18 HPLC and the product was gained as yellow powder (16 mg, 4.02 µmol, 8.0% yield).

HRMS: m/z: 1148.5795 $[M+3H]^{3+}$ (calc. 1148.6129 m/z); 861.6882 $[M+4H]^{4+}$ (calc. 861.7117 m/z).

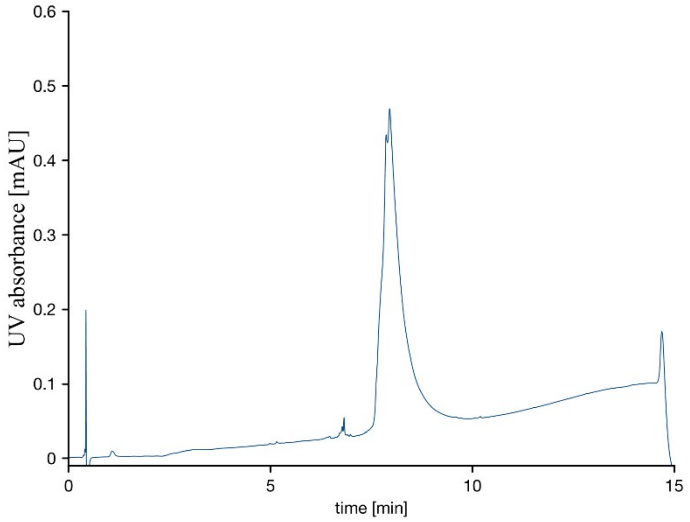

4.23. General procedure 4 for synthesis of BCL9-peptides

The BCL9 peptide was synthesized in a 0.1 mmol scale on a Rink Amide Resin with a loading of 0.78 mmol/g. The synthesis was carried out on a PTI synthesizer with a single coupling of each standard amino acid (5 eq. amino acid for 40 min). Fmoc-Azidohomoalanin (2 eq.) was coupled with HATU (2 eq.) for four hours. Fmoc deprotection was accomplished by treating the peptide with 20% piperidine in DMF for 3 minutes two to three times according to UV read out. N-terminal acetylation was done by incubation with a mixture of lutidine:acetic acid:DMF (6%:5%:89%;v;v;v) for 10 minutes. Final cleavage from solid support was carried out by incubating the resin with 4 ml of a TFA:TIS:H2O (95:2.5:2.5) mixture for two hours and precipitated in cold diethylether.

4.24. Synthesis of BCL9-Nle-Aha-LCys peptide 8a

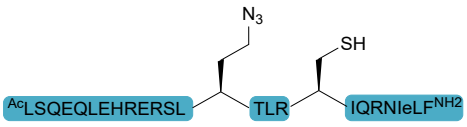

The Peptide was synthesized according to general procedure 4. The crude peptide was purified by preparative reverse phase C18 HPLC (0-5 min 95/5, water (0.1%TFA)/MeCN (0.1%TFA); 5-60 min 10/90, water (0.1%TFA)/MeCN (0.1%TFA)). The product **8a** was gained as white powder (35 mg as TFA-salt, 9.7 µmol, 9.7 % yield).

HRMS: m/z: 1012.5317 $[M+3H]^{3+}$ (calc. 1012.5532 m/z).

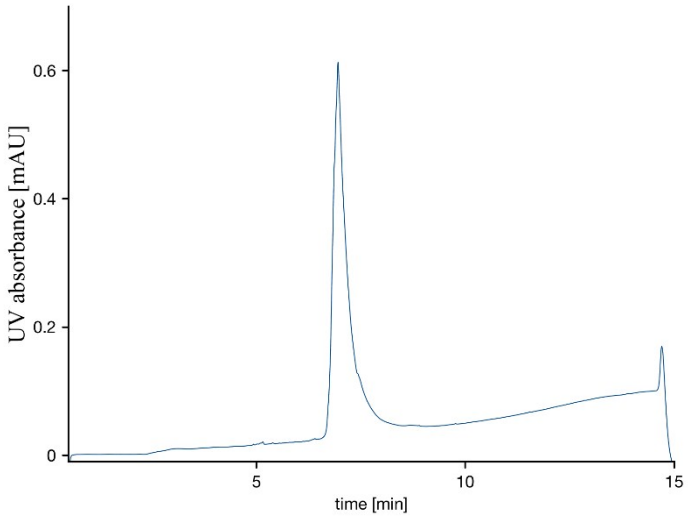

4.25. Synthesis of BCL9-Nle-Aha-DCys 8b

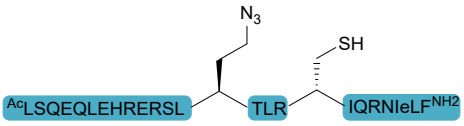

The Peptide was synthesized according to general procedure 4. The crude peptide was purified by preparative reverse phase C18 HPLC (0-5 min 95/5, water (0.1%TFA)/MeCN (0.1%TFA); 5-60 min 10/90, water (0.1%TFA)/MeCN (0.1%TFA)). The product was gained as white powder (50.5 mg as TFA-salt, 14.0 µmol, 14 % yield).

HRMS: m/z: 1012.5383 $[M+3H]^{3+}$ (calc. 1012.5532 m/z).

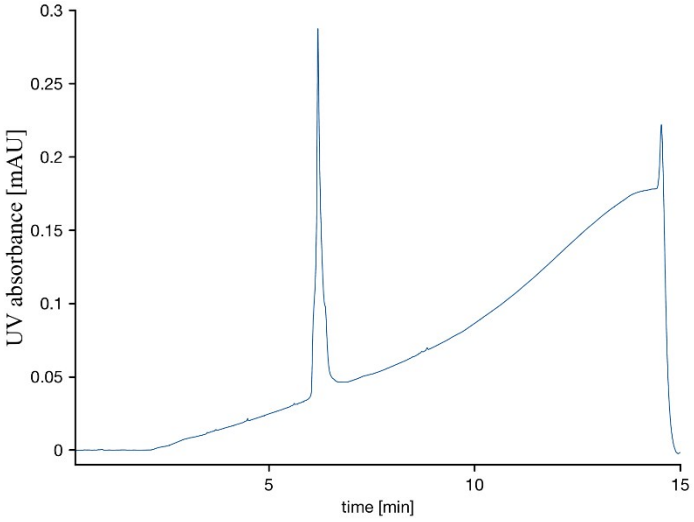

4.26. Synthesis of FAM-BCL9-Nle-Aha-DCys peptide (8b-CF)

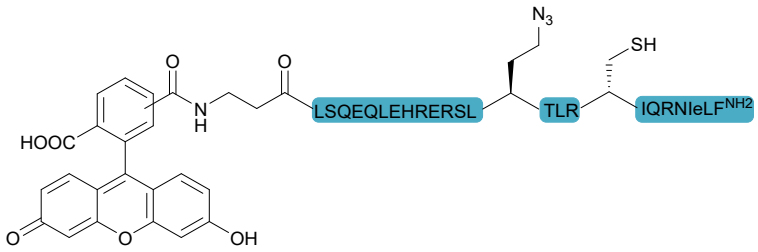

The Peptide was synthesized according to general procedure 4. After the final regular amino acid coupling and Fmoc-deprotection, Fmoc-β-Alanine (5 eq.) was coupled manually with HATU (5 eq.) and DIPEA (10 eq.) as activating base for one hour. After Fmoc-deprotection 5-(6)-carboxyfluorescein succinimidyl ester (2 eq.) was coupled with DIPEA (3 eq.) as activating base for four hours. Final cleavage from solid support was carried out by incubating the resin with 4 ml of a TFA:TIS:H2O (95:2.5:2.5) mixture for two hours and precipitated in cold diethylether. The crude peptide was purified by preparative reverse phase C18 HPLC (0-5 min 95/5, water (0.1%TFA)/MeCN (0.1%TFA); 5-60 min 10/90, water (0.1%TFA)/MeCN (0.1%TFA)). The product was gained as yellow powder (42.0 mg as TFA-salt, 10.2 µmol, 10.2 % yield).

HRMS: m/z: 1141.5472 [M+3H]3+ (calc. 1141.5780 m/z); 856.4244 [M+4H]4+ (calc. 856.4355 m/z).

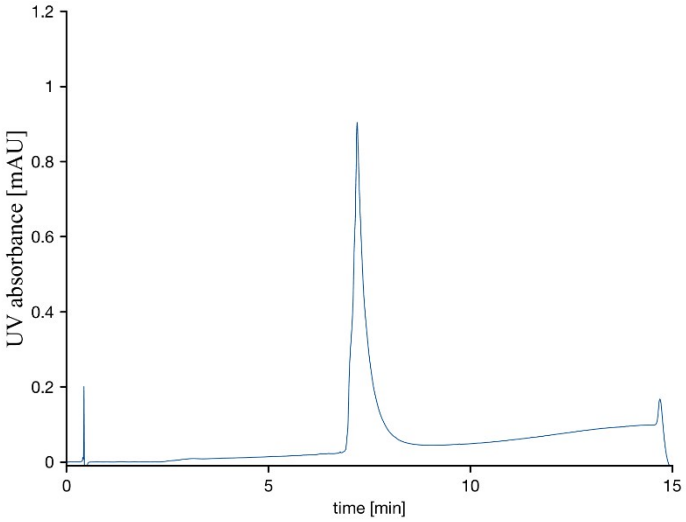

4.27. General procedure 5 for the Staudinger induced peptide cyclization

Vinyl magnesium bromide in THF (1 M, 2 ml, 2 mmol, 1 eq.) was cooled to -78°C in a flame dried schlenk flask and diethylchlorophosphite (0.286 ml, 2 mmol, 1 eq.) was added. The solution was stirred for 10 minutes at -78°C and let warm to room temperature and stirred for another 90 minutes. The full consumption of starting material was confirmed by 31P-NMR and used as crude in the following Staudinger reaction with an azido-peptide.

Purified azido-peptide was dissolved in DMSO at a 3 mM concentration and dried in a flame-dried flask for one hour prior to adding five equivalents of bisethoxyalkene-phosphonite (volume according to percentage of product determined by NMR). After the reaction mixture was stirred over night at room temperature and full conversion was observed by UPLC-UV/MS, water was added and the reaction mixture directly lyophilized. The crude product was purified by preparative HPLC.

4.28. Synthesis of cyclic-BCL9-Nle-Aha-LCys peptide 9a

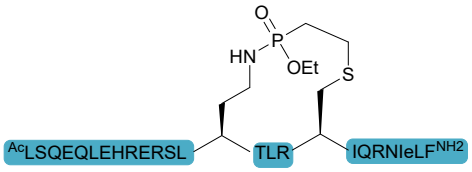

Peptide 8a (15 mg, 4.16 µmol, 1eq.) was reacted according to the general procedure 5. The crude peptide was purified by preparative reverse phase C18 HPLC (0-5 min 95/5, water (0.1%TFA)/MeCN (0.1%TFA); 5-60 min 10/90, water (0.1%TFA)/MeCN (0.1%TFA)). The product 7a was gained as white powder (7 mg as TFA-salt, 1.89 µmol, 45.4 % yield).

HRMS: m/z: 1043.1953 [M+3H]3+ (calc. 1043.2292 m/z).

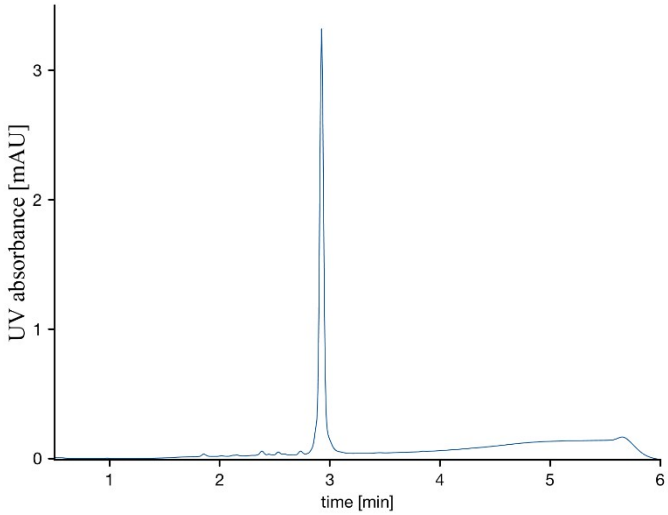

4.29. Synthesis of Cyclic-BCL9-Nle-Aha-DCys peptide synthesis 9b

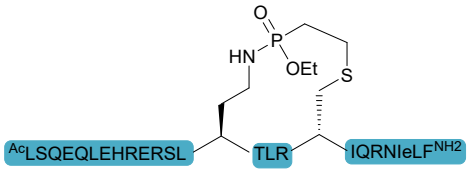

Peptide 8b (34 mg, 9.43 µmol, 1eq.) was reacted according to the general procedure 5. The crude peptide was purified by preparative reverse phase C18 HPLC (0-5 min 95/5, water (0.1%TFA)/MeCN (0.1%TFA); 5-60 min 10/90, water (0.1%TFA)/MeCN (0.1%TFA)). The product 8b was gained as white powder (15 mg as TFA-salt, 4.06 µmol, 43.1 % yield).

HRMS: m/z: 1043.2085 [M+3H]3+ (calc. 1043.2292 m/z).

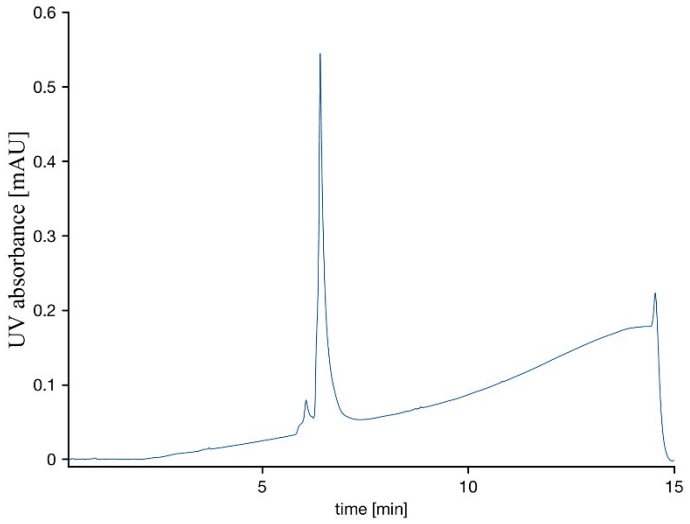

4.30. FAM labeled cyclic-BCL9-Nle-Aha-DCys peptide synthesis (9b-CF)

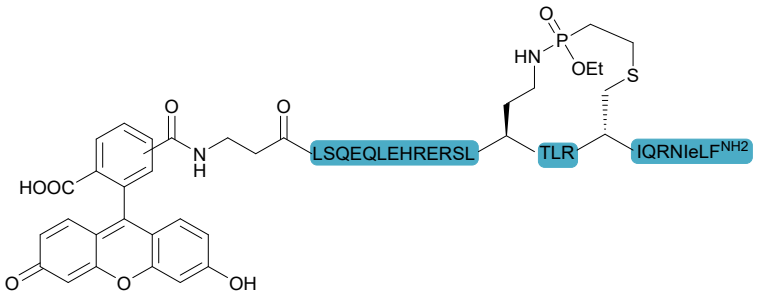

Peptide 8b-CF(21 mg, 5.1 µmol, 1eq.) was reacted according to the general procedure 5. The crude peptide was purified by preparative reverse phase C18 HPLC (0-5 min 95/5, water (0.1%TFA)/MeCN (0.1%TFA); 5-60 min 10/90, water (0.1%TFA)/MeCN (0.1%TFA)). The product 8b-CF was gained as yellow powder (12 mg as TFA-salt, 2.9 µmol, 56.9 % yield).

HRMS: m/z: 1172.1996 [M+3H]3+ (calc. 1172.2539 m/z); 879.4191 [M+4H]4+ (calc. 879.4424 m/z).

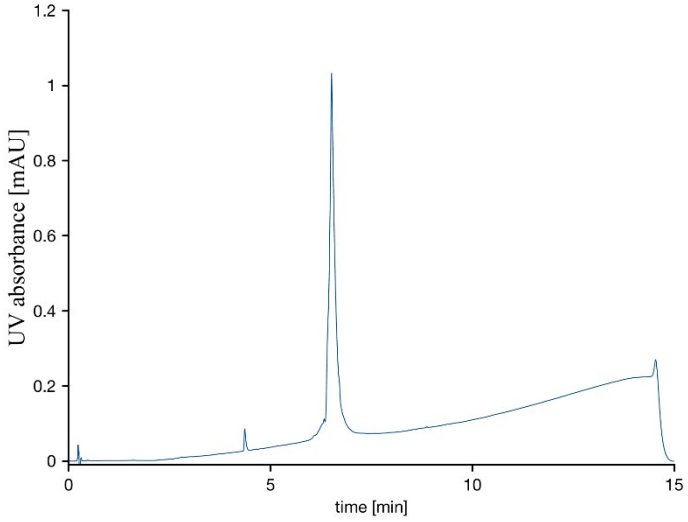

4.31. Alkylated-BCL9-Nle-Aha-LCys peptide synthesis 10

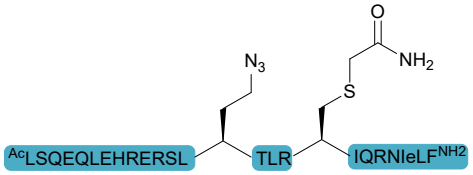

Peptide 8a (43.2 mg, 12.0 µmol) was incubated with iodoacetamide (22.2 mg, 120 µmol, 10eq.) in a mixture of ammoniumbicarbonate buffer and acetonitrile (6:2) with a final pH of 8.5. After one hour the mixture was purified by preparative HPLC 0-5 min 95/5, water (0.1%TFA)/MeCN (0.1%TFA); 5-60 min 10/90, water (0.1%TFA)/MeCN (0.1%TFA)). The product was gained as white powder (25 mg as TFA-salt, 6.8 µmol, 57 % yield).

HRMS: m/z: 1031.5342 [M+3H]3+ (calc. 1031.5604 m/z).

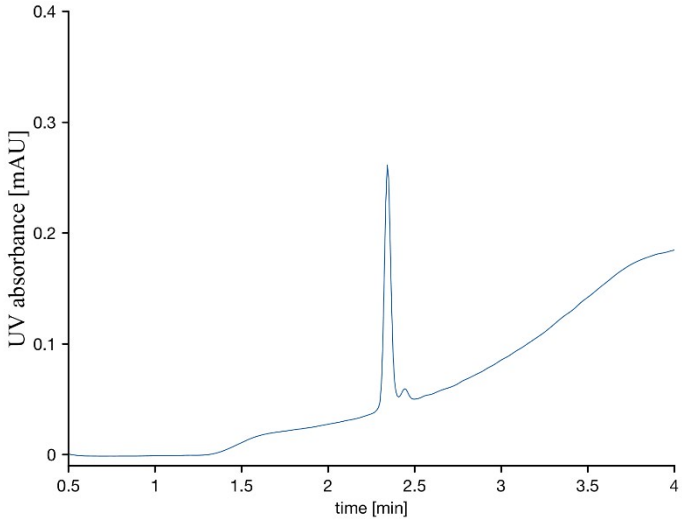

4.32. Synthesis of cyclic-benzylphosphonamidate-BCL9-Nle-Aha-DCys peptide 13

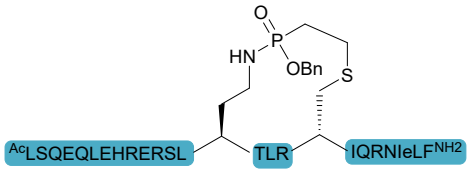

Bis(diisopropylamino) chlorophosphine (267 mg, 1 mmol, 1 eq.) was given into a flame dried schlenk flask and dried under vacuo for 30 minutes. Vinyl magnesium bromide in THF (1 M, 1.1 ml, 1.1 mmol, 1.1 eq.) was added at -78°C and the reaction mixture was stirred for 10 minutes. Then the reaction was let to warm up to room temperature and stirred for another 30 minutes. First tetrazole in acetonitrile (0.45 M, 5.56 ml, 2.5 mmol, 2.5 eq.) was added to the reaction mixture followed by benzylalcohol (0.26 ml, 2.5 mmol, 2.5 eq.). The reaction was stirred for 16 hours and used further as crude after confirmation of product formation *via* ^{31}P-NMR (product at 164.2 ppm). Peptide **8b** (15 mg, 4.04 µmol, 1eq.) was solubilized in DMSO and reacted with the crude phosphonite (24.2 µmol, 6 eq.) in a final concentration of 10 mM. The reaction mixture was stirred for 16 hours at 40°C and the crude peptide was purified by preparative reverse phase C18 HPLC (0-5 min 95/5, water (0.1%TFA)/MeCN (0.1%TFA); 5-60 min 10/90, water (0.1%TFA)/MeCN (0.1%TFA)). The product **13** was gained as white powder (5 mg as TFA-salt, 1.33 µmol, 32.9 % yield). HRMS: m/z: 1063.8917 $[M+3H]^{3+}$ (calc. 1063.9010 m/z).

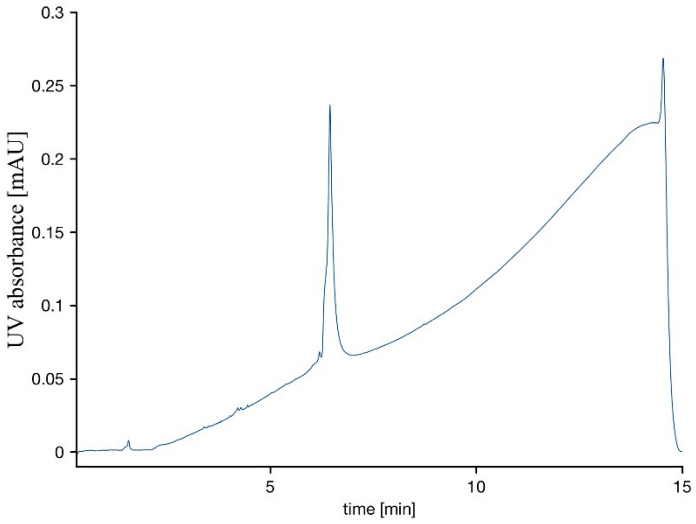

4.33. Synthesis of FAM labeled cyclic- benzylphosphonamidate-BCL9-Nle-Aha-DCys peptide (13-CF)

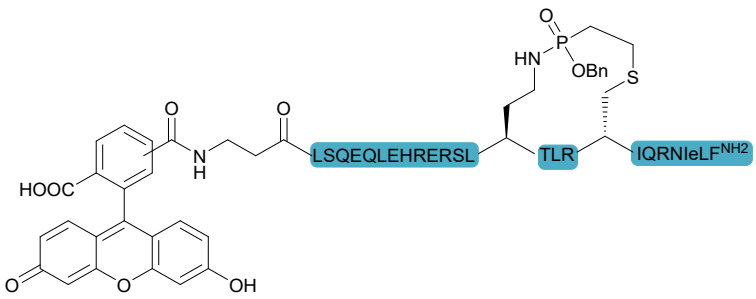

Bis(diisopropylamino) chlorophosphine (267 mg, 1 mmol, 1 eq.) was given into a flame dried schlenk flask and dried under vacuo for 30 minutes. Vinyl magnesium bromide in THF (1 M, 1.1 ml, 1.1 mmol, 1.1 eq.) was added at -78°C and the reaction mixture was stirred for 10 minutes. Then the reaction was let to warm up to room temperature and stirred for another 30 minutes. First tetrazole in acetonitrile (0.45 M, 5.56 ml, 2.5 mmol, 2.5 eq.) was added to the reaction mixture followed by benzylalcohol (0.26 ml, 2.5 mmol, 2.5 eq.). The reaction was stirred for 16 hours and used further as crude after confirmation of product formation *via* ^{31}P-NMR (product at 164.2 ppm). Peptide **8b-CF** (22 mg, 5.93 µmol, 1eq.) was solubilized in DMSO and reacted with the crude phosphonite (35.6 µmol, 6 eq.) in a final concentration of 10 mM. The reaction mixture was stirred for 16 hours at 40°C and the crude peptide was purified by preparative reverse phase C18 HPLC (0-5 min 95/5, water (0.1%TFA)/MeCN (0.1%TFA); 5-60 min 10/90, water (0.1%TFA)/MeCN (0.1%TFA)). The product **13-CF** was gained as yellow powder (3.1 mg as TFA-salt, 0.75 µmol, 12.6 % yield).

LRMS: m/z: 1193.11 $[M+3H]^{3+}$ (calc. 1192.9258 m/z).

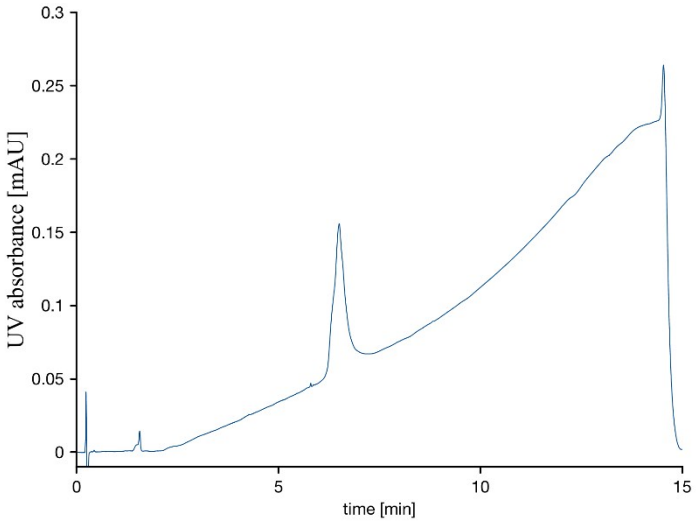

4.34. Linear-(R_{10})-Aha-Cys 15

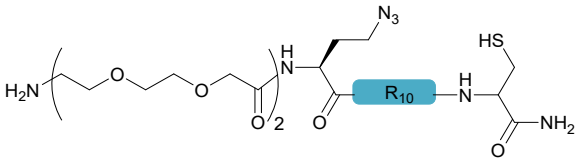

The cyclic-(R10)-azido peptide was synthesized in a 0.1 mmol scale on a Rink Amide Resin with a loading of 0.78 mmol/g. The synthesis was carried out on a PTI synthesizer with double couplings of each amino acid (5 eq. amino acid for 40 min) in DMF apart from Fmoc-azidohomoalanin, which (2eq.) was coupled with HATU (2 eq.) for four hours in presence of NMM (4 eq.) as activating base. SPPS was ending with an Fmoc deprotection step to yield the free *N*-terminal amine. Final cleavage from resin was accomplished in two cleavage steps. First the peptide was cleaved from resin with a mixture of TFA:TIS:H_2O (92:4:4;v:v:v) for 2.5 hours, followed by a second cleavage of not fully cleaved protecting groups with TFA:TIS:DTT:Thioanisole (88:2:2:8;v:v:v:v) for one hour. The crude peptide was purified by preparative reverse phase C18 HPLC (0-5 min 95/5, water (0.1%TFA)/MeCN (0.1%TFA); 5-60 min 10/90, water (0.1%TFA)/MeCN (0.1%TFA)). The product **15** was gained as white powder (78 mg as TFA-salt, 24.1 µmol, 24.1 % yield).

HRMS: m/z: 700.0462 $[M+3H]^{3+}$ (calc. m/z: 700.0908).

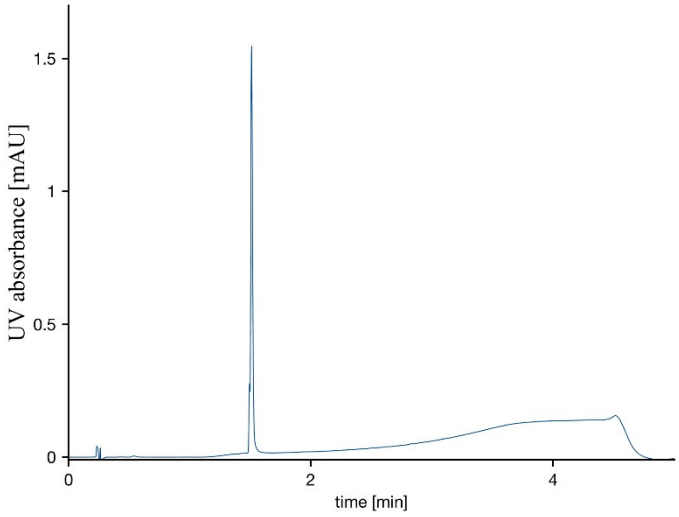

4.35. Cyclic-R10-Staudinger-Macrocycle 16

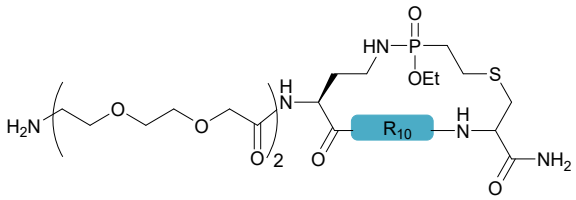

Peptide **15** was reacted according to general procedure 5 with the deviation that the reaction was carried out at 50°C instead of room temperature. The crude peptide was purified by preparative reverse phase C18 HPLC (0-5 min 95/5, water (0.1%TFA)/MeCN (0.1%TFA); 5-60 min 10/90, water (0.1%TFA)/MeCN (0.1%TFA)). The product **16** was gained as white powder (10.7 mg as TFA-salt, 3.2 µmol, 26.8 % yield).

HRMS: m/z: 730.7141 $[M+3H]^{3+}$ (calc. 730.7668 m/z).

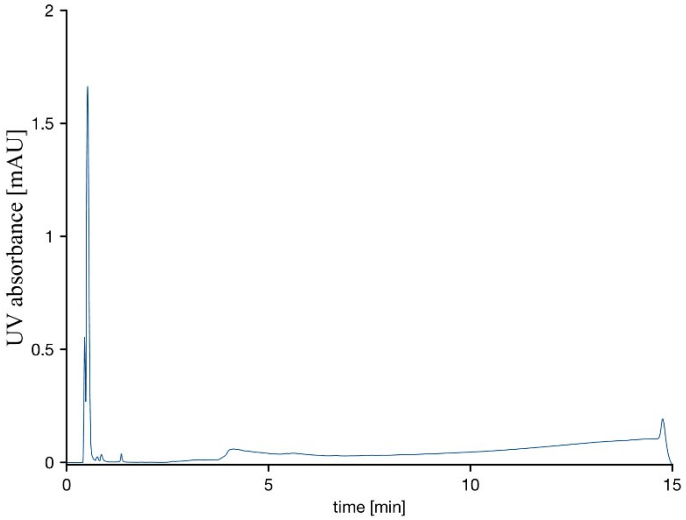

4.36. Alkyne-Cyclic-R_{10}-Staudinger-Macrocycle 18

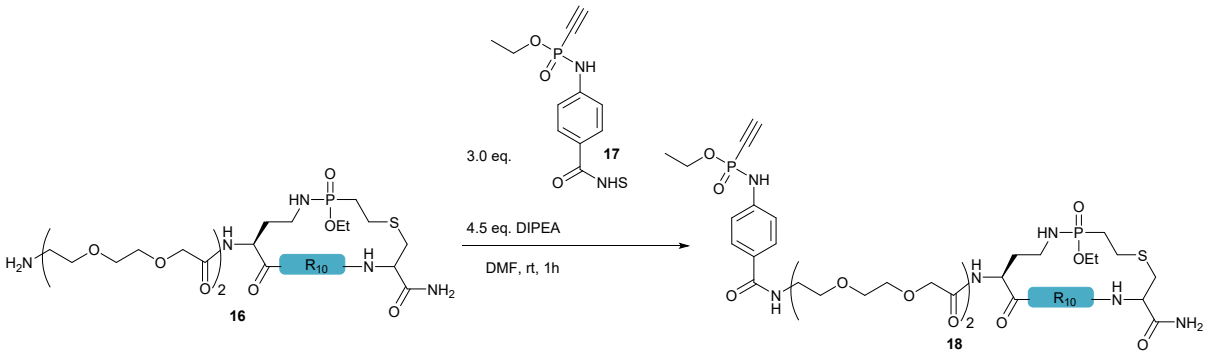

Peptide **16** (20 mg, 6 µmol, 1 eq.) solubilized in DMF (400 µl, c = 15 mM) was incubated with NHS-phosphonamidate alkyne **17** (6.3 mg, 18.0 µmol, 3eq.) in presence of DIPEA (4.68 µl, 26.9 µmol, 4.5 eq.) for one hour. After confirmation of product formation by LC-MS, the crude was diluted with water and purified by preparative HPLC. The product **18** was gained as white powder (9.8 mg as TFA salt, 2.8 µmol, 46 %yield).

LRMS: m/z: 809.0552 $[M+3H]^{3+}$ (calc. 809.1134 m/z).

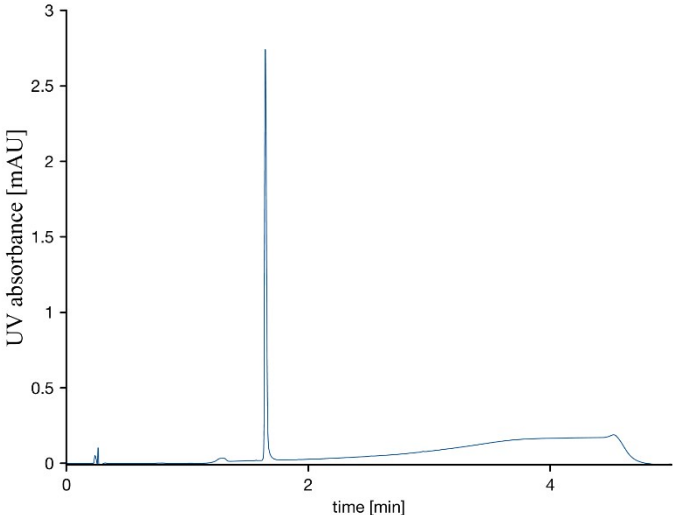

5. NMR spectra

Di(2-nitrobenzyl) vinylphosphonite borane (**1b**)

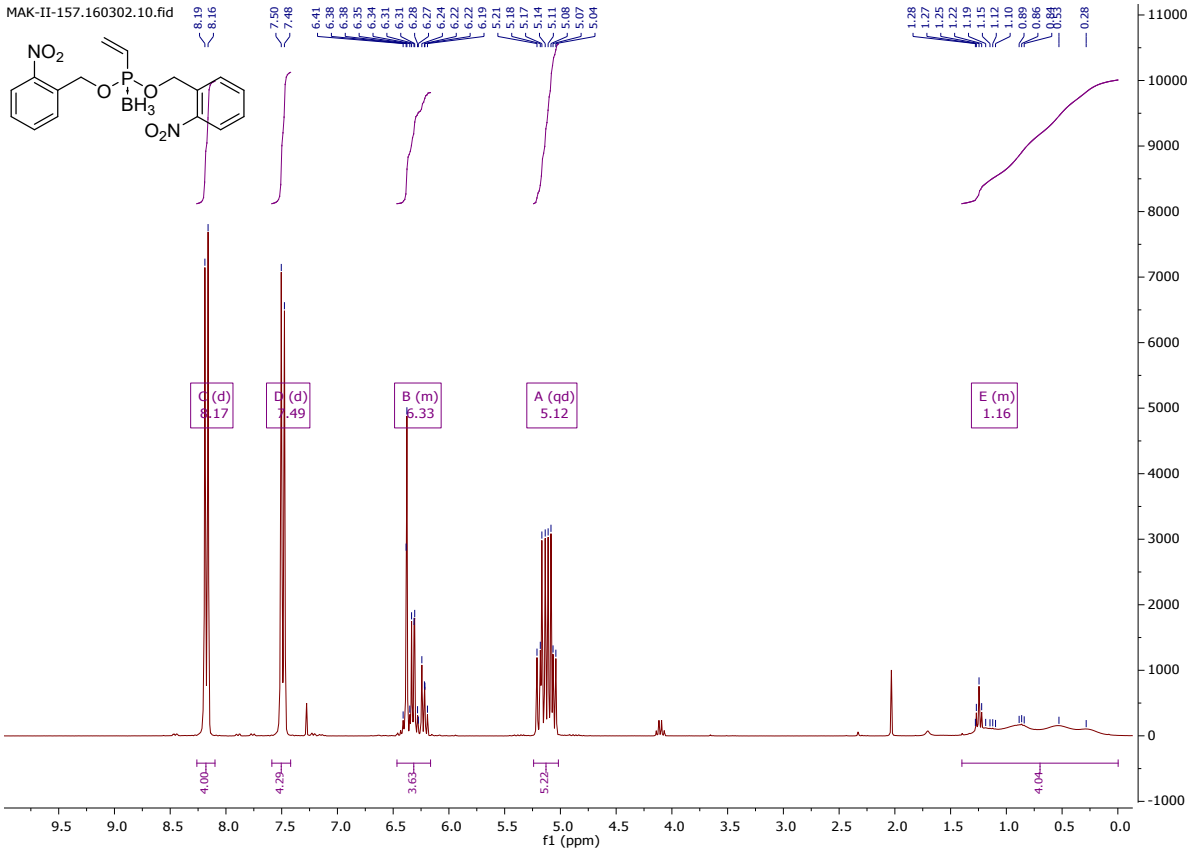

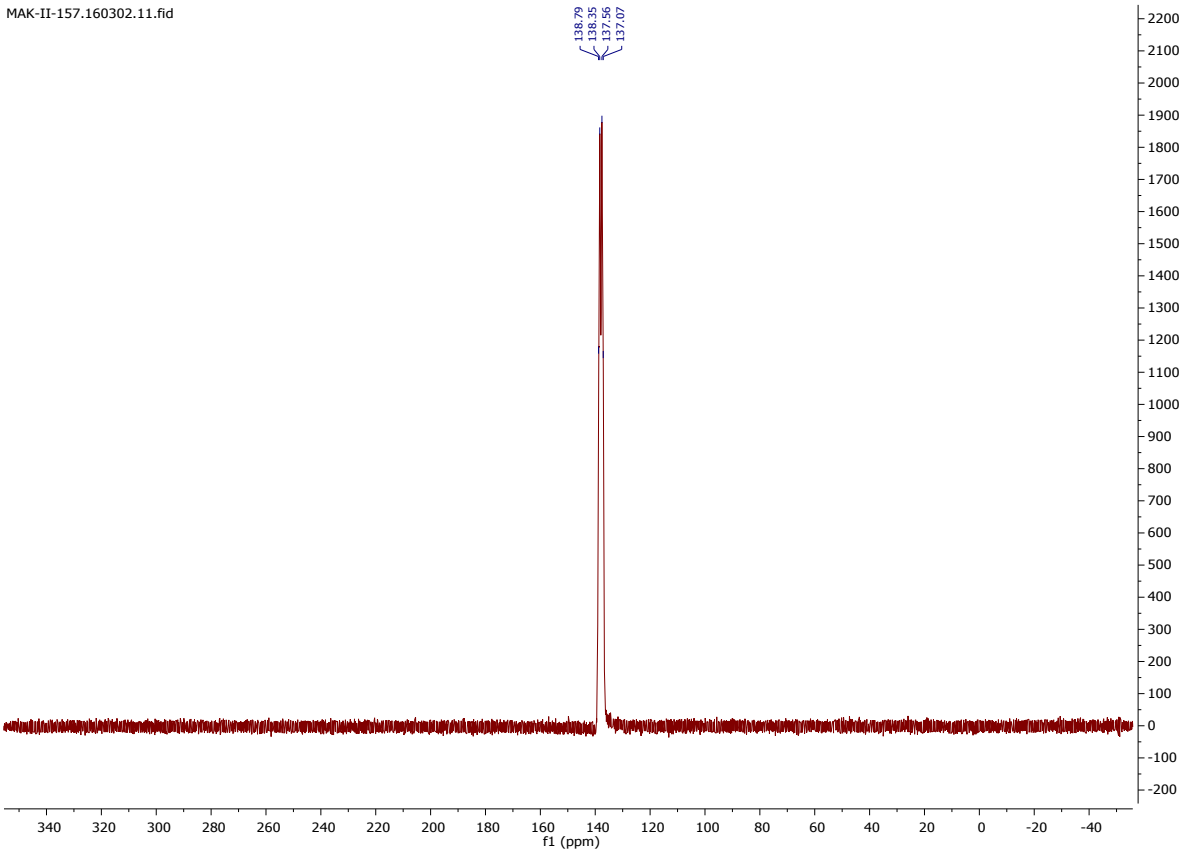

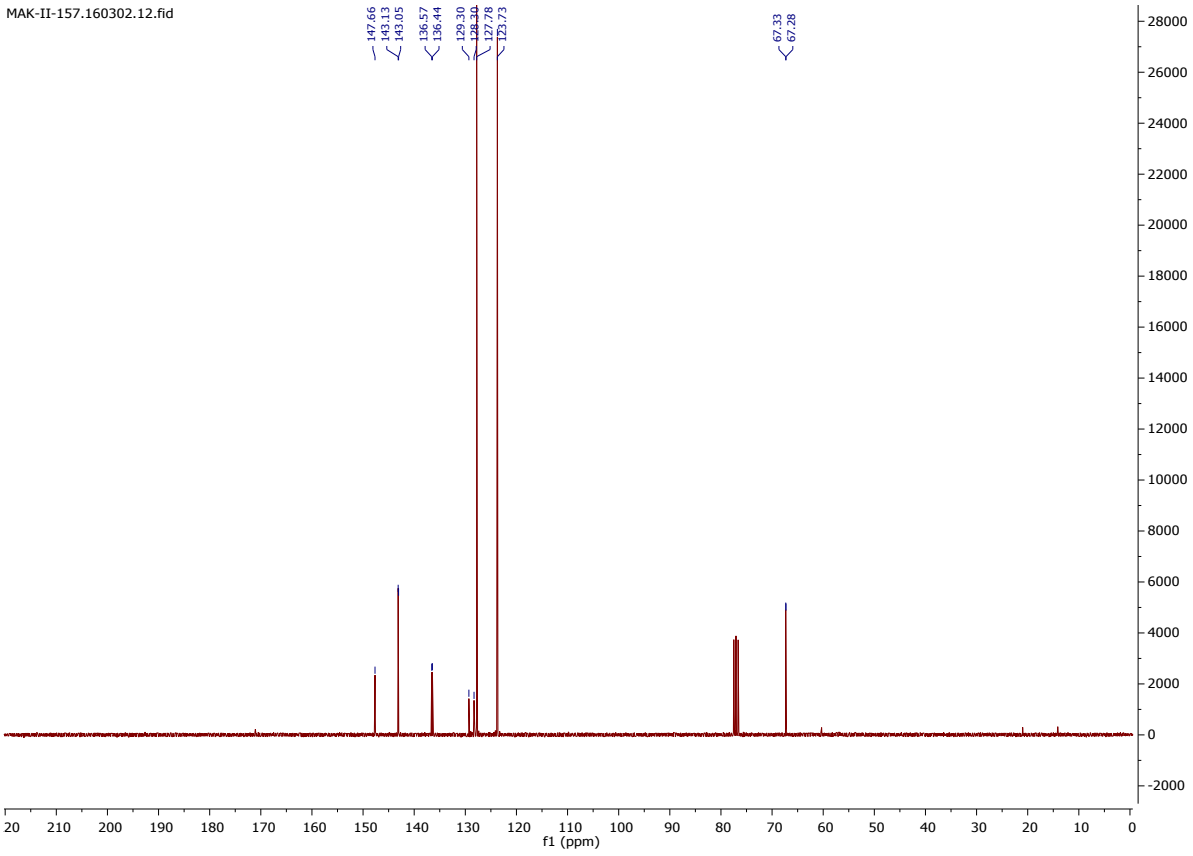

Diphenyl vinylphosphonite borane (**1c**)

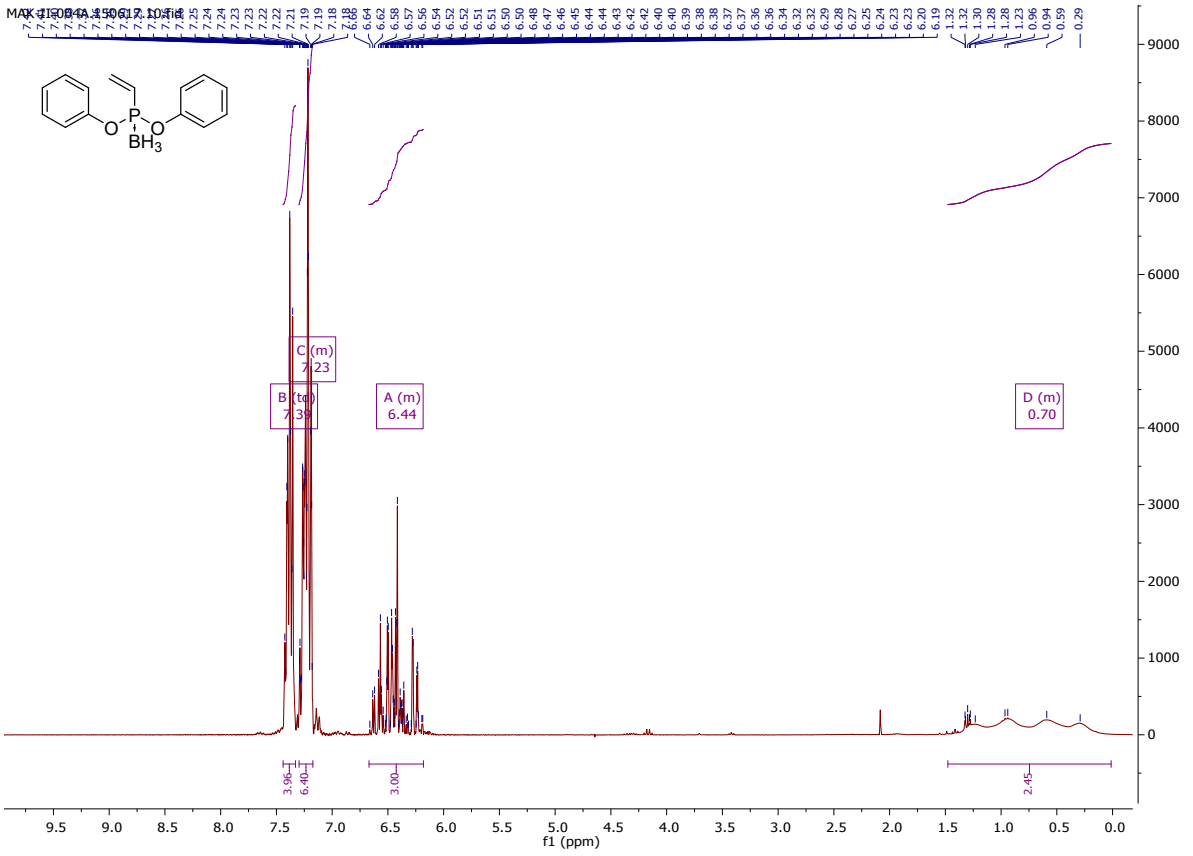

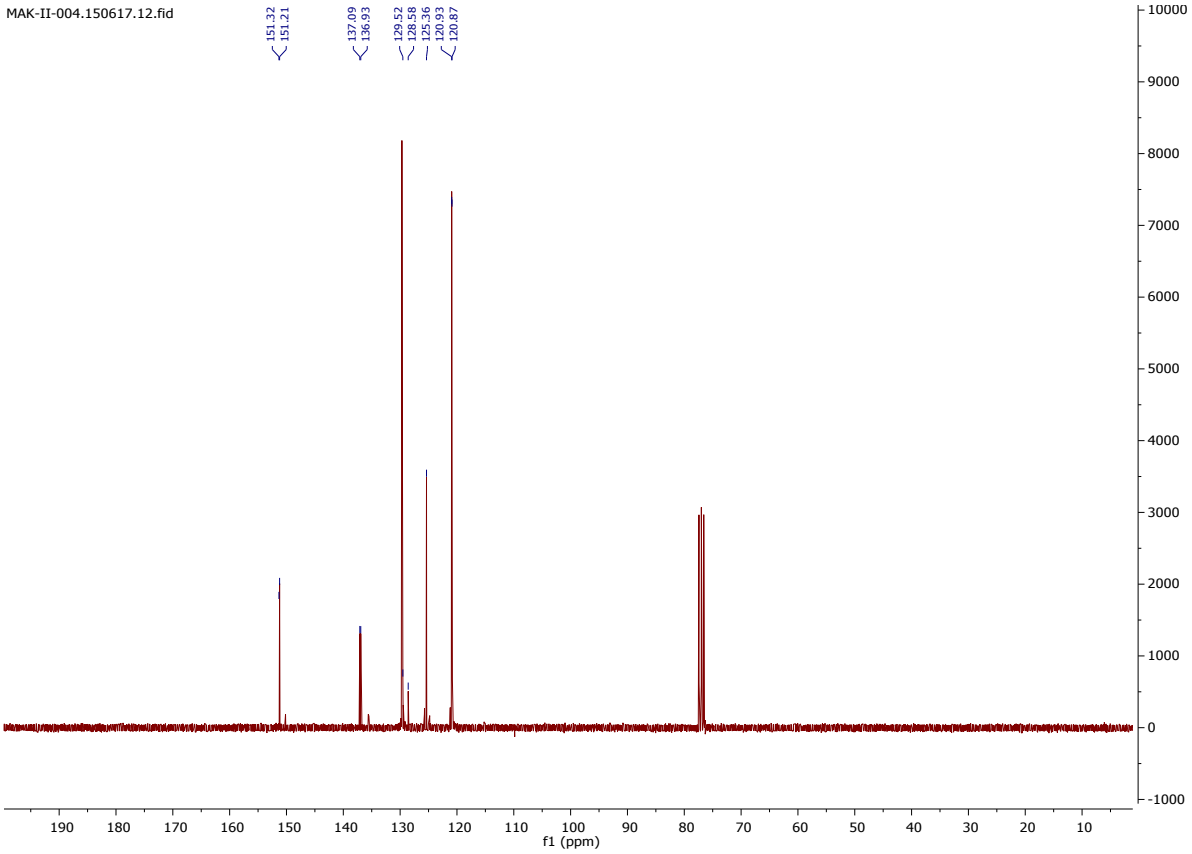
MAK-II-004.150617.12.fid
151.32
151.21
137.09
136.93
129.52
128.58
125.36
120.93
120.87
f1 (ppm)

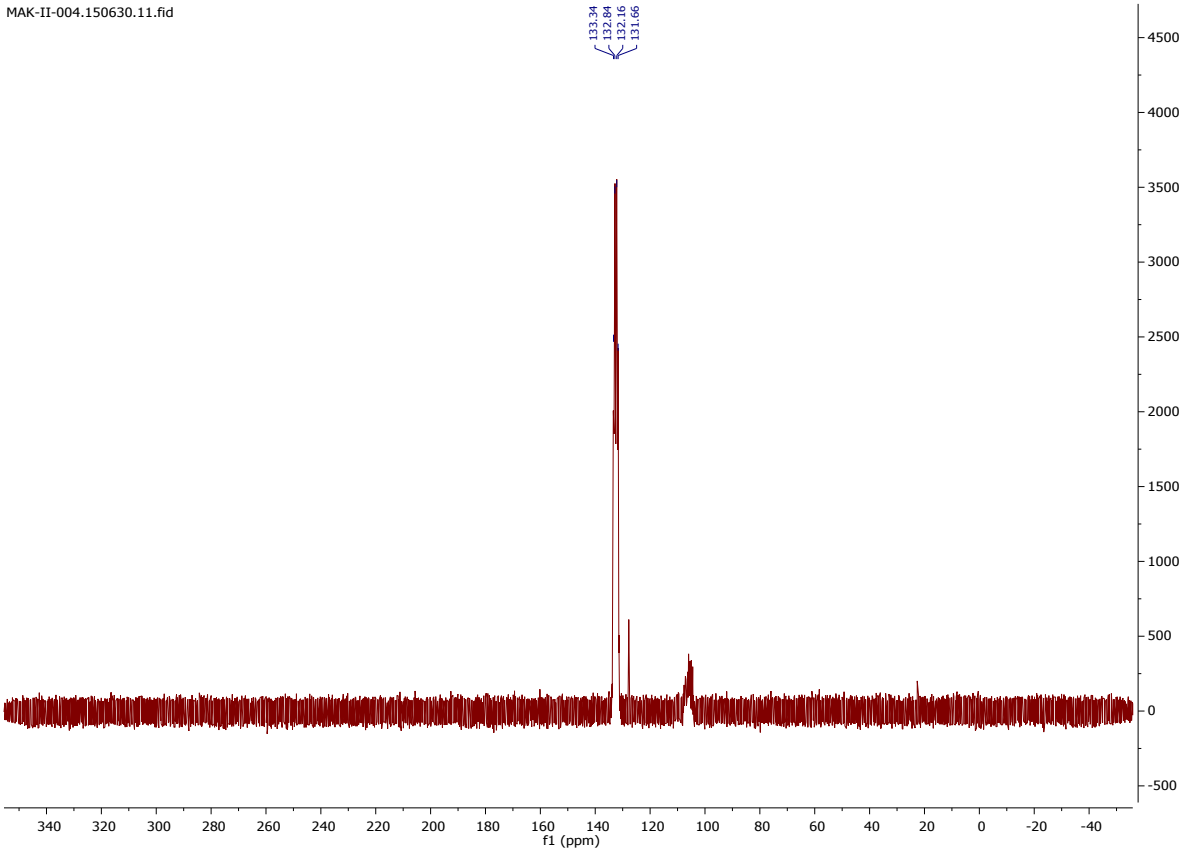
MAK-II-004.150630.11.fid
133.34
132.84
132.16
131.66
f1 (ppm)

Bis(2,2,2-trifluoroethyl) vinylphosphonite borane (**1d**)

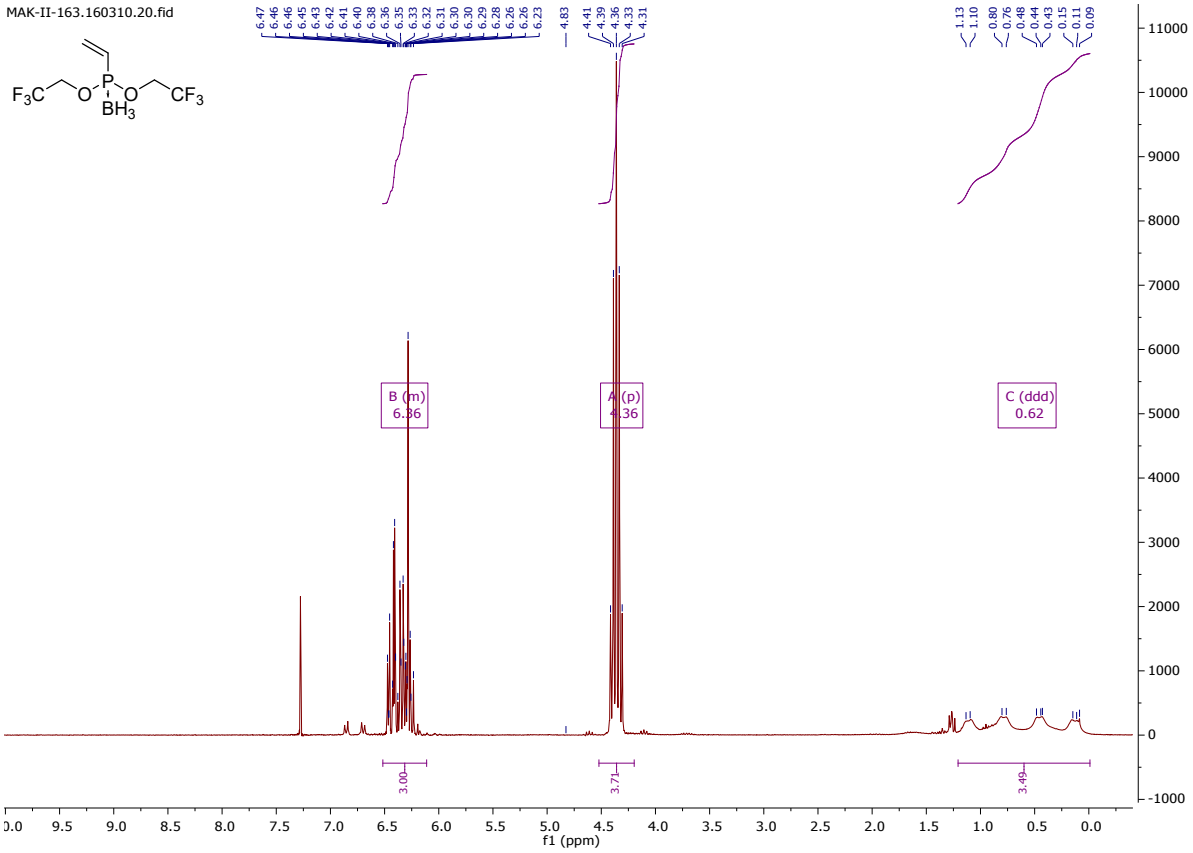

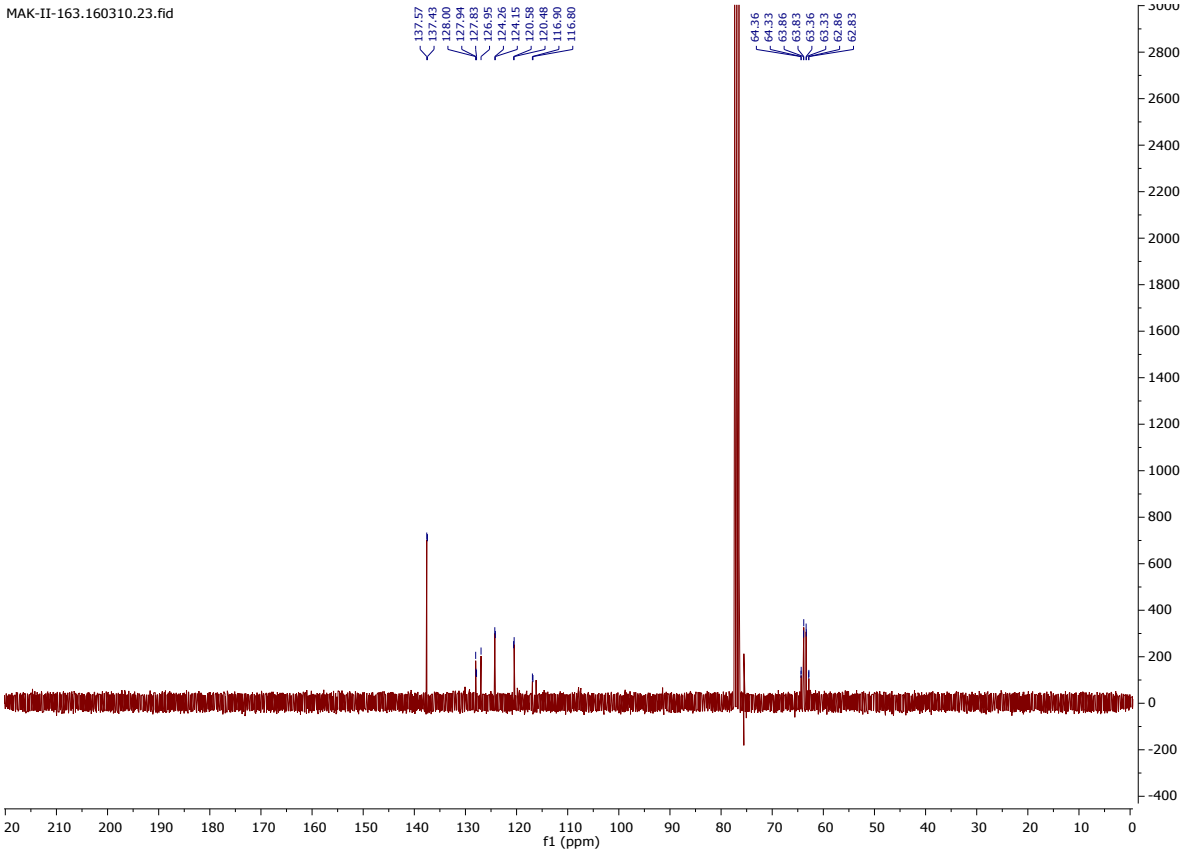

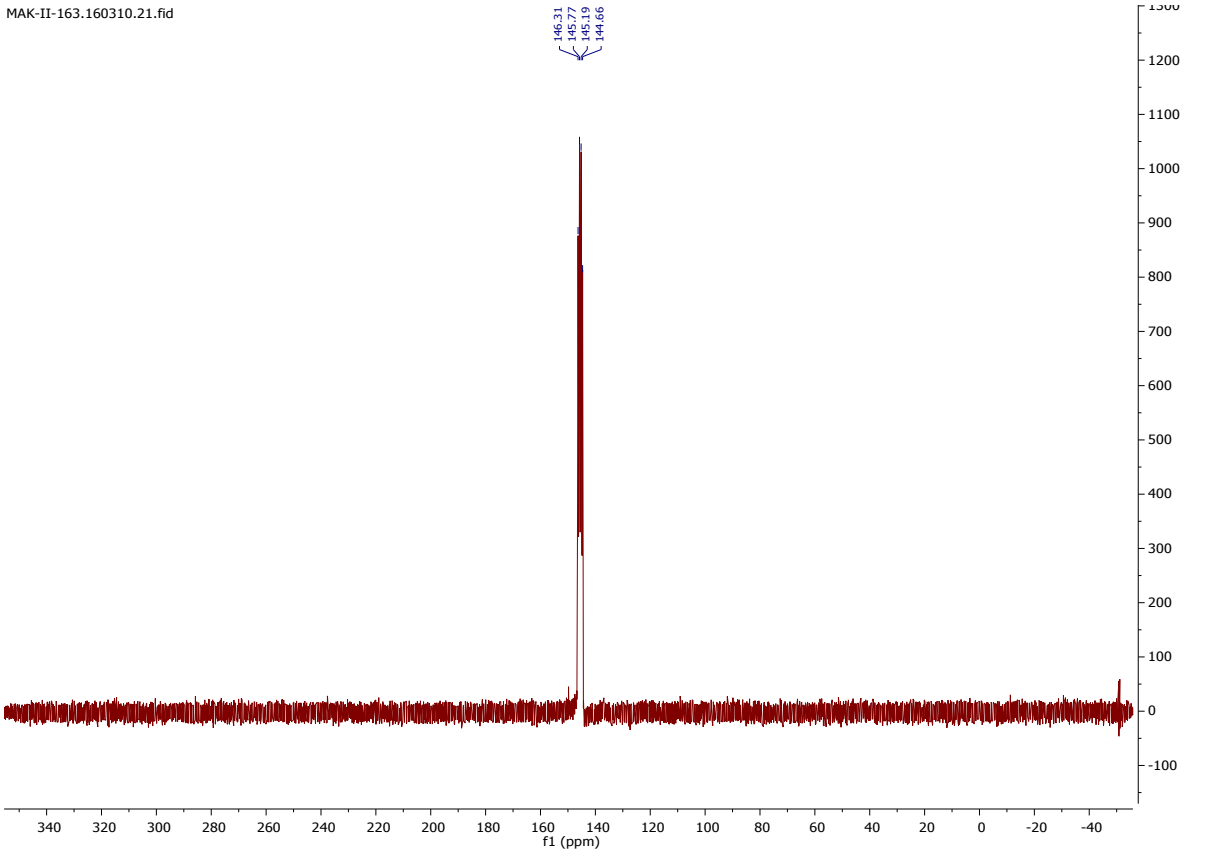
MAK-II-163.160310.21.fid
146.31
145.77
145.19
144.66
f1 (ppm)

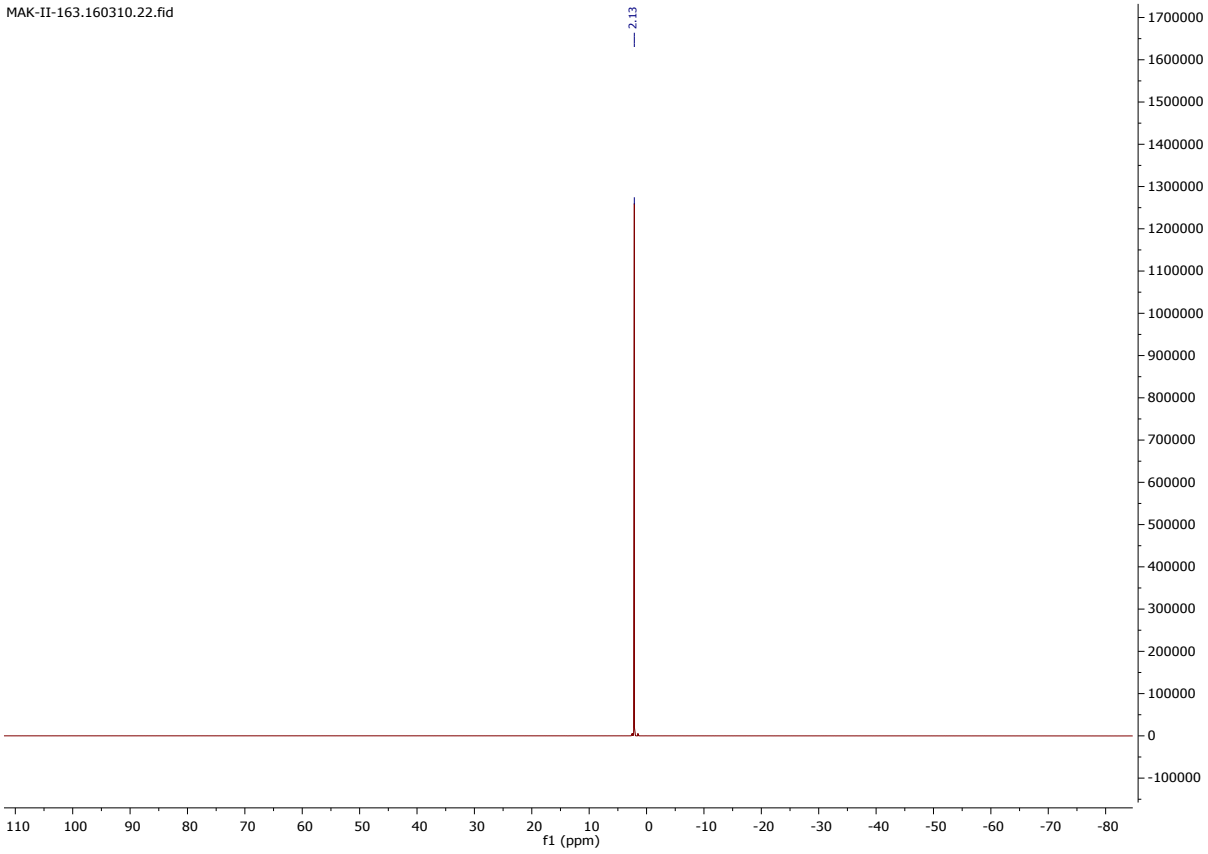
MAK-II-163.160310.22.fid
2.13
f1 (ppm)

Ethyl-N-phenyl-P-vinylphosphonamidate (**4a**)

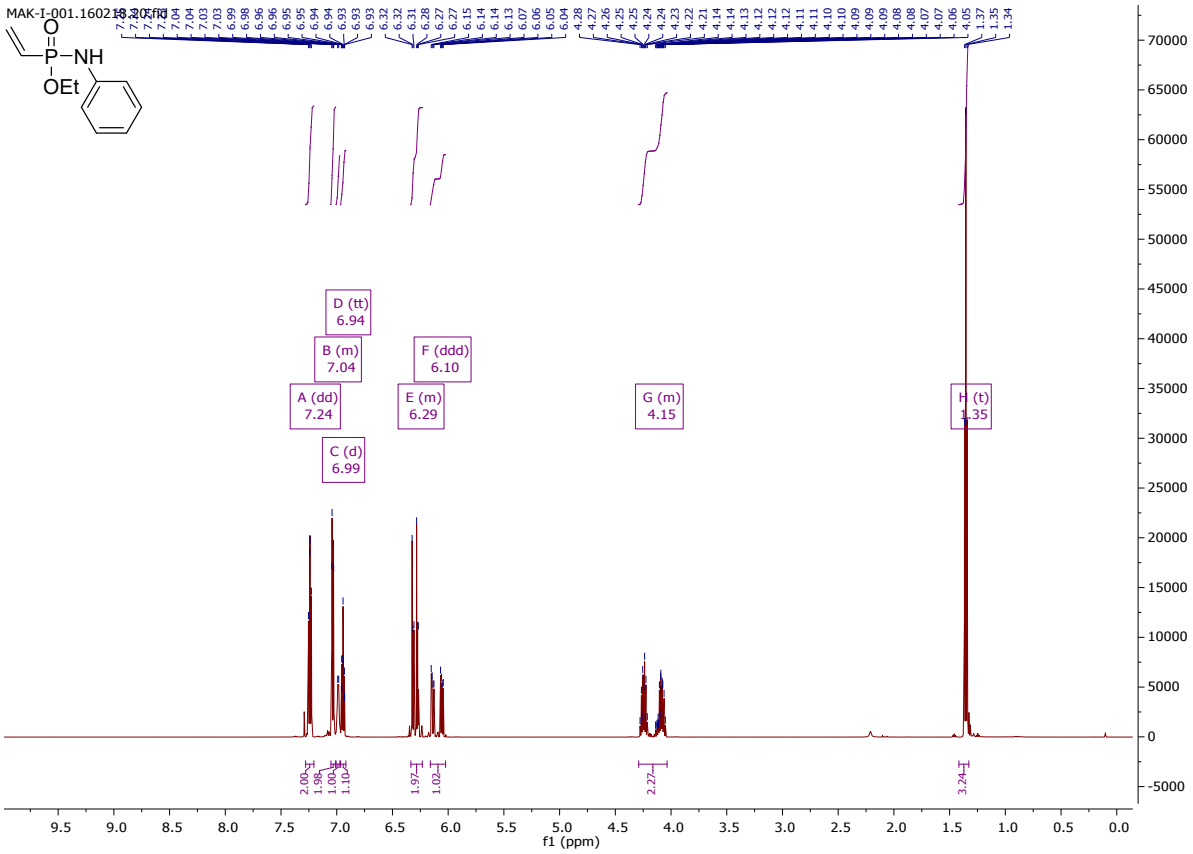

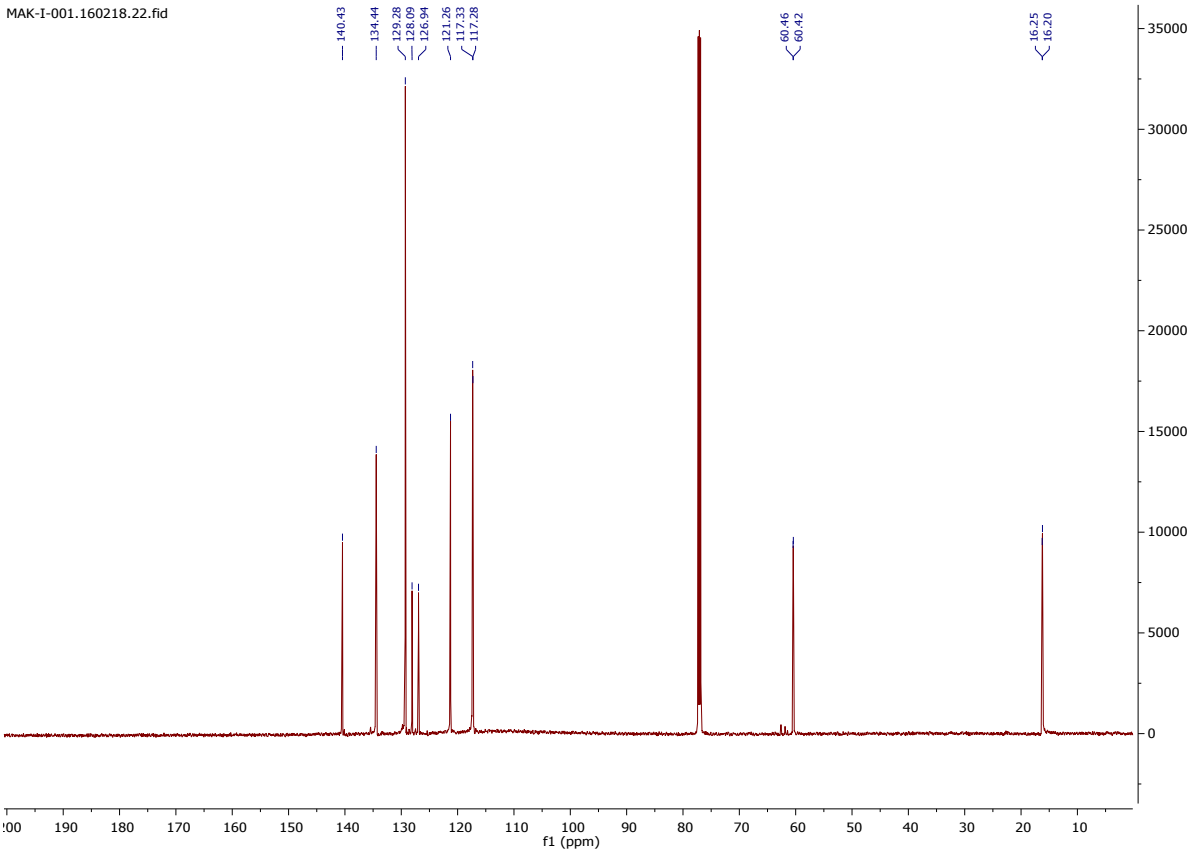

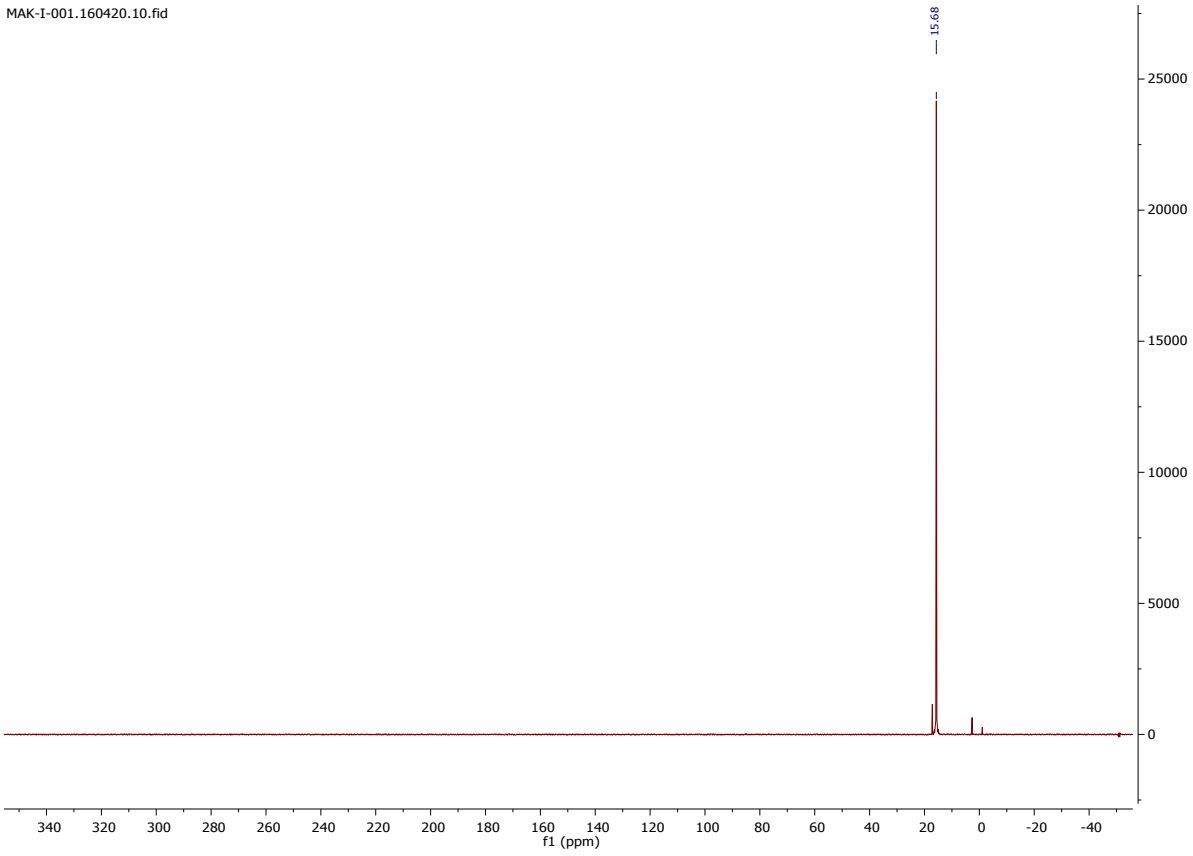

Ethyl-N-(3-phenyl-propyl)-P-vinyl-phosphonamidate (**5a**)

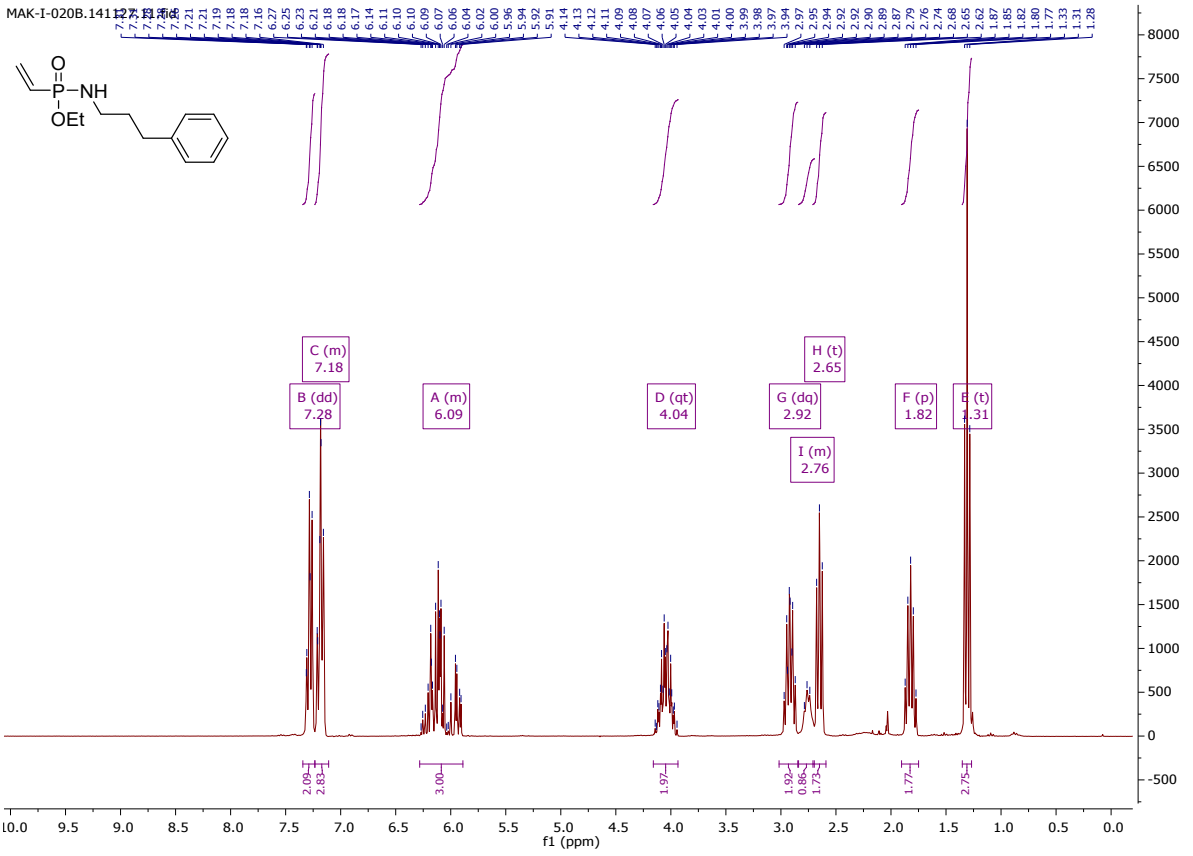

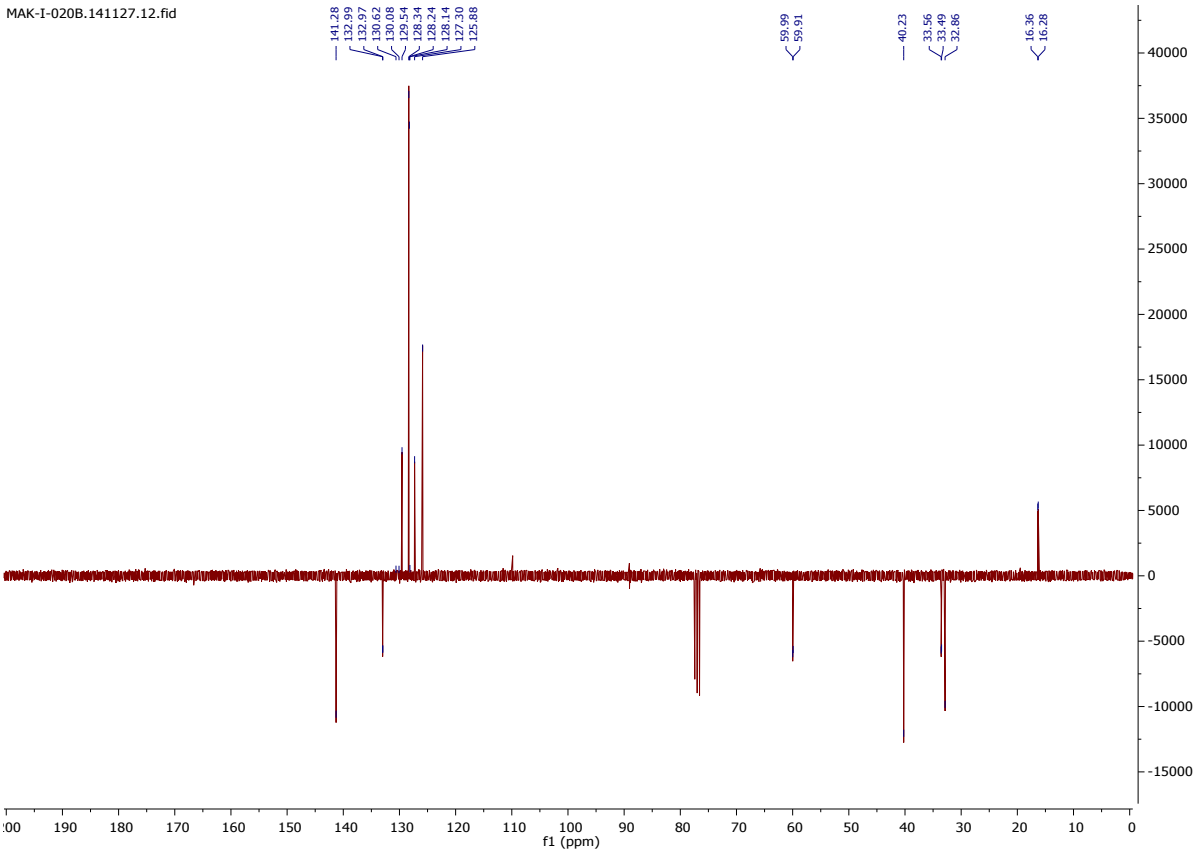
MAK-I-020B.141127.12.fid
141.28
132.99
132.97
130.62
130.08
129.54
128.34
128.24
128.14
127.30
125.88
59.99
59.91
40.23
33.56
33.49
32.86
16.36
16.28
f1 (ppm)

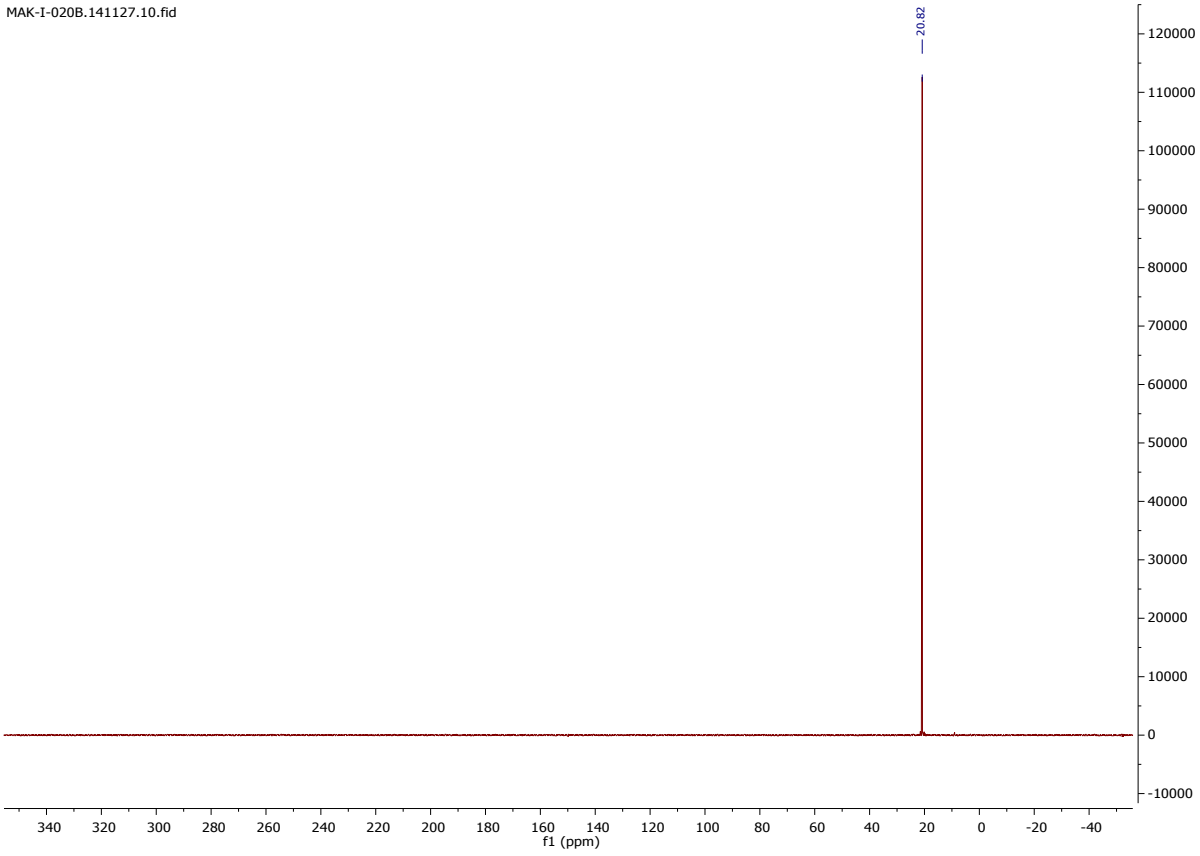
MAK-I-020B.141127.10.fid
20.82
f1 (ppm)

2-Nitrobenzyl-*N*-phenyl-*P*-vinylphosphonamidate (**4b**)

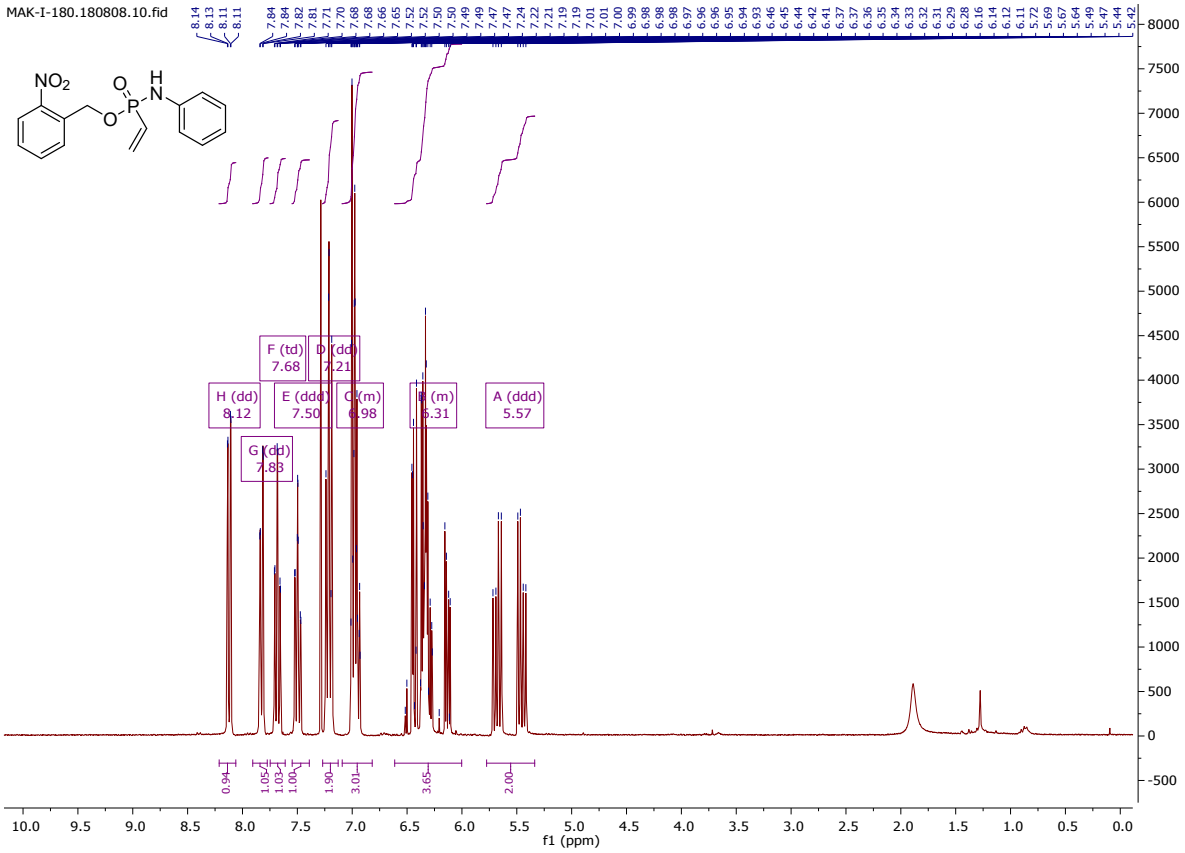

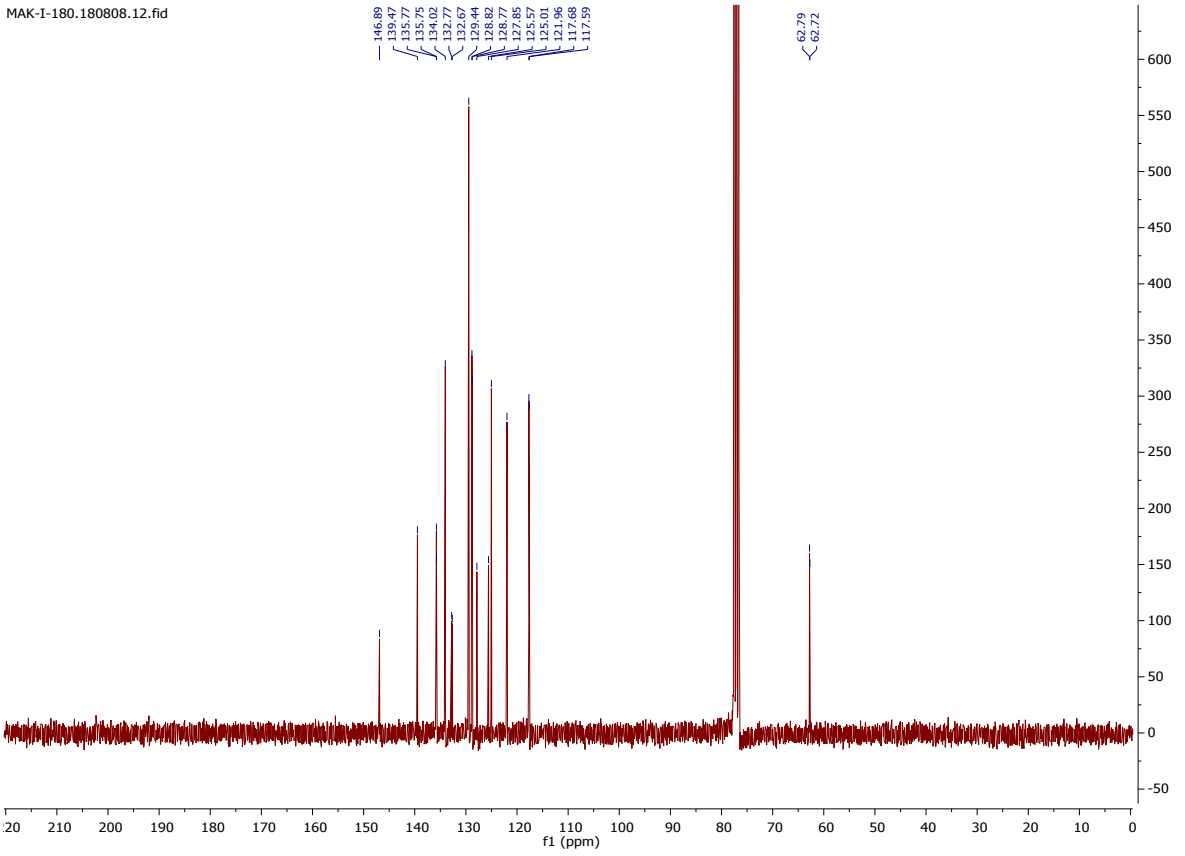

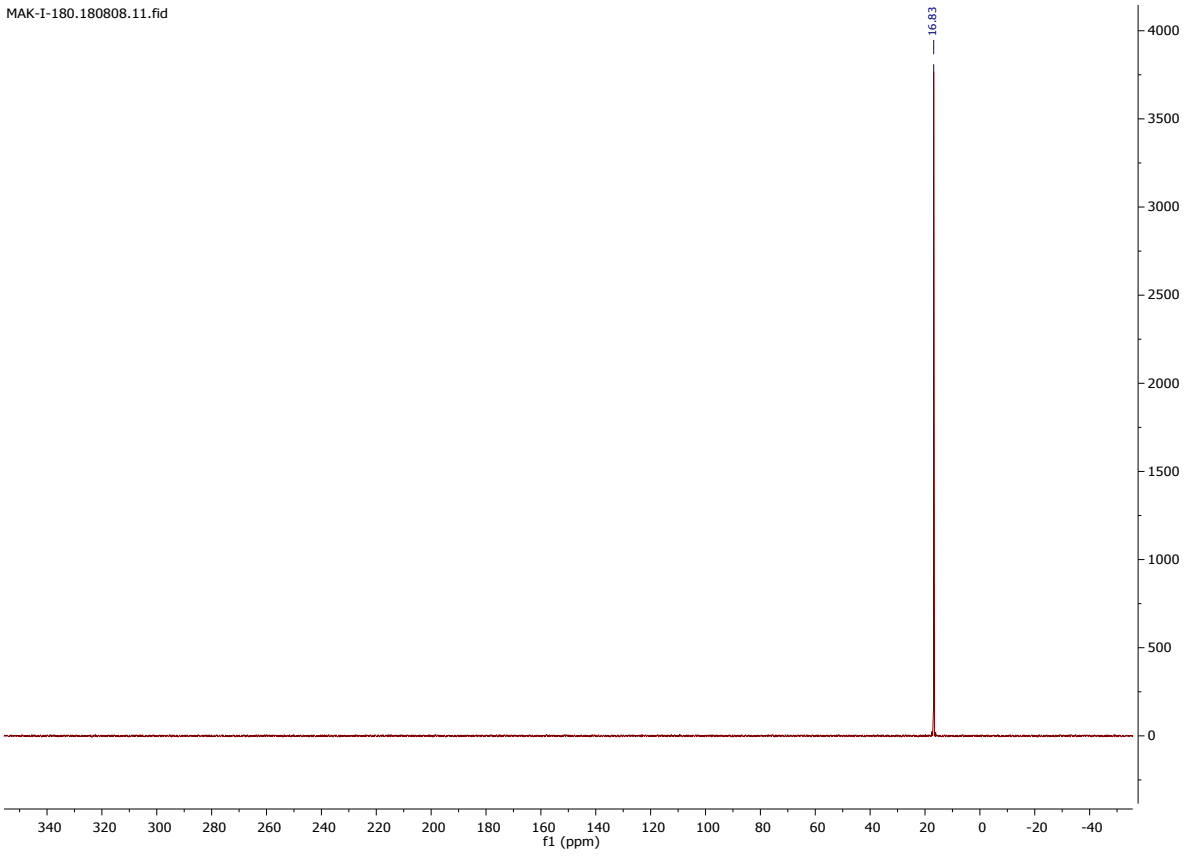

2-Nitrobenzyl-*N*-(3-phenyl-propyl)-*P*-vinylphosphonamidate (**5b**)

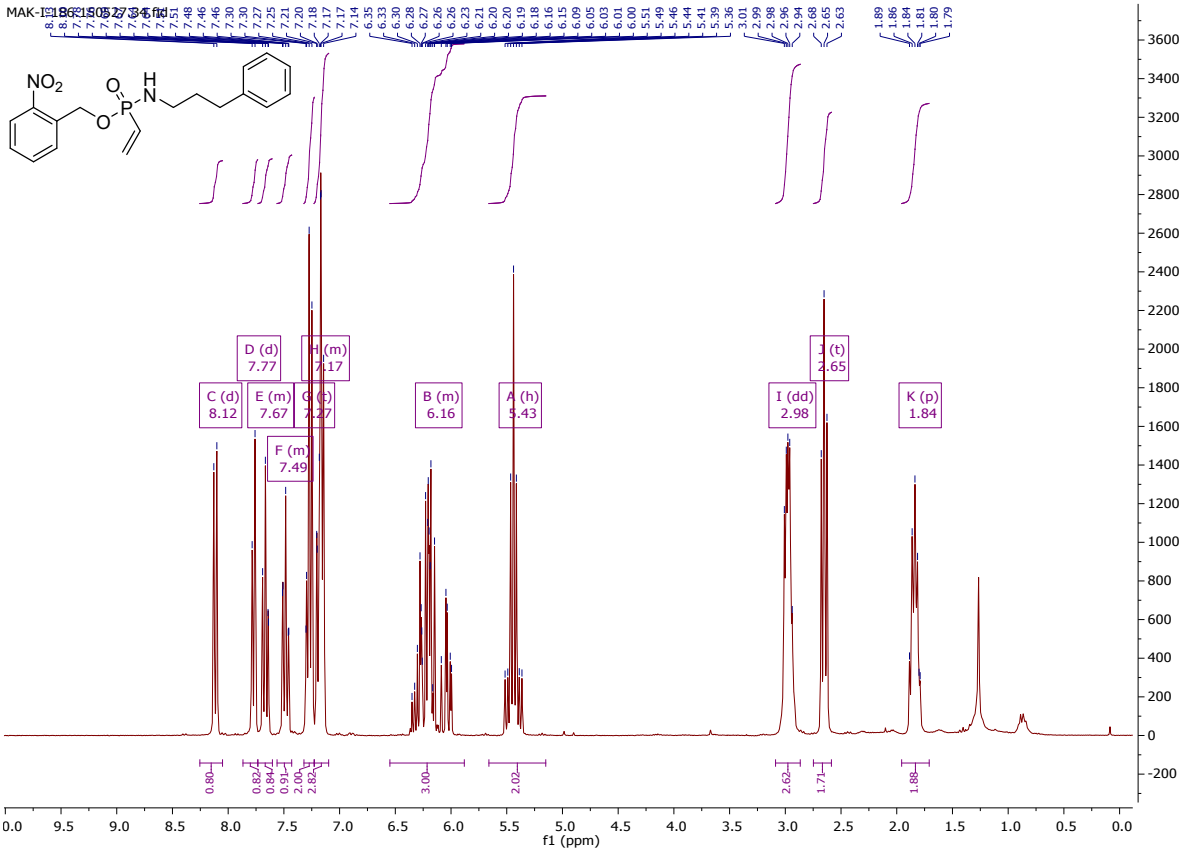

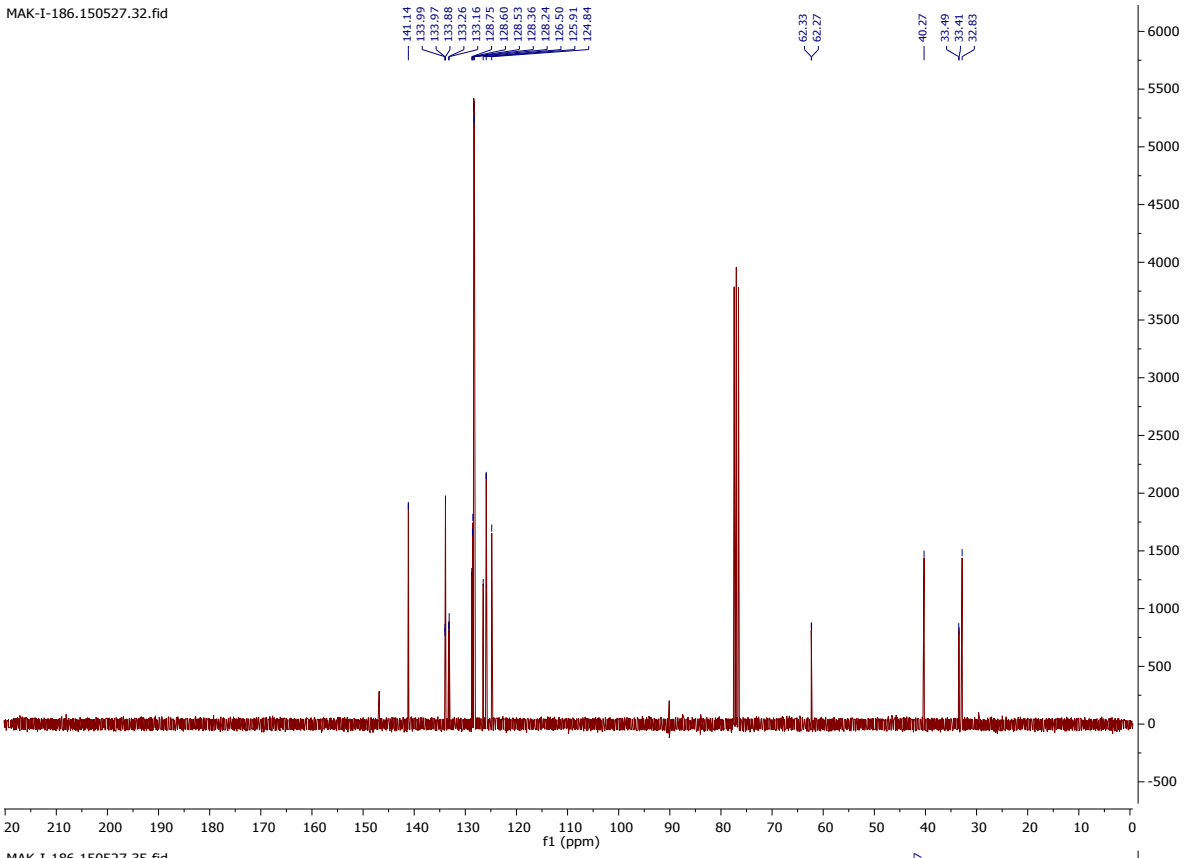
MAK-I-186.150527.32.fid
141.14
133.99
133.97
133.88
133.26
133.16
128.75
128.60
128.53
128.36
128.24
126.50
125.91
124.84
62.33
62.27
40.27
33.49
33.41
32.83
f1 (ppm)

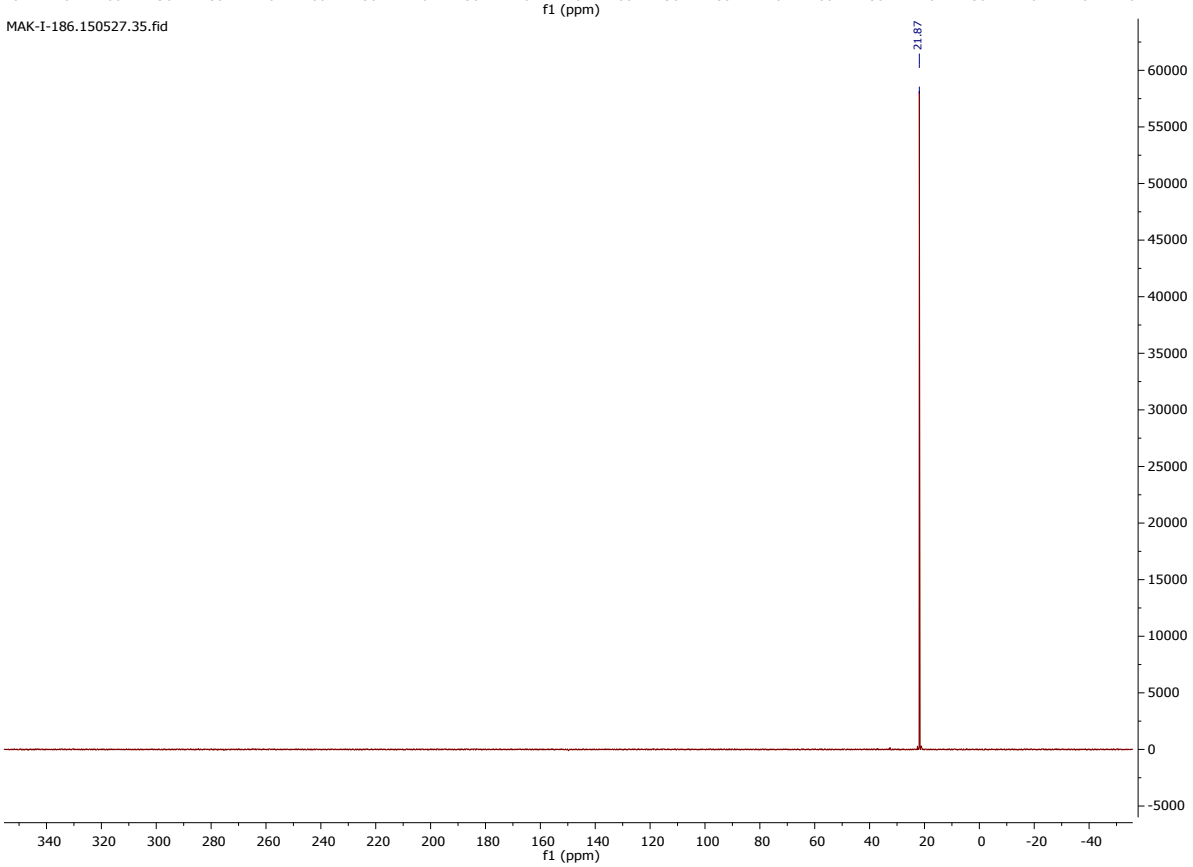
MAK-I-186.150527.35.fid
21.87
f1 (ppm)

phenyl-*N*-phenyl-*P*-vinylphosphonamidate (**4c**)

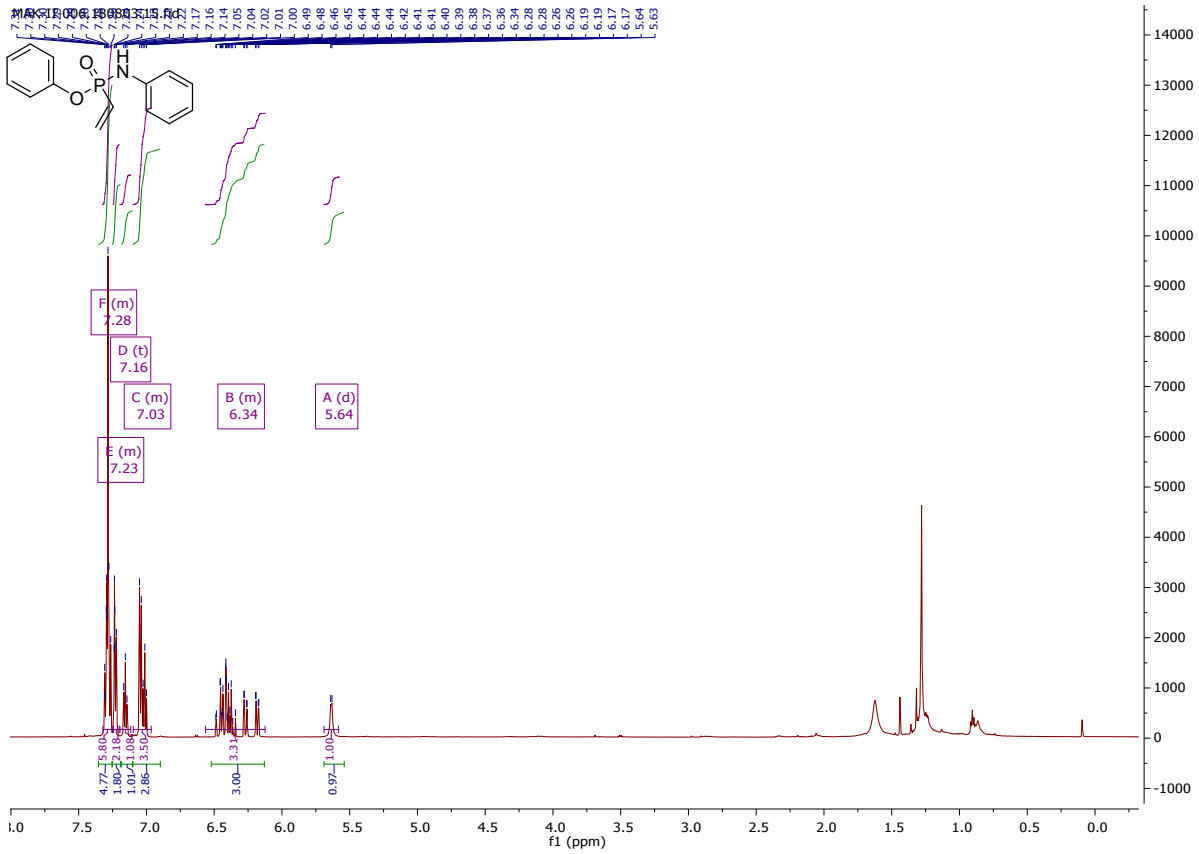

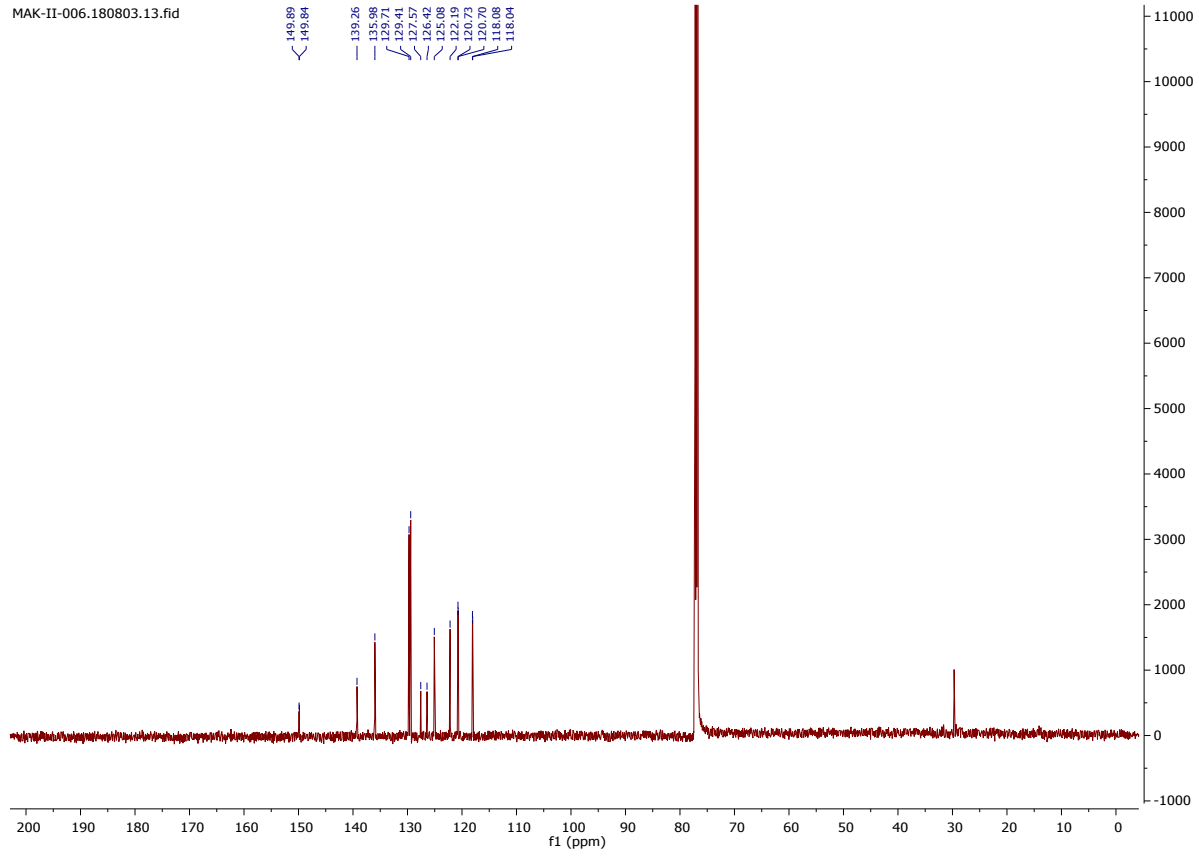

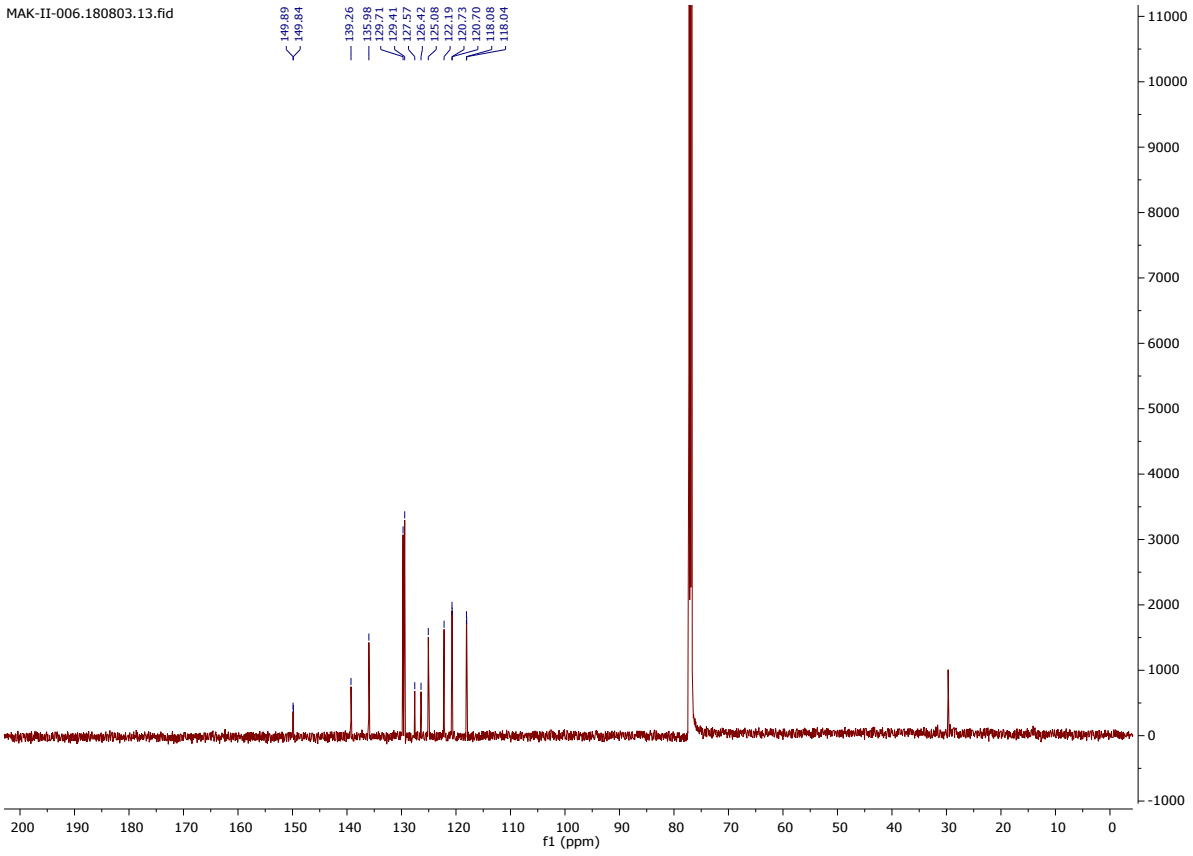

Phenyl-*N*-(3-phenyl-propyl)-*P*-vinylphosphonamidate (**5c**)

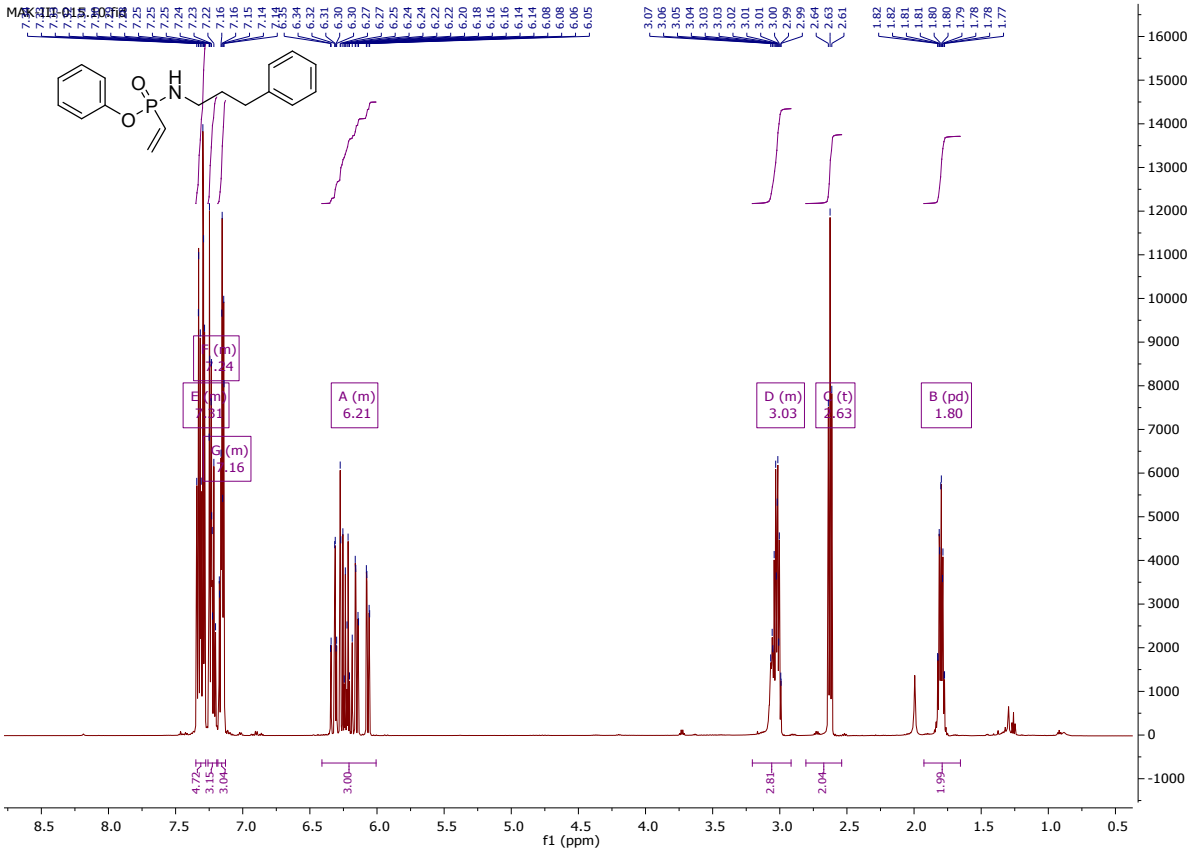

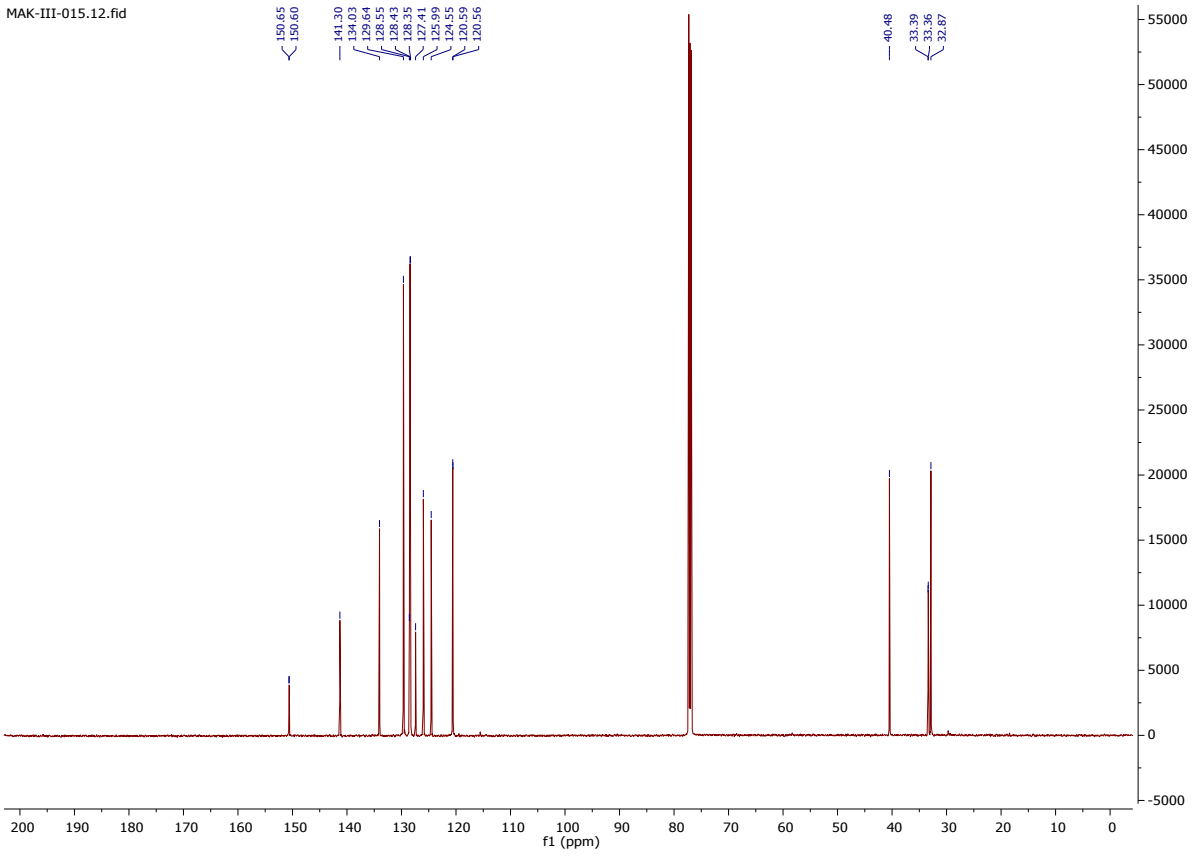
MAK-III-015.12.fid
150.65
150.60
141.30
134.03
129.64
128.55
128.43
128.35
127.41
125.99
124.55
120.59
120.56
40.48
33.39
33.36
32.87
f1 (ppm)

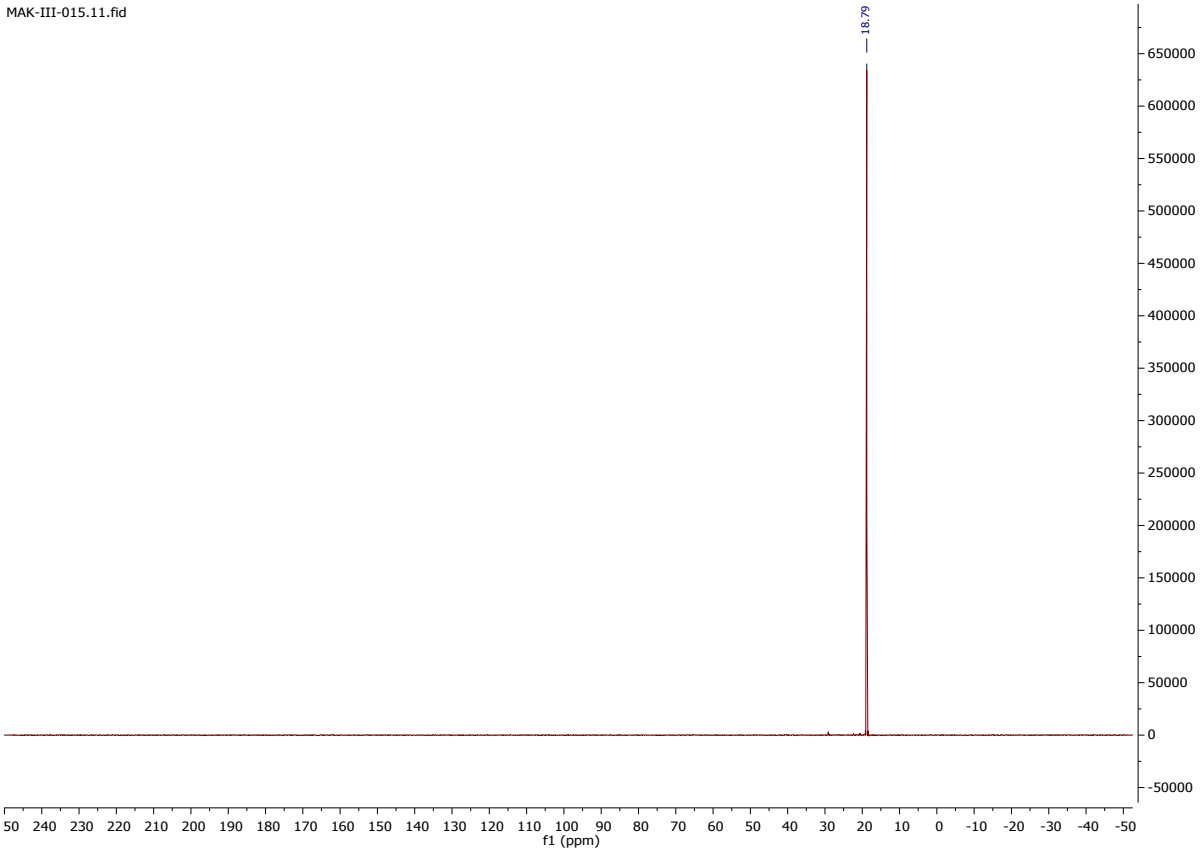
MAK-III-015.11.fid
18.79
f1 (ppm)

2,2,2-trifluoroethyl-*N*-phenyl-*P*-vinylphosphonamidate (**4d**)

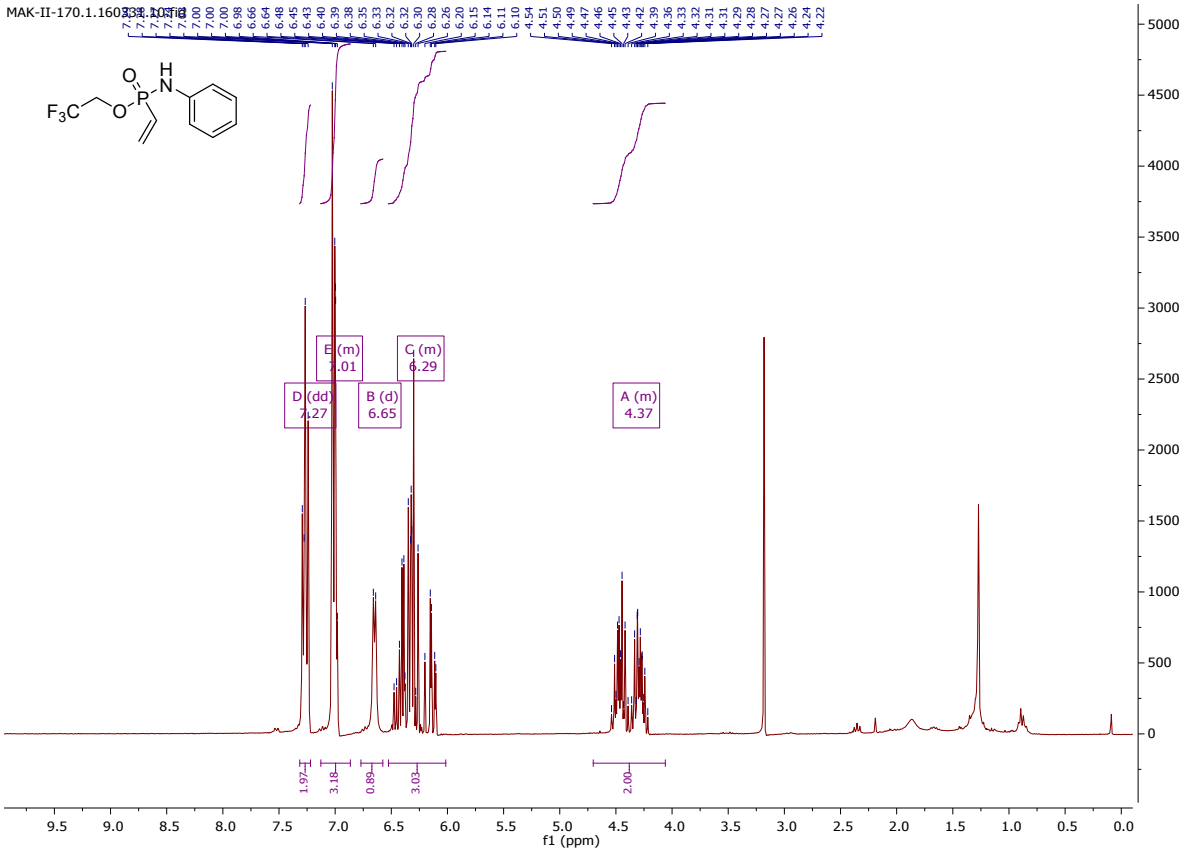

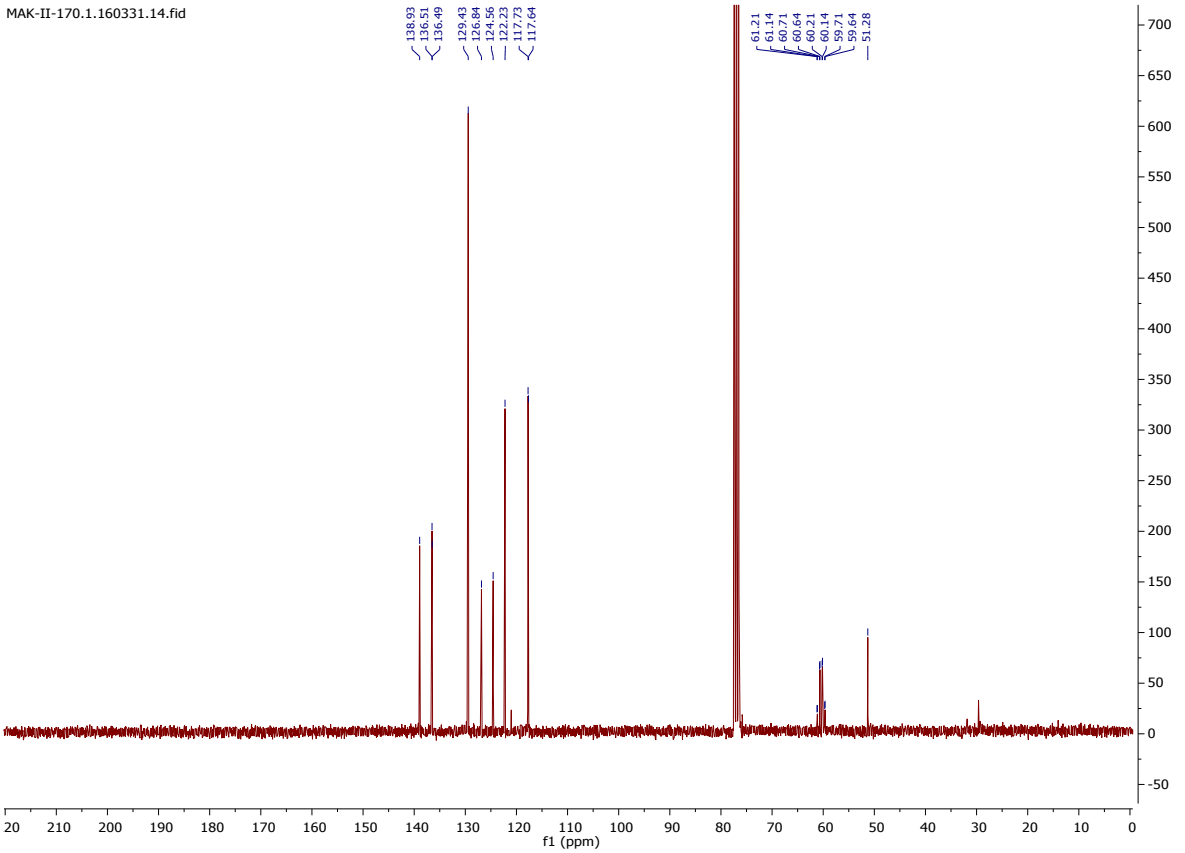

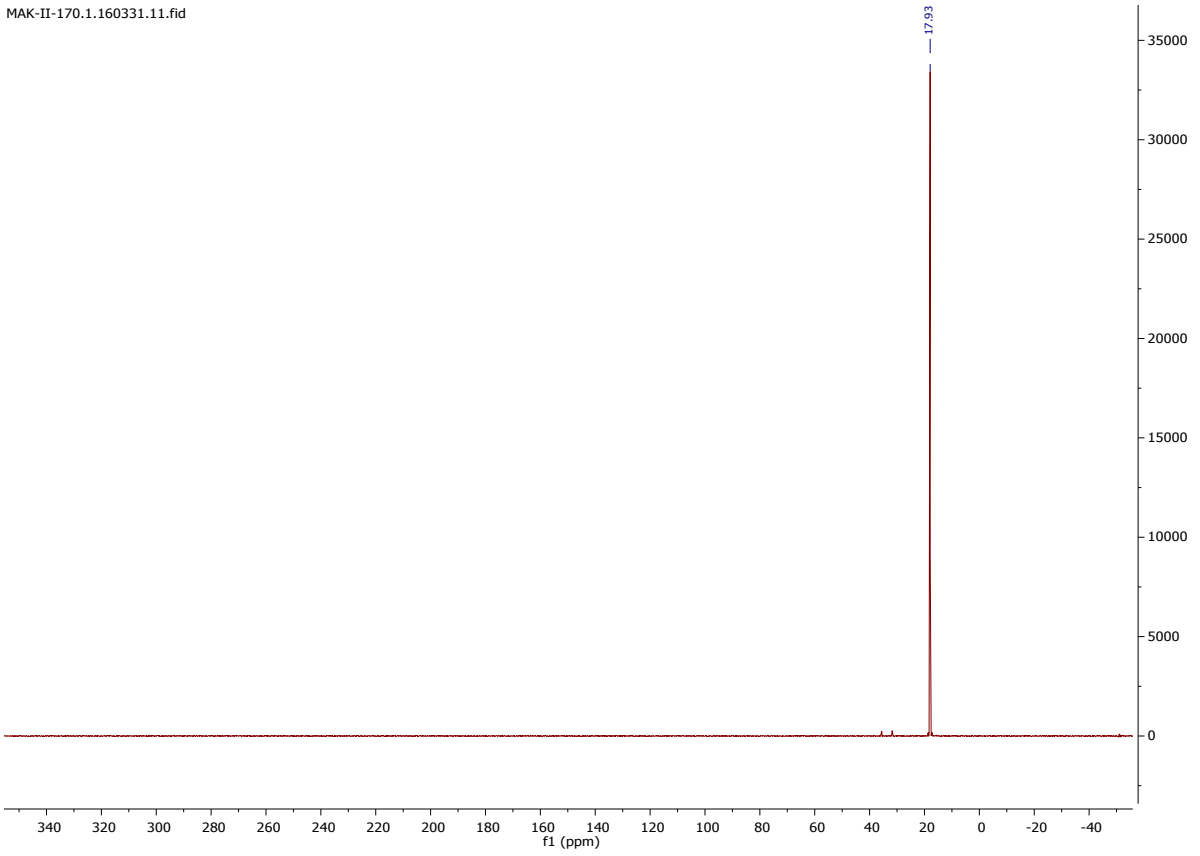
MAK-II-170.1.160331.11.fid
17.93
35000
30000
25000
20000
15000
10000
5000
0
340 320 300 280 260 240 220 200 180 160 140 120 100 80 60 40 20 0 -20 -40
f1 (ppm)

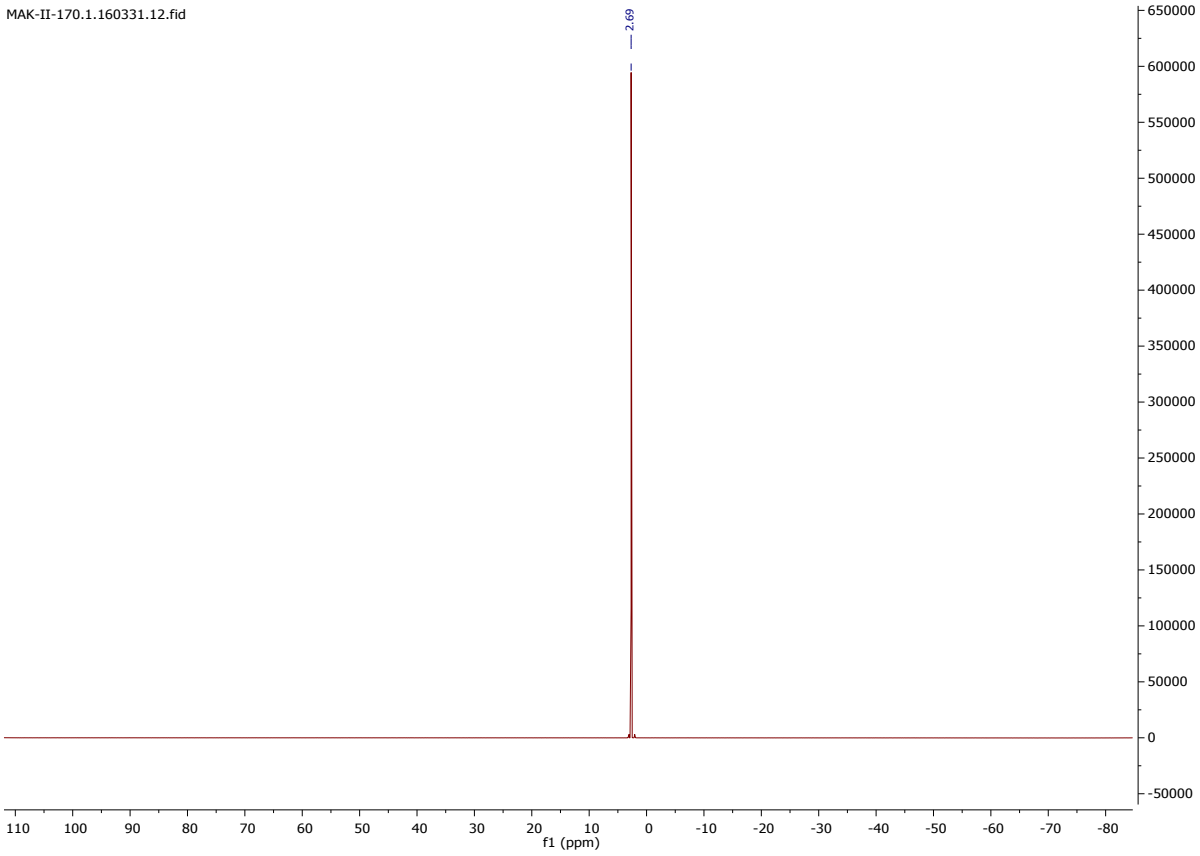
MAK-II-170.1.160331.12.fid
2.69
650000
600000
550000
500000
450000
400000
350000
300000
250000
200000
150000
100000
50000
0
-50000
110 100 90 80 70 60 50 40 30 20 10 0 -10 -20 -30 -40 -50 -60 -70 -80
f1 (ppm)

2,2,2-trifluoroethyl-*N*-(3-phenyl-propyl)-phenyl-*P*-vinyl-phosphonamidate (**5d**)

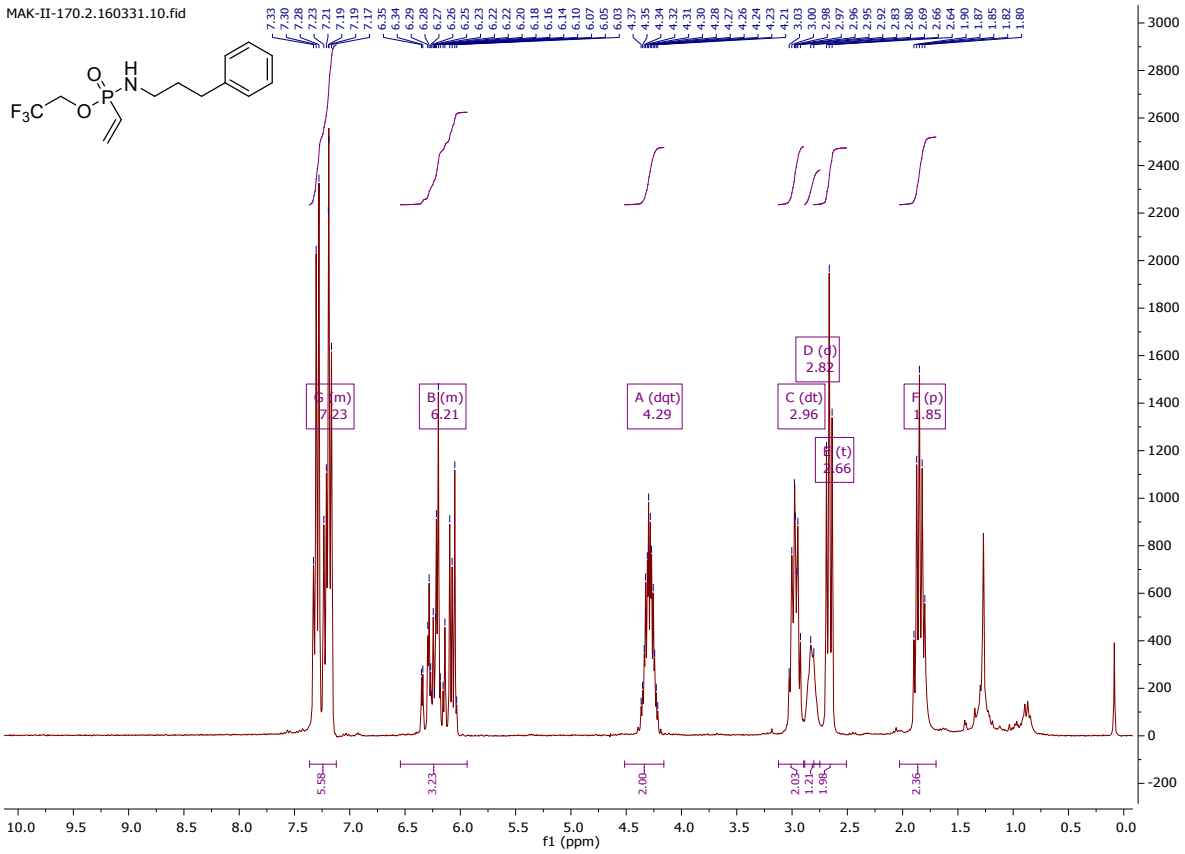

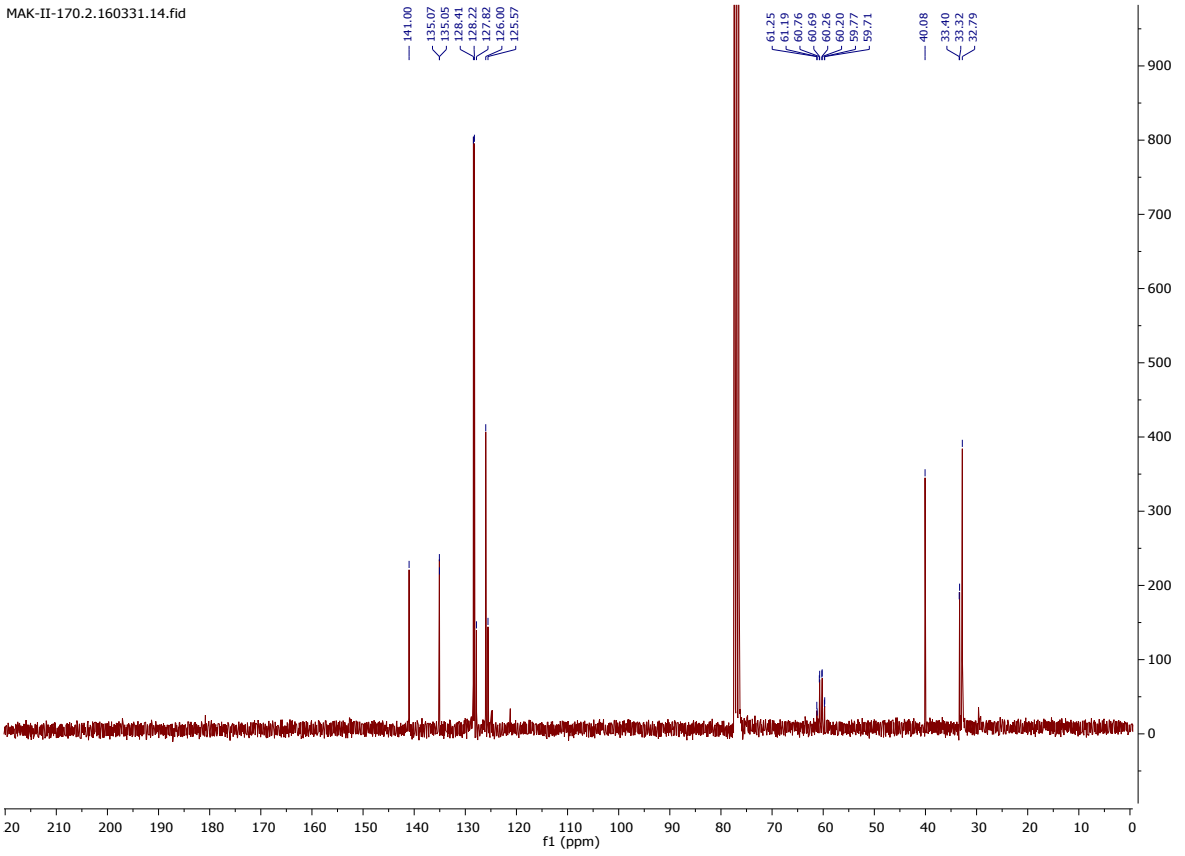

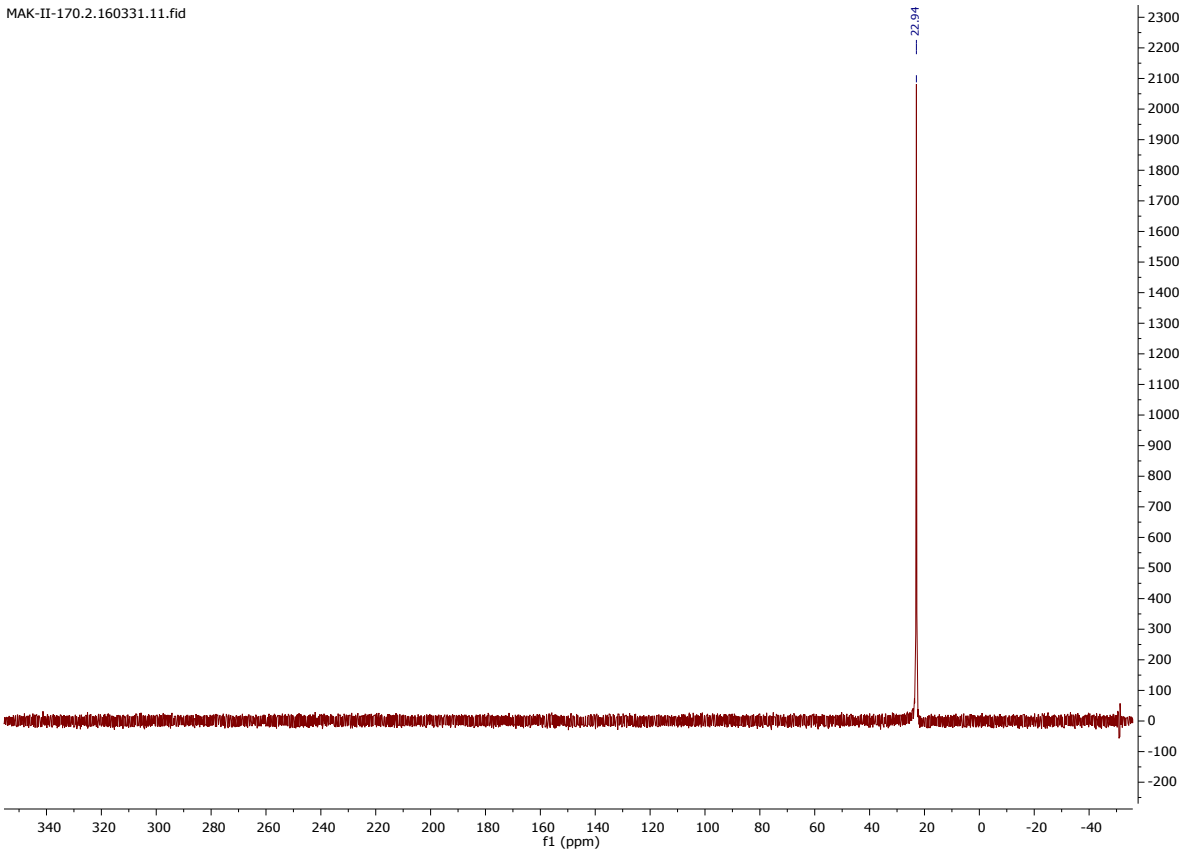
MAK-II-170.2.160331.11.fid
22.94
f1 (ppm)

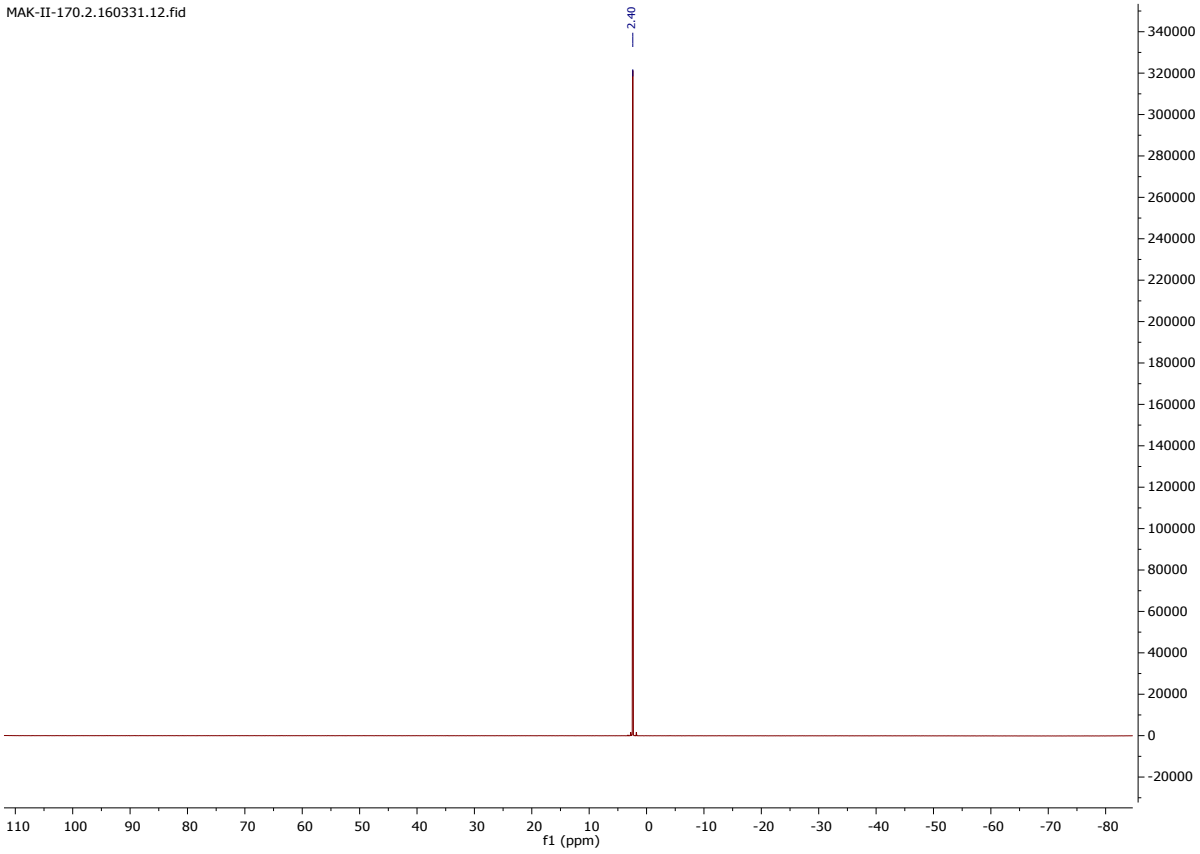
MAK-II-170.2.160331.12.fid
2.40
f1 (ppm)

Ethyl-*N*-phenyl-*P*-(2-(glutathionyl-thio)ethyl)-phosphonamidate

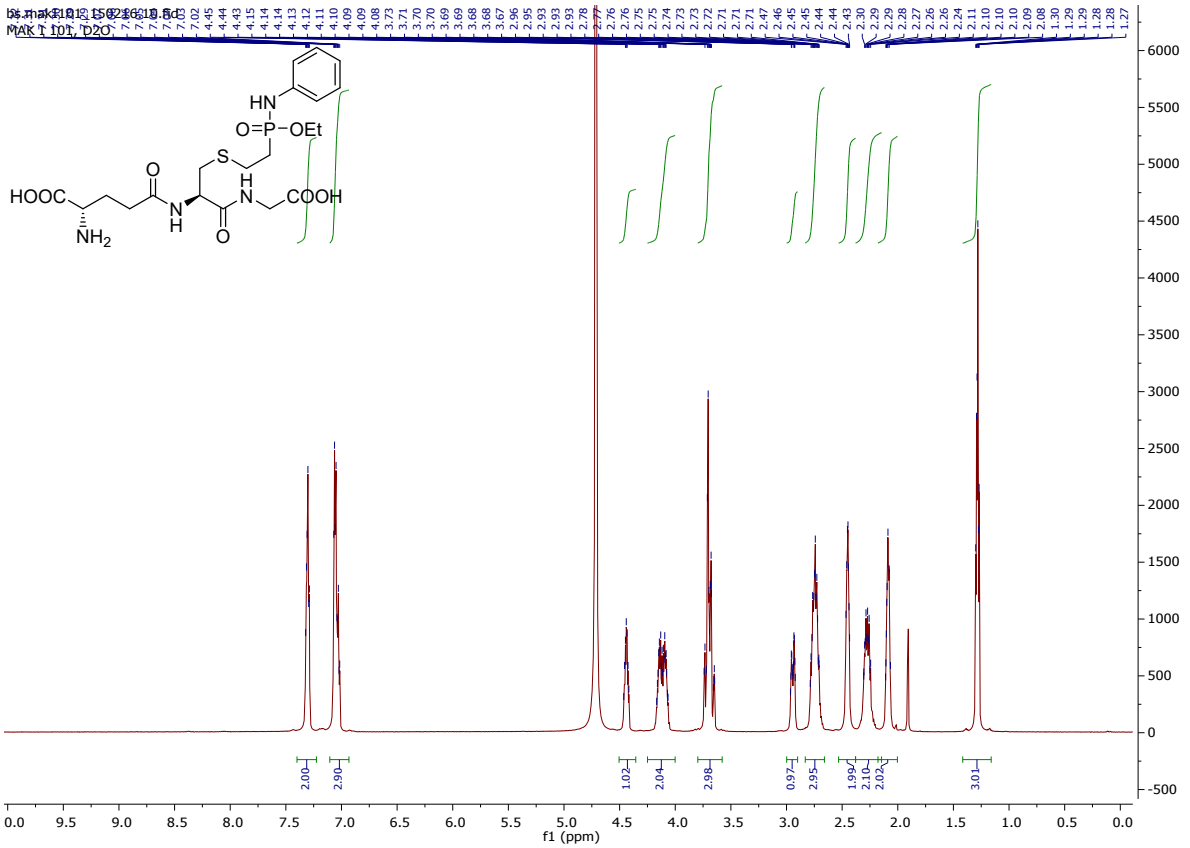

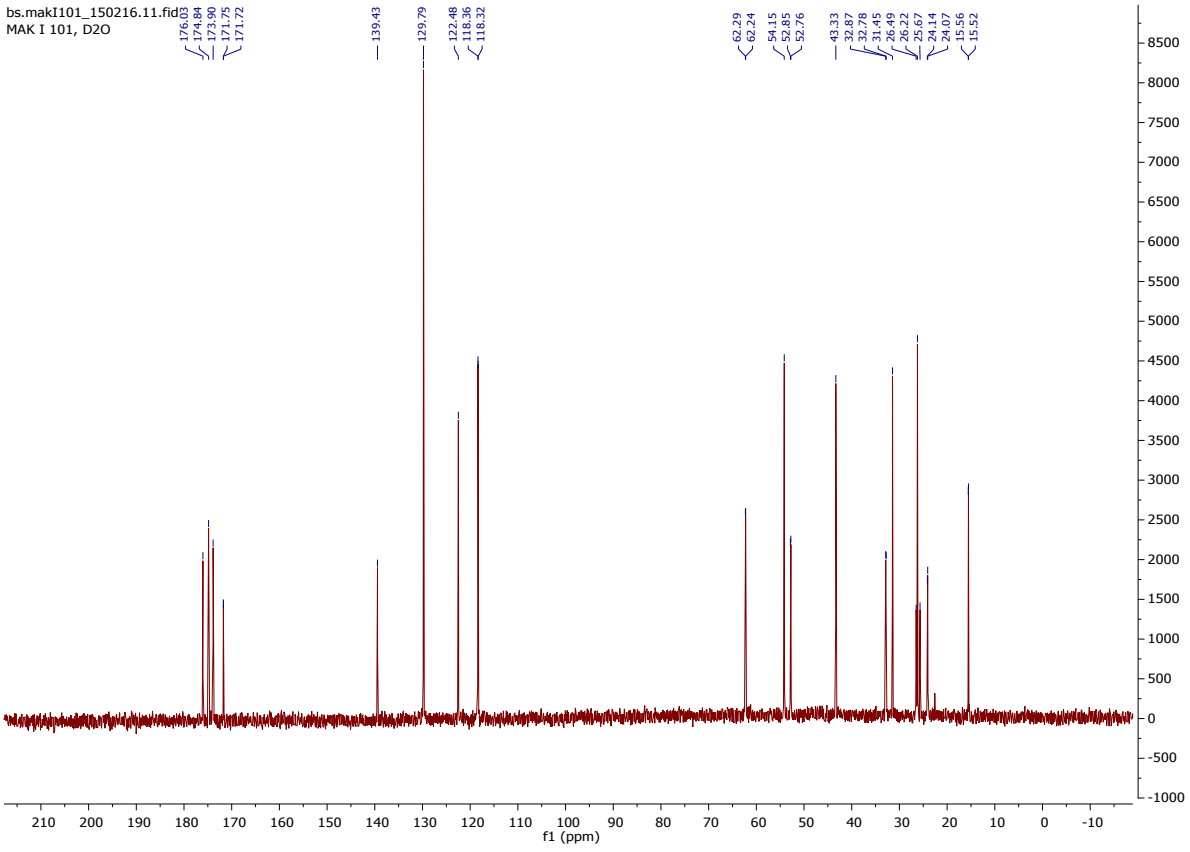

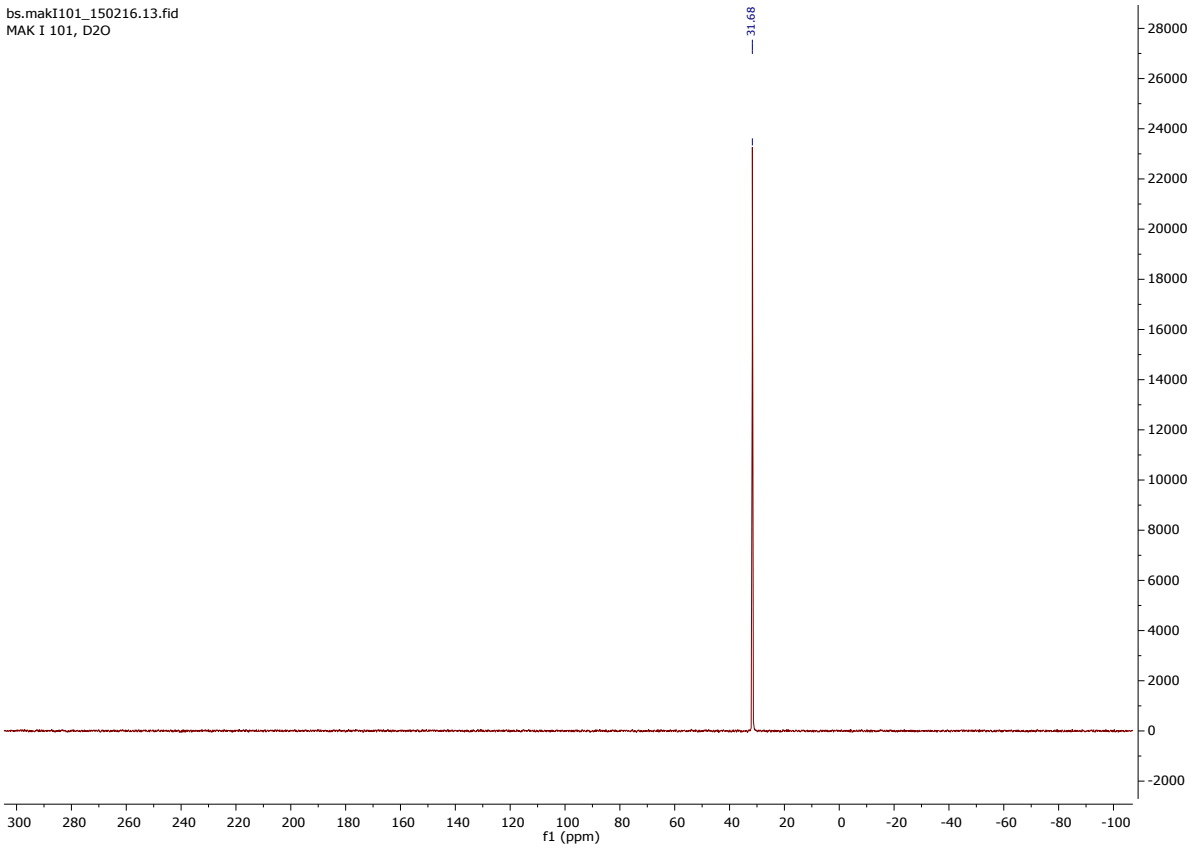

2,2,2-trifluoroethyl-*N*-phenyl-*P*-(2-(glutathionyl-thio)ethyl)-phosphonamidate

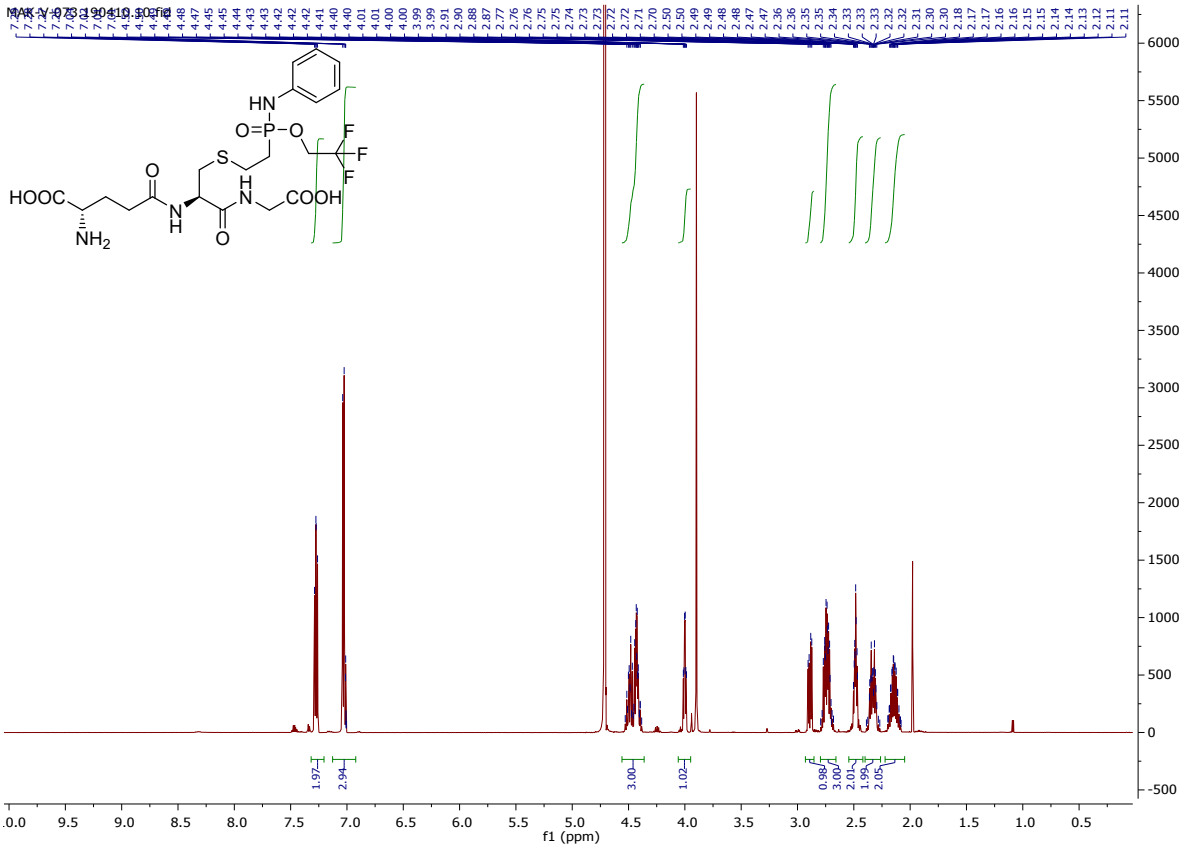

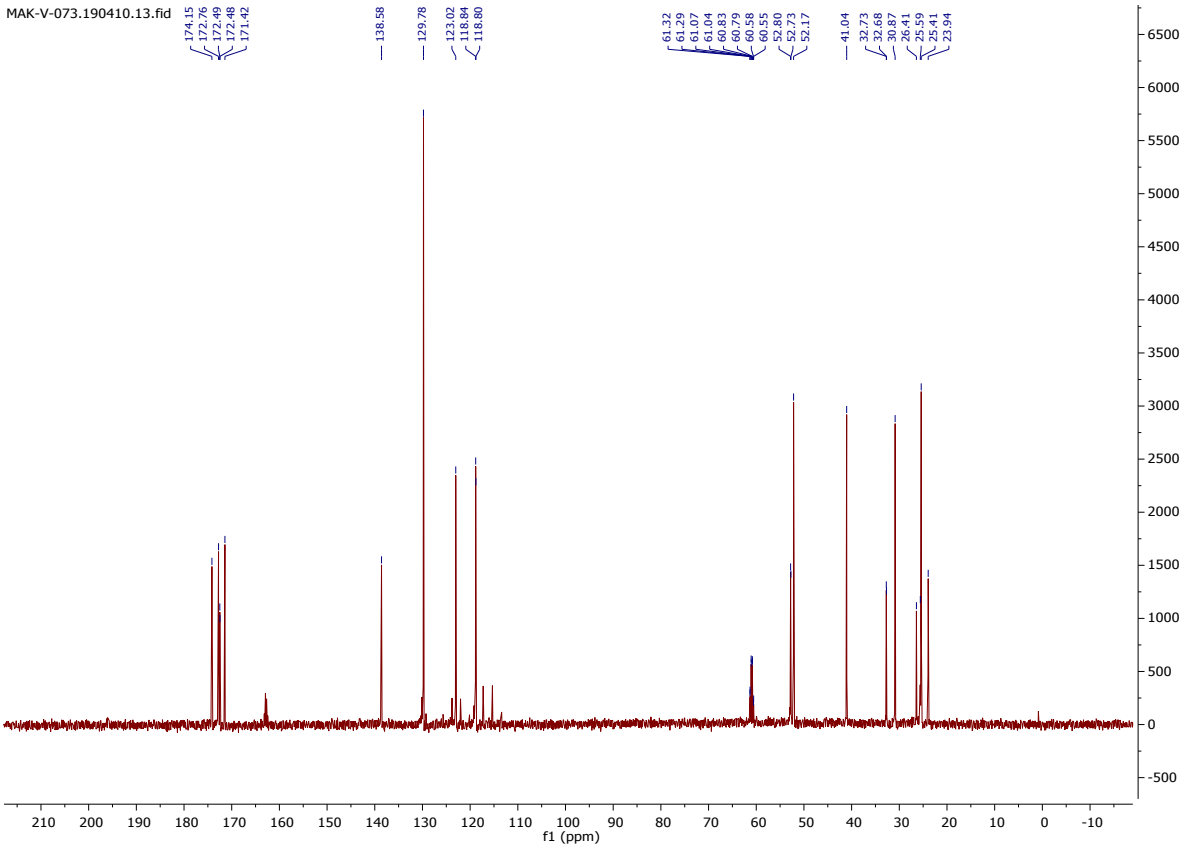
MAK-V-073.190410.13.fid
174.15
172.76
172.49
172.48
171.42
138.58
129.78
123.02
118.84
118.80
61.32
61.29
61.07
61.04
60.83
60.79
60.58
60.55
52.80
52.73
52.17
41.04
32.73
32.68
30.87
26.41
25.59
25.41
23.94
f1 (ppm)

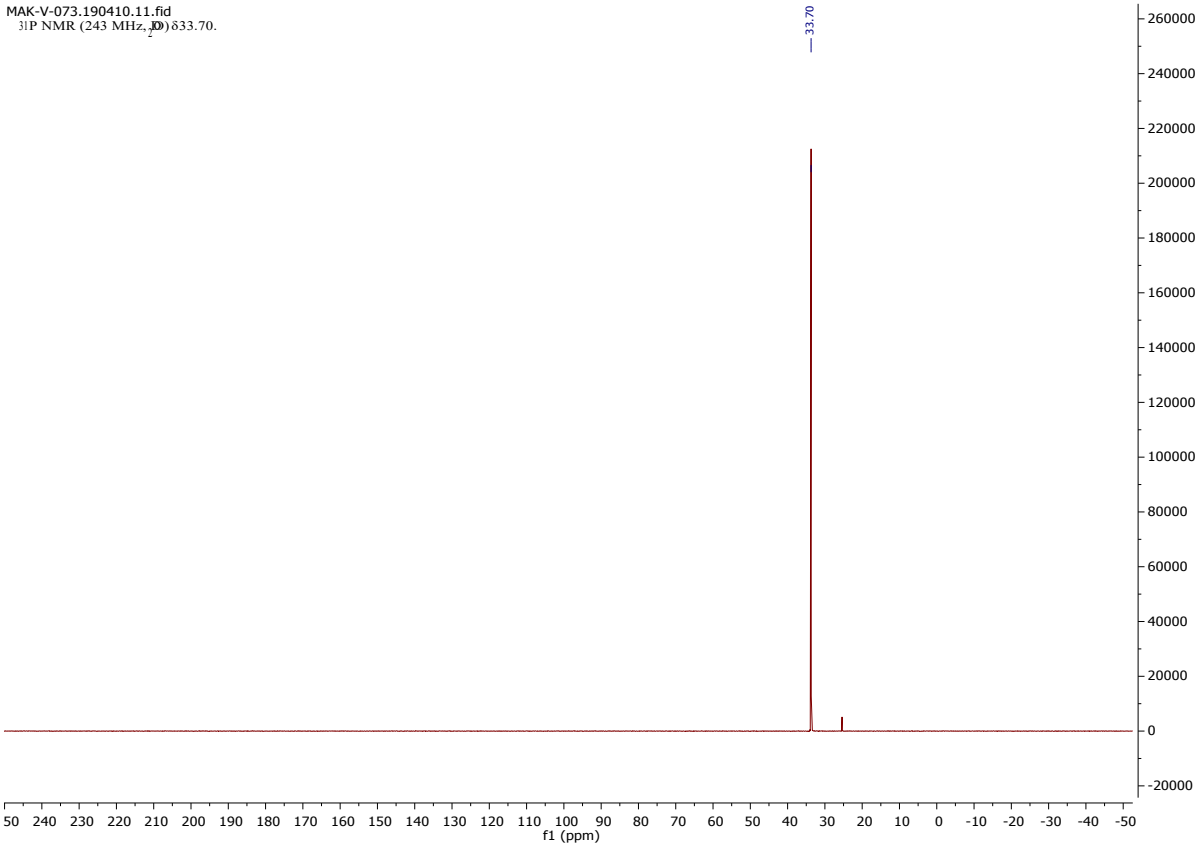
MAK-V-073.190410.11.fid
31P NMR (243 MHz, D2O) δ33.70.
33.70
f1 (ppm)

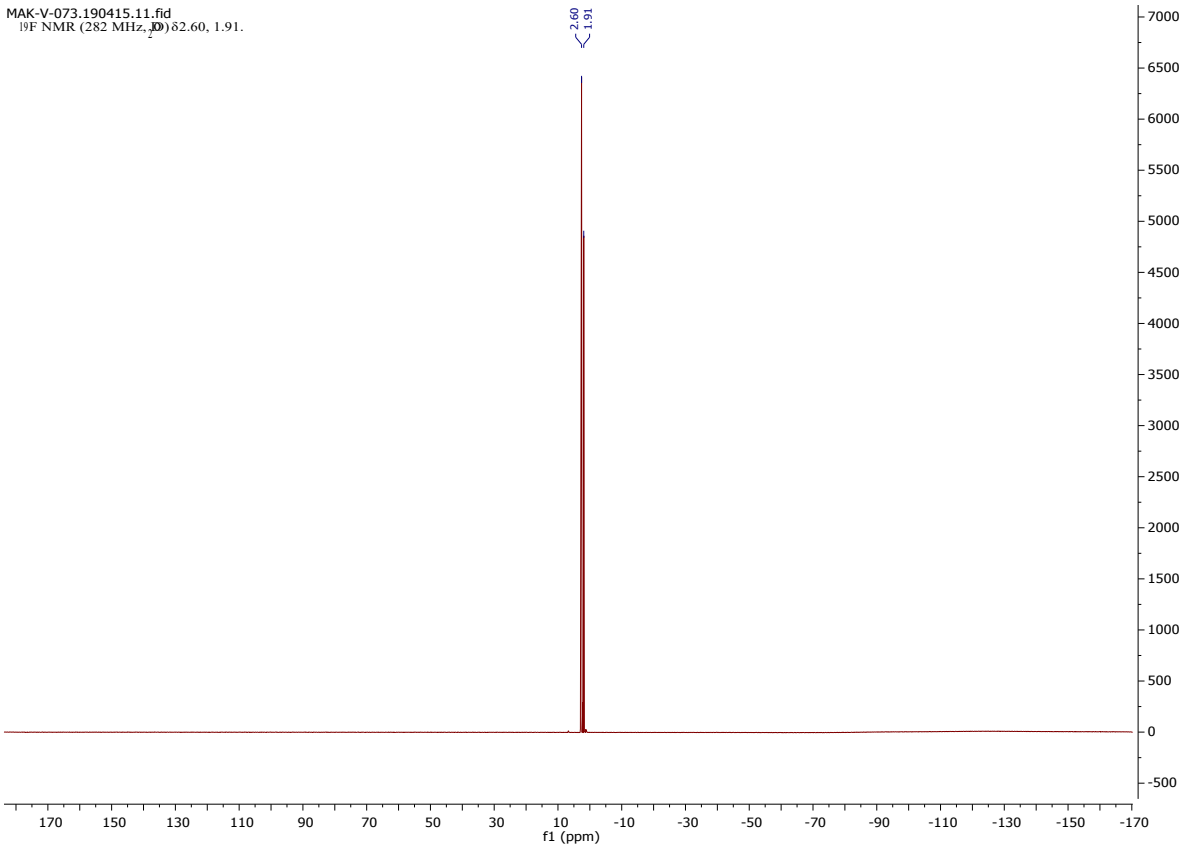

Trifluorethyl-N-(4-(2,5-dioxo-1-pyrrolidinyl)oxy-carbonyl-phenyl)-P-vinylphosphonamidate

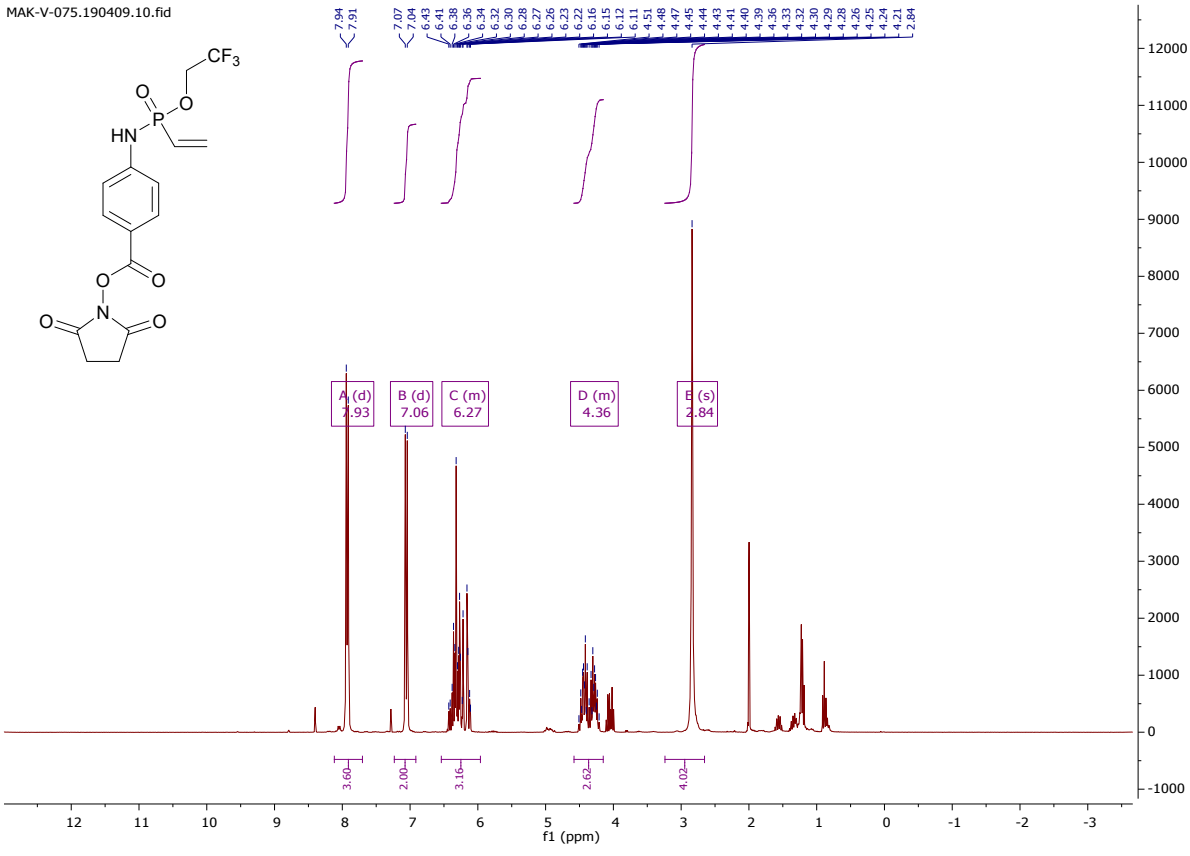

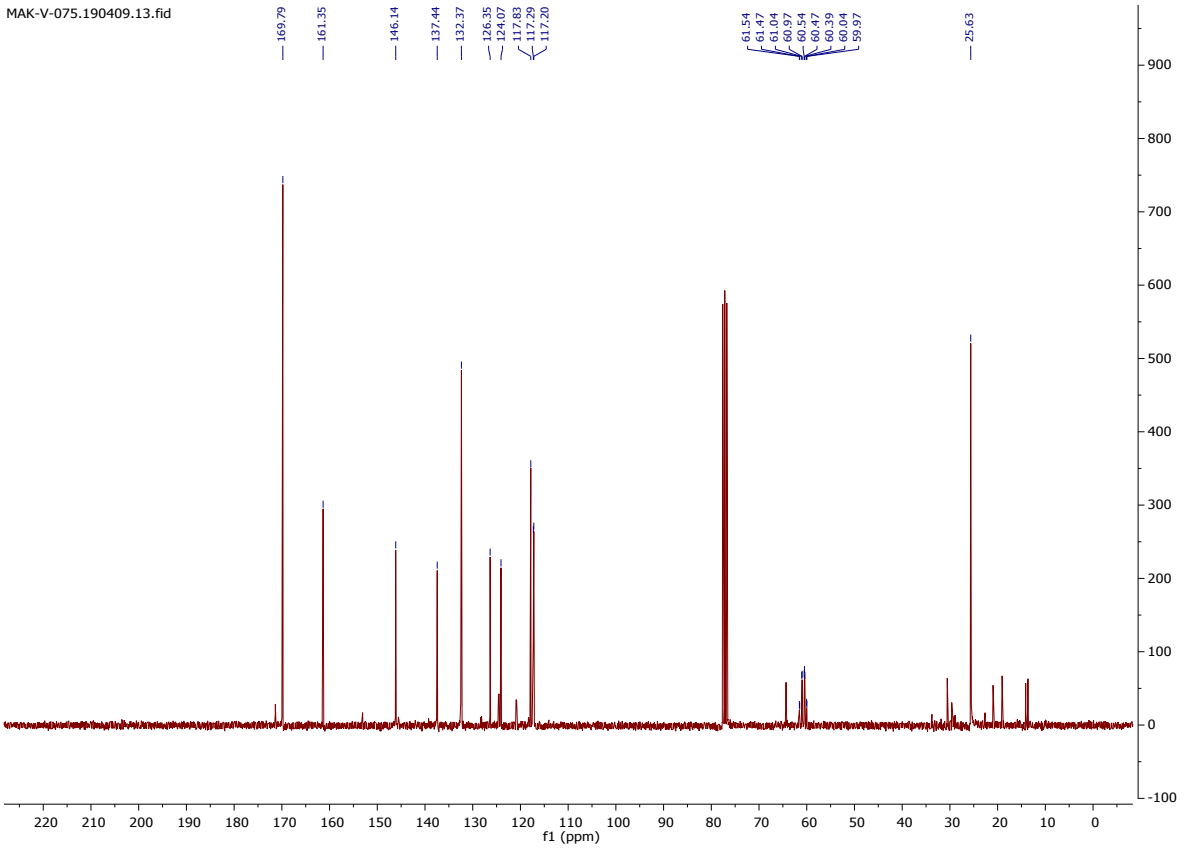
MAK-V-075.190409.13.fid
169.79
161.35
146.14
137.44
132.37
126.35
124.07
117.83
117.29
117.20
61.54
61.47
61.04
60.97
60.54
60.47
60.39
60.04
59.97
25.63
f1 (ppm)

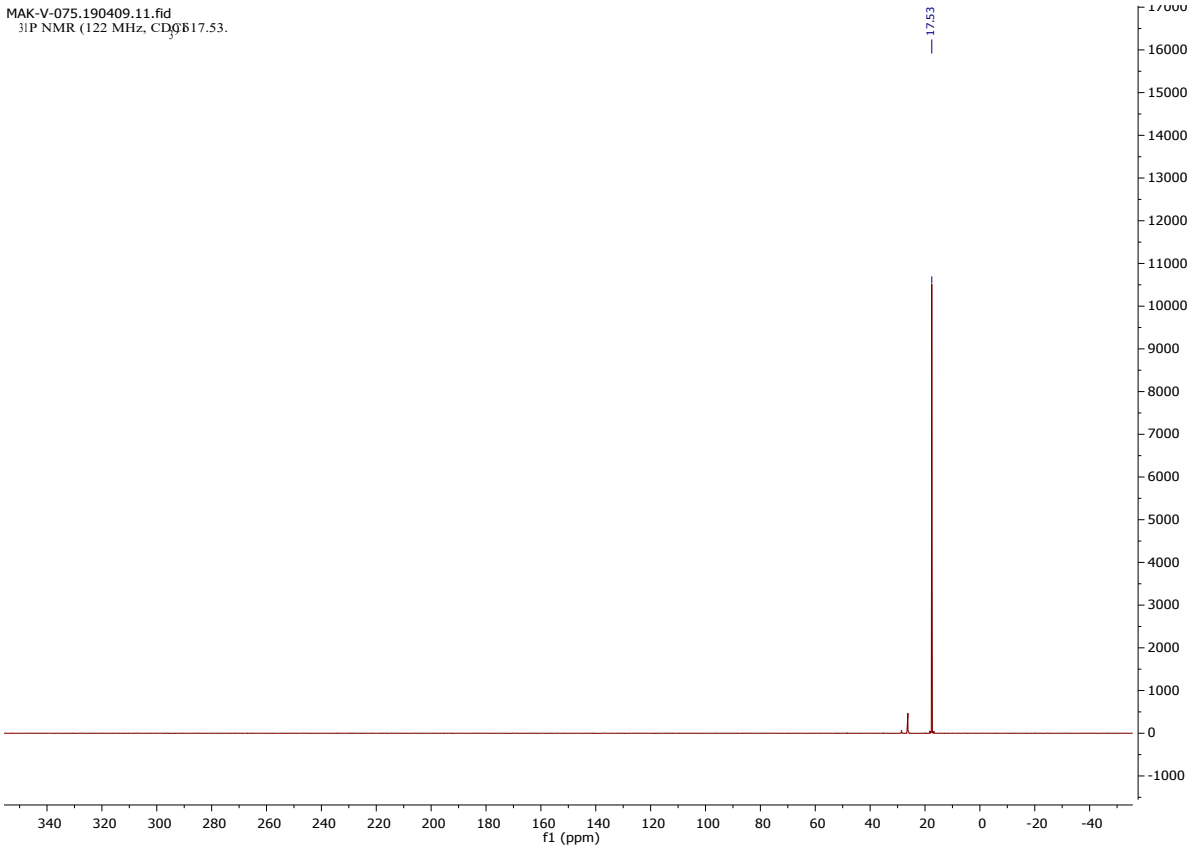
MAK-V-075.190409.11.fid
31P NMR (122 MHz, CDCl3) δ 17.53.
17.53
f1 (ppm)

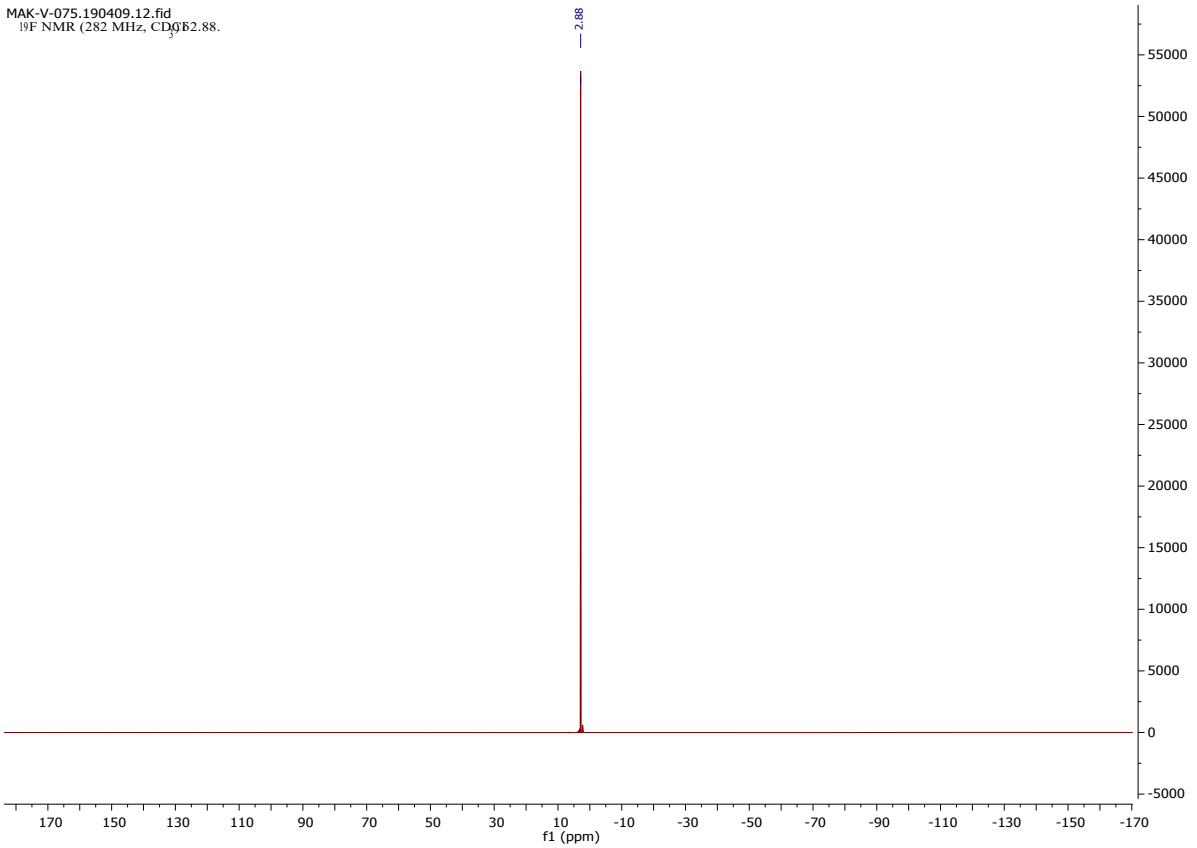

5-((2-(O-trifluorethyl-P-vinyll-phosphonamidato-N-benzoyl)ethyl)amino)naphthalene-1-sulfonic acid (**6**)

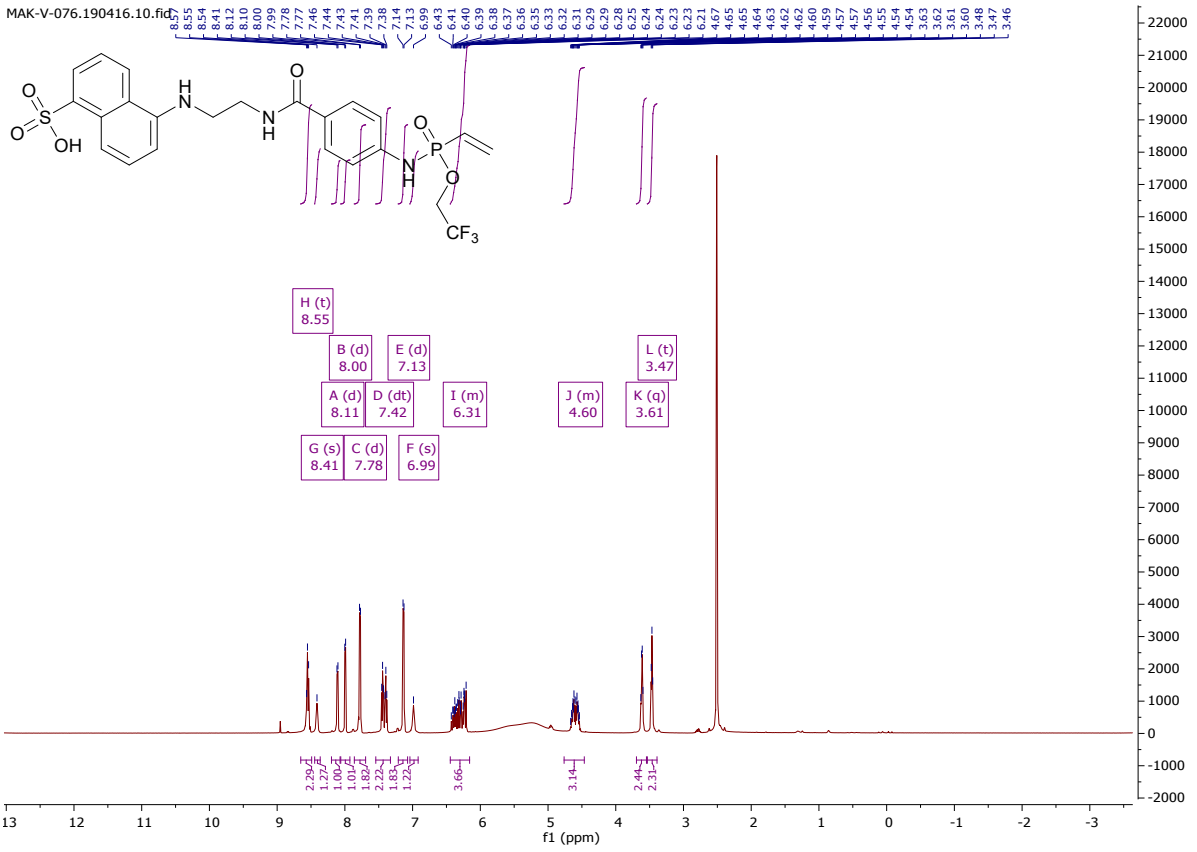

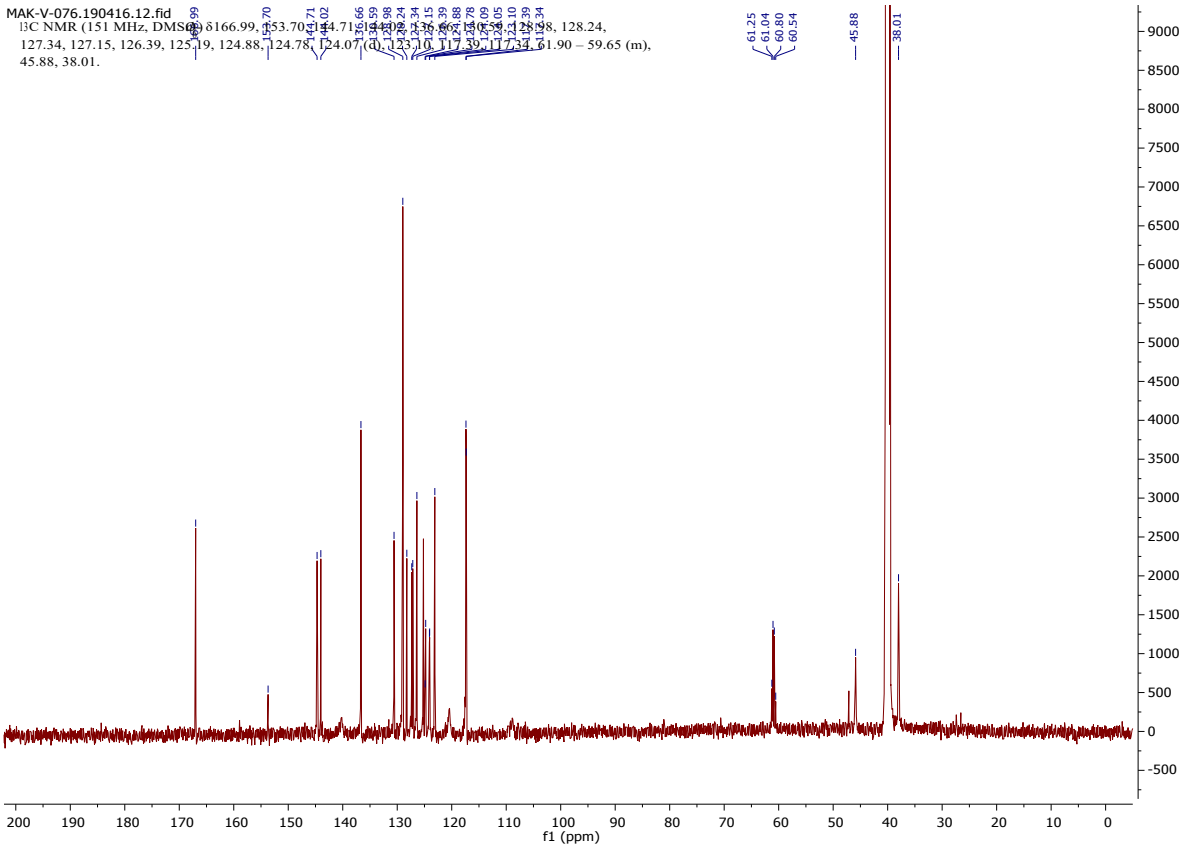
MAK-V-076.190416.12.fid
13C NMR (151 MHz, DMSO) δ166.99, 153.70, 144.71, 144.02, 135.66, 134.78, 128.24, 127.34, 127.15, 126.39, 125.19, 124.88, 124.78, 124.07 (d), 123.10, 117.39, 117.34, 61.90 – 59.65 (m), 45.88, 38.01.
f1 (ppm)

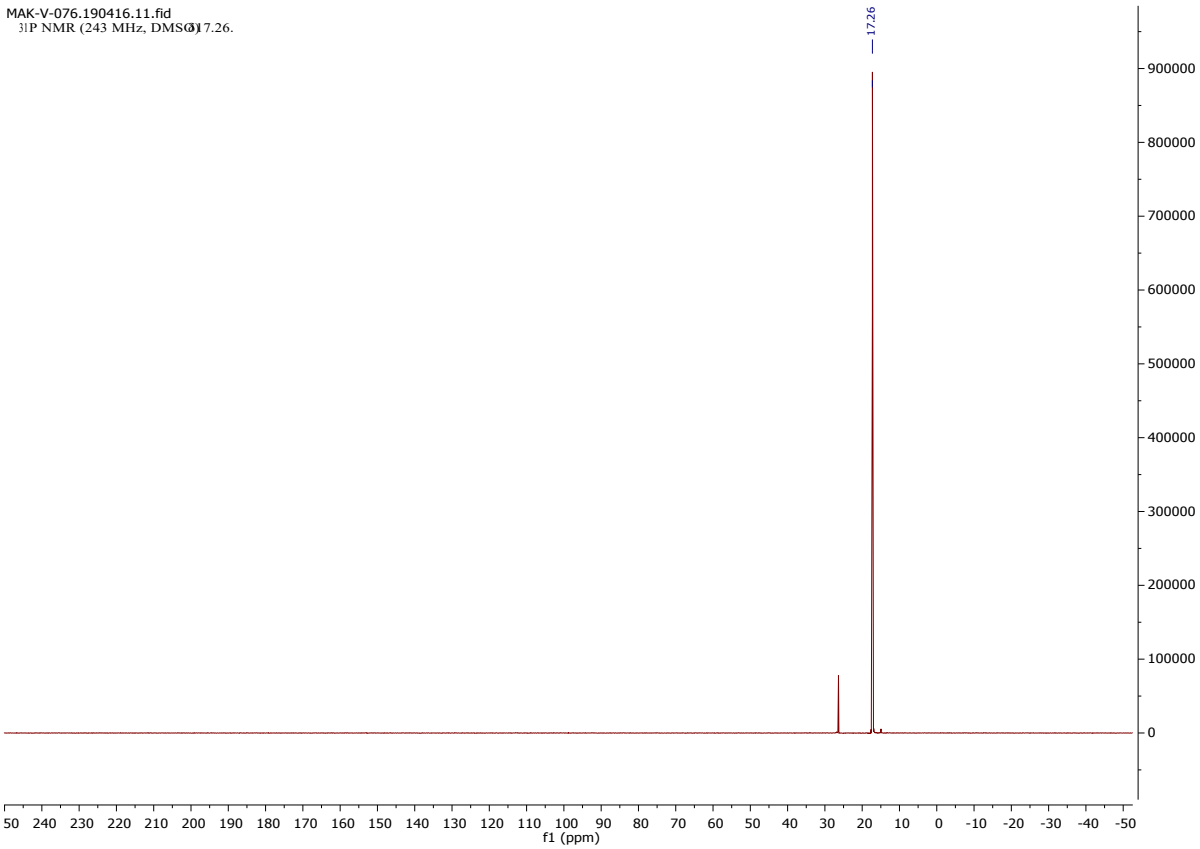
MAK-V-076.190416.11.fid
31P NMR (243 MHz, DMSO) 17.26.
f1 (ppm)

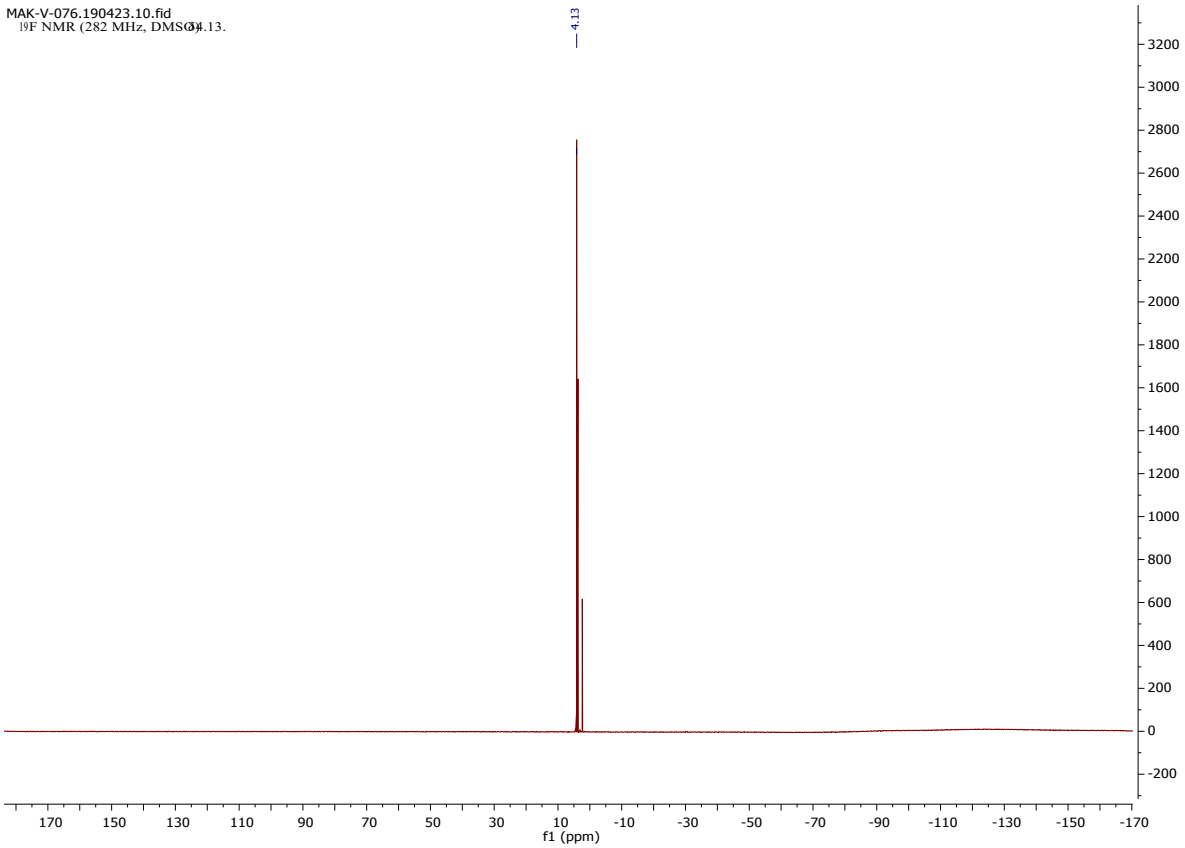

2-Nitrobenzyl-*N*-(4-biotinamido-phenyl)-*P*-vinyl phosphonamidate

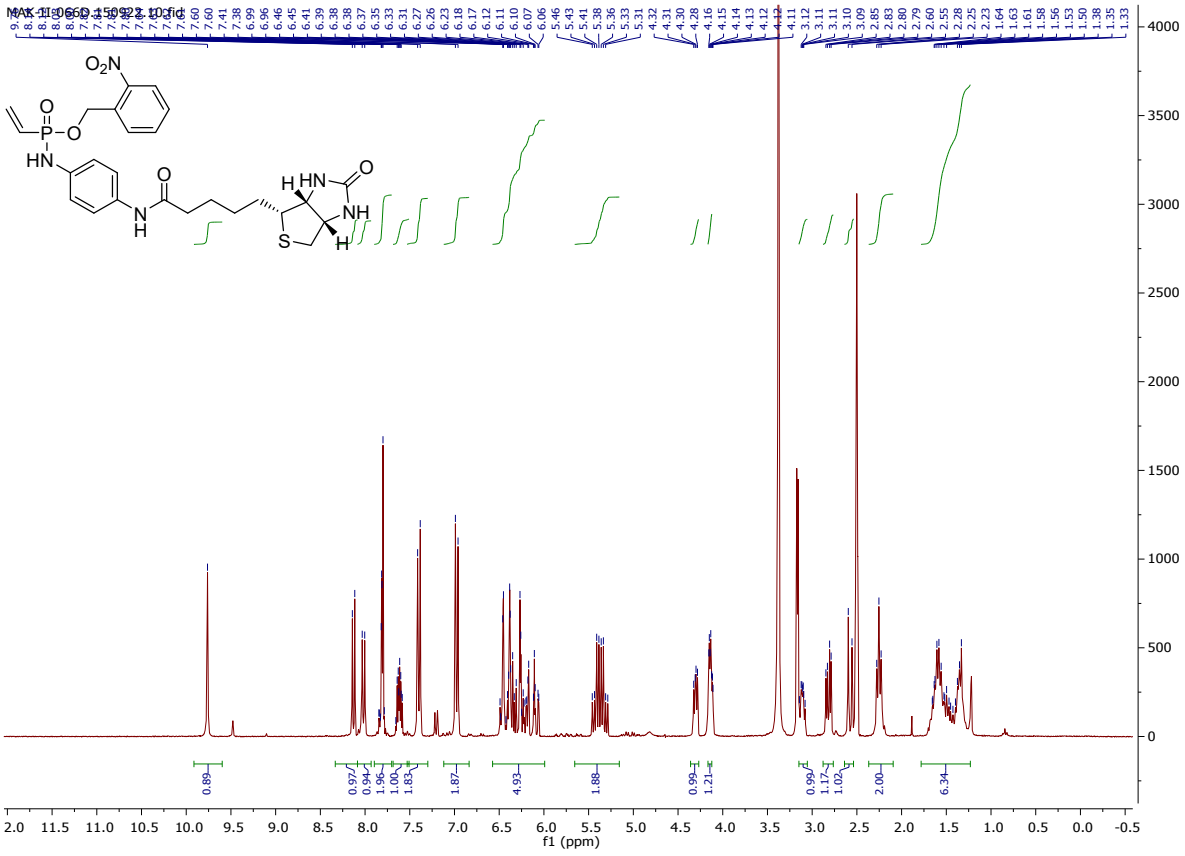

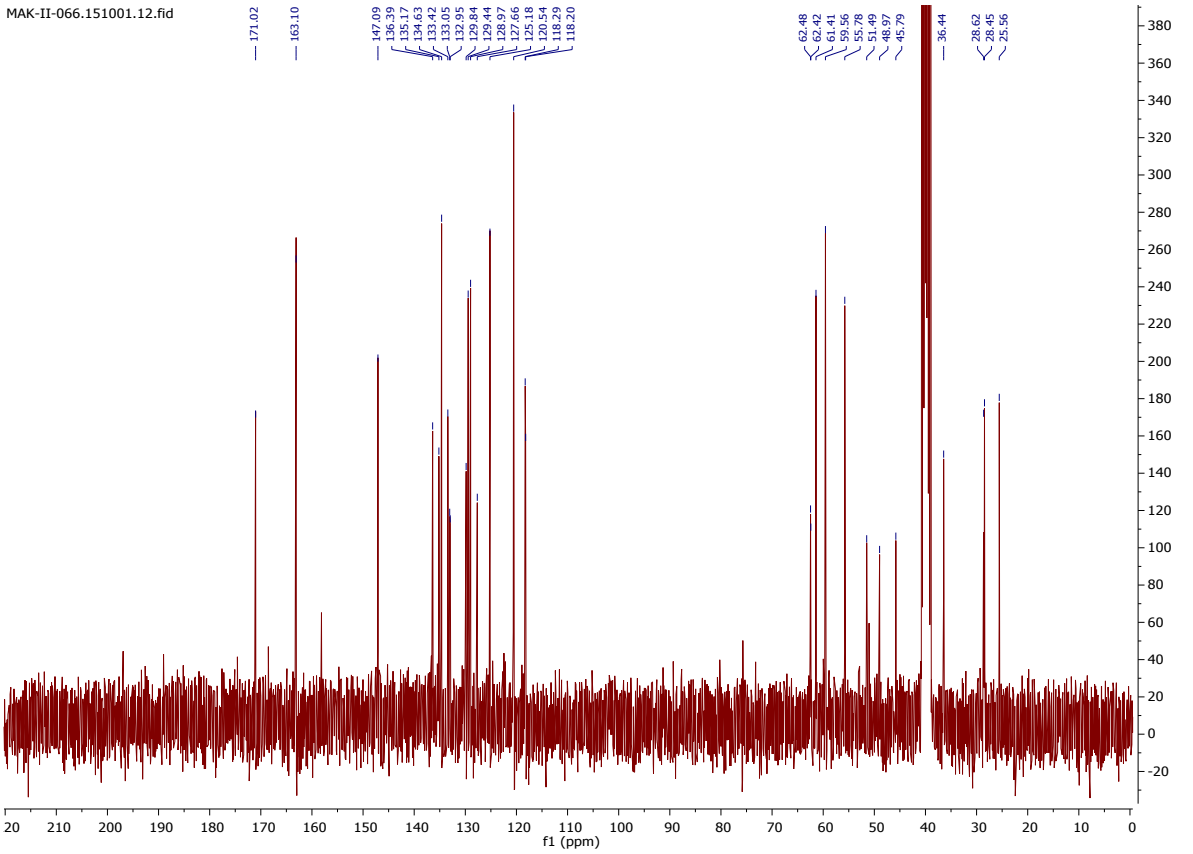
MAK-II-066.151001.12.fid
171.02
163.10
147.09
136.39
135.17
134.63
133.42
133.05
132.95
129.84
129.44
128.97
127.66
125.18
120.54
118.29
118.20
62.48
62.42
61.41
59.56
55.78
51.49
48.97
45.79
36.44
28.62
28.45
25.56
f1 (ppm)

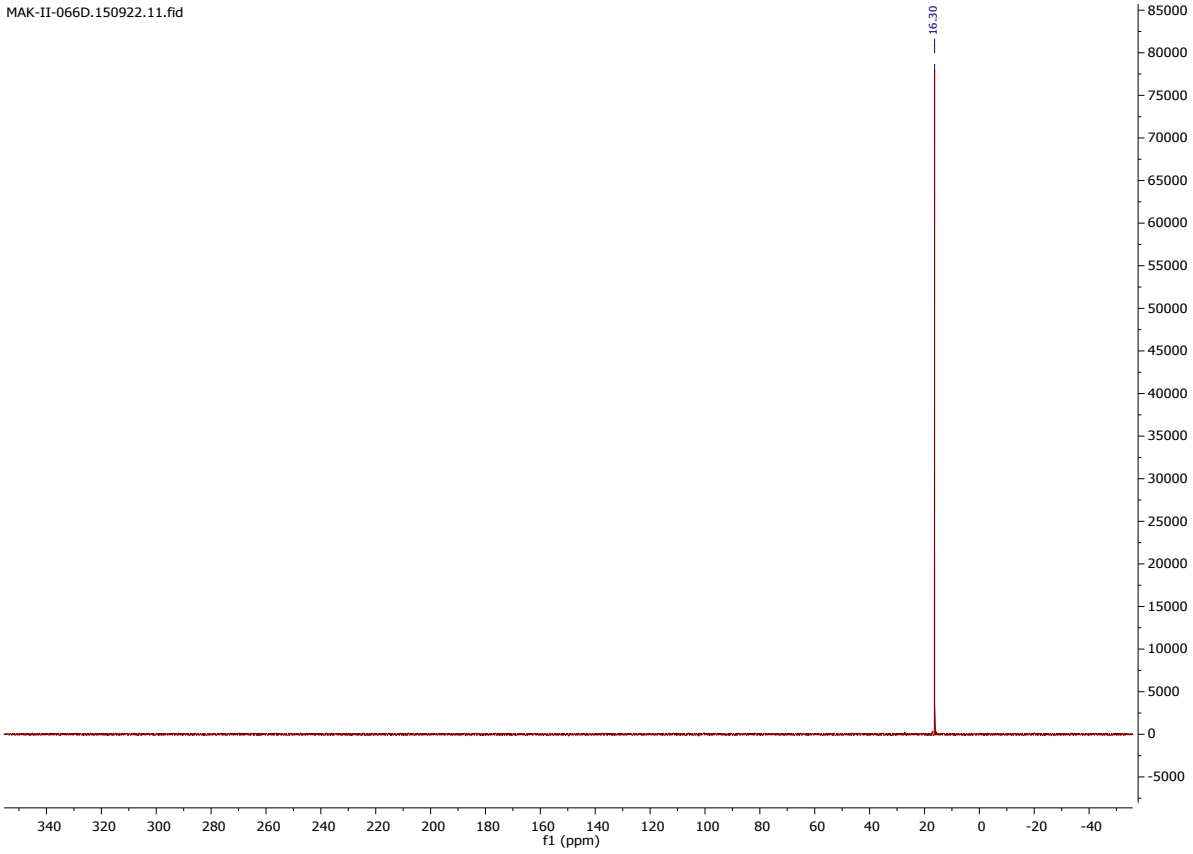
MAK-II-066D.150922.11.fid
16.30
f1 (ppm)

6. References

1. A. Shevchenko, H. Tomas, J. Havli, J. V. Olsen and M. Mann, *Nat. Protoc.*, 2007, **1**, 2856.
2. M.-A. Kasper, M. Glanz, A. Stengl, M. Penkert, S. Klenk, T. Sauer, D. Schumacher, J. Helma, E. Krause, M. C. Cardoso, H. Leonhardt and C. Hackenberger, *Angew. Chem. Int. Ed.*, in press doi:10.1002/anie.201814715.
3. M. R. J. Vallée, L. M. Artner, J. Dernedde and C. P. R. Hackenberger, *Angew. Chem. Int. Ed.*, 2013, **52**, 9504-9508.
4. S. p. Ortial and J.-L. Montchamp, *Org. Lett.*, 2011, **13**, 3134-3137.

6.2.2. Scope of the SPhR with vinylphosphonites and further variation of the phosphonamidate ester residue

In the previous chapter, only two small molecule azides without any functional groups attached have been used in the SPhR with vinylphosphonites. Furthermore, protein modification reactions were solely performed with cetuximab. To broaden the scope of vinylphosphonamidates in terms of applicability for protein modifications, the aim of this research project was to synthesize further vinylphosphonites and –phosphonamidates with increased complexity to facilitate thiol addition to various proteins with different functionalities attached to the *O*- and the *N*-substituent.

6.2.2.1. Synthesis of various vinylphosphonamidates

In addition to the two *O*-ethyl-vinylphosphonamidate derivatives that have been described in the previous chapter, more azides have been used in the one-pot synthesis protocol, starting from diethyl chlorophosphite **47** and vinylmagnesium bromide followed by azide addition and hydrolysis. The desired vinylphosphonamidates **48**-**51** were isolated in good to moderate overall yields (Scheme 54). It could be shown that carboxylic acids are tolerated in the reaction and electron-rich as well as electron-poor azides yield the desired vinylphosphonamidates. With compound **48**, a vinylphosphonamidate with increased water solubility was synthesized that can be also further used as modular building block to attach the vinylphosphonamidate moiety to other functional amine containing molecules via amide coupling.

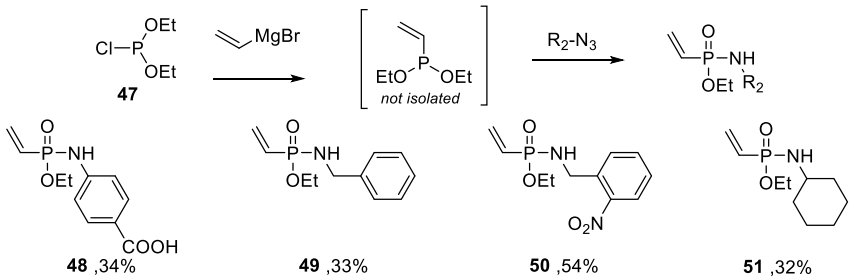

Scheme 54: One-Pot-Procedure for the synthesis of vinylphosphonamidates via alkylation of diethyl chlorophosphite (**47**), followed by SPhR with different azides. Stated are isolated yields.*

To further vary the phosphonamidate ester residue of vinylphosphonamidates, several vinylphosphonites, carrying different functional groups were synthesized. Since some alcohols are not compatible with subsequent addition of the highly reactive vinylmagnesium bromide reagent, the vinylphosphonites described in this chapter were synthesized, starting with vinylation of bis(diisopropylamino)chlorophosphine (**2**) followed by tetrazole mediated exchange of the diisopropylamine of **52** with the desired alcohol and borane protection, as described in the previous

* Compound **50** was synthesized and characterized by Jan Ole Kaufmann as part of his internship in the Hackenberger laboratory under the supervision of the author

chapter. Among others, it was possible to synthesize light cleavable vinylphosphonites carrying terminal alkynes with electron withdrawing 2-nitrobenzyl substituents (**53** and **54**). Other than that, it could be shown that electron-rich substituents such as 4-hydroxy phenyl in **55** as well as electron withdrawing substituents in **56** are well tolerated in the phosphonite synthesis (Scheme 55).

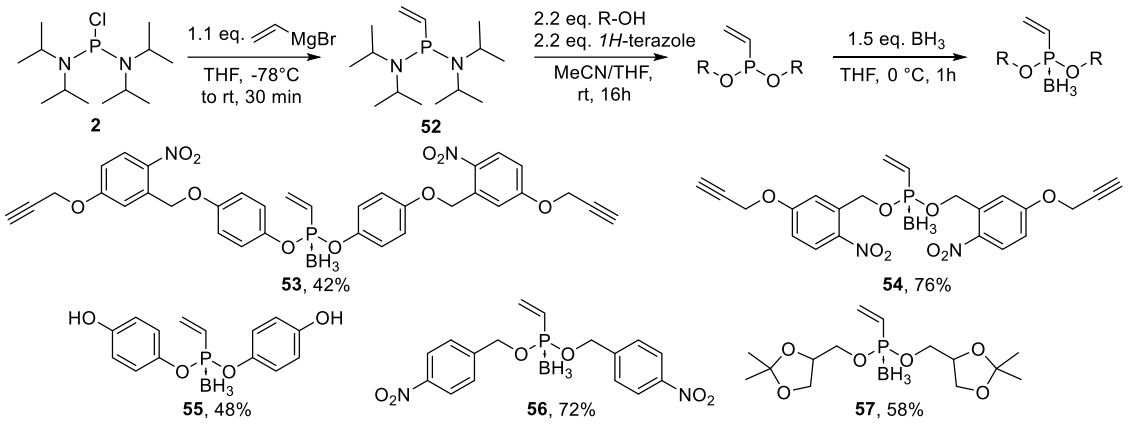

Scheme 55: One-Pot-Procedure for the synthesis of various borane protected vinylphosphonites from bis(diisopropylamino)chlorophosphine. Stated are isolated yields.

Next, the synthesized phosphonites were applied to SPhR with phenyl azide after borane deprotection with DABCO as described in the previous chapter. All of the tested phosphonites reacted smoothly under the tested conditions and could be isolated in decent to moderate yields. Electron withdrawing phosphonite-substituents were as well tolerated as electron donating groups.

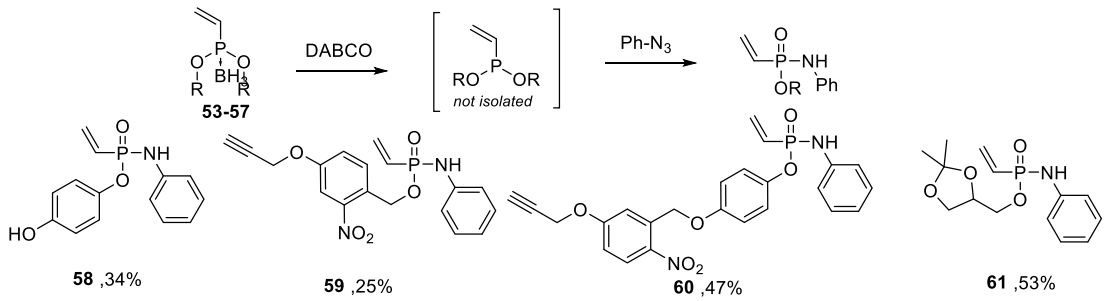

Scheme 56: SPhR with various phosphonites after borane deprotection with different phenyl azides. Reactions with phenyl azide were carried out, peptides were reacted in THF/DMF mixtures to ensure solubility. Stated are isolated yields

Compound **61** was synthesized to generate a polar water-soluble vinylphosphonamidate diol after removal of the ketal. However, all attempts hydrolyze the acetonide under acidic conditions and with acidic cation exchange resins failed due to decomposition of the starting material. The functionality of the substituents of the compounds **59** and **60** will be further evaluated in the next chapter.

6.2.2.2. Vinylphosphonamidates modification of proteins.

Encouraged by the decent reactivity of vinylphosphonamidates towards glutathione in aqueous buffer and the successful modification of antibodies via reduction and alkylation protocols, described in chapter 6.1.1, the modification of cysteine residues on other proteins was evaluated in the next step.

At first, the aforementioned eGFP C70M S147C, carrying a single accessible cysteine residue was incubated at room temperature with the water-soluble phosphonamidate **48** in basic buffer. The reaction mixture was analyzed by MALDI-TOF/MS after overnight incubation, and an indicative shift of 255 dalton with respect to the starting could be observed after 16 hours (Figure 21). However, in contrast to the experiments with ethynylphosphonamidates described in chapter 6.1.1 full conversion of the eGFP C70M S147C could not be achieved, even with prolonged reaction times and strong basic conditions of pH 9. This might be explained by slower reaction kinetics of *O*-ethyl-vinylphosphonamidates in the reaction with cysteine, as described in chapter 6.2.1.

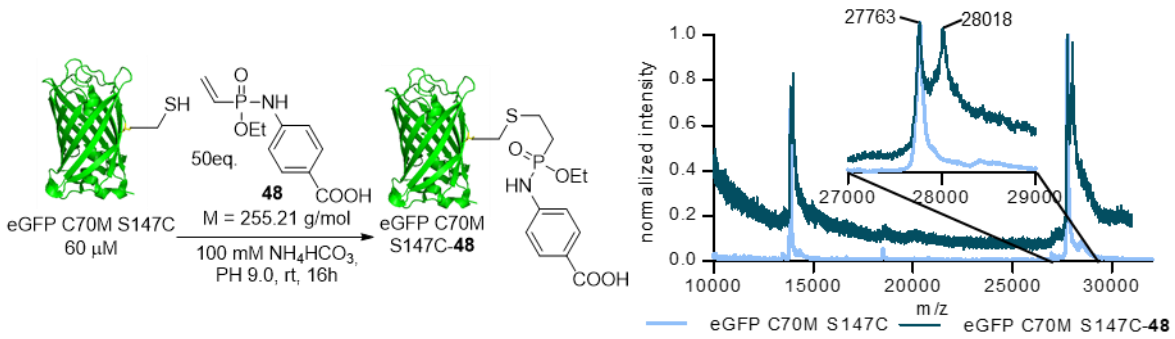

Figure 21: Addition of the vinylphosphonamidate **48** to eGFP C70M S147C. MALDI-TOF/MS for the eGFP C70M S147C starting material (light blue) and the phosphonamidate adduct (cyan). Spectra are normalized.

To overcome the issue of low conversions of cysteine residues on proteins, either the phosphonamidate equivalents with respect to the protein could be increased or the reactivity of the vinylphosphonamidates by attaching electron withdrawing *O*-substituent, as demonstrated in chapter 6.2.1. To circumvent problems arising from limited solubility of the phosphonamidate at higher concentrations, all the following protein modification reactions were carried out using vinylphosphonamidates with electron-deficient *O*-substituents.

For further labelling experiments of eGFP, a far-red-fluorescent Cy5-vinylphosphonamidate **63** that can be detected by in-gel fluorescence[336] and has been applied to cellular- and in-vivo imaging[337] was synthesized from Cy5-azide **45** and phosphonite **62** (Figure 22a). The desired 2-nitrobenzyl substituted Cy5 vinylphosphonamidate could be isolated by column chromatography and protein reactivity was probed with eGFP C70M S147C (Figure 22b).

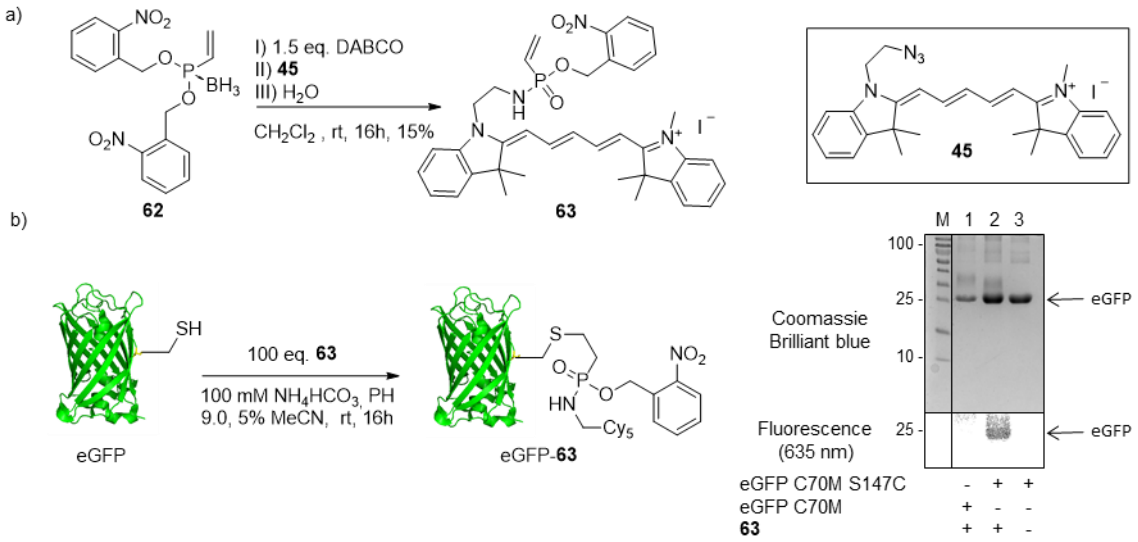

Figure 22: Synthesis of an *O*-2-nitrobenzyl-Cy5-vinylphosphonamidate **63** and labelling of eGFP C70MS147C. a) Synthetic scheme for the synthesis of **63** via SPhR. b) Addition of **63** to two different eGFP mutants. Gel analysis with fluorescent readout; lane 1: Reaction with eGFP C70M (no addressable cysteine); lane 2: Reaction with eGFP C70M S147C; lane 3: eGFP C70M S147C starting material.

In gel fluorescence with excitation at 635 nm revealed successful labelling of eGFP C70M S147C. To proof the chemoselectivity of the vinylphosphonamidate labelling for cysteine residues, the reaction was carried out with the eGFP mutant C70M that doesn't carry any addressable cysteine.* Under the tested conditions at pH 9.0, an excellent selectivity for cysteine residues was observed, since no fluorescence signal was detected even after 16 hours of incubation (Figure 22c).

6.2.2.3. Selectivity of vinylphosphonamidates for cysteine residues

In chapter 6.2.1 it was shown that *O*-trifluoroethyl substituted vinylphosphonamidates can cross-react with lysine residues, when a large excess is used in the reaction. In order to elucidate the dependence of this phenomenon on the nature of the phosphonamidate ester substituent, modification of cetuximab with a large excess of 100 equivalents of the *O*-phenyl substituted phosphonamidate **64** was performed, similar as described in chapter 6.2.1, employing the protocol of reducing and alkylating the interchain disulfide bonds.[70a] Cysteine selectivity was afterwards investigated by MS/MS analysis after trypsin digestion of the modified antibody with and without prior reduction with DTT.†

* eGFP C70M was designed and cloned by Dr. Dominik Schumacher as part of his PhD thesis. Expression was performed by Kristin Kemnitz-Hassanin.

† MS/MS analysis was performed by Martin Penkert as part of his PhD thesis and Dr. Michael Schümann.

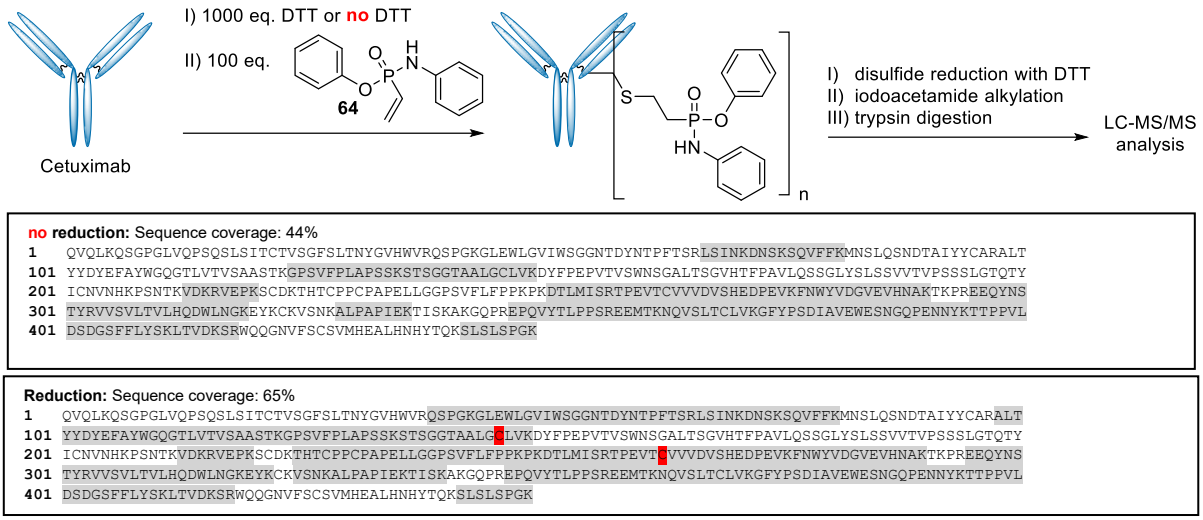

Figure 23: Cetuximab modification with **64**, followed by trypsin digestion and LC-MS/MS analysis. Shown are the results of the Mascot search on cetuximab's heavy chain after incubation with 100 eq. of **64** with (top) and without (bottom) prior reduction of the disulfide bonds. Identified peptides are highlighted in grey. Amino acid residues modified with **64** are highlighted in red. Oxidation of methionine, alkylation of cysteine via iodoacetamide and the phosphonamidate on Y, S, T, C, K, H & R were searched as variable modifications.

Two phosphonamidate modified sites on the heavy chain of cetuximab on Cys 146 and Cys 264 could be identified and confirmed via HCD-MS/MS. Those two cysteines were only modified after reduction and alkylation with **64** and no modification on any other nucleophilic amino acid was found without prior reduction (Figure 23). This observation suggests that the cross-reactivity of other nucleophilic side chains is lower for the *O*-phenyl-substituted vinylphosphonamidates when compared to the *O*-trifluoroethyl substituent that modified several lysine sides when used in a large excess of 100 equivalents. It should be noted that a comparison to the experiment described in chapter 6.2.1 is difficult since labelling was performed here at 4 °C and an antibody concentration of 1.5 mg/ml whereas the previous experiment was performed at room temperature and increased antibody concentration of 5 mg/ml. However, the experiments described here clearly show that a highly selective labelling of cysteine residues with *O*-phenyl-vinylphosphonamidates is possible under the conditions applied in this experiment.

6.2.2.4. Vinylphosphonamidates for light cleavable triple conjugations

The substituents of the phosphonites **53** and **54** allow for the attachment of an additional functionality to the terminal alkyne via CuAAC to the conjugated protein, similar as described in chapter 6.1.2.3. The 2-nitrobenzyl substituent furthermore facilitates a triggered release of this substituent by light irradiation[338] and acts as an electron-withdrawing substituent that increases the reaction rate of the thiol addition. Release of the phosphonamidate ester residue to liberate a phosphonamidic acid has been shown to increase the lability of the *P*-*N*-bond.[322] This would cause a detachment of both functionalities, attached to the *O*- and the *N*-substituent of the phosphonamidate, from the protein. To overcome this limitation, a second substituent has been synthesized with an additional

hydroquinone moiety between the 2-nitrobenzyl group and the phosphonamidate for applications were cleavage of both substituents is undesired (Scheme 57). Here, light mediated cleavage would yield a stable *O*-4-hydroxy-phenyl phosphonamidate similar to compound **58** that has been described in chapter 6.2.2.1.

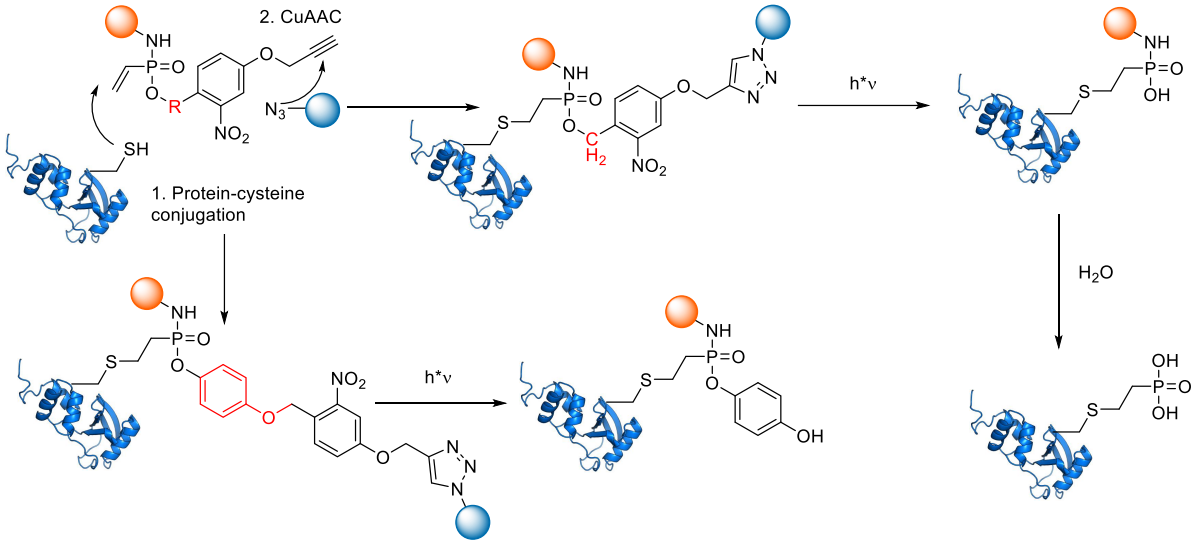

Scheme 57: 2-Nitrobenzyl Phosphonamidate ester substituents modified with terminal alkynes facilitate a light cleavable triple conjugation. Principle of the attachment and light mediated release. Direct attachment of the 2-nitrobenzyl group to the phosphonamidate facilitates a cleavage of both modifications from the protein whereas the hydroquinone spacer (red) releases only the alkyne handle.

In order to test the possibility to incorporate the two different substituents into phosphonamidates with subsequent modification of a protein's cysteine residue, a model peptide was reacted with the two phosphonites **53** and **54** after borane deprotection. The model peptide **65** was chosen due to its good water solubility and the ability to induce a gel-shift of a protein in a SDS-PAGE analysis. The two desired peptides could be isolated by preparative HPLC. Since the peptide contained unprotected alcohols, amines and carboxylic acids, this result underlines again a good functional group tolerance of the SPhR with vinylphosphonamidates. (Figure 24a).

Next, the ability of the peptides to modify cysteine residues on proteins was evaluated. For this, a single cysteine containing ubiquitin mutant ubiquitin G75C was chosen as a model protein, which was incubated with 25 equivalents of the peptides in basic buffer at 4 °C overnight and the conjugation mixture was analyzed by SDS/PAGE (Figure 24b and c). A conversion of approximately 60% could be observed under these conditions for both of the peptides, estimated by the intensities of the two protein bands of starting material and product.

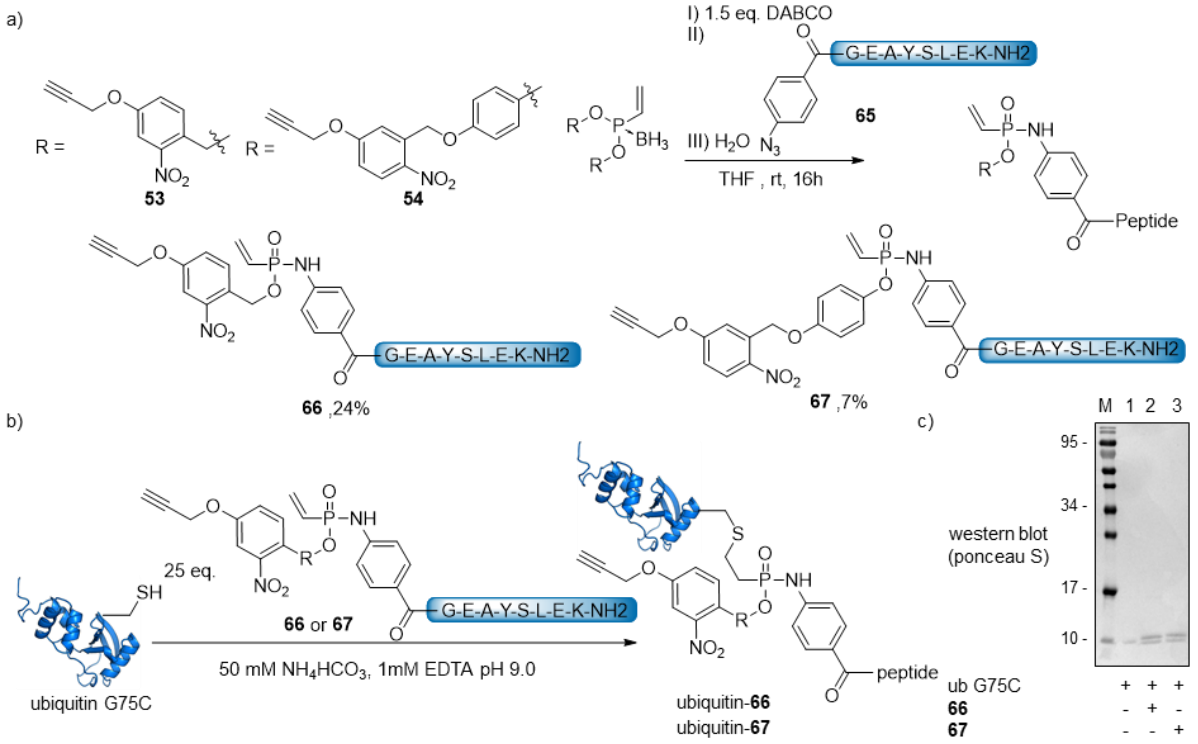

Figure 24: Synthesis of protein-peptide conjugates with alkyne modified 2-nitrobenzyl substituted phosphonamidate. a) Installation of the two different phosphonamidate moieties on an azide-containing model peptide. b) Synthetic scheme of the attachment of **66** and **67** to ubiquitin G75C. c) Western blot analysis of the reaction mixtures of ubiquitin G75C with **66** and **67**.

With the peptide-protein conjugate ubiquitin-**66** in hands, CuAAC with a biotin azide was performed to attach a cleavable immobilization handle to the protein construct. Successful cycloaddition was confirmed by intact protein MS, which showed complete consumption of the starting material. Next, immobilization of the peptide-protein-biotin constructs on streptavidin beads followed by light irradiation was attempted (Figure 25). Incubation of the conjugation mixture that still contained unmodified protein with streptavidin beads and analysis of the supernatant demonstrated significantly reduced amount of conjugated ubiquitin, due to immobilization of the clicked peptide conjugate. This is further confirmed by the observation that a protein that is shifted to higher masses is released after washing and boiling of the beads. Next, the resin was irradiated for 20 minutes in PBS and the supernatant subjected to SDS/PAGE analysis. It was observed that this irradiation releases a protein with a gel shift close to the starting material, whereas the un-irradiated, boiled beads only showed a single band that is shifted towards higher masses.

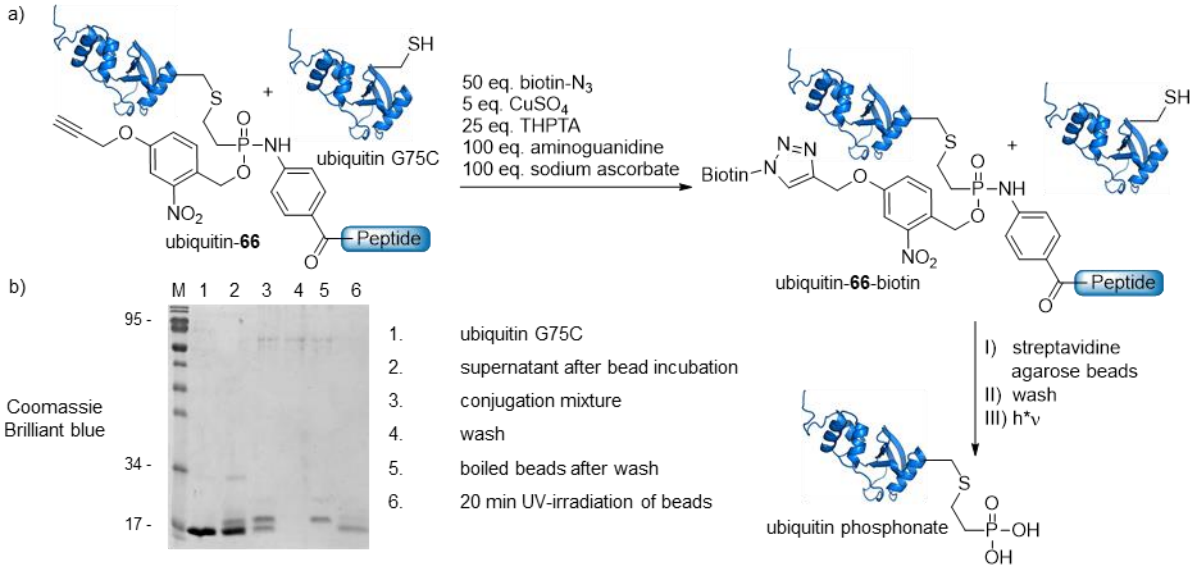

Figure 25: Ubiquitin-**66** can be modified with a biotin azide via CuAAC, immobilized on streptavidin beads and released by UV-irradiation. a) Scheme for the attachment of a biotin azide, immobilization and photorelease. b) SDS/PAGE analysis of the different fractions of the pull-down experiment. All steps were performed in PBS.

The fact that the protein is released from the beads by UV-irradiation suggests a cleavage of the biotin moiety and the gel shift points towards an additional loss of the peptide from the protein, most probably due to *P*-*N*-hydrolysis. This shift is not observed in the boiled beads fraction, suggesting that the peptide is still attached, which underlines the hypothesis of simultaneous *P*-*O*- and *P*-*N*-hydrolysis by UV-irradiation. These experiments demonstrate that the attachment of a peptide to a protein with an additional light cleavable CuAAC-handle at a vinylphosphonamidate is in principle possible. The observations on the behavior after light irradiation can be explained by the mechanism that is proposed in scheme 56. Further investigations with the hydroquinone spacer have to be undertaken to provide further evidence for this proposed principle.

6.3. Ethynylphosphonamidates for the cysteine-selective synthesis of Antibody-Drug-Conjugates

Requirements on linker technology for the attachment of cytotoxic drugs to antibodies to generate ADCs that effectively deliver the payload to the malignant cell are exceptionally high. The conjugation strategy determines factors such as linkage stability during blood circulation, overall hydrophobicity that is added to the antibody and homogeneity of the antibody conjugates that are important for the safety profile of the final product. As an alternative to conjugation methods that rely on elaborative antibody engineering, drug attachment to native antibodies via reduction of the interchain disulfide bonds and alkylation of the liberated cysteine residues is a very attractive strategy (see chapter 4.3.1.3). Due to the remarkable linkage stability that has been described for cysteine conjugates in chapter 6.1 and 6.2, the aim of the work described in this chapter was to apply unsaturated phosphonamidates to the construction of ADCs. It was anticipated that phosphonamidates linkages facilitate an excellent linkage stability during blood circulation. Furthermore, the ability to vary the phosphonamidate's *O*-substituent was exploited to improve linker properties in terms of hydrophilicity. Ethynylphosphonamidates were used, since they combine superior selectivity for cysteine with faster reaction kinetics when directly compared to their vinyl counterparts. The following main goals were defined to evaluate the ethynylphosphonamidate-cysteine conjugation reaction as a general tool for the synthesis of efficacious ADCs, starting from native unengineered antibodies:

a) Synthetic attachment of the phosphonamidate moiety to cytotoxic drugs and incorporation of hydrophilic *O*-substituents to increase water solubility of the linker-drug constructs.
b) Development of synthesis protocols for the construction of ADCs from native antibodies and ethynylphosphonamidates via disulfide reduction and alkylation strategies.
c) Evaluation of the phosphonamidate-linked ADCs in terms of linkage stability during blood circulation, selective cytotoxic activity on antigen positive cell lines *in vitro* and efficacy in tumor xenograft mouse models *in vivo*.

6.3.1. Synthesis and biochemical *in vitro* and *in vivo* evaluation of phosphonamidate-linked Antibody-Drug-Conjugates

This chapter was published in the following journal:

Marc-André Kasper, Andreas Stengl, Philipp Ochtrop, Marcus Gerlach, Tina Stoschek, Dominik Schumacher, Jonas Helma, Martin Penkert, Eberhard Krause, Heinrich Leonhardt* and Christian P. R. Hackenberger*

"Ethynylphosphonamidates for the rapid and cysteine selective generation of efficacious Antibody-Drug-Conjugates"

Angew. Chem. Int. Ed. **2019**, *58* (34), 11631-11636.
Publication date (online): June 28th, 2019
The article is available online at:
https://onlinelibrary.wiley.com/doi/10.1002/anie.201904193

*Corresponding authors

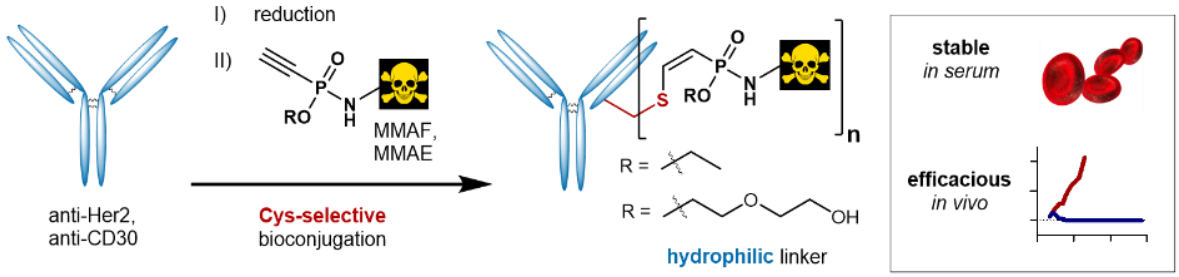

Figure 26: Ethynylphosphonamidates facilitate straightforward synthesis of ADC via reduction and alkylation of the interchain disulfide bonds of native antibodies. Phosphonamidate-linked ADC are stable in rat serum, and efficacious in tumor xenograft mouse models.

Abstract

Requirements for novel bioconjugation reactions for the synthesis of Antibody-Drug-Conjugates (ADCs) are exceptionally high, since selectivity of the conjugation as well as stability and hydrophobicity of linkers and payloads drastically influence the performance and safety profile of the

final product. Herein we describe Cys-selective ethynylphosphonamidates as new reagents for the rapid generation of efficacious ADCs from native non-engineered monoclonal antibodies, applying a simple one-pot reduction and alkylation protocol. Ethynylphosphonamidates can be easily substituted with hydrophilic residues, giving rise to electrophilic labelling reagents with tunable solubility properties. We demonstrate that ethynylphosphonamidate-linked ADCs have excellent properties for next generation antibody therapeutics in terms of serum stability and *in vivo* antitumor activity.

Responsibility assignment

Christian P. R. Hackenberger designed and conceived the project. Heinrich Leonhardt, Jonas Helma and Dominik Schumacher designed and conceived the *in vitro* and *in vivo* efficacy studies. The author designed the synthetic strategies for the attachment of phosphonamidates to the drug molecules and synthesized and characterized all phosphonites, phosphonamidates, drug-linker constructs and synthetic precursors thereof. The author furthermore developed the antibody-drug conjugation protocols, synthesized, purified and characterized all ADCs and conceived and performed the DAR analysis studies as well as the serum stability analyses. Andreas Stengl expressed and purified trastuzumab and performed all cellular imaging and cell-based proliferation assays. Philipp Ochtrop performed the solubility assay and synthesized drug-linker constructs. Marcus Gerlach performed cell viability assays and size-exclusion analyses of the ADCs and developed the ADC concentration determination. Tina Stoschek expressed and purified brentuximab. Martin Penkert and Eberhard Krause performed intact protein MS of the trastuzumab conjugates. The author wrote the manuscript supported by Christian P. R. Hackenberger, Dominik Schumacher, Philipp Ochtrop and Andreas Stengl.

Summary of content

Cysteine selective ethynylphosphonamidates have been applied to the synthesis and evaluation of ADCs via reduction and alkylation of the interchain disulfide bonds of native IgG antibodies. The Her2-binding antibody trastuzumab was at first modified with the cytotoxic drug MMAF followed by evaluation of cell-viability on different Her2-positive and -negative cell lines. Here, the antibody concentrations leading to fifty percent of maximal growth inhibition (IC_{50}) of trastuzumab could be improved by MMAF attachment by 81-fold for SKBR3 cells (Her2++), whereas an MDAMB468 cell line (Her2-) was mostly unaffected. Afterwards, a second antibody-drug pair was synthesized from the cytotoxic auristatin MMAE and the monoclonal antibody brentuximab, to synthesize an ADC that is structurally analogous to the FDA approved Adcetris® with the maleimide linkage exchanged by a phosphonamidate. Since MMAE is even more unpolar than the MMAF used in the first study, a small diethylene glycol chain was incorporated to the phosphonamidate's *O*-substituent to increase water-solubility of the drug-linker pair. Optimization of the subsequent antibody conjugation procedure lead

to the development of two ADC synthesis protocols that facilitate an average drug loading of approximately four drug molecules per antibody exactly like in Adcetris®, requiring only minimal excess of the drug molecules. One protocol is relying on complete reduction with an excess of DTT, followed by DTT removal and drug conjugation, whereas the other makes use of partial disulfide reduction with low amounts of TCEP in the presence of the phosphonamidate modified drug in a one-pot manner. With these protocols, a phosphonamidate linked brentuximab-MMAE with an average of four drug molecules was synthesized and directly compared to its structurally related Adcetris® in terms of linkage stability in serum, selective decrease of the viability *in vitro* and finally anti-tumor efficacy *in vivo*. It could be shown that the phosphonamidate is much more stable in the presence of rat serum, resulting in 90% intact linkage after seven days, whereas the maleimide decreased to 25% already after three days. Both ADCs showed a similar behavior on cell viability *in vitro* and an excellent efficacy in an *in vivo* tumor xenograft mouse model system, with tumor remission for all mice treated twice with 1 mg/kg ADC already a few days after the treatments. In a final *in vivo* experiment, a reduced dosage of twice 0.5 mg/kg was administered in the same xenograft model. Here it could be shown that the median survival of the mice treated with Adcetris® increased from 21 to 48 days for the phosphonamidate linked ADC, which corresponds to a factor of 2.3. Correlating this increased efficacy at lower ADC doses with the superior linkage stability in serum of phosphonamidates when directly compared to maleimides in Adcetris®, one can speculate that the stable phosphonamidate linkage facilitates a prolonged drug delivery to the side of the tumor and therefore an increased antitumor activity.

Manuscript and supporting information

Bioconjugation

International Edition: DOI: 10.1002/anie.201904193
German Edition: DOI: 10.1002/ange.201904193

Ethynylphosphonamidates for the Rapid and Cysteine-Selective Generation of Efficacious Antibody–Drug Conjugates

Marc-André Kasper, Andreas Stengl, Philipp Ochtrop, Marcus Gerlach, Tina Stoschek, Dominik Schumacher, Jonas Helma, Martin Penkert, Eberhard Krause, Heinrich Leonhardt, and Christian P. R. Hackenberger**

Dedicated to Professor Sam Gellman on the occasion of his 60th birthday

Abstract: *Requirements for novel bioconjugation reactions for the synthesis of antibody–drug conjugates (ADCs) are exceptionally high, since conjugation selectivity as well as the stability and hydrophobicity of linkers and payloads drastically influence the performance and safety profile of the final product. We report Cys-selective ethynylphosphonamidates as new reagents for the rapid generation of efficacious ADCs from native non-engineered monoclonal antibodies through a simple one-pot reduction and alkylation. Ethynylphosphonamidates can be easily substituted with hydrophilic residues, giving rise to electrophilic labeling reagents with tunable solubility properties. We demonstrate that ethynylphosphonamidate-linked ADCs have excellent properties for next-generation antibody therapeutics in terms of serum stability and in vivo antitumor activity.*

Antibody conjugates consisting of a drug linked to a tumor-selective antibody, so called antibody–drug conjugates (ADCs), are an emerging class of targeted therapeutics.[1] While most of the ADCs in clinical development contain cytotoxic molecules, recent studies also include the treatment of infectious diseases with antibody–antibiotic conjugates (AACs).[2] ADCs are particular interesting for the treatment of cancer, since they combine the high potency of cytotoxic molecules with the tumor specificity of monoclonal antibodies. ADCs thus have the potential to significantly broaden the therapeutic window compared to standard chemotherapy.[1,3] Recent progress in clinical development include the approval of inotuzumab ozogamicin (Besponsa)[4] and the re-approval of gemtuzumab ozogamicin (Mylotarg).[5] Nevertheless, challenges remain, especially in improving the linkage between drug and antibody.[6] Commonly used linker systems face problems such as insufficient serum stability and undesired aggregation behavior, which limits the number of drug molecules linked to an antibody and leads to undesired off-target toxicity.[7]

Maleimides have become the prime linker reagents for the generation of ADCs, including two approved ADCs: trastuzumab emtansine (Kadcyla) and brentuximab vedotin (Adcetris).[8] Maleimides can be applied to either modify native IgG antibodies through interchain-disulfide reduction and alkylation[9] or to engineered antibodies through addition to an additionally incorporated cysteine (Thiomab technology).[7a] Nevertheless, one of the biggest drawbacks of maleimide linkages is their susceptibility towards retro-Michael additions, which leads to premature drug cleavage during circulation and reattachment to cysteine-containing proteins like albumin.[7a,10] Even though consequences arising from such payload transfer are not yet fully understood, it is anticipated that the anti-tumor efficacy might be lowered due to decreased drug delivery to targeted cells. Furthermore toxic side effects might occur.[11] Several compound classes have been developed to overcome this issue, including self-hydrolyzing maleimides[11] and structurally refined Michael-type acceptors such as carbonyl acrylic derivatives[12] or exocyclic maleimides.[13] All of these methods yield stable sulfhydryl adducts; however, synthetic incorporation of these electrophiles into functional molecules remains challenging.[14]

Undesired aggregation of ADCs is another challenge, since many drugs used in the context of ADCs are hydrophobic.[15] The addition of organic co-solvents to the conjugation mixture is commonly employed to enable the conjugation of hydrophobic drugs, which however may affect the structural integrity of the antibody.[16] Additionally, the hydrophobic nature of drugs increases the formation of

[*] M.-A. Kasper, P. Ochtrop, Dr. D. Schumacher, M. Penkert, Prof. Dr. C. P. R. Hackenberger
Chemical Biology Department
Leibniz-Forschungsinstitut für Molekulare Pharmakologie (FMP)
Robert-Rössle-Strasse 10, 13125 Berlin (Germany)
E-mail: hackenbe@fmp-berlin.de

M.-A. Kasper, Dr. D. Schumacher, M. Penkert, Dr. E. Krause, Prof. Dr. C. P. R. Hackenberger
Department of Chemistry, Humboldt Universität zu Berlin
Brook-Taylor-Str. 2, 12489 Berlin (Germany)

A. Stengl, Dr. M. Gerlach, T. Stoschek, Dr. D. Schumacher, Dr. J. Helma, Prof. Dr. H. Leonhardt
Department of Biology II, and Center for Integrated Protein Science Munich, Ludwig-Maximilians-Universität München
Großhadenerstr. 2, 82152 Martinsried (Germany)
E-mail: h.leonhardt@lmu.de

Supporting information and the ORCID identification number(s) for the author(s) of this article can be found under: https://doi.org/10.1002/anie.201904193.

high-molecular-weight species (HMWS) in the final product.[17] Those aggregates impair the pharmacokinetic profile and efficacy[18] of ADCs and often limit the drug-to-antibody ratio (DAR) to a maximum of 4.[19] To overcome this issue, hydrophilic polyethylene glycol (PEG) linkers have been developed that compensate for the lipophilic nature of the drug.[20] However, it has recently been shown that PEG can negatively affect pharmacokinetics when incorporated as a linear spacer between antibody and drug.[21] Increasing the solvent exposure of the drug most likely facilitates unspecific hydrophobic interactions. This unwanted effect has been successfully mitigated by side-chain attachment of the solubilizing polymer.[21]

Based on our recently reported phosphonamidite-based labelling method,[22] we applied ethynylphosphonamidates as a novel compound class for the generation of stable Cys-linked ADCs. We initiated our studies by conjugating the antimitotic agent Monomethyl auristatin F (MMAF)[23] to the Her2-targeting antibody trastuzumab by using phosphonamidate functionalized cathepsin B cleavable linker **4**, which was synthesized based on previously published procedures for Fmoc-protected Val-Cit dipeptides[24] (Figure S1 in the Supporting Information). In a first proof-of-concept study, we conjugated **4** to trastuzumab following our previously established method by applying 10 equiv labeling reagent per Cys,[22] giving an average DAR of 4.6 (Figure 1 a and Figure S2 in the Supporting Information). To validate the functionality of trastuzumab–**4**, it was evaluated in a Her2-based proliferation assay with two Her2-overexpressing cell lines (BT474 and SKBR3) as well as a Her2-negative cell line as a control (MDAMB468).[25] Since trastuzumab alone exhibits antiproliferative potency, cell viability was measured via a sensitive, high-content assay to asses retained antibody functionality after exposure to the conjugation procedure. The antibody concentrations leading to half maximal growth inhibition (IC_{50}) decreased with trastuzumab–**4** compared to trastuzumab alone by 81-fold, from 900 to 11 pM, for SKBR3 cells (Her2++) and by 42-fold, from 800 to 19 pM, for BT474 cells (Her2+). An effect on the proliferation of the control cell line MDAMB468 was only observed at very high ADC concentrations ($IC_{50} > 100$ nM). Notably, trastuzumab–**4** inhibits the proliferation of close to 100% of cell population for SKBR3 cells, while trastuzumab alone only inhibits up to 50%. As an additional control, trastuzumab was treated with **4** without prior disulfide reduction. Those constructs behaved in a similar manner to the non-modified antibodies, thus highlighting the high Cys-selectivity, efficient removal of excessive toxin, and gentle reaction conditions of our method (Figure 1 b). We additionally validated our measured IC_{50} values in a standard cell viability assay and obtained similar IC_{50} growth inhibition constants for trastuzumab–**4** (Figure S3 in the Supporting Information). The mode of action of MMAF is the destabilization of microtubules through inhibition of tubulin polymerization.[26] Along these lines, we observed by fluorescence microscopy a disturbance of tubulin organization in BT474 cells upon treatment with 0.3 nM trastuzumab–**4** for 4 days in contrast to proper spindle formation in untreated mitotic control cells (Figure 1 c and Figure S4 in the Supporting Information).

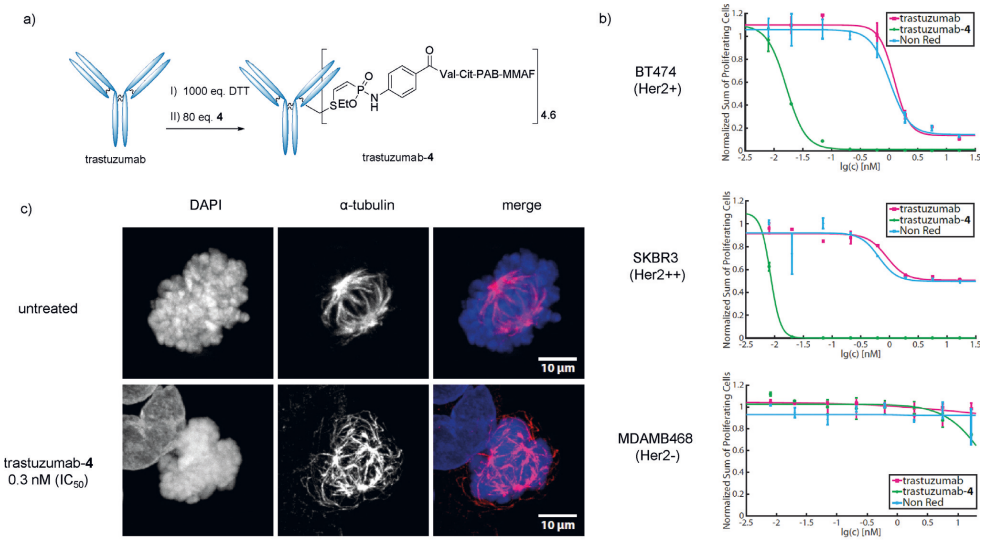

Figure 1. a) Synthetic scheme for the attachment of **4** to trastuzumab. b) Antiproliferative potency of trastuzumab–**4** on two Her2-overexpressing cell lines (SKBR3, BT474) and a control (MDAMB468). Plots depict the number of proliferating cells after 4 days of antibody treatment against antibody concentration. Non-Red-trastuzumab treated with **4** without prior disulfide reduction. c) Effect of trastuzumab–**4** treatment on mitotic tubulin organization in BT474 (Her2+) cells. Shown are representative images of mitotic BT474 cells after 4 days of treatment with 0.3 nM trastuzumab–**4** compared to untreated cells.

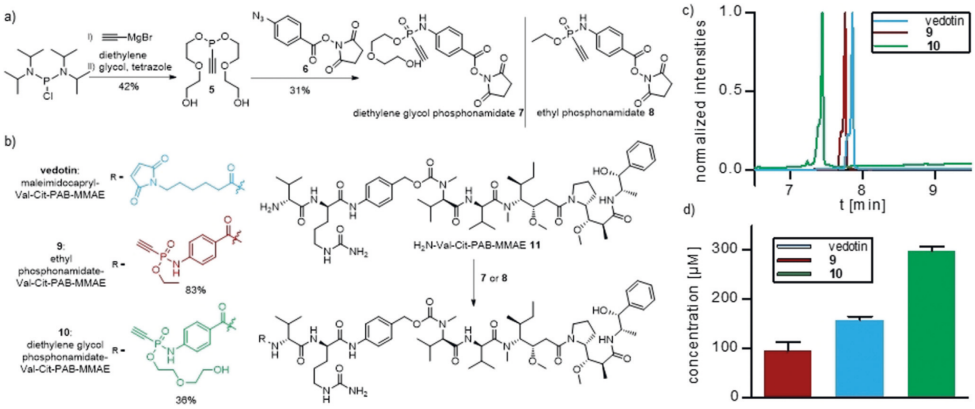

Figure 2. a) Synthesis of ethylene glycol substituted ethynylphosphonamidate building block **7** and structural comparison to the corresponding ethyl-substituted **8**.[22] b) Structure of vedotin and synthesis of ethyl (**9**) and diethylene glycol (**10**) phosphonamidate-based vedotin analogues. c) RP-HPLC analysis of vedotin and analogues **9** and **10**. d) Solubility in PBS with 5% DMSO of vedotin and analogues **9** and **10**. Error bars calculated from three independent measurements.

Furthermore, we anticipated that ethynylphosphonamidates bearing O-substituents with increased hydrophilicity might serve as powerful building blocks to increase the polarity of the whole linker system without increasing the overall linker length. Since the Staudinger-phosphonite reaction (SPhR) comprises a very convenient synthetic route to incorporate the ethynylphosphonamidate moiety into a given molecule, we focused on the synthesis of a hydrophilic phosphonite. Following our previous methods, we were able to synthesize the diethylene glycol substituted phosphonite **5** in a one-pot procedure.[27] Subsequent SPhR was performed with the NHS-modified azide **6** and yielded the desired diethyleneglycol-phosphonamidate **7** in 31% yield (Figure 2a).

To demonstrate the versatility of our method, we proceeded with the construction of a second antibody–drug pair. Since we wanted to directly compare our linkage technology with the maleimide linkage used in Adcetris, we continued our studies with phosphonamidate-linked ADCs that are structurally as close to Adcetris as possible. In addition to the MMAF constructs used in the previous study, two ethynylphosphonamidate MMAE derivatives were synthesized, one with an ethyl substituent at the phosphorous (**9**) and one with a diethylene glycol substituent (**10**; Figure 2b). RP-HPLC analysis showed a reduced retention time for compound **10**, when compared to **9** or vedotin (Figure 2c). Solubility measurements revealed that the aqueous solubility of the conjugates is drastically increased by the diethylene glycol substituent, from 95 µM (**9**) to 298 µM (**10**). The aqueous solubility of **10** is also twice as high as vedotin (Figure 2d and Figure S5 in the Supporting Information) Based on these observations we decided to proceed with the hydrophilic compound **10** for subsequent conjugation studies to antibodies.

Next, we tried to optimize our conjugation method to reduce the number of drug equivalents needed for sufficient conjugation. Since Adcetris is modified with an average of four vedotin molecules per antibody,[28] we started by screening different amounts of **10** to achieve similar modification and analyzed the DAR by intact protein MS (Figure S6 in the Supporting Information). We estimated that 16 equiv of **10** per antibody (2 equiv per Cys-residue) are needed to reach a DAR of 4 at 1 mg mL^{-1} antibody concentration. We attribute the required excess of phosphonamidate to slower reaction kinetics of ethynylphosphonamidates compared to maleimides.[22] To compensate for the slower kinetics, we increased the antibody concentration in the conjugation reaction to 5 mg mL^{-1}, a concentration that was previously also used for maleimide conjugations.[9] With this, we were able to use as little as 4.5 equiv of **10** per antibody to achieve a DAR of 4.0 (Figure S7 in the Supporting Information). After this, upscaling of the conjugation reaction to 2.4 mg brentuximab was performed at 1 or 5 mg mL^{-1} followed by a preparative size-exclusion chromatography step to ensure complete removal of the toxin prior to subsequent functional evaluations, yielding 1.6 mg of the desired ADC brentuximab–**10** with a DAR of 3.8–4.0. To furthermore simplify the conjugation process, we applied partial reduction of the interchain disulfide bonds with TCEP.[29] By screening TCEP equivalents needed to modify brentuximab, we found out that a partial reduction method with 3 equiv TCEP, 5 equiv **10**, and 5 mg mL^{-1} brentuximab, applied in a one pot process, produces an ADC with a DAR of 3.9 without the need for removal of reducing agent prior payload conjugation (Figure S8 in the Supporting Information). This one-pot process can be problematic with other cysteine-labelling reagents, since it has been shown that maleimides and vinyl sulfones for instance, irreversibly react with TCEP.[30]

Taking advantage of our ADC synthesis methods, we then evaluated commercially available Adcetris in comparison to our analogue brentuximab–**10** (Figure 3a). We started with a cell-based viability assay with a CD30-overexpressing cell

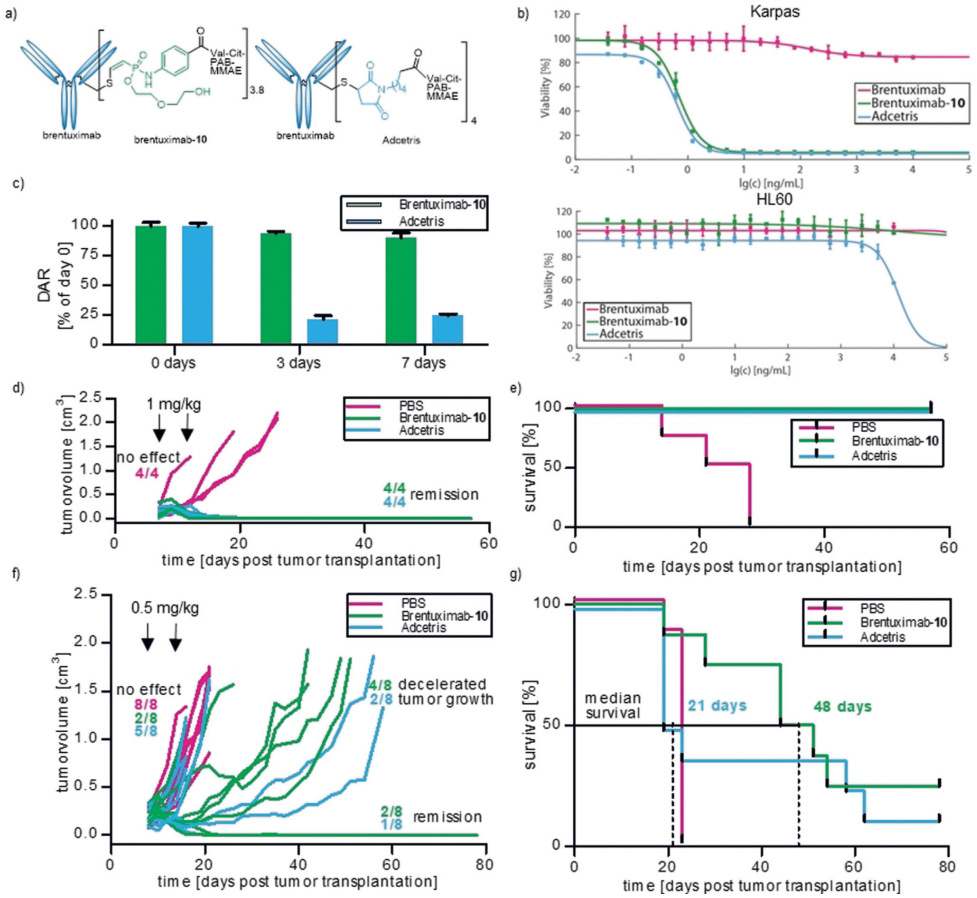

Figure 3. a) Structural comparison of Adcetris with brentuximab–**10.** b) Cell viability assays with a CD30-overexpressing cell line (Karpas299, top) and a control (HL60, bottom) for brentuximab–**10**, Adcetris· and brentuximab alone. c) Linkage-stability studies in rat serum. ADCs were incubated in rat serum for 0, 3, and 7 days at 37 °C and analyzed by MS after pulldown, deglycosylation, and reduction. Shown is the DAR relative to the average DAR of day 0 for brentuximab–**10** and Adcetris. d) Antitumor activity of brentuximab–**10** and Adcetris and a PBS control in a Karpas 299 tumor xenograft model in SCID mice. Treatment of 1 mg kg^{-1} was administered twice at day 7 and day 10 after tumor transplantation. Tumor volumes of the four mice per group are shown separately. e) Kaplan–Meier survival analysis of the study shown in (d). f) Treatment of 0.5 mg kg^{-1} at day 8 and day 12 after tumor transplantation. Tumor volumes of the eight mice per group are shown separately. g) Kaplan–Meier survival analysis of the study shown in (f).

line Karpas299 and a CD30-negative cell line HL60 as a control. Both ADCs showed similar IC_{50} growth inhibition constants in the range of 0.9 ng mL^{-1} in the antigen-positive cell line. Whereas Adcetris slightly affected the antigen-negative cell line at high ADC concentrations, we observed no such effect for brentuximab–**10**. (Figure 3b).

As mentioned earlier, increased stability of the linkage between drug and antibody in serum might improve the properties of ADCs in terms of off-target toxicity and anti-tumor efficacy.[11] In our experiment, we observed that 90% of the phosphonamidate-linked MMAE was still connected to brentuximab after 7 days of incubation in rat serum at 37 °C, as measured by intact-protein MS after pulldown of the ADC from serum. Under the same incubation conditions, Adcetris lost more than 70% of its payload after three days. (Figure 3c and Figure S9 in the supporting information). This data is in accordance with previous observations that describe a drastic DAR decrease of similar maleimide linked ADCs following 6 days of incubation in serum at 37 °C.[31] Although hydrolysis of maleimides was shown to improve conjugate stability and

generates ADCs with increased in vivo potency,[11,32] the occurrence of incomplete hydrolysis of many maleimides may limit this approach.[33] Taken together, the stability experiments in serum clearly underlines our previously reported data on the excellent stability of the phosphonamidate linkage,[22] in particular when compared to maleimide-linked ADCs. Additionally, we performed storage tests with brentuximab–**10** to analyze the formation of HMWS, as reported previously.[34] Size-exclusion chromatography revealed less than 9% HMWS formation with respect to the monomeric species after storage at 40 °C over two weeks. No significant increase in HMWS was observed after two weeks of storage at 4 °C (Figure S10 in the Supporting Information).

Finally, brentuximab–**10** was evaluated in vivo in a Karpas 299 derived tumor xenograft model in immunodeficient female CB17-SCID mice in a similar manner as previously reported.[35] In a first study, four mice were treated twice, at day 7 and day 10, with 1 mg ADC per kg bodyweight with brentuximab–**10**, Adcetris, or only PBS as a control. All 4 mice treated with brentuximab-**10** or Adcetris showed an excellent response to the treatment. Treated mice were in tumor remission already a few days after ADC injection and no relapse was observed over the whole observation period of 58 days, while the untreated control showed uncontrolled tumor growth and had to be sacrificed within three weeks after tumor transplantation (Figure 3d and Figure S11 in the Supporting Information). It was previously reported that an ADC with an average of four MMAE molecules connected to brentuximab via maleimides is significantly less efficacious in a tumor xenograft model when the dosing is lowered from 1 to 0.5 mg kg^{-1}.[35] From our serum stability studies (Figure 3c), we anticipated that phosphonamidite-linked ADCs might still be active at lower doses due to prolonged drug delivery in circulation. Therefore, we initiated a second in vivo study, with three groups of eight mice treated with either 0.5 mg kg^{-1} brentuximab–**10** or Adcetris or only PBS twice at day 8 and day 12. As expected, we observed decreased antitumor activity for both constructs when compared to the first study, leading to tumor remission in two mice for brentuximab–**10** and only one for Adcetris. However, five out of eight mice did not show any observable response to the treatment with Adcetris, and the tumor growth was as fast as in the PBS-treated control group. In contrast, this was only observed in two mice treated with brentuximab–**10** (Figure 3f and Figure S11 in the Supporting Information). Hence, we were able to show a drastic increase in median survival from 21 days for commercial Adcetris to 48 days for brentuximab–**10** (Figure 3g). This increase by a factor of 2.3 in comparison to Adcetris indicates promising antitumor activity for our novel phosphonamidate-linked ADCs. It should be noted that none of the mice, treated with either construct, showed significant changes in bodyweight over the observation period (Figure S11 in the Supporting Information).

In summary, we present ethynylphosphonamidates as cysteine-reactive handles for the construction of next-generation cancer therapeutics. By making use of the SPhR, we obtained a new modular diethyleneglycol-modified ethynylphosphonamidate building block for the synthesis of hydrophilic Cys-selective linker systems for the conjugation of unpolar payloads. With this method, we synthesized an ADC from brentuximab and MMAE, and demonstrated appropriate linkage stability combined with beneficial in vivo antitumor activity, resulting in an increased median survival from 21 days for Adcetris to 48 days for the phosphonamidate linkage. The conjugation method is straightforward, using only minimal drug excesses, and facilitates one-pot synthesis of ADCs starting from native antibodies. Taken together, the ethynylphosphonamidates described herein facilitate the straightforward construction of ADCs for cancer therapeutics and show great promise for other pharmacological targets.

Acknowledgements

We thank K. K. Hassanin for excellent technical assistance. This work was supported by grants from the Deutsche Forschungsgemeinschaft (DFG) (SPP1623) to C.P.R.H. and (HA 4468/9-1), (LE 721/13-2) and (SFB1243/A01) to H.L., the Einstein Foundation Berlin (Leibniz-Humboldt Professorship), the Boehringer-Ingelheim Foundation (Plus 3 award) and the Fonds der Chemischen Industrie to C.P.R.H, by the Leibniz Association with the Leibniz Wettbewerb to C.P.R.H and H.L., by the German Federal Ministry for Economic Affairs and Energy and the European Social Fund with grants to D.S. and J.H. (EXIST FT I) and by the Bavarian Ministry of Economic Affairs, Regional Development and Energy with grants to D.S., J.H., H.L. and C.P.R.H. (m^4-Award). A.S. was trained and supported by the graduate school RTG1721 of the DFG.

Conflict of interest

The technology described in the manuscript is part of a pending patent application by M.-A.K., D.S., J.H., A.S, H.L. and C.P.R.H.

Keywords: ADCs · antibodies · bioconjugation · bioorganic chemistry · drug delivery

How to cite: *Angew. Chem. Int. Ed.* **2019**, *58*, 11631 – 11636
Angew. Chem. **2019**, *131*, 11757 – 11762

[1] V. Chudasama, A. Maruani, S. Caddick, *Nat. Chem.* **2016**, *8*, 114 – 119.
[2] S. Mariathasan, M.-W. Tan, *Trends Mol. Med.* **2017**, *23*, 135 – 149.
[3] D. Schumacher, C. P. R. Hackenberger, H. Leonhardt, J. Helma, *J. Clin. Immunol.* **2016**, *36*, 100 – 107.
[4] N. Uy, M. Nadeau, M. Stahl, A. M. Zeidan, *J. Blood Med.* **2018**, *9*, 67 – 74.
[5] F. R. Appelbaum, I. D. Bernstein, *Blood* **2017**, *130*, 2373 – 2376.
[6] P. Agarwal, C. R. Bertozzi, *Bioconjugate Chem.* **2015**, *26*, 176 – 192.
[7] a) B.-Q. Shen, K. Xu, L. Liu, H. Raab, S. Bhakta, M. Kenrick, K. L. Parsons-Reponte, J. Tien, S.-F. Yu, E. Mai, D. Li, J. Tibbitts, J. Baudys, O. M. Saad, S. J. Scales, P. J. McDonald, P. E. Hass, C. Eigenbrot, T. Nguyen, W. A. Solis, R. N. Fuji, K. M. Flagella, D. Patel, S. D. Spencer, L. A. Khawli, A. Ebens, W. L. Wong, R. Vandlen, S. Kaur, M. X. Sliwkowski, R. H. Scheller, P. Polakis, J. R. Junutula, *Nat. Biotechnol.* **2012**, *30*, 184 – 189; b) P. J. Burke,

J. Z. Hamilton, S. C. Jeffrey, J. H. Hunter, S. O. Doronina, N. M. Okeley, J. B. Miyamoto, M. E. Anderson, I. J. Stone, M. L. Ulrich, J. K. Simmons, E. E. McKinney, P. D. Senter, R. P. Lyon, *Mol. Cancer Ther.* **2017**, *16*, 116.
[8] A. Beck, L. Goetsch, C. Dumontet, N. Corvaïa, *Nat. Rev. Drug Discovery* **2017**, *16*, 315.
[9] S. O. Doronina, B. E. Toki, M. Y. Torgov, B. A. Mendelsohn, C. G. Cerveny, D. F. Chace, R. L. DeBlanc, R. P. Gearing, T. D. Bovee, C. B. Siegall, J. A. Francisco, A. F. Wahl, D. L. Meyer, P. D. Senter, *Nat. Biotechnol.* **2003**, *21*, 778 – 784.
[10] J. F. Ponte, X. Sun, N. C. Yoder, N. Fishkin, R. Laleau, J. Coccia, L. Lanieri, M. Bogalhas, L. Wang, S. Wilhelm, W. Widdison, J. Pinkas, T. A. Keating, R. Chari, H. K. Erickson, J. M. Lambert, *Bioconjugate Chem.* **2016**, *27*, 1588 – 1598.
[11] R. P. Lyon, J. R. Setter, T. D. Bovee, S. O. Doronina, J. H. Hunter, M. E. Anderson, C. L. Balasubramanian, S. M. Duniho, C. I. Leiske, F. Li, P. D. Senter, *Nat. Biotechnol.* **2014**, *32*, 1059.
[12] B. Bernardim, P. M. S. D. Cal, M. J. Matos, B. L. Oliveira, N. Martínez-Sáez, I. S. Albuquerque, E. Perkins, F. Corzana, A. C. B. Burtoloso, G. Jiménez-Osés, G. J. L. Bernardes, *Nat. Commun.* **2016**, *7*, 13128.
[13] D. Kalia, P. V. Malekar, M. Parthasarathy, *Angew. Chem. Int. Ed.* **2016**, *55*, 1432 – 1435; *Angew. Chem.* **2016**, *128*, 1454 – 1457.
[14] O. Koniev, A. Wagner, *Chem. Soc. Rev.* **2015**, *44*, 5495 – 5551.
[15] C. D. Medley, J. Kay, Y. Li, J. Gruenhagen, P. Yehl, N. P. Chetwyn, *Anal. Chim. Acta* **2014**, *850*, 92 – 96.
[16] J. R. McCombs, S. C. Owen, *AAPS J.* **2015**, *17*, 339 – 351.
[17] a) I. Hollander, A. Kunz, P. R. Hamann, *Bioconjugate Chem.* **2008**, *19*, 358 – 361; b) A. Wakankar, Y. Chen, Y. Gokarn, F. S. Jacobson, *mAbs* **2011**, *3*, 161 – 172.
[18] A. Saluja, D. S. Kalonia, *Int. J. Pharm.* **2008**, *358*, 1 – 15.
[19] A. Mullard, *Nat. Rev. Drug Discovery* **2013**, *12*, 329.
[20] R. Y. Zhao, S. D. Wilhelm, C. Audette, G. Jones, B. A. Leece, A. C. Lazar, V. S. Goldmacher, R. Singh, Y. Kovtun, W. C. Widdison, J. M. Lambert, R. V. J. Chari, *J. Med. Chem.* **2011**, *54*, 3606 – 3623.
[21] R. P. Lyon, T. D. Bovee, S. O. Doronina, P. J. Burke, J. H. Hunter, H. D. Neff-LaFord, M. Jonas, M. E. Anderson, J. R. Setter, P. D. Senter, *Nat. Biotechnol.* **2015**, *33*, 733.
[22] M.-A. Kasper, M. Glanz, A. Stengl, M. Penkert, S. Klenk, T. Sauer, D. Schumacher, J. Helma, E. Krause, M. C. Cardoso, H. Leonhardt, C. P. R. Hackenberger, *Angew. Chem. Int. Ed.* **2019**, https://doi.org/10.1002/anie.201814715; *Angew. Chem.* **2019**, https://doi.org/10.1002/ange.201814715.
[23] S. O. Doronina, B. A. Mendelsohn, T. D. Bovee, C. G. Cerveny, S. C. Alley, D. L. Meyer, E. Oflazoglu, B. E. Toki, R. J. Sanderson, R. F. Zabinski, A. F. Wahl, P. D. Senter, *Bioconjugate Chem.* **2006**, *17*, 114 – 124.
[24] a) I. Rillat, M. Perez, L. Goetsch, M. Broussas, C. Beau-Larvor, J.-F. Haeuw, WO2015162293, WO2015162293 (A1), **2015**; b) L. Liang, S.-W. Lin, W. Dai, J.-K. Lu, T.-Y. Yang, Y. Xiang, Y. Zhang, R.-T. Li, Q. Zhang, *J. Controlled Release* **2012**, *160*, 618 – 629.
[25] A. Stengl, D. Hörl, H. Leonhardt, J. Helma, *SLAS Discov.* **2017**, *22*, 309 – 315.
[26] A. B. Waight, K. Bargsten, S. Doronina, M. O. Steinmetz, D. Sussman, A. E. Prota, *PLoS One* **2016**, *11*, e0160890.
[27] a) M. R. J. Vallée, P. Majkut, I. Wilkening, C. Weise, G. Müller, C. P. R. Hackenberger, *Org. Lett.* **2011**, *13*, 5440 – 5443; b) K. D. Siebertz, C. P. R. Hackenberger, *Chem. Commun.* **2018**, *54*, 763 – 766.
[28] S. M. Ansell, *Blood* **2014**, *124*, 3197 – 3200.
[29] C. Bahou, E. A. Love, S. Leonard, R. J. Spears, A. Maruani, K. Armour, J. R. Baker, V. Chudasama, *Bioconjugate Chem.* **2019**, *30*, 1048 – 1154.
[30] T. Kantner, A. G. Watts, *Bioconjugate Chem.* **2016**, *27*, 2400 – 2406.
[31] C. Wei, G. Zhang, T. Clark, F. Barletta, L. N. Tumey, B. Rago, S. Hansel, X. Han, *Anal. Chem.* **2016**, *88*, 4979 – 4986.
[32] L. N. Tumey, M. Charati, T. He, E. Sousa, D. Ma, X. Han, T. Clark, J. Casavant, F. Loganzo, F. Barletta, J. Lucas, E. I. Graziani, *Bioconjugate Chem.* **2014**, *25*, 1871 – 1880.
[33] S. D. Fontaine, R. Reid, L. Robinson, G. W. Ashley, D. V. Santi, *Bioconjugate Chem.* **2015**, *26*, 145 – 152.
[34] N. S. Beckley, K. P. Lazzareschi, H.-W. Chih, V. K. Sharma, H. L. Flores, *Bioconjugate Chem.* **2013**, *24*, 1674 – 1683.
[35] K. J. Hamblett, P. D. Senter, D. F. Chace, M. M. C. Sun, J. Lenox, C. G. Cerveny, K. M. Kissler, S. X. Bernhardt, A. K. Kopcha, R. F. Zabinski, D. L. Meyer, J. A. Francisco, *Clin. Cancer Res.* **2004**, *10*, 7063 – 7070.

Manuscript received: April 5, 2019
Revised manuscript received: May 9, 2019
Accepted manuscript online: June 28, 2019
Version of record online: July 18, 2019

Angewandte Chemie
Eine Zeitschrift der Gesellschaft Deutscher Chemiker

Supporting Information

Ethynylphosphonamidates for the Rapid and Cysteine-Selective Generation of Efficacious Antibody–Drug Conjugates

Marc-André Kasper, Andreas Stengl, Philipp Ochtrop, Marcus Gerlach, Tina Stoschek, Dominik Schumacher, Jonas Helma, Martin Penkert, Eberhard Krause, Heinrich Leonhardt, and Christian P. R. Hackenberger**

anie_201904193_sm_miscellaneous_information.pdf

Table of contents

1. Supplementary Figures

1.1. Figure S1

Synthesis of a phosphonamidate modified, cathepsin B cleavable MMAF **4**. Compound **1** was synthesized based on previously published procedures for Fmoc-protected Val-Cit dipeptides.[1] **1** was afterwards converted into the phosphonamidate **2** via Staudinger-phosphonite reaction and activated as a carbonate (Scheme 1). The resulting compound **3** constitutes a modular building block to install a cathepsin B cleavable phosphonamidate into any primary or secondary amine-containing payload. Here we used 3 for the synthesis of a phosphonamidate modified cleavable MMAF **4**.

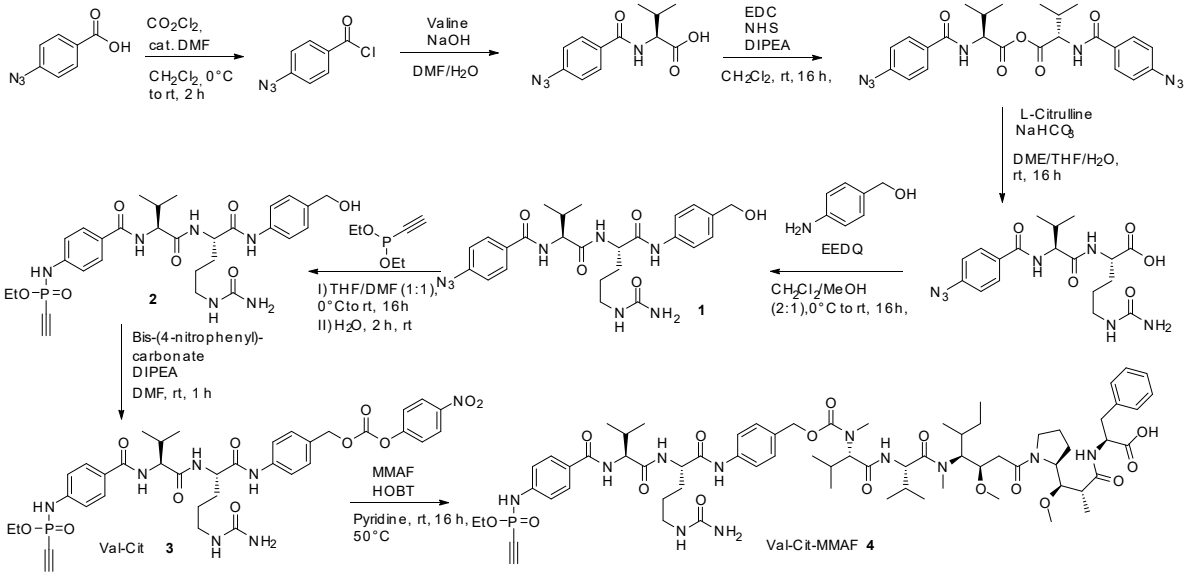

1.2. Figure S2

Synthetic scheme for the attachment of **4** to trastuzumab. Deconvoluted spectrum of deglycosylated and reduced trastuzumab-**4**. LC: Light chain, HC: Heavy Chain. DAR: Drug to Antibody Ratio.

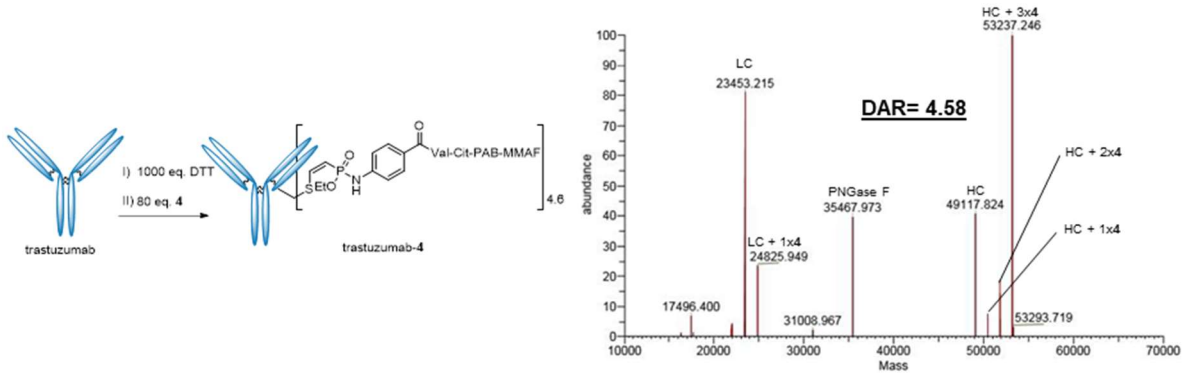

1.3. Figure S3

Increased cytotoxicity of MMAF linked trastuzumab on a Her2 overexpressing cell line (SKBR3) and a control (MDAMB468), demonstrated in a Resazurin assay. Plots depict cell viability after antibody treatment in dependency of the antibody concentration. Trastuzumab alone (pink) and trastuzumab-**4** (green). (See chapter 3.4 for details)

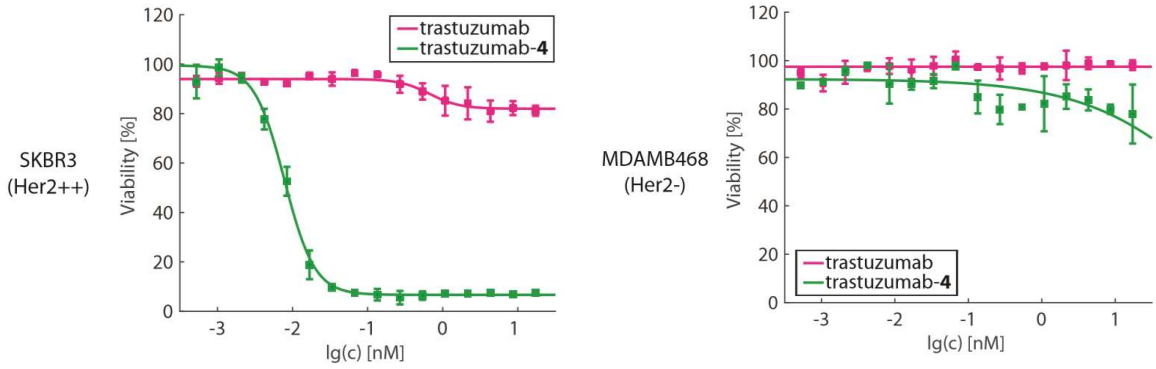

1.4. Figure S4

Effect of trastuzumab-**4** treatment on mitotic tubulin organization in BT474 (Her2+) cells. Shown are three representative images of mitotic BT474 cells after 4 days of treatment with 0.3 nM trastuzumab-**4** (a) and untreated (b). DAPI stain visualizes DNA condensation. Anti α-tubulin immunostaining visualizes spindle organization in untreated mitotic cells. Cells treated with trastuzumab-**4** show DNA condensation but a strongly altered and distorted α-tubulin pattern.

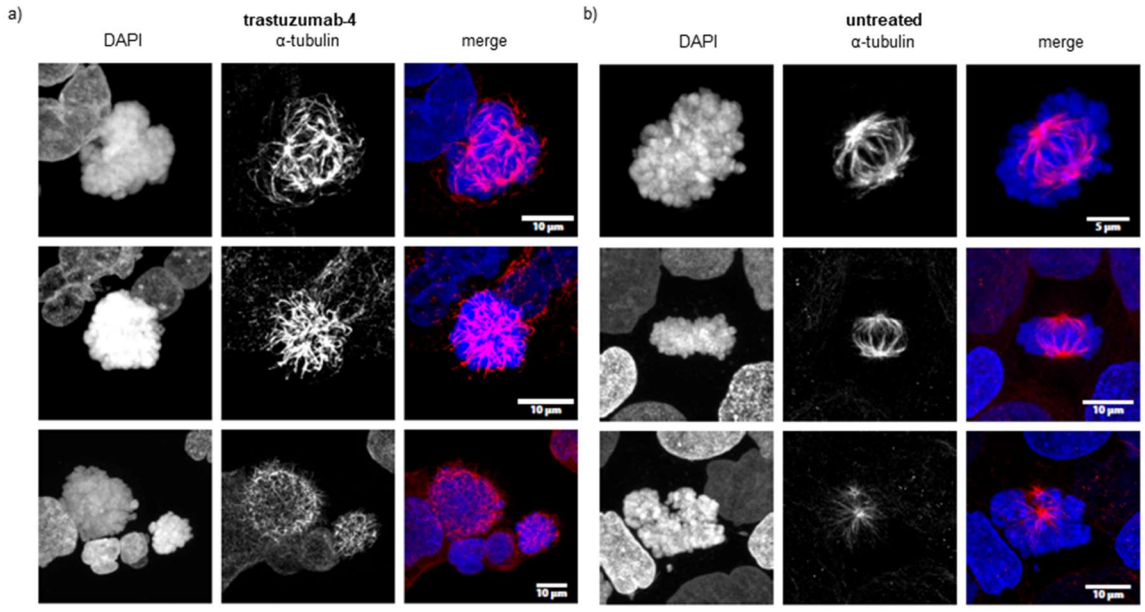

1.5. Figure S5

Solubility measurements of **9** (red), **10** (green) and vedotin (cyan) in PBS with 5% DMSO and Inosine as an internal standard. (See chapter 3.5 for details) a) Calibration curves of different analyte concentrations (5, 10, 50, 100 and 200 µM) were recorded by UPLC/UV by peak integration of the analyte in relation to Inosin as an internal standard. Shown are error bars from three independent measurements (black) and a linear fit. Values that were out of the concentration range and therefore not in the linear region were excluded from the fit (grey). b) Three independent measurements of saturated solutions and concentration calculation with the linear equation, estimated in a.

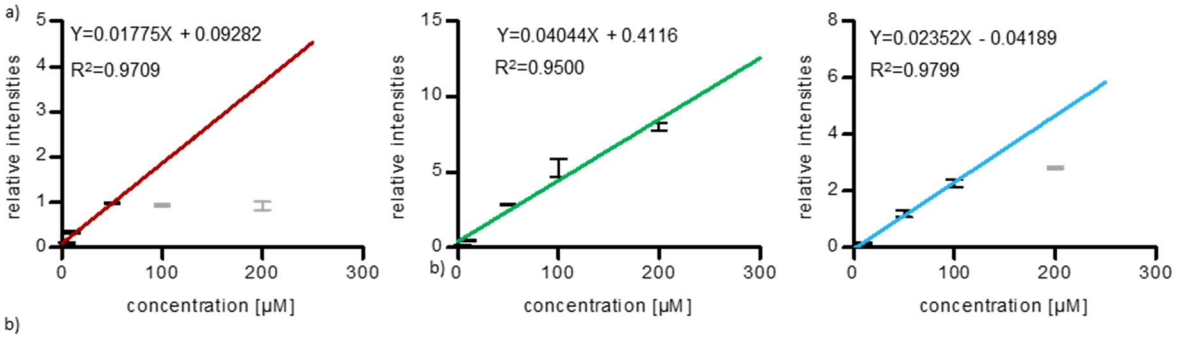

b)

relative intensities	concentration [µM]	relative intensities	concentration [µM]	relative intensities	concentration [µM]
1.47054541	78	12.19842	291	3.57240427	154
1.75660984	93	12.9149908	309	3.87751283	167
2.10353633	113	12.2324009	292	3.53587418	152

1.6. Figure S6

Modification of brentuximab at **1 mg/ml** with varying equivalents of the vedotin analog **10** delivers ADCs with different DARs. (See chapter 3.7 for details) a) SDS-PAGE of brentuximab, reduced with 1000 eq. DTT and alkylated with **10**. Modification was carried out under the same conditions for every reaction: 1 mg/ml antibody, 50 mM tris-buffer, 1 mM EDTA pH 8.5 and 5% DMSO; reaction over-night at 14°C as described in chapter 3.6. b) Exemplary MS-spectrum and calculated DAR of sample in lane 5 (modification carried out with 10 eq. **10**), as described in chapter 3.9. HC: heavy chain, LC: light chain. *deconvolution artefacts (half mass of HC species and double mass of LC species) c) Plot of phosphonamidate equivalents against the measured DAR. Shown are results of 20 independent experiments (dots) and an exponential fit (solid line, R^2= 0.9540). Red line marks the theoretical equivalents (16 in this case) to reach a DAR of 4.

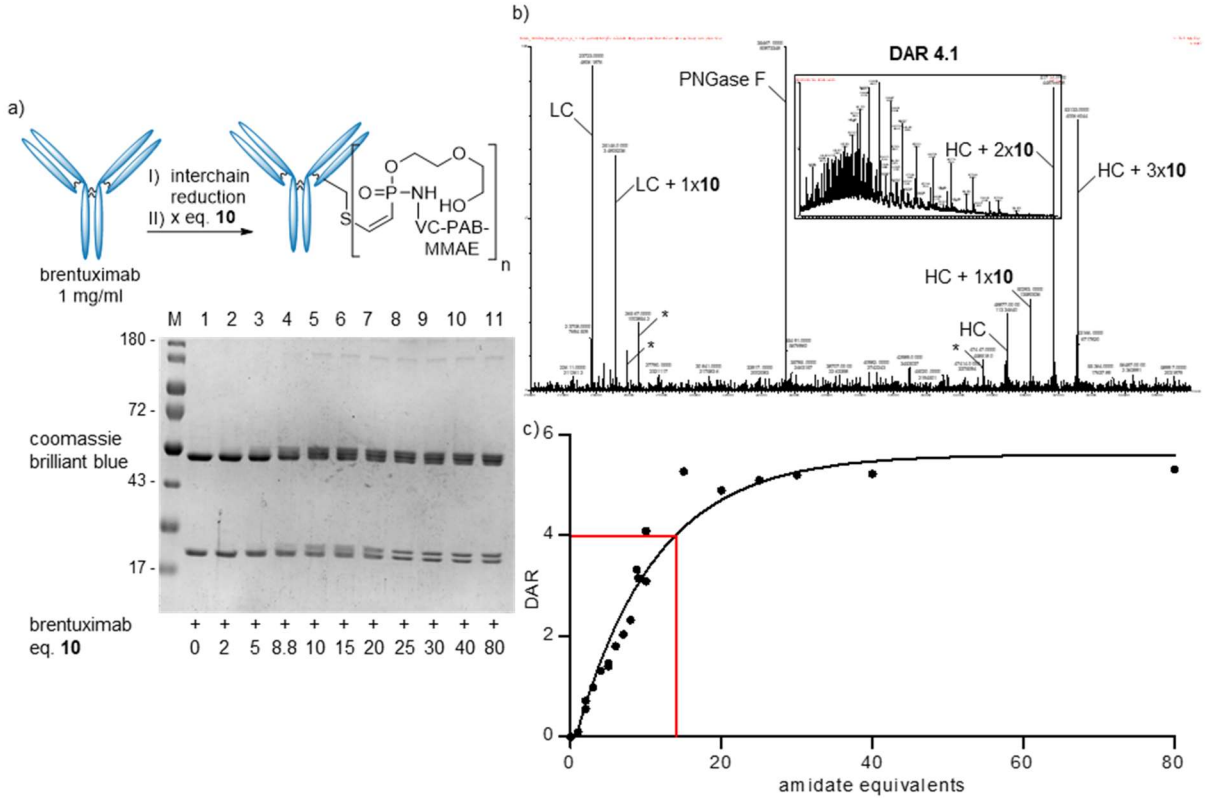

1.7. Figure S7

Increased conjugation efficiency can be observed at **5 mg/ml** brentuximab. (See chapter 3.8 for details) a) DAR-analysis of brentuximab, reduced with 200 eq. of DTT and alkylated with **10**. Modification was carried out under the same conditions for every reaction: 5 mg/ml antibody, 50 mM tris-buffer, 1 mM EDTA pH 8.5 and 5% DMSO; reaction over-night at 14°C as described in chapter 3.7. DAR-analysis was carried as described in chapter 3.9. b) Exemplary MS-spectrum and calculated DAR of sample in lane 2 (modification carried out with 6 eq. **10**). HC: heavy chain, LC: light chain.

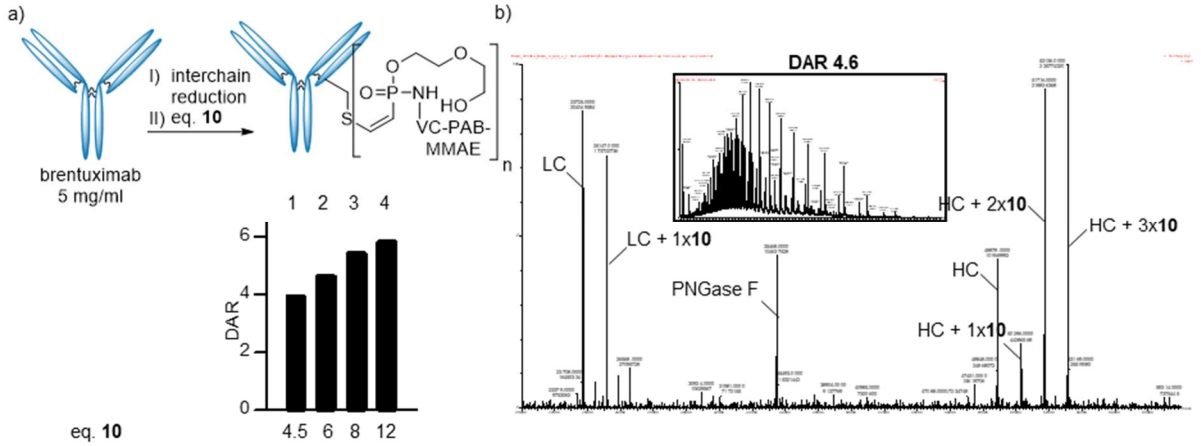

1.8. Figure S8

Partial reduction of the interchain disulfides with small excess of TCEP yields ADCs with a high conjugation effiency in a one-step procedure. (See chapter 3.9 for details) a) DAR-analysis of brentuximab, reduced and alkylated with **10**. Modification was carried out under the same conditions for every reaction with varying equivalents of TCEP: 5 mg/ml antibody, 50 mM tris-buffer, 100 mM NaCl, 1 mM EDTA pH 8.5, 167 µM **10** (5.0 eq.) and 5% DMSO; reaction over-night at 14°C as described in chapter 3.8. DAR-analysis was carried as described in chapter 3.9. b) Exemplary MS-spectrum and calculated DAR of sample in lane 3 (modification carried out with 3 eq. TCEP). HC: heavy chain, LC: light chain.

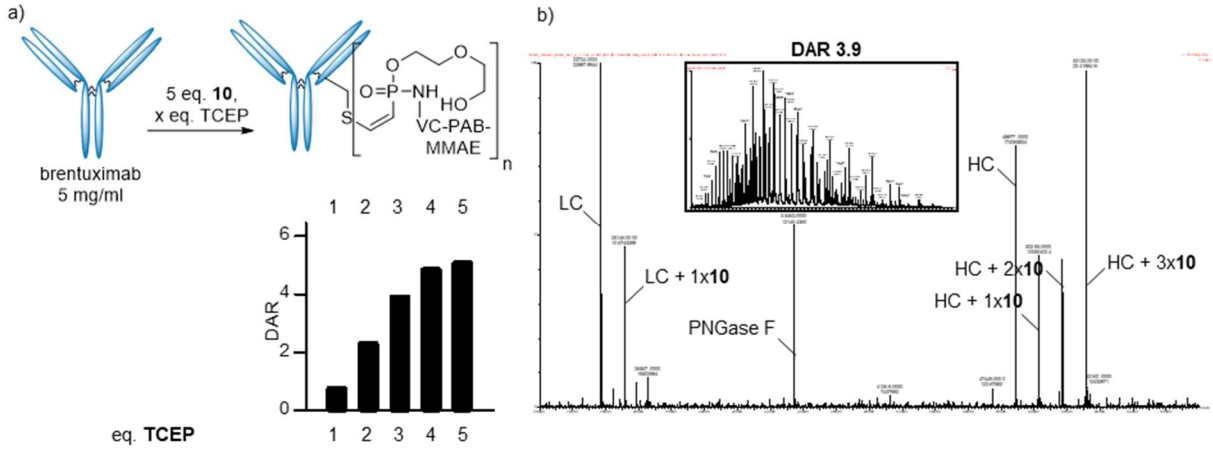

1.9. Figure S9

DAR analysis of brentuximab-**10** (a, green) and Adcetris® (b, cyan) after incubation in rat serum for 0, 3 and 7 days as described in chapter 3.12. Shown are values from three independent measurements for each time point. We measured a DAR of 3.05 (mean of three measurements) for Adcetris at Day 0, even though, Adcetris is known to be modified with an average of 4 drug molecules.[2] We attribute this to a loss of modification during the analysis process of pulldown, deglycosylation, reduction and MS-analysis. Since this sample-preparation was conducted in the same way for day 0, 3 and 7, this should not influence the relative values, given in the main manuscript. c) MS analysis of two Adcetris® measurements (day 0 top and day 3 bottom) indicating hydrolysis of the vedotin molecules that are still attached to the antibody. From this we concluded complete hydrolysis of maleimides to the open ring form at day 3, resulting in no further retro-Michael addition and associated payload loss until day 7

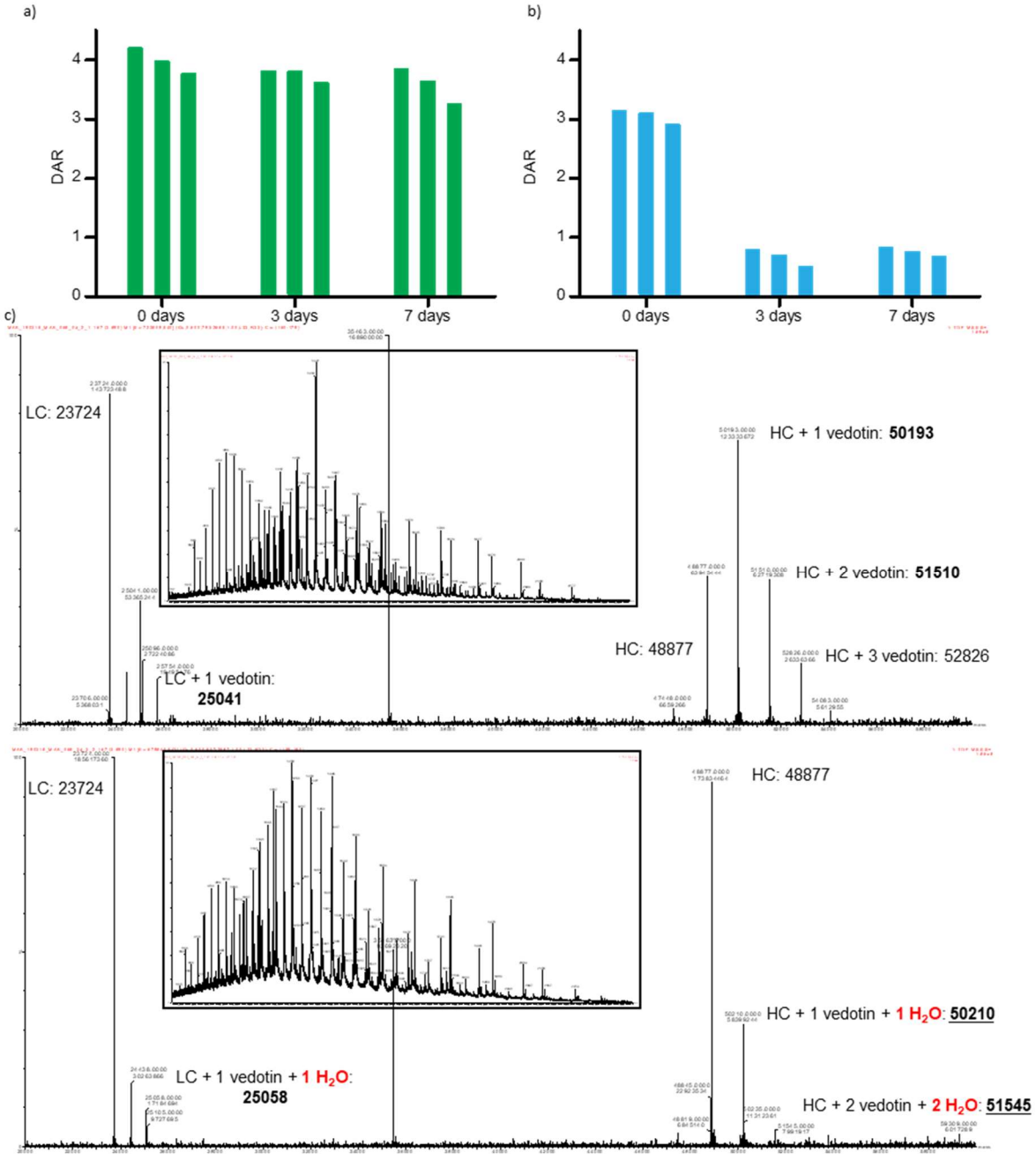

1.10. Figure S10

Size-exclusion HPLC analysis of Brentuximab-**10** after storage at different temperatures in PBS. Chromatograms were recorded after 0, 7 and 14 days. Chromatograms are normalized to the maximal intensity. (See chapter 3.13 for details)

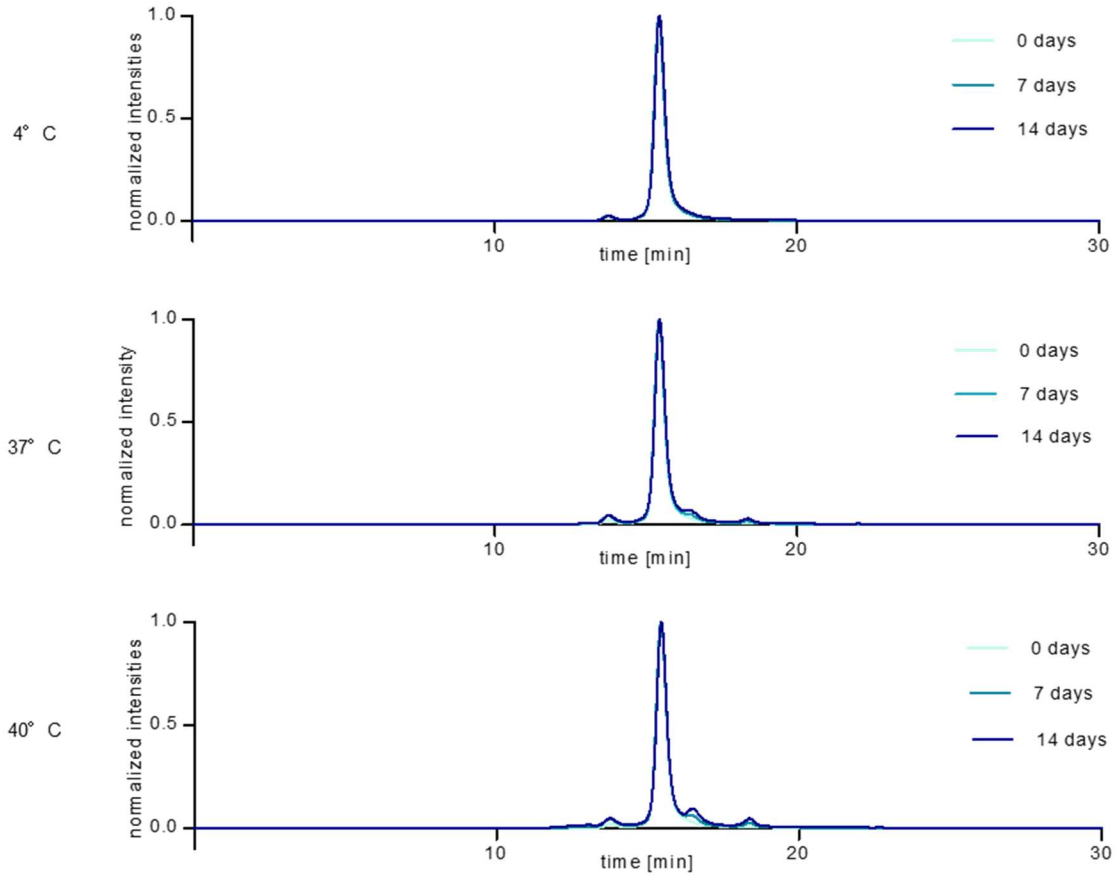

1.11. Figure S11

Changes in bodyweight (top) and tumorvolumes (bottom) of SCID mice with a Karpas 299 tumor xenograft after treatment with PBS (magenta), Brentuximab-**10** (blue) or PBS (green). Shown are tumor volumes of eight mice per group separately. a) 1. Study: Shown are tumor volumes of four mice per group separately treated at day 7 and 10 with 1 mg/kg ADC. b) 2. Study: Shown are tumor volumes of eight mice per group separately treated at day 8 and 11 with 0.5 mg/kg ADC. (See chapter 3.14 for details)

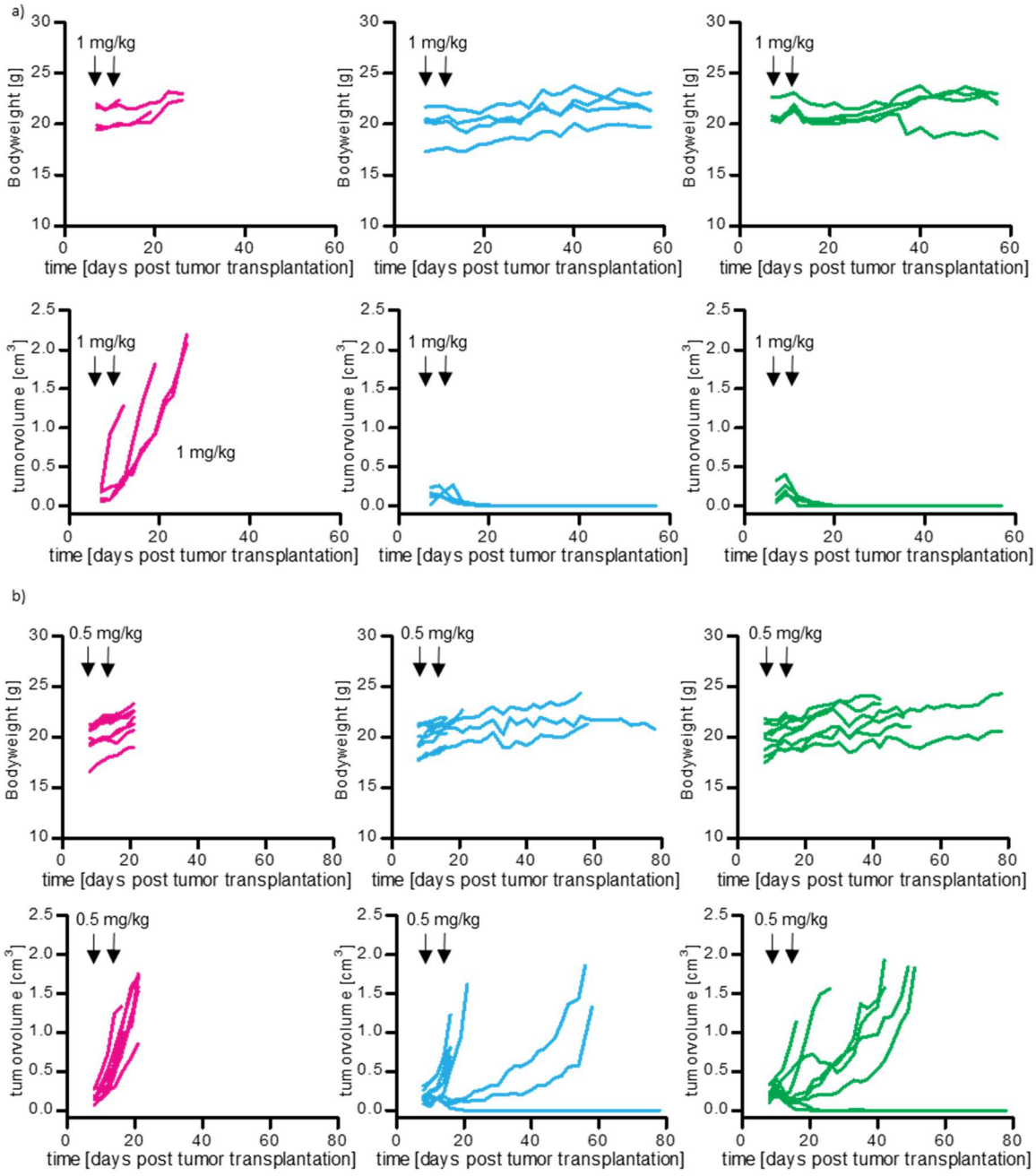

2. General Information

2.1. Chemicals and solvents

Chemicals and solvents were purchased from Merck (Merck group, Germany), TCI (Tokyo chemical industry CO., LTD., Japan) and Acros Organics (Thermo Fisher scientific, USA) and used without further purification. Dry solvents were purchased from Acros Organics (Thermo Fisher scientific, USA). Adcetris was obtained from Takeda.

2.2. Flash- and thin layer chromatography

Flash column chromatography was performed, using NORMASIL 60® silica gel 40-63 µm (VWR international, USA). Glass TLC plates, silica gel 60 W coated with fluorescent indicator F254s were purchased from Merck (Merck Group, Germany). Spots were visualized by fluorescence depletion with a 254 nm lamp or manganese staining (10 g K_2CO_3, 1.5 g $KMnO_4$, 0.1 g NaOH in 200 ml H_2O), followed by heating.

2.3. Preparative HPLC

Preparative HPLC was performed on a Gilson PLC 2020 system (Gilson Inc, WI, Middleton, USA) using a VP 250/32 Macherey-Nagel Nucleodur C18 HTec Spum column (Macherey-Nagel GmbH & Co. Kg, Germany). The following gradients were used: Method C: (A = H_2O + 0.1% TFA (trifluoroacetic acid), B = MeCN (acetonitrile) + 0.1% TFA, flow rate 30 ml/min, 5% B 0-5 min, 5-90% B 5-60 min, 90% B 60-65 min. Method D: (A = H_2O + 0.1% TFA, B = MeCN + +0.1% TFA), flow rate 30 ml/min, 5% B 0-5 min, 5-25% B 5-10 min, 25%-45% B 10-50 min, 45-90% 50-60 min, 90% B 60-65 min. Method E: 0.1% TFA, flow rate 18 ml/min, 5% B 0-5 min, 5-90% B 5-60 min, 90% B 60-65 min, using a VP 250/21 Macherey-Nagel Nucleodur C18 HTec Spum column (Macherey-Nagel GmbH & Co. Kg, Germany)

2.4. Semi-preparative HPLC

Semi-preparative HPLC was performed on a Shimadzu prominence HPLC system (Shimadzu Corp., Japan) with a CBM20A communication bus module, a FRC-10A fraction collector, 2 pumps LC-20AP, and a SPD-20A UV/VIS detector, using a VP250/10 Macherey-Nagel Nucleodur C18 HTec Spum column (Macherey-Nagel GmbH & Co. Kg, Germany). The following gradients were used: Method F: (A = H_2O + 0.1% TFA, B = MeCN + +0.1% TFA), flow rate 5 ml/min, 30% B 0-5 min, 30-99% B 5-65 min, 99% B 65-75 min.

2.5. NMR

NMR spectra were recorded with a Bruker Ultrashield 300 MHz spectrometer and a Bruker Avance III 600 MHz spectrometer (Bruker Corp., USA) at ambient temperature. Chemical shifts δ are reported in ppm relative to residual solvent peak ($CDCl_3$: 7.26 [ppm]; DMSO-d6: 2.50 [ppm] for ^{1}H-spectra and $CDCl_3$: 77.16 [ppm]; DMSO-d6: 39.52 [ppm] for ^{13}C-spectra . Coupling constants *J* are stated in Hz. Signal multiplicities are abbreviated as follows: s: singlet; d: doublet; t: triplet; q: quartet; m: multiplet.

2.6. HR-MS

High resolution ESI-MS spectra were recorded on a Waters H-class instrument equipped with a quaternary solvent manager, a Waters sample manager-FTN, a Waters PDA detector and a Waters column manager with an Acquity UPLC protein BEH C18 column (1.7 µm, 2.1 mm x 50 mm). Samples were eluted with a flow rate of 0.3 mL/min. The following gradient was used: A: 0.01% FA in H_2O; B: 0.01% FA in MeCN. 5% B: 0-1 min; 5 to 95% B: 1-7min; 95% B: 7 to 8.5 min. Mass analysis was conducted with a Waters XEVO G2-XS QTof analyzer.

2.7. UPLC-UV/MS

UPLC-UV/MS traces were recorded on a Waters H-class instrument equipped with a quaternary solvent manager, a Waters autosampler, a Waters TUV detector and a Waters Acquity QDa detector with an Acquity UPLC BEH C18 1.7 µm, 2.1 x 50 mm RP column with a flow rate of 0.6 mL/min (Waters Corp., USA). The following gradient was used for purity analyses: A: 0.1% TFA in H_2O; B: 0.1% TFA in MeCN. 5% B 0 - 1.5 min, 5-95% B 1.5-11 min, 95% B 11-13 min, 5% B 13-15 min. The following gradient was used in the solubility assay: A: 0.1% TFA in H_2O; B: 0.1% TFA in MeCN. 5% B 0 - 0.5 min, 5-95% B 0.5-3 min, 95% B 3-3.9 min, 5% B 3.9-5 min.

2.8. Intact protein MS (trastuzumab conjugates only)

Reduced antibody subunits were analyzed using a reversed-phase liquid chromatography system (Dionex Ultimate 3000 NCS-3500RS Nano, Thermo Scientific) connected to an Orbitrap Fusion mass spectrometer (Thermo Scientific). Chromatographic separation was performed with an Acquity UPLC protein BEH C4 column (300 Å, 1.7 µm, 2.1 mm x 50 mm). Component A of the mobile phase was 0.01% formic acid in water and component B consist of Acetonitrile with 0.01% formic acid. Separation was performed with a flow rate of 300 µL/min within 7.5 min linear gradient starting with 0% and ending with 40% of component B, followed by a flushing step until 80% of component B. Proteins were ionized in positive ion mode applying a spray voltage of 4.5 kV, using sheath gas (75 Arb), aux gas (12 Arb), sweep gas (1 Arb) and a vaporizer temperature of 300°C. Ionized proteins were analyzed in intact protein mode with a resolution of 15000 (FWHM), 10 microscans and a scan range of m/z 500-3000. The maximum injection time was set to 100 ms to reach an AGC-Target value of 5e5.

Raw data were analyzed with ProteinDeconvolut version 3.0 (Thermo Scientific), considering a m/z range of 800-3000 and charge states ranging from 10-100. 30000 was used as a targeted mass and the intact protein model was chosen. The output mass range was 10000-70000.

2.9. Intact protein MS (all brentuximab conjugates)

Intact proteins were analyzed using a Waters H-class instrument equipped with a quaternary solvent manager, a Waters sample manager-FTN, a Waters PDA detector and a Waters column manager with an Acquity UPLC protein BEH C4 column (300 Å, 1.7 µm, 2.1 mm x 50 mm). Proteins were eluted with a flow rate of 0.3 mL/min. The following gradient was used: A: 0.01% FA in H_2O; B: 0.01% FA in MeCN. 5-95% B 0-6 min. Mass analysis was conducted with a Waters XEVO G2-XS QTof analyzer. Proteins were ionized in positive ion mode applying a cone voltage of 40 kV. Raw data was analyzed with MaxEnt 1.

2.10. Preparative size-exclusion chromatography

Protein purification by size-exclusion chromatography was conducted with an ÄKTA FPLC system (GE Healthcare, United States) equipped with a P-920 pump system, a UPC-900 detector and a FRAC-950 fraction collector.

2.11. Analytical size-exclusion chromatography

Analytical size-exclusion chromatography (A-SEC) of the ADCs was conducted on a Vanquish Flex UHPLC System with a DAD detector, Split Sampler FT (4°C), Column Compartment H (25°C) and binary pump F (Thermo Fisher Scientific, USA) using a MAbPac SEC-1 300 Å, 4 x 300 mm column (Thermo Fisher Scientific, USA) with a flow rate of 0.15 mL/min. Separation of different ADC/mAb populations have been achieved during a 30 minute isocratic gradient using a phosphate buffer at pH 7 (20 mM Na_2HPO_4/NaH_2PO_4, 300 mM NaCl, 5% v/v isopropyl alcohol as a mobile phase. 8 µg ADC/mAb where loaded onto the column for A-SEC analysis.

UV chromatograms were recorded at 220 and 280 nm. Quantification of monomer and HMWS was achieved after integration of the peak area at 220 nm.

3. Experimental procedures

3.1. Trastuzumab production

Trastuzumab expression and purification was executed as previously published with an additional final purification by gel filtration on a Superdex 200 Increase 10/300 from GE (GE life sciences, USA) with PBS and flow rate of 0.75 ml/min.[3]

3.2. Synthesis and analysis of trastuzumab-MMAF conjugates

Trastuzumab modification was carried out by incubating freshly expressed antibody (0.5 mg/ml, 3.33 µM) with 1000 eq. of DTT in a buffer containing 50 mM sodium borate in PBS (pH 8.0) with a total volume of 80 µl at 37 °C for 40 min. Excess DTT removal and buffer exchange to a solution containing 50 mM NH_4HCO_3 and 1mM EDTA (pH 8.5) was conducted afterwards using 0.5 mL Zeba™ Spin Desalting Columns with 7K MWCO (Thermo Fisher Scientific, USA). 4 µl of *O*-Ethyl-*P*-ethynyl-phosphonamidate-VC-PAB-MMAF **4**, dissolved in DMSO (5.33 mM) were added quickly to reach a final DMSO content of 5% and 80 eq. phoshonamidate with respect to the antibody. The mixture was shaken at 850 rpm and 14 °C for 16 hours. Excess reagent was again removed by buffer exchange to sterile PBS using 0.5 mL Zeba™ Spin Desalting Columns with 7K MWCO.

For SDS-page-analysis, 2 µl of the crude reaction mixture were mixed with 10 µl of ultrapure water and 4 µl Laemmli sample buffer (Bio-Rad Laboratories, USA) containing 0.4 µl 2-mercaptoethanol. Samples were heated to 95 °C for 15 minutes and completely loaded to the SDS-PAGE gel.

For MS analysis: The modified antibody was rebuffered to 100 mM NH_4HCO_3 and 500 mM NaCl using 75 µL Zeba™ Spin Desalting Columns with 7K MWCO (Thermo Fisher Scientific, USA). 8 µl of this solution were treated with 1 µl RapiGest™ (Waters Corp., USA) solution (1% in H_2O) and heated to 60 °C for 30 min. The solution was allowed to cool to room temperature, 1 µl PNGase-F solution (Pomega, Germany, Recombinant, cloned from Elizabethkingia miricola 10 u/µl) was added and the solution was incubated at 37 °C over night. Remaining disulfide bridges were reduced by addition of 1 µl DTT solution (50 mM in H_2O) and incubation at 37°C for 30 min. Samples were diluted with 1% HCl subjected to MS analysis with the Orbitrap Fusion system. (See chapter 2.8)

MS spectrum shows the ion series, which was deconvoluted to obtain the spectrum in Figure 1b.

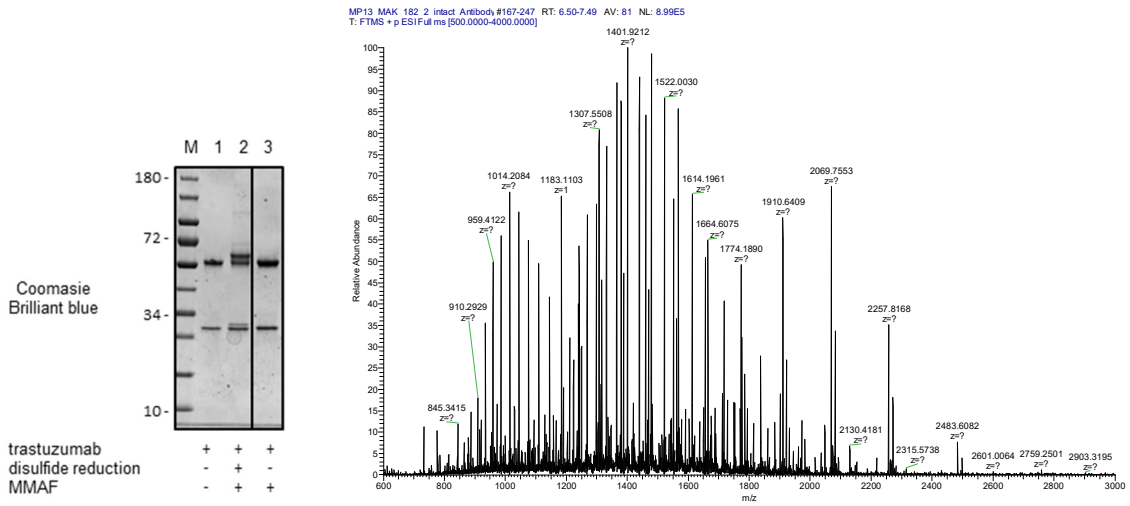

3.3. Cell based antiproliferation assays

Antiproliferation assays were conducted as previously reported[3] with the following minor changes:

- For MDAMB468 cells, a reduced amount of $2*10^3$ cells were seeded in each well of a 96-well optical cell culture plate supplemented with 100 µL culture media.
- Images were acquired with an Operetta High-Content Imaging system (PerkinElmer, Waltham, MA, USA) equipped with a 20× high NA objective.
- Cell counts were calculated from duplicates

3.4. Resazurin assay

HL60 and Karpas cell lines were cultured in RPMI-1640 supplemented with 10% FCS and 0.5% Penicillin-Streptomycin. SKBR3 and MDAMB468 cell lines were cultured in DMEM/F12 supplemented with 10% FCS and 0.5% Penicillin-Streptomycin. Cells were seeded at a density of 5*10^3 cells/well (SKBR3, HL60 and Karpas) or 1*10^3 cells/well (MDAMB468) in 96-well cell culture microplate. 1:4 serial dilutions of ADCs or antibodies were performed in cell culture medium starting at 3 µg/mL final concentration and transferred in duplicates to respective wells on the microplate. Plates were incubated for 96 h at 37°C 5 % CO_2. Subsequently, resazurin was added to a final concentration of 50 µM followed by incubation for 3 – 4 h at 37°C, 5% CO_2. Metabolic conversion of resazurin to resorufin is quantified by the fluorescent signal of resorufin (λ_{EX} = 560 nm and λ_{EM} = 590 nm) on a Tecan Infinite M1000 micro plate reader. Mean and standard deviation was calculated from duplicates, normalized to untreated control and plotted against antibody concentration. Data analysis was performed with MatLab R2016 software.

3.5. Solubility assay

The aqueous solubility of compounds **9**, **10** and vedotin was determined using a shake flask solubility assay. Saturated solutions of the compounds in 5% DMSO/PBS at pH 7.4 were prepared in triplicates by adding 2 µL of compound (40 mM in DMSO) to 38 µL PBS, pH 7.4 containing 50 µM inosine as internal standard. The samples were incubated at 25°C for 2h and subsequently subjected to high-speed centrifugation (10 minutes, 16873 rcf). The supernatant was analyzed by UPLC/UV and the concentration was determined using a standard curve. For the standard curves, serial dilutions in 5% DMSO/PBS at pH 7.4 containing 50 µM Inosine were prepared in triplicates with final compound concentrations of 5 µM, 10 µM, 50 µM, 100 µM and 200 µM. The samples were incubated at 25°C for 2 h and subsequently subjected to high-speed centrifugation (10 minutes, 16873 rcf). The supernatant was analyzed by UPLC/UV and the peak area of compound and internal standard were integrated. The normalized peak

areas (integrated area compound divided by integrated area standard) were plotted against the concentration and a linear fit was applied within the respective solubility range.

3.6. Brentuximab production

Brentuximab expression and purification was executed in analogy to trastuzumab with final purification by gel filtration on a Superdex 200 Increase 10/300 from GE (GE life sciences, USA) with PBS and flow rate of 0.75 ml/min.

3.7. Procedure for the modification of brentuximab (1mg/ml) with different equivalents of 10

35 µl of a 70 mM solution of DTT in 50 mM sodium borate in PBS (pH 8.0) was added to 350 µl of a brentuximab solution of 1.0 mg/ml in 50 mM sodium borate in PBS (pH 8.0) and the mixture was incubated at 37 °C for 40 min. Excess DTT removal and exchange to the conjugation buffer (50 mM Tris, 1 mM EDTA, 100 mM NaCl, pH 8.5 at 14°C) was conducted afterwards using 2 mL Zeba™ Spin Desalting Columns with 7K MWCO (Thermo Fisher Scientific, USA). 50 µl of the reduced antibody solution (0.91 mg/ml, 6.07 µM antibody) were mixed quickly afterwards with the desired amount of *O*-2-(2-Hydroxyethoxy)ethyl-*P*-ethynyl-phosphonamidate-VC-PAB-MMAE **10** dissolved in DMSO to give a final amount of 5% DMSO. The mixture was shaken at 850 rpm and 14 °C for 16 hours. For SDS-page-analysis, 2 µl of the crude reaction mixture were mixed with 10 µl of ultrapure water and 4 µl Laemmli sample buffer (Bio-Rad Laboratories, USA) containing 0.4 µl 2-mercaptoethanol. Samples were heated to 95 °C for 15 minutes and completely loaded to the SDS-PAGE gel.

3.8. Procedure for the modification of brentuximab (5.0 mg/ml) with different equivalents of 10

5 µl of a 70 mM solution of DTT in 50 mM sodium borate in PBS (pH 8.0) was added to 50 µl of a brentuximab solution of 5.0 mg/ml in 50 mM sodium borate in PBS (pH 8.0) and the mixture was incubated at 37 °C for 40 min. Excess DTT removal and exchange to the conjugation buffer (50 mM Tris, 1 mM EDTA, 100 mM NaCl, pH 8.5 at 14°C) was conducted afterwards using 0.5 mL Zeba™ Spin Desalting Columns with 7K MWCO (Thermo Fisher Scientific, USA). 50 µl of the reduced antibody solution (4.55 mg/ml, 30.30 µM antibody) were mixed quickly afterwards with desired amount of *O*-2-(2-Hydroxyethoxy)ethyl-*P*-ethynyl-phosphonamidate-VC-PAB-MMAE **10** dissolved in DMSO to give a final amount of 5% DMSO. The mixture was shaken at 850 rpm and 14 °C for 16 hours.

3.9. Procedure for the partial reduction of brentuximabs interchain disulfide bonds with TCEP

50 µl of a brentuximab solution of 5.0 mg/ml in conjugation buffer (50 mM Tris, 1 mM EDTA, 100 mM NaCl, pH 8.5 at 14°C) were mixed with 5 µl of a TCEP solution in conjugation buffer containing the appropriate amount of TCEP. Directly afterwards, 2.75 µl of a 3.03 mM solution of *O*-2-(2-Hydroxyethoxy)ethyl-*P*-ethynyl-phosphonamidate-VC-PAB-MMAE **10** (5.0 eq. with respect to the antibody) dissolved in DMSO were added to give a final amount of 5% DMSO. The mixture was shaken at 850 rpm and 14 °C for 16 hours.

3.10. Procedure for DAR determination of brentuximab conjugates by intact protein MS

a)

40 µl of the crude antibody modification mixture were purified by size-exclusion chromatography with a 5 ml HiTrap® desalting column and a flow of 1.5 ml/min eluting with

100 mM $NaHCO_3$ and 500 mM NaCl over two column volumes. An exemplary chromatogram is shown below.

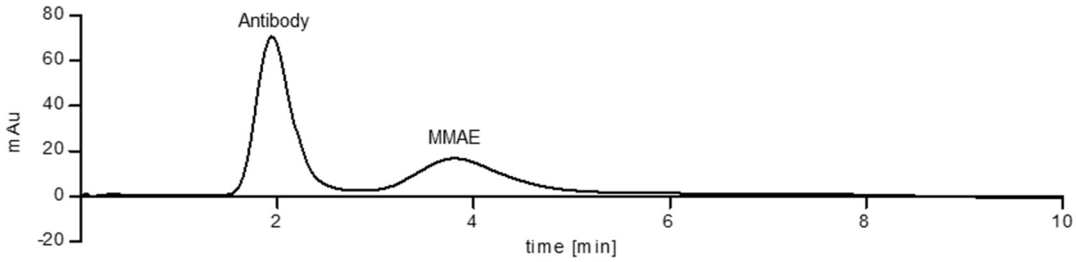

The antibody containing fractions were pooled and concentrated by spin-filtration to 40 µl (MWCO: 10 kDa, 0.5 ml, Sartorius, Germany).

b)

2 µl RapiGest™ solution (1% in H_2O) (Waters Corp., USA) were added and the solution was heated to 60 °C for 30 min. The solution was allowed to cool to room temperature, 1 µl PNGase-F solution (Pomega, Germany, Recombinant, cloned from Elizabethkingia miricola 10 u/µl) was added and the solution was incubated at 37 °C for at least 2 hours. Disulfide bridges were reduced by addition of 2 µl DTT solution (70 mM in H_2O) and incubation at 37°C for 30 min. Samples were diluted with 120 µl 1% HCl and subjected to intact protein MS (see chapter 2.9), injecting 5 µl for each sample.

c) For Adcetris pulldown samples from serum, 1 µl PNGase-F solution (Pomega, Germany, Recombinant, cloned from Elizabethkingia miricola 10 u/µl) was added to 20 µl of Adcetris in PBS and the solution was incubated at 37 °C for at least 2 hours. Disulfide bridges were reduced by addition of 2 µl DTT solution (70 mM in H_2O) and incubation at 37°C for 30 min. 10 µl of the samples were diluted with 190 µl of pure water and subjected to intact protein MS (see chapter 2.9), injecting 3 µl for each sample.

After deconvolution of the crude spectra, the DAR was determined with the following formula, were **I** corresponds to the mass intensities of the respective species.

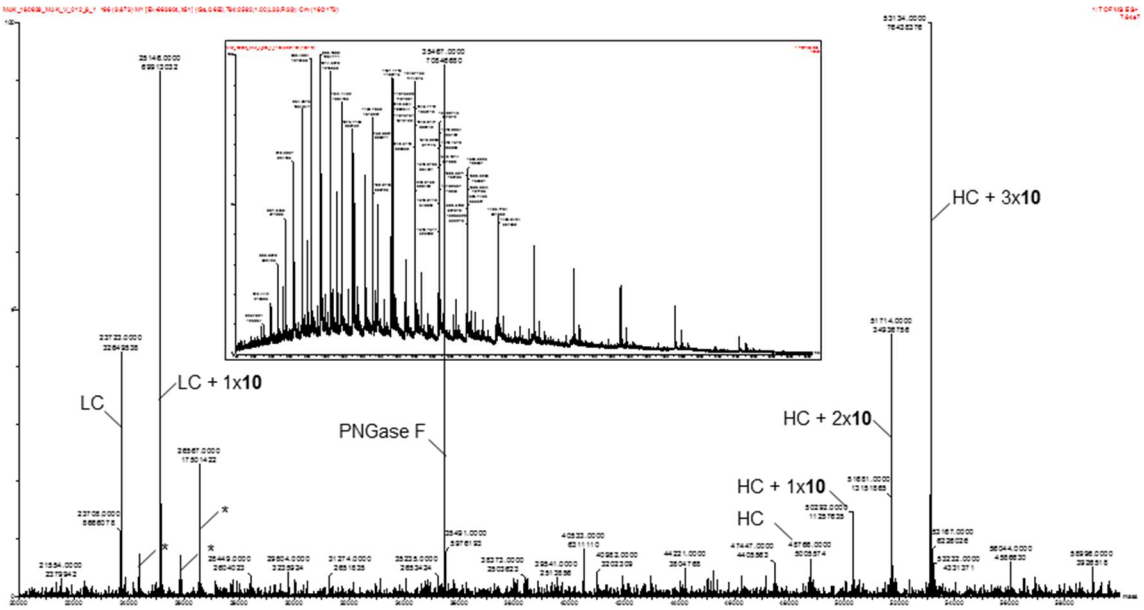

$$\mathrm{DAR} = 2 \times \frac{\mathrm{I}(LC+1x\mathbf{10})}{\mathrm{I}(LC)+\mathrm{I}(LC+1x\mathbf{10})} + 2 \times \frac{\mathrm{I}(HC+1x\mathbf{10})+2\times\mathrm{I}(HC+2x\mathbf{10})+3\times\mathrm{I}(HC+3x\mathbf{10})}{\mathrm{I}(HC)+\mathrm{I}(HC+1x\mathbf{10})+\mathrm{I}(HC+2x\mathbf{10})+\mathrm{I}(HC+3x\mathbf{10})}$$

3.11. Synthesis and purification of an ADC from brentuximab and 10.

240 µl of a 70 mM solution of DTT in 50 mM sodium borate in PBS (pH 8.0) were added to 2.4 ml of a brentuximab solution of 1.0 mg/ml in 50 mM sodium borate in PBS (pH 8.0) and the mixture was incubated at 37 °C for 40 min. Excess DTT removal and exchange to the conjugation buffer was conducted afterwards using 10 mL Zeba™ Spin Desalting Columns with 7K MWCO (Thermo Fisher Scientific, USA). The reduced antibody solution (0.91 mg/ml, 6.07 µM) was mixed quickly afterwards with 132 µl of a 1.94 mM solution of *O*-2-(2-Hydroxyethoxy)ethyl-*P*-ethynyl-phosphonamidate-VC-PAB-MMAE **10** dissolved in DMSO to give a final amount of 5% DMSO and 16 eq. phosphonamidate. The solution was shaken at 850 rpm and 14 °C for 16 hours. Afterwards, the mixture was concentrated to 900 µl by spin-filtration (MWCO: 10 kDa, 0.5 ml, Sartorius, Germany)

Alternatively, 48 µl of a 70 mM solution of DTT in 50 mM sodium borate in PBS (pH 8.0) was added to 480 µl of a brentuximab solution of 5.0 mg/ml in 50 mM sodium borate in PBS (pH 8.0) and the mixture was incubated at 37 °C for 40 min. Excess DTT removal and exchange to the conjugation buffer was conducted afterwards using 2 mL Zeba™ Spin Desalting Columns with 7K MWCO (Thermo Fisher Scientific, USA). The reduced antibody solution (4.55 mg/ml, 30.35 µM) was mixed quickly afterwards with 27.5 µl of a 2.73 mM solution of *O*-2-(2-Hydroxyethoxy)ethyl-*P*-ethynyl-phosphonamidate-VC-PAB-MMAE **10** dissolved in DMSO to give a final amount of 5% DMSO and 4. eq. phosphonamidate. The solution was shaken at 850 rpm and 14 °C for 16 hours.

The reaction mixtures were purified in two portions by size-exclusion chromatography with a 25 ml Superose™ 6 Increase 10/300GL (GE healthcare, United States) and a flow of 0.8 ml/min eluting with sterile PBS (Merck, Germany). The antibody containing fractions were pooled and concentrated by spin-filtration (MWCO: 10 kDa, 6 ml, Sartorius, Germany). For DAR analysis, 10 µl of this sample were mixed with 30 µl of a buffer containing 500 mM NaCl and 100 mM $NaHCO_3$and the sample was processed further as described under 3.9b. The final concentration was determined in a 96-well plate with a Pierce™ Rapid Gold BCA Protein Assay Kit (Thermo Fisher Scientific, USA) and a Bradford reagent B6916 (Merck, Germany) with pre-diluted protein assay standards of bovine gamma globulin (Thermo Fisher Scientific, USA). Results of both Assays were arithmetically averaged.

The ADC was analyzed by analytical size exclusion chromatography (a) and intact protein MS (b) before subsequent experiments. HC: heavy chain, LC: light chain. *deconvolution artefacts (half mass of HC species and double mass of LC species). It should be noted that no species was detected in the MS that could be assigned to any form of unconjugated MMAE.

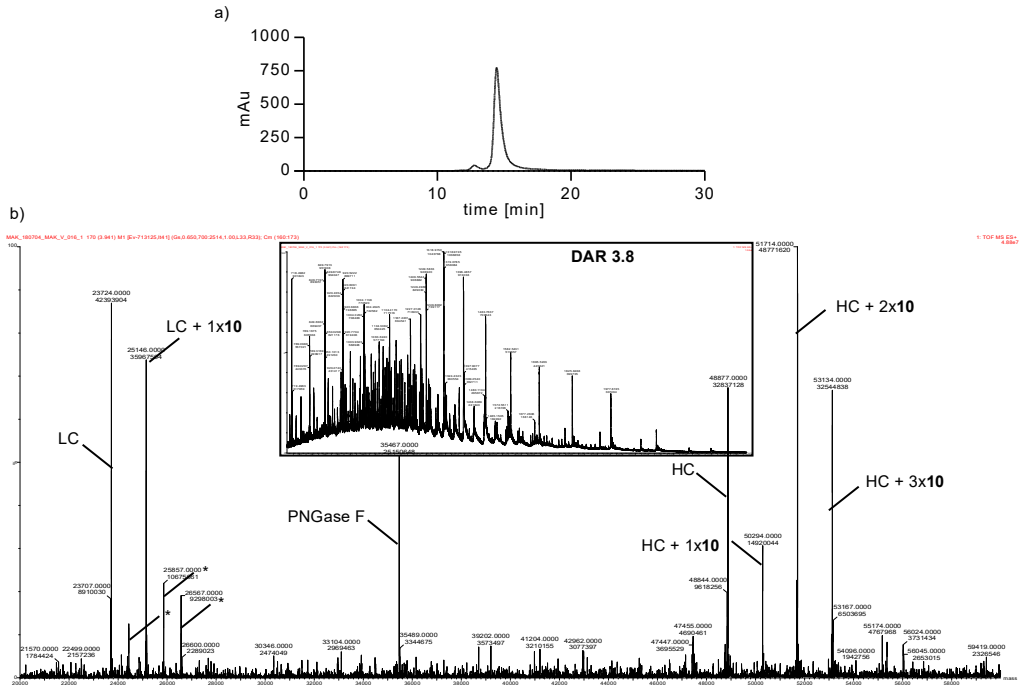

3.12. Stability studies in rat serum: ADC incubation serum and analysis of the DAR after antibody pulldown

In an Eppendorf-tube, 200 µl rat serum (Sigma Aldrich, United States) were mixed with 50 µl Brentuximab-**10** (2.0 mg/ml) or Adcetris® for each sample individually to give a final solution of 0.4 mg/ml ADC in 80% rat serum. Samples were sterile filtered with UFC30GV0S centrifugal filter units (Merck, Germany) and incubated at 37°C for 3 and 7 days. Samples for day 0 were directly processed further.

The supernatant of 50 µl anti human igG (Fc-Specific) agarose slurry (Sigma Aldrich, United States) was removed by centrifugation and the remaining resin washed three times with 200 µl PBS. The resin was incubated with 240 µl of the serum-ADC mix for 30 min at room temperature. Afterwards, the supernatant was removed and the resin washed 5 times with 200 µl PBS. Following by incubation for 5 minutes with 200 µl IgG elution buffer (Thermo-Fisher, United States) at room temperature. Now the supernatant was transferred into a Spin filter (MWCO: 10 kDa, 0.5 ml, Sartorius, Germany), rebuffered to a buffer containing 500 mM NaCl and 100 mM $NaHCO_3$, concentrated to 40 µl and processed further as described under 3.9b for the Brentuximab-**10** samples. Since we observed decomposition of the maleimide linkage in Adcetris® under our standard deglycosylation conditions, all Adcetris® samples were rebuffered to PBS, concentrated to 100 µl and processed further as described under 3.9c. All measurements were performed in triplicates (n=3). MS Spectra that were obtained after 0, 3 and 7 days are shown below. HC: heavy chain, LC: light chain.

0 days of incubation of brentuximab-**10** in rat serum at 37°C:

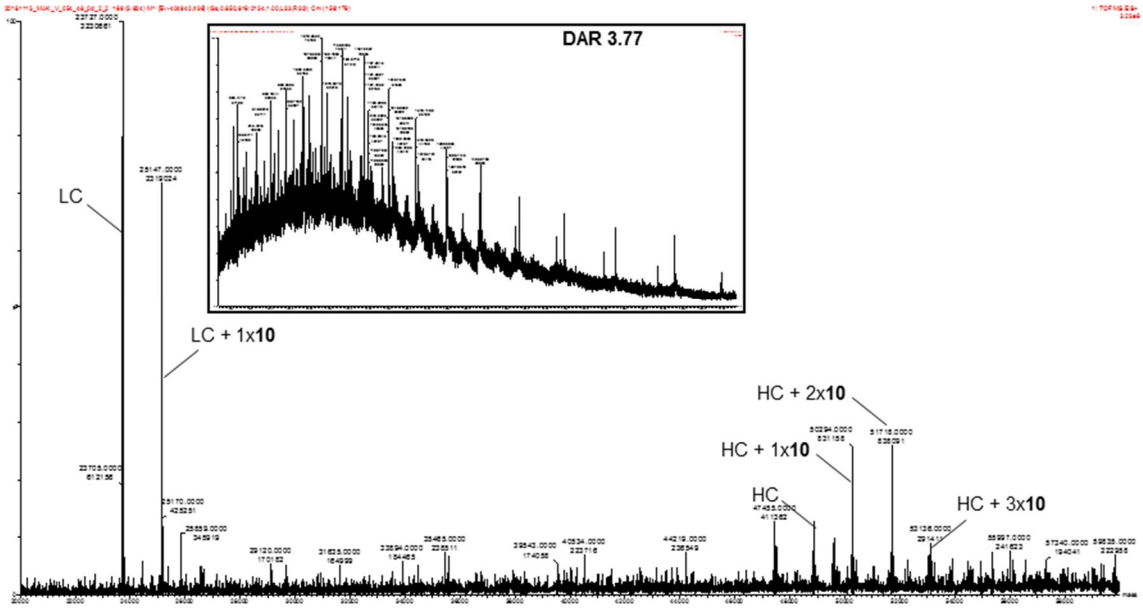

3 days of incubation of brentuximab-**10** in rat serum at 37°C:

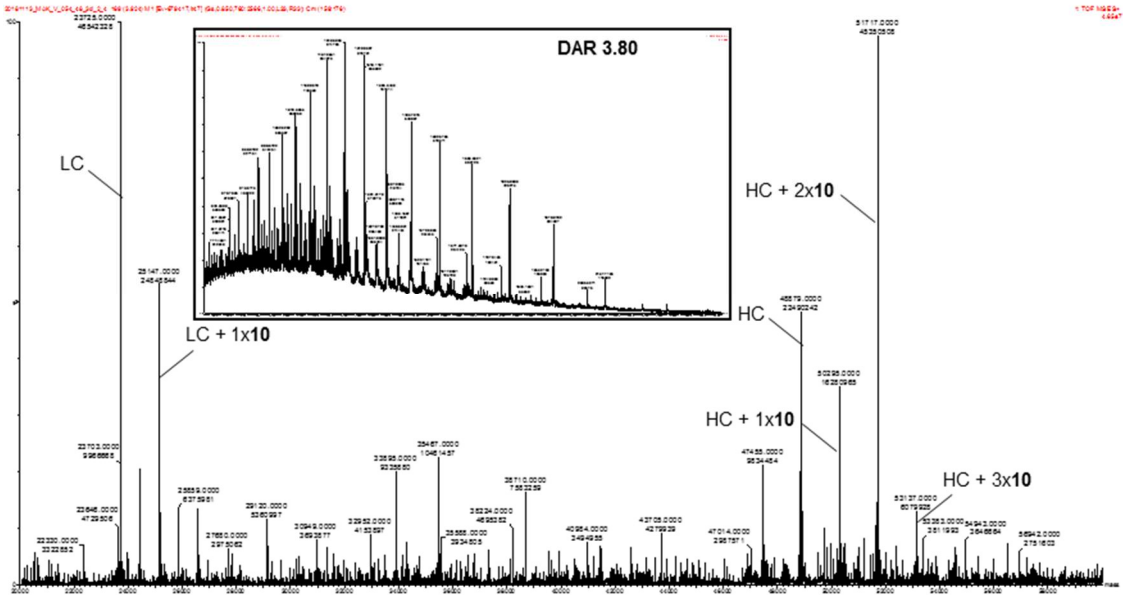

7 days of incubation of brentuximab-**10** in rat serum at 37°C:

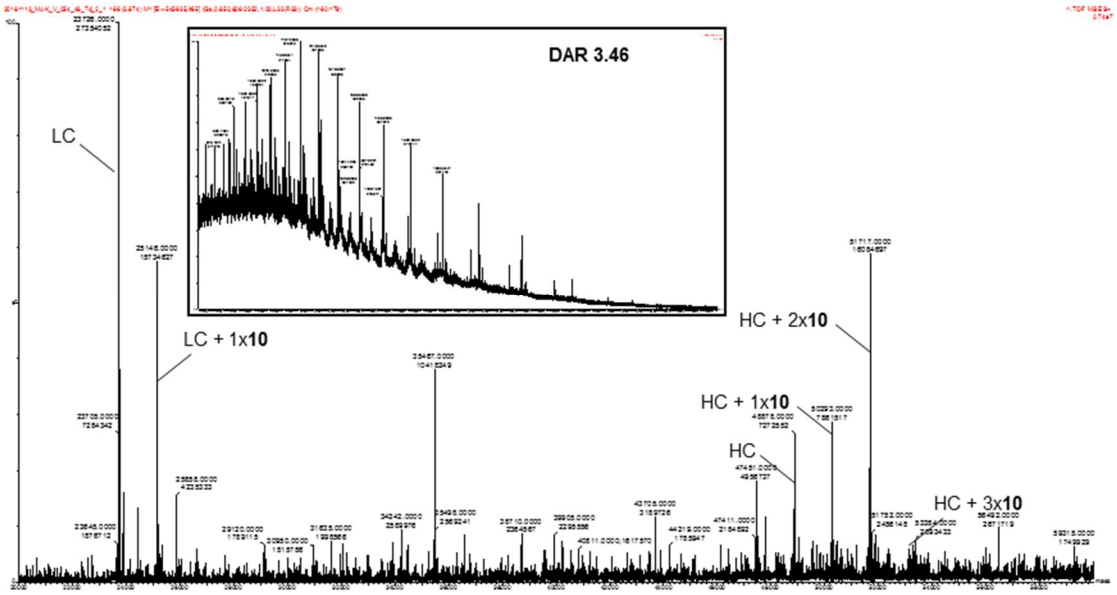

0 days of incubation of Adcetris® in rat serum at 37°C:

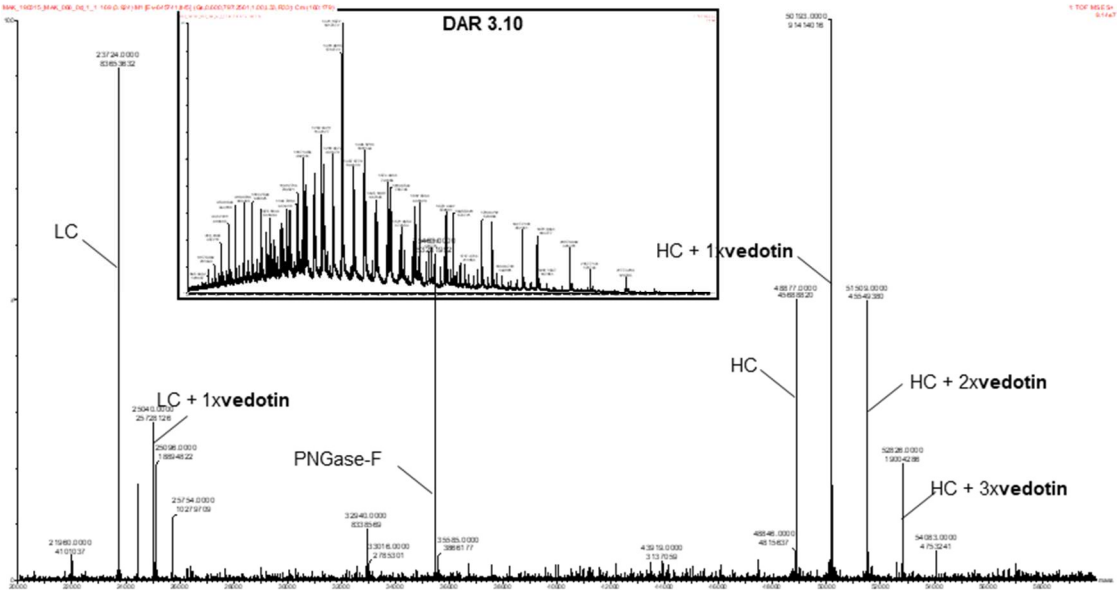

3 days of incubation of Adcetris® in rat serum at 37°C:

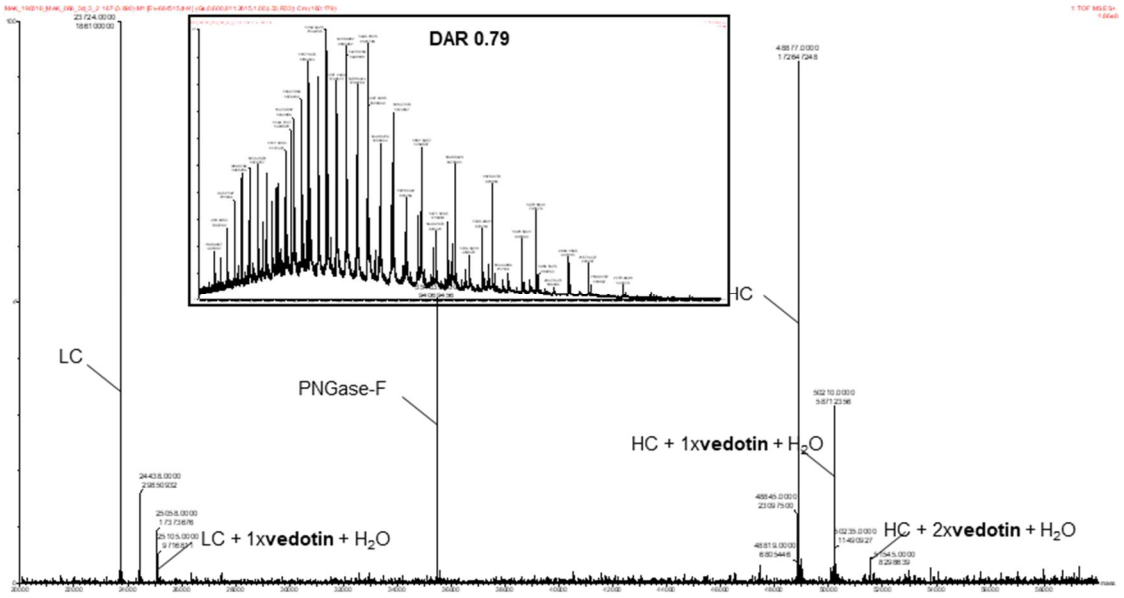

7 days of incubation of Adcetris® in rat serum at 37°C:

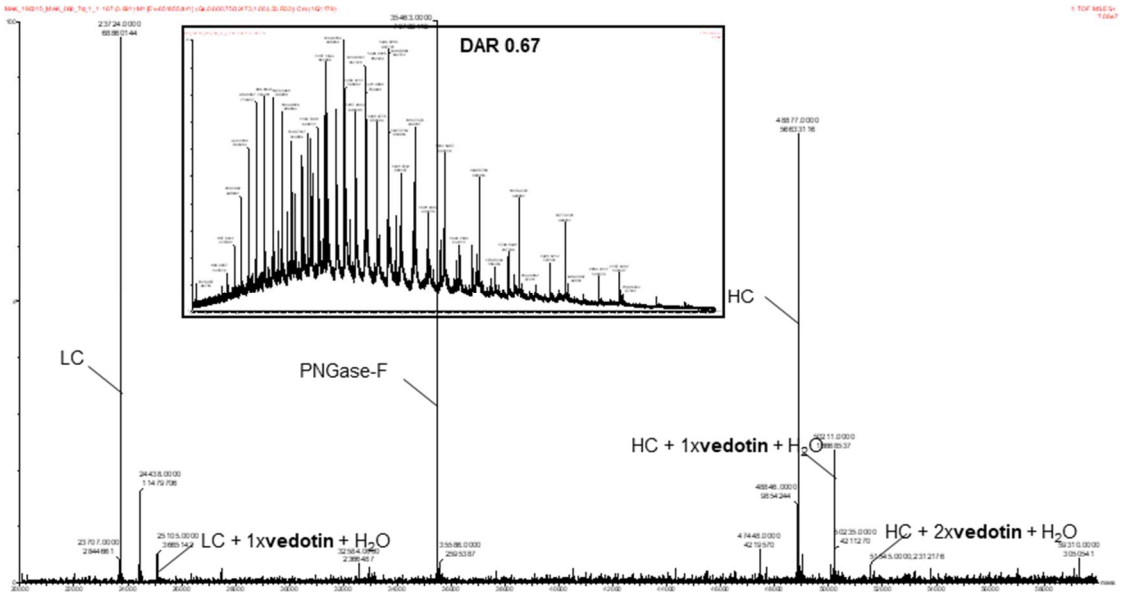

3.13. Stability assessment of ADCs with A-SEC

Brentuximab-**10** was adjusted to a protein concentration of 1 mg/mL in PBS (Dulbeccos Phospahte Bufferd Saline, Sigma-Aldrich Merck KGaA) and filtered sterile (Ultrafree-MC Centrifugal filter units, Merck Millipore). Samples were stored at 4-8°C, 37°C and 40°C for up to 14 days. For samples stored at elevated temperatures, it was ensured that no condensate was formed. Before analysis via A-SEC the samples where centrifuged at 4°C, 4000 x g for 4 minutes.

3.14. In vivo xenograft model

The *in vivo* evaluations were performed at EPO GmbH. All animal experiments were conducted in accordance with German animal welfare law and approved by local authorities. In brief, $1x10^7$ Karpas 299 cells were subcutaneously injected to CB17-Scid mice at day 0. Treatment was initiated when tumors reached a mean tumor volume of 0.136±0.087 cm^3 at day 7 (study

1) and day 8 (study 2). Following randomization of mice into treatment and control groups, 1 mg/kg of brentuximab-**10** or Adcetris as well as vehicle (PBS) were administered as intravenous injection on days 7 and 10 for the first study and 0.5 mg/kg of brentuximab-**10** or Adcetris as well as vehicle (PBS) on days 8 and 12 for the second study. Tumor volumes, body weights and general health conditions were recorded throughout the whole study.

4. Organic synthesis

4.1. *N*-(4-azidobenzoyl)-*L*-valine

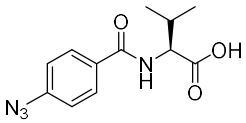

A 50-ml Schlenk-flask was charged with 1.00 g of 4-azidobenzoic acid (6.13 mmol, 1.00 eq.) and suspended in 8.5 ml of dry CH_2Cl_2 together with a drop of DMF under argon. 630 µl of oxalylchloride were added drop-wise at 0 °C and the reaction mixture was stirred at room temperature for 2 h until the solution became clear. All volatiles were removed under reduced pressure and the corresponding solid was redissolved in 4 ml of DMF. The corresponding solution was added drop-wise at 0 °C to a solution of 720 mg *L*-valin (6.13 mmol, 1.00 eq.) and 612 mg sodium hydroxide (15.33 mmol, 2.50 eq.) in 8 ml water and stirred for 2 more hours. The solution was acidified with 1 N HCl and extracted three times with diethylether. The organic fractions were pooled, dried ($MgSO_4$) and the solvents were removed under reduced pressure. Pure product was obtained by flash column chromatography on silicagel (30% EtOAc, 0.5% formic acid in *n*-hexane) as colourless fume. (954 mg, 4.96 mmol, 80.9%)

^{1}H NMR (600 MHz, Chloroform-*d*) δ = 10.12 (s, 1H), 7.79 (d, *J*=8.6, 2H), 7.05 (d, *J*=8.6, 2H), 6.79 (d, *J*=8.5, 1H), 4.76 (dd, *J*=8.5, 4.9, 1H), 2.33 (pd, *J*=6.9, 4.9, 1H), 1.03 (d, *J*=6.9, 3H), 1.01 (d, *J*=6.9, 3H). ^{13}C NMR (151 MHz, $CDCl_3$) δ = 175.82, 167.28, 144.03, 130.17, 129.13, 119.20, 77.16, 57.79, 31.40, 19.16, 17.99. HR-MS for $C_{12}H_{15}N_4O_3^+$ $[M+H]^+$ calcd.: 263.1139, found 263.1151.

4.2. *N*-(4-azidobenzoyl)-*L*-valine-anhydride

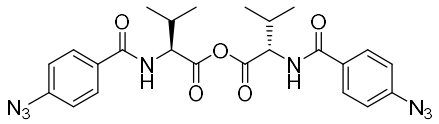

In a 100-ml round-bottom flask, 954 mg *N*-(4-azidobenzoyl)-*L*-valine (3.64 mmol, 1.00 eq.), 750 mg dicyclohexylcarbodiimide (3.64 mmol, 1.00 eq.), 418 mg *N*-hydroxysuccinimide (3.64 mmol, 1.00 eq.) and 9 mg 4-(dimethylamino)-pyridine (0.07 mmol, 0.02 eq.) were dissolved in 25 ml of THF and stirred over night at room temperature. The reaction mixture was filtered, the solids were washed several times with THF, the solvent was removed under reduced pressure and the crude product was purified by flash column chromatography on silicagel (20 to 40% EtOAc in *n*-hexane). The compound was isolated as white powder (513 mg, 1.01 mmol, 55.7%)

^{1}H NMR (600 MHz, Chloroform-*d*) δ = 8.01 (d, *J*=8.7, 2H), 7.13 (d, *J*=8.7, 2H), 4.29 (d, *J*=4.6, 1H), 2.39 (heptd, *J*=6.9, 4.6, 1H), 1.16 (d, *J*=6.9, 3H), 1.03 (d, *J*=6.9, 3H). ^{13}C NMR (151 MHz, $CDCl_3$) δ = 177.52, 160.90, 144.51, 129.60, 122.43, 119.30, 70.68, 31.28, 18.76, 17.57.

4.3. *N*-(4-azidobenzoyl)-*L*-valine-*L*-citrulline

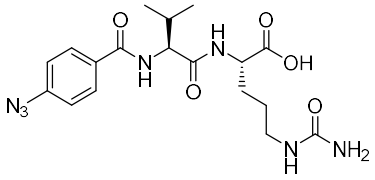

In a 50-ml round-bottom flask, 380 mg *N*-(4-azidobenzoyl)-*L*-valine-anhydride (0.75 mmol, 1.00 eq.) were dissolved in 2 ml of 1,2-Dimethoxyethane and cooled to 0 °C. A solution of 351 mg *L*-citrulline (1.50 mmol, 2.00 eq.) and 144 mg sodium hydrogencarbonate (2.25 mmol, 3.00 eq.) in 4 ml H_2O and 2 ml THF was added dropwise and stirred over night at room temperature. All volatiles were removed under reduced pressure and the crude product was purified by flash column chromatography on silicagel (10% MeOH, 0.5% formic acid in CH_2Cl_2). The compound was isolated as colourless oil (312 mg, 0.74 mmol, 99.0%).

^{1}H NMR (600 MHz, DMSO-d_6) δ = 8.31 (d, *J*=8.8, 1H), 8.27 – 8.21 (m, 1H), 7.96 (d, *J*=8.6, 2H), 7.20 (d, *J*=8.6, 2H), 6.05 (t, *J*=5.5, 1H), 5.47 (s, 2H), 4.37 (t, *J*=8.3, 1H), 4.18 (td, *J*=8.1, 5.1, 1H), 2.98 (q, *J*=6.4, 2H), 2.15 (dq, *J*=13.6, 6.8, 1H), 1.78 – 1.68 (m, 1H), 1.68 – 1.56 (m, 1H), 1.51 – 1.35 (m, 2H), 0.96 (d, *J*=6.8, 3H), 0.94 (d, *J*=6.8, 3H). ^{13}C NMR (151 MHz, DMSO) δ = 174.09, 171.54, 165.99, 159.40, 142.77, 131.36, 129.93, 119.23, 59.31, 52.57, 49.07, 30.77, 29.01, 27.07, 19.75, 19.28. HR-MS for $C_{18}H_{26}N_7O_5^+$ $[M+H]^+$ calcd.: 420.1990, found 420.1990.

4.4. *N*-(4-azidobenzoyl)-*L*-valine-*L*-citrulline-4-aminobenzyl alcohol (1)

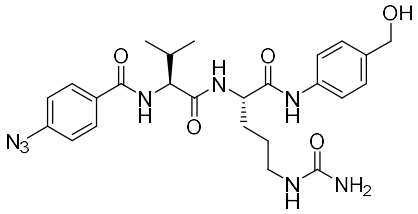

In a 50-ml round-bottom flask, 330 mg *N*-(4-azidobenzoyl)-*L*-vaine-*L*-citrulline (0.787 mmol, 1.0 eq.) and 107 mg 4-aminobenzyl alcohol (0.866 mmol, 1.10 eq.) were dissolved in 8 ml CH_2Cl_2 and 4 ml MeOH under an argon atmosphere and cooled to 0 °C. 390 mg N-Ethoxycarbonyl-2-ethoxy-1,2-dihydroquinoline (1.574 mmol, 2.00 eq.) were added portion-wise and the resulting solution was allowed to warm to room temperature overnight. All volatiles were removed under reduced pressure and the crude product was isolated by flash column chromatography on silicagel (10% to 15% MeOH in CH_2Cl_2) and obtained as white solid (164 mg, 0.313 mmol, 39.8%). Enantiomeric pure compound was isolated by preparative HPLC (Method D) and obtained as a white solid after lyophilisation.

^{1}H NMR (600 MHz, DMSO-d_6) δ = 9.93 (s, 1H), 8.32 (d, *J*=8.4, 1H), 8.21 (d, *J*=7.6, 1H), 7.96 (d, *J*=8.6, 2H), 7.55 (d, *J*=8.6, 2H), 7.24 (d, *J*=8.6, 2H), 7.21 (d, *J*=8.6, 2H), 6.12 (bs, 2H), 4.44 (s, 2H), 4.46 – 4.40 (m, 1H), 4.36 (t, *J*=8.1, 1H), 3.09 – 2.93 (m, 2H), 2.24 – 2.04 (m, *J*=6.7, 1H), 1.84 – 1.58 (m, 2H), 1.55 – 1.34 (m, 2H), 0.95 (d, *J*=6.7, 3H), 0.94 (d, *J*=6.7, 3H). ^{13}C NMR (151 MHz, DMSO) δ = 171.62, 170.79, 166.15, 159.46, 142.83, 137.95, 137.91, 131.29, 129.96, 127.38, 119.34, 119.26, 63.07, 59.56, 53.64, 39.20, 30.61, 29.88, 27.16, 19.79, 19.37. HR-MS for $C_{25}H_{33}N_8O_5^+$ $[M+H]^+$ calcd.: 525.2568, found 525.2563. $[\alpha]_D^{24}$ = –49.6 (c = 0.81; MeOH)

4.5. *N*-(4-(*O*-Ethyl-*P*-ethynyl-phosphonamidato-*N*-benzoyl)-*L*-valine-*L*-citrulline-4-aminobenzyl-4-nitrophenyl carbonate (2)

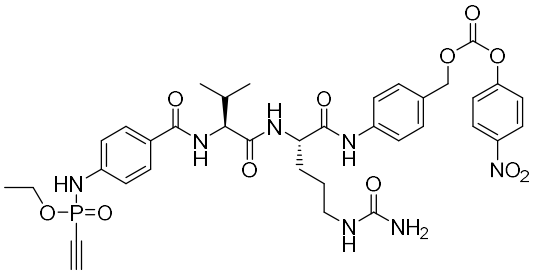

A 5-ml round-bottom flask was charged with 31 mg *N*-(4-(*O*-Ethyl-*P*-ethynyl-phosphonamidato-*N*-benzoyl)-*L*-valine-*L*-citrulline-4-aminobenzyl alcohol (**1**) (0.050 mmol, 1.00 eq.) and 31 mg Bis(4-nitrophenyl) carbonate (0.101 mmol, 2.00 eq.). The solids were dissolved in 140 µl of DMF and 17.4 µl DIPEA (0.101 mmol, 2.00 eq.) were added. The yellow solution was stirred for 1 h at room temperature and the solution was added to 30 ml of ice-cold diethyl ether. The precipitate was collected by centrifugation, redissolved in DMF and again precipitated with ether. The procedure was conducted three times in total and finally the solid was dried under high vacuum conditions. The compound was isolated in quantitative yields and sufficiently pure for the next step. Analytical pure material was purified by preparative HPLC using method C.

^{1}H NMR (600 MHz, DMSO-d_6) δ = 10.10 (s, 1H), 8.79 (d, *J*=8.5, 1H), 8.32 (d, *J*=9.1, 1H), 8.23 (d, *J*=7.4, 1H), 8.07 (dd, *J*=8.5, 2.2, 1H), 7.81 (d, *J*=8.7, 2H), 7.66 (d, *J*=8.5, 2H), 7.57 (d, *J*=9.1, 1H), 7.42 (d, *J*=8.5, 2H), 7.13 (d, *J*=8.7, 2H), 5.25 (s, 2H), 4.47 – 4.40 (m, 2H), 4.34 (t, *J*=8.0, 1H), 4.20 – 4.05 (m, 2H), 3.01 (ddt, *J*=47.1, 13.4, 6.8, 2H), 2.20 – 2.09 (m, *J*=6.8, 1H), 1.80 – 1.59 (m, 2H), 1.55 – 1.35 (m, 2H), 1.30 (t, *J*=7.0, 3H), 0.95 (d, *J*=6.7, 3H), 0.93 (d, *J*=6.7, 3H). ^{13}C NMR (151 MHz, DMSO-d_6) δ = 171.79, 171.17, 166.58, 159.44, 155.75, 152.42, 145.63, 143.50, 139.83, 129.95, 129.77, 129.30, 127.59, 125.86, 123.08, 119.51, 117.24 (d, *J*=7.8), 91.67 (d, *J*=45.6), 77.26 (d, *J*=261.0), 70.71, 62.26 (d, *J*=5.0), 59.31, 53.68, 39.14, 30.71, 29.76, 27.19, 19.80, 19.30, 16.41 (d, *J*=6.9). ^{31}P NMR (243 MHz, DMSO) δ = -10.39, -10.44. HR-MS for $C_{36}H_{43}N_7O_{11}P^+$ $[M+H]^+$ calcd.: 780.2753, found 780.2744.

4.6. *N*-(4-(*O*-Ethyl-*P*-ethynyl-phosphonamidato-*N*-benzoyl)-L-valine-L-citrulline-4-aminobenzyl-4-nitrophenyl carbonate (3)

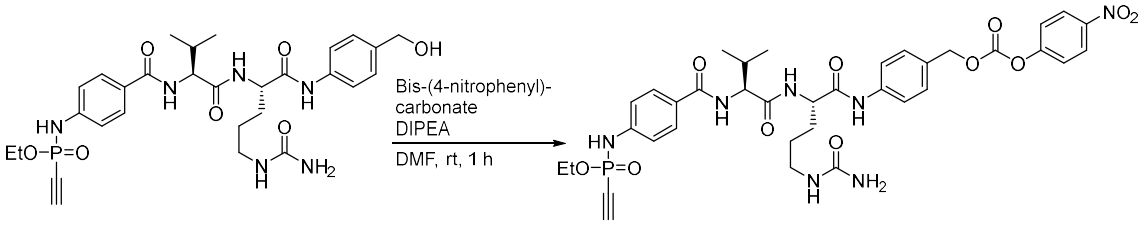

A 5-ml round-bottom flask was charged with 31 mg *N*-(4-(*O*-Ethyl-*P*-ethynyl-phosphonamidato-*N*-benzoyl)-*L*-valine-*L*-citrulline-4-aminobenzyl alcohol (**2**) (0.050 mmol, 1.00 eq.) and 31 mg Bis(4-nitrophenyl) carbonate (0.101 mmol, 2.00 eq.). The solids were dissolved in 140 µl of DMF and 17.4 µl DIPEA (0.101 mmol, 2.00 eq.) were added. The yellow solution was stirred for 1 h at room temperature and the solution was added to 30 ml of ice-cold diethyl ether. The precipitate was collected by centrifugation, redissolved in DMF and again precipitated with ether. The procedure was conducted three times in total and finally the solid was dried under high vacuum conditions. The compound was isolated in quantitative yields and sufficiently pure for the next step. Analytical pure material was purified by preparative HPLC using method C.

^{1}H NMR (600 MHz, DMSO-d_6) δ = 10.10 (s, 1H), 8.79 (d, *J*=8.5, 1H), 8.32 (d, *J*=9.1, 1H), 8.23 (d, *J*=7.4, 1H), 8.07 (dd, *J*=8.5, 2.2, 1H), 7.81 (d, *J*=8.7, 2H), 7.66 (d, *J*=8.5, 2H), 7.57 (d, *J*=9.1, 1H), 7.42 (d, *J*=8.5, 2H), 7.13 (d, *J*=8.7, 2H), 5.25 (s, 2H), 4.47 – 4.40 (m, 2H), 4.34 (t, *J*=8.0, 1H), 4.20 – 4.05 (m, 2H), 3.01 (ddt, *J*=47.1, 13.4, 6.8, 2H), 2.20 – 2.09 (m, *J*=6.8, 1H), 1.80 – 1.59 (m, 2H), 1.55 – 1.35 (m, 2H), 1.30 (t, *J*=7.0, 3H), 0.95 (d, *J*=6.7, 3H), 0.93 (d, *J*=6.7, 3H). ^{13}C NMR (151 MHz, DMSO-d_6) δ = 171.79, 171.17, 166.58, 159.44, 155.75, 152.42, 145.63, 143.50, 139.83, 129.95, 129.77, 129.30, 127.59, 125.86, 123.08, 119.51, 117.24 (d, *J*=7.8), 91.67 (d, *J*=45.6), 77.26 (d, *J*=261.0), 70.71, 62.26 (d, *J*=5.0), 59.31, 53.68, 39.14, 30.71, 29.76, 27.19, 19.80, 19.30, 16.41 (d, *J*=6.9). ^{31}P NMR (243 MHz, DMSO) δ = -10.39, -10.44. HR-MS for $C_{36}H_{43}N_7O_{11}P^+$ [M+H]$^+$ calcd.: 780.2753, found 780.2744.

4.7. *O*-Ethyl-*P*-ethynyl-phosphonamidate-VC-PAB-MMAF 4

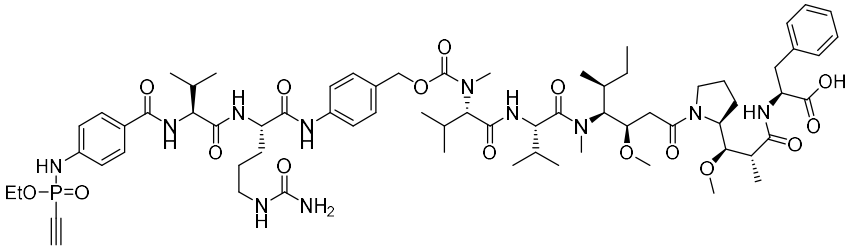

A screw-cap vial was charged with 14.35 mg *N*-(4-(*O*-Ethyl-*P*-ethynyl-phosphonamidato-*N*-benzoyl)-*L*-valine-*L*-citrulline-4-aminobenzyl-4-nitrophenyl carbonate (**3)** (0.0184 mmol, 1.00 eq.), 0.50 mg 1-Hydroxybenzotriazol (0.0037 mmol, 0.20 eq.) and 13.15 mg MMAF (0.0184 mmol, 1.00 eq.). The solids were dissolved in 250 µl dry DMF and 25 µl pyridine and heated to 60 °C over-night. All volatiles were removed under reduced pressure, the crude product was purified by preparative HPLC using method E and the desired compound obtained as a white solid after lyophilization. (4.84 mg, 0.0035 mmol, 19.2 %). HR-MS for $C_{69}H_{104}N_{11}O_{16}P^{2+}$ [M+2H]$^{2+}$ calcd.: 686.8695, found 686.8694.

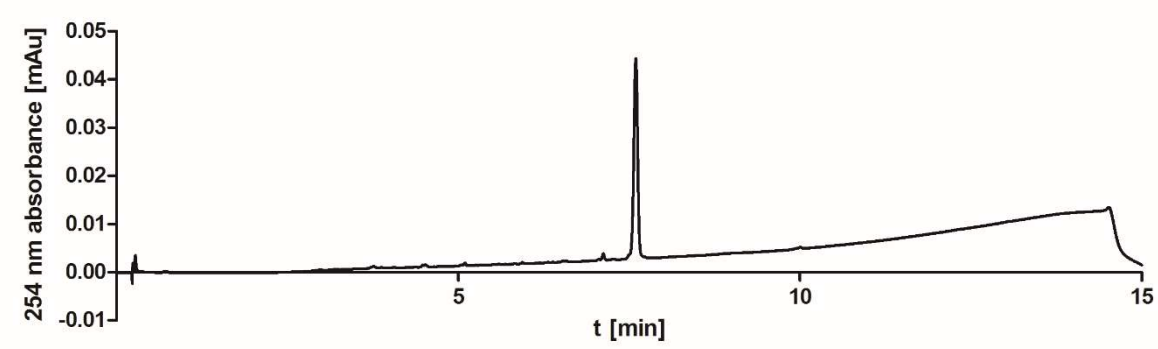

4.8. Di-(2-(2-Hydroxyethoxy)ethyl) ethynylphosphonite (5)

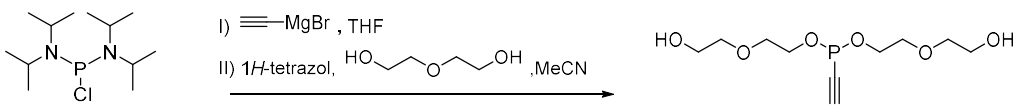

A 25-ml Schlenk flask was charged with 267 mg bis(diisopropylamino)chlorophosphine (1.00 mmol, 1.00 eq.) under an argon atmosphere, cooled to 0 °C and 2.20 ml ethynylmagnesium bromide solution (0.5 M in THF, 1.10 mmol, 1.10 eq.) was added drop wise. The yellowish solution was allowed to warm to room temperature and stirred for further 30 minutes. 1.06 g diethylene glycol (10.00 mmol, 10.00 eq.), dissolved in 5.56 ml 1H-tetrazole solution (0.45 M in MeCN, 2.50 mmol, 2.50 eq.) were added and the white suspension was stirred over night at room temperature. The reaction mixture was directly placed on a silica gel flash column for

purification (5% MeOH in CH_2Cl_2). The desired compound was obtained as a yellowish oil. (112 mg, 0.421 mmol, 42.1%).

^{1}H NMR (300 MHz, Chloroform-*d*) δ = 4.14 – 3.98 (m, 4H), 3.65 – 3.59 (m, 4H), 3.58 – 3.49 (m, 8H), 3.15 (d, *J*=2.4, 1H) ^{13}C NMR (75 MHz, Chloroform-*d*) δ = 92.51 (d, *J*=1.4), 84.30 (d, *J*=46.8), 72.60, 70.72 (d, *J*=4.0), 67.20 (d, *J*=6.0), 61.44. ^{31}P NMR (122 MHz, $CDCl_3$) δ = 131.97.

4.9. 2-(2-Hydroxyethoxy)ethyl-*N*-(4-benzoic-acid-*N*-hydroxysuccinimideester)-*P*-ethynyl phosphonamidate (8)

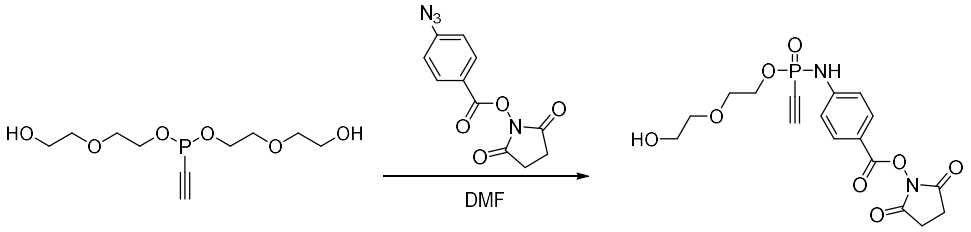

In a 5 ml round-bottom-flask, 93 mg Di-(2-(2-Hydroxyethoxy)ethyl) ethynylphosphonite (**5**) (0.192 mmol, 1.00 eq.) and 91 mg 4-azidobenzoic-acid-*N*-hydroxysuccinimide ester (**6**) (0.192 mmol, 1.00 eq.) were dissolved in 1 ml of DMF and the solution was stirred overnight. All volatiles were removed under reduced pressure and the residue purified by column chromatographie on silicagel (100% EtOAc). The compound was obtained as colourless oil. (45 mg, 0.109 mmol, 31.4%).

^{1}H NMR (300 MHz, Chloroform-*d*) δ 8.02 (d, *J* = 8.7 Hz, 2H), 7.79 (d, *J* = 7.6 Hz, 1H), 7.21 (d, *J* = 8.8 Hz, 2H), 4.30 (dp, *J* = 13.6, 4.5 Hz, 2H), 3.89 – 3.67 (m, 6H), 3.09 (d, *J* = 13.3 Hz, 1H), 2.89 (s, 4H). ^{13}C NMR (75 MHz, Chloroform-*d*) δ 169.67, 161.45, 145.78 (d, *J* = 1.6 Hz), 132.32, 118.04, 117.66 (d, *J* = 8.1 Hz), 89.29 (d, *J* = 50.1 Hz), 75.34 (d, *J* = 294.4 Hz), 72.59, 69.44 (d, *J* = 5.1 Hz), 66.19 (d, *J* = 5.9 Hz), 61.35, 25.68. ^{31}P NMR (122 MHz, $CDCl_3$) δ -9.66. HRMS for $C_{17}H_{20}N_2O_8P^+$ $[M+H]^+$ calcd.: 411.0952, found: 411.0951.

4.10. *O*-ethyl-*P*-ethynyl-phosphonamidate-VC-PAB-MMAE 9

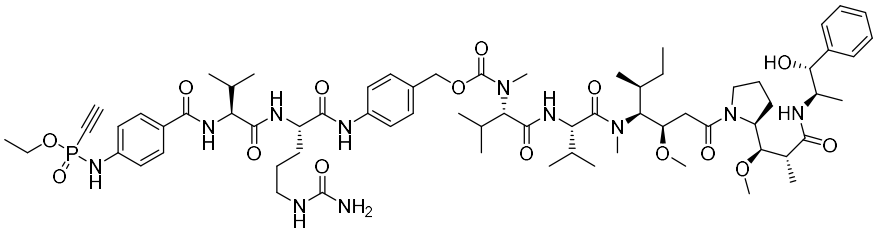

In a screw-cap-vial equipped with a stirring bar, 5 mg of H_2N-Val-Cit-PAB-MMAE **11** (4.452 µmol, 1.00 eq.) and 3.12 mg 2-ethyl-*N*-(4-benzoic-acid-*N*-hydroxysuccinimideester)-*P*-ethynyl phosphonamidate (**7**) (8.904 µmol, 2.00 eq.) were dissolved in 50 µl DMF. 3.1 µl DIPEA (17.808 µmol, 4.00 eq.) were added and the solution was stirred overnight at room temperature. The solution was diluted with 4 ml 30% MeCN in H_2O and subjected to semi-preparative HPLC purification using method F and the desired compound obtained as a white solid after lyophilization. (5.00 mg, 3.681 µmol, 82.7%). HR-MS for $C_{69}H_{105}N_{11}O_{15}P^+$ $[M+H]^+$ calcd.: 1358.7524, found 1358.7518.

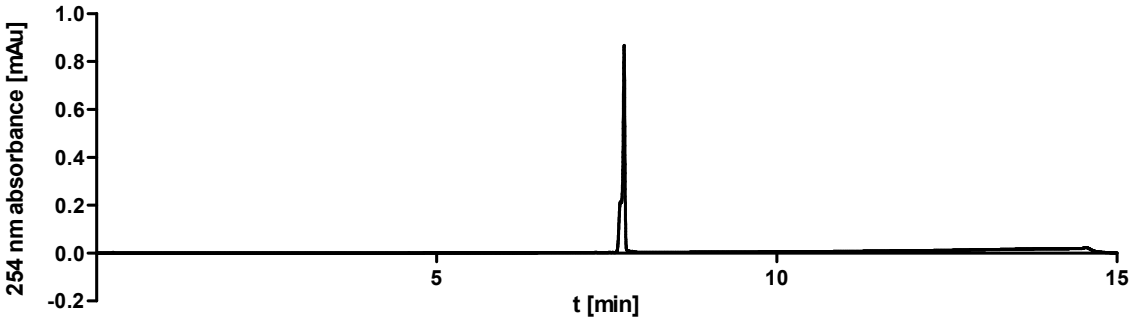

4.11. *O*-2-(2-Hydroxyethoxy)ethyl-*P*-ethynyl-phosphonamidate-VC-PAB-MMAE 10

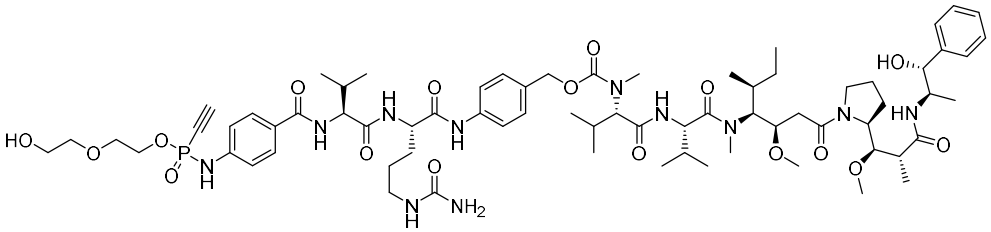

In a screw-cap-vial equipped with a stirring bar, 5 mg of H_2N-Val-Cit-PAB-MMAE **11** (4.452 µmol, 1.00 eq.) and 3.65 mg 2-(2-Hydroxyethoxy)ethyl-*N*-(4-benzoic-acid-*N*-hydroxysuccinimideester)-*P*-ethynyl phosphonamidate (**8**) (8.904 µmol, 2.00 eq.) were dissolved in 50 µl DMF. 3.1 µl DIPEA (17.808 µmol, 4.00 eq.) were added and the solution was stirred overnight at room temperature. The solution was diluted with 4 ml 30% MeCN in H_2O and subjected to semi-preparative HPLC purification using method F and the desired compound obtained as a white solid after lyophilization. (2.73 mg, 1.589 µmol, 35.7%). HR-MS for $C_{71}H_{109}N_{11}O_{17}P^+$ $[M+H]^+$ calcd.: 1418.7735, found 1418.7729.

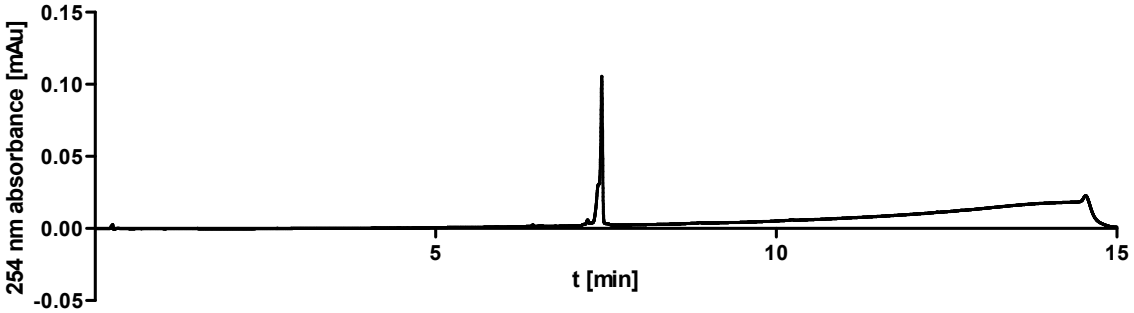

5. NMR spectra

N-(4-azidobenzoyl)-*L*-valine

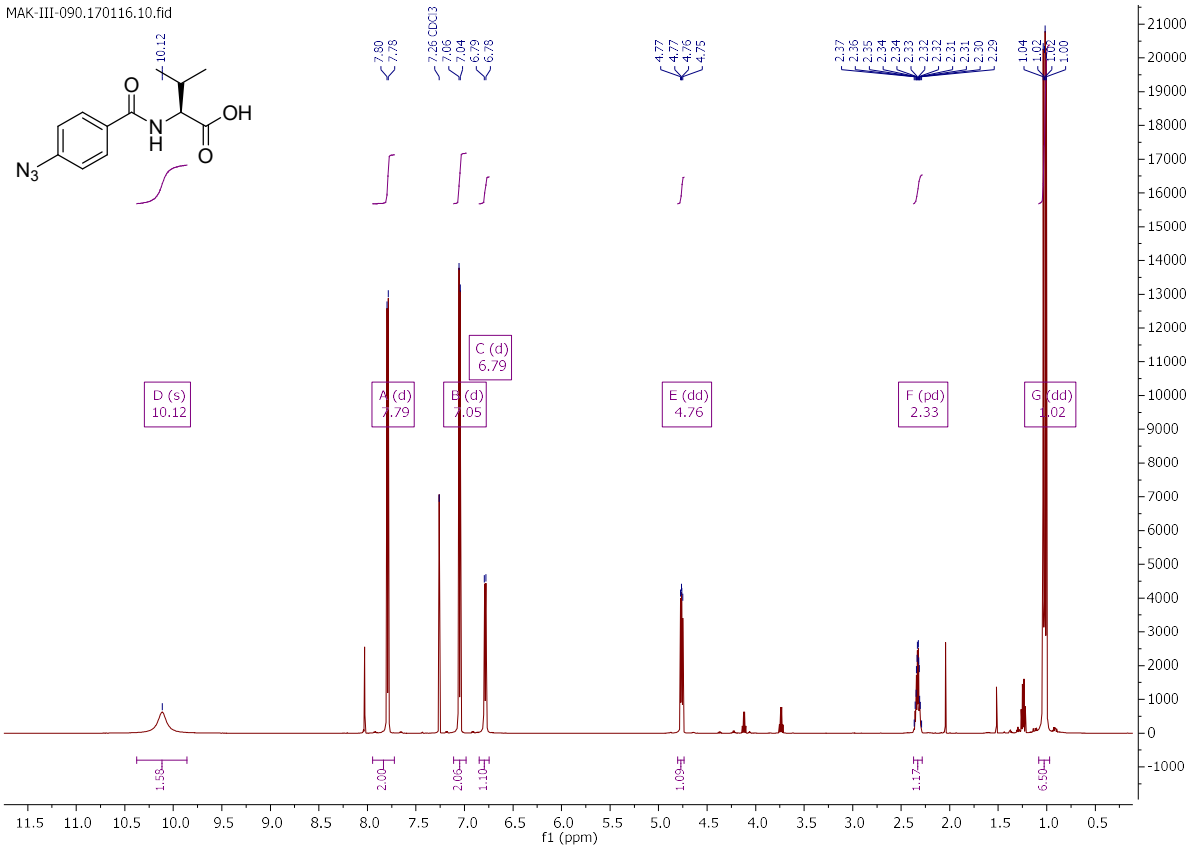

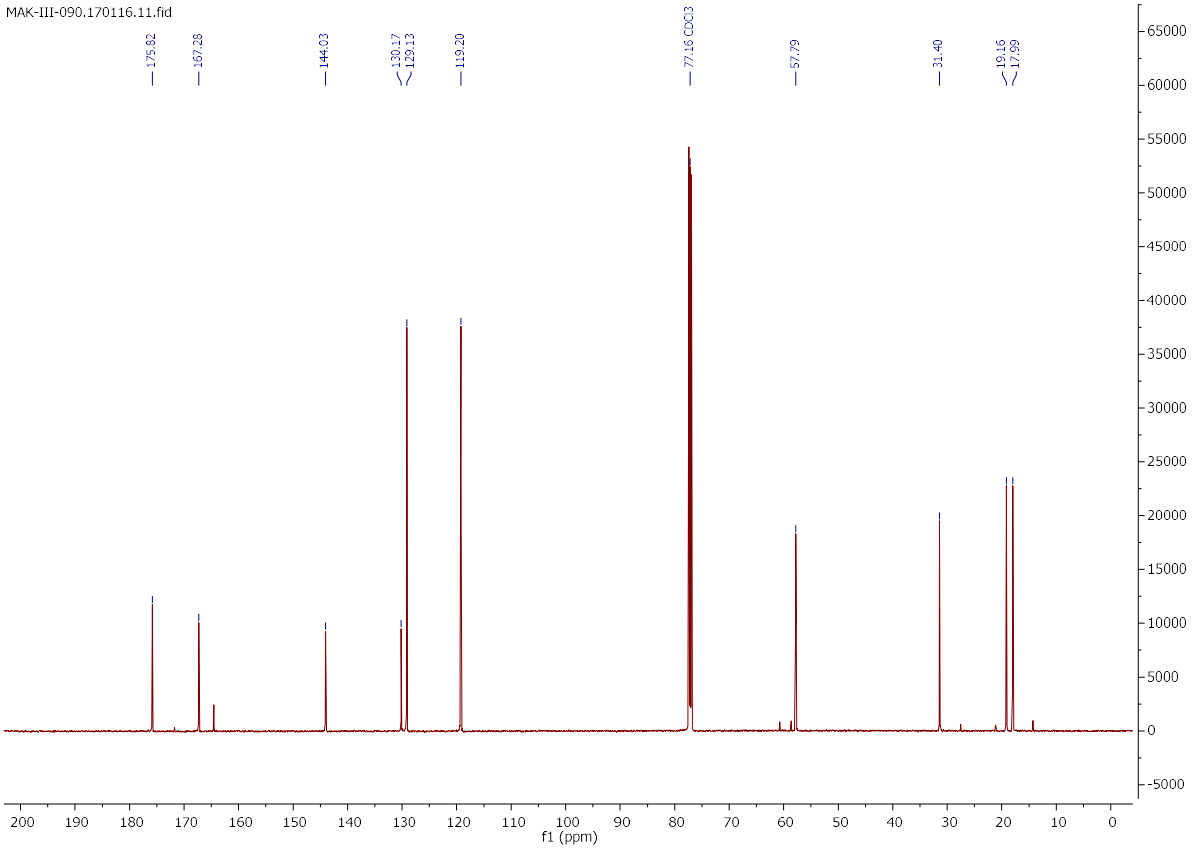

N-(4-azidobenzoyl)-*L*-valine-anhydride

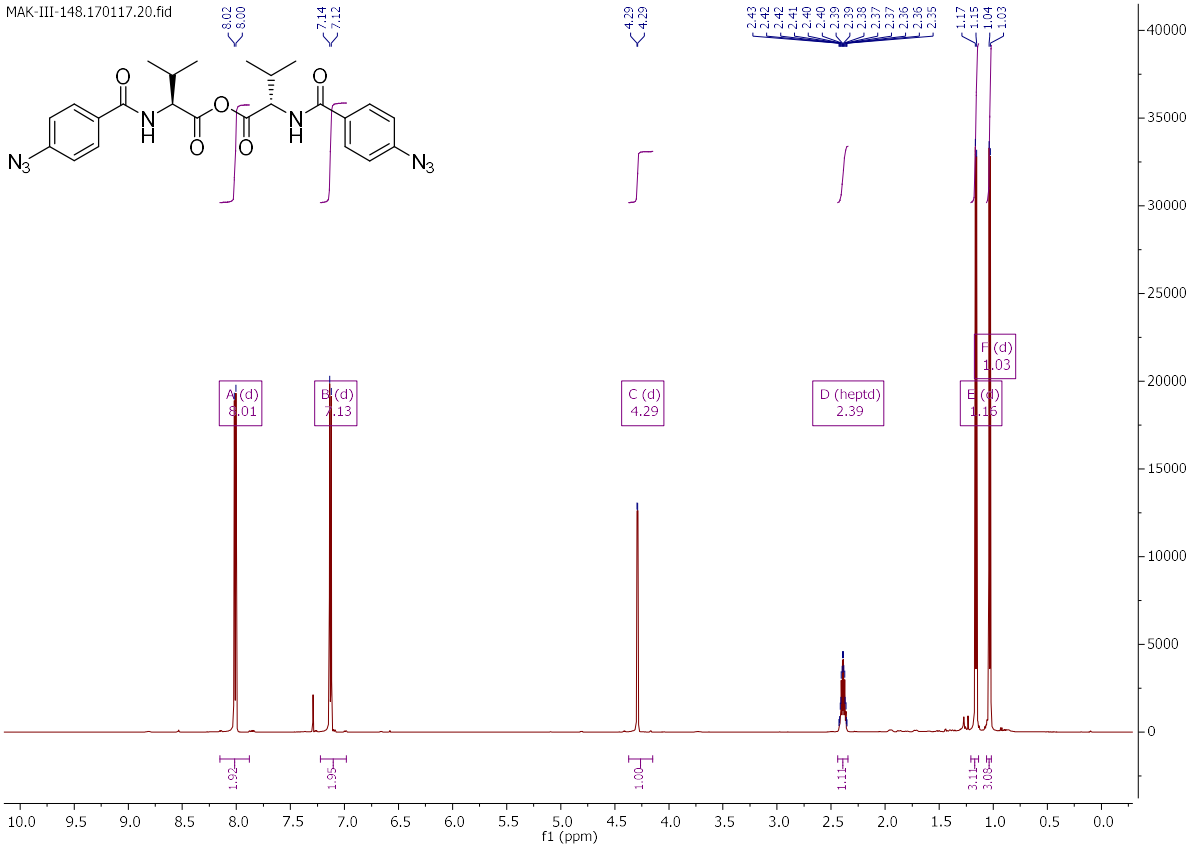

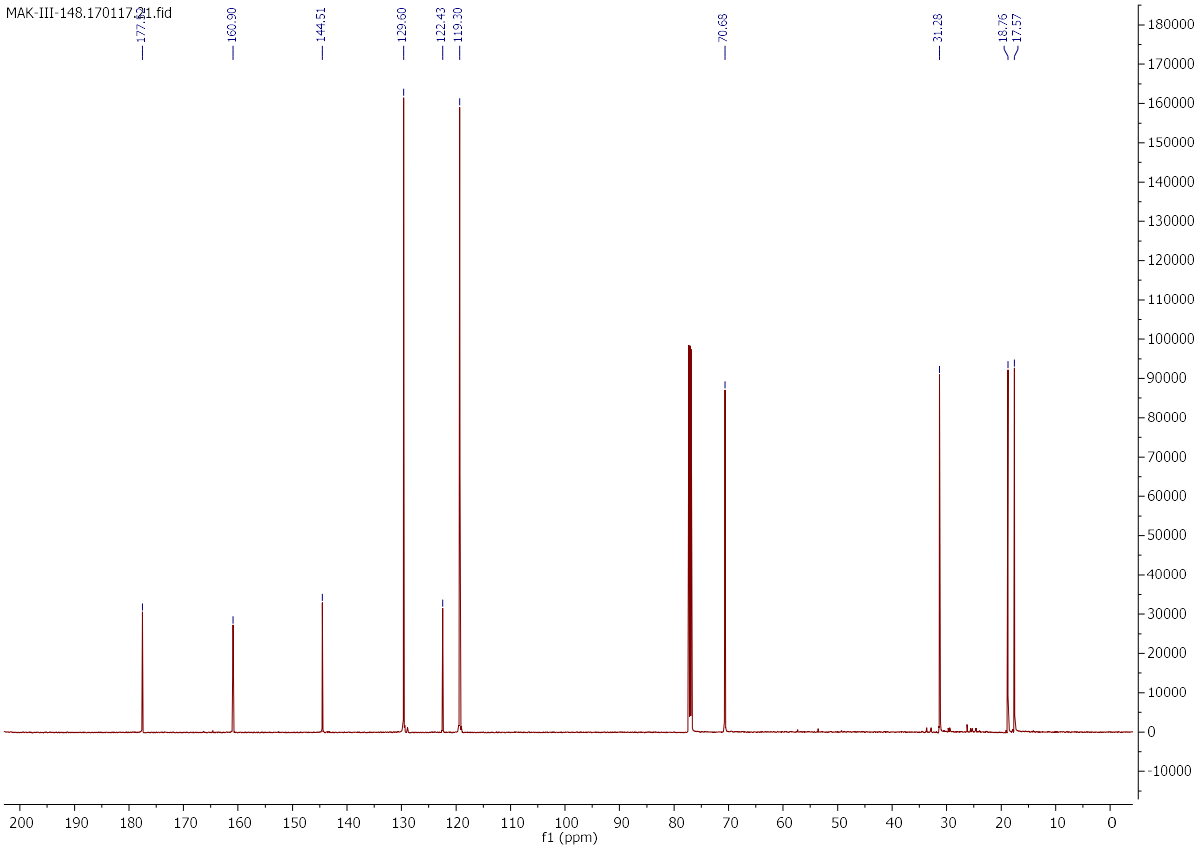

N-(4-azidobenzoyl)-*L*-valine-*L*-citrulline

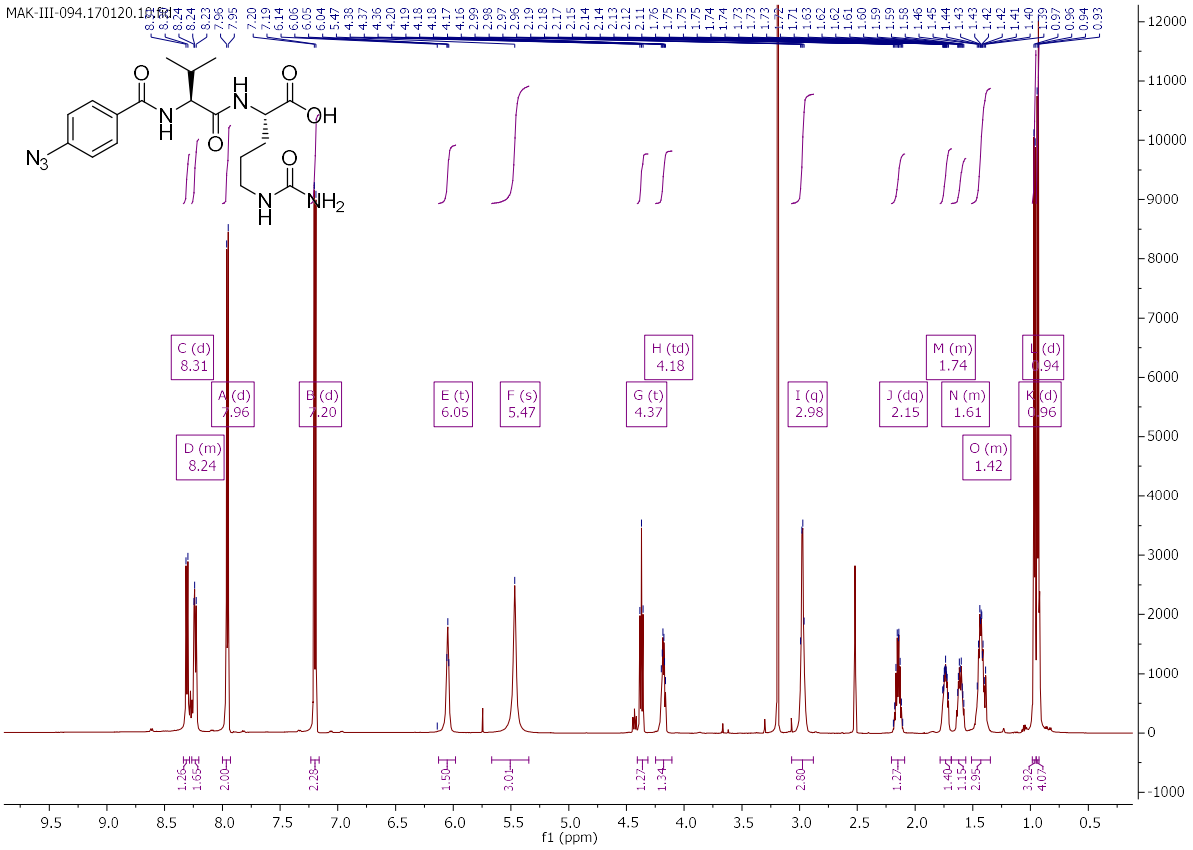

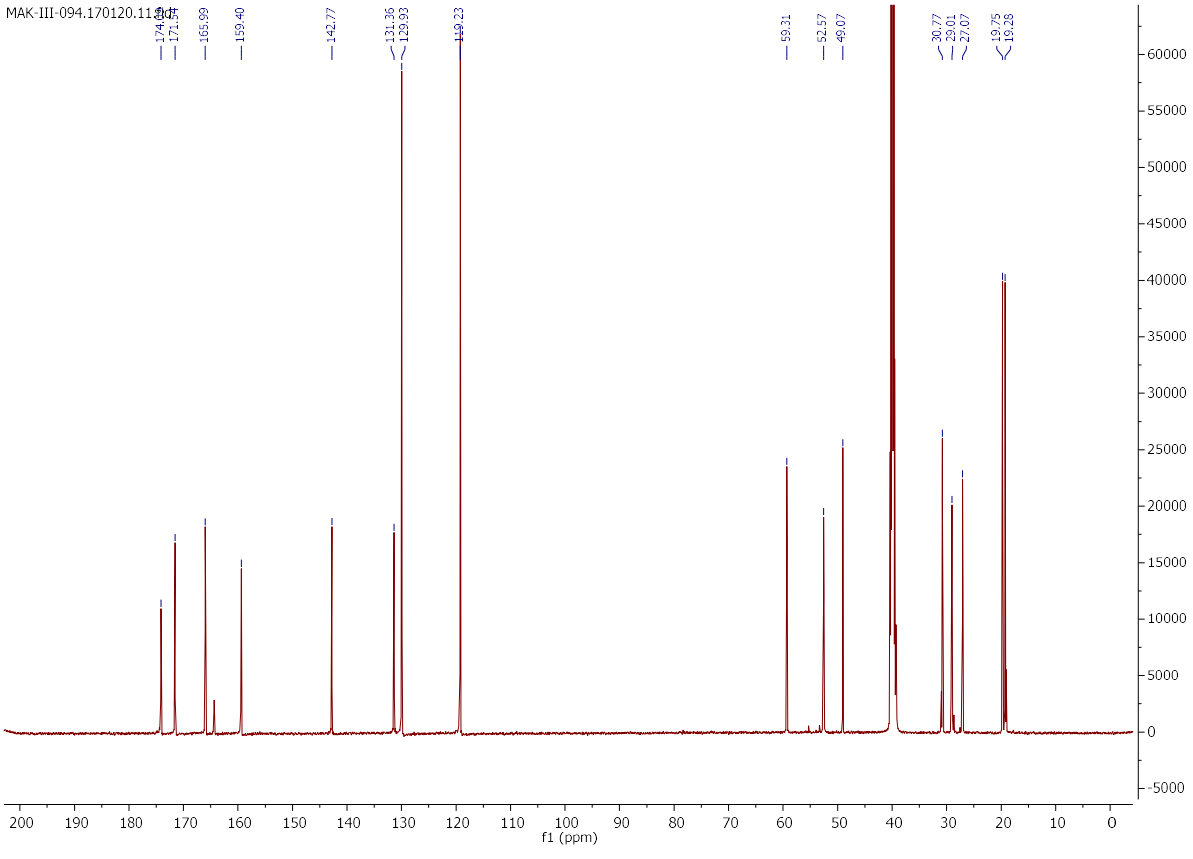

N-(4-azidobenzoyl)-*L*-valine-*L*-citrulline-4-aminobenzyl alcohol **(2)**

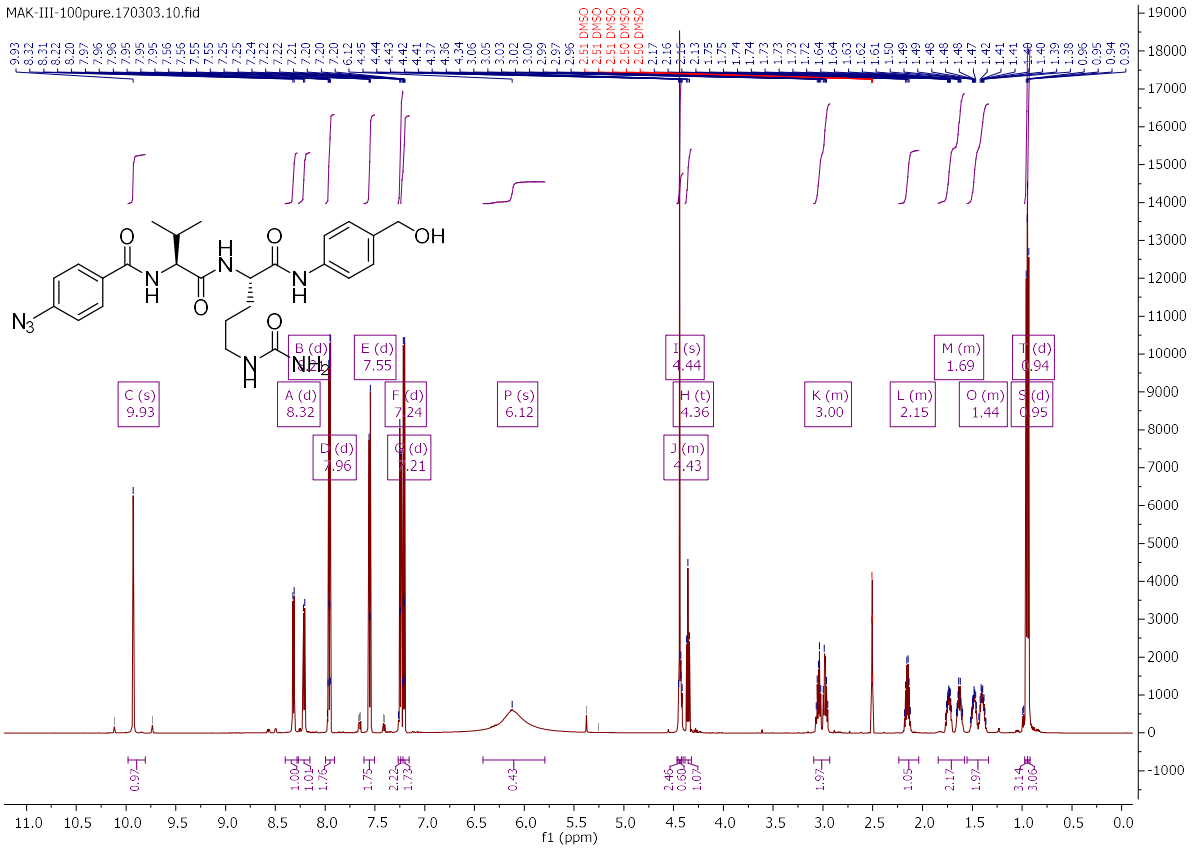

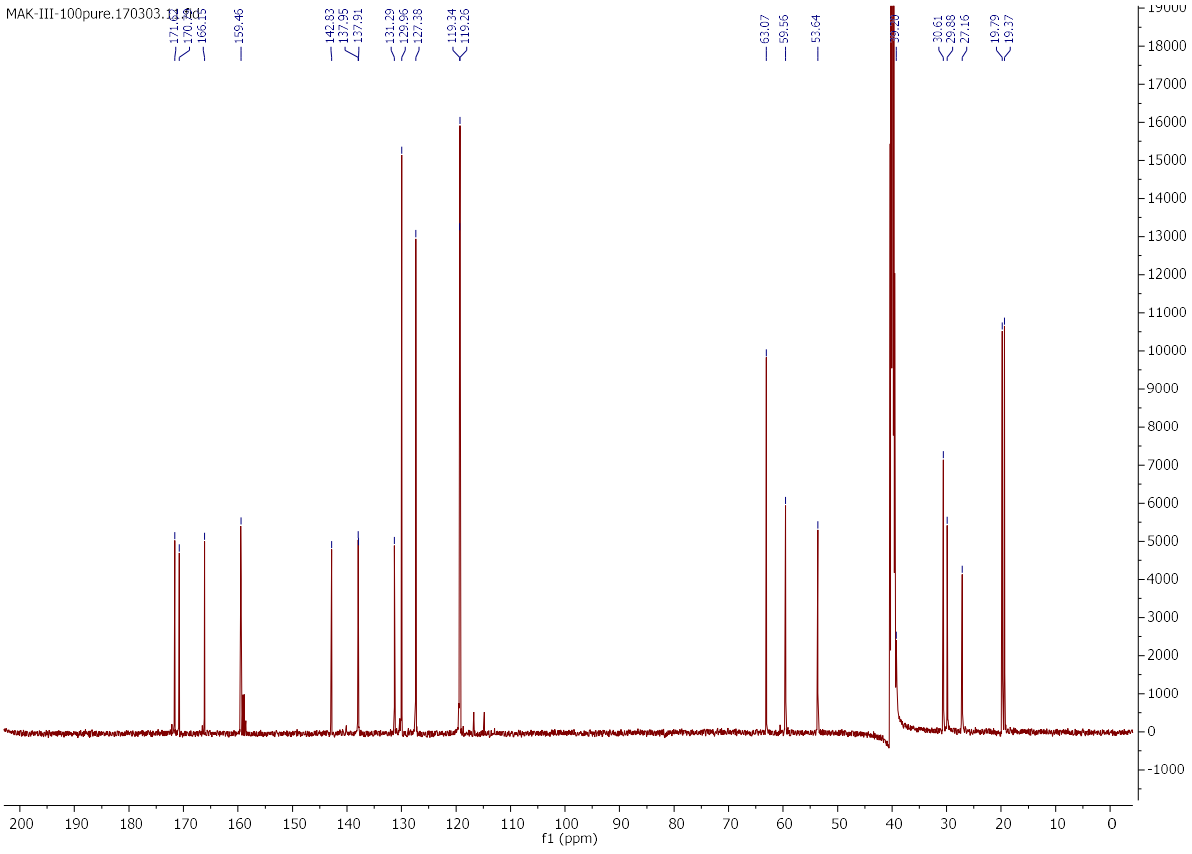

N-(4-(*O*-Ethyl-*P*-ethynyl-phosphonamidato-*N*-benzoyl)-*L*-valine-*L*-citrulline-4-aminobenzyl alcohol **(2)**

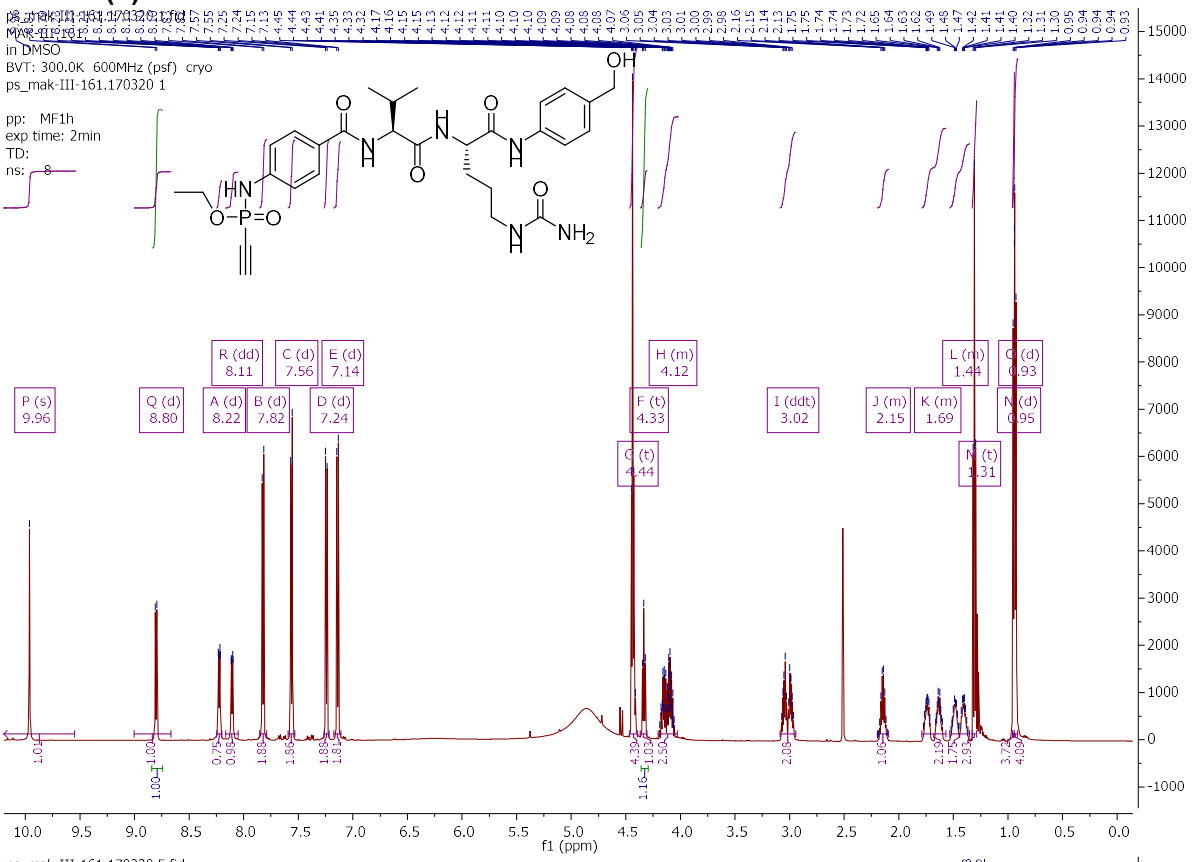

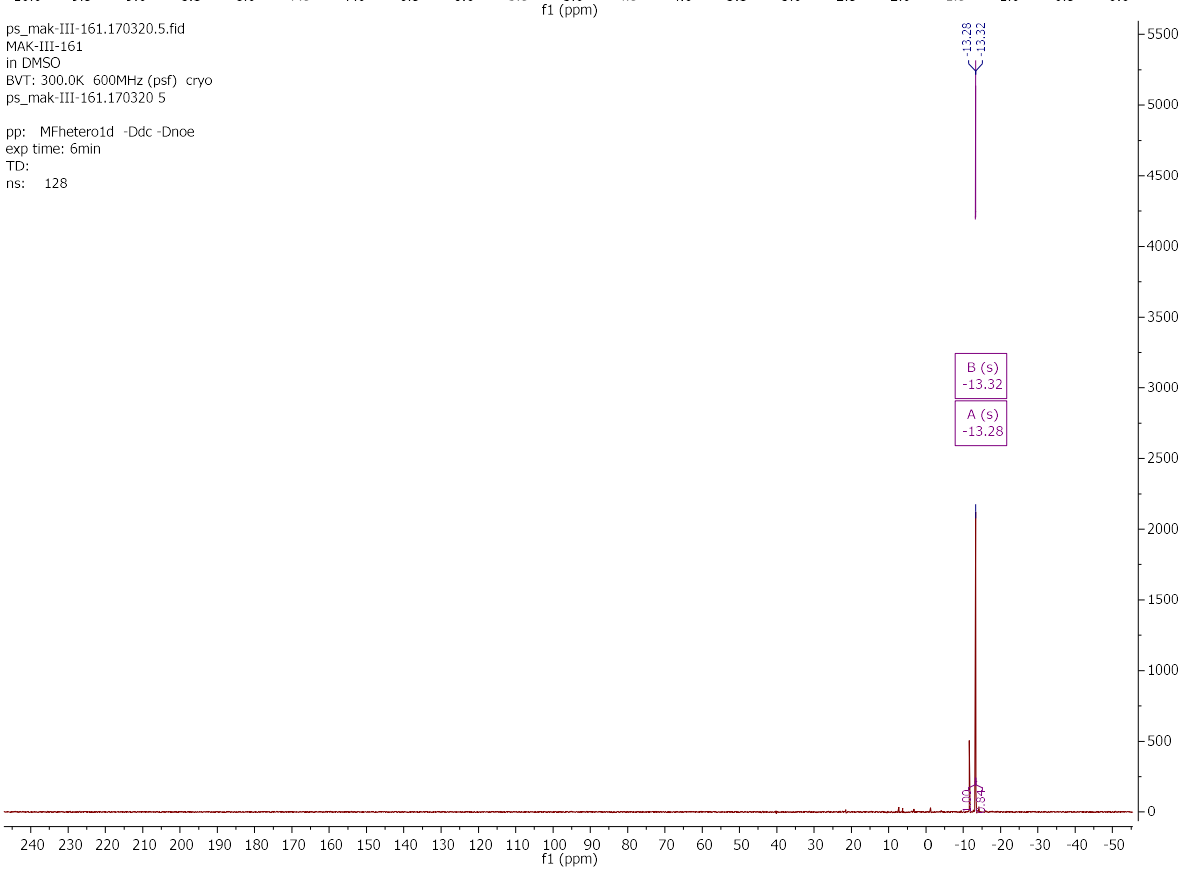

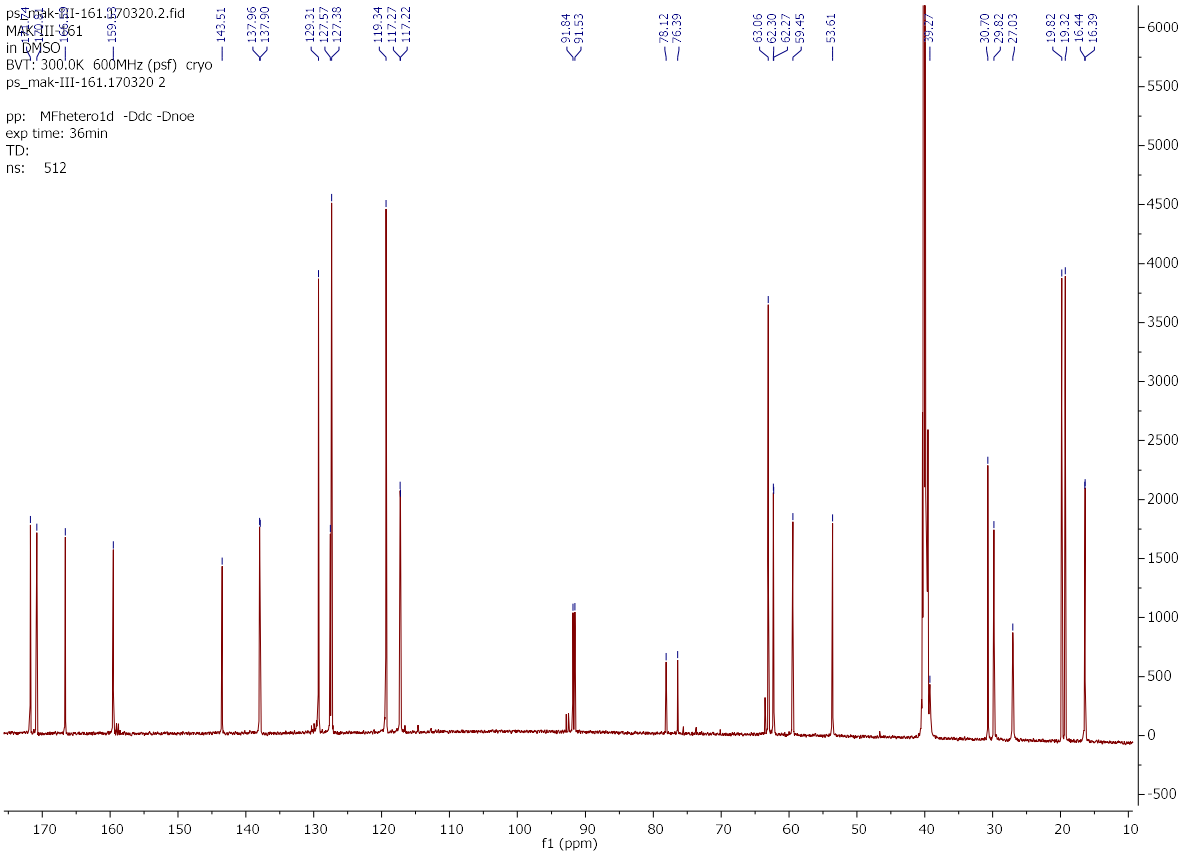

N-(4-(*O*-Ethyl-*P*-ethynyl-phosphonamidato-*N*-benzoyl)-*L*-valine-*L*-citrulline-4-aminobenzyl-4-nitrophenyl carbonate **(3)**

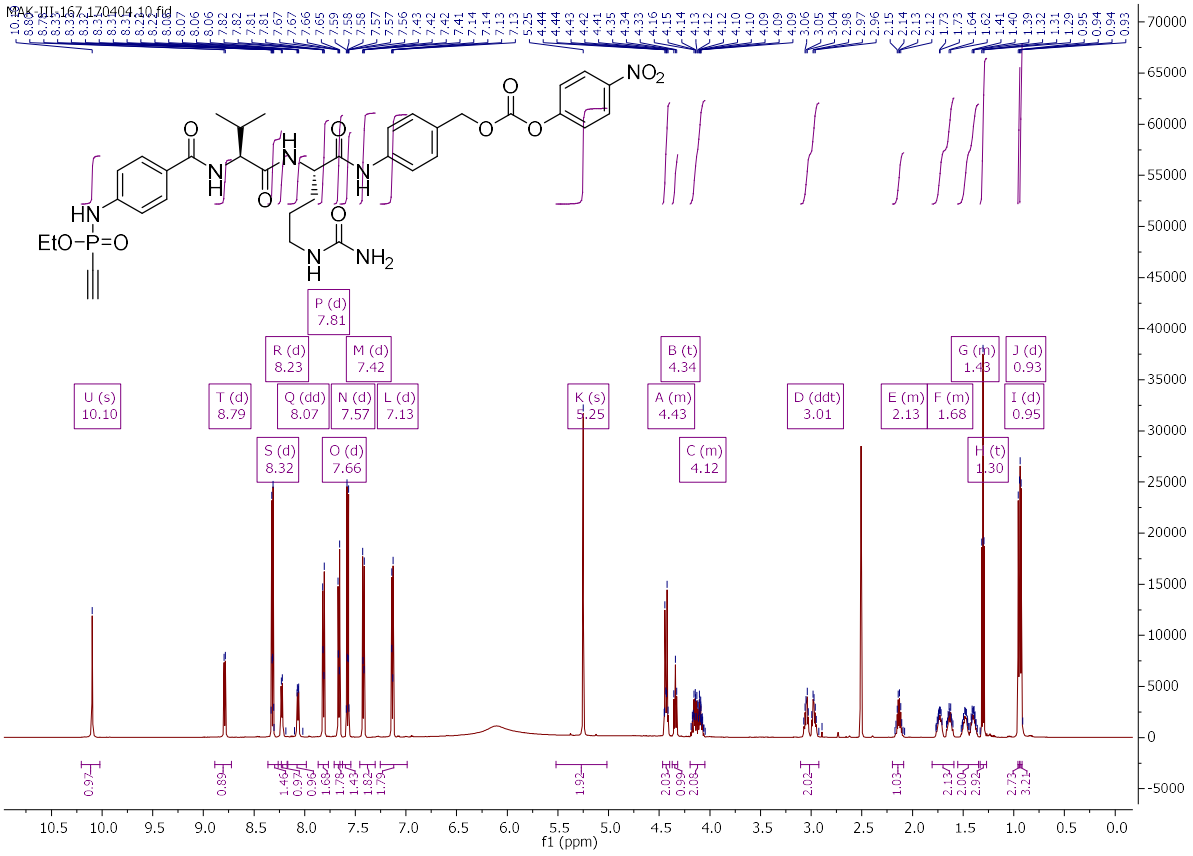

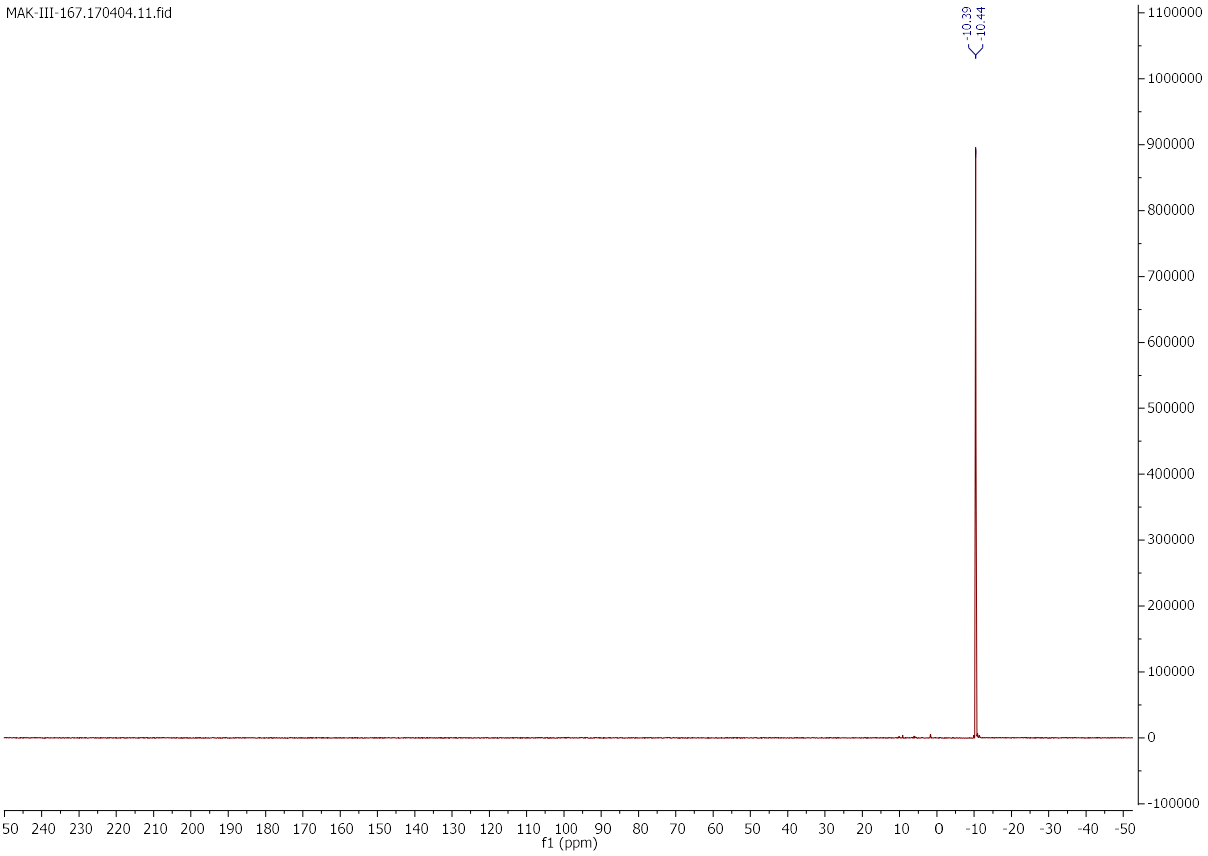
MAK-III-167.170404.11.fid
10.39
10.44
f1 (ppm)

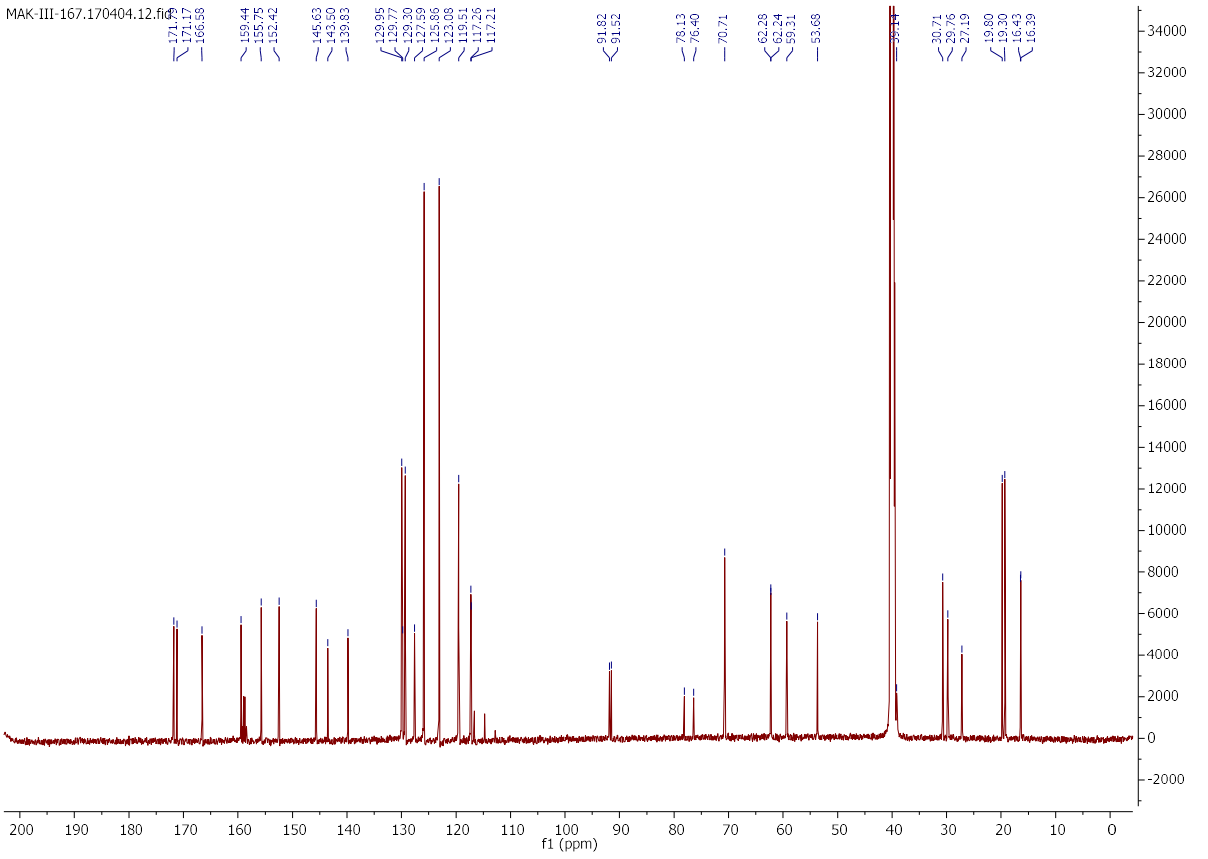
MAK-III-167.170404.12.fid
171.17
166.58
159.44
155.75
152.42
145.63
143.50
139.83
129.95
129.77
129.30
127.59
125.86
123.08
119.51
117.26
117.21
91.82
91.52
78.13
76.40
70.71
62.28
62.24
59.31
53.68
39.14
30.71
29.76
27.19
19.80
19.30
16.43
16.39
f1 (ppm)

Di-(2-(2-Hydroxyethoxy)ethyl) ethynylphosphonite (**5**)

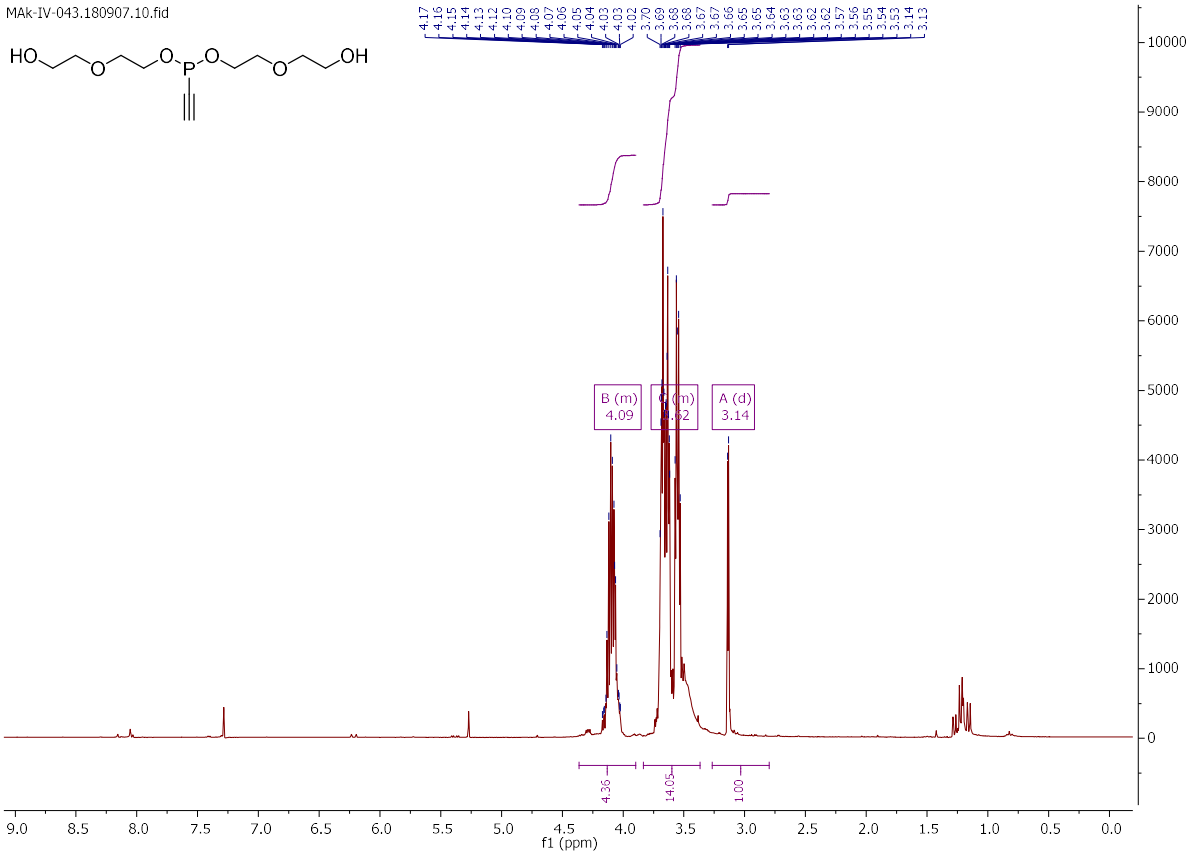

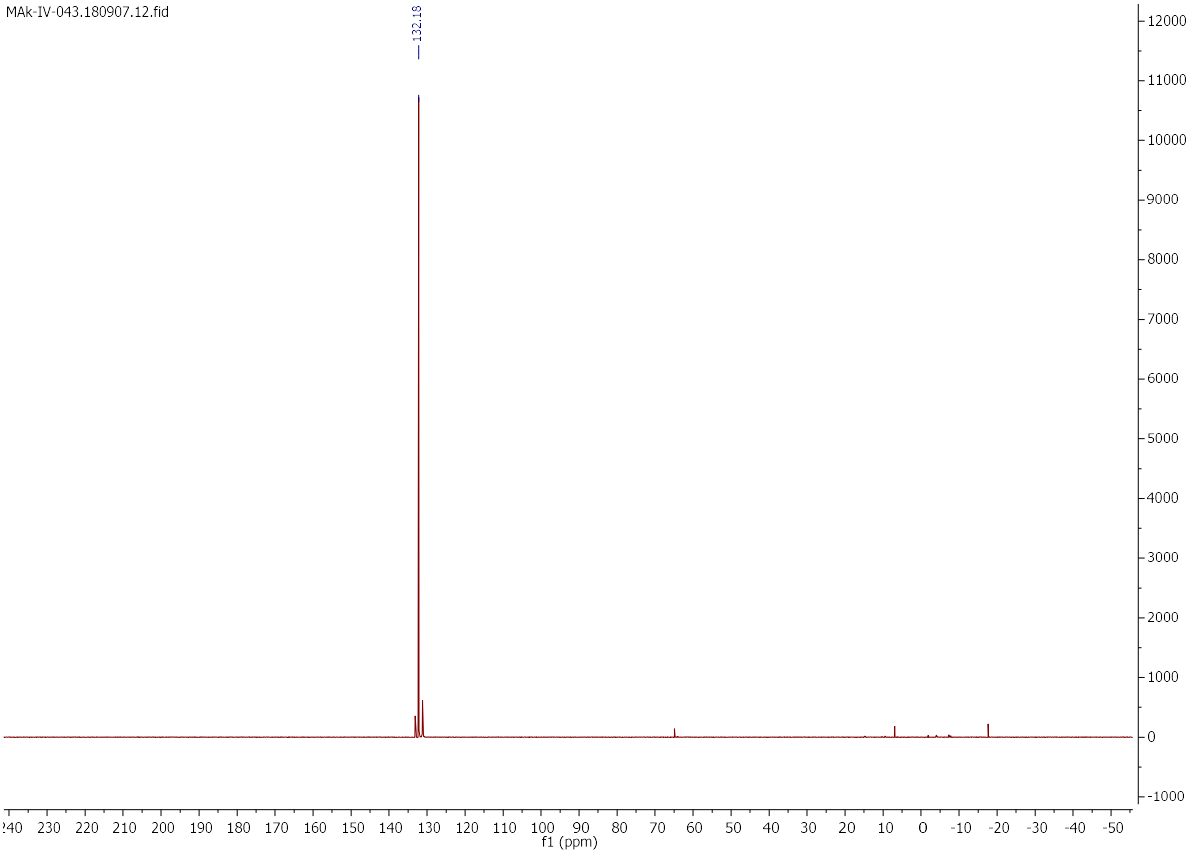

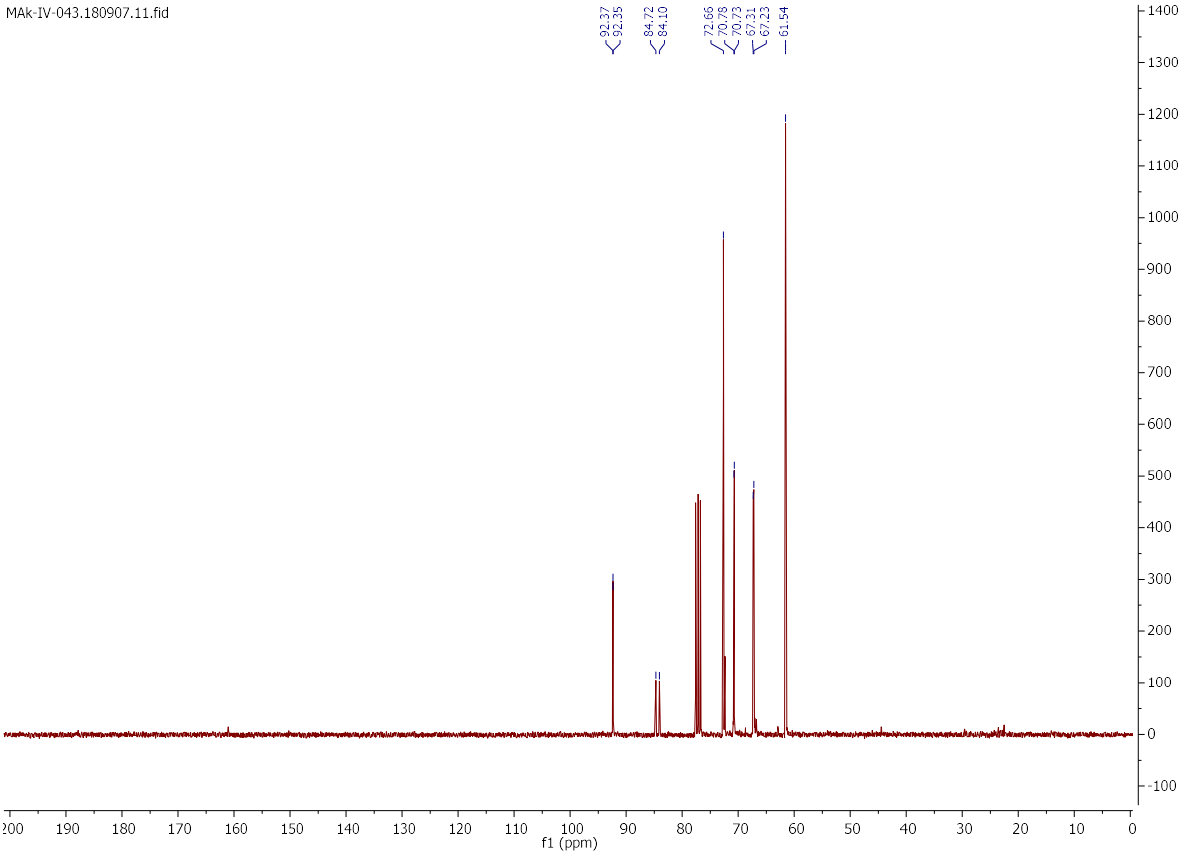

Di-(2-(2-Hydroxyethoxy)ethyl)-*N*-(4-benzoic-acid-*N*-hydroxysuccinimideester)-*P*-ethynyl phosphonamidate (**8**)

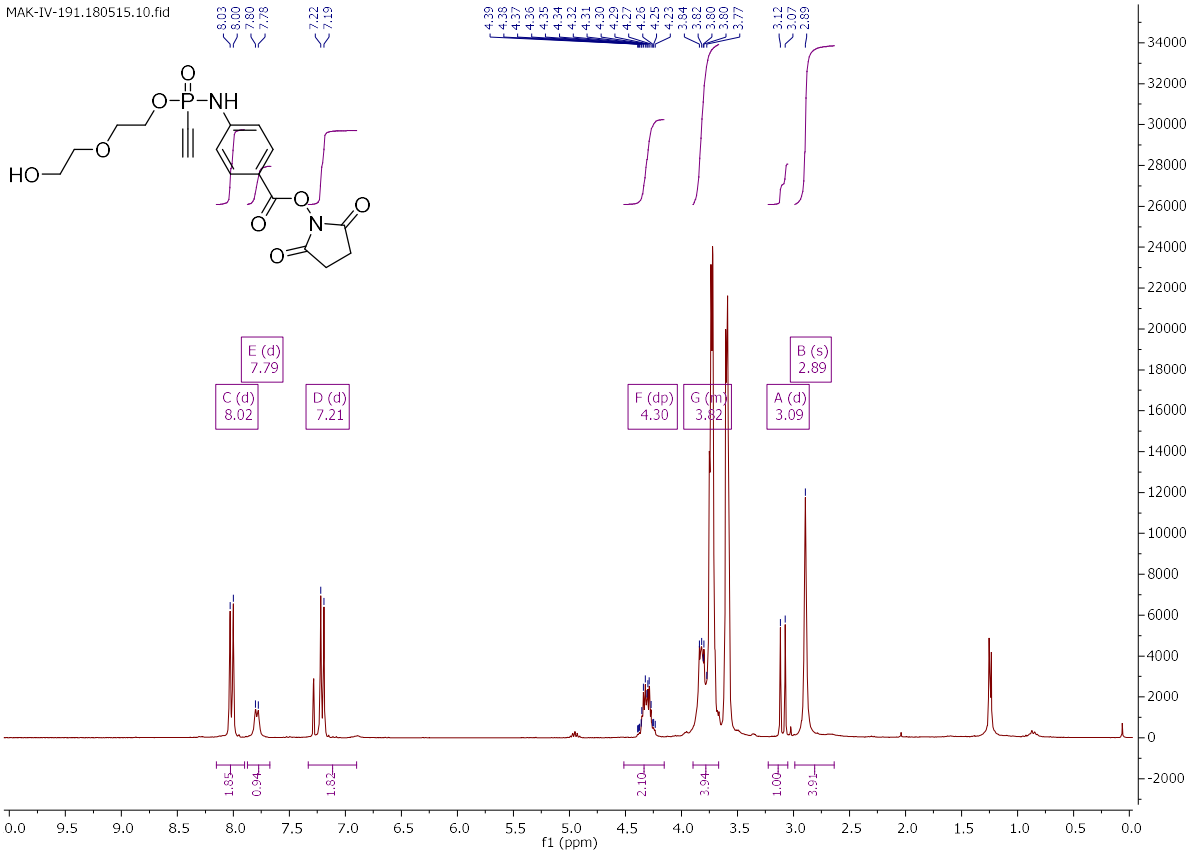

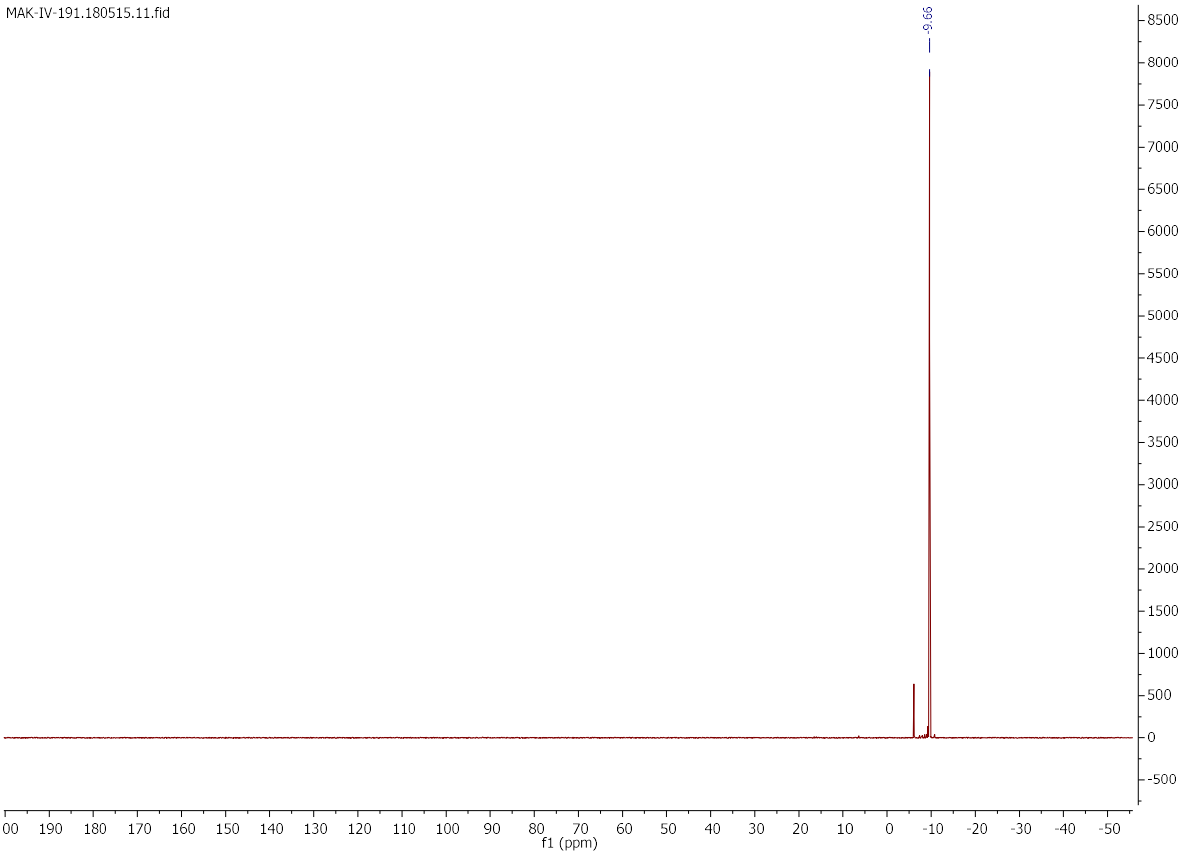
MAK-IV-191.180515.11.fid
-9.66
f1 (ppm)

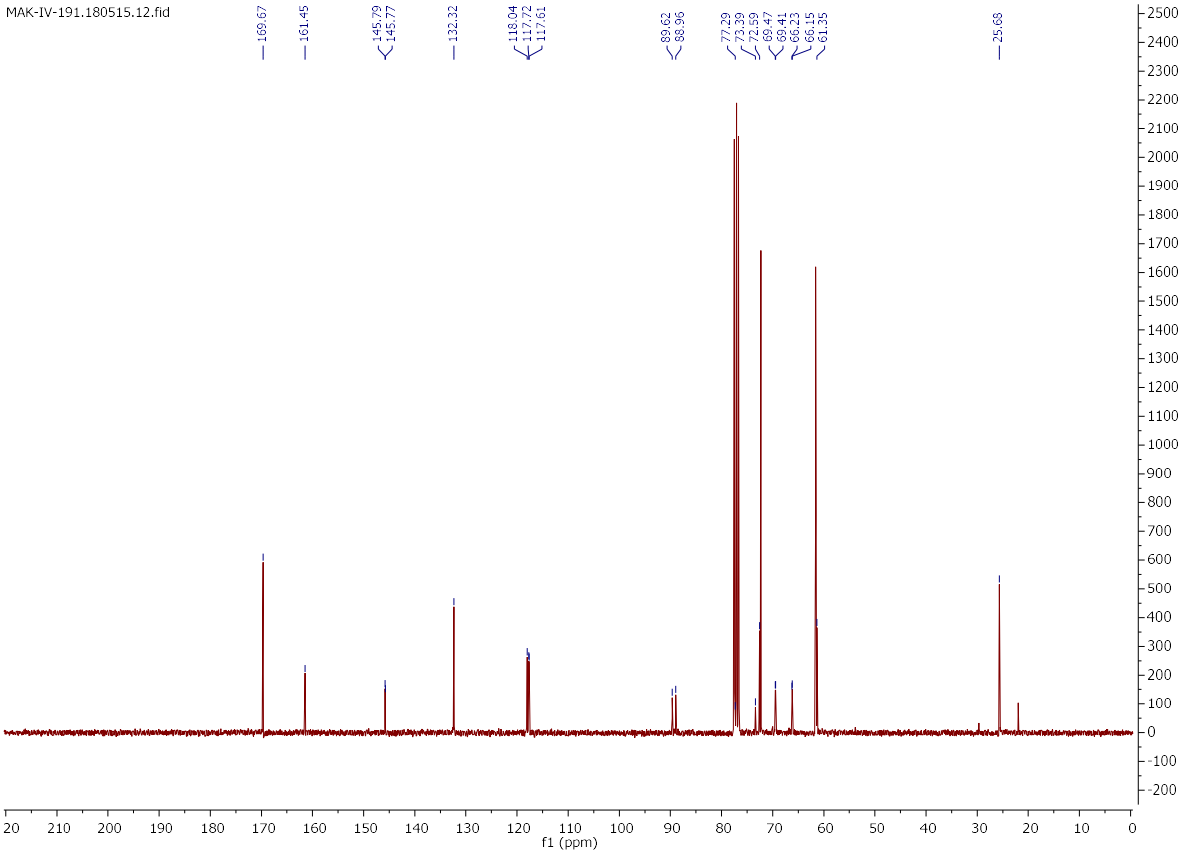
MAK-IV-191.180515.12.fid
169.67
161.45
145.79
145.77
132.32
118.04
117.72
117.61
89.62
88.96
77.29
73.39
72.59
69.47
69.41
66.23
66.15
61.35
25.68
f1 (ppm)

6. References

[1] I. Rillat, M. Perez, L. Goetsch, M. Broussas, C. Beau-Larvor, J.-F. Haeuw*, Vol. WO2015162293*, WO2015162293 (A1) ed., **2015**.

[2] S. M. Ansell, *Blood* **2014**, *124*, 3197-3200.

[3] A. Stengl, D. Hörl, H. Leonhardt, J. Helma, *SLAS Discov.* **2017**, *22*, 309-315.

7. Summary and Outlook

Within the present work, a novel cysteine selective protein- and antibody modification method based on electrophilic phosphonamidate reagents has been established. Additionally, it was demonstrated that the cysteine reactive vinyl- and ethynylphosphonamidates can be chemoselectively installed into a given azide modified molecule by means of the Staudinger-phosphonite reaction with vinyl- and ethynylphosphonites yielding electron-deficient phosphorus-(V) compounds. This chemoselective reaction chemically induces reactivity for the subsequent cysteine modification on proteins. The reaction sequence thereby constitutes an unprecedented modular strategy for the attachment of highly complex functional molecules to proteins. Furthermore, it was shown in several independent experiments, employing various model systems that the thiol adducts to the electrophilic phosphonamidate reagents are formed irreversibly under physiological conditions. Since linkage integrity is crucial for the safety and efficacy of functional drug conjugates that facilitate a selective delivery of a pharmacophore in the body towards the side of action, the phosphonamidate linker system has been applied to link cytotoxic payloads to monoclonal antibodies. The resulting ADCs were extensively evaluated *in vitro* and *in vivo*, which revealed a superior stability of the linker system paired with an increased antitumor efficacy in mice when directly compared to standard maleimide linkages in a FDA-approved ADC.

7.1. Chemically induced cysteine modification of proteins and antibodies with ethynylphosphonamidates

Previous research that dealt with the development of the SPhR for the chemoselective modification of azide containing proteins and for the modular conjugation of two azide containing building blocks using borane protected ethynylphosphonites has been continued within the present work. This lead to the establishment of a novel modular reaction sequence that employs the SPhR for the synthesis of ethynylphosphonamidates that subsequently undergo cysteine modification on proteins and antibodies. A synthetic procedure has been developed that facilitates the synthesis of ethynylphosphonamidates from various azide containing building blocks in the presence of several functional groups. Incorporation into a variety of different molecules has been performed in very good yields, including biotin derivatives, fluorescent dyes and unprotected peptides. Subsequent thiol addition studies revealed a second order rate constant of 0.62 $M^{-1}s^{-1}$ that is reasonably fast for cysteine modification on proteins. After method development, the technique was applied to the synthesis of various functional protein and antibody conjugates from fluorescent dyes, peptides and biotin derivatives (Figure 27), which generated the desired conjugates with an unprecedented selectivity for cysteine and good conjugation yields. Stability measurements revealed an excellent cysteine conjugate

stability under physiological conditions in the presence of large thiol excess, cellular lysate and human serum. In strong contrast to standard maleimide linkages, it was shown that antibodies modified with phosphonamidates do not transfer the attached payload to other cysteine containing proteins like albumin and phosphonamidate-cysteine linkages are generally less prone to retro-thiol addition once the conjugates are formed.

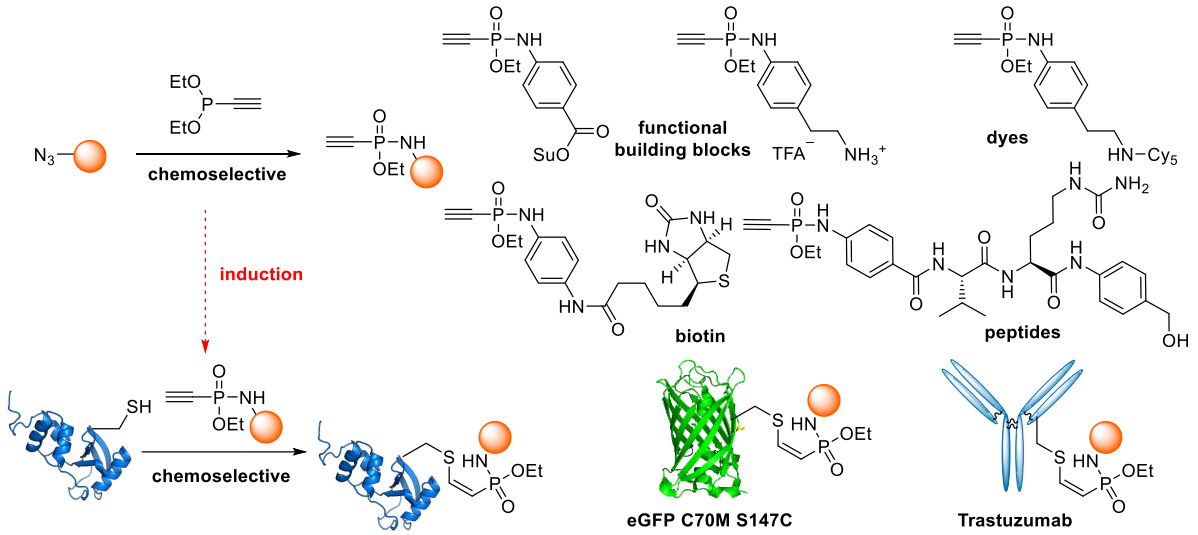

Figure 27: Principle of the SPhR with ethynylphosphonites that induces thiol reactivity for the subsequent cysteine selective modification on proteins. Shown are chosen ethynylphosphonamidates that have been synthesized and proteins that have been modified within the present work.

Furthermore, the synthetic incorporation of different *O*-substituents to the phosphonamidates has been performed within the current work. Several different phosphonites were prepared, carrying various functional handles and have been subsequently used in the SPhR with azides. Thereby it was possible to attach moieties to the *O*-substituent that expand the functionality of the final conjugate. It could be demonstrated that small ethylene glycol chains increase the water solubility of ethynylphosphonamidate modified hydrophobic payloads, which leads to a better cysteine conjugation efficiency to antibodies In addition to that, a terminal alkyne has been attached that allows for the attachment of a third functionality to the system via CuAAC. Finally, different tags have been synthetically attached to the phosphonamidate that allow a stimulated release of the *O*-substituent by light, esterase activity or reductive conditions to generate phosphonamidic acids with increased *P-N*-lability (Figure 28). Here, intracellularly cleavable handles could facilitate a traceless release of a primary amine after cellular uptake, which makes those substituents in particular interesting for drug delivery applications.

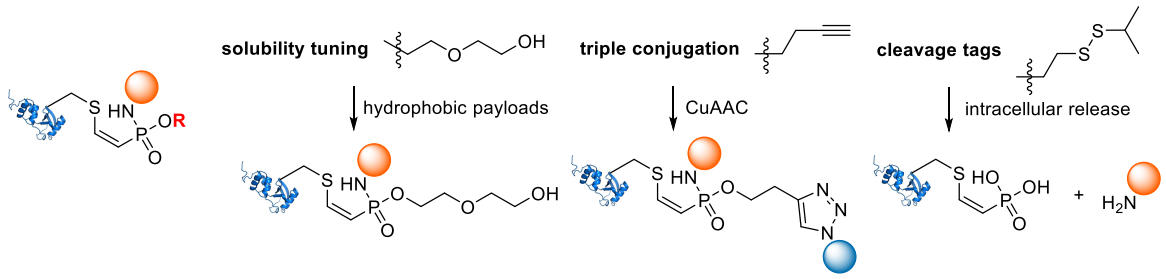

Figure 28: Attachment of different handles to the phosphonamidate ester residue expands the functionality of the final conjugate. Shown are chosen substituents that have been synthetically incorporated and evaluated within this work.

The current work described the synthesis of phosphonamidates with cleavable substituents and provides preliminary data that support the mechanistic principle of an intracellular release. Further investigations include intensive stability studies on the intact phosphonamidates and the released phosphonamidic acids intracellularly and during blood circulation to finally construct a drug-conjugate that is stably linked via a cleavable phosphonamidate and releases its payload only upon cellular uptake. The groundwork towards such a conceptually novel, phosphonamidate based cleavage side has been laid by the work described in this thesis.

7.2. Variation of the *O*-substituent of vinylphosphonamidates facilitate reactivity tuning of the thiol-addition

To further expand the scope of the methodology, the SPhR was also carried out with vinylphosphonites to synthesize electrophilic vinylphosphonamidates for subsequent cysteine modifications on proteins and antibodies. To overcome much slower reaction kinetics of vinylphosphonamidates when compared to their ethynyl counterparts, several vinylphosphonites with different electron-withdrawing substituents have been synthesized, transformed into vinylphosphonamidates via SPhR and tested in the reactivity with glutathione. It could be shown that various electron-withdrawing phosphonamidate ester residues exert increasing effects on the kinetics of the thiol addition. With a second-order rate constant of 0.021 $M^{-1}s^{-1}$, the *O*-trifluoroethyl substituted reagent was the fastest vinylphosphonamidate tested (Figure 29). Even though this is one order of magnitude slower than the standard ethyl-substituted ethynylphosphonamidate, the reaction is still fast enough to modify cysteine residues on proteins, as exemplified by modification of the antibody cetuximab with an EDANS-fluorophore. Further functional cysteine reactive vinylphosphonamidates that have been synthesized within the current work include peptides, a biotin derivative and Cy5-fluorophore. Vinylphosphonamidates have been successfully conjugated to various proteins and antibodies, including eGFP, ubiquitin and cetuximab.

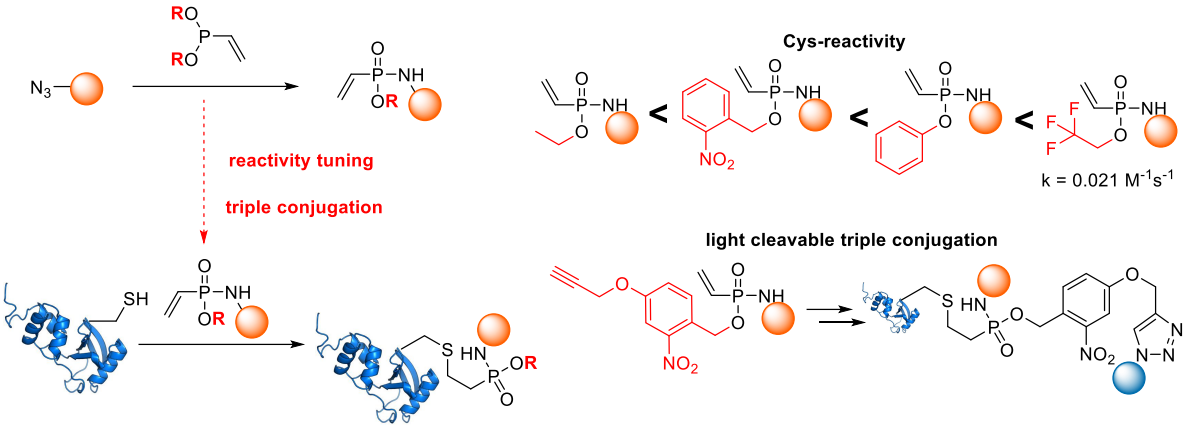

Figure 29: Principle of the SPhR with vinylphosphonites and subsequent cysteine addition. Variation of the *O*-substituent facilitates tuning of the vinylphosphonamidate's reactivity for cysteine or enable a light-cleavable triple conjugation via CuAAC.

Similar to ethynylphosphonamidates, the attachment of an additional terminal alkyne to the phosphonamidate ester residue that enables further CuAAC-modifications could also be accomplished for vinylphosphonamidates (Figure 29). The additional incorporation of a 2-nitrobenzyl substituent between the phosphonamidate and the alkyne handle facilitates both, increased thiol addition kinetics due to the electron-withdrawing nature and furthermore a controlled light-mediated release of the substituent after conjugation.

The fine tuning of the cysteine reactivity by variation of the phosphonamidate ester residue is giving rise to novel cysteine reactive probes for applications where a narrow reactivity window is crucial, as in covalent enzyme inhibitors for active center cysteines, for instance. Other than that, future investigations include further application of the light mediated triple conjugation for example to protein catch and release strategies or defined light mediated release of a cargo from a protein in cellular imaging applications.

7.3. Ethynylphosphonamidates facilitate a simple synthetic access to efficacious ADCs

One important aspect in tumor directed drug delivery is linkage stability between the targeting unit and the drug to prevent premature release during blood circulation that can cause severe side effects. This is in particular important for drug delivery systems that are big in size such as ADCs due to long circulation times in the body. Since ethynylphosphonamidates exhibit excellent cysteine selectivity, good reaction kinetics and outstanding linkage stability, they were chosen in the present work to synthesize ADCs via interchain disulfide reduction and alkylation. It could be demonstrated in several *in vitro* experiments that phosphonamidate linked ADCs from two therapeutically relevant antibodies, brentuximab and trastuzumab linked to two cytotoxic payloads MMAF and MMAE efficiently reduce the viability of targeted cell lines. Incorporation of a diethylene glycol unit to the phosphonamidate ester residue significantly enhanced the water solubility of the less polar MMAE and thereby also the

conjugation efficiency to antibodies. It was shown that only 4.5 equivalents of the drug are needed to achieve an average antibody loading of 4. Further development of this already very efficient conjugation reaction resulted in a most simple one-pot reduction and alkylation protocol for the synthesis of efficacious ADCs from native antibodies in a single step.

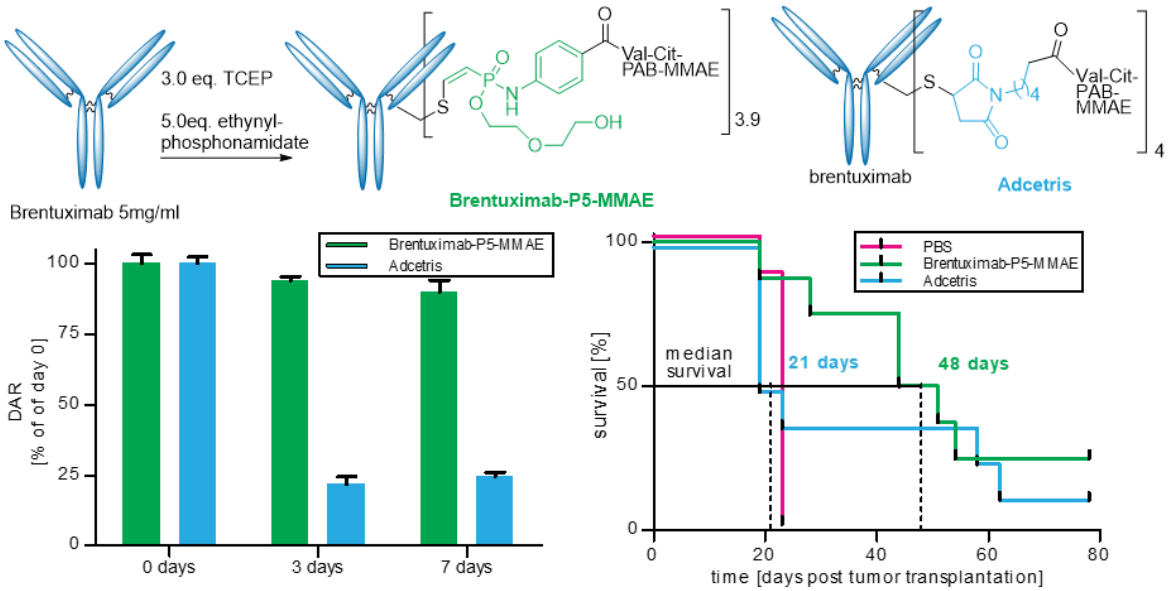

Figure 30: Phosphonamidate linked Brentuximab-MMAE that has been synthesized in a highly efficient one-pot protocol within this thesis. Phosphonamidate linkage has been shown to improve linkage stability of maleimide linked Adcetris® in rat serum (left) and lead to an increase in median survival in mice bearing a tumor xenograft by a factor of 2.3 (right).

Having the synthetic protocols established, an ADC analogously to the FDA-approved Adcetris® was synthesized from brentuximab and cathepsin B cleavable MMAE with the only difference being a phosphonamidate- instead of a maleimide linkage. It was shown that the phosphonamidate linked ADC exhibits a superior linkage stability in serum with only 10% of payload loss after seven days over commercial Adcetris® that lost 75% of its payload already after three days. In addition to that, it was shown that a group of tumor bearing mice, treated twice with 0.5 mg/kg ADC showed an increase in median survival from 23 to 48 days, which corresponds to a factor of 2.3 for the phosphonamidate linked ADC when compared to commercially available Adcetris®.

Next steps include further validation of the superior pharmacologic properties of the phosphonamidate linkage in the context of ADCs, conducting *in vivo* pharmacokinetic and *in vivo* linkage stability measurements and investigating the maximum tolerated dose in a direct comparison to maleimide linked ADCs. The final goal is the establishment of ethynylphosphonamidates as a new linker class for safer and more efficacious Antibody-Drug-Conjugates, to develop a new generation of cancer treatment.

8. Experimental part

8.1. General information

8.1.1. Chemicals and solvents

Chemicals and solvents were purchased from Merck (Merck group, Germany), TCI (Tokyo chemical industry CO., LTD., Japan) and Acros Organics (Thermo Fisher scientific, USA) and used without further purification. Dry solvents were purchased from Acros Organics (Thermo Fisher scientific, USA).

8.1.2. Flash- and thin layer chromatography

Flash column chromatography was performed, using NORMASIL 60® silica gel 40-63 µm (VWR international, USA). Glass TLC plates, silica gel 60 W coated with fluorescent indicator F254s were purchased from Merck (Merck Group, Germany). Spots were visualized by fluorescence depletion with a 254 nm lamp or manganese staining (10 g K2CO3, 1.5 g KMnO4, 0.1 g NaOH in 200 ml H2O), followed by heating.

8.1.3. Semi-preparative HPLC

Semi-preparative HPLC was performed on a Shimadzu prominence HPLC system (Shimadzu Corp., Japan) with a CBM20A communication bus module, a FRC-10A fraction collector, 2 pumps LC-20AP, and a SPD-20A UV/VIS detector, using a VP250/21 Macherey-Nagel Nucleodur C18 HTec Spum column (Macherey-Nagel GmbH & Co. Kg, Germany) eluting with 10 ml/min. Compounds with a sample-size of less than 10 mg were purified using a VP250/21 Macherey-Nagel Nucleodur C18 HTec Spum column eluting with 5 ml/min. The following gradients were used: Method A: (Solvent A = H_2O + 0.1% TFA, solvent B = MeCN + +0.1% TFA), 5% B 0-5 min, 5-99% B 5-65 min, 99% B 65-75 min. Method B: (Solvent A = H_2O + 0.1% TFA, solvent B = MeCN + +0.1% TFA), 25% B 0-5 min, 25-99% B 5-65 min, 99% B 65-75 min.

8.1.4. NMR

NMR spectra were recorded with a Bruker Ultrashield 300 MHz spectrometer and a Bruker Avance III 600 MHz spectrometer (Bruker Corp., USA) at ambient temperature. Chemical shifts δ are reported in ppm relative to residual solvent peak ($CDCl_3$: 7.26 [ppm]; DMSO-d6: 2.50 [ppm]; acetone-d6: 2.05 [ppm]; CD_3CN 1.94 [ppm]; 4.79 D_2O [ppm] for 1H-spectra and $CDCl_3$: 77.16 [ppm]; DMSO-d6: 39.52 [ppm]; acetone-d6: 29.84 [ppm]; CD_3CN 1.32 [ppm]; for 13C-spectra . Coupling constants J are stated in Hz. Signal multiplicities are abbreviated as follows: s: singlet; d: doublet; t: triplet; q: quartet; m: multiplet.

8.1.5. UPLC-UV/MS

UPLC-UV/MS traces were recorded on a Waters H-class instrument equipped with a quaternary solvent manager, a Waters autosampler, a Waters TUV detector and a Waters Acquity QDa detector with an Acquity UPLC BEH C18 1.7 µm, 2.1 x 50 mm RP column with a flow rate of 0.6 mL/min (Waters Corp., USA). The following gradient was used: A: 0.1% TFA in H_2O; B: 0.1% TFA in MeCN. 5% B 0 - 0.5 min, 5-95% B 0.5-3 min, 95% B 3-3.9 min, 5% B 3.9-5 min. Analytical method: 5% B 0 – 1.5 min, 5-95% B 1.5-13 min, 95% B 13-13.9 min, 5% B 13.91-15 min.

8.1.6. HR-MS

High resolution ESI-MS spectra were recorded on a Waters H-class instrument equipped with a quaternary solvent manager, a Waters sample manager-FTN, a Waters PDA detector and a Waters column manager with an Acquity UPLC protein BEH C18 column (1.7 µm, 2.1 mm x 50 mm). Samples were eluted with a flow rate of 0.3 mL/min. The following gradient was used: A: 0.01% FA in H_2O; B: 0.01% FA in MeCN. 5% B: 0-1 min; 5 to 95% B: 1-7min; 95% B: 7 to 8.5 min. Mass analysis was conducted with a Waters XEVO G2-XS QTof analyzer.

8.1.7. Intact protein MS

Intact proteins were analyzed using a Waters H-class instrument equipped with a quaternary solvent manager, a Waters sample manager-FTN, a Waters PDA detector and a Waters column manager with an Acquity UPLC protein BEH C4 column (300 Å, 1.7 µm, 2.1 mm x 50 mm) at a column temperature of 80 °C. Proteins were eluted with a flow rate of 0.3 mL/min. The following gradient was used: A: 0.01% FA in H_2O; B: 0.01% FA in MeCN. 5-95% B 0-6 min. Mass analysis was conducted with a Waters XEVO G2-XS QTof analyzer. Proteins were ionized in positive ion mode applying a cone voltage of 80 kV. Raw data was analyzed with MaxEnt 1.

8.1.8. Preparative size-exclusion chromatography

Protein purification by size-exclusion chromatography was conducted with an ÄKTA FPLC system (GE Healthcare, United States) equipped with a P-920 pump system, a UPC-900 detector and a FRAC-950 fraction collector.

8.1.9. MALDI-TOF MS

MALDI-TOF MS of intact protein samples was conducted with a Bruker Microflex™ LT benchtop system (Bruker, United States). Using a matrix of saturated DHAP (2',6'-Dihydroxyacetophenone) in acetonitrile.

8.2. Procedures and compound characterizations

General procedure 1 for the synthesis of *O*-substituted ethynylphosphonites from bis(diisopropylamino)chlorophosphine

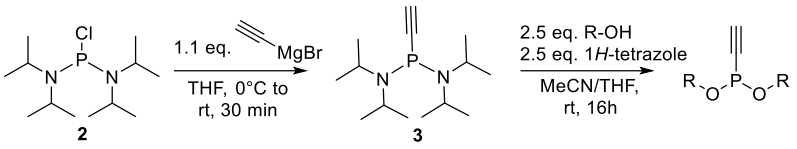

A 25-ml Schlenk flask was charged with 267 mg bis(diisopropylamino)chlorophosphine (**2**) (1.00 mmol, 1.00 eq.) under an argon atmosphere, cooled to 0 °C and 2.20 ml ethynylmagnesium bromide solution (0.5 M in THF, 1.10 mmol, 1.10 eq.) was added drop wise. The yellowish solution was allowed to warm to room temperature and stirred for further 30 minutes. The desired alcohol, dissolved in 5.56 ml 1H-tetrazole solution (0.45 M in MeCN, 2.50 mmol, 2.50 eq.) was added and the white suspension was stirred overnight at room temperature. The reaction mixture was directly placed on a silica gel flash column for purification. It should be noted, that mass analysis of phosphonites failed for all of the tested compounds, possibly due to decomposition under ESI-conditions.

2-Hydroxyethyl isopropyldisulfide

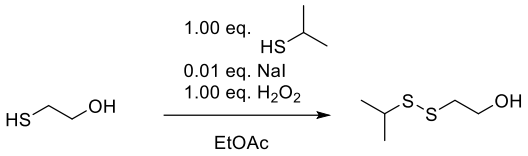

A 250 ml-round bottom flask was charged with 2.00 ml isopropylthiol (21.53 mmol, 1.00 eq.), 1.52 ml 2-mercaptoethanol (21.53 mmol, 1.00 eq.), 32 mg sodium iodide (0.21 mmol, 0.01 eq.) and 40 ml EtOAc and cooled to 0°C. The mixture was rapidly stirred and 10 mmol of a solution of 30% H_2O_2 in water was added drop-wise. 2.44 ml hydrogen peroxide solution (aqueous, 30%) (21.53 mmol, 1.00 eq.) were added dropwise, the mixture was allowed to warm to room temperature and stirred for 1 h. All volatiles were removed under reduced pressure and the disulfide was isolated by column chromatography on silica (10% EtOAc in hexane) yielding 1.10 g of a colorless liquid (7.22 mmol, 33.6%).

^{1}H NMR (300 MHz, Chloroform-*d*) δ = 3.88 (m, 2H), 3.02 (hept, *J*=6.7, 1H), 2.85 (t, *J*=5.9, 2H), 2.37 (m, 1H), 1.32 (d, *J*=6.7, 6H). ^{13}C NMR (75 MHz, $CDCl_3$) δ = 60.48, 41.94, 41.14, 22.54.

Di-(2-isopropyl disulfido)ethyl) ethynylphosphonite (4)

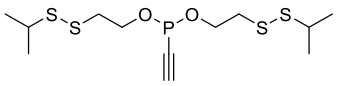

The compound was synthesized according to the general procedure 1 from 213 mg bis(diisopropylamino)chlorophosphine (**2**) (0.80 mmol, 1.00 eq.), 1.76 ml ethynylmagnesium bromide solution (0.5 M in THF, 0.88 mmol, 1.10 eq.), 370 mg 2-Hydroxyethyl isopropyldisulfide (2.00 mmol, 2.50 eq.), 4.44 ml 1*H*-tetrazole solution (0.45 M in MeCN, 2.00 mmol, 2.50 eq.) and purified by flash column chromatography on silica gel (10% EtOAc in hexane). The compound was obtained as yellowish oil. (183 mg, 0.51 mmol, 63.9%).

^{1}H NMR (300 MHz, Chloroform-*d*) δ = 4.21 (dt, *J*=8.0, 6.8, 4H), 3.15 (d, *J*=2.3, 1H), 3.04 (p, *J*=6.7, 2H), 2.94 (t, *J*=6.8, 4H), 1.33 (d, *J*=6.7, 12H). ^{13}C NMR (75 MHz, Chloroform-d) δ 92.47 (d, J = 1.0 Hz), 84.15 (d, J = 47.9 Hz), 66.24 (d, J = 6.1 Hz), 41.18, 40.13 (d, J = 4.4 Hz), 22.58. ^{31}P NMR (122 MHz, $CDCl_3$) δ = 130.40.

Di-(2-*tert*-butyl disulfido)ethyl) ethynylphosphonite (5)

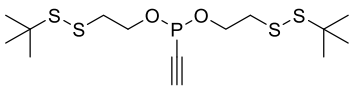

The compound was synthesized according to the general procedure 1 from 167 mg bis(diisopropylamino)chlorophosphine (**2**) (0.63 mmol, 1.00 eq.), 1.38 ml ethynylmagnesium bromide solution (0.5 M in THF, 0.69 mmol, 1.10 eq.), 260 mg 2-Hydroxyethyl *tert*-butyl disulfide (1.57 mmol, 2.50 eq.), 3.48 ml 1*H*-tetrazole solution (0.45 M in MeCN, 1.57 mmol, 2.50 eq.) and purified by flash column chromatography on silica gel (10% EtOAc in hexane). The compound was obtained as yellowish oil. (190 mg, 0.49 mmol, 78.5%).

^{1}H NMR (300 MHz, Chloroform-d) δ = 4.20 (dt, J=7.9, 6.9, 4H), 3.14 (d, J=2.2, 1H), 2.95 (t, J=6.9, 4H), 1.36 (s, 18H). ^{13}C NMR (75 MHz, Chloroform-d) δ = 92.35 (d, J=1.0), 84.21 (d, J=47.8), 66.37 (d, J=6.1), 47.98, 40.77 (d, J=4.3), 29.89. ^{31}P NMR (122 MHz, $CDCl_3$) δ = 130.28.

2-(3-Hydroxypropyl) isopropyl disulfide

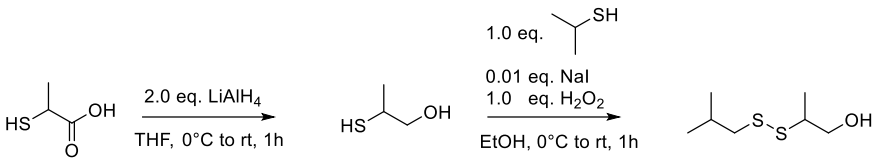

A 500-ml round-bottom flask was charged with 2.00 ml thiolactic acid (23.55 mmol, 1.00 eq.) and 150 ml dry THF. At 0 °C, 1.60 g Lithium aluminum hydride (47.10, 2.0 eq.) were added portion-wise. The mixture was stirred at room temperature for 1 h, cooled again to 0 °C and quenched carefully with 6 N HCl. The aqueous phase was extracted with twice with 100 ml EtOAc, the organic fractions pooled, dried ($MgSO_4$) and all volatiles were removed under reduced pressure. The resulting colorless oil was redissolved in 20 ml EtOH and 2.18 ml isobutyl thiol (23.55 mmol, 1.00 eq.), 55 mg sodium iodide (0.24 mmol, 0.01 eq.) were added and the solution cooled to 0°C. 2.70 ml hydrogen peroxide solution (aqueous, 30%) (23.55 mmol, 1.00 eq.) were added and the yellowish solution was stirred for another hour at room temperature. Volatiles were removed under reduced pressure and the above stated disulfide isolated by column chromatography on silica (20% EtOAc in hexane) as colorless oil. Yield: 1.15 g (6. 928 mmol, 29.4%)

^{1}H NMR (300 MHz, Chloroform-*d*) δ = 3.69 (dd, *J*=5.8, 3.2, 2H), 3.08 – 2.83 (m, 2H), 1.37 – 1.25 (m, 9H). ^{13}C NMR (75 MHz, CDCl3) δ = 65.49, 48.70, 41.66, 22.60, 22.51, 16.89.

Di-((2-isopropyl disulfido)-3-propyl) ethynylphosphonite (6)

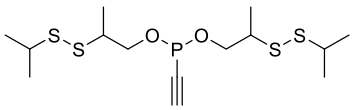

The compound was synthesized according to the general procedure 1 from 267 mg bis(diisopropylamino)chlorophosphine (**2**) (1.00 mmol, 1.00 eq.), 2.20 ml ethynylmagnesium bromide solution (0.5 M in THF, 1.10 mmol, 1.10 eq.), 415 mg 2-(3-Hydroxypropyl) isopropyl disulfide (2.50 mmol, 2.50 eq.), 5.55 ml 1*H*-tetrazole solution (0.45 M in MeCN, 2.50 mmol, 2.50 eq.) and purified by flash column chromatography on silica gel (0-10% EtOAc in hexane). The compound was obtained as a diastereomeric mixture as a yellowish oil. (91 mg, 0.235 mmol, 23.5%).

^{1}H NMR (300 MHz, Chloroform-*d*) δ = 4.28 – 4.06 (m, 2H), 3.99 – 3.81 (m, 2H), 3.21 – 3.10 (m, 1H), 3.07-2.95 (m, 4H), 1.37 – 1.28 (m, 18H). ^{13}C NMR (75 MHz, Chloroform-*d*) δ = 92.39 (d, *J*=3.6), 84.32 (d, *J*=49.3), 71.18 (d, *J*=4.9), 48.18 – 44.79 (m), 41.65, 22.55 (d, *J*=6.5), 17.12. ^{31}P NMR (122 MHz, $CDCl_3$) δ = 130.56, 130.32, 130.10.

Di-(3-Butinyl) ethynylphosphonite (7)

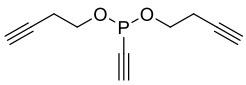

The compound was synthesized according to the general procedure 1 from 267 mg bis(diisopropylamino)chlorophosphine (**2**) (1.00 mmol, 1.00 eq.), 2.20 ml ethynylmagnesium bromide solution (0.5 M in THF, 1.10 mmol, 1.10 eq.), 189 µl 3-Butyn-1-ol (2.50 mmol, 2.50 eq.), 5.56 ml 1*H*-tetrazole solution (0.45 M in MeCN, 2.50 mmol) and purified by flash column chromatography on silica gel (10% EtOAc in n-hexane). The compound was obtained as a colorless oil. (152 mg, 0.774 mmol, 77.4%).

^{1}H NMR (300 MHz, Chloroform-d) δ = 4.07 (dtd, J=8.1, 7.0, 1.5, 4H), 3.14 (d, J=2.3, 1H), 2.56 (tdd, J=7.0, 2.7, 0.6, 4H), 2.03 (t, J=2.7, 2H). ^{13}C NMR (75 MHz, Chloroform-d) δ = 92.42 (d, J=1.3), 83.92 (d, J=47.1), 80.24, 70.02, 65.81 (d, J=6.5), 21.28 (d, J=4.7). ^{31}P NMR (122 MHz, $CDCl_3$) δ = 130.15.

Di-(2-(2-Hydroxyethoxy)ethyl) ethynylphosphonite (8)

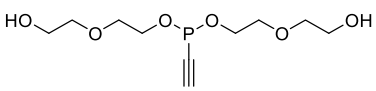

The compound was synthesized according to the general procedure 1 from 267 mg bis(diisopropylamino)chlorophosphine (**2**) (1.00 mmol, 1.00 eq.), 2.20 ml ethynylmagnesium bromide solution (0.5 M in THF, 1.10 mmol, 1.10 eq.), 1.06 g diethylene glycol (10.00 mmol, 10.00 eq.), 5.56 ml 1*H*-tetrazole solution (0.45 M in MeCN, 2.50 mmol) and purified by flash column chromatography on silica gel (5% MeOH in CH_2Cl_2). The compound was obtained as a yellowish oil. (112 mg, 0.421 mmol, 42.1%).

^{1}H NMR (300 MHz, Chloroform-*d*) δ = 4.14 – 3.98 (m, 4H), 3.65 – 3.59 (m, 4H), 3.58 – 3.49 (m, 8H), 3.15 (d, *J*=2.4, 1H) ^{13}C NMR (75 MHz, Chloroform-*d*) δ = 92.51 (d, *J*=1.4), 84.30 (d, *J*=46.8), 72.60, 70.72 (d, *J*=4.0), 67.20 (d, *J*=6.0), 61.44. ^{31}P NMR (122 MHz, $CDCl_3$) δ = 131.97.

Di-(2-diethylamino benzyl) ethynylphosphonite (9)

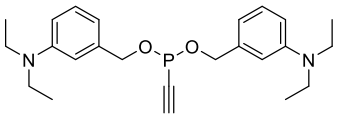

The compound was synthesized according to the general procedure 1 from 267 mg bis(diisopropylamino)chlorophosphine (**2**) (1.00 mmol, 1.00 eq.), 2.20 ml ethynylmagnesium bromide solution (0.5 M in THF, 1.10 mmol, 1.10 eq.), 433 mg 2-diethylamino benzylalcoho (2.50 mmol, 2.50

eq.), 5.56 ml 1*H*-tetrazole solution (0.45 M in MeCN, 2.50 mmol) and purified by flash column chromatography on silica gel (20% EtOAc in hexane). The compound was obtained as a yellowish oil. (200 mg, 0.485 mmol, 48.5%).

^{1}H NMR (300 MHz, Chloroform-*d*) δ 7.34 – 7.16 (m, 2H), 6.74 – 6.62 (m, 6H), 5.08 – 4.86 (m, 4H), 3.39 (q, *J* = 7.0 Hz, 8H), 3.18 (d, *J* = 2.4 Hz, 1H), 1.20 (t, *J* = 7.1 Hz, 12H). ^{13}C NMR (75 MHz, Chloroform-*d*) δ 147.98, 138.84 (d, *J* = 4.2 Hz), 129.41, 114.74, 111.44, 111.02, 92.07, 85.08 (d, *J* = 49.0 Hz), 70.65 (d, *J* = 6.3 Hz), 44.36, 12.63. ^{31}P NMR (122 MHz, $CDCl_3$) δ 129.82.

Di-(4-acetoxy benzyl) ethynylphosphonite (10)

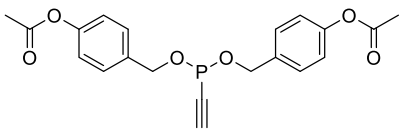

The compound was synthesized according to the general procedure 1 from 267 mg bis(diisopropylamino)chlorophosphine (**2**) (1.00 mmol, 1.00 eq.), 2.20 ml ethynylmagnesium bromide solution (0.5 M in THF, 1.10 mmol, 1.10 eq.), 415 mg 4-Acetoxybenzyl alcohol (2.50 mmol, 2.50 eq.), 5.55 ml 1*H*-tetrazole solution (0.45 M in MeCN, 2.50 mmol, 2.50 eq.) and purified by flash column chromatography on silica gel (30% EtOAc in hexane). The compound was obtained as a as colorless oil. (118 mg, 0.306 mmol, 30.6%).

^{1}H NMR (300 MHz, Chloroform-*d*) δ = 7.34 (d, *J*=8.5, 4H), 7.08 (d, *J*=8.5, 4H), 4.95 (dd, *J*=8.4, 1.7, 4H), 3.20 (d, *J*=2.3, 1H), 2.32 (s, 6H). ^{13}C NMR (75 MHz, Chloroform-*d*) δ = 169.44, 150.37, 135.31 (d, *J*=4.3), 128.89, 121.68, 92.68, 84.40 (d, *J*=47.6), 69.35 (d, *J*=6.8), 21.16. ^{31}P NMR (122 MHz, $CDCl_3$) δ = 131.09.

Di (4-(diazophenyl)-benzyl) ethynylphosphonite (11)

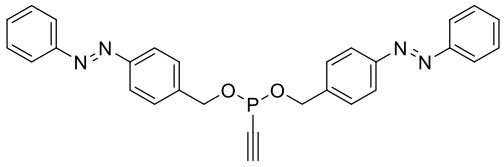

The compound was synthesized according to the general procedure 1 from 98 mg bis(diisopropylamino)chlorophosphine (**2**) (0.37 mmol, 1.00 eq.), 0.80 ml ethynylmagnesium bromide solution (0.5 M in THF, 0.4 mmol, 1.10 eq.), 195 mg 1-(4-(hydroxymethyl)phenyl)-2-phenyldiazene (0.93 mmol, 2.50 eq.), 2.00 ml 1*H*-tetrazole solution (0.45 M in MeCN, 0.93 mmol, 2.50 eq.) and purified by flash column chromatography on silica gel (0-10% EtOAc in hexane). The compound was obtained as orange solid. (82 mg, 0.171 mmol, 46.3%).

^{1}H NMR (300 MHz, Chloroform-*d*) δ = 7.98 – 7.86 (m, 8H), 7.59 – 7.44 (m, 10H), 5.08 (d, *J*=8.5, 4H), 3.24 (d, *J*=2.3, 1H). ^{13}C NMR (75 MHz, Chloroform-*d*) δ = 152.60, 152.27, 140.55 (d, *J*=4.3), 131.07, 129.09, 128.24, 123.03, 122.90, 92.89, 84.35 (d, *J*=47.2), 69.54 (d, *J*=6.9). ^{31}P NMR (122 MHz, $CDCl_3$) δ = 131.77.

General procedure 2 for the synthesis of borane protected ethynylphosphonites from Bis(diisopropylamino)chlorophosphine

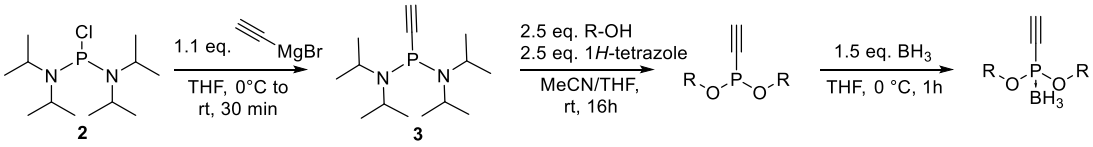

A flame-dried Schlenk flask was charged with 1.0 mmol (1.0 eq.) Bis(diisopropylamino)-chlorophosphine, dissolved in 200 µl of dry THF and cooled to 0 °C. 1.10 mmol (1.1eq.) of ethynyl magnesiumbromide (1.0 M in THF) was added and the reaction was stirred at room temperature for 30 minutes. A solution of 2.5 mmol vacuum dried alcohol (2.5 eq.) in 1 ml of dry THF or MeCN and 2.5 mmol (2.5 eq.) 1*H*-tetrazole (0.45 M in MeCN) was added. The resulting suspension was stirred at room temperature overnight. Finally 1.5 mmol (1.5 eq.) of borane (1.0 M in THF) were added at 0 °C and stirred for another hour. The crude product was dry packed on a silica column for purification. It should be noted, that mass analysis of phosphonites failed for all of the tested compounds, possibly due to decomposition under ESI-conditions.

Diphenyl ethynylphosphonite borane (12)

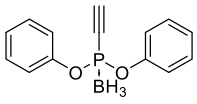

The compound was synthesized according to the general procedure 2 from Bis(diisopropylamino)chlorophosphine (267 mg, 1.00 mmol). The crude borane protected phosphonite was purified by flash column chromatography (30% CH_2Cl_2 in hexane) and obtained as a colorless oil. (90 mg, 0.351 mmol, 35.1%)

^{1}H NMR (300 MHz, Chloroform-*d*) δ 7.41 (dd, *J* = 8.7, 7.0 Hz, 4H), 7.34 – 7.20 (m, 6H), 3.28 (d, *J* = 7.5 Hz, 1H), 1.77 – 0.20 (m, 3H). ^{13}C NMR (75 MHz, Chloroform-*d*) δ 151.11 (d, *J* = 10.0 Hz), 129.88 (d, *J* = 1.3 Hz), 125.98 (d, *J* = 1.5 Hz), 120.89 (d, *J* = 4.6 Hz), 95.75 (d, *J* = 24.7 Hz), 76.01 (d, *J* = 119.5 Hz). ^{31}P NMR (122 MHz, Chloroform-*d*) δ 107.02 – 103.45 (m).

Di(2-nitrobenzyl) ethynylphosphonite borane (13)

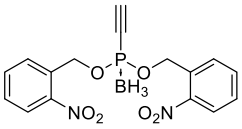

The compound was synthesized according to the general procedure 2 from Bis(diisopropylamino)chlorophosphine (534 mg, 2.00 mmol). The crude borane protected phosphonite was purified by flash column chromatography (20% EtOAc in hexane) and obtained as a colorless solid. (677 mg, 1.810 mmol, 90.5%)

^{1}H NMR (300 MHz, Chloroform-*d*) δ 8.36 – 8.12 (m, 2H), 7.87 – 7.67 (m, 4H), 7.62 – 7.45 (m, 2H), 5.76 – 5.49 (m, 4H), 3.33 (d, *J* = 7.3 Hz, 1H), 1.78 – 0.18 (m, 3H). ^{13}C NMR (75 MHz, Chloroform-*d*) δ 146.46, 134.23, 131.83 (d, *J* = 7.5 Hz), 129.02, 128.36, 125.04, 94.63 (d, *J* = 24.6 Hz), 66.54 (d, *J* = 5.3 Hz), 62.49. ^{31}P NMR (122 MHz, Chloroform-*d*) δ 109.92 (dd, *J* = 152.1, 47.5 Hz).

Bis(2,2,2-trifluoroethyl) ethynylphosphonite borane (14)

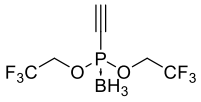

The compound was synthesized according to the general procedure 2 from Bis(diisopropylamino)chlorophosphine (267 mg, 1.00 mmol). The crude borane protected phosphonite was purified by flash column chromatography (10% EtOAc in hexane) and obtained as a colorless oil. (158 mg, 0.590 mmol, 59.0%)

^{1}H NMR (300 MHz, Chloroform-*d*) δ 4.59 – 4.24 (m, 4H), 3.43 (d, *J* = 7.8 Hz, 1H), 1.54 – 0.03 (m, 3H). ^{13}C NMR (75 MHz, Chloroform-*d*) δ 122.14 (d, *J* = 286.1 Hz), 95.97 (d, *J* = 28.2 Hz), 64.09 (qd, *J* = 38.4, 4.5 Hz). ^{31}P NMR (122 MHz, Chloroform-*d*) δ 121.41 – 114.01 (m). ^{19}F NMR (282 MHz, $CDCl_3$) δ 2.58.

General procedure 3 for the synthesis of *O*-substituted ethynylphosphonamidates from unprotected ethynylphosphonites and 4-azidobenzoic acid NHS-ester

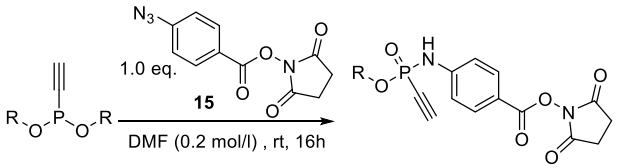

1.00 mmol of an 4-azidobenzoic acid NHS-ester **15** (1.00 eq.) was stirred together with 1.00 mmol of an ethynylphosphonite (1.00 eq.) in 5 ml DMF overnight. The organic solvent was removed under reduced pressure and the residue purified by column chromatography on silica.

2-Isopropyl-disulfido-ethyl-*N*-(4-benzoic-acid-*N*-hydroxysuccinimideester)-*P*-ethynylphosphonamidate (16)

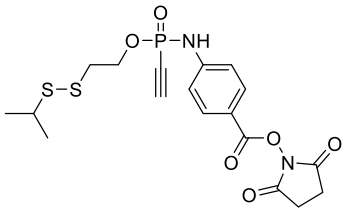

The compound was synthesized according to the general procedure 3 from 147 mg Di-(2-isopropyl disulfido)ethyl) ethynylphosphonite (**4**) (0.411 mmol, 1.00 eq.) and 106 mg 4-azidobenzoic-acid-*N*-hydroxysuccinimide ester (**15**) (0.411 mmol, 1.00 eq.) and purified by flash column chromatography on silica gel (60% EtOAc in hexane). The compound was obtained as colorless oil. (80 mg, 0.175 mmol, 42.6%).

^{1}H NMR (300 MHz, Chloroform-*d*) δ = 8.08 (d, *J*=8.7, 2H), 7.20 (d, *J*=8.8, 2H), 7.13 (d, *J*=7.5, 1H), 4.63 – 4.18 (m, 2H), 3.23 – 2.76 (m, 8H), 1.31 (dd, *J*=6.7, 1.0, 6H). ^{13}C NMR (75 MHz, Chloroform-*d*) δ 169.10 (d, *J* = 55.1 Hz), 161.37, 145.27, 132.42, 118.41, 117.66 (d, *J* = 7.9 Hz), 89.15 (d, *J* = 50.2 Hz), 75.07 (d, *J* = 278.6 Hz), 64.26 (d, *J* = 5.2 Hz), 41.24, 38.75 (d, *J* = 7.5 Hz), 25.62 (d, *J* = 11.8 Hz), 22.51. ^{31}P NMR (122 MHz, $CDCl_3$) δ = -10.16. HRMS for $C_{18}H_{21}N_2NaO_6PS_2^+$ $[M+Na]^+$ calcd.: 479.0471, found: 479.0471.

2-*tert*-butyl-disulfido-ethyl-*N*-(4-benzoic-acid-*N*-hydroxysuccinimideester)-*P*-ethynylphosphonamidate (17)

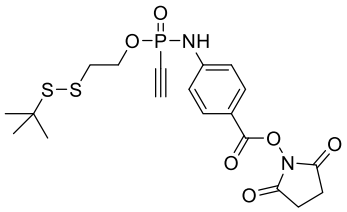

The compound was synthesized according to the general procedure 3 from 50 mg Di-(2- *tert*-butyl disulfido)ethyl) ethynylphosphonite (**5**) (0.129 mmol, 1.00 eq.) and 33 mg 4-azidobenzoic-acid-*N*-hydroxysuccinimide ester (**15**) (0.129 mmol, 1.00 eq.) and purified by flash column chromatography on silica gel (70% EtOAc in hexane). The compound was obtained as colorless solid. (29 mg, 0.0638 mmol, 47.4%).

^{1}H NMR (300 MHz, Chloroform-*d*) δ = 8.06 (d, *J*=8.7, 2H), 7.49 (d, *J*=7.5, 1H), 7.21 (d, *J*=8.7, 2H), 4.58 – 4.26 (m, 2H), 3.09 – 2.81 (m, 7H), 1.33 (s, 9H). ^{13}C NMR (75 MHz, Chloroform-*d*) δ 169.50, 161.40, 145.32, 132.40, 118.34, 117.68 (d, *J* = 8.0 Hz), 89.19 (d, *J* = 50.2 Hz), 75.06 (d, *J* = 278.6 Hz), 64.38 (d, *J*

= 5.1 Hz), 48.28, 39.38 (d, *J* = 7.5 Hz), 29.83, 25.70. ^{31}P NMR (122 MHz, $CDCl_3$) δ = -9.98. HRMS for $C_{19}H_{22}N_2NaO_6PS_2^+$ $[M+Na]^+$ calcd.: 493.0627, found: 493.0628.

2-isopropyldisulfido-3-propyl-*N*-(4-benzoic-acid-*N*-hydroxysuccinimideester)-*P*-ethynylphosphonamidate (18)

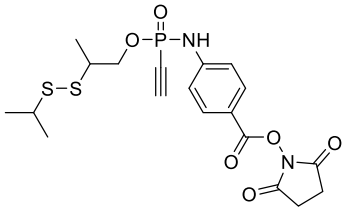

The compound was synthesized according to the general procedure 3 from 61 mg Di-((2-isopropyl disulfido)-3-propyl) ethynylphosphonite (**6**) (0.158 mmol, 1.00 eq.) and 40 mg 4-azidobenzoic-acid-*N*-hydroxysuccinimide ester (**15**) (0.158 mmol, 1.00 eq.) and purified by flash column chromatography on silica gel (70% EtOAc in hexane). The compound was obtained as mixture of diastereomers as colorless oil. (32 mg, 0.068 mmol, 43.0%).

^{1}H NMR (300 MHz, Chloroform-*d*) δ = 8.05 (d, *J*=8.7, 2H), 7.84 – 7.74 (m, 1H), 7.21 (d, *J*=8.8, 2H), 4.57 – 4.27 (m, 2H), 3.20 – 2.66 (m, 7H), 1.46 – 1.21 (m, 9H). ^{31}P NMR (122 MHz, $CDCl_3$) δ = -9.87. 13C NMR (75 MHz, Chloroform-d) δ 169.46, 161.37, 145.30, 132.41, 118.40, 117.63 (d, J = 7.9 Hz), 89.17 (dd, J = 50.1, 10.0 Hz), 72.01 – 66.52 (m), 45.32 (d, J = 8.1 Hz), 41.70 (d, J = 4.1 Hz), 25.70, 22.56, 22.45, 16.90 (d, J = 1.3 Hz). HRMS for $C_{19}H_{22}N_2NaO_6PS_2^+$ $[M+Na]^+$ calcd.: 493.0627, found: 493.0628.

3-Butinyl-*N*-(4-benzoic-acid-*N*-hydroxysuccinimideester)-*P*-ethynylphosphonamidate (19)

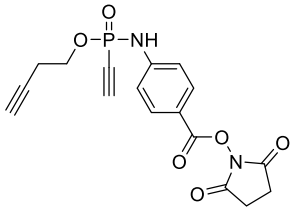

The compound was synthesized according to the general procedure 3 from 61 mg Di-(3-Butinyl) ethynylphosphonite (**7**) (0.192 mmol, 1.00 eq.) and 50 mg 4-azidobenzoic-acid-*N*-hydroxysuccinimide ester (**15**) (0.192 mmol, 1.00 eq.) and purified by flash column chromatography on silica gel (70% EtOAc in hexane). The compound was obtained as colorless oil. (55 mg, 0.147mmol, 76.6%).

^{1}H NMR (300 MHz, Chloroform-*d*) δ 8.02 (d, *J* = 6.9 Hz, 2H), 7.21 (d, *J* = 8.8 Hz, 2H), 4.42 – 4.04 (m, 2H), 3.06 (d, *J* = 13.2 Hz, 1H), 2.89 (s, 4H), 2.65 (td, *J* = 6.7, 2.7 Hz, 2H), 2.07 (t, *J* = 2.6 Hz, 1H). ^{13}C NMR (75 MHz, Chloroform-*d*) δ 169.61, 145.52, 132.30, 118.19, 117.72 (d, *J* = 8.1 Hz), 89.38 (d, *J* = 50.0 Hz),

75.22 (d, *J* = 315.3 Hz), 70.94, 63.92 (d, *J* = 5.0 Hz), 31.48, 25.69, 20.57 (d, *J* = 8.2 Hz). ^{31}P NMR (122 MHz, $CDCl_3$) δ -9.74. HRMS for $C_{17}H_{16}N_2O_6PS^+$ $[M+H]^+$ calcd.: 375.0740, found: 375.0740.

2-(2-Hydroxyethoxy)ethyl-*N*-(4-benzoic-acid-*N*-hydroxysuccinimideester)-*P*-ethynylphosphonamidate (8)

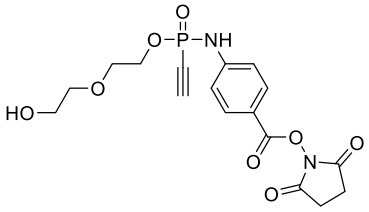

The compound was synthesized according to the general procedure 3 from 93 mg Di-(2-(2-Hydroxyethoxy)ethyl) ethynylphosphonite (**20**) (0.192 mmol, 1.00 eq.) and 91 mg 4-azidobenzoic-acid-*N*-hydroxysuccinimide ester (**15**) (0.192 mmol, 1.00 eq.) and purified by flash column chromatography on silica gel (100% EtOAc). The compound was obtained as colorless oil. (45 mg, 0.109 mmol, 31.4%).

^{1}H NMR (300 MHz, Chloroform-*d*) δ 8.02 (d, *J* = 8.7 Hz, 2H), 7.79 (d, *J* = 7.6 Hz, 1H), 7.21 (d, *J* = 8.8 Hz, 2H), 4.30 (dp, *J* = 13.6, 4.5 Hz, 2H), 3.89 – 3.67 (m, 6H), 3.09 (d, *J* = 13.3 Hz, 1H), 2.89 (s, 4H). ^{13}C NMR (75 MHz, Chloroform-*d*) δ 169.67, 161.45, 145.78 (d, *J* = 1.6 Hz), 132.32, 118.04, 117.66 (d, *J* = 8.1 Hz), 89.29 (d, *J* = 50.1 Hz), 75.34 (d, *J* = 294.4 Hz), 72.59, 69.44 (d, *J* = 5.1 Hz), 66.19 (d, *J* = 5.9 Hz), 61.35, 25.68. ^{31}P NMR (122 MHz, $CDCl_3$) δ -9.66. HRMS for $C_{17}H_{20}N_2O_8P^+$ $[M+H]^+$ calcd.: 411.0952, found: 411.0951.

4-acetoxy-benzyl-*N*-(4-benzoic-acid-*N*-hydroxysuccinimide ester)-*P*-ethynylphosphonamidate (21)

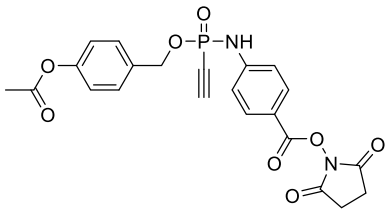

The compound was synthesized according to the general procedure 3 from 103 mg Di-(4-acetoxy benzyl) ethynylphosphonite (**10**) (0.267 mmol, 1.00 eq.) and 69 mg 4-azidobenzoic-acid-*N*-hydroxysuccinimide ester (**15**) (0.267 mmol, 1.00 eq.) and purified by flash column chromatography on silica gel (70% EtOAc in hexane). The compound was obtained as colorless oil. (36 mg, 0.077 mmol, 28.7%).

^{1}H NMR (300 MHz, Chloroform-*d*) δ = 7.53 – 7.34 (m, 2H), 7.20 – 6.99 (m, 7H), 5.14 (d, *J*=8.8, 2H), 3.01 (d, *J*=13.3, 1H), 2.91 (s, 4H), 2.32 (s, 3H). ^{13}C NMR (75 MHz, Chloroform-*d*) δ 169.52, 162.61, 161.39,

151.05, 145.42, 132.35, 129.69, 122.00, 119.31, 118.24, 117.58 (d, *J* = 8.0 Hz), 89.14 (d, *J* = 50.3 Hz), 75.32 (d, *J* = 293.0 Hz), 67.27 (d, *J* = 4.8 Hz), 25.69, 21.12. ^{31}P NMR (122 MHz, $CDCl_3$) δ = -10.33. HRMS for $C_{22}H_{20}N_2O_8P^+$ $[M+H]^+$ calcd.: 471.0952, found: 471.0956.

4-Diazophenyl-benzyl-*N*-(4-benzoic-acid-*N*-hydroxysuccinimideester)-*P*-ethynylphosphonamidate (22)

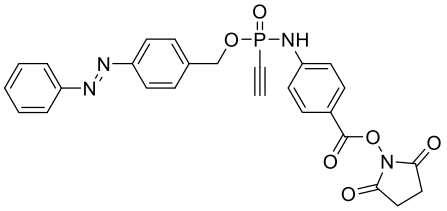

The compound was synthesized according to the general procedure 3 from 71 mg Di (4-(diazophenyl)-benzyl) ethynylphosphonite (**11**) (0.148 mmol, 1.00 eq.) and 39 mg 4-azidobenzoic-acid-*N*-hydroxysuccinimide ester (**15**) (0.148 mmol, 1.00 eq.) and purified by flash column chromatography on silica gel (50% EtOAc in hexane). The compound was obtained as orange solid. (58 mg, 0.112 mmol, 75.8%).

^{1}H NMR (600 MHz, DMSO-d_6) δ = 9.44 (d, *J*=8.6, 1H), 8.02 (d, *J*=8.8, 2H), 7.96 – 7.89 (m, 4H), 7.67 (d, *J*=8.5, 2H), 7.64 – 7.57 (m, 3H), 7.33 (d, *J*=8.8, 2H), 5.28 (ddd, *J*=45.1, 12.5, 8.7, 2H), 4.61 (d, *J*=13.0, 1H), 2.88 (s, 4H). ^{13}C NMR (151 MHz, DMSO-d_6) δ = 170.90, 161.75, 152.36, 152.23, 147.36, 139.31 (d, *J*=7.6), 132.33, 132.17, 129.97, 129.41, 123.14, 123.08, 118.17 (d, *J*=8.1), 117.25, 93.06 (d, *J*=46.9), 76.49 (d, *J*=265.4), 66.88, 25.98. ^{31}P NMR (243 MHz, DMSO) δ = -10.42. HRMS for $C_{26}H_{22}N_4O_6P^+$ $[M+H]^+$ calcd.: 517.1271, found: 517.1278.

General procedure 4 for the amide bond formation between phosphonamidate-NHS esters and EDANS

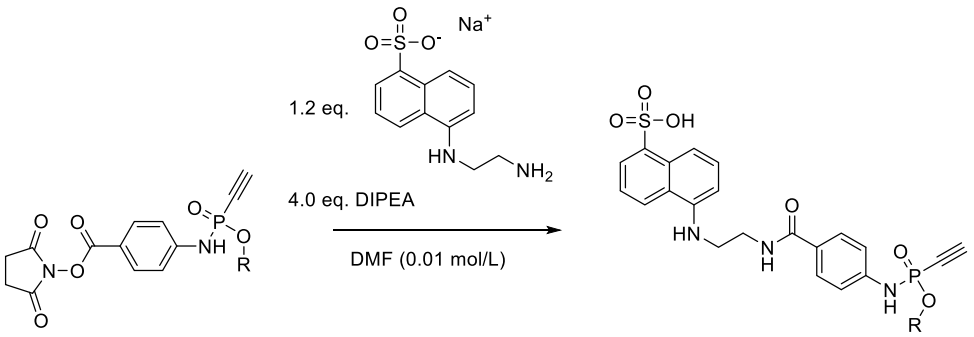

0.1 mmol NHS-phosphonamidate (1.00 eq.) and 0.12 mmol 5-((2-Aminoethyl)aminonaphthalene-1-sulfonate (EDANS) sodium salt (1.20 eq.) were dissolved in 10 mL DMF. 0.40 mmol of DIPEA (4.0 eq.)

was added and the mixture stirred for 3 hours at room-temperature. All volatiles were removed under reduced pressure and the crude mixture was purified by semi preparative HPLC using Method A.

5-((2-(*O*-(2-Isopropyl-disulfido-ethyl)-*P*-ethynylphosphonamidato-*N*-benzoyl)ethyl)amino)naphthalene-1-sulfonic acid (23)

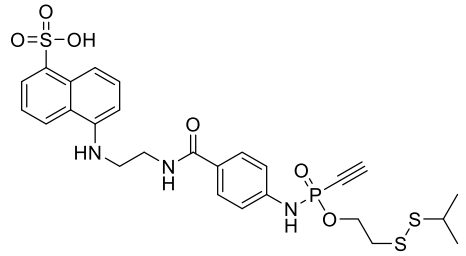

The compound was synthesized according to the general procedure 4 from 72 mg 2-Isopropyl-disulfido-ethyl-*N*-(4-benzoic-acid-*N*-hydroxysuccinimide ester)-*P*-ethynylphosphonamidate (**16**) (0.157 mmol, 1.00 eq.), 54 mg EDANS sodium salt (0.188 mmol, 1.20 eq.) and 109 µl DIPEA (0.628 mmol, 4.0 eq.) and purified by semi-preparative HPLC (method A). The compound was obtained as white solid. (62 mg, 0.102 mmol, 64.9%).

^{1}H NMR (600 MHz, DMSO-d_6) δ = 8.90 (d, *J*=8.8, 1H), 8.61 (t, *J*=5.6, 1H), 8.56 (d, *J*=8.6, 1H), 8.13 (d, *J*=8.3, 1H), 8.04 (dd, *J*=7.2, 1.1, 1H), 7.82 (d, *J*=8.7, 2H), 7.60 – 7.31 (m, 2H), 7.17 (d, *J*=8.8, 2H), 4.51 (d, *J*=12.8, 1H), 4.37 – 4.17 (m, 2H), 3.65 (q, *J*=6.3, 2H), 3.52 (t, *J*=6.5, 2H), 3.07 (p, *J*=6.7, 1H), 3.03 (t, *J*=6.3, 2H), 1.24 (dd, *J*=6.7, 2.8, 6H). ^{13}C NMR (151 MHz, DMSO-d_6) δ = 167.03, 144.53, 143.31, 130.53, 129.02, 127.63, 126.33, 125.44, 125.15, 124.70, 123.21, 117.55, 117.50, 92.38 (d, *J*=45.7), 76.79 (d, *J*=262.5), 63.85 (d, *J*=4.7), 46.85, 40.77, 39.01 (d, *J*=7.7), 37.65, 22.72. ^{31}P NMR (243 MHz, DMSO) δ = -9.84. HRMS for $C_{26}H_{31}N_3O_6PS_3^+$ $[M+H]^+$ calcd.: 608.1107, found: 608.1107.

5-((2-(*O*-(2-*tert*-butyl-disulfido-ethyl)-*P*-ethynylphosphonamidato-*N*-benzoyl)ethyl)amino)naphthalene-1-sulfonic acid (24)

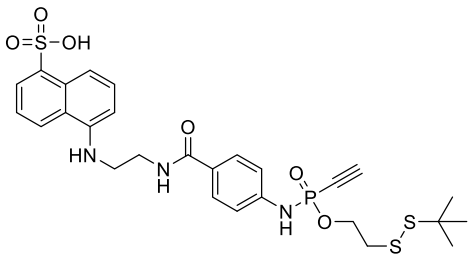

The compound was synthesized according to the general procedure 4 from 10 mg 2-*tert*-butyl-disulfido-ethyl-*N*-(4-benzoic-acid-*N*-hydroxysuccinimide ester)-*P*-ethynylphosphonamidate (**17**) (0.021 mmol, 1.00 eq.), 7 mg EDANS sodium salt (0.025 mmol, 1.20 eq.) and 15 µl DIPEA (0.084 mmol,

4.0 eq.) and purified by semi-preparative HPLC (method A). The compound was obtained as white solid. (8 mg, 0.013 mmol, 62,3%).

^{1}H NMR (600 MHz, DMSO-d_6) δ = 8.87 (d, *J*=8.7, 1H), 8.57 (t, *J*=5.8, 1H), 8.21 (d, *J*=8.6, 1H), 8.10 (d, *J*=8.5, 1H), 7.94 (dd, *J*=7.1, 1.2, 1H), 7.80 (d, *J*=8.7, 2H), 7.36 (dd, *J*=8.5, 7.1, 1H), 7.31 (dd, *J*=8.7, 7.5, 1H), 7.14 (d, *J*=8.8, 2H), 6.74 (d, *J*=7.6, 1H), 4.49 (d, *J*=12.8, 1H), 4.37 – 4.11 (m, 2H), 3.60 (q, *J*=6.4, 2H), 3.40 (t, *J*=6.5, 2H), 3.03 (t, *J*=6.5, 2H), 1.29 (s, 9H). ^{13}C NMR (151 MHz, DMSO-d_6) δ 166.87, 144.74, 143.15, 130.64, 128.93, 127.87, 126.55, 124.89, 124.24, 123.20, 123.08, 117.52, 117.47, 92.34 (d, *J* = 45.8 Hz), 76.82 (d, *J* = 261.9 Hz), 63.92, 48.31, 44.55, 38.50, 29.98. ^{31}P NMR (243 MHz, DMSO) δ = -9.87. HRMS for $C_{27}H_{33}N_3O_6PS_3^+$ $[M+H]^+$ calcd.: 622.1264, found: 622.1265.

5-((2-(*O*-2-isopropyl disulfido-3-propyl)-*P*-ethynylphosphonamidato-*N*-benzoyl)ethyl)amino)naphthalene-1-sulfonic acid (25)

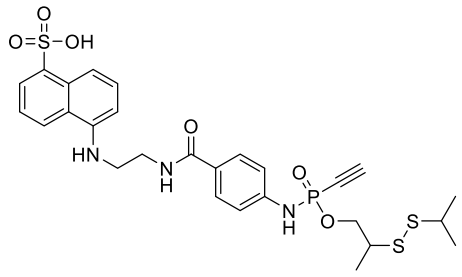

The compound was synthesized according to the general procedure 4 from 29 mg 2-isopropyl disulfido-3-propyl-*N*-(4-benzoic-acid-*N*-hydroxysuccinimide ester)-*P*-ethynylphosphonamidate (**18**) (0.061 mmol, 1.00 eq.), 21 mg EDANS sodium salt (0.073 mmol, 1.20 eq.) and 42 µl DIPEA (0.244 mmol, 4.0 eq.) and purified by semi-preparative HPLC (method A). The compound was obtained as a mixture of diastereomers as white solid. (15 mg, 0.024 mmol, 39.5%).

^{1}H NMR (600 MHz, DMSO-d_6) δ = 8.88 (d, *J*=8.8, 1H), 8.58 (t, *J*=5.7, 1H), 8.35 (d, *J*=8.6, 1H), 8.10 (dt, *J*=8.6, 1.1, 1H), 7.98 (dd, *J*=7.1, 1.1, 1H), 7.81 (d, *J*=8.7, 2H), 7.39 (ddd, *J*=31.3, 8.6, 7.3, 2H), 7.15 (d, *J*=8.8, 2H), 6.91 (d, *J*=7.5, 1H), 4.51 (dd, *J*=12.9, 1.8, 1H), 4.25 – 4.13 (m, 1H), 4.13 – 3.98 (m, 1H), 3.61 (q, *J*=6.4, 2H), 3.45 (t, *J*=6.6, 2H), 3.18 (dtd, *J*=10.6, 6.8, 5.2, 1H), 3.03 (h, *J*=6.7, 1H), 1.30 – 1.19 (m, 9H). ^{13}C NMR (151 MHz, DMSO-d_6) δ = 166.92, 144.74, 143.21, 130.61, 128.96, 127.79, 126.43, 125.10, 124.61, 123.82, 123.09, 117.50 (d, *J*=7.5), 92.58 (d, *J*=9.5), 92.28 (d, *J*=9.4), 76.76 (d, *J*=262.3), 68.10 (d, *J*=4.9), 45.48, 41.32 (d, *J*=8.6), 38.15, 22.74, 17.14 (d, *J*=4.1). ^{31}P NMR (243 MHz, DMSO) δ = -9.76, -9.79. HRMS for $C_{27}H_{33}N_3O_6PS_3^+$ $[M+H]^+$ calcd.: 622.1264, found: 622.1264.

5-(3-Butinyl)-*P*-ethynylphosphonamidato-*N*-benzoyl)ethyl)amino)naphthalene-1-sulfonic acid (26)

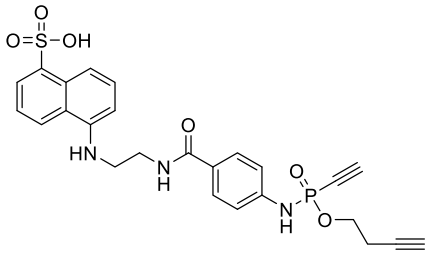

The compound was synthesized according to the general procedure 4 from 19.42 mg 3-Butinyl-*N*-(4-benzoic-acid-*N*-hydroxysuccinimide ester)-*P*-ethynylphosphonamidate (**19**) (0.052 mmol, 1.00 eq.), 18 mg EDANS sodium salt (0.062 mmol, 1.20 eq.) and 36 µl DIPEA (0.628 mmol, 4.0 eq.) and purified by semi-preparative HPLC (method A). The compound was obtained as white solid. (20 mg, 0.039 mmol, 74.3%).

^{1}H NMR (300 MHz, DMSO-d_6) δ 8.88 (d, *J* = 8.8 Hz, 1H), 8.58 (t, *J* = 5.7 Hz, 1H), 8.26 (d, *J* = 8.6 Hz, 1H), 8.10 (d, *J* = 8.5 Hz, 1H), 7.95 (dd, *J* = 7.1, 1.0 Hz, 1H), 7.80 (d, *J* = 8.6 Hz, 2H), 7.36 (ddd, *J* = 17.3, 8.6, 7.4 Hz, 2H), 7.15 (d, *J* = 8.7 Hz, 2H), 6.81 (d, *J* = 7.6 Hz, 1H), 4.49 (d, *J* = 12.9 Hz, 1H), 4.22 – 3.93 (m, 2H), 3.60 (q, *J* = 6.3 Hz, 2H), 3.42 (t, *J* = 6.5 Hz, 2H), 2.96 (t, *J* = 2.6 Hz, 1H), 2.61 (td, *J* = 6.3, 2.7 Hz, 2H). ^{13}C NMR (75 MHz, DMSO-d_6) δ 166.91, 144.66, 143.16, 130.59, 129.28, 128.95, 127.83, 126.55, 124.97, 124.34, 123.43, 123.13, 117.53, 117.43, 92.30 (d, *J* = 45.9 Hz), 81.01, 76.76 (d, *J* = 262.2 Hz), 73.46, 63.94 (d, *J* = 4.9 Hz), 44.81, 38.34, 20.39 (d, *J* = 8.2 Hz). ^{31}P NMR (122 MHz, DMSO) δ -9.90. HRMS for $C_{25}H_{25}N_3O_6PS^+$ $[M+H]^+$ calcd.: 526.1196, found: 526.11968.

5-(2-(2-Hydroxyethoxy)ethyl-)-*P*-ethynylphosphonamidato-*N*-benzoyl)ethyl)amino)naphthalene-1-sulfonic acid (27)

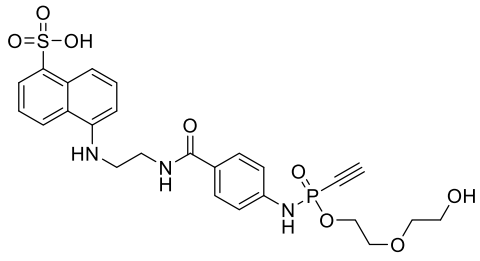

The compound was synthesized according to the general procedure 4 from 16.3 mg 2-(2-Hydroxyethoxy)ethyl-*N*-(4-benzoic-acid-*N*-hydroxysuccinimideester)-*P*-ethynylphosphonamidate (**20**) (0.040 mmol, 1.00 eq.), 13.7 mg EDANS sodium salt (0.048 mmol, 1.20 eq.) and 27 µl DIPEA

(0.160 mmol, 4.0 eq.) and purified by semi-preparative HPLC (method A). The compound was obtained as white solid. (12.5 mg, 0.022 mmol, 56.0%).

^{1}H NMR (300 MHz, DMSO-d_6) δ 8.84 (d, *J* = 8.7 Hz, 1H), 8.60 (t, *J* = 5.6 Hz, 1H), 8.40 (dd, *J* = 8.7, 2.6 Hz, 1H), 8.12 (d, *J* = 8.5 Hz, 1H), 7.99 (dd, *J* = 7.2, 0.9 Hz, 1H), 7.80 (d, *J* = 8.7 Hz, 2H), 7.60 – 7.34 (m, 2H), 7.16 (d, *J* = 8.7 Hz, 2H), 7.00 (dd, *J* = 7.8, 3.0 Hz, 1H), 4.47 (d, *J* = 12.8 Hz, 1H), 4.28 – 3.97 (m, 2H), 3.82 – 3.56 (m, 4H), 3.57 – 3.37 (m, 6H). ^{13}C NMR (75 MHz, DMSO-d_6) δ 167.00, 144.63, 143.37, 143.36, 130.56, 128.97, 127.64, 126.43, 125.21, 124.76, 124.74, 124.12, 124.09, 123.16, 117.43 (d, *J* = 7.9 Hz), 92.09 (d, *J* = 45.6 Hz), 76.95 (d, *J* = 262.1 Hz), 72.72, 69.54 (d, *J* = 7.6 Hz), 65.20 (d, *J* = 5.3 Hz), 60.62. ^{31}P NMR (122 MHz, DMSO) δ -9.71. HRMS for $C_{25}H_{29}N_3O_8PS^+$ [M+H]$^+$ calcd.: 562.1407, found: 562.1407.

5-((2-(*O*-(4-acetoxybenzyl)-*P*-ethynylphosphonamidato-*N*-benzoyl)ethyl)amino)naphthalene-1-sulfonic acid (28)

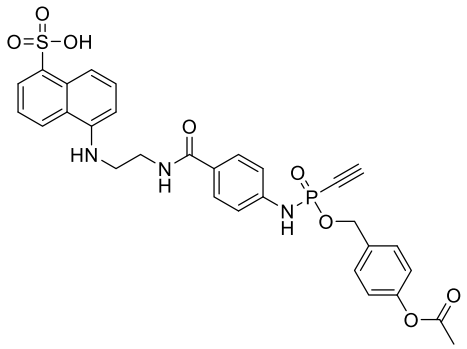

The compound was synthesized according to the general procedure 4 from 36 mg 4-acetoxy-benzyl-*N*-(4-benzoic-acid-*N*-hydroxysuccinimide ester)-*P*-ethynylphosphonamidate (**21**) (0.076 mmol, 1.00 eq.), 22 mg EDANS sodium salt (0.095 mmol, 1.20 eq.) and 53 µl DIPEA (0.284 mmol, 4.0 eq.) and purified by semi-preparative HPLC (method A). The compound was obtained as white solid. (14 mg, 0.023 mmol, 30.4%).

^{1}H NMR (600 MHz, DMSO-d_6) δ = 8.92 (d, *J*=8.6, 1H), 8.56 (t, *J*=5.7, 1H), 8.32 (d, *J*=8.7, 1H), 8.10 (d, *J*=8.5, 1H), 8.03 – 7.92 (m, 1H), 7.80 (d, *J*=8.6, 2H), 7.47 (d, *J*=8.5, 2H), 7.41 (dd, *J*=8.5, 7.2, 1H), 7.36 (t, *J*=8.1, 1H), 7.17 (d, *J*=6.7, 2H), 7.15 (d, *J*=6.7, 2H), 6.88 (d, *J*=7.5, 1H), 5.25 – 5.05 (m, 2H), 4.49 (d, *J*=12.8, 1H), 3.61 (q, *J*=6.3, 2H), 3.44 (t, *J*=6.6, 2H), 2.28 (s, 3H). ^{13}C NMR (151 MHz, DMSO-d_6) δ = 169.61, 166.95, 150.96, 144.73, 143.29, 133.66 (d, *J*=7.7), 130.61, 129.81, 128.99, 127.82, 126.47, 125.06, 124.53, 123.68, 123.10, 122.42, 117.44 (d, *J*=7.9), 92.28 (d, *J*=45.6), 77.01 (d, *J*=261.8), 66.59 (d, *J*=4.4), 45.26, 38.24, 21.31. ^{31}P NMR (243 MHz, DMSO) δ = -9.87. LC-MS for $C_{30}H_{29}N_3O_8PS^+$ [M+H]$^+$ calcd.: 622.14, found: 622.15.

5-((2-(*O*-(4-Diazophenyl-benzyl)-*P*-ethynylphosphonamidato-*N*-benzoyl)ethyl)amino)naphthalene-1-sulfonic acid (29)

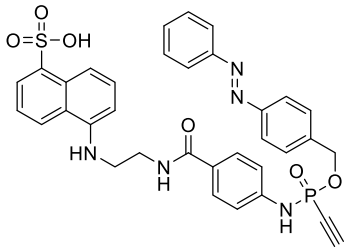

The compound was synthesized according to the general procedure 4 from 27 mg 4-Diazophenyl-benzyl-*N*-(4-benzoic-acid-*N*-hydroxysuccinimide ester)-*P*-ethynylphosphonamidate (**22**) (0.053 mmol, 1.00 eq.), 15 mg EDANS sodium salt (0.064 mmol, 1.20 eq.) and 37 µl DIPEA (0.212 mmol, 4.0 eq.) and purified by semi-preparative HPLC (method A). The compound was obtained as orange solid. (18 mg, 0.027 mmol, 50.9%).

^{1}H NMR (600 MHz, DMSO-d_6) δ = 8.98 (d, *J*=8.7, 1H), 8.57 (t, *J*=5.7, 1H), 8.36 (d, *J*=8.6, 1H), 8.11 (d, *J*=8.5, 1H), 7.98 (d, *J*=7.1, 1H), 7.97 – 7.88 (m, 4H), 7.81 (d, *J*=8.8, 2H), 7.66 (d, *J*=8.5, 2H), 7.64 – 7.52 (m, 4H), 7.42 (dd, *J*=8.5, 7.1, 1H), 7.37 (t, *J*=8.1, 1H), 7.18 (d, *J*=8.7, 2H), 6.92 (d, *J*=7.5, 1H), 5.37 – 5.04 (m, 2H), 4.53 (d, *J*=12.8, 1H), 3.61 (q, *J*=6.4, 2H), 3.45 (t, *J*=6.6, 2H). ^{13}C NMR (151 MHz, DMSO-d_6) δ = 166.95, 152.36, 152.18, 144.75, 143.27, 139.56, 139.51, 132.15, 130.61, 129.97, 129.32, 129.01, 127.84, 126.44, 125.11, 124.62, 123.83, 123.13, 123.07, 117.49 (d, *J*=8.0), 92.47 (d, *J*=45.9), 76.95 (d, *J*=262.7), 66.56 (d, *J*=4.4), 45.47, 38.15. ^{31}P NMR (243 MHz, DMSO) δ = -9.68. HRMS for $C_{34}H_{31}N_5O_6PS^+$ $[M+H]^+$ calcd.: 668.1727, found: 668.1733.

General procedure 5 for the synthesis of *O*-substituted ethynylphosphonamidates from borane protected ethynylphosphonites

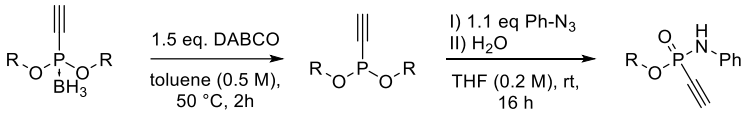

A flame-dried Schlenk flask was charged with 1.0 mmol (1.0 eq.) of the borane protected ethynylphosphonite under an argon atmosphere and dissolved in 2 ml of dry toluene. In an argon stream, DABCO (1.50 mmol, 1.5 eq.) was added and the solution was heated to 50 °C for 2 hours. The mixture was allowed to cool to room temperature and a solution of 1.1 mmol of the azide (1.1 eq.) in 3 ml dry THF or dry DMF was added. The resulting solution was stirred at room temperature overnight. Finally 1 ml of water was added and stirred for another two hours. The crude product was purified by column chromatography.

Ethyl-*N*-phenyl-*P*-ethynylphosphonamidate

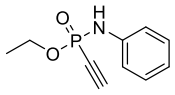

The compound was synthesized according to the General procedure 5 from 85 mg Diethyl ethynylphosphonite borane (0.531 mmol, 1.00 eq.), 90 mg DABCO (0.797 mmol, 1.50 eq.) and 70 mg phenyl azide (0.584 mmol, 1.1 eq.). The compound was purified by flash column chromatography on silica gel (100% EtOAc) and obtained as colorless solid. (22 mg, 0.104 mmol, 19.5%)

^{1}H NMR (600 MHz, Chloroform-*d*) δ = 7.33 – 7.25 (m, 2H), 7.20 (d, *J*=7.6, 1H), 7.16 – 7.10 (m, 2H), 7.05 – 6.94 (m, 1H), 4.35 – 4.10 (m, 2H), 2.91 (d, *J*=12.9, 1H), 1.39 (t, *J*=7.1, 3H). ^{13}C NMR (151 MHz, Chloroform-*d*) δ = 139.18, 129.28, 122.23, 118.16 (d, *J*=7.6), 87.77 (d, *J*=48.8), 76.39 (d, *J*=272.9), 62.13 (d, *J*=5.1), 16.17 (d, *J*=7.4). ^{31}P NMR (243 MHz, Chloroform-*d*) δ = -8.75. HR-MS for $C_{10}H_{13}NO_2P^+$ $[M+H]^+$ calcd.: 210.0678, found 210.0680.

Phenyl-*N*-phenyl-*P*-(2-phenyloxyvinyl)phosphonamidate (31)

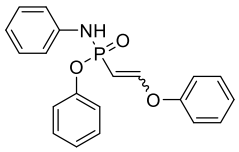

The compound was synthesized according to the General procedure 5 from 30 mg Diphenyl ethynylphosphonite borane (**12**) (0.117 mmol, 1.00 eq.), 20 mg DABCO (0.175 mmol, 1.50 eq.) and 15 mg phenyl azide (0.128 mmol, 1.1 eq.). The compound was purified by flash column chromatography on silica gel (100% EtOAc) and obtained as colorless solid. (27 mg, 0.028 mmol, 24.3%)

^{1}H NMR (300 MHz, Chloroform-*d*) δ 7.51 (dd, *J* = 13.2, 11.0 Hz, 1H), 7.40 – 6.91 (m, 15H), 6.04 (d, *J* = 6.4 Hz, 1H), 5.65 – 5.31 (t, *J* = 13.2, 1H). ^{13}C NMR (75 MHz, Chloroform-*d*) δ 160.56, 160.26, 155.56, 149.99 (d, *J* = 8.0 Hz), 139.54, 129.94, 129.71, 129.44, 125.02, 122.02, 120.84 (d, *J* = 4.7 Hz), 118.15, 118.05 (d, *J* = 6.7 Hz), 95.74 (d, *J* = 189.7 Hz). ^{31}P NMR (122 MHz, $CDCl_3$) δ 15.62. HR-MS for $C_{20}H_{19}NO_3P^+$ $[M+H]^+$ calcd.: 352.1097, found 352.1105.

General procedure 6 for the addition of a Cys-DABCYL peptide to different *O*-Substituted EDANS phosphonamidates

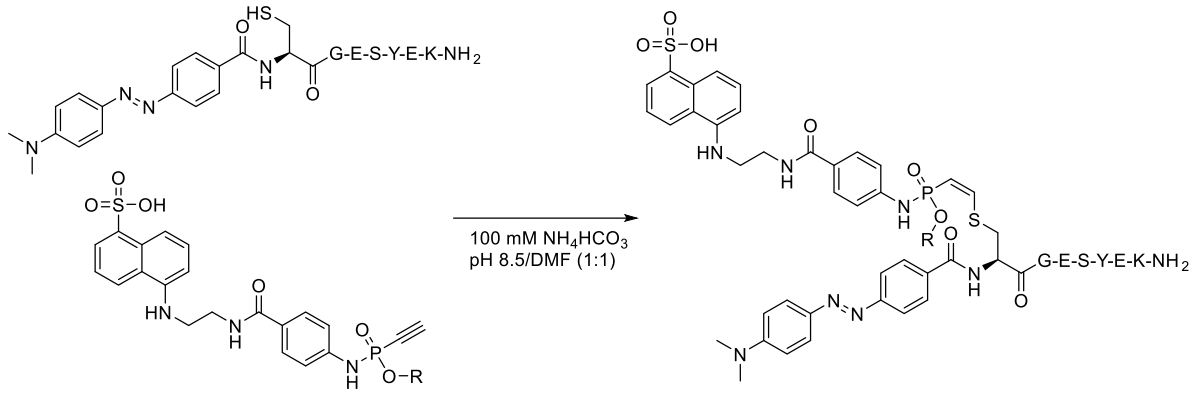

Equal volumes of a 5 mM solution of the respective EDANS-phosphonamidate in DMF and a 5 mM solution of the above stated DABCYL-Modified Cys-peptide in 100 mM NH_4HCO_3-Buffer (pH 8.5) were freshly prepared, mixed and shaken at room temperature for 3 hours. All volatiles were removed under reduced pressure and the thiol adducts isolated by semi-preparative HPLC (method A).

DABCYL-Cys peptide *O*-(2-Isopropyl-disulfido-ethyl)-phosphonamidate EDANS adduct (32)

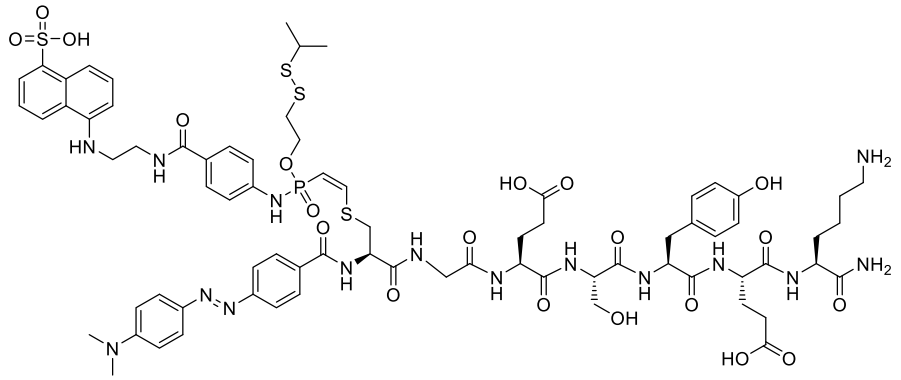

The above stated compound was synthesized according to the general procedure 6 from 452 µl of a 5 mM solution of 5-((2-(*O*-(2-Isopropyl-disulfido-ethyl)-*P*-ethynylphosphonamidato-*N*-benzoyl)ethyl)amino)naphthalene-1-sulfonic acid (**23**) in DMF and 452 µl of a 5 mM solution of the DABCYL-Cys peptide in 100 mM NH_4HCO_3-Buffer (pH 8.5). The peptide was obtained as a red solid (2.98 mg, 39.4%). HR-MS for $C_{74}H_{96}N_{15}O_{20}PS_4^{2+}$ $[M+2H]^{2+}$ calcd.: 836.7783, found 836.7783.

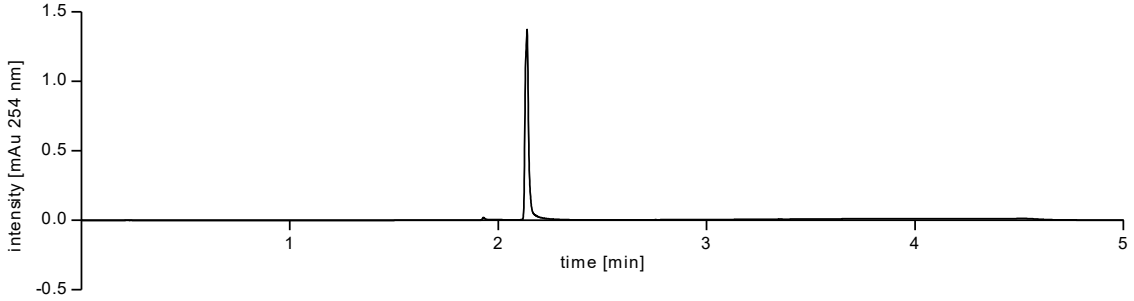

DABCYL-Cys peptide *O*-(2-*tert*-butyl-disulfido-ethyl)-phosphonamidate EDANS adduct (33)

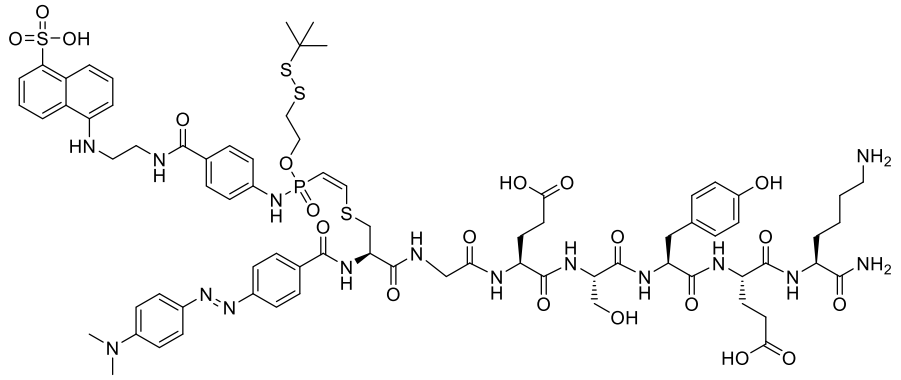

The above stated compound was synthesized according to the general procedure 6 from 403 µl of a 5 mM solution of 5-((2-(*O*-(2-*tert*-butyl-disulfido-ethyl)-*P*-ethynylphosphonamidato-*N*-benzoyl)ethyl)amino)naphthalene-1-sulfonic acid (**24**) in DMF and 403 µl of a 5 mM solution of the DABCYL-Cys peptide in 100 mM NH_4HCO_3-Buffer (pH 8.5). The peptide was obtained as a red solid (3.04 mg, 44.7%). HR-MS for $C_{75}H_{98}N_{15}O_{20}PS_4^{2+}$ $[M+2H]^{2+}$ calcd.: 843.7861, found 843.7863.

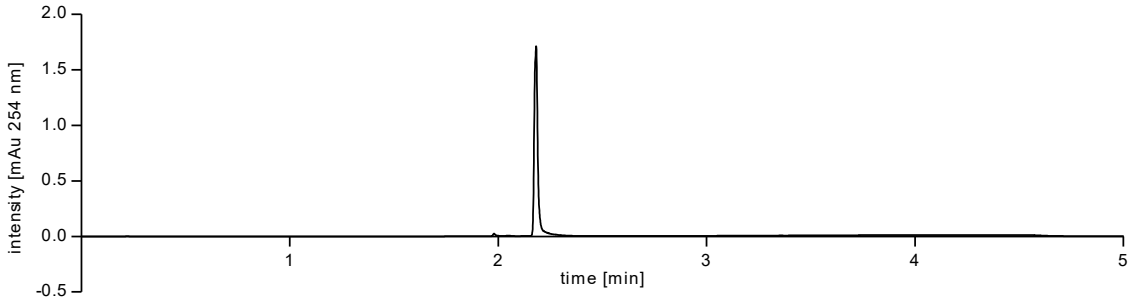

DABCYL-Cys peptide *O*-*(*2-isopropyl-disulfido-3-propyl)-phosphonamidate EDANS adduct (34)

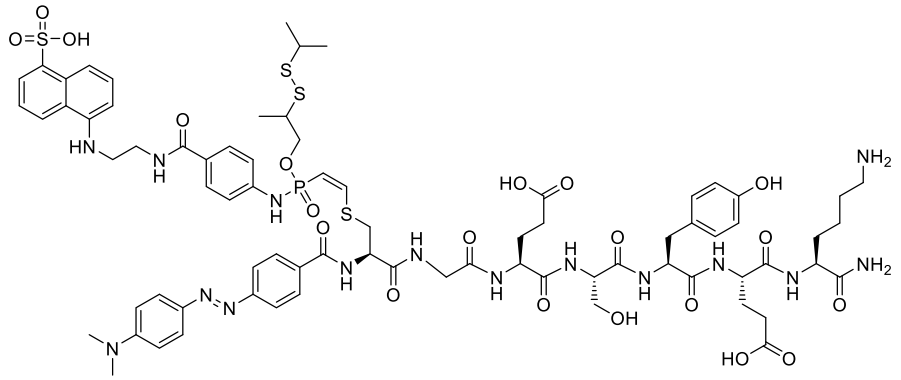

The above stated compound was synthesized according to the general procedure 6 from 1.04 ml of a 5 mM solution of 5-((2-(*O*-*(*2-isopropyl-disulfido-3-propyl)-*P*-ethynylphosphonamidato-*N*-benzoyl)ethyl)amino)naphthalene-1-sulfonic acid (**25**) in DMF and 1.04 ml of a 5 mM solution of the

DABCYL-Cys peptide in 100 mM NH_4HCO_3-Buffer (pH 8.5). The peptide was obtained as a red solid (2.16 mg, 24.5%). HR-MS for $C_{75}H_{98}N_{15}O_{20}PS_4^{2+}$ $[M+2H]^{2+}$ calcd.: 843.7861, found 843.7858.

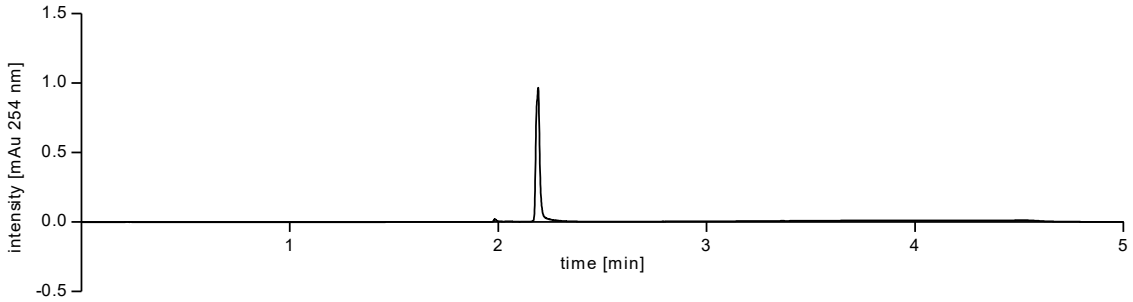

DABCYL-Cys peptide *O*-(4-acetoxybenzyl)-phosphonamidate EDANS adduct (35)

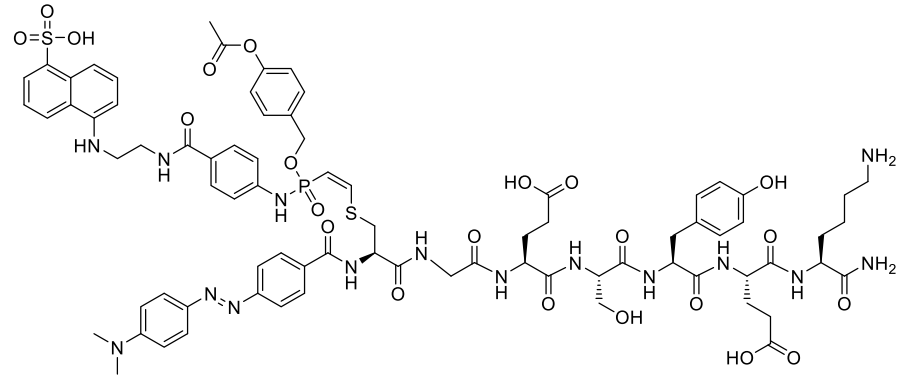

The above stated compound was synthesized according to the general procedure 6 from 1.03 ml of a 5 mM solution of 5-((2-(*O*-(4-acetoxybenzyl)-*P*-ethynylphosphonamidato-*N*-benzoyl)ethyl)amino)naphthalene-1-sulfonic acid (**26**) in DMF and 1.03 ml of a 5 mM solution of the DABCYL-Cys peptide in 100 mM NH_4HCO_3-Buffer (pH 8.5). The peptide was obtained as a red solid (2.27 mg, 26.1%). HR-MS for $C_{78}H_{92}N_{15}O_{222}PS_2^{2+}$ $[M+2H]^{2+}$ calcd.: 843.7933, found 843.7934.

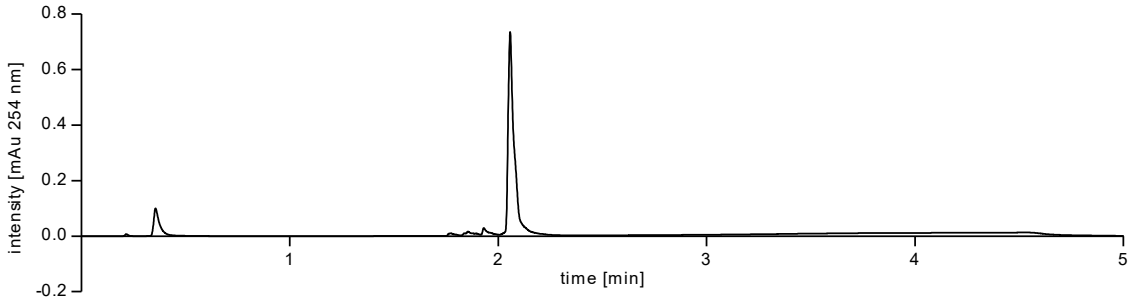

DABCYL-Cys peptide *O*-ethyl-phosphonamidate EDANS adduct (36)

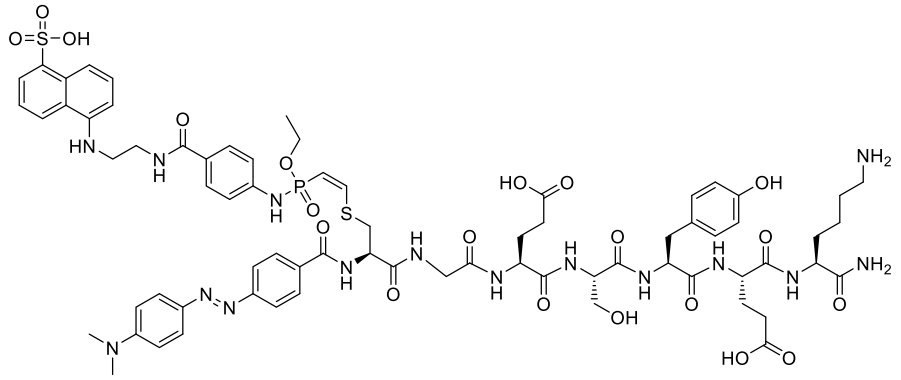

The above stated compound was synthesized according to the general procedure 6 from 430 µl of a 5mM solution of 5-((2-(*O*-ethyl-*P*-ethynylphosphonamidato-*N*-benzoyl)ethyl)amino)naphthalene-1-sulfonic acid in DMF and 430 µl of a 5 mM solution of the DABCYL-Cys peptide in 100 mM NH_4HCO_3-Buffer (pH 8.5). The peptide was obtained as a red solid (3.39 mg, 50.4%). HR-MS for $C_{71}H_{90}N_{15}O_{20}PS_2^{2+}$ $[M+2H]^{2+}$ calcd.: 783.7827, found 783.7804.

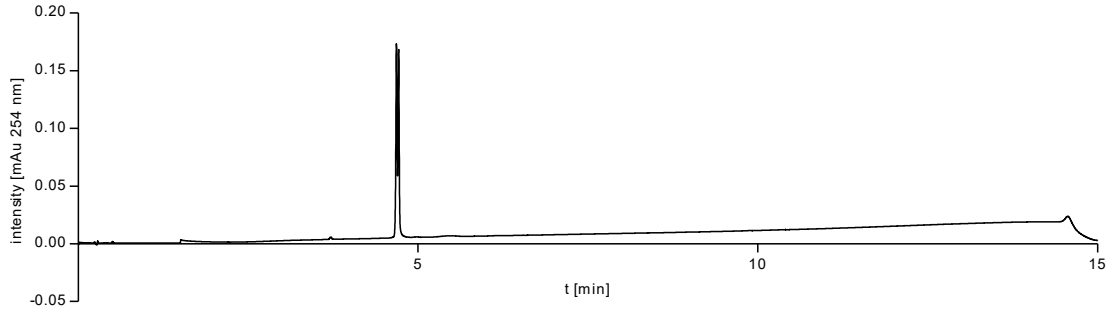

Procedure for the exposure of compounds 32-34 and 36 to TCEP

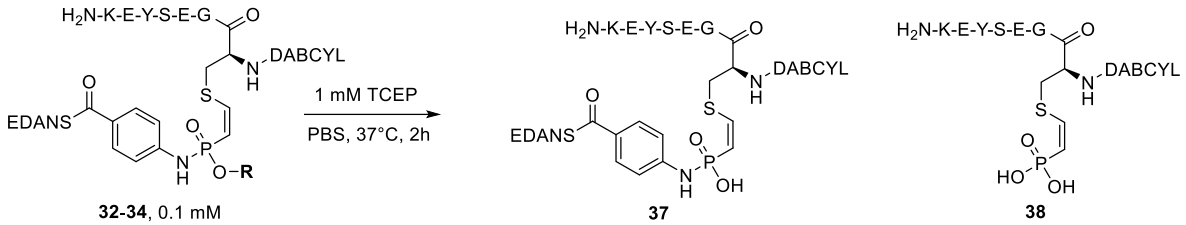

10 µl of a 1 mM stock solution of the peptide (**32**-**34** and **36**) in PBS was premixed with 80 µl of PBS. 10 µl of a 10 mM stock solution of TCEP in PBS was added and the solutions were shaken at 37°C for

two hours. Control reactions were shaken in PBS only. 15 µl samples were drawn afterwards, diluted with 15 µl of 2% TFA solution in water and subjected to UPLC-MS analysis.

Procedure for the exposure of compounds 35 and 36 to HeLa cell lysate

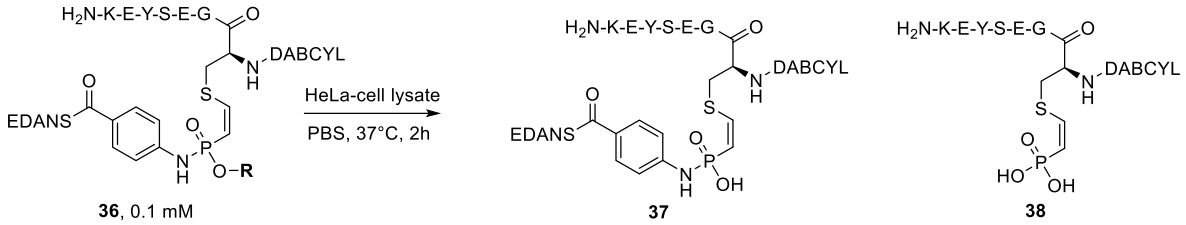

10 µl of a 1 mM stock solution of the peptide **35** and **36** in PBS was premixed with 90 µl of freshly prepared HeLa-lysate in PBS. HeLa-cell lysate was generated from approximately 3,9*10^7 cells, lysed in 2 mL PBS by sonification (final protein concentration: 1.7 mg/ml). Cells were grown on three 75 cm^2 cell culture plates, washed twice with PBS and harvested with a cell scraper. The solutions was shaken at 37°C for two hours. Control reactions were shaken in PBS only. A 15 µl sample was drawn afterwards, diluted with 15 µl of 2% TFA solution in water and subjected to UPLC-MS analysis.

Fluorescence measurements of the DABCYL-EDANS adducts

Stability studies were conducted in 96-well plate (Corning 3615, black with clear, flat bottom). 5 µl of a 200 µM Stock solution of compound **32** and **36** and 95 µl of 100 µM TCEP solution were added to a well. Fluorescence was measured on a Tecan Safire plate reader. Excitation: 360 nm, emission: 508 nm, bandwidth: 5nm at 20 °C.

5-(3-Butinyl)-*P*-ethynylphosphonamidato-*N*-benzoyl)-cR$_{10}$ (40)

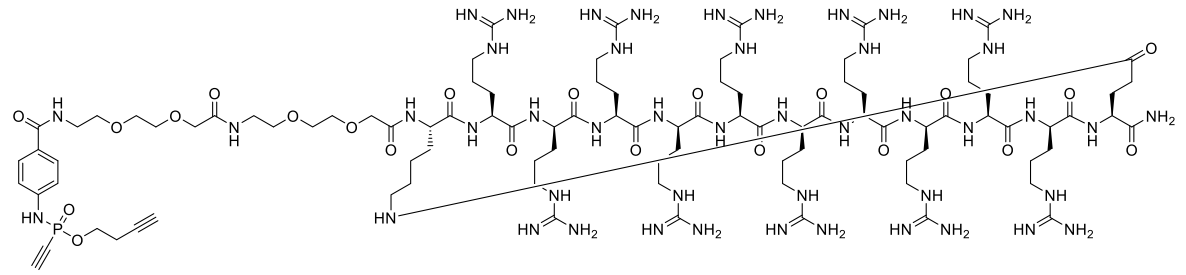

SPPS of cyclic R_{10}-NH_2 was carried out exactly as previously described.[167] An Eppendorf-tube was charged with 11.2 mg (3.324 mmol, 1.0 eq.) of cR$_{10}$-NH_2 **39**, 2.5 mg 3-Butinyl-*N*-(4-benzoic-acid-*N*-hydroxysuccinimideester)-*P*-ethynylphosphonamidate (**19**) (6.648 mmol, 2.0 eq.), 2.3 µl DIPEA (13.296 mmol, 4.0 eq.) and 50 µl DMF. The yellowish mixture was shaken overnight at room temperature and the desired product isolated by semi-preparative HPLC (method A) as a white powder

after lyophilization (3.34 mg, 0.994 mmol, 29.9%). HR-MS for $C_{96}H_{175}N_{47}O_{22}P^{3+}$ $[M+3H]^{3+}$ calcd.: 790.1258, found 790.1271.

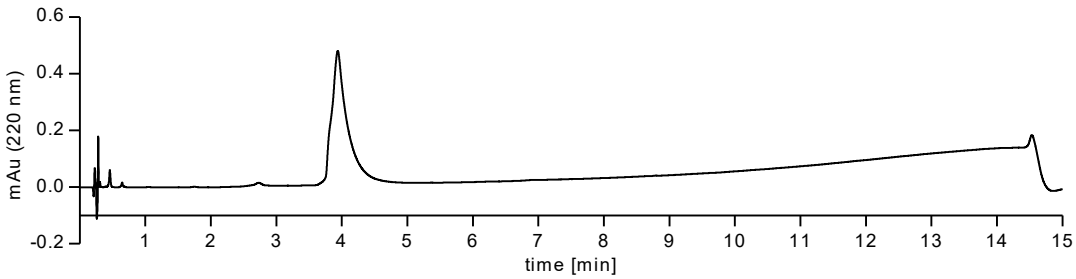

Addition of eGFP C70M S147C to 40

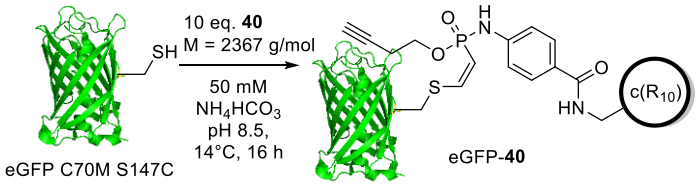

An Eppendorf-tube was charged with 500 µl eGFP in PBS (c=86 µM), 50 µl of a 86 mM solution of DTT in PBS were added and the solution was incubated at 37°C for 30 minutes. Excess DTT removal and buffer exchange to a solution containing 50 mM NH_4HCO_3 and 1mM EDTA (pH 8.5) was conducted afterwards using 2 mL Zeba™ spin Desalting Columns with 7K MWCO (Thermo Fisher Scientific, USA). Afterwards, 55 µl of a 8 mM solution of **40** in PBS were added and the solution was incubated at 14 °C overnight. Excess **40** removal and buffer exchange to PBS was conducted afterwards using 2 mL Zeba™ spin Desalting Columns with 7K MWCO (Thermo Fisher Scientific, USA). The product was analyzed by intact protein MS and SDS-PAGE. Raw spectra of the eGFP-starting material (left) and the product (right) that have been deconvoluted to produce the spectra in Figure 17e can be found below:

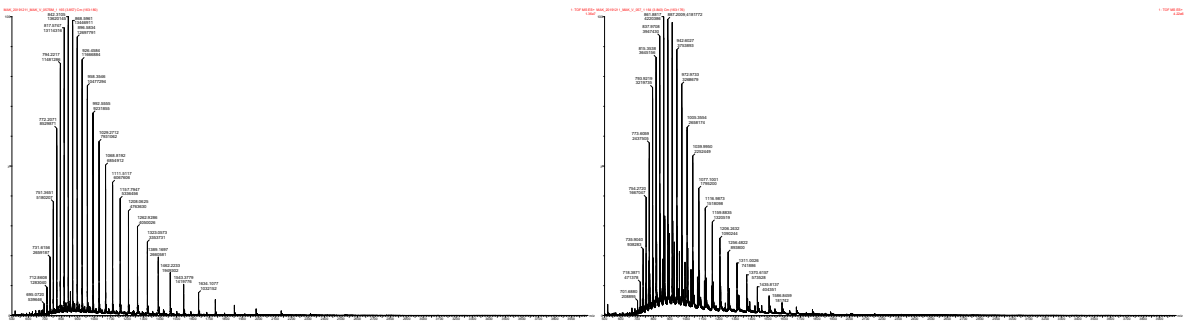

1-(2-azidoethyl)-3,3-Dimethyl-2-methyleneindoline (43)

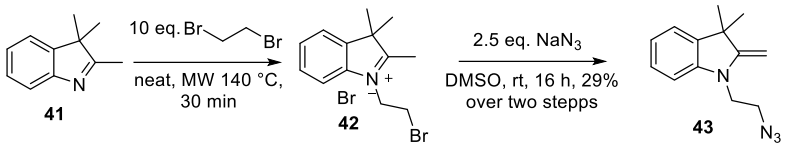

A 5-ml sealed microwave tube was charged with 500 µl **41** (3.140 mmol, 1.00 eq.), 2.7 ml 1,2-Dibromoethane (31.40 mmol, 1.00 eq.) and a stirring bar and heated to a constant temperature of 140 °C by microwave irradiation for 30 minutes. The mixture was cooled to room temperature and poured into ice-cold diethyl ether. The precipitate was collected by centrifugation, redissolved in methanol, precipitated with diethyl ether and collected by centrifugation again. 904 mg of a red solid were obtained after vacuum drying and used in the next step without further purification. A 50-ml round-bottom flask was charged with the residual substance, dissolved in 5 ml dry DMSO and 408 mg sodium azide (6.280 mmol, 2.0 eq.) were added. The red solution was stirred overnight, poured into 100 ml saturated sodium bicarbonate solution and extracted three times with 50 ml EtOAc. The organic fractions were pooled, dried over $MgSO_4$ and all volatiles were removed under reduced pressure. The crude mixture was purified by flash chromatography on silica (10% EtOAc in hexane) yielding 207 mg of a yellow oil (0.910 mmol, 29.0 %).

^{1}H NMR (300 MHz, Chloroform-d) δ 7.24 – 7.08 (m, 2H), 6.84 (td, J = 7.4, 0.8 Hz, 1H), 6.67 (d, J = 7.8 Hz, 1H), 4.07 – 3.88 (m, 2H), 3.77 (t, J = 6.2 Hz, 2H), 3.54 (t, J = 6.1 Hz, 2H), 1.38 (s, 6H). ^{13}C NMR (75 MHz, $CDCl_3$) δ 161.11, 145.43, 137.43, 127.61, 122.09, 119.09, 105.18, 74.01, 47.71, 44.29, 42.26, 30.05.

Cy5 azide 45

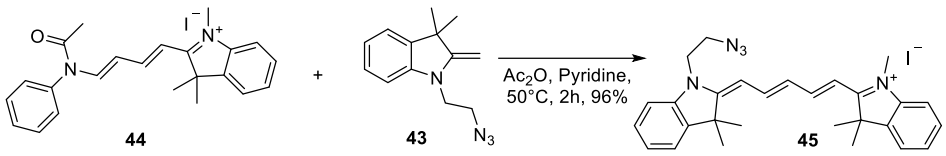

Cy5 azide **45** was synthesized from 908 mg 1,3,3-trimethyl-2-((1E,3E)-4-(N-phenylacetamido)buta-1,3-dien-1-yl)-3H-indolium iodide (**44**) (1.924 mmol, 1.08 eq.) and 405 mg 1-(2-azidoethyl)-3,3-Dimethyl-2-methyleneindoline (**43**) (1.776 mmol, 1.00 eq.) by heating in a mixture of 15 ml acetic anhydride and 15 ml pyridine for 2 hours under an argon atmosphere. All volatiles were removed under reduced pressure and the crude product was purified by flash chromatography on silica (0-5% MeOH in CH_2Cl_2) yielding 963 mg of a deep blue solid (1.705 mmol, 96.0 %).

^{1}H NMR (300 MHz, Chloroform-*d*) δ 8.08 (td, *J* = 13.0, 2.5 Hz, 2H), 7.37 (m, 4H), 7.30 – 7.11 (m, 4H), 6.96 (t, *J* = 12.5 Hz, 1H), 6.60 (d, *J* = 13.4 Hz, 1H), 6.34 (d, *J* = 13.7 Hz, 1H), 4.43 (t, *J* = 5.4 Hz, 2H), 3.92

(t, *J* = 5.3 Hz, 2H), 3.69 (s, 3H), 1.75 (s, 6H), 1.73 (s, 6H). ^{13}C NMR (75 MHz, $CDCl_3$) δ 173.87, 172.42, 153.83, 153.42, 142.45, 142.22, 140.93, 140.62, 128.63, 128.49, 126.83, 125.42, 124.89, 122.14, 122.09, 110.67, 110.62, 104.49, 104.05, 49.41, 49.24, 49.14, 44.10, 32.30, 28.17, 27.88, 20.90. HR-MS for $C_{28}H_{32}N_5^+$ $[M]^+$ calcd.: 438.2652, found 438.2652.

CuAAC of Cy5-N_3 45 to eGFP, modified with 40

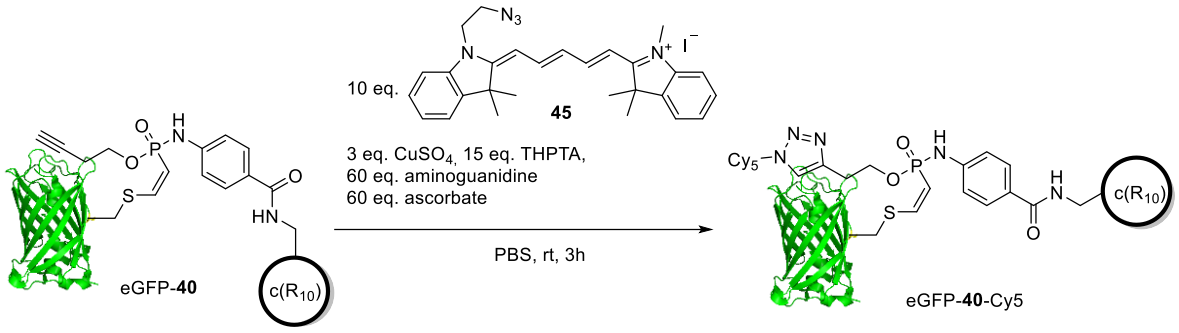

A solution containing 78 µM eGFP-**40**, 0.8 mM Cy5-N_3, 0.25 mM Copper(II) sulfate, 0.125 mM THPTA, 5 mM amino guanidine and 5 mM sodium ascorbate in PBS with 10% DMSO was shaken for 3 hours at room temperature. The crude protein modification mixture was purified by size-exclusion chromatography with a 5 ml HiTrap® desalting column and a flow of 1.5 ml/min eluting with PBS over two column volumes. The protein containing fractions were pooled and concentrated by spin-filtration (MWCO: 10 kDa, 0.5 ml, Sartorius, Germany). The product was analyzed by intact protein MS and SDS-PAGE. Raw spectrum of the product that has been deconvoluted to produce the spectra in Figure 18c can be found below:

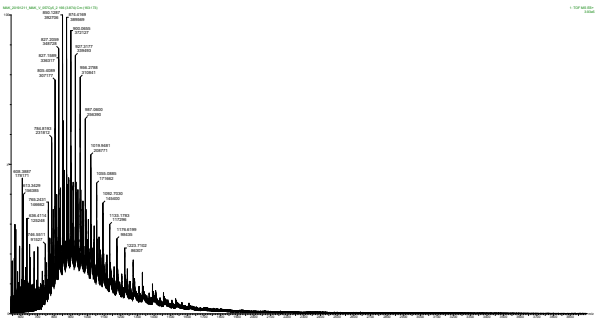

Enantiomer separation of Ethyl-N-(4-(2,5-dioxo-1-pyrrolidinyl)oxy-carbonyl-phenyl)-P-ethynylphosphonamidate (46)

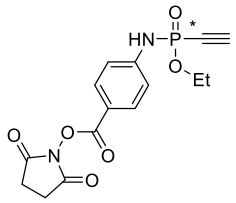

Enantiomers were separated by semi-preparative chiral HPLC eluting with 30% isopropanol in hexane with a Chiralpak® IA column (Chiral Technologies Europe, France) and analyzed with the same column type and isocratic gradient, eluting with 1 ml/min.

Enantiomer A: $[\alpha]_D^{24}$ = –30.1 (c = 0.76; $CHCl_3$)

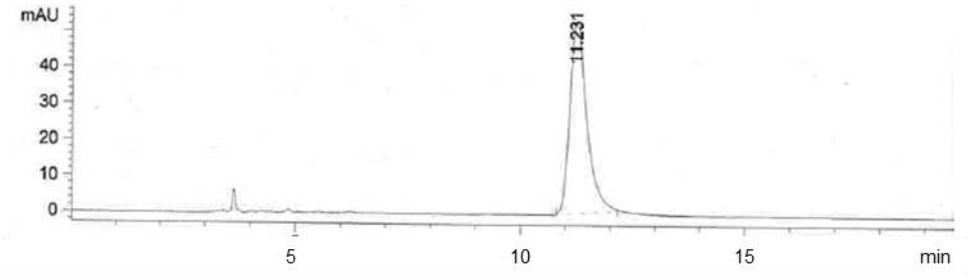

Enantiomer B: $[\alpha]_D^{24}$ = +28.6 (c = 0.88; $CHCl_3$)

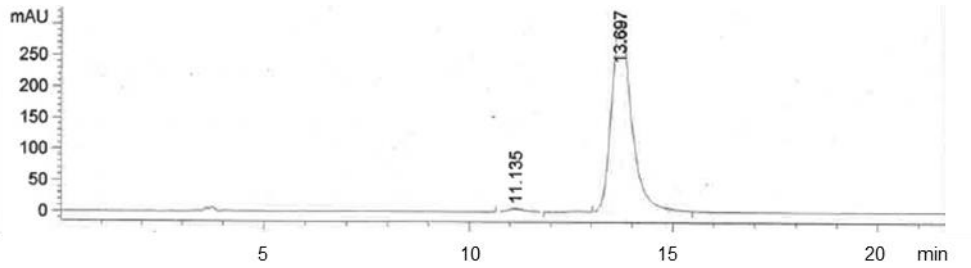

General procedure 7: One-pot protocol for the synthesis of vinylphosphonamidates from crude diethyl vinylphosphonites.

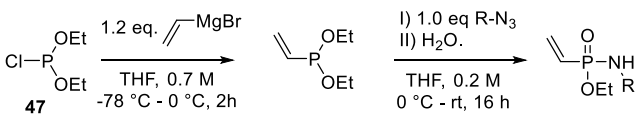

A 25-ml Schlenk flask was charged with 1.71 ml vinylmagnesium bromide (0.7 M in THF, 1.20 mmol, 1.2 eq.) under an argon atmosphere, cooled to -78 °C and 140 µl diethyl chlorophosphite (1.00 mmol, 1.0 eq.) were added drop wise. The yellowish solution was allowed to warm to 0 °C, stirred for another two hours and 1.00 mmol of azide (1.0 eq.) dissolved in 3.2 ml of THF was added and stirred overnight

at room temperature. 5 ml of water were added and stirred for another 24 h. The solvents were removed under reduced pressure and the crude product was purified by flash column chromatography on silica gel.

Ethyl-*N*-(4-carboxy-phenyl)-*P*-vinylphosphonamidate (48)

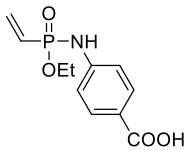

The compound was synthesized according to the general procedure 7 from 288 µl diethyl chlorophosphite (2 mmol). The crude phosphonamidate was purified by flash column chromatography (10-20% MeOH in CH2Cl2) and obtained as a white solid. (173 mg, 0.68 mmol, 34.0%)

^{1}H NMR (600 MHz, DMSO-d6) δ = 8.37 (d, J=7.9, 1H), 7.80 (d, J=8.7, 2H), 7.12 (d, J=8.7, 2H), 6.42 – 6.04 (m, 3H), 4.11 – 3.94 (m, 2H), 1.26 (t, J=7.0, 3H). ^{13}C NMR (151 MHz, DMSO-d6) δ = 167.56, 146.36, 135.00, 131.21, 129.04 (d, J=165.8), 123.06, 117.00 (d, J=6.9), 60.84 (d, J=5.7), 16.61 (d, J=6.3). ^{31}P NMR (122 MHz, DMSO-d6) δ = 14.36. HRMS for $C_{11}H_{15}NO_4P^+$ $[M+H]^+$ calcd.: 256.0733, found: 256.0723.

Ethyl-*N*-benzyl-*P*-vinylphosphonamidate (49)

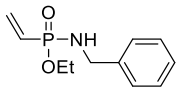

The compound was synthesized according to the general general procedure 7 from 290 µl diethyl chlorophosphite (2 mmol). The crude phosphonamidate was purified by flash column chromatography (EtOAc) and obtained as a colorless oil. (155 mg, 0.69 mmol, 34.3%)

^{1}H NMR (300 MHz, Chloroform-d) δ = 7.36 – 7.21 (m, 5H), 6.33 – 5.88 (m, 3H), 4.16 – 3.90 (m, 4H), 3.21 (d, J=8.5, 1H), 1.28 (t, J=7.1, 3H). ^{13}C NMR (75 MHz, Chloroform-d) δ = 139.65 (d, J=5.9), 133.21 (d, J=1.5), 129.45, 128.46, 127.20, 127.17, 60.11 (d, J=5.7), 44.58, 16.27 (d, J=6.7). 31P NMR (122 MHz, Chloroform-d) δ = 20.52. HRMS for $C_{11}H_{17}NO_2P^+$ $[M+H]^+$ calcd.: 226.0991, found: 226.1003.

Ethyl-*N*-(2-nitro-Benzyl)-*P*-vinylphosphonamidate (50)

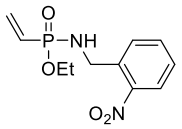

The Compound was synthesized according general procedure 7 from 120 µl diethyl chlorophosphite (0.83 mmol). The crude phosphonamidate was purified by flash column chromatography (2% MeOH in CH2Cl2) and obtained as a brown oil. (125 mg, 0.46 mmol, 55.4%)

^{1}H NMR (300 MHz, Chloroform-d) δ = 8.03 (d, J=8.1, 1H), 7.73 – 7.57 (m, 2H), 7.45 (t, J=7.6, 1H), 6.31 – 5.83 (m, 3H), 4.39 (dd, J=11.2, 7.7, 2H), 4.12 – 3.85 (m, 2H), 3.65 (q, J=8.6, 1H), 1.26 (t, J=7.1, 3H). ^{13}C NMR (75 MHz, Chloroform-d) δ = 148.09, 135.45 (d, J=4.2), 133.83, 133.52 (d, J=1.6), 131.10, 128.41, 128.26 (d, J=169.7), 124.95, 60.35 (d, J=5.7), 42.42 (d, J=1.3), 16.22 (d, J=6.7). ^{31}P NMR (122 MHz, Chloroform-d) δ = 20.63. HRMS for $C_{11}H_{16}N_2O_4P^+$ $[M+H]^+$ calcd.: 271.0842, found: 271.0851.

Ethyl-*N*-cyclohexyl-*P*-vinylphosphonamidate (51)

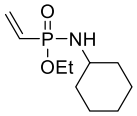

The compound was synthesized according to the general procedure 7 from 140 µl diethyl chlorophosphite (1 mmol). The crude phosphonamidate was purified by flash column chromatography (1.5% MeOH in CH_2Cl_2) and obtained as a colorless oil. (70 mg, 0.32 mmol, 32.2%)

^{1}H NMR (600 MHz, Chloroform-d) δ = 6.25 – 5.93 (m, 3H), 4.14 – 3.97 (m, 2H), 2.96 (dqd, J=13.8, 9.6, 8.1, 4.2, 1H), 2.51 (t, J=9.6, 2H), 1.97 – 1.84 (m, 2H), 1.74 – 1.65 (m, 1H), 1.57 (dt, J=13.0, 3.9, 1H), 1.32 (t, J=7.1, 3H), 1.30 – 1.09 (m, 5H). ^{13}C NMR (75 MHz, Chloroform-d) δ = 132.56 (d, J=1.8), 129.30 (d, J=168.8), 59.80 (d, J=5.9), 49.71, 36.03, 25.24, 24.96, 16.32 (d, J=6.8). ^{31}P NMR (122 MHz, Chloroform-d) δ = 19.34. HRMS for $C_{10}H_{21}NO_2P^+$ $[M+H]^+$ calcd.: 218.1304, found: 218.1302.

General procedure 8 for the synthesis of vinylphosphonites from Bis(diisopropylamino)chlorophosphine

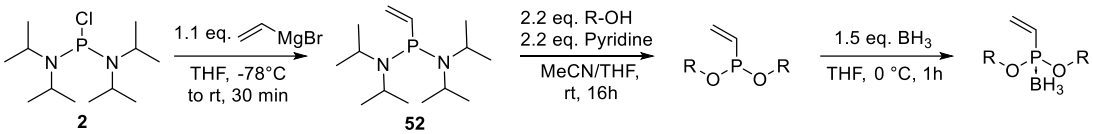

A flame-dried Schlenk flask was charged with 1.0 mmol (1.0 eq.) Bis(diisopropylamino)-chlorophosphine, dissolved in 200 µl of dry THF and cooled to -78 °C. 1.10 mmol (1.1eq.) of vinyl

magnesiumbromide (1.0 M in THF) was added and the reaction was stirred at room temperature for 30 minutes. A solution of 2.2 mmol vacuum dried alcohol (2.2 eq.) in 1 ml of dry THF or MeCN and 2.2 mmol (2.2 eq.) Tetrazole (0.45 M in MeCN) was added. The resulting suspension was stirred at room temperature overnight. Finally 1.50 mmol (1.5 eq.) of borane (1.0 M in THF) were added at 0 °C and stirred for another hour. The crude product was dry packed on a silica column for purification. It should be noted, that mass analysis of phosphonites failed for all of the tested compounds, possibly due to decomposition under ESI-conditions.

4-(2-nitro-5-(oxypropargyl)benzyloxy)phenol

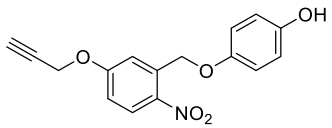

A flame dried Schlenk-tube, 400 mg of 2-nitro-5-(oxypropargyl)benzyl alcohol (1.93 mmol, 1.0 eq.), together with 850 mg hydroquinone (7.72 mmol, 4.0 eq.) and 750 mg of triphenylphosphine (2.90 mmol, 1.5 eq.) were dissolved in 10 ml of dry THF. The solution was cooled to 0 °C and 1.33 ml of diethyl azodicarboxylate (40% solution in Toluene) (2.90 mmol, 1.5 eq.) were added dropwise and the reaction was allowed to warm to room temperature overnight. The crude product was dry packed on a silica column for purification, eluting with Hexane/EtOAc (7:3 to 3:2), yielding 505 mg of a yellow solid. (1.68 mmol, 87.5 %)

^{1}H NMR (300 MHz, Chloroform-d) δ = 8.26 (d, J=9.1, 1H), 7.51 (d, J=2.8, 1H), 7.00 (dd, J=9.2, 2.9, 1H), 6.89 (d, J=9.0, 2H), 6.80 (d, J=9.0, 2H), 5.46 (s, 2H), 4.79 (d, J=2.4, 2H), 2.54 (t, J=2.4, 1H). ^{13}C NMR (75 MHz, Chloroform-d) δ = 161.86, 152.11, 150.03, 140.10, 137.71, 127.69, 116.11, 116.03, 113.88, 113.69, 76.95, 76.68, 67.66, 56.20. HRMS for C16H14NO5+ $[M+H]^+$ calcd.: 300.0866, found: 300.0871.

Di(4-(2-nitro-5-(oxypropargyl)benzyloxy)phenyl) vinylphosphonite borane (53)

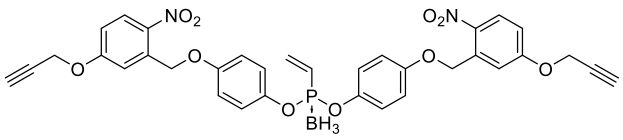

The compound was synthesized according to the general procedure 8 from Bis(diisopropylamino)chlorophosphine (71 mg, 0.27 mmol). The crude borane protected phosphonite was purified by flash column chromatography (Hexane/ CH_2Cl_2, 1:1) and obtained as a yellowish solid. (75 mg, 0.11 mmol, 41.9%)

^{1}H NMR (300 MHz, Chloroform-d) δ = 8.25 (d, J=9.1, 2H), 7.47 (d, J=2.8, 2H), 7.17 – 6.87 (m, 10H), 6.62 – 6.14 (m, 3H), 5.48 (s, 4H), 4.78 (d, J=2.4, 4H), 2.55 (t, J=2.4, 2H), 1.51 - 0.24 (m, 3H). ^{13}C NMR (75 MHz, Chloroform-d) δ = 161.89, 155.27 (d, J=1.3), 145.34 (d, J=8.4), 140.04, 137.08 (d, J=12.6), 136.97, 129.06 (d, J=71.3), 127.77, 121.93 (d, J=4.0), 115.74 (d, J=1.1), 113.85, 113.79, 76.89, 76.89, 67.37, 56.24. ^{31}P NMR (122 MHz, Chloroform-d) δ = 136.36 – 131.69 (m).

Di(2-nitro-5-(oxypropargyl)benzyl) vinylphosphonite borane (54)

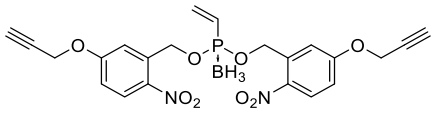

The compound was synthesized according to the general procedure 8 from Bis(diisopropylamino)chlorophosphine (513 mg, 1.92 mmol). The crude borane protected phosphonite was purified by flash column chromatography (Hexane/CH2Cl2, 4:1) and obtained as a yellowish solid. (704 mg, 1.45 mmol, 75.6%)

^{1}H NMR (300 MHz, Chloroform-d) δ = 8.19 (d, J=9.1, 2H), 7.31 (d, J=2.8, 2H), 7.00 (dd, J=9.2, 2.8, 2H), 6.58 – 6.22 (m, 3H), 5.49 (qd, J=15.5, 7.4, 4H), 4.81 (d, J=2.4, 4H), 2.62 (t, J=2.4, 2H), 1.31 – 0.12 (m, 3H). 13C NMR (75 MHz, Chloroform-d) δ = 161.86, 139.86, 136.92 (d, J=10.4), 135.78 (d, J=6.8), 128.43 (d, J=73.2), 127.79, 114.10, 113.92, 76.95, 76.89, 65.54 (d, J=3.6), 56.31. ^{31}P NMR (122 MHz, Chloroform-d) δ = 136.32 (d, J=107.0).

Di-(4-Hydroxyphenyl) vinylphosphonite borane (55)

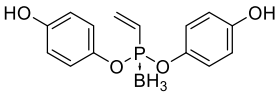

The compound was synthesized according to the general procedure 8 from Bis(diisopropylamino)chlorophosphine (534 mg, 2.00 mmol) and hydroquinone (2.20 g, 10 eq.). The crude borane protected phosphonite was purified by flash column chromatography (Hexane/EtOAc, 4:1 to 1:1) and obtained as a colorless solid. (280 mg, 0.96 mmol, 48.3%)

^{1}H NMR (300 MHz, DMSO-d6) δ = 9.49 (s, 2H), 6.96 (d, J=8.5, 4H), 6.74 (d, J=8.9, 4H), 6.63 – 6.22 (m, 3H), 1.20 – -0.12 (m, 3H). ^{31}P NMR (122 MHz, DMSO-d6) δ = 131.80.

Di(4-nitrobenzyl) vinylphosphonite borane (56)

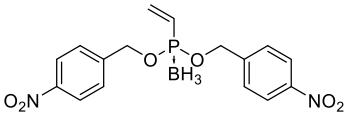

The compound was synthesized according to the general procedure 8 from Bis(diisopropylamino)chlorophosphine (533 mg, 2.00 mmol). The crude borane protected phosphonite was purified by flash column chromatography (Hexane/CH2Cl2, 9:1 to 4:1) and obtained as a white solid. (540 mg, 1.44 mmol, 71.8%)

^{1}H NMR (300 MHz, Chloroform-d) δ = 8.17 (d, J=8.6, 4H), 7.49 (d, J=8.5, 4H), 6.47 – 6.16 (m, 3H), 5.12 (qd, J=13.2, 8.3, 4H), 1.40 - 0.00 (m, 3H). ^{13}C NMR (75 MHz, Chloroform-d) δ = 147.66, 143.09 (d, J=6.1), 136.50 (d, J=10.2), 128.80 (d, J=76.0), 127.78, 123.73, 67.30 (d, J=3.8). ^{31}P NMR (122 MHz, Chloroform-d) δ = 137.95 (d, J=95.6). ^{13}C NMR (151 MHz, DMSO-d_6) δ 155.22, 143.60 (d, *J* = 8.8 Hz), 137.79 (d, *J* = 10.7 Hz), 129.63 (d, *J* = 69.9 Hz), 122.00 (d, *J* = 3.8 Hz), 116.43.

Di(1,2-isopropylidene glyceryl) vinylphosphonite borane (57)

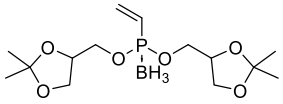

The compound was synthesized according to the general procedure 8 from Bis(diisopropylamino)chlorophosphine (533 mg, 2.00 mmol). The crude borane protected phosphonite was purified by flash column chromatography (20% EtOAc in hexane) and obtained as a mixture of diastereomers as a colorless oil. (380 mg, 1.14 mmol, 57.9%)

^{1}H NMR (300 MHz, Chloroform-*d*) δ 6.45 – 6.05 (m, 3H), 4.30 (p, *J* = 5.7 Hz, 2H), 4.13 – 3.92 (m, 6H), 3.79 (td, *J* = 8.6, 5.6 Hz, 2H), 1.42 (s, 6H), 1.35 (s, 6H). 1.20 – -0.34 (m, 3H) ^{13}C NMR (75 MHz, Chloroform-*d*) δ 135.62 (q, *J* = 10.4, 9.8 Hz), 129.11 (dt, *J* = 75.3, 9.5 Hz), 111.91 – 108.56 (m), 74.21 (dd, *J* = 8.2, 6.6 Hz), 67.04 (ddd, *J* = 35.7, 4.9, 2.3 Hz), 66.45 – 65.34 (m), 27.87 – 26.18 (m), 25.18. ^{31}P NMR (122 MHz, Chloroform-*d*) δ 137.23 – 132.50 (m).

General procedure 9 for the synthesis of vinylphosphonamidates from borane protected phosphonites.

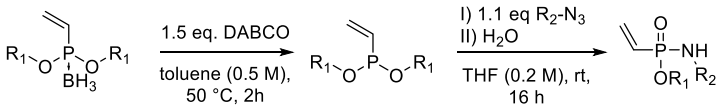

A flame-dried Schlenk flask was charged with 1.0 mmol (1.0 eq.) of the borane protected phosphonite under an argon atmosphere and dissolved in 2 ml of dry toluene. In an argon stream, DABCO (1.50 mmol, 1.5 eq.) was added and the solution was heated to 50 °C for 2 hours. The mixture was allowed to cool to room temperature and a solution of 1.1 mmol of the azide (1.1 eq.) in 3 ml dry THF or dry DMF was added. The resulting solution was stirred at room temperature overnight. Finally 1 ml of

water was added and stirred for another two hours. The crude product was purified by column chromatography.

4-Hydroxyphenyl-*N*-phenyl-*P*-vinylphosphonamidate (58)

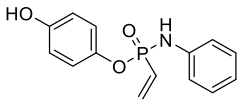

The compound was synthesized according to the General procedure 9 from 55 mg Di-(4-Hydroxyphenyl) vinylphosphonite borane (**55**) (0.189 mmol). The crude phosphonamidate was purified by flash column chromatography (50 to 100% EtOAc in hexane) and obtained as a white solid. (13 mg, 0.047 mmol, 25.0%)

^{1}H NMR (600 MHz, DMSO-d_6) δ 9.33 (s, 1H), 8.16 (d, *J* = 8.2 Hz, 1H), 7.21 (dd, *J* = 8.5, 7.3 Hz, 2H), 7.14 – 7.04 (m, 2H), 6.99 (dd, *J* = 8.9, 1.4 Hz, 2H), 6.93 – 6.82 (m, 1H), 6.70 (d, *J* = 8.9 Hz, 2H), 6.49 – 6.03 (m, 3H). ^{13}C NMR (151 MHz, DMSO-d_6) δ 154.72, 142.58 (d, *J* = 7.9 Hz), 141.32, 135.49, 129.47, 129.04 (d, *J* = 166.3 Hz), 121.93 (d, *J* = 4.3 Hz), 121.31, 118.09 (d, *J* = 6.9 Hz), 116.23. ^{31}P NMR (243 MHz, DMSO) δ 13.07. HRMS for $C_{14}H_{15}NO_3P^+$ $[M+H]^+$ calcd.: 276.0784, found: 276.0785.

2-nitro-5-(oxypropargyl)benzyl-*N*-phenyl-*P*-vinylphosphonamidate (59)

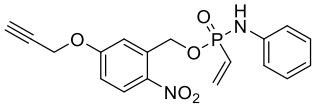

The compound was synthesized according to the general procedure 9 from 28 mg Di(2-nitro-5-(oxypropargyl)benzyl) vinylphosphonite borane (**54**) (0.058 mmol). The crude phosphonamidate was purified by flash column chromatography (30% EtOAc in hexane) and obtained as a yellow solid. (10 mg, 0.027 mmol, 46.7%)

^{1}H NMR (300 MHz, Chloroform-*d*) δ 8.20 (d, *J* = 9.1 Hz, 1H), 7.40 (d, *J* = 2.8 Hz, 1H), 7.22 (t, *J* = 7.8 Hz, 2H), 7.08 – 6.89 (m, 4H), 6.55 – 5.97 (m, 4H), 5.58 (ddd, *J* = 62.8, 15.6, 7.4 Hz, 2H), 4.76 (d, *J* = 2.4 Hz, 2H), 2.59 (t, *J* = 2.4 Hz, 1H). ^{13}C NMR (75 MHz, Chloroform-*d*) δ 161.75, 140.10, 139.29, 136.07 (d, *J* = 7.7 Hz), 135.74, 129.39, 127.77, 127.72, 125.49, 121.96, 117.63, 117.54, 114.13, 113.86, 62.90 (d, *J* = 4.5 Hz), 56.21. 31P NMR (122 MHz, CDCl3) δ 16.43. HRMS for $C_{18}H_{18}N_2O_5P^+$ $[M+H]^+$ calcd.: 373.0981, found: 373.0979.

4-(2-nitro-5-(oxypropargyl)benzyloxy)phenyl-*N*-phenyl-*P*-vinylphosphonamidate (60)

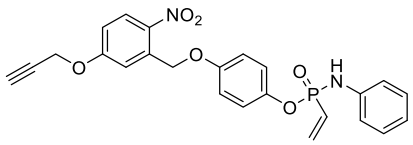

The compound was synthesized according to the general procedure 9 from 21 mg Di(4-(2-nitro-5-(oxypropargyl)benzyloxy)phenyl) vinylphosphonite borane (**53**) (0.031 mmol). The crude phosphonamidate was purified by flash column chromatography (30% EtOAc in hexane) and obtained as a yellow solid. (5 mg, 0.011 mmol, 34.2%)

^{1}H NMR (300 MHz, Chloroform-*d*) δ 8.25 (d, *J* = 9.1 Hz, 1H), 7.42 (d, *J* = 2.8 Hz, 1H), 7.32 – 7.19 (m, 2H), 7.12 (dd, *J* = 9.0, 1.5 Hz, 2H), 7.05 – 6.94 (m, 4H), 6.85 (d, *J* = 9.0 Hz, 2H), 6.54 – 6.00 (m, 3H), 5.82 (d, *J* = 5.7 Hz, 1H), 5.44 (s, 2H), 4.77 (d, *J* = 2.4 Hz, 2H), 2.54 (t, *J* = 2.4 Hz, 1H). ^{13}C NMR (75 MHz, Chloroform-*d*) δ 161.85, 155.07, 143.74, 143.62, 140.03, 139.21, 137.14, 135.98, 129.35, 127.73, 126.74 (d, *J* = 173.4 Hz), 122.03, 121.80, 121.75, 117.79 (d, *J* = 6.5 Hz), 115.73, 113.96, 113.59, 67.31, 56.16. ^{31}P NMR (122 MHz, $CDCl_3$) δ 13.18. HRMS for $C_{24}H_{22}N_2O_6P^+$ $[M+H]^+$ calcd.: 465.1210, found: 465.1227.

Procedure for Cys-modification of eGFP (C70M or C70M S147C) with vinylphosphonamidates

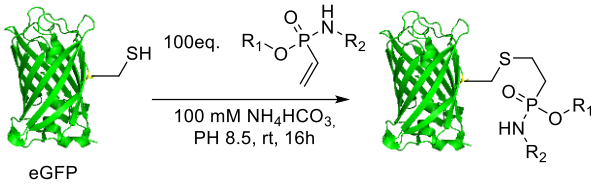

The storage buffer of eGFP (PBS) was exchanged to 100 mM NH_4HCO_3, pH 8.5 using Amicon spin filters with a 10 kDa MWCO (Sartorius, Germany). The protein was filtered three times with the reaction buffer at 14000 rpm for 5 minutes to give a typical concentration of 50 µM. 2.5µl of a 100 mM solution of the vinylphosphonamidate (100 eq.) in MeCN, DMSO or DMF, depending on the solubility, were added to 50 µl of the protein. The reaction mixture was shaken at 25 °C and 850 rpm overnight. The excess phosphonamidate was removed by spin filtration using Amicon spin filters with a 10 kDa MWCO (Sartorius, Germany) and analyzed by MALDI-MS or SDS-PAGE.

Cy5-*O*-2-nitrobenzyl-*P*-vinylphosphonamidate 63

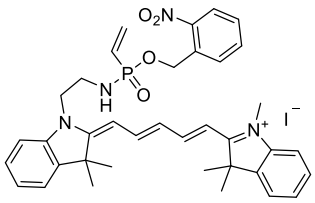

The compound was synthesized according to the general procedure 9 from 37 mg Di(2-nitrobenzyl) vinylphosphonite borane (**62**) (0.097 mmol, 1.10 eq.) in DMF. The crude phosphonamidate was purified by flash column chromatography (0-5% MeOH in CH_2Cl_2) and obtained as deep blue solid. (10 mg, 0.013 mmol, 14.8%)

^{1}H NMR (600 MHz, Chloroform-*d*) δ 8.08 (dd, *J* = 8.2, 1.3 Hz, 1H), 7.99 – 7.90 (m, 2H), 7.84 – 7.71 (m, 2H), 7.51 – 7.31 (m, 7H), 7.25 (t, *J* = 7.5 Hz, 1H), 7.20 (t, *J* = 7.4 Hz, 2H), 7.11 – 6.99 (m, 2H), 6.44 – 5.91 (m, 3H), 5.48 – 5.39 (m, 2H), 5.36 (dt, *J* = 14.5, 7.7 Hz, 1H), 4.60 (dt, *J* = 14.5, 7.4 Hz, 1H), 4.41 (m, 1H), 3.68 – 3.57 (m, 1H), 3.52 (s, 3H), 3.50 – 3.43 (m, 1H), 1.74 (s, 3H), 1.72 (s, 3H), 1.70 (s, 6H). ^{13}C NMR (151 MHz, Chloroform-*d*) δ 174.93, 171.18, 154.32, 151.65, 146.35, 142.94, 141.94, 141.03, 140.41, 134.54, 133.87, 129.20, 129.15, 128.87, 128.57, 128.08, 128.04, 126.81, 125.79, 124.58, 124.41, 122.06, 121.94, 112.01, 109.64, 106.75, 102.53, 70.45 (d, *J* = 92.1 Hz), 62.56 (d, *J* = 4.2 Hz), 50.71, 49.68, 48.62, 46.46, 37.81, 28.16, 28.11, 27.98, 27.96. ^{31}P NMR (243 MHz, $CDCl_3$) δ 23.21. HRMS for $C_{37}H_{42}N_4O_4P^+$ $[M]^+$ calcd.: 637.2938, found: 637.2940.

Modification of cetuximab's interchain disulfide bonds with 64 and MS/MS analysis

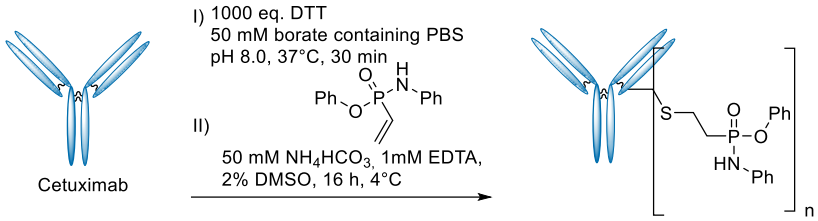

Cetuximab modification was carried out by incubating the antibody (typical concentration c = 1.5 mg/ml, 10 µM) in a buffer containing 50 mM sodium borate and 4 mM DTT in PBS (pH 8.0) with a total volume of 80 µl at 37 °C for 30 min. Excess DTT removal and buffer exchange to a solution containing 50 mM NH_4HCO_3 and 1mM EDTA (pH 8.5) was conducted afterwards using 0.5 mL Zeba™ spin Desalting Columns with 7K MWCO (Thermo Fisher Scientific, USA). 1 µl of a solution containing 50 mM *N*-phenyl-*P*-vinylphosphonamidate (**64**) in DMSO were added quickly to 50 µl of the reduced antibody solution. The mixture was shaken at 800 rpm and 4 °C for 16 hours. Excess reagent was again removed by buffer exchange to sterile PBS using 0.5 mL Zeba™ spin Desalting Columns with 7K MWCO.

Afterwards, 10 µl of the antibody solution were mixed with 10 µl of a 10 mM DTT solution and incubated at 55 °C for 30 minutes. After cooling to room temperature, 10 µl of a 55 mM iodoacetamide solution was added and the mixture was incubated for further 30 minutes in the dark. Finally, 10 µl of a solution of 0.1 mg/ml trypsin in 1 mM HCl was added, the mixture was incubated at 37°C overnight and subjected to MS/MS-analysis.

Shown below are the results of the Mascot search on cetuximab's heavy- and light chain after incubation with 100 eq. of **64** with prior reduction of the disulfide bonds. Matched Peptides are highlighted in grey. Amino acid residues modified with **64** are highlighted in red. Oxidation of methionine, alkylation of cysteine via iodoacetamide and the phosphonamidate on Y, S, T, C, K, H & R were searched as variable modifications.

reduction:
light chain sequence coverage: 69%
1 DILLTQSPVILSVSPGERVSFSCRASQSIGTNIHWYQQRTNGSPRLLIKYASESISGIPSRFSGSGSGTDFTLSINSVESEDIADYYCQQNNNWPTTFGA
101 GTKLELKRTVAAPSVFIFPPSDEQLKSGTASVVCLLNNFYPREAKVQWKVDNALQSGNSQESVTEQDSKDSTYSLSSTLTLSKADYEKHKVYACEVTHQG
201 LSSPVTKSFNRGEC

heavy chain sequence coverage: 65%
1 QVQLKQSGPGLVQPSQSLSITCTVSGFSLTNYGVHWVRQSPGKGLEWLGVIWSGGNTDYNTPFTSRLSINKDNSKSQVFFKMNSLQSNDTAIYYCARALT
101 YYDYEFAYWGQGTLVTVSAASTKGPSVFPLAPSSKSTSGGTAALGCLVKDYFPEPVTVSWNSGALTSGVHTFPAVLQSSGLYSLSSVVTVPSSSLGTQTY
201 ICNVNHKPSNTKVDKRVEPKSCDKTHTCPPCPAPELLGGPSVFLFPPKPKDTLMISRTPEVTCVVVDVSHEDPEVKFNWYVDGVEVHNAKTKPREEQYNS
301 TYRVVSVLTVLHQDWLNGKEYKCKVSNKALPAPIEKTISKAKGQPREPQVYTLPPSREEMTKNQVSLTCLVKGFYPSDIAVEWESNGQPENNYKTTPPVL
401 DSDGSFFLYSKLTVDKSRWQQGNVFSCSVMHEALHNHYTQKSLSLSPGK

Next, the MS spectrum of the phosphonamidate-modified peptide 136-149, highlighted above in yellow is shown.

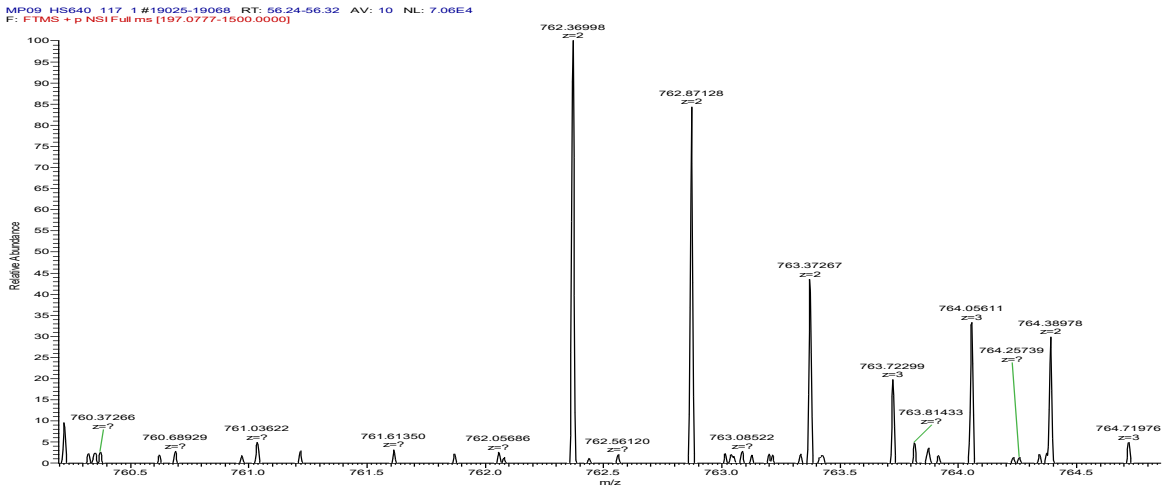

Next, the MS/MS spectrum with HCD fragmentation of the phosphonamidate-modified peptide 136-149, highlighted above in yellow is shown. The signal series 778.28-1335.85 show the y5-y12-fragments, carrying the modification. y3 was detected as a small signal at 359.26, demonstrating modification at Cys146.

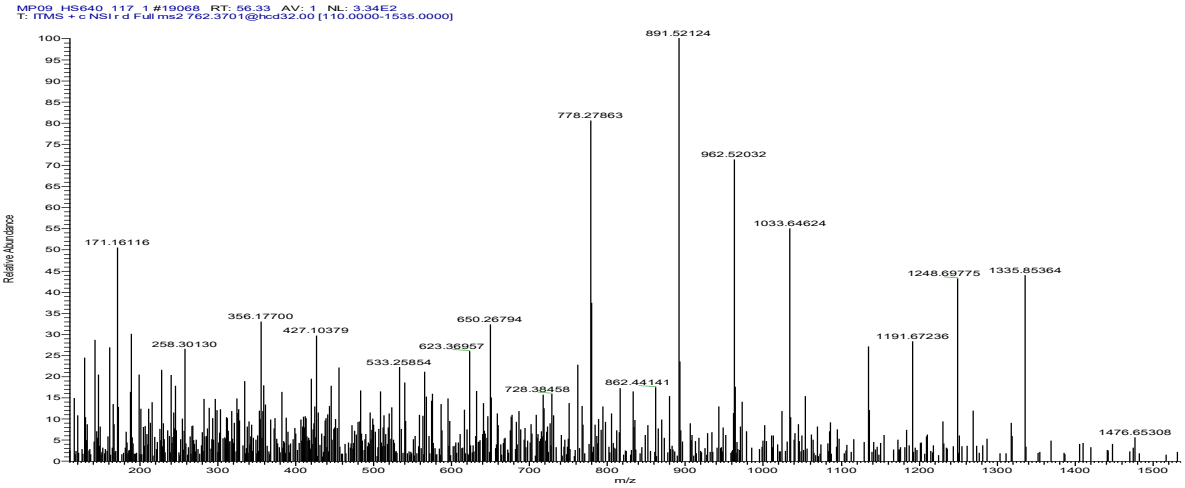

Shown below are the results of the Mascot search on cetuximab's heavy- and light chain after incubation with 100 eq. of **64** without prior reduction of the disulfide bonds. Matched Peptides are highlighted in grey. Amino acid residues modified with **64** are highlighted in red.

no reduction:

light chain sequence coverage: 71%

```
1   DILLTQSPVILSVSPGERVSFSCRASQSIGTNIHWYQQRTNGSPRLLIKYASESISGIPSRFSGSGSGTDFTLSINSVESEDIADYYCQQNNNWPTTFGA
101 ASESISGIPSRFSGSGSGTDFTLSINSVESEDIADYYCQQNNNWPTTFGAGTKLELKRTVAAPSVFIFPPSDEQLKSGTASVVCLLNNFYPREAKVQWKV
201 DNALQSGNSQESVTEQDSKDSTYSLSSTLTLSKADYEKHKVYACEVTHQGLSSPVTKSFNRGEC
```

heavy chain sequence coverage: 44%

```
1   QVQLKQSGPGLVQPSQSLSITCTVSGFSLTNYGVHWVRQSPGKGLEWLGVIWSGGNTDYNTPFTSRLSINKDNSKSQVFFKMNSLQSNDTAIYYCARALT
101 YYDYEFAYWGQGTLVTVSAASTKGPSVFPLAPSSKSTSGGTAALGCLVKDYFPEPVTVSWNSGALTSGVHTFPAVLQSSGLYSLSSVVTVPSSSLGTQTY
201 ICNVNHKPSNTKVDKRVEPKSCDKTHTCPPCPAPELLGGPSVFLFPPKPKDTLMISRTPEVTCVVVDVSHEDPEVKFNWYVDGVEVHNAKTKPREEQYNS
301 TYRVVSVLTVLHQDWLNGKEYKCKVSNKALPAPIEKTISKAKGQPREPQVYTLPPSREEMTKNQVSLTCLVKGFYPSDIAVEWESNGQPENNYKTTPPVL
401 DSDGSFFLYSKLTVDKSRWQQGNVFSCSVMHEALHNHYTQKSLSLSPGK
```

Synthesis of the *O*-2-nitro-5-(oxypropargyl)benzyl-P-vinyl modified peptide 66

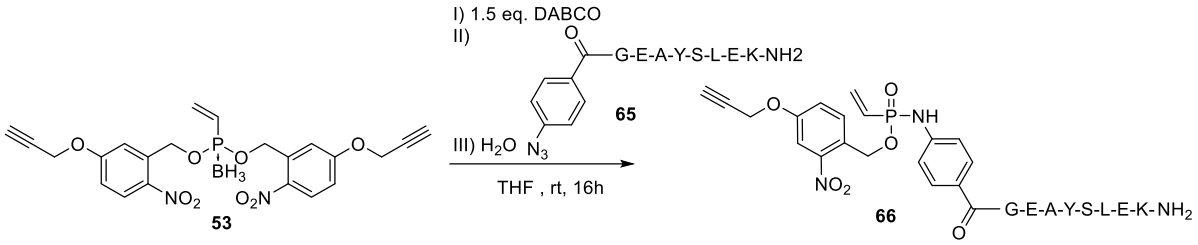

A 5-ml round-bottom-flask was charged with 4 mg Di(2-nitro-5-(oxypropargyl)benzyl) vinylphosphonite borane (**53**) (8.264 µmol, 1.5 eq.) and 1.8 mg DABCO (16.528 µmol, 3.0 eq.) dissolved in 400 µl dry THF under an argon atmosphere. The solution was heated to 50 °C for three hours, cooled to room temperature and 5.7 mg of the azido modified peptide **65** (5.510 µmol, 1.0 eq.), dissolved in 200 µl of dry DMF was added. The solution was stirred overnight at room temperature, 200 µl of water were added and the mixture purified by semi-preparative HPLC. The desired product was obtained as white powder after lyophilization (1.7 mg, 1.322 µmol, 24.0%). HR-MS for $C_{58}H_{79}N_{12}O_{20}P^{2+}$ $[M+2H]^{2+}$ calcd.: 647.2630, found 647.2644.

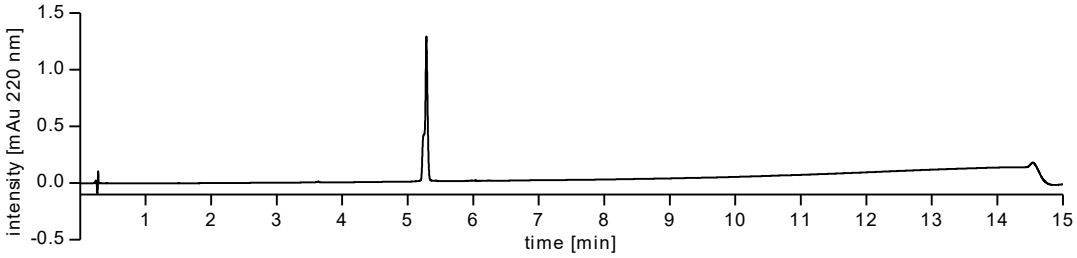

Synthesis of the *O*-(2-nitro-5-(oxypropargyl)benzyloxy)phenyl-P-vinyl modified peptide 67

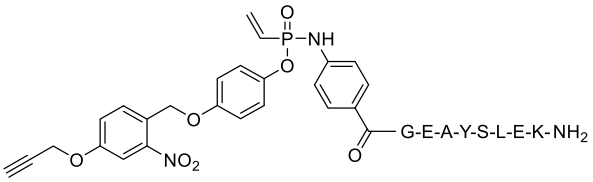

A 5-ml round-bottom-flask was charged with 5.5 mg Di(4-(2-nitro-5-(oxypropargyl)benzyloxy)phenyl) vinylphosphonite borane (**54**) (8.233 µmol, 1.5 eq.) and 1.8 mg DABCO (16.466 µmol, 3.0 eq.) dissolved in 400 µl dry THF under an argon atmosphere. The solution was heated to 50 °C for three hours, cooled to room temperature and 5.7 mg of the azido modified peptide **65** (5.489 µmol, 1.0 eq.), dissolved in 200 µl of dry DMF was added. The solution was stirred overnight at room temperature, 200 µl of water were added and the mixture purified by semi-preparative HPLC. The desired product was obtained as white powder after lyophilization (0.5 mg, 0.357 µmol, 6.5%). HR-MS for $C_{64}H_{83}N_{12}O_{21}P^{2+}$ $[M+2H]^{2+}$ calcd.: 693.2761, found 693.2773.

Ubiquitin G75C conjugation to peptides 66 and 67

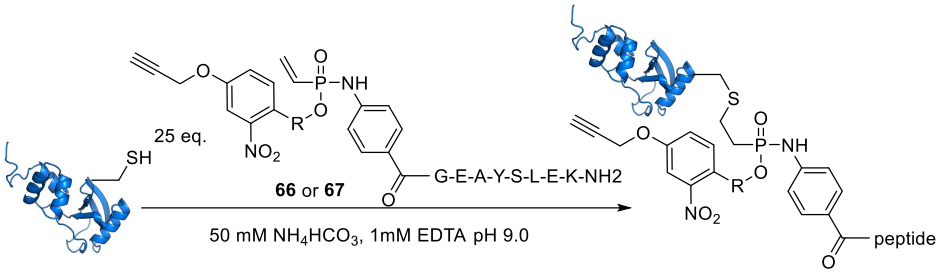

A 32 µM solution of Ubiquitin G75C and 0.8 mM **66** or **67** in a buffer containing 50 mM NH_4HCO_3 and 1 mM EDTA at pH 9.0 was shaken at 4 °C overnight. The solution was rebuffered to PBS by spin filtration using Amicon spin filters with a 3 kDa MWCO (Sartorius, Germany).

Biotin-azide conjugation via CuAAC to Ubiquitin-66

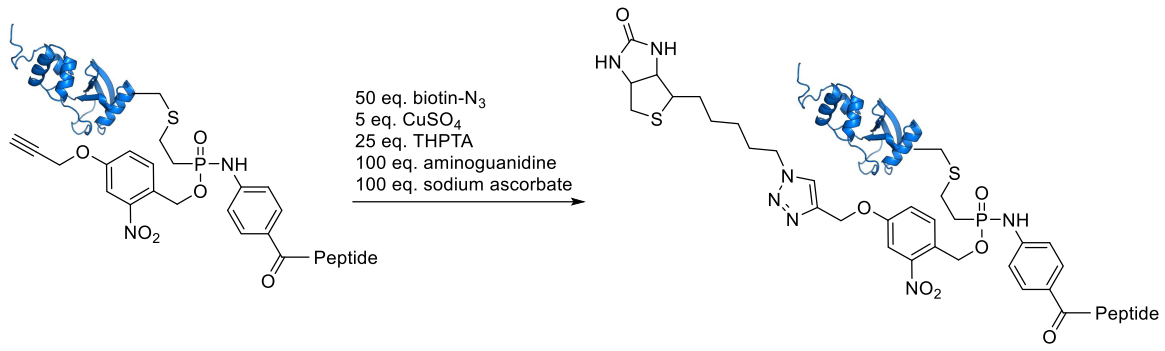

CuAAC was performed based on a previously published protocol with slight variations.[339] 4.2 µl of 5 mM solution of CuSO4 was premixed with 4.2 µl of a 25 mM solution of THPTA, 4.2 µl amino guanidine and 3 µl PBS. The mixture was added to a 70 µl solution of ubiquitin-**66** in PBS and 4.2 µl of a 50 mM solution of biotin azide in DMSO were added. Finally, 4.2 µl of a 100 mM solution of sodium ascorbate were added to start the reaction. The mixture was incubated overnight at 37 °C. Reagent excesses were removed by spin filtration to PBS using Amicon spin filters with a 3 kDa MWCO (Sartorius, Germany).

Ubiquitin-66-biotin pulldown experiment

25 µl of a suspension of streptavidin immobilized on agarose (Solulink N-1000-005, Trilink, United States) was washed five times with 100 µl PBS and incubated for 2 hours at room temperature with 11 µl of a 100 µM solution of ubiquitin-**66**-biotin. 10 µl of the supernatant were subjected to SDS-PAGE analysis. Beads were washed with PBS three times and 10 µl of the last wash fraction were subjected to SDS-PAGE analysis. Half of the beads were subjected to SDS-PAGE analysis and the other half was resuspended in 200 µl of PBS and UV-irradiated for 15 minutes at room temperature. The supernatant was concentrated by vacuum centrifugation and subjected to SDS-PAGE analysis.

9. References

[1] International Agency for Research on Cancer, Press Release N° 263, https://www.who.int/cancer/PRGlobocanFinal.pdf, **2018**.
[2] R. L. Siegel, K. D. Miller, A. Jemal, *CA: Cancer J. Clin.* **2018**, *68*, 7-30.
[3] O. W. Brawley, T. Gansler, R. C. Wender, *CA: Cancer J. Clin.* **2018**, *68*, 327-328.
[4] M. Arruebo, N. Vilaboa, B. Sáez-Gutierrez, J. Lambea, A. Tres, M. Valladares, A. González-Fernández, *Cancers* **2011**, *3*, 3279-3330.
[5] V. T. DeVita, E. Chu, *Cancer Res.* **2008**, *68*, 8643-8653.
[6] B. A. Chabner, T. G. Roberts Jr, *Nat. Rev. Cancer* **2005**, *5*, 65.
[7] N. Tsesmetzis, B. C. Paulin, G. S. Rudd, N. Herold, *Cancers* **2018**, *10*, 240.
[8] A. Imran, A. W. Waseem, S. Kishwar, H. Ashanul, *Anti-Cancer Agents Med. Chem.* **2013**, *13*, 296-306.
[9] A. L. Demain, P. Vaishnav, *Microb. Biotechnol.* **2011**, *4*, 687-699.
[10] P. G. Corrie, *Medicine* **2008**, *36*, 24-28.
[11] V. Malhotra, M. C. Perry, *Cancer Biol. Ther.* **2003**, *2*, 1-3.
[12] R. V. J. Chari, M. L. Miller, W. C. Widdison, *Angew. Chem. Int. Ed.* **2014**, *53*, 3796-3827.
[13] J. M. Drake, J. K. Lee, O. N. Witte, *Mol. Cell. Biol.* **2014**, *34*, 1722-1732.
[14] C. Sawyers, *Nature* **2004**, *432*, 294.
[15] C. L. Sawyers, *Genes Dev.* **2003**, *17*, 2998-3010.
[16] J. F. Gainor, A. T. Shaw, *J. Clin. Oncol.* **2013**, *31*, 3987-3996.
[17] M. I. Davis, J. P. Hunt, S. Herrgard, P. Ciceri, L. M. Wodicka, G. Pallares, M. Hocker, D. K. Treiber, P. P. Zarrinkar, *Nat. Biotechnol.* **2011**, *29*, 1046.
[18] F. C. Breedveld, *The Lancet* **2000**, *355*, 735-740.
[19] A. M. Scott, J. D. Wolchok, L. J. Old, *Nat. Rev. Cancer* **2012**, *12*, 278-287.
[20] a) P. Sharma, J. P. Allison, *Science* **2015**, *348*, 56-61; b) X. Zang, *Genes Dis* **2018**, *5*, 302-303.
[21] V. Chudasama, A. Maruani, S. Caddick, *Nat. Chem.* **2016**, *8*, 114-119.
[22] J. T. PENTO, *Anticancer Res.* **2017**, *37*, 5935-5939.
[23] M. Srinivasarao, P. S. Low, *Chem. Rev.* **2017**, *117*, 12133-12164.
[24] P. Ehrlich, *Br. Med. J.* **1913**, *2*, 353-359.
[25] E. C. Calvaresi, P. J. Hergenrother, *Chem. Sci.* **2013**, *4*, 2319-2333.
[26] K. Seidi, R. Jahanban-Esfahlan, H. Monhemi, P. Zare, B. Minofar, A. Daei Farshchi Adli, D. Farajzadeh, R. Behzadi, M. Mesgari Abbasi, H. A. Neubauer, R. Moriggl, N. Zarghami, T. Javaheri, *Oncogene* **2018**, *37*, 3967-3980.
[27] J. Roy, T. X. Nguyen, A. K. Kanduluru, C. Venkatesh, W. Lv, P. V. N. Reddy, P. S. Low, M. Cushman, *J. Med. Chem.* **2015**, *58*, 3094-3103.
[28] N. Parker, M. J. Turk, E. Westrick, J. D. Lewis, P. S. Low, C. P. Leamon, *Anal. Biochem.* **2005**, *338*, 284-293.
[29] K. V. Waller, K. M. Ward, J. D. Mahan, D. K. Wismatt, *Clin. Chem.* **1989**, *35*, 755-765.
[30] P. L. Turecek, M. J. Bossard, F. Schoetens, I. A. Ivens, *J. Pharm. Sci.* **2016**, *105*, 460-475.
[31] J. Pan, W. Chen, Y. Ma, G. Pan, *Chem. Soc. Rev.* **2018**, *47*, 5574-5587.
[32] X. Guo, L. Wang, X. Wei, S. Zhou, *Journal of Polymer Science Part A: Polymer Chemistry* **2016**, *54*, 3525-3550.
[33] G. Zhu, G. Niu, X. Chen, *Bioconjugate Chem.* **2015**, *26*, 2186-2197.
[34] X. Chen, G. Ding, Q. Gao, J. Sun, Q. Zhang, L. Du, Z. Qiu, C. Wang, F. Zheng, B. Sun, J. Ni, Z. Feng, J. Zhu, *PLoS One* **2013**, *8*, e63093.
[35] R. A. Root, W. Cao, B. Li, P. LaPan, C. Meade, J. Sanford, M. Jin, C. O'Sullivan, E. Cummins, M. Lambert, D. A. Sheehan, W. Ma, S. Gatto, K. Kerns, K. Lam, M. A. D'Antona, L. Zhu, A. W. Brady, S. Benard, A. King, T. He, L. Racie, M. Arai, D. Barrett, W. Stochaj, R. E. LaVallie, R. J. Apgar, K. Svenson, L. Mosyak, Y. Yang, R. G. Chichili, L. Liu, H. Li, S. Burke, S. Johnson, R.

Alderson, J. W. Finlay, L. Lin, S. Olland, W. Somers, E. Bonvini, H.-P. Gerber, C. May, A. P. Moore, L. Tchistiakova, L. Bloom, *Antibodies* **2016**, *5*.

[36] Y. Safdari, V. Ahmadzadeh, M. Khalili, H. Z. Jaliani, V. Zarei, V. Erfani-Moghadam, *Mol. Med.* **2016**, *22*, 258-270.

[37] M. Altai, H. Liu, H. Ding, B. Mitran, P.-H. Edqvist, V. Tolmachev, A. Orlova, T. Gräslund, *J. Control. Release* **2018**, *288*, 84-95.

[38] S. D. Goldberg, R. M. F. Cardoso, T. Lin, T. Spinka-Doms, D. Klein, S. A. Jacobs, V. Dudkin, G. Gilliland, K. T. O'Neil, *Protein Eng., Des. Sel.* **2016**, *29*, 563-572.

[39] D. Schumacher, C. P. R. Hackenberger, H. Leonhardt, J. Helma, *J. Clin. Immunol.* **2016**, *36*, 100-107.

[40] A. Beck, L. Goetsch, C. Dumontet, N. Corvaïa, *Nat. Rev. Drug Discov.* **2017**, *16*, 315.

[41] N. Uy, M. Nadeau, M. Stahl, A. M. Zeidan, *J. Blood Med.* **2018**, *9*, 67-74.

[42] F. R. Appelbaum, I. D. Bernstein, *Blood* **2017**, *130*, 2373-2376.

[43] P. A. Szijj, C. Bahou, V. Chudasama, *Drug Discov. Today* **2018**, *30*, 27-34.

[44] L. J. Harris, S. B. Larson, K. W. Hasel, A. McPherson, *Biochemistry* **1997**, *36*, 1581-1597.

[45] B. C. Laguzza, C. L. Nichols, S. L. Briggs, G. J. Cullinan, D. A. Johnson, J. J. Starling, A. L. Baker, T. F. Bumol, J. R. F. Corvalan, *J. Med. Chem.* **1989**, *32*, 548-555.

[46] D. J. Elias, L. E. Kline, B. A. Robbins, H. C. Johnson, K. Pekny, M. Benz, J. A. Robb, L. E. Walker, M. Kosty, R. O. Dillman, *Am. J. Respir. Crit. Care Med.* **1994**, *150*, 1114-1122.

[47] B. H. Petersen, S. V. DeHerdt, D. W. Schneck, T. F. Bumol, *Cancer Res.* **1991**, *51*, 2286.

[48] J. M. Lambert, A. Berkenblit, *Annu. Rev. Med.* **2018**, *69*, 191-207.

[49] A. H. Staudacher, M. P. Brown, *Br. J. Cancer* **2017**, *117*, 1736.

[50] S. I. Rudnick, J. Lou, C. C. Shaller, Y. Tang, A. J. P. Klein-Szanto, L. M. Weiner, J. D. Marks, G. P. Adams, *Cancer Res.* **2011**, *71*, 2250-2259.

[51] J. T. Ryman, B. Meibohm, *CPT Pharmacometrics Syst. Pharmacol.* **2017**, *6*, 576-588.

[52] P. W. H. I. Parren, P. J. Carter, A. Plückthun, *mAbs* **2017**, *9*, 898-906.

[53] I. S. Arif, C. L. Hooper, F. Greco, A. C. Williams, S. Y. Boateng, *Br. J. Pharmacol.* **2013**, *169*, 1178-1188.

[54] A. W. Tolcher, S. Sugarman, K. A. Gelmon, R. Cohen, M. Saleh, C. Isaacs, L. Young, D. Healey, N. Onetto, W. Slichenmyer, *J. Clin. Oncol.* **1999**, *17*, 478-478.

[55] S. Parmley, *Science-Business eXchange* **2014**, *7*, 1397-1397.

[56] P. J. Burke, P. D. Senter, D. W. Meyer, J. B. Miyamoto, M. Anderson, B. E. Toki, G. Manikumar, M. C. Wani, D. J. Kroll, S. C. Jeffrey, *Bioconjugate Chem.* **2009**, *20*, 1242-1250.

[57] R. P. Lyon, T. D. Bovee, S. O. Doronina, P. J. Burke, J. H. Hunter, H. D. Neff-LaFord, M. Jonas, M. E. Anderson, J. R. Setter, P. D. Senter, *Nat. Biotechnol.* **2015**, *33*, 733.

[58] A. Lucas, L. S. L. Price, A. Schorzman, M. Storrie, J. A. Piscitelli, J. Razo, W. C. Zamboni, *Factors Affecting the Pharmacology of Antibody–Drug Conjugates, Vol. 7*, **2018**.

[59] A. Mullard, *Nat. Rev. Drug Discov.* **2013**, *12*, 329.

[60] S. C. Alley, N. M. Okeley, P. D. Senter, *Curr. Opin. Chem. Biol.* **2010**, *14*, 529-537.

[61] N. G. Caculitan, J. dela Cruz Chuh, Y. Ma, D. Zhang, K. R. Kozak, Y. Liu, T. H. Pillow, J. Sadowsky, T. K. Cheung, Q. Phung, B. Haley, B.-C. Lee, R. W. Akita, M. X. Sliwkowski, A. G. Polson, *Cancer Res.* **2017**, *77*, 7027-7037.

[62] Y. V. Kovtun, V. S. Goldmacher, *Cancer Lett.* **2007**, *255*, 232-240.

[63] L. R. Staben, S. G. Koenig, S. M. Lehar, R. Vandlen, D. Zhang, J. Chuh, S.-F. Yu, C. Ng, J. Guo, Y. Liu, A. Fourie-O'Donohue, M. Go, X. Linghu, N. L. Segraves, T. Wang, J. Chen, B. Wei, G. D. L. Phillips, K. Xu, K. R. Kozak, S. Mariathasan, J. A. Flygare, T. H. Pillow, *Nat. Chem.* **2016**, *8*, 1112-1119.

[64] A. M. Wu, P. D. Senter, *Nat. Biotechnol.* **2005**, *23*, 1137.

[65] P. D. Senter, *Curr. Opin. Chem. Biol.* **2009**, *13*, 235-244.

[66] L. Ducry, B. Stump, *Bioconjugate Chem.* **2010**, *21*, 5-13.

[67] T. H. Pillow, J. D. Sadowsky, D. Zhang, S.-F. Yu, G. Del Rosario, K. Xu, J. He, S. Bhakta, R. Ohri, K. R. Kozak, E. Ha, J. R. Junutula, J. A. Flygare, *Chem. Sci.* **2017**, *8*, 366-370.

[68] D. Zhang, T. H. Pillow, Y. Ma, J. d. Cruz-Chuh, K. R. Kozak, J. D. Sadowsky, G. D. Lewis Phillips, J. Guo, M. Darwish, P. Fan, J. Chen, C. He, T. Wang, H. Yao, Z. Xu, J. Chen, J. Wai, Z. Pei, C. E. C. A. Hop, S. C. Khojasteh, P. S. Dragovich, *ACS Med. Chem. Lett.* **2016**, *7*, 988-993.

[69] G. M. Dubowchik, R. A. Firestone, L. Padilla, D. Willner, S. J. Hofstead, K. Mosure, J. O. Knipe, S. J. Lasch, P. A. Trail, *Bioconjugate Chem.* **2002**, *13*, 855-869.

[70] a) S. O. Doronina, B. E. Toki, M. Y. Torgov, B. A. Mendelsohn, C. G. Cerveny, D. F. Chace, R. L. DeBlanc, R. P. Gearing, T. D. Bovee, C. B. Siegall, J. A. Francisco, A. F. Wahl, D. L. Meyer, P. D. Senter, *Nat. Biotechnol.* **2003**, *21*, 778-784; b) S. M. Ansell, *Blood* **2014**, *124*, 3197-3200.

[71] S. C. Jeffrey, J. B. Andreyka, S. X. Bernhardt, K. M. Kissler, T. Kline, J. S. Lenox, R. F. Moser, M. T. Nguyen, N. M. Okeley, I. J. Stone, X. Zhang, P. D. Senter, *Bioconjugate Chem.* **2006**, *17*, 831-840.

[72] K. Dudgeon, R. Rouet, I. Kokmeijer, P. Schofield, J. Stolp, D. Langley, D. Stock, D. Christ, *Proc. Natl. Acad. Sci. U.S.A.* **2012**, *109*, 10879-10884.

[73] A. Saluja, D. S. Kalonia, *Int. J. Pharm.* **2008**, *358*, 1-15.

[74] a) S. Kumar, S. K. Singh, X. Wang, B. Rup, D. Gill, *Pharm. Res.* **2011**, *28*, 949; b) K. D. Ratanji, J. P. Derrick, R. J. Dearman, I. Kimber, *J. Immunotoxicol.* **2014**, *11*, 99-109.

[75] P. J. Burke, J. Z. Hamilton, S. C. Jeffrey, J. H. Hunter, S. O. Doronina, N. M. Okeley, J. B. Miyamoto, M. E. Anderson, I. J. Stone, M. L. Ulrich, J. K. Simmons, E. E. McKinney, P. D. Senter, R. P. Lyon, *Mol. Cancer Ther.* **2017**, *16*, 116.

[76] M. T. Kim, Y. Chen, J. Marhoul, F. Jacobson, *Bioconjugate Chem.* **2014**, *25*, 1223-1232.

[77] J. R. Junutula, H. Raab, S. Clark, S. Bhakta, D. D. Leipold, S. Weir, Y. Chen, M. Simpson, S. P. Tsai, M. S. Dennis, Y. Lu, Y. G. Meng, C. Ng, J. Yang, C. C. Lee, E. Duenas, J. Gorrell, V. Katta, A. Kim, K. McDorman, K. Flagella, R. Venook, S. Ross, S. D. Spencer, W. Lee Wong, H. B. Lowman, R. Vandlen, M. X. Sliwkowski, R. H. Scheller, P. Polakis, W. Mallet, *Nat. Biotechnol.* **2008**, *26*, 925.

[78] S. Lin, X. Yang, S. Jia, A. M. Weeks, M. Hornsby, P. S. Lee, R. V. Nichiporuk, A. T. Iavarone, J. A. Wells, F. D. Toste, C. J. Chang, *Science* **2017**, *355*, 597-602.

[79] P. M. S. D. Cal, G. J. L. Bernardes, P. M. P. Gois, *Angew. Chem. Int. Ed.* **2014**, *53*, 10585-10587.

[80] M. M. C. Sun, K. S. Beam, C. G. Cerveny, K. J. Hamblett, R. S. Blackmore, M. Y. Torgov, F. G. M. Handley, N. C. Ihle, P. D. Senter, S. C. Alley, *Bioconjugate Chem.* **2005**, *16*, 1282-1290.

[81] L. M. Hinman, P. R. Hamann, R. Wallace, A. T. Menendez, F. E. Durr, J. Upeslacis, *Cancer Res.* **1993**, *53*, 3336-3342.

[82] P. Dennler, A. Chiotellis, E. Fischer, D. Brégeon, C. Belmant, L. Gauthier, F. Lhospice, F. Romagne, R. Schibli, *Bioconjugate Chem.* **2014**, *25*, 569-578.

[83] a) J. Ohata, Z. T. Ball, *J. Am. Chem. Soc.* **2017**, *139*, 12617-12622; b) A. Perols, M. Arcos Famme, A. Eriksson Karlström, *ChemBioChem* **2015**, *16*, 2522-2529.

[84] J. Y. Axup, K. M. Bajjuri, M. Ritland, B. M. Hutchins, C. H. Kim, S. A. Kazane, R. Halder, J. S. Forsyth, A. F. Santidrian, K. Stafin, Y. Lu, H. Tran, A. J. Seller, S. L. Biroc, A. Szydlik, J. K. Pinkstaff, F. Tian, S. C. Sinha, B. Felding-Habermann, V. V. Smider, P. G. Schultz, *Proc. Natl. Acad. Sci. U.S.A.* **2012**, *109*, 16101.

[85] a) N. Krall, F. P. da Cruz, O. Boutureira, G. J. L. Bernardes, *Nat. Chem.* **2015**, *8*, 103; b) E. M. Sletten, C. R. Bertozzi, *Angew. Chem. Int. Ed.* **2009**, *48*, 6974-6998.

[86] a) C. D. Spicer, B. G. Davis, *Nat. Commun.* **2014**, *5*, 4740; b) Y. Takaoka, A. Ojida, I. Hamachi, *Angew. Chem. Int. Ed.* **2013**, *52*, 4088-4106.

[87] a) K. Lang, J. W. Chin, *Chem. Rev.* **2014**, *114*, 4764-4806; b) E. Baslé, N. Joubert, M. Pucheault, *Chem. Biol.* **2010**, *17*, 213-227.

[88] S. Sakamoto, I. Hamachi, *Anal. Sci.* **2019**, *35*, 5-27.

[89] R. Wetzel, R. Halualani, J. T. Stults, C. Quan, *Bioconjugate Chem.* **1990**, *1*, 114-122.

[90] D. R. Dempsey, H. Jiang, J. H. Kalin, Z. Chen, P. A. Cole, *J. Am. Chem. Soc.* **2018**, *140*, 9374-9378.
[91] G. D. Lewis Phillips, G. Li, D. L. Dugger, L. M. Crocker, K. L. Parsons, E. Mai, W. A. Blättler, J. M. Lambert, R. V. J. Chari, R. J. Lutz, W. L. T. Wong, F. S. Jacobson, H. Koeppen, R. H. Schwall, S. R. Kenkare-Mitra, S. D. Spencer, M. X. Sliwkowski, *Cancer Res.* **2008**, *68*, 9280-9290.
[92] O. Boutureira, G. J. L. Bernardes, *Chem. Rev.* **2015**, *115*, 2174-2195.
[93] T. Nakamura, Y. Kawai, N. Kitamoto, T. Osawa, Y. Kato, *Chem. Res. Toxicol.* **2009**, *22*, 536-542.
[94] N. Jentoft, D. G. Dearborn, *J. Biol. Chem.* **1979**, *254*, 4359-4365.
[95] K. Tanaka, T. Masuyama, K. Hasegawa, T. Tahara, H. Mizuma, Y. Wada, Y. Watanabe, K. Fukase, *Angew. Chem. Int. Ed.* **2008**, *47*, 102-105.
[96] M. J. Matos, B. L. Oliveira, N. Martínez-Sáez, A. Guerreiro, P. M. S. D. Cal, J. Bertoldo, M. Maneiro, E. Perkins, J. Howard, M. J. Deery, J. M. Chalker, F. Corzana, G. Jiménez-Osés, G. J. L. Bernardes, *J. Am. Chem. Soc.* **2018**, *140*, 4004-4017.
[97] P. Dawson, T. Muir, I. Clark-Lewis, S. Kent, *Science* **1994**, *266*, 776-779.
[98] T. W. Muir, D. Sondhi, P. A. Cole, *Proc. Natl. Acad. Sci. U.S.A.* **1998**, *95*, 6705-6710.
[99] H. Liu, X. Li, *Acc. Chem. Res.* **2018**, *51*, 1643-1655.
[100] K. F. Geoghegan, J. G. Stroh, *Bioconjugate Chem.* **1992**, *3*, 138-146.
[101] J. M. Gilmore, R. A. Scheck, A. P. Esser-Kahn, N. S. Joshi, M. B. Francis, *Angew. Chem. Int. Ed.* **2006**, *45*, 5307-5311.
[102] A. Miseta, P. Csutora, *Mol. Biol. Evol.* **2000**, *17*, 1232-1239.
[103] G. Bulaj, T. Kortemme, D. P. Goldenberg, *Biochemistry* **1998**, *37*, 8965-8972.
[104] a) J. M. Chalker, G. J. L. Bernardes, Y. A. Lin, B. G. Davis, *Chem. Asian J.* **2009**, *4*, 630-640; b) S. B. Gunnoo, A. Madder, *ChemBioChem* **2016**, *17*, 529-553.
[105] G. Bulaj, *Biotechnol. Adv.* **2005**, *23*, 87-92.
[106] S. Ariyasu, H. Hayashi, B. Xing, S. Chiba, *Bioconjugate Chem.* **2017**, *28*, 897-902.
[107] J. Katz, J. E. Janik, A. Younes, *Clin. Cancer Res.* **2011**, *17*, 6428-6436.
[108] B. D. Mather, K. Viswanathan, K. M. Miller, T. E. Long, *Prog. Polym. Sci.* **2006**, *31*, 487-531.
[109] B. H. Northrop, S. H. Frayne, U. Choudhary, *Polym. Chem.* **2015**, *6*, 3415-3430.
[110] F. Saito, H. Noda, J. W. Bode, *ACS Chem. Biol.* **2015**, *10*, 1026-1033.
[111] a) J. E. Moore, W. H. Ward, *J. Am. Chem. Soc.* **1956**, *78*, 2414-2418; b) T. C. Tsao, K. Bailey, *Biochim. Biophys. Acta* **1953**, *11*, 102-113.
[112] N. Goel, S. Stephens, *mAbs* **2010**, *2*, 137-147.
[113] C.-W. Wu, L. R. Yarbrough, F. Y. H. Wu, *Biochemistry* **1976**, *15*, 2863-2868.
[114] S. Kurono, T. Kurono, N. Komori, S. Niwayama, H. Matsumoto, *Bioorg. Med. Chem.* **2006**, *14*, 8197-8209.
[115] C. F. Brewer, J. P. Riehm, *Anal. Biochem.* **1967**, *18*, 248-255.
[116] J. Václavík, R. Zschoche, I. Klimánková, V. Matoušek, P. Beier, D. Hilvert, A. Togni, *Chem. Eur. J.* **2017**, *23*, 6490-6494.
[117] A. D. Baldwin, K. L. Kiick, *Bioconjugate Chem.* **2011**, *22*, 1946-1953.
[118] S. C. Alley, D. R. Benjamin, S. C. Jeffrey, N. M. Okeley, D. L. Meyer, R. J. Sanderson, P. D. Senter, *Bioconjugate Chem.* **2008**, *19*, 759-765.
[119] a) B.-Q. Shen, K. Xu, L. Liu, H. Raab, S. Bhakta, M. Kenrick, K. L. Parsons-Reponte, J. Tien, S.-F. Yu, E. Mai, D. Li, J. Tibbitts, J. Baudys, O. M. Saad, S. J. Scales, P. J. McDonald, P. E. Hass, C. Eigenbrot, T. Nguyen, W. A. Solis, R. N. Fuji, K. M. Flagella, D. Patel, S. D. Spencer, L. A. Khawli, A. Ebens, W. L. Wong, R. Vandlen, S. Kaur, M. X. Sliwkowski, R. H. Scheller, P. Polakis, J. R. Junutula, *Nat. Biotechnol.* **2012**, *30*, 184-189; b) J. F. Ponte, X. Sun, N. C. Yoder, N. Fishkin, R. Laleau, J. Coccia, L. Lanieri, M. Bogalhas, L. Wang, S. Wilhelm, W. Widdison, J. Pinkas, T. A. Keating, R. Chari, H. K. Erickson, J. M. Lambert, *Bioconjugate Chem.* **2016**, *27*, 1588-1598.
[120] a) P. Knight, *Biochem. J.* **1979**, *179*, 191-197; b) S. D. Fontaine, R. Reid, L. Robinson, G. W. Ashley, D. V. Santi, *Bioconjugate Chem.* **2015**, *26*, 145-152.

[121] L. N. Tumey, M. Charati, T. He, E. Sousa, D. Ma, X. Han, T. Clark, J. Casavant, F. Loganzo, F. Barletta, J. Lucas, E. I. Graziani, *Bioconjugate Chem.* **2014**, *25*, 1871-1880.
[122] R. P. Lyon, J. R. Setter, T. D. Bovee, S. O. Doronina, J. H. Hunter, M. E. Anderson, C. L. Balasubramanian, S. M. Duniho, C. I. Leiske, F. Li, P. D. Senter, *Nat. Biotechnol.* **2014**, *32*, 1059.
[123] O. Koniev, A. Wagner, *Chem. Soc. Rev.* **2015**, *44*, 5495-5551.
[124] D. Kalia, P. V. Malekar, M. Parthasarathy, *Angew. Chem. Int. Ed.* **2016**, *55*, 1432-1435.
[125] L. M. Tedaldi, M. E. B. Smith, R. I. Nathani, J. R. Baker, *Chem. Commun.* **2009**, 6583-6585.
[126] C. Marculescu, H. Kossen, R. E. Morgan, P. Mayer, S. A. Fletcher, B. Tolner, K. A. Chester, L. H. Jones, J. R. Baker, *Chem. Commun.* **2014**, *50*, 7139-7142.
[127] F. F. Schumacher, M. Nobles, C. P. Ryan, M. E. B. Smith, A. Tinker, S. Caddick, J. R. Baker, *Bioconjugate Chem.* **2011**, *22*, 132-136.
[128] P. Moody, M. E. B. Smith, C. P. Ryan, V. Chudasama, J. R. Baker, J. Molloy, S. Caddick, *ChemBioChem* **2012**, *13*, 39-41.
[129] a) M. E. B. Smith, M. B. Caspersen, E. Robinson, M. Morais, A. Maruani, J. P. M. Nunes, K. Nicholls, M. J. Saxton, S. Caddick, J. R. Baker, V. Chudasama, *Org. Biomol. Chem.* **2015**, *13*, 7946-7949; b) C. P. Ryan, M. E. B. Smith, F. F. Schumacher, D. Grohmann, D. Papaioannou, G. Waksman, F. Werner, J. R. Baker, S. Caddick, *Chem. Commun.* **2011**, *47*, 5452-5454.
[130] J. P. M. Nunes, V. Vassileva, E. Robinson, M. Morais, M. E. B. Smith, R. B. Pedley, S. Caddick, J. R. Baker, V. Chudasama, *RSC Advances* **2017**, *7*, 24828-24832.
[131] L. Castañeda, Z. V. F. Wright, C. Marculescu, T. M. Tran, V. Chudasama, A. Maruani, E. A. Hull, J. P. M. Nunes, R. J. Fitzmaurice, M. E. B. Smith, L. H. Jones, S. Caddick, J. R. Baker, *Tetrahedron Lett.* **2013**, *54*, 3493-3495.
[132] a) A. Maruani, M. E. B. Smith, E. Miranda, K. A. Chester, V. Chudasama, S. Caddick, *Nat. Commun.* **2015**, *6*, 6645; b) C. Bahou, D. A. Richards, A. Maruani, E. A. Love, F. Javaid, S. Caddick, J. R. Baker, V. Chudasama, *Org. Biomol. Chem.* **2018**, *16*, 1359-1366.
[133] A. Maruani, S. Alom, P. Canavelli, M. T. W. Lee, R. E. Morgan, V. Chudasama, S. Caddick, *Chem. Commun.* **2015**, *51*, 5279-5282.
[134] D. P. Nair, M. Podgórski, S. Chatani, T. Gong, W. Xi, C. R. Fenoli, C. N. Bowman, *Chem. Mater.* **2014**, *26*, 724-744.
[135] D. C. Brune, *Anal. Biochem.* **1992**, *207*, 285-290.
[136] B. Bernardim, P. M. S. D. Cal, M. J. Matos, B. L. Oliveira, N. Martínez-Sáez, I. S. Albuquerque, E. Perkins, F. Corzana, A. C. B. Burtoloso, G. Jiménez-Osés, G. J. L. Bernardes, *Nat. Commun.* **2016**, *7*, 13128.
[137] S. Brocchini, S. Balan, A. Godwin, J.-W. Choi, M. Zloh, S. Shaunak, *Nat. Protocols* **2006**, *1*, 2241-2252.
[138] H. Khalili, A. Godwin, J.-w. Choi, R. Lever, S. Brocchini, *Bioconjugate Chem.* **2012**, *23*, 2262-2277.
[139] H.-Y. Shiu, T.-C. Chan, C.-M. Ho, Y. Liu, M.-K. Wong, C.-M. Che, *Chem. Eur. J.* **2009**, *15*, 3839-3850.
[140] M. S. Masri, M. Friedman, *J. Protein Chem.* **1988**, *7*, 49-54.
[141] Z. Wu, L. Li, S. Liu, F. Yakushijin, K. Yakushijin, D. Horne, P. S. Conti, Z. Li, F. Kandeel, J. E. Shively, *J. Nucl. Med.* **2014**, *55*, 1178-1184.
[142] T. A. Modro, *Can. J. Chem.* **1977**, *55*, 3681-3685.
[143] F. Gao, X. Yan, K. Auclair, *Chem. Eur. J.* **2009**, *15*, 2064-2070.
[144] D. R. Goddard, L. Michaelis, *J. Biol. Chem.* **1935**, *112*, 361-371.
[145] N. Lundell, T. Schreitmüller, *Anal. Biochem.* **1999**, *266*, 31-47.
[146] T. Müller, D. Winter, *Mol. Cell. Proteom.* **2017**, *16*, 1173-1187.
[147] M. L. Nielsen, M. Vermeulen, T. Bonaldi, J. Cox, L. Moroder, M. Mann, *Nat. Methods* **2008**, *5*, 459-460.
[148] M. Sunbul, L. Nacheva, A. Jäschke, *Bioconjugate Chem.* **2015**, *26*, 1466-1469.

[149] B. D. Smith, J. J. Higgin, R. T. Raines, *Bioorg. Med. Chem. Lett.* **2011**, *21*, 5029-5032.
[150] J. M. Chalker, C. S. C. Wood, B. G. Davis, *J. Am. Chem. Soc.* **2009**, *131*, 16346-16347.
[151] E. V. Vinogradova, C. Zhang, A. M. Spokoyny, B. L. Pentelute, S. L. Buchwald, *Nature* **2015**, *526*, 687.
[152] K. K.-Y. Kung, H.-M. Ko, J.-F. Cui, H.-C. Chong, Y.-C. Leung, M.-K. Wong, *Chem. Commun.* **2014**, *50*, 11899-11902.
[153] R. Kundu, Z. T. Ball, *Chem. Commun.* **2013**, *49*, 4166-4168.
[154] N. Gupta, J. Kancharla, S. Kaushik, A. Ansari, S. Hossain, R. Goyal, M. Pandey, J. Sivaccumar, S. Hussain, A. Sarkar, A. Sengupta, S. K. Mandal, M. Roy, S. Sengupta, *Chem. Sci.* **2017**, *8*, 2387-2395.
[155] A. M. Spokoyny, Y. Zou, J. J. Ling, H. Yu, Y.-S. Lin, B. L. Pentelute, *J. Am. Chem. Soc.* **2013**, *135*, 5946-5949.
[156] A. Celine, S. Claudio, *Curr. Med. Chem.* **2002**, *9*, 963-978.
[157] a) L. D. Walensky, A. L. Kung, I. Escher, T. J. Malia, S. Barbuto, R. D. Wright, G. Wagner, G. L. Verdine, S. J. Korsmeyer, *Science* **2004**, *305*, 1466-1470; b) L. D. Walensky, G. H. Bird, *J. Med. Chem.* **2014**, *57*, 6275-6288.
[158] S. Kalhor-Monfared, M. R. Jafari, J. T. Patterson, P. I. Kitov, J. J. Dwyer, J. M. Nuss, R. Derda, *Chem. Sci.* **2016**, *7*, 3785-3790.
[159] C. Zhang, A. M. Spokoyny, Y. Zou, M. D. Simon, B. L. Pentelute, *Angew. Chem. Int. Ed.* **2013**, *52*, 14001-14005.
[160] C. Zhang, M. Welborn, T. Zhu, N. J. Yang, M. S. Santos, T. Van Voorhis, B. L. Pentelute, *Nat. Chem.* **2015**, *8*, 120.
[161] R. Frei, M. D. Wodrich, D. P. Hari, P.-A. Borin, C. Chauvier, J. Waser, *J. Am. Chem. Soc.* **2014**, *136*, 16563-16573.
[162] D. Abegg, R. Frei, L. Cerato, D. Prasad Hari, C. Wang, J. Waser, A. Adibekian, *Angew. Chem.* **2015**, *127*, 11002-11007.
[163] J. Charpentier, N. Früh, A. Togni, *Chem. Rev.* **2015**, *115*, 650-682.
[164] L. Brülisauer, M. A. Gauthier, J.-C. Leroux, *J. Control. Release* **2014**, *195*, 147-154.
[165] G. L. Ellman, *Arch. Biochem. Biophys.* **1959**, *82*, 70-77.
[166] C. Chatterjee, R. K. McGinty, B. Fierz, T. W. Muir, *Nat. Chem. Biol.* **2010**, *6*, 267.
[167] H. D. Herce, D. Schumacher, A. F. L. Schneider, A. K. Ludwig, F. A. Mann, M. Fillies, M.-A. Kasper, S. Reinke, E. Krause, H. Leonhardt, M. C. Cardoso, C. P. R. Hackenberger, *Nat. Chem.* **2017**, 762–771.
[168] a) G. J. L. Bernardes, G. Casi, S. Trüssel, I. Hartmann, K. Schwager, J. Scheuermann, D. Neri, *Angew. Chem.* **2012**, *124*, 965-968; b) T. List, G. Casi, D. Neri, *Mol. Cancer Ther.* **2014**, *13*, 2641-2652.
[169] J. Bertran-Vicente, M. Penkert, O. Nieto-Garcia, J.-M. Jeckelmann, P. Schmieder, E. Krause, C. P. R. Hackenberger, *Nat. Commun.* **2016**, *7*, 12703.
[170] J. M. Chalker, S. B. Gunnoo, O. Boutureira, S. C. Gerstberger, M. Fernandez-Gonzalez, G. J. L. Bernardes, L. Griffin, H. Hailu, C. J. Schofield, B. G. Davis, *Chem. Sci.* **2011**, *2*, 1666-1676.
[171] C. J. M., L. Lukas, R. N. R., S. C. J., D. B. G., *Angew. Chem. Int. Ed.* **2012**, *51*, 1835-1839.
[172] N. Haj-Yahya, H. P. Hemantha, R. Meledin, S. Bondalapati, M. Seenaiah, A. Brik, *Org. Lett.* **2014**, *16*, 540-543.
[173] T. H. Wright, B. J. Bower, J. M. Chalker, G. J. L. Bernardes, R. Wiewiora, W.-L. Ng, R. Raj, S. Faulkner, M. R. J. Vallée, A. Phanumartwiwath, O. D. Coleman, M.-L. Thézénas, M. Khan, S. R. G. Galan, L. Lercher, M. W. Schombs, S. Gerstberger, M. E. Palm-Espling, A. J. Baldwin, B. M. Kessler, T. D. W. Claridge, S. Mohammed, B. G. Davis, *Science* **2016**, *354*.
[174] J. M. Chalker, B. G. Davis, *Curr. Opin. Chem. Biol.* **2010**, *14*, 781-789.
[175] R. Meledin, S. M. Mali, S. K. Singh, A. Brik, *Org. Biomol. Chem.* **2016**, *14*, 4817-4823.
[176] C. E. Hoyle, C. N. Bowman, *Angew. Chem. Int. Ed.* **2010**, *49*, 1540-1573.
[177] C. E. Hoyle, A. B. Lowe, C. N. Bowman, *Chem. Soc. Rev.* **2010**, *39*, 1355-1387.

[178] H. C. Kolb, M. G. Finn, K. B. Sharpless, *Angew. Chem.* **2001**, *113*, 2056-2075.
[179] N. Floyd, B. Vijayakrishnan, J. R. Koeppe, B. G. Davis, *Angew. Chem.* **2009**, *121*, 7938-7942.
[180] D. Weinrich, P.-C. Lin, P. Jonkheijm, U. T. T. Nguyen, H. Schröder, C. M. Niemeyer, K. Alexandrov, R. Goody, H. Waldmann, *Angew. Chem.* **2010**, *122*, 1274-1279.
[181] E. M. Valkevich, R. G. Guenette, N. A. Sanchez, Y.-c. Chen, Y. Ge, E. R. Strieter, *J. Am. Chem. Soc.* **2012**, *134*, 6916-6919.
[182] F. Li, A. Allahverdi, R. Yang, G. B. J. Lua, X. Zhang, Y. Cao, N. Korolev, L. Nordenskiöld, C.-F. Liu, *Angew. Chem. Int. Ed.* **2011**, *50*, 9611-9614.
[183] J. M. Antos, M. B. Francis, *J. Am. Chem. Soc.* **2004**, *126*, 10256-10257.
[184] J. M. Antos, J. M. McFarland, A. T. Iavarone, M. B. Francis, *J. Am. Chem. Soc.* **2009**, *131*, 6301-6308.
[185] Y. Seki, T. Ishiyama, D. Sasaki, J. Abe, Y. Sohma, K. Oisaki, M. Kanai, *J. Am. Chem. Soc.* **2016**, *138*, 10798-10801.
[186] N. S. Joshi, L. R. Whitaker, M. B. Francis, *J. Am. Chem. Soc.* **2004**, *126*, 15942-15943.
[187] S. D. Tilley, M. B. Francis, *J. Am. Chem. Soc.* **2006**, *128*, 1080-1081.
[188] K. L. Seim, A. C. Obermeyer, M. B. Francis, *J. Am. Chem. Soc.* **2011**, *133*, 16970-16976.
[189] H. Ban, J. Gavrilyuk, C. F. Barbas, *J. Am. Chem. Soc.* **2010**, *132*, 1523-1525.
[190] J. Gavrilyuk, H. Ban, M. Nagano, W. Hakamata, C. F. Barbas, *Bioconjugate Chem.* **2012**, *23*, 2321-2328.
[191] J. J. Bruins, A. H. Westphal, B. Albada, K. Wagner, L. Bartels, H. Spits, W. J. H. van Berkel, F. L. van Delft, *Bioconjugate Chem.* **2017**, *28*, 1189-1193.
[192] S. Li, M. Hong, *J. Am. Chem. Soc.* **2011**, *133*, 1534-1544.
[193] X. Li, H. Ma, S. Dong, X. Duan, S. Liang, *Talanta* **2004**, *62*, 367-371.
[194] S. R. Adusumalli, D. G. Rawale, U. Singh, P. Tripathi, R. Paul, N. Kalra, R. K. Mishra, S. Shukla, V. Rai, *J. Am. Chem. Soc.* **2018**, *140*, 15114-15123.
[195] J. R. Kramer, T. J. Deming, *Chem. Commun.* **2013**, *49*, 5144-5146.
[196] M. T. Taylor, J. E. Nelson, M. G. Suero, M. J. Gaunt, *Nature* **2018**, *562*, 563-568.
[197] a) D. G. Hoare, D. E. Koshland, *J. Am. Chem. Soc.* **1966**, *88*, 2057-2058; b) E. Valeur, M. Bradley, *Chem. Soc. Rev.* **2009**, *38*, 606-631.
[198] N. A. McGrath, K. A. Andersen, A. K. F. Davis, J. E. Lomax, R. T. Raines, *Chem. Sci.* **2015**, *6*, 752-755.
[199] S. Tsukiji, H. Wang, M. Miyagawa, T. Tamura, Y. Takaoka, I. Hamachi, *J. Am. Chem. Soc.* **2009**, *131*, 9046-9054.
[200] S.-h. Fujishima, R. Yasui, T. Miki, A. Ojida, I. Hamachi, *J. Am. Chem. Soc.* **2012**, *134*, 3961-3964.
[201] C. C. Hughes, Y.-L. Yang, W.-T. Liu, P. C. Dorrestein, J. J. L. Clair, W. Fenical, *J. Am. Chem. Soc.* **2009**, *131*, 12094-12096.
[202] Y. Koshi, E. Nakata, M. Miyagawa, S. Tsukiji, T. Ogawa, I. Hamachi, *J. Am. Chem. Soc.* **2008**, *130*, 245-251.
[203] C. G. Acevedo-Rocha, N. Budisa, *Microb. Biotechnol.* **2016**, *9*, 666-676.
[204] D. B. Cowie, G. N. Cohen, *Biochim. Biophys. Acta* **1957**, *26*, 252-261.
[205] J. C. M. van Hest, K. L. Kiick, D. A. Tirrell, *J. Am. Chem. Soc.* **2000**, *122*, 1282-1288.
[206] A. J. Link, M. K. S. Vink, D. A. Tirrell, *J. Am. Chem. Soc.* **2004**, *126*, 10598-10602.
[207] J. W. Chin, *Annu. Rev. Biochem.* **2014**, *83*, 379-408.
[208] K. Wals, H. Ovaa, *Front. Chem.* **2014**, *2*, 15-15.
[209] A. Bianco, F. M. Townsley, S. Greiss, K. Lang, J. W. Chin, *Nat. Chem. Biol.* **2012**, *8*, 748.
[210] C. C. Liu, P. G. Schultz, *Annu. Rev. Biochem.* **2010**, *79*, 413-444.
[211] T. S. Young, P. G. Schultz, *J. Biol. Chem.* **2010**, *285*, 11039-11044.
[212] M. Rashidian, J. K. Dozier, M. D. Distefano, *Bioconjugate Chem.* **2013**, *24*, 1277-1294.
[213] J. S. Rush, C. R. Bertozzi, *J. Am. Chem. Soc.* **2008**, *130*, 12240-12241.
[214] N. Pishesha, J. R. Ingram, H. L. Ploegh, *Annu. Rev. Cell Dev. Biol.* **2018**, *34*, 163-188.

[215] B. Spolaore, S. Raboni, A. Ramos Molina, A. Satwekar, N. Damiano, A. Fontana, *Biochemistry* **2012**, *51*, 8679-8689.
[216] D. Schumacher, J. Helma, F. A. Mann, G. Pichler, F. Natale, E. Krause, M. C. Cardoso, C. P. R. Hackenberger, H. Leonhardt, *Angew. Chem. Int. Ed.* **2015**, *54*, 13787-13791.
[217] N. K. Devaraj, *ACS Central Science* **2018**, *4*, 952-959.
[218] K. Lang, J. W. Chin, *ACS Chem. Biol.* **2014**, *9*, 16-20.
[219] L. K. Mahal, K. J. Yarema, C. R. Bertozzi, *Science* **1997**, *276*, 1125-1128.
[220] K. Rose, *J. Am. Chem. Soc.* **1994**, *116*, 30-33.
[221] D. Rideout, *Cancer Investig.* **1994**, *12*, 189-202.
[222] J. Shao, J. P. Tam, *J. Am. Chem. Soc.* **1995**, *117*, 3893-3899.
[223] S. Ulrich, D. Boturyn, A. Marra, O. Renaudet, P. Dumy, *Chem. Eur. J.* **2014**, *20*, 34-41.
[224] J. A. Prescher, C. R. Bertozzi, *Nat. Chem. Biol.* **2005**, *1*, 13.
[225] B. L. Oliveira, Z. Guo, G. J. L. Bernardes, *Chem. Soc. Rev.* **2017**, *46*, 4895-4950.
[226] D. L. Boger, *Chem. Rev.* **1986**, *86*, 781-793.
[227] a) M. L. Blackman, M. Royzen, J. M. Fox, *J. Am. Chem. Soc.* **2008**, *130*, 13518-13519; b) N. K. Devaraj, R. Weissleder, S. A. Hilderbrand, *Bioconjugate Chem.* **2008**, *19*, 2297-2299.
[228] A. Niederwieser, A.-K. Späte, L. D. Nguyen, C. Jüngst, W. Reutter, V. Wittmann, *Angew. Chem. Int. Ed.* **2013**, *52*, 4265-4268.
[229] K. Lang, L. Davis, S. Wallace, M. Mahesh, D. J. Cox, M. L. Blackman, J. M. Fox, J. W. Chin, *J. Am. Chem. Soc.* **2012**, *134*, 10317-10320.
[230] D. M. Patterson, L. A. Nazarova, B. Xie, D. N. Kamber, J. A. Prescher, *J. Am. Chem. Soc.* **2012**, *134*, 18638-18643.
[231] S. Eising, F. Lelivelt, K. M. Bonger, *Angew. Chem. Int. Ed.* **2016**, *55*, 12243-12247.
[232] R. Rossin, S. M. van den Bosch, W. ten Hoeve, M. Carvelli, R. M. Versteegen, J. Lub, M. S. Robillard, *Bioconjugate Chem.* **2013**, *24*, 1210-1217.
[233] M. T. Taylor, M. L. Blackman, O. Dmitrenko, J. M. Fox, *J. Am. Chem. Soc.* **2011**, *133*, 9646-9649.
[234] A. Darko, S. Wallace, O. Dmitrenko, M. M. Machovina, R. A. Mehl, J. W. Chin, J. M. Fox, *Chem. Sci.* **2014**, *5*, 3770-3776.
[235] T. Peng, H. C. Hang, *J. Am. Chem. Soc.* **2016**, *138*, 14423-14433.
[236] C. Uttamapinant, J. D. Howe, K. Lang, V. Beránek, L. Davis, M. Mahesh, N. P. Barry, J. W. Chin, *J. Am. Chem. Soc.* **2015**, *137*, 4602-4605.
[237] T. S. Elliott, F. M. Townsley, A. Bianco, R. J. Ernst, A. Sachdeva, S. J. Elsässer, L. Davis, K. Lang, R. Pisa, S. Greiss, K. S. Lilley, J. W. Chin, *Nat. Biotechnol.* **2014**, *32*, 465.
[238] H. Wu, N. K. Devaraj, *Acc. Chem. Res.* **2018**, *51*, 1249-1259.
[239] P. Griess, *Proc. Royal Soc. Lond.* **1864**, *13*, 377-384.
[240] R. J. Griffin, *Prog. Med. Chem.* **1994**, *31*, 121-232.
[241] G. W. Preston, A. J. Wilson, *Chem. Soc. Rev.* **2013**, *42*, 3289-3301.
[242] D. Huang, G. Yan, *Adv. Synth. Catal.* **2017**, *359*, 1600-1619.
[243] A. Michael, *J. prakt. Chem.* **1893**, *48*, 94-95.
[244] R. Huisgen, *Angew. Chem. Int. Ed.* **1963**, *2*, 565-598.
[245] V. D. Bock, H. Hiemstra, J. H. van Maarseveen, *Eur. J. Org. Chem.* **2006**, *1*, 51-68.
[246] a) V. V. Rostovtsev, L. G. Green, V. V. Fokin, K. B. Sharpless, *Angew. Chem. Int. Ed.* **2002**, *41*, 2596-2599; b) C. W. Tornøe, C. Christensen, M. Meldal, *J. Org. Chem.* **2002**, *67*, 3057-3064.
[247] H. C. Kolb, K. B. Sharpless, *Drug Discov. Today* **2003**, *8*, 1128-1137.
[248] Q. Wang, T. R. Chan, R. Hilgraf, V. V. Fokin, K. B. Sharpless, M. G. Finn, *J. Am. Chem. Soc.* **2003**, *125*, 3192-3193.
[249] A. E. Speers, B. F. Cravatt, *ChemBioChem* **2004**, *5*, 41-47.
[250] T. S. Seo, X. Bai, D. H. Kim, Q. Meng, S. Shi, H. Ruparel, Z. Li, N. J. Turro, J. Ju, *Proc. Natl. Acad. Sci. U.S.A.* **2005**, *102*, 5926-5931.
[251] L. Liang, D. Astruc, *Coord. Chem. Rev.* **2011**, *255*, 2933-2945.

[252] E. Haldón, M. C. Nicasio, P. J. Pérez, *Org. Biomol. Chem.* **2015**, *13*, 9528-9550.
[253] a) S. Li, L. Wang, F. Yu, Z. Zhu, D. Shobaki, H. Chen, M. Wang, J. Wang, G. Qin, U. J. Erasquin, L. Ren, Y. Wang, C. Cai, *Chem. Sci.* **2017**, *8*, 2107-2114; b) M. Yang, A. S. Jalloh, W. Wei, J. Zhao, P. Wu, P. R. Chen, *Nat. Commun.* **2014**, *5*, 4981.
[254] L. Jin, D. R. Tolentino, M. Melaimi, G. Bertrand, *Sci. Adv.* **2015**, *1*, e1500304.
[255] Z. Chen, H. Meng, G. Xing, C. Chen, Y. Zhao, G. Jia, T. Wang, H. Yuan, C. Ye, F. Zhao, Z. Chai, C. Zhu, X. Fang, B. Ma, L. Wan, *Toxicol. Lett.* **2006**, *163*, 109-120.
[256] Z. Li, T. S. Seo, J. Ju, *Tetrahedron Lett.* **2004**, *45*, 3143-3146.
[257] G. Wittig, A. Krebs, *Chem. Ber.* **1961**, *94*, 3260-3275.
[258] N. J. Agard, J. A. Prescher, C. R. Bertozzi, *J. Am. Chem. Soc.* **2004**, *126*, 15046-15047.
[259] J. Steflova, G. Storch, S. Wiesner, S. Stockinger, R. Berg, O. Trapp, *J. Org. Chem.* **2018**, *83*, 604-613.
[260] J. A. Codelli, J. M. Baskin, N. J. Agard, C. R. Bertozzi, *J. Am. Chem. Soc.* **2008**, *130*, 11486-11493.
[261] N. J. Agard, J. M. Baskin, J. A. Prescher, A. Lo, C. R. Bertozzi, *ACS Chem. Biol.* **2006**, *1*, 644-648.
[262] J. M. Baskin, J. A. Prescher, S. T. Laughlin, N. J. Agard, P. V. Chang, I. A. Miller, A. Lo, J. A. Codelli, C. R. Bertozzi, *Proc. Natl. Acad. Sci. U.S.A.* **2007**, *104*, 16793-16797.
[263] X. Ning, J. Guo, M. A. Wolfert, G.-J. Boons, *Angew. Chem. Int. Ed.* **2008**, *47*, 2253-2255.
[264] E. M. Sletten, H. Nakamura, J. C. Jewett, C. R. Bertozzi, *J. Am. Chem. Soc.* **2010**, *132*, 11799-11805.
[265] M. F. Debets, S. S. van Berkel, S. Schoffelen, F. P. J. T. Rutjes, J. C. M. van Hest, F. L. van Delft, *Chem. Commun.* **2010**, *46*, 97-99.
[266] a) J. C. Jewett, E. M. Sletten, C. R. Bertozzi, *J. Am. Chem. Soc.* **2010**, *132*, 3688-3690; b) C. G. Gordon, J. L. Mackey, J. C. Jewett, E. M. Sletten, K. N. Houk, C. R. Bertozzi, *J. Am. Chem. Soc.* **2012**, *134*, 9199-9208.
[267] J. Dommerholt, S. Schmidt, R. Temming, L. J. A. Hendriks, F. P. J. T. Rutjes, J. C. M. van Hest, D. J. Lefeber, P. Friedl, F. L. van Delft, *Angew. Chem. Int. Ed.* **2010**, *49*, 9422-9425.
[268] K. E. Beatty, J. D. Fisk, B. P. Smart, Y. Y. Lu, J. Szychowski, M. J. Hangauer, J. M. Baskin, C. R. Bertozzi, D. A. Tirrell, *ChemBioChem* **2010**, *11*, 2092-2095.
[269] S. T. Laughlin, J. M. Baskin, S. L. Amacher, C. R. Bertozzi, *Science* **2008**, *320*, 664-667.
[270] P. V. Chang, J. A. Prescher, E. M. Sletten, J. M. Baskin, I. A. Miller, N. J. Agard, A. Lo, C. R. Bertozzi, *Proc. Natl. Acad. Sci. U.S.A.* **2010**, *107*, 1821-1826.
[271] H. Tian, T. P. Sakmar, T. Huber, *ChemBioChem* **2015**, *16*, 1314-1322.
[272] R. van Geel, G. J. M. Pruijn, F. L. van Delft, W. C. Boelens, *Bioconjugate Chem.* **2012**, *23*, 392-398.
[273] E. M. Sletten, C. R. Bertozzi, *Org. Lett.* **2008**, *10*, 3097-3099.
[274] F. Friscourt, P. A. Ledin, N. E. Mbua, H. R. Flanagan-Steet, M. A. Wolfert, R. Steet, G.-J. Boons, *J. Am. Chem. Soc.* **2012**, *134*, 5381-5389.
[275] X. Ning, R. P. Temming, J. Dommerholt, J. Guo, D. B. Ania, M. F. Debets, M. A. Wolfert, G.-J. Boons, F. L. van Delft, *Angew. Chem. Int. Ed.* **2010**, *49*, 3065-3068.
[276] H. Staudinger, J. Meyer, *Helv. Chim. Acta* **1919**, *2*, 635-646.
[277] Y. G. Gololobov, I. N. Zhmurova, L. F. Kasukhin, *Tetrahedron* **1981**, *37*, 437-472.
[278] S. Ayesa, B. Samuelsson, B. Classon, *Synlett* **2008**, *2008*, 97-99.
[279] M. Köhn, R. Breinbauer, *Angew. Chem. Int. Ed.* **2004**, *43*, 3106-3116.
[280] E. Saxon, C. R. Bertozzi, *Science* **2000**, *287*, 2007-2010.
[281] K. L. Kiick, E. Saxon, D. A. Tirrell, C. R. Bertozzi, *Proc. Natl. Acad. Sci. U.S.A.* **2002**, *99*, 19-24.
[282] G. A. Lemieux, C. L. de Graffenried, C. R. Bertozzi, *J. Am. Chem. Soc.* **2003**, *125*, 4708-4709.
[283] B. L. Nilsson, L. L. Kiessling, R. T. Raines, *Org. Lett.* **2000**, *2*, 1939-1941.
[284] E. Saxon, J. I. Armstrong, C. R. Bertozzi, *Org. Lett.* **2000**, *2*, 2141-2143.
[285] B. L. Nilsson, L. L. Kiessling, R. T. Raines, *Org. Lett.* **2001**, *3*, 9-12.
[286] M. B. Soellner, B. L. Nilsson, R. T. Raines, *J. Org. Chem.* **2002**, *67*, 4993-4996.

[287] O. David, W. J. N. Meester, H. Bieräugel, H. E. Schoemaker, H. Hiemstra, J. H. van Maarseveen, *Angew. Chem.* **2003**, *115*, 4509-4511.
[288] R. Kleineweischede, C. P. R. Hackenberger, *Angew. Chem. Int. Ed.* **2008**, *47*, 5984-5988.
[289] R. W. Rudolph, R. W. Parry, C. F. Farran, *Inorg. Chem.* **1966**, *5*, 723-726.
[290] M. Mühlberg, D. s. M. M. Jaradat, R. Kleineweischede, I. Papp, D. Dechtrirat, S. Muth, M. Broncel, C. P. R. Hackenberger, *Bioorg. Med. Chem.* **2010**, *18*, 3679-3686.
[291] B. L. Nilsson, R. J. Hondal, M. B. Soellner, R. T. Raines, *J. Am. Chem. Soc.* **2003**, *125*, 5268-5269.
[292] M. I. Kabachnik, V. A. Gilyarov, *Bull. Acad. Sci. USSR, Div. Chem. Sci.* **1956**, *5*, 809-816.
[293] L. Kasukhin, M. Ponomarchuk, T. Klepa, R. Yurchenko, *Phosphorus Sulfur Silicon Relat. Elem.* **1981**, *10*, 339-341.
[294] C.-g. Shin, Y. Yonezawa, K. Watanabe, J. Yoshimura, *Bull. Chem. Soc. Jpn.* **1981**, *54*, 3811-3814.
[295] T. Sakakura, T.-A. Kobayashi, T. Hayashi, Y. Kawabata, M. Tanaka, I. Ogata, *J. Organomet. Chem.* **1984**, *267*, 171-177.
[296] W. W. Metcalf, W. A. van der Donk, *Annu. Rev. Biochem.* **2009**, *78*, 65-94.
[297] a) B. Chen, A. K. Mapp, *J. Am. Chem. Soc.* **2004**, *126*, 5364-5365; b) B. Chen, A. K. Mapp, *J. Am. Chem. Soc.* **2005**, *127*, 6712-6718.
[298] B. C. Challis, J. A. Challis, J. N. Iley, *J. Chem. Soc., Perkin Trans. 2* **1978**, 813-818.
[299] I. Wilkening, G. del Signore, C. P. R. Hackenberger, *Chem. Commun.* **2008**, *25*, 2932-2934.
[300] I. Wilkening, G. del Signore, W. Ahlbrecht, C. P. R. Hackenberger, *Synthesis* **2011**, *17*, 2709-2720.
[301] R. L. Letsinger, G. A. Heavner, *Tetrahedron Lett.* **1975**, *16*, 147-150.
[302] R. Serwa, I. Wilkening, G. Del Signore, M. Mühlberg, I. Claußnitzer, C. Weise, M. Gerrits, C. P. R. Hackenberger, *Angew. Chem. Int. Ed.* **2009**, *48*, 8234-8239.
[303] R. A. Serwa, J.-M. Swiecicki, D. Homann, C. P. R. Hackenberger, *J. Pept. Sci.* **2010**, *16*, 563-567.
[304] a) R. Serwa, P. Majkut, B. Horstmann, J.-M. Swiecicki, M. Gerrits, E. Krause, C. P. R. Hackenberger, *Chem. Sci.* **2010**, *1*, 596-602; b) N. Nischan, A. Chakrabarti, R. A. Serwa, P. H. M. Bovee-Geurts, R. Brock, C. P. R. Hackenberger, *Angew. Chem. Int. Ed.* **2013**, *52*, 11920-11924; c) E. Hoffmann, K. Streichert, N. Nischan, C. Seitz, T. Brunner, S. Schwagerus, C. P. R. Hackenberger, M. Rubini, *Mol. BioSyst.* **2016**, *12*, 1750-1755.
[305] J. Bertran-Vicente, R. A. Serwa, M. Schümann, P. Schmieder, E. Krause, C. P. R. Hackenberger, *J. Am. Chem. Soc.* **2014**, *136*, 13622-13628.
[306] D. s. M. M. Jaradat, H. Hamouda, C. P. R. Hackenberger, *Eur. J. Org. Chem.* **2010**, *26*, 5004-5009.
[307] V. Böhrsch, T. Mathew, M. Zieringer, M. R. J. Vallée, L. M. Artner, J. Dernedde, R. Haag, C. P. R. Hackenberger, *Org. Biomol. Chem.* **2012**, *10*, 6211-6216.
[308] a) V. Böhrsch, R. Serwa, P. Majkut, E. Krause, C. P. R. Hackenberger, *Chem. Commun.* **2010**, *46*, 3176-3178; b) N. Nischan, M. A. Kasper, T. Mathew, C. P. R. Hackenberger, *Org. Biomol. Chem.* **2016**, *14*, 7500-7508.
[309] A. Michaelis, R. Kaehne, *Ber. Dtsch. Chem. Ges.* **1898**, *31*, 1048-1055.
[310] A. K. Bhattacharya, G. Thyagarajan, *Chem. Rev.* **1981**, *81*, 415-430.
[311] W.-S. Hwang, J. T. Yoke, *J. Org. Chem.* **1980**, *45*, 2088-2091.
[312] M. R. J. Vallée, P. Majkut, I. Wilkening, C. Weise, G. Müller, C. P. R. Hackenberger, *Org. Lett.* **2011**, *13*, 5440-5443.
[313] M. R. J. Vallée, L. M. Artner, J. Dernedde, C. P. R. Hackenberger, *Angew. Chem. Int. Ed.* **2013**, *52*, 9504-9508.
[314] M. R. J. Vallée, P. Majkut, D. Krause, M. Gerrits, C. P. R. Hackenberger, *Chem. Eur. J.* **2015**, *21*, 970-974.
[315] G. M. Clore, J. Iwahara, *Chem. Rev.* **2009**, *109*, 4108-4139.
[316] Kelly N. Chuh, Anna R. Batt, Matthew R. Pratt, *Cell Chem. Biol.* **2016**, *23*, 86-107.

[317] P. Gong, G. A. Davidson, W. Gui, K. Yang, W. P. Bozza, Z. Zhuang, *Chem. Sci.* **2018**, *9*, 7859-7865.
[318] R. D. Row, J. A. Prescher, *Acc. Chem. Res.* **2018**, *51*, 1073-1081.
[319] G. Leriche, L. Chisholm, A. Wagner, *Bioorg. Med. Chem.* **2012**, *20*, 571-582.
[320] R. M. Kaake, X. Wang, L. Huang, *Mol. Cell. Proteom.* **2010**, *9*, 1650-1665.
[321] C. J. Choy, J. J. Geruntho, A. L. Davis, C. E. Berkman, *Bioconjugate Chem.* **2016**, *27*, 824-830.
[322] K. D. Siebertz, C. P. R. Hackenberger, *Chem. Commun.* **2018**, *54*, 763-766.
[323] B. Stewart, A. Harriman, L. J. Higham, *Organometallics* **2011**, *30*, 5338-5343.
[324] J. A. Burns, J. C. Butler, J. Moran, G. M. Whitesides, *J. Org. Chem.* **1991**, *56*, 2648-2650.
[325] S. p. Ortial, J.-L. Montchamp, *Org. Lett.* **2011**, *13*, 3134-3137.
[326] B. Kevin, W. Robert, G. Iain, D. Kevin, *Curr. Drug Metab.* **2003**, *4*, 461-485.
[327] Y.-Y. Yang, M. Grammel, A. S. Raghavan, G. Charron, H. C. Hang, *Chem. Biol.* **2010**, *17*, 1212-1222.
[328] A. Sorkin, M. von Zastrow, *Nat. Rev. Mol. Cell Biol.* **2002**, *3*, 600-614.
[329] N. Nischan, H. D. Herce, F. Natale, N. Bohlke, N. Budisa, M. C. Cardoso, C. P. R. Hackenberger, *Angew. Chem. Int. Ed.* **2015**, *54*, 1950-1953.
[330] F. Shabanpoor, M. J. Gait, *Chem. Commun.* **2013**, *49*, 10260-10262.
[331] R. L. Simmons, R. T. Yu, A. G. Myers, *J. Am. Chem. Soc.* **2011**, *133*, 15870-15873.
[332] S. Kobayashi, J. Kadokawa, I. F. Yen, S. Shoda, *Macromolecules* **1989**, *22*, 4390-4392.
[333] C. Pierra Rouvière, A. Amador, E. Badaroux, T. Convard, D. Da Costa, D. Dukhan, L. Griffe, J.-F. Griffon, M. LaColla, F. Leroy, M. Liuzzi, A. G. Loi, J. McCarville, V. Mascia, J. Milhau, L. Onidi, J.-L. Paparin, R. Rahali, E. Sais, M. Seifer, D. Surleraux, D. Standring, C. Dousson, *Bioorg. Med. Chem. Lett.* **2016**, *26*, 4536-4541.
[334] C. Beermann, G. Schneider, K. Seeger, H. J. Kleiner, E. Schrinner, in *DE 2024250*, **1971**.
[335] C.-F. Yen, J. Yuang, C.-H. R. King, in *US 2010 0120719*, **2010**.
[336] J. Park, S. Oh, S. B. Park, *Angew. Chem. Int. Ed.* **2012**, *51*, 5447-5451.
[337] Z.-H. Jin, J. Razkin, V. Josserand, D. Boturyn, A. Grichine, I. Texier, M.-C. Favrot, P. Dumy, J.-L. Coll, *Mol. Imaging* **2007**, *6*, 43-45.
[338] V. N. Rajasekharan Pillai, *Synthesis* **1980**, *1980*, 1-26.
[339] S. I. Presolski, V. P. Hong, M. G. Finn, *Curr. Protoc. Chem. Biol.* **2011**, *3*, 153-162.

10. Appendix

10.1. NMR spectra

2-Hydroxyethyl isopropyldisulfide

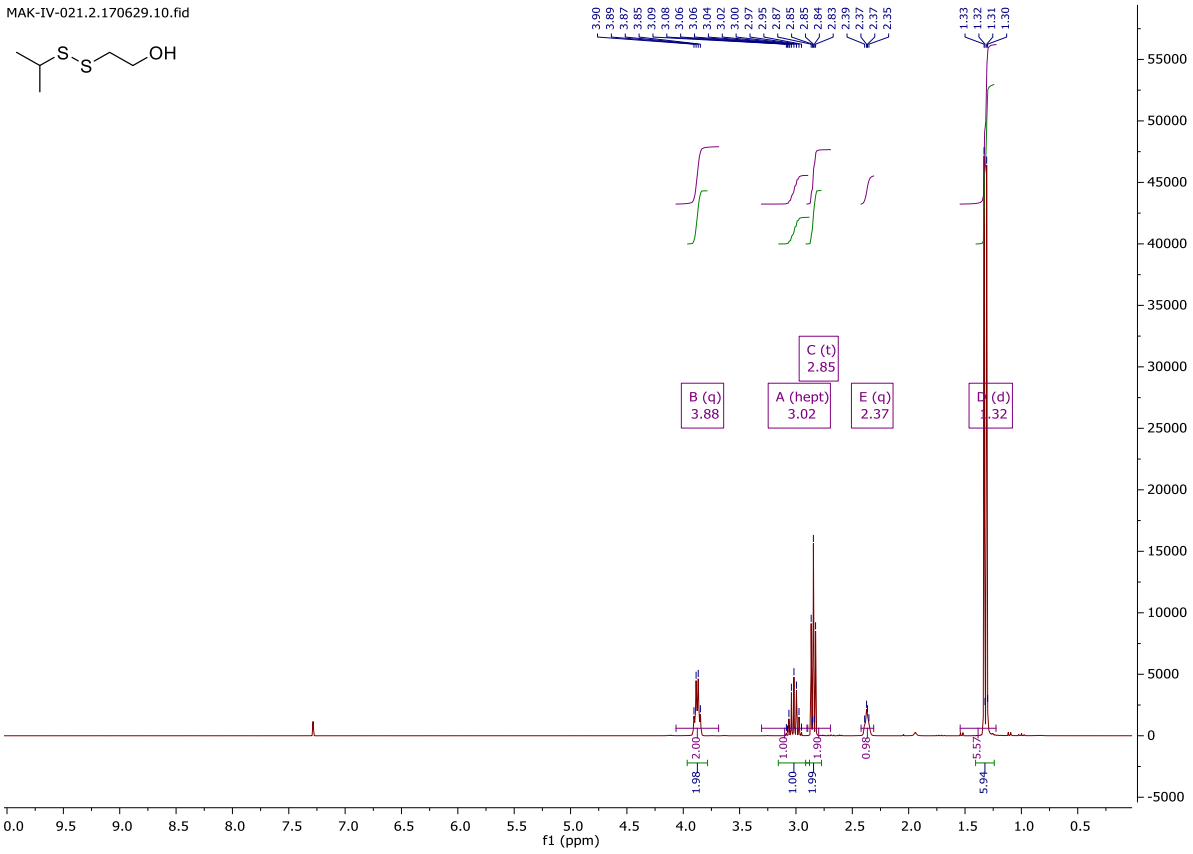

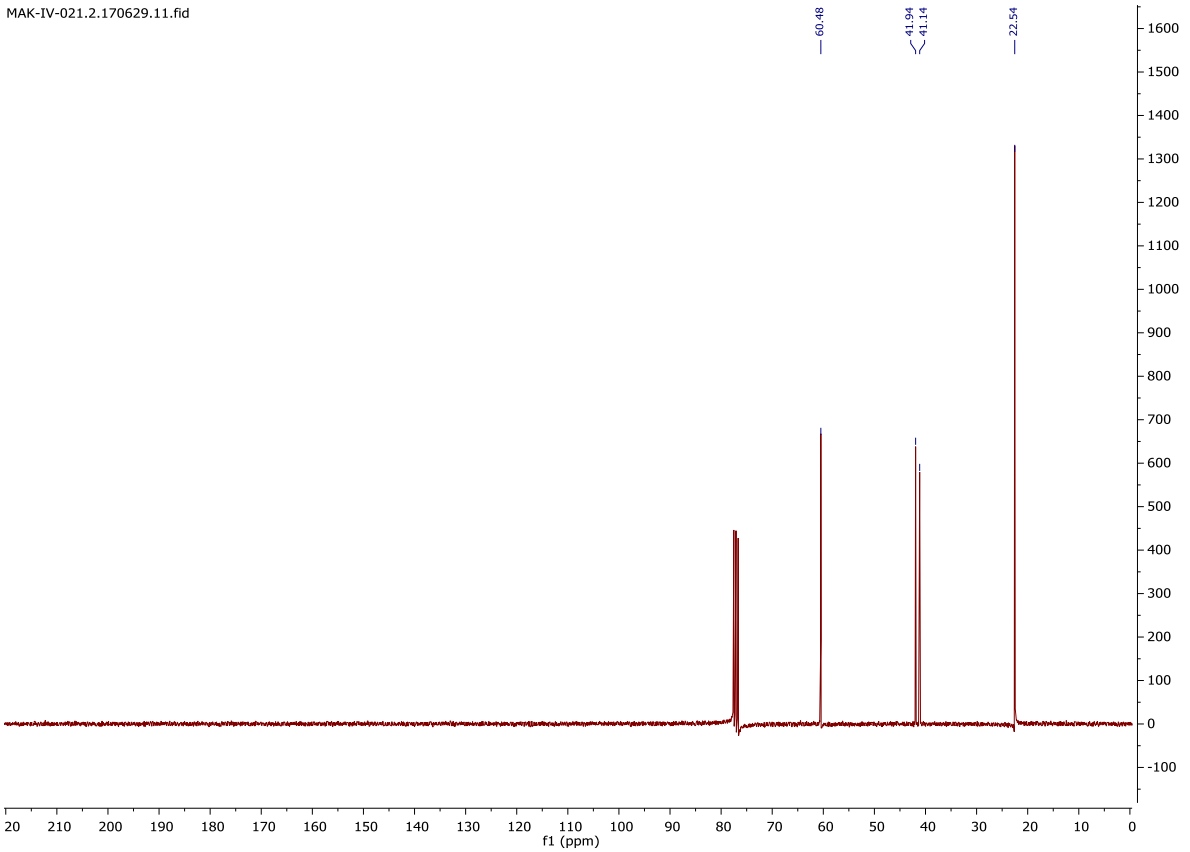

Di-(2-isopropyl disulfido)ethyl) ethynylphosphonite (**4**)

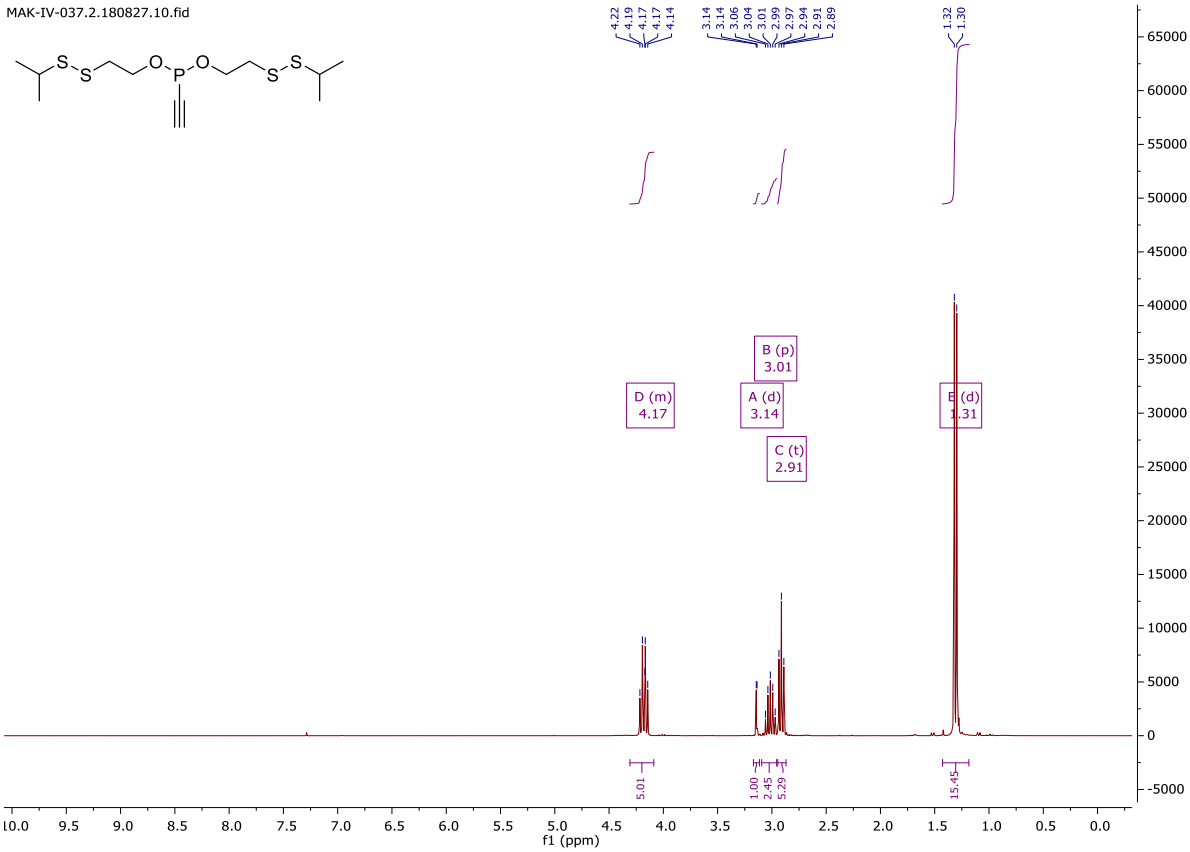

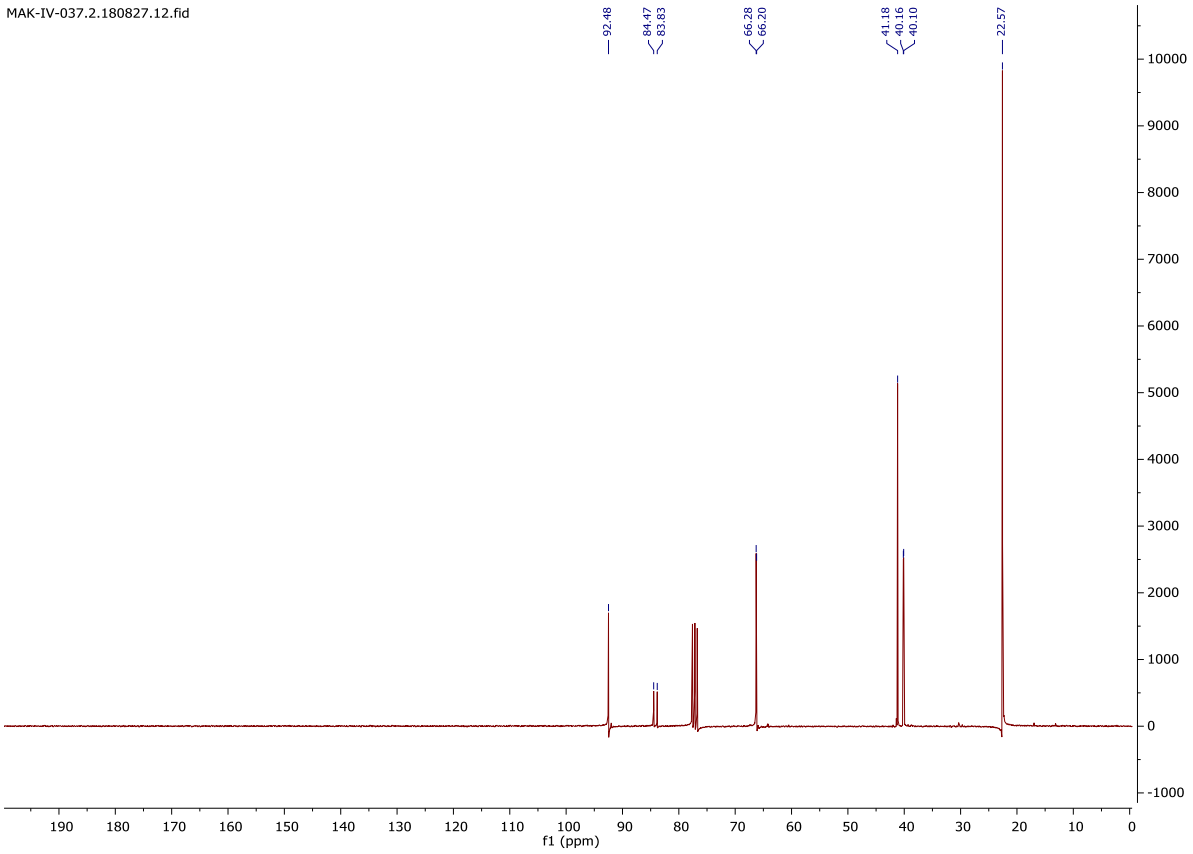
MAK-IV-037.2.180827.12.fid
92.48
84.47
83.83
66.28
66.20
41.18
40.16
40.10
22.57
f1 (ppm)

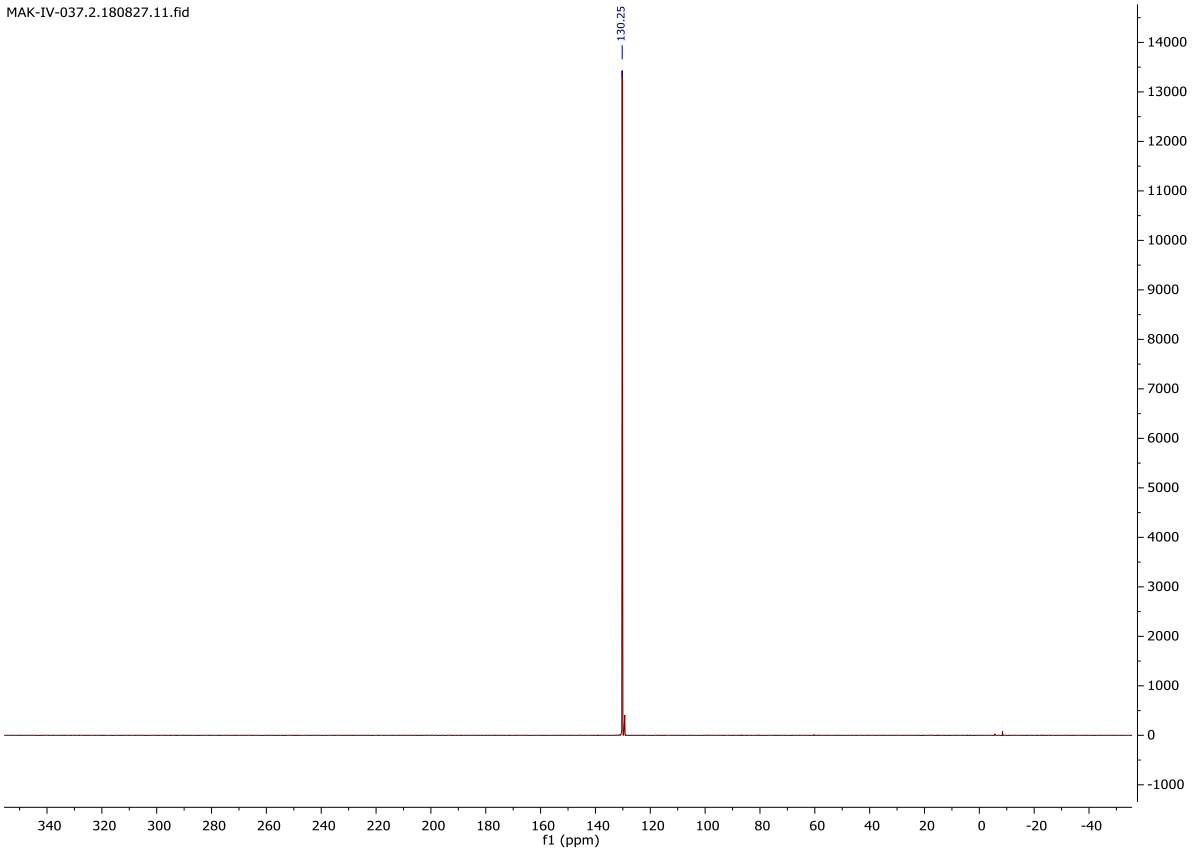
MAK-IV-037.2.180827.11.fid
130.25
f1 (ppm)

Di-(2-*tert*-butyl disulfido)ethyl) ethynylphosphonite (**5**)

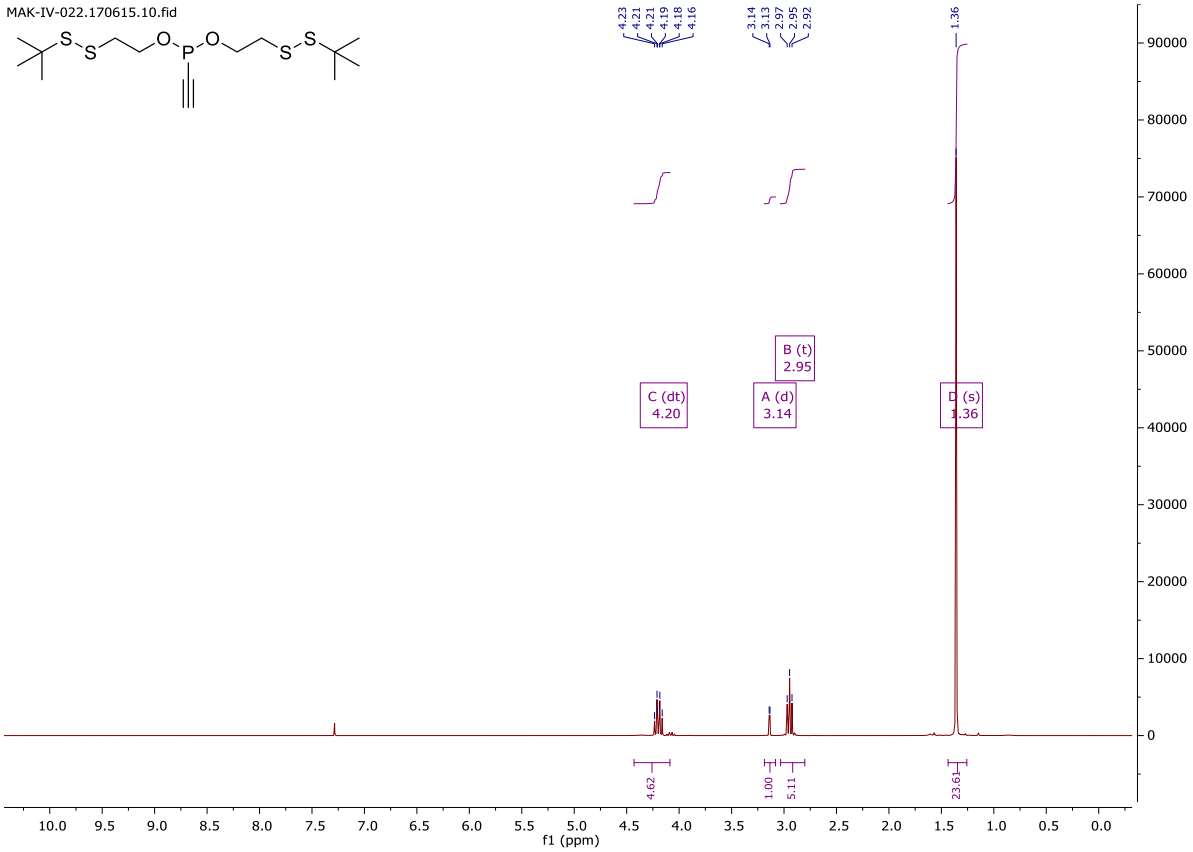

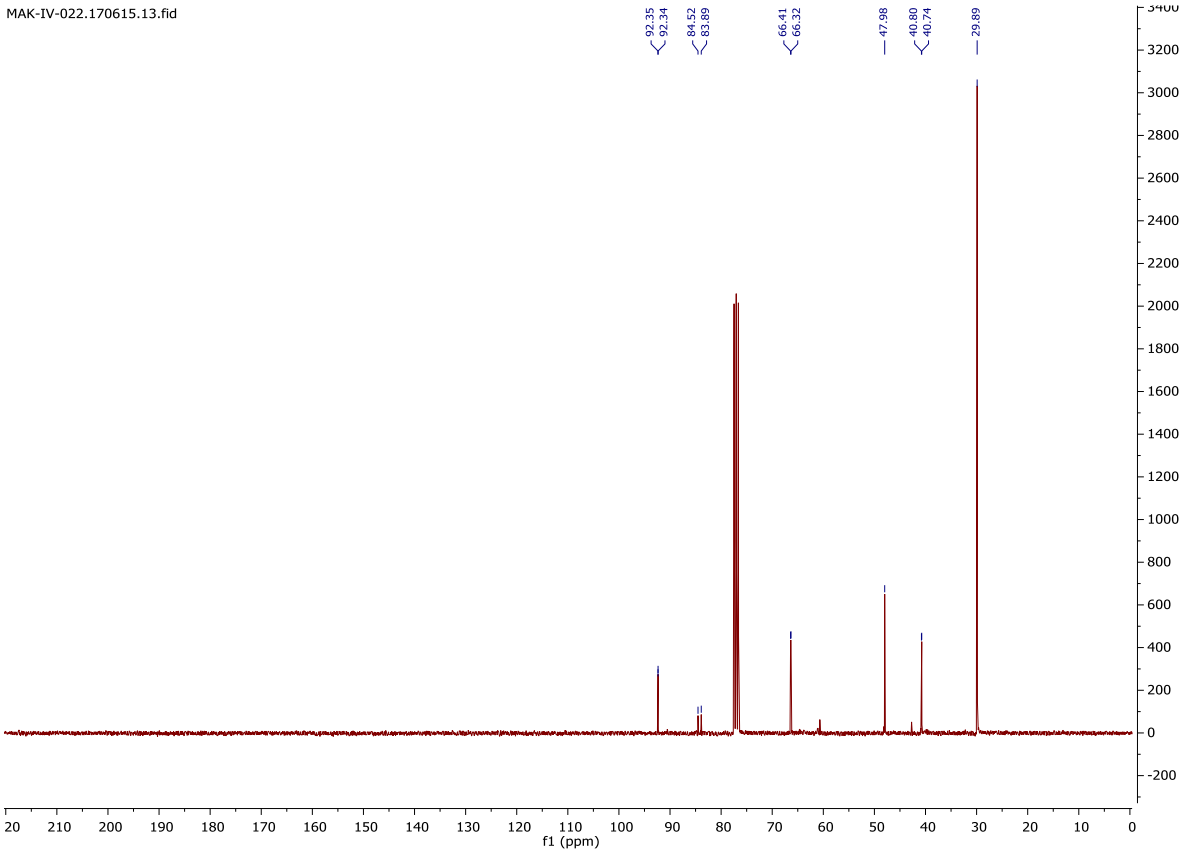

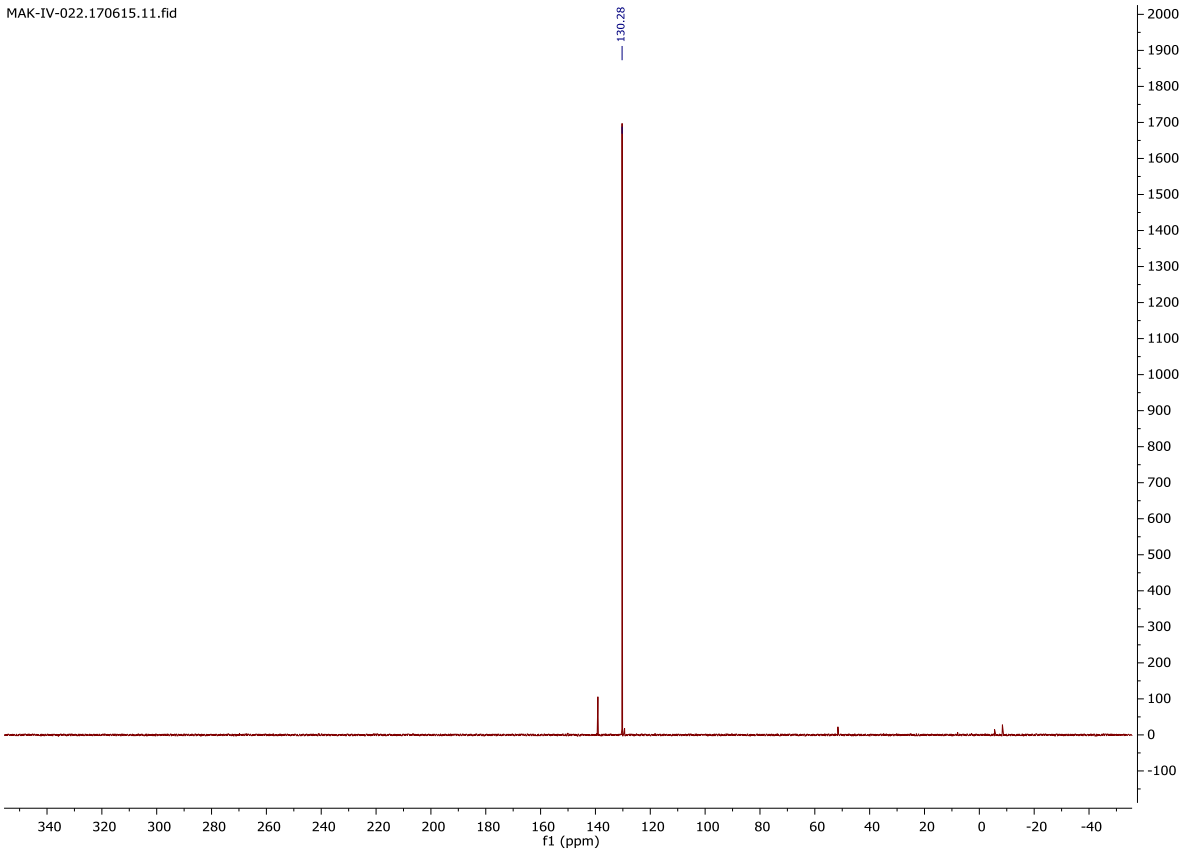

2-(3-Hydroxypropyl) isopropyl disulfide

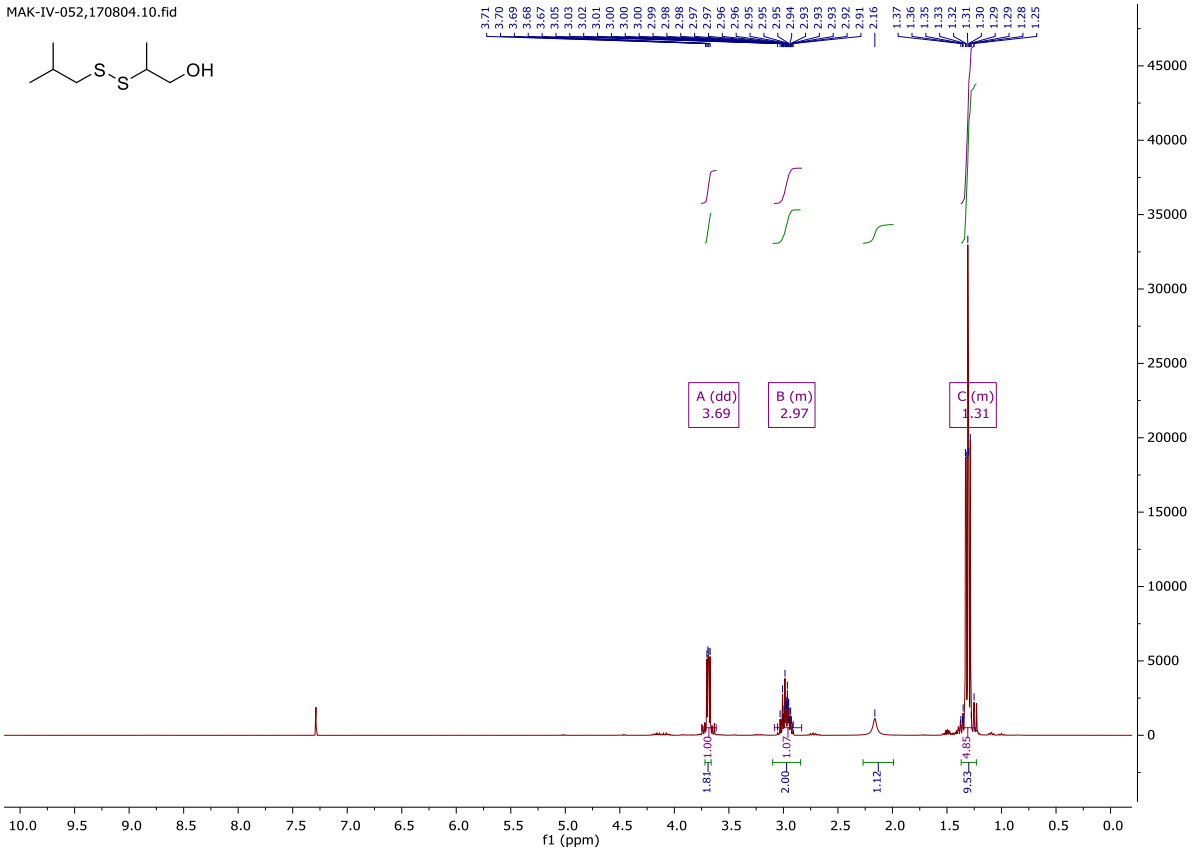

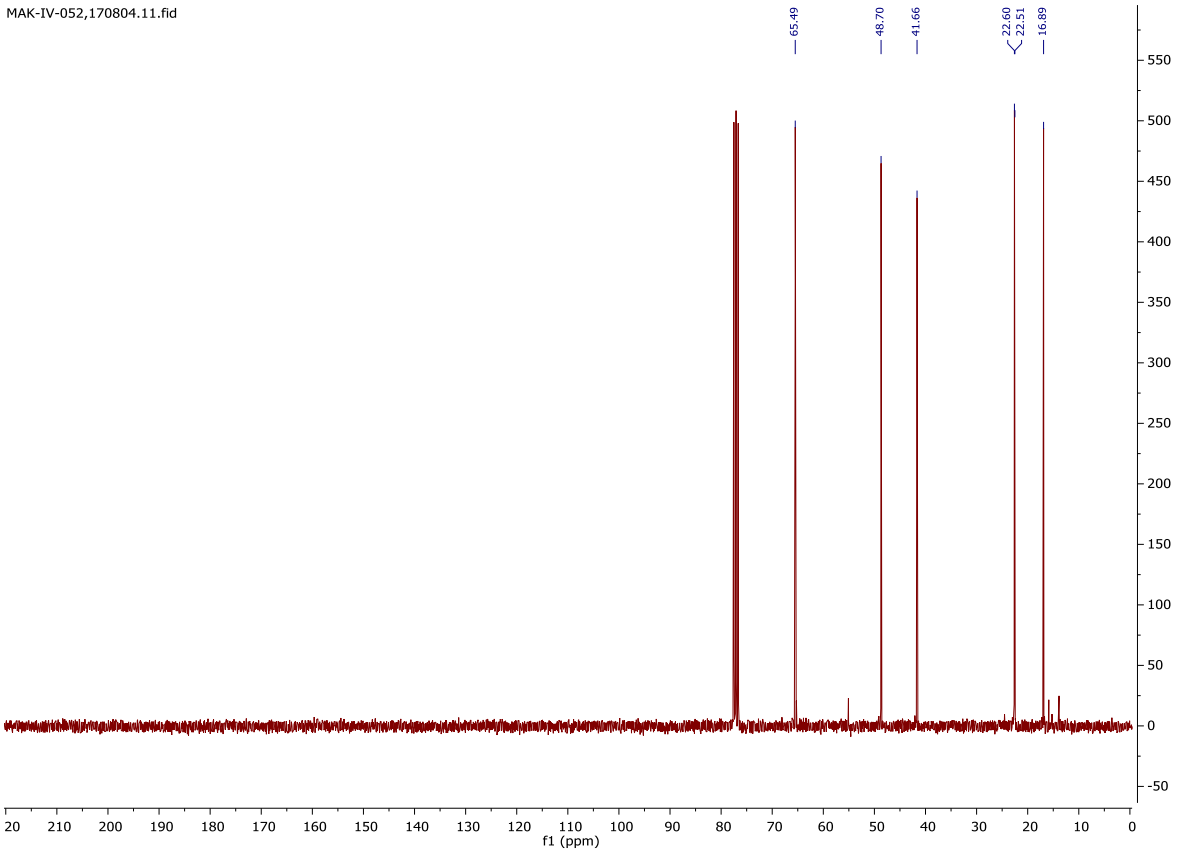

Di-((2-isopropyl disulfido)-3-propyl) ethynylphosphonite (**6**)

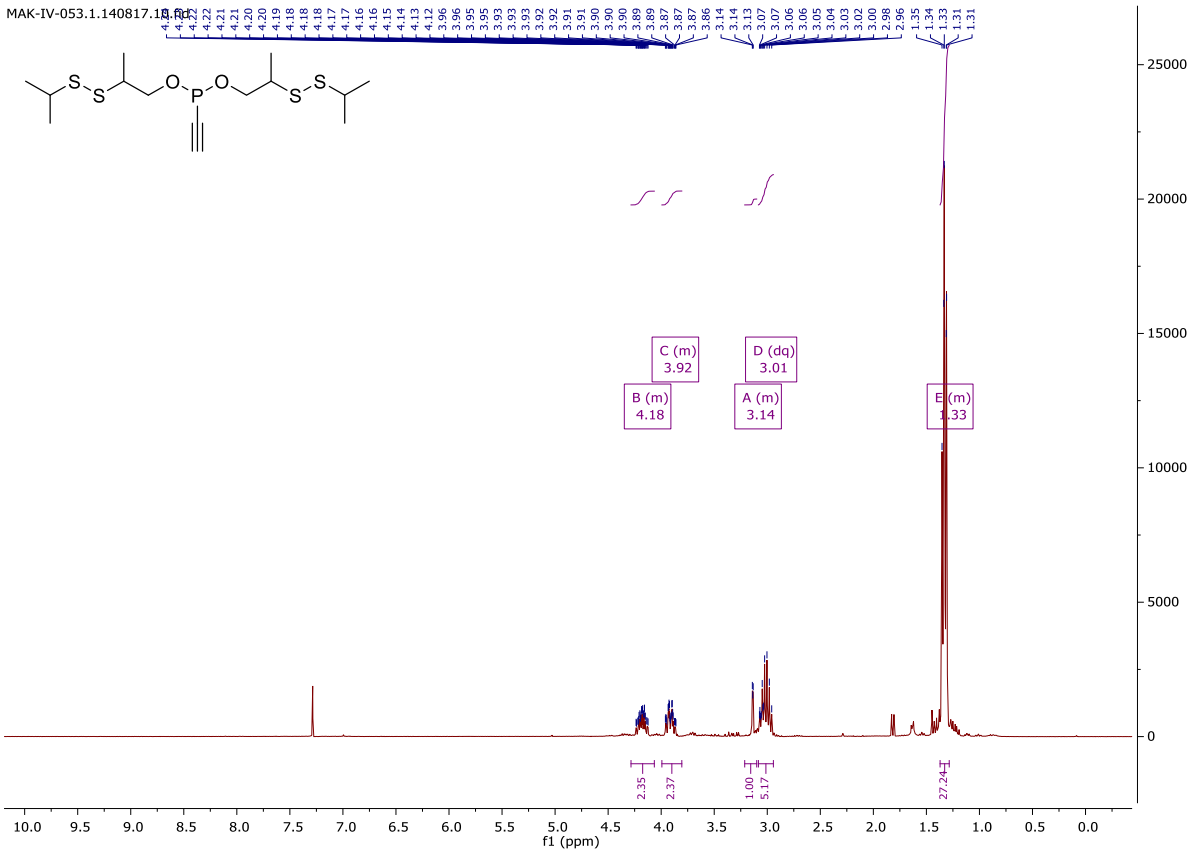

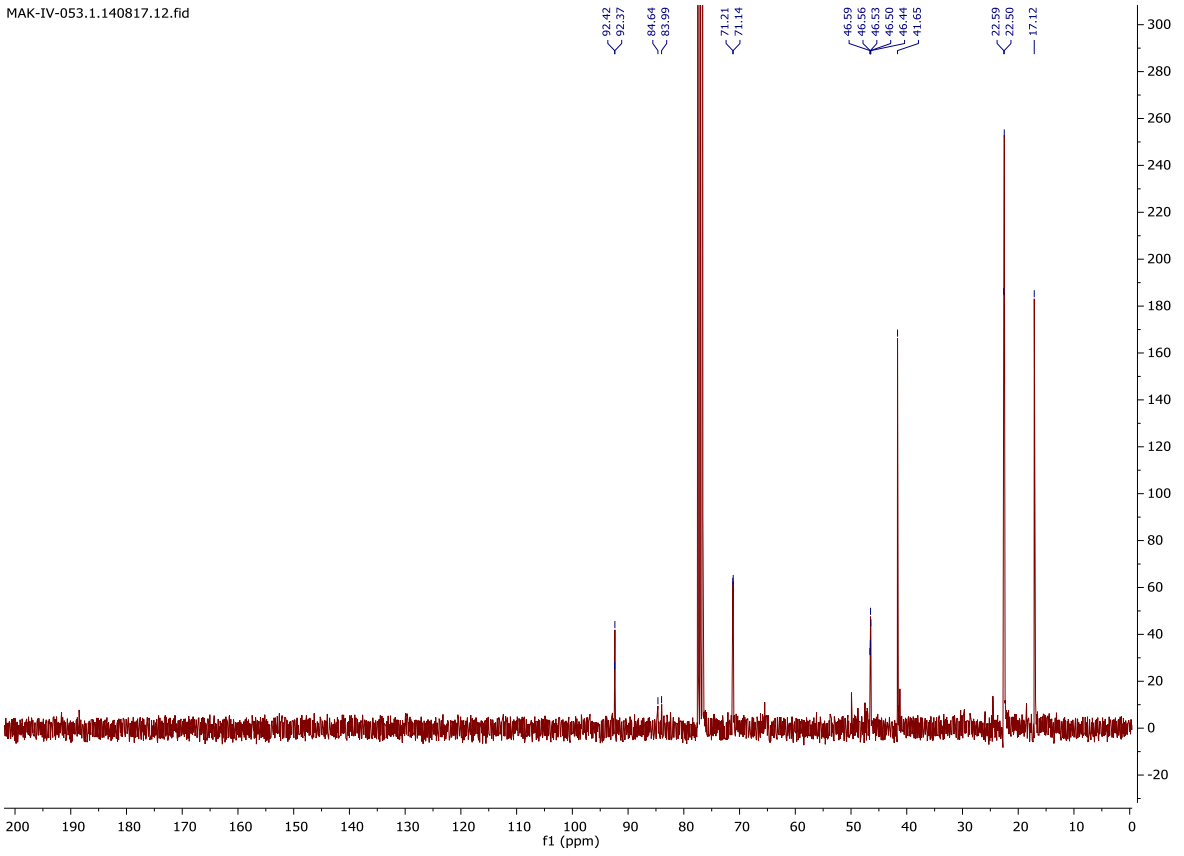
MAK-IV-053.1.140817.12.fid
92.42
92.37
84.64
83.99
71.21
71.14
46.59
46.56
46.53
46.50
46.44
41.65
22.59
22.50
17.12
f1 (ppm)

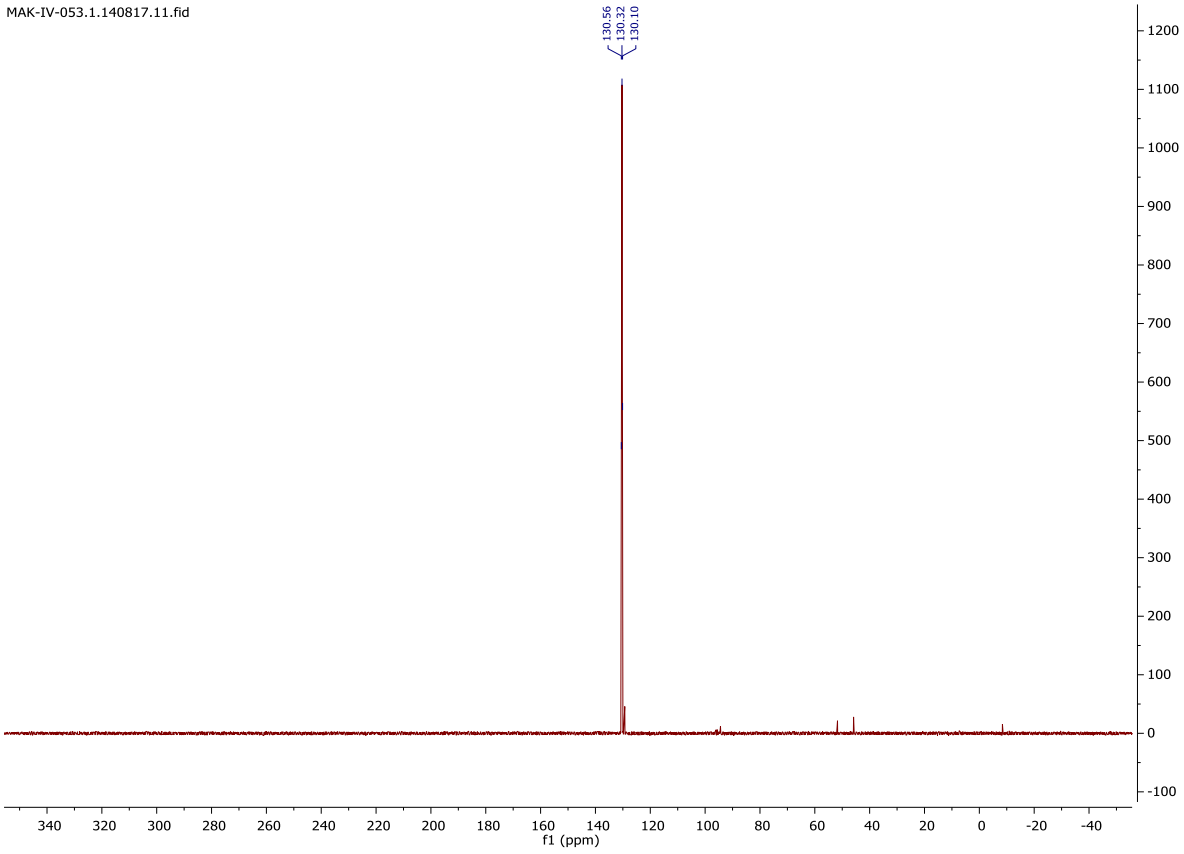
MAK-IV-053.1.140817.11.fid
130.56
130.32
130.10
f1 (ppm)

Di-(3-Butinyl) ethynylphosphonite (**7**)

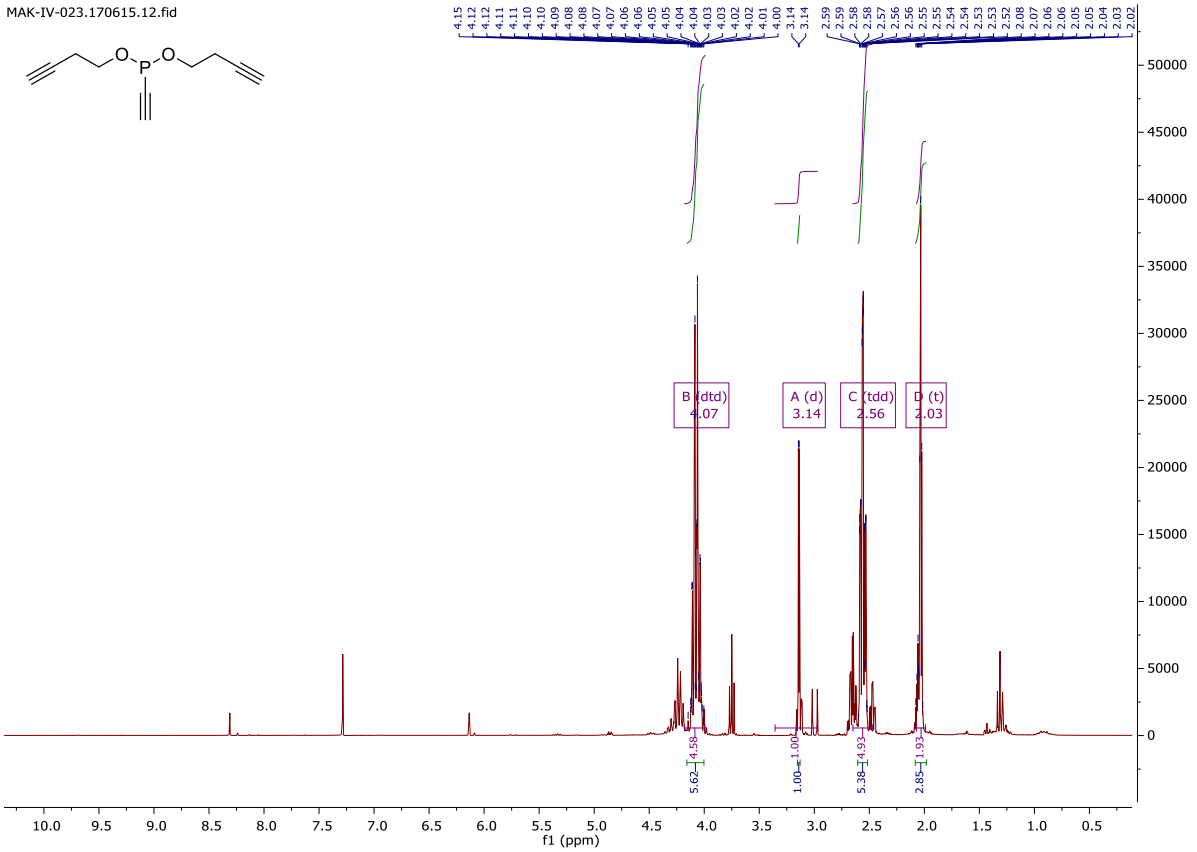

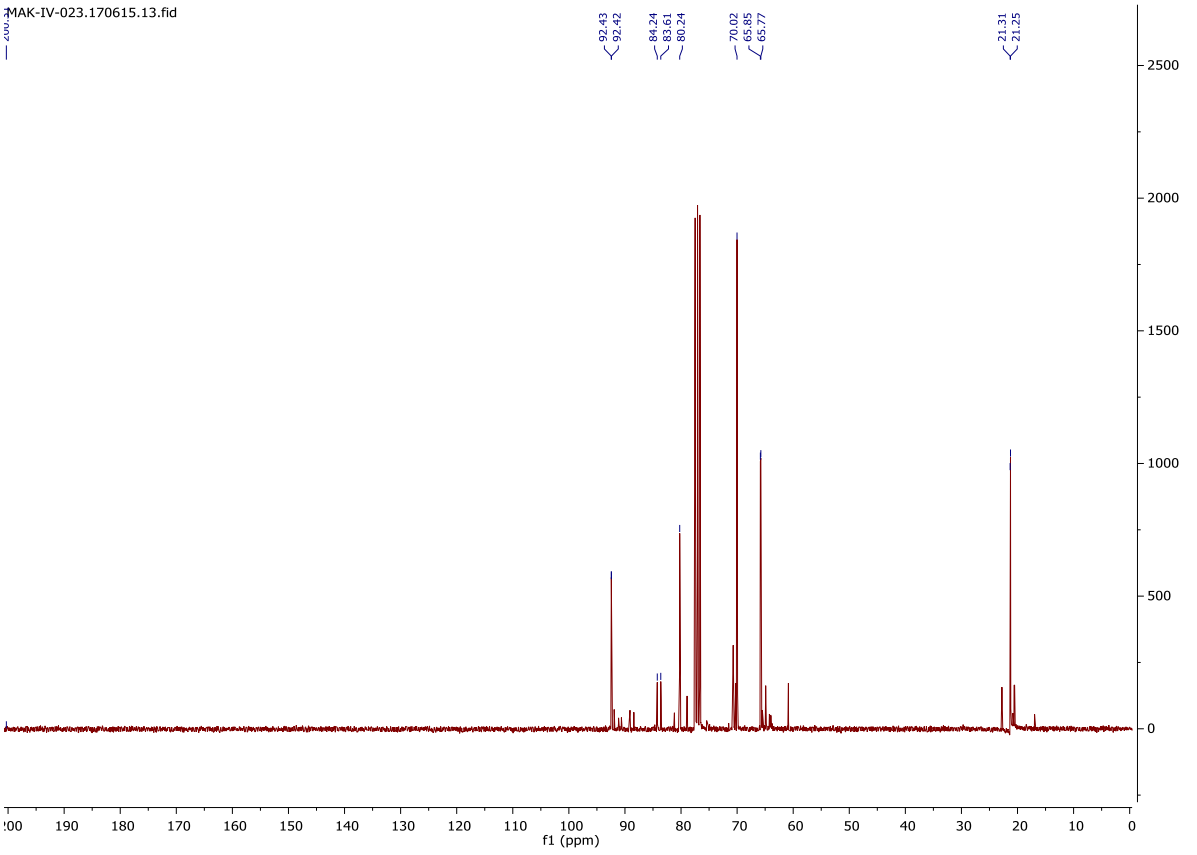

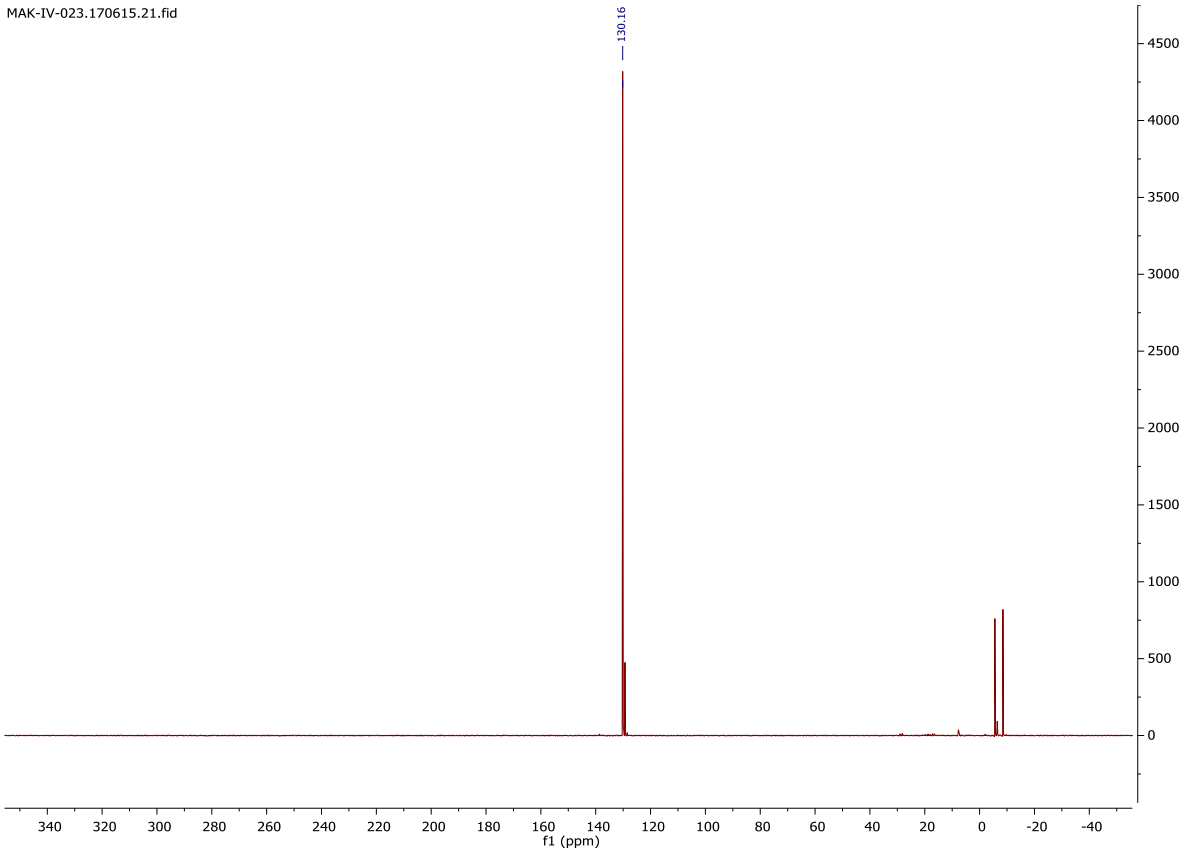

Di-(2-diethylamino benzyl) ethynylphosphonite (**9**)

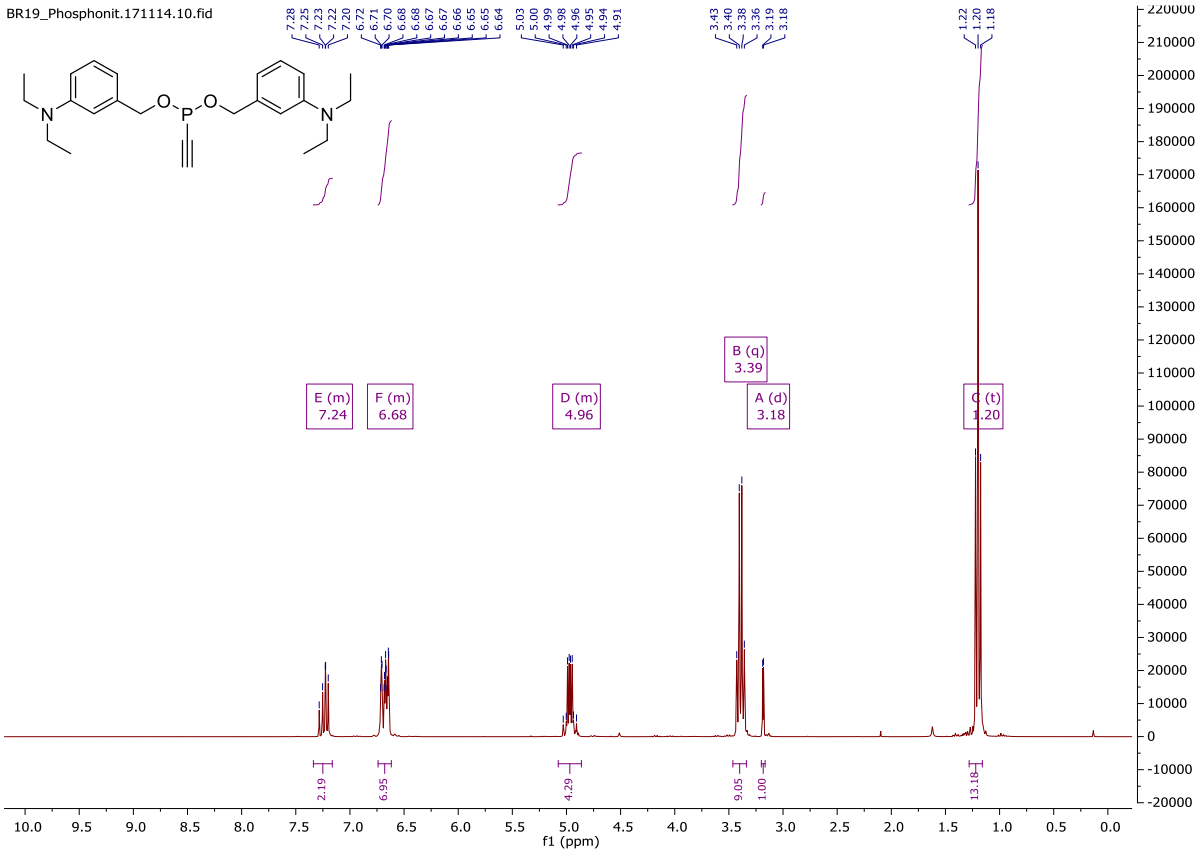

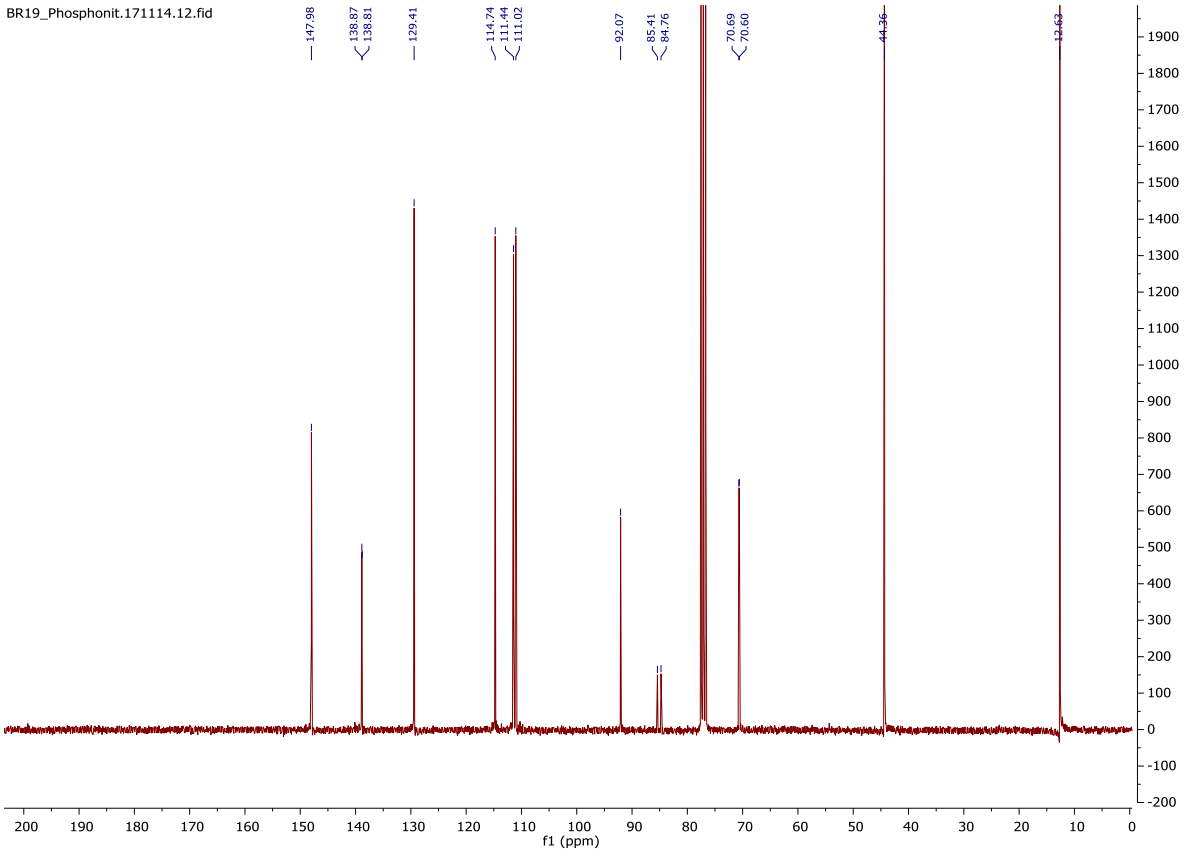
BR19_Phosphonit.171114.12.fid
147.98
138.87
138.81
129.41
114.74
111.44
111.02
92.07
85.41
84.76
70.69
70.60
44.36
12.62
f1 (ppm)

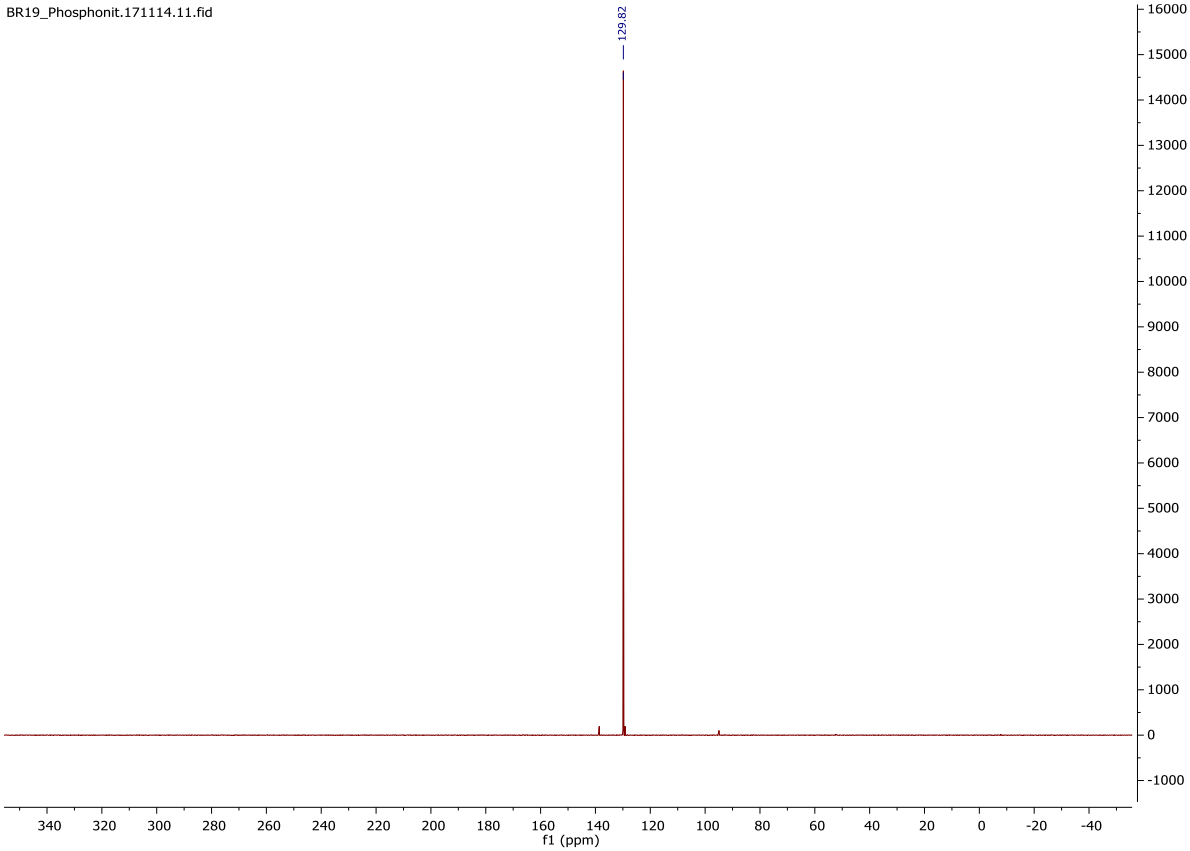
BR19_Phosphonit.171114.11.fid
129.82
f1 (ppm)

Di-(4-acetoxy benzyl) ethynylphosphonite (**10**)

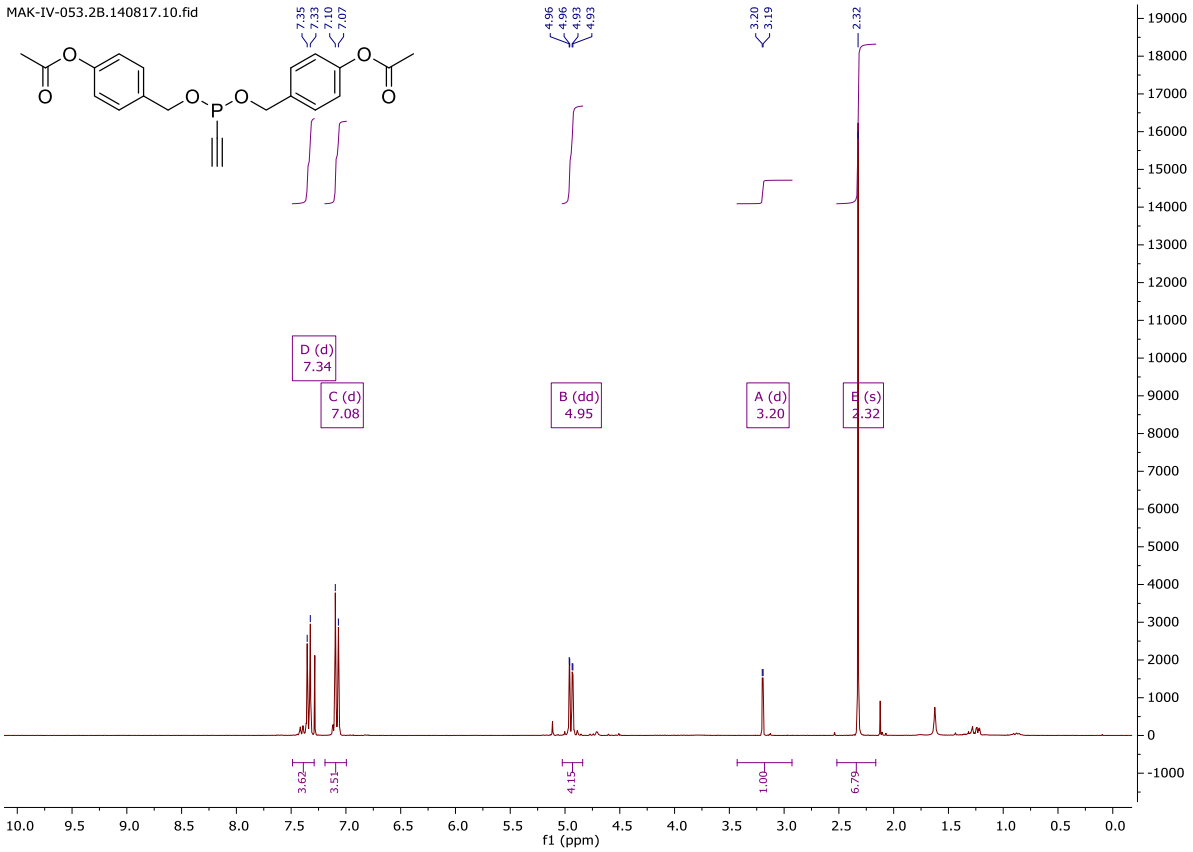

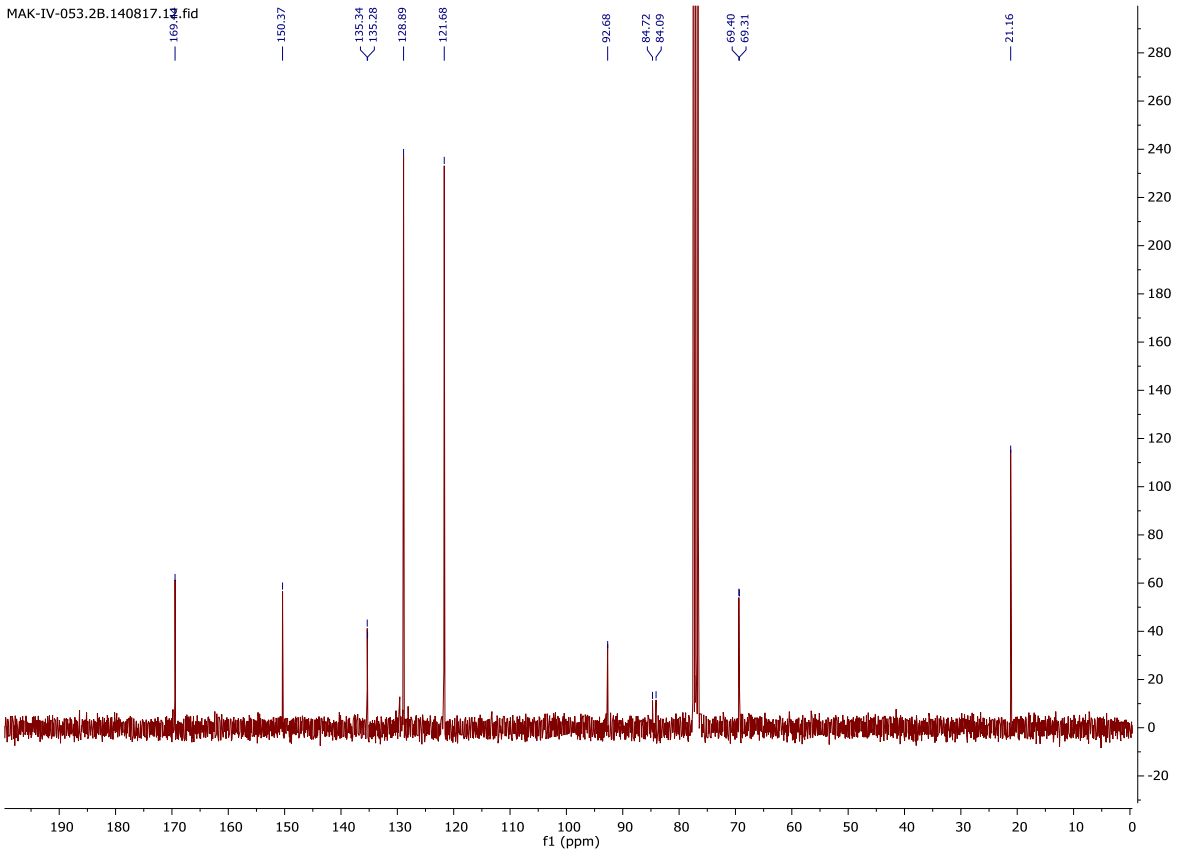

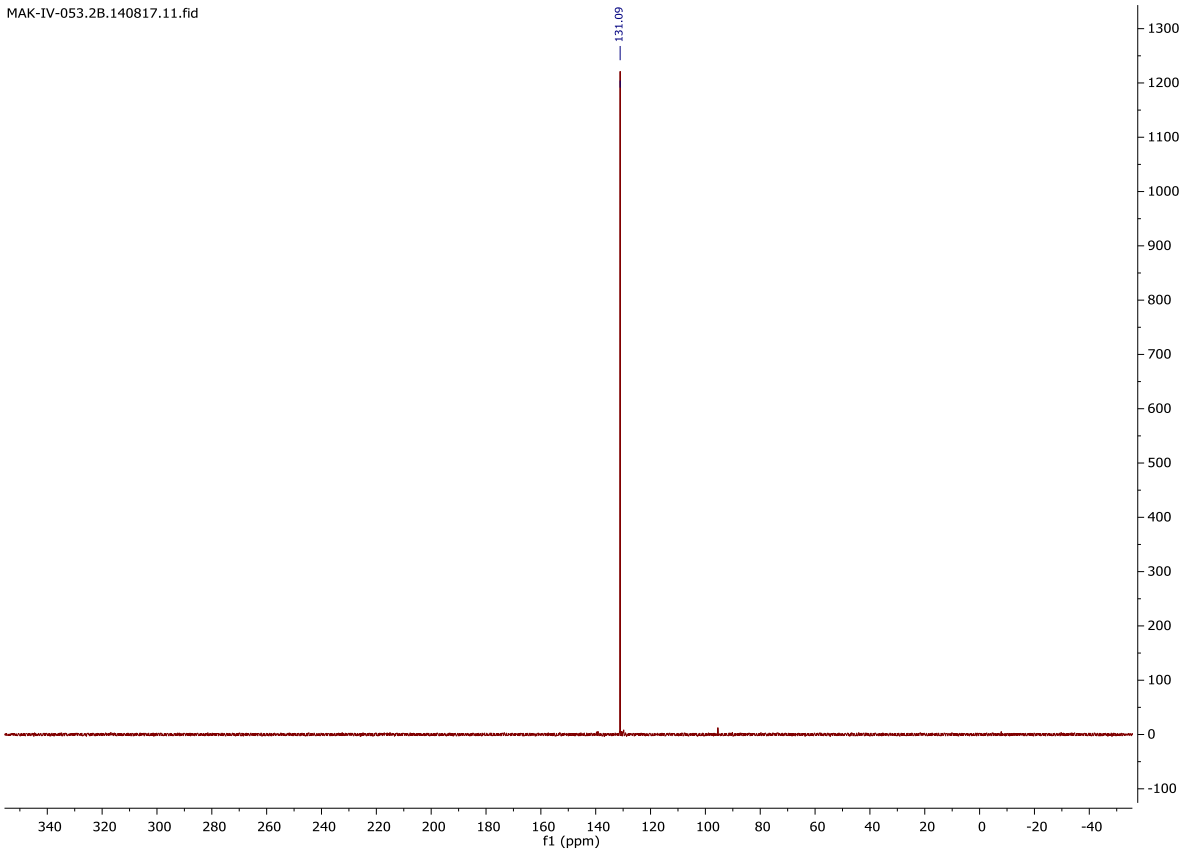

Di (4-(diazophenyl)-benzyl) ethynylphosphonite (**11**)

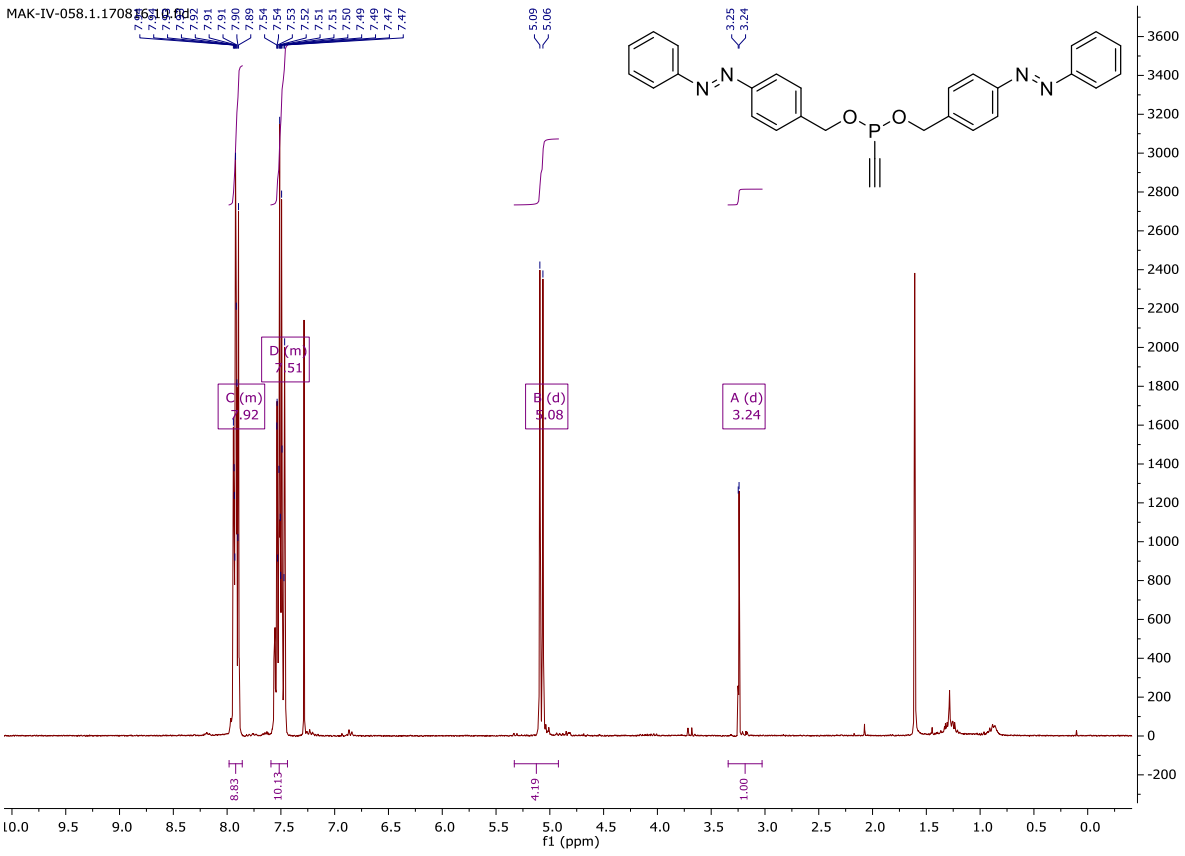

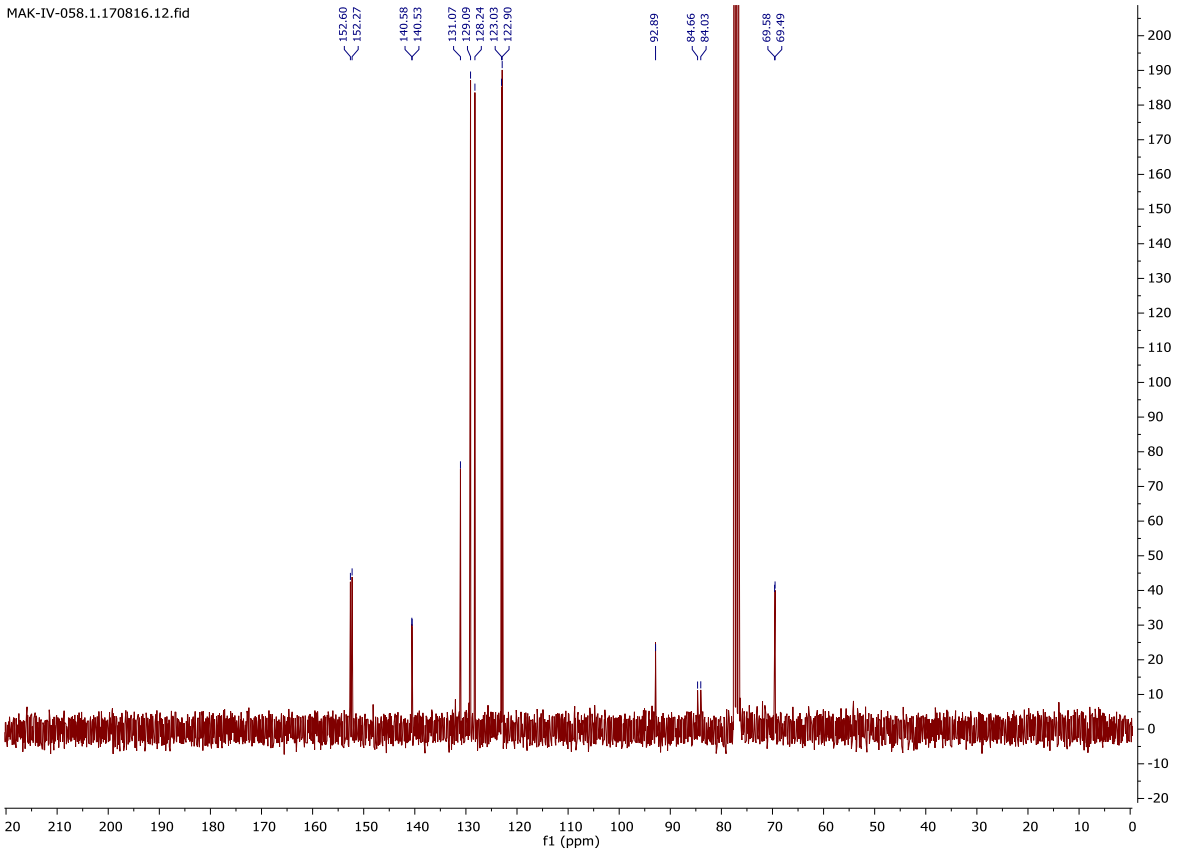
MAK-IV-058.1.170816.12.fid
152.60
152.27
140.58
140.53
131.07
129.09
128.24
123.03
122.90
92.89
84.66
84.03
69.58
69.49
f1 (ppm)

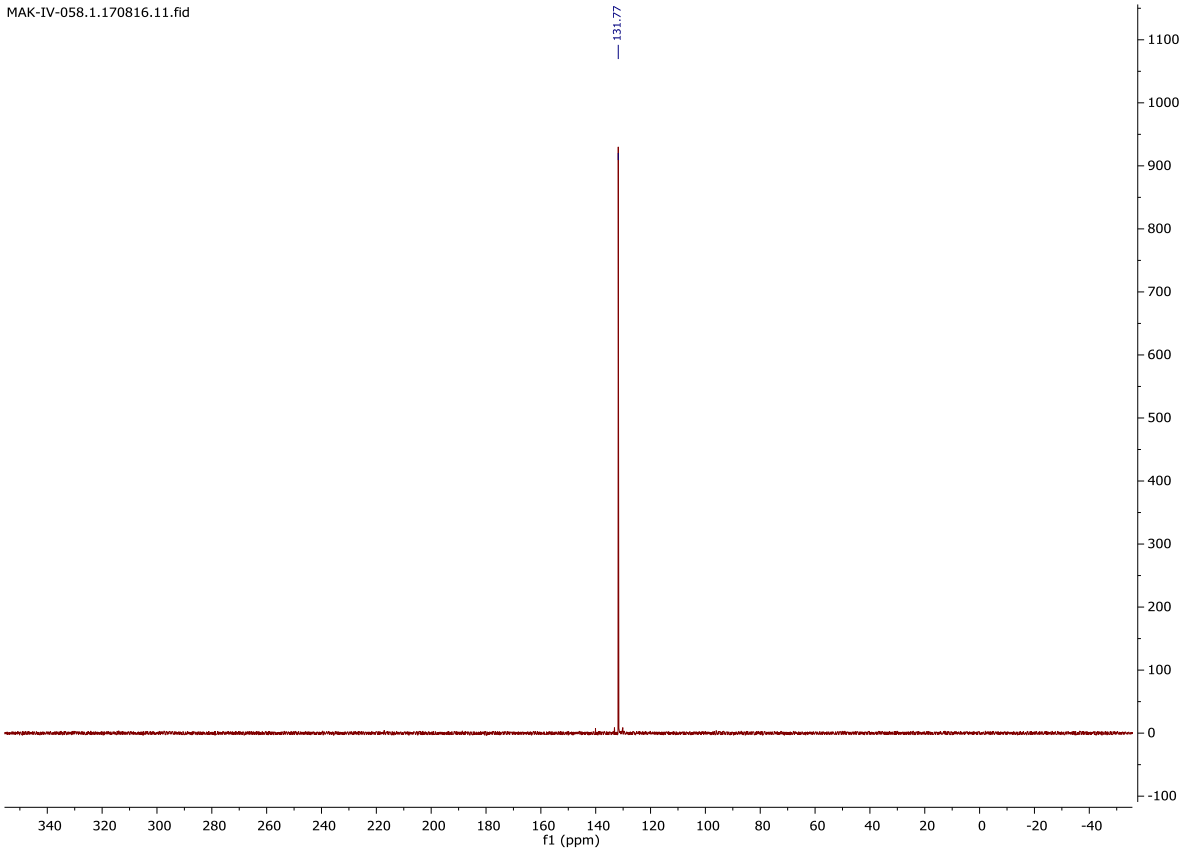
MAK-IV-058.1.170816.11.fid
131.77
f1 (ppm)

Diphenyl ethynylphosphonite borane (**12**)

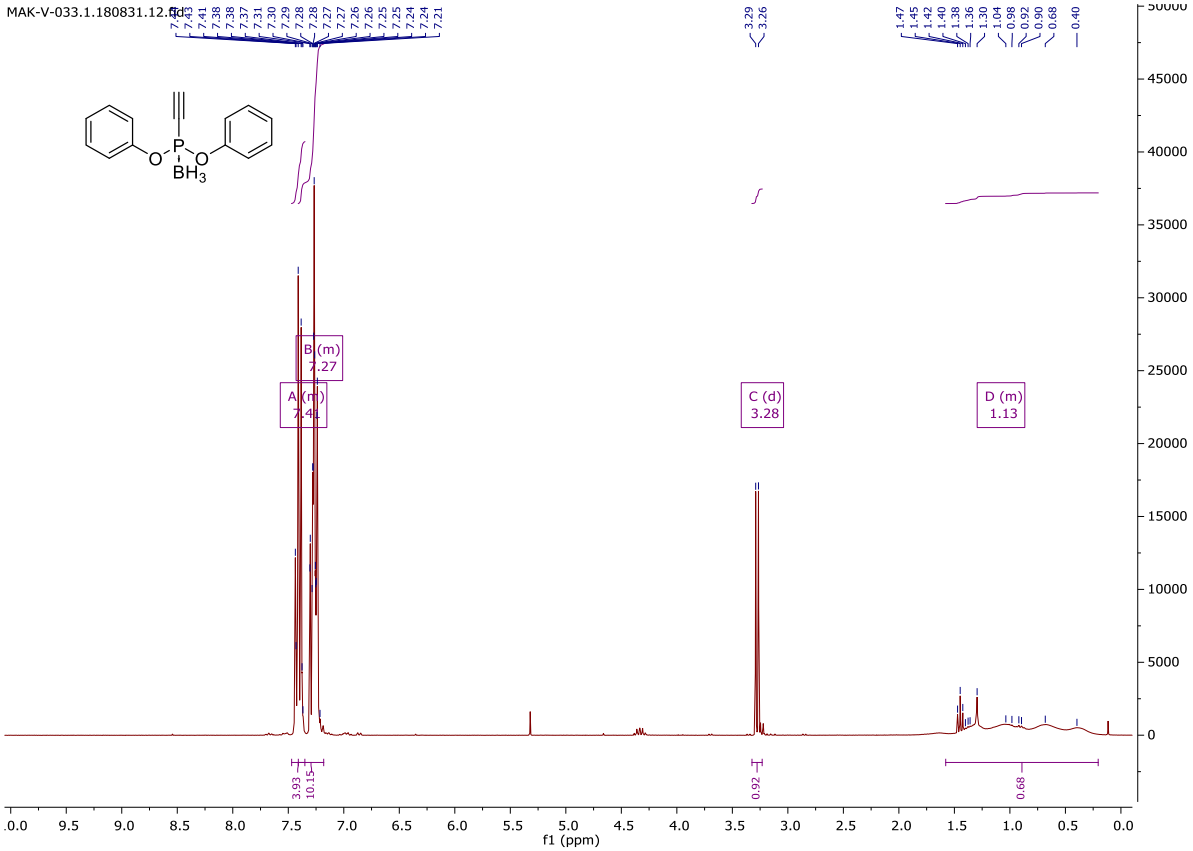

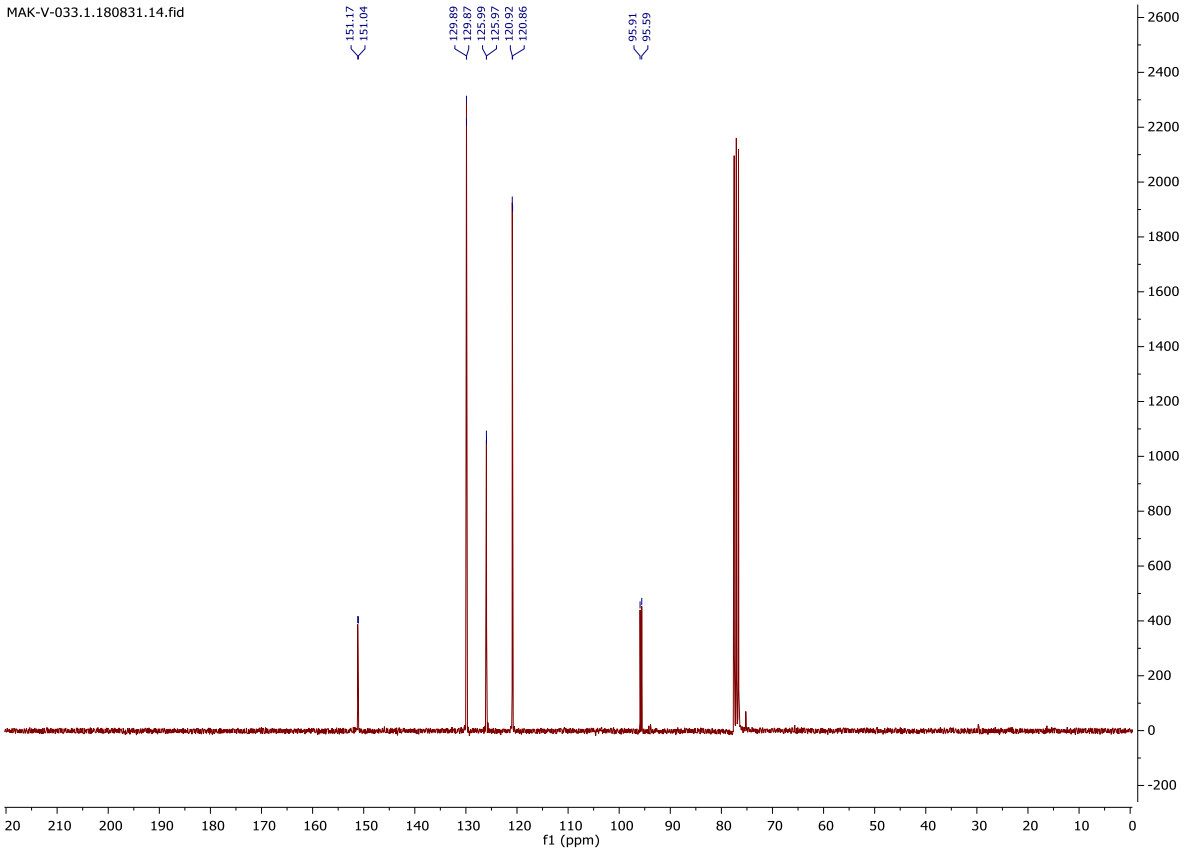

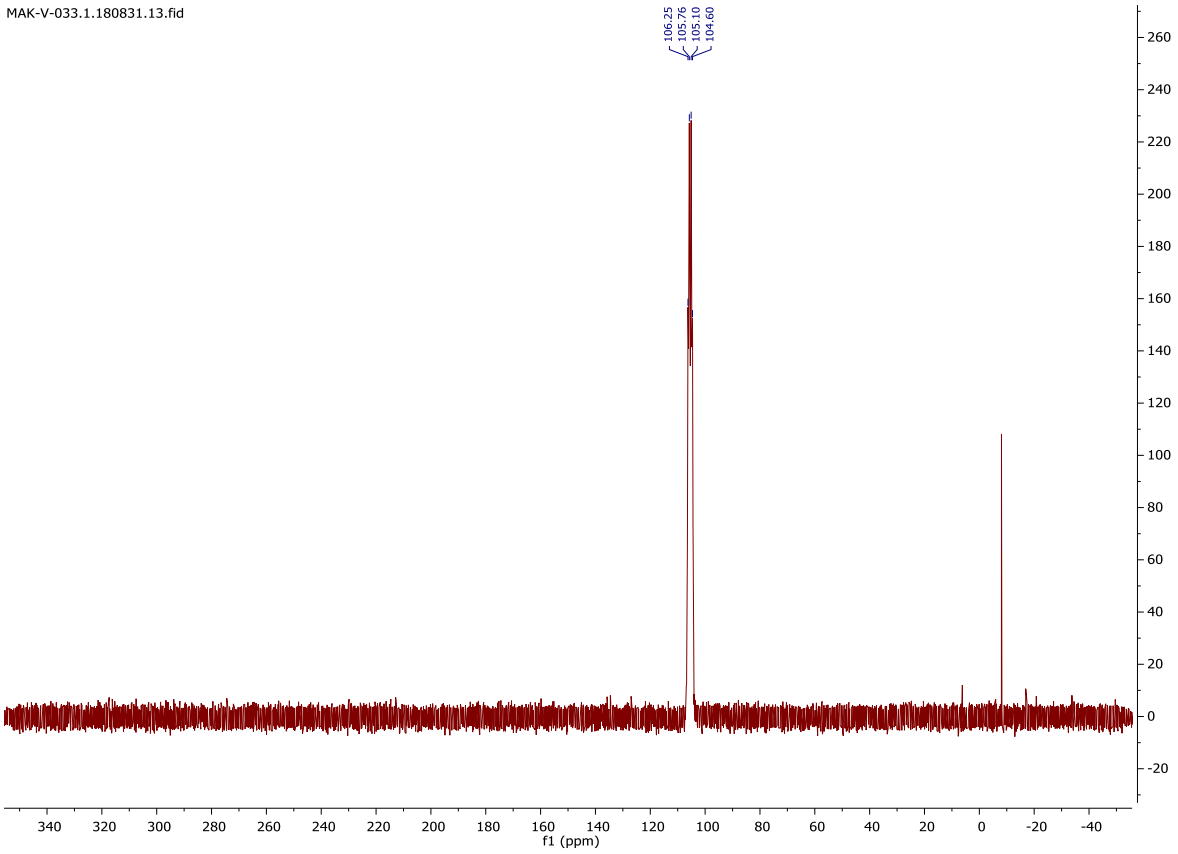

Di(2-nitrobenzyl) ethynylphosphonite borane (**13**)

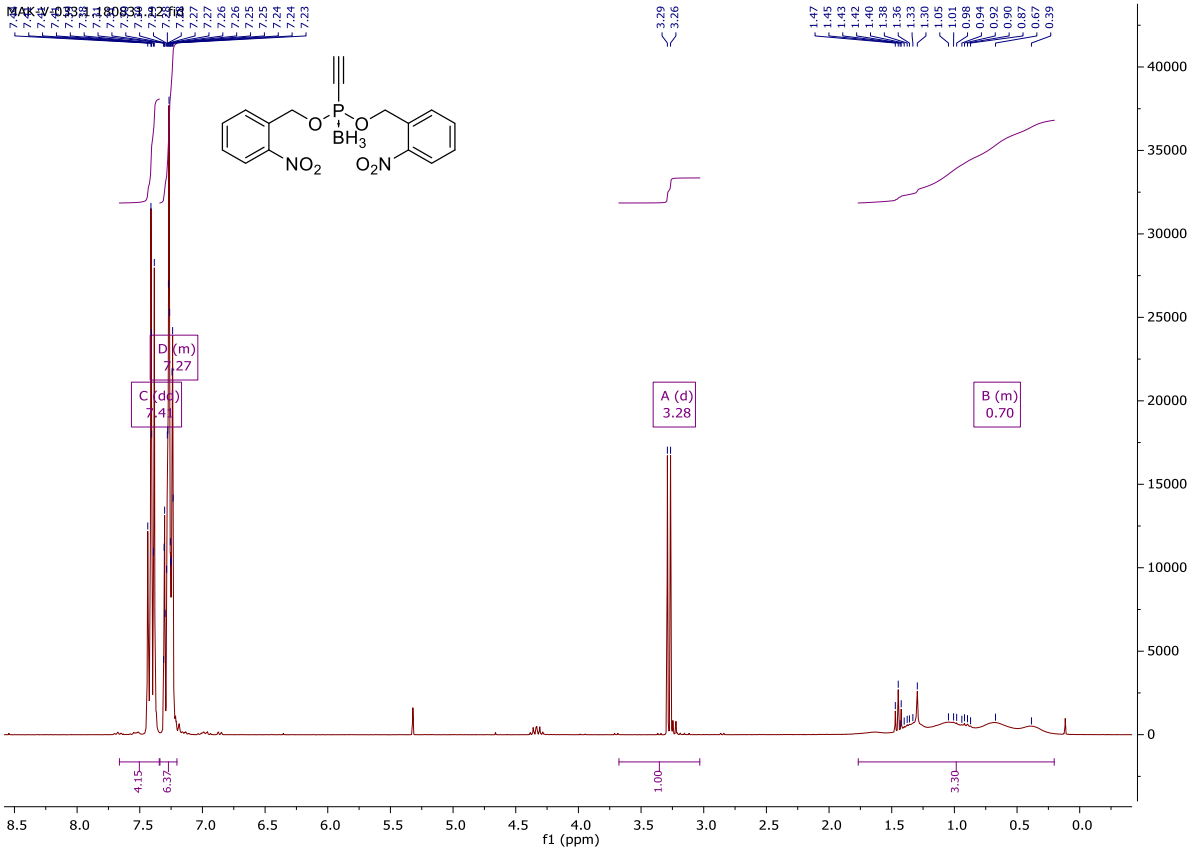

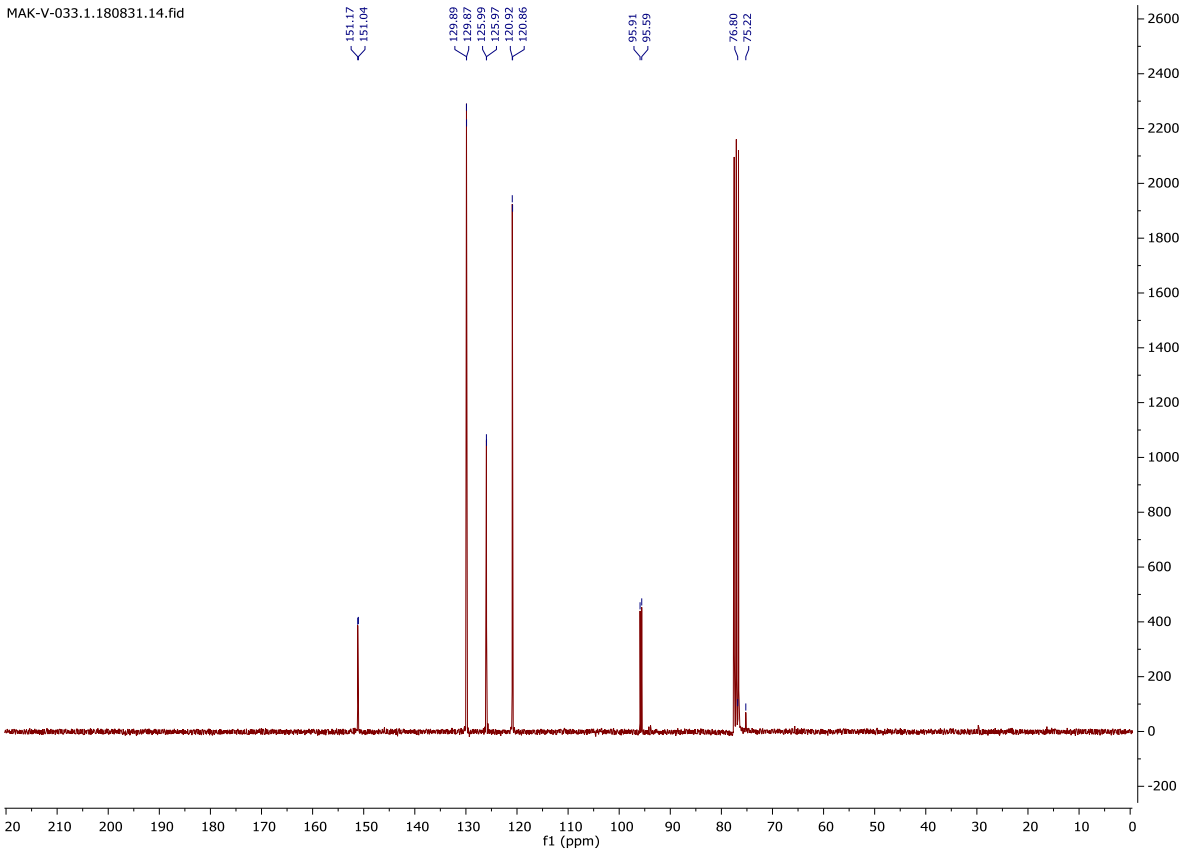
MAK-V-033.1.180831.14.fid
151.17
151.04
129.89
129.87
125.99
125.97
120.92
120.86
95.91
95.59
76.80
75.22
f1 (ppm)

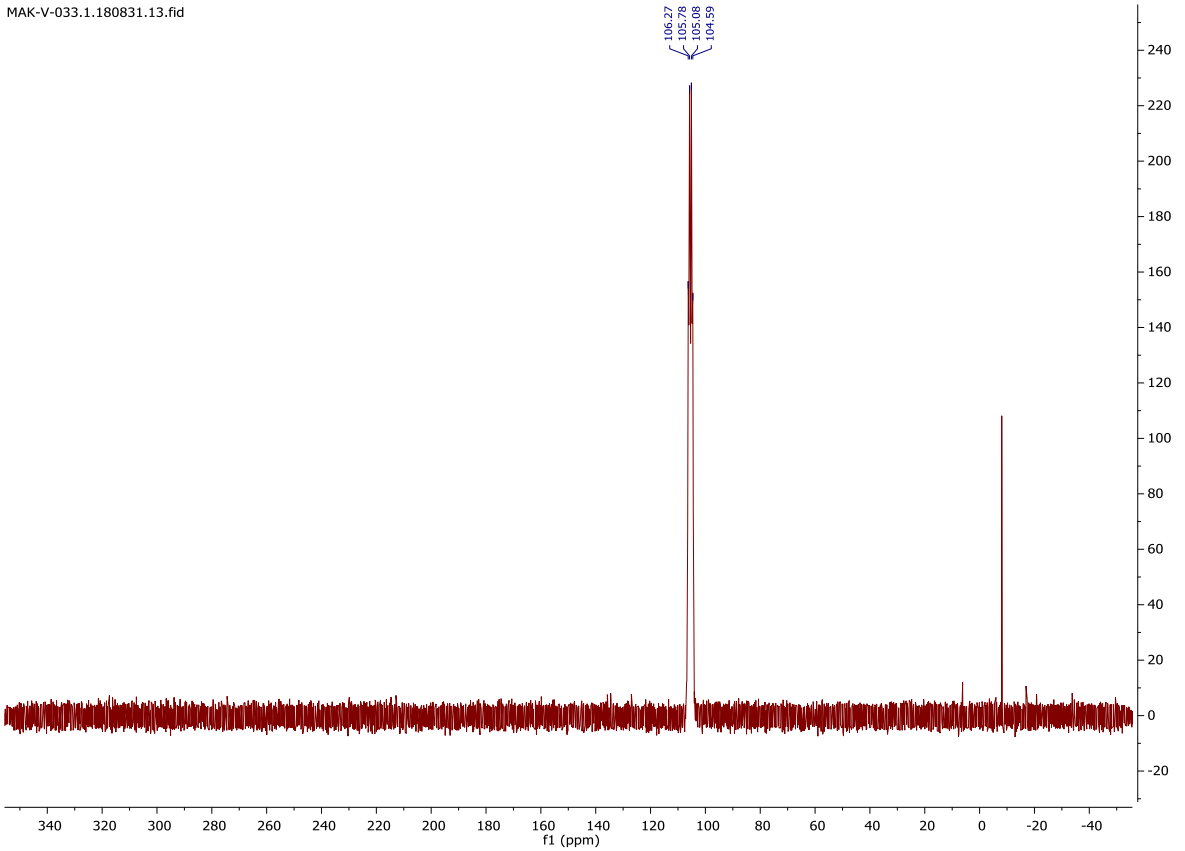
MAK-V-033.1.180831.13.fid
106.27
105.78
105.08
104.59
f1 (ppm)

Bis(2,2,2-trifluoroethyl) ethynylphosphonite borane (**14**)

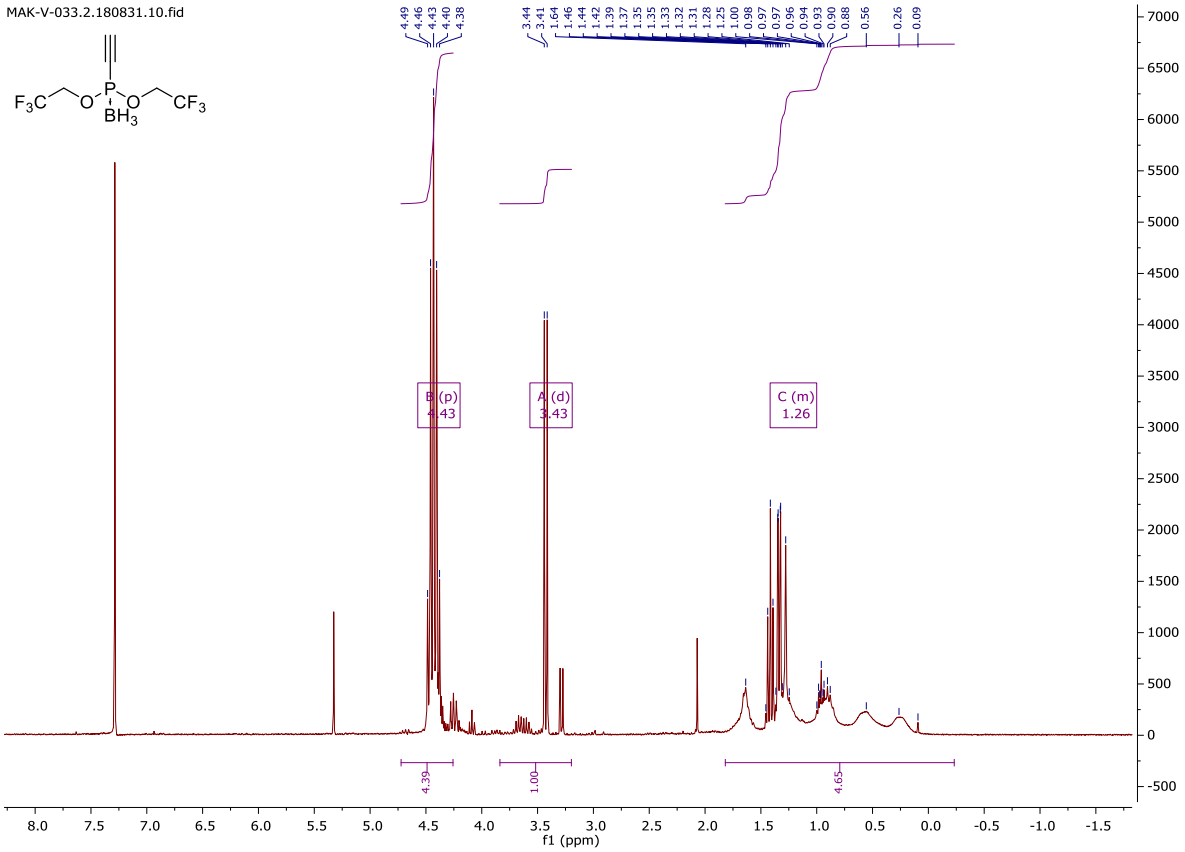

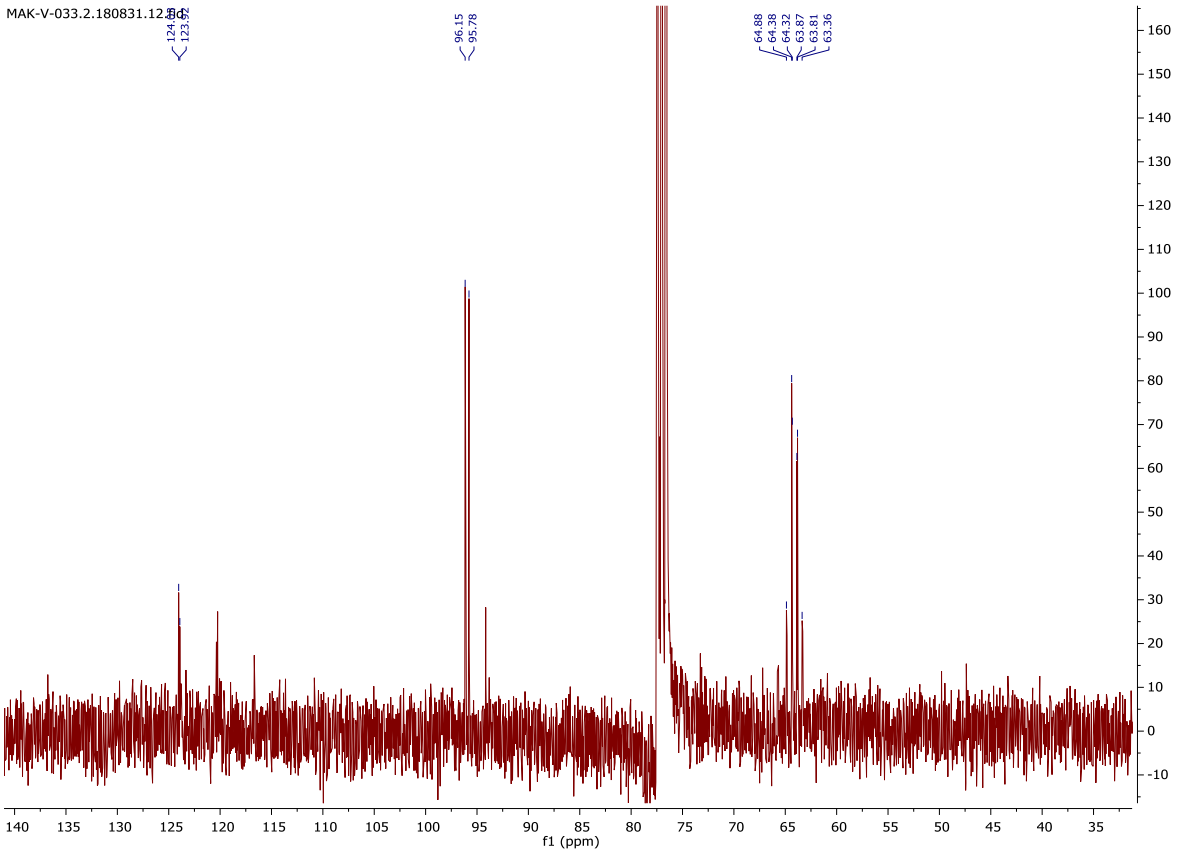

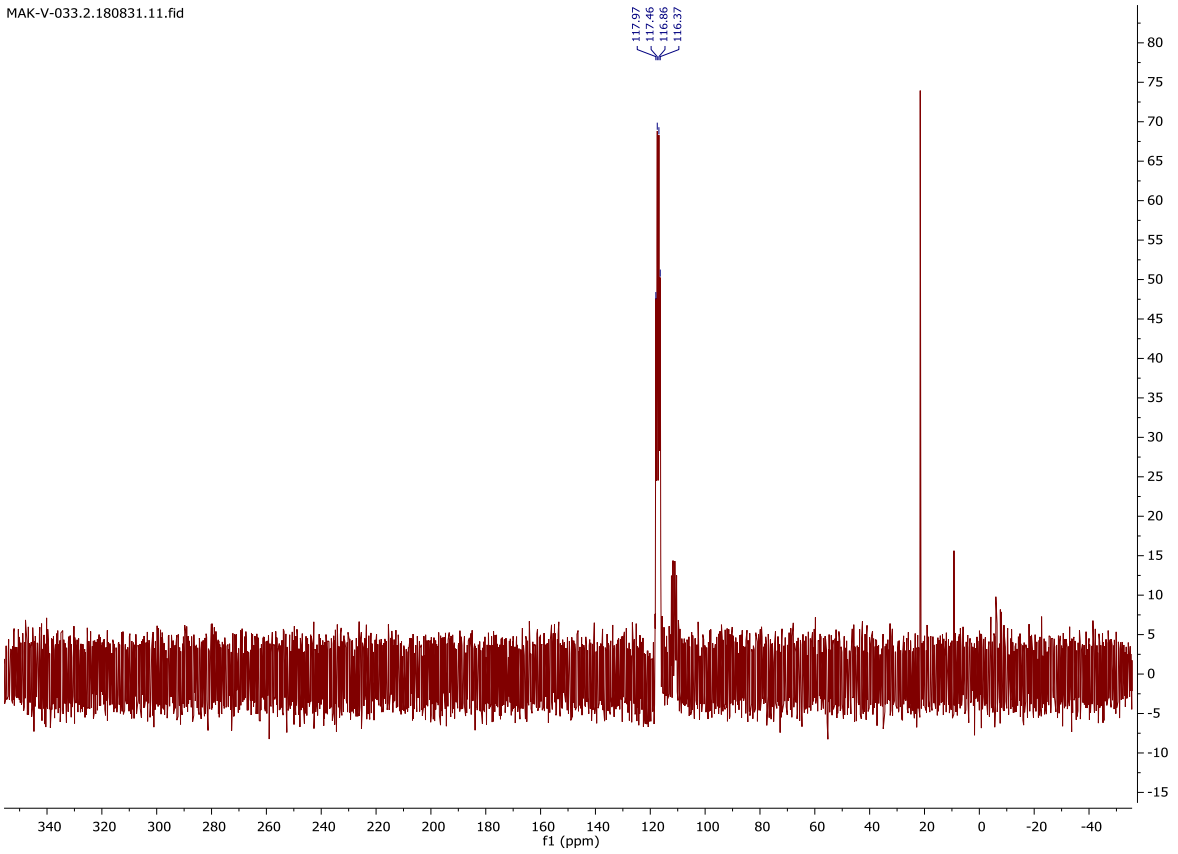
MAK-V-033.2.180831.11.fid
117.97
117.46
116.86
116.37
f1 (ppm)

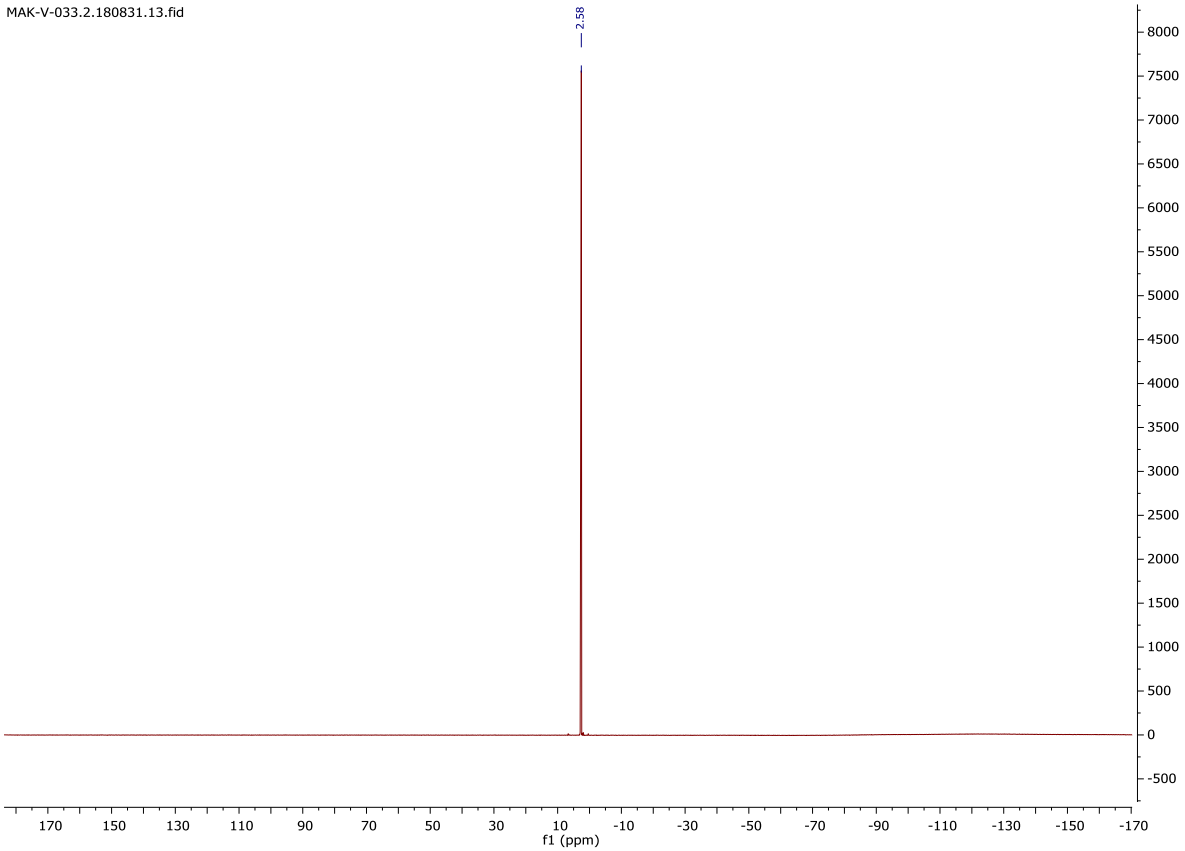
MAK-V-033.2.180831.13.fid
2.58
f1 (ppm)

2-Isopropyl-disulfido-ethyl-*N*-(4-benzoic-acid-*N*-hydroxysuccinimideester)-*P*-ethynylphosphonamidate (**16**)

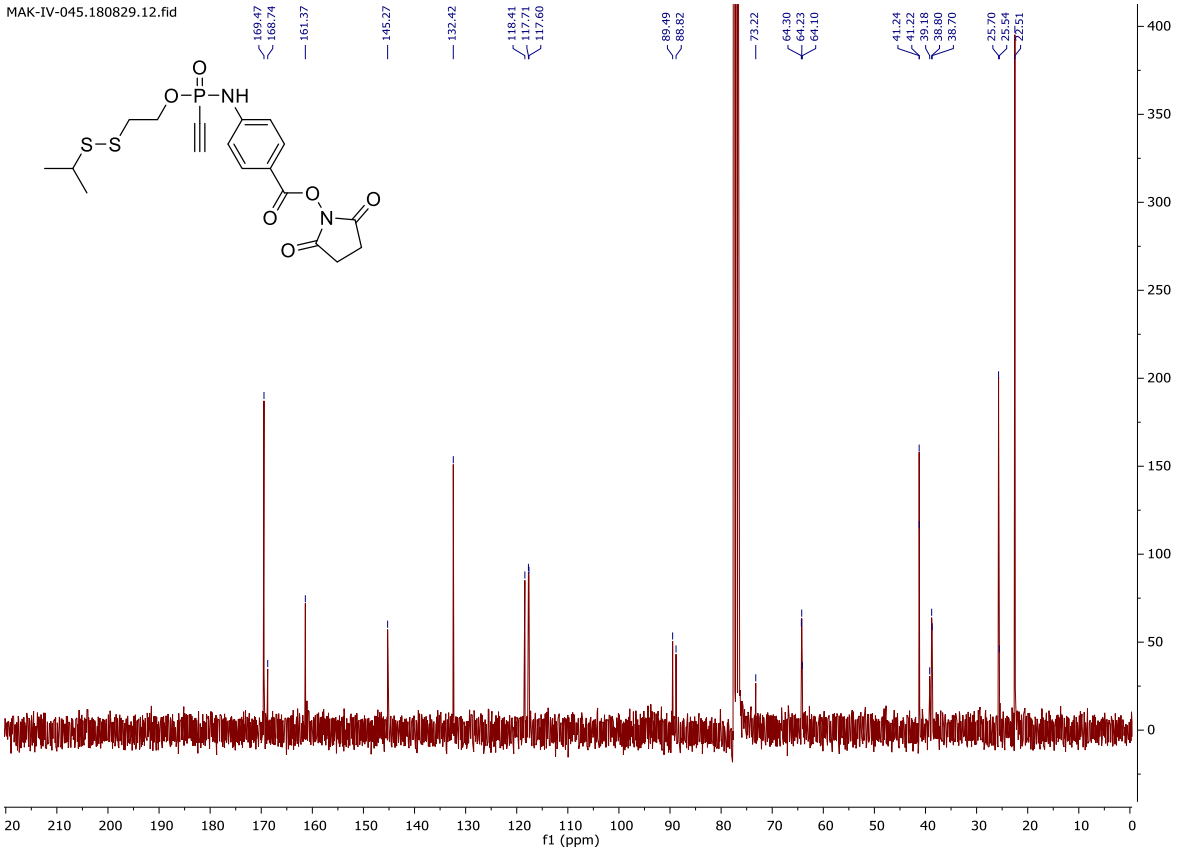

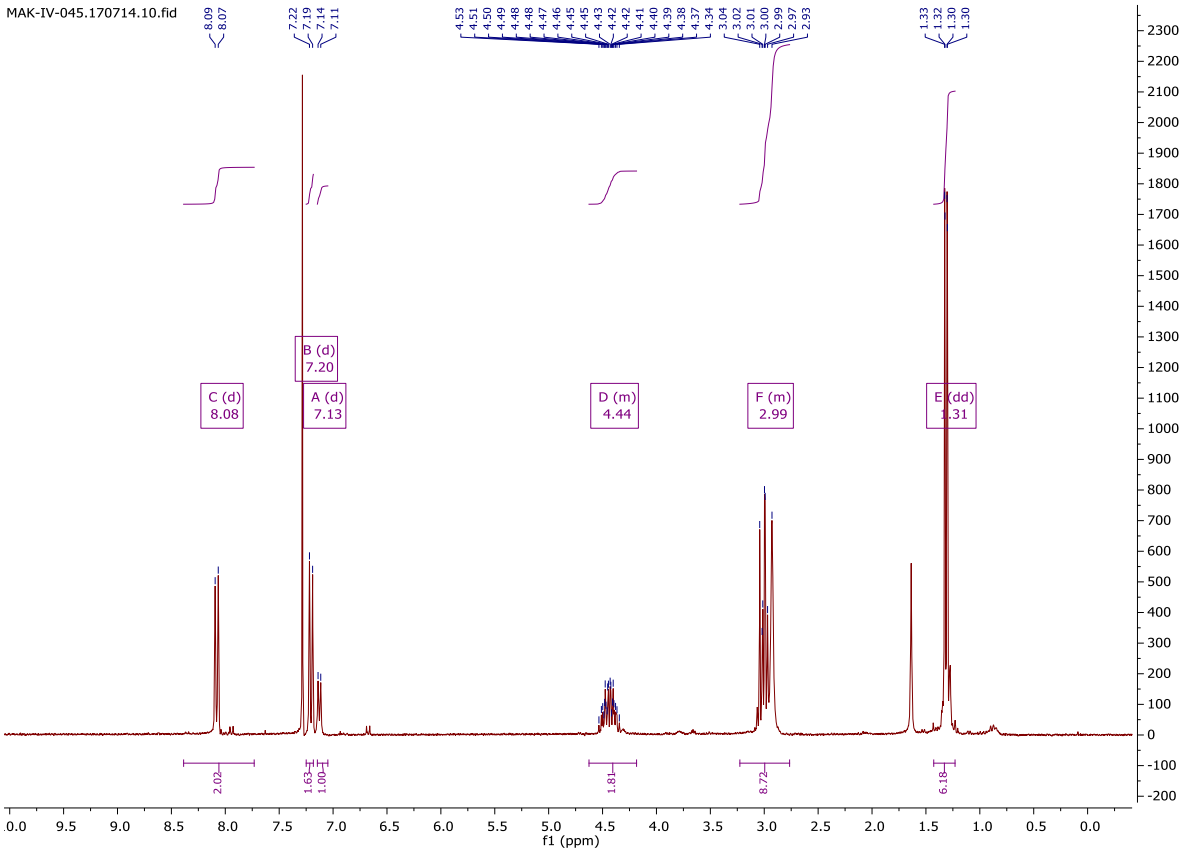

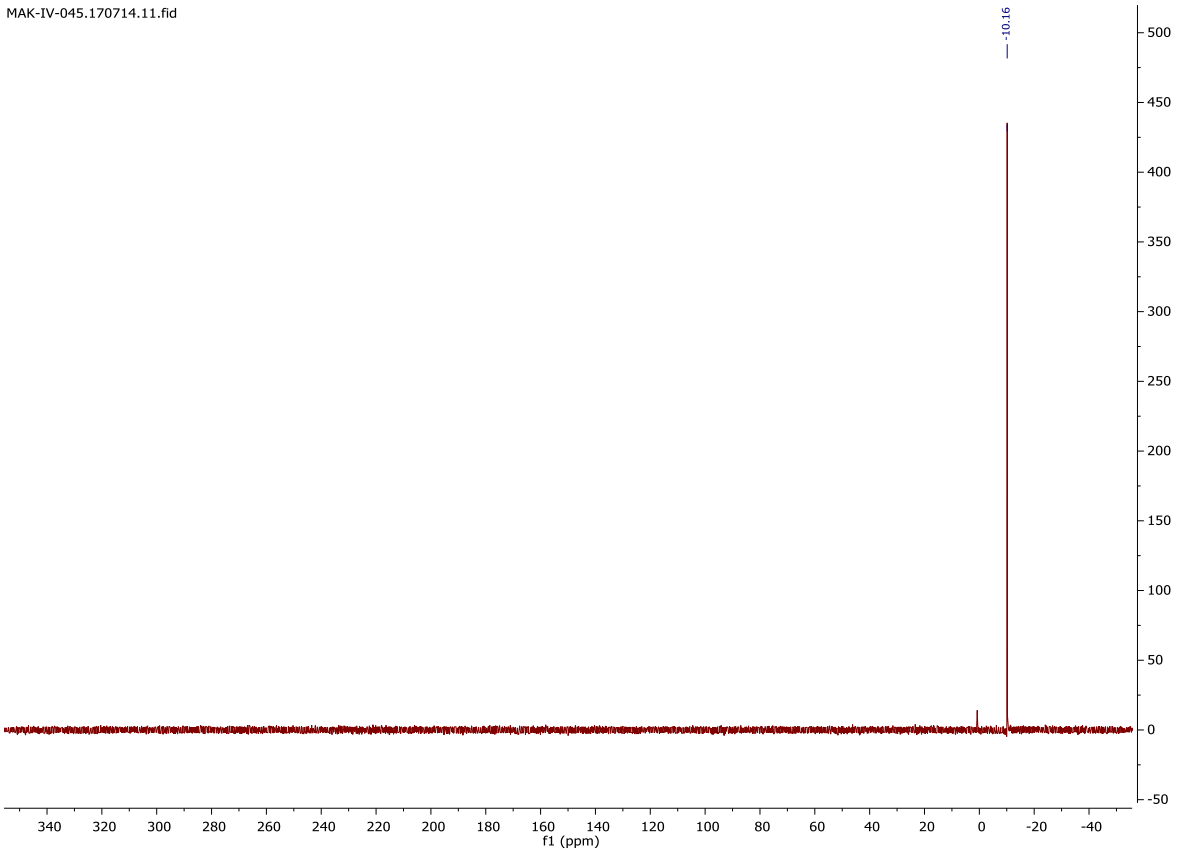

2-*tert*-butyl-disulfido-ethyl-*N*-(4-benzoic-acid-*N*-hydroxysuccinimideester)-*P*-ethynylphosphonamidate (**17**)

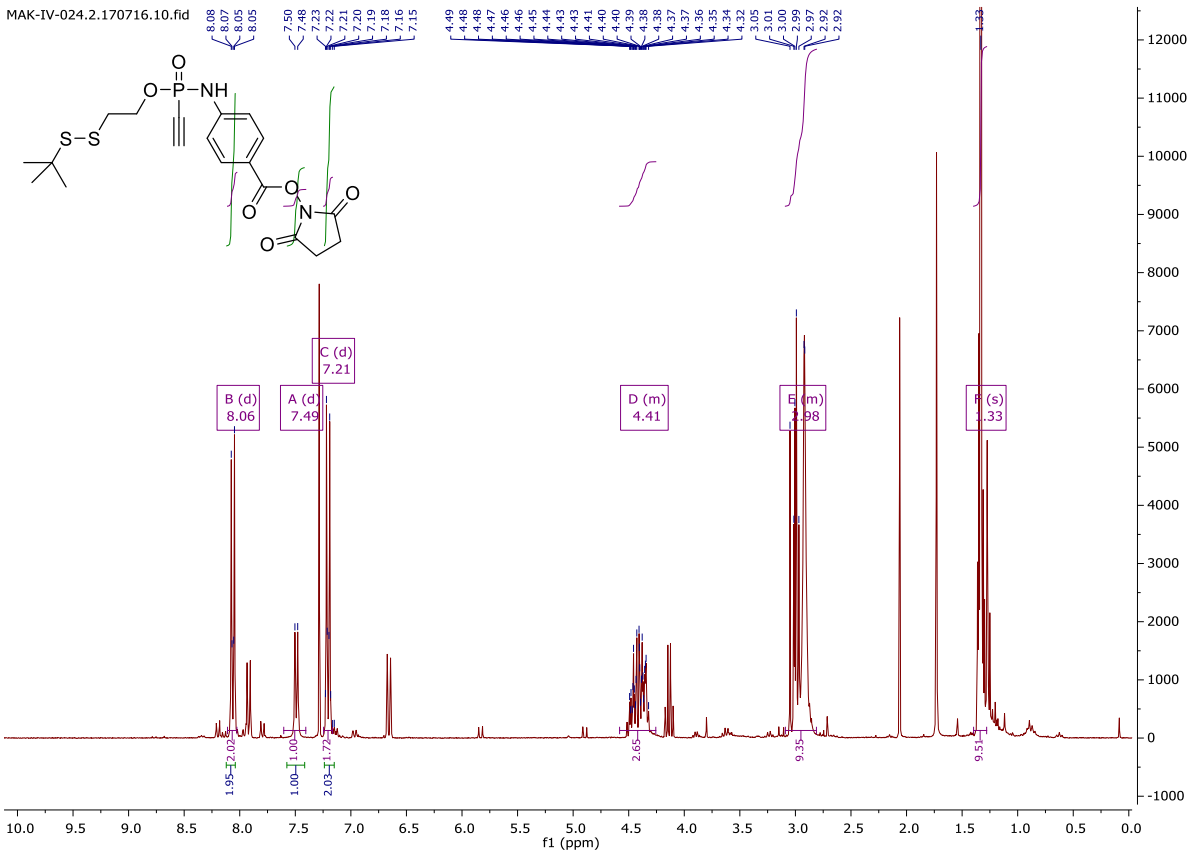

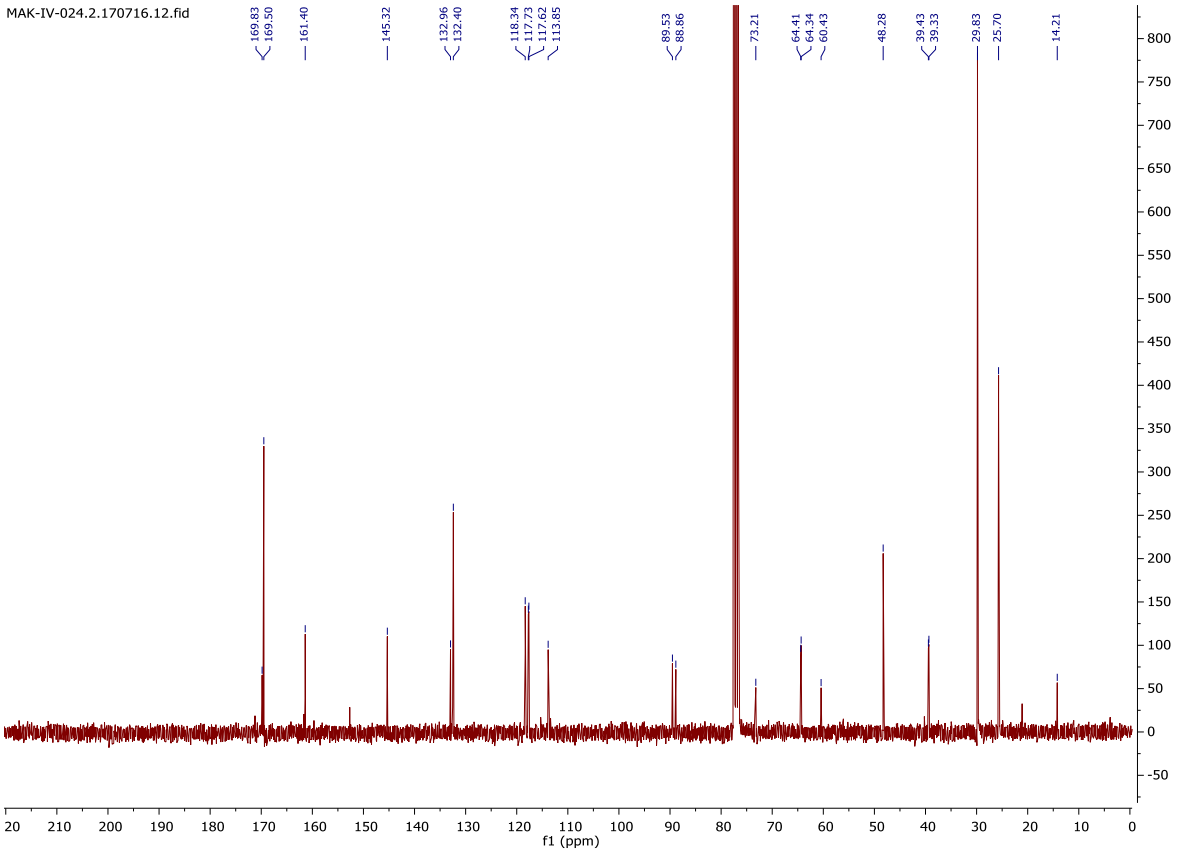
MAK-IV-024.2.170716.12.fid
169.83
169.50
161.40
145.32
132.96
132.40
118.34
117.73
117.62
113.85
89.53
88.86
73.21
64.41
64.34
60.43
48.28
39.43
39.33
29.83
25.70
14.21
f1 (ppm)

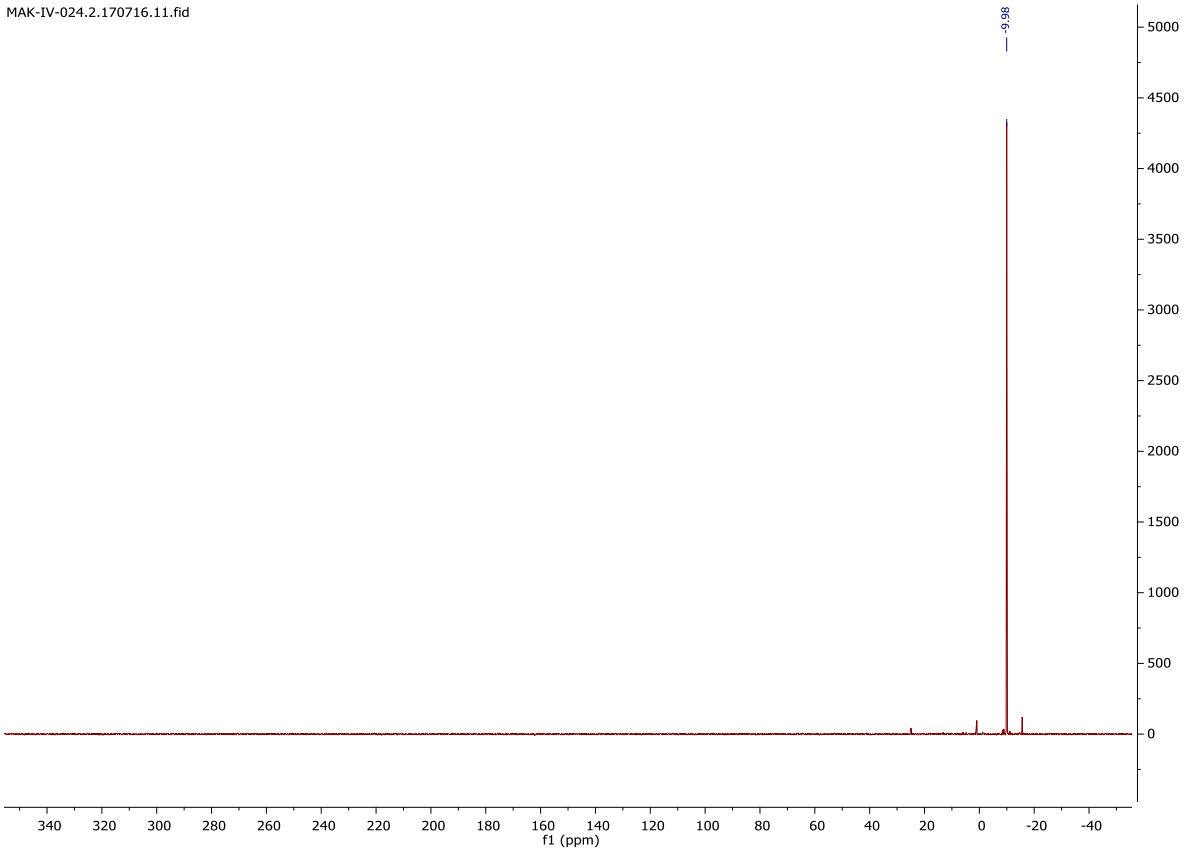
MAK-IV-024.2.170716.11.fid
-9.98
f1 (ppm)

2-isopropyldisulfido-3-propyl-*N*-(4-benzoic-acid-*N*-hydroxysuccinimideester)-*P*-ethynylphosphonamidate (**18**)

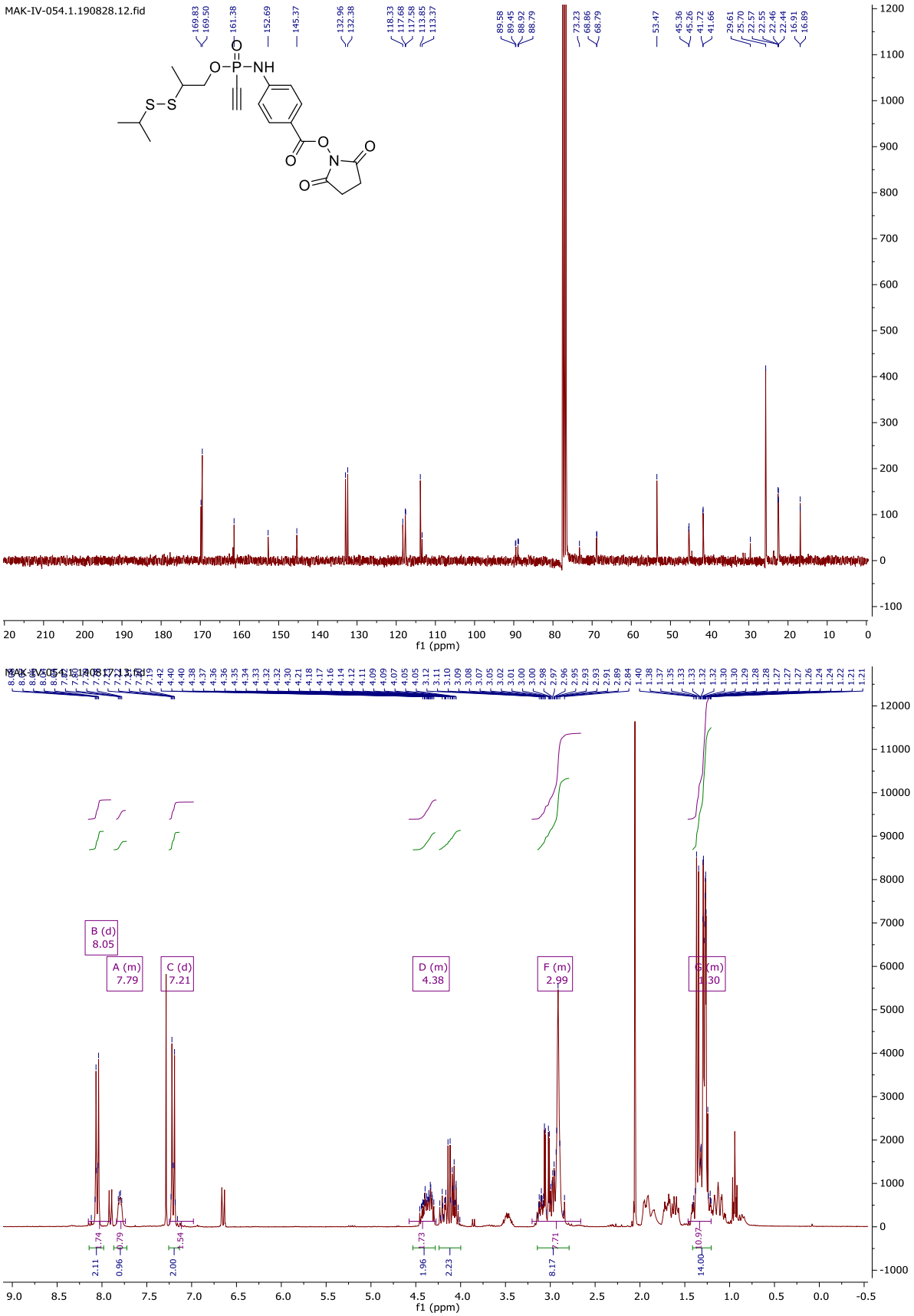

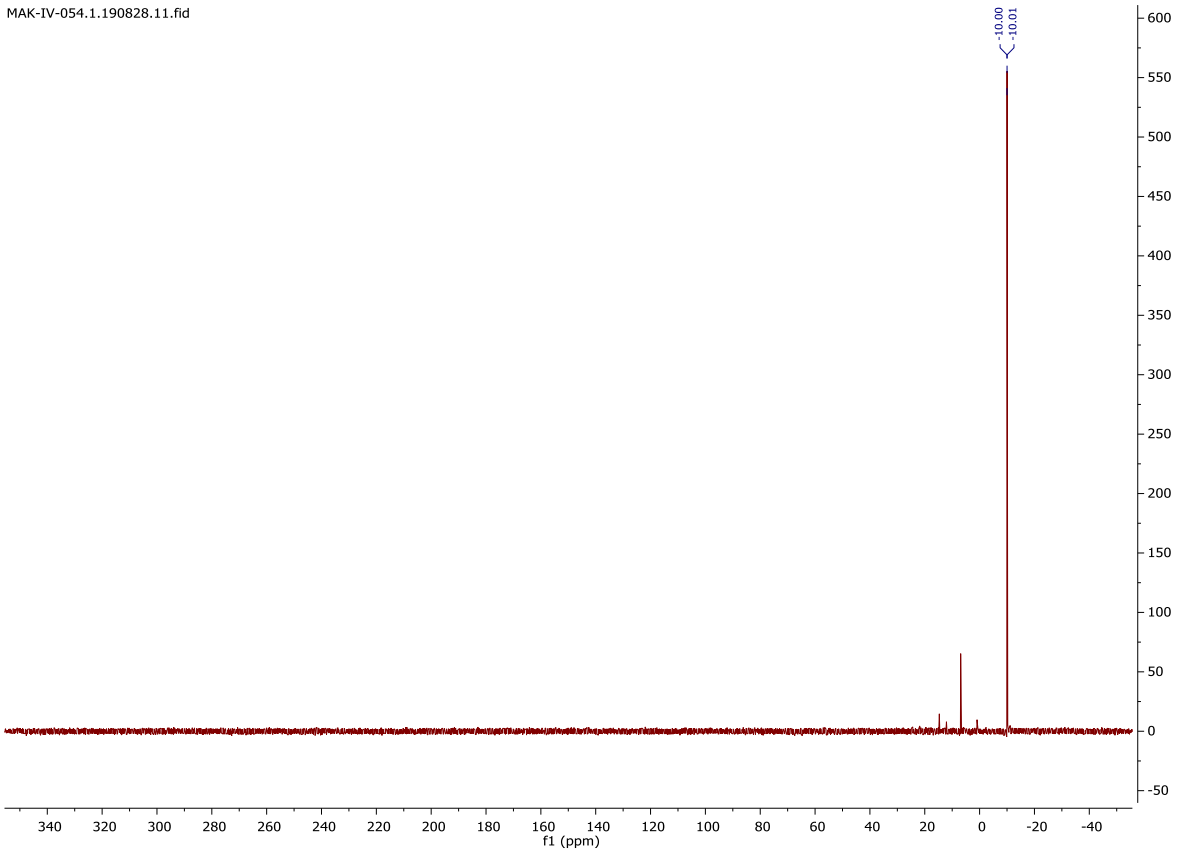

3-Butinyl-*N*-(4-benzoic-acid-*N*-hydroxysuccinimideester)-*P*-ethynylphosphonamidate (**19**)

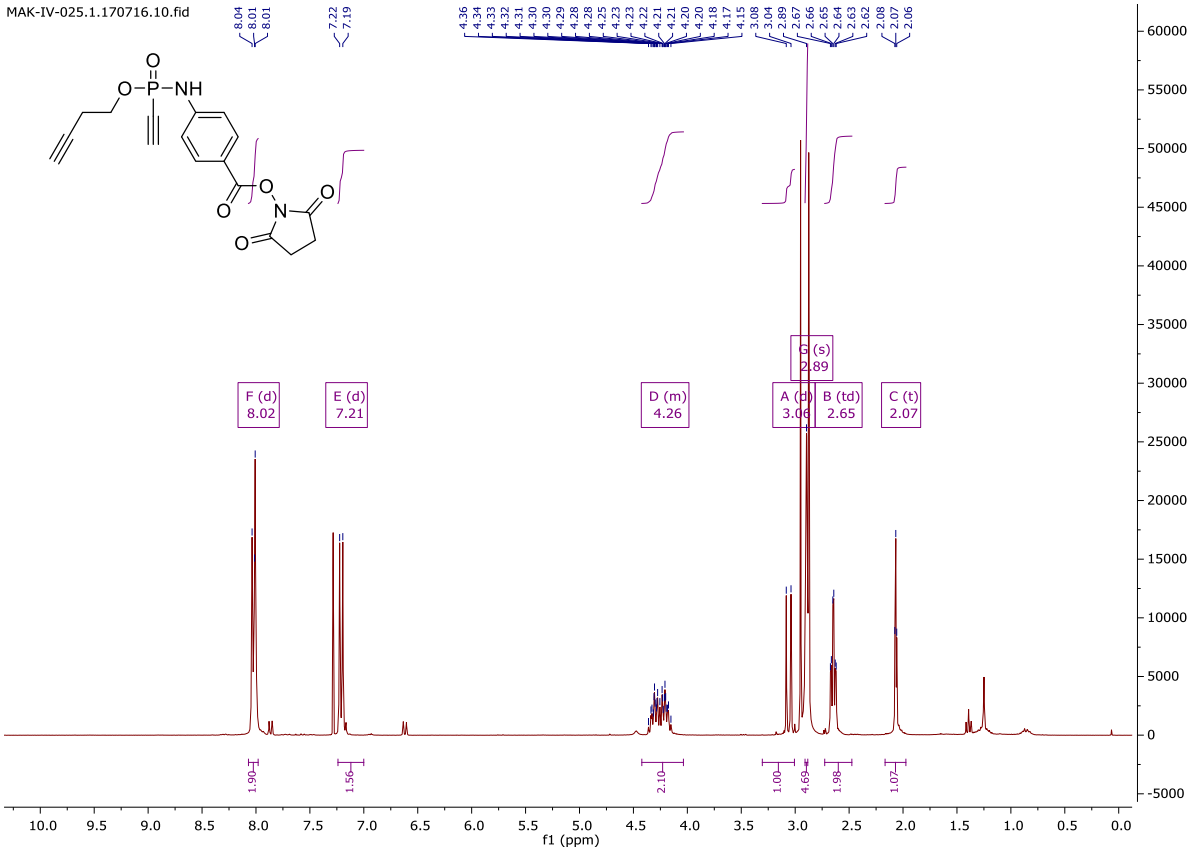

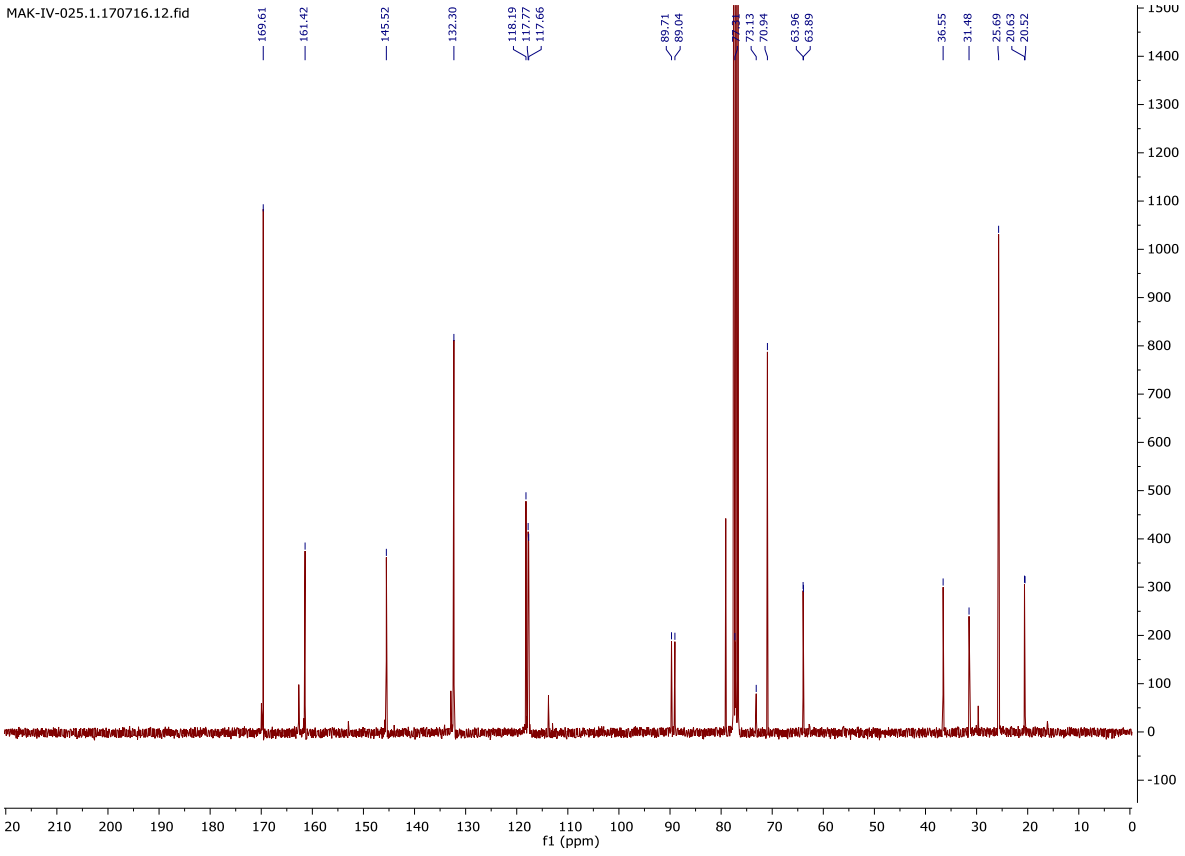
MAK-IV-025.1.170716.12.fid
169.61
161.42
145.52
132.30
118.19
117.77
117.66
89.71
89.04
73.13
70.94
63.96
63.89
36.55
31.48
25.69
20.63
20.52
f1 (ppm)

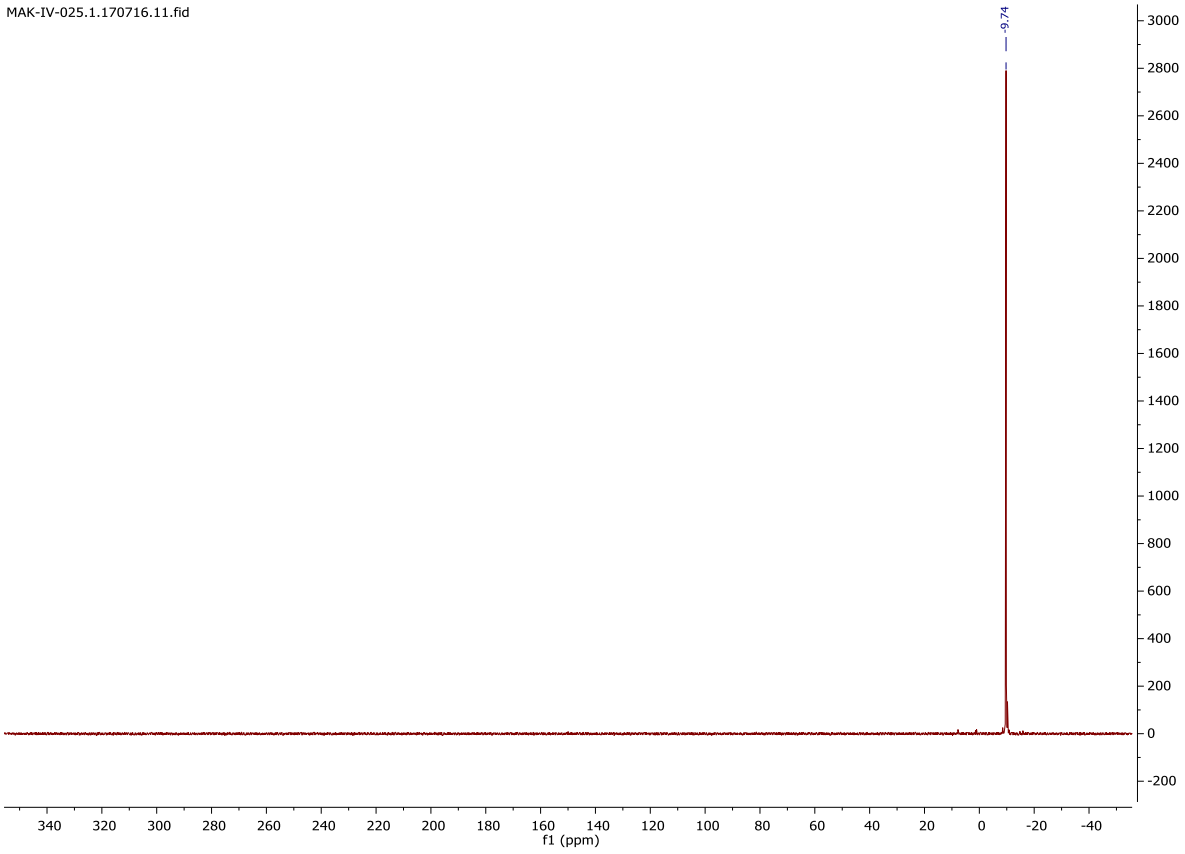
MAK-IV-025.1.170716.11.fid
-9.74
f1 (ppm)

4-acetoxy-benzyl-*N*-(4-benzoic-acid-*N*-hydroxysuccinimide ester)-*P*-ethynylphosphonamidate (**21**)

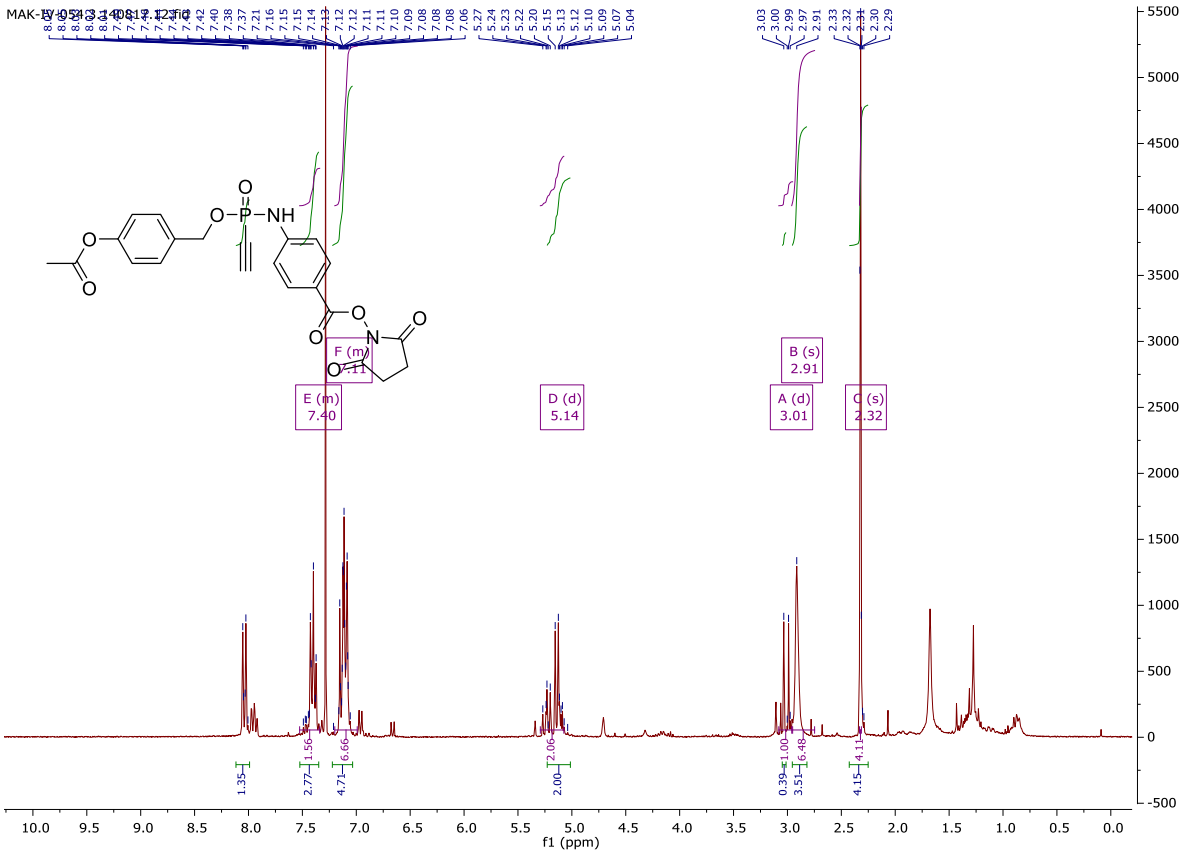

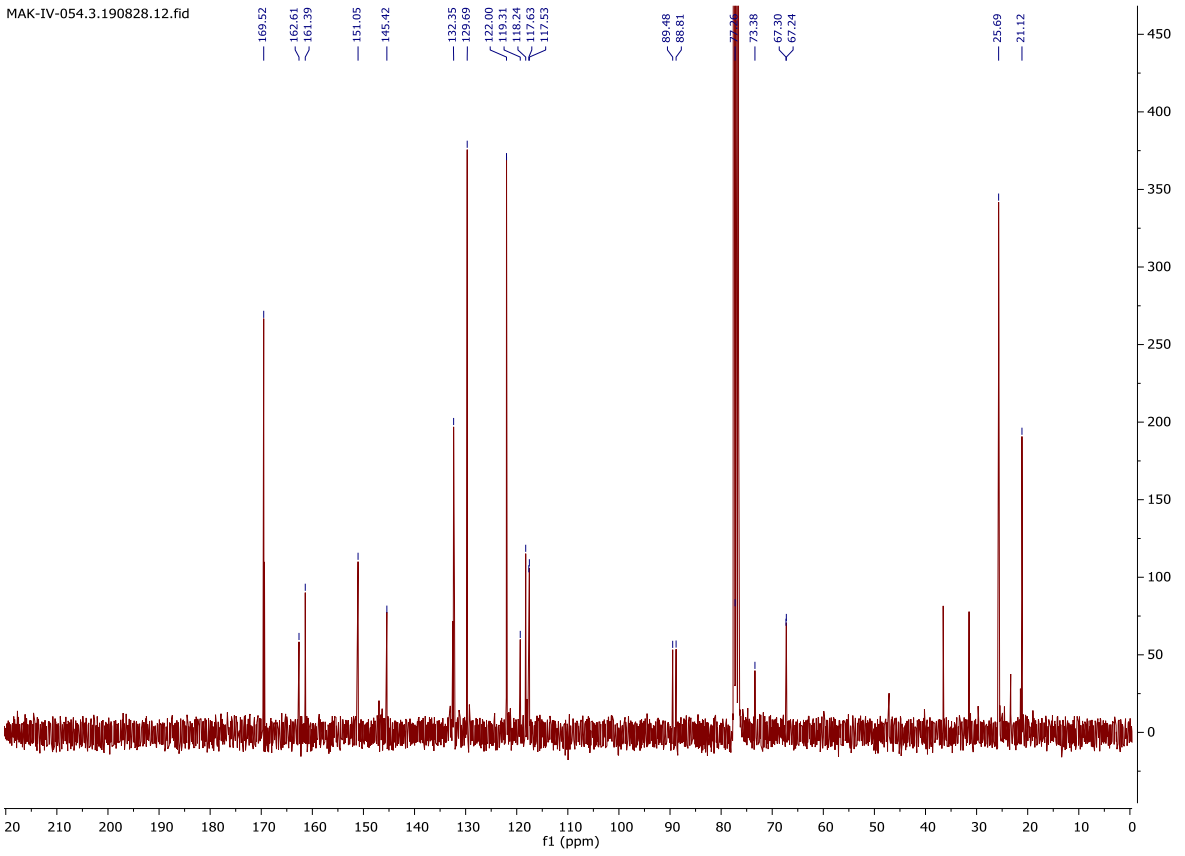

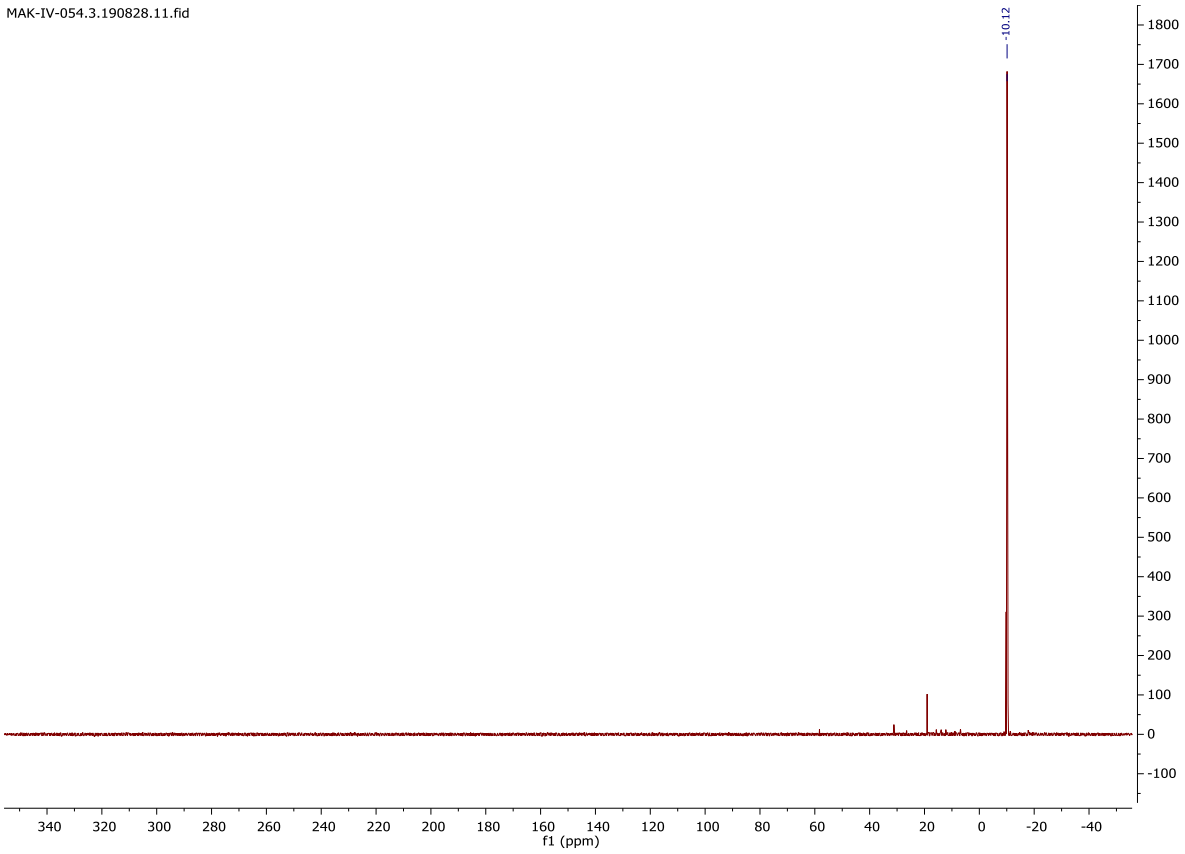

4-Diazophenyl-benzyl-*N*-(4-benzoic-acid-*N*-hydroxysuccinimide ester)-*P*-ethynylphosphonamidate (**22**)

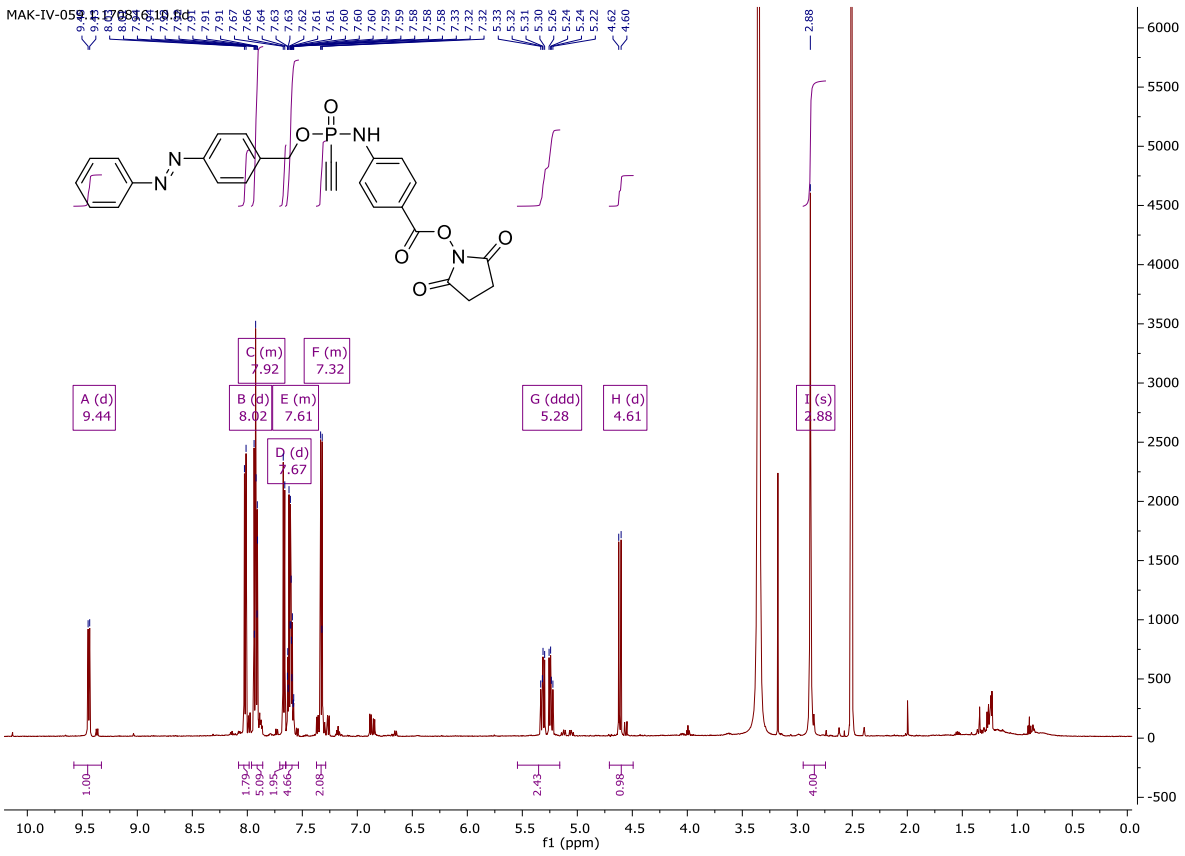

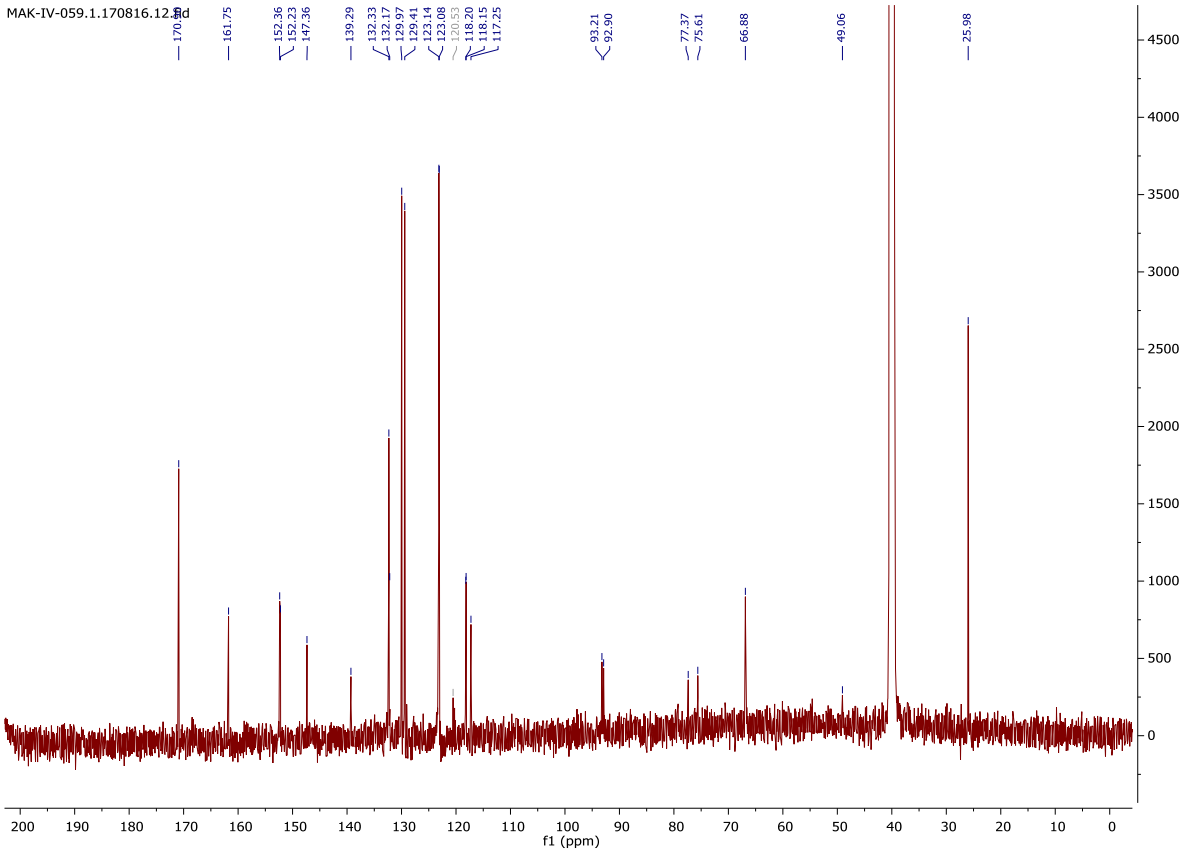
MAK-IV-059.1.170816.12.fid
170.44
161.75
152.36
152.23
147.36
139.29
132.33
132.17
129.97
129.41
123.14
123.08
120.53
118.20
118.15
117.25
93.21
92.90
77.37
75.61
66.88
49.06
25.98
f1 (ppm)

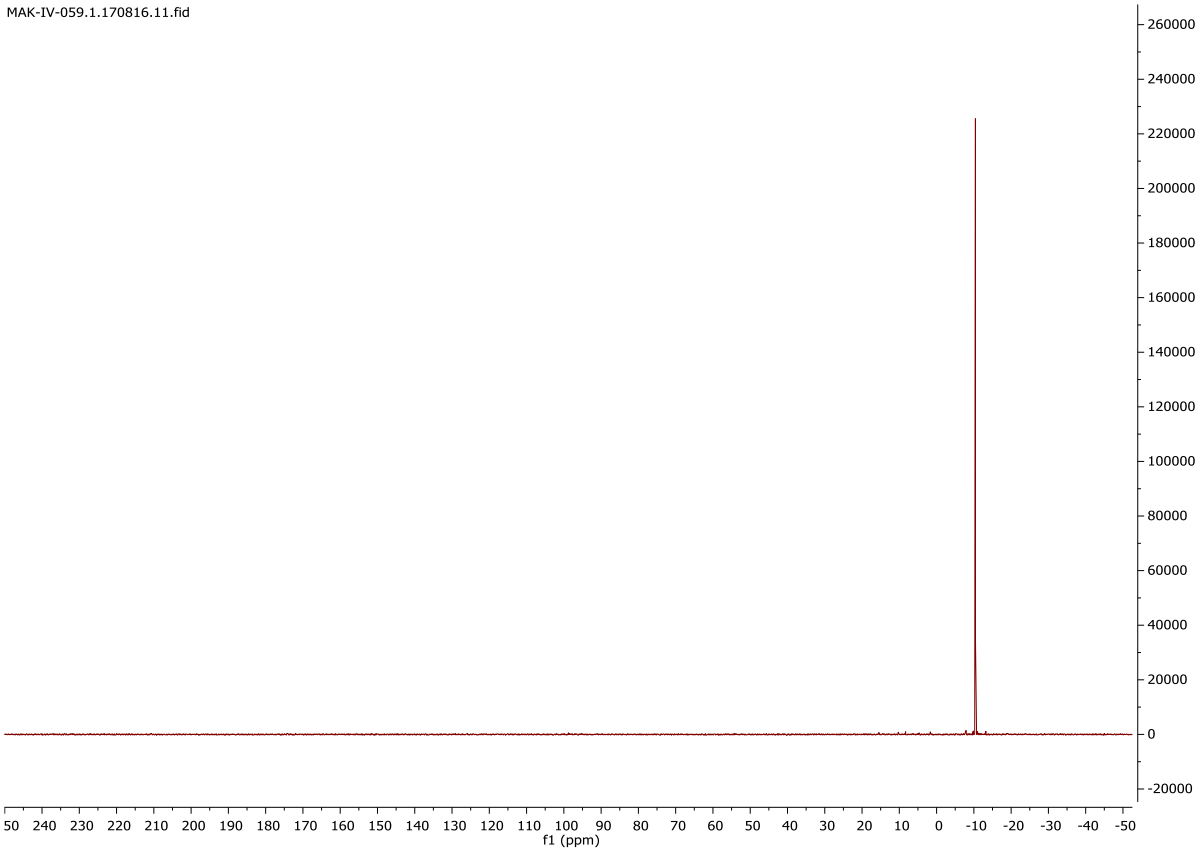
MAK-IV-059.1.170816.11.fid
f1 (ppm)

5-((2-(*O*-(2-Isopropyl-disulfido-ethyl)-*P*-ethynylphosphonamidato-*N*-benzoyl)ethyl)amino)naphthalene-1-sulfonic acid (**23**)

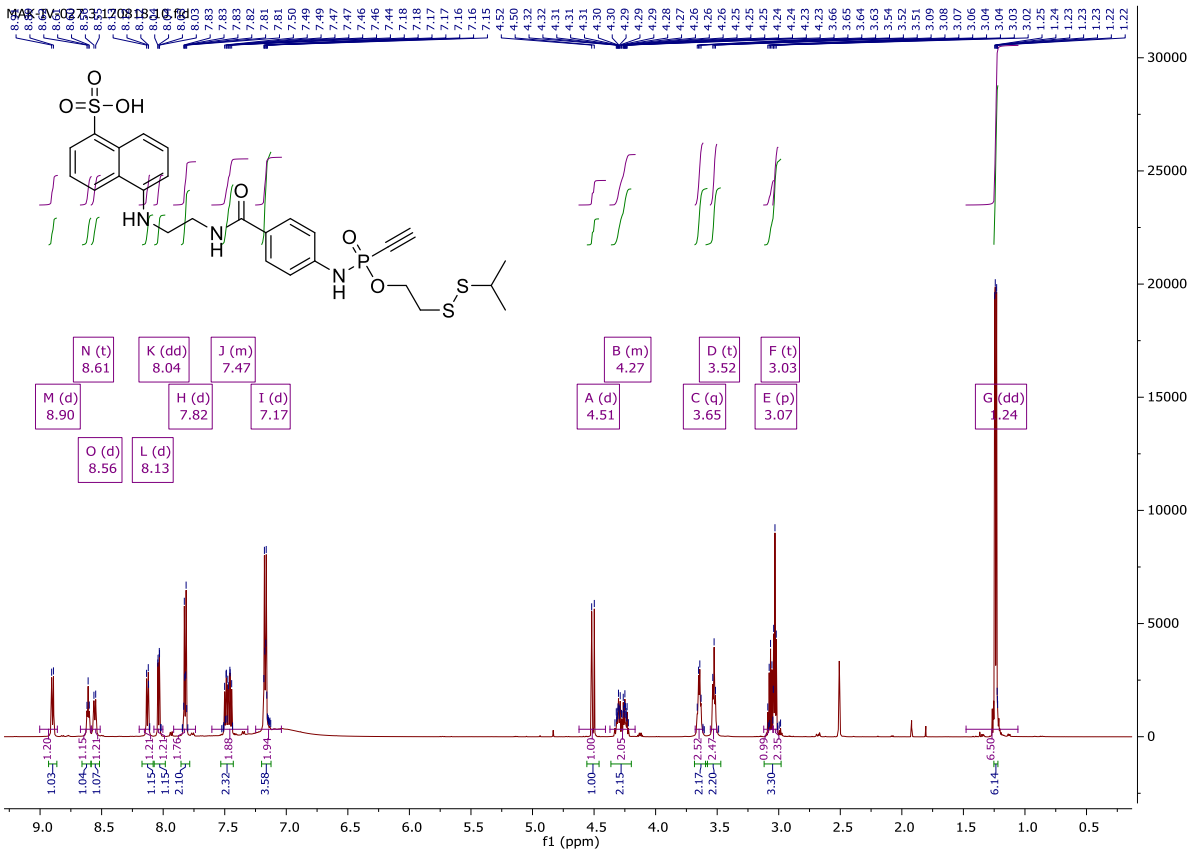

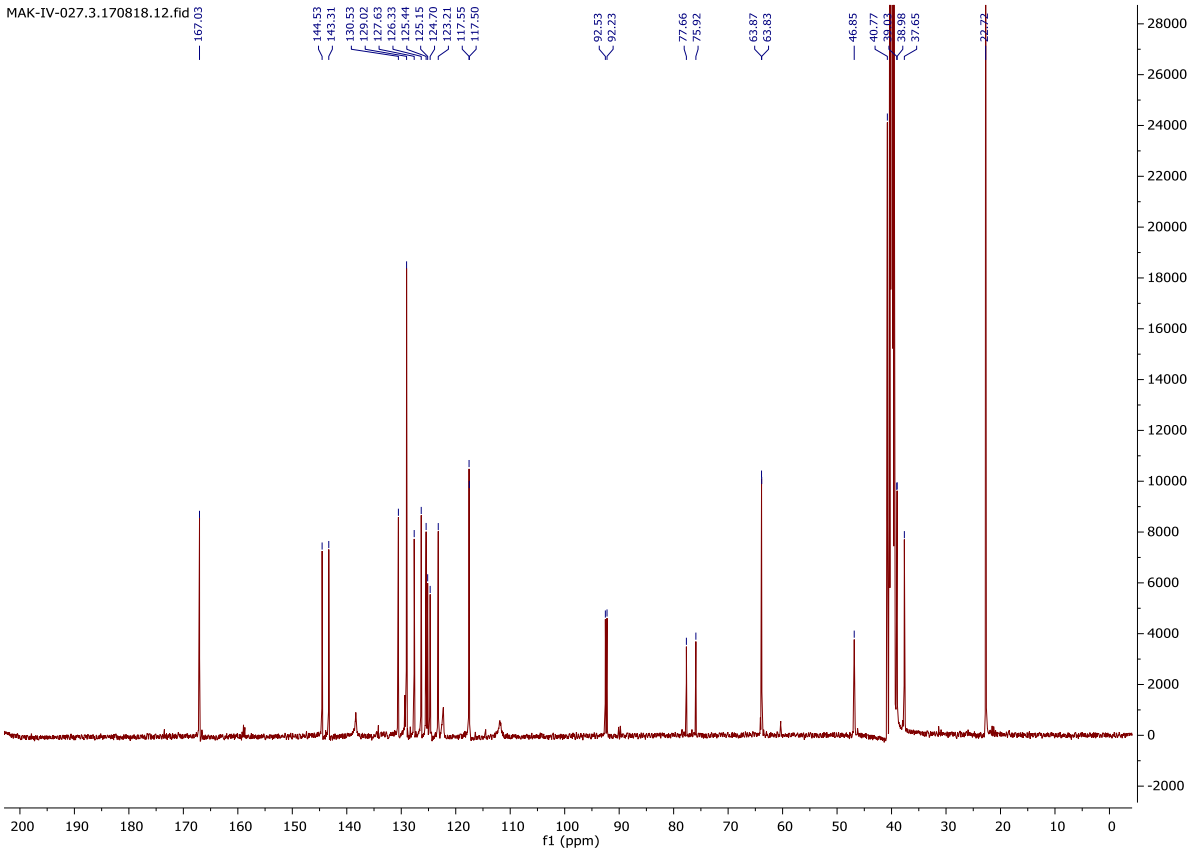

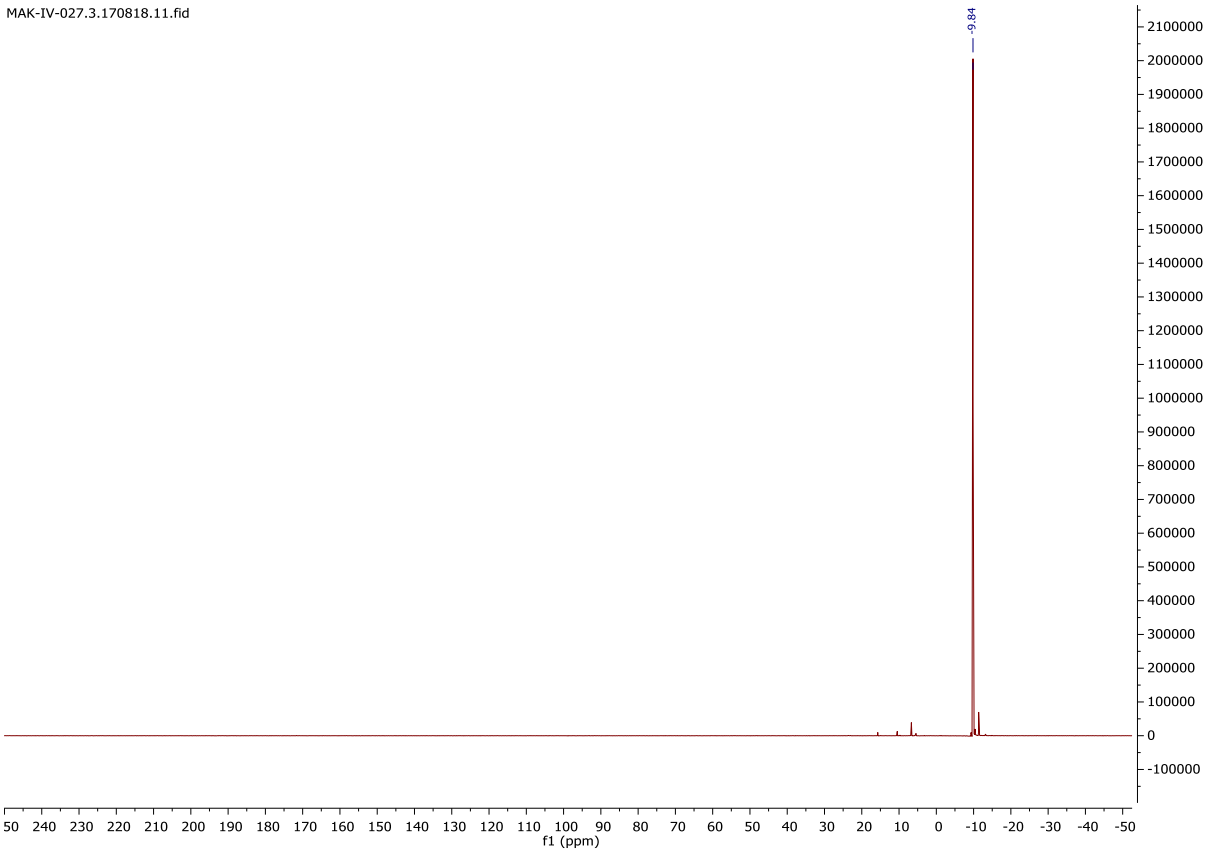

5-((2-(*O*-(2-*tert*-butyl-disulfido-ethyl)-*P*-ethynylphosphonamidato-*N*-benzoyl)ethyl)amino)naphthalene-1-sulfonic acid (**24**)

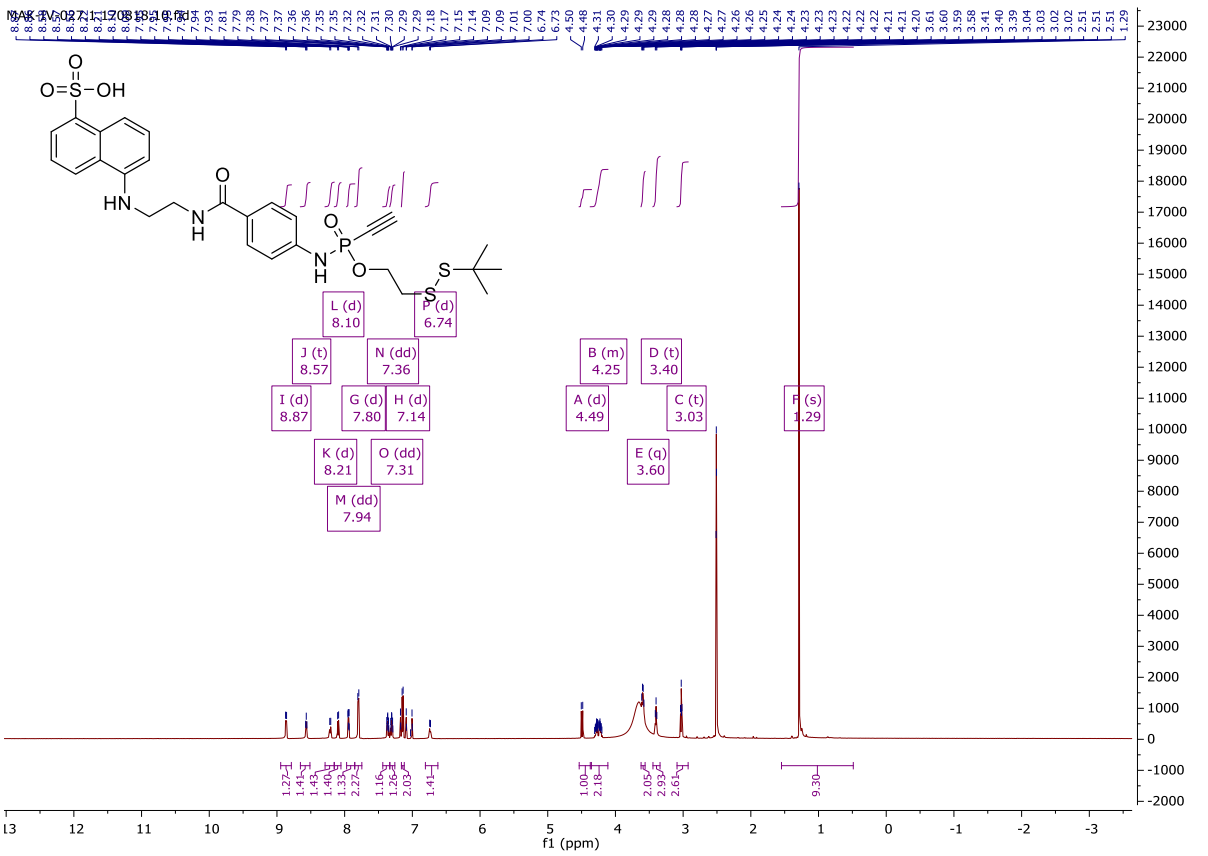

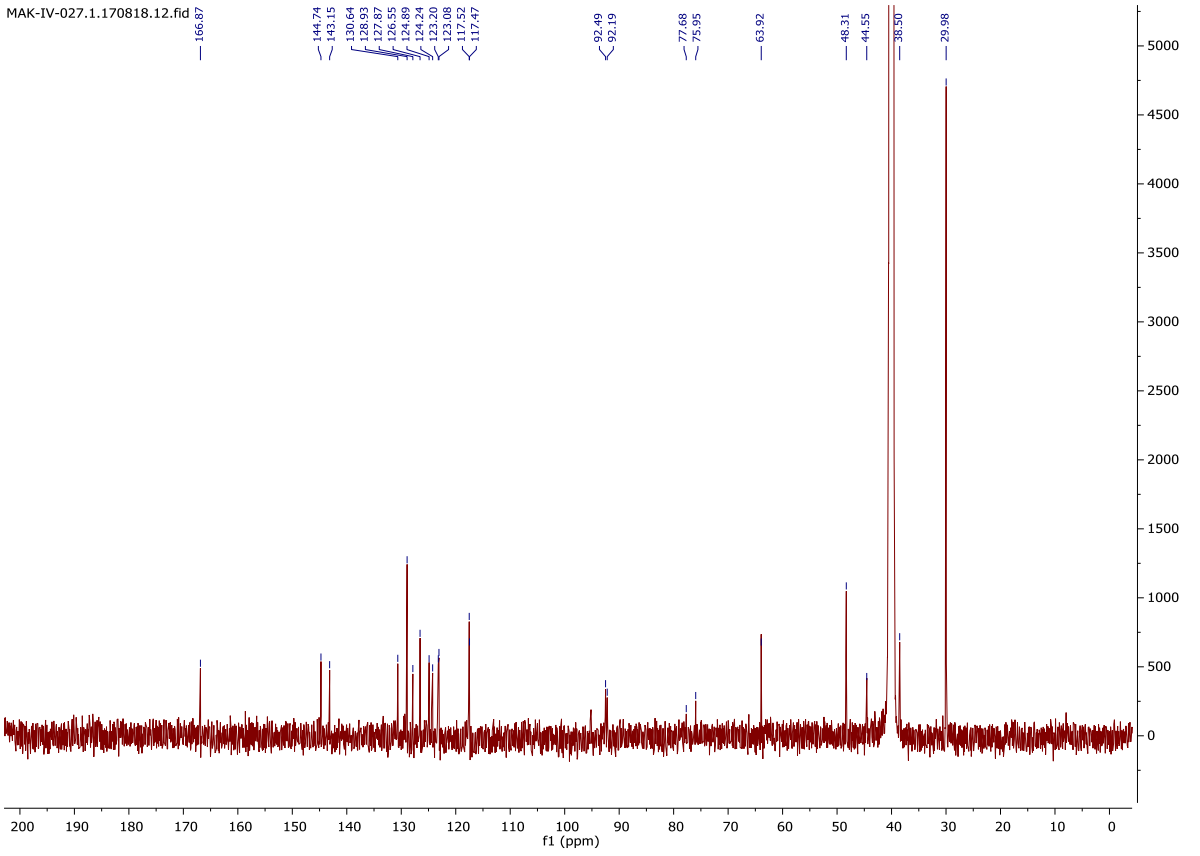
MAK-IV-027.1.170818.12.fid
166.87
144.74
143.15
130.64
128.93
127.87
126.55
124.89
124.24
123.20
123.08
117.52
117.47
92.49
92.19
77.68
75.95
63.92
48.31
44.55
38.50
29.98
f1 (ppm)

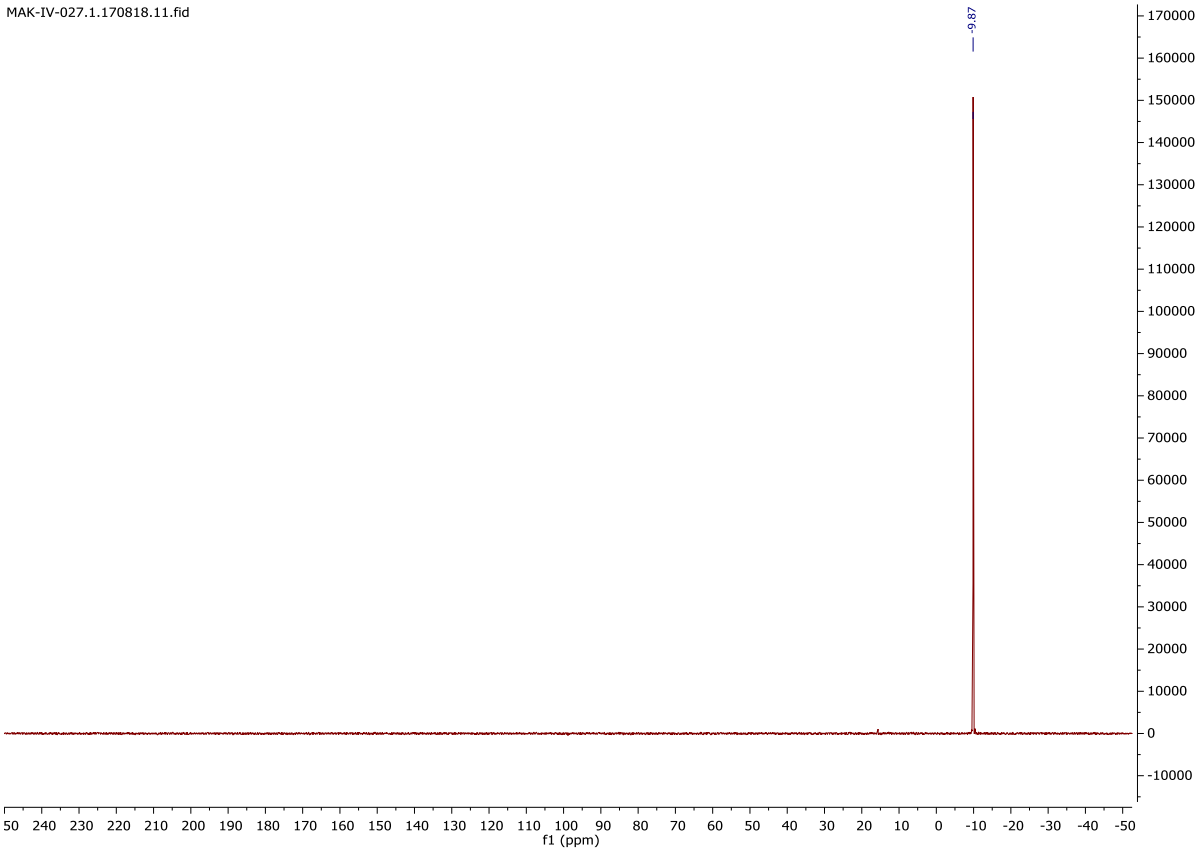
MAK-IV-027.1.170818.11.fid
-9.87
f1 (ppm)

5-((2-(*O*-2-isopropyl disulfido-3-propyl)-*P*-ethynylphosphonamidato-*N*-benzoyl)ethyl)amino)naphthalene-1-sulfonic acid (**25**)

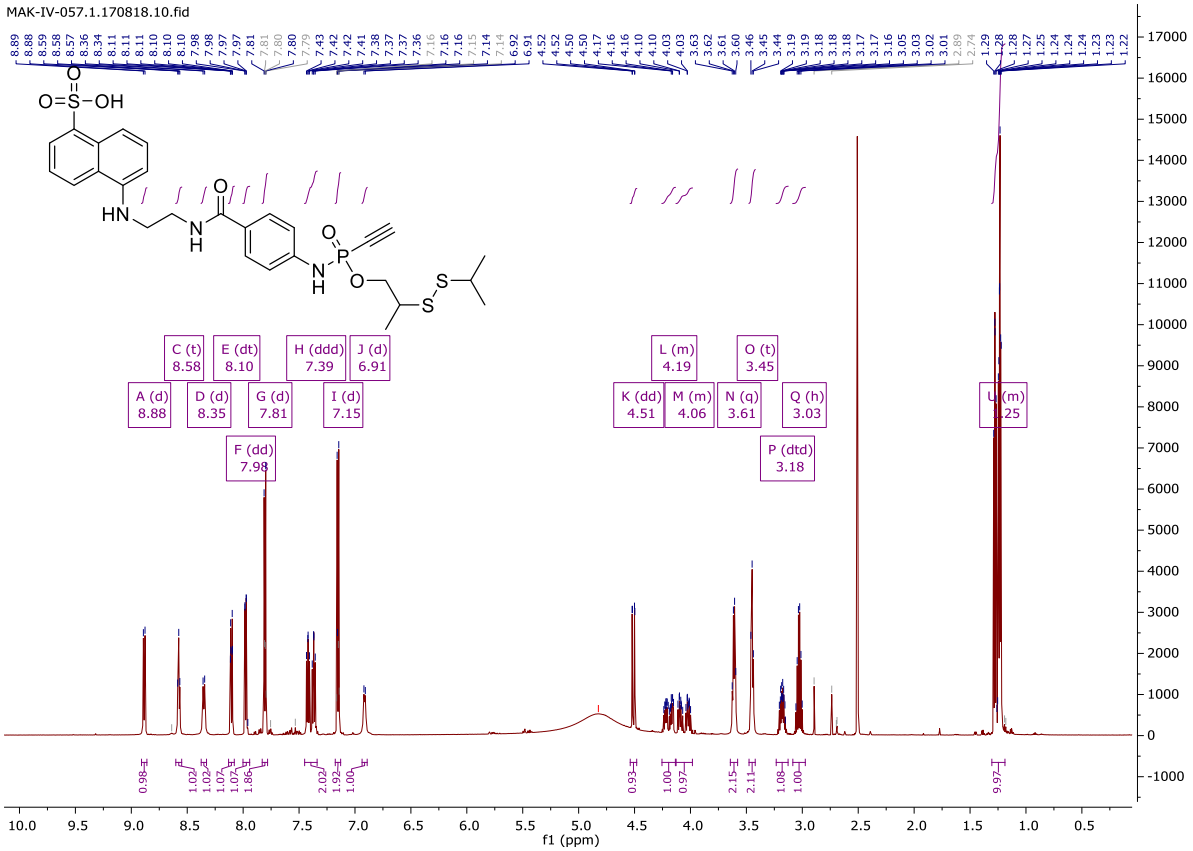

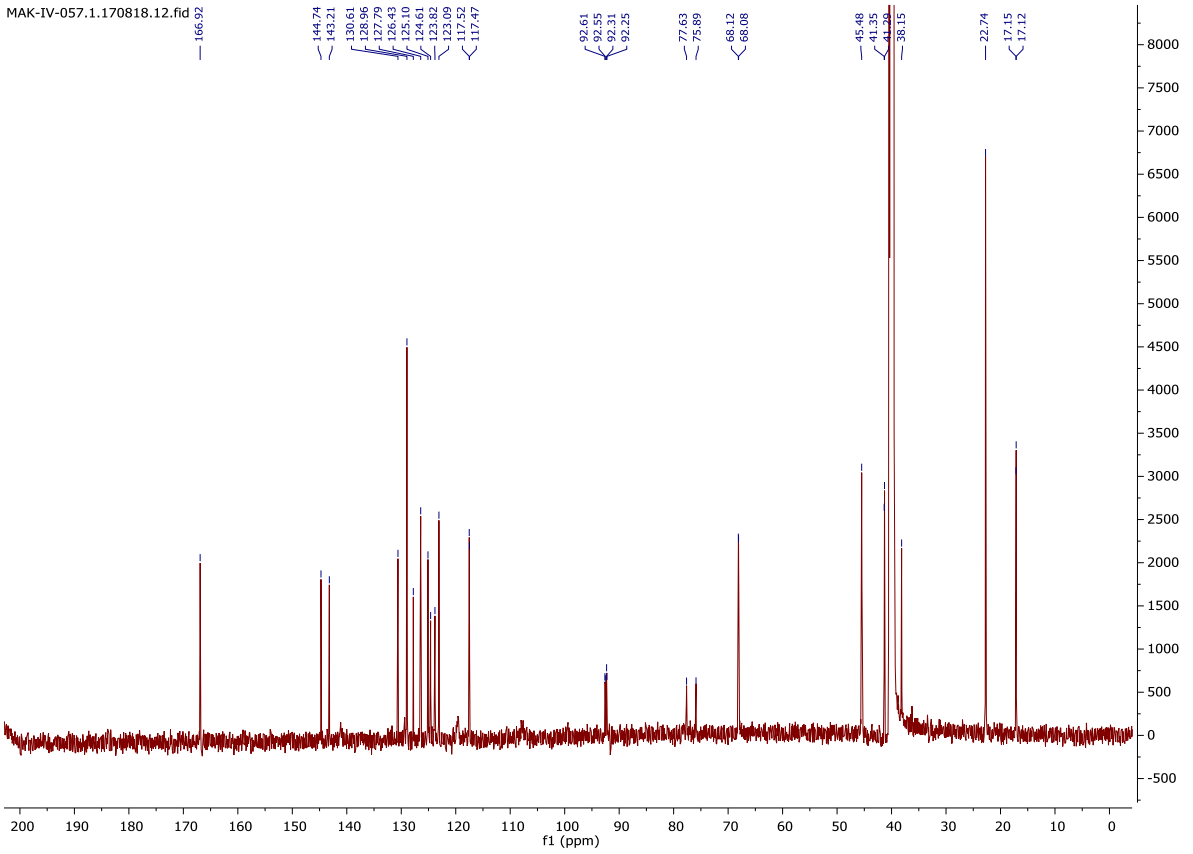

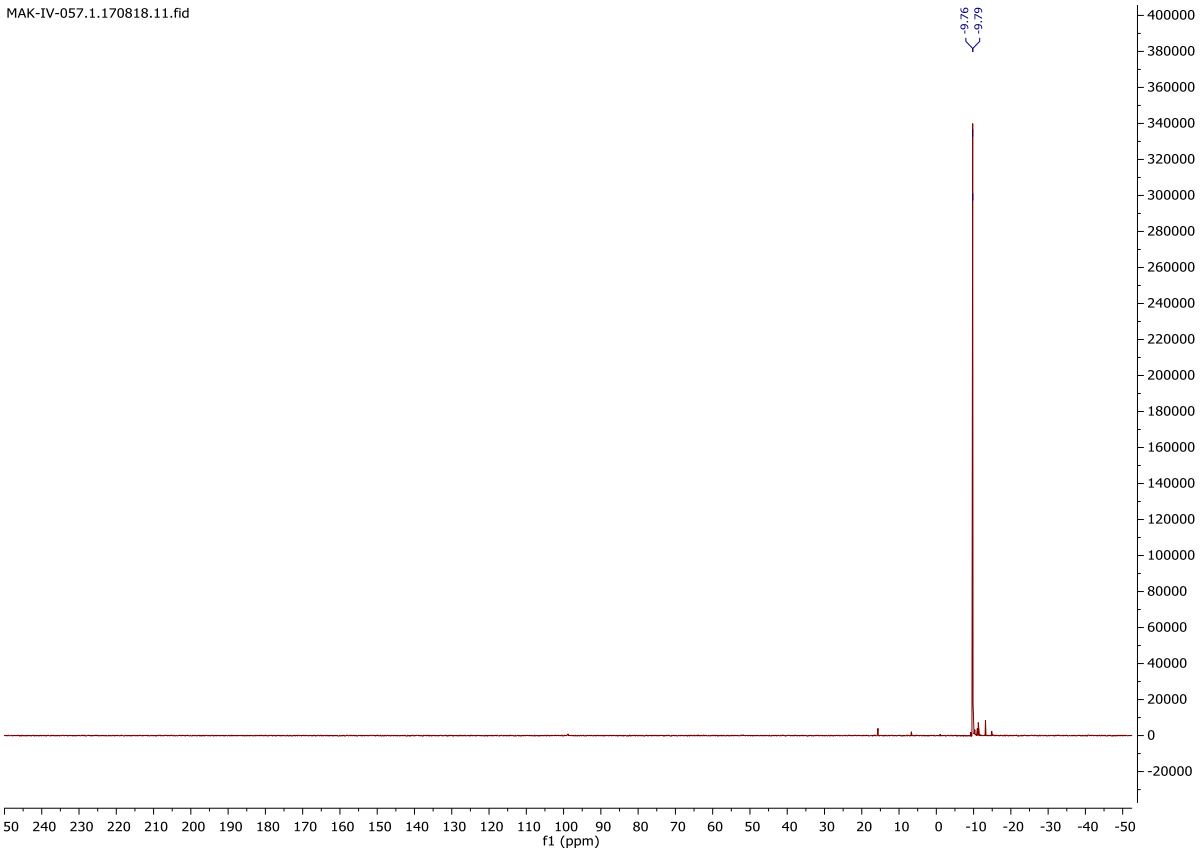

5-(3-Butinyl)-*P*-ethynylphosphonamidato-*N*-benzoyl)ethyl)amino)naphthalene-1-sulfonic acid (**26**)

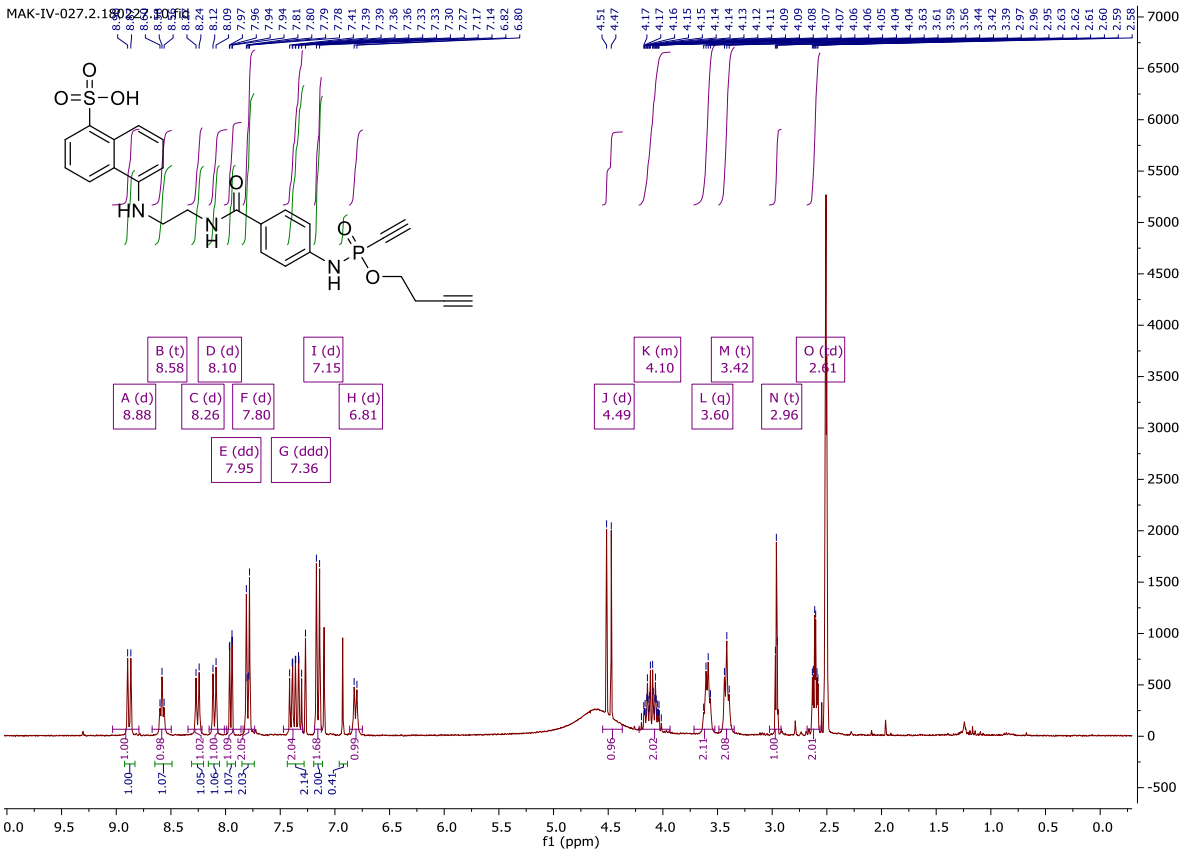

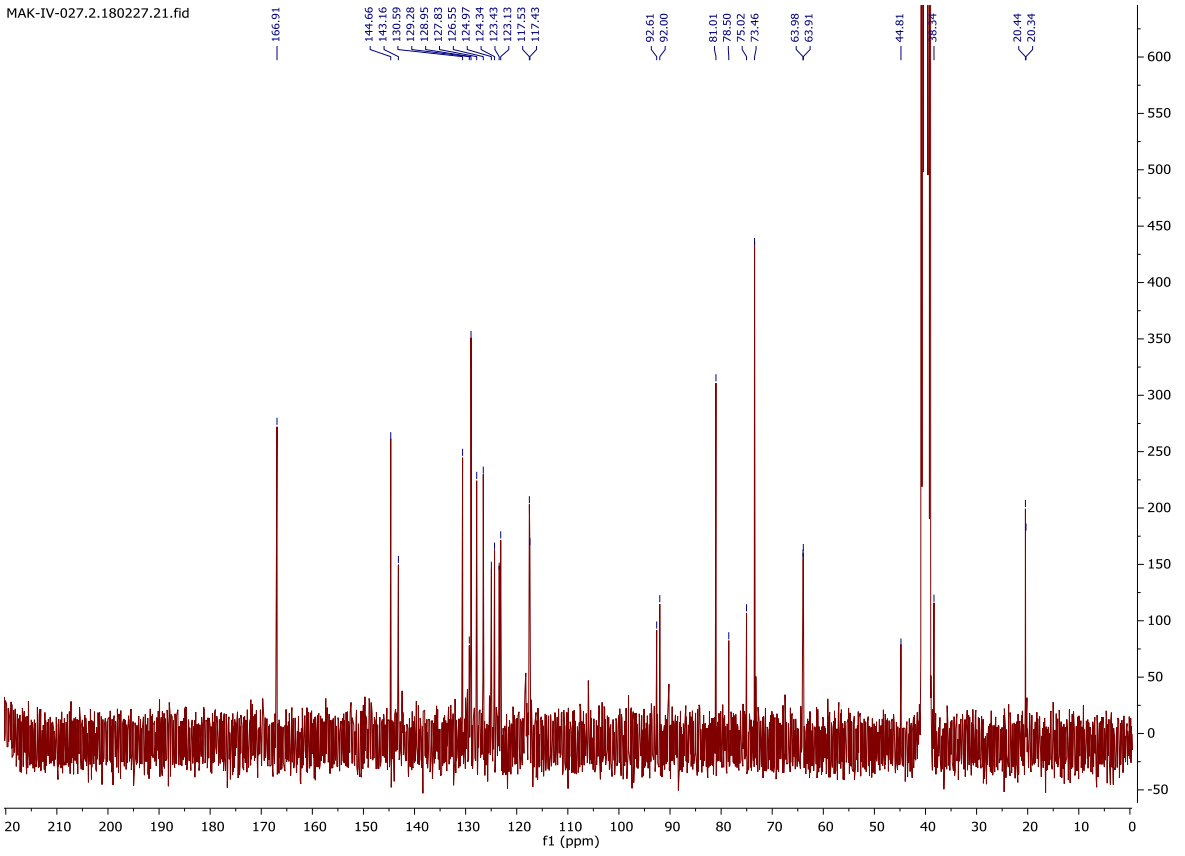
MAK-IV-027.2.180227.21.fid
166.91
144.66
143.16
130.59
129.28
128.95
127.83
126.55
124.97
124.34
123.43
123.13
117.53
117.43
92.61
92.00
81.01
78.50
75.02
73.46
63.98
63.91
44.81
38.34
20.44
20.34
f1 (ppm)

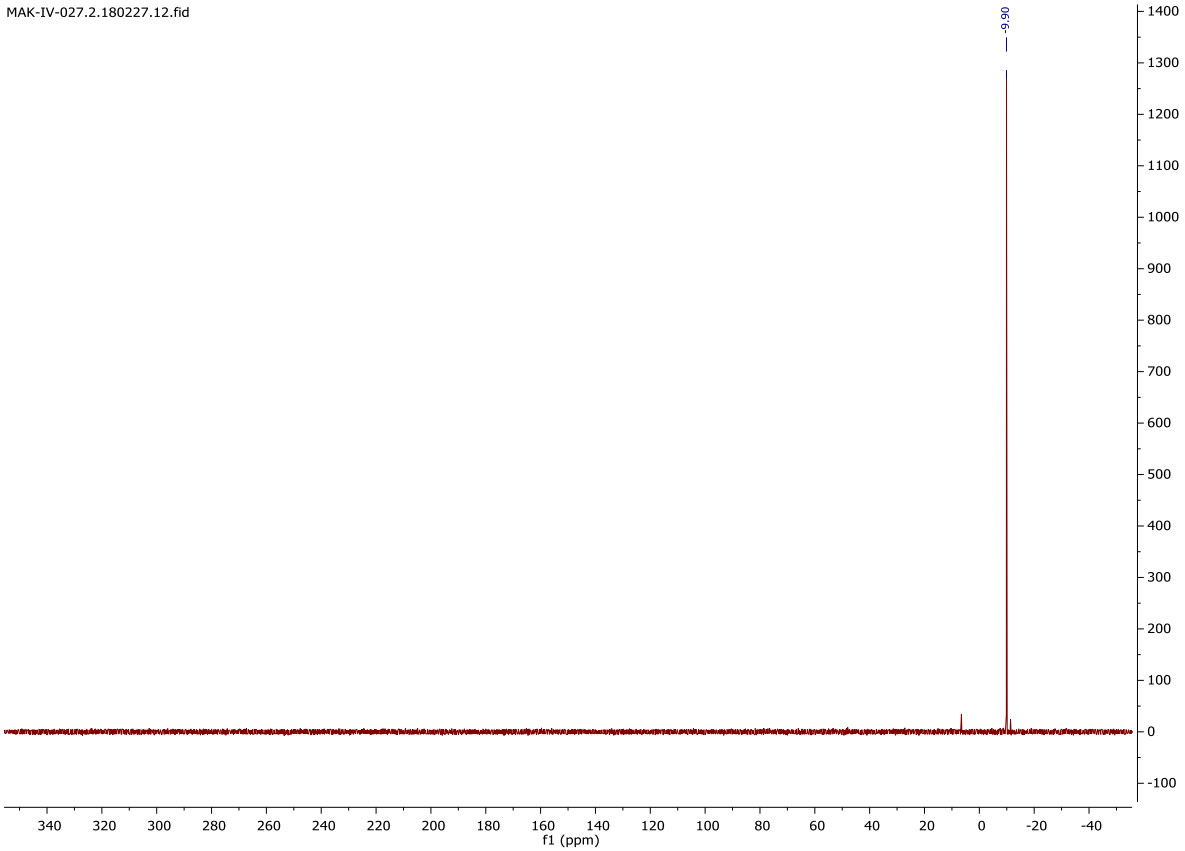
MAK-IV-027.2.180227.12.fid
-9.90
f1 (ppm)

5-(2-(2-Hydroxyethoxy)ethyl-)-*P*-ethynylphosphonamidato-*N*-benzoyl)ethyl)amino)naphthalene-1-sulfonic acid (**27**)

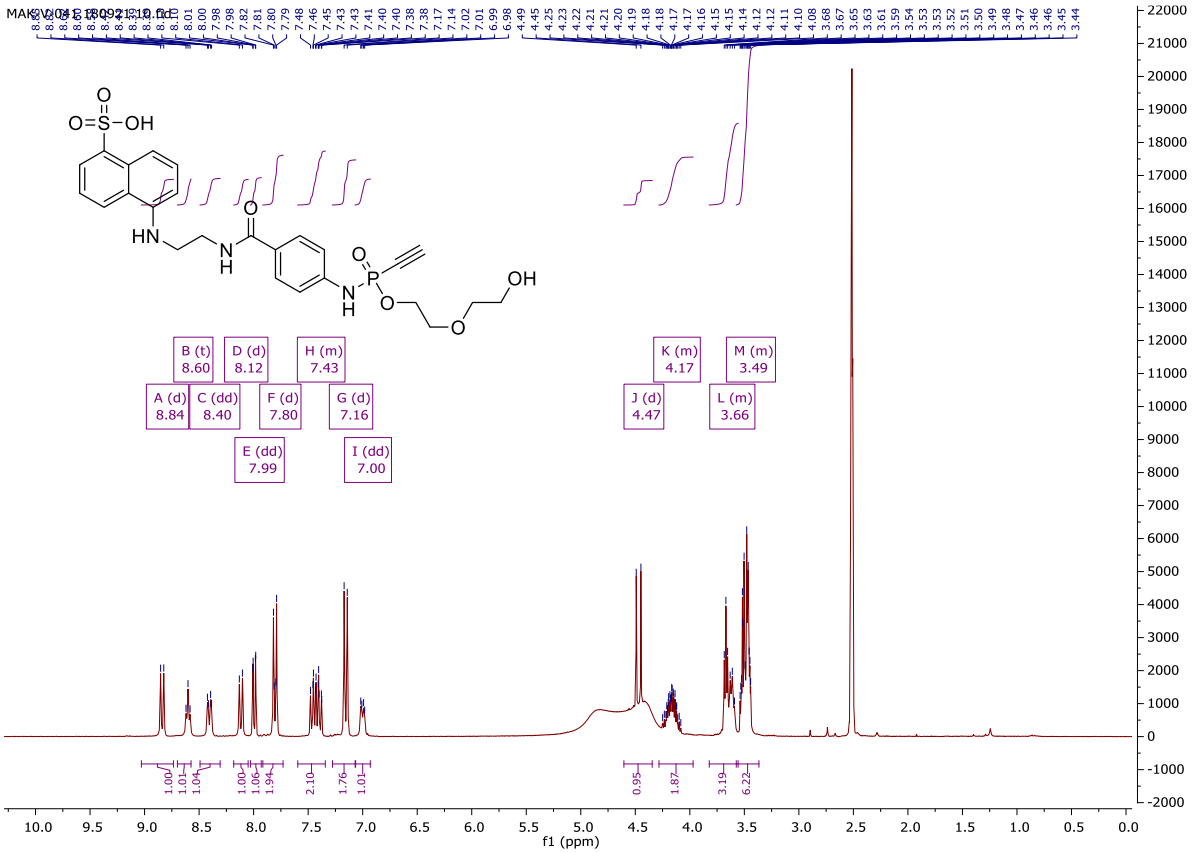

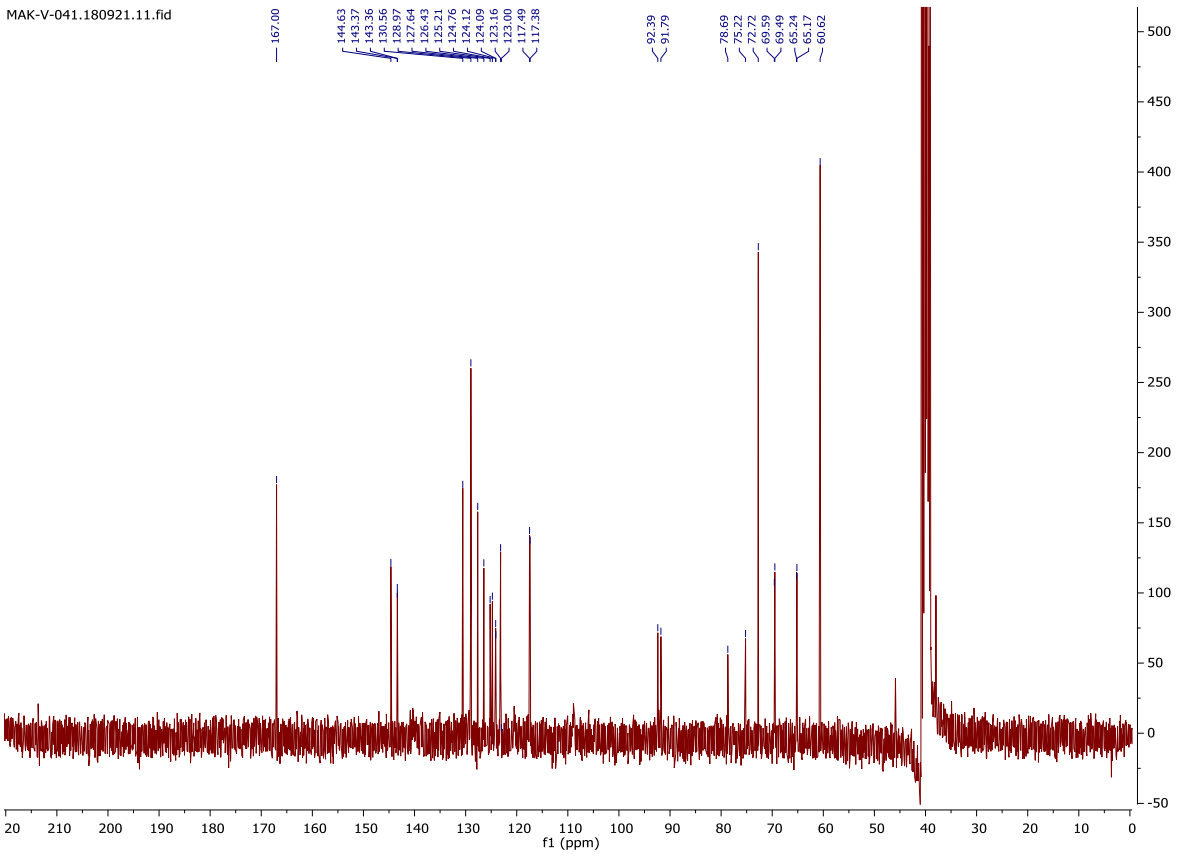

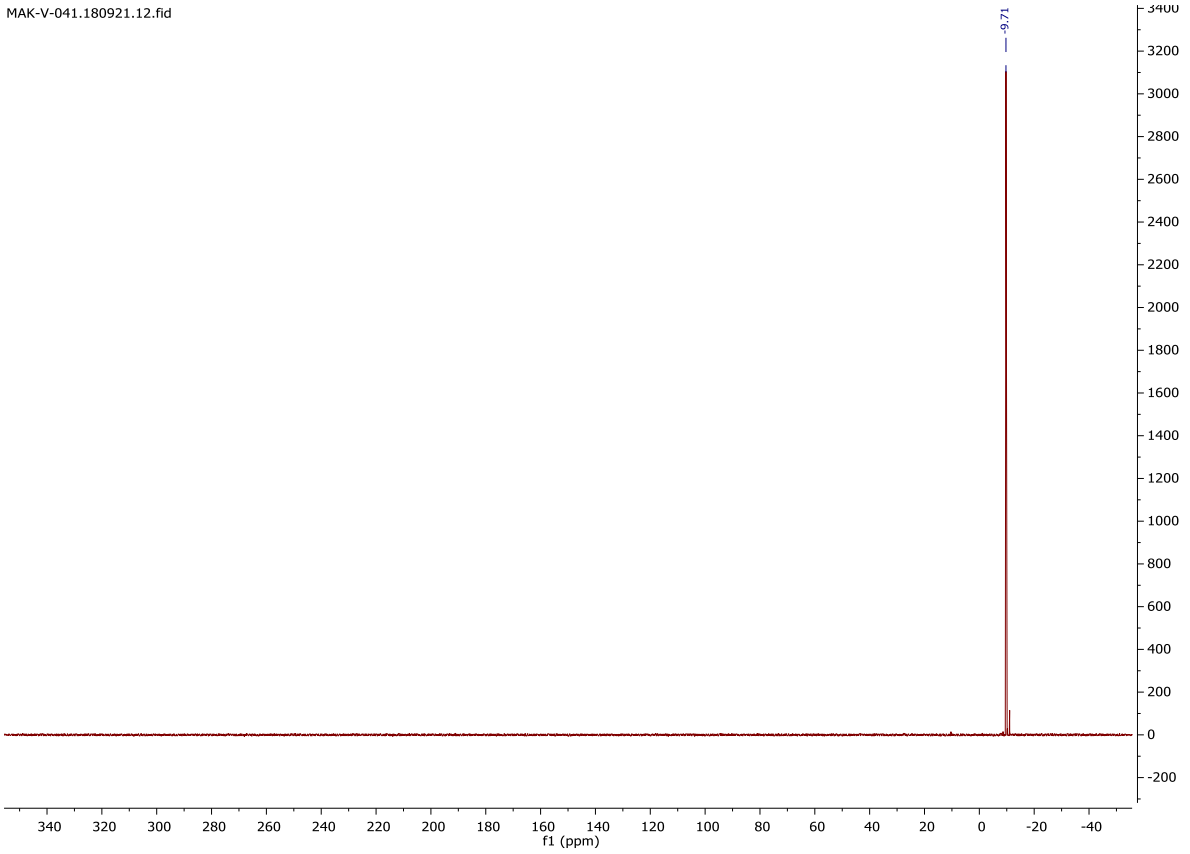

5-((2-(*O*-(4-acetoxybenzyl)-*P*-ethynylphosphonamidato-*N*-benzoyl)ethyl)amino)naphthalene-1-sulfonic acid (**28**)

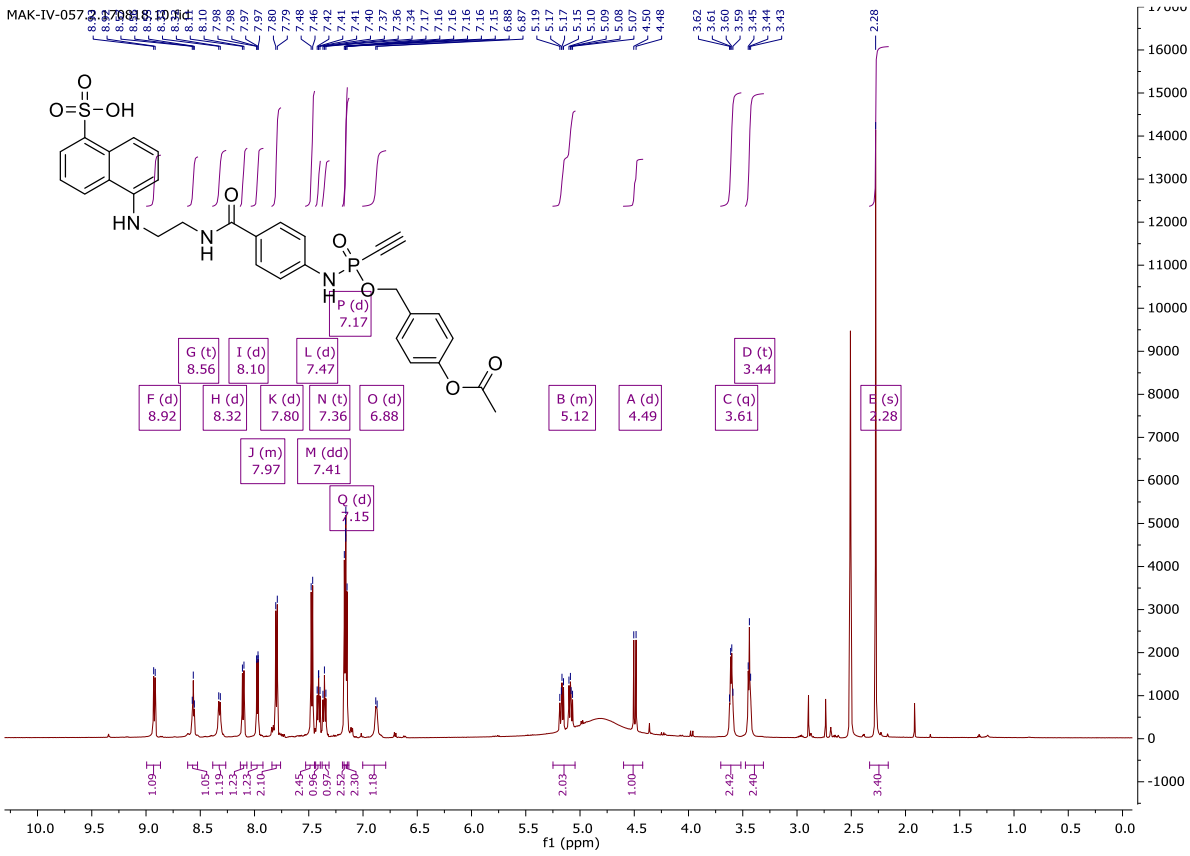

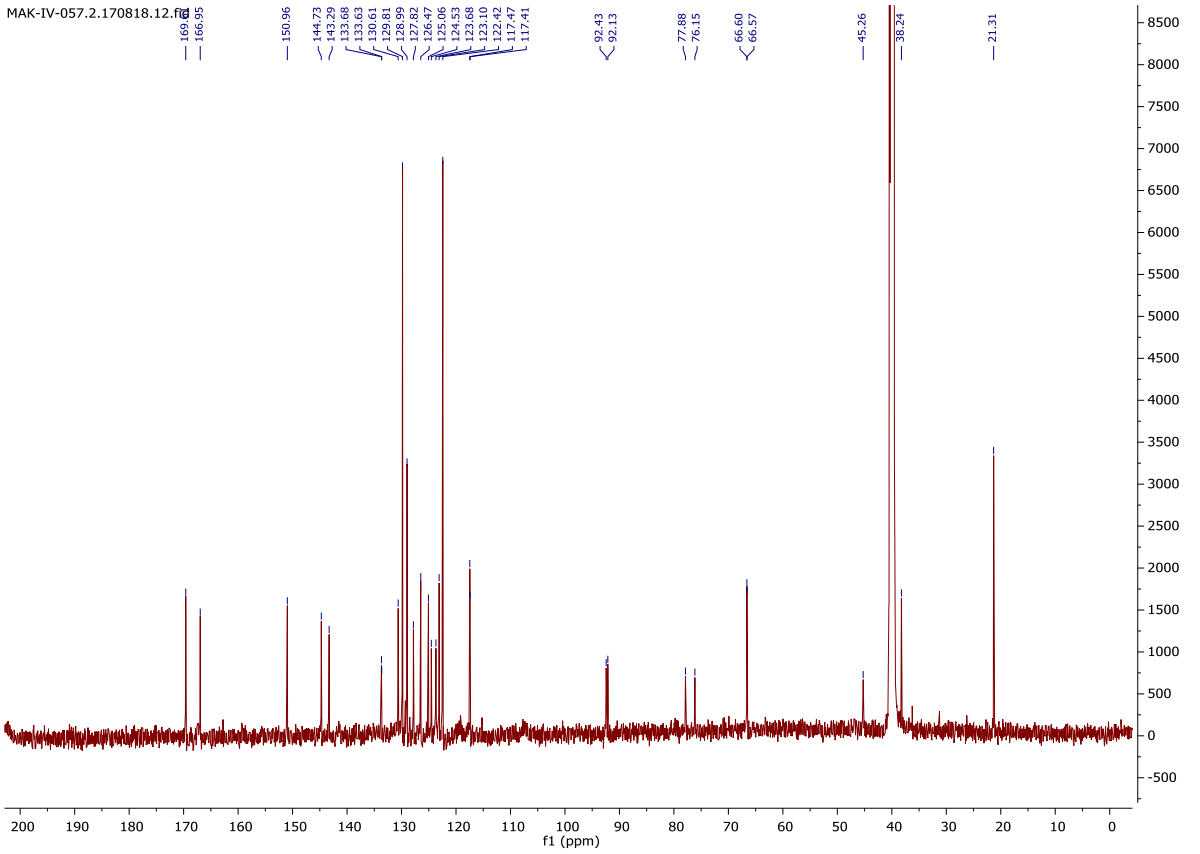
MAK-IV-057.2.170818.12.fid
169.76
166.95
150.96
144.73
143.29
133.68
133.63
130.61
129.81
128.99
127.82
126.47
125.06
124.53
123.68
123.10
122.42
117.47
117.41
92.43
92.13
77.88
76.15
66.60
66.57
45.26
38.24
21.31
f1 (ppm)

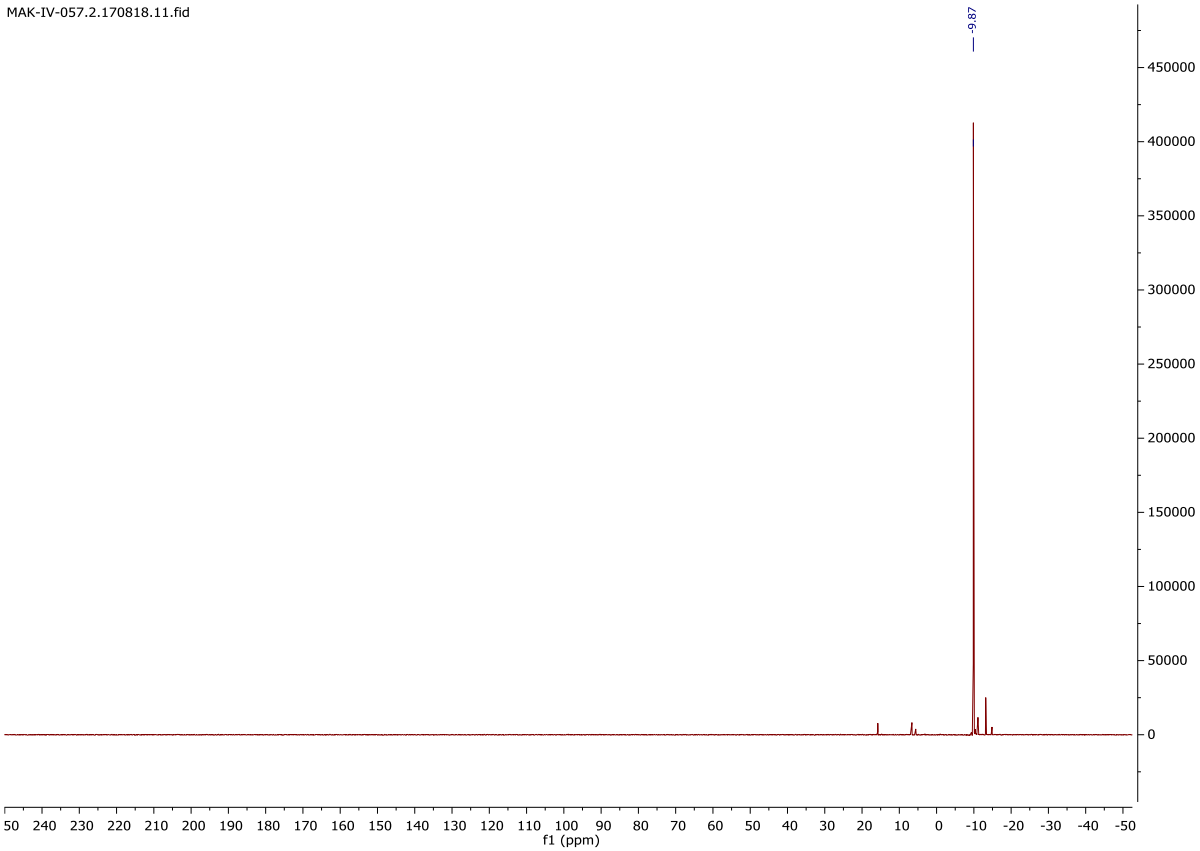
MAK-IV-057.2.170818.11.fid
-9.87
f1 (ppm)

5-((2-(*O*-(4-Diazophenyl-benzyl)-*P*-ethynylphosphonamidato-*N*-benzoyl)ethyl)amino)naphthalene-1-sulfonic acid (**29**)

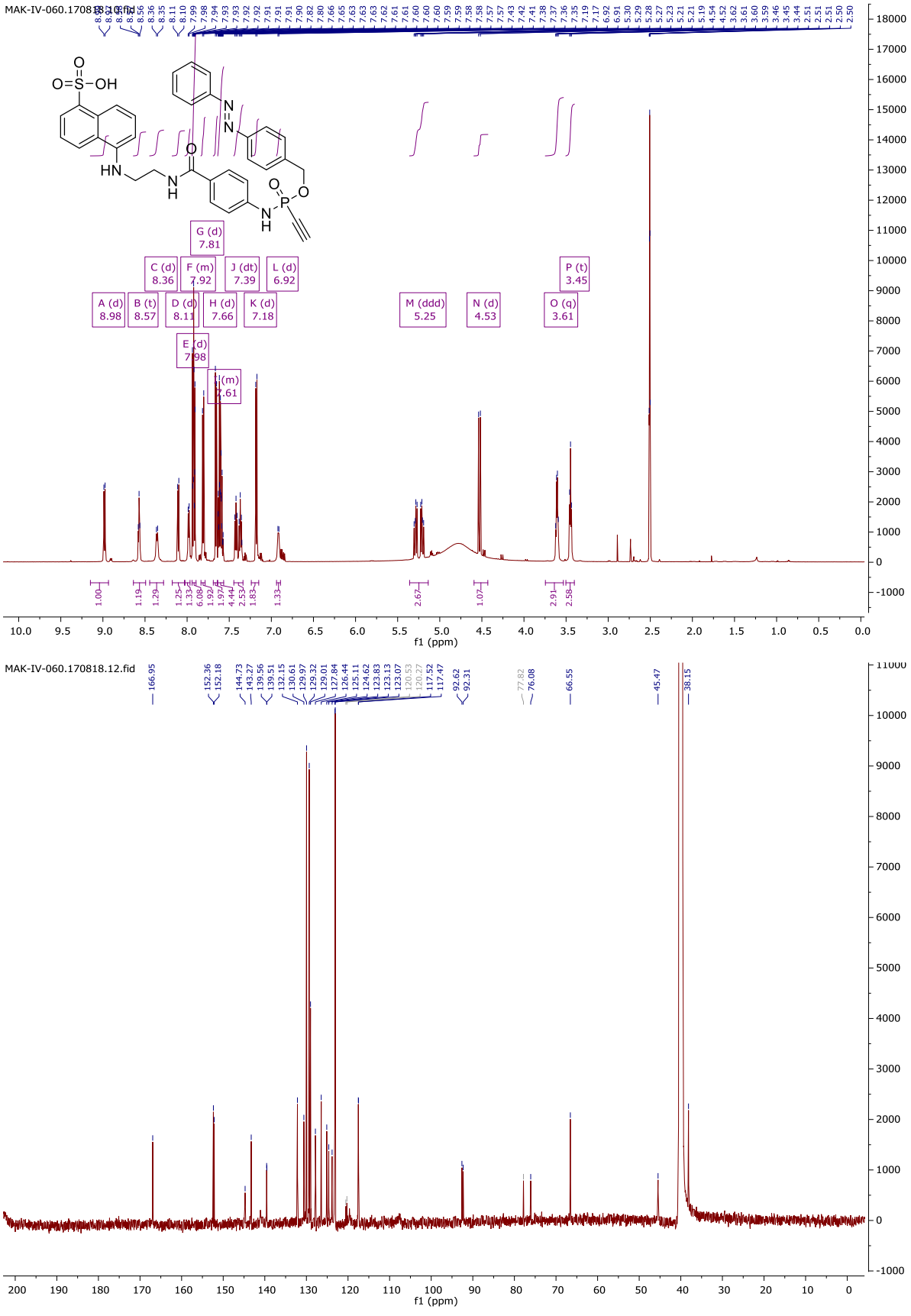

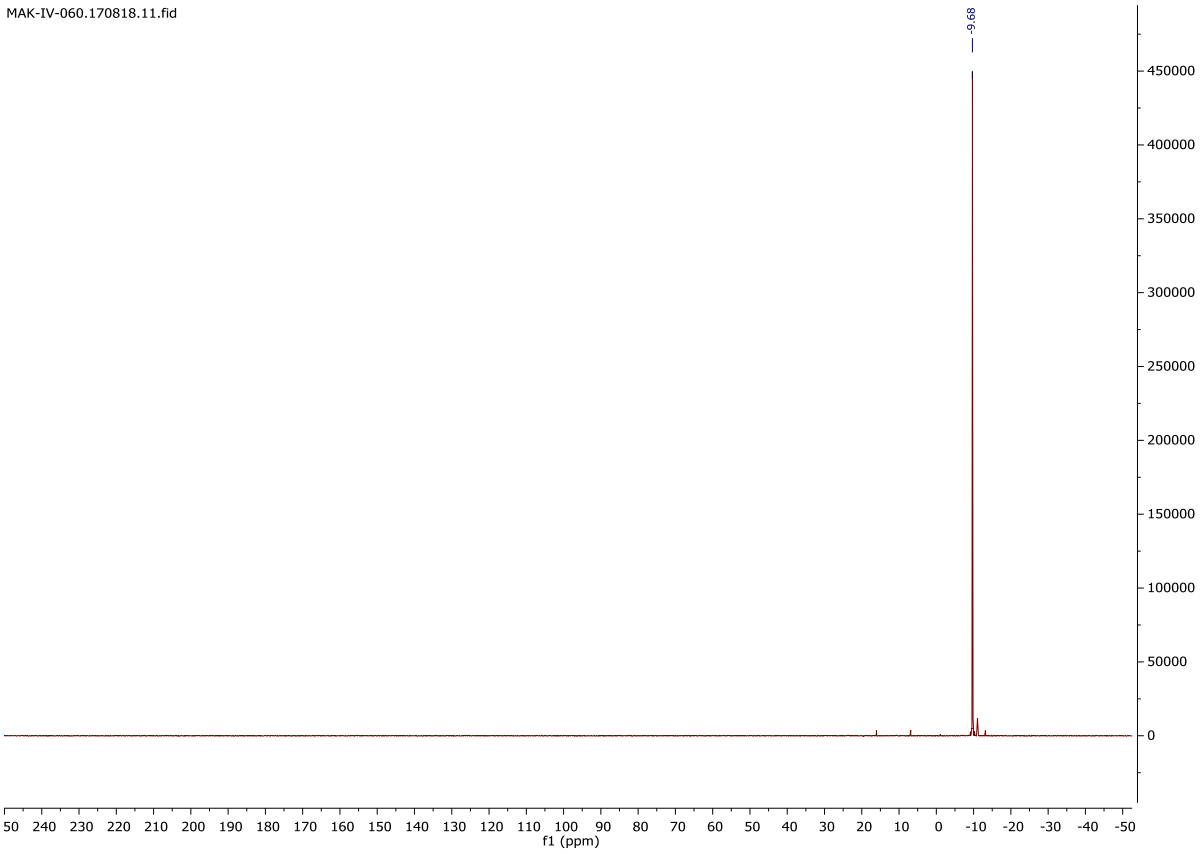

Phenyl-*N*-phenyl-*P*-(2-phenyloxyvinyl)phosphonamidate (**31**)

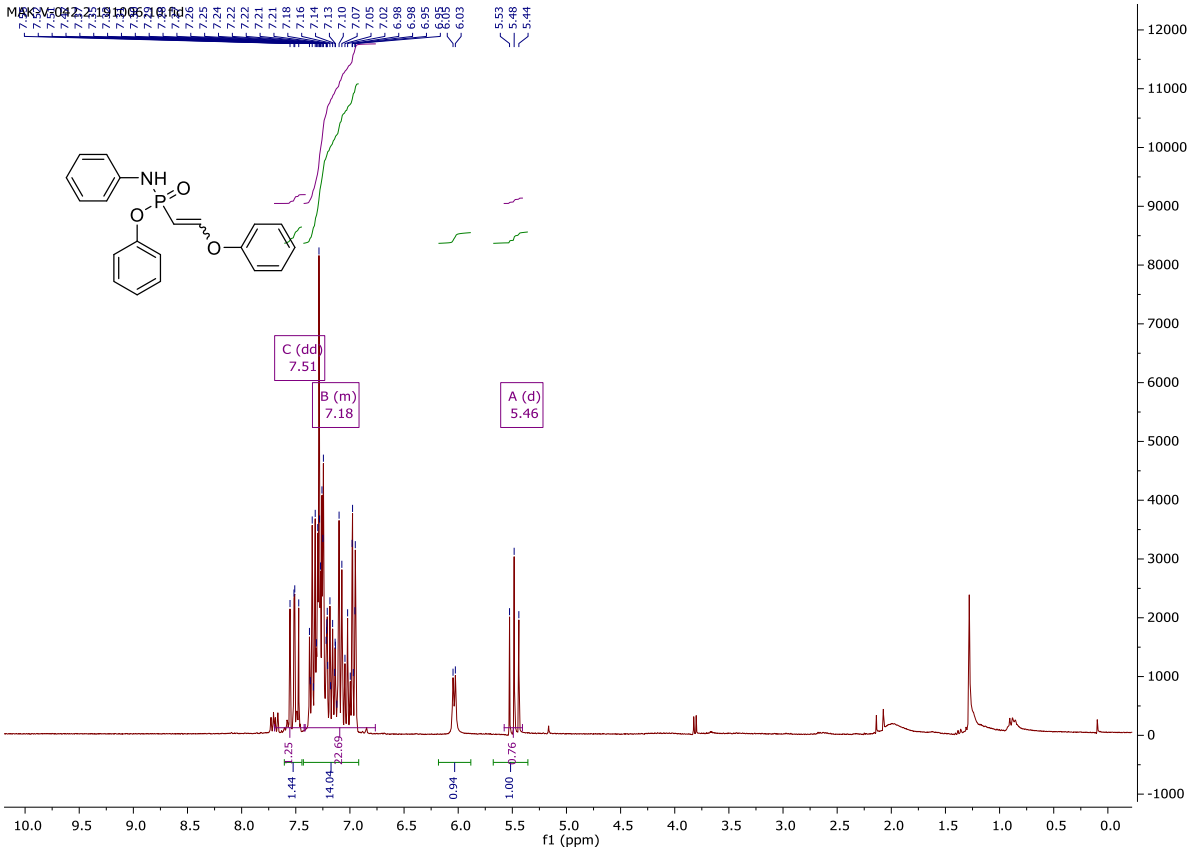

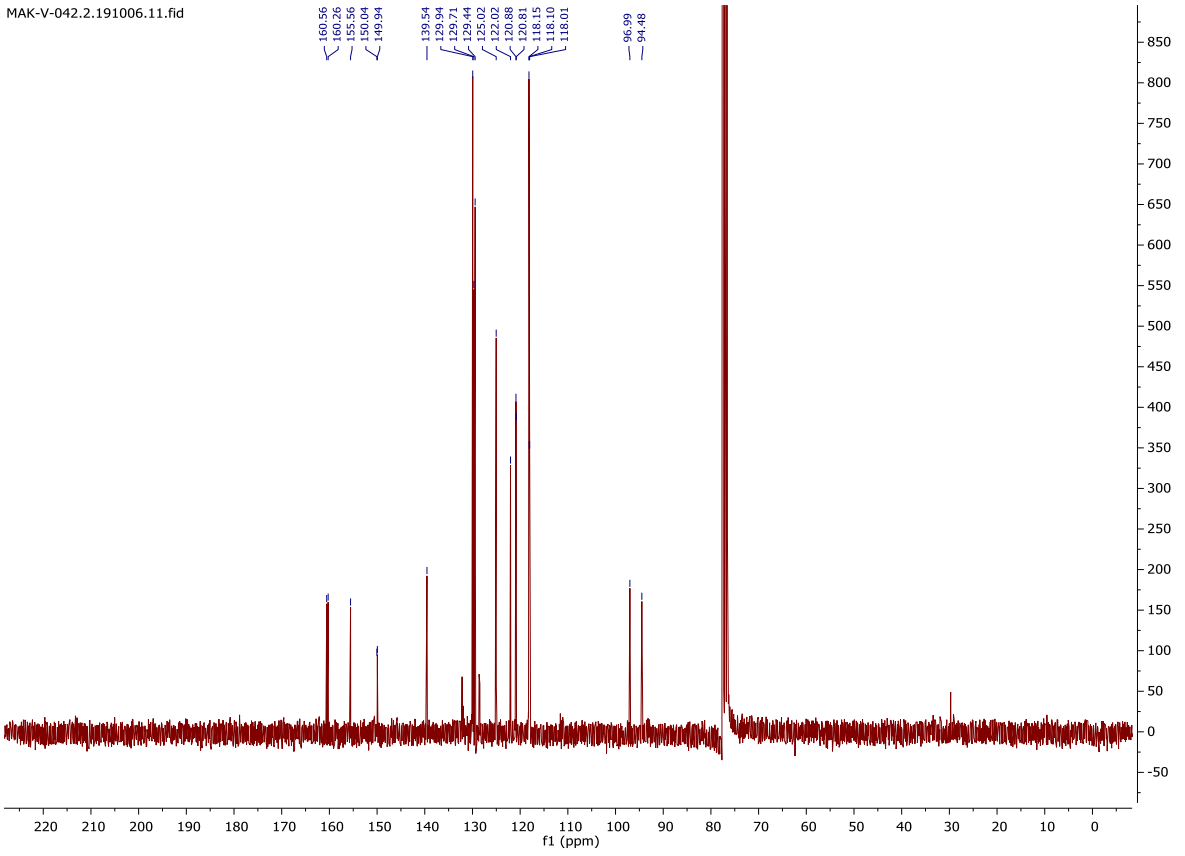
MAK-V-042.2.191006.11.fid
160.56
160.26
155.56
150.04
149.94
139.54
129.94
129.71
129.44
125.02
122.02
120.88
120.81
118.15
118.10
118.01
96.99
94.48
f1 (ppm)

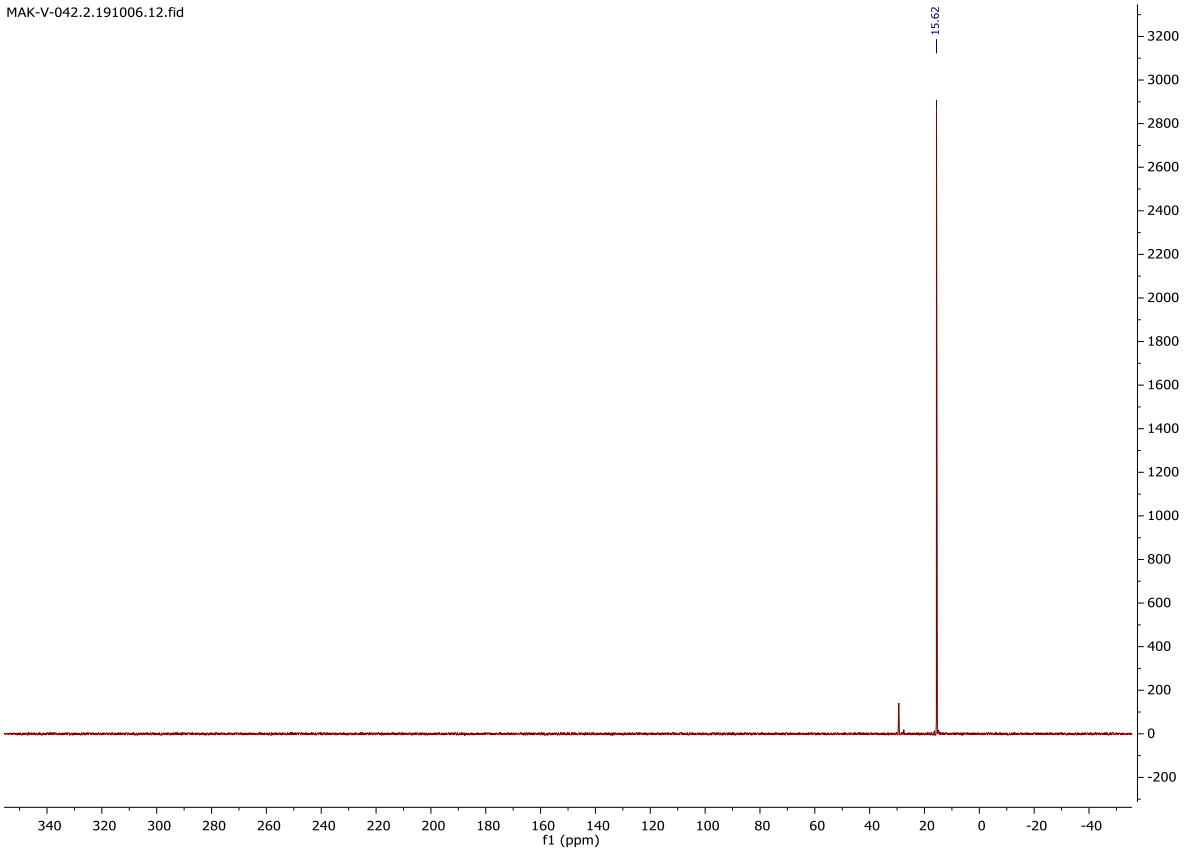
MAK-V-042.2.191006.12.fid
15.62
f1 (ppm)

1-(2-azidoethyl)-3,3-Dimethyl-2-methyleneindoline (**43**)

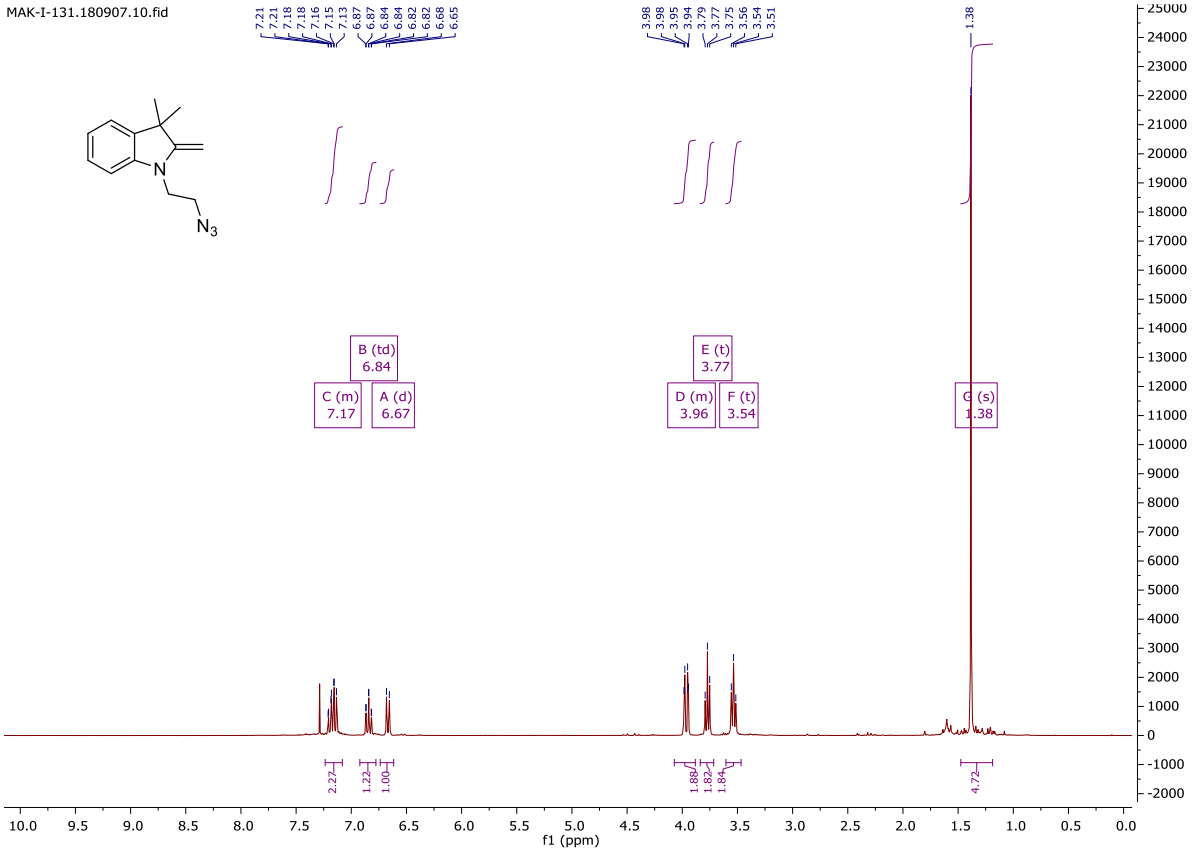

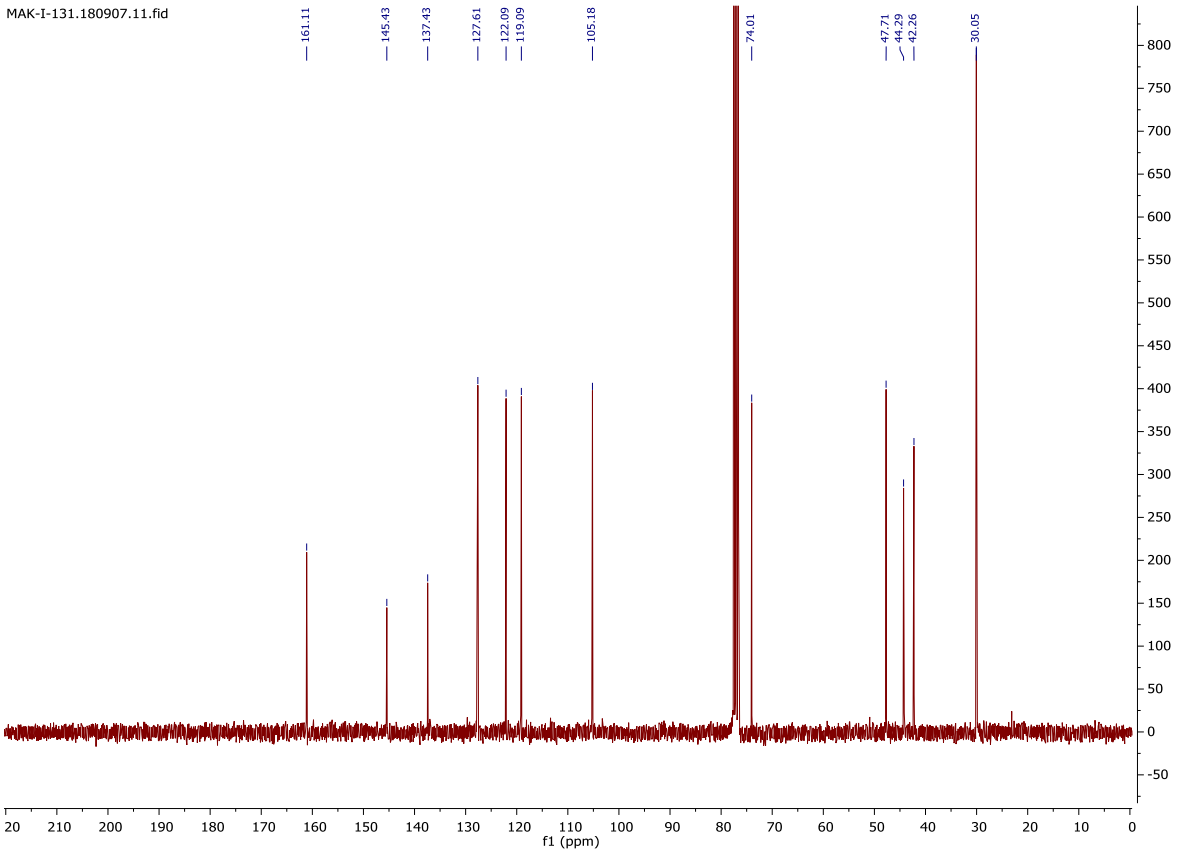

Cy5 azide **45**

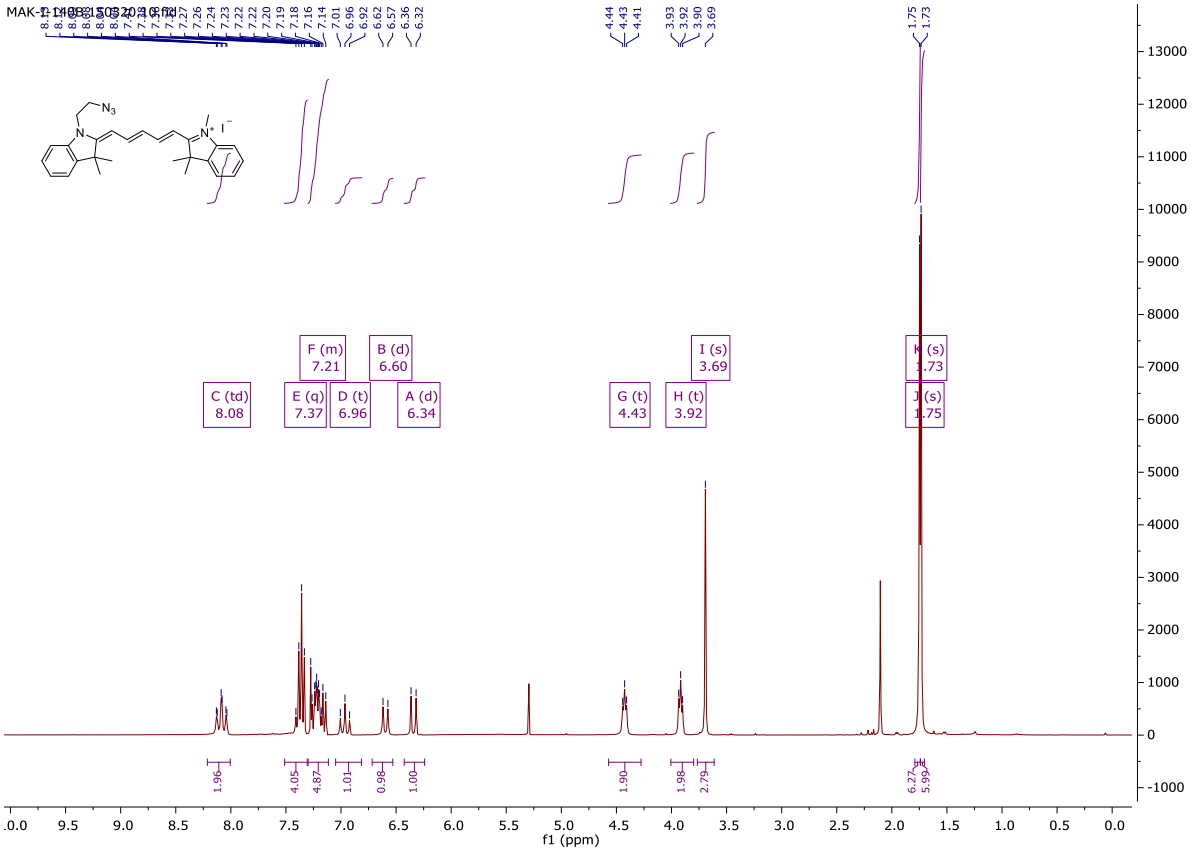
MAK-I-140B.150320.16.fid
F (m) 7.21
B (d) 6.60
I (s) 3.69
K (s) 1.73
C (td) 8.08
E (q) 7.37
D (t) 6.96
A (d) 6.34
G (t) 4.43
H (t) 3.92
J (s) 1.75
f1 (ppm)

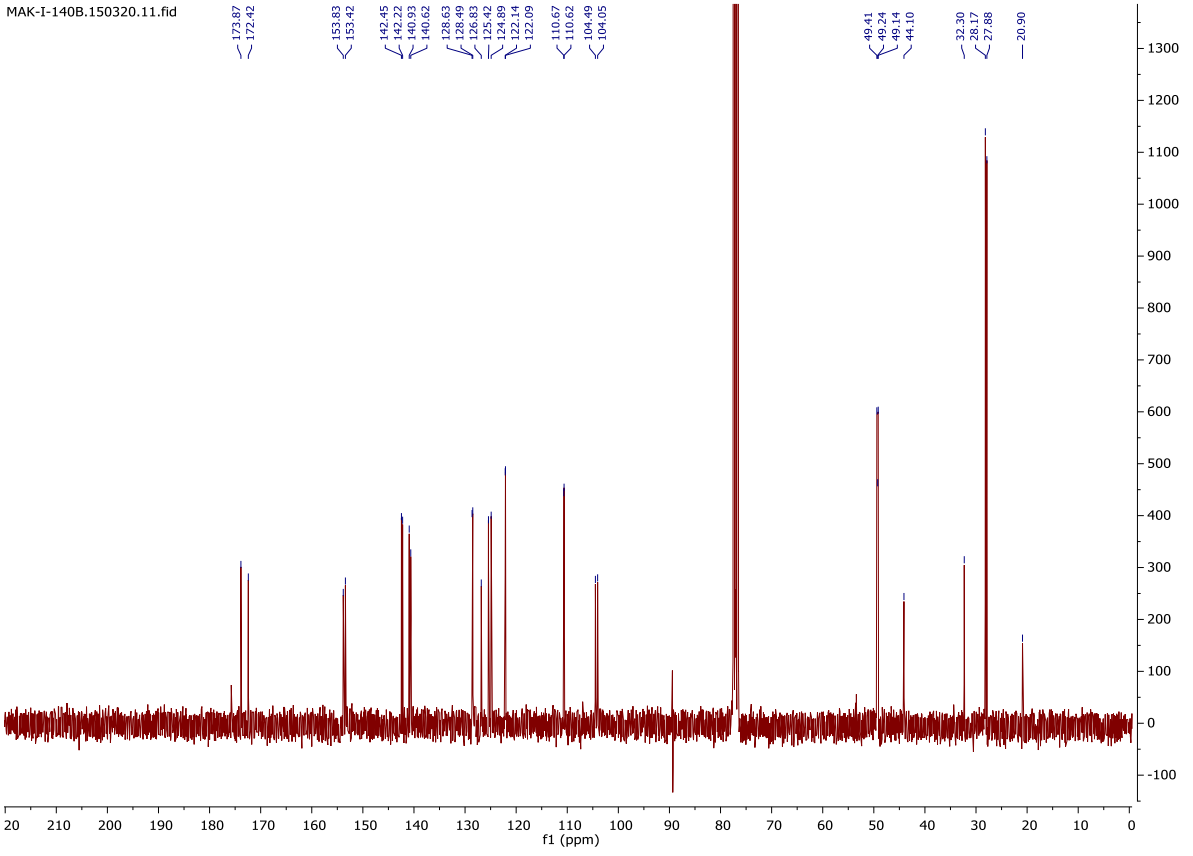
MAK-I-140B.150320.11.fid
f1 (ppm)

Ethyl-*N*-(4-carboxy-phenyl)-*P*-vinyl-phosphonamidate (**48**)

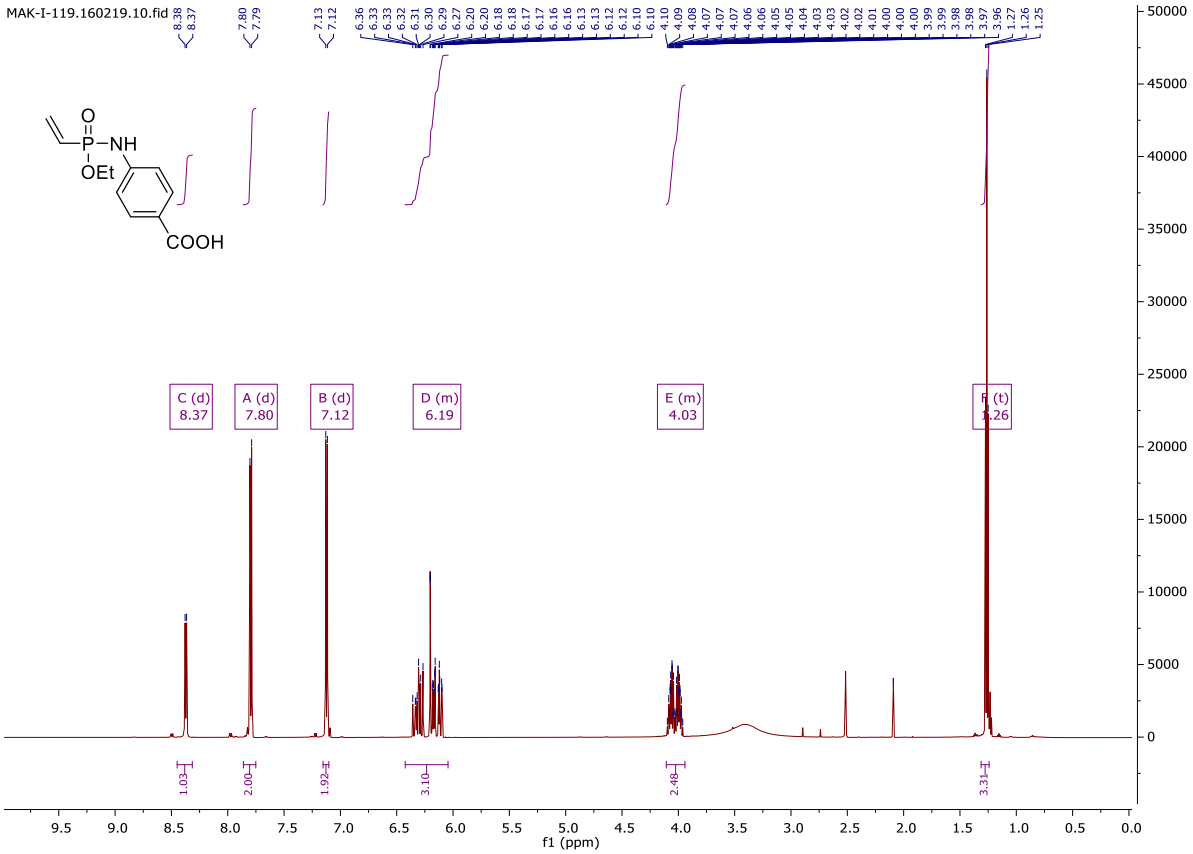

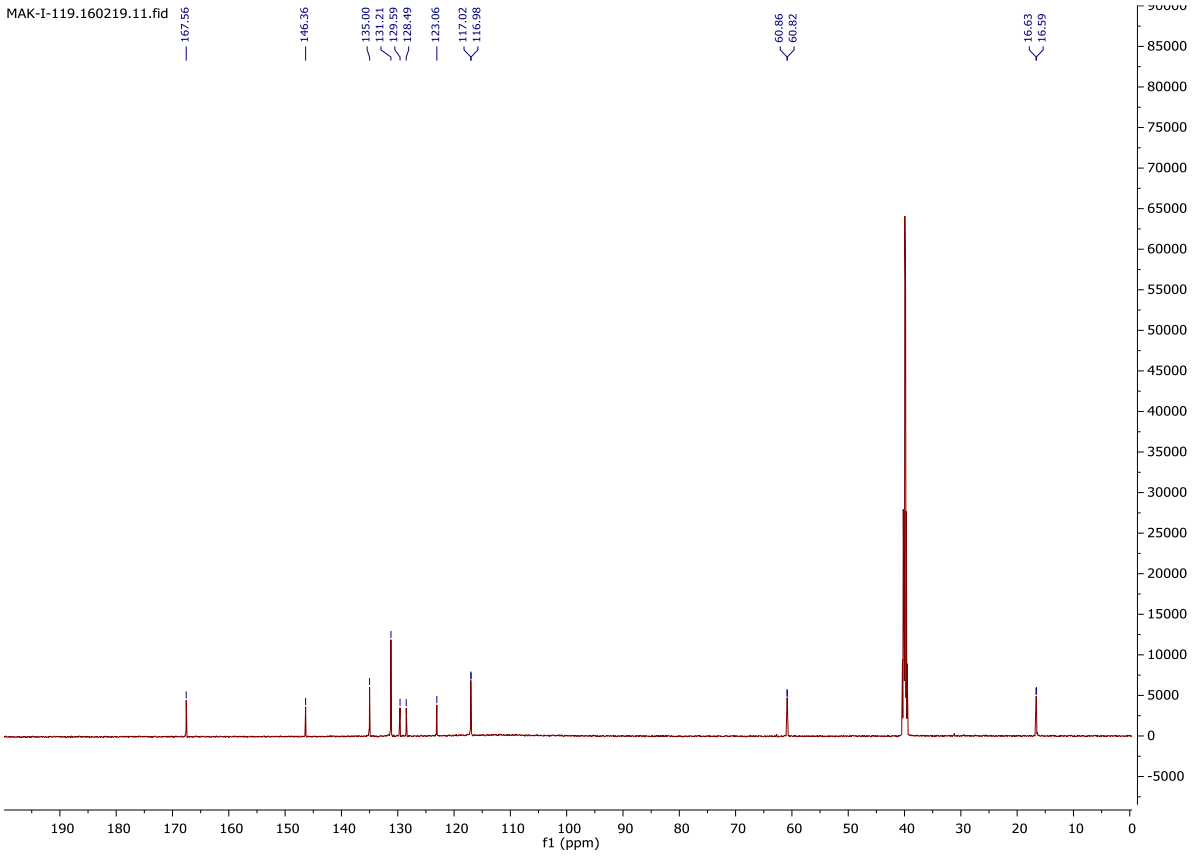

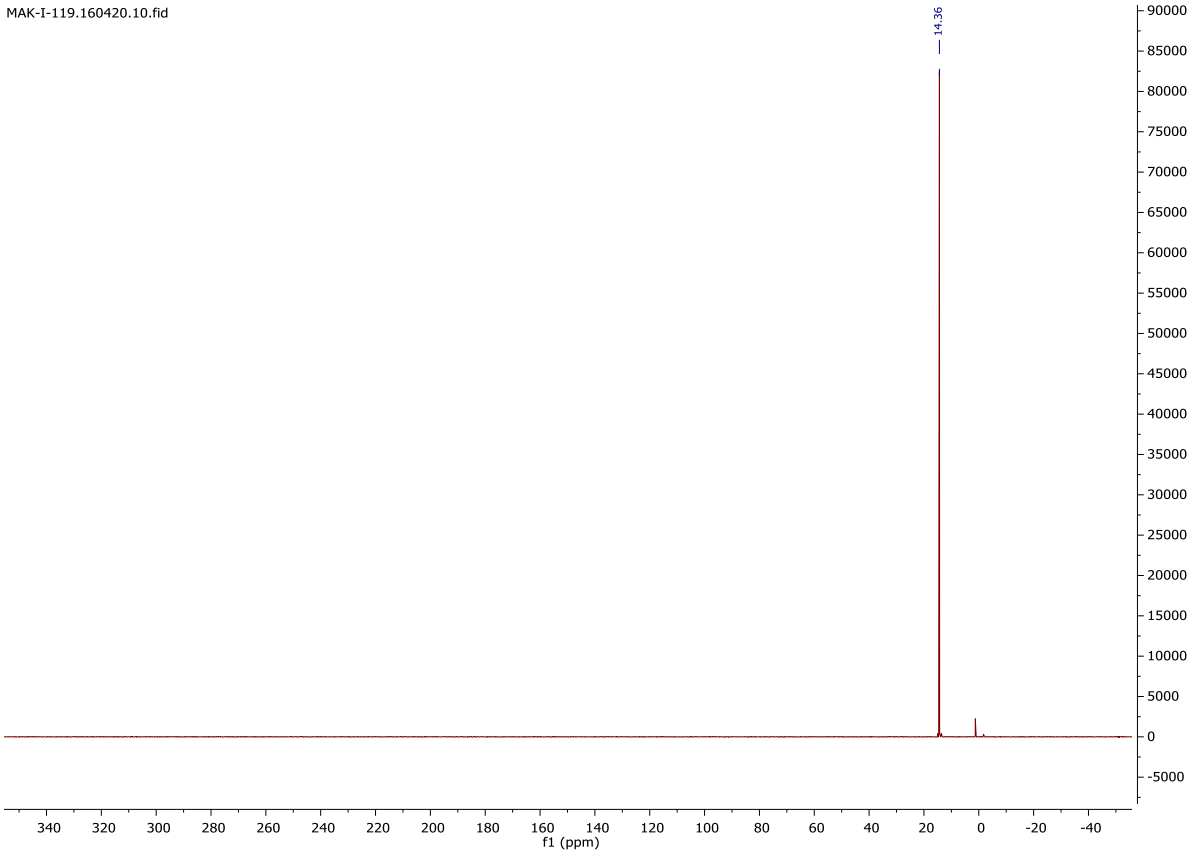

Ethyl-*N*-benzyl-*P*-vinyl-phosphonamidate (**49**)

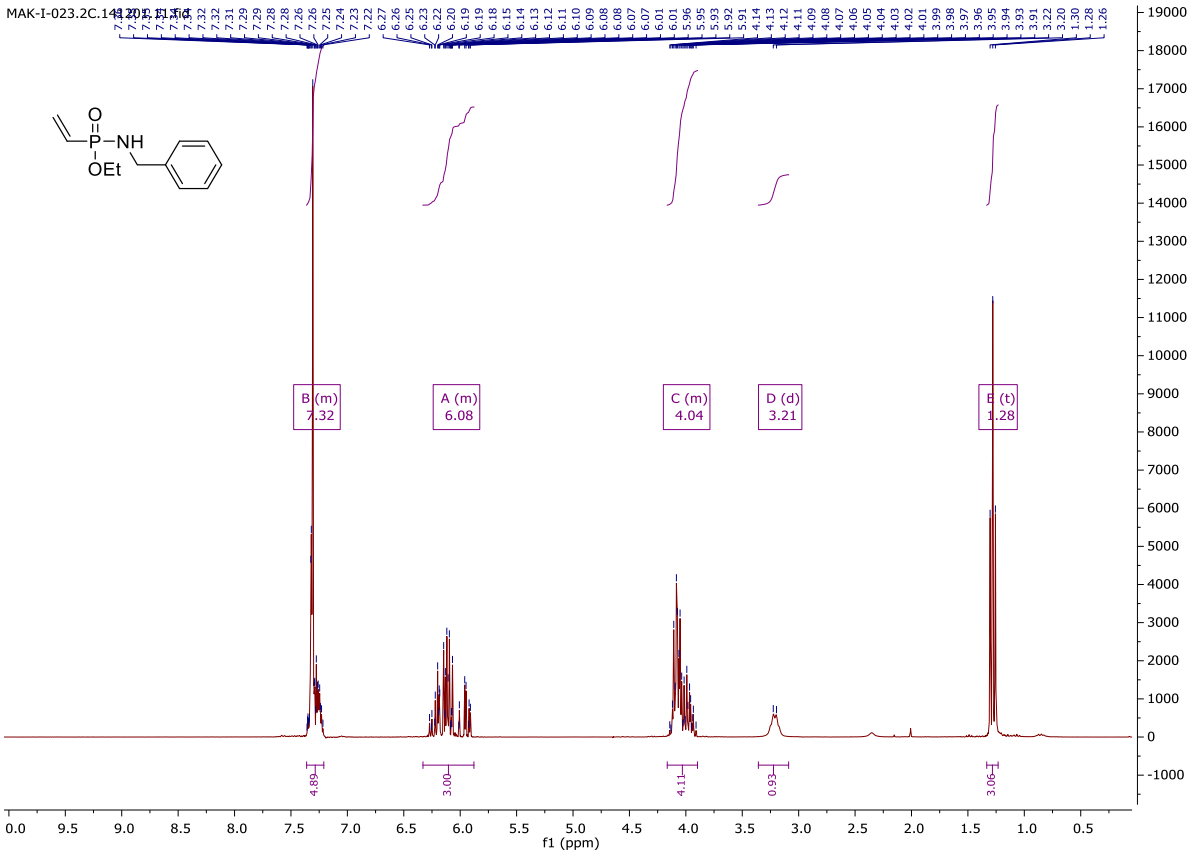

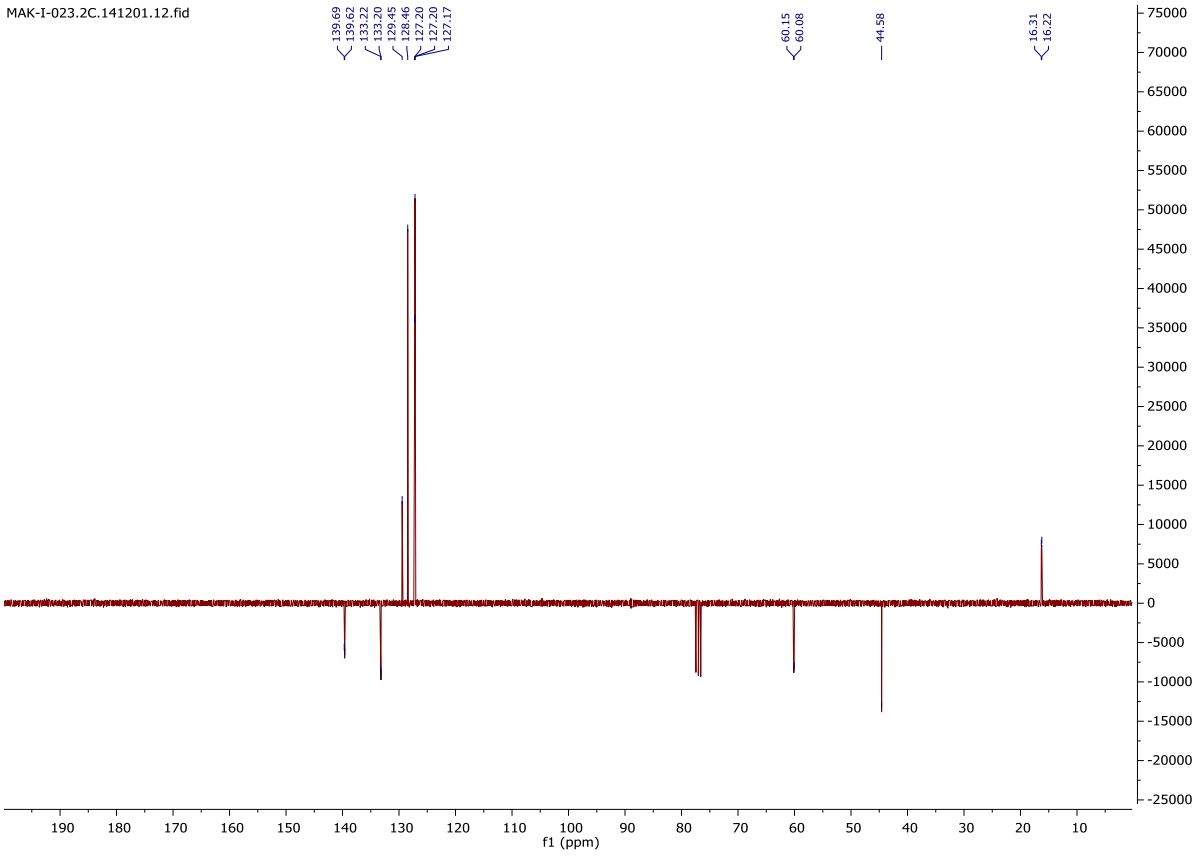
MAK-I-023.2C.141201.12.fid
139.69
139.62
133.22
133.20
129.45
128.46
127.20
127.20
127.17
60.15
60.08
44.58
16.31
16.22
f1 (ppm)

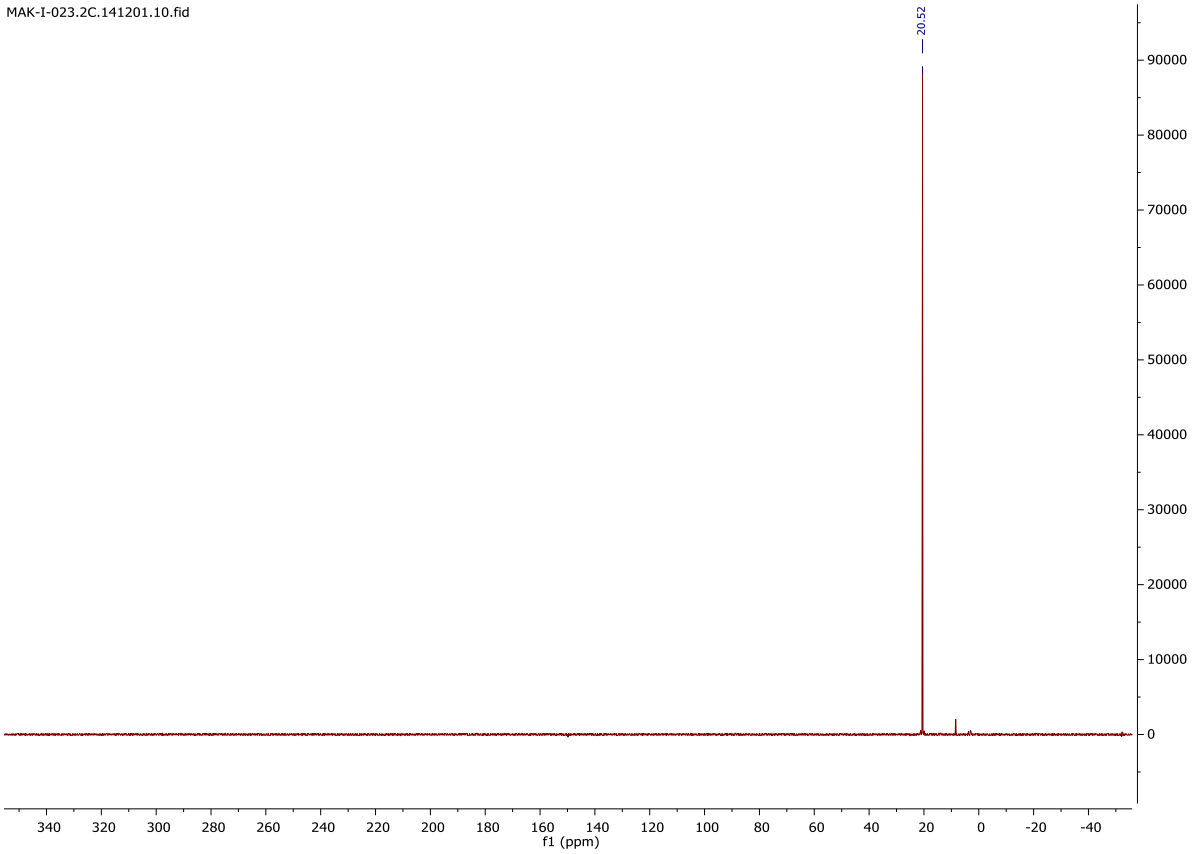
MAK-I-023.2C.141201.10.fid
20.52
f1 (ppm)

Ethyl-*N*-(2-nitro-Benzyl)-*P*-vinyl-phosphonamidate (**50**)

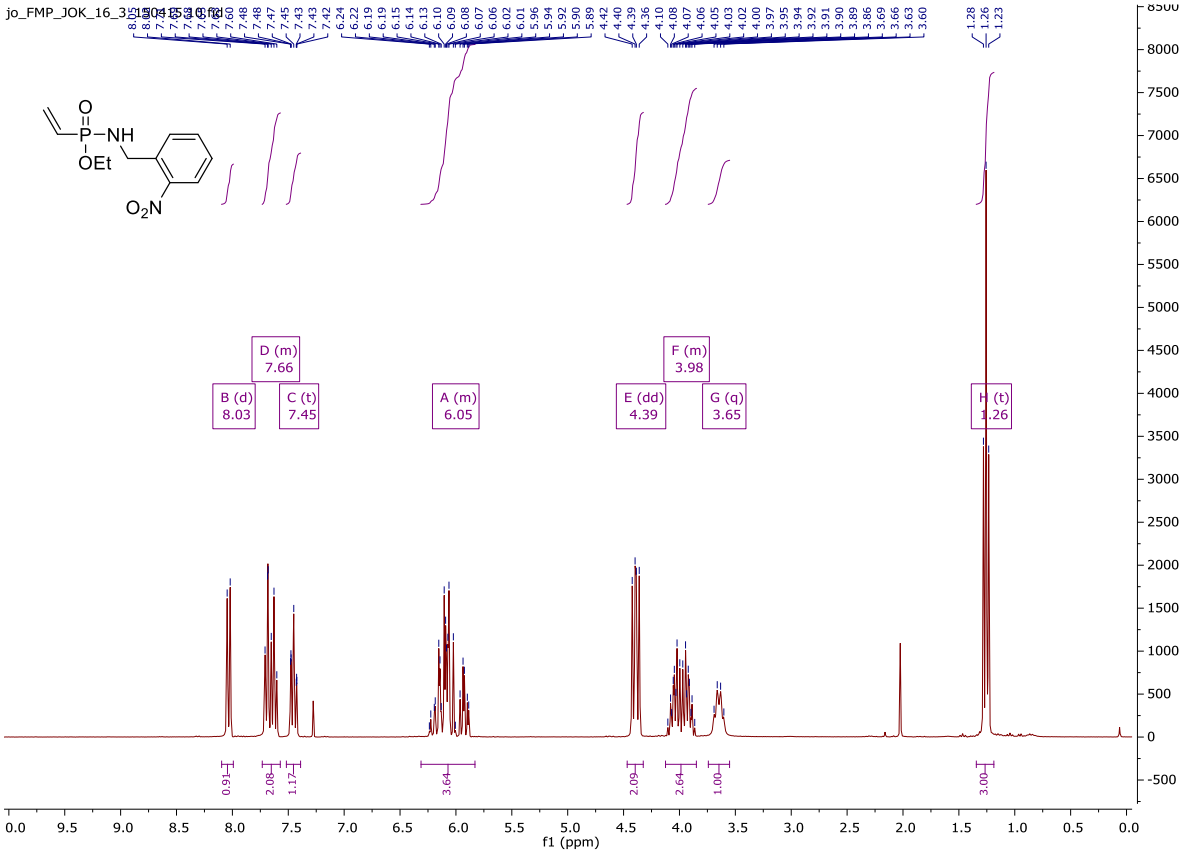

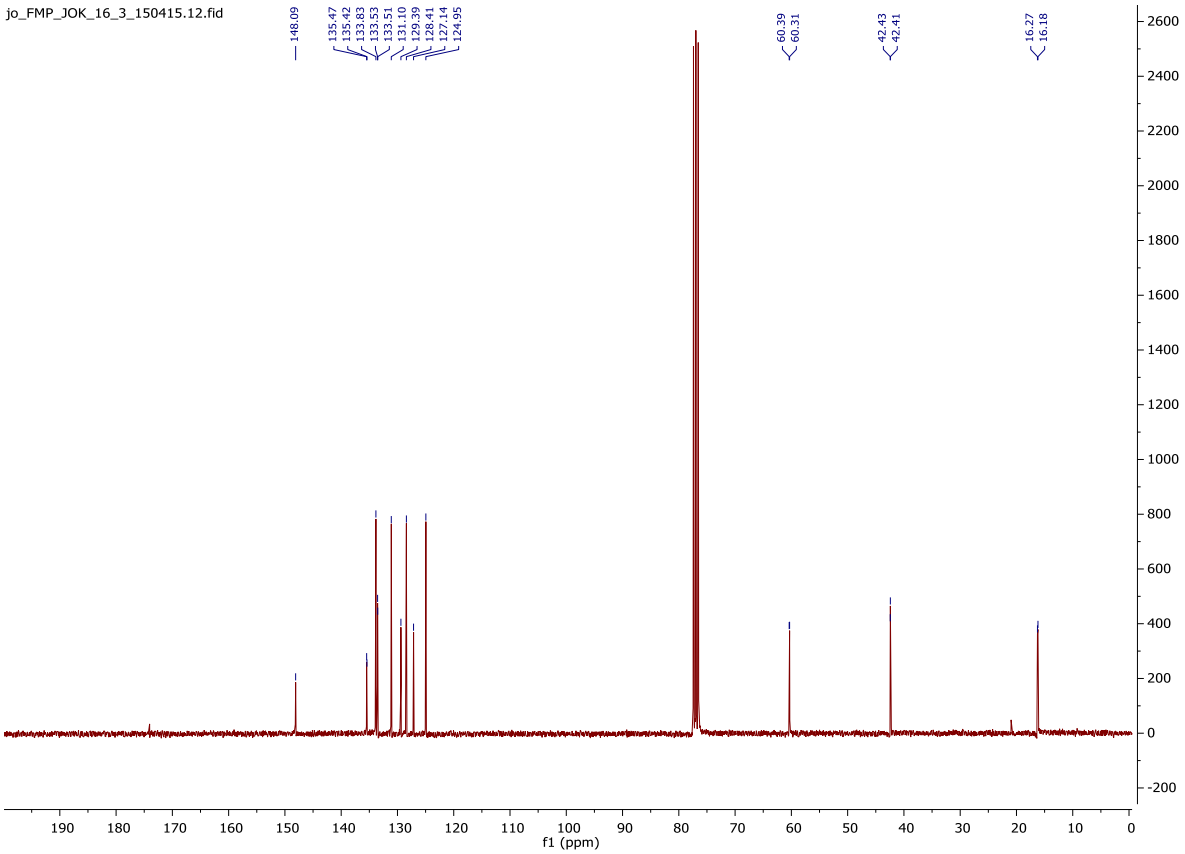

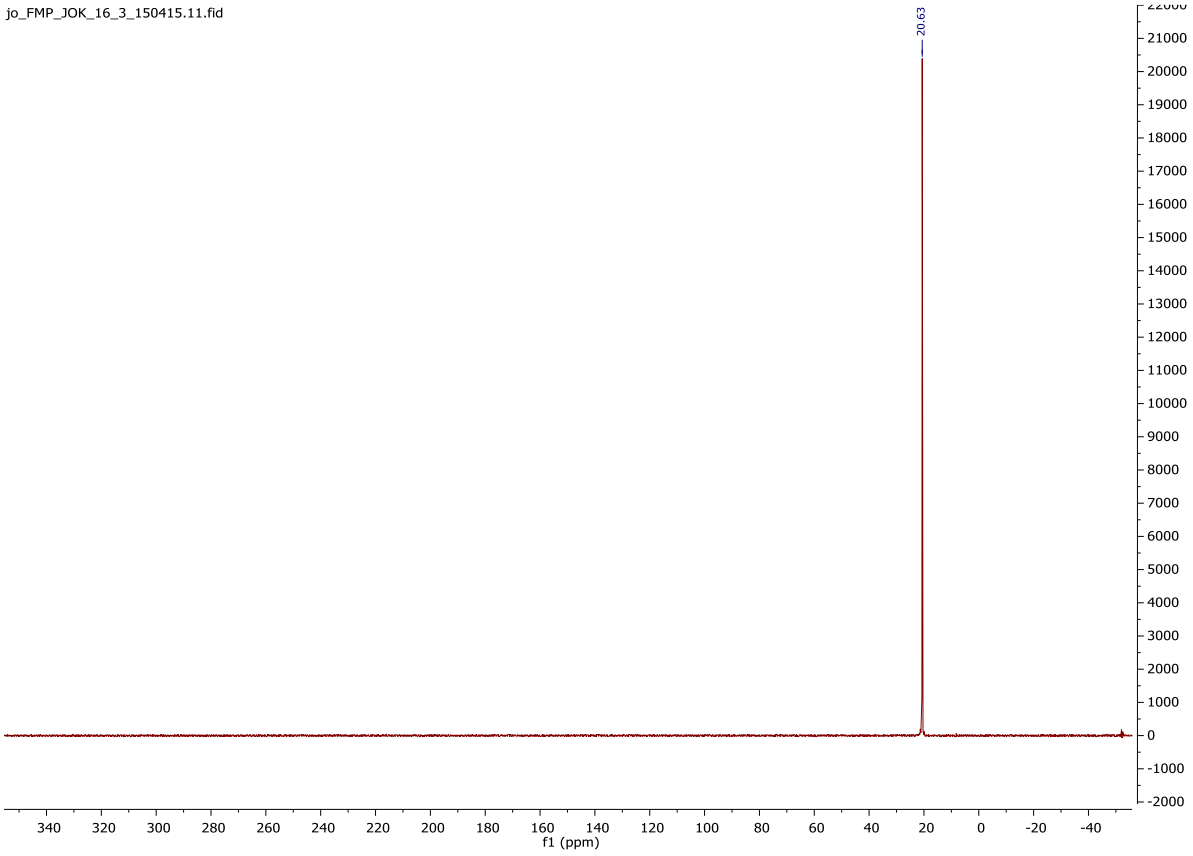

Ethyl-*N*-cyclohexyl-*P*-vinyl-phosphonamidate (**51**)

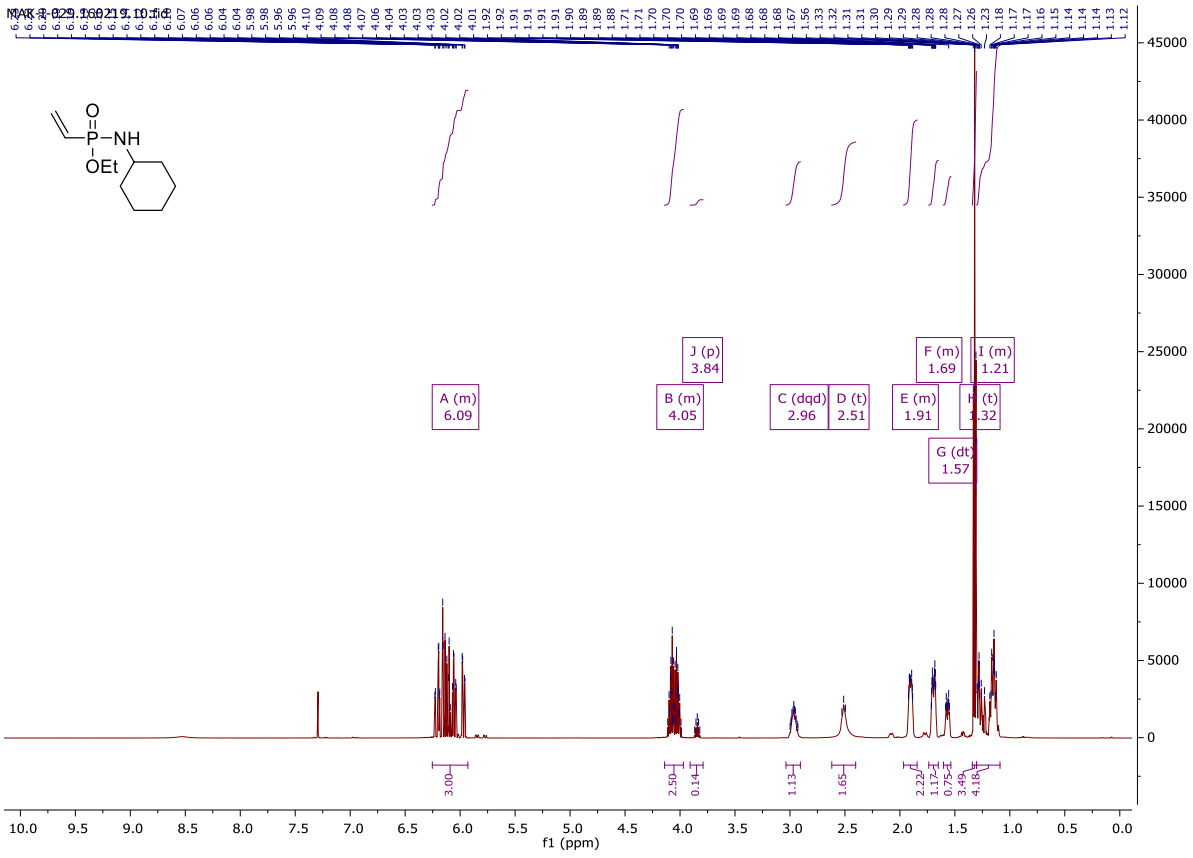

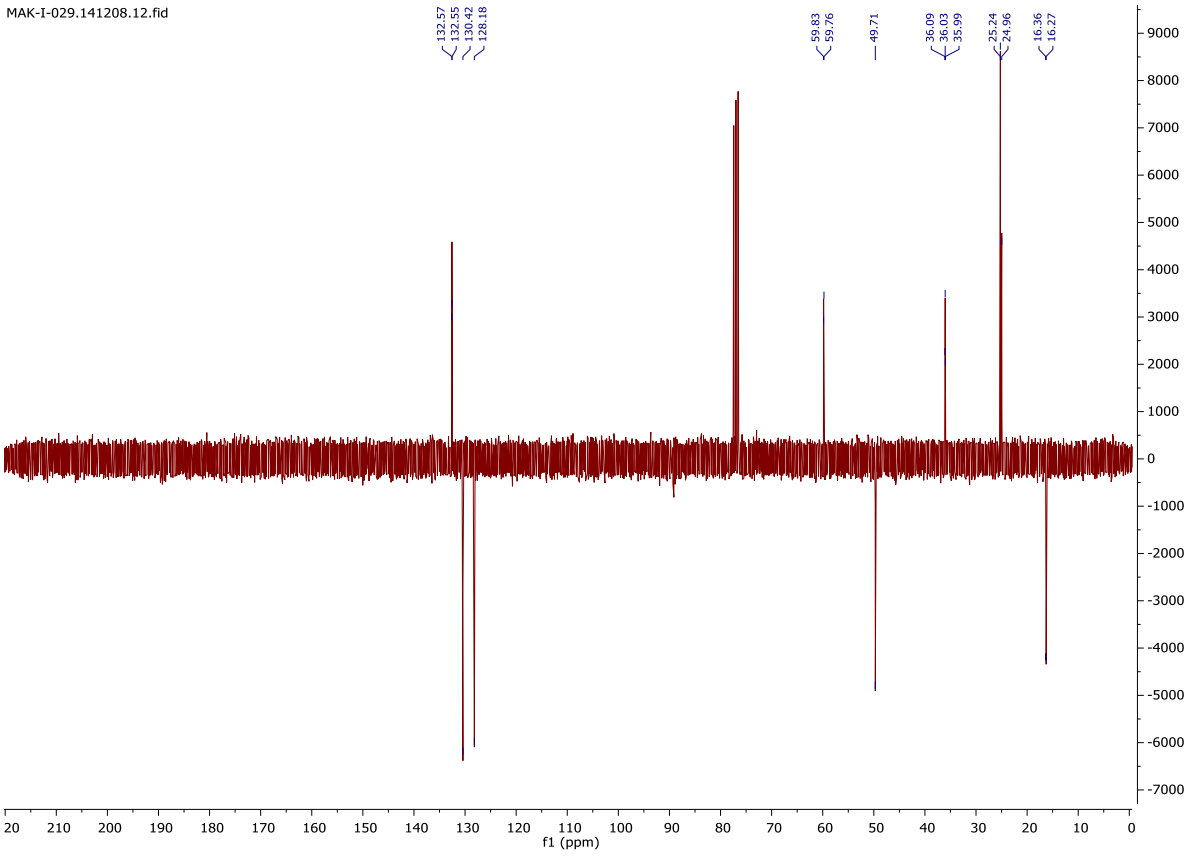
MAK-I-029.141208.12.fid
132.57
132.55
130.42
128.18
59.83
59.76
49.71
36.09
36.03
35.99
25.24
24.96
16.36
16.27
f1 (ppm)

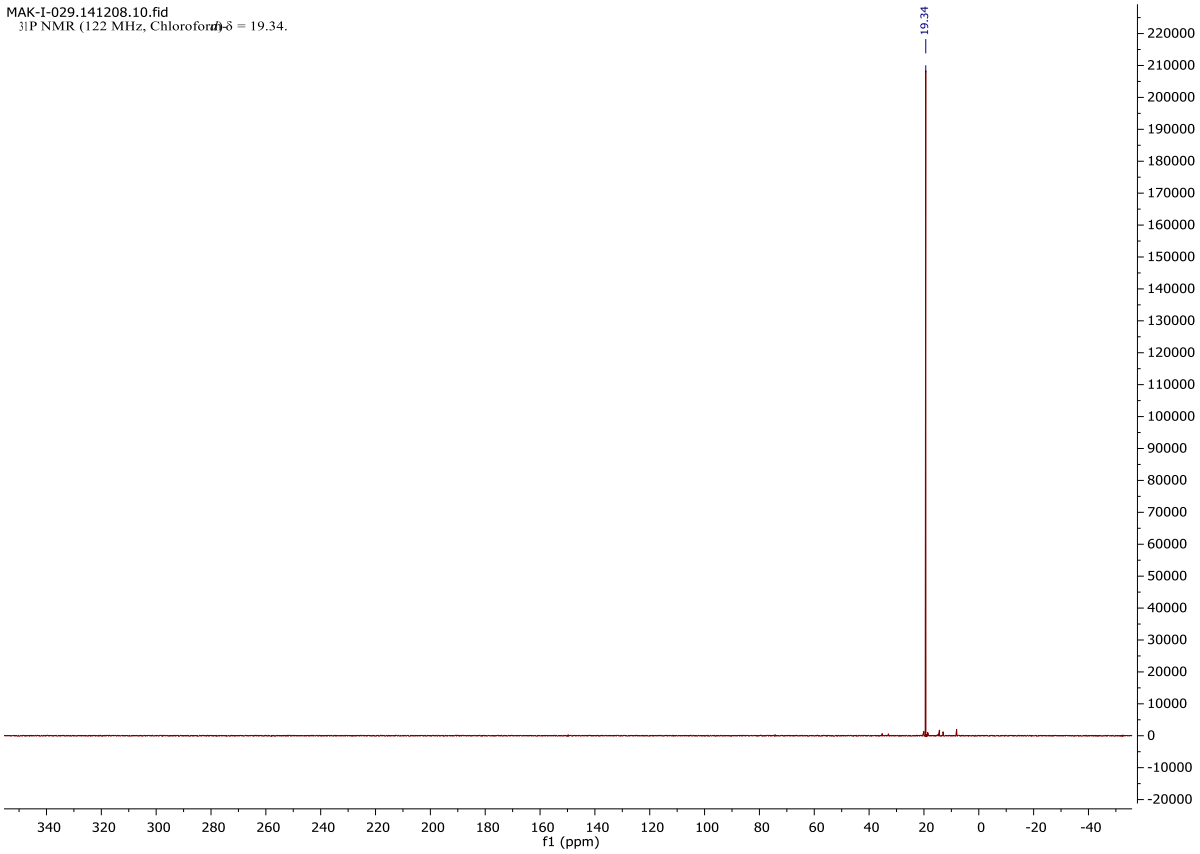
MAK-I-029.141208.10.fid
31P NMR (122 MHz, Chloroform-d) δ = 19.34.
19.34
f1 (ppm)

4-(2-nitro-5-(oxypropargyl)benzyloxy)phenol

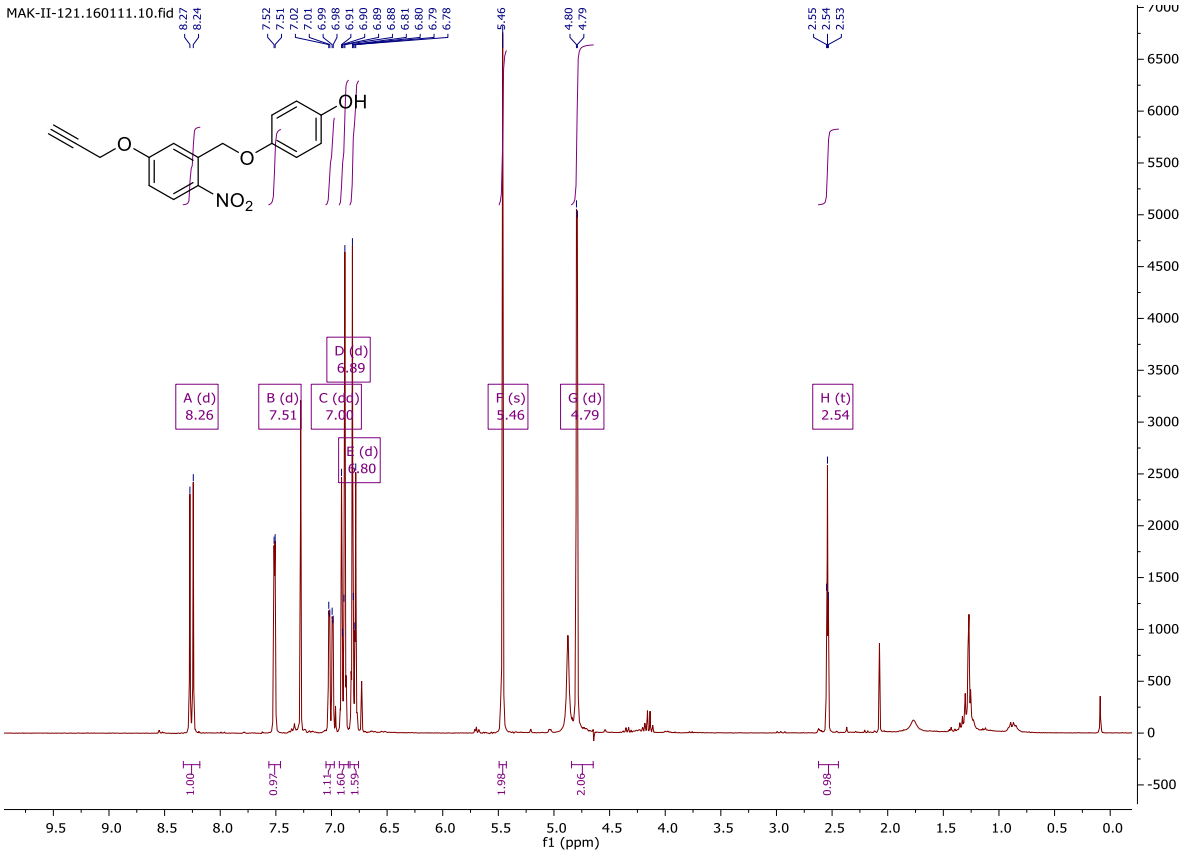

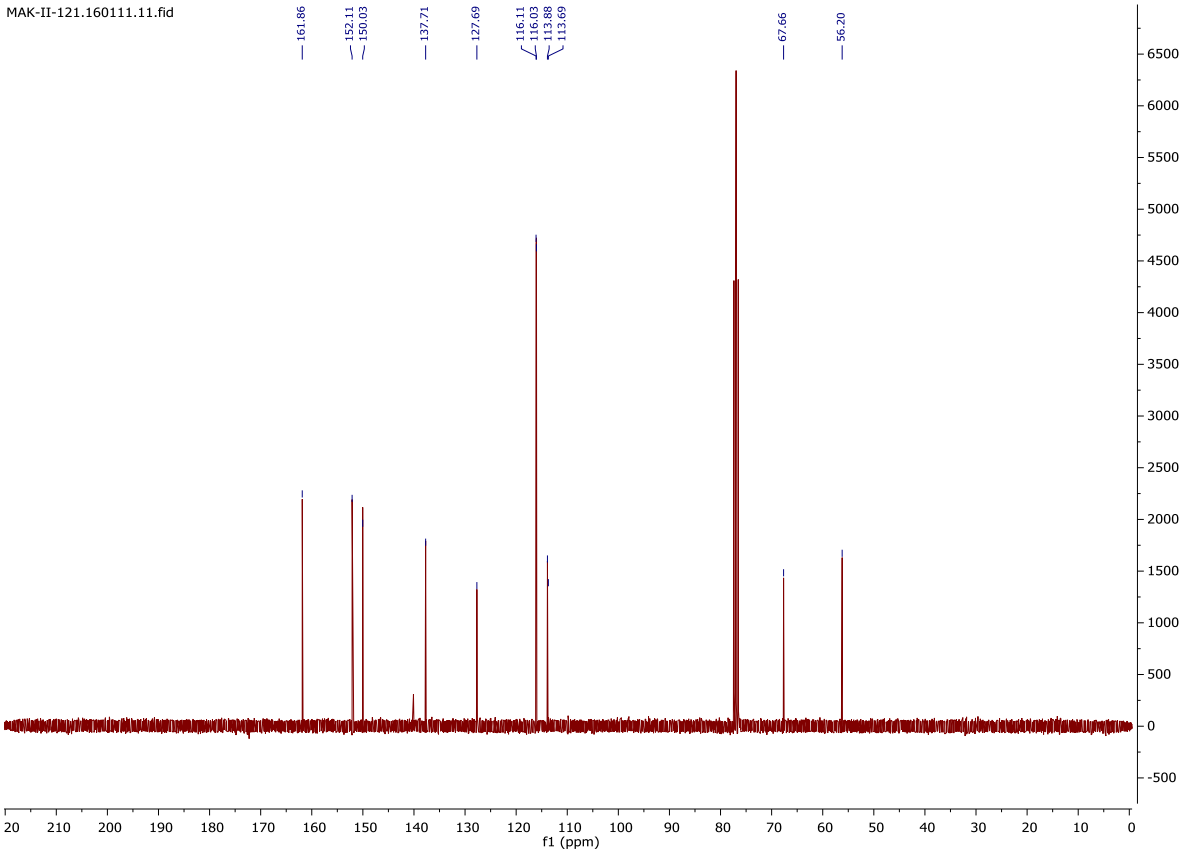

Bis(4-(2-nitro-5-(oxypropargyl)benzyloxy)phenyl) vinyl phosphonite borane (**53**)

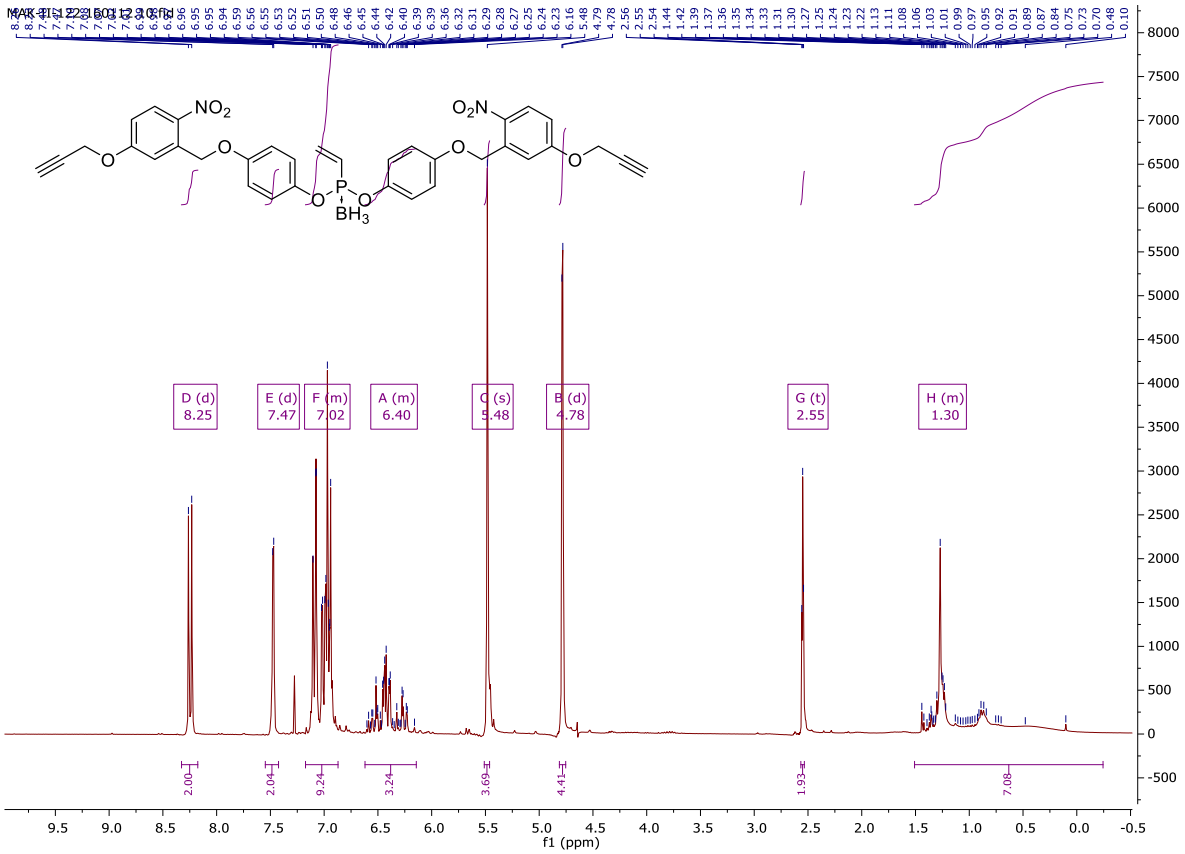

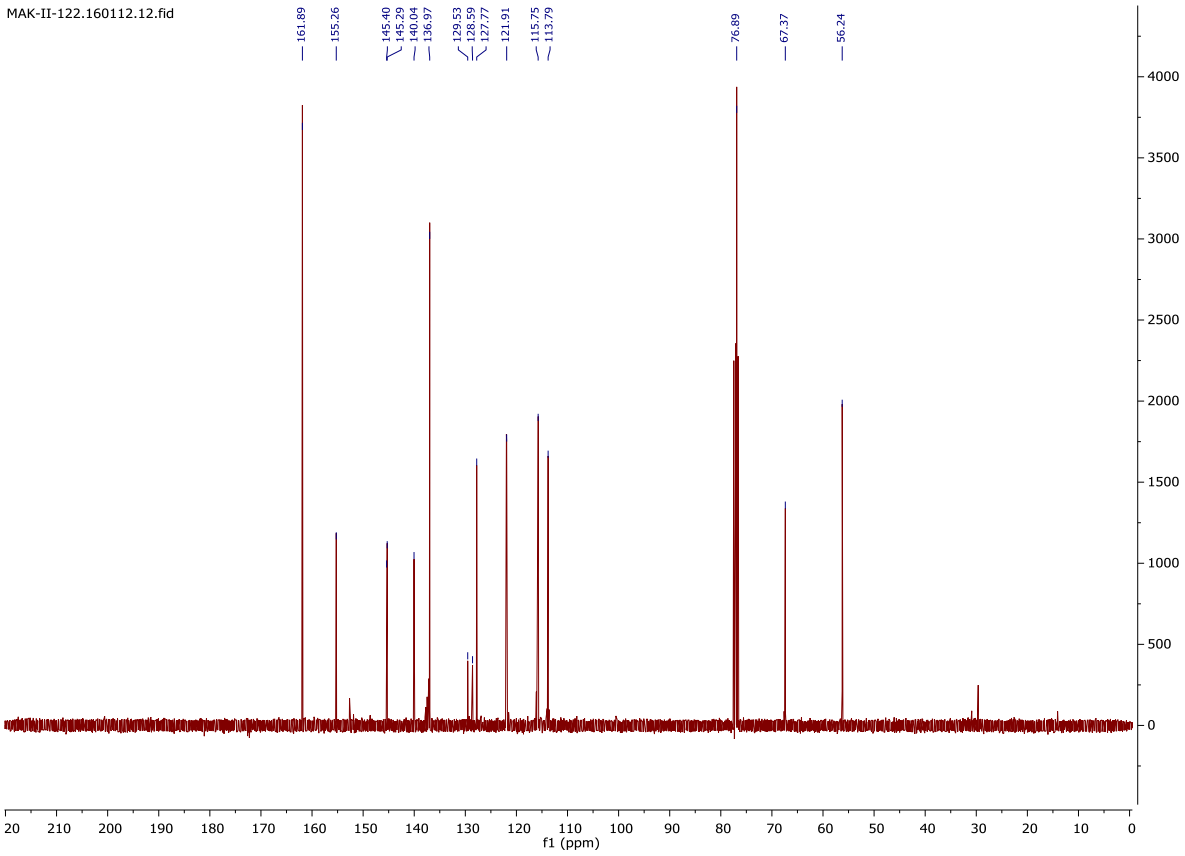

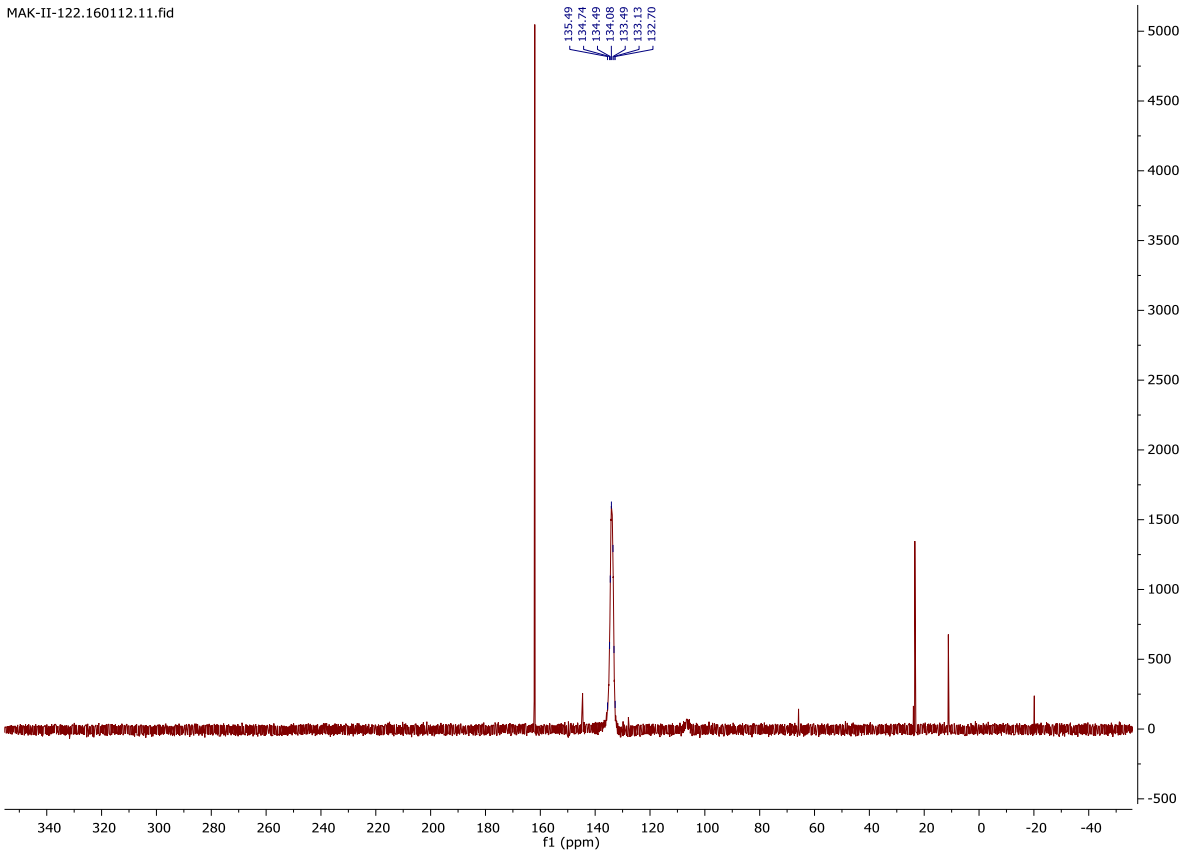

Bis(2-nitro-5-(oxypropargyl)benzyl) vinyl phosphonite borane (**54**)

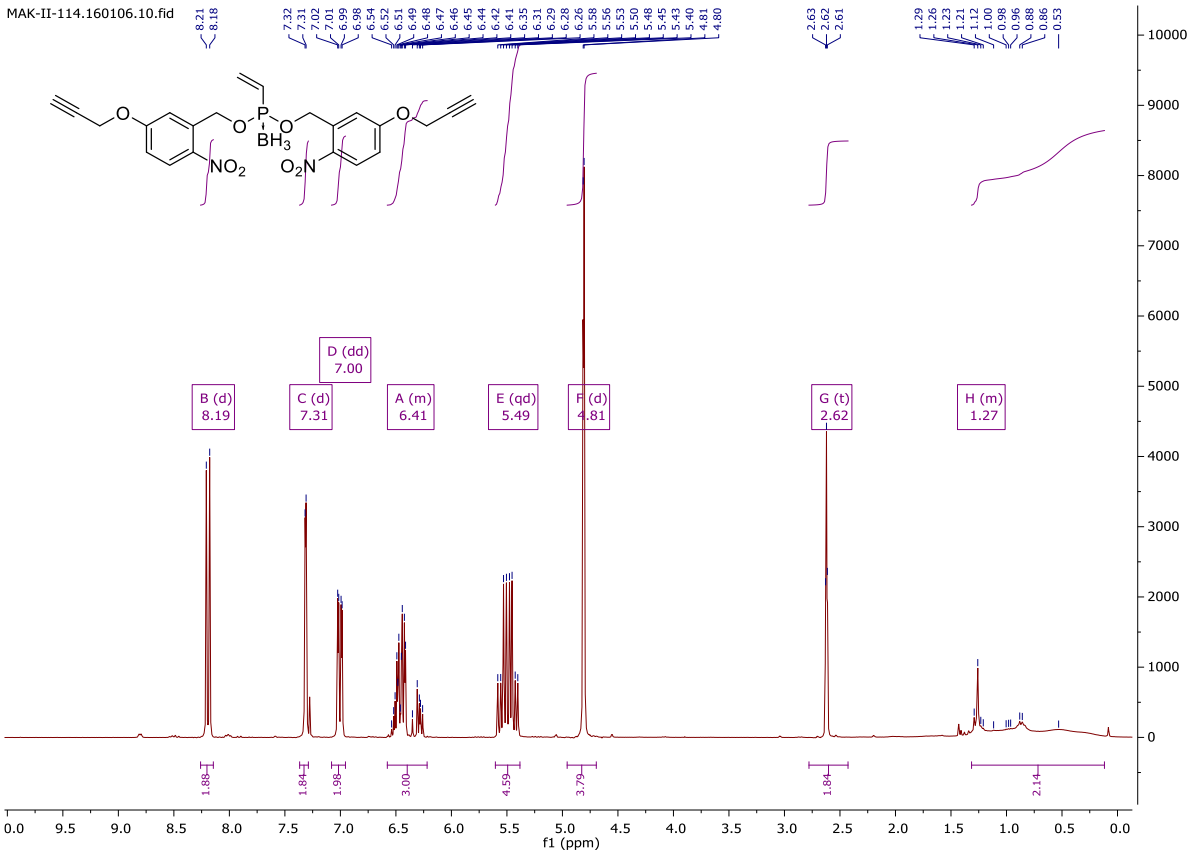

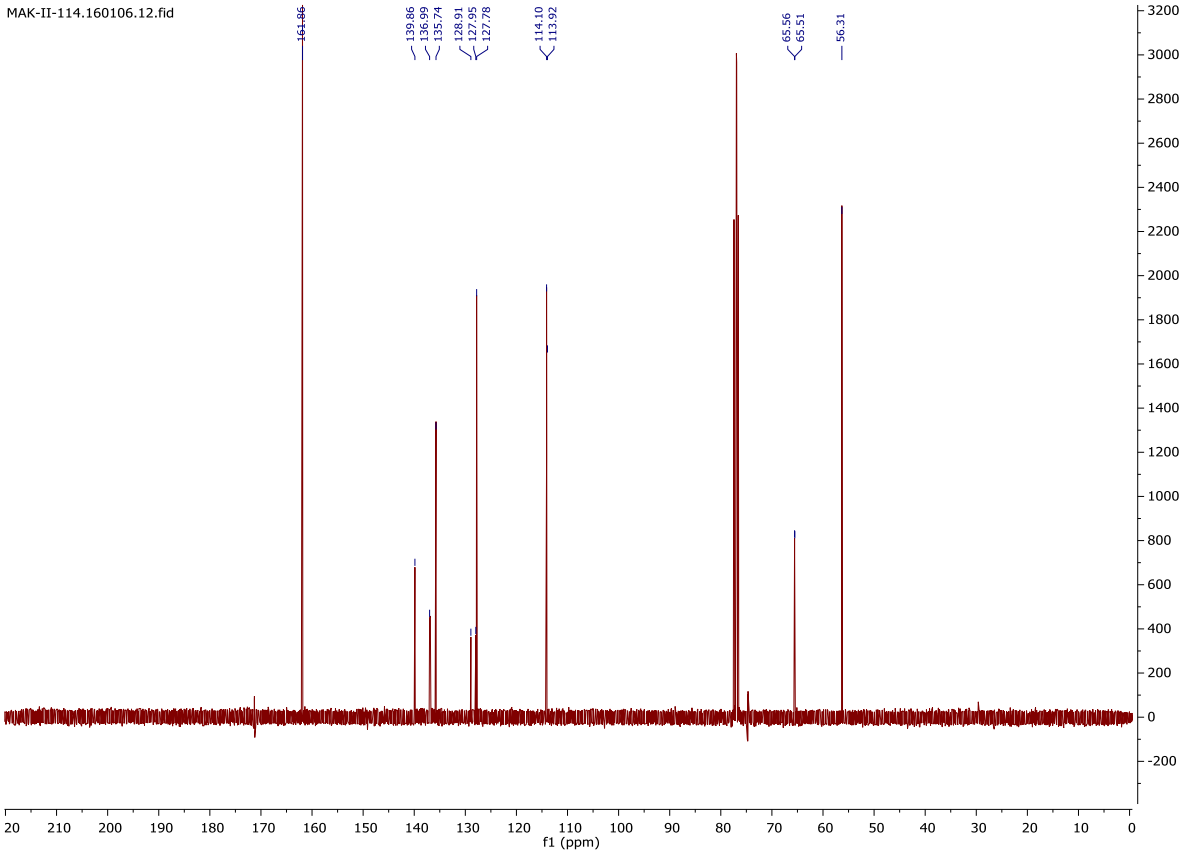
MAK-II-114.160106.12.fid
161.86
139.86
136.99
135.74
128.91
127.95
127.78
114.10
113.92
65.56
65.51
56.31
f1 (ppm)

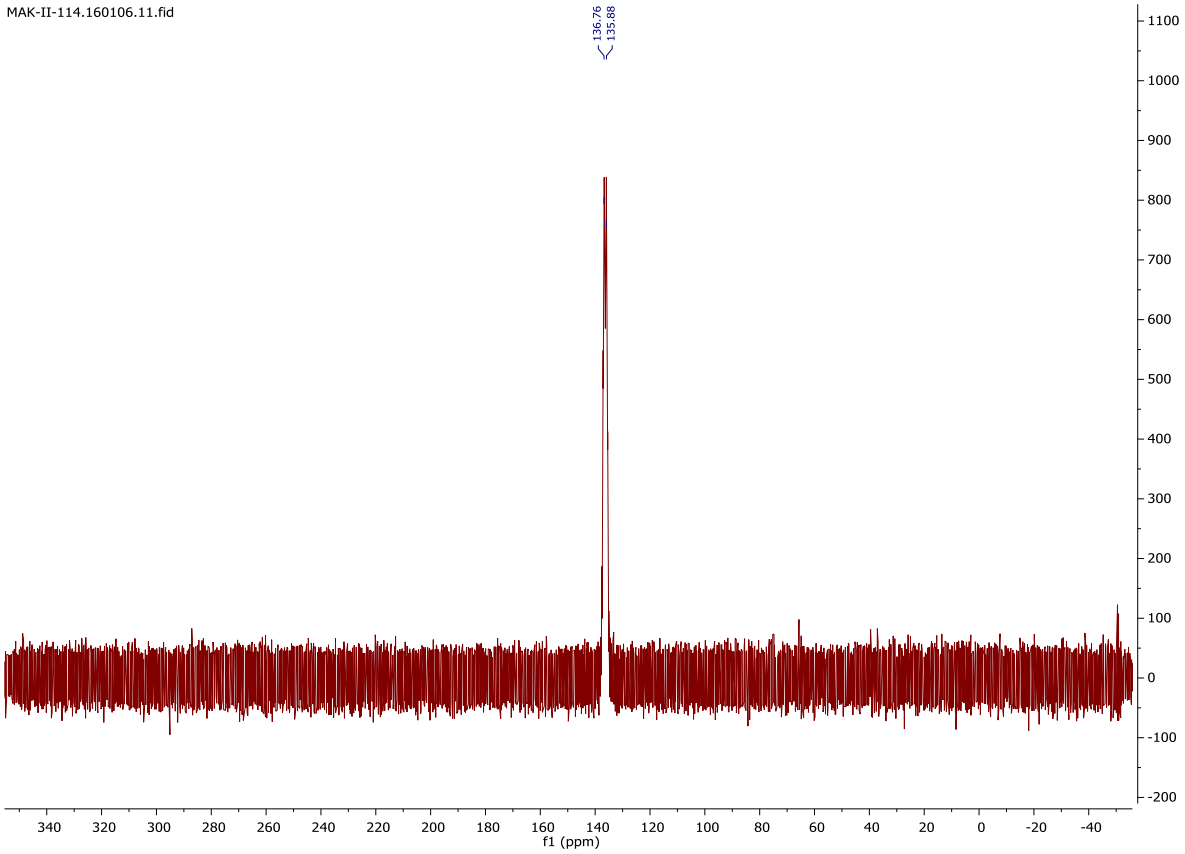
MAK-II-114.160106.11.fid
136.76
135.88
f1 (ppm)

Bis-(4-Hydroxyphenyl) vinyl phosphonite borane (**55**)

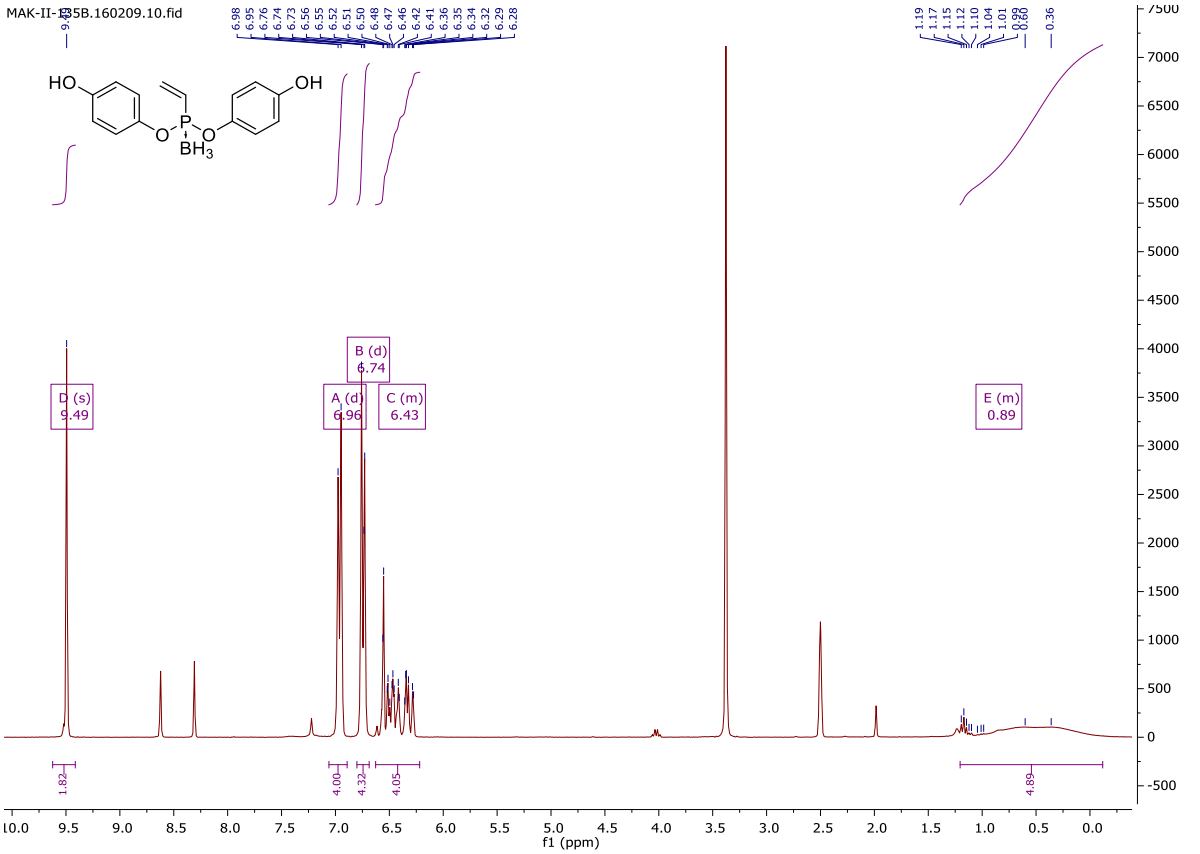

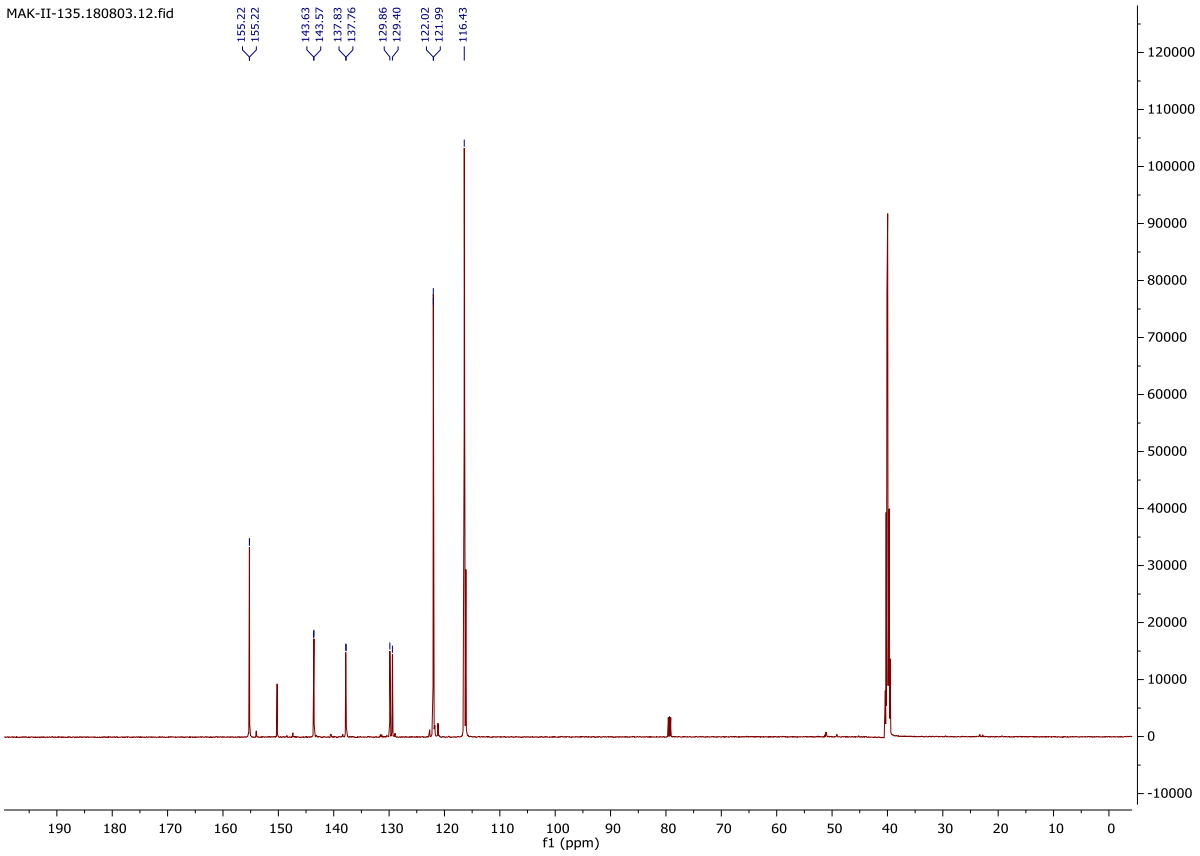

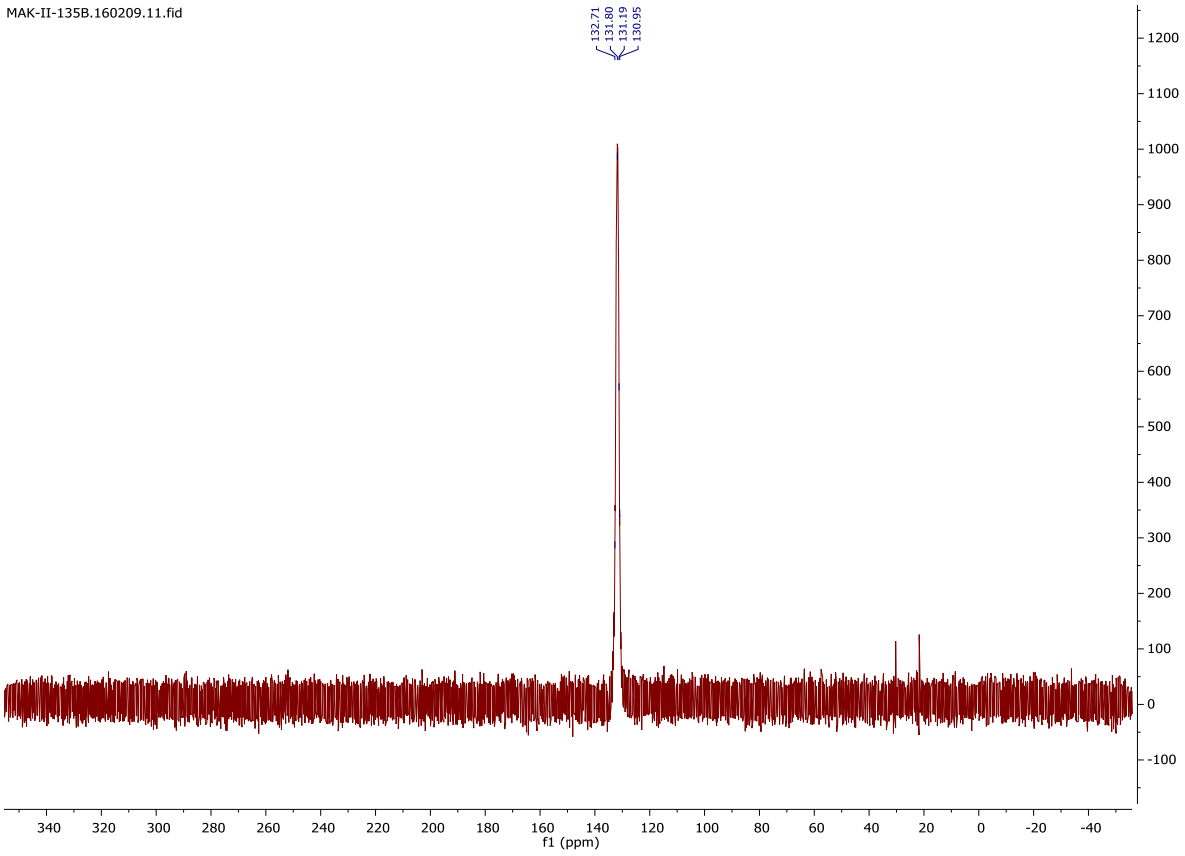

Di(4-nitrobenzyl) vinylphosphonite borane (**56**)

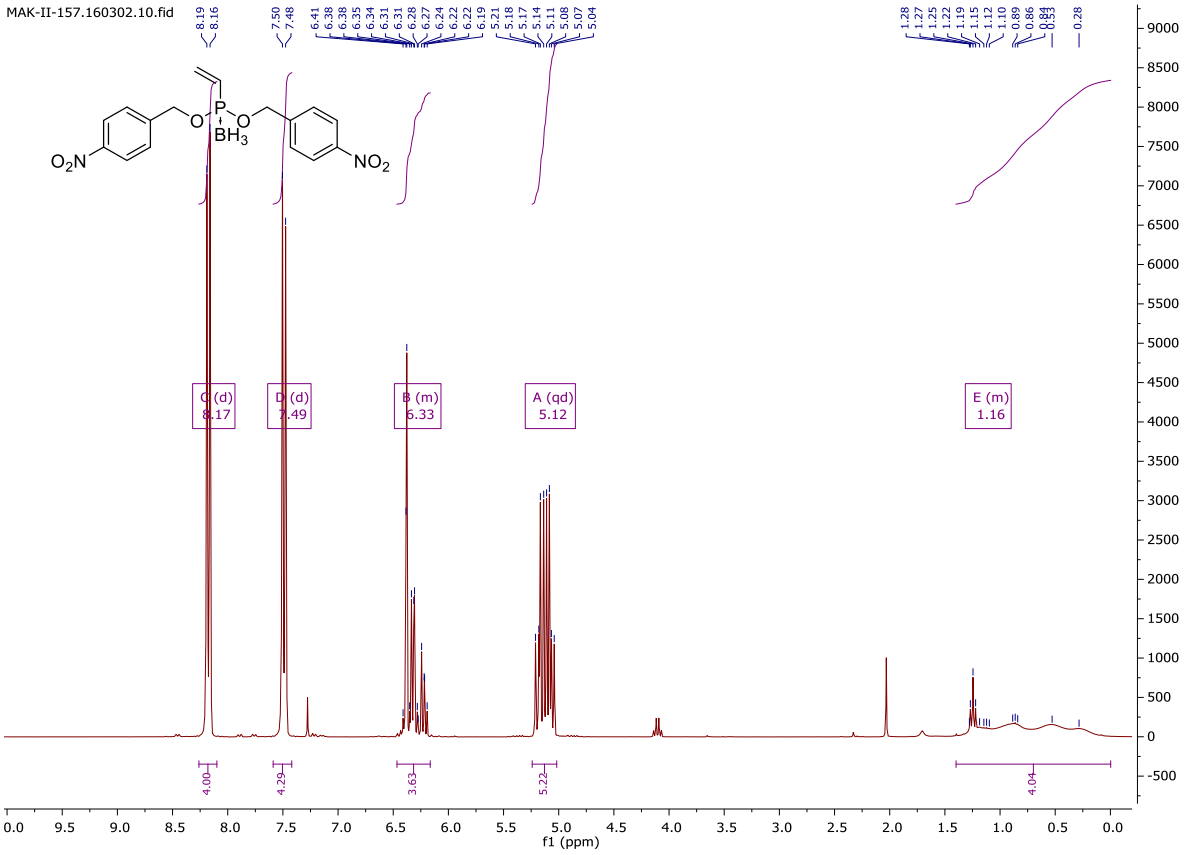

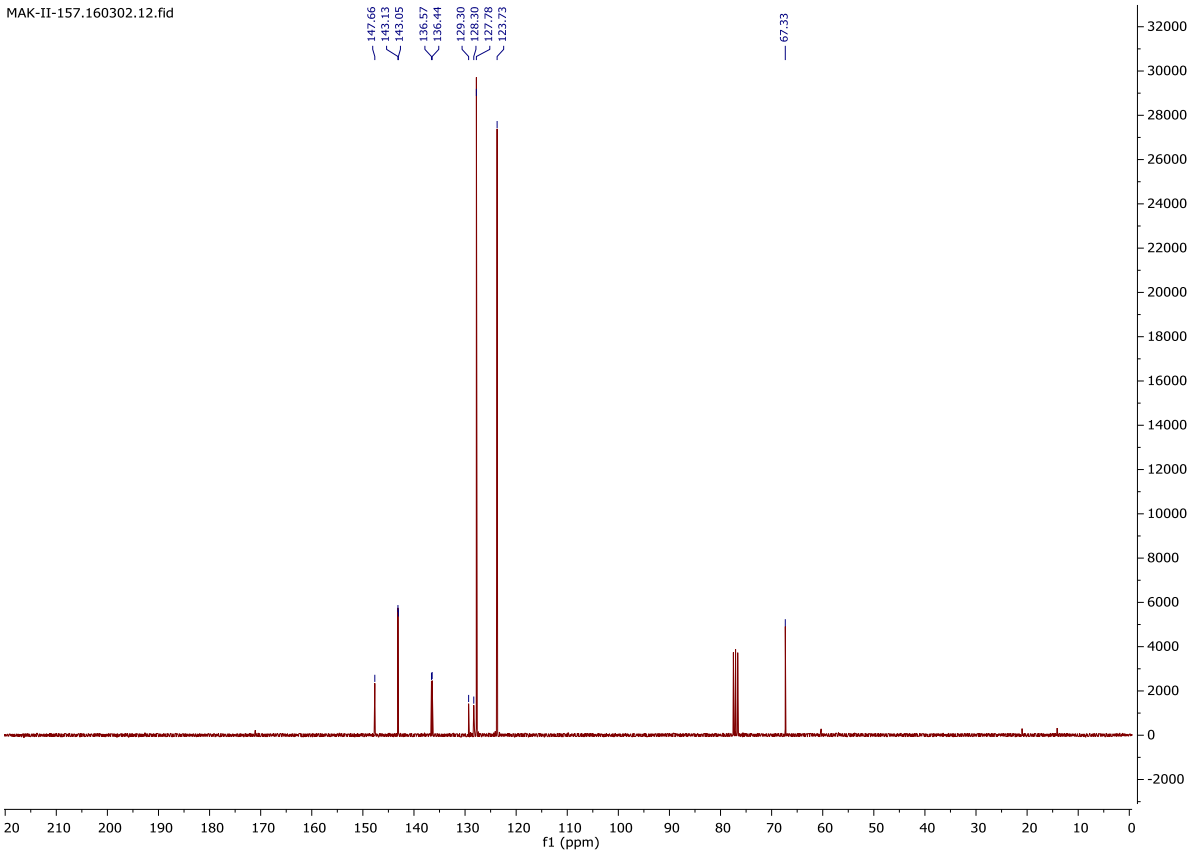
MAK-II-157.160302.12.fid
147.66
143.13
143.05
136.57
136.44
129.30
128.30
127.78
123.73
67.33
f1 (ppm)

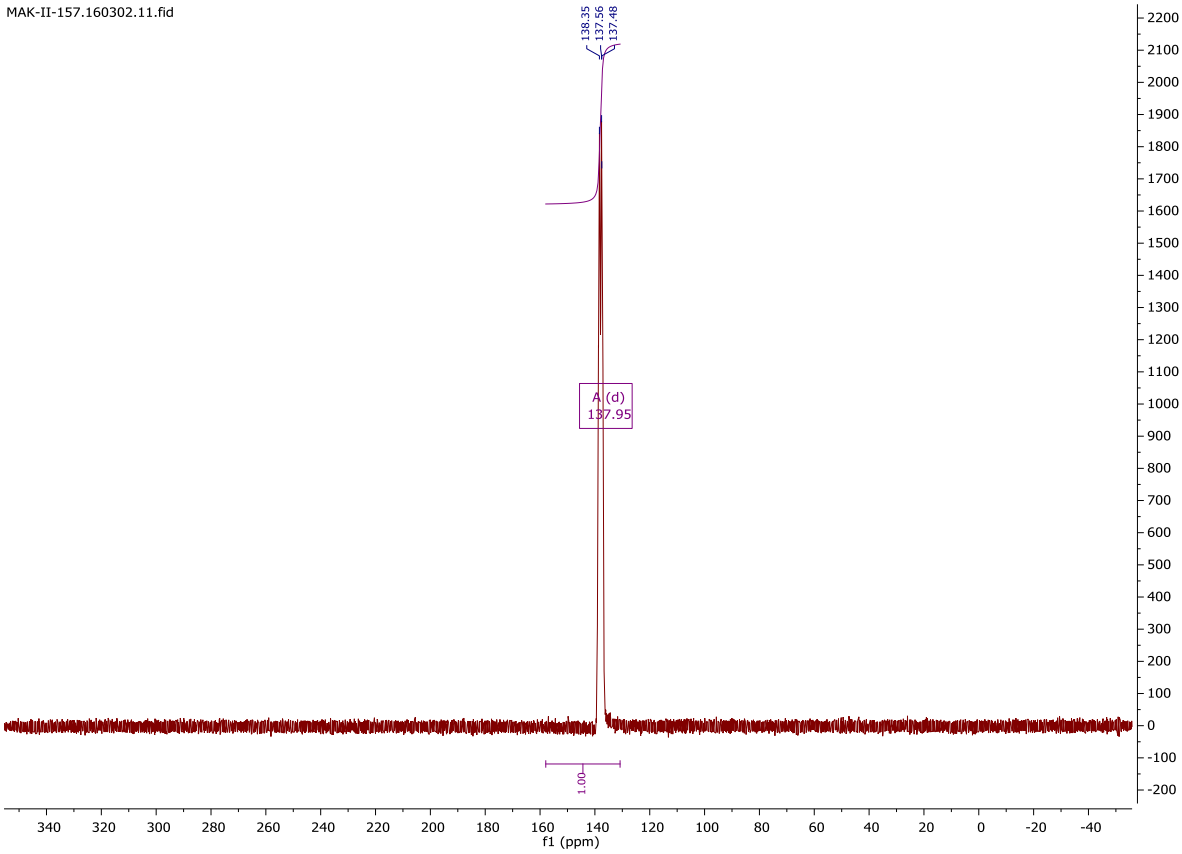
MAK-II-157.160302.11.fid
138.35
137.56
137.48
A (d)
137.95
1.00
f1 (ppm)

Di(1,2-isopropylidene glyceryl) vinyl phosphonite borane (**57**)

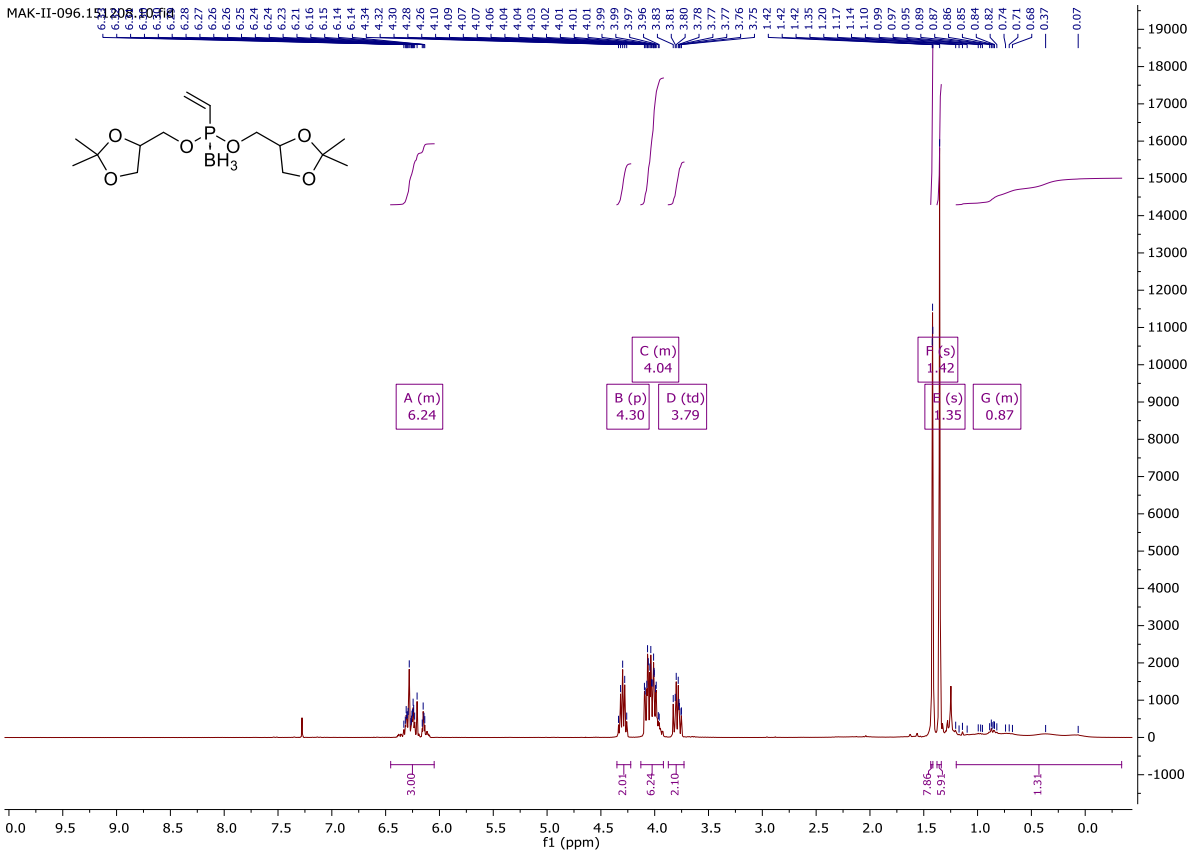

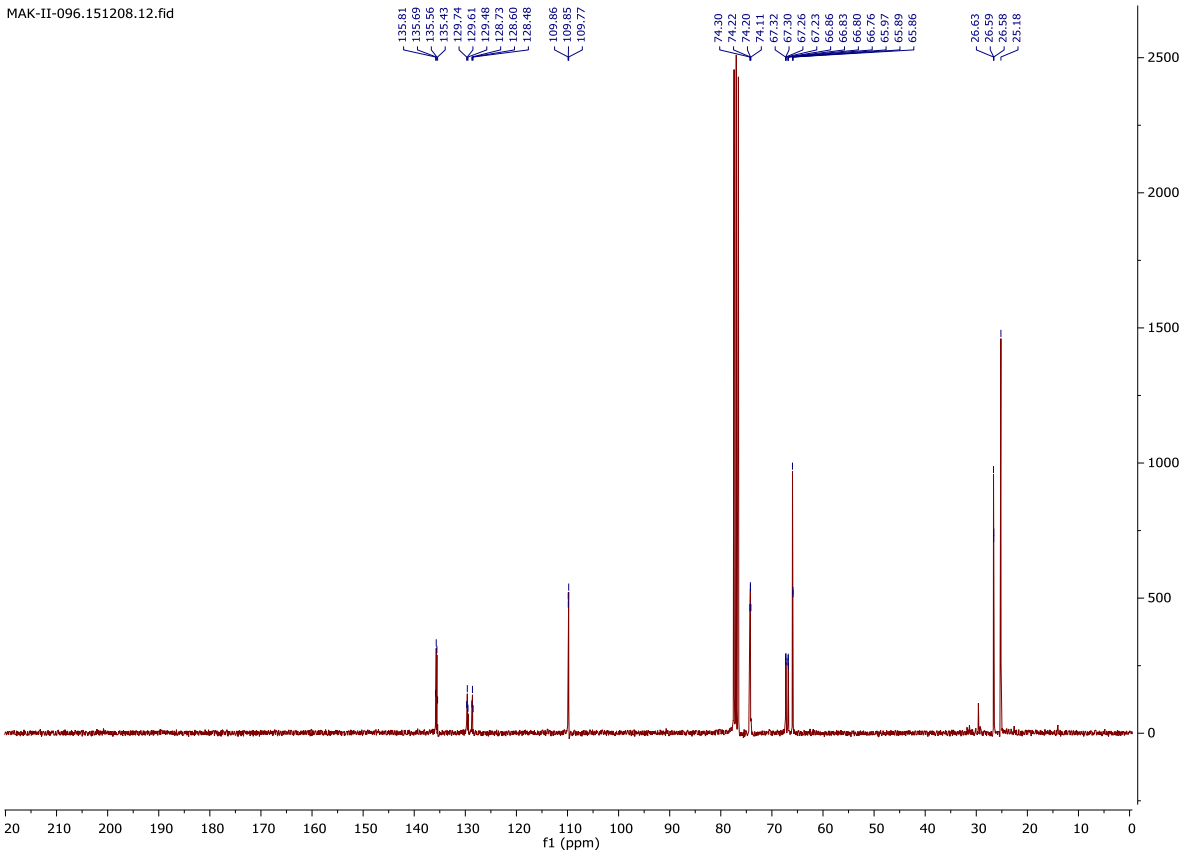

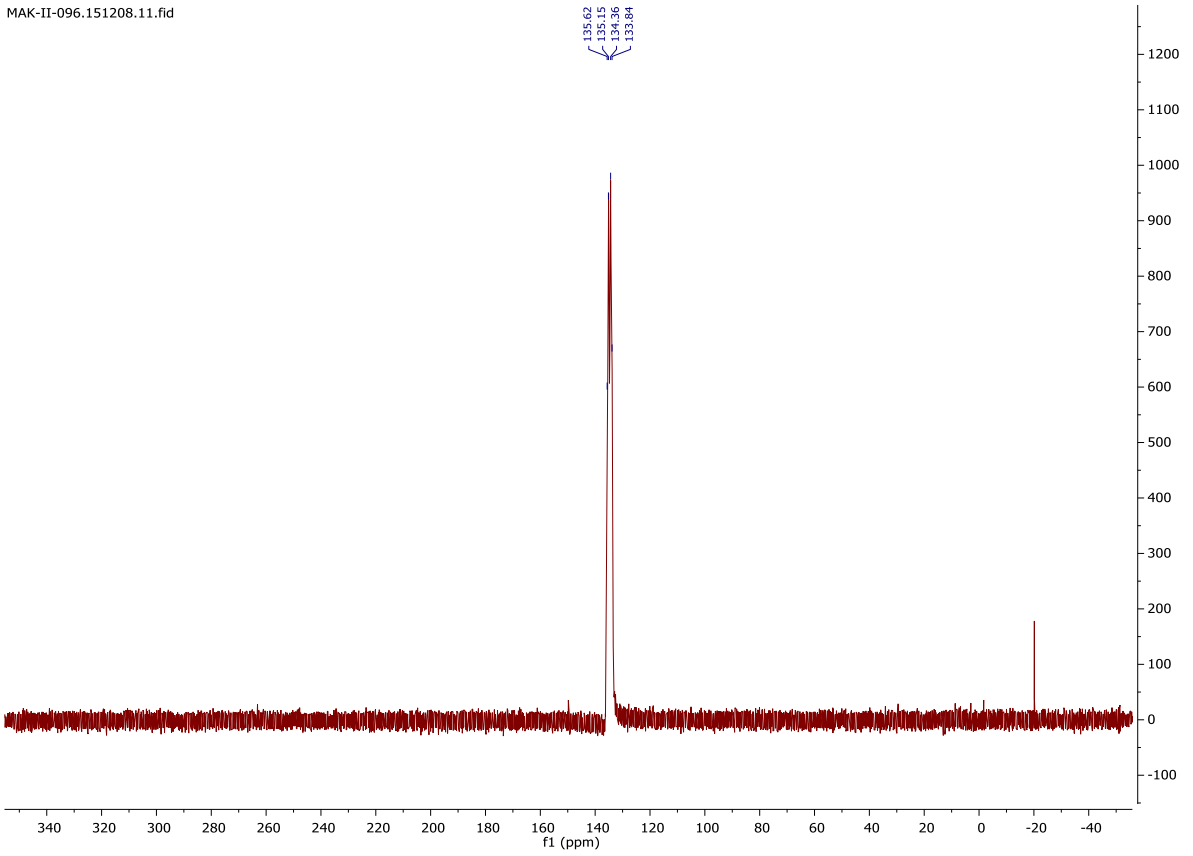

4-Hydroxyphenyl -*N*-phenyl-*P*-vinyl-phosphonamidate (**58**)

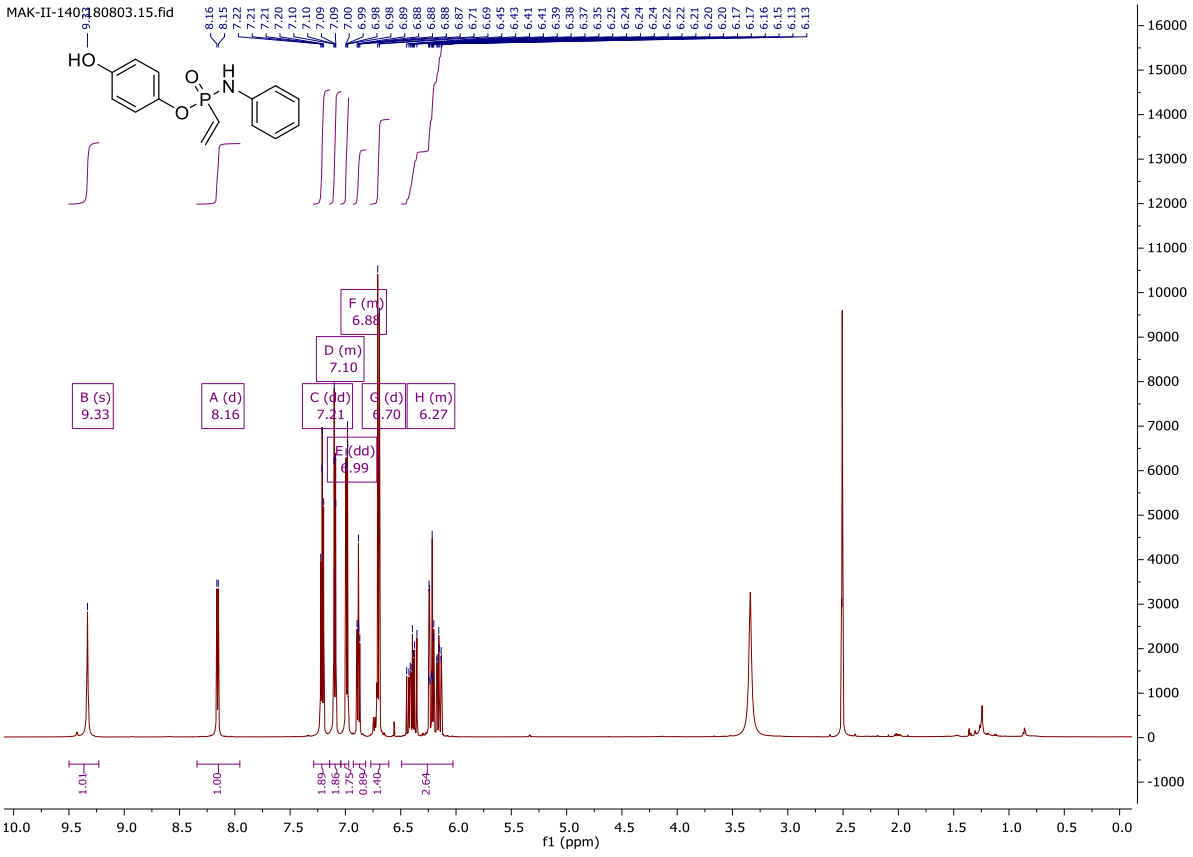

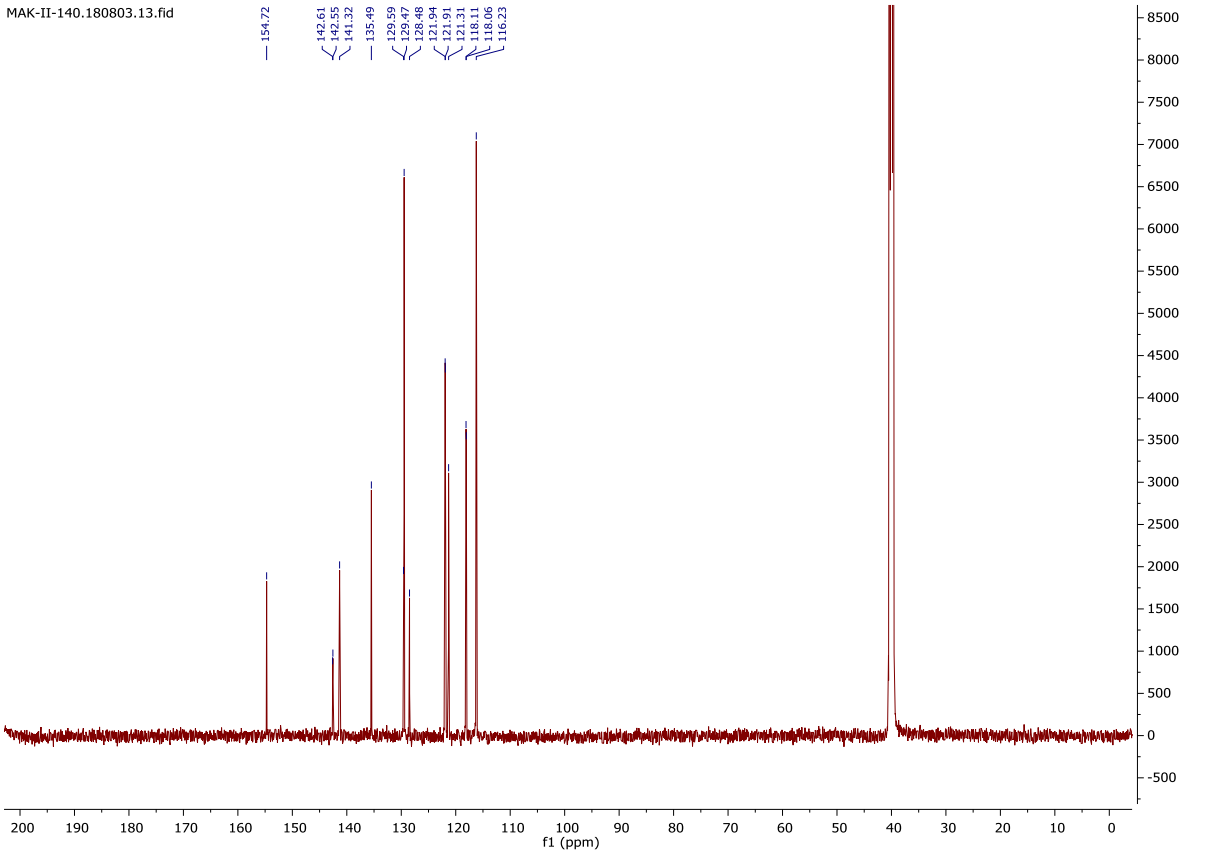
MAK-II-140.180803.13.fid
154.72
142.61
142.55
141.32
135.49
129.59
129.47
128.48
121.94
121.91
121.31
118.11
118.06
116.23
f1 (ppm)

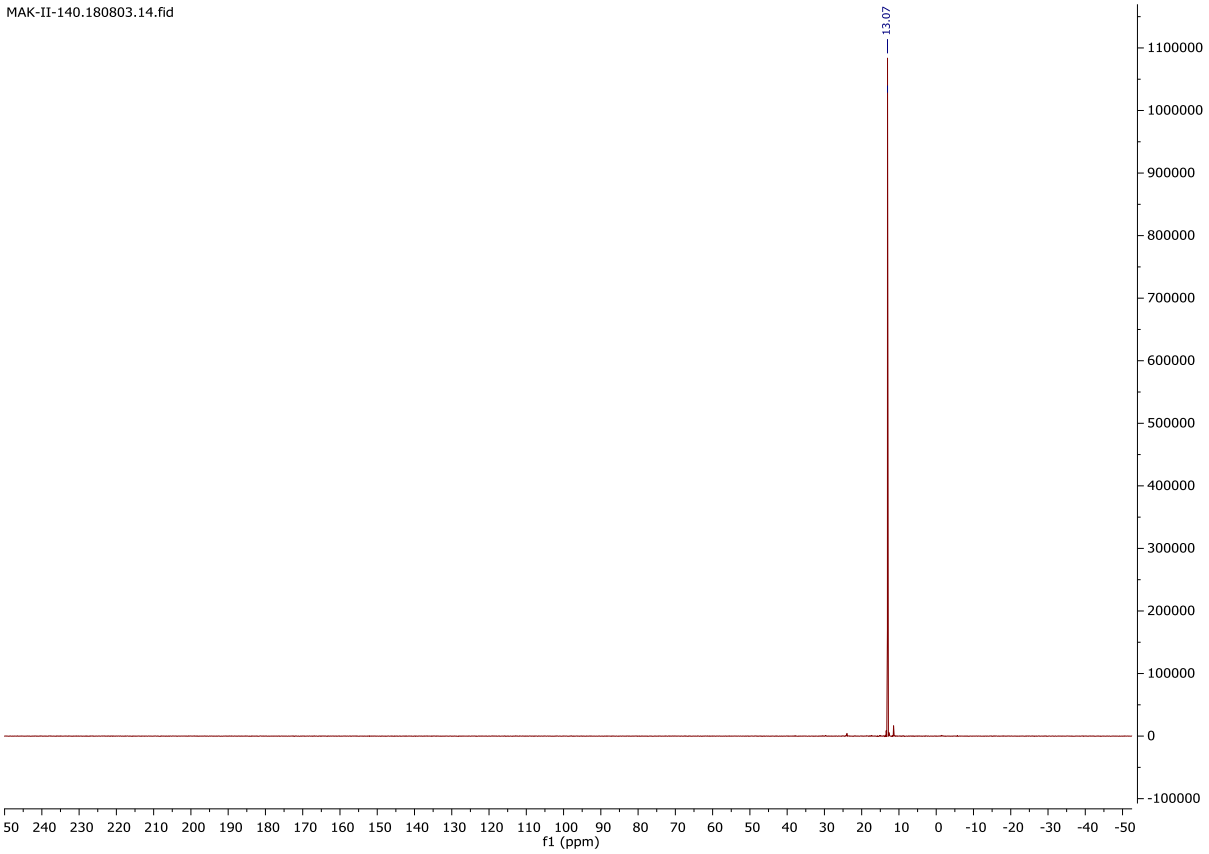
MAK-II-140.180803.14.fid
13.07
f1 (ppm)

2-nitro-5-(oxypropargyl)benzyl-*N*-phenyl-*P*-vinyl-phosphonamidate (**59**)

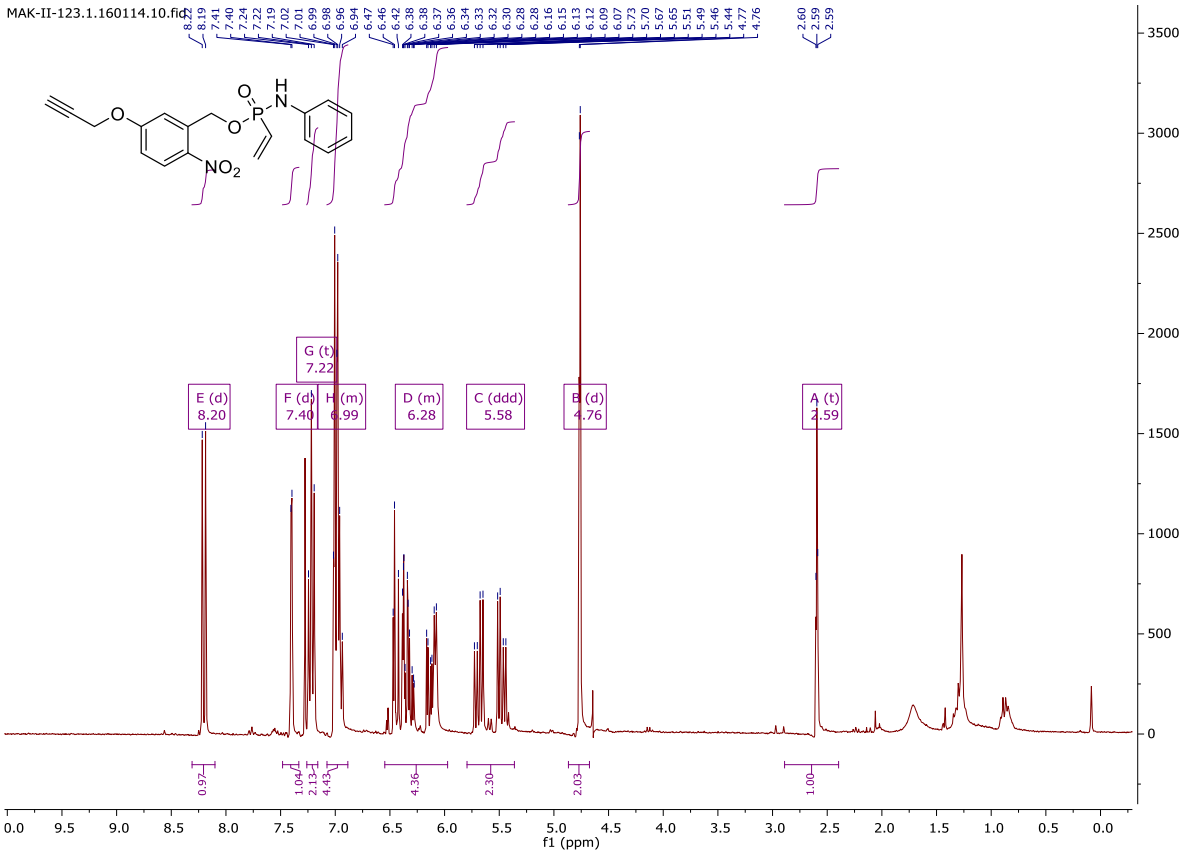

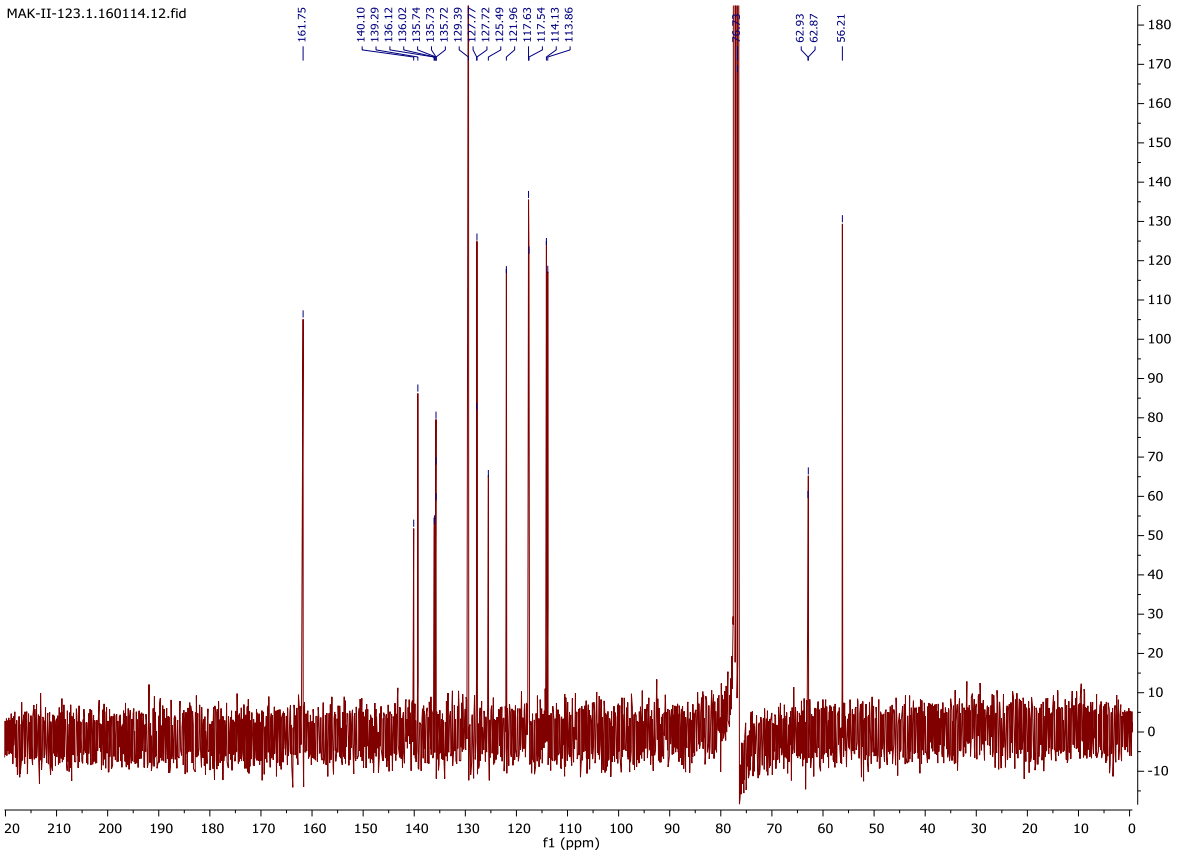

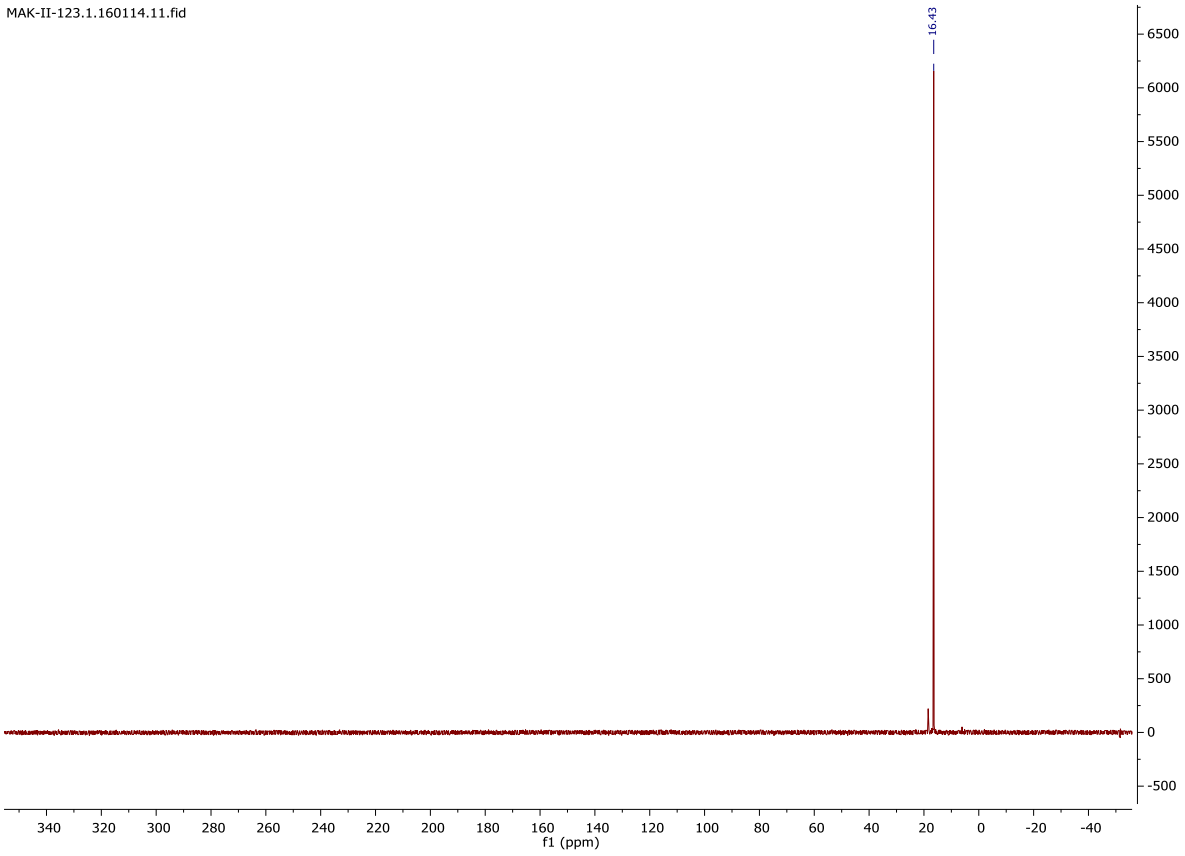

4-(2-nitro-5-(oxypropargyl)benzyloxy)phenyl-*N*-phenyl-*P*-vinyl-phosphonamidate (**60**)

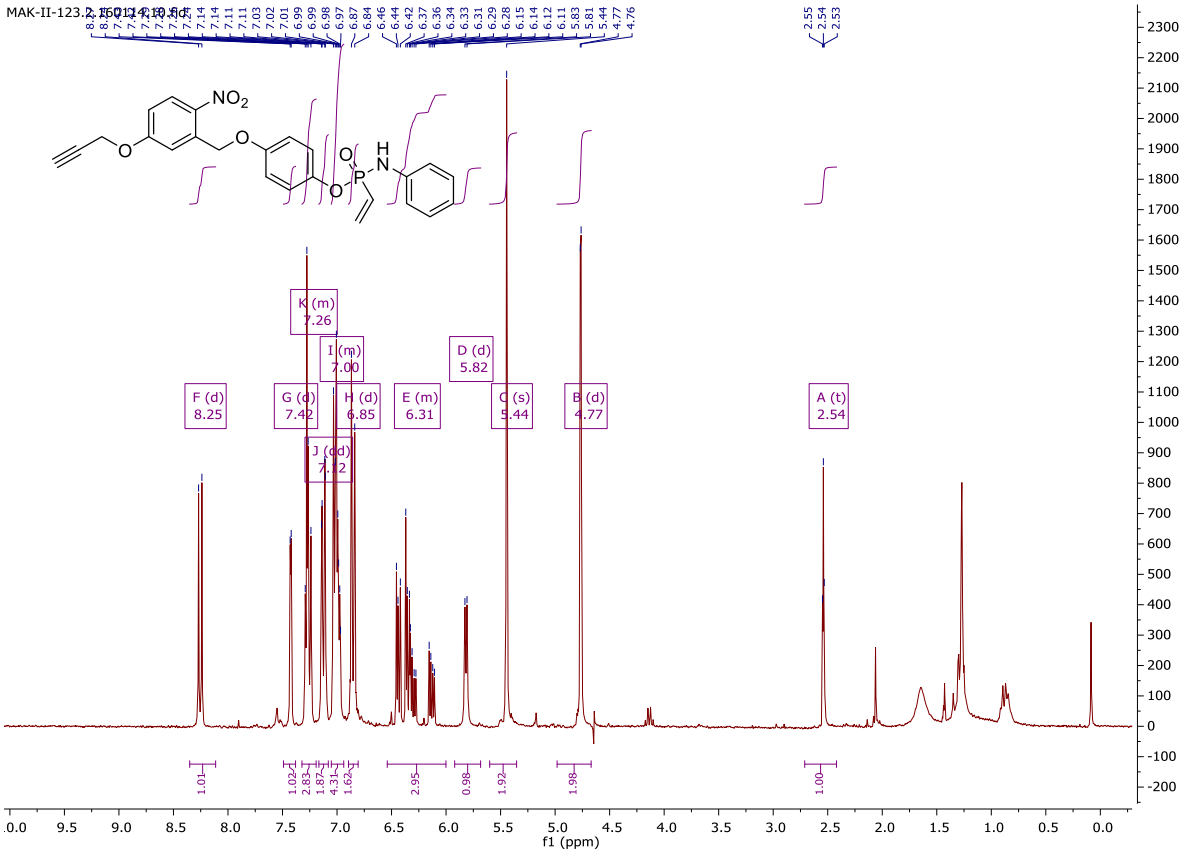

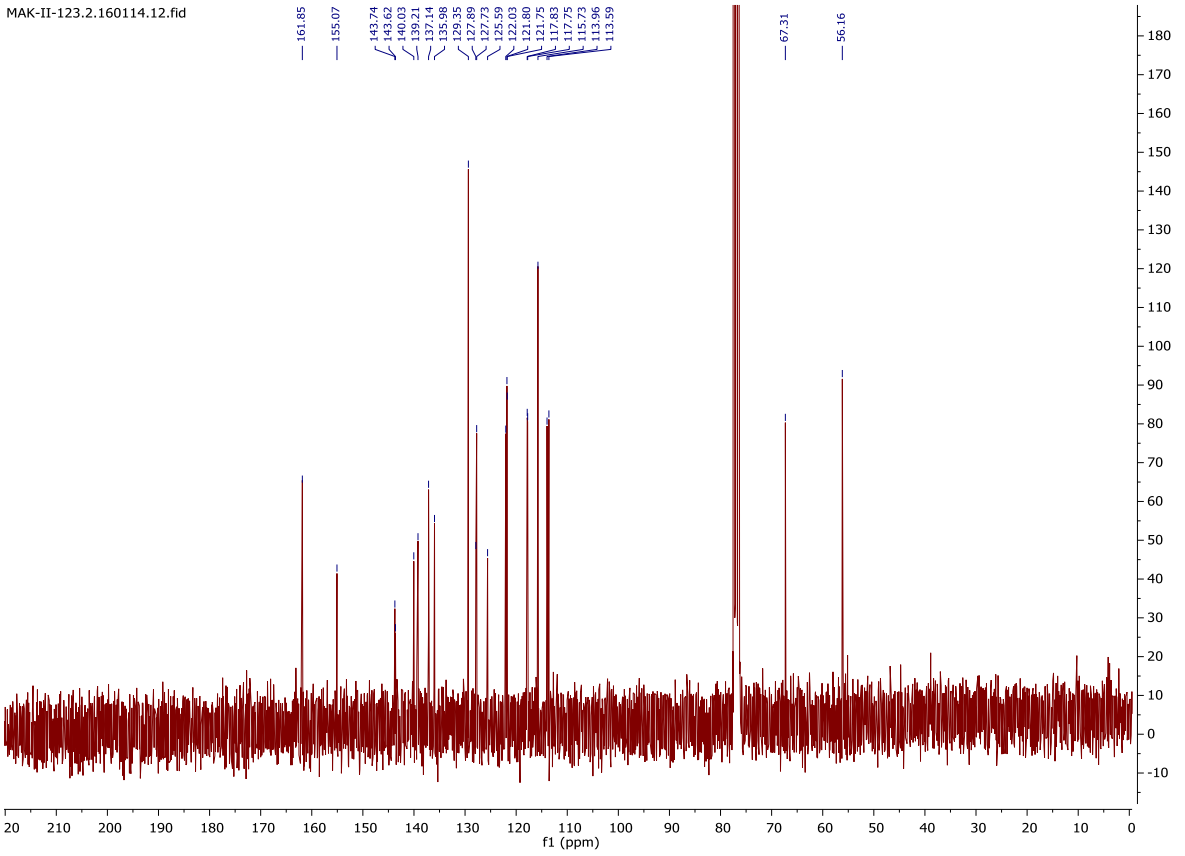
MAK-II-123.2.160114.12.fid
161.85
155.07
143.74
143.62
140.03
139.21
137.14
135.98
129.35
127.89
127.73
125.59
122.03
121.80
121.75
117.83
117.75
115.73
113.96
113.59
67.31
56.16
f1 (ppm)

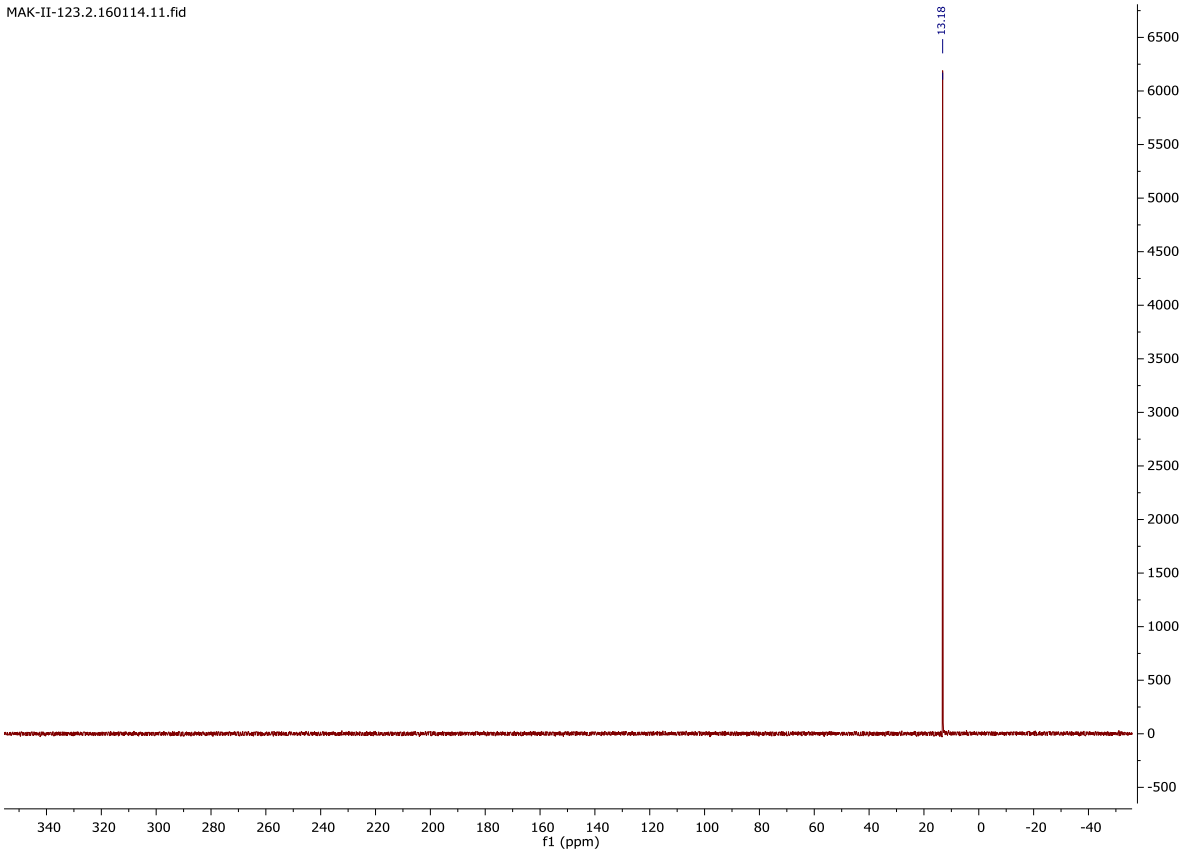
MAK-II-123.2.160114.11.fid
13.18
f1 (ppm)

Cy5-*O*-2-Nitrobenzyl-*P*-vinyl-phosphonamidate **63**

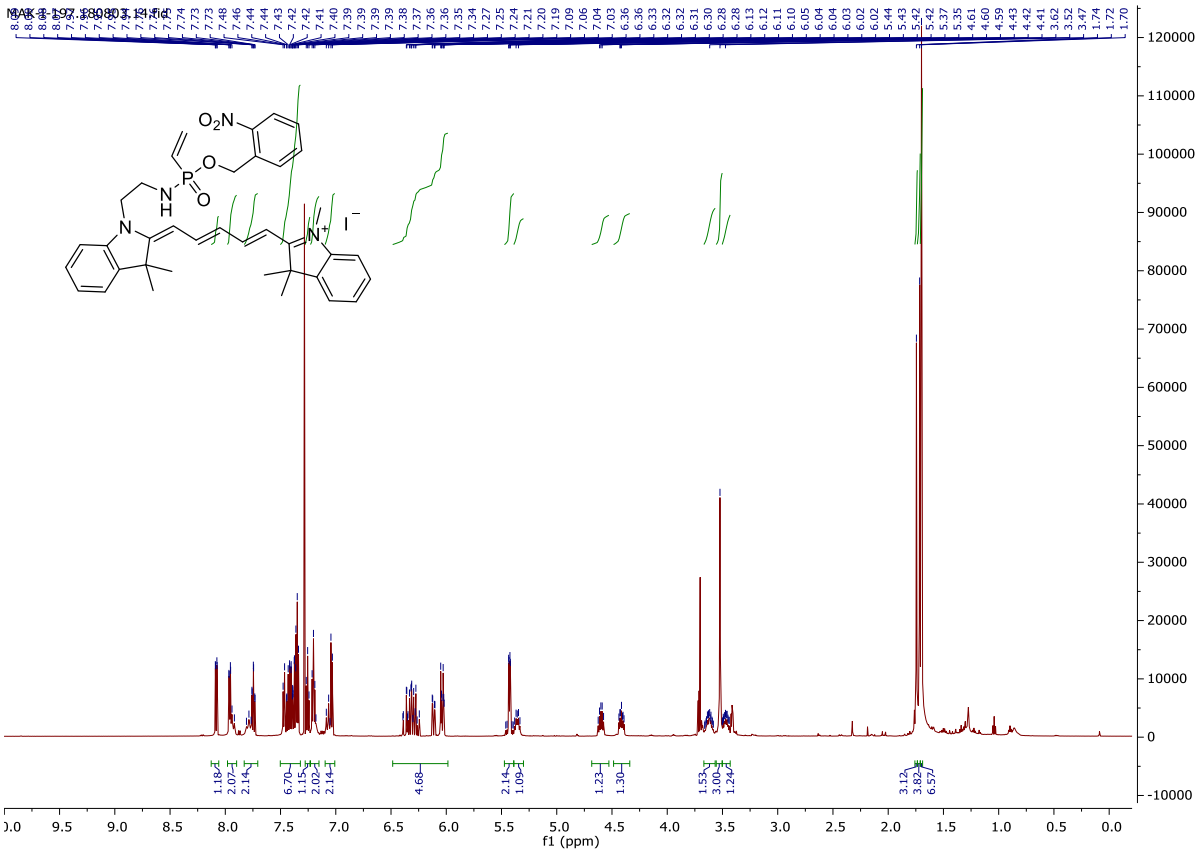

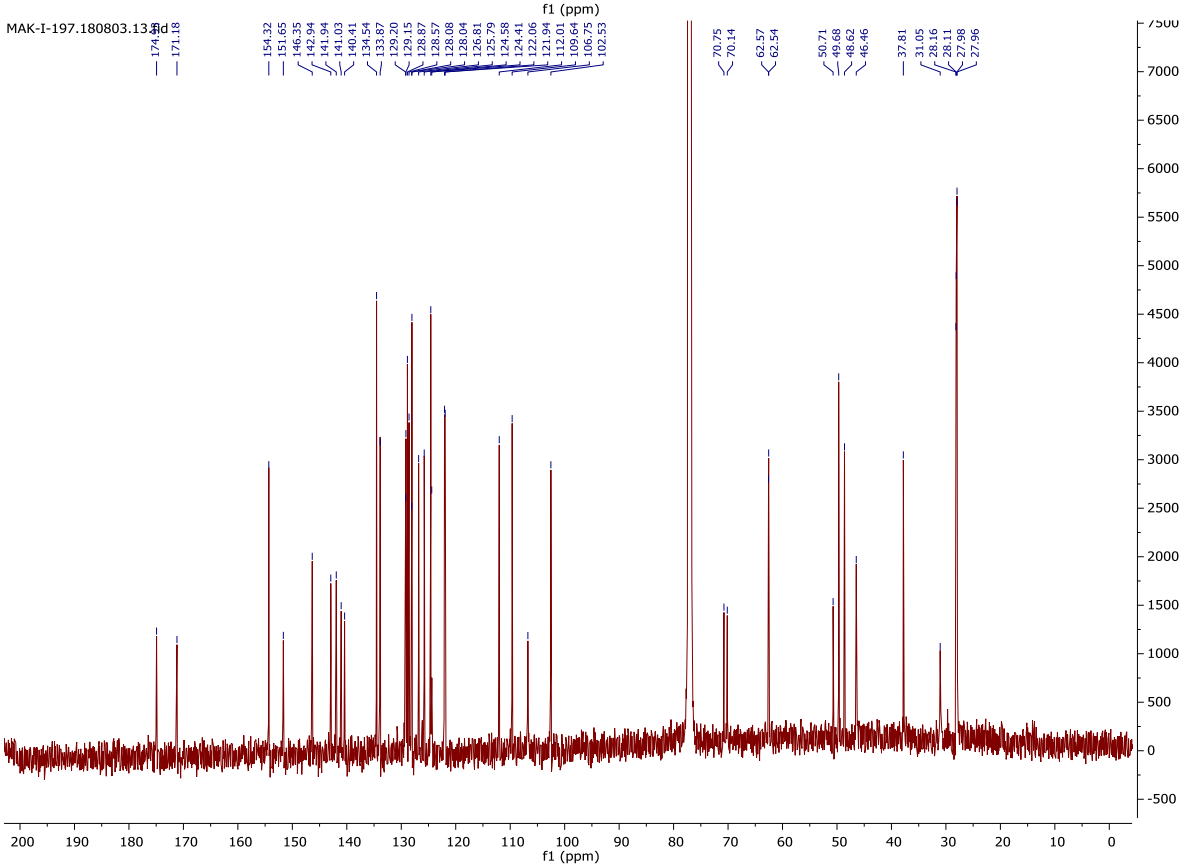

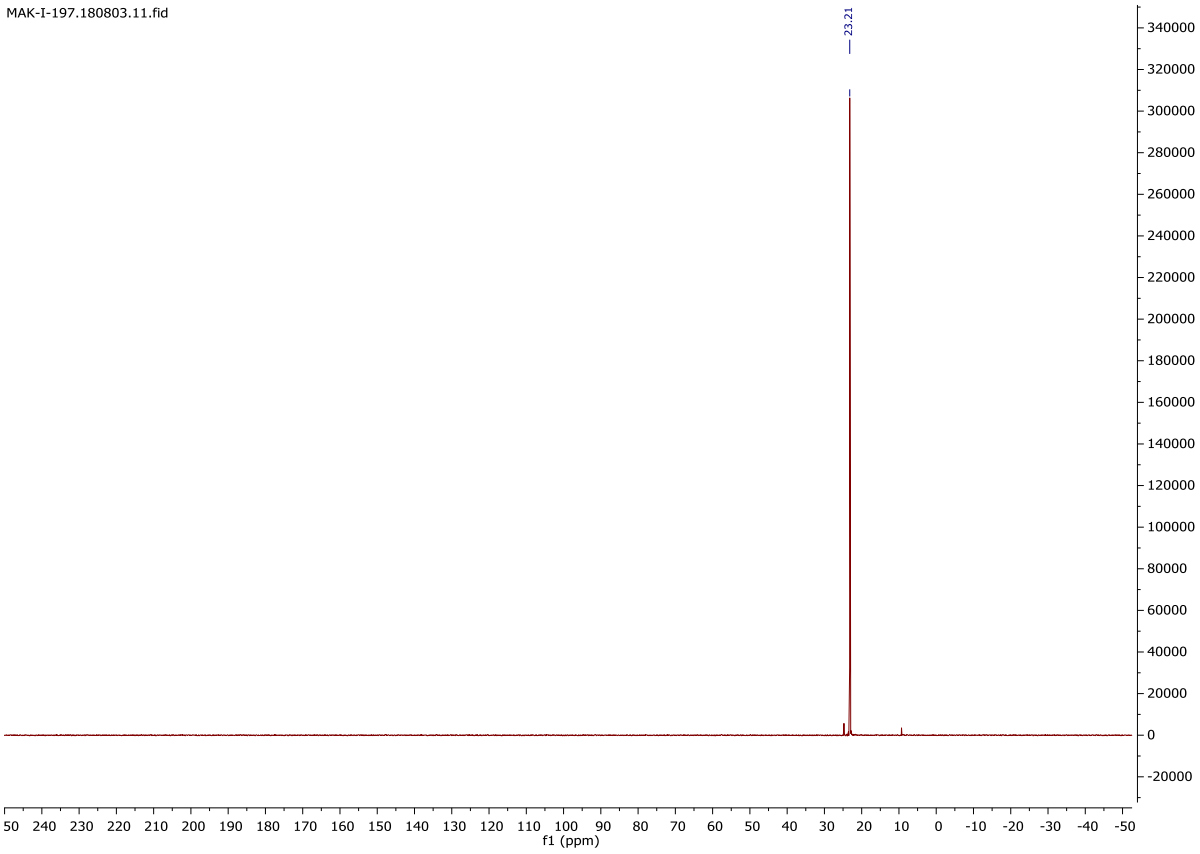
MAK-I-197.180803.11.fid
23.21
340000
320000
300000
280000
260000
240000
220000
200000
180000
160000
140000
120000
100000
80000
60000
40000
20000
0
-20000
50 240 230 220 210 200 190 180 170 160 150 140 130 120 110 100 90 80 70 60 50 40 30 20 10 0 -10 -20 -30 -40 -50
f1 (ppm)